ENGINEERING-TRANSPORTATION
LIBRARY

Indexes

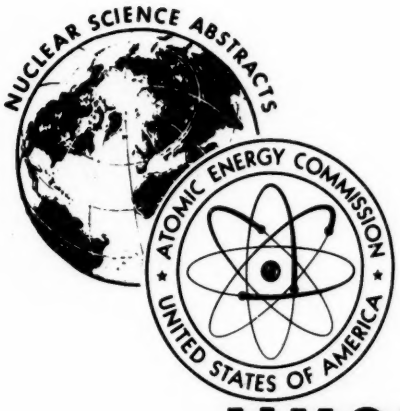

THE UNIVERSITY OF MICHIGAN
JUN 7 1966
ENGINEERING LIBRARY

NUCLEAR SCIENCE ABSTRACTS

Volume 20 Number 9

Abstracts 14231–16157

May 15, 1966

UNITED STATES ATOMIC ENERGY COMMISSION
Division of Technical Information

DEPOSITED BY THE
UNITED STATES OF AMERICA

USAEC DEPOSITORY LIBRARIES

Collections of USAEC reports are maintained in the libraries of the organizations listed below for reference use by the general public. Facilities for making photocopies are available. The USAEC also makes available through these libraries atomic energy reports of countries other than the U. S. that are abstracted in *Nuclear Science Abstracts*.

ALABAMA
Auburn, Auburn University
ALASKA
College, University of Alaska
ARIZONA
Tucson, University of Arizona
ARKANSAS
Fayetteville, University of Arkansas
CALIFORNIA
Berkeley, University of California
Davis, University of California
Los Angeles, University of California
San Diego, Public Library
Stanford, Stanford University
COLORADO
Boulder, University of Colorado
Denver, Public Library
CONNECTICUT
New Haven, Yale University
DELAWARE
Newark, University of Delaware
DISTRICT OF COLUMBIA
Washington, Library of Congress
FLORIDA
Coral Gables, University of Miami
Gainesville, University of Florida
Tallahassee, The Florida State University
GEORGIA
Atlanta, Georgia Institute of Technology
HAWAII
Honolulu, University of Hawaii
ILLINOIS
Chicago, John Crerar Library
Chicago, University of Chicago
Evanston, Northwestern University
Urbana, University of Illinois
INDIANA
Bloomington, Indiana University
Lafayette, Purdue University
IOWA
Ames, Iowa State University
KANSAS
Manhattan, Kansas State University
KENTUCKY
Lexington, University of Kentucky
Louisville, University of Louisville
LOUISIANA
Baton Rouge, Louisiana State University
New Orleans, Tulane University
MARYLAND
Baltimore, Johns Hopkins University
College Park, University of Maryland
MASSACHUSETTS
Cambridge, Harvard University
Cambridge, Massachusetts Institute of Technology
MICHIGAN
Ann Arbor, University of Michigan
Detroit, Public Library
East Lansing, Michigan State University
MINNESOTA
Minneapolis, University of Minnesota
MISSISSIPPI
State College, Mississippi State University
MISSOURI
Kansas City, Linda Hall Library
Rolla, University of Missouri School of Mines and Metallurgy
St. Louis, Washington University
MONTANA
Bozeman, Montana State College
NEVADA
Las Vegas, Nevada Southern University
Reno, University of Nevada
NEW JERSEY
Princeton, Princeton University
Teaneck, Fairleigh Dickinson University
NEW MEXICO
Albuquerque, University of New Mexico
NEW YORK
Albany, The University of the State of New York
Buffalo, State University of New York at Buffalo
Ithaca, Cornell University
New York, Atomic Industrial Forum, Inc.
New York, Columbia University
New York, New York University
Rochester, University of Rochester
Schenectady, Union College
Syracuse, Syracuse University
Troy, Rensselaer Polytechnic Institute
NORTH CAROLINA
Charlotte, Public Library of Charlotte and Mecklenburg County
Durham, Duke University
Raleigh, North Carolina State College
NORTH DAKOTA
Grand Forks, University of North Dakota
OHIO
Cincinnati, University of Cincinnati
Cleveland, Public Library
OHIO (CONT.)
Columbus, Ohio State University
Toledo, University of Toledo
Youngstown, Youngstown University
OKLAHOMA
Norman, University of Oklahoma
Stillwater, Oklahoma State University
OREGON
Corvallis, Oregon State University
Portland, Reed College
PENNSYLVANIA
Philadelphia, University of Pennsylvania
Pittsburgh, Carnegie Library
University Park, Pennsylvania State University
PUERTO RICO
Rio Piedras, University of Puerto Rico
RHODE ISLAND
Providence, Brown University
SOUTH CAROLINA
Columbia, University of South Carolina
TENNESSEE
Knoxville, University of Tennessee
Memphis, Public Library
Nashville, Joint University Libraries
Oak Ridge, Oak Ridge Associated Universities
TEXAS
Austin, University of Texas
College Station, Texas A & M University
Dallas, Southern Methodist University
Houston, Rice University
Lubbock, Texas Technological College
San Antonio, Public Library
UTAH
Salt Lake City, University of Utah
VIRGINIA
Blacksburg, Virginia Polytechnic Institute
Charlottesville, University of Virginia
Norfolk, Old Dominion College
WASHINGTON
Pullman, Washington State University
Seattle, University of Washington
WEST VIRGINIA
Morgantown, West Virginia University
WISCONSIN
Madison, University of Wisconsin
Milwaukee, Public Library
WYOMING
Laramie, University of Wyoming

Volume 20, Number 9, May 15, 1966

NUCLEAR SCIENCE ABSTRACTS

A semimonthly publication of the USAEC Division of Technical Information, Edward J. Brunenkant, Director. Published by the USAEC Division of Technical Information Extension, Robert L. Shannon, Extension Manager.

Nuclear Science Abstracts covers the international literature on nuclear science and technology and provides the only comprehensive abstracting and indexing of this body of information. Published twice each month since 1947, *NSA* covers technical reports of the U. S. Atomic Energy Commission and its contractors, technical reports of U. S. Government agencies and other governments, universities, industrial and research organizations, as well as patents, books, and journal literature on a world-wide basis. Nearly 350,000 abstracts have appeared in *NSA* through Volume 19. The subject matter covered in *NSA* is described in issue Number 1 and in TID-4552, *Subject Scope of Nuclear Science Abstracts*, available free from the U. S. Atomic Energy Commission, Division of Technical Information Extension, P. O. Box 62, Oak Ridge, Tennessee 37830.

Abstracts are arranged according to a number of subject categories and subcategories. Definitions of categories appear in issues Number 1 and 13. If the language of the original item is not English, the language will be indicated. Translations are not abstracted where an abstract of the original item has appeared in *NSA*.

INDEXES TO NSA

Corporate author, personal author, subject, and report number indexes appear in each issue and are cumulated quarterly, semiannually, and annually. Multi-volume cumulations have been issued as indicated on the following page. Report number indexes for all volumes (1–18) were issued at the end of Vol. 18. At the end of Vol. 19, the indexes for Vols. 1–15 were reissued to include additional public availability information. This cumulation will be a permanent shelf item and will not be reissued. Report number indexes for Vol. 19 are included as a cumulation beginning with Vol. 16.

AVAILABILITY OF PUBLICATIONS ABSTRACTED

The public availability of all U. S. Atomic Energy Commission reports is indicated in the report number indexes. The availability of other reports, when known, is also indicated. The availability of some unnumbered reports is given in the abstract.

Dissertations abstracted in *Dissertation Abstracts* and included in *NSA* are available from University Microfilms, Inc., 315 N. First Street, Ann Arbor, Michigan 48103.

Most of the published literature abstracted in *NSA* is on deposit at the Library, Oak Ridge Associated Universities, Oak Ridge, Tennessee, (a USAEC depository library) and is available through interlibrary loan. When requesting papers from this source, it is important that *NSA* volume and abstract number be cited.

HOW TO OBTAIN NUCLEAR SCIENCE ABSTRACTS

NSA is available on an exchange basis to universities, research institutions, industrial firms, and publishers of scientific information. Inquiries should be directed to the U. S. Atomic Energy Commission, Division of Technical Information Extension, P. O. Box 62, Oak Ridge, Tennessee 37830.

Government agencies may obtain *NSA* free of charge.

NSA is available to the general public on a subscription basis from the Superintendent of Documents, U. S. Government Printing Office, Washington, D. C. 20402, as follows:

For the 24 regular issues, $30.00 domestic, $37.00 foreign. A single issue costs $1.75, plus 25 per cent for foreign mailing. Domestic rates apply to the United States, Canada, Mexico, and Central and South American countries except Argentina, Brazil, British and French Guiana, Surinam, and British Honduras. Foreign rates apply to the countries excepted above and to all other countries throughout the world.

For the quarterly, semiannual, and annual indexes, $22.00 domestic, $25.00 foreign.

Multivolume subject and author indexes are available as follows:

Vols. 1–4 (1948–1950) Johnson Reprint Corporation, 111 Fifth Avenue, New York, N. Y. 10003, $30.00.

Vols. 5–10 (1951–1956) Superintendent of Documents, U. S. Government Printing Office, Washington, D. C. 20402, $5.25.

Vols. 11–15, Subjects, Superintendent of Documents, U. S. Government Printing Office, Washington, D. C. 20402, $19.00.

Vols. 11–15, Personal Authors, Superintendent of Documents, U. S. Government Printing Office, Washington, D. C. 20402, $14.25.

Vols. 11–15, Corporate Authors, Superintendent of Documents, U. S. Government Printing Office, Washington, D. C. 20402, $2.50.

Cumulative Report Number Index, Vols. 1–15, Revised, is available from the Superintendent of Documents, U. S. Government Printing Office, Washington, D. C. 20402, $4.00.

Cumulative Report Number Index, Vols. 16–19, is available from the Superintendent of Documents, U. S. Government Printing Office, Washington, D. C. 20402, $2.50.

Annual Indexes are available separately from the U. S. Government Printing Office as follows:

Vol. 16, Subject and Authors, $9.75.
Vol. 17, Subject and Authors, $12.25.
Vol. 18, Subject and Authors, $12.50.
Vol. 19, Subject and Authors, $12.50.

ACKNOWLEDGMENTS

Agreements between the United States Atomic Energy Commission and the following organizations with regard to providing continuing services and specific literature coverage for *Nuclear Science Abstracts* are gratefully acknowledged:

American Institute of Physics; Atomic Energy of Canada Limited; Atomic Energy Research Establishment, United Kingdom; European Atomic Energy Community (EURATOM); Gmelin Institute; International Atomic Energy Agency; Japan Atomic Energy Bureau—Japan Atomic Energy Research Institute; Netherlands Patent Office; Reactor Centrum Nederland.

DEPOSITED BY THE
UNITED STATES OF AMERICA

TABLE OF CONTENTS

Volume 20, Number 9, May 15, 1966

Category	Page
BIOLOGY AND MEDICINE	1751
General	1751
Ecology	1751
Metabolism, Tissue Distribution, and Toxicology	1752
Radiation Effects on Biochemicals	1755
Radiation Effects on Tissues	1759
Radiation Effects Therapy and Countermeasures	1773
Radiation Hazards and Protection	1775
Radiotherapy and Radiodiagnosis	1775
CHEMISTRY	1779
General	1779
Analytical Procedures	1779
Inorganic and Physical Chemistry	1789
Organic Chemistry	1798
Radiation Chemistry	1798
Radiochemistry	1805
Separation Processes and Procedures	1806
ENGINEERING	1810
General	1810
Applications of Nuclear Explosions	1810
Facilities and Equipment	1810
Heat Transfer and Fluid Flow	1813
Materials Testing	1815
Protective Structures	1818
Space Propulsion	1819
Vacuum Engineering	1820
GEOLOGY, METEOROLOGY, AND MINERALOGY	1821
General	1821
Meteorology	1821
Natural Radioactivity and Fallout	1821
Techniques and Equipment	1823
Thorium and Uranium Minerals	1828
HEALTH AND SAFETY	1830
INSTRUMENTATION	1834
General	1834
Radiation Detection	1837
Radiation Effects	1845
ISOTOPE TECHNOLOGY	1847
General	1847
Industrial Applications	1847
Power Application	1849
Separation and Production	1849
MATHEMATICS AND COMPUTERS	1850
METALS, CERAMICS, AND OTHER MATERIALS	1851
General	1851
Corrosion	1853
Fabrication	1856
Properties and Structure	1860
Radiation Effects	1872
PHYSICS	1875
General	1875
Accelerators	1876
Astrophysics and Cosmology	1879
Atomic Physics	1885
Cosmic Radiation	1890
Direct Energy Conversion	1891
Elementary Particles and Radiations	1893
Field Theory, Scattering Theory, and Symmetries	1906
Fluid Physics and Thermodynamics	1917
Geophysics	1920
Gravitation, Quantum Mechanics, and Relativity Theory	1925
Low Temperature Physics	1927
Neutron Physics	1930
Nuclear Properties and Reactions	1933
Plasma Physics and Thermonuclear Processes	1951
Shielding	1958
Solid State Physics	1960
REACTOR TECHNOLOGY	1967
General	1967
Auxiliaries and Components	1967
Criticality Studies	1969
Design and Feasibility	1972
Fuels	1973
Power and Power-Breeder Reactors	1974
Process Heat Reactors	1979
Propulsion and Space	1980
Research and Test Reactors	1981
WASTE DISPOSAL AND PROCESSING	1983
GENERAL AND MISCELLANEOUS	1985
CORPORATE AUTHOR INDEX	INDEX-1
PERSONAL AUTHOR INDEX	INDEX-12
SUBJECT INDEX	INDEX-53
REPORT NUMBER INDEX	INDEX-134

STAFF OF NUCLEAR SCIENCE ABSTRACTS

MANAGING EDITOR

John W. Norris

ASSISTANT MANAGING EDITOR

Donald D. Davis

ASSOCIATE EDITORS

Lawrence T. Whitehead
David E. Bost
Robert C. Kelly
Lee M. Thompson

SUBJECT INDEX EDITOR

Everett J. Hoffman

EVALUATORS

William D. Matheny
John H. Mitchell
Mary H. Newman

ABSTRACTORS

F. S. Armstrong (AECL)
Jane G. Buchanan
D. Lamar Cason
Bennie G. Di Bona
Helen G. Donald
James R. Dulaney
Wells L. Green
Mary Catherine Grissom
Fernando J. Hamilton
Phyllis C. Hansen
Carolyn D. Houston
Rose V. Jermain
Betty L. McDowell
Jean F. Peckham
Mona H. Raridon
Julia Redford
Francis L. Sachs
Lila B. Smith
Charles E. Stuber
Martha J. Thomas
Anne G. Ward
David C. West
Milton O. Whitson
Gabriel O. Ycaza

SUBJECT HEADING SPECIALIST

Robert E. Upchurch

CORPORATE AUTHOR SPECIALIST

Clara L. Fox

DESCRIPTIVE CATALOGING SPECIALIST

J. Paul Meredith

SCHEDULING AND PUBLISHING COORDINATOR

Brainard L. Patton

Communication concerning the editorial policy and content of *NSA* should be addressed to the Managing Editor, *Nuclear Science Abstracts*, AEC Division of Technical Information Extension, P. O. Box 62, Oak Ridge, Tennessee 37830.

Use of funds for printing this publication approved by the Director of the Bureau of the Budget, May 20, 1963

Volume 20, Number 9 May 15, 1966

NUCLEAR SCIENCE ABSTRACTS

BIOLOGY AND MEDICINE

General

Refer also to abstracts 14320 and 14950.

14231 (BNL-931) GENETIC CONTROL OF DIFFERENTIATION. Report of Symposium held June 7-9, 1965. Brookhaven Symposia in Biology, Number 18. (Brookhaven National Lab., Upton, N. Y.). Contract AT(30-2)-Gen-16. 275p. (CONF-650665). Dep. mn. CFSTI $3.00 cy, $1.50 mn.

The genetic control of differentiation is discussed in 15 papers representing the disciplines of cytogenetics, biochemistry, microbiology, embryology, and morphology. The discussions present common or divergent viewpoints, theories, and conclusions. Author and subject indexes are included. (C.H.)

14232 (LA-3440) COMPUTER ANALYSIS OF CELL VOLUME DISTRIBUTIONS. Dean, Phillip N. (Los Alamos Scientific Lab., Univ. of California, N. Mex.). Nov. 1965. Contract W-7405-eng-36. 51p. Dep. mn. CFSTI $3.00 cy, $0.50 mn.

Two computer programs were written to analyze blood cell volume distributions measured with a Coulter type of cell spectrometer. One of the programs, called AVØL, is used to calculate the mean cell volume of any type of distribution and to plot the data in various formats. The other program, called CELVØL, uses an iterative least-squares technique to fit either normal, log-normal, or skewed-normal distributions to the data. Either single- or double-peak distributions can be fitted. The program also converts the results of the fit to cell concentration in each peak in cells per cubic millimeter, standard deviation in cubic microns, and mean cell volume in cubic microns. For red blood cells the mean cell volume is also calculated from the hematocrit and included in the data output listing. (auth)

14233 (UCRL-16566) PHOTOBIOCHEMISTRY—DEHYDRATION CONDENSATION IN AQUEOUS SOLUTION [Thesis]. Steinman, Gary David (Lawrence Radiation Lab., Univ. of California, Berkeley). Jan. 1966. Contract W-7405-eng-48. 211p. Dep. mn. CFSTI $6.00 cy, $1.25 mn.

The results reported from many laboratories over the past decade make it clear that monomers necessary for biogenesis could have been formed under conditions believed to have existed on the primitive Earth. Mechanisms by which the biological monomers may have condensed in aqueous solution to produce more complex compounds, such as phosphates, acetates, pyrophosphates and peptides are discussed with emphasis on the role of dicyandiamide and dicyanamide in the types of condensations occurring on the primitive Earth. Results are reported from studies of the mechanism of dipeptide synthesis promoted by dicyanamide under conditions of simple, relatively stable reactants, moderate temperature, and dilute, aqueous solutions. It is postulated that this study demonstrates one means by which essential biochemicals could have been formed on the primitive Earth, thus providing materials needed for the origin of living systems. (C.H.)

14234 AIMS AND STANDARDS OF STERILIZATION TREATMENTS. Artandi, C. pp 85-94 of Ionising Radiation for the Sterilization of Medical Products. London, Panel on Gamma and Electron Irradiation, 1965.

Sterilization is discussed with respect to definition, production, measurement, maintenance, and minimization of changes induced in materials by the sterilization process. It is concluded that good manufacturing practices, high professional standards of the manufacturer, efficient methods of sterilization, and eternal vigilance are prerequisite for superior, sterile products. (H.G.D.)

Ecology

14235 (SAN-584-1) BATHYPHOTOMETRIC STUDIES OF THE LIGHT REGIME OF ORGANISMS OF THE DEEP SCATTERING LAYERS. Final Report. Clarke, William D. (General Motors Corp., Santa Barbara, Calif. Defense Research Labs.). Jan. 1966. Contract AT(04-3)-584. 50p. (TR-66-02). Dep. mn. CFSTI $2.00 cy, $0.50 mn.

The swimming capabilities of marine organisms make them important agents for the distribution and transportation of radioisotopes. Since the organisms associated with the deep scattering layers of the ocean move across density gradients such as the thermocline and the halocline, which normally inhibit physical mixing, and since these organisms provide forage for commercially-harvested fish, they may transfer radioactive substances from ocean waters to the food-chain of man. Results are reported from a study of the migrating mesopelagic organisms associated with the deep scattering layers of the Santa Barbara Channel, Calif. This area is part of that studied by the AEC in connection with the Vandenberg Air Force Base missile launching site. The principal phytogenic groups of migrating organisms were sampled at constant light levels, or isolumes, and plankton were sampled from the different strata of water between the maximum sampling depths and the surface. Sampling methods and equipment are described in detail. The migrating mesopelagic organisms associated with the deep scattering layers of the Santa Barbara Channel appear to form a series of partially overlapping layers that are correlated most closely with light intensity in their vertical distributions. Data are included on the distribution of the various species found. (C.H.)

14236 ^{90}Sr, STABLE STRONTIUM AND CALCIUM IN THE SOIL AND VEGETABLE FOOD PRODUCTS. Pavlotskaya, F. I.; Tyuryukanova, E. B.; Zatsepina, L. N.; Babicheva, E. V.; Baranov, V. I. (Vernadskii Inst. of Geochemistry and Analytical Chemistry, Moscow). Gig. Sanit., 11: 54-63(1965). (In Russian).

The distribution and content of ^{90}Sr in the arable stratum of turf-podzolic grey-forest and chernozem soil depends

on the strontium mobility and the agricultural technique used. A higher content of this isotope was noted at the depth of 10 to 20 cm. Stable strontium and calcium are more evenly distributed in the arable stratum of these soils. No relation could be traced between the ^{90}Sr content of the soil and that of the plants, as it depends on a great number of factors: first of all there may be a direct contamination of the parts of plants above the soil; in 1961, for example, the portion of plants contaminated above the soil comprised on the average 36%, the portion of isotope entering the plant through the root system amounted to 64%. The amount of ^{90}Sr removed by the plants did not exceed 3% of its content in the soil. (auth)

14237 SYMPOSIUM ON RADIATION AND TERRESTRIAL ECOSYSTEMS. Hungate, F. P. Nucl. Safety, 7: 92-9; 102(Fall 1965). (BNWL-SA-219).

A symposium on Radiation and Terrestrial Ecosystems was held May 3–5, 1965, in Richland, Wash. The symposium consisted basically of three parts: sources of radionuclides and how these radionuclides enter a food chain through plants; ecological paths and rates of nuclide transfer; and radiation as an environmental factor. Tracers of all kinds were utilized in the studies, those of natural origin, those widely dispersed as fallout, those intentionally introduced into the system, and even nonradioactive simple mineral constituents. It was pointed out that radiation produces both stimulatory and inhibitory effects, depending on levels used and features of the system observed. (auth)

Metabolism, Tissue Distribution, and Toxicology

Refer also to abstract 14372.

14238 (CONF-650560-13) THE AUTOMATIC HANDLING OF DATA FROM A LARGE-SCALE DOG RADIATION EXPERIMENT USING A GENERAL PURPOSE COMPUTER. Dipert, Merlin H.; Norris, W. P.; Pagels, Jeanne A. (Argonne National Lab., Ill.). [nd]. Contract W-31-109-eng-38. 13p. Dep. mn. CFSTI $1.00 cy, $0.50 mn.

From 13th Annual Meeting of the Radiation Research Society, Philadelphia.

The techniques of using a G.E. 225 digital computer and a Cal-Comp on-line plotter for the storage, retrieval, reduction and display of data are discussed. Our current experience includes over 1000 dogs with approximately one million words of information. The data from the dog radiation experiment are stored on magnetic tape in an open-end file which can be automatically updated, examined, and displayed with direct on-line printing and plotter facilities. The following items selected from those of current interest are discussed: census-table; food intake—calories consumed; weight; tables and plots; breeding-history tables; age-weight graphs; theoretical curves and plots; necropsy records; and calculation and display of radionuclide injection data. (auth)

14239 (JUL-312-ST) UEBER DEN NACHWEIS VON INKORPORIERTEM PLUTONIUM. (The Detection of Incorporated Plutonium). Jacobs, H. (Kernforschungsanlage, Juelich (West Germany). Zentralabteilung Strahlenschutz). Oct. 1965. 27p. Dep. mn.

A review is given on the present state of plutonium in men on the basis of a bibliographic study. For a better understanding of the methods and for evaluation of the results, some general properties of plutonium and its metabolism in the body are briefly described. The literature of the last 10 years is considered, but no claim to completeness is made. (144 references) (tr-auth)

14240 (NP-15670) UTILIZATION OF ^{14}C-LABELED UREA AND ^{32}P-LABELED PHOSPHATE TO INVESTIGATE THE PRACTICABILITY OF FOLIAR-APPLIED FERTILIZER FOR RICE GROWING IN RECLAIMED TIDAL LANDS. Report No. 2 (Final Part 2). Ku, Yuen-liang; Shih, Ching-yuan; Chu, Chun (National Taiwan Univ., Taipei (China). Dept. of Agronomy). Nov. 1963. Contract 102/OB. 27p. Dep. mn.

The practicability of the foliar fertilization of rice growing on reclaimed tidal lands was studied using ^{32}P-phosphates and ^{14}C-urea. Preliminary results are reported of studies on the response of rice seedlings and plants to foliar sprays of urea or phosphate fertilizers after being subjected to saline treatments in pot cultures, and factors that might affect the rate of absorption and translocation of nutrients. (C.H.)

14241 (TID-21437) METABOLISM OF METHYL PALMITATE, A PHAGOCYTIC AND IMMUNOLOGIC DEPRESSANT, AND ITS INFLUENCE ON TISSUE LIPIDS. Blickens, D. A.; Di Luzio, N. R. (Tennessee Univ., Memphis. Dept. of Physiology and Biophysics). [1964]. Contract AT(40-1)-1999. 26p. Dep. mn. CFSTI $2.00 cy, $0.50 mn.

The metabolism of methyl palmitate, a lipid which selectively impairs phagocytic and immunologic activity, was investigated to elucidate the mechanism of macrophage depression. An emulsion of methyl palmitate, labeled in either the methyl position or in the fatty acid position, was employed. The early tissue distribution of the methyl palmitate was not comparable to the classical distribution of other colloids known to be phagocytized by the reticuloendothelial system. The absence of a competitive effect of colloidal carbon on the vascular clearance of the labeled methyl palmitate preparation further indicates that methyl palmitate is not removed from the vascular system by a phagocytic process. Phagocytic depression induced by methyl palmitate is not due to hydrolysis of methyl palmitate and the formation of methanol. Rapid hydrolysis of the methyl carbon in methyl palmitate was suggested by the high level of expired $^{14}CO_2$. Tissue radioactivity 24 hours after injection of the radioactive methyl palmitate preparations and tissue lipid analyses revealed no profound storage of methyl palmitate; nor a measurable alteration in tissue lipid levels, indicating that methyl palmitate does not induce phagocytic or immunologic paralysis by a physical saturation of reticuloendothelial cells with lipid. (auth)

14242 (TID-22591) A STUDY OF THE EFFECTS OF AGE AND IONIZING RADIATION ON NUCLEIC ACID METABOLISM AND PROTEIN SYNTHESIS IN VISCERAL AND CENTRAL NERVOUS SYSTEM TISSUES. Technical Progress Report, March 15, 1965–January 1, 1966. Wulff, Verner J. (Masonic Medical Research Lab., Utica, N. Y.). Contract AT(30-1)-3518. 11p. Dep. mn. CFSTI $1.00 cy, $0.50 mn.

The metabolism of ribonucleic acid in the liver of young and adult rats was studied after the intraperitoneal injection of ^{3}H-cytidine one hr prior to killing. The RNA and DNA content of liver nuclei from young and old rats was determined. The turnover of RNA in liver nuclei was measured in vitro in diced liver obtained after administration of ^{3}H-cytidine or ^{3}H-orotic acid to intact animals. Labeling techniques using ^{3}H-orotic acid or ^{3}H-cytidine were developed for use in studies of RNA metabolism in the brain of young and old rats. Preliminary results are included from studies of RNA metabolism in parabiotic rats. (C.H.)

14243 (TID-22626) FISSION PRODUCT METABOLISM AND RESPONSE IN LABORATORY AND DOMESTIC ANIMALS AND PLANNING STUDY FOR EVALUATION OF RADIOACTIVE CONTAMINATION OF THE FOOD CHAIN. Progress Report, January 1, 1964–December 31, 1965. Comar, C. L.; Lengemann, F. W.; Wasserman, R. H.; Thompson, J. C. Jr. (New York State Veterinary Coll., Ithaca, N. Y. Dept. of Physical Biology). Contract AT(30-1)-2147. 155p. Dep. mn. CFSTI $5.00 cy, $1.00 mn.

Progress is reported in the evaluation of the levels of certain fissile and fission products in the food chain; investigation of factors governing the movement of certain fission products in the food chain; study of fundamental physiological processes that determine the levels of fission products that will occur in the human population; estimation of radiation dosage to tissues from ingested radionuclides and from

external radiation; study of the transport of materials across biological membranes; and certain aspects of genetics and its relation to the functioning of the organism. Emphasis was placed on the alkaline earth metals, particularly calcium and strontium. These studies include the relation of strontium retention to age; the relation of urinary strontium to dietary levels; the incorporation of calcium and strontium into human chromosomes; the transport of calcium, strontium, and barium across the intestinal wall; and the investigation of the effect of Vitamin D upon calcium absorption. The predictive equation for iodine consumption from milk by a human population was further refined and data are included from an assessment of radio-contamination in the food chain and man. The current appraisals include variability of fluid milk consumption; nutritional assessments; ^{90}Sr and ^{137}Cs in selected vegetables and, radionuclide prediction studies. (105 references) (C.H.)

14244 PLACENTAL TRANSFER OF ^{85}Sr IN MICE. **Nelson, Arne; Roennbaeck, Curt; Sjoeden, Ann-Marie (Research Inst. of National Defence, Sundbyberg, Swden). Acta Radiol. Therapy, Phys., Biol., 3: 477-83(Dec. 1965).**

The placental transfer of ^{85}Sr in mice was examined. If the strontium is administered before mating, the fetal uptake is low. The rate of uptake by the fetuses after fetal injection on the 12th, 14th, or 16th day of gestation is dependent on the growth of the fetus. The high uptake on the 18th day is due to the ossification of the fetal skeleton. (auth)

14245 AUTORADIOGRAPHIC STUDIES OF THE UPTAKE OF ^{131}I AND $^{35}SCN^-$ IN THYROID, SALIVARY GLANDS, TRACHEA, AND OTHER ORGANS OF THE GUINEA PIG. **Kleine, T. O. (Univ., Heidelberg). Arch. Exp. Pathol. Pharmakol., 251: 125-6(1965). (In German).**

Autoradiography of guinea pig organs was performed by dry stripping, reversal stripping, or alcohol stripping to detect ^{131}I (or ^{125}I) within thyroid follicles, follicular epithelium, interstitium, and in the border zones. In the parotid and sublingual glands it was detected in the lumen, as well as intra- and periepithelially in the proximal duct, and in the lumen and end piece of the distal duct. It was detected in the epithelial cells and cytoplasm of the trachea after in vivo administration, and decreasingly from the outer epithelial cells toward the lumen when added to the trachea in vitro. It was found in the lumen and intracellularly in the foveola, and in the neck and body of the glandular cells of the gastric mucosa. $^{35}SCN^-$ was detected within the thyroidal follicle cells, in the boundary zone, and in the follicular epithelium. It was also detected in the connective tissue and blood vessels of the thyroid. In the parotid and sublingual salivary glands the distribution of $^{35}SCN^-$ was identical to that observed with ^{131}I. After in vivo administration the distribution of $^{35}SCN^-$ in trachea was similar to that of ^{131}I, but it was, in addition, detected in the perichondrium, and diffusely in the epithelium, connective tissue, and cartilage. In the gastric mucosa its distribution was also found in the interstitial vessels. $^{35}SCN^-$ was detected in the epithelial cells of the esophagus, and in roots and shafts of hairs located in epidermal cells of the snout. (BBB)

14246 EFFECT OF PYRIDOXAL ON THE STRONTIUM CONTENT OF THE SKELETON. **Zipf, K.; Schenkel, R.; Schmid, A. Arch. Exp. Pathol. Pharmakol., 251: 190-2 (1965). (In German).**

After subcutaneous administration of pyridoxal-HCl doses ranging from 49 to 1964 μmole/kg body wt, the Sr content in representative samples of compact and spongy bone from rats was reduced in proportion to the amount of pyridoxal administered, except at the highest dose where it increased. Pyridoxal administration decreased the Sr content more in spongy bone than in compact bone. The authors assumed that this difference was related to the greater exchangeability of Sr in spongy bone and the smaller fraction of fixed Sr. On this basis, pyridoxal may be less able to affect the fraction of Sr that is fixed. Increased fixation of Sr at high doses of pyridoxal may depend on increased fixation of Sr by bone. At the higher doses pyridoxal administration gave rise to saluresis that was proportional to the dose of pyridoxal administered, but this did not seem to have a strictly diuretic effect. (BBB)

14247 MEASUREMENT OF ^{47}Ca ABSORPTION BY WHOLE-BODY GAMMA SPECTROMETRY. **Deller, D. J.; Worthley, B. W.; Martin, Heather (Univ. of Adelaide). Austral. Ann. Med., 14: 223-31(Aug. 1965).**

Absorption of calcium from the gastrointestinal tract was studied using ^{47}Ca and a whole-body counter. The physical characteristics of the isotope and the design and efficiency of the whole-body counter are described. Calculations showed that the total-body irradiation following the administration of 1 μC of ^{47}Ca to a standard man is less than 10 mrad and for the ^{45}Ca contaminant less than 7 mR to bone, values within the range of natural background radiation. Results of 86 studies carried out on 53 subjects with normal or disturbed calcium metabolism are presented. Absorption of ^{47}Ca as estimated by whole-body counting correlated well with the clinical state and experimental condition. Advantages and disadvantages of the technique are discussed. (TCO)

14248 A METHOD FOR STUDYING THE MATURATION TIME OF AN AVERAGE BONE MARROW CELL IN RAT USING ^{32}P AS TRACER. **Lahiri, S. K.; Udupa, K. B.; Nag, B. D. (Saha Inst. of Nuclear Physics, Calcutta). Indian J. Exp. Biol., 3: 149-53(July 1965).**

A method was developed for determining the maturation time of bone marrow cells and a mathematical model was developed to interpret the experimental results. Data for rats given 1 μC/70 g ^{32}P as tracer were used to examine the model. It was concluded that, by using differential techniques for separation of marrow cell types, the same principle can be used for determination of maturation types of different series of cells. A similar technique, using ^{59}Fe as tracer, can give maturation time of erythroid series cells. (BBB)

14249 STUDIES IN IODINE METABOLISM. III. THREE-POOL SYSTEMS OF EXTRATHYROIDAL THYROXINE KINETICS. **Sharney, Lena; Segal, Robert Lloyd; Dumont, Allan E.; Girolami, Antonio; Silver, Solomon (Mt. Sinai Hospital, New York). J. Mt. Sinai Hosp. N. Y., 32: 396-420(May-June 1965).**

Various earlier models used to interpret radioiodine metabolism in extrathyroidal compartments are discussed and a new three-pool model is developed from mathematical considerations for radiothyroxine metabolism. The results of experiments in dogs and humans are discussed in detail. Plasma thyroxine disappearance experiments were conducted with ^{131}I-labeled thyroxine, and blood specimens were collected every five minutes, then hourly, and finally daily. Stool specimens were also collected over a week or more, and the cumulative activity extrapolated to obtain the total fraction of initial activity eventually excreted as thyroxine or its derivatives in feces. Urines were also collected and counted. The elimination of errors in the estimation of the rate of hormone degradation, due either to the blocking of the gland by ^{127}I or the recycling of ^{131}I, by means of the double isotope technique is discussed. Several three-pool models of extrathyroidal thyroxine metabolism are formulated after the outline of the theoretical aspects of iodide metabolism, and on the basis of these clinical data. (BBB)

14250 STUDIES IN IODINE METABOLISM. IV. FORMULATION AND ANALYSIS OF THREE-POOL SYSTEMS. **Sharney, Lena; Feitelberg, Sergei; Segal, Robert Lloyd; Mittelmann, Alice (Mt. Sinai Hospital, New York). J. Mt. Sinai Hosp. N. Y., 32: 421-36(May-June 1965).**

Three-pool models applicable to radioiodine and radiothyroxine kinetics are formulated mathematically and their use in interpreting clinical data is discussed. Before formulating these mathematical models or analogues of this metabolic system, it was necessary to define fundamental assumptions about the distribution and movement of these metabolites within the body. When tracer substances are used as the principal tool of investigation, these assumptions or postulates must be consistent with the known physiological properties of the metabolite, and permit predictions about the dynamic behavior of the tracer. In practice

only a limited number of the compartments or pools of a metabolic system are accessible to instantaneous introduction of a tracer substance, and to its subsequent sampling and measurement. Tracer behavior in certain metabolic systems can be best approximated by sums of exponential functions with constant coefficients. These functions form solutions of linear homogeneous differential equations with constant coefficients. Therefore, the tracer behavior within a workable mathematical model of a metabolic system was described by a set of such differential equations. These equations were solved in the standard manner by means of the Laplace transforms. The general methodology underlying the formulation of multiple-pool models, and their mathematical treatment are discussed prior to formulating and handling three-pool models which are directly applicable to either iodide or thyroxine kinetics. (BBB)

14251 DECREMENT IN RADIOSTRONTIUM RETENTION FOLLOWING STABLE STRONTIUM PREFEEDING IN THE GROWING RAT. **Teree, Thomas M.; Gusmano, Ernest A.; Cohn, Stanton H. (Western Reserve Univ., Cleveland). J. Nutr., 87: 399-406(Dec. 1965).**

The value of stable Sr prefeeding in lowering tissue retention of ^{90}Sr after exposure was investigated in rats. Young, growing rats were fed varying amounts of stable Sr lactate (zero, 2, 4, and 6%) mixed with diet for 5 days prior to the intraperitoneal injection of both ^{85}Sr and ^{47}Ca. Whole-body retentions of both radioisotopes were determined by in vivo counting techniques, and Ca and Sr were determined in the bones and sera at the conclusion of the study. Maximal decrement in ^{85}Sr retention was obtained by the feeding of the 6% diet. Since the inclusion of 2% Sr lactate in the diet failed to alter ^{90}Sr retention, there appears to be a threshold to this effect located between levels achievable by the 2% and 4% diets. (TCO)

14252 THE DEPOSITION OF RADIOACTIVE Ba AND Sr IN THE AORTIC WALL. **Lamberts, H. B.; Van Andel, J. G. (Univ. of Groningen, Netherlands). Koninkl. Ned. Akad. Wetensch. Proc., Ser. C, 68: 311-19(1965).**

Rats were given one subcutaneous injection of 30 μC $^{140}BaSO_4$ in neutralized saline with a small excess of stable $BaSO_4$. After suitable intervals animals were killed and samples of aorta, skin, lungs, and tibia were analyzed for γ activity. It was seen that the ^{140}Ba bone content, after 3 weeks, rose steadily up to 12 weeks; after this a decrease occurred. Among the soft tissues, skin and lung sections did not show high specific activity but the aortic wall did. Rats each received 30 μC of $^{85}SrSO_4$ subcutaneously, and tissue samples were taken every two weeks. With Sr also, a preferential localization in the aortic wall was found, but contrary to the binding of ^{140}Ba, the Sr deposition was not periodic, at least not in the 11-week period studied. (TCO)

14253 SKIN CONTAMINATION BY RADIOACTIVE SUBSTANCES. **Kaneyasu, Yoshiko; Yoshizawa, Yasuo (Tokyo Univ.). Nuclear Eng. (Tokyo), 11: 51-4(Jan. 1965). (In Japanese).**

Sorptive properties of rat skin were studied, using carrier-free ^{32}P, ^{90}Y, and ^{198}Au. For nuclides having an ionic form, only about 5% of the amount administered was absorbed from the intact skin. When the epithelium, cerium, or subcutaneous tissues were injured, sorption from the wound was 35, 50, and 85%, respectively. The effects of tannic acid and epinephrine on skin absorption were investigated. It was concluded that the amount of radioisotopes absorbed into the body may be controlled by inhibiting the skin absorption temporarily by the local administration of epinephrine, and by incising in the meantime the contaminated skin or treating it by other appropriate methods. (TCO)

14254 RADIUM ISOTOPE ACCUMULATION IN ANIMAL THYROIDS. **Van Middlesworth, L. (Univ. of Tennessee, Memphis); Correa, Pelayo; Perkins, R. W.; Keane, A. T. Science, 151: 453-4(Jan. 28, 1966).**

Uranium and thorium daughters are ten times more concentrated in thyroids from some bovine animals than in the teeth of the same animals. These radioactive isotopes are believed to be from natural sources, but their resulting annual dosage of thyroid radiation has exceeded that from ^{131}I fallout. (auth)

14255 TRANSFERS OF WATER AND ELECTROLYTES ACROSS GRANULATION TISSUE IN PATIENTS FOLLOWING BURNS. **Moser, Manny H.; Robinson, David W.; Schloerb, Paul R. (Univ. of Kansas, Kansas City). Surg. Gynecol. Obstet., 118: 984-8(May 1964).**

The transfer of ^3H_2O, ^{22}Na, and ^{36}Cl across burned skin was studied in 19 patients. Solutions of the radioisotopes were applied directly to the skin and local loss of radioactivity was measured. Absorption of all three isotopes from the solution exposed to the burn granulation tissue was rapid, ranging from 11 to 56% in 30 min. No absorption from normal skin was detected. Tritiated water transfers were consistently higher than radiosodium, but not higher than radiochloride. Net chloride-36 absorption was almost double that of ^{22}Na. Sodium-22 absorption was 8.2 ± 1.1 (standard deviation) mequiv per cm^2 per min, although net absorption was only 1.1 ± 0.5. Because of transfers from the granulating tissue surface, net chloride-36 absorption was 2.6 ± 0.9 mequiv per cm^2 per min. Results indicated that water was transferred from the granulating tissue surface at nearly the same rate at which it was absorbed. Data show: large transfers of water and electrolyte across burned tissue; that absorption is concentration dependent; and suggest that a more physiologic solution should have electrolyte concentrations approximating those of the extracellular fluid. (TCO)

14256 EFFECTS OF CHELATING AGENTS IN MAN. **Spencer, Herta; Rosoff, Betty (Veterans Administration Hospital, Hines, Ill.). pp 34-65 in Chelation Therapy, Soffer, A. (ed.). Springfield, C. C Thomas, 1964.**

An extensive survey, with 50 references, is provided of the effects of chelating agents and their use in facilitating radioisotope excretion in man. Data are provided on excretion of rare earth elements and radiostrontium in chelated form. Toxicity of these agents is also reviewed. The relation between the amount of excess chelate and the magnitude of the urinary excretion of the yttrium chelate is discussed. Use of chelating agents to modify the distribution and excretion of trace metals of biological importance is also considered. (TCO)

14257 EFFECTS OF EXERCISE AND INHALED YTTRIUM OXIDE ON BLOOD LACTIC ACID, ERYTHROCYTE VOLUME, AND LUNG HISTOLOGY IN DOGS [Thesis]. **Reece, William Omar. Ames, Iowa, Iowa State Univ. of Science and Tech., 1965. 143p.**

Eighteen beagle dogs, 6–9 months of age, were subjected to treadmill exercise and exposure to a chamber atmosphere of yttrium oxide. The exposure period lasted for 30 days (180 exposure hours) and treadmill exercise was accomplished for 10 minutes per day throughout the experiment. Postexercise blood lactate concentration was determined twice weekly and erythrocyte volume, plasma volume, hemoglobin concentration, and leukocyte counts were determined before the exposure period began and again at its termination. Analysis was based upon a paired experiment and a significant increase was noted in blood lactic acid concentration and total leukocyte counts. A slightly significant decrease was noted in erythroctye volume. No significant difference was noted in plasma volume and hemoglobin concentration. In those dogs that showed a marked elevation in postexercise blood lactate concentration, a notable decrease was observed in the erythrocyte volume. Hypertrophy, hyperplasia, and desquamation of the alveolar epithelial cells and leukocyte infiltration were noted in the lungs. No connective tissue increase was observed. It appears that concentration of blood lactic acid following treadmill exercise might be useful for the evaluation of materials where the toxicity becomes apparent when a greater functional activity is demanded of certain systems of the body. (Dissertation Abstr.)

Radiation Effects on Biochemicals

See also CHEMISTRY — Radiation Chemistry

14258 (AD-627569) SYSTEMIC FACTOR IN RECOVERY OF RAT KIDNEY FROM X IRRADIATION: THYMIDINE-^{3}H INCORPORATION STUDIES. Wachtel, L. W.; Phillips, T. L.; Cole, L. J. (Naval Radiological Defense Lab., San Francisco, Calif.). Dec. 13, 1965. 21p. (USNRDL-TR-945). CFSTI $1.00 cy, $0.50 mn.

The effect of x-irradiation on thymidine-^{3}H incorporation into kidney cells (thymidine index) was measured at 4 to 8 hour intervals up to 96 hours in unilaterally nephrectomized female weanling rats. A sharp drop in the thymidine index occurred during the first 16 hours after the kidney only was irradiated with 1000 rad, and also after the kidney was irradiated with 125 rad or 500 rad at the same time the body received 500 rad. Irradiation of the body, but with the kidney completely shielded had no apparent inhibitory effect on kidney thymidine incorporation. The ability of the irradiated kidney to incorporate thymidine reappeared in 24 hours if the remainder of the body was not irradiated. When both the body and the kidney were irradiated, recovery of thymidine uptake depended on the amount of radiation received by each. An explanation for the above observations is offered on the basis of a postulated systemic factor, the formation or induction of which could be affected by radiation and which is essential for thymidine incorporation in the kidney. (auth)

14259 (NP-15855) A STUDY OF THE MECHANISM OF INITIAL RADIATION EFFECTS. Final Report, November 1, 1963-October 31, 1965. Report No. 6. Skreb, Yvette (Yugoslav Academy of Sciences and Arts, Zagreb. Inst. for Medical Research). Contract 217/R1/RB. 44p. Dep. mn.

Results are reported from studies on the effects of γ and uv radiations on the content of DNA, RNA, and proteins in whole amoeba, amoeba fragments with the nucleus, and amoeba fragments without the nucleus at various time intervals after exposure. The uptake of ^{14}C-adenine, ^{14}C-phenylalanine, ^{14}C-uracil, ^{3}H-cytidine, and ^{3}H-thymidine during the synthesis of these constituents were followed autoradiographically. (C.H.)

14260 (NP-15856) X-RAY INACTIVATION OF LAMBDA PHAGES. I. THE DAMAGES ON ADSORPTION AND INJECTION. II. REACTIVATION PROCESSES. Hradecna, Zdenka (Geneva Univ. (Switzerland). Biophysical Lab.). [1964]. 28p. Dep. mn.

Reactivation possibilities for the x-ray inactivation of λ phages were studied. All reactivation processes can be divided into two groups: photoreactivation and host cell reactivation which are of enzymatic nature, and multiplicity reactivation and cross reactivation which are due to genetic recombination. It was found that only little enzymatic reactivation occurs. Therefore, the phage seems not to carry a measurable proportion of lesions resembling uv lesions. The only marked reactivation phenomenon observed with x-ray inactivated phages is a certain marker rescue. Undamaged parts of the irradiated genome are incorporated to a measurable extent into simultaneously infecting, non-irradiated phages. (auth)

14261 THE RATE OF PEROXIDATION OF HOMOGENIZED TISSUES DURING THEIR IRRADIATION IN VITRO. Furnica, M.; Spiridon, M. (Institutul Oncologic, Bucharest). Acad. Repub. Pop. Rom., Stud. Cercet. Biochim., 5: 447-52(1962). (In Rumanian).

Rat tissues were irradiated in vitro with doses of 12,500 and 25,000 R. Peroxide formation was analyzed by the spectrophotometric method based on 2-thiobarbituric acid immediately after irradiation, 1 hour afterwards, and 2 hours afterwards. The % increase in peroxide above normal values is given for assays immediately after irradiation of 12,500 and 25,000 R respectively: brain, 71%, 156%; kidneys, 64%, 61%; intestinal mucosa, 39%, 77%; liver, 0%, 0%; spleen, 3%, 7%; Jensen's tumor, 20%, 43%. For assays after 1 hour: brain, 60%, 136%; kidneys, 36%, 51%; intestinal mucosa, 39%, 45%; liver, 52%, 48%; spleen, 0%, 7%; Jensen's tumor, 27%, 51%. For assays after 2 hours: brain, 80%, 93%; kidneys, 42%, 56%; intestinal mucosa, 38%, 51%; liver, 66%, 97%; spleen, 7%, 31%; tumor, —, 40%. These differences are interpreted in relation to the effects observed during local irradiation of various organs. (BBB)

14262 THE EARLY AND LATE REACTION OF THE FINE STRUCTURES IN THE FETAL RAT LIVER CELL TO A WHOLE-BODY IRRADIATION OF 400 R. Franke, H.; Goetze, E. (Friedrich-Schiller-Univ., Jena, Ger.). Acta Biol. Med. Ger., 14: 556-69(1965). (In German).

Early and late reactions of the fine structures in fetal liver cells of rats exposed to 400 R of whole-body x irradiation during the seventeenth day of development were studied. No changes were observed in the fine structures of the cells. However, lipid droplets appearing 12 min post-irradiation increased rapidly in size until 72 hrs post-irradiation when the lipid inclusions occupied almost the entire cellular volume of newly-formed erythroblasts. At 72 hrs post-irradiation lipid concentrations in the liver cells began to decrease, returning almost to normal by the fifth day post-irradiation. (H.G.D.)

14263 OBSERVATIONS ON BIOCHEMICAL CHANGES IN IRRADIATED SPORES OF BACILLUS CEREUS. Farkas, J.; Kiss, I. (Central Food Research Inst., Budapest). Acta Microbiol. Acad. Sci. Hung., 12: 15-28(1965).

The dipicolinic acid content of resting Bacillus cereus spores contained in a dense aqueous suspension was investigated after x irradiation. Spectrophotometry and chromatography were used to study substances leaking from bacterial cells after irradiation with lethal doses (up to 2000 krad). It was established that the pseudo-germination observed in the resting spores after irradiation with high doses is correlated with the increased permeability of the cell wall. It is suggested that as an effect of irradiation the chelate breaks down and the leakage of free amino acids precedes that of dipicolinic acid. After lethal heat treatment (90°C, 100 min) very few ninhydrin-positive compounds appeared in the amino acid chromatogram of the spores as compared with the chromatogram of irradiated spores. From a comparison of the amino acid chromatograms of vegetative spores and of resting spores, it appears that in the supernatant of irradiated vegetative spore suspensions the proportion of certain amino acids (methionine, tyrosine, valine, leucine) exceeds that of other amino acids. Radioresistance of resting B. cereus cells rapidly decreased to the sensitivity level of vegetative cells, when they were induced to germinate. (TCO)

14264 ON THE INFLUENCE OF X RAYS ON THE PHOSPHATE METABOLISM OF PHYCOMYCES. Brucker, W. (Ernst-Moritz-Arndt-Univ., Greifswald, Ger.). Ber. Deut. Bot. Ges., 78: 183-92(July 30, 1965). (In German).

Germinating spores of Phycomyces blakesleeanus were irradiated with x rays (20 and 50 KR). Visible germination of the mycelium was retarded 2 or 3 days by irradiation, but after 12 days the differences in dry weight of fungus disappeared. Analyses of six phosphate fractions from 12-day-old thalli showed radiogenic alterations in orthophosphate (40% increase), phosphate soluble in organic acid (20% decrease), total nucleic acid phosphate (15% decrease), and DNA phosphate (50% decrease). (TCO)

14265 BREAKDOWN OF DNA IN X-IRRADIATED ESCHERICHIA COLI. McGrath, R. A.; Williams, R. W.; Swartzendruber, D. C. (Oak Ridge National Lab., Tenn.). Biophys. J., 6: 113-22(Jan. 1966). (CONF-650221-4).

A comparison of differences in incorporation and loss of radioactivity between two strains of Escherichia coli shows that: three times as much irradiation is necessary to produce the same reduction in incorporation of ^{3}H-thymidine in B/r, the resistant strain, as in B_{s-1}, the sensitive one; radioactivity is lost from the DNA of previously labeled bacteria during the first few cell generations after x-ray exposure, and even though the initial rate of loss is similar for all strains, the sensitive one loses much more label;

loss of DNA is a complicated function of dose. Losses increase with dose up to 25 or 50 kR in both strains; with higher doses, losses decrease in B_{s-1} but are unchanged in B/r. Since in both strains labeled RNA is retained in irradiated cells, lysis has not occurred, but the DNA is broken down into small pieces that leak from each cell. Losses from either strain do not occur at ice-bath temperature, indicating that breakdown is a function of metabolic processes. A proposed mechanism for x-ray damage and repair is advanced. (auth)

14266 INDIVIDUAL DIFFERENCES IN THE RADIATION MORTALITY OF MICE AS PREDICTED FROM THE PRE-IRRADIATION STRESS RESPONSES. Pospisil, M. Sikulova, J. (Czechoslovak Academy of Sciences, Brno). Int. J. Radiat. Biol., 9: 597-600(1965).

Electrolytic balance as an indirect indicator of regulatory functions was measured in the urine of normal mice that were subsequently exposed to 760 R x-ray doses. A higher mortality rate was observed in animals having Na/K ratios below or above the norm. Results proved the importance of the applied indicator of stress readiness of the individuals for the prediction of the degree of radiation damage. (H.G.D.)

14267 REPAIR OF DAMAGE INDUCED BY A MONOFUNCTIONAL ALKYLATING AGENT IN A TRANSFORMABLE, ULTRAVIOLET-SENSITIVE STRAIN OF BACILLUS SUBTILIS. Reiter, H.; Strauss, B. (Univ. of Chicago). J. Mol. Biol., 14: 179-94(Nov. 1965).

Mechanisms of repair of uv-induced inactivation of this bacteria were investigated. The lethal effects of uv irradiation are determined both by the dose of radiation administered and by the capacity of the irradiated organism to repair the damage, repair being defined as the restoration of the biological activity of damaged DNA. A uv-sensitive, transformable strain of B. subtilis (uvr^-) was unable to carry out host cell reactivation of the virulent bacteriophage SPO1. The ratio of the slopes (k_{uvr^-}/k_{uvr^+}) of the uv-inactivation curves was 6 to 8 for cells or for whole phage, and 2 to 3 for indole transforming DNA or for SPO1 phage DNA measured in a transforming system. Whole phage inactivated with nitrogen mustard showed greater survival on uvr^+ cells than on uvr^-; there was no such difference for whole phage inactivated with methyl methanesulfonate (MMS). Whole uvr^+ cells recovered from uv-induced damage, as determined by an increase in extractable transforming activity during a period of incubation in which net DNA synthesis did not occur. Uvr^- cells were unable to recover from uv-induced damage but they did recover from MMS-induced damage in similar experiments. Density-labeled $^2H^{15}N$-MMS-treated uvr^+ cells incubated in $^1H^{14}N$ medium containing ^3H-thymidine showed a three-fold increase in extractable transforming activity, with no formation of new DNA molecules as determined by pycnometric analysis. The repair of damage induced by uv irradiation differs by at least one step from the repair of damage induced by MMS. Thus, B. subtilis has two separable recovery mechanisms, both of which can repair DNA containing a specific lesion. It is suggested that one of the mechanisms may repair damage due to the insertion of single-strand breaks while the other repairs DNA damaged by some agent which deforms the DNA or produces cross-links. Alternately, the repair of a single-strand break may occur as a later step in the repair of uv damage. The existence of MMS-sensitive strains which are also uv-sensitive, is prediced, if this be so. (BBB)

14268 VARIATIONS OF THE HEPATIC LIPID COMPONENTS IN THE MOUSE AFTER WHOLE-BODY IRRADIATION WITH A LETHAL DOSE. Del Favero, A.; Pasotti, C.; Nicrosini, F. (Univ., Pavia, Italy). Minerva Radiol., Fisioterap. Radiobiol., 10: 381-5(Sept. 1965). (In Italian).

The effects of a lethal whole-body irradiation on the lipid contents of liver tissue were investigated in the white mouse. The effect of tissue hydration on the same components was also investigated. After 6 days of observation, a slight increase of the total tissue lipids, attributable to an increase of the glyceride and steroid fractions, were observed in all groups of animals. The findings are described and the pathogenesis of the findings observed is discussed. (tr-auth)

14269 URINARY EXCRETION OF PSEUDOURIDINE IN THE COURSE OF X-RAY THERAPY. Drahovsky, D.; Winkler, A.; Skoda, J. (Cancer Research Inst., Bratislava). Neoplasma, 12: 561-4(1965).

A marked increase of urinary excretion of pseudouridine during x-ray therapy in patients with malignant disease was observed. This increase is particularly marked when lymphatic nodes, e.g., spleen, are irradiated. The ratio of urinary nucleic acids catabolites (pseudouridine : uric acid) after irradiation of certain organs changes with the ratio of the content of soluble ribonucleic acid (s-RNA) to the whole content of nucleic acids in the particular organ. (auth)

14270 THE INFLUENCE OF X-RADIATION, METHIONINESULFOXIMINE, BURNS, AND CYTOSTATIC AGENT TS 160 (SPOFA) ON THE URINARY EXCRETION OF INORGANIC PHOSPHATES AND AMMONIA AND ON THE LEVEL OF ADENINE NUCLEOTIDES IN BLOOD AND LIVER OF RATS. Kolousek, J.; Jiracek, V.; Zicha, B.; Dienstbier, Z. (Charles Univ., Prague). Neoplasma, 12: 565-83(1965).

The effect of x radiation, methioninesulfoximine, cytostatic agent TS 160-Spofa (tris-chlorethyl-amine hydrochloride), and of burns on the excretion of inorganic phosphates and ammonia nitrogen in the urine of experimental rats was studied. Further the influence of x-radiation (1000 R) and of L-methioninesulfoximine on the levels of adenine nucleotides (ATP, ADP, AMP) in the liver and in the blood of rats was studied. The x-radiation (600 R) increased the phosphate diuresis from the 48th hour and the ammonia diuresis in the period of 72 to 96 hrs after the irradiation. On the contrary, methioninesulfoximine decreased the inorganic phosphate contents and increased the ammonia nitrogen in the urine in the period of 0 to 24 hrs after the application. The cytostatic agent TS 160-Spofa increased the phosphate diuresis in the period of 0 to 48 hrs and the ammonia diuresis only in the period of 0 to 24 hrs after the application. The burns influenced the phosphate diuresis similarly as the x radiation, whereas the ammonia contents were increased in the period of 0 to 24 hrs after the intervention. The x-radiation (1000 R) decreased the ATP contents partly immediately (in the liver), partly 24 hours after the irradiation (in the liver and in the blood). The AMP contents in the liver were increased in the period of 0 to 12 hrs after the irradiation. Methioninesulfoximine in the liver first decreases the ATP contents and increases the AMP contents (6 hrs after the application), later it increases the ATP and decreases the AMP contents (24 to 48 hrs after the application). (auth)

14271 SUPPRESSION OF PHAGE T4 BY COINFECTION WITH UV-INACTIVATED HOMOLOGOUS PHAGE. Harm, Walter (Univ., Cologne). Photochem. Photobiol., 4: 569-73(June 1965).

Viable phage, infecting cells of E. coli B which are coinfected with several uv irradiated homologous phages, may fail to produce progeny. This phenomenon, termed suppression, was evident for multiplicities higher than 5 of uv irradiated T4, and for multiplicities higher than 8 of uv irradiated T2. These earlier results were interpreted as a consequence of limited participation of phage in intracellular growth. At uv doses much higher than those originally applied, suppression of T4 was noticed even at lower multiplicities of infection of the irradiated phage. Further experimental data concerning suppression of phage T4 are presented and their possible interpretation discussed. The results showed that unirradiated phage $T4v_1$ may fail to produce viable progeny in cells which are coinfected with uv irradiated homologous particles. The extent of this suppression is positively correlated with the multiplicity of infection of the irradiated phage and with the uv dose. The suppression reaches a max level at about 300 to 600 lethal hits. Quantitative evaluation of the results shows that in some complexes one irradiated phage particle is

sufficient to suppress an unirradiated phage. Two hypotheses are discussed to explain the results. One, lethal uv damages are incorporated into the unirradiated phage genome by genetic recombination; two, genetic subunits (e.g., cistrons or operons) of the uv irradiated phage produce informationally incorrect messenger RNA molecules, which compete with the correct ones from the unirradiated phage in the protein-synthetizing system. Hypothesis two appears to be more adequate to explain the experimental results. (BBB)

14272 EFFECT OF AMINO ACIDS ON THYMINE DIMERIZATION. **Balis, M. Earl (Sloan-Kettering Inst. for Cancer Research, New York). Photochem. Photobiol., 4: 587-92(June 1965).**

A primary result of the action of uv light on DNA is the formation of pyrimidine dimers, and it has been suggested previously that the chemical reaction involved is analogous to the low temperature dimerization of thymine. Such hypotheses do not, however, take into account the possible effects of alterations in the milieu in which the DNA might exist. DNA is associated in the nucleus with basic proteins, and the nature of these proteins might influence the photodimerization. Therefore, the dimerization of thymine in the presence of several amines was examined. The effect of the amines on the uv-catalyzed dimerization of thymine was determined at 25 and −20°C. Most amino acids and EDTA had no effect. Histidine, phosphoserine, and phosphoethanolamine increased the net yield of dimer at 25°C, but decreased the yield at −20°C. Histidine stimulates the cleavage of dilute solutions of thymine dimer at 25°C. It is suggested that these compounds might prevent the orientation of thymine molecules necessary for their photoactivation. These findings stress the potential role of the surrounding medium in photoreactions involving DNA both in vitro and in vivo. Attempts to cause photodimerization of thymine with proflavin as photoactivator were unsuccessful. This is contrasted with the observed effects of this dye on DNA which mimic those of uv. (BBB)

14273 INACTIVATION AND INDUCTION OF FREE RADICALS IN DRIED TRYPSIN. **Brustad, T.; Steen, H. B.; Dyrset, J. (Norsk Hydro's Inst. for Cancer Research, Montebello, Norway). Radiat. Res., 27: 217-28(Feb. 1966).**

An investigation was carried out of inactivation and induction of stable free radicals in crystalline trypsin exposed to ultraviolet light at about 10°C or irradiated with ^{60}Co γ rays at about 0°C. It was found that the ESR signal induced by γ rays is surprisingly similar to that induced by ultraviolet light. The results suggest that enzymes may be inactivated by ultraviolet light of certain wavelengths without concomitant induction of stable radicals, and/or that the radicals detected at room temperature after completion of the exposure represent merely the last step in chains of reactions initiated by the primary absorption events, and that the injury is related to earlier steps in these sequences of events, which are likely to be different for the two types of radiation. (auth)

14274 QUANTUM YIELD STUDIES OF THE DYE-SENSITIZED PHOTOINACTIVATION OF TRYPSIN. **Glad, Blaine W.; Spikes, John D. (Univ. of Utah, Salt Lake City). Contract AT(11-1)-875. Radiat. Res., 27: 237-49(Feb. 1966). (COO-875-43).**

The quantum yield of the photodynamic inactivation of trypsin was studied with methylene blue, eosin Y, and FMN as sensitizers. The reaction was studied for each dye with respect to several kinetic variables: light intensity, dye concentration, trypsin concentration, pH and ionic strength, and temperature. Further, the effects of several protective agents, including sodium iodide, histidine, AET, and egg albumin, were examined. Quantum yields for inactivation under the reaction conditions used were 0.0014 with methylene blue, 0.0027 with eosin Y, and 0.0023 with FMN, and were essentially independent of light intensity. With increasing dye concentration, the quantum yields increased rapidly, attained a maximum, and then decreased; the yields increased with increasing enzyme concentration. No inactivation occurred below pH 6 with methylene blue and eosin Y. As pH was increased above this value, quantum yields rose sharply and then leveled off. With FMN, the same behavior was observed above pH 6, but, in contrast, appreciable inactivation occurred below pH 6. With all three dyes, the quantum yields increased slightly as the temperature was raised from 4 to 33°C. Histidine and egg albumin protected trypsin against photodynamic inactivation with all three dyes; sodium iodide protected with eosin Y and FMN, and AET protected with methylene blue and FMN. (auth)

14275 BIOCHEMICAL EFFECTS OF X-IRRADIATION ON ERYTHROCYTES. **Myers, D. K.; Bide, R. W. (Atomic Energy of Canada Ltd., Chalk River, Ont.). Radiat. Res., 27: 250-63(Feb. 1966).**

The degree of hemolysis in irradiated erythrocyte suspensions after incubation was found to depend on the concentration of cells and on the composition of the extracellular fluid during x irradiation. Potassium loss from the irradiated cells during incubation at 4°C was not affected by these factors and seemed to depend primarily on radiation damage inside the erythrocyte. Radiation doses which eventually result in hemolysis caused an immediate loss of intracellular glutathione and of membrane antioxidants together with peroxidation of membrane lipids. Glutathione levels were rapidly restored to normal, but lipid peroxidation and hemolysis increased during subsequent incubation of the irradiated cells, particularly at 37°C. The damage causing potassium loss was also repaired when the irradiated cells were incubated at 37°C. Elimination of most of the erythrocyte sulfhydryl groups by reaction with N-ethylmaleimide produced a threefold increase in the sensitivity of the cells to subsequent irradiation. (auth)

14276 EFFECTS OF EXPERIMENTAL DYSPROTIDEMIA ON THE HOMOLSKY'S TEST RESPONSES. **Sciascia, R.; Cabassa, N. (Universita, Bologna). Radiobiol. Radioterap. Fis. Med., 20: 221-8(May-June 1965). (In Italian).**

The behavior of Hamolsky's test in rats exposed to a whole-body irradiation of 1000 R (^{60}Co) administered in a single dose was studied. A remarkable reduction in the values of the erythrocyte uptake of $T_3 - ^{131}I$ was observed in the irradiated rats in comparison with the control animals. This result is attributed to the profound disturbance of the plasmatic protein picture induced by irradiation. The mechanisms through which dysprotidemia interferes with the test response are discussed. The value of this test as a real expression of the thyroid function in many physiological and pathological conditions, associated to a more or less degree with dysprotidemia, is also considered. (tr-auth)

14277 EFFECTS OF IONIZING RADIATION ON DNA IN THE NUCLEOPROTEIN COMPLEX. **Usakovskaya, T. S. (Inst. of Experimental Biology, Academy of Medical Sciences, USSR). Radiobiologiya, 5: 791-6(1965). (In Russian).**

The data presented indicates that during irradiation of DNA in DNP compounds, a series of structural and local damage occurs in the DNA molecule at doses from 2.5 to 15 kr. The albumin found in the DNA complex partially protects it from damage. (tr-auth)

14278 PHOSPHOLIPIDS OF MITOCHONDRIA OF LIVER AND SMALL INTESTINE MUCOSA CELLS IN RABBITS UNDERGOING WHOLE-BODY γ IRRADIATION. **Simonov, V. V. Radiobiologiya, 5: 907-8(1965). (In Russian).**

To determine whether radiation-induced changes in mitochondria are physical or chemical, tissues of different radiation sensitivity were irradiated and the mitochondria phospholipids were analyzed. The phospholipids in the mitochondria from the livers of rabbits (3 to 4 kg) sacrificed 24 hr after 800 R of ^{60}Co gamma irradiation were normal both in total amount and in the amounts in the various fractions. Those from the small-intestine mucosa were slightly lower in total amount, 32% lower in lysocephalins, and 50% higher in polyglycerophosphatides than normal. (TTT)

14279 LIPASE ACTIVITY IN THE FATTY TISSUES AND LIVER FOLLOWING γ IRRADIATION. Lomova, M. A. Radiobiologiya, 5: 908-10(1965). (In Russian).

The problem of determining the activity of lipolytic enzymes was evaluated in rat, mouse, and rabbit liver tissue and epididymal fatty tissue. Rabbits and rats were x-irradiated to 800 R and the mice to 700 R at a rate of 250 R/min. The fatty tissue lipase activity increased in the mice to 27% above normal in 30 min and in the rabbits to 45% and the rats to 30% in 2 hr. There was then a decrease to about normal in all, with values first going below normal in the rats and mice but returning to normal in 1 and 3 days, respectively. In the liver homogenates after 2 hr lipase activity was highest in the mouse tissues and lowest in the rabbit. The results, considered with earlier ones on tributyrinase and those of other workers, show that there are at least two lipolytic enzymes in fatty tissue. Irradiation selectively activates the lipase in the fatty tissue and the tributyrinase in the liver. The results are of interest in radiation sickness studies. (TTT)

14280 AN EARLY REACTION OF THE ADRENAL CORTEX IN DOGS EXPOSED TO IRRADIATION. Stashkov, A. M. (Inst. of Experimental Medicine, Leningrad). Radiobiologiya, 5: 913(1965). (In Russian).

Two hours after 600 or 700 R (whole-body) x-irradiation of dogs, the concentration of 17-oxycorticosteroid in the peripheral blood plasma was up to 300 per cent higher than normal in four of eight animals studied. In three of the animals the increase was small and in one there was a slight decrease. After 24 hr, in the 600 R group values were essentially normal, but in the 700 R group two were normal and two were about 50 per cent below normal. These observations indicate an initial increase in the adrenal cortex function. (TTT)

14281 X-RADIATION INFLUENCE ON SMALLPOX VACCINE VIRUS IN CHICKEN EMBRYO. Kamalyan, L. A.; Ter-Pogosyan, R. A.; Vartevanyan, Zh. Ts. (Dept. of Radiobiology, Erevan). Radiobiologiya, 5: 919-21(1965). (In Russian).

In 8- to 10-day-old chick embryos x-irradiated to 700 to 900 R (60 R/min) 96 or 48 hr before inoculation with smallpox virus vaccine, the radiation sickness symptoms were aggravated by the inoculation. Of 650 subjects, those from the 700 R group that hatched showed petechiae in the dorsal region and on the extremities; the others showed large hemorrhagic areas on the bodies and heads. All weighed less than the controls. Most of the 900 R groups and 20 to 30% of the 700- and 800 R groups that hatched died within 20 to 30 days. Irradiation with 800 or 900 R 48 hr before inoculation decreased virus multiplication. Increasing the time to 96 hr decreased the virus growth in the 700 R group. Other workers have observed the opposite effect, i.e., increased virus growth with irradiation of 250 to 1000 R. The difference may be due to differences in conditions. (TTT)

14282 STUDIES OF POTASSIUM RELEASE FROM γ-IRRADIATED CELLS. Burdin, K. S.; Koltunov, Yu. B.; Parkhomenko, I. M. (Moscow State Univ.). Radiobiologiya, 5: 922-3(1965). (In Russian).

Damage to the walls of cells, suspended in isotonic glucose, by gamma irradiation (^{60}Co) to 5 to 60 kR at 1200 R/min was studied with a K^+ selective electrode. Release of potassium through the cell walls began with a dose of 10 kR and increased with increasing dose. The change in the potassium activity occurred 6 hr after the irradiation. Initially 3.16×10^{-5}M, the solution potassium concentration was 6.9×10^{-5}M after 50 min and 1.1×10^{-4}M after 6 hr. Vinyl pyrrolidone completely inhibited the release of potassium ion through the cell walls, but AET increased the release to 2.2×10^{-3}M after 5 hr. (TTT)

14283 INVESTIGATIONS ON THE RADIOSENSITIVITY OF DESOXYRIBONUCLEIC ACID. PART III. BREAKAGE AND CROSSLINKING POLYMERIZATION AFTER DIRECT IRRADIATION. Hagen, Ulrich; Wellstein, Hans (Univ., Freiburg i. B.). Strahlentherapie, 128: 565-76(Dec. 1965). (In German).

Dry DNA was exposed to 20,000 rad of x radiation in vacuum, air, and oxygen in order to determine the direct radiation effect on DNA. Determining the viscosity of native as well as denatured DNA, the number of single and double breaks in the DNA helix can be calculated. The distribution of the sedimentation was also determined. The results were used to determine the number of cross linkings formed between the single molecules. The G-values for the different reactions are given. With vacuum irradiation, each third event on a single chain is a cross linking, two thirds are breaks. Using oxygen, the number of single breaks resulted in a 5 fold increase, the cross linking formations decreased to a half. Double breaks are only slightly influenced by irradiating in the presence of O_2. (tr-auth)

14284 INFLUENCE OF RADIATION ON THE ACTIVITY OF SOME DEHYDROGENASES IN LIVER HOMOGENATES AND IN MITOCHONDRIA OF RATS. Zicha, Blahoslav (Charles Univ., Prague). Vet. Med. (Prague), No. 11, 671-80(1965). (In Czech).

Dehydrogenase activity was followed by reduction of triphenyltetrazolium salts in homogenates and in mitochondria of liver of Wistar rats after whole-body irradiation with a dose 800 R of ^{60}Co γ rays. Reduction of triphenyltetrazolium in the presence of various substrates was determined at 6, 12, 24, 48, and 72 hr postirradiation. In homogenate of liver, no change in dehydrogenase activity was detected with either endogenous substrate or added succinic acid at any of these intervals. However, with glutamate, α-ketoglutarate, pyruvate, and lactate significant decreases in dehydrogenase activity was noted 12 hr postirradiation; slight decreases at other intervals were not significant. With α-glycerophosphate, activity was lower than that in controls at 12 and 24 hr after irradiation, but above normal levels at 72 hr postirradiation. Succinic dehydrogenase activity was not affected in liver homogenate at any time following irradiation. Results in liver mitochondria also showed succinic dehydrogenase activity to be unaltered by irradiation. However, in mitochondria at 24 hr postirradiation dehydrogenase activity was below the normal level at 24 hr postirradiation when α-ketoglutarate and α-glycerophosphate were added as substrates. (BBB)

14285 THE FATE OF DNA INJECTED INTO THE HOST CELL FROM UV IRRADIATED T4 BACTERIOPHAGES. Shahn, Ezra. Pittsburgh, Pa., Univ. of Pennsylvania, 1965. 101p.

The fate of DNA injected into the host cell from uv inactivated T4 bacteriophages was investigated. In all cases where irradiated phages were used, infection was accompanied by simultaneous infection with viable, light, nonradioactive "rescuing" phages. With respect to nonirradiated phages, the amount of DNA transferred from phages subjected to 100 phage lethal hits of uv irradiation was only one-third. Second cycle growth with a low multiplicity of infection and no rescuing phage showed that these progeny were all viable. The DNA extracted from progeny phages was, in different experiments, sheared under a variety of conditions, denatured, and analyzed in both cesium chloride and sucrose gradients. The results indicate that transfer of DNA occurs in a manner that is basically semi-conservative, restores the continuity of the polynucleotide chains of the progeny DNA molecules, and leaves no inheritable scars. Increasing uv doses result in a decrease in net transfer from parent to progeny populations, a decrease in the average parental contribution per progeny phage, a decrease in the size of the individual subunits of parental origin within each phage, and an increase in the number of such subunits in each phage. An experiment bearing on the mechanism of this rescue indicated that polymerase is unable to act on the DNA from irradiated phages beyond certain points of uv-induced damage. Rescue is effected when a material exchange occurs between this partially replicated (and blocked) molecule and another complex being primed by either a molecule of DNA from a rescuing phage, or a replica of such a molecule. It is suggested, further, that recombinase is responsible for this material ex-

change, which, it is believed, cannot occur in the absence of replication. (A.G.W.)

Radiation Effects on Tissues

Refer also to abstract 14936.

14286 (AD-625837) A COMPARISON BETWEEN THE EFFECTS OF EXPOSURE TO A MIXED FISSION SPECTRUM DELIVERED IN A SINGLE "PULSE" AND X-RAYS DELIVERED AT A SLOWER RATE UPON THE CONDITIONED AVOIDANCE BEHAVIOR OF PRIMATES. Technical Report No. 4. Sharp, Joseph C.; Keller, Barbara K. (Walter Reed Army Inst. of Research, Washington, D. C. Behavioral Radiology Lab.). Oct. 1965. 16p.

Radiation effects on conditioned behavior was studied in 19 young male primates (Macaca mulatta) exposed to a mixed fission source delivered in a single pulse or to x rays delivered at a slower rate. Prior to irradiation at doses ranging from 1,000 to 65,000 rads, the animals were conditioned for shock avoidance. Television monitors permitted observation of response to the shock stimulus that was applied before irradiation, continuing during exposure and until complete incapacitation. It was concluded that the debilitating effects of massive doses of a mixed fission spectrum of radiation delivered in a single brief instant occur sooner than when x rays are delivered at slower rates. Depending on the dose, and following a pulse, there is an increased probability of an initial period of incapacitation, then a period of quite effective response followed by the sudden onset of permanent incapacitation and death. A marked absence of the usual signs and symptoms associated with radiation sickness was observed when the primates were exposed to a pulse. (H.G.D.)

14287 (AD-626996) TIME HISTORY OF BIOLOGICAL RESPONSE TO IONIZING RADIATION. Laumets, E. (Naval Radiological Defense Lab., San Francisco, Calif.). Nov. 22, 1965. 42p. (USNRDL-TR-905). CFSTI $2.00 cy, $0.50 mn.

Exposure of personnel to initial ionizing radiation from a nuclear air or surface burst can cause both prompt and delayed casualties. Their percentages and times to incapacitation (or combat ineffectiveness, in a military sense) after exposure can be of major significance in military operations. Although adequate data are lacking for the determination of dose-effect relationships vs time after exposure, quantitative estimates are needed nevertheless for guidance in battle-field predictions and decision-making. Available nuclear-accident data and other data on human exposures were used to obtain curves to represent the estimated time history of the acute radiation syndrome as a function of dose received in a very short time. The sources of data are clinical records of nuclear-accident casualties from 1945 to 1958, followup records of radiotherapy patients, and casualty studies on the atomic explosions at Hiroshima and Nagasaki. Emphasis is put on the time after exposure of the onset of the initial stage of radiation sickness (nausea, vomiting, malaise, etc.), duration of the initial stage, start and duration of the following asymptomatic latent period, time of onset of the second (or manifest illness) stage, and time of eventual recuperation or death. The estimated time history is depicted graphically with two other time histories for comparison. Analytical expressions are derived for the three time histories for use in estimating any of these syndrome times or periods. (auth)

14288 (AD-627986) ISOLATION OF STREPTOCOCCUS EQUI FROM BURROS. Wisecup, W. G.; Schroder, C. M.; Page, N. P. (Naval Radiological Defense Lab., San Francisco, Calif.). Dec. 28, 1965. 14p. (USNRDL-TR-960). CFSTI $1.00 cy, $0.50 mn.

An insidious disease was found in an experimental herd of burros in which the primary manifestations were debilitation and the presence of abscesses in abdominal lymph nodes. Streptococcus equi was isolated from these abscesses and also from the nares of many affected animals. A comparison of the frequency of S. equi in x irradiated, control, and newly purchased burros showed an incidence in irradiated animals approximately twice that of the controls. (C.H.)

14289 (BNL-9509) CHANGES IN LEAVES OF QUERCUS ALBA EXPOSED TO CHRONIC GAMMA RADIATION [Thesis]. Brower, Moonyean S. (Brookhaven National Lab., Upton, N. Y.). May 28, 1965. Contract AT(30-2)-Gen-16. 45p. ORAU.

Submitted to Massachusetts Univ., Amherst.

Leaves of Quercus alba L. were collected from the experimental forest at Brookhaven National Laboratory to study anatomical and morphological changes resulting from exposure to chronic gamma irradiation. Effects of increased solar radiation were also investigated since trees at radiation levels greater than 3R/20 hour day have a reduced number of leaves. High levels of chronic gamma radiation increased thickness and weight of the leaf blade, and also increased the number of stomata and chlorophyll content per unit of epidermal area. Exposure of leaves to full sunlight produced a similar syndrome of anatomical and morphological modifications. The effects of the two types of radiation were found to be additive. (auth)

14290 (NYO-1800-12) ATTEMPTS TO DELINEATE INBORN ANEMIAS IN MICE. Progress Report, February 1, 1965-January 31, 1966. Russell, Elizabeth S.; Bernstein, Seldon E. (Roscoe B. Jackson Memorial Lab., Bar Harbor, Maine). Feb. 10, 1966. Contract AT(30-1)-1800. 21p. Dep. mn. CFSTI $1.00 cy, $0.50 mn.

The existence in the mouse of 11 different non-allelic mutant genes whose actions lead to serious anemias demonstrates that there are at least 11 different internal physiological processes that are important for erythrocyte production, maintenance, or both. Results are reported from a comparison of colony-forming units in the marrow of various genotypes. New methods of analysis were used in the analysis of gene action pathways in hereditary defects of hematopoiesis, the state of the marrow, and its complement of blood-forming cells. Preliminary observations are presented for 8 different genotypes that indicate that mice of some anemic genotypes are not deficient in the number of stem cells, mice of several anemic genotypes are severely deficient, and still others are intermediate. Results are reported from studies on the effects of the implantation of hematopoietic tissues and exogenous erythropoietin on modifications of the anemias, biochemical and genetic studies of anemic mice, the effects of parabiosis on erythrocyte size and count, and preliminary observations on the influence of genotype on sensitivity of mice to x radiation and the relation of stem-cell deficiency to radiosensitivity of anemic mice. (C.H.)

14291 (TID-22494) RADIOAUTOGRAPHIC, HISTOCHEMICAL AND BIOCHEMICAL STUDIES OF THE EFFECTS OF IRRADIATION IN CARTILAGE AND BONE. Progress Report, December 15, 1963-December 31, 1964. Hirschman, Albert (State Univ. of New York, Brooklyn, Dept. of Anatomy). Contract AT(30-1)-2960. 14p. Dep. mn. CFSTI $1.00 cy, $0.50 mn.

Results are reported from studies on the effects of x radiation on the antigenic properties of extracts of irradiated rat epiphyseal cartilage, histochemical studies of fresh epiphyseal cartilage, the effects of irradiation on thymidine uptake and cytology, and a comparison of the effects of irradiation and mechanical injury on rat tibias. (C.H.)

14292 (TID-22563) [PROGRESS REPORT ON CARDIAC DAMAGE, FINAL, 1965]. Guyton, Arthur C. (Mississippi Univ., Jackson, Dept. of Physiology and Biophysics). Contract AT(40-1)-3111. 11p. Dep. mn. CFSTI $1.00 cy, $0.50 mn.

A summary is given of studies on: progressive changes in cardiac function following irradiation of the myocardium in dogs; procedures for measuring various fluid spaces in the lungs; and assessment of different indirect methods for measuring pulmonary blood volume. The procedure used for determining cardiac function curves at progressive intervals both before and after irradiation is described. Ventricular function was assessed by quantitative means during

all stages of progressive heart failure, from normal cardial function all the way to lethal congestive heart failure. The methods developed for measuring fluid and blood volume in the lungs are described. (P.C.H.)

14293 FORMATION OF LIPID PEROXIDES IN THE TISSUES OF IRRADIATED AND RADIOPROTECTED RATS. Costachel, O.; Furnica, M.; Dragon, V. (Institutul Oncologic, Bucharest). Acad. Repub. Pop. Rom., Stud. Cercet. Biochim., 5: 219-26(1962). (In Rumanian).

Rats were irradiated with doses of 1000 R; peroxides in various organs were determined spectrophotometrically after reaction with 2-thiobarbituric acid. Peroxides appeared in the spleen after 24 hours, in the liver after 3 days, and in the brain after 4 days. The peroxides reached maximum values at the end of 4 days in the spleen, at the end of 5 days in the brain, and at the end of 7 days in the liver; values attained were 115% greater than normal in the spleen, 118% in the brain, and 218% in the liver. Afterwards the peroxides declined again, reaching a normal value in the brain on the seventh day, but not in the spleen or liver within 8 days. A set of animals protected by Largactil (5 mg/kg, 10 min before irradiation) did not show any delay in appearance of peroxides. However, the amounts formed were smaller (85% increase in the spleen, 48% in the brain, 67% in the liver). (BBB)

14294 SUBMICROSCOPIC STUDIES ON THE EFFECT OF RADIATION IN A WHOLE-BODY DOSE OF 1000 R ON THE LIVER CELLS OF PREGNANT RATS AND THEIR FETUSES. Franke, H.; Goetze, E. (Univ., Jena, Ger.). Acta Biol. Med. Ger., 14: 792-808(Sept. 1965). (In German).

Adult female Wistar rats were given single doses of 400, 600, 800, and 1000 R of x rays on the 17th day of pregnancy, and electron microscopic studies were made of maternal and fetal liver 4 and 8 hr postirradiation. The fine structure of maternal liver organelles showed injury of varying degrees, dependent on the dose of radiation delivered. The degree of injury often showed wide variation from one cell to another. After 800 R, the ergastoplasm either showed only partial break-down by fragmentation or was destroyed completely, in which latter case the entire endoplasmic reticulum consisted of a microvesiculated framework. The mitochondria also demonstrated widely varying degrees of swelling. Their internal structure was destroyed in only a few instances. After 1000 R, the endoplasmic reticulum in most of the liver cells was highly vacuolated, and residual double membranes were seen in irregular arrangements or the intralamellar space was greatly dilated. In part, the matrix of the mitochondria was very dense, with internal structure destroyed in many cases. In addition, giant mitochondria appeared. After both 800 R and 1000 R doses, electron-opaque liver cells appeared, some with very dense cytoplasm. Surprisingly, no changes were visible in the fine structure of the fetal liver cells even after 1000 R, 4 to 8 hr after irradiation, aside from changes in the radiation-sensitive erythroblasts. However, lipid inclusions were increased in both cell nuclei and cytoplasm. (BBB)

14295 AUTORADIOGRAPHIC AND FLUORESCENCE MICROSCOPIC STUDIES OF AORTIC MUCOPOLYSACCHARIDE AFTER LOCAL EXPOSURE TO ^{90}Sr-^{90}Y RADIATION. Kunz, J. (Humboldt Univ., Berlin). Acta Histochem., 22: 16-26(1965). (In German).

Sulfate-^{35}S incorporation in aortic mucopolysaccharides (MPS) and their staining reactions were examined in rabbits. A 40 C β radiation source with an active surface of 1 cm^2 was inserted in the abdominal aorta. The $^{90}Sr-^{90}Y$ source giving a surface dose rate of 18 rad/sec was used to provide local aorta irradiation doses of 3, 15, and 30 krad. The animals were sacrificed 4, 10, or 30 days (and in one case 4 month) after irradiation. Two days before sacrifice the rabbits were injected intravenously with 2 μC of $Na_2{}^{35}SO_4$, enabling synthesis of sulfated MPS to be followed by autoradiography. After the 3-krad dose the incorporation of ^{35}S into MPS was stimulated at all periods tested, that is, higher than normal MPS synthesis occurred. In contrast, after the two higher doses (15 and 30 krad) MPS synthesis was depressed. Correlating histological and histochemical studies showed proliferation of intimal endothelium and fibroblasts in certain zones near the radiation source, and increased ^{35}S uptake in these cells was seen autoradiographically. Increasing radiation dose in the aorta wall was associated with increased incidence or frequency of the following histologic changes: intimal proliferation, intramural leukocyte infiltration, fragmentation of eleastic membranes, ground substance alterations, muscle cell disappearance, and periaortic fibrosis. (BBB)

14296 ISOTOPE TESTS OF KIDNEY FUNCTION IN PELVIC AND ABDOMINAL IRRADIATION. Green, J. P.; Bruneau, R.; Rubin, P. (Univ. of Rochester Medical Center, N. Y.). Acta Radiol. Therapy, Phys., Biol., 3: 418-24(Dec. 1965).

The results of the isotope test of the kidney function in 48 patients undergoing irradiation for pelvic and abdominal neoplasms are reviewed. The isotope test seems to be a reliable, economical, and rapid screening test. (auth)

14297 CHOROIDO-RETINAL DAMAGE AS A COMPLICATION OF RADIOTHERAPY. Perrers-Taylor, Marjorie; Brinkley, Diana; Reynolds, Tegwedd (Addenbrooke's Hospital, Cambridge, Eng.). Acta Radiol. Therapy, Phys., Biol., 3: 431-40(Dec. 1965).

A description is given of choroido-retinal changes occurring after irradiation treatments near the eye. Details are given of six cases with illustration of the fundi. When treating skin lesions in certain sites around the orbit, it seems difficult to avoid quite large doses of radiation reaching the choroid and retina when standard forms of radiotherapy are used. It appears that these doses of irradiation of the order of 1500 R upwards are sufficient in some cases to cause permanent choroido-retinal damage, probably by initially affecting the small blood vessels. (auth)

14298 VESICO-URETERIC REFLUX IN CONNECTION WITH SUPERVOLTAGE THERAPY FOR BLADDER CARCINOMA. Edsmyr, Folke; Nilson, Arne E. (Karolinska Sjukhuset, Stockholm). Acta Radiol. Therapy, Phys., Biol., 3: 449-56(Dec. 1965).

An investigation of the occurrence of reflux following ^{60}Co therapy for vesical carcinoma in 76 patients is reported. Reflux was evident in a large proportion of the ureteric orifices involved by the tumor, but in few of the others. Dilatation of the upper urinary tract was present in only 3 of the 25 patients with reflux. No implantation metastases were discovered in the upper urinary tract. (auth)

14299 INFLUENCE OF TOTAL DOSE AND OF AGE ON EFFECTS OF PROTON IRRADIATION OF SPINAL CORDS OF YOUNG RATS. Gilmore, Shirley Ann (Univ. of Uppsala). Acta Radiol. Therapy, Phys., Biol., 3: 463-76(Dec. 1965).

Single doses of high-energy protons ranging from 0.75 krad to 12 krad were administered to limited portions of spinal cords of neonatal rats when 3 to 5, 9 to 11, or 14 to 16 days of age. The incidence of neurologic abnormalities in the hindlimbs and the time between irradiation and onset of these abnormalities were studied and are discussed with respect to age when irradiated and amount of radiation. The microscopically pathologic changes of the spinal cords are reported and discussed in relation to age, dose, and the neurologic status of the animal. (auth)

14300 MALIGNANT MIXED MUELLERIAN NEOPLASMS (MIXED MESODERMAL TUMORS). Krupp, P. J.; Sternberg, W. H.; Clark, W. H.; St. Romain, M. J.; Smith, R. C. (Tulane Univ., New Orleans). Amer. J. Obstet. Gynecol., 81: 959-69(May 1961).

Fifty-one cases of mixed mesodermal tumor are surveyed, and data are provided that suggest possible implication of ionizing radiation in tumorigenesis. Thus, it was noted that two patients had previous irradiation for carcinoma of the cervix 11 and 13 years before diagnosis of malignant mixed Muellerian tumor. Although there is no conclusive evidence that uterine sarcoma can be induced by previous irradiation, especially for benign conditions, the incidence rate seems to be too high to be coincidental.

It appears that there are basic factors inherent at the time of the benign condition for which radiotherapy was given that led to the eventual formation of the tumor. (TCO)

14301 MIXED HETEROLOGOUS MESENCHYMAL SARCOMAS (MIXED MESODERMAL SARCOMAS) OF THE UTERUS: ADDITION OF 7 CASES. Edwards, David L.; Sterling, Lehman N.; Keller, Richard H.; Nolan, James F. (Los Angeles Tumor Inst., Calif.). Amer. J. Obstet. Gynecol., 85: 1002-11(Apr. 15, 1963).

The possible implication of prior radiotherapy in the induction of tumors is discussed in considering seven cases of mixed heterologous mesenchymal sarcoma (mixed mesodermal sarcomas) of the uterus. Sixty-one cases reported in the literature are reviewed. The incidence of 2 tumors out of 7 cases (28.7%) in the present group is in keeping with the figures given earlier and supports the view that prior irradiation may be important in the pathogenesis of some of these tumors. Therapy for these patients is also considered. However, radiation as a mode of therapy proved disappointing. (TCO)

14302 PATHOLOGIC ALTERATIONS PRODUCED BY TOTAL BODY X-IRRADIATION IN MONKEYS. Allen, J. R.; Van Lancker, J. L.; Wolf, R. C. (Univ. of Wisconsin, Madison). Amer. J. Pathol., 48: 317-31(Feb. 1966).

Forty of 51 adult monkeys were given 700 R, 800 R, or 1,000 R total body x-irradiation. During the post-irradiation period the monkeys developed leukopenia, thrombocytopenia, anemia, hypergammaglobulinemia, and bacteremia. The mean survival time for those that died was 11 days for the animals that received 1,000 R, 15 days for those given 800 R, and 16 days for those receiving 700 R. One monkey given 700 R and 4 that received 800 R survived 30 days. In all cases, the monkeys that died survived the acute intestinal phase and died during the bone marrow syndrome of irradiation sickness. The differences in the response and the histologic alterations observed in the tissue of monkeys that received total body x-irradiation are discussed. (auth)

14303 A COMPARISON OF WOUND HEALING BETWEEN IRRADIATED AND NONIRRADIATED PATIENTS AFTER RADICAL NECK DISSECTION. Vanden Berg, Henry J. Jr.; Chen, Shek C.; Blatt, Charles J.; Berkas, Ernest M. (Wayne State Univ., Detroit). Amer. J. Surg., 110: 557-61(Oct. 1965).

Wound complications after radical neck dissection were compared between patients irradiated with conventional 250-kv x-ray therapy and nonirradiated patients. Among 124 preoperatively irradiated and 170 nonirradiated patients who underwent neck dissections or composite operations, fistula, slough, or infection occurred in 29% of the irradiated group and in 44% of the nonirradiated group. Wound complication rate was lowest (18%) for patients operated upon within two months of radiation therapy. (TCO)

14304 HOST RESPONSE TO EGGS OF SCHISTOSOMA MANSONI. IV. FLUORESCENT ANTIBODY TITERS IN MICE INFECTED WITH NORMAL CERCARIAE, GAMMA-RADIATED CERCARIAE AND WITH PURIFIED EGGS. Jaimes, Salvador (Hospital San Juan de Dios, Santa Ana, El Salvador); Lichtenberg, Franz V. Amer. J. Trop. Med. Hyg., 14: 727-35(Sept. 1965).

Serial determinations of fluorescent cercarial antibody titers (FCAT) were performed in mice with Schistosoma mansoni infections, and in mice infected with: ^{60}Co γ-irradiated cercariae; purified eggs; and irradiated cercariae followed by purified eggs. The findings were correlated with worm and egg burdens and with the pathological changes at successive stages of infection. All four types of infection induced antibody titers of varying levels and durations. Mild elevations of titer were first noted two to three weeks after primary stimulation, regardless of the type of schistosome antigen used. Successive stimulation with worms and with eggs resulted in an accelerated antibody response. Infections with worms or eggs, alone or in succession, resulted in much lower antibody titers than did full-scale infection with normal cercariae. Correlation of data on antigen destruction and on antibody formation in experimental schistosome pseudotubercles, obtained with immunofluorescent tests, showed that catabolism of stainable schistosome antigen and granuloma formation precede the appearance of fluorescent antibody in host serum. It was concluded that intraperitoneal infection with γ-irradiated cercariae was a much weaker stimulus, as regards FCAT, than full-scale infection. (TCO)

14305 THE EFFECT OF γ-RADIATION ON SOME WOOD-BORING INSECTS. Bletchly, J. D. (Forest Products Research Lab., Princes Risborough, Eng.). Ann. Appl. Biol., 49: 362-70(June 1961).

Eradication of wood-boring insect infestations frequently presents special problems, particularly in large timbers where restricted access to all surfaces renders treatment difficult. Gamma radiation appeared to offer possibilities of treating large timbers, so that studies were made on the effects of ^{60}Co radiation on eggs, larvae, pupae, and adults of several wood-boring insects. Oviposition was obtained on suitable egg-laying blocks (oak sapwood veneers for Lyctus, Corsican, or Scots, pine sapwood blocks for Anobium, and decayed oak sapwood for Xestobium). Larvae were either irradiated free (Lyctus) or within oak sapwood blocks (Lyctus), or pine (Anobium) or decayed oak sapwood (Xestobium). Pupae were treated free (Anobium) or within decayed oak sapwood (Xestobium); adults were irradiated free or within infested wood. Studies were made of subsequent fertility and viability of eggs. Initial studies showed that high doses were needed to kill Lyctus larvae in a short time or to prevent emergence of beetles (>72,000 R) when the adult stage had been reached. Since such doses would involve severe hazards in practice, effects of lower doses were investigated. Results showed that a method could be devised for controlling wood-boring insect infestations if treatments are carried out at doses adequate to prevent completion of development or to produce sterile adults. About 10,000 R is needed, although further information is required on the survival of larvae hatching from irradiated eggs. It appears that the mechanical difficulties of providing adequate shielding for a radioactive source preclude the use of γ radiation for controlling wood-boring insect infestations in timbers in situ in most instances. (BBB)

14306 ADULT EMERGENCE OF THE HOUSE FLY, MUSCA DOMESTICA, FROM X-IRRADIATED PUPAE. Rockstein, M.; Dauer, M.; Bhatnagar, Prem Lata (Univ. of Miami School of Medicine, Coral Gables, Fla.). Ann. Entomol. Soc. Amer., 58: 375-9(May 1965).

Between 36 and 48 hr following pupation, Musca pupae were exposed to a single dose of x rays, which varied from 10,000 to 30,000 rad (at 250 kvp). Of the pupae exposed to 10,000 rad, 90.1% emerged successfully, and none showed any externally detectable effects of the **x** irradiation. Emergence was: 73.9 after 15,000 rad; 42.5 after 20,000 rad; and 19.5% at 30,000 rad. In nonirradiated controls 96.3% emerged. Irradiation favored male emergence, particularly at the higher doses (15,000 rad up). Results suggest that, irrespective of the fact that various biochemical processes continue from the pupal into the adult stage, at least two mechanisms govern the emergence of the irradiated flies: Termination of the pupal stage and a second initiating the actual process of emergence of the imago. (H.G.D.)

14307 INHIBITORY EFFECT OF X-IRRADIATION ON THE DEVELOPMENT OF THE OVARIES OF THE FISH, ORYZIAS LATIPES, IN SEXUALLY INACTIVE SEASONS. Egami, Nobuo; Hyodo, Yasuko (National Inst. of Radiological Sciences, Chiba, Japan). Annot. Zool. Jap., 38: 8-11(Mar. 1965).

The inhibitory effect of whole-body x irradiation on the development of the ovaries of adult fish (Oryzias latipes) maintained in a warm environment in sexually inactive seasons was investigated. Irradiations were performed with 2- or 8-kR doses of x rays. When the fish were irradiated with 2 kR of x rays on the day of transfer to warm water, the development of ovaries was strongly inhibited. The inhibition of the ovarian development seems to be attributable to a depression of the release of gonadotropins from the pituitary gland, since implantation of desiccated pituitary glands diminished the inhibitory effect of x irra-

diation on the ovaries. If irradiation with 2 kR of x rays was postponed to 12 or 13 days after transfer to warm environment, the development of the ovaries was not disturbed. Irradiation with 8 kR of x rays destroyed ovarian oocytes resulting in a decrease in weight of warmed fish, even if it were given after 12- or 13-day exposure to 26°C. The 8-kR dose exerted an acute lethal effect, all irradiated fish dying within 16 days after irradiation, while the 2-kR dose was tolerated, most of irradiated fish surviving more than 30 days. In summer fish, grown oocytes in the ovaries underwent degeneration after irradiation with 8 kR. (TCO)

14308 THE ATTENUATION OF VIRULENT TREPONEMA PALLIDUM BY MEANS OF GAMMA IRRADIATION. Miller, J. N. (National Inst. of Public Health, Utrecht). Antonie Van Leeuwenhoek, J. Microbiol. Serol., 31: 223 (1965).

Attempts to produce antisyphilis immunity with radioinactivated spirochetes are described. Both rabbits and man infected with Treponema pallidum develop a relatively high degree of resistance to re-infection during the course of the disease. However, attempts to induce this immunity in rabbits using antigens extracted from T. pallidum or related organisms and T. pallidum inactivated by heat, mapharsen, penicillin, or lyophilization have failed. These investigations suggest that more than one antigen may be responsible for conferring protection and that these antigenic components may be irreversibly altered by the inactivation procedures. Furthermore, since a loss in virulence and corresponding immunogenicity of freshly isolated treponemes appears to be closely associated with a loss in motility, it is conceivable that immunogenic antigens are altered by procedures which also cause immobilization of the organisms. Thus, the hypothesis was advanced that freshly isolated T. pallidum rendered avirulent but retaining motility would be an effective immumizing agent, thereby implying complete and intact antigenicity. It was further postulated that such organisms might be useful in the study of the mechanism whereby immunity develops. In light of this knowledge and speculation a series of experiments were carried out to determine whether treponemas could be modified in this manner by γ radiation. It was found that T. pallidum could be rendered noninfectious by a high dosage of γ rays without affecting its motility or its observable morphologic and staining characteristics. Although injection of relatively small numbers of these organisms failed to elicit a significant serologic response, the T. pallidum immobilization (TPI) antigen or antigens, thought to play a role in the development of host resistance, remained intact. (BBB)

14309 PHOTOBIOLOGY OF LUPUS ERYTHEMATOSUS. Baer, Rudolf L.; Harber, Leonard C. (New York Univ. Schools of Medicine, N. Y.). Arch. Dermatol., 92: 124-8 (Aug. 1965).

The role of the uv component of sunlight in the induction and exacerbation of lupus erythematosus is reviewed and 29 cases are reported. The cutaneous effects of uv irradiation were studied in 23 patients with localized chronic discoid lupus erythematosus (DLE), five with acute systemic lupus erythematosus (SLE). No differences in the erythema response were observed in the 23 DLE patients when compared with that in the control group of normal volunteers. On the basis of clinical reports and experimental evidence presently available, the probable effects of sunlight in lupus erythematosus are estimated. Repeated exposures of the same site to uv radiation may well be a test method for selecting those cases which are most likely to exacerbate with exposures to sunlight. It is possible also that in patients with SLE, irradiation of larger skin areas with uv light would cause systemic effects which were not noted after exposure of only a few small test sites. (TCO)

14310 ULTRAVIOLET ERYTHEMA. Everett, Mark Allen; Olsen, Robert L.; Sayer, Robert M. (Univ. of Oklahoma, Oklahoma City). Arch. Dermatol., 92: 713-19 (Dec. 1965).

A high pressure, xenon arc, grating monochromator was used to study the erythema reaction spectrum in 36 subjects in the spectral region 250 to 310 mμ. The resultant erythema action spectrum was characterized by continuously decreasing efficiency from a maximum at 250 mμ. A second max at 297 mμ and a minimum at 280 mμ as reported previously were not observed, and are believed to be an artifact of the method used earlier. (TCO)

14311 DEOXYRIBONUCLEASE II AND DEOXYRIBONUCLEIC ACID IN RAT THYMUS AFTER THE ACTION OF RADIOMIMETIC DRUGS AND X IRRADIATION. Tempel, K.; Roessner, W.; Zipf, K. (Univ., Munich). Arch. Exp. Pathol. Pharmakol., 251: 116-17(1965). (In German).

The in vitro activity of deoxyribonuclease II was measured in the thymuses of 500 adult rats 4 hr to 28 days after 365- and 730-R doses of whole-body x irradiation or a single injection of 0.75 and 1.5 mg/kg of the radiomimetic drug Sinalost, or 0.8 and 1.6 mg/kg of triethylenemelamine. All of the treatments increased the enzymatic activity within 8 to 16 hr after administration. A maximum of 2 to 4 times the original activity was observed within 24 hr after irradiation. A similar increase was observed within 3 days after the drugs were administered. The values returned to normal several days later in the animals that had been irradiated or that had received triethylenemelamine, but in the animals that had received Sinalost it required 10 days before the activity returned to normal. The DNA concentrations in thymus were almost inversely proportional to the activity of the enzyme. The concentrations decreased to a minimum of 10 to 15% of the starting value within 48 hr after irradiation, but this low value was reached only after 7 days following the drug administration. After 4 weeks the total DNA in thymus of irradiated animals was still depressed, but its concentration had increased within 10 days. The total amount and the concentrations both returned to normal in the drug treated animals within 3 or 4 weeks. (BBB)

14312 EFFECT OF RADIOMIMETIC DRUGS AND X IRRADIATIONS ON THE PERMEABILITY OF THE BLOOD-BRAIN BARRIER TO EVANS BLUE. Roessner, W.; Tempel, K. (Univ., Munich). Arch. Exp. Pathol. Pharmakol., 251: 139-40(1965). (In German).

The degree of damage suffered by the blood-brain barrier after administration of a lethal dose of 730 R of x irradiation to adult male rats reached a maximum within 3 days after administration, but a maximum was not reached until 7 days after 365 R was administered. Lethal doses (1.5 to 1.6 mg/kg) of Sinalost and sublethal doses (0.75 to 8 mg/kg) of triethylenemelamine also resulted in maximum blood-brain barrier damage 3 days later. Regeneration of the barrier was complete by 10 days after the drugs were administered. It required 21 days before the blood-brain barrier damage appeared to be repaired in the animals that received 365 R of x irradiation. The latent time for appearance of increased permeability of the blood-brain barrier to Evans blue dye appeared to depend on the amount of radiomimetic drug or irradiation administered. Sinalost was more toxic to the central nervous system, as measured in these terms, than was triethylenemelamine. The increase in permeability of the blood-brain barrier to Evans blue was reversible when a lethal amount of x irradiation was administered. In contrast to the other reactions, this could be a primary effect of irradiation. The results appeared to be in accord with the concept that the central nervous system is not radioresistant, as was once thought. (BBB)

14313 MORPHOLOGIC AND PHYSIOLOGIC CHANGES IN STAPHYLOCOCCI FROM STREPTOMYCIN AND ^{60}Co TREATMENT. Winterhoff, D. H.; Ritzerfeld, W. (Westfaelische Wilhelms-Univ., Muenster, Ger.). Arch. Hyg. Bakteriol., 149: 680-93(Dec. 1965). (In German).

Staphylococcus aureus (SG511) was treated with antibiotic and ^{60}Co γ radiation at a dose rate of 235 R/min on agar plates. The total radiation dose was about 80,000 R. Populations of staphylococci irradiated with ^{60}Co grew either as small colorless colonies without hemolysis or

as hemolyzing colonies with pigmentation. In the normal case, the dwarf forms are capable of mutation. The behavior of the different forms under the action of streptomycin, during the measurement of oxygen consumption, in gram staining, and in multiple biochemical reactions, was also tested. The findings are discussed and compared with recent reports in this field. (BBB)

14314 HEMATOLOGICAL CHANGES IN RADIATION SICKNESS. V. CHANGES IN THE PERIPHERAL BLOOD SYSTEM. Dienstbier, Z.; Pospisil, J.; Arient, M.; Vitek, F.; Kofranek, Vl. (Charles Univ., Prague). Atompraxis, 11: 666-70(Nov.-Dec. 1965). (In German).

The quantitative hematological changes found in the peripheral blood system of various species of experimental animals after single and repeated external irradiation and incorporation of ^{24}Na, ^{32}P, ^{131}I, and ^{198}Au are described. The changes observed were related to the radiation dose, and from this a scheme for individual dosimetric diagnostics was derived. Special attention is called to the possibility of diagnosing the incorporation of radionuclides by hematological methods, and of differentiating between incorporation and exposure to external radiation by means of the protracted reticulocytosis and neutrophilia which appear in the former case. In both cases the extent of lymphopenia is used for a quantitative evaluation of radiation damage. (auth)

14315 EFFECTS OF X-IRRADIATION UPON POSTNATAL GROWTH IN THE MOUSE. Nash, Donald J.; Gowen, John W. (Iowa State Univ., Ames). Biol. Bull., 122: 115-36(Feb. 1962).

The effect of x irradiation of mouse embryos on their postnatal development was measured by several responses: body weight changes from birth to maturity, lifetime fecundity, and total lifespan. Three genetically differentiated inbred strains of mice (Ba, K, and S) and all their possible hybrids, including reciprocals, were used. Pregnant females were exposed to single, whole-body, 250-kv x-ray doses from 20 to 320 R on day $6\frac{1}{2}$, $10\frac{1}{2}$, $14\frac{1}{2}$, and $17\frac{1}{2}$ of gestation. In addition, mice were irradiated on the day of birth without previous irradiation of the maternal organism. Postnatal growth was followed from birth to 75 days of age. Body weight response was found to be dependent on both levels of irradiation and embryologic age at irradiation. Evaluation of these results emphasizes the importance of considering both immediate and delayed effects in assessing damage induced by embryonic irradiation. (BBB)

14316 THE OCCURRENCE OF SQUAMOUS CARCINOMA AND OSTEOSARCOMA IN YOUNG RABBITS INJECTED WITH ^{90}Sr (50-100 μC/kg.). Kshirsagar, Sharad; Vaughan, Janet; Williamson, Margaret (Churchill Hospital, Oxford). Brit. J. Cancer, 19: 777-86(Dec. 1965).

The development of squamous carcinomas of the external auditory meatus after a long latent period in rabbits given a low initial dose (50 to 100 μC/kg) of ^{90}Sr is described together with radiation dose measurements and estimations of ^{90}Sr retention. It is suggested that accumulated radiation dose may be more important than dose rate in carcinogenesis from bone-seeking isotopes. The importance of the retention of radioactive bone-seeking isotopes in sites where there is little remodeling and only slow loss of ^{90}Sr from the bone adjacent to sensitive tissue is stressed. Such areas may be more important than hot spots away from sensitive tissues. Proliferating squamous epithelium adjacent to bone is as much a tissue at risk from bone-seeking isotopes as the endosteal osteogenic connective tissue. (auth)

14317 STERILIZATION OF THE CARROT RUST FLY BY IRRADIATION WITH ^{137}Cs. McClanahan, R. J. (Canada Dept. of Agriculture, Chatham, Ont.). Can. Entomol., 97: 1042-5(Oct. 1965).

In the use of the sterile male technique of eradication of certain field crop insects, several factors must be considered in appraising the possibilities of controlling an insect. The carrot rust fly Psila rosae meets some of the requirements. This insect is confined to reasonably small isolated areas, and sterilized adults would disperse among the natural population. A known rearing method could be used to accumulate large numbers of diapausing pupae. Therefore, laboratory studies were conducted with carrot rust flies to determine if irradiation of pupae would cause sterility in adults, the effect on emergence and longevity, and the degree of competitiveness of treated males with normal males. The pupae were treated 15 days after emergence, at about the mid-point of pupal duration, by irradiation from ^{137}Cs. Irradiation at 95 R/min with 1.4, 2.8, and 4.3 kR did not adversely affect emergence. Treated females caged with normal males laid a few sterile eggs when the treatment was 1.4 kR but none at the higher doses. Normal females caged with treated males laid a normal complement of eggs, and the per cent hatch was 10, 2, and 0 with treatments of 1.4, 2.8, and 4.3 kR, respectively. When flies of both sexes from pupae treated at 3.0 kR were mixed with normal flies in a ratio of 6:1, the number of larvae was reduced by 93%. The reduction in larval production with only a 6:1 ratio of treated to normal flies is considered a favorable one, and it is suggested that, despite the fact that carrot rust flies mate repeatedly, the sterile sperm are competitive with sperm from normal males. These experiments demonstrate the feasibility of field trials of sterile male releases. The difficulty lies in the problem of assessing the numbers of the natural population which can be expected in a given area. (BBB)

14318 THE EFFECT OF X-IRRADIATION ON THE CELL SIZE DISTRIBUTION OF THYMUS LYMPHOCYTES. Vittorio, P. V.; Blehm, S.; Linkletter, D. (Defence Chemical Biological and Radiation Labs., Ottawa). Can. J. Physiol. Pharmacol., 44: 77-87(Jan. 1966).

The effect of x irradiation on the cell size distribution of thymic lymphocytes was studied with the aid of an electronic Coulter cell counter. In the thymus the small lymphocytes were the most radioresistant and the large lymphocytes were repopulated before the medium-sized lymphocytes. As the radiation dose was increased from 50 to 400 R, there was a decrease in the large to small thymocyte ratio, and a longer time period was required for a return to the normal ratio. Single and repeated doses of x irradiation produced much the same type of effect on the large to small ratio of both thymus and spleen lymphocytes, and it was concluded that the effects of x irradiation on the cell size distribution of lymphocytes in the thymus and spleen were similar. (auth)

14319 CHILDHOOD CANCER IN TWINS. Hewitt, David; Lashof, Joyce C.; Stewart, Alice M. (Oxford Univ.). Cancer, 19: 157-61(Feb. 1966).

A statistical study of the first 5763 deaths covered by the Oxford Survey of Childhood Cancers showed that the number of twin-born cases was below expectation and that this applied especially to members of like-sex pairs. This may reflect prenatal selection against embryos (especially males) with a disposition to develop cancer in childhood. (auth)

14320 A NATURALLY OCCURRING HAPLOID EMBRYO IN THE COCONUT PALM (COCOS NUCIFERA L.). Ninan, C. A.; Raveendranath, T. G. (Univ. of Kerala, Trivandrum, India). Caryologia, 18: 619-23(Oct.-Dec. 1965).

A haploid embryo with 16 chromosomes was bound in a West Coast tall palm growing near Trivandrum, India. It was postulated that the embryo originated by haploid parthenogenesis. Experiments on induced haploidy in coconuts are reported. Pollination with irradiated pollen (50,000 R) gave up to 65% setting of nuts compared to 14% in the controls when a number of female flowers were removed before the others were pollinated. (H.G.D.)

14321 SYSTEMATIC MICROSCOPIC STUDY OF THE EFFECT OF IONIZING RADIATION ON ANIMAL CELLS IN CULTURE. II. EFFECT OF LOW DOSES OF X RAYS. Driessens, J.; Cappelaere, P.; Giaux, G.; Herbin, Y. (Institut de Recherches sur le Cancer, Lille. Section Physique du Centre Anticancereux, Lille). Compt. Rend. Soc. Biol., 159: 1161-3(1965). (In French).

The x irradiation with low doses (500, 1000, and 5000 R) of a culture of striated muscle cells from 9-day-old chicken

embryo causes lesions of exactly the same type as those caused by a massive application (38,000 R). Sharp variations in low and high dose groups have very interesting nuances for the further study of the modes of molecular effects of ionizing radiations in living matter. In particular, the rapid cellular degeneration observed after 38,000 R doses is detected, with all of its attributes in the lower dose groups. Therefore, it is concluded that irradiation induces a generalized type of response in the cytoplasm. (tr-auth)

14322 RADIATION AND INFANTS' TEETH. Binford, Robert T. Jr.; Burnett, George W. Dent. Progr., 1: 108-14(Jan. 1961).

Experiments were conducted in newborn Wistar rats to determine the threshold at which x-ray doses cause dental damage, to obtain data applicable to problems encountered in radiotherapy of children. Head-only or whole-body exposures to 250-kv x rays were begun within 12 hr after birth. Doses extended from 50 to 1000 R for head, and from 100 to 500 R for whole-body irradiation. All the animals were sacrificed at 13 days of age, and half-sections were made of the heads. The most sensitive histologic indicator of radiation-induced changes in developing teeth was irregularities of the dentino-enamel junction. These were barely visible at 400 R and distinctive at about 500 R. Except for hemorrhage within the tooth germ, the dental alterations after total-body irradiation were similar to those produced by head-only irradiation. It was found that x rays alter the development of teeth in ways that somewhat resemble the effects of removal of thyroid and pituitary glands. Histological examination of the x-rayed rats showed that the thyroid glands were normal. The net result of the alteration was to interfere with the generation of enamel in the affected area. Dentin germ cells were much more sensitive. The more prominent effects of radiation were the formation of osteodentin; disorganization of the dentin germ cell layers; and dentin germ cells that resembled bone germ cells. It is concluded that head irradiation at 500 to 1000 R can seriously affect the subsequent nature of developing teeth that have not yet erupted; the implications in the radiotherapy of infant humans are suggested. (TCO)

14323 ELECTRON MICROSCOPIC STUDIES OF TEETH IRRADIATED WITH ULTRAHARD RADIATION. Osswald, M. (Ernst-Moritz-Arndt-Univ., Griefswald, Ger.). Deut. Stomatol., 11: 855-63(1961). (In German).

In older patients it is difficult to ascertain whether dental defects that appear after irradiation are phenomena due to irradiation or to continuation of destructive process already in progress. Results of irradiation with a ^{60}Co source were studied in a 24-yr-old patient under treatment for a throat sarcoma. Starting at about ½ yr after the start of irradiation treatment chalky areas appeared over the entire circumference of the teeth. These resembled early symptoms of developing caries. The crowns of the teeth became dull and brown-colored. The surfaces of the molars became flat and abraded. The enamel layers tended to become abraded and the dentine became exposed. The anatomical form of the dentine retained its shape if it were not abraded by chewing. The changes observed were not characteristic of caries. The dentine acquired a cartilaginous character, similar to that deserved in teeth decalcified in vitro. It became somewhat elastic to applied pressure. It gave a smothered sound when struck. Progressive changes in the enamel structure were studied serially by the electron microscope. The enamal was brittle and chalky over broad areas. The photographs taken demonstrated that the archetechtonic surface structure was markedly and increasingly altered by the ^{60}Co irradiation treatments. (BBB)

14324 INJURIES IN THE MOUTH-JAW REGION FOLLOWING IRRADIATION. Dorhbrack, G.; Osswald, M. (Ernst-Moritz-Arndt-Univ., Griefswald, Ger.). Deut. Stomatol., 13: 731-4(1963). (In German).

Radiation injuries appeared in 15% of the patients irradiated with 1500 to 15,000 R doses of x ray or Ra, and appeared as destruction of the enamel and cementum. The injuries differed from caries symptoms in that they were found on all of the smooth surfaces and on the neck of the tooth. The enamel became raw, porous, and brittle. The enamel was easily removed from the chewing surfaces. The dentine became dark colored, acquired a cartilaginous consistency, and became extremely plastic. The cementum essentially disappeared. The pulp was replaced by amorphous chalky deposits. A persistent gingivitis appeared, with discoloration, swelling, and ulceration. Teleangiectases appeared in the oral mucosa and gums of the side irradiated. Osteoradionecrosis appeared in 2 patients. To prevent many irradiation injuries in the mouth and jaw region, the teeth and bone should be protected with Pb sheets as much as possible, and the oral cavity should be kept as clean as possible. (TCO)

14325 ON KIDNEY FUNCTION IN CASES OF SUBCUTANEOUS TRAUMA COMBINED WITH RADIATION SICKNESS. Tovstoles, K. V. Eksp. Khir. Anesteziol., 8: 70-1(May-June 1963). (In Russian).

An experiment was conducted on renal function in 104 rabbits after subcutaneous trauma combined with radiation sickness. Subcutaneous trauma was inflicted over one kidney of half of the rabbits and x irradiation in doses of 400, 600, and 800 R was given. Radiation sickness of three degrees of severity developed in these rabbits, observed up to one year from the time of trauma. Renal function was evaluated by various urinanalyses, a dye excretion test, and intravenous urography, that is, by tests made use of in everyday urologic practice. After irradiation without trauma the volume of urine somewhat exceeded normal in the first 24 hr, and from the third day slowly diminished, returning to the initial level the third week. After trauma of the kidney without irradiation the daily urine volume had fallen to 50% on the following day, and returned to the initial level after a month. With renal trauma in unirradiated animals combined with infection, hematuria lasted one to five days. Twenty rabbits died from traumatic shock, hemorrhage, acute and chronic irradiation injury, and its sequelae (pneumonia and peritonitis), but renal impairment was not regarded as a direct cause of death of the animals. It is concluded that depressed kidney function alterations owing to the combined action of trauma and x-irradiation depends primarily on the severity of physical injury and secondarily on radiation injury. (TCO)

14326 EARLY ACTION OF GAMMA RADIATIONS ON ELECTRICAL BRAIN ACTIVITY AND BEHAVIOR IN THE RABBIT. Monnier, Marcel; Krupp, P. (Univ., Basel). Exp. Neurol., 3: 419-31(May 1961).

The previous concept that the central nervous system is highly resistant to ionizing radiations is contradicted by this investigation. Electrophysiologic studies demonstrated that low doses of ^{60}Co γ irradiation of the rabbit head produce early transitory brain alterations. Irradiation of the head (400 or 600 R) was followed by slightly hyperactive motor behavior with oral patterns of rhinencephalic type and definite EEG alterations: desynchronization in the neocortex, with slight activation of the reticular ascending system, and hyperactivity in the archicortex. On the contrary, stronger irradiation doses (900 R) to the rabbit head slightly moderated motor behavior, as well as neocortical activity (high-voltage, slow-wave syndrome) and reticular excitability, whereas a precritical hyperactivity developed in the hippocampal archicortex. The reversibility of the electrographic and motor symptoms after weak irradiation suggests an early and transitory action of radiation on neuronal and synaptic activities in the neocortex and archicortex. Stronger doses alter these structures more severely and depress slightly the electrical activity of the neocortex. The increased high-voltage slow-wave activity suggests a diminished activation power of the reticular system upon the neocortex. The sharp waves and spike potentials discharged in the hippocampus can be considered as premonitory symptoms of convulsant processes developing under influence of stronger irradiations. These ob-

servations after irradiation with 900 R correspond to earlier results in monkeys irradiated with 1500 R. The electrical alterations and the behavioral changes following weak irradiation of the head alone show a tendency to decrease after 6 hr. This suggests a partly reversible mechanism, which is indicated by the fact that the sharp waves in the neocortex and the spike potentials discharged in the hippocampus are suppressed by arousal reactions following sensory or electrical stimulation of the ascending reticular system. (BBB)

14327 RECOMBINATION AMONG UV-INDUCED ADENINE-1 MUTANTS OF SCHIZOSACCHAROMYCES POMBE. Clarke, C. H. (Medical Research Council, Edinburgh). Experientia, 21: 582-3(1965).

Ten uv-induced adenine-1 mutants of Schizosaccharomyces pombe were tested for recombination. The results indicate that damage had occurred at 10 distinct sites within the adenine-1 locus. The recombination frequencies obtained were not strictly additive. (C.H.)

14328 STIMULATION OF RECOMBINATION IN MULTIPLICITY-REACTIVATED BICOMPLEXES AND THE GENETIC MAP LENGTH OF PHAGE T4. Barricelli, Nils Aall; Caplan, Charles (Univ. of Washington, Seattle). Genetics, 53: 275-9(Feb. 1966).

The assumption (Barricelli 1956) that multiplicity reactivation (MR) in phage T4 is due to the elimination of damages by crossovers is used to derive a method for estimating the map length of the genome of phage T4. Epstein's 1958 data on MR bicomplexes are used to compute the length, resulting in estimates ranging from 843 to 2006 map units, corrected for high negative interference. (auth)

14329 MODIFICATION OF CONJUGATION IN ESCHERICHIA COLI K-12 BY ULTRAVIOLET IRRADIATION. Joset, F.; Wood, T. H. (Service de Radiologie et de Cancerologie, Paris. Univ. of Pennsylvania, Philadelphia). Contract AT(30-1)2803. Genetics, 53: 343-56(Feb. 1966).

Ultraviolet irradiation before mating of either the donor parent (HfrH) or the recipient one (PA 309) greatly affects conjugation in Escherichia coli K-12. Ultraviolet irradiation of the male results in the production of at least two types of lesions: the first prevents the transfer of the male chromosome to the female; the second prevents the formation of an effective union between donor and recipient. Irradiation of the female parent, on the other hand, does not affect detectably the transfer step but affects primarily the steps of union and integration. In the production of recombinants there is a selective utilization of genetic information from the nonirradiated male parent as if there were a selective advantage conferred on those zygotes that receive larger portions of the male chromosome during mating. This results in an apparent increase in linkage between the male markers. (TCO)

14330 CALCULATION OF RADIATION DOSE FROM PROTONS AND NEUTRONS TO 400 Mev. Neufeld, Jacob; Snyder, W. S.; Turner, J. E.; Wright, Harvel (Oak Ridge National Lab., Tenn.). Health Phys., 12: 227-37(Feb. 1966). (ORNL-P-1584).

A computer code utilizing Monte Carlo techniques was developed and used to calculate particle histories corresponding to various nuclear interactions which a high-energy neutron or proton may undergo during the slowing process within a tissue phantom. The phantom was assumed to be composed of H, C, N, and O in approximately the proportions of standard man and of density about 1 g/cm^3. It was assumed to have the form of a slab 30 cm thick and infinite in extent, and was assumed to be uniformly exposed to the radiation over one face. Calculations were made for both normal incident and isotropical monoenergetic neutron and proton fluxes. By computing a large number of particle histories in an unbiased manner, a statistical sample of the physical interactions which would occur due to the incident neutron or proton flux was obtained. This basic information was then analyzed in order to find the absorbed dose at various depths in the tissue slab. The dose equivalent at various depths in tissue was computed on the basis of QF-LET relationships for routine occupational exposure. (C.H.)

14331 THE EVALUATION OF RISK FROM RADIATION. Russell, R. Scott; Doll, W. R. S.; Dunster, H. J. (and others). Health Phys., 12: 239-302(Feb. 1966).

Available data are summarized on the genetic and somatic effects of low-dose γ and x radiation on human populations. It is pointed out that medical exposure is in the interest of the individual and some occupational exposure is in the economic interest of the individual and the community. Somatic effects are evident only in the exposed generation while genetic effects may be evident not only in the first generation offspring of exposed persons but in later generations also. The evaluation of the total detriment from exposure to radiation demands the consideration of both somatic and genetic consequences. Somatic damage from low dose radiation is considered to result mainly from malignant conditions while genetic damage includes not only a great many known hereditary defects but also an unknown number of functional disturbances with some genetic component. The sum of the present evidence on somatic damage is inconclusive, although there is a possibility that small doses of radiation have a non-specific and deleterious effect on life expectancy. It is concluded that, in the present state of knowledge, any evaluation of genetic risks from radiation is beset with much uncertainty, largely because it is necessary to rely on much indirect evidence obtained from experimental animals. (143 references.) (C.H.)

14332 IRRADIATION WITH ^{90}Sr OF A SUPERIOR SYMPATHETIC CERVICAL GANGLION OF THE RAT IN VITRO. Welti, H.-J.; Berger, J.-P.; Lerch, P. (Univ. de Lausanne, Switzerland). Helv. Physiol. Pharmacol. Acta, 23: 68-9(1965). (In French).

The authors describe a procedure whereby nerve tissue can be immobilized in a solution containing Krebs solution and be irradiated by a source containing ^{90}Sr. This radioisotope has the advantage of long half life, high β energy, and simple shielding problems to protect the investigator from the irradiation emitted. The ^{90}Sr used was in the form of applicators ordinarily used for contact therapy, with an activity of 20 mC. The absorbed dose at the surface was 7.2 ± 1.4 R/sec. Two of these sources were placed in the cylindrical cavity of a Plexiglas block. They were held by two horizontal rods which could be moved to adjust the location of the sources. The ganglion to be irradiated could be positioned so that it was directly at the point of intersection of the axis of the cavity and the two ^{90}Sr sources. The total irradiation dose administered to the sample of ganglionic tissue was proportional to the duration of irradiation and the dose rate, as evaluated from an appropriate curve. The electrode system used with the ganglion provided for electrical stimulation of the ganglion and recording of the action current produced at various times during the course of irradiation with the ^{90}Sr sources. (BBB)

14333 X-RAY AND FAST NEUTRON SURVIVAL RESPONSE OF 5-BROMO-DEOXYCYTIDINE-TREATED BONE MARROW CELLS. Silini, G. (C.S.N.-Casaccia, Rome); Maruyama, Y. Int. J. Radiat. Biol., 9: 605-10 (1965).

Analog sensitization of mouse bone marrow cells assayed by the spleen-nodule technique of Till and McCulloch was studied. It was shown that radiosensitization to x rays can be achieved by means of interrupted schedules of drug administration in vivo, despite transport to a remote tissue through the circulatory system; and that the radiosensitization observed with low LET radiations such as x ray is negligible when fast neutrons (6 Mev) having higher LET are used. (H.G.D.)

14334 FREQUENCY AND SPECTRUM OF CHLOROPHYLL MUTATIONS FOLLOWING ETHYLENIMINE TREATMENT OF SECOND GENERATION SEEDS OF γ-IRRADIATED BARLEY. Shangin-Berezovskii, G. N. (Inst. of Genetics, Moscow). Izv. Akad. Nauk SSSR, Ser. Biol., No. 6, 859-70(1965). (In Russian).

Pre-sowing treatment of barley seeds with a weak solu-

tion of ethylenimine increases the frequency and widens the spectrum of radioinduced recessive chlorophyll mutations. That ethylenimine can reduce the rate of seed germination through an increased level of variability is not associated with a selective elimination of seeds sensitive to ethylenimine treatment. Dose-exposure curves of variability allow distinction between two types of mutations related to the extent of cell damage in the mutation-bearing organism. The actual level of variability in the population may not agree with its potential level. A complete transformation of mutability into variability can be realized only by optimal effectiveness of the modifying agent. An analysis of the data regarding modification of barley radiation mutagenesis by means of seed treatment with ethylenimine suggests that mutations may develop when protected from restoration processes. (TCO)

14335 THE ROLE OF THE MITOCHONDRIAL APPARATUS OF LYMPHOCYTES IN THEIR RESPONSE TO IONIZING RADIATION. Manteifel', V. M.; Meisel', M. N. (Inst. of Molecular Biology, Moscow). Izv. Akad. Nauk SSSR, Ser. Biol., No. 6, 884-97(1965). (In Russian).

Electron microscopy of lymphatic nodes of animals irradiated with large doses or at higher dose rates revealed ultrastructural lymphocytic lesions appearing 4 to 5 min after irradiation. The lesions primarily affect lipoprotein membranes of cellular organelles (mitochondrial crystae and membranes and nuclear membranes) and involve stratification and vacuolization of two-layer membranes and destruction of mitochondrial crystae. Development in mitochondria is earlier than in nuclei. Fusion of damaged mitochondria together with the fact of their increasing contact with nuclear membranes has been convincingly proven. A comparison of the results obtained with the literature data on early structural and ultrastructural lesions and functional damage in mitochondria and nuclei of irradiated radiosensitive cells suggests their interdependence. An important role in radiosensitivity of lymphocytes and other cells similarly responding to irradiation belongs to damageability of a relatively limited number of mitochondria and, consequently, to disturbances in the cellular metabolic rates that in turn promote radiation pathology and prevent reparation of radioinduced lesions. (auth)

14336 SPERM PRODUCTION BY CHRONICALLY IRRADIATED BULLS. Welch, P. R.; Murphree, R. L. (Univ. of Tennessee, Oak Ridge). J. Animal Sci., 24: 1045-50(Nov. 1965).

The effects of fractionated doses of whole-body γ radiation on sperm production and testicular histology in bulls were investigated. Based on sperm production and histologic data, two doses of 50 R per week were more deleterious than a single dose of 100 R per week. An accumulated dose of 600 R was as deleterious as 1100 R when both were delivered at the same rate. Despite histologic evidence of severe damage to the seminiferous epithelium, the irradiated bulls were producing sufficient numbers of motile and morphologically normal sperm that it is presumed they would have been fertile. Hemoglobin, hematocrit, and platelet values were not affected; leukocyte numbers were depressed for 2 years following the initial exposure. (TCO)

14337 SKELETAL DEFECTS IN PRENATALLY IRRADIATED SHEEP, CATTLE AND SWINE. McFee, A. F.; Murphree, R. L.; Reynolds, R. L. (Univ. of Tennessee, Oak Ridge). J. Animal Sci., 24: 1131-5(Nov. 1965).

Whole-body doses of 200 to 400 R of γ radiation administered to ewes between days 22 and 25 of gestation produced deformities of the thoracic limbs in most lambs. Exposure between days 23 and 27 caused a high incidence of defective pelvic limbs. Similar anomalies of the thoracic limbs were produced by γ irradiation of cattle on the 32nd day of pregnancy and by neutron exposure of swine on day 21 of gestation. The minimum dose to the dam at which anomalies were produced was 200 R in sheep and 300 R in cattle. In sheep fetuses damage during days 23 to 25 is specific for the humero-radial joint. Organs which are developing most rapidly at the time of exposure are the most readily damaged; differentiation of the various components of the forelimb has not yet begun. Thus at this stage primordial cells which are destined to form the humero-radial joint, but are not yet histologically distinguishable, are highly radiosensitive. The observed time period for the induction of tail deformities in pigs by neutron irradiation falls within the range previously established, that is, for γ irradiation, between the 12th and 19th days of gestation. The affected tails had missing and fused vertebrae, the fusion usually occurring at an angle which resulted in a kinked and shortened tail. Of the five pigs with leg deformities, four showed bilateral fusion of the humero-radial joint similar to that seen in sheep, except that the ulna was present and normal. Affected legs were typically shortened by the tendency of the radius to fuse to the shaft of the humerus and by a general underdevelopment in length of these bones as well as the carpals. (BBB)

14338 HYPOTHYROIDISM FOLLOWING ^{131}I TREATMENT FOR HYPERTHYROIDISM. Einhorn, Jerzy; Wicklund, Harriet (Karolinska Sjukhuset, Stockholm). J. Clin. Endrocrinol. Metab., 26: 33-6(Jan. 1966).

Thyroid response to thyrotropin (TSH) was studied in 44 cases of hypothyroidism that had developed more than 1 yr after ^{131}I treatment. In those responding to TSH a systematic attempt was made to withdraw the thyroid substitution therapy. Hypothyroidism was found to be permanent in all but 1 of the 44 cases. Hypothyroidism that had developed more than 1 yr after radioiodine treatment was not transient, and the high incidence of this hypothyroidism reported previously cannot be attributed to overdiagnosis. (auth)

14339 MORPHOLOGIC RESPONSE OF THE MUCOSA OF HUMAN SMALL INTESTINE TO X-RAY EXPOSURE. Trier, Jerry S.; Browning, Thomas H. (Veterans Administration Hospital, Madison, Wis. Univ. of Wisconsin, Madison). J. Clin. Invest., 45: 194-204(Feb. 1966).

Peroral biopsies were serially obtained from patients before, during, and after abdominal x-ray therapy from small bowel within the irradiated field. Biopsies were studied by light and electron microscopic techniques. Histological changes included: a reduction of mitoses in the crypts to 25 to 51% of control levels; marked shortening of the villi with a resultant 39 to 48% reduction of epithelial surface length; megaloblastosis and megalocytosis of epithelial cells; heavy infiltration of the lamina propria with plasma cells and polymorphonuclear leukocytes; and occasional crypt abscess formation. Electron microscopy further revealed cytologic epithelial cell changes including: swelling and dilatation of mitochondria and endoplasmic reticulum; irregular distribution and shortening of microvilli; and a scalloped nuclear border and the presence of huge nucleoli. The data indicate that extensive morphologic damage of the small intestinal mucosa of man is regularly induced by therapeutic doses of abdominal x-ray therapy. This is associated with surprisingly few symptoms, is rapidly reversible, and appears localized to the bowel in the field of irradiation. (TCO)

14340 EGG MORTALITY AFTER GAMMA IRRADIATION OF ADULTS OF THE OMNIVOROUS LEAF ROLLER. Jacklin, S. W.; Smith, F. F.; Boswell, A. L. (Dept. of Agriculture, Beltsville, Md.). J. Econ. Entomol., 58: 1168-9(Dec. 1965).

Since the omnivorous leaf roller Platynota stultana attacks both greenhouse and outdoor crops and is difficult to control with insecticides, the possibility of developing a sterility technique was examined and a study made of its biology, rearing techniques, and effects of γ radiation upon it. Radiation treatment of adults and subsequent effects upon egg hatching are described. Male and female moths, sexed in the pupal stage, were subjected to ^{60}Co radiation within 24 hr after eclosion, then mated individually to normal moths within 24 hr. Treated and untreated control pairs were followed for development and hatching of individual eggs in masses on the smooth interior surface. The radiation treatment results, as well as those of oviposition and hatching, are tabulated for doses ranging from 4 to 32 kR. With both male-treated and

female-treated pairings, the percentage of pairings which produced viable eggs decreased as the dose increased. At the highest doses used, hatching was nearly eliminated without reducing the numbers of eggs laid/female. The observed egg mortalities showed that treatments of 16 kR for females and 32 kR for males produced over 99% egg mortality. (BBB)

14341 RADIATION-INDUCED MUTATIONS IN SOUTHERN PEAS. **Jones, Sam T. (Auburn Univ., Ala.). J. Heredity, 56: 273-6(Nov.-Dec. 1965).**

Southern peas, Vigna sinensis, were irradiated with varying doses of x rays and thermal neutrons. The neutron doses ranged from 0.7×10^{12} to 6.5×10^{12}/cm^2. The x-ray doses ranged from 5000 to 25,000 R. The seeds were planted individually in sterile soil in peat pots in a greenhouse within 30 days of irradiation. After 20 days, the percentage germinating was determined and the height of the emerged seedlings was measured. Surviving X_1 seedlings were transplanted to the field for observation. There were no significant differences in percentage of germination between any of the treatments except of the highest dose of thermal neutrons (28.8% germination compared to 86.1% for the control). Seedling vigor, however, appeared to be closely related to the dose both for thermal-neutron and x-ray treatments. There was some stimulating effect on seedling height of thermal-neutron doses up to 1.4×10^{12} n/cm^2. A dose of 6.5×10^{12} n/cm^2 resulted in a drastic reduction in vigor. A significant stimulating effect of x rays on seedling height was noted for the lowest (5000 R) treatment. High doses (20,000 and 25,000 R) resulted in a marked reduction in seedling vigor. No mutant types were observed among the 5000 controls, but among the 15,000 X_2 plants from the two highest-dose x-ray and neutron treatments six heritable mutants were found. The mutant types observed were an albino, a dwarf, a crinkle leaf, a browneye, an early fruiting, and an extra-long peduncle type. The albino was lethal. All others produced normal seed and were homozygous for the mutant character. The dwarf mutant proved to be determined by a single gene (df) recessive to normal. (BBB)

14342 RENAL CONCENTRATING DEFECT IN CANINE RADIATION NEPHRITIS. **Coburn, Jack W.; Rubini, Milton E.; Kleeman, Charles R. (Wadsworth Hospital, Los Angeles. Cedars-Sinai Medical Center, Los Angeles. Univ. of California, Los Angeles). J. Lab. Clin. Med., 67: 209-23(Feb. 1966).**

In an effort to characterize the polyuria observed early in the course of experimental radiation nephritis, the study of canine radiation nephritis was extended to the ability to concentrate urine. Dogs received 2,700 to 3,000 R to the left kidney after prior contralateral nephrectomy. Concentrating ability (maximum urine plasma osmolality and T^cH_2O) fell within 2 to 3 weeks, while glomerular filtration rate (GFR) was normal. Later (4 to 8 weeks), diluting ability (minimum U/P osmolality and C_{H_2O}) was impaired and salt wasting followed sodium deprivation coincident with GFR reduction to less than 50 per cent of control values. The abilities to dilute and to conserve Na were similar to those of normal dogs under urea osmotic diuresis when the data were compared at solute excretion rates adjusted to GFR(U_{Osm} V/GFR). Concentrating ability, similarly compared, remained abnormal. Such impaired concentrating ability with near normal diluting capacity and over-all normal reabsorption of sodium is consistent with an impaired medullary countercurrent concentrating mechanism. This might be produced by either unresponsiveness of the collecting duct to antidiuretic hormone activity or grossly reduced medullary hypertonicity. Ineffective transport of sodium into the medulla or altered medullary blood flow could bring about a reduction in medullary hypertonicity. (auth)

14343 THE DEVELOPMENT OF DOMINANT LETHALITY IN FRUIT FLIES EXPOSED TO VIBRATION, ACCELERATION, AND GAMMA RADIATION. **Parfenov, G. P. Kosm. Issled., 3: 643-51(July-Aug. 1965). (In Russian).**

The combined and individual effects of vibration, acceleration, and 500 R doses of gamma radiation on fruit flies were studied using Domodedovo-18 and -32 strains. In each test, one thousand males were mated to the same number of virgin females 1 hr after exposure to a stress. The eggs of these females were subsequently collected and examined for lethality. It was found that various vibration frequencies did not injure the mature sperm of fruit flies. Egg lethality following exposure to vibration was attributed to lowered male sexual activity. Vibration with a frequency of 70 cps for 2 hr or longer caused injury during the spermatid phase resulting in zygote lethality after fertilization. Regardless of the sequence, the total effect of vibration combined with radiation did not exceed the sum of each of the individual stressors. Exposure to 40 g for 20 min did not have a mutagenic effect or influence the radiation effect. A higher magnitude of acceleration (4000 g for 20 min) did not affect the spermatids but did affect mature germ cells. The effect was analogous to that of 200 to 250 r of γ rays. The mechanism of the cellular effect of 4000 g was probably nonnuclear. Radiation followed by acceleration (4000 g) had a total effect equal to the sum of the individual effects. When the order was reversed, the radiation effect was modified. (TCO)

14344 EFFECTS OF RADIOTHERAPY ON ARTIFICIAL GRAFTS OF THE THORACIC AORTA: EXPERIMENTAL STUDY. **Bertho, Emile; Genest, Leopold; Prive, Lucien; Aranguren, Visitacion; Perez, Alberto Perez y (Hotel-Dieu Saint-Valier, Chicoutimi, Quebec). Laval Med., 36: 239-48(Mar. 1965). (In French).**

A study was made of the radiotherapy effects on artificial arterial grafts implanted after resection of the thoracic aorta in 15 dogs. This study originated as a result of a clinical case of implantation of a left aortofemoral artificial graft in a 49-year-old man with an ileal bladder, malignant latero-aortic lymphoma, and Leriche syndrome. The graft was irradiated with a dose of 3000 R without deleterious effect. The present study was made on nine woven Teflon grafts (Edwards type), three knitted Dacron grafts (De Bakey type), one woven-knitted Dacron graft, one woven Mersilene graft, and one woven Teflon-Dacron graft. The daily doses of radiotherapy used on the dogs were the same as those commonly used on adult humans in radiation treatment. X ray doses were 250 R, 1800 R, or 3000 R in three dogs but in all others ranged from 4500 to 8100 R. Clinical studies made on the living dogs showed retention of good circulation below the graft. However, in most instances where high doses were used, the dogs suffered weight loss, anemia, and diarrhea, even though appetite was usually excellent. Bone marrow examination showed a lasting hypoplasia. Macroscopic and microscopic studies of the artificial aortic grafts on the irradiated animals revealed a more accentuated state of degeneration of the elastic fibers of the vascular media at the ends of the graft in comparison with those of the nonirradiated animals. The results indicate that subsequent irradiation is not likely to impair the integrity of vascular grafts. (BBB)

14345 RESPONSE TO RADIOTHERAPY OF AN AORTIC-FEMORAL PROSTHESIS. **Bertho, E.; Genest, L.; Bruneau, J.; Perez, A. Perez y; Aranguren, V. (Hotel-Dieu St.-Vallier, Chicoutimi, Quebec). Lyon Chir., 61: 359-63(May 1965). (In French).**

Data are reported on a man who required an arterial graft of dacron and later underwent radiation treatment given in the area of the graft. Function and integrity of the vascular graft were not impaired by radiotherapy. A brief review of radiation effects on blood vessels is presented. Preliminary studies are also reported wherein dogs with artificial arterial grafts were x irradiated with total doses up to 7000 R (in 200-R daily fractions). No deleterious effects on the grafts were noted. (TCO)

14346 OXFORD SURVEY OF CHILDHOOD CANCERS PROGRESS REPORT III: LEUKEMIA AND DOWN'S SYNDROME. **Lashof, Joyce C.; Stewart, Alice. Mon. Bull. Ministry Health (London), 24: 136-43(June 1965).**

During the course of the Oxford Survey several associations were detected that show that preconception, prenatal

and postnatal influences, including ionizing irradiation, play diverse roles in the etiology of childhood cancers. The most powerful of these is the one that links leukemia with trisomy of chromosome 21. For the 98 cases of leukemia associated with mongolism that were compared with 2848 cases of childhood leukemia, each group contained the same proportion of myeloid leukemias. In both there was a peak incidence during early childhood. The modal age at death was earlier for mongols (second year) than nonmongols (fourth year), and the proportion of males was lower for mongols than nonmongols. In respect of leukemia incidence and cell types, there were no differences between mongols with old and young mothers. The significance of these findings is discussed in relation to current theories on the origin of leukemia. (TCO)

14347 X-RAY INDUCED FEMALE STERILITY IN PHASEOLUS MUNGO. Jana, Manas K. (Indian Inst. of Tech., Kharagpur, India). Naturwissenschaften, 52: 646(1965).

The occurrence of female sterility in the X_2 generation of plants of Phaseolus mungo, the seeds of which were irradiated with x rays to 60,000 r, is reported. To determine the causes of sterility and the stage at which degeneration begins, megasporogenesis was studied in buds of different sizes both in female-sterile and normal plants. The lack of development of normal integument was suggested as a possible cause of the failure of embryo development. A genetic study showed that the disorder was due to a single factor. (J.S.R.)

14348 EVALUATION FOR GENETIC DAMAGE IN OFFSPRING OF WOMEN WITH HIGH-LEVEL GONADAL IRRADIATION. Whelton, James A. (Temple Univ., Phildelphia); Ingall, David; Bamford, Sophia; Smedal, Magnus I.; Wright, Kenneth. New Engl. J. Med., 273: 1266-7(Dec. 2, 1965).

Chromosome analyses were conducted in three children of women whose ovaries had been irradiated during the course of cancer therapy. The children were born 4, 6, and 9 yrs after ovarian exposure. Neither clinical nor cytogenetic investigations indicated any genetic damage to the offspring. (H.G.D.)

14349 EFFECTS OF RADIATION ON SEEDS OF PHLEUM PRATENSE L. RELATION BETWEEN ELECTRON SPIN RESONANCE CONCENTRATION AND RADIOBIOLOGICAL EFFECTS. Sato, Tadashi (Sapporo Medical College). Nippon Igaku Hoshasen Gakkai Zasshi, 25: 251-6(July 1965). (In Japanese).

Dormant seeds of Phleum pratense L. were exposed to x- and γ-irradiation. Germination tests were conducted immediately after and at irregular specified intervals following storage at room temperature. The radiation damage in terms of germinating rate and seedling height was measured on the 15th day. The percent germination did not change up to 50,000 R. Seeds germinated immediately after irradiation showed reduction in seedling height at 5,000 R, the maximal effect being about 20,000 R. Damage increased with the time of storage following irradiation for a period up to 1 month. The water content of the seeds showed a definite influence on the radiosensitivity. The seedling height was least affected around a 17% of water content while an increase in damage was seen at lesser or larger water contents. Free radicals were revealed by ESR even in seeds irradiated with 5,000 R, but the resonance spectra showed almost no change up to 100,000 R, and/or in the seeds examined soon after irradiation or stored for periods up to 1 month in room temperature or in dry-ice ether. No relationship between the ESR concentration and the radiobiological effects were observed. (TCO)

14350 ELECTROENCEPHALOGRAPHIC STUDIES ON THE EFFECTS OF IONIZING RADIATION TO THE CENTRAL NERVOUS SYSTEM. EFFECTS OF HEAD IRRADIATION TO EEG AFTERREACTION. Ono, Yoshimi (Yokohama Univ., Japan). Nippon Igaku Hoshasen Gakkai Zasshi, 25: 325-36(Aug. 1965). (In Japanese).

The effects of ^{60}Co γ rays on the central nervous system in rabbits were studied electroencephalographically. (1) The phenomena of elevated threshold for inducing EEG after reaction (EA) was observed constantly above 100 R whole-head irradiation. Intensity of elevated threshold and recovery process were found highly dose-dependent. Significant effects could be observed as low as 20 R, although individual variation predominated under 100 R. (2) Spontaneous EA was inhibited transitionally by single-head exposure over 1000 R. The ratio of spontaneous EA stage to EEG spindle burst stage was found to be a sensitive indicator. (3) The effects of head-irradiation on animal behavior were also studied. (TCO)

14351 THE RADIOSENSITIVITY AND NONPROTEIN SH COMPOUNDS IN MAMMALIAN TISSUES. Ueno, Yori; Sugahara, Tsutomu (Kyoto Univ.). Nippon Igaku Hoshasen Gakkai Zasshi, 25: 370-3(Aug. 1965). (In Japanese).

The correlation between the radiosensitivity and the contents of nonprotein sulfydryl and disulfide groups (SH compounds) determined by polarography was studied in mammalian cells with different in vivo radiosensitivities. The ratio of nonprotein SH compounds (NPSH) to protein SH compounds seemed to be larger in the spleen and bone marrow cells in a radioresistant strain of mice. A similar correlation was found after the intraperitoneal injection of AET. The mechanisms were discussed. (auth)

14352 EFFECT OF LOW-INTENSITY RADIATION ON MAN. Jankowski, F. J. (Rutgers Univ., New Brunswick, N. J.). Nucl. Safety, 7: 12-14(Fall 1965).

The ratio of radiation-dose-rate threshold for somatic damage to the normal background dose rate is of the order of a few hundred (100 to 500). This is shown to be in the range of the ratio of harmful concentration of several chemicals to the amount needed or believed to be needed for health. The question as to whether all radiation is harmful, is considered. Experiments at low or very low (below background) dose rates are suggested. (auth)

14353 RADIATION DOSE FROM RADIUM D TO THE HUMAN BONES. Jaworowski, Zbigniew (Inst. of Nuclear Research, Warsaw). Nukleonika, 10: 735-7(1965).

The radiation dose absorbed by tissue in the haversian canals from RaD is calculated on the basis of the mean value of the RaD concentrations found in Poland and Germany in 1964. (L.B.S.)

14354 THE RESPONSE TO AN ANTIGEN STIMULUS BY THE LYMPHORETICULAR SYSTEM. Cottier, H. (Univ., Bern). Oncologia, 19: 170-9(1965). (In German).

The present knowledge concerning the fate of injected antigen, the possible role of the reticulohistiocytic system in antibody responses, and the morphologic basis of primary and secondary antibody responses is briefly reviewed. The rapid de novo formation and growth of germinal centers during secondary, but not during primary antibody responses to tetanus toxoid are discussed in relation to the accelerated and efficient antibody production in the course of an anamnestic response. The effects of ionizing whole-body irradiation and perinatal thymectomy on the immune competence of the organism are considered in the light of some recent experimental results. (auth)

14355 METABOLISM OF NUCLEIC ACIDS IN UV-IRRADIATED L-STRAIN CELLS TREATED WITH NATIVE DEOXYRIBONUCLEIC ACID. Kostic, Lj.; Djordjevic, O.; Kanazir, D. (Inst. of Nuclear Sciences Boris Kidric, Belgrade). Photochem. Photobiol., 4: 515-20(June 1965).

Isologous DNA-^{14}C was incorporated into the DNA of normal and irradiated recipient cells. The rate of DNA-^{14}C label incorporation in the DNA of irradiated recipient cells was slower than in the unirradiated controls. The presence of thymidine in the incubation media reduces the incorporation rate of DNA-^{14}C. When the irradiated cells were growing in a medium containing isologous DNA in presence of thymidine or heterologous DNA, the recovery effect was not observed. The recovery of irradiated cells treated with native DNA was studied. These experiments

represented an attempt to get a better insight in the molecular mechanism(s) leading to the recovery of irradiated cells. Earlier, it was observed that after uv irradiation DNA synthesis was temporarily depressed, nucleic acid precursors accumulated in the acid-soluble fraction, the irradiated cells lost the capacity to divide, and giant cells appeared. When irradiated cells were cultivated in suspension in the medium containing isologous DNA, the number of cells significantly increased, i.e., the treated cells were dividing at a rate more rapid than irradiated non-treated controls. The recovery effect was observed in suspension as well as when L cells were plated to form colonies. In experiments on these cells grown in medium containing 0.01 μC thymidine-^{14}C per ml, DNA labeled with ^{14}C was prepared. (BBB)

14356 INFLUENCE OF pH AND OXYGEN ON 315 mμ INACTIVATION AND THYMINE DIMERIZATION IN MUTANTS OF BACTERIOPHAGE T4. Haug, A.; Sauerbier, W. (Univ., Cologne). Photochem. Photobiol., 4: 555-61(June 1965).

It was shown that irradiation with 315-mμ uv-irradiation inactivates phage T4v$^-$x$^+$, and T4v$^-$x$^-$, and forms thymine dimers in their DNA. Both the rates of inactivation and of thymine dimerization depend upon pH and gaseous environment during irradiation. The photoreactivable sectors also depend upon the environmental conditions at 315-mμ inactivation. The molecular basis of these findings is discussed. It is concluded that, besides thymine dimer, at least one other lethal photoproduct (probably a photoproduct of cytosine) is involved in photoreactivation. (TCO)

14357 HOST-CELL REACTIVATION OF NON-LETHAL ULTRAVIOLET EFFECTS. Harm, Walter (Southwest Center for Advanced Studies, Dallas). Photochem. Photobiol., 4: 575-85(June 1965).

Experiments were carried out with the following phage types: T1, λvir, T4, and T4x. The host-cell reactivating (HCR(+)) strain E. coli B and the non-host-cell reactivating (HCR(−)) mutant strain E. coli B$_{S-1}$ were used as host bacteria for T1, T4, and T4x. Delay of intracellular growth of uv-irradiated T1 and λ phage was compared in HCR(+) and HCR(−) bacterial strains. At a given phage survival level, intracellular growth delay occurs to the same extent in HCR(+) and HCR(−) strains; at a given absolute uv dose, this delay is considerably more expressed in HCR(−) than in HCR(+) strains. Therefore, it does not reflect the time required for the HCR repair of otherwise lethal uv lesions. The results rather suggest that uv causes, besides lethal lesions, stable photoproducts in the DNA, which are a priori nonlethal, and which are recognized and efficiently eliminated by the HCR repair system. The HCR enzymes likewise act on (nonlethal) uv photoproducts causing prophage induction in lysogenic cells. Consequently, one obtains the maximum induction effect in a lysogenic HCR(−) strain at a much lower uv dose than in the corresponding lysogenic HCR(+) strain. In contrast, uv damage causing loss of the host cell's capacity to support growth of unirradiated phage is not affected by HCR. (BBB)

14358 PHOTOPROTECTION AGAINST GENETIC DAMAGE IN NEUROSPORA CAUSED BY X-RAYS. Klein, Deana T.; Klein, Richard M. (Albert Einstein Coll. of Medicine, New York). Photochem. Photobiol., 4: 623-4 (June 1965).

Conidia of the purple-adenineless mutant (38701) of Neurospora crassa were exposed for 15 min to 1000 ft-candle of white light from either fluorescent lamps or from incandescent lamps whose radiation was filtered through both a cellulose acetate filter and a 1% copper sulfate solution. The fluorescent lamps transmitted light to 705 mμ and the incandescent lamp system transmitted radiations only between 385 and 695 mμ. Immediately following visible irradiation, the conidia were irradiated with 280 kv x rays. No differences in response were seen when Neurospora conidia were irradiated with 2.5×10^4 rad at either 245 rad/min or 3660 rad/min. Neither fluorescent nor filtered incandescent light protected Neurospora conidia against genetic damage measured as the ability to form colonies following irradiation with low or high dose rates of x rays. Independent of the dose rate of x radiation both types of visible light photoprotected against genetic damage measured as a reduction in the frequency of reversions to adenine phototropy. Filtered incandescent light was not photoprotective against genetic damage measured by aberrant colony formation when given prior to irradiation with either low or high dose rates of x rays; fluorescent light was effective in combination with both low and high dose rates of x rays. These data confirm the existence of photoprotection against x-ray damage and extend the phenomenon to include genetic markers. (BBB)

14359 A METABOLIC THEORY OF CELL SURVIVAL CURVES. Orr, J. S. (Western Regional Hospital Board, Glasgow); Hope, C. S.; Wakerley, Sheila E.; Stark, J. M. Phys. Med. Biol., 11: 103-8(Jan. 1966).

A metabolic theory of cell survival after irradiation is presented and developed in the form of a mathematical model. The parameters which fit the model to some published experimental data are given. The effects on survival of environmental changes are considered in terms of the model. (auth)

14360 EXPERIMENTAL RADIATION CARCINOGENESIS. Casarett, George W. (Univ. of Rochester, N. Y.). Progr. Exp. Tumor Res., 7: 49-82(1965).

This review encompasses experimental data and observations which shed light upon the mechanism of radiation carcinogenesis and their relation to known carcinogenic influences and mechanisms in general. (120 references.) (TCO)

14361 VARIATIONS OF RESISTANCE AGAINST α RADIATIONS WITH THE TIME OF DAY. Hofer, Kurt; Biebl, Richard (Univ., Vienna). Protoplasma, 59: 506-21(1965). (In German).

Diurnal variations in resistance to α irradiation from a ^{210}Po source of about 20 mC were studied in the internal and external epidermis of onion bulb scales of Allium cepa and in leaves of the moss Mnium cuspidatum. The unit used for evaluation of the comparative radiosensitivity was the product of the source strength in mC times the duration of irradiation in seconds, and the criterion of effect was complete or partial death of the tissues irradiated. For the epidermal tissues of the onion the maximum radiosensitivity occurred at 12 noon, and the minimum was at about 10 p.m. Mnium cuspidatum had maximum resistance at 12 midnight, with a minimum between 12 noon and 4 p.m. The sizes of the cell nuclei also showed diurnal variations. The maximum size of the nuclei was observed at 12 noon, and the minimum was observed at 8 p.m., when the volume decreased to $\sim^2/_5$. Comparison showed that when the resistance of the internal epidermis was greatest, the nuclei were largest. This was true in reverse, also, because when the nuclei were smallest in size the radioresistance was least. The changes in the daily variations of radioresistance were probably due to alterations in the cytoplasmic environment. These are more closely related to early death of cells, while death of cells more than 24 hr after irradiation is probably due to injury to nuclei. (BBB)

14362 THE ACTIVITY OF PYRIDINE NUCLEOTIDASE IN WHOLE-BODY X-IRRADIATED RATS. Hilgertova, Jirina; Sonka, Jiri; Pospisil, Jan; Dienstbier, Zdenek (Charles Univ., Prague). Radiat. Res., 27: 211-16(Feb. 1966).

The fall in specific pyridine nucleotidase activity of rat spleen and liver was assayed up to 24 hours after whole-body x irradiation (800 R). A temporary increase in this enzyme to preirradiation levels was found between the fourth and sixth hour after irradiation. A corresponding decrease in pyridine nucleotide levels may be partly the result of the enhanced activity of this enzyme. (auth)

14363 INACTIVATION OF ISOLATED ESCHERICHIA COLI RIBOSOMES BY GAMMA IRRADIATION. Kucan, Zeljko (Inst. Ruder Boskovic, Zagreb). Radiat. Res., 27: 229-36(Feb. 1966).

The inactivation of isolated Escherichia coli ribosomes

by γ irradiation was studied by measuring their ability to support the polyuridylic-acid-directed synthesis of polyphenylalanine in a cell-free system from the same bacterium. The radiation-sensitive molecular weight of 2.7×10^6, derived from the experiments with lyophilized ribosomes, was in a good agreement with the data obtained by other methods. Irradiation of ribosomes in suspension gave an increased radiosensitivity; in the case of ribosomes dissociated into 50 S and 30 S subunits this apparent high sensitivity could not be explained only by the indirect effect of radiation. (auth)

14364 RECOVERY OF THE INTESTINAL MUCOSA IN THE RAT AFTER X-IRRADIATION OF THE EXTERIORIZED INTESTINE. Wiernik, G.; Creamer, B.; Shorter, R. G. (St. Thomas' Hospital and Medical School, London). Radiat. Res., 27: 264-71(Feb. 1966).

Exteriorized loops of rat jejunum were x irradiated with a dose of 1000 R. Histological assessment of the architecture of the mucosa, the epithelial appearances, and mitotic activity showed that these had returned to normal at 1 week postirradiation. Cells labeled with tritiated thymidine revealed a similar epithelial cell turnover from 1 to 4 weeks after irradiation, and this corresponds closely to previously published work in normal animals. (auth)

14365 CELLULAR ASPECTS OF THE MAMMALIAN RADIATION SYNDROME. II. CELL DEPLETION IN BONE MARROW, SPLEEN, AND THYMUS OF YOUNG MICE. Puck, T. T. (Univ. of Colorado, Denver). Radiat. Res., 27: 272-83(Feb. 1966).

Quantitative studies of the time course of nucleated cell depletion in the spleen and thymus of young Swiss mice after total-body γ irradiation were carried out. These organs resemble the bone marrow in showing no measurable depletion after doses below 50 rads, and then a depletion rate increasing with dose until a dose of 200 to 300 rads has been achieved, after which further increase of dose has no effect up to 1500 rads. The limiting cell depletion rates of these two organs are greater than that of the bone marrow, although they are achieved at the same limiting dose of irradiation. These results support the theory that the cells of all three tissues have similar single-cell survival curves with respect to reproductive inhibition, and that the principal action during the first 45 hours after irradiation is the suppression of normal reproduction without any appreciable action on the rate of cell destruction or removal from these tissues for the dose range studied. This theory of reproductive inhibition correctly predicted that cell depletion of irradiated bone marrow, thymus, and spleen during the first 40 hours follows the same course in each case, regardless of whether the total body was irradiated or only the part containing the sampled tissue. (C.H.)

14366 SPATIAL AVOIDANCE IN A PARADIGM IN WHICH IONIZING IRRADIATION PRECEDES SPATIAL CONFINEMENT. Martin, Joan C. (Florida State Univ., Tallahassee). Radiat. Res., 27: 284-9(Feb. 1966).

Spatial avoidance in a shuttle-box was investigated when the noxious stimulus (x irradiation) preceded confinement on either the black or gray side. Sixty-four Sprague-Dawley rats were assigned to one of four groups and received a cumulative dosage of 0, 178, 340, or 500 R at a rate of 2 R/min over 8 days. An analysis of variance was performed on the differences between preirradiation and postirradiation preference scores. This was in terms of the time spent by an animal on the side on which he had been confined after irradiation. Treatment effects were significant beyond the 0.01 level. It was suggested that the postirradiation effects of the exposure, possibly a physiological change or disturbance, acted as the unconditioned stimulus. (auth)

14367 STUDY OF MECHANISMS OF RADIATION-INDUCED REPRODUCTIVE DEATH OF MAMMALIAN CELLS IN CULTURE: ESTIMATION OF STAGE AT CELL DEATH AND BIOLOGICAL DESCRIPTION OF PROCESSES LEADING TO CELL DEATH. Watanabe, Ikuo; Okada, Shigefumi (Univ. of Rochester, N. Y.). Radiat. Res., 27: 290-306(Feb. 1966).

Mouse leukemic L5178Y cells were irradiated with 1000 R of γ radiation. After irradiation, the cell number, the percentage of M-stage cells, the percentage of S-stage cells, the percentage of eosin staining, and the rate of cell passage from G_1 to S and from S to G_2 were studied at various postirradiation times. (C.H.)

14368 A PERSISTENT METABOLIC EFFECT OF X-RAYS OR NEUTRONS. Osborn, G. K.; Jones, D. C.; Kimeldorf, D. J. (Naval Radiological Defense Lab., San Francisco). Radiat. Res., 27: 307-17(Feb. 1966).

Body weights and the consumption of food, oxygen, and water were determined in male rats at intervals of 6 months after whole-body irradiation with single doses of 430 or 680 rads of x rays or 230 or 320 rads of fast neutrons at 101 days of age. These measurements for irradiated groups were compared to those obtained in simultaneously aging littermate controls. Results indicate that the consequences of the acute phase of damage and repair after radiation exposure may be extended and accentuated in later life. Differentiation from simultaneously aging controls was more surely predictable in animals irradiated with doses potentially lethal with respect to the 30-day mortality. Thus, irradiation early in life may be viewed as resulting in the permanent loss of a fraction of the animal, which is reflected in oxygen and food consumption decrements proportional to the decrement in metabolic size. Later in life, the degenerative processes normally seen in control animals at a more advanced chronological age give rise to decreased efficiency in food utilization and increased water intake. (auth)

14369 COSTAL FRACTURES AS A CONSEQUENCE OF RADIATION TREATMENT OF BREAST CANCER. Peracchia, G.; Schippisi, G. Gagnoni; Bocchi, R. (Univ., Parma, Italy). Radiobiol. Radioterap. Fis. Med., 20: 327-80(Sept.-Oct. 1965). (In Italian).

The literature on radioinduced costal bone fractures is reviewed, and case histories are presented for twelve patients who developed costal fractures after breast cancer radiotherapy. Etiologic, pathogenic, and genetic aspects of costal fractures are discussed. Time and dosimetry factors are analyzed, and prognosis and therapy are considered. (H.G.D.)

14370 DPN DEGRADATION AND SYNTHESIS OF LYMPHOSARCOMA ASCITES CELLS AFTER X IRRADIATION. Altenbrunn, H. J.; Steenbeck, L.; Schleichors, H.; Ehrhardt, E.; Schmaglowski, S. (Robert-Roessle-Klinik, Berlin). Radiobiol. Radiotherap. (Berlin), 5: 494-500 (1964). (In German).

The cause of reduction of the pyridine diphosphate nucleoside (DPN) concentration of lymphosarcoma ascites by x irradiation was studied with enzymatic and chemical methods in ascites cell homogenates and suspensions. After irradiation with 10,000 R of x irradiation the DPN concentration of mouse ascites cells is decreased to only 30% of its original value within 24 hr. Similar concentration differences were observed in testes, liver, and spleen. These results may have been caused by decreased DPN synthesis or increased DPN loss from the cells caused by increased activity of the DPNase or increased cell membrane permeability. For measurement of DPN degradation washed ascites cells were homogenized and incubated. DPN degradation increased with the amount of homogenate prepared. It was inhibited by nicotinic acid amide. Compared with liver DPNase the DPNase of ascites cells was much less active. The DPNase reaction in ascites cell homogenates was inhibited in spite of an excess of DPN, and did not show any increased DPN use after irradiation. A great increase in DPN degradation was shown after irradiation only when the homogenates had been incubated for short intervals. Washed irradiated and nonirradiated ascites cells were incubated with isotonic KCl solutions of DPN. DPN utilization was related to irradiation with 5000 R. The results suggested increased cell membrane permeability. The authors concluded that irradiation alters cell permeability and increases DPNase activity. (BBB)

14371 UNCONDITIONAL REFLEXES OF LUNGS TO THE ACTIVITY OF THE CARDIOVASCULAR SYSTEM DURING NORMAL CONDITIONS AND DURING RADIATION INJURIES. Bachurina, T. I. (Kirov Military-Medical Academy, Leningrad). Radiobiologiya, 5: 916-19(1965). (In Russian).

The course of acute radiation sickness was shown to be characterized by a change in the reflexes from the lungs. Cardiovascular responses to stimulation of the lung receptors by acetylcholine, chloroform, ether, CO_2, and pressure were studied for 1 to 2 months in cats x-irradiated to 400 R. The nerve connection of the isolated lungs of the anesthetized animals was retained. In the irradiated animals the number of cases where reflexes were absent was higher, especially for stimulation with carbon dioxide and acetylcholine in 1 : 10,000 dilution. Chloroform and acetylcholine solution in 1 : 1000 and 1 : 100 dilution were ineffective stimulants. As distinct from the reaction in the intact animal, the irradiated animals showed rapid changes in the reflexes on repeated stimulation. Changing the stimulant concentration in most cases had a compensating effect. In some cases changing the stimulant reversed the effect. Blood pressure tracings are shown. (TTT)

14372 PLACENTAL TRANSFER OF FISSION PRODUCTS AND EFFECTS ON FETAL DEVELOPMENT. Sternberg, Joseph (Univ. of Montreal). Radioisotopes (Tokyo), 14: 534-42(Nov. 1965).

Radiation hazards to the human fetus are reviewed. Natural and artificial sources must be considered in determining fetal exposure to ionizing radiation. Whether the radioactive environment of the fetus is due to external sources or internal contaminations plays a significant role in the type of hazard to which the fetus is subject. Time of exposure is particularly influential in determining fetal defects, for damage will be greatest in those tissues undergoing rapid growth. Fission product metabolism is discussed, and the role of the placenta in determining fetal exposure is emphasized. (H.G.D.)

14373 RADIATION CARCINOGENESIS: THE SEQUENCE OF EVENTS. Cole, Leonard J.; Nowell, Peter C. Science, 150: 1782-6(Dec. 31, 1965).

Concepts on carcinogenesis are reviewed and a proposed sequence of events and related factors for radiation carcinogenesis is presented. Results are reported from a study of neoplastic and hyperplastic liver lesions in x irradiated mice (500 rad) treated with carbon tetrachloride. It is concluded that the complex interplay of many factors and mechanisms of carcinogenesis makes a simple dose-response relationship untenable. (C.H.)

14374 FUNCTION OF THE RETICULOENDOTHELIAL SYSTEM AFTER LOCAL RADIATION BURDEN TO THE LIVER. Fridrich, Raimund (Buergerspital, Basel). Strahlentherapie, 128: 549-57(Dec. 1965). (In German).

The RES function after local x irradiation of the liver of mice was tested by the intravasal elimination rate, the liver uptake, and the storage of colloidal radiogold in liver, spleen, bone marrow, and lungs. No recognizable inhibition of the RES function is observed after a single irradiation with 500 or 1000 R. This function is significantly reduced, however, after 2000 R or 2 × 1000 R even in spite of the compensationally increased storage in the spleen. Splenectomy, performed prior to irradiation, results in a 20% increase in storage rate of the Kupffer's star cells; storage of radiogold in the bone marrow and lungs is not changed. The importance of the relationship between liver and spleen in the RES function is discussed in detail. (tr-auth)

14375 EXPERIMENTAL INVESTIGATIONS ON HeLa CELLS AFTER SEPARATED AND COMBINED USE OF DECORTILEN AND X RADIATION. Peters, Karl; Bauer, Robert (Univ., Tuebingen, Ger.). Strahlentherapie, 128: 577-85(Dec. 1965). (In German).

Decortilen (16-methylenprednisolon) Merck causes significant mitosis inhibition in tissue cultures of HeLa cells. In combination with x radiation, the mitosis inhibition caused by Decortilen is maintained. Decortilen causes no decrease or increase of the radiation induced irreversible changes, including pathological mitoses, cytolysis, and nuclear pyknosis. (tr-auth)

14376 BEHAVIOR OF SUCCINIC ACID DEHYDROGENASE AND NADH-CYTOCHROME-c REDUCTASE IN LIVER, SPLEEN, AND THYMUS MITOCHONDRIA OF RATS AFTER IRRADIATION IN VIVO. Waldschmidt, Marianne (Univ., Freiburg i. B.). Strahlentherapie, 128: 586-94 (Dec. 1965). (In German).

Mitochondria were isolated from liver, spleen, and thymus 2 to 40 hours after x irradiation of rats with 300 R. The activity of succinic acid dehydrogenase was always found to decrease in mitochondria obtained from the spleen; in mitochondria obtained from the thymus a significant decrease was observed 8 hours post irradiation. After 8 hours post radiation a slight decrease in NADH-cytochrome-c-reductase activity was observed in mitochondria obtained from the spleen; the activity of this enzyme was unchanged after irradiation, however, in mitochondria obtained from thymus. The activity of both of these enzymes as well as the P/O ratio was not changed by irradiation in liver mitochondria. (tr-auth)

14377 URINARY COMPLICATIONS FOLLOWING COMBINED INTERSTITIAL RADIATION AND NODE DISSECTION THERAPY FOR CERVICAL CANCER. Landsteiner, Ernest K.; McDuff, Henry C. Jr. (Rhode Island Hospital, Providence). Trans. New Engl. Obstet. Gynecol. Soc., 17: 57-65(1963).

Results of 48 cases of cervical carcinoma treated by a combination of radium, x-ray, and pelvic node dissection are reported. Five-year improvement as well as complications are described. It was shown that disease, infection, radium, and x-ray treatment, and surgery all predispose to circulatory change and endarteritis and as a natural consequence to increased complications. Among the 48 patients, there were 20 major complications in all. Of these, 15% were medical, 20% cardiovascular, 25% intestinal, and 40% urinary tract complications. Severe ureteral obstruction not commonly seen in patients undergoing radium and x-ray therapy or pelvic lymphadenectomy alone was observed, and it appeared that the combined insults of surgery and radiation were responsible. (TCO)

14378 INFLUENCE OF THE CORTISONE AND ACTH TREATMENT ON THE SERUM GLYCOPROTEIN LEVELS IN X-IRRADIATED RATS. Zicha, Blahoslav; Kucera, Karel (Charles Univ., Prague). Vet. Med. (Prague), No. 6, 369-76(1965). (In Czech).

Serum glycoprotein concentrations were followed for 30 days after x irradiation of adult Wistar rats. Doses of 450, 500, and 600 R were administered over the whole body with 180-kv x rays delivered at a dose rate of 33 R/min. These doses resulted in a 30-day mortality rate of 28, 72, and 92%, respectively. ACTH and cortisone injections increased the mortality rate, i.e., after 450R, it rose to 56 and 68%, respectively, compared with 28% after saline injection. Hormone treatment was given intramuscularly for 10 days. The hormones also appeared to accelerate the development of the the radiation syndrome. Elevations of serum glycoproteins caused by irradiation were significantly enhanced by both hormones. It is suggested that this synergistic action of radiation and the hormones is a nonspecific one and unrelated to selective tissue injury. (BBB)

14379 OXIDATION PRODUCTS OF UNSATURATED FATTY ACIDS IN THE IRRADIATED ORGANISM. Zicha, Blahoslav; Benes, Jiri (Charles Univ., Prague). Vet. Med. (Prague), No. 11, 681-90(1965). (In Czech).

The influence of x radiation on the formation of oxidation products of unsaturated fatty acids was followed by reaction with 2-thiobarbituric acid (TBA). In vivo studies were conducted in adult Wistar rats receiving whole-body x ray (250-kv, 70 R/min) doses up to 1400 R, and in vitro experiments were performed on rat tissue components exposed to doses up to 10,000 R. The tissue content of oxidation products did not increase in liver of rats after a whole-body irradiation. The TBA reaction in homogenate of the small intestine of normal rats was lower than that in liver and after a dose of 1400 R the TBA substances increased at both

intervals studied (after 12 and 48 hr) following irradiation. Antioxidation capacity of the small intestine was significantly diminished for 48 hr after whole-body irradiation with a dose of 1400 R in vitro. No significant inhibition of antioxidation capacity was seen after in vitro irradiation with a dose reaching 10,000 R. The amount of oxidation products of unsaturated fatty acids rose significantly in mitochondria isolated from liver of the rats irradiated with a whole-body dose of 1400 R. This phenomenon was noted immediately after irradiation and up to 6 hr after exposure to x rays in the doses employed. (BBB)

14380 X IRRADIATION IN PREGNANCY. Wichtl, O. (Siemmelweis-Frauenklinik, Vienna). Wien. Klin. Wochenschr., 77: 313-18(May 7, 1965). (In German).

The use of x irradiation during pregnancy is infrequent, but varies somewhat between areas and clinics. It is used in pregnant women at a rate as low as 0.5% in some clinics, but as much as 10% or more in others. The application of x irradiation is surveyed in each of these fields, and its usefulness and diagnostic value are evaluated. No more than 100 mR should be administered during pregnancy. Although the irradiation exposure that might be used during pregnancy contributes a large proportion of the irradiation dose received by the gonads, relative to the total medical irradiation burden, studies made in the pelvic region represent only a small percentage. (TCO)

14381 SOME EFFECTS OF ACCUMULATED RADIUM ON THE PRODUCTIVITY OF ALGAE [Thesis]. Angelovic, Joseph W. Logan, Utah, Utah State Univ., 1965. 149p.

Three genera of algae were cultured in media containing different amounts of dissolved radium. Each experiment was designed for statistical analysis and contained five treatment levels of radium, four to six replications of each level, and four time periods. After exposure to radium for a predetermined length of time, the algae were analyzed either for radium content or changes in productivity. Radium analyses showed the algae accumulated radium to varying degrees. Patterns of uptake and concentration varied between algae and statistical tests confirmed that the differences were real. The measurements used to determine changes in productivity were carbon fixation, respiration, oxygen production, dry weight, total nitrogen, and total lipids. Each of these production characteristics demonstrated some change. Response patterns were extremely variable but it was shown statistically that either the amount of radium or the length of exposure affected each parameter. In low concentrations radium sometimes accelerated certain of the metabolic processes while it retarded others, but in higher concentrations all activities were depressed. Carbon fixation was decreased as the radium concentrations increased from the control to 160 pC/l, respiration was increased in concentrations between 25 and 125 pC/l, while oxygen production was inhibited in all concentrations of radium. Algal growth was stimulated at 6 pC/l while the nitrogen content of algae was higher in all concentrations of radium than in the controls. From these experiments it appeared that radium may either stimulate, inhibit, or have no effect on productivity measurements and the response from a particular measurement can vary between algae. (Dissertation Abstr.)

14382 PHYSIOLOGICAL AND BIOCHEMICAL STUDIES OF INCOMPATIBILITY IN OENOTHERA ORGANENSIS [Thesis]. Kumar, Sudhir. Pullman, Wash., Washington State Univ., 1965. 64p.

Investigations indicated that the stamens of O. organensis do not provide substances that promote the growth of the styles. Emasculation had no effect on the development of selfed pollen tubes. The stamens either do not contribute to the incompatibility substances of the styles, or the styles themselves produce a sufficient quantity of these substances to inhibit the growth of tubes from selfed pollen. Ultraviolet treatment of self-incompatible style prior to self-pollination promoted the development of pollen tubes. The best results were obtained with 4 hours of ultraviolet treatment. The lability of the stylar component of incompatibility to ultraviolet, x-ray, and elevated temperature treatments suggests that the inhibitory substance is probably of a proteinaceous nature. The addition of boric acid or calcium, or both boric acid and calcium to the warm water in which the styles were treated led to a further enhancement of pollen tube growth in otherwise incompatible styles. It was established that developing pollen tubes of O. organensis obtain sugar from the stylar tissue through which they grow. The rate of this utilization of exogenous sugar was stimulated by the addition of boric acid. A relationship was noted between the deposition of callose and the rate of growth of the pollen tubes. More callose was formed in the slower growing incompatible tubes than in the rapidly developing compatible tubes. Less callose was formed in otherwise incompatible tubes growing through styles treated so as to inactivate the inhibitory substances. Studies on the amount of bound and free amino acids indicated that proline was present in much larger quantity in the anthers than in the styles. More glutamic acid accumulated in anthers and styles of incompatible than in compatible clones of O. organensis. (Dissertation Abstr.)

14383 ORGANIZATION AND METABOLISM IN CULTURED PLANT CELLS: EFFECTS OF RADIATION AND OTHER FACTORS ON GROWTH INDUCTION [Thesis]. Holsten, Richard David. Ithaca, N. Y., Cornell Univ., 1965. 312p.

The biological effect of radiation that can be transmitted via various external media was studied with a view to identifying the substances by which the effect in cells was mediated. Since the process of growth induction, during which the sensitivity of the cells to radiation changes markedly, should involve the nucleic acids, these constituents were investigated quantitatively. Protein synthesis as related to growth induction and especially to nucleic acids was submitted to investigation with special reference to the ability of cell free preparations to incorporate ^{14}C-labeled substrates into a product recognizable and recoverable as protein. It was found that the indirect effects of radiation on growing cells are elicited by radiolysis products of sugar. Other evidence shows that indirect radiation effects are obtainable on other systems. The changes in nucleic content per cell as the resting tissue passes into active growth were traced. It is shown that cells exposed to a full culture medium that lacks only the factors that promote cell division synthesize the nucleic acids (RNA and also DNA) normally regarded as necessary for growth and protein synthesis. The cell division factors intervene to make this system effective in protein synthesis and the radiation effects intervene to antagonize them. Since a specific inhibitor of RNA synthesis (actinomycin D) affects the system in a manner analogous to the radiolysis products, it is believed that the site of the action of the latter concerns the nucleic acids. Other events in growing cells set in train when the cells commence to grow may be similarly affected by the radiation possibly acting through the nucleic acids. The work on protein synthesis was carried out with aseptic precautions. Attempts were made to demonstrate net synthesis of protein (by increase of amino acid N in a hydrolysate) and recovery of ^{14}C amino acids from the protein. Evidence which could be interpreted as net protein synthesis was obtained using particles prepared from actively growing cells. The bearing of all this upon current concepts of a protein synthesis is discussed. (Dissertation Abstr.)

14384 BIOLOGICAL EFFECTS OF MULTIPLE TREATMENTS WITH RADIATION AND DIETHYL SULFATE ON BARLEY [Thesis]. Mohan Rao, Pendurty Krishna. Pullman, Wash., Washington State Univ., 1965. 148p.

Several biological effects induced by multiple treatments with radiation (x or gamma rays) and diethyl sulfate (dES) (as pre- or post-treatment) on barley seeds, Hordeum vulgare var. Himalaya, were analyzed. The influences of hydrolyzed diethyl sulfate (HdES) on radiation-induced damage and of pH on radiation- and dES-induced damage in single and multiple treatments were analyzed. Both pre- and post-radiation treatments with 0.0038M and 0.0076M dES for 2 hours at 30°C produced a positive

interaction (synergistic effect) for M_1 seedling injury and mitotic chromosome fragment frequency and a negative interaction (protective effect) for M_1 plant lethality and M_1 spike sterility. The mutation frequency per 100 M_2 seedlings in pre- and post-radiation treatments with 0.0038M dES (the multiple treatments) was nearly additive at all the radiation doses studied; whereas, the mutation frequencies per 100 M_1 plants and 100 M_1 spikes were less than additive at the radiation doses above 20 kR. Post-x-radiation treatments with 0.1M HdES for 2 hours at 30°C exhibited the same type of interactions as did pre- and post-radiation treatments with dES. However, pre-x-radiation treatments with 0.1M HdES for 2 hours at 30°C exhibited near additivity for the amount of M_1 seedling injury and the frequency of chromosome aberrations. The action of radiation (gamma rays) and dES in single and multiple treatments depended upon the pH of the treatment. The type of interaction between radiation and dES in multiple treatments differed with the biological effect measured. The near additivity of the mutation frequencies per 100 M_2 seedlings induced by the two mutagens suggests an independent action that might involve different mechanisms. It is suggested that low pH influences the radiation-induced chromosome aberration frequency by either modifying the properties of radiation-induced radicals or the activity of enzymes concerned with the development and/or subsequent behavior of the chromosome breaks. (A.G.W.)

14385 THE ANIMAL CELL IN CELL CULTURES. Schindler, R. Recent Results in Cancer Research. Volume 1. Berlin, Springer-Verlag, 1965. 88p.

The sensitivity of many cultured normal or neoplastic cells toward irradiation depends on whether they have diploid or polyploid chromosomal structure. In the intact organism the lethal effects of irradiation depend largely on its proliferative effects on the cell populations of the bone marrow and intestinal mucosa. Irradiation of cells results in two phenomena: a transient and reversible cessation of cell division and an irreversible loss of capacity to proliferate. Recovery from irradiation appears to require synthesis of ribonucleic acid. The primary injury that cells suffer during irradiation appears to take place in the genetic structures. A dose sufficient to cause loss of proliferation capacity produces recognizable histological chromosomal changes, leading to reduced mitosis. After irradiation with greater doses, mutations are frequently observed, with changes in cellular morphology, chromosomal structure, lengthening of reproduction time, and increased radiosensitivity. Studies with halogenated pyrimidines substantiate the possibility that irreversible cell damage after irradiation is related to changes in structure of deoxyribonucleic acid, possibly by production of breaks in the chain structure of the molecule. Development of giant cells after less than lethal doses of irradiation suggests that mitosis is blocked, but that synthesis of macromolecular cell components, such as proteins, ribonucleic acid, and deoxyribonucleic acid is not. Changes or inhibition of mitotic activity sometimes appear after doses as low as 10 to 30 R. Sensitivity of mitotic activity to these and other doses of irradiation varies with the stage of division occurring when the cell is irradiated. (764 references.) (BBB)

14386 USE OF IONIZING RADIATION FOR MEASURING BIOLOGICAL PHENOMENA. Nelson, Neal S.; Rust, John H. (Univ. of Chicago). pp 59-170 of Methods of Animal Experimentation. Vol. 2. Gay, William I. (ed.). New York, Academic Press, 1965.

Practical aspects of biological experimentation with radiation are reviewed. Topics considered include: laboratory design and construction, handling of radioisotopes, administration of radiation or radioisotopes to the experimental animal, collection of samples, and uses of radioisotopes for chromatography, ion exchange, labeling, isotope dilution, autoradiography, and radioactivation analysis. (TCO)

14387 THE EFFECT OF IONIZING RADIATION IN PRODUCING STERILITY IN PHARMACEUTICAL PRODUCTS: WITH SPECIAL REFERENCE TO VIRUSES. Pollard, E. C. pp 25-30 of Ionising Radiation for the Sterilization of Medical Products. London, Panel on Gamma and Electron Irradiation, 1965.

Theories underlying the basic nature of virus inactivation are considered. Review of research on the effects of ionizing radiation on viruses indicates that ionizing radiation does remove infectivity. Viral survival depends on the volume ionized. The inactivation volume appears to bear some relationship to the nucleic acid content of the virus in the single-stranded viruses. Experiments with the single-stranded R_{17} phage and the double-stranded T1 showed that the mechanism of inactivation is not the same in single-stranded and double-stranded viruses. It is suggested that the ultimate sensitivity of a double-stranded virus may be in the part of the B strand that is transcribed to make a new enzyme to enable viral DNA to replicate. Methods for eliminating a clump of viruses is discussed, and the relationship between viral inactivation by direct and indirect means is considered. Numerical conclusions are presented. (H.G.D.)

14388 THE EFFECT OF IONIZING RADIATION IN PRODUCING STERILITY IN PHARMACEUTICAL PRODUCTS: WITH SPECIAL REFERENCE TO VEGETATIVE CELLS. Brynjolfsson, A. pp 33-45 of Ionising Radiation for the Sterilization of Medical Products. London, Panel on Gamma and Electron Irradiation, 1965.

General characteristics of radiation effects on vegetative bacteria and the influence of culture and irradiation media on bacterial radiosensitivity are reviewed. Mathematical models for the effects of radiation on vegetative cells are presented and compared with the experimental results of Christensen et al. on Micrococcus radiodurans. (H.G.D.)

14389 THE EFFECTS OF IONIZING RADIATIONS IN PRODUCING STERILITY IN PHARMACEUTICAL PRODUCTS WITH SPECIAL REFERENCE TO SPORES. Ley, F. J. pp 51-65 of Ionising Radiation for the Sterilization of Medical Products. London, Panel on Gamma and Electron Irradiation, 1965.

Research on the effects of ionizing radiation on various bacterial spores is summarized. Both aerobic and anaerobic spores were used as test organisms. Pharmaceutical products contaminated with bacterial spores were sterile after irradiation with 2.5 Mrad doses. (H.G.D.)

14390 POTENTIAL MODIFYING FACTORS IN STERILIZATION AND INACTIVATION. Charlesby, A. pp 66-74 of Ionising Radiation for the Sterilization of Medical Products. London, Panel on Gamma and Electron Irradiation, 1965.

Variables affecting the sterilization process are considered. Research on radiation mechanisms for bacterial inactivation, and the means by which these can be changed by such factors as type of radiation, the presence or absence of oxygen, water and other chemical compounds, and temperature are discussed. (H.G.D.)

Radiation Effects Therapy and Countermeasures

14391 BIOCHEMICAL STUDY ON RADIOPROTECTION PROCESSES. Furnica, M.; Furnica, G. (Institutul Oncologic, Bucharest). Acad. Repub. Pop. Rom., Stud. Cercet. Biochim., 5: 251-61(1962). (In Rumanian).

The influence of radioprotectors (AET, Largactil) on a lethal dose of radiation is examined. The restoration of leukocyte count/mm^3 by a combination of AET and Largactil within 10 days after a small dose (500 R for rats) is charted. Consumption of O_2 in spleen tissues after administration of AET, aminothiazole, and cysteamine is tabulated; an increase is noted (from 69 to 87 μl/100 mg tissue/hour) for AET. Largactil decreases O_2 consumption particularly in the brain and kidneys in relation to its dose, but not so much in the liver; 2.5 mg Largactil/100 mg tissue drop O_2 consumption from 92 to 13.7 in the brain, from 181 to 54 μl/100 mg tissue/hour in the kidneys. The action of radioprotectors on serum and blood cholinesterase

runs from 0% inhibition for glutathione to 92% serum enzyme inhibition for Largactil. Greater dependence on pH for Largactil blood enzyme inhibition is noted (pH 7.4 30%, 6.4 76%; 8.4 40%) than serum enzyme inhibition (all about 44%). Decrease of cholinesterase activity on irradiation of the brain and liver is enhanced by AET, particularly in the liver. No single mechanism applies. The nervous system is involved whether one uses a protector directly affecting the nervous system or one which acts radiolytically. Radiolytic compounds have a max protection of 70% in tests with synthetic polyelectrolytic macromolecules. (BBB)

14392 EVALUATION OF THE RADIOPROTECTIVE ACTION OF METHYLANDROSTENOLONE IN THE COURSE OF POSTRADIATION DISEASE CAUSED BY DIFFERENT DOSES OF X RAYS. Danysz, A.; Panek, R. Acta Physiol. Pol., 16: 893-902(1965). (In Polish).

The radioprotective action of methylandrostenolone on young rats irradiated with different doses of x rays was investigated. Administration of methylandrostenolone in the dose of 1 mg/kg for 20 days before and 20 days after irradiation decreased the mortality rate of irradiated animals, inhibited the decrease in lymphatic leukocytic index, and inhibited the postradiation increase in gas metabolism. (auth)

14393 PROTECTION OF THE MOUSE AGAINST LETHAL EFFECTS OF X RAYS BY SODIUM HYPOSULFITE. Maldague, P.; Duplan, J. F. (Institut du Radium, Paris). Compt. Rend. Soc. Biol., 159: 1063-6(1965). (In French).

Sodium hyposulfite, injected intravenously in mice at a dose of 6 g/kg, protects 65% of the mice exposed to x radiation at a dose of 1000 R. The dose reduction coefficient is approximately 1.6 if the LD_{50} of the control mice (675 R) is compared with that of the treated mice (1075 R). With the exception of a transitory hypothetical anoxia, no known mechanism can explain the mechanism of this protective agent. (tr-auth)

14394 SPECULATIONS CONCERNING RELATIONSHIPS BETWEEN CHEMICAL PROTECTION AGAINST X-IRRADIATION AND THE PROTECTION OF CELLS FROM FREEZING DAMAGE. Ashwood-Smith, M. J. (Medical Research Council Radiobiological Research Unit, Harwell, Eng.). Cryobiology, 1: 242-3(Jan.-Feb. 1965).

Some correlations of research findings in cryobiological and radiobiological research are discussed. Removal of water from many biological systems leads to an increased resistance to radiation damage. Studies showing that the survival of the bacterium Pseudomonas after freezing and thawing in saline is altered by the presence of substances known to influence the course of radiation damage or to disturb hydrogen bonds are reported. Glutathione (0.05M) and thiourea (0.15M) protect cells from radiation damage, but increase freezing damage in Pseudomonas 2 to 4 fold. Experiments with Pseudomonas have failed to demonstrate any difference in freezing sensitivity between samples frozen either under anoxic conditions or in the presence of pure oxygen. (TCO)

14395 EFFECT OF IRRADIATION TEMPERATURE ON THE RADIOSENSITIZING ACTIVITY OF VITAMIN K_5. Chandler, H. K. (Army Natick Lab., Mass.); Licciardello, J. J.; Goldblith, S. A. J. Food Sci., 30: 893-7(Sept.-Oct. 1965).

A study was undertaken to determine the feasibility of destroying salmonellae in liquid egg through the combined use of vitamin K_5 and γ irradiation from a ^{60}Co source. Salmonella typhimurium was irradiated in phosphate buffer, pH 7.6, containing various levels of vitamin K_5 over a temperature range of 32 to 120°F either in air or under vacuum. Vitamin K_5 exerted a radiosensitizing effect under vacuum and a radioprotective effect in air. The radiosensitizing effect decreased with increasing temperature, being maximum at 32°F. It is suggested that vitamin K_5, was rapidly destroyed at the high irradiation temperatures, and hence was available for sensitization. Vitamin K_5, in whole egg irradiated in air or vacuum, had little or no effect on the survival of S. typhimurium over the temperature range investigated. (TCO)

14396 POLYVINYLPYRROLIDONE IN THE TREATMENT OF RADIATION SICKNESS. RADIOTOXINS. Nuvolone, U. (Ospedale Maggiore, Novara, Italy). Minerva Radiol., Fisioterap. Radiobiol., 10: 385-90(Sept. 1965). (In Italian).

The principal pathogenic hypotheses on radiation sickness are briefly described, and the role of radionecrotoxins is especially considered. The literature on the radioprotective properties of polyvinylpyrrolidone is reviewed. The results obtained in 31 patients, having symptoms of radiation sickness during Co or x-ray therapy and treated with PVP, are described. Favorable results were obtained in a high proportion of the cases. (tr-auth)

14397 THE EFFECTS OF HIGHLY POLYMERIZED HETEROLOGOUS RIBONUCLEIC ACID (RNA) ON IRRADIATED HEALTHY ANIMALS AND ON IRRADIATED ANIMALS BEARING ASCITE TUMORS. D'Acunazo, L.; Giudici, G.; Pini, M. (Univ., Trieste, Italy. Ospedale Maggiore, Trieste, Italy). Minerva Radiol., Fisioterap. Radiobiol., 10: 390-2(Sept. 1965). (In Italian).

The radioprotective action of RNA was investigated in healthy animals exposed to a 700 R whole-body doses of electron irradiation. A marked survival 30 days after the irradiation was observed. Animals with Ehrlich ascites cancer that were irradiated showed a very rapid drop in the mitotic index both in treated and untreated groups. It is suggested that RNA protects healthy tissues but not tumorous tissues. (tr-auth)

14398 THE INFLUENCE OF 5-HYDROXYTRYPTAMINE (SEROTONIN) ON THE RADIOINDUCED MUTATION RATE IN DROSOPHILA MELANOGASTER. Kuenkel, H. A.; Trams, A.; Henke, H. (Univ., Hamburg). Naturwissenschaften, 52: 650(1965). (In German).

The mutagenic effects of serotonin in conjunction with x radiation was investigated. Drosophila melanogaster were exposed to doses of 3000 r. Some of the flies were treated with serotonin 10 min before the radiation. Irradiation alone caused a 7.9% increase in the mutation rate. The combined treatment of serotonin and radiation caused an increase in the mutation rate of recessive sex-linked lethal factors of 15.8%. (J.S.R.)

14399 OXYGEN EFFECT ON THE POST-IRRADIATION RESTORATION OF YEAST CELLS. Barsukov, V. S.; Malinovskii, O. V.; Mityushova, N. M. (Pavlov Inst. of Physiology, Leningrad). Radiobiologiya, 5: 860-6(1965). (In Russian).

The presence of oxygen during irradiation causes an abrupt decrease in the speed of post-irradiation recovery in yeast cells. The presence of oxygen during irradiation altered the magnitude of the percentage of survival and the speed of restoration in water but did not modify the shape of the dose dependence curves. The oxygen effect on the survival and the speed of restoration in water is the same at all dose ranges and equals approximately 3. (tr-auth)

14400 SERUM CONCENTRATION: EFFECTS ON CYCLE AND X-RAY SENSITIVITY OF MAMMALIAN CELL. Hahn, George M.; Bagshaw, Malcolm A. (Stanford Univ., Palo Alto, Calif.). Science, 151: 459-61(Jan. 28, 1966).

If the content of serum in the culture medium of exponentially growing Chinese hamster cells is below optimum (15%), the doubling time and the resistance to x-irradiation of the cells are increased. In synchronously dividing populations the increase in doubling time is primarily caused by increase in duration of the postmitotic (G_1) phase of the cells; this phase is relatively radiation resistant. The response of the cells growing synchronously is related quantitatively to the response of the cells dividing randomly. (auth)

14401 INVESTIGATIONS ON THE RADIOPROTECTIVE EFFECTS OF RIBONUCLEIC ACID ON NORMAL AND TUMOR TISSUES. Pini, Mario; D'Acunzo, L.; Giudici, G. (Ospedale Maggiore, Trieste, Italy). Strahlentherapie, 128: 558-64(Dec. 1965). (In German).

Heterologous and highly polymerized ribonucleic acid was used as a radiation protective substance. This substance produced a high recovery ability in mice which received 700 R total-body x irradiation and in tissues which

were damaged by local irradiation. Experiments done with inoculation tumors showed that this protective effect is not present in neoplastic tissue. (tr-auth)

14402 INVESTIGATIONS OF THE EFFECTIVE MECHANISM OF THE RADIOPROTECTIVE SUBSTANCE METHANDROSTENOLON. PART II. THE DEPENDENCE OF THE RADIATION PROTECTION ON THE HYPOXEMIC EFFECT OF METHANDROSTENOLON. Danysz, Andrzej; Panek, Ryszard; Proniewski, Henryk; Kruszewska, Jadwiga (Pharmakologische Institut der Medizinischen Akademie Bialystok, Poland). Strahlentherapie, 128: 610-16(Dec. 1965). (In German).

A radioprotective effect in rats, resulting in an increase in the LD_{50}, was found after a continuous application of methandrostenolon (1 mg/kg). The radioprotective effect is proportional to the duration of application during the 5 to 20 day period prior to irradiation. A relationship between the radioprotective effect and the inhibition in oxygen consumption was observed during the 5 to 15 application days. Further application of methandrostenolon did not increase the inhibition of oxygen consumption; however, the radioprotective effect was increased. The radioprotective effect of methandrostenolon seems to depend, to a certain extent, on the reduction in the oxygen consumption by tissue and partly on the direct anticatabolic and anabolic effect of this steroid. (tr-auth)

Radiation Hazards and Protection

See also HEALTH AND SAFETY

14403 (NP–15714) DISINTEGRATION RATE MULTIPLIERS IN BETA-EMITTER DOSE CALCULATIONS. Brown, Stephen L. (Stanford Research Inst., Menlo Park, Calif.). Aug. 1965. Contract N228(62479)65702. 169p.

The possible biological doses from external beta emitters are discussed and are compared with those from external gamma emitters. A detailed analysis is made of the dose distribution in tissue to be expected from individual beta-emitting radionuclides in contact dose or beta bath plane geometries. Simplified models are also discussed. Disintegration rate multipliers, which convert contamination levels in dis/sec-cm^2 to dose rates in rad/sec, are given for nearly 400 radioisotopes and for several depths in tissue and widths of air gap. Comparisons are made with the simplified results and with a simplified gamma model. The conclusion is reached that beta radiation can be a serious hazard in comparison with gamma radiation if there are unprotected radiosensitive tissues at shallow depths in the exposed organism. (auth)

14404 PROTECTIVE EFFECTS OF STREPTOMYCIN AGAINST RADIATION DAMAGE OF THE CHROMOSOMES OF GERMINAL CELLS OF MAMMALS. Shao, Wei; Wang, Tu-kung; Chang, Han. Sci. Sinica (Peking), 13: 1523-5 (1964). (In Russian).

An experiment was conducted to detect the possible protective effects of a low concentration of streptomycin on the chromosomes of the germinal cells of male mice, weighing 20 to 25 g. Eight hr before irradiation a solution of the antibiotic at different concentrations was introduced into the stomachs of the mice which were then subjected to x rays at a dose rate of 31 R/min. At 16 hr after irradiation the percentage of spermatocytes with chromosome aberrations was 10.4%, and after 38 hours 9.18%, while in nonirradiated mice the percentage of sperm cells with chromosome aberrations was only 0.13%. The frequency of aberrations of chromosomes in animals treated with streptomycin before irradiation was lowered to some extent. Protective effects of the antibiotic, as seen in samples taken 16 hr after irradiation, reached 63.8% and after 38 hours, 49.6%. Changes in the frequency of aberration of chromosomes in antibiotic-treated nonirradiated mice were insignificant, except in cells examined 46 hr after a high dose (5 mg). The protective effect of streptomycin may be related to its ability to form a complex with DNA. The protective effects are probably not connected with its antibacterial effect, but rather with its chemical structure. For example, streptidine, which does not have a bacteriostatic effect, has protective effects, indicating the importance of chemical structure in this activity. (BBB)

Radiotherapy and Radiodiagnosis

Refer also to abstract 14883.

14405 (COO–1305-2) BLOOD SUPPLY TO HEPATIC V2 CARCINOMA IMPLANTS AS MEASURED BY RADIOACTIVE MICROSPHERES. Blanchard, Robert J. W.; Grotenhuis, Ivan; LaFave, James W.; Perry, John F. Jr. (Ancker Hospital, St. Paul, Minn. Minnesota Univ., Minneapolis. Medical School). [1964]. Contract AT(11-1)-1305. 10p. Dep. mn. CFSTI $1.00 cy, $0.50 mn.

Ceramic or plastic microspheres 15μ in diameter and containing tracer doses of ^{46}Sc, suspended in a solution of dextran, were used as tracers to measure the blood supply to hepatic carcinoma implants in rabbits. The findings demonstrate that radioactive microspheres lodge in tumors in higher concentrations than in the surrounding liver when infused into the hepatic artery, while the opposite is true if the microspheres are infused into the portal system. Applications in the use of intravascular introduction of chemotherapeutic or radioactive materials in tumor therapy are discussed. (C.H.)

14406 RADIOISOTOPES IN INTERNAL RADIATION THERAPY. Gregorio, Reynaldo G. (Univ. of the Philippines Medical Center, Manila). Acta Med. Philippina, 1: Ser. 2, 96-104(Oct.-Dec. 1964).

Development of the uses of radioisotopes in cancer radiation therapy is reviewed. Intracavitary applicators are described and illustrated. Cancer of the uterine cervix offers especially favorable conditions for intracavitary applicator therapy, because the tumor can be cross-fired from the uterus and vagina and because these two organs tolerate high radiation doses well. The value of intracavitary applicator therapy in comparison with external x-ray therapy for cervix cancer is probably greatly underrated. However, with isotopes used in combination with external x-ray therapy, a very favorable dose distribution can be achieved with the dose max automatically placed in the proper location. The rationale of internal mammary radioisotope implants is discussed. (TCO)

14407 FIELD CONTROL OF TELECOBALT THERAPY BY GAMMA-RAY TELEVISION. Malven, R.; Rosengren, B.; Wallman, H. (Univ. of Gothenberg, Sweden). Acta Radiol. Therapy. Phys., Biol., 3: 425-30(Dec. 1965).

The field control of telecobalt therapy based on a special system of γ-ray television is described. Its advantages are discussed. (auth)

14408 RECORD FORM FOR EXTERNAL BEAM THERAPY DESIGNED SPECIALLY FOR ^{60}Co TREATMENT WITH STATIONARY FIELDS. Lindgren, Martin; Nordberg, Ulla-Brita (Univ. of Lund, Sweden). Acta Radiol. Therapy, Phys., Biol., 3: 457-62(Dec. 1965).

A record form for external ^{60}Co irradiation is described in detail. The form together with supplementary cross-section diagrams of the target volume allows a complete description of technical data, treatment planning, and dose distribution within the irradiated region. (auth)

14409 PELVIC LYMPH NODE DISSECTION FOLLOWING RADIOTHERAPY FOR CANCER OF THE CERVIX: RE-EVALUATION. Gray, Mary Jane (Univ. of Vermont, Burlington); Frick II, Henry Clay. Amer. J. Obstet. Gynecol., 93: 110-14(Sept. 1, 1965).

Use of radiotherapy following surgery for 72 patients with cervical carcinoma (Stages I and II) is reported. The patients received two applications of radium using the Corscaden applicator followed by external radiotherapy by a 250-kv x-ray machine and a supervoltage unit. Complications occurred in 18 patients. The results of this combination therapy did not yield survival rates that were

significantly better than those obtained by either radiotherapy or operation alone. (TCO)

14410 SUPERVOLTAGE X-IRRADIATION OF EPITHELIAL TUMOURS OF THE LACRIMAL GLAND. Mortada, Aly (Cairo Univ.). Brit. J. Ophthalmol., 48: 601-8(Nov. 1964).

The different histopathological types of epithelial tumor of the lacrimal gland and the effects of supervoltage x irradiation on them were studied in eight cases. For recurrent or malignant epithelial tumors, the Lederman method of giving 6000 R of supervoltage x irradiation in 6 weeks with indirect ocular protection gave good results. Recent views on the use of radiation for treatment of epithelial tumors of the lacrimal gland are summarized. (TCO)

14411 VESICO-URETERAL REFLUX AFTER IRRADIATION OF THE URINARY BLADDER. Zingg, E.; Camponovo, F.; Wirth, W. (Universitaetsklinik, Zurich). Helv. Chir. Acta, 4: 478-83(Oct. 1965). (In German).

Intracavitary ^{60}Co irradiation, betatron irradiation, or telecobalt irradiation was administered to 24 patients with recurrent bladder papillomatosis, and several types of carcinomas. The total ^{60}Co γ irradiation dose given amounted to 7000 R, and the betatron irradiation was ~6000 R. Vesicoureteral reflux with cystitis was observed in all patients who received ^{60}Co irradiation as one of several symptoms of postirradiation injury. Reflux was observed in one of two patients who received telecobalt irradiation. Only four out of 17 who received betatron irradiation developed reflux. (TCO)

14412 RADIATION TOLERANCE OF THE PATIENT IN EXTRA-ORAL RADIOGRAPHY. Sonnabend, E. (Univ. Goettingen, Ger.). Int. Dent. J., 13: 495-502(Sept. 1963).

The doses received on the surface of the skin and in the area of the gonads during different types of extraoral radiography were determined by an ionization chamber and film. Measurements were carried out during diagnostic radiography of 10 different facial areas. Dose values in extraoral radiography published previously are tabulated. Measurements of doses in various types of radiographs of the lower jaw are discussed. The different types of radiographs of the other bones of face showed on the whole the same dose as in the radiographs of the lower jaw. It is concluded that the doses differ greatly in different extraoral methods of x-ray photography. (TCO)

14413 REVIEW OF CHEMOTHERAPEUTIC AGENTS AND RADIOISOTOPES IN THE NONOPERATIVE TREATMENT OF GYNECOLOGIC CANCERS. Sherman, Alfred I. (Washington Univ., St. Louis). J. Int. Coll. Surg., 43: 259-65(Mar. 1965).

The present status of chemotherapeutic drugs and radioisotopes in the treatment of gynecologic cancers is surveyed, along with a consideration of some new forms of radiation, such as neutron bombardment, and a variety of newer technics, such as hyperbaric irradiation. (TCO)

14414 ADVANCED CANCER OF THE BLADDER: MANAGEMENT WITH IRRADIATION. Ball, Ottis G.; Hickman, Bernard T. (Univ. of Mississippi School of Medicine, Jackson). J. Miss. State Med. Ass., 6: 345-9 (Sept. 1965).

An analysis was made of 55 cases of bladder carcinoma treated with rotational ^{60}Co teletherapy from 1955 to 1964. A 6000-R tumor dose was delivered to the entire bladder in about six weeks. The complications secondary to radiation that were encountered were not a significant deterrent to therapy for cure. Good palliation of even far advanced lesions was achieved, and occasional five-yr cures obtained in far advanced lesions. No significant advantage of combining chemotherapy with irradiation was noted. It is concluded that supervoltage irradiation (such as with ^{60}Co) therapy should be offered to early cases, particularly because of its decreased morbidity and increased effectiveness compared to conventional x-ray therapy. (TCO)

14415 RELATIONSHIP BETWEEN HEMATOCRIT AND SOLUBILITY OF ^{133}Xe IN BLOOD. Andersen, Anne Marie; Ladefoged, Jorgen (Glostrup Hospital, Copenhagen). J. Pharm. Sci., 54: 1684-5(Nov. 1965).

The relation between the hematocrit (hct) and the solubility of ^{133}Xe in blood at 37°C was measured in 64 samples. The hct varied from 0 to 88%. An excellent linear correlation between the partition coefficients (in g/g) against the hematocrit was found. The slope of the correlation line was 0.0112 (standard deviation, 0.0004), and the intercept (for hct = 0) was 1.0 (standard deviation, 0.02). The standard deviation of the estimate was 0.08. These values indicate a partition coefficient plasma/water of 1.02 (in g/g) and erythrocytes/water of 2.14 (in g/g). From known values of the specific weight of plasma and erythrocytes, the following formula for the partition coefficient of tissue/blood in g/ml (λ) at changing hematocrits was calculated: $\lambda hct_x = \lambda hct_{50}\ (1.69/1.05 + 0.013\ hct_x)$; where λhct_{50} is the partition coefficient of the tissue at hematocrit 50%, and λhct_x is the partition coefficient of the tissue at hematocrit x %. The higher solubility of ^{133}Xe in plasma and blood rather than in water is explained by the high affinity of ^{133}Xe for lipids and hemoglobin. The solubility of ^{133}Xe in plasma and erythrocytes has been previously investigated in vitro, with resulting partition coefficients (in g/g) of erythrocytes and plasma to water of 3.75 and 1.45, respectively. However, these measurements were carried out at a temperature of 21°, and the figures are therefore not directly comparable with the present ones. For whole blood (hemoglobin content 15 g/l), the partition coefficient of blood/water in vivo was 2.10, a figure not confirmed by the present findings. Earlier measurements were carried out at 25 mm Hg partial pressure of xenon. The results reported here show that estimations of the blood flow from clearance values of ^{133}Xe without correction of the partition coefficient of tissue to blood for the hematocrit may induce a random error of about 10%. (BBB)

14416 TONSIL AND PALATINE ARCH CANCER-TREATMENT BY RADIOTHERAPY. Schulz, M. D. Laryngoscope, 75: 958-67(June 1965).

Data on effectiveness of various dose levels and incidence of complication are presented in a report of x-ray treatment of 305 patients. A gross three-year cure rate of 22% was achieved in the treatment by irradiation of all squamous cell carcinomas, regardless of site of origin. Local control by irradiation was largely a function of tumor dose, increasing by a factor of almost 1.5 in the control of the primary tumor when the dose was 5000 R or more as compared to that achieved by doses of less than 5000 R, and by 2.6 in the control of regional metastases. When the dose was more than 5000 R, primary cancer was controlled for the duration of the patient's life in almost 80% of instances (158 of 203). Control in 10 of 48 cases was achieved with doses less than 5000 R. (TCO)

14417 THE ROLE OF RADIATION THERAPY IN THE TREATMENT OF CHEMODECTOMAS OF THE GLOMUS JUGULARE. Grubb, William B. Jr.; Lampe, Isadore (Univ. of Michigan, Ann Arbor). Laryngoscope, 75: 1861-71(Dec. 1965).

Data on 20 cases of chemodectomas of the glomus jugulare are reported, some were treated with surgery and others with radiation therapy, or both. Emphasis is placed on the generally inadequate results obtained with surgery alone and the fact that the tumors can be controlled fairly well by radiotherapy. (TCO)

14418 ON THE TREATMENT OF HEMANGIOMA OF THE SKIN. Osterland, G.; Schondorf, K.-W.; Gerstenberg, E. (Univ., Freien, Berlin). Med. Klin., 60: 772-4(May 7, 1965). (In German).

Safety procedures for radiotherapy of skin hemangiomas are discussed, and treatment methods are considered. (H.G.D.)

14419 EFFECTIVE CONTROL OF X-RAY EXPOSURE IN DENTISTRY. Blatz, Hanson (New York City Office of Radiation Control). N. Y. State Dent. J., 31: 250-5 (June 1965).

Findings of the x-ray inspection program in New York City are reported. An attempt was made to ascertain that all dentists have equipment that meets mechanical standards of the National Committee on Radiation Protection, and that it is used in a manner to minimize the exposure of operators and patients. Reinspections in New York City have shown that most of the deficiencies originally found in dental x-ray installations have now been corrected. However, there is evidence that most dentists have not conducted self-examinations of their procedures, to determine whether they could effect a reduction in their contribution to the population dose. Two simple methods are proposed by which most dentists can reduce such exposures significantly. (TCO)

14420 RADIATION TREATMENT OF CANCER OF THE LUNG. **Muta, Nobuyoshi; Morita, Kazuo (Sapporo Medical College). Nippon Igaku Hoshasen Gakki Zasshi, 25: 292-7(July 1965). (In Japanese).**

Twenty-four cases of lung cancer treated with γ or x radiation are reviewed. Evaluation of treatment methods, though hindered by the advanced state of most patients at the onset of therapy, indicated that telecobalt therapy was somewhat better than other procedures. (H.G.D.)

14421 DEVELOPMENT AND DOSIMETRY OF AN "EPITHERMAL" NEUTRON BEAM FOR POSSIBLE USE IN NEUTRON CAPTURE THERAPY. II. ABSORBED DOSE MEASUREMENTS IN A PHANTOM MAN. Fairchild, R. G. (Brookhaven National Lab., Upton, N. Y.); Goodman, L. J. Phys. Med. Biol., 11: 15-30(Jan. 1966).

In order to evaluate the usefulness of an epithermal neutron beam (0.5 ev to 10 kev) for the neutron capture therapy procedure, a tissue equivalent chamber was used to determine separately the depth-dose distributions from γ rays, fast neutrons, and the $^{14}N(n,p)^{14}C$ reaction in a phantom man. Results showed that tumors deeper than 2.5 cm could not be treated with a thermal beam (assuming 35 μg of ^{10}B per gram of tumor, and a ratio of ^{10}B in tumor to ^{10}B in tissue of 3 to 1) because the ratio of tumor dose to maximum normal tissue dose (advantage factor) would have been less than unity. With the epithermal beam on the other hand advantage factors of 1.4 to 1.9 were obtained at all depths greater than 1.5 cm in the phantom head, assuming the same conditions as with the thermal beam. Advantage factors were found to be more sensitive to the absolute ^{10}B concentration than to the ^{10}B ratio in tumor to normal tissue. Improved depth-dose curves generated by the epithermal beam can solve the problem of rapid neutron attenuation encountered with thermal neutron beams. (auth)

14422 A WHOLE-BODY COUNTER FOR CLINICAL MEASUREMENTS UTILIZING THE "SHADOW SHIELD" TECHNIQUE. Warner, G. T.; Oliver, R. (Churchill Hospital, Oxford). Phys. Med. Biol., 11: 83-94(Jan. 1966).

Two 4 in. sodium-iodide crystals are mounted one above and the other below a motorized couch. The detectors view a field 20 in. across and either 6 or 12 in. along the couch, further lead protection being provided to eliminate direct background radiation. As the total weight is only 4½ tons, installation within the hospital was possible and the equipment is now in routine use for clinical measurement of uptake of ^{58}Co and ^{59}Fe. The "traverse count," obtained as the couch drives between the detectors, varied by not more than ±8% with position of a small source in a body phantom, and by not more than 3% with variation of distribution of activity in any one patient. Good agreement was demonstrated between percentage retention derived from whole-body counts and from measurement of fecal activity. The average ratio obtained was 1.01 ± 0.12. (auth)

14423 THE USE OF ^{99m}Tc AS A CLINICAL TRACER ELEMENT. Herbert, R.; Kulke, W.; Shepherd, R. T. H. (Liverpool Radium Inst.). Postgrad. Med. J., 41: 656-62 (Nov. 1965).

Properties of the ideal radioisotope for clinical diagnosis are considered. The physical properties, metabolism, and radiation dose of ^{99m}Tc are discussed and compared with those of ^{123}I, ^{125}I, ^{131}I, and ^{132}I. Plasma clearance tests were performed on three human subjects using ^{99m}Tc as pertechnetate in isotonic saline, by intravenous injection while the same dose was given orally to a third. After two hr the plasma concentration was in each case between 3% and 5% per liter and the mean long-term component was 3.5% per liter with a half clearance time of 9 hr. Urine excretion accounted for 30% of the dose at 24 hr and 40% at two days, while 10% was collected in the feces in two days. The data were used to estimate the radiation hazard resulting from a tracer dose of ^{99m}Tc. It is shown that with ^{99m}Tc the highest in vivo counting rates are obtained for a given internal radiation dose, so that measurements of high statistical accuracy may safely be made. Since the γ-ray energy is near optimum for scanning, transients may be observed using light-weight collimators. (TCO)

14424 ATRIAL FIBRILLATION IN THYROTOXICOSIS TREATED WITH RADIOIODINE. **Staffurth, J. S.; Gibberd, M. C.; Hilton, P. J. (Lewisham Hospital, London). Postgrad. Med. J., 41: 663-71(Nov. 1965).**

Thirty-nine patients with atrial fibrillation (AF) and thyrotoxicosis who had been referred for ^{131}I treatment are reviewed, with particular reference to reversion to sinus rhythm, the ultimate cardiac status, and risk of embolism. Radioiodine doses in patients with small or impalpable glands were 4 to 6 mC, those with moderate goiters 8 to 10 mC, those with large goiters from 12 to 15 mC; in two very severe cases, 25 mC was given in divided doses initially. Eighteen patients had been made euthyroid with carbimazole before ^{131}I treatment, after which the drug was continued in decreasing dosage for three months. Of the 170 subjects in the main series, 39 (23%) had AF confirmed by electrocardiogram (ECG) at some stage of their illness. In eight subjects the AF was paroxysmal before definitive treatment was given and in one it occurred for the first time three months after the first dose of ^{131}I. After completion of treatment half of the patients were in sinus rhythm but when those with paroxysmal AF were excluded the proportion was reduced to one third. These results compare unfavorably with earlier surgical experiences and possible reasons for this are discussed. The cardiac status after treatment is described and attention drawn to a persistent form of heart disease which is not uncommon and which, it is suggested, should be called postthyrotoxic cardiomyopathy. Four instances of suspected cerebral emboli are described and attention drawn to the possibility of this complication in thyrotoxicosis with AF. The use of antithyroid drugs before or after radioiodine is discussed with emphasis on the necessity for care in management of this entails. It is concluded that all subjects with thyrotoxicosis and AF should be treated energetically whatever method is chosen. (TCO)

14425 HIGH-ENERGY RADIATIONS IN FRANCE. (PRESENT EQUIPMENT AND FUTURE PROSPECTS). **Lalanne, C. M. (Institut Gustave Roussy, Villejuif, France); Dutreix, J.; Amalric, R. Radiaz. Alta Energia, 4: 183-92(July 1965). (In Italian).**

The availability in France of telecobalt devices, telecesium devices, and high-energy accelerators for therapeutic purposes are indicated. The therapeutic indications for the use of each of these devices are summarized. The possibility for the future development and construction of additional radiation facilities is considered. (J.S.R.)

14426 MOVING-FIELD IRRADIATION WITH WEDGE FILTERS IN ^{60}Co TELETHERAPY. **Welker, Klaus (Robert-Roessle-Klinik, Berlin). Strahlentherapie, 128: 514-25(Dec. 1965). (In German).**

A large dose maximum and a rapid dose decrease involving healthy tissue was obtained using wedge filters during ^{60}Co-moving field irradiation. A displacement in the dose maximum was not observed. Necessary wedge filters were determined for different pendulum angles. Patient profile, pendulum-axis depth, and field size were shown to have only a small influence on the size of the wedge angle. These results show that standardization of wedge filters is possible for fixed focus-wedge distance and fixed focus-point of rotation distance. (tr-auth)

14427 NUCLEAR MEDICINE'S TWO EXPLOSIVE DECADES. **Breeling, Jim. Today's Health, 43: 54-9; 66-9(July 1965).**

A general review is provided of the medical aspects of the development of nuclear materials, particularly radioisotopes. Medical diagnostic and research uses of isotopes are outlined. Genetic studies in continuously irradiated animals are described and fallout hazards are considered. (TCO)

CHEMISTRY

General

Refer also to abstract 15133.

14428 (ORNL–3889) ANALYTICAL CHEMISTRY DIVISION ANNUAL PROGRESS REPORT FOR PERIOD ENDING NOVEMBER 15, 1965. Raaen, Helen P. (comp. and ed.) (Oak Ridge National Lab., Tenn.). Jan. 1966. Contract W-7405-eng-26. 167p. Dep. mn. CFSTI $5.00 cy, $1.00 mn.

Information concerning research-associated activities is presented in nineteen sections. Separate abstracts were prepared for thirteen sections. The sections for which no abstracts were prepared are concerned with quality control, mass spectrometric analysis, spectrochemical laboratory, process analyses, ORNL master analytical manual, activities related to educational institutions, and publications. (J.R.D.)

For abstracts of individual sections see: 14452–14461, 14511, 14576, and 14581.

14429 PREHLED CHEMICKE TECHNOLOGIE JADERNEHO PRUMYSLU. (Survey of Chemical Technology in the Nuclear Industry). Neumann, Leo; Rypar, Vratislav. Prague, State Publishing House of Technical Literature. 1964. 219p.

The size of the nuclear chemical industry is reviewed, and the following subjects are discussed: nuclear reactor fuels; physical and chemical separation of uranium, thorium, protactinium, and radium from ores; isotope separation, e.g., by diffusion, distillation, gas centrifugation, and electromagnetic methods; moderators, e.g., heavy water, graphite, various phenyl compounds, and beryllium; special materials such as zirconium, hafnium, magnesium, niobium, sodium, and calcium and their properties; and processing of irradiated fuels, after cooling and decladding, by extraction (e.g., methyl isobutyl ketone and tributyl phosphate), cation and anion exchange, pyrometallurgy, inorganic ion exchange, fractional distillation of fluorides, selective oxidation, liquid metal extraction, halogenation, or electrolysis to recover the fissionable material and of waste by such methods as deacidification, removal of cesium and strontium, incorporation of residue in concrete, adsorption on soils, ion exchange, fusion, disposal in the sea, and precipitation. (TTT)

Analytical Procedures

See also Separation Processes and Procedures

Refer also to abstracts 14239, 14509, 14662, 14871, 14963, 15044, 15872, 15959, 16046, and 16133.

14430 (AD–620219) RADIOCHEMICAL PROCEDURES FOR SELECTED RADIONUCLIDES IN ENVIRONMENTAL SAMPLES. Instrumentation Papers (Scientific Report). Pecci, Joseph; Drevinsky, Peter J.; Couble, Edward; Dimond, Noreen A.; Kalkstein, Marvin I. (Air Force Cambridge Research Labs., L. G. Hanscom Field, Mass.). June 1965. 73p. (AFCRL–65–410; IP–68). CFSTI $3.00 cy, $0.75 mn.

Methods are presented for the radiochemical analysis of precipitation, air-filter, and impactor-filter samples for: fission products (Sr-89, Sr-90, Zr-95, Ba-140, Ce-141, and Ce-144); induced radioactivities (Mn-54, Ag-110, W-181, and W-185); high-altitude tracers (Rh-102 and Cd-109); cosmic-ray spallation products (Be-7, Na-22, P-32, P-33 and S-35); and natural radioactivity (Pb-210). (auth)

14431 (ANL–7078) CORRECTIONS FOR X-RAY INTENSITY DATA OBTAINED FROM ELECTRON MICROPROBES. Hart, Raymond K. (Argonne National Lab., Ill.). Nov. 1965. Contract W-31-109-eng-38. 12p. Dep. mn. CFSTI $1.00 cy, $0.50 mn.

The chemical composition of a specimen can be determined quantitatively by electron microprobe analysis, providing suitable corrections are applied to the instrumental data. Corrections to be made fall into two groups: instrumental, and those associated with the interaction of electrons and x rays with the specimen. The nature and application of these corrections to experimental data are discussed. (auth)

14432 (ANL–7123) GLOVEBOX AMALGAMATION FOR THE DETERMINATION OF OXYGEN IN ALKALI METALS. Holt, Ben D. (Argonne National Lab., Ill.). Dec. 1965. Contract W-31-109-eng-38. 10p. Dep. mn. CFSTI $1.00 cy, $0.50 mn.

The use of a new type of amalgamation vessel for the determination of oxygen in sodium and potassium is described. The metal is amalgamated immediately after sampling inside a helium-filled glovebox, thereby terminating the risk of significant oxygen contamination by subsequent handling and exposure to the glovebox atmosphere. Endpoint sensitivity is enhanced by titrating the oxide residue in the same vessel, thus avoiding dilution by wash water that would be required in the transfer to a titration flask. The described technique yielded generally lower and more reproducible values in the low-ppM range than did the older, vacuum-line, amalgamation procedures. (auth)

14433 (BAW–298) RADIOCHEMISTRY OF NUCLEAR FUELS. Quarterly Progress Report No. 4, May 1–July 31, 1965. Bishop, W. N. (Babcock and Wilcox Co., Lynchburg, Va.). Contract AT(30-1)-3376. 24p. Dep. mn. CFSTI $1.00 cy, $0.50 mn.

Experiments were performed to improve the accuracy of neutron flux measurement; samples from two rolls of cobalt-aluminum alloy flux wire were analyzed for cobalt content by chemical and activation techniques. The results showed no variations between samples from the same roll, and small variations between those from different rolls of wire. In a new procedure developed to separate Mn-54 from irradiated iron flux wires, manganese is eluted from an anion exchange column with 50 ml of 7 N HCl. This fraction is free of Fe-59 and Co-60. The addition of up to 20 mg of manganese and up to 50 mg of iron has no adverse effect on the separation. (auth)

14434 (BNWL–180) ADSORPTION OF TRACE IONS FROM INTERMEDIATE-LEVEL RADIOACTIVE WASTES BY ION EXCHANGE. Mercer, B. W. (Battelle-Northwest, Richland, Wash. Pacific Northwest Lab.). Jan. 1966. Contract AT(45-1)-1830. 33p. Dep. mn. CFSTI $2.00 cy, $0.50 mn.

Trace cesium and strontium selectivity coefficients were determined for 16 cation exchangers. Mass action equations were derived for determining the cesium and strontium equilibrium distribution coefficients for solutions containing several competing cations. Good agreement was obtained between computed and experimental distribution coefficients. The computed 1% cesium breakthrough points were within 20% of the actual 1% cesium breakthrough points determined previously for two waste treatment pilot plant ion exchange columns with a plant condensate waste. The slopes of the computed breakthrough curves agreed well with the actual curves for the range covered. A plant condensate waste was steam stripped, filtered, and decontaminated by ion exchange on a pilot plant scale. The inadvertent introduction of bacteria into the plant condensate re retention tank complicated the decontamination of this condensate by increasing the filtration requirement. The steam stripped condensate waste containing bacterial residue was successfully filtered with a horizontal plate filter by using diatomaceous earth filter aid. The use of a fine particle zeolite as both a filtration and an ion exchange media for the horizontal plate filter was apparently unsatisfactory because only a fraction of the zeolite ion-exchange capacity was used before the bed became plugged. (auth)

14435 (BNWL-SA-503) CHEMICAL ANALYSIS OF SPENT POWER REACTOR FUELS. Roberts, F. P.; Van Tuyl, H. H. (Battelle-Northwest, Richland, Wash. Pacific Northwest Lab.). Dec. 27, 1965. Contract AT(45-1)-1830. 7p. (CONF-660305-11). Dep. mn. CFSTI $1.00 cy, $0.50 mn.

From American Nuclear Society Topical Meeting, Augusta, Ga.

The isotopic composition of Pm in typical spent power reactor fuels was evaluated. Also, the amounts of a number of fission product and heavy element isotopes were determined for the purpose of lending factual support for calculations of the value of these isotopes in spent reactor fuels. Four samples of fuel from the Yankee Reactor (a typical pressurized water reactor) and three from the Vallecitos Boiling Water Reactor were analyzed. The results showed that Pm from power reactors of the type studied will not contain intolerable amounts of ^{146}Pm. For the worst case (Yankee), the Pm would require no more shielding than ^{238}Pu for many source sizes and applications. Data from the analyses of actinide elements and pertinent fission products in the fuels provide a basis for predicting the production rates of various reactor by-products. (P.C.H.)

14436 (BNWL-SA-504) FISSION PRODUCT RECOVERY RESEARCH AT BATTELLE-NORTHWEST. Moore, R. L. (Battelle-Northwest, Richland, Wash. Pacific Northwest Lab.). Dec. 27, 1965. Contract AT(45-1)-1830. 9p. (CONF-660305-6). Dep. mn. CFSTI $1.00 cy, $0.50 mn.

From American Nuclear Society Topical Meeting, Augusta, Ga.

The major recent developments in fission product recovery at the Pacific Northwest Laboratory (formerly Hanford Laboratories) are described. Process optimization studied for the compact band ion exchange separation of individual light rare earth elements, using DTPA, EDTA, or HEDTA as eluting agents. Equipment for purifying kilogram quantities of promethium has been installed recently, and was applied to the preparation of 62,500 Curies of very high-purity promethium. A process for recovery of fission product rhodium has been developed, and used for the purification of one gram of rhodium. Earlier work at Hanford Laboratories is briefly summarized by specific fission product, with respect to scientific and technical contributions, as well as the large-scale manufacturing production program which has resulted from application of this new technology. (auth)

14437 (CEA-R-2879) VOLTAMMETRIE DU CHLORURE D'URANYLE DANS L'EUTECTIQUE LiCl-KCl. (Voltammetry of Uranyl Chloride in the LiCl-KCl Eutectic). Fondanaiche, Jean-Claude (Commissariat a l'Energie Atomique, Fontenay-aux-Roses (France). Centre d'Etudes Nucleaires). Oct. 1965. 58p. Dep. mn.

Quantitative analysis of a uranyl chloride solution in LiCl-KCl eutectic at 400°C was performed using voltammetry (a large area graphite indicator electrode was employed). The precision obtained was about 6 per cent for concentrations below 10^{-2} M. Precision decreased slightly for more concentrated solutions. The study of polarization curves indicated a reduction mechanism for the UO_2^{2+} ion. For dilute solutions, this reduction proceeded through the UO_2^{+} ion. Interpretation of current-potential curves was made difficult by the dismutation reaction of the UO_2^{+} ion and by the fact that the surface of the indicator electrode was not renewed. (J.B.)

14438 (CEND-540) ANALYTICAL AND EXPERIMENTAL METHODS OF DETERMINING HEAVY-ISOTOPE CONTENT OF OPERATING FUEL ELEMENTS. Valerino, Michael F.; Roszstoczy, Zoltan R. (Combustion Engineering, Inc., Windsor, Conn. Nuclear Div.). Sept. 30, 1965. Contract AT(38-1)-207. 156p. Dep. mn. CFSTI $5.00 cy, $1.00 mn.

Available methods for calculating isotopic content of operating fuel elements in power reactors were investigated. The feasibility of developing simple methods for testing the results of nuclear loss and production calculations in power reactors, using the maximum amount of actual reactor operating data as input was the specific aim of the investigation. A comprehensive evaluation of published data and associated methods of analyses is presented for calculations. Information supplied through specific requests from the various reactor designers and operators is included in the evaluation. Where available, experimental data that were obtained from operating power reactors were factored into the evaluation. These data include experimental measurements of flux and power distributions, exposures, and spent fuel isotopic composition as a function of exposure. Heavy-isotope cross-section data used by the various reactor designers were compared to obtain an indication of their relative consistency. Available computer codes used for fuel depletion and heavy-isotope buildup are described and appended. (P.C.H.)

14439 (GA-5556) APPLICATION OF NEUTRON ACTIVATION ANALYSIS IN SCIENTIFIC CRIME DETECTION. 18-Month Summary Report for the Period May 1, 1962–October 31, 1963. Bryan, D. E.; Guinn, V. P. (General Atomic, San Diego, Calif. John Jay Hopkins Lab. for Pure and Applied Science). July 27, 1964. Contract AT(04-3)-167. 94p. Dep. mn. CFSTI $3.00 cy, $0.75 mn.

Developments in the use of high-flux neutron activation analysis (NAA) in the field of scientific crime detection are reported. A highly reliable NAA method was devised for the detection of gunshot residues on the gunhand of a person who has recently fired a gun, based on the detection of microgram and submicrogram traces of barium and antimony deposited on the back of the gunhand from the detonation of the cartridge primer. A wide variety of manufactured products, such as automobile grease, automobile tire rubber, glass, paper, paint, and plastics from different manufacturers of essentially the same product were found to display clearly recognizable differences in their minor-constituent and trace-level element contents. These findings have considerable potential application in the investigation of hit-and-run, burglary, and various other types of criminal cases. It was also found that numerous naturally occurring materials of forensic interest, such as soils and hair, also display characterizing differences in their trace-element compositions when examined by means of high-flux NAA. Emphasis was placed, wherever possible, on the use of the purely instrumental, nondestructive form of NAA, based upon multichannel gamma spectrometry of activated samples, since this technique is faster than the more detailed radiochemical-separation form of the method, it preserves the samples (for possible introduction in court), and its results lend themselves readily to graphical presentation in court. (auth)

14440 (LA-3452) THE DETERMINATION OF NITRIDE NITROGEN IN PLUTONIUM METAL, ALLOYS, AND COMPOUNDS. Hakkila, E. A.; Waterbury, G. R. (Los Alamos Scientific Lab., Univ. of California, N. Mex.). Jan. 14, 1966. Contract W-7405-eng-36. 12p. Dep. mn. CFSTI $1.00 cy, $0.50 mn.

Nitride nitrogen in plutonium metal, alloys, or compounds is separated by steam distillation as ammonia, trapped in a boric acid solution, and measured either spectrophotometrically using Nessler's reagent or by titration with standardized acid, depending upon the quantity of nitrogen present. The samples are dissolved and digested in a mixture of hydrochloric and perchloric acids, and the solutions are made strongly alkaline prior to the steam distillation. For the spectrophotometric measurement, the color-forming reagent is added to the boric acid solution, and the absorbance is measured at a wavelength of 410 mμ. The molar absorptivity of the colored species is 3500. The standard deviations in measuring 1 to 100 μg. of nitrogen spectrophotometrically in 1-gram samples range from 30 to 3%. For the titrimetric measurement, the boric acid solution containing the ammonia is titrated directly with dilute standardized hydrochloric acid. The relative standard deviations of the titration method in measuring 100 to 2000 μg. of nitrogen are in the range from 6 to 0.7%. Results for nitrogen in plutonium metals obtained by the spectrophotometric method are essentially

equal to the values obtained by a Dumas method, indicating that the nitrogen exists predominantly in the combined or nitride form. (auth)

14441 (MCW-1493) PROCESS DEVELOPMENT QUARTERLY PROGRESS REPORT, JULY–SEPTEMBER 1965. (Mallinckrodt Chemical Works, Weldon Spring, Mo. Uranium Div.). Nov. 1, 1965. Contract W-14-108-eng-8. 27p. Dep. mn. CFSTI $2.00 cy, $0.50 mn.

Information on process development is presented in three sections. Separate abstracts were prepared for each section. (J.R.D.)

For abstracts of individual sections see: 14442, 14443, and 15044.

14442 (MCW-1493, pp 5-13) AN ENERGY DISPERSION SYSTEM FOR LIGHT ELEMENT ANALYSIS WITH THE ELECTRON MICROPROBE. Fergason, L. A.; Neumann, N. F. (Mallinckrodt Chemical Works, Weldon Spring, Mo. Uranium Div.).

A system for energy dispersion analysis was assembled and used with the Cambridge electron microprobe. This system included a high-resolution flow counter with an ultra-thin Formvar window, a low-noise Tennelac preamplifier, and a Packard 400-channel analyzer. One of its primary purposes was to facilitate the analysis of elements that have atomic numbers lower than Mg. With this equipment, rates as high as 87,000 counts per second were observed for C K_α x-rays emitted by high-density graphite. Carbides and oxides of U were identified by analysis of the light elements. (auth)

14443 (MCW-1493, pp 27-30) A SPECTROCHEMICAL METHOD FOR THE SIMULTANEOUS DETERMINATION OF CALCIUM, LITHIUM, AND POTASSIUM IN HIGH-PURITY THORIUM COMPOUNDS. Nelms, J. R.; Vogel, R. S. (Mallinckrodt Chemical Works, Weldon Spring, Mo. Uranium Div.).

A spectrochemical method was developed for simultaneous determination of Ca, Li, and K in high-purity Th compounds. The method is implemented by a focal-plane filter mounted at the photographic plate location of K 7698.98 Å. This arrangement eliminates second-order cyanogen band interference and permits the simultaneous determination of the three listed elements in one efficient spectrogram. (auth)

14444 (MLM-1268) MOUND LABORATORY PROGRESS REPORT FOR JUNE 1965. Eichelberger, J. F.; Grove, G. R.; Jones, L. V. (Mound Lab., Miamisburg, Ohio). June 21, 1965. Contract AT(33-1)-Gen-53. 37p. Dep. mn. CFSTI $2.00 cy, $0.50 mn.

Developments are reported for studies on: uranium-234 recovery; measurement of 2.3-kev isomeric state in lead-205; semiconductor radiation detectors; hydrolysis of plutonyl ions; plutonium-238 alpha sources; neutron spectrometry; increase in neutron yields; carbon isotope separation; stable gaseous isotopes; thermal diffusion research; helium vapor pressure thermometry; controlled-potential coulometric determination of uranium in uranyl acetylacetonate salts; emission spectroscopy; and calorimetry. (P.C.H.)

14445 (MSAR-66-10) DEVELOPMENT OF TECHNIQUES FOR MEASUREMENT OF IMPURITIES IN SODIUM. Quarterly Progress Report, October–December 1965. Rodgers, S. J.; Andrews, R. C. (MSA Research Corp., Callery, Pa.). Jan. 20, 1966. Contract AT(11-1)-765. 16p. Dep. mn. CFSTI $1.00 cy, $0.50 mn.

Developments in laboratory methods for the determination of impurities in sodium are reported. The methods include: surface tension; organic solvent extraction; and mass spectrometry during high-temperature refluxing. Preliminary measurements with the surface tension method were made on potassium. A difference in surface tension between pure potassium and oxygen-contaminated potassium was noted. In other experiments, high-purity sodium samples were run using naphthalene as a reactant and tetrahydrofuran as a solvent medium and diluent. The high-vacuum reflux distillation unit and the mass spectrometer connection are illustrated. (P.C.H.)

14446 (N64-25607) APPLICATIONS AUX ALLIAGES NIOBIUM–ZIRCONIUM DE LA METHODE D'ANALYSE SPECTROGRAPHIQUE DES SOLUTIONS SUR GRAPHITE A MECHE. (Some Applications to Niobium–Zirconium Alloys of the Method of Spectrographic Analysis of Solutions on Cored Graphite. Technical Note No. 76). Malamand, Frima (Office National d'Etudes et de Recherches Aerospatiales, Chatillon-sous-Bagneux (France)). 1964. 28p. Dep. mn.

The principle of a new method for spectrographic analysis of solutions is described. A graphite electrode with a porous core in its center and previously submitted to outgassing is impregnated during a well known interval of time with the solution to be analyzed. Thus the core acts as storage tank for the liquid which continuously feeds the gap of the spark or of the arc. The effects of various factors on the emission of lines from the solution elements and on the accuracy of results were studied. By means of this method very accurate titration of zirconium in niobium-zirconium alloys is possible for a large concentration range (0.6 to 62%). The results show the advantages of the method of analysis of solutions on cored electrodes. (auth)

14447 (NBL-231) EVALUATION OF THE METHODS IN TID-7029, "SELECTED MEASUREMENT METHODS FOR PLUTONIUM AND URANIUM IN THE NUCLEAR FUEL CYCLE." Lerner, M. W. (New Brunswick Lab. (AEC), N. J.). Feb. 15, 1966. 132p. Dep. mn. CFSTI $4.00 cy, $1.00 mn.

A compilation and statistical analysis of the results of analyses for Pu and U in standardized materials by different laboratories using the methods contained in TID-7029 is presented. (W.L.G.)

14448 (NLCO-970, pp 1.1-22) DEVELOPMENT OF A THORIUM PURIFICATION SYSTEM. Kispert, R. C.; Tolos, W. P.; Rector, J. W.; Mueller, J. H.; Leist, N. R. (National Lead Co. of Ohio, Cincinnati).

Thorium distribution coefficients were determined in the laboratory for the tributyl phosphate (TBP)–thorium nitrate and the diamyl amylphosphonate (DAAP–thorium nitrate systems. The data developed in these tests were used in pilot-scale (2-in.-dia perforated-plate pulse columns) development tests of a liquid-liquid extraction process for the purification of thorium. This process was subsequently implemented in semiworks extraction equipment. DAAP was found to be the superior extractant. Two additional solvent extraction systems were studied for the separation of thorium and uranium and/or rare earth elements to supplement the DAAP extraction system. Both of these extractants, di-sec-butyl phenylphosphonate (DSBPP) and TBP, were evaluated in pulse column tests for the production of a thorium nitrate solution which contained less than 5 ppM uranium on a thorium basis. (auth)

14449 (NLCO-970, pp 7.1-5) THE DETERMINATION OF ^{235}U BY GAMMA-RAY SPECTROSCOPY. Twitty, B. L.; Humphrey, H. W.; Fritz, K. M. (National Lead Co. of Ohio, Cincinnati).

A gamma spectrometric method was developed for the rapid measurement of ^{235}U in uranium solution samples. The 184-kev gamma ray of ^{235}U is measured after ^{238}U decay products have been removed by liquid-liquid extraction. Total analysis time is less than 2 hours, and the precision is better than ±0.02 wt % ^{235}U up to the 5% ^{235}U level. Standards need be run only occasionally since the count rate is corrected for drift by means of a special ^{235}U standard. Only a minimum of training is necessary. (auth)

14450 (NLCO-970, pp 8.1-4) THE DETERMINATION OF BETA ACTIVITIES IN PLANT EFFLUENTS. Twitty, B. L.; Humphrey, H. W. (National Lead Co. of Ohio, Cincinnati).

Two methods were devised for determining the beta activity of plant effluents containing uranium and thorium decay products. The lower detection level was 3 d/m/ml of effluent water. The first method, developed for laboratories, utilizes a barium coprecipitation at high pH, followed by gross beta counting with an antracene crystal.

The second method, developed for plants, utilizes a detector head consisting of four Geiger-Müller tubes which are submersed for counting in a known volume of effluent. The count is compared with that of a standardized europium-152, -154 solution. (auth)

14451 (NYO-2586-2) FEASIBILITY OF A SHORT-LIVED RADIOISOTOPE TRACER SYSTEM FOR DETECTION OF HIDDEN MATERIALS. Jordan, E. D. (Catholic Univ. of America, Washington, D. C. Div. of Nuclear Science and Engineering). Dec. 1964. Contract AT(30-1)-2586. 56p. Dep. mn. CFSTI $3.00 cy, $0.50 mn.

The feasibility of detecting hidden materials by the addition of low activity radioactive tracers was investigated. All gamma-emitting isotopes with half lives between 5 and 36 hours were considered with As-76, Cu-64, Eu-152m, Pr-142, Na-24, and W-187 investigated in detail because of their gamma emission spectra and neutron absorption cross section. Ten americium–beryllium neutron sources, placed in a water moderator to produce a maximum thermal neutron flux of 1.3×10^5 n/cm^2/sec was used as a neutron irradiator. It appears that Eu-152m is the preferred isotope because of its 9.3-hr half life, 1700-barn cross section, and gamma emission spectra. A portable radiation detection probe with sodium iodide crystal, amplifier, power supply, and transmitter was designed, constructed, and tested. The detector was self-sustained with battery power supplies. A receiver could pick up transmitted count rate meter signals, transmitting on citizen band frequencies, at various distances from the probe. A reactor was used to irradiate europium nitrate impregnated samples, including United States currency. Measurements were made under both idealized conditions as well as with europium activated currency in tagged letters in mail sacks. It was determined that the detector signals were both linear as well as reproducible. A 50-μC source could be detected more than 4 feet away from the mail sack with a signal to background ratio of about 5. Consideration was given to safety and licensing problems in the use of radioactive tracers in the postal system. Technical feasibility of the use of a radioactive tracer was established. (P.C.H.)

14452 (ORNL-3889, pp 1-12) ANALYTICAL INSTRUMENTATION. Kelley, M. T.; Fisher, D. J. (Oak Ridge National Lab., Tenn.).

Activities are summarized in research on instrumentation and techniques such as those for compensated chronopotentiometers, comparative amperometric d-c polarography, ORNL model Q-2792 d-c polarograph-voltameter, ORNL model Q-2564 coulometric titrator, polarographic determination of U in tri-n-octylphosphine oxide, analytical uses of controlled-potential polarography and coulometry, derivative chronopotentiometry, controlled-potential voltammeter circuitry, ^{60}Co source sample-irradiation assembly, computer programs, square-wave polarographs, and controlled-potential differential d-c polarography. (J.R.D.)

14453 (ORNL-3889, pp 12-14) ANALYTICAL STUDIES OF MOLTEN-SALT SYSTEMS. White, J. C. (Oak Ridge National Lab., Tenn.).

Spectral and electrochemical studies were continued in a program on analytical studies of molten-salt systems. Reflectance spectra of the solid state and absorption spectra of the molten state were obtained on samples of irradiated $LiF-BeF_2-ZrF_4-ThF_4-UF_4$ in an attempt to determine the oxidation state of the U in the salt. Little evidence of the presence of trivalent U was observed. Transmission spectra of small crystals (0.1-mm diam) and diffuse-reflectance spectra were obtained to aid in elucidating the symmetry and coordination of light-absorbing solid-state species. Solidified UF_3 and UF_4 were examined at 250 to 1200 mμ wavelength. A paper was published on the reversible deposition of Fe and Ni on Ag and pyrolytic-graphite electrodes from molten-fluoride-salt media. The experimental data agreed satisfactorily with the published theory of Berzins and Delahay. (auth)

14454 (ORNL-3889, pp 17-24) ANALYTICAL CHEMISTRY FOR REACTOR PROJECTS. Kelley, M. T.; White, J. C.; Corbin, L. T. (Oak Ridge National Lab., Tenn.).

Analytical research and development is being done for the Molten-Salt Reactor Experiment, Transuranium Element Processing Program, and Medium-Power Reactor Experiment. Brief summaries are presented of these investigations. Included are discussions of several projects that were done as part of the Nuclear Safety Program. Among these are investigations of the presence of nonelemental I compounds originating from fission-product-produced I_2. Gas chromatography and spectrophotometry are the methods primarily used in this work. (auth)

14455 (ORNL-3889, pp 25-32) SPECIAL RESEARCH AND DEVELOPMENT PROBLEMS. White, J. C. (Oak Ridge National Lab., Tenn.).

A two-column gas chromatographic apparatus with a scintillation detector was assembled for the study of the exchange reaction between tritiated water and methane. Relative concentrations of the pyrolysis products (methane, ethylene, benzene, toluene, ethylbenzene, and styrene) of the dielectric films from acceptable and defective dosimeters were determined by gas chromatography. Electrochemical studies with solid electrodes of pyrolytic graphite and glassy carbon showed that these materials are useful in voltammetry, differential titrimetry, and chronopotentiometry. Titanium in seawater was determined by a concentration step followed by a polarographic estimation; the limit of detection is 0.5 ppB. Niobium–iron alloys were analyzed polarographically for trace quantities of Cu, Bi, Pb, and Zn. The selectivity of arsenazo III for the spectrophotometric determination of U was improved by use of cyclodiaminetetraacetic acid as masking agent and maleic acid as a buffer. Dissolutions or decompositions of organic materials were accomplished by means of various acid mixtures. The oxidizing ability of hydrolyzed xenon hexafluoride was studied. Miscellaneous special determinations included: nitrite in a neutral solution of potassium iodide and potassium nitrate, degree of nitration of BAMBP, I_2, and F_2 in KIO_2F_2, and U^{6+} in UO_2-ThO_2 fuels. The interference of fluoride in the spectrophotometric determination of Nb was obviated by use of Al. The problem of color instability in the spectrophotometric heteropoly-blue method for Si was corrected. Nitrate was determined by controlled-potential coulometric titration; alkylbenzenesulfonate detergents were analyzed for Na^+, Cl^-, SO_4^{2-}, HCO_3^-, and water. (J.R.D.)

14456 (ORNL-3889, pp 32-5) ANALYTICAL BIOCHEMISTRY. White, J. C. (Oak Ridge National Lab., Tenn.).

A program to separate and purify transfer ribonucleic acids (tRNA) from Escherichia coli bacteria is reported. Special attention was given to establishing the optimum conditions for the phenylalanine-phenylalanyl tRNA charging reaction in order to achieve quantitative determinations of the nucleic acid. Pyrolytic products of purines and pyrimidines at 880°C were analyzed by gas chromatography. Methyl cyanide was identified in significant concentrations from uracil, in addition to traces of ethyl cyanide. Cytosine also produced significant amounts of methyl cyanide; the other nitrogenous bases produced comparatively small amounts of methyl cyanide. (J.R.D.)

14457 (ORNL-3889, pp 36-9) X-RAY AND SPECTROCHEMICAL ANALYSES. (Oak Ridge National Lab., Tenn.).

A program was written to perform the calculations for analyzing eight-component alloys by x-ray fluorescence. Analyses were very accurate when polished specimens were used. The lattice spacing of the lead stearate film on the mica crystal in the Philips electron probe analyzer was measured, thus making possible the use of wavelength tables to identify low-Z elements. The areal density of Au coatings on Si radiation detectors was measured by x-ray fluorescence and by atomic absorption; results by the two methods agreed to within experimental errors. The limits of detection (μg/ml) for the atomic absorption method were: Au, 0.03; Cu, 0.01; Ag, 0.01. A method was developed for isolating traces of Cr from MSRE salt and determining the Cr spectrographically. Di-(2-ethylhexyl)phosphoric acid was studied as a reagent for separating Cm from contaminant metals. It was found that

when $MgNH_4PO_4$ is formed in tap water, it coprecipitates Ba almost completely, especially if Ca is present; this coprecipitation is the basis of a technique for collecting Ba from tap water for flame photometric determination. In the tissue-analysis program, a technique was worked out for homogenizing large samples of muscle, fat, or bone; contamination during the homogenization was negligible. A survey of universally applicable methods of emission spectrographic analysis was begun. For visual estimation of impurity concentrations, the Kroonen-Vader (Li_2CO_3-base) method appears to be more accurate than graphite-base methods. A solution technique was established for determining five elements on filter papers from air samples; the Paschen Direct Reader is used. (auth)

14458 (ORNL–3889, pp 39-43) MASS SPECTROMETRY. Cameron, A. E. (Oak Ridge National Lab., Tenn.).

An MS-7 spark-source mass spectrograph was used for survey and semiquantitative determinations of trace elements in a variety of materials. Nonconductors are mixed with a powdered metal matrix and are isostatically pressed in a mold of naphthalene, which is later removed with hot acetone. The laboratory cooperated in the analysis of a standard copper sample. The TRU mass spectrometry laboratory made isotopic determinations on the transplutonium elements up to and including Cf. The half-lives of the Cf isotopes were checked by mass spectrometric analyses. Investigation of a real, but relatively small, isotope discrimination effect observed in U samples in the nanogram range showed that the effect seems not to be temperature dependent. At temperatures above ~2200°K the production of U ions from a molecular beam of UF_4 impinging on a filament follows the Saha-Langmuir equation. Below that temperature there are marked deviations. A study of the lower-temperature region is contemplated with control of amounts of impurities admitted to the ionization region. The isotopic composition of lead from tektites and in material from impact craters that appear to be contemporaneous was studied. The data were not evaluated thoroughly, but the similarity between lead from Ivory Coast tektites and from Lake Bosumtwi phyllite suggests that the tektites were formed from terrestrial material during the formation of the crater. (auth)

14459 (ORNL–3889, pp 44-6) INFRARED AND NUCLEAR MAGNETIC RESONANCE SPECTROMETRY. White, J. C.; Thomason, P. F. (Oak Ridge National Lab., Tenn.).

The NMR spectra of a wide variety of organic compounds were obtained and were recorded for reference. A considerable and diversified number of organic and inorganic compounds were also examined by infrared spectrometry. These techniques are used primarily to identify organic compounds and to ascertain relative degrees of purity. Quantitative analyses are done when feasible, particularly for functional groups, for oil in waters from various sources, and for water in engine and lubrication oils. (J.R.D.)

14460 (ORNL–3889, pp 46-8) OPTICAL AND ELECTRON MICROSCOPY. Kelley, M. T.; Willmarth, T. E.; Harmon, T. G.; Wright, H. W. (Oak Ridge National Lab., Tenn.).

Examination of radioactive materials by electron microscopy has been in progress since December 1964 at the new microscopy facility in Building 3019. Assistance to research groups concerned with the Nuclear Safety Program continued. A variety of methods were developed for replicating powders, extracting inclusions from metals, and observing particulates collected on cellulose triacetate filters. Optical and electron microscopy and electron diffraction services were provided to other divisions when knowledge of the internal and external ultrastructure or microstructure of a wide variety of materials was important. Members of the group attended special classes in ultramicrotomy and ultrafiltration methods. (auth)

14461 (ORNL–3889, pp 48-70) NUCLEAR AND RADIOCHEMICAL ANALYSES. White, J. C.; Lyon, W. S. (Oak Ridge National Lab., Tenn.).

Information and data are presented on nuclear properties of radionuclides, activities in the cooperative isotopes program, measurement of radioactivity, results of radiochemical research, development and use of liquid scintillators, computer applications, applications of radioisotopes in analytical chemistry, development and uses of activation analysis, and performance of 14-Mev neutron generator. (J.R.D.)

14462 (ORNL–3890) FLOODING IN PERFORATED-PLATE PULSED EXTRACTION COLUMNS: A SURVEY OF REPORTED EXPERIMENTAL DATA AND CORRELATIONS, AND THE PRESENTATION OF NEW CORRELATIONS WITH PHYSICAL PROPERTIES, OPERATING VARIABLES, AND COLUMN GEOMETRY. Groenier, W. S.; McAllister, R. A.; Ryon, A. D. (Oak Ridge National Lab., Tenn.). Mar. 1966. Contract W-7405-eng-26. 312p. Dep. mn. CFSTI $7.00 cy, $1.50 mn.

All of the readily available flow capacity data for pulsed perforated-plate extraction columns were compiled and correlated with physical properties, mode of operation, and column parameters. About 2200 data points representing over 20 different chemical systems having a wide range of physical properties were used in the correlations for both aqueous- and organic-continuous operation in a variety of columns. Exact equations describing flooding due to insufficient pulsation are presented for 9 different modes of flow control in and out of the column. In each case, the flow capacity is a function only of flow ratio and pulse velocity. Flooding in the emulsion regime, however, is much more complex. Correlations were made by combining the variables of physical properties, pulse, and column geometry in dimensionless groups and determining the coefficients by multiple regression. A number of equations gave nearly equal success. Using the best equation, the calculated flow capacity is, on the average, 8.6% higher than experimental, with a standard deviation of 45. The new correlations were compared to several in the literature which had been derived from a much narrower range of the variables. (130 references). (auth)

14463 (PAEC(D)CH–652) STUDIES ON COCONUT OIL. II. GAS CHROMATOGRAPHIC ANALYSIS OF THE VARIOUS COMMERCIALLY AVAILABLE OILS FROM THE COCONUT. Pascual, O. S.; Cunanan, S. A. (Philippine Atomic Energy Commission, Manila). Aug. 1965. 18p. Dep. mn.

Various oils from the coconut were analyzed by gas chromatography. The oils included: copra oil; oil from coconut water; parings oil; and desiccated-coconut oil. The results showed that commercial parings oil contains at least twice the total unsaturated fatty acids (oleic and linoleic) content of either desiccated coconut or copra oil. The oil from coconut water has a fatty acid content between that of desiccated-coconut oil and that of parings oil. Since it was difficult to distinguish copra oil from desiccated-coconut oil by fatty acid composition alone, trace metal analysis was found to be useful in differentiating them. The chlorine content of copra oil was almost ten times that of desiccated-coconut oil while sodium was barely detectable in the latter. Data are tabulated. (P.C.H.)

14464 (RFP–599) THE IMPURITY ANALYSIS OF PLUTONIUM PEROXIDE AND PLUTONIUM FLUORIDE. Johnson, A. J.; Vejvoda, E. (Rocky Flats Div., Dow Chemical Co., Golden, Colo.). Feb. 4, 1966. Contract AT(29-1)-1106. 12p. Dep. mn. CFSTI $1.00 cy, $0.50 mn.

A review was made on the spectrographic methods used for the impurity analysis of plutonium peroxide and plutonium fluoride. For comparison purposes, the impurity analyses on nitrate feeds, peroxides, fluorides, and metal buttons are reported. (auth)

14465 (RFP–657) IMPROVED ELECTRODELESS TOROIDAL CONDUCTIVITY ANALYZER. Johnson, C. M.; Hart, G. E. (Rocky Flats Div., Dow Chemical Co., Golden, Colo.). Feb. 11, 1966. Contract AT(29-1)-1106. 17p. Dep. mn. CFSTI $1.00 cy, $0.50 mn.

An improved electrodeless toroidal conductivity analyzer was designed and constructed. Improvements in the in-

strument sensitivity were achieved by frequency tuning, modified toroidal configuration, and increased core mass. Improvements in instrument design were achieved by transistorized circuitry, including automatic temperature compensation. (auth)

14466 (RL-SA-58) STORAGE OF LONG-LIVED FISSION PRODUCTS ON ALUMINO-SILICATE ZEOLITES. Mercer, B. W. (Battelle-Northwest, Richland, Wash. Pacific Northwest Lab.); Schmidt, W. C. (General Electric Co., Richland, Wash. Hanford Atomic Products Operation). Dec. 3, 1965. Contract AT(45-1)-1851. 12p. (CONF-660208-3). Dep. mn. CFSTI $1.00 cy, $0.50 mn.

From Symposium on Solidification and Long-Term Storage of Highly Radioactive Wastes, Richland, Wash.

Technology for the encapsulation and storage of long-lived radioisotopes ^{137}Cs and ^{90}Sr was developed. This technology includes adsorption of the isotopes on alumino-silicate zeolites, drying the zeolites to prevent excessive pressure after a container is sealed, sealing the containers by welding, and elution of the containers to recover the isotopes. Several alumino-silicate zeolites that possess the chemical properties to adsorb these cations (1.5 to 2 equiv/kg) from the mother liquor were investigated. Dehydration was found to be a satisfactory method of reducing the moisture content of the zeolite to less than 0.5 wt %. Purging the container with helium prior to final closure increased the thermal conductivity of the zeolite and permitted use of the mass spectrometer for detecting minute leaks after final closure. Final closure was made by tungsten inert gas welding to form a container which is capable of withstanding several hundred pounds per square inch pressure without yielding. (P.C.H.)

14467 (RT/PROT(64)-20) CONTROLLO DEI POLIFENILI NEGLI AMBIENTI DI LAVORO DETERMINAZIONE SPETTROFOTOMETRICA DEI PRODOTTI PURI E DELLE LORO MISCELE. (The Control of Polyphenyls in Work Environments. Spectrophotometric Determination of Pure Products and Their Mixtures). Testa, C.; Masi, G. (Comitato Nazionale Energia Nucleare, Rome (Italy). Divisione di Biologia e Protezione Sanitaria). Oct. 1964. 56p. Dep. mn.

Methods for sampling and determination of polyphenyls in working environments are reported. Silica-gel tubes for rapid controls, and cellulose powder beds, for long period samplings, were used to retain the organic vapors. Quantitative analysis was performed either by colorimetry or by ultraviolet spectrophotometry: the latter method was found to be very effective also for the determination of components percentages in some polyphenyl mixtures. Terphenyl concentrations, found in the ROSPO reactor room for the period June 1963–March 1964, are reported. (auth)

14468 (TID-22505) ATTEMPTED DETERMINATION OF NITRATE IN FIRED THORIA USING INFRARED TECHNIQUES. Technical Report No. XXVII. Olsen, C. S.; Olson, F. A.; Wadsworth, M. E. (Utah Univ., Salt Lake City. Inst. of Metals and Explosives Research). Sept. 1, 1965. Contract W-7405-eng-26, Subcontract 2176. 12p. Dep. mn. CFSTI $1.00 cy, $0.50 mn.

For Oak Ridge National Lab., Tenn.

Using infrared spectroscopy, a quantitative method of determining nitrate in fired thoria was attempted. The KBr pellet technique was based upon the conversion of a covalent nitrate in the thoria to an ionic nitrate. This method was unsuccessful because the exchange was not quantitative. Mull methods were also unsuccessful due to the low concentration of nitrate in thoria and low absorbance of the nitrato bands. (auth)

14469 (TID-22650) ION EXCHANGE SEPARATION OF URANIUM AND THORIUM IN MIXED AND NON-AQUEOUS SOLVENTS. Final Technical Report. Korkisch, J. (Vienna Univ. (Austria). Analytisches Institut). Oct. 1965. Contract 67/US. 163p. Dep. mn. CFSTI $5.00 cy, $1.00 mn.

Includes Additional Report to Final Technical Report, Dec. 1965.

All important data hitherto reported on the cation and anion exchange behavior of uranium, thorium, lanthanides, and other metal ions in mixed and nonaqueous solvents containing mineral or organic acids as complexing agents for these elements are summarized. Based on equilibrium studies carried out in mixtures consisting of organic solvents such as the aliphatic alcohols, ketones, ethers, organic acids and of acids such as hydrochloric, hydrobromic, nitric, and sulfuric acids, the most suitable conditions for analytical separations of uranium, thorium, etc., were worked out. The methods thus developed are applicable for the isolation of microgram and milligram quantities of these elements in a variety of materials such as minerals, rocks, sediments, steel, high purity materials, etc. Also the application of a number of azo dyes of the Solochrome class for the spectrophotometric determination of uranium, thorium, rare earth elements, and other metal ions in hydrochloric or nitric acid-methanol media is described. The methods make possible the accurate and rapid quantitative determination of microgram amounts of these elements. A method for the separation of uranium by combined ion exchange-solvent extraction in 90% tetrahydrofuran and 10% 6$\underline{N}$ HNO_3 is also described. Using this method, uranium in amounts ranging from micrograms to grams can be completely separated from practically all elements except bismuth. The method is assumed to be based on a competition for the uranyl ion by the cation exchange resin and the tetrahydrofuran–nitric acid mixture acting as a liquid anion exchanger. (205 references). (P.C.H.)

14470 (UCRL-7873) SOME ANALYTICAL METHODS FOR EXPLOSIVES AND EXPLOSIVE SIMULANTS. Selig, Walter (Lawrence Radiation Lab., Univ. of California, Livermore). May 1964. Contract W-7405-eng-48. 68p. Dep. mn. CFSTI $3.00 cy, $0.75 mn.

Methods for the analysis of explosives and explosive stimulants are compiled. With the exception of one method, all were prepared for routine analysis and an attempt was made to keep them as simple as possible by using solvent extraction. One method involves nonaqueous titrimetry. Extrusible explosives, plastic-bonded explosives, and explosive simulants are covered. (P.C.H.)

14471 DETERMINATION OF TRACE ELEMENTS IN IRON BY NEUTRON-ACTIVATION TECHNIQUES. Malvano, R.; Grosso, P. Anal. Chim. Acta, 34: 253-68 (Mar. 1966).

A systematic analytical procedure for determination of some trace impurities in iron matrices was developed by employing both direct and destructive neutron-activation techniques. Irradiations in fast neutron fluxes, selective activation by epithermal neutrons, and coincidence γ spectrometry measurements were used in some cases, in order to improve the sensitivity for nondestructive analysis; for destructive methods, radiochemical separations based on ion exchange, and solvent extraction were applied. Procedures are described, and some results of the determination of low concentrations of Al, Mn, Ti, V (nondestructive), P, S, Zn (destructive, and As, Co, Cr, Cu, Mo, Ni, Sc, W (both methods) in iron are reported and discussed. (auth)

14472 THE MICROCHEMICAL ANALYSIS OF DUST SAMPLES FOR LONG-LIVED URANIUM FISSION PRODUCTS. Loley, F.; Malissa, H. Anal. Chim. Acta, 34: 278-93 (Mar. 1966). (In German).

A microchemical qualitative and quantitative separation process for long-lived radionuclides from uranium fission (Cs, Sr, Ce, Zr, and Ru) in dust samples is described. The loaded dust filter was moistened with carrier solution and with borax–sodium carbonate, and ashed in an electrically heated platinum spiral; the dust was thus decomposed, forming beads. The solution of the bead in dilute acid was concentrated in a ring with the ring oven. The paper bearing the radioactive ring was cut into sectors and a specific precipitation reaction was applied for each nuclide in separate sectors. Identification and determination were carried out by autoradiography of the sectors. Practical testing was done with a 2.5-year old dust sample origi-

nating from nuclear studies in 1961 to 1962; radioactive Cs, Sr, and Ru were detected in 1.7 mg of dust ash. The quantitative evaluation of ^{90}Sr of the order of 10^{-12} C showed the sensitivity of the method. The range of application of the method is indicated. (auth)

14473 DIRECT SPECTROGRAPHIC DETERMINATION OF IMPURITIES IN URANIUM TETRAFLUORIDE. Podobnik, B.; Spenko, M. (Nuclear Inst. J. Stefan, Ljubljana, Yugoslavia). Anal. Chim. Acta, 34: 294-301(Mar. 1966).

A direct spectrographic method for determination of some impurities in UF_4 is described. The sample in the graphite electrode was covered with a layer of alumina before the arc was struck; alumina prevented the volatilization of UF_4. To stabilize the discharge, a controlled atmosphere of argon and oxygen was used. The impurity elements were divided into 3 categories according to their volatility: high (B, Si), medium (Co, Mn, V, Mo, Ti, etc.), and low (Ni, Pb, alkaline earths, etc.). Impurities of high and medium volatility could be determined with germanium or aluminum as internal standard. The sensitivities found for this method generally agreed with those of the carrier distillation method. The coefficients of variation varied from 8 to 25% at the 25 ppM level. (auth)

14474 A RAPID METHOD FOR THE SIMULTANEOUS DETERMINATION OF TOTAL CARBON AND ^{14}C IN SMALL SAMPLES. van der Laarse, J. D.; van Leuven, H. C. E. (Shell Research, Amsterdam). Anal. Chim. Acta, 34: 370-1(Mar. 1966).

The radioactivity and carbon content of samples were measured simultaneously by a rapid micro-method involving: combustion of the sample in a quartz tube, absorption of the carbon in a combined absorption-scintillation liquid, titration of carbon dioxide, and determination of the radioactivity. The precision of the carbon determination is ~0.5%. Twenty analyses can be carried out in a single day. (F.J.H.)

14475 THE DETERMINATION OF GOLD IN COSMIC DUST COLLECTION BY NUCLEAR ACTIVATION ANALYSIS. Choy, Thomas K. (Univ. of California, San Diego). Anal. Chim. Acta, 34: 372-4(Mar. 1966).

The determination of gold in cosmic dust is discussed. The dust was collected on a greased petrolatum nylon mesh previously washed with detergent solution and then distilled water with an efficiency of about 50%. The samples were removed from the mesh and processed. Magnetic particles were removed from the solution with a strong magnet. The dust samples were irradiated for 30 min together with a gold reference standard, in a reactor with a flux of 1.8×10^{12} n/cm^2/sec. The samples were allowed to decay for 30 hr before actual counting in order to circumvent interferences. Gamma spectra of the samples were obtained. The ^{198}Au photopeak with a maximum at 0.412 Mev and a half life of 2.7 days was measured. The amount of gold found in various collections was of the same order of magnitude. (F.J.H.)

14476 SPECTROFLUORIMETRIC DETERMINATION OF MICROGRAM AMOUNTS OF SCANDIUM. PART II. SEPARATION BY SOLVENT EXTRACTION. Kirkbright, G. F.; West, T. S.; Woodward, C. (Imperial Coll. of Science and Tech., London). Analyst, 91: 23-6(Jan. 1966).

The spectrofluorimetric method previously described for determining scandium and based on the use of salicylaldehyde semicarbazone as reagent was modified by incorporation of a solvent extraction separation procedure to permit the determination of scandium in the presence of the few other ions that also produce fluorescent species, i.e., aluminum, yttrium, etc. Chromium(III), titanium(IV), and zirconium produced low results, while tellurium(IV) and tin(IV) completely suppressed the fluorescence of the scandium complex. (auth)

14477 RADIOACTIVATION ANALYSIS AS AN ANALYTICAL TOOL. Lyon, W. S. (Oak Ridge National Lab., Tenn.). Ann. N. Y. Acad. Sci., 137: 311-22(Jan. 20, 1966).

Advantages, disadvantages, and techniques of activation analysis are discussed. Nondestructive activation analysis begins with simultaneous irradiation of sample and standard. Following removal from the reactor, the sample is placed above a NaI(Tl) crystal cemented to a photomultiplier tube. This detector is electronically coupled to a multichannel analyzer. Spectra of radiation emitted when neutrons are captured by the target nuclei are obtained. Some examples of the use of activation analysis are considered. (M.C.G.)

14478 NAPOLEON'S ILLNESS 1816–1821 IN THE LIGHT OF ACTIVATION ANALYSES OF HAIRS FROM VARIOUS DATES. Forshufvud, Sten; Smith, Hamilton; Wassen, Anders. Arch. Toxicol., 20: 210-19(May 27, 1964).

Clinical data analyzed from reports of Napoleon's terminal illness suggested that progressive arsenic poisoning was the cause of his death. Neutron activation analysis of Napoleon's hair clippings was used to substantiate this newly advanced reason for his death. Smaller sections of hair were analyzed. The usual irradiation conditions in the reactor used (BEPO, Harwell) afforded a sensitivity of detection of about 10^{-10} g at the maximum neutron flux of about 10^{12} neutrons/cm^2/sec. The hair was cut into 1 cm lengths and sealed in silica capillaries with an ID just greater than the diameter of the hair. The hair sections were finally analyzed by the Smith method. Results are described for millimeter pieces of hairs from the lock shaved from Napoleon's head on 6th May, 1821, and kept as a souvenir by his valet. From these results it was concluded that Napoleon was undoubtedly exposed to arsenic on many occasions between the summer of 1820 and April, 1821. Other studies on hairs cut in 1816 showed particularly high concentrations of arsenic which must have been deposited before Napoleon was exiled to St. Helena. (TCO)

14479 IMPROVED METHODS FOR LIQUID SCINTILLATION ASSAY OF (A) ^{14}C-COMPOUNDS ON PAPER CHROMATOGRAMS AND (B) ^{14}C-PROTEIN. Bartley, J. C.; Abraham, S. (Univ. of California, Berkeley). Atomlight, 49: 1-8(Nov. 1965).

Methods for liquid scintillation assay of ^{14}C-labeled compounds isolated by paper chromatography and of ^{14}C-labeled protein are described. The ^{14}C-labeled compound is oxidized by persulfate on the paper chromatogram and assayed as $^{14}CO_2$. The efficiency of this method was 40.9%. The compounds can be assayed after being located by indicator-spray reagents that do not remove carbon from the compound. Experiments also indicated that reactions that lead to decarboxylation of organic and amino acids can be performed on samples isolated on paper chromatograms provided that absorption of the aldehydic product by the organic base is avoided. A method of liquid scintillation assay of ^{14}C-labeled protein, which allows determination of the amount of protein and the ^{14}C content on aliquots from the same solution, is described. A formic acid solution of protein is added to a liquid scintillator for ^{14}C counting. The protein is determined by either the biuret procedure or spectrophotometry. (M.C.G.)

14480 DETERMINATION OF HYDROGEN IN HYDROCARBONS BY NEUTRON ACTIVATION. Kovar, M.; Hynst, A.; Koza, F. (Zapototskii Military Academy, Brno). Chem. Zvesti, 19: 833-9(1965). (In Czech).

A method for determination of the hydrogen content of hydrocarbons using neutron irradiation from a Ra–Be source was developed. The intensity of the protons leaving the material being studied after interaction of the neutrons with hydrogen atoms was measured. The hydrogen content was calculated on the basis of a derived linear relation on a calibration line. The measured intensity value was not affected by the specific weight of the hydrocarbon investigated so that the measurement was made simply as in the radiometric hydrogen determination by means of absorption measurements of the β radiation. In the measurements, approximately a 10-ml probe was used and the measurements took approximately 15 min each. The relative error was under 2%. In the presence of other elements the relation for determination of the hydrogen content was not directly usable. The method described can lead to a considerable simplification of the analysis of liquid hydro-

carbons and is also applicable to continuous measurements. (tr-auth)

14481 COMPLEXES OF URANYL WITH PHENOLIC LIGANDS. III. SPECTROPHOTOMETRIC STUDIES OF REACTIONS WITH 2,3-DIHYDROXYNAPHTHALENE-6-SULFONIC ACID AND CHROMOTROPIC ACID. Sommer, L.; Sepel, T.; Kurilova, L. (Univ., Brno). Collec. Czech. Chem. Commun., 30: 3426-54(Oct. 1965). (In German).

The step-wise formation of mononuclear complexes was detected by analysis of extinction curves in solutions. The component ratio of the complexes depended on the ligand concentration and on the pH of the solution. In solutions with excessive ligands no multinuclear or hydrolytic complexes were found. Both reagents were suitable for the spectrophotometric determination of uranium under rigid reaction conditions. (tr-auth)

14482 URANYL COMPLEXES WITH PHENOLIC LIGANDS. IV. SPECTROPHOTOMETRIC INVESTIGATION OF THE REACTION WITH TIRON AND PYROCATECHIN. Sommer, L.; Sepel, T.; Kurilova, L. (Purkyne-Univ., Brno). Collect. Czech. Chem. Commun., 30: 3834-60(Nov. 1965). (In German).

The equilibrium in solutions of uranyl salts with pyrocatechol and tiron were followed spectrophotometrically. In systems with pyrocatechol a regular series of mononuclear complexes were formed with the component ratios M:R of 1:1, 1:2, and 1:3, whereas in systems of tiron only the formation of the 1:1 complexes in the pH range from 1 to 3.5 could be detected spectrophotometrically with certainty. The complexing agents investigated were not suitable for the spectrophotometric determination of uranium in aqueous solutions. (tr-auth)

14483 DETERMINATION OF RADIOCESIUM IN THE ENVIRONMENT. Petrukhin, N. V.; Pokrovsky, S. I.; Tikhomirov, V. R.; Ryadov, V. G. Gig. Sanit. 11: 86-91 (1965). (In Russian).

A survey is given of methods for preparing samples of ^{137}Cs for analysis, the determination of ^{137}Cs content using isotopic carriers, the separation of ^{137}Cs from solutions by means of ion exchange, and the determination of ^{137}Cs by radiometric methods. Tables are presented of the properties of several reagents used for the radiochemical separation of cesium and of the characteristics of some ion-exchange materials. (M.J.T.)

14484 CONDUCTOMETRIC DETERMINATION OF LANTHANUM AS THE NORMAL SELENITE. Prasad, Sarju; Garg, Virendra Nath (Banaras Hindu Univ., Varanasi, India). J. Electroanal. Chem., 11: 72-4(Jan. 1966).

Conductometric titration of lanthanum nitrate with selenious acid was carried out at 25 ± 0.5°C. Lanthanum concentrations between 4.053×10^{-4} and 9.727×10^{-4}M in ethanol were successfully titrated with selenious acid (0.04237M). Ethanol concentrations ranging from 30 to 35% gave the best results. The method is reproducible and has an accuracy of 0.5 to 1%. The conductometric curves are given. (F.J.H.)

14485 THE SPECTROPHOTOMETRIC DETERMINATION OF THORIUM(IV) WITH CHROMAZUROL S. Ishida, Ryoei (Hokkaido Gakugei Univ., Sapporo). Nippon Kagaku Zasshi, 86: 1169-73(Nov. 1965). (In Japanese).

Chromazurol S, in the slightly acidic medium, reacts with the thorium ion to give a reddish violet complex. The results of a spectrophotometric study of the thorium–chromazurol S complex and the application of this reagent for determining trace amounts of thorium are described. Several conditions for the color development were investigated, and the composition of colored complex and the influence of coexisting ions are considered. The maximum absorption of the complex in the solution was found at 554 mμ for the reagent blank, and absorption curves had an isosbestic point at about 485 mμ according to the amount of reagent for water blank. The optimum pH of the color development was at about 5.6. Beer's Law was obeyed up to about 7.0 μg of thorium per milliliter at 554 mμ. The molar extinction coefficient of the complex was found to be 32000 at the same wave length. The mole ratio of thorium and chromazurol S in the complex was determined spectrophotometrically, that is, by the continuous variation method and the mole ratio method, and found to be 1:2. Moreover, this complex has a formation constant of 2.0×10^{11} under the conditions studied. Anions such as phosphate, EDTA, etc., inhibited the color development of the complex, and cations such as Al(III), Fe(II,III), and Be(II), etc., caused overestimation of the thorium. (auth)

14486 GASCHROMATOGRAPHIC DETERMINATION OF SCANDIUM AS ACETYLACETONATE AND TRIFLUOROACETYLACETONATE. Fujinaga, Taitiro; Kumamoto, Tooru; Ono, Yusuke (Kyoto Univ.). Nippon Kagaku Zasshi, 86: 1294-9(Dec. 1965). (In Japanese).

The gas phase chromatography of metal chelates of acetylacetone(AA) and trifluoroacetylacetone(TFA) was investigated. The chelates of the fluorine-containing β-diketones were more volatile and could be eluted at much lower column temperatures than corresponding chelates of acetylacetone. The AA of scandium was eluted quantitatively at a column (containing glass microbeads coated with 0.5% Apiezon-L grease) temperature of 220°C but the separation of scandium, aluminum, and beryllium was not complete. The TFA of scandium was eluted at a column (containing Chromosorb-W coated with 10% Silicone Oil) temperature of 185°C and could be quantitatively determined as low as several micrograms of scandium within an error of ±4%. Conditions were established for the complete separation of scandium, aluminum, and beryllium. This method was applied to the determination of scandium in the presence of the other two. These metal ions were extracted from aqueous solution with benzene after the addition of trifluoroacetylacetone and an aliquot of the extract was chromatographed. The feasibility of gas chromatographic analysis of these metals was found. (auth)

14487 DEBALANCING OF DIFFERENTIAL X-RAY FILTERS. Dziunikowski, Bohdan; Niewodniczanski, Jerzy (Inst. of Nuclear Techniques, Krakow). Nukleonika, 10: 675-80(1965).

The effect of debalancing of the differential Ross filters due to the variation of the disturbing element contents is considered. This effect was observed in the case of the fluorescence determination of copper in ore samples containing different admixtures of iron. A physical explanation of this effect, confirmed by experimental results, is given. (auth)

14488 APPLICATION OF SEVERAL RADIOACTIVE ISOTOPES IN RADIOCHEMICAL ANALYSIS. Glazov, V. M. Radiokhimiya, 7: 475-9(1965). (In Russian).

The use of several radioisotopes in radiochemical analysis is discussed. The identification of radioisotopes with any form of radiation may be determined relatively simply by using a universal scintillation counter. The count rate from a multicomponent radioactive tagging with simultaneous use of α, β, and γ isotopes is conducted as follows: the count rate is obtained for the alpha-emitting isotopes using a detector based on ZnS (Ag); the γ background is obtained with a detector that has a stilbene crystal, by placing an aluminum absorber between the counter and the sample, which absorbs all β; the plate is removed and the total β + γ is measured from which β is obtained by the difference; and the γ count is obtained with the first scintillation counter, which has a NaI(Tl) crystal. It is possible to use beta-emitting isotopes with complex spectra as well as isotopes in equilibrium with daughter decay products. The accuracy of the experiment depends to a great extent on the stability of the scintillation spectrometer. Experiments showed that stability of the scintillation spectrometer was achieved after a 4 to 5 hr warm up. Scalers did not affect the stability of the spectrometer and were turned on 30 min before operation. Under these conditions the accuracy of measurement of the count rate from each of the two radioactive isotopes in the chemical compound was 2 to 3%. (CFSTI)

14489 QUANTITATIVE DETERMINATION OF NICKEL AND IRON IN FERROMAGNETIC FILMS BY NEUTRON

ACTIVATION. Naumova, I. I. Radiokhimiya, 7: 502-4 (1965). (In Russian).

A method was developed for the quantitative analysis of films consisting of 83% Ni and 17% Fe, which contain about 10 μg of this alloy. The samples and standards were put into a reactor in aluminum vials where they were irradiated in a 2×10^{13} n/cm^2·sec beam for approximately 1 month. Specimens were processed 1 week after irradiation. The calculated sensitivities for the determination of iron from ^{59}Fe and nickel from ^{63}Ni were 6×10^{-9} and 1.4×10^{-8} g, respectively. After dissolution of the sample in 1:1 nitric acid and introduction of inert carriers, iron was precipitated with NH_4OH and separated by centrifuging. Nickel was separated by dimethylglyoxime precipitation. After precipitation samples were subjected to radiochemical purification and counted. The mean error for the determination of iron was 0.5 to 3%. The standard deviation in the determination of nickel was 1%. Cobalt was also determined in amounts ranging from 10^{-5} to 10^{-6}%. Analogous amounts of nickel and iron may be determined by irradiation of samples with 14-Mev neutrons in an accelerator, and measuring ^{56}Mn, produced by the reaction of ^{56}Fe(n,p) ^{56}Mn ($T_{½}$ = 2.6 hrs); and ^{57}Ni, produced by the reaction ^{58}Ni(n,2n)^{57}Ni ($T_{½}$ = 36 hrs). (CFSTI)

14490 NEW YTTERBIUM COMPOUNDS WITH ORGANIC ACIDS. Spacu, P.; Mavrodin, Maria (Inorganic Chemistry Center, Bucharest). Rev. Rom. Chim., 10: 973-7(Oct. 1965). (In Rumanian).

A series of compounds of ytterbium with mono- and dibasic acids (chloromandelic acid, bromomandelic acid, mucic acid, adipic acid, dihydroxymaleic acid, and saccharic acid) are presented. The utilization of chloromandelic acid as a reagent to determine and separate ytterbium from Sm and Eu was investigated. Bromomandelic acid and mucic acid were also used as reagents for the determination of Yb. (tr-auth)

14491 DETERMINATION OF THORIUM IN DIFFERENT MONAZITE ORE SAMPLES. Georgescu, Iulia I. (Polytechnic Inst. Gheorghe Gheorghiu-Dej, Bucharest); Ciohodaru, Lucia; Cojocaru, V. Rev. Roum. Phys., 10: 755-67(1965).

Various analysis methods, i.e., mineralogical, spectral, and chemical methods, as well as x-ray diffraction are applied, and it is shown that the ore samples under study are monazite ores with rare cerium earths of the light lanthanons group mixed with cerium oxides. In all analyzed samples uranium was completely lacking. For the determination of thorium in non-concentrated monazite ore samples, the following physical methods were applied: emanation method, autoradiography with nuclear emulsions, and gamma spectrometry. Meanwhile, measurements were made on Norwegian monazite mineral ore samples. It is deduced that in the monazite ore samples under study the percentage of thorium content varies from 0.75 to 7.28. (auth)

14492 PLASMA JET APPLIED SPECTROSCOPIC SOURCE FOR ALKALI EARTH ANALYSIS. Ishida, Ryohei (Government Chemical Industrial Research Inst., Tokyo). Sci. Light (Tokyo), 12: 16-27(July 1963).

A plasma jet applied spectroscopic source was found to be suited to the determination of alkaline earth elements (Mg, Ca, Sr, Ba) with a sensitivity of spectrum lines better than that obtained from flame sources. In the plasma jet generator used, sample solutions were atomized by compressed nitrogen gas in a Perkin-Elmer type atomizer chamber and the nitrogen stream with an atomized fog of sample solution was carried into the plasma jet. From observations of the Mg spectrum, the temperature of the plasma was found to be a little higher at the base and a little lower at the top of the plasma jet, but as a whole almost the same as that of an arc discharge column. The sensitivity in the spectrographic determinations of alkaline earth elements was found to be much higher with the plasma jet source than with customary flame sources. The plasma jet source was generally more stable than the arc source but less stable than the flame source. This apparatus can be used for the study of vaporization and excitation mechanisms as well as for analysis of other elements and various sorts of samples. In the plasma jet spectroscopic source it is possible to use inert gases such as nitrogen and argon to avoid the presence of oxygen and emission of the carbon monoxide band. The sites of vaporization and excitation are separated. Temperatures higher than those of chemical flames can be obtained as desired by control of the electric current. (BBB)

14493 MEASUREMENT OF THE ASH CONTENT OF LIGNITE BY THE γ IRRADIATION TECHNIQUE WITH THE RADIONUCLIDE ^{170}Tm. Koch, Siegfried; Windelband, Rolf (Technische Universitaet, Dresden). Wiss. Z. Tech. Univ. Dresden, 13: 23-30(1964). (In German).

The sensitivity of ash analyses by the γ irradiation method was studied as a function of detector radiation collimation, thickness of sample, and spectral composition of the radiation from the ^{170}Tm source. Data are presented for relative radiation intensity as a function of ash content for different diameters of the detector collimator and relative intensity as a function of ash content for different thicknesses of the lignite sample. Similar data are presented for the results of K_α radiation with ordinary and very large samples. The recorded radiation was also studied as a function of sample moisture for several ash contents. The best results were obtained when measurement of the characteristic radiation of the ^{170}Tm preparation was limited and the thickness of the sample was increased for increasing ash content. The diameter of the collimator bore was decreased and the thickness of the coal sample increased for maximum sensitivity. Experimental errors are discussed. (BBB)

14494 REPORT ON THE DETERMINATION OF TRACE IMPURITIES IN UO_2 FUEL MATERIALS. Neeb, Karl Heinz; Duda, Renate; Franke, Renate; Seyfarth, Rudolf; Stoeckert, Heinz (Siemens-Schuckertwerke AG, Erlangen, Ger.). Z. Anal. Chem., 215: 161-75(1966). (In German).

Analytical methods were developed for the determination of trace amounts of phosphorus, silicon, fluorine, chlorine, lithium, sodium, calcium, and carbon in UO_2 of nuclear purity. By combination of simple and rapid separation procedures (extraction, pyrohydrolysis) with highly sensitive methods of determination (spectrophotometry, flame photometry, coulometric titration) detection limits of 0.1 to 10 ppM were obtained with sample sizes of 0.5 to 1 g. In order to reduce the time needed for analysis, some of the above elements are determined simultaneously. The methods described were successfully applied to the purity control of nuclear fuels. (auth)

14495 ACTIVATION ANALYTICAL DETERMINATION OF VERY SMALL IRIDIUM CONTENTS IN URANIUM OXIDE. Ruf, H.; von Baeckmann, A. (Kernforschungszentrum, Karlsruhe, Ger.). Z. Anal. Chem., 215: 176-81 (1966). (In German).

Very small amounts of iridium in uranium oxide were quantitatively determined by neutron-activation analysis. Iridium was separated from uranium prior to irradiation by means of an anion-exchange resin. After a decay period of twelve days the activity of ^{192}Ir in the undestroyed silica ampoule was measured in a well-type crystal without any chemical operation. (auth)

14496 DETERMINATION OF VERY SMALL HAFNIUM CONTENTS IN ZIRCONIUM DIOXIDE PREPARATIONS BY MEANS OF X-RAY SPECTRAL ANALYSIS AFTER ENRICHMENT BY MEANS OF A PARTITION PROCESS. Fischer, Werner; Biesenberger, Kurt; Boehmer, Winfried; Reinhardt, Kalus (Technische Hochschule, Hanover). Z. Anal. Chem., 216: 61-5(1966). (In German).

Low concentrations of HfO_2 in the range from 0.002% and up in zirconium dioxide may be determined by x-ray fluorescence analysis after a preceding enrichment process. In this process the oxide is melted with $Na_2S_2O_7$, the melt dissolved in an aqueous NH_4SCN solution, and this solution subjected to a 3 stage liquid-liquid extraction process. (auth)

14497 ON THE X-RAY FLUORESCENCE ANALYSIS OF TECHNETIUM AND MOLYBDENUM IN SOLUTIONS. Lux, Franz; Ammentorp-Schmidt, Frits; Opavsky, Werner. Z. Anorg. Allg. Chem., 341: 172-82(Dec. 1965). (In German).

With a view to simplicity, safe handling, and the possibility of determining smaller amounts of technetium compounds, an x-ray fluorescence method for their measurement in solution was developed. The analytical conditions were established by means of the nonradioactive neighboring element molybdenum, which is easier to handle. At concentrations of less than 1.0 mg Tc and Mo, respectively, per ml, there were no interelement effects due to the other components of the compound to be analyzed. In this range it was therefore possible to determine compounds that are soluble in water or dioxane without chemical decomposition, and to use aqueous solutions of pertechnetate and molybdate, respectively, or solutions of, e.g., technetium and molybdenum carbonyl, respectively, in dioxane as standards without corrections. The detection limit is about 4 μg Tc (Mo). The standard deviation is ±0.4%. (auth)

14498 EVALUATION OF GAMMA-EMITTER ACTIVITY IN X-RAY ABSORPTION ANALYSIS. Plaksin, I. N.; Nikitin, F. V. Zavodsk. Lab., 31: 1461-5(1965). (In Russian).

A method is proposed for calculation of the activity of the γ emitter for x-ray absorption analysis with radioisotopes using given concentrations of the elements being studied. The method takes into consideration the time of the operation of the emitter and the absorption characteristics of the experiment. Examples of the calculation of the emitter for a series of radioisotopes are given for the case of x-ray absorption determination of Ag. (tr-auth)

14499 I. PROPERTIES AND INFRARED SPECTRA OF SEVERAL METAL CHELATES. II. ANALYTICAL GAS CHROMATOGRAPHY OF METAL CHELATES [Thesis]. Tackett, James Edwin. Riverside, Calif., University of California, 1964. 171p.

The infrared spectra of ethylenediaminetetraacetic acid and its chelates of the alkaline earth ions, cobalt(II), nickel(II), copper(II), zinc(II), cadmium(II), manganese(II), lead(II), bismuth(III), cerium(III), aluminum(III), iron(III), chromium(III), thorium(IV), and vanadium(IV) in deuterium oxide solutions were studied as a function of solution acidity. On the basis of the shift in peak position and area for the carboxylate-carboxylic acid absorption bands, the positions of the acidic protons on the ligand molecule in solution were established. Infrared spectra were recorded for ethylenediaminetetraacetic acid and its chelates in the solid phase in the 11- to 25-micron region. Assignments are made for the major absorption bands. The effect of hydration on the spectra of the chelates is discussed along with evidence for uncoordinated carboxylate groups. The infrared spectra in the 11- to 25-micron region of 8-quinolinol and its chelates of the alkaline earth ions, manganese(II), cobalt(II), nickel(II), copper(II), zinc(II), cadmium(II), lead(II), aluminum(III), iron(III), thorium(IV), and uranium(VI) were recorded and band assignments are made. A consideration of the spectral shifts are used to study the structures of the divalent metal chelates in the solid phase. The thermal properties of the acetylacetone and 8-quinolinol chelate systems were studied to determine the usefulness of these reagents in forming chelates that can be separated by gas chromatography. Although some of the chelates are sufficiently thermally stable to be eluted from a column, in general, they can not be vaporized without some decomposition under the conditions necessary for gas chromatography. (Dissertation Abstr.)

14500 ANALYTICAL CHEMISTRY OF SELECTED METALLIC ELEMENTS. Lingane, James J. Reinhold Chemistry Textbook Series. New York, Reinhold Publishing Corp., 1966. 150p. $3.50.

Techniques and methods for analyzing metallic compounds are discussed in terms of classical and instrumental inorganic analytical chemistry. Topics covered include: alkali metals (lithium, sodium, potassium, rubidium, cesium, and francium), alkaline earth metals (calcium, strontium, and barium), aluminum, antimony, arsenic, bismuth, cadmium, chromium, cobalt, copper, iron, lead, magnesium, manganese, mercury, molybdenum, nickel, silver, tin, titanium, tungsten, uranium, vanadium, and zinc. (F.J.H.)

14501 METODY ANALIZA RADIOAKTIVNYKH PREPARATOV. (Methods for Analysis of Radioactive Preparations). Kharlamov, V. (ed.). Moscow, Atomizdat, 1965. 176p.

Nineteen papers are included on the control of the quality of radioactive isotopes and their labeled compounds, radiochemical composition of some halide derivatives of fluorescein labeled with ^{131}I and their quantitative determination, paper electrophoresis for the analysis of labeled carbohydrates, polarographic determination of hexavalent and trivalent Cr in preparations labeled with ^{51}Cr, polarographic method of analysis of some labeled organic materials, paper chromatography for determining the change of radiochemical composition of preparations of methionine labeled ^{35}S during its storage, quantitative determination of cardiotrast and o-iodohippuran labeled with ^{131}I, analysis of preparations of adenine and adenosine labeled with ^{14}C, quantitative determination of Y in preparations containing ^{90}Y, analysis of preparations of sodium chromate and chromium chloride labeled with ^{51}Cr, spectrophotometric determination of sodium tetraiodophenolphthalein labeled with ^{131}I and determination of its radiochemical composition, identification of the products of stabilization of radiophosphorus in the target $CCl_4 + C_2H_5OH$, thin-layer chromatography on silica gel for the analysis of neohydrin labeled with ^{203}Hg, comparison of properties of several types of paper chromatography used for the analysis of labeled preparations, apparatus for automatic recording of the distribution of activity in paper chromatography, methods of analysis of cysteine labeled with ^{35}S, thin-layer chromatography for the analysis of thiophosphamides labeled with ^{35}S, radiochemical composition of colloidal solution of gold labeled with ^{198}Au, and quantitative determination of labeled amino acids using paper chromatography. (M.J.T.)

14502 DERIVATIVE NEUTRON ACTIVATION ANALYSIS. Harmison, Lowell T. (Hittman Associates, Inc., Baltimore); Lakshmanan, S.; Duffey, Dick. 10p. (CONF-650602-62). Gmelin, AED-CONF-65-125-44.

From American Nuclear Society, 11th Annual Meeting, Gatlinburg, Tenn.

The detection of elements with extremely small activation cross sections is no longer an impossibility by using derivative neutron activation. Also, the constraints of short half life or energy or type of emitted radiation are no longer factors that comprise the effectiveness of activation analysis because atoms can be selected that afford optimum properties for both activation and detection. For example, zinc was determined at trace levels below the direct activation sensitivity with lower neutron fluxes and shorter irradiation periods. Hence, this method makes possible the extension of activation analysis to other laboratories, which do not have direct access to a high flux reactor or elaborate radiation detection equipment. (auth)

14503 APPARATUS FOR CONCENTRATION AND MEASUREMENT OF LOW TRITIUM ACTIVITIES. Cameron, J. F.; Payne, B. R. (International Atomic Energy Agency, Vienna). 17p. (CONF-650652-1). Gmelin, AED-CONF-65-158-6.

From International ^{14}C and ^{3}H Dating Conference, Pullman, Wash.

An apparatus was designed for routine concentration and measurement of a maximum number of samples with activities greater than 0.5 T.U. with an accuracy of about ±5% or ±0.5 T.U. The electrolytic concentration of the samples are accomplished with systems consisting of electrolytic cells and cooling and isolating systems. In the gas counting system, water samples are converted to ethane, which is counted in proportional counters. Gas preparation, counter construction, shielding, electronic circuitry,

counter characteristics, standards and backgrounds, and comparisons of counters are discussed. The scintillation counter was used for measuring enriched spiked samples from the electrolytic cells and samples from tracer experiments. A minimum error of ±80 T.U. (±0.2 cpm) was observed on all samples measured by scintillation counting. Organization of measurements of low-tritium activities and processing of data are discussed. Costs of measurements are given. (F.J.H.)

14504 THE NONDESTRUCTIVE MEASUREMENT OF BURNUP BY γ-RAY SPECTROSCOPY. Rasmussen, N. C.; Sovka, J. A.; Mayman, S. (Massachusetts Inst. of Tech., Cambridge). Vienna, International Atomic Energy Agency, 1965, Preprint No. SM-67/45, 31p. (CONF-650803-40). ORINS.

From IAEA Symposium on Nuclear Materials Management, Vienna.

Two types of γ spectroscopy are being used to study spent reactor fuel at this laboratory. Considerable work was done using bent quartz crystal spectrometers. With these instruments the γ spectrum up to about 500 kev was resolved after cooling times as short as 12 hr. It was possible to determine the relative intensity of the 133-kev γ ray of ^{144}Ce as a function of position along an MITR fuel element. The relative burnup determined from this data agreed with values obtained with a computer code called MITBURN, which uses the neutron flux distribution calculated by a two-group diffusion code, TWENTY GRAND. Because of uncertain half life and self-absorption corrections no attempt was made to determine the absolute burnup. Li-drifted Ge solid-state γ detectors were developed and employed to study the higher energy part of the spectrum. With these detectors it was possible to identify the 662-kev line of ^{137}Cs after as little as two weeks cooling time. Spectra were obtained with a detector measuring about 1.5 by 2.2 cm, having a depletion depth of 4 mm and operating at liquid nitrogen temperature with a bias of 200 volts. The measured energy resolution of the detector and associated electronics was 5.8-kev for the 662 kev ^{137}Cs line. Work is now underway to determine absolute burnup from the intensity of the ^{137}Cs line and to correlate it with the theoretical predictions. (auth)

14505 IMPROVEMENTS IN OR RELATING TO RADIOMETRIC ANALYSIS TECHNIQUES. Rhodes, John Rathbone (to United Kingdom Atomic Energy Authority). British Patent 1,017,595. Jan. 19, 1966. Filed June 20, 1962.

An apparatus and process are patented for testing a sample to determine the concentration of a required element by determining two absorption coefficients of the sample by using two energies of incident x rays selected so as to be close to the top and bottom respectively of an absorption edge of the required element. The apparatus includes a continuous spectrum source of radiation, two targets constituted by elements having respectively a characteristic radiation energy within 5% of the top and bottom of an absorption of the required element, and a different pair of differential filters for association with each target. One of the pair of filters is essentially opaque to the characteristic radiation of the associated target, and the other filter of the pair is essentially transparent to the radiation thereby permitting the isolation of substantially monochromatic fluorescent x rays that have passed from the target through the sample. The absorption by the sample of the monochromatic x rays from the targets is determined by means of x-ray detection in the form of a counter located at the side of the sample remote from the targets. (B.L.M.)

Inorganic and Physical Chemistry

Refer also to abstracts 14669 and 15853.

14506 (CRDL-SP-5-7) SEVENTEENTH MATERIALS REVIEW. Lyem, Arthur (Chemical Research and Development Labs., Edgewood Arsenal, Md. Experimental Engineering Div.). Apr. 1965. 93p.

Important scientific and technical highlights regarding materials research, principally in the polymer and plastics fields, are reviewed. The materials covered include: high polymers; plastics; synthetic fibers; miscellaneous organic and inorganic compounds; and metals and alloys. (319 references). (P.C.H.)

14507 (LA-3399) THERMODYNAMIC PROPERTIES OF Pu COMPOUNDS FROM EMF MEASUREMENTS. I. Pu VERSUS Ag IN LiCl-KCl EUTECTIC. Campbell, G. M.; Leary, J. A. (Los Alamos Scientific Lab., Univ. of California, N. Mex.). Sept. 16, 1965. Contract W-7405-eng-36. 18p. Dep. mn. CFSTI $1.00 cy, $0.50 mn.

The EMF of the cell $Pu/Pu^{+3}(x_1)$, LiCl-KCl // LiCl-KCl, $Ag^+(x_2)/Ag$ was determined over the temperature range 697 to 729°K and over a Pu^{+3} mole fraction (x_1) range of from 5.94×10^{-4} to 21.5×10^{-4}. The Ag^+ concentration in the reference electrode was maintained at a constant mole fraction of 5.68×10^{-4}. The reversible EMF of the cell can be expressed as $E_T = (2.19 - 1.004 \times 10^{-3}T) + (RT/3F) \ln x$. In addition, the EMF of the cell Ag/Ag^+ (x_2) LiCl-KCl/Cl_2,C was measured. By combining the data of the first cell with that of the last cell, the free energy of formation of $PuCl_3$ in LiCl-KCl solution was found to be represented by the equation $-\Delta F_T = 224 - 0.046\ T$ (kcal/mole). (auth)

14508 (N65-20481) RATES OF HYDROGEN-GRAPHITE REACTION BETWEEN 1550 DEG AND 2260 DEG C. Sanders, William A. (National Aeronautics and Space Administration, Cleveland, Ohio. Lewis Research Center). Apr. 1965. 11p. (NASA-TN-D-2738). CFSTI $1.00 cy, $0.50 mn.

The rates of reaction of a pitch-free, petroleum coke-base graphite with purified hydrogen were determined in the temperature range 1550 to 2660°C. Experimental weight losses agreed very well above 1800°C with calculations based on thermodynamic data for the hydrogen-graphite theoretical equilibrium compositions, where acetylene was calculated to be the major reaction product. Although the experimental curve and the theoretical curve diverge below 1800°C, equilibrium might be achieved at temperatures below 1800°C if slower hydrogen flow rates were employed. (STAR)

14509 (NP-15826) PRAEPARATIVE UND ROENTGENOGRAPHISCHE UNTERSUCHUNGEN AN STARK RADIOAKTIVEN STOFFEN [Theses]. (Preparation and Roentgenographic Study of Highly Radioactive Material [Thesis]). Weigel, Fritz (Munich Univ. (West Germany)). 1965. 301p. Dep. mn.

Information is given on: methods and techniques used in the separation of ^{238}Pu and ^{241}Am; properties of Am compounds; isolation of Cm and Pm in microquantities; Cm(111) precipitation as the phosphate and determined by its x-ray diagram; $CmPO_4$ crystallization in the monoclinic form; methods used for the purification of Pm and for the production of metallic Pm; and the preparation and crystallography of 16 compounds of Pm, including the fluoride, oxyfluoride, chloride, monoxide, oxide, hydroxide, nitrate, hydrated phosphate, water-free phosphate, arsenate, iodate, oxalate, and carbonate. (202 references). (P.C.H.)

14510 (NP-15834) BIBLIOGRAFIA SOBRE LA CONVERSION DE AGUAS SALADAS Y SALOBRES EN AGUA DULCE (1954-1964). (Bibliography on the Conversion of Salt and Brackish Waters into Fresh Water (1954-1964)). Gurza, Tomas; Zamora, Pedro (comps.) (Comision Nacional de Energia Nuclear, Mexico City (Mexico)). Nov. 1965. 178p. Dep. mn.

References (955) are given to various methods and equipment used for the desalination of water are given to reports, journals, and books published from 1954 through 1964. A separate author index is included. (P.C.H.)

14511 (ORNL-3889, pp 71-3) INORGANIC PREPARATIONS. Kelley, M. T.; LaValle, D. E.; Quincy, R. B. (Oak Ridge National Lab., Tenn.).

Continued routine preparation of fused salts is reported, and high-purity KCl was prepared along with alkali metal oxides such as KO_2, RbO_2, Na_2O, and K_2O. Samples of $LiOBr \cdot H_2O$ and K_2ReCl_6 were also prepared. Rare earth nitrides, phosphides, and sulfides were produced. Uranium trihalides were produced along with iron-substituted alums. (J.R.D.)

14512 (ORNL-TM-1418) VAPOR PRESSURES OF GASEOUS PRODUCTS FROM CHEMICAL REACTIONS OF SOL-GEL FUELS. Gens, T. A. (Oak Ridge National Lab., Tenn.). Feb. 10, 1966. Contract W-7405-eng-26. 13p. Dep. mn. CFSTI $1.00 cy, $0.50 mn.

Calculations were made on the partial pressures of gases expected to be formed in various reactor fuel materials. The calculations are based on data from the chemical literature. The CO pressure due to reaction between coating and oxide inside carbon-coated UO_2 and ThO_2 microspheres will reach 450 psi when the temperatures are 2400 and 2300°C, respectively. Nitrogen pressures from thermally decomposing UN and PuN microspheres will reach equilibrium values of 450 psi at 3000 and 2800°C, respectively. This is the helium pressure expected in the TARGET gas-cooled reactor. Therefore, it appears that these coated fuel microspheres would not develop excessive internal pressures at the pressure and respective temperatures listed above. Pressures expected at other temperatures are also tabulated. (auth)

14513 (RFP-688) CRITICAL TEMPERATURE OF PLUTONIUM-CHLORINATED SOLVENT REACTIONS. Pitts, S. H. Jr. (Rocky Flats Div., Dow Chemical Co., Golden, Colo.). Feb. 18, 1966. Contract AT(29-1)-1106. 10p. Dep. mn. CFSTI $1.00 cy, $0.50 mn.

Critical temperatures were determined for some plutonium-chlorinated solvent reactions. The critical temperature is defined as the lowest temperature at which plutonium reacts with the solvent to yield an exothermic reaction accompanied by light emission. These temperatures were determined by heating plutonium samples to a known temperature in argon and dropping them into various solvents while visually watching for a reaction. The solvents used were carbon tetrachloride, trichloroethylene, perchloroethylene, and Freon TB-1. A correlation was established between the critical temperature and surface area for unalloyed and 1 wt % gallium alloyed plutonium in several chlorinated solvents. The critical temperature decreased as the specific surface area was increased. (P.C.H.)

14514 (UCRL-11821) THE THERMODYNAMIC PROPERTIES OF METALS AND ALLOYS [Thesis]. Anderson, Philip Douglass (Lawrence Radiation Lab., Univ. of California, Berkeley). Jan. 1966. Contract W-7405-eng-48. 136p. Dep. mn. CFSTI $4.00 cy, $1.00 mn.

The concentration dependence of the free energy of formation of forty-seven binary liquid alloys was studied by examining nine hundred experimental values of the partial molar free energy given in the literature. These values were selected from less reliable ones. The method of least squares was used to fit the data to ten different solution models of varying degree of complexity, containing from one to three adjustable parameters. The resulting tables presented in this work allow a number of conclusions to be reached at significant confidence levels regarding the concentration dependence of the excess free energy, providing that the alloy systems are divided into two different classes, depending on the sign of the deviation from ideality. Correlation of the magnitude of the deviation from ideality with certain physical parameters was also found. The magnitude of the excess entropy of formation was examined for forty-eight binary liquid alloys. It was found that $-1.0 < \Delta S^{xs} < 1.0$ unless the alloy system has a large exothermic heat of formation, in which case large negative excess entropies are to be expected. The results indicate that configurational contributions to this entropy are unimportant compared to other (presumably vibrational) causes. (auth)

14515 (UCRL-16649) VAPORIZATION STUDIES OF LANTHANUM FLUORIDE [Thesis]. Mar, Raymond W. (Lawrence Radiation Lab., Univ. of California, Berkeley). Jan. 26, 1966. Contract W-7405-eng-48. 24p. Dep. mn. CFSTI $1.00 cy, $0.50 mn.

The sublimation pressure of lanthanum fluoride was measured in the temperature range 1325 to 1650°K by the torsion-effusion method. The pressure data are represented by the expression $\log_{10} P_{atm} = -(2.174 \pm 0.009) \times (10^4/T) + 9.608 \pm 0.065$ where the quoted errors are standard deviations from the least squares fit. The heat of sublimation at 298.15°K was found to be 107.45 ± 4 kcal/mole by the Second-Law method and 103.48 ± 4 kcal/mole by the Third-Law method. Assigning equal weights for the two methods, the heat of sublimation was taken as the average, 105.5 ± 5 kcal/mole. (auth)

14516 STUDIES ON THE FAILURE OF THE FIRST BORN APPROXIMATION IN ELECTRON DIFFRACTION. I. URANIUM HEXAFLUORIDE. Seip, Hans M. (Univ. of Oslo). Acta Chem. Scand., 19: 1955-68(1965).

The structure of uranium hexafluoride was studied by electron diffraction. There was no evidence for deviation from O_h symmetry. The U−F bond length is 1.999 Å with a standard deviation of 0.003 Å. The root-mean-square amplitudes of vibration are the same as found from spectroscopic data within experimental error limits. Scattering amplitudes calculated by different authors were used. It is demonstrated that the theoretical values fit the experimental data reasonably well. (auth)

14517 ROTATIONAL ANALYSIS OF THE PERTURBED C AND D STATES OF BaH AND BaD. Kopp, Ingvar; Aslund, Nils; Edvinsson, Gunnar; Lindgren, Bo. (Univ. of Stockholm). Arkiv Fys., 30: 321-57(1965).

The absorption spectra of BaH and BaD in the region 3300−4500 Å were photographed using a King furnace and a 10.685-meter concave-grating spectrograph. The strongly perturbed 0−0 band of the $C^2\Sigma - X^2\Sigma$ transition was reanalyzed, and the main perturbations were attributed to interactions with a new state $D^2\Sigma$. Computer methods were used for picking out and numbering the branches and for fitting mathematical models to the term values of the states. The equilibrium constants derived for BaH are given. (auth)

14518 THE EXCHANGE REACTION OF H AND H_2. Micha, David A. (Uppsala Univ.). Arkiv Fys., 30: 425-36(1965).

The exchange reaction of a hydrogen atom and hydrogen molecule was studied with a quantum mechanical model for systems under aligning forces. Consideration of nuclear spins to describe the para-ortho conversion introduced a factor $^3/_4$ in the coordinate-dependent cross sections. An analytical expression was obtained for the total cross-section σ by using a piecewise interaction potential and computational simplifications. Calculations of σ as a function of the initial relative wavenumber k, for $k \lesssim 7.00$ au showed a threshold for σ followed by an oscillatory behavior around a mean $\sigma_{av} = 0.50$ au. This function was shifted to larger k with increasing potential strength and the initial molecular angular momentum, but only slightly in this last case. The value for σ was noticeably changed by varying the range of the chemical interaction and the hard-core radius of the H_3 potential. The mean value σ_{av} increased when the hard-core radius increased but seemed fairly independent of the other parameters. (auth)

14519 ENRICHMENT OF DEUTERIUM THROUGH HIGH-PRESSURE ISOTOPIC EXCHANGE BETWEEN HYDROGEN AND LIQUID AMMONIA IN A HOT/COLD INSTALLATION. Walter, S. (Friedrich Uhde GmbH, Dortmund, Ger.); Schindewolf, U. Chem.-Ing.-Tech., 37: 1185-91(Dec. 1965). (In German).

The enrichment of deuterium by high-pressure isotope exchange between hydrogen and liquid ammonia with dissolved potassium amide as catalyst offers advantages with respect to other known methods because of the high elementary isotopic displacement and the favorable chemical properties of the reaction partners. In a semi-industria installation working on the dual-temperature principle, enrichment studies were carried out for more than several hundred hours. In these studies a six-fold enrichment of the deuterium was obtained in the hydrogen and in the ammonia a twenty-fold enrichment of deuterium was found in the feed hydrogen. The enrichment of deuterium with the hydrogen/ammonia exchange system in the dual-temperature process is considered possible in industrial quantities (tr-auth)

14520 PRODUCTION OF RARE EARTHS FROM KOLA-APATITE. Richter, Herfried; Krause, Albert. Chem. Tech. (Leipzig), 17: 707-10(Dec. 1965). (In German).

The possibilities for the production of rare earths from apatite from the Kola Peninsula (USSR) are discussed on the basis of literature data and unpublished works of the VEB Nitrogen Works of Piesteritz. Results indicated that a commercially feasible production of rare earths is possible by precipitating them as phosphates during the production of multinutrient fertilizers by the Odda method and the lime nitrophosphate method. (tr-auth)

14521 NEW COMPLEXES. III. POLAROGRAPHIC DETERMINATION OF STABILITY CONSTANTS OF MESO-2,3-DIAMINOBUTANE-N,N,N′,N′-TETRAACETIC ACID WITH LANTHANIDES. Novak, V.; Maier, Ya.; Svichekova, M. (Komensky Univ., Bratislava). Chem. Zvesti, 19: 817-25(1965). (In Czech).

Studies of the chelating properties of meso-2,3-diaminobutane-N,N,N′,N′-tetraacetic acid (meso-DBTA) were continued by an investigation of the complexes of meso-DBTA with additional central atoms. The values of the logarithms of the stability constants of normal complexes of meso-DBTA with lanthanides were determined in KNO_3 media (μ = 0 and 10 and t = 20°C) by polarographic studies of exchange equilibrium systems. For calculation of the stability constants, the values of 43 equilibrium constants of exchange equilibrium systems were used. These values were determined polarographically. In this manner the accuracy of the determination of the stability constants were considerably increased. The basic value for all constants was the potentiometrically determined value of the Cd(II) complex of meso-DBTA of 16.77 ± 0.04 at μ = 0 and 10 (KNO_3) and t = 20°C. The values of the stability constants of the lanthanide complexes investigated were significantly lower than those of the complexes with EDTA. Graphic representation of the logarithms of the stability constants of the lanthanides as a discontinuous function of the atomic number of the central atom lanthanide showed an increase of four units of log K with a characteristic nick at Gd. (tr-auth)

14522 COMPLEXES OF URANYL WITH PHENOLIC LIGANDS. II. POTENTIOMETRIC STUDIES OF PYROCATECHIN-5-SULFONIC ACID AND PYROCATECHIN-3,5-DISULFONIC ACID COMPLEXES. Bartusek, M.; Stankova, O. (Univ., Brno). Collec. Czech. Chem. Commun., 30: 3415-25(Oct. 1965). (In German).

In weakly acid solutions of approximately 10^{-3} M uranyl salts, in the presence of pyrocatechin monosulfonic acid and pyrocatechin disulfonic acids, complexes of the type NRH and M_2R_2OH are formed. The existence of the complexes MR and $M_3R_3(OH)_2$ reported earlier could not be confirmed. (tr-auth)

14523 COMPLEXES OF XENON OXIDE TETRAFLUORIDE. Selig, Henry (Argonne National Lab., Ill.). Inorg. Chem., 5: 183-6(Feb. 1966).

Xenon oxide tetrafluoride bears a strong resemblance to the halogen fluorides both in physical properties and chemical behavior. Xenon oxide tetrafluoride is a clear, colorless liquid freezing at −46.2°C. Its electrical conductivity at 24°C is 1.03×10^{-5} ohm^{-1} cm^{-1} and its dielectric constant is 24.6 at 24°C. It is miscible with anhydrous HF, but its conductivity is not enhanced in such a solution. The addition of CsF or RbF to $XeOF_4$ increases its conductivity markedly. Xenon oxide tetrafluoride forms a series of addition compounds with the heavier alkali fluorides. The following complexes were isolated: $CsF \cdot XeOF_4$, $3RbF \cdot 2XeOF_4$, and $3KF \cdot XeOF_4$. No reaction occurred with NaF. Thermogravimetric studies showed that a number of intermediates are formed before final decomposition to the alkali fluorides. Xenon oxide tetrafluoride reacted with SbF_5 to form a complex of composition $XeOF_4 \cdot 2SbF_5$. A reaction also occurred with AsF_5 at −78°C, but the complex was unstable at room temperature. (auth)

14524 THE STRUCTURE REFINEMENT OF La_2Te_3, A Th_3P_4 TYPE STRUCTURE. Cox, W. L.; Steinfink, H.; Bradley, W. F. (Univ. of Texas, Austin). Inorg. Chem., 5: 318-19(Feb. 1966).

The importance of the Th_3P_4 structure in rare earth compounds prompted an investigation of La_2Te_3 single crystals to determine the exact value of the positional parameter of the 16-fold position of the ion in space group $I\bar{4}3d$. There were two different La−Te bond distances, 3.244 ± 0.0028 and 3.418 ± 0.0028 Å, in the structure. The coordination polyhedron around La could be described in terms of two tellurium tetrahedra, an elongated one and a flat one. Relative bond strengths were determined. (M.C.G.)

14525 THE EXCHANGE OF ^{18}O BETWEEN WATER AND ORTHOTUNGSTATE AND BETWEEN WATER AND 12-TUNGSTOCOBALTATE(III). Geier, Gerhard; Brubaker, C. H. Jr. (Michigan State Univ., East Lansing). Contract AT(11-1)-1001. Inorg. Chem., 5: 321-2(Feb. 1966). (COO-1001-6).

The oxygen exchange between water and orthotungstate and water and 12-tungstocobaltate(III) at 25°C was studied by means of an ^{18}O tracer. Data from the experiments carried out on the ^{18}O content of $BaWO_4$ precipitated at 25°C from Na_2WO_4 solution are given. There was a relatively rapid exchange (within a few minutes) of ^{18}O between water and orthotungstate at 25°C. There seemed to be no appreciable exchange of oxygen between water and 12-tungstocobaltate(III). (F.J.H.)

14526 ELECTRONIC SPECTRA OF SOLUTIONS OF EUROPIUM AND YTTERBIUM IN LIQUID AMMONIA. Thompson, D. S.; Schaefer, D. W.; Waugh, J. S. (Massachusetts Inst. of Tech., Cambridge). Inorg. Chem., 5: 325-6(Feb. 1966).

The electronic spectra of solutions of europium and ytterbium in liquid ammonia at −45°C are shown. The approximate mole ratios for the metals are $Eu/NH_3 = 9 \times 10^{-5}$ and $Yb/NH_3 = 5 \times 10^{-5}$. The absorptions in divalent Eu ascribed to transitions between the $^8S_{7/2}$ ground state with its seven optical electrons in the 4f shell and the excited states having one of these 4f electrons in a 5d, 6s, or 6p state. The two broad bands observed in the visible and near-ultraviolet are characteristic of both divalent europium and ytterbium. The integrated intensities of the paramagnetic resonance signals of both the Eu species and the solvated electron species showed similar linear decays with time. (F.J.H.)

14527 PHOTOCHEMICAL FORMATION OF KRYPTON DIFLUORIDE FROM KRYPTON AND FLUORINE OR OXYGEN DIFLUORIDE. Streng, L. V.; Streng, A. G. (Temple Univ., Philadelphia). Contracts AF 04(611)-9555; Nonr 3085(01). Inorg. Chem., 5: 328-9(Feb. 1966).

Photochemical formation of KrF_2 from equimolar mixtures of Kr and F_2 or Kr and OF_2 by exposing them to sunlight for 5 weeks in dry glass flasks at room temperature and at a total pressure of 1 atm absolute is reported. When the same flasks with $Kr-F_2$ or $Kr-OF_2$ mixtures were kept in the dark for the same period of time there was no formation of krypton fluoride crystals. The products were analyzed by thermal decomposition and measuring and analyzing the gas evolved. (F.J.H.)

14528 THE REFRACTIVE INDEX AND MOLAR REFRACTION OF XENON OXIDE TETRAFLUORIDE. Selig, H.; Chernick, C. L.; Williams, C. W. (Argonne National Lab., Ill.). Inorg. Nucl. Chem. Lett., 1: 17-20(1965).

The refractive index and density of $XeOF_4$ were measured. The $XeOF_4$ was prepared by partial hydrolysis of XeF_6. The refractive index on two samples was 1.4279 at 4861Å, 1.424 at 5460Å, and 1.4215 at 5893Å. The density at 30.50°C was 3.071 g/cm^3 and the measurements obeyed the equation $d = 3.168 - 0.0032t$. (M.C.G.)

14529 RAMAN POLARIZATION STUDIES OF SEVERAL NITRATO COMPLEXES. Ferraro, J. R.; Walker, A.; Cristallini, C. (Argonne National Lab., Ill.). Inorg. Nucl. Chem. Lett., 1: 25-7(1965).

Raman polarization measurements on the liquid complex $Th(NO_3)_4 \cdot 2TBP$ and several rare earth $(NO_3)_3 \cdot 3TBP$ indicated that the high-frequency bands at about 1550 cm^{-1} are polarized and that the low-frequency bands at about 1300 cm^{-1} are depolarized. It was concluded that in this complex the bonding to the nitrate is definitely bridging or bidentate. (F.J.H.)

14530 ROENTGENOGRAPHIC STUDIES OF LANTHANUM TELLURIDES. Eliseev, A. A.; Yarembash, E. I.; Kuznetsov, L. I.; Antonova, L. I.; Stoyantsova, Z. P. (Kurnakov Inst. of General and Inorganic Chemistry, Academy of Sciences, USSR). Izv. Akad. Nauk SSSR, Neorg. Mater., 1: 1027-38(July 1965). (In Russian).

In the lanthanum–tellurium system the phases LaTe, $La_{3-x}Te_4$, $LaTe_{2-x}$, and $LaTe_{3-x}$ were confirmed and the phases $LaTe_{1.71x}$ and La_2Te_5 were established for the first time. For all these phases the range of homogeneity was determined and the phase diagram of the La–Te system was constructed. LaTe with the cubic structure type NaCl (a = 6.422 ± 0.001 Å) has a very narrow range of homogeneity. $La_{3-x}Te_4$ with a cubic structure of the Th_3P_4 type has a homogeneity range in the interval from La_3Te_4 (a = 9.621 ± 0.001 Å) to La_2Te_3 (a = 9.619 ± 0.001 Å) with vacancies in the La position. $LaTe_{1.71x}$ with a rhombic lattice (a = 4.622 ± 0.003, b = 4.497 ± 0.002, and c = 9.142 ± 0.003 Å) with the space group Pmmn and unknown structure has a range of homogeneity in the interval from $LaTe_{1.6}$ to $LaTe_{1.78}$ (61.0 to 64.0 at. % Te). $LaTe_{2-x}$ with a tetragonal laminated structure of the Cu_2Sb type (a = 4.552 ± 0.003 and b = 9.178 ± 0.006 Å and c/a = 2.017) has a range of homogeneity in the interval from $LaTe_{1.8}$ to $LaTe_2$(64.0 to 66.5 at. % Te) with vacancies in the 2(a) tellurium position. $LaTe_{3-x}$ with a tetragonal lattice in the space group $p4_2/n$ and unknown structure (a = 4.405 and c = 25.90 ± 0.10 Å and c/a = 5.9) has a range of homogeneity in the interval from $LaTe_{2.55}$ to $LaTe_3$ (71.4 to 75.0 at. % Te) with supposed vacancies in the tellurium position. On the basis of crystallochemical analogy with compounds of the MTe, M_3Te_4, and MTe_2 type, the existence of phases of the type $MTe_{1.71x}$ and M_2Te_5 was assumed in the tellurides of other rare earth elements from La to Sm. (tr-auth)

14531 CHEMICAL AND THERMAL STABILITY OF SCANDIUM BORIDES. Lyutaya, M. D.; Akinina, Z. S. (Inst. of Problems in Metallography, Academy of Sciences, Ukrainian SSR). Izv. Akad. Nauk SSSR, Neorg. Mater., 1: 1039-43(July 1965). (In Russian).

The interaction of ScB_2 and ScB_{12} with concentrated and dilute acids was investigated. The chemical stability of scandium borides seemed to be connected with their crystalline structure; with complication of the structure elements from the boron atoms the chemical stability increased. Scandium diboride was less stable; it readily reacted with salts and acids. The stability of scandium dodecaboride was much higher with respect to the same acids. This property of different stabilities was used for the separation of pure phases of ScB_{12}. The thermal stability of scandium borides was also investigated. It is shown that scandium borides, during heating in air, are stable at temperatures up to 600°C. At 700°C scandium boride gradually began to decompose and the decomposition was accompanied by formation of scandium oxyborides. (tr-auth)

14532 NEW TERNARY COMPOUNDS WITH $W_2Cr_{21}C_6$ TYPE STRUCTURE. Kuz'ma, Yu. B.; Voroshilov, Yu. V.; Cherkashin, E. E. (Lvov State Univ.). Izv. Akad. Nauk SSSR, Neorg. Mater., 1: 1109-11(July 1965). (In Russian).

By the method of x-ray structure analysis, the existence of the compounds $Sb_2Co_{21}B_6$, $Sb_2Ni_{21}B_6$, $U_2Co_{21}B_6$, and $U_2Ni_{21}B_6$, having the structure type $W_2Cr_{21}C_6$, was established. The lattice parameters of these compounds were determined and tabulated. For the compositions $R_2X_{21}B_6$ (R = Y, Cd, Ag, and Pb and X = Co and Ni), $R_2Fe_{21}B_6$ (R = V, Zr, Nb, Mo, and W), and $R_2Cu_{21}B_6$ (R = Mn, Zr, Nb, and Mo), compounds isostructural with the τ-phases were not detected. It was established that the ratio of the atomic radii r_R/r_X of the type $W_2Cr_{21}B_6$ borides was in the interval 1.04 to 1.31 (R component with large atomic radius and X = Co and Ni). (tr-auth)

14533 ZIRCONIUM–COBALT–BORON SYSTEM. Kuz'ma, Yu. B.; Lakh, V. I.; Voroshilov, Yu. V.; Stadnykh, B. I. (Lvov State Univ.). Izv. Akad. Nauk SSSR, Neorg. Mater., 1: 1112-14(July 1965). (In Russian).

The systems Zr–Co and Zr–Co–B were investigated by the method of x-ray structure analysis. In the system Zr–Co the existence of the compounds Zr_6Co_{23}, with the structure type Th_6Mn_{23} and a = 11.53 Å, and Zr_3Co was established. For the system Zr–Co–B, the isothermal profile at 800°C was constructed. In this system two ternary compounds exist: the τ-phase $Zr_2Co_{21}B_6$ (structure type $W_2Cr_{21}B_6$ and a = 10.597 Å) and ρ-phase with the approximate composition $ZrCo_3B$. (tr-auth)

14534 SYNTHESIS AND PROPERTIES OF INTERMEDIATE LANTHANUM, CERIUM, PRASEODYMIUM, AND NEODYMIUM TUNGSTATES. Plyushchev, V. E.; Amosov, V. M. (Moscow State Univ.). Izv. Akad. Nauk SSSR, Neorg. Mater., 1: 1155-61(July 1965). (In Russian).

Formation of La, Ce, Pr, and Nd tungstates by high-temperature synthesis was studied and the physical and chemical properties of $La_2O_3 \cdot 3WO_3$, $Ce_2O_3 \cdot 3WO_3$, $Pr_2O_3 \cdot 3WO_3$, and $Nd_2O_3 \cdot 3WO_3$ are described. (tr-auth)

14535 REACTIONS OF LANTHANUM NITRATE WITH AMMONIUM CARBONATE IN SOLUTION. Golub, A. M.; Maidukova, T. P. (Inst. of Reagents and Highly Pure Substances, USSR). Izv. Akad. Nauk SSSR, Neorg. Mater., 1: 1166-70(July 1965). (In Russian).

The system $La(NO_3)_3$–$(NH_4)_2CO_3$–H_2O was investigated by solubility, potentiometry, and conductometry and by measurements of the apparent total sedimentation. It was established that the interaction of lanthanum nitrate with ammonium carbonate proceeds in one stage with the formation of intermediate $La_2(CO_3)_3 \cdot 8H_2O$. This was confirmed by chemical, thermal, and microscopic analysis of the separated precipitates. (tr-auth)

14536 STRUCTURE, ELECTRIC CONDUCTIVITY, AND CONDUCTIVITY CHARACTERISTICS IN THE TERNARY SYSTEM (0.75 CeO_2–0.25 ZrO_2)–CaO. Volchenkova, Z. S.; Strekalovskii, V. N.; Pal'guev, S. F. (Inst. of Electrochemistry, Academy of Sciences, USSR). Izv. Akad. Nauk SSSR, Neorg. Mater., 1: 1171-6(July 1965). (In Russian).

The specific electric conductivity of samples of ternary oxides of the system (0.75 CeO_2–0.25 ZrO_2)–CaO was examined in a composition interval from 0 to 100 mol % CaO and a temperature interval from 500 to 1000°C. The temperature coefficient of the total electric conductivity of these samples was calculated. The phase constituents of samples of different composition were determined by x-ray analysis. The wide range of existence of solid solutions with structures of the floride type was established. It is shown that with increasing additions of calcium oxide a change of the parameters of the elementary cell of the solid solution occurred. This phenomenon was examined in the light of data on the effect of the total electric conductivity and data on the determination of the transfer number of ions and electrons. (tr-auth)

14537 MORE ON THE POLYMORPHISM OF RARE EARTH PYROSILICATES. Lazarev, A. N.; Tenisheva, T. F.; Bondar, I. A. (Grebenshchikova Inst. of Silicate Chemistry, USSR). Izv. Akad. Nauk SSSR, Neorg. Mater., 1: 1207-9(July 1965). (In Russian).

The high-temperature modification of the crystal $Y_2Si_2O_7$ is similar to the structure of the pyrosilicates of Gd to Ho, but the low-temperature modification is similar to the pyrosilicates of Er to Lu and Sc. The form of the antisymmetric oscillation band Si–O–Si in the infrared spectrum of $Sc_2Si_2O_7$ indicates the flexibility of this bond. There is significant freedom of internal rotation and deformation of the Si–O–Si angle. The growth, in comparison with $Sc_2Si_2O_7$, of the elementary cells of isostructural $Er_2Si_2O_7$ and $Y_2Si_2O_7$ is possible. (tr-auth)

14538 REACTIONS OF VANADIUM WITH LIQUID ELEMENTS OF THE PERIODIC TABLE. Efimov, Yu. V. (Baikov Inst. of Metallurgy, USSR). Izv. Akad. Nauk SSSR, Neorg. Mater., 1: 1298-1305(Aug. 1965). (In Russian).

The possibility of interaction in the liquid state in binary systems of V was analyzed for 83 elements. On the basis of one Hildebrand factor or Mott number, the existence of miscibility or immiscibility with V could be predicted for

electropositive and transition metals only. The comparison of the Hildebrand inequality and the Mott number is necessary to derive the fusion temperature of the metals considered. The evaluation of this criterion at room temperature gives the least precise and incomplete results. With electropositive and transition metals, miscibility with V was observed at: $\frac{1}{2}(V_1 + V_2)(\delta_1 - \delta_2)^2 < 2RT$, or $k < 2$; and immiscibility was observed at: $\frac{1}{2}(V_1 + V_2)(\delta_1 - \delta_2)^2 < 6RT$, where V is the atomic volumes and δ is the square root of the heat of sublimation divided by V. At $2 < k < 6$ miscibility is partial. At $2RT < \phi < 6RT$ in systems where the miscibility is the greatest, the formation of simple eutectics is characteristic. The interaction at $2 < k < 6$ depends on the size of the factors. Statistical curves for the Mott numbers calculated at the fusion temperature of V were constructed. From the Hildebrand factor vs absolute magnitude of the difference of the electronegativity diagram the miscibility of V and the electronegative metals and metalloids could be successfully analyzed. The solubility of electronegative metals and metalloids in liquid V is connected to the formation of compounds in this system. This method of analysis makes it possible to evaluate not only the interaction in the liquid state, but in some cases to predict the general outline of the constitution diagram. (tr-auth)

14539 ON THE FORMATION OF LANTHANUM, PRASEODYMIUM AND NEODYMIUM ALUMINATES. Godina, N. A.; Keler, E. K. (Grebenshchikov Inst. of Chemistry of Sieicates, Academy of Sciences, USSR). Izv. Akad. Nauk SSSR, Ser. Khim., 1: 24-31(1966). (In Russian).

In the systems $La_2O_3-Al_2O_3$, $Pr_2O_3-Al_2O_3$, and $Nd_2O_3-Al_2O_3$, two types of compounds are formed: $Ln_2O_3 \cdot Al_2O_3$ and $Ln_2O_3 \cdot 11Al_2O_3$. The conditions for the formation of compounds during the reaction of the oxides of La, Pr, and Nd with α-alumina and aluminum nitrate and in coprecipitated solutions containing Al and La ions were investigated. The process for the formation of compounds $Ln_2O_3 \cdot 11Al_2O_3$ appeared to be a step process. In the reaction of aluminum oxide with the oxides of the rare earth metals the monoaluminate appeared in the intermediate stages and reacted with aluminum oxide to form the compound $Ln_2O_3 \cdot 11Al_2O_3$ after an additional temperature increase. The production of monoaluminate from α-Al_2O_3 and the rare earth oxides requires temperatures of 1600 to 1650°C whereas the utilization of aluminum nitrate in the synthesis occurs at 1200°C. In coprecipitation of equal molecular compositions, chemical compounds were formed in x-ray amorphous gels at 400°C but did not crystallize up to temperatures of 800°C. An hypothesis on the formation of compounds in the coprecipitation process is given. The γ form of Al_2O_3 formed during the decomposition of the aluminum nitrate in the presence of rare earth oxides was stable up to 1300°C. (tr-auth)

14540 CONDUCTANCE OF IONS IN LIGHT AND HEAVY WATER AT 25 deg. Swain, C. Gardner; Evans, D. Fennell (Massachusetts Inst. of Tech., Cambridge). J. Amer. Chem. Soc., 88: 383-90(Feb. 5, 1966).

Conductances of potassium fluoride, potassium chloride, potassium bromide, potassium iodide, sodium chloride, cesium chloride, potassium benzoate, potassium p-toluenesulfonate, and tetra-n-butylammonium bromide were determined in the range from $5-90 \times 10^{-4}$ M in both protium oxide and deuterium oxide at 25°C, using 1 liter of solvent for each salt. Limiting ionic equivalent conductance ratios, calculated by combining these data for the salts with the transference numbers of Longsworth, varied from 1.198 for potassium and cesium ions to 1.229 for tetra-n-butylammonium and 1.235 for fluoride ions. These limiting conductance ratios are treated as solvent isotope effects arising from changes in zero-point librational energy of the solvating waters on going from the ground state to the transition state. Assuming four solvating waters in the ground state, the librational frequencies were calculated for various numbers of water molecules around the ion at the transition state. Since the average librational frequency was less for the transition state than for the reactant ions, three waters appeared unreasonable. An addition-elimination mechanism for conductance is proposed in which the ion has five solvating water molecules at the transition state. (auth)

14541 THE FLUORIDES AND OXIDES OF HELIUM AND NEON. Allen, Leland C.; Lesk, Arthur M.; Erdahl, Robert M. (Princeton Univ., N. J.). J. Amer. Chem. Soc., 88: 615-16(Feb. 5, 1966).

High-accuracy, many-electron, valence-bond wave functions were obtained for HeF, HeO, NeF, NeF_2, and NeO. The potential energy curves for all of these species were repulsive. The valence-bond wave functions were constructed using the exact Hamiltonian with simultaneous inclusion of all the electrons. The NeO wave function includes the chemical structures NeO, Ne^+O^-, and $Ne^{2+}O^{2+}$, and is composed of 16 states made up from twenty-four 18×18 determinants. The chemically significant terms in the wave functions for the various species are given. Among the singly ionized states there are three in NeO and one in HeO that significantly lower the energy through formation of electron-pair bonds between open shells on each atom. Hybridization in the ionic states is discussed for these compounds. (F.J.H.)

14542 CATALYTIC ACTIVITY OF NOBLE ALLOYS. METHANE-DEUTERIUM EXCHANGE AND PROPANE CRACKING ON PLATINUM-PALLADIUM AND PALLADIUM-RHODIUM ALLOYS. McKee, D. W.; Norton, F. J. (General Electric Research Lab., Schenectady, N. Y.). J. Catalysis, 3: 252-67(June 1964).

The exchange reaction between methane and deuterium and the cracking of propane in the temperature range 100 to 200°C were used to study variations in catalytic activity in the Pt–Pd and Pd–Rh alloy series. Stepwise exchange was exhibited by both Pt and Pd, CH_3D being the most abundant initial product and the other deuteromethanes appearing in order. Rhodium showed predominantly multiple exchange at the higher temperatures with the initial appearance of CD_4. Stepwise exchange was the most important mechanism with all alloy samples although the contribution of multiple exchange increased with increasing temperature. The order of activity of the pure metals followed the sequence Pt > Rh > Pd at 150° for both exchange and cracking reactions and the binary alloys showed intermediate activities. A rough correlation between atomic radius and exchange mechanism was observed and the mechanism of the exchange reaction is discussed. It appears that stepwise exchange proceeds via the initial dissociation of a C–H bond and the formation of chemisorbed methyl radicals on the metal surface. As the metal is initially covered with strongly adsorbed deuterium atoms, it is likely that this dissociation arises from a Rideal-Eley type of interaction between gas phase methane and surface D atoms. (BBB)

14543 ELECTRON CORRELATION AND THE NUCLEAR SPIN-SPIN COUPLING CONSTANT. I. AN ALTERNANT MOLECULAR ORBITAL DESCRIPTION OF NUCLEAR SPIN-SPIN COUPLING. Barfield, Michael (Univ. of Arizona, Tucson). J. Chem. Phys., 44: 1836-44 (Mar. 1, 1966).

A theoretical description of contact nuclear spin–spin coupling is presented in terms of the density-matrix formalism and the approximation of an average excitation energy. For a molecular system in a singlet state the density of spin coupling is proportional to the difference between the correlation functions for electrons of the same and opposite spins. Application of the one-parameter alternant molecular orbital (AMO) method, which includes both types of correlation in an easily visualizable manner, yields expressions for the density of spin coupling in alternant systems of 2n electrons. In the case of directly bonded systems of two electrons, correlation between electrons of antiparallel spins make a significant contribution to the coupling constant. Coupling constants between nuclei separated by two and three bonds were examined by the AMO expressions in the tight-binding approximation. In contrast to the single-determinant results, a long-range spin

correlation is implicit in the AMO description, and, depending on whether the nuclei are in the same or different subsets of the alternant system, this term alternates in sign. (auth)

14544 TEMPERATURE-INDEPENDENT FACTOR IN ISOTOPIC RATE-CONSTANT RATIOS. Gatz, Carole R. (Portland State Coll., Oregon). J. Chem. Phys., 44: 1861-4(Mar. 1, 1966).

A general expression is given for the temperature-independent factor (TIF) in isotopic rate-constant ratios, in terms of the reaction coordinate (a linear combination of internal displacement coordinates) and the G matrix for the transition state. Values of TIF for some three-center carbon models are given for reaction coordinates that include simultaneous changes in bond angle and bond lengths. (auth)

14545 LOW-ENERGY ATOMIC COLLISIONS. I. THE SCHROEDINGER EQUATION FOR H+-H. Kouri, Donald J.; Curtiss, C. F. (Univ. of Wisconsin, Madison). J. Chem. Phys., 44: 2120-30(Mar. 1, 1966).

The Schrödinger equation for the system H^+-H is considered. After the usual separation of the center-of-mass coordinates, group theoretic methods were used to eliminate three degrees of freedom associated with the rotational motion of the system. This was done in a manner that treats the protons symmetrically, thereby enabling the symmetry character of the wave functions to be easily established. The result is in a form that is convenient in the study of scattering. (auth)

14546 MEASUREMENT OF THE LATTICE CONSTANT IN THE DIHYDRIDES OF GADOLINIUM–YTTRIUM ALLOYS. Uhrich, David L. (Univ. of Pittsburgh). J. Chem. Phys., 44: 2202-3(Mar. 1, 1966).

The lattice parameters of several compounds of the approximate composition $[Gd_xY_{1-x}]H_2$ were determined at room temperature using x-ray-diffraction techniques. The pure dihydrides of the alloys exhibited a linear decrease in the lattice parameters as Gd content was reduced. For x = 1 and x = 0.5 a lattice contraction of ≈0.01Å was observed as the hydrogen-to-metal ratio was increased from 2.0 to 2.99. This was consistent with similar contractions observed in other lanthanide hydrides. (F.J.H.)

14547 EPR STUDIES OF DEFECT SITES IN THULIUM ETHYLSULFATE CRYSTALS. Dearman, Henry H. (Univ. of Chicago). J. Chem. Phys., 44: 2218-19(Mar. 1, 1966).

Results of an EPR study of defect sites in undiluted crystals of thulium ethylsulfate crystals, $Tm(C_2H_5SO_4)_3 \cdot 9H_2O$, are reported. Two low-field doublets were observed at 4.2°K. They obeyed the relation H sin Θ = constant, where Θ is the angle between the magnetic-field direction and the c axis of the crystal. Crystal alignment was effected by making use of the angular dependence of the EPR spectra of known-impurity rare-earth ions, that were present in the sample. At the microwave frequency of 8732 mC sec^{-1} the centers of the doublets occurred at 419.5 and 450.5G. The splitting of both doublets at Θ = 90° was 228 ± 1G. The four lines had normal Lorentzian line shapes. The width of an individual line varied from 9G at Θ = 90° to 250G at Θ = 3.3°, which corresponded to resonances at the highest magnetic field (~12 KG). The intensity of each component of a doublet was the same; however the lower-field doublet was usually about twice as intense as the higher. The intensity ratio varied slightly in different crystals. All lines increased in intensity with decreasing temperature. These results indicated that there were two slightly different defect sites of low symmetry in the crystal. (F.J.H.)

14548 STUDY BY DIFFERENTIAL THERMAL ANALYSIS, RADON RELEASE, AND RADIOCRYSTALLOGRAPHY OF THE THERMAL DECOMPOSITION OF β LEAD DIOXIDES OF DIFFERENT TEXTURE. Fouque, Daniel; Fouilloux, Pierre; Bussiere, Paul; Weigel, Dominique; Prettre, Marcel (CNRS, Villeurbanne, France). J. Chim. Phys., 62: 1088-94(Oct. 1965). (In French).

The thermal evolution, during linear increases in temperature in nitrogen atmosphere at atmospheric pressure of two lead dioxides of the β type with different texture was studied. One had a specific surface of 1.3 m^2/g and the other 18.5 m^2/g. The first decomposed by the scheme $\beta\text{-}PbO_2 \rightarrow \alpha\text{-}PBO_x \rightarrow Pb_3O_4 \rightarrow PbO$ at 400 to 600°C. The second had the following transformation scheme: $\beta\text{-}PbO_2 \rightarrow \alpha\text{-}PbO_x \rightarrow \beta\text{-}PbO_x \rightarrow PbO$ at 350 to 500°C. A topochemical decomposition process was detected for the second. (tr-auth)

14549 A SUGGESTED MODIFICATION TO THE PERIODIC CHART. Villar, G. E. (Univ. of Montevideo, Uruguay). J. Inorg. Nucl. Chem., 28: 25-9(Jan. 1966).

Study of the emission spectra of the actinide elements proved that their electronic structures are characterized by the successive additions of electrons to an inner 5*f* shell. Therefore, the actinide elements constitute an *f*-transition series corresponding to a special place in the periodic chart, outside of the d-transition series where the actinide elements are often situated. For this reason modifications to the periodic chart are suggested: the places occupied by the lanthanide elements and the actinide elements would be occupied only by lutetium and lawrencium, which would be not *f*-transition elements but d-transition elements. The places of lanthanide and actinide elements would be between barium and lutetium, and between radium and lawrencium. (auth)

14550 THE HEAT CONTENT OF CRYSTAL-BAR THORIUM. Levinson, L. S. J. Nucl. Mater., 19: 50-2 (Apr. 1966). (LA-DC-7136).

The heat contents of α- and β-phase thorium were measured between 1269 and 1650°K and 1667 and 1991°K respectively, and that of molten thorium at 2069 and 2100°K, using a drop calorimeter. Estimates of the heat of transition, $\beta \rightarrow \alpha$-phase, 857 ± 28 cal/mole and the heat of fusion, $3.3 \times 10^3 \pm 300$ cal/mole, were made. (auth)

14551 THE WETTING OF UC BY COPPER AND GOLD. Nicholas, M.; Poole, D. M. (United Kingdom Atomic Energy Authority, Harwell, Eng.). J. Nucl. Mater., 19: 117-19(Apr. 1966). (AERE-R-4843).

A contact angle of 128° was observed between Cu and UC at 1100°C. Increasing the temperature caused the contact angle to decrease, values of less than 90° were observed above 1350°C. A sluggish chemical reaction occurred if the samples were held at temperature, causing the contact angle to decrease slowly with time in a complex manner. The behavior of Au was similar, but much more time- and temperature-dependent. (W.L.G.)

14552 PRODUCTION OF URANIUM DIOXIDE BY ELECTROCHEMICAL REDUCTION OF U(VI) IN SODIUM CARBONATE SOLUTIONS AT A MERCURY CATHODE. II. CHEMICAL PROCESSES OCCURRING IN CARBONATE SOLUTIONS AFTER THE REDUCTION OF U(VI). Perec, M. (Instytut Badan Jadrowych, Warsaw). Nukleonika, 10: 693-703(1965). (In Polish).

Investigations on the precipitation of UO_2 from carbonate solutions after the reduction of U(VI) were carried out with the use of polarographic techniques for process control. U(V) disproportionation in solutions of sodium carbonates was found to be reversible. At pH 9.5 the precipitation of hydrated UO_2 occurs between the U^{4+} ion present in equilibrium with the $[U(CO_3)_5]^{6-}$ complex and OH^- ions. At pH values over 10.6 the precipitation of UO_2 results probably from the exchange between the OH^- ions and the CO_3^{2-} groups in the aquo- and aquohydroxyuranium carbonate complexes. The U(V) and U(VI) ions do not take part in the process of precipitation of UO_2. (auth)

14553 ABSORPTION SPECTRUM OF Ce^{3+}-IONS AND CRYSTAL FIELD IN La(Ce)Cl. Hellwege, K. H.; Orlich, E.; Schaack, G. Phys. Kondens. Mater., 4: 196-206 (1965). (In German).

The absorption spectrum of single crystals of $La_{(1-x)}Ce_xCl_3$ (x = 0.05 ... 0.005) was observed at low temperatures in the region of the 4f → 4f infrared transitions. Values for the crystal-field parameters V_2^0, V_4^0, V_6^0, and V_6^6 and for the spin-orbit coupling constant of the ion in the crystalline environment were determined by fitting the observed splittings of the multiplet-components $^2F_{5/2}$ and $^2F_{7/2}$ in the crystal

field. The parameters were found to be consistent with values extrapolated from rare earth ions with neighboring atomic numbers in the same host-lattice. The only exception was the parameter V_6^6, which was found to be smaller in La(Ce)Cl_3 than in other rare earth trichlorides ($V_6^6/V_6^0 = -6.23$ in La($CeCl_3$, $V_6^6/V_6^0 \approx -10$ in other trichlorides). The correct relation V_6^6/V_6^0 in La(Ce)Cl_3 was obtained by fitting the parameters to the observed crystal-field splitting of the $^2F_{5/2}$ component and to the observed Zeeman-splitting factors taken from the literature. The discrepancies between the two fitting procedures are explained by an effect of nonlinear shielding of the crystal field. (auth)

14554 STUDY OF NIOBIUM AND TANTALUM SULFIDES. Obolonchik, V. A.; Rodzikovskaya, S. V.; Bukhanevich, V. F. (Inst. of Problems in Metallography, Academy of Sciences, Ukrainian SSR). Porosh. Met., Akad. Nauk Ukr. SSR, 11: 9-14(1965). (In Russian).

The reaction of metallic niobium and tantalum powders with hydrogen sulfide was investigated. At 1000 to 1300°C niobium sulfide $NbS_{1.6}$ was obtained, and at 1400°C tantalum disulfide. The parameters of the lattices and the pycnometric density were determined; the resistance in various media and the oxidation resistance were studied. (auth)

14555 INTERACTION OF DIBORIDES OF VANADIUM, NIOBIUM AND TANTALUM WITH CARBON. Levinskii, Y. V.; Salibekov, S. E.; Levinskaya, M. Kh. Porosh. Met., Akad. Nauk Ukr. SSR, 11: 66-9(1965). (In Russian).

Thermal, metallographic, and roentgen analyses showed that the systems vanadium diboride–carbon, niobium diboride–carbon, and tantalum diboride–carbon are pseudobinary and eutectic in nature. The temperature and composition of the eutectic were established. In obtaining compact parts from powders of vanadium, niobium, and tantalum diborides by pressing in graphite molds, the pressing temperature must not exceed 2500 to 2600°K. (auth)

14556 FORMATION OF PENTAVALENT NEPTUNIUM COMPLEXES IN LACTATE AND GLYCOLATE SOLUTIONS. Moskvin, A. I.; Mefod'eva, M. P. Radiokhimiya, 7: 410-19(1965). (In Russian).

Data were obtained on the complex formation of NpO_2^+ ion with lactic and glycolic acids. The distribution of Np(V) between the cationite KU-2 and lactic acid solutions of different concentrations was studied. The equilibrium concentration of different forms of Np(V) as a function of the concentration of lactic acid is shown. The concentration of lactic acid was varied from 0.005 to 0.2M. The ionic strength values were $\mu = 0.05$ and $\mu = 0.2$. Two lactate complexes were discovered: $[NpO_2Lact]^0$ and $[NpO_2(Lact)_2]$. The concentration stability constants for these two complexes are: $\beta_1 = 51 \pm 1$, $\beta_2 = (3.0 \pm 1.0) \cdot 10^2$ ($\mu = 0.05$) and $\beta_1 = 36 \pm 1$, $\beta_2 = (1.6 \pm 0.1) \cdot 10^2$ ($\mu = 0.2$), respectively. Electrophoresis produced distribution curves, which showed that in lactate solutions the neutral complex is predominant. In glycolate solutions of complexes only an electrically neutral complex of Np(V) was formed. The stability constant of this complex was 40 ± 7. The thermodynamic equilibrium constants were calculated and are listed with those of other neptunyl complexes. (CFSTI)

14557 STUDY OF THE $NaBeF_3$–$NaPO_3$ SYSTEM BY THE EMANATION METHOD. Levina, M. E.; Shershev, B. S.; Zaborenko, K. B. Radiokhimiya, 7: 480-2(1965). (In Russian).

Studies were made to determine more accurately the phase diagram of the $NaBeF_3$–$NaPO_3$ system, which was previously studied by means of thermal analysis, and to investigate chemical reactions of mixtures in the solid state, which would give additional data concerning this system. The phase diagram of the $NaBeF_3$–$NaPO_3$ system consist of a continuous series of solid solutions. Radiothorium chloride was introduced as an alcoholic solution into finely ground $NaBeF_3$ powder, which was then thoroughly mixed and dried. The active $NaBeF_3$ was mixed in appropriate molar ratios with $NaPO_3$. The mixture was placed into a Pt crucible and heated in the metal block of an electric furnace. The temperature was measured with a Pt–Pt/Rh thermocouple. The ionization chamber was used for measuring the α activity of thoron. The experimental data obtained by this method verified the existence of a liquidus curve of the continuous series of solid solutions in the investigated system. (CFSTI)

14558 STUDY OF THE $KBeF_3$–KPO_3 SYSTEM BY THE EMANATION METHOD. Levina, M. E.; Shershev, B. S.; Zaborenko, K. B. Radiokhimiya, 7: 483-6(1965). (In Russian).

The phase diagram and solid-state chemical reactions of the $KBeF_3$–KPO_3 system were studied by the radioactive emission method with emphasis on the region of the diagram in the 10 to 40 mole % KPO_3 range. The beryllium glasses formed in this region are the most transparent in ultraviolet or infrared spectral regions, and the most weatherproof of all the glasses in the system. The curves of emissive power versus temperature of the sample indicated that a chemical reaction in the solid state started at 200 to 220°C. Earlier DTA data obtained are confirmed, indicating the formation of a $KBeF_3$–KPO_3 compound with a melting point of 495 to 500°C, which formed two eutectics with the pure components of the system. The peaks of the emission curves from the eutectic mixtures containing 20 to 35 mole % KPO_3 indicated that the melting begins at 295 to 300°C for all these mixtures and ends at a temperature varying with the composition. The latter temperature data coincided with data determined earlier from the liquidus curve extrapolated because it was impossible to obtain experimental DTA data for this part of the phase diagram. (CFSTI)

14559 THIRD-ORDER POTENTIAL CONSTANTS OF BENT XY_2 MOLECULES. Kuchitsu, Kozo; Morino, Yonezo (Tokyo Univ.). Spectrochim. Acta, 22: 33-46 (Jan. 1966).

In pursuit of a method for predicting the cubic constants and the vibration-rotation interaction constants α of polyatomic molecules, the physical significance of the third-order constants (the cubic coefficients of the expansion of the internuclear potential function in terms of the internal coordinates) of the bent XY_2 molecule was studied. An anharmonic potential function of the valence-force type (which includes general quadratic force constants and a third-order coefficient of the bond-stretching displacements) is supplemented by a function that depends on the Y–Y distance as an empirical model, and the third-order constants are considered in relation to this function. The calculations, which make use of several empirical functions for the hydrogen–hydrogen and neon–neon interactions taken from the literature, showed that the signs (negative in most cases) and the orders of magnitude for the third-order constants of H_2O, D_2O, H_2S, H_2Se, D_2Se, SO_2, and OF_2 can be accounted for fairly satisfactorily by this model. This model is also able to make correct order-of-magnitude estimations for many of the cubic and the α constants of these molecules. In particular, the estimates of the α_2^A and α_2^B constants of H_2O, D_2O, SO_2, and OF_2 appeared in better agreement with the corresponding experimental values than those based on the valence-force model. The predictions based on the nonbonded interaction model, however, were found to be poor in some cases, for example, for the $f_{\tau\tau'\alpha}$ and α_1^A constants of OF_2. (auth)

14560 SPECTROSCOPIC INVESTIGATIONS OF SOME NEODYMIUM COMPLEXES. Sinha, S. P. (Cyanamid European Research Inst., Geneva). Spectrochim. Acta, 22: 57-62(Jan. 1966).

The solution and reflection spectra of some neodymium complexes containing ligands having oxygen donors and nitrogen donors were investigated. The red shifts of the visible and the near infrared bands were correlated with the covalency parameter δ. The carboxylates and β-diketonates showed weak covalent bonding. In the solid state, the nitrogen donor heterocyclic ligands and the oxide systems indicated strong metal-ligand covalent binding. In methanol solution, however, the nitrogen heterocyclic ligands are weakly bonded to the neodymium ion. The solvent effect on the spectrum of trivalent neodymium is also discussed. (auth)

14561 POLARIZATION IN ANODIC DISSOLUTION OF CERIUM METAL IN A FUSED EUTECTIC MIX OF LITHIUM AND POTASSIUM CHLORIDES. Sokolovskii, Yu. S.; Smirnov, N. V. Tr. Inst. Elektrokhim., Akad. Nauk SSSR, Ural. Filial, No. 5, 17-22(1964). (In Russian).

Polarization of the Ce-anode during electrolysis of a fused eutectic mix LiCl–KCl over current densities of 1.10 to 4–5 amp/cm^2 at 418 and 612°C is described. At densities above the metal dissolution point, anodic polarization of Ce is governed by the diffusion of its ions from the electrode layer into the deeper layers of the electrolyte. The anode potential is described by a linear equation for concentration polarization. At relatively low temperatures and high current densities (0.2–0.4 amp/cm^2) intense polarization occurs, with considerable fluctuation in potential due to the formation of solid salt phases on the anode surface. (Rev. Metal Lit.)

14562 POLARIZATION OF A MOLYBDENUM CATHODE IN ELECTROLYSIS OF THE SYSTEMS LiCl–KCl AND NaCl–KCl CONTAINING CERIUM TRICHLORIDE. Sokolovskii, Yu. S.; Smirnov, M. V. Tr. Inst. Elektrokhim., Akad. Nauk SSSR, Ural. Filial, No. 5, 23-31(1964). (In Russian).

Polarization of the Mo cathode in fused mixtures of LiCl–KCl at 400–600°C and NaCl–KCl at 700 to 900°C was studied. Ce deposition on the cathode is preceded by considerable residual currents caused chiefly by transformation of the alkali metal cations to subions and reduction of the additives. Ce metal deposits on the cathode at potentials close to the equilibrium at suitable concentrations and temperatures due to the direct charging of its ions. Its deposition can be accompanied by the reduction of the Ce ions alongside the cathode by the alkali metal subions and the formation of a suspension of metal in the electrolyte. Joint deposition of Ce and alkali metal occurs in fused LiCl–KCl with 3.5–10 wt % $CeCl_3$ at 400°C and current densities of 0.1–1 amp/cm^2 at 400°C and 0.2–2 amp/cm^2 at 600°C. Joint deposition also occurs in an equimolar mixture of NaCl–KCl with 1.5–7 wt % $CeCl_3$, at 700°C and 0.2–1 amp/cm^2 and 0.6–4 amp/cm^2 at 800°C. The limiting diffusion Ce ion discharge current is not reached with 15–20 wt % $CeCl_3$ and above. (Rev. Metal Lit.)

14563 REACTION OF TRIVALENT CERIUM IONS WITH FLUORIDE ANIONS IN A MEDIUM COMPOSED OF THE FUSED EUTECTIC LiCl–KCl. Smirnov, M. V.; Sokolovskii, Yu. S. Tr. Inst. Elektrokhim., Akad. Nauk SSSR, Ural. Filial, No. 5, 33-40(1964). (In Russian).

Equilibrium potentials were measured for Ce in fused eutectic LiCl–KCl containing 2.5–20 wt % LiF and 1.09–8.53 wt % $CeCl_3$ at 600–750°C. An equation was derived showing the relation between the equilibrium potential of Ce and temperature and Ce and F ion concentration in a fused system LiCl–KCl, in relation to a chloride reference electrode. In fluoride–chloride systems with (F)/(Ce) ratios of 5–40, trivalent Ce forms fluoride cation complexes between 850–1050°K. Experimental data afforded an expression for the instability constant of the mean statistical complex CeF_m. The constant is about 10^{-3}, which indicates the low strength of fluoride complexes of Ce in the fused eutectic mix LiCl–KCl. (Rev. Metal Lit.)

14564 ELECTRODE PROCESSES IN ELECTROLYSIS OF CERIUM IN CHLORIDE–FLUORIDE SYSTEMS. Sokolovskii, Yu. S.; Smirnov, M. V. Tr. Inst. Elektrokhim., Akad. Nauk SSSR, Ural. Filial, No. 5, 47-51(1964). (In Russian).

The polarization of a Ce anode in fused eutectic LiCl–KCl with additions of 5 and 10 wt % LiF at 617 and 733°C is described. Addition of F to the electrolyte does not have a marked effect on the polarization of the Ce anode in comparison with Cl systems, despite displacement of its potential to the negative side, 0.12 V at 617°C and 10 wt % LiF. Polarization of a Mo cathode in electrolysis of systems LiCl–KCl with 0–12 wt % $CeCl_3$ and 5–10 wt % LiF showed that the potentials of the Ce deposition sectors correspond to the equilibrium sectors as measured under the same conditions of temperature and Ce and F concentration in the fused system. (Rev. Metal Lit.)

14565 LANTHANUM TRICHLORIDE REACTION WITH A FUSED EUTECTIC MIX OF LITHIUM AND POTASSIUM CHLORIDES. Smirnov, M. V.; Krasnov, Yu. N.; Khazemov, F. F. Tr. Inst. Elektrokhim., Akad. Nauk SSSR, Ural. Filial, No. 5, 53-60(1964). (In Russian).

La passes into the system chiefly in the trivalent state. The equilibrium potentials of La in fused LiCl–KCl systems containing 0.348, 0.798, 1.70, 3.68, 7.17, 15.8, and 39.3 mole % $LaCl_3$ were measured over the 400–650°C range. With an La content up to 5 mole % in fused $LaCl_3$–LiCl–KCl systems, the latter behave like ideal diluted solutions. At higher concentrations there is a positive deviation from the ideal. An equation is derived showing temperature dependence of the equilibrium potential for fused systems containing up to 5 mole % $LaCl_3$ as related to a chloride reference electrode. From experimental and literature data on the thermodynamic aspects, the change in the Gibbs potential when liquid La trichloride is mixed with the fused eutectic LiCl–KCl were evaluated and activity coefficients were calculated for La^{3+} in fused systems. (Rev. Metal Lit.)

14566 PRECIPITATION OF SCANDIUM FROM HYDROCHLORIC ACID SOLUTIONS BY SODIUM SILICOFLUORIDE. Samodelov, A. P.; Merkulov, A. G.; Berseneva, G. T. Uch. Zap. Tsentr. Nauch. Issled. Inst. Olovyan Prom-Sti., No. 2, 46-9(1964). (In Russian).

Precipitation of Sc from solution by sodium silicofluoride was studied and the composition of the compound formed determined. The studies were based on the investigation of equilibrium in the system with constant metal concentration and variable precipitant concentration. It was found that, during precipitation of Sc from solution, a composite Sc fluoride of ScF_3–$3NaF_3$ type is formed in the residue with silicic acid impurities. In studying the effect of impurities on the degree of Sc recovery from sodium silicofluoride solutions, it was observed that such impurities as Fe, Mn, and Ti do not affect Sc precipitation while the presence of alkaline earth metals, particularly Ba, increases recovery from solution. In the presence of Al, precipitation of Sc from solutions is incomplete. (Rev. Metal Lit.)

14567 MOESSBAUER EFFECT IN TIN. Bontschev, Zv.; Christov, D.; Burin, Kl.; Mandzukov, Iv. (Univ., Sofia). Z. Phys., 190: 278-85(1966). (In German).

The results are presented of an investigation on SnH_4, analogous to methane, by means of the Mössbauer effect. A line was observed in the spectrum of the chemical whose width, extropolated to zero thickness of the absorber, corresponds to the characteristic width of the gamma line. The effect on broadening of the line was found to agree with the model for the tetrahedral structure of these types of molecules and with the SP-hybridization of the valence electrons. The isomer shift of –1.0 to 0.1 mm/s compared with beta-tin was found to be larger than the isomer shift for the chemical compound, –0.6 mm/s, determined from a nomogram. This is explained by the higher degree of ionic character of the Sn–H bond, which was determined also from the nomogram. The small effects, f' = 0.025 at –196°C, indicated that in this case the theory of Kagan is not applicable, in spite of which, for SnH_4 the maximum possible distinction between the measurements of both atomic forms was obtained. The temperature dependence of the effect for tin dissolved in ether tends to zero at about –120°C. Since the tin nucleus itself is not arranged in the lattice of the solid ether, but the molecule SnH_4, it is concluded that the temperature dependence of the resonance absorption of the molecule as a whole must be treated instead of the tin nucleus. (tr-auth)

14568 INFRARED SPECTRA OF PRODUCTS OF Nd_2O_3 REACTION WITH WATER. Glushkova, V. B.; Suglubov, D. N. Zh. Strukt. Khim., 6: 837-42(1965). (In Russian).

The infrared absorption spectra of neodymium hydroxide $Nd(OH)_3$, the oxide monohydrate, $Nd_2O_3 \cdot H_2O$, the compound $3Nd_2O_3 \cdot 2H_2O$, and the A-form of neodymium oxide, together with the analogous deuterated compounds, were investigated in the range from 400 to 4000 cm^{-1}. It is shown

that in the compounds studied water does not seem to crystallize, but is present in the form of hydroxyl groups, between which weak hydrogen bonds exist. (tr-auth)

14569 VISIBLE SPECTRA OF THE TWO STABLE ISOTOPIC SPECIES OF YTTRIUM MONOCHLORIDE [Thesis]. Janney, Gareth Maynard. Washington, D. C., Georgetown Univ., 1965. 129p.

Emission spectra of YCl^{35} and YCl^{37} were observed in the wavelength region 6300 to 6930 angstroms. The sources used were electrodeless discharge lamps containing either anhydrous YCl_3^{35} or YCl_3^{37} and helium at a pressure of 2 to 3 torr. The lamps were operated in an electric furnace at a temperature of approximately 800°C. The spectra were recorded in a Wadsworth mounting spectrograph using a 6-in. grating with a radius of 21 feet. The grating has 15,000 lines per inch and was used in the second order. The reciprocal dispersion in the observed wavelength region was approximately 2.0 angstroms per millimeter. The spectrum of each isotopic species of YCl consists of a single system of single headed bands shaded toward longer wavelengths. The wavelengths of sixteen band heads of the YCl^{35} spectrum and fourteen band heads of the YCl^{37} spectrum were measured and a vibrational analysis was made for each spectrum. The (0,0), (0,1), and (1,0) bands of both spectra contained some well-resolved rotational structure. Rotational analyses were made for these bands. The bands consist of single R and P branches, indicating that the electronic transition is of the $^1\Sigma$ to $^1\Sigma$ type. The dissociation limits were calculated by extrapolation from the vibrational data. The difference in the two dissociation limits is approximately equal to the excitation energy of the first excited state of atomic yttrium. The lower molecular state can be correlated with the two atomic ground states: $Cl(^2P) + Y(^2D)$. The upper molecular state can be correlated with the ground state of chlorine and the first excited state of yttrium: $Cl(^2P) + Y(^2D)$. The lower molecular state is probably the ground state of the molecule. The constants of YCl^{35} and YCl^{37} are given. (Dissertation Abstr.).

14570 THE ACCELERATION OF THE URANIUM(IV)–(VI) ELECTRON EXCHANGE REACTION BY HYDROCHLORIC ACID. Kakihana, H. (Tokyo Inst. of Tech.); Tomiyasu, H.; Gonda, K. Vienna, International Atomic Energy Agency, 1965, Preprint No. SM-64/8, 14p. (CONF-650549–4). ORINS.

From IAEA Symposium on Exchange Reactions, Upton, N. Y.

The homogeneous exchange reaction between natural uranium(IV) and depleted uranium(VI) was studied in various concentrations of HCl at 30, 50, and 70°C. At several steps of the exchange process of each experiment uranium(VI) was separated from uranium(IV) by solvent extraction and the ratio of uranium isotopes was determined by a mass spectrometer. The exchange reaction was found to be catalyzed by large concentrations of chloride, while inhibited by small concentrations of HCl. The exchange rates at 30°C were 1.34×10^{-4}, 3.50×10^{-3}, and 2.85×10^{-2} M^{-1} min^{-1} for 6M, 8M, and 10M HCl, respectively, while practically no exchange reaction was observed in 2M and 4M HCl. The activation energies were estimated as 25.3, 24.5, and 23.8 kcal/mole for 6M, 8M, and 10M HCl respectively. The increased rate above 6M HCl was about twelfth order in chloride concentration and fifth order in chloride activity. The concentration of uranium(VI) had no appreciable influence on the exchange rate in 8M HCl, while the rate was first order in uranium(IV) concentration. This exchange process was explained by assuming the formation of highly reactive activated complexes containing uranium(IV), uranium(VI), and both bridging and nonbridging chloride ions. (auth)

14571 THE CHLORIDE ION CATALYZED IRON(II) + IRON(III) ISOTOPE EXCHANGE IN DIMETHYLSULFOXIDE. Wada, G.; Reynolds, W. L. (Univ. of Illinois, Urbana). Vienna, International Atomic Energy Agency, 1965, Preprint No. SM-64/15, 11p. (CONF-650549–10). ORINS.

From IAEA Symposium on Exchange Reactions, Upton, N. Y.

The iron(II) + iron(III) isotope exchange reaction in dimethylsulfoxide is catalyzed by chloride ions. In the absence of chloride ions the apparent second-order rate constant in perchloric acid-sodium perchlorate-dimethylsulfoxide media was approximately 18 ± 2 liter $mole^{-1}$ sec^{-1} at 20°C and was independent of acid concentration when no water was added. At low acid concentrations the apparent second-order rate constant increased rapidly as water was added indicating that hydroxide ions replace dimethylsulfoxide in the first co-ordination sphere and that the rate constant for a hydrolyzed species is greater than that for the solvated ions. At high acid concentrations the apparent rate constant decreased as water was added indicating that water competes successfully for first-co-ordination-sphere positions and that the rate constants for the partially hydrated ions are smaller than that for the solvated ions. Over the range of chloride ion concentrations $1.5 \times 10^{-4}\underline{M} \leq [Cl^-] \leq 6.0 \times 10^{-4}\underline{M}$ the apparent second-order rate constant is given by $k(M^{-1}\ sec^{-1}) = k_0 + k_1\ [Cl^-]$ where k_1, the product of the rate constant k_f for the activated complex of empirical formula $(Fe_2Cl)^{+4}$ and the formation constant K_{31} of $FeCl^{+2}$, is equal to 3.1×10^5 liter $mole^{-1}$ sec^{-1} within an error of approximately 20%. Attempts to measure K_{31} failed because β_{32}, the overall formation constant of $FeCl_2^+$, is approximately 4×10^4 $(mole/liter)^{-2}$ and the ratio (K_{31}/β_{32}) is less than 10^{-6}. An upper limit of approximately 0.05 for K_{31} gives a lower limit of approximately 6×10^6 liter $mole^{-1}$ sec^{-1} for k_1. The very large change from the value for the solvated species indicates an inner-sphere mechanism for the monochloro-activated complex. (auth)

14572 KINETICS AND MECHANISM OF HETEROGENEOUS EXCHANGE REACTIONS ON THE SURFACE OF IONIC CRYSTALS. Lieser, K. H. (Technische Hochschule, Darmstadt, Ger.). Vienna, International Atomic Energy Agency, 1965, Preprint No. SM-64/11, 13p. (CONF-650549–7). ORINS.

From IAEA Symposium on Exchange Reactions, Upton, N. Y.

The following formula was derived for the rate of heterogeneous exchange reactions: $\ln(1-\lambda) = -kf(n_0 + n_L)t$, where λ is the exchange fraction (as in the McKay equation), f the area equivalent of an exchanging ion, n_0 the number of exchanging ions on the surface of the crystals ($n_0 \cdot f$ the total surface area of the crystals), n_L the number of exchanging ions in the solution, and t the time. To prove the validity of this equation, the rate of isotopic exchange in the systems $BaSO_4(s)/^{35}SO_4^{2-}(aq)$, $BaSO_4(s)/^{140}Ba^{2+}(aq)$, $AgCl(s)/^{36}Cl^-(aq)$, and $AgCl(s)/^{110m}Ag^+(aq)$ was measured by determination of the half times of exchange. The number of ions on the surface, n_0, and the number of the ions in solution, n_L, were varied over a wide range. The results of these experiments were in agreement with the formula. By varying the temperature, the activation energy of the exchange reactions in the systems $BaSO_4(s)/^{35}SO_4^{2-}(aq)$, $BaSO_4(s)/^{140}Ba^{2+}(aq)$, $SrSO_4(s)/^{35}SO_4^{2-}(aq)$ and $SrSO_4(s)/^{85}Sr^{2+}(aq)$ was found to be in the range of 7 to 15 kcal/mole. These high values are explained by the fact that the water molecules forming the hydration shell of an ion must be stripped off when the ion passes from the solution into the surface of the crystals. In addition the rates for diffusion-controlled heterogeneous reactions were calculated for the experimental conditions and compared with the rate constants observed. The values differed by several orders of magnitude. This was another proof of the fact that in the systems investigated the surface reaction is the rate-determining step for the exchange. (auth)

14573 KINETICS OF TRIHALIDE EXCHANGE. Myers, O. E. (Convair Scientific Research Lab., San Diego, Calif.). Vienna, International Atomic Energy Agency, 1965, Preprint No. SM-64/28, 9p. (CONF-650549–18). ORINS.

From IAEA Symposium on Exchange Reactions, Upton, N. Y.

Data are presented concerning the broadening of the NMR absorption lines for ^{79}Br and ^{81}Br in aqueous NaBr and KBr solutions on addition of elemental bromine. The

enhanced relaxation rate results from quadrupolar coupling and must be associated with the presence of the tribromide ion in the system. It was observed that the broadening effect of bromine, measured by the slope of a graph of $1/T_2$ vs $\{Br_2\}/[Br^-]$, is greater for ^{79}Br than for ^{81}Br, approximately in the ratio of the square of the quadrupole moments. Also, the effect is shown to be dependent on the correlation time. Whatever the responsible chemical event, its duration is therefore too short to ensure relaxation of the bromide ion. The behavior of the triiodide system is similar where such comparison is possible with ^{127}I resonance observations only. Iodine was much less effective than bromine at broadening the bromide ion resonance. Nor could reliable data be obtained for the chlorine-chloride system, in keeping with the small quadrupole moment of the chlorine isotopes. All processes that enhance the relaxation rate of the halide in the presence of added halogen will contribute to the observed NMR line width. The approximations and assumptions used to estimate limiting values for several rate constants were examined. (auth)

14574 THE INFLUENCE OF COMPLEX STABILITIES ON ELECTRON TRANSFER REACTIONS. Baechmann, K.; Lieser, K. H. (Technische Hochschule, Darmstadt, Ger.). Vienna, International Atomic Energy Agency, 1965, Preprint No. SM-64/10, 20p. (CONF-650549-6). ORINS.

From IAEA Symposium on Exchange Reactions, Upton, N. Y.

The rate of exchange in solutions containing sulfate ions was measured in the system Fe(II)/Fe(III) at different temperatures with ^{59}Fe as a tracer. At 25°C and an ionic strength of 1 the rate constants were: $k_1[FeSO_4^+/Fe^{2+}] = 295$ and $k_2[(SO_4)_2^-/Fe^{2+}] = 17{,}500$ liter mole^{-1} sec^{-1}. The activation energies were $E_1 = 13.8$ and $E_2 = 15$ kcal/mole. For the rate constants of the electron exchange between different complexes of Fe^{3+} and Fe^{2+} the following relation was found: $\log_{10} k = 1.1 + 0.5\,\Delta \log_{10} k$, where $\Delta \log_{10} k$ is the difference between the logarithms of the stability constants of the Fe(III) and Fe(II) complexes with the same ligands. In the system Ce(III)/Ce(IV) a first order reaction with respect to Ce(III) contributed to the exchange reaction. This was explained by the formation of excited Ce(III) ions. The rate constant was $k_5 = 4.45 \times 10^{-4}$ sec^{-1} (0°C). At 0°C the rate constants for the second order reactions were: $k_1[CeSO_4^{2+}/Ce^{3+}] = 0.10$, $k_2[Ce(SO_4)_2^+/Ce^{3+}] = 0.11$, $k_3[Ce(SO_4)_3^{2-}/Ce^{3+}] = 0.17$, and $k_4[Ce^{4+}/Ce^{3+}] = 5.05 \times 10^{-3}$ liter mole^{-1} sec^{-1}. The electron exchange was accelerated by sulfate ions, but not to the same extent as in the system Fe(II)/Fe(III). The rate constants in the system Ce(III)/Ce(IV) also followed a relation of the form $\log k = a + b\,\Delta \log k$. The constants a and b were found to be −2.3 and 0.4, respectively. In the system U(IV)/U(VI), in the absence of light, the rate of the electron exchange in solutions containing sulfate ions was proportional to the concentrations of U(IV) and U(VI) and inversely proportional to the third power of the H^+ concentration. The rate determining step was the disproportionation of U(V), which was present in small quantities in equilibrium with U(IV) and U(VI). The rate constant was found to be 2.6×10^{-4} l^2 mole^{-2} sec^{-1} (25°C, ionic strength 2). This value was higher by a factor of 1220 than the rate constant in a solution containing perchlorate ions instead of sulfate ions. The activation energy was found to be 10.2 kcal/mole. (auth)

14575 PRODUCTION OF SPHERICAL URANIUM NUCLEAR FUEL SUBSTANCES. Akimoto, Yumi; Suehiro, Yoshiyuki; Suehiro, Yosie (to Mitsubishi Kinzoku Kogyo Kabushiki Kaisha). U. S. Patent 3,228,749. Jan. 11, 1966. Priority date Feb. 23, 1962, Japan.

In a method of producing spherical uranium nuclear fuel substances, a uranium compound that is difficult to dissolve in water and that is capable of forming a hydrate is dispersed in an oil medium, and the oil medium containing the U is agitated with an aqueous phase consisting of water or water mixed with an affinitizing agent to transfer the U to the aqueous phase in the form of spherical granules. The affinitizing agent is effective to moisten the surface of the powdered U compound and to facilitate its movement to the aqueous phase. (B.L.M.)

Organic Chemistry

14576 (ORNL–3889, pp 73-7) ORGANIC PREPARATIONS. White, J. C.; Thomason, P. F.; Holsopple, H. L. (Oak Ridge National Lab., Tenn.).

Special organic compounds, most of which are not available commercially, were synthesized. Compounds such as benzyltributylphosphonium bromide, benzyltributylphosphonium chloride, 2,6-dioximinocyclohexanone, ^{10}B diborane, methyl methanesulfonate, heptadecylamine, Calcichrome, and chlorophosphonazo III were prepared. (J.R.D.)

14577 KINETIC ISOTOPE EFFECTS AND THEIR ROLE IN THE STUDY OF THE MECHANISM OF ELECTROPHILIC AROMATIC SUBSTITUTIONS. Olah, George A. (Dow Chemical Co., Farmingham, Mass.). J. Tenn. Acad. Sci., 40: 77-91(July 1965).

The role of kinetic hydrogen isotope effects on the mechanism of electrophilic aromatic substitutions is discussed. Nitration, Friedel-Crafts akylation, halogenation, acylation, nitrosation, Friedel-Crafts cyclizations, sulfonation, sulfonylation, and azo coupling are considered. Relation of the occurrence of isotope effects to the position of the transition state along the reaction coordinate and to the general energy profile was attempted. Nitration, alkylation, or bromination by positive species having early transition states showed no primary isotope effects only small secondary ones. In acylations, nitrosations, azo couplings, etc., which have late transition states, primary kinetic isotope effects were observed. Data are presented in tables (38 references). (M.C.G.)

Radiation Chemistry

See also BIOLOGY AND MEDICINE — Radiation Effects on Biochemicals Radiation Effects on Tissues

Refer also to abstracts 14730, 14870, and 16053–16055.

14578 (EUR–2435.f) INFLUENCE DE LA STRUCTURE MOLECULAIRE SUR LA DECOMPOSITION PAR AUTO-IRRADIATION DES STEROIDES EN SOLUTION. (Influence of Molecular Structure on the Decomposition of Steroids in Solution by Auto-Irradiation). Osinski, P. (Hopital St. Pierre, Louvain (Belgium). Laboratoire de Recherches de la Clinique Medicale). 1965. 14p. Dep. mn.

The influence of molecular structure on the decomposition of steroids in solution by auto-irradiation was investigated. The steroids were deposited in different conditions in regard to solvent, temperature, and radioactive concentration. It was noted that as the oxygen atoms contained in the molecules tend to increase in number, they have an adverse effect on the storage of the steroids, irrespective of the position of the groups which carry this oxygen. The various structures of the A-nucleus did not seem to have any effect on the nature and degree of decomposition of the tritiated products. In order to study the way in which the decomposition of tritiated steroids is affected by the structure of the side-chain, comparisons were made between hydrocortisone and cortexolone on one hand and corticosterone and deoxycorticosterone on the other. These two pairs of steroids differ only by the presence of a hydroxyl group in the 11 position in the hydrocortisone and corticosterone molecules, this group being absent in the cortexolone and deoxycorticosterone molecules. The presence of the hydroxyl group is favorable to the storage of hydrocortisone, whereas on the other hand the decomposition of corticosterone is more pronounced than that of deoxycorticosterone. The storage properties of corticosterone are inferior to those of aldosterone, whose molecule contains an aldehyde group in the 18 position, whereas in the cor-

ticosterone molecule this position is occupied by a methyl. (auth)

14579 (NYO-2383-15) STUDIES OF THE RADIATION CHEMISTRY OF ORGANIC COMPOUNDS. Progress Report, February 1, 1965–January 31, 1966. Lichtin, Norman N. (Boston Univ., Mass.). Feb. 21, 1966. Contract AT(30-1)-2383. 11p. Dep. mn. CFSTI $1.00 cy, $0.50 mn.

Developments are reported for studies on: effects of acid on gamma radiolysis of deaerated methanol; radiolytic trans-cis isomerization of stilbene in methanol solution; effects of acid on $G(H_2O_2)$ and $G(CH_2O)$ from the ^{60}Co-gamma radiolysis of aerated methanol; absorption spectrum of methanol before and after gamma radiolysis; and photolysis of methanolic H_2O_2. (P.C.H.)

14580 (ORNL-2764) RADIATION DENSITIES AND TBP RADIOLYSIS DURING THOREX SHORT DECAY RUNS. Davis, Wallace Jr. (Oak Ridge National Lab., Tenn.). Aug. 20, 1959. Contract W-7405-eng-26. 17p. Dep. mn. CFSTI $1.00 cy, $0.50 mn.

A general equation was derived to calculate the total radiation dose received by the solvent in a pulsed column, assuming ideal mixing of organic and aqueous phases. With this equation and data from the Thorex short-decay runs, radiation dose densities and the amount of TBP that might be decomposed by radiation in the first cycle extraction column were calculated. The average radiation densities were 0.13–0.24 watt-hr/liter, which would decompose 0.01% of the TBP in the 40% TBP-Amsco 125-82 extractant. The amount of acidic radiolysis products would probably be inadequate to precipitate thorium dibutyl phosphate in the 1A column at equilibrium, but would probably cause precipitation if the extractant residence time in the extraction section was increased by a factor of 3 over the 1.2–1.5 min that prevailed during the short-decay runs. (auth)

14581 (ORNL-3889, pp 14-16) EFFECTS OF RADIATION ON ANALYTICAL METHODS. White, J. C. (Oak Ridge National Lab., Tenn.).

The effects of gamma radiolysis of acid chloride solutions were investigated using the spectrophotometric determination of Zr with arsenazo III as the test medium. At dosages below 1000 rads, no deleterious effect is observed. The role of methanol as an inhibitor of the formation of free Cl during irradiation was confirmed; however, depletion of free acid was not arrested, and the rate of acid loss was unaffected by the presence of methanol. Gas chromatographic analyses of the gaseous products of irradiation showed the presence of much methyl chloride and traces of methane and ethane. Studies on a high-temperature chemical dosimeter using deaerated ferrous sulfate at 150, 200, and 250°C were made that showed G values lower by about 10% than the accepted value of 8.2 at 25°C. Modifications were made to the ^{60}Co source used in the study of effects of radiation on analytical methods. (auth)

14582 (SGAE-CH-25/1965) STRAHLENCHEMISCHE CARBOXYLIERUNG VON POLYCHLORVERBINDUNGEN ZU TRICHLORESSIGSAEURE. (Radiation Chemical Carboxylation of Polychloride Compounds for Trichloroacetic Acid). Guetlbauer, F.; Bildstein, H.; Wess, K. (Oesterreichische Studiengesellschaft fuer Atomenergie G.m.b.H., Seibersdorf. Institut fuer Chemie). [1965]. 19p. Dep. mn.

Trichloroacetic acid was formed as a main product by γ-irradiation aqueous, CO_2-saturated solutions of CCl_4 or $CHCl_3$. The radioinduced carboxylation process was studied by means of these systems in respect to its dependence on the radiation dose and pH. The formation of trichloroacetic acid can be explained by reactions of the primary species of the radiolysis of water. (auth)

14583 (TID-21634) CHORAL HYDRATE 800 RAD DOSIMETER. Boyd, W.; Brownell, L. E.; Farvar, M. A. (Michigan Univ., Ann Arbor). Jan. 1965. Contract AT(11-1)-1259. 8p. Dep. mn. CFSTI $1.00 cy, $0.50 mn.

In order to explore the usefulness of chloral hydrate solutions for measuring doses of 800 rads or less, 0.2 M solutions were irradiated with various doses over a range of 80 to 800 rads, with exposures given at different dose rates. Temperature during irradiation was found to have a significant effect. The pH of the chloral hydrate solutions was found to be temperature dependent, and independent of the dose-rate in the range of 20 to 140 rad/min. The solutions must be prepared freshly as the initial pH decreases with time. Also, the change is more rapid if exposed to sunlight. It was concluded that chloral hydrate solutions can be useful for low-dose chemical dosimetry. (P.C.H.)

14584 (TID-22444) LOW ENERGY INVESTIGATIONS OF RADIATION CHEMISTRY. Final Report, February 1, 1964–May 14, 1965. Kiser, Robert W. (Kansas State Univ., Manhattan. Dept. of Chemistry). Nov. 15, 1965. Contract AT(11-1)-751. 23p. Dep. mn. CFSTI $1.00 cy, $0.50 mn.

Developments are reported for studies on: mass spectrometry of organic compounds, transition metals, and organometallics; negative ions, and multiple charged ions; and hot-atom chemistry studies on the $^{59}Co(n,\gamma)^{60}Co$ system with coordination compounds and the $^{32}S(n,p)^{32}P$ systems. (P.C.H.)

14585 (TID-22652) THE INFRARED SPECTRA OF NEOPRENE BEFORE AND AFTER GAMMA IRRADIATION [Thesis]. Moore, Barry Hilton (Georgia Univ., Athens). 1965. Contract AT(40-1)-2418. 40p. Dep. mn. CFSTI $2.00 cy, $0.50 mn.

The infrared spectra of Neoprenes, types W, CG, and GN-M2, were measured and vibrational assignments were made for the observed bands. A high degree of crystallinity was observed in Neoprene type CG, a much smaller degree in types W- and GN-M2. Irradiation with gamma rays of Neoprene type W at doses of 6.7×10^7, 2.5×10^8, and 8.7×10^8 rads, of type CG at 5.5×10^8 rads, and of type GN-M2 at 9.2×10^8 rads produced new bands at 965, 1243, and 1715 cm^{-1} together with shifting of the methylene stretching bands to higher frequencies. The predominant effects were the formation of trans-vinylene unsaturation and crosslinking. Formation of methyl groups and double bond conjugation were also observed. It was concluded that trans-vinylene growth is a zero order reaction followed by first-order decay of trans-vinylene groups. The decay constant k_2, the initial growth rate G_0, and the concentration at infinite dose were calculated to be 4.9×10^{-23} g/ev, 2.1, and 7.2×10^{-4} moles/g, respectively. Irradiation with doses higher than 2.5×10^8 rads eliminated crystallinity in Neoprene and crosslinking was postulated as the cause. It was determined that Neoprene oxidized slightly in conjunction with irradiation. Exposure to air enormously increased the oxidation of irradiated Neoprene. (auth)

14586 INVESTIGATIONS IN THE FIELD OF RADIATION-INDUCED SOLID STATE POLYMERIZATION. IX. γ-RAY INITIATED POLYMERIZATION OF TRIALLYL CYANURATE IN THE LIQUID AND SOLID STATE. Hardy, Gy.; Nagy, L. (Research Inst. for the Plastics Industry, Budapest). Acta Chim. Acad. Sci. Hung., 46: 345-55(1965).

The initial stage in γ-radioinduced polymerization of triallyl cyanurate had kinetically a linear character in both the liquid and the solid states. In the solid state the rate of polymerization increased in the vicinity of the melting point. The activation energy in the liquid phase was 6.00 kcal/mole and in the solid phase 2.42 kcal/mole. Under suitable conditions the presence of diphenylpicrylhydrazyl or p-benzoquinone resulted in decreased rate of polymerization in the solid state, which was an indication of the radical character of the process. Depending on the conditions of the polymerization, an insoluble cross-linked polymer was formed above a certain conversion either in the liquid or the solid phase. The swelling of this polymer in acetone was characteristically different depending on whether the polymer was made in the solid or in the liquid phase, and changes with the degree of conversion, too.(auth)

14587 DAMAGE TO PROTEINS, ENZYMES, AND AMINO ACIDS BY PEROXIDIZING LIPIDS. Roubal, W. T.; Tappel, A. L. (Univ. of California, Davis). Arch. Biochem. Biophys., 113: 5-8(Jan. 1966).

Transient free-radicals are produced in peroxidizing lipid-protein reaction systems. The pattern of damage to proteins, induced by these radicals, is similar to that observed in the case of radiation damage; proteins and enzymes lose solubility and constituent amino acids are destroyed. Lipid peroxidation damage appears to be about one-tenth as effective as radiation damage. Amino acid destruction was measured in lipid-peroxidation damaged γ-globulin, catalase, serum albumin, hemoglobin, and ovalbumin. Among the most labile amino acids are methionine, histidine, cystine, and lysine. Major products of lipid peroxidation-cysteine interaction are hydrogen sulfide and cystine. (auth)

14588 RADIATION DEGRADATION OF POLYAMINO ACIDS IN THE SOLID STATE. Hayden, G. A.; Rogers, S. C.; Friedberg, F. (Howard Univ. Medical School, Washington, D. C.). Arch. Biochem. Biophys., 113: 247-50(Jan. 1966).

Solid polyamino acids were exposed in vacuo to 40-Mrad doses of ^{60}Co γ rays. Viscosity measurements were taken for each polyamino acid at concentrations of 1.5, 1.2, and 0.9%. At the dose used, amino acid transformations similar to those reported for polyamino acids irradiated in aqueous media were not detected. It is concluded that viscosity and molecular weight determinations on proteins irradiated by γ rays in the solid state indicate degradative action by the ray if the protein is fibrous, and unfolding or non-degradative action if the protein is globular. (H.G.D.)

14589 YIELD OF MOLECULAR HYDROGEN IN γ-IRRADIATED ALKALINE SOLUTIONS OF CHROMITE(III) AND CHROMATE(VI). Kalecinski, J. (Inst. of Structural Research, Polish Academy of Sciences, Wroclaw). Bull. Acad. Pol. Sci., Ser. Sci. Chim., 13: 717-22(1965).

Molecular hydrogen formed during radiolysis of alkaline chromite and chromate was determined. Solutions of chromate or chromite in KOH were degassed in a calibrated irradiation vessel and irradiated, using a cobalt source, at dose rates of 4.8×10^{18} and 9.1×10^{18} ev/ml/hr. Gases evolved during radiolysis were analyzed on a mass spectrometer. In irradiated chromite solutions the gas evolved contained only hydrogen. The quantity of hydrogen was a linear function of dose. The yield of hydrogen from irradiated chromate solutions decreased slightly with increasing dose. (M.C.G.)

14590 THE RADIOLYSIS OF TRIFLUOROETHANOL. Russell, J. C.; McCallum, K. J. (Univ. of Alberta, Edmonton, Can.). Can. J. Chem., 44: 243-7(Jan. 15, 1966).

Gamma radiation from a ^{60}Co source was used both on pure trifluoroethanol and on an aqueous solution. The radiolysis gave results very similar to those obtained for ethanol but quite different from those of the related halogenated compounds. Trifluoroethanol is thus best regarded as a modified ethanol rather than an analog of the other halogenated compounds. (F.S.A.)

14591 RADIATION-INDUCED BROMINATION OF 2,3-DIMETHYLBUTANE. Wheeler, Owen H.; Batlle de Pabon, Hilda (Puerto Rico Nuclear Center, Mayaguez). Can. J. Chem., 44: 407-9(Feb. 1, 1966).

Gamma-induced (^{60}Co) bromination was studied and compared with photochemical bromination. The high G-value (2760 ± 130) (molecules reacted per 100 ev) indicated that the reaction proceeds by an initial chain mechanism. The photochemical and radioinduced halogenations of organic compounds seemed to produce the same products and probably proceed by similar mechanisms. (F.S.A.)

14592 THE RADIORESISTANCE OF NUCLEOHISTONE. Van de Vorst, Albert; Richir, Marc; Krsmanovic-Simic, Draga (Univ., Liege). Compt. Rend., 261: 5682-5 (Dec. 20, 1965). (In French).

The yields in free radicals formed by the action of x rays on nucleohistone in the solid phase and the yields characterizing the components isolated were determined. The comparison of the results showed an increase of the radioresistance of the proteic complex with respect to the value that can be predicted in possible interactions between the constituents are not taken into consideration. The free radicals formed are not located in the proteic part of the molecule. (tr-auth)

14593 EFFECT OF X RAYS ON THE REVERSIBILITY OF COLLAGEN GEL. van Caneghem, P.; Lapiere, C. M. (Univ., Liege). Compt. Rend. Soc. Biol., 159: 1250-2 (1965). (In French).

The speed of dissolution of an irradiated collagen gel decreases when the radiation dose is increased. The phenomenon is not reversible. It appears to be bound to a modification of the structure of the collagen. (tr-auth)

14594 RADIATION POLYMERIZATION OF VINYL CHLORIDE IN SOLID SOLUTIONS AT LOW TEMPERATURES. Gerasimov, G. N.; Sabirova, T. M.; Khomikovskii, P. M.; Abkin, A. D. (Karpov Inst. of Physics and Chemistry, USSR). Dokl. Akad. Nauk SSSR, 164: 365-7(Sept. 11, 1965). (In Russian).

The polymerization of vinyl chloride was carried out in mineral oil at a dose rate of 70 rad/sec (^{60}Co) and temperatures of −78 and −196°C. Considerable postpolymerization was found to take place during tha ing of the solutions, so that the latter was carried out very rapidly when kinetic data were taken. The kinetic curves obtained showed that at −196°C the reaction rate decreases sharply during the first stage, and the polymerization practically ceases at 15 to 20% conversion. The yield of polymer was markedly reduced when the vinyl chloride content increased from 6 to 15%. At −78°C, the reaction rate increased sharply at first, then reached a maximum, and declined rapidly at 50 to 60% conversion. The products formed were low-molecular polymers. It was postulated on the basis of the kinetic data that the polymerization of vinyl chloride in a solid mineral oil solution is determined by a definite ordered arrangement of vinyl chloride molecules. The structure of the frozen systems also affected the polymerization process. In contrast to amorphous solutions of vinyl chloride in low-molecular paraffins, the solid vinyl chloride-mineral oil system was a microheterogeneous one; in the presence of microheterogeneity, significant kinetic effects can take place. (CFSTI)

14595 DISTRIBUTION OF ENERGY OF IONIZING RADIATION IN MOLECULAR MIXTURES. Kaplan, I. G. (Karpov Inst. of Physics and Chemistry, USSR). Dokl. Akad. Nauk SSSR, 164: 842-5(Oct. 1, 1965). (In Russian).

The phenomena of absorption and transfer of energy during irradiation of chemical substances by ionizing radiation are discussed. From the reported theoretical and experimental data, it was concluded that of the total number of primary elementary ionization events occurring during irradiation of a system with fast electrons or ^{60}Co gamma rays, about 50% are induced by fast electrons if dN(E) designates the number of elementary events produced by electrons with an energy in the range of E + dE. Then, after a steady-state distribution is established, the following equality is approximately fulfilled: $\int_0^{E = 100\ ev} dN(E) \approx \int_{E = 100\ ev}^{E_0} dN(E)$, where E_0 designates the maximum energy of the electron beam. The estimates given are qualitative, but the contribution of fast electrons to the total number of elementary events will always be substantial. (CFSTI)

14596 CIS-TRANS ISOMERIZATION IN SOLID MATRICES BY γ IRRADIATION. Brown, W. G.; Jankowski, S. (Argonne National Lab., Ill.). J. Amer. Chem. Soc., 88: 233-5(Jan. 20, 1966).

The conversion of α-phenyl-cis-cinnamic acid to the trans isomer occurred in the solid phase under γ irradiation when the solid was in intimate contact with an alkali metal bromide. A similar effect was produced in contact with hexabromoethane but not with hexabromobenzene. Cuprous bromide, thallium bromide, potassium chloride, and potassium iodide were inactive. The effect was attributed to bromine atom catalysis. Potassium bromide similarly triggered the solid-state conversion of cis-dibenzoylethylene to the trans isomer but was without effect on maleic or fumaric acid. The liquid phase isomerization of dimethyl maleate under γ-irradiation was subject to marked accel-

eration of a less specific nature by contact with various solids, thallium bromide being the most active of those tested. (auth)

14597 ELECTRON SPIN RESONANCE SPECTRA OF γ-IRRADIATED POLYCRYSTALLINE ALKYL IODIDES. Fenrick, Harold W.; Willard, John E. (Univ. of Wisconsin, Madison). J. Amer. Chem. Soc., 88: 412-16(Feb. 5, 1966). (COO-32-114).

It was previously shown that polycrystalline C_2H_5I, γ irradiated at 77°K, gives an unexpectedly complex ESR spectrum with more than 32 lines spread over 1000 gauss. Similar complexity with varying spreads was found for the polycrystalline forms of other normal alkyl iodides having an even number of carbon atoms per molecule, but not for the odd-carbon-number species or for the glassy forms. To assist in determining the cause of the complex signals, spectra were obtained for C_2H_5I prepared from ^{129}I, rather than the naturally occurring ^{127}I, and for C_2D_5I, to learn whether changes in the spins and nuclear magnetic moments of the iodine and hydrogen atoms affect the pattern. The spectrum of the polycrystalline $C_2H_5{}^{129}I$ was indistinguishable from that of $C_2H_5{}^{127}I$, while that of $C_2D_5{}^{127}I$ had the wide spread of the latter, but fewer and broader lines. These data were interpreted to indicate that the breadth of the spectra results from coupling of the spin of the unpaired electron with orbital angular momentum on the iodine to give radicals with anisotropic apparent g values ranging from about 1.7 to 2.3. The lines are the result of superposition of the hydrogen hyperfine splitting spectra of radicals oriented to give different apparent g values. Similar complex spectra were produced in $(C_2H_5)_3SnI$ (1000 gauss) and CH_2I_2 (700 gauss). Momentary warming from 77°K to a temperature slightly under the melting point, followed by return to 77°K, causes the complex spectra of C_2H_5I and i-C_3H_7I to decrease while a simpler spectrum grew. This occurred only in those samples frozen to the polycrystalline form following supercooling and not in those frozen slowly from a seed crystal, suggesting that a dissociative neutralization process may be favored by release of strain energy. (auth)

14598 ELECTRON SPIN RESONANCE STUDY OF RADICAL PAIRS TRAPPED IN X-IRRADIATED SINGLE CRYSTALS OF DIMETHYLGLYOXIME-O, O-d_2, GLYOXIME, AND METHYLGLYOXIME AT LIQUID-NITROGEN TEMPERATURE. Kurita, Yukio; Kashiwagi, Michio (Toyo Rayon Co., Ltd., Kamakura, Japan). J. Chem. Phys., 44: 1727-8(Mar. 1, 1966).

The ESR spectra of x-irradiated single crystals of dimethylglyoxime-O, O-d_2, glyoxime, and methylglyoxime were measured at 77°K. An analysis of the spectra revealed the presence of radical pairs $R_1-CR_2\dot{N}O\ldots R_1-CR_2\dot{N}O$, where $R_1 = C(CH_3)NOD$ and $R_2 = CH_3$ for dimethylglyoxime-d_2 (the average distance between the unpaired electrons R = 5.4 Å), $R_1 = CHNOH$ and $R_2 = H$ for glyoxime (R ≤ 4.8 Å), and $R_1 = CHNOH$ and $R_2 = CH_3$ for methylglyoxime (R ≤ 5.2 Å). Radical pairs decayed in dimethylglyoxime faster than in dimethylglyoxime-d_2. This fact showed that the iminoxy radicals $CR_1NOH-CR_2\dot{N}O$ diffuse by hydrogen-atom abstraction from nearby hydroxyl groups. (auth)

14599 GAS-PHASE RADIOLYSIS OF CYCLOPENTANE. RELATIVE RATES OF H_2^--TRANSFER REACTIONS FROM VARIOUS HYDROCARBONS TO $C_3H_6^+$. Doepker, R. D.; Ausloos, P. (National Bureau of Standards, Washington, D. C.). J. Chem. Phys., 44: 1951-8(Mar. 1, 1966).

The radiolysis of cyclo-C_5D_{10} was investigated in the presence of various saturated and unsaturated perprotonated hydrocarbons. On the basis of the isotopic analysis of the propanes formed in these mixtures and several other experimental observations it was concluded that the $C_3D_6^+$ ion, which is the major ion produced in the fragmentation of $C_5D_{10}^+$, reacts with various saturated hydrocarbons (AH_2) as follows: $C_3D_6^+ + AH_2 \rightarrow CD_3CDHCD_2H + A^+$. Rates of this process relative to that of the reference reaction, $C_3D_6^+$ + cyclo-$C_5D_{10} \rightarrow C_3D_8 + C_5D_8^+$, were measured with an accuracy of better than 2%. It is suggested that the saturated hydrocarbons also transfer an H^- ion to $C_3D_6^+$ according to the following reaction: $C_3D_6^+ + AH_2 \rightarrow C_3D_6H + AH^+$. Although in agreement with theory the total rate of reaction of $C_3D_6^+$ with AH_2 generally increased with an increase in molecular weight of AH_2, there were appreciable variations in the rates of the H_2^- transfer reaction versus that of the H^--transfer reaction with a change in structure of the hydrocarbon molecule. The H^--transfer reaction is usually favored when AH_2 is a branched hydrocarbon, except for neopentane, which is entirely unreactive toward $C_3D_6^+$. Unsaturated hydrocarbons do not transfer an H_2^- ion to $C_3D_6^+$ but probably undergo a condensation-type process. The radiolysis of cyclopentane was also investigated in the presence of O_2, NO, and $(CH_3)_3N$. It was demonstrated that the $C_3H_6^+$ and $C_5H_{10}^+$ ions transfer their charge to NO, or $(CH_3)_3N$ and that at a pressure of 20 torr approximately 20% of the parent ions undergo ring opening prior to the charge-transfer process. (auth)

14600 GAMMA RADIOLYSIS OF ALKALINE AND NEUTRAL SOLUTIONS. I. ALKALINE SOLUTIONS OF SODIUM PHOSPHITE. Haissinsky, Moise (Laboratoire Curie, Paris). J. Chim. Phys., 62: 1141-8(Oct. 1965). (In French).

The γ irradiation of alkaline solutions of sodium phosphite, Na_2HPO_3, aerated or traversed by a current of oxygen, leads to oxidation in a chain reaction due to an electron transfer between the intermediary HPO_3^- and O_2. Studies of the degassed solutions irradiated in the presence of various hydrated electron captors and H atoms, at pH 11.8, gave the following primary results: $G_e = 2.65$, $G_H = 0.55$, and $G_{H_2} = 0.45$. The oxidation yield of the irradiated phosphite alone in degassed alkaline solutions was $G(P^V) = G(H_2) = 1.85$. Analysis of this value showed that a part of the hydrated electrons react with the tetravalent phosphorus, which results in an equivalent loss of oxidizing radiolytic products. Analogous losses explained without doubt the low radical and molecular yields obtained by irradiation of alkaline solutions of other solutes where the transformation passed through an intermediate oxidation state. (tr-auth)

14601 GAMMA RADIOLYSIS OF ALKALINE AND NEUTRAL SOLUTIONS. II. EFFECT OF pH ON THE YIELDS. Haissinsky, Moise (Laboratoire Curie, Paris). J. Chim. Phys., 62: 1149-54(Oct. 1965). (In French).

The γ radiolysis of solutions of sodium phosphite, Na_2HPO_3, in the presence of $NaNO_3$ and at pH's between 6.3 and 13.9, led to the formation of phosphate, nitrite, and hydrogen. Measurements of the yields of these products permit calculations of G_{H_2}, G_H, G_e, G_{-H_2O}, and indirectly G_{OH}. The radical and molecular yields did not vary between pH 6.3 and 11.8; G_E and G_{OH} increased with the pH whereas G_H decreased. The decomposition yield of water seemed to be constant in the pH region studied: $G_{-H_2O} = 4.10$. The velocity constant of the reaction $HPO_3^{2-} + H$ at pH 13 was 1.8×10^9 $M^{-1}sec^{-1}$. The mechanism of the decomposition of water at all the pH's studied (from 0 to 14) is represented by a single scheme. (tr-auth)

14602 A NUCLEAR MAGNETIC RESONANCE STUDY OF DECOMPOSITION IN NEUTRON-IRRADIATED LiF. Knutson, C. D.; Hooper, H. O.; Bray, P. J. (Brown Univ., Providence). J. Phys. Chem. Solids, 27: 147-61(Jan. 1966).

The decomposition of LiF produced by neutron irradiation in a reactor was studied by nuclear magnetic resonance (NMR) techniques. Several sets of crystals and powdered samples were irradiated at a variety of temperatures for total neutron doses between 10^{15} and 2×10^{19} n/cm^2. In several cases the temperature of the sample during irradiation was measured by means of thermocouples. The temperature of a sample during the irradiation was usually between 120 and 300°C. After irradiation, distinctive lines were found superimposed on the characteristic NMR spectrum of LiF. Through a detailed study of their properties, the additional lines were shown to be due to ^{19}F nuclei in a molecular fluorine phase probably trapped in small cavities in the crystals, and to ^7Li nuclei in a metallic lithium phase. The concentration of molecular fluorine in the samples was found to increase with dose when the

specimen temperature during irradiation (T_s) did not rise above approximately 300°C, reaching an ultimate concentration of from 1 to 2% of all fluorine in the sample at doses above 10^{18} n/cm^2. However, the concentration was a strong function of T_s if T_s was near or above 300°C. The concentration of lithium metal observable by NMR may be even more sensitive to T_s. No mass loss due to escape of fluorine was observed when T_s was kept below 300°C. Disagreements between measurements of lattice expansion in neutron-irradiated LiF by x-ray and density studies may arise from the heterogeneous nature of the damage; conflicting results from measurements of linear expansion and density (on different specimens) may arise from different values of T_s. (auth)

14603 THERMAL HISTORY OF LiF SINGLE CRYSTALS DURING NEUTRON IRRADIATION. Greene, A. C.; Hooper, H. O.; Bray, P. J. (Brown Univ., Providence). J. Phys. Chem. Solids, 27: 163-9(Jan. 1966).

The temperatures of single crystals of LiF and LiBr were monitored during neutron irradiation by means of thermocouples and chemical indicators. For thermal neutron fluxes between approximately 7 and 12×10^{12} n/cm^2/sec, the temperature during irradiation normally rose to a value between 130 and 300°C. The temperature of a given sample in the reactor facility is shown to depend on such factors as the neutron flux (n/cm^2/sec), total time in the reactor, the packaging of the sample, and the cooling employed in the reactor facility. Various inconsistencies and disagreements in the literature concerning changes in properties of LiF after reactor irradiation can be attributed to these thermal effects. (auth)

14604 PHOTOCHEMISTRY OF V CENTERS IN ALKALI HALIDES X-RAYED NEAR 200 deg K. Itoh, N. (Princeton Univ., N. J.). J. Phys. Chem. Solids, 27: 197-203(Jan. 1966).

Photochemical and dichroic studies were made of the V_4 band in KBr and of the V band at 240 mμ in KCl both of which are produced by irradiation with x radiation around 200°K. It was found that H centers are produced by photoexcitation of the V bands at low temperatures and that both are excited strongly by light polarized along a ⟨100⟩ direction. Measurements were also made of the recovery of the photochemically destroyed V_4 band in KBr. It was suggested that these V bands correspond to the same center that is associated with an interstitial halogen atom. Plausible models are proposed and it was concluded that a di-interstitial halogen molecule or a Cl_3^- molecule (Christy's V_3 center) is consistent with the experimental facts. (auth)

14605 F-BANDS IN NaBr–NaCl MIXED CRYSTALS. Thyagarajan, R. (Solid State Physics Lab., Delhi). J. Phys. Chem. Solids, 27: 218-20(Jan. 1966).

The behavior of F-bands in mixed crystals of NaCl–NaBr is discussed. Mixed crystals of 20, 56.4, and 76.5 mol % NaBr in NaCl were grown by Kyropoulos method and cooled over a prolonged period to reduce growth defects and thermal strains. The crystals were exposed to Cu K α radiation at 30 kv and 15 mA. The specimens were irradiated ~8 hr in the dark at a distance of 2 cm from the window. Absorption measurements were made for optical densities at room temperature at about 27°C. The variation of the F-band peak position with the increasing proportion of NaBr in NaCl is shown. The change in the intensity half width of the F-bands with composition is also shown. The half widths changed rapidly with increasing mol % of NaBr in NaCl and attained a maximum for the composition at ~75 mol % NaBr in NaCl. It was concluded that the increased broadening of the F-bands is connected with the density of Schottky defects. (F.J.H.)

14606 ESR STUDY OF FREE RADICALS FORMED BY γ-IRRADIATION OF POLY(ETHYLENE TEREPHTHALATE). Araki, K.; Campbell, D.; Turner, D. T. (Research Triangle Inst., Durham, N. C.). J. Polymer Sci. Pt. B, 3: 993-6(Dec. 1965).

The formation of free radicals on γ irradiation of poly(ethylene terephthalate) (PET) (single-crystal and film) at −78°C and of ethylene glycol dibenzoate (single-crystal) at 30°C with 10 Mrad was studied. ESR spectra of the free radicals were obtained. The ESR signal from an irradiated amorphous sample of PET (in the form of Mylar film) decayed rapidly but a long-lived signal was obtained from other normal Mylar samples. The identities of two free radicals were concluded from the experiments using the ethylene glycol dibenzoate as a model compound. (F.J.H.)

14607 ELECTRON BEAM PRODUCED LICHTENBERG FIGURES. Tanner, Raymond L. (Univ. of California, Los Angeles); Fingerhut, Aaron G. J. Tenn. Acad. Sci., 40: 110-12(July 1965).

Lucite blocks were irradiated with 6-Mev electrons. Lichtenberg figures (trees) were produced. During irradiation the blocks emitted a white fluorescent glow. Coloration preceded tree formation and increased with dose. The tree-like discharge pattern was formed during irradiation if a scratch or crack was present or if a sharp instrument was used to form a small surface fracture. Lightning-like flashes were observed superimposed on the fluorescent glow. The tree location, like the thickness of the colored region depends on the incident electron energy. Formation of the tree-like pattern is due to dielectric breakdown caused by the large localized space charge of electrons and the high electric field intensity surrounding the sharp point that initiates a spark discharge. (M.C.G.)

14608 RADIATION-INDUCED COPOLYMERIZATION OF TETRAFLUOROETHYLENE WITH ISOBUTYLENE. I. SYNTHESIS OF THE COPOLYMER. Ishigure, Kenkichi; Tabata, Yoneho; Oshima, Keichi; Sobue, Hiroshi (Tokyo Univ.). Kogyo Kagaku Zasshi, 68: 558-61(Mar. 1965). (In Japanese).

Low-temperature (−78°C) γ-irradiation with ^{60}Co was used to promote the copolymerization of tetrafluoroethylene with isobutylene to form a crystalline alternating copolymer over a wide range of the monomer composition. The dose range studied varied from 4 to 30×10^4 R/hr, at 71 mole % C_2F_4. The monomer reactivity ratios for C_4H_8 and C_2F_4, determined from the elementary analysis of copolymers, were 0.2 to 0, respectively. The alternating tendency of this copolymer was apparently due to the opposite polarities of the monomers, that is, the electron-withdrawing property of the fluorine atoms of tetrafluoroethylene and the electron-donating property of methyl groups of isobutylene. It is suggested on the basis of the monomer composition dependency of copolymerization rates that isobutylene plays an important role in the termination reaction at its high concentration in the monomer mixtures. A stepwise sequence of possible reactions in the mechanism of copolymerization is outlined, along with dissociation constants. (BBB)

14609 EFFECT OF PREIRRADIATION ON ACTIVATED CHARCOAL. Mitsutani, Akio (Kurashiki Rayon Co., Ltd., Osaka). Kogyo Kagaku Zasshi, 68: 1070-4 (June 1965). (In Japanese).

Attempts were made to enhance the catalytic activity of activated charcoal, which is one of the main components of the catalyst for vapor phase synthesis of vinyl acetate. It was irradiated with ^{60}Co γ rays and the electron beam of a Van de Graaff accelerator. Preirradiated charcoal was used as the catalyst for vinyl ester synthesis after being impregnated with zinc salts. The activity of charcoal as a catalyst for vinyl acetate and propionate synthesis was markedly enhanced by the preirradiation, and an irradiation dose of 10^7 to 10^8 R was found to be suitable. The presence of oxygen during irradiation did not affect the catalytic activity. The main cause of such enhancement induced by irradiation was considered to be an increase of carbonyl groups on the charcoal, accompanied by an increase of chemisorbed zinc acetate. To explain the increased catalytic activity, the action of radiation, such as in the change of interaction between zinc acetate and charcoal and the change of number of unpaired electrons in the charcoal, was considered. Electron spin resonance studies showed a linear increase of the number of unpaired electrons with radiation dose, and a decrease of unpaired electrons with the Zn acetate-activated charcoal (wt/wt ratio). (BBB)

14610 THE RADIATION CHEMISTRY OF CYCLIC DIENES. I. THE RADIOLYSIS OF 1,3- AND 1,4-CYCLOHEXADIENES IN LIQUID PHASE. Okada, Takuji; Takamuku, Setsuo; Sakurai, Hiroshi (Osaka Univ.). Nippon Kagaku Zasshi, 86: 1118-23(Nov. 1965). (In Japanese).

Gamma radiolysis of 1,3- and 1,4-cyclohexadienes (CHD) was studied at doses from 0.7 to 6.4×10^{20} ev/g at room temperature. Hydrogen, benzene, cyclohexene, isomeric CHD, dimer, and polymer were identified as the products in both 1,3- and 1,4-CHD's and their G values were determined. The formations of cyclohexene and the dimeric compounds, which may be produced by the addition of hydrogen atoms to CHD, as well as ESR spectra of irradiated CHD's suggest that the main primary process is the dissociation of the allylic C–H bonds in both 1,3- and 1,4-CHD's. The hydrogen atoms thus formed are added to CHD or attract hydrogen atoms from CHD, leading to the formation of secondary products. The mechanism of these two decompositions seemed to be similar but not the same, because the ESR spectrum of the 1,4-CHD irradiated at –196°C showed the presence of cyclohexadienyl radicals, while 2-cyclohexenyl radicals, which may be formed by the addition of hydrogen atoms to 1,3-CHD, were identified as the main intermediate radical in the radiolysis of 1,3-CHD. The behavior as the radical scavenger of these CHD's was also investigated by the radiolysis of cyclohexane–CHD mixtures. (auth)

14611 THE DEPENDENCE OF THE SPECTRAL COMPOSITION OF RADIOLUMINESCENCE ON THE INTENSITY OF THE EXCITING RADIATION. Chornii, Z. P.; Lyskovich, A. B. Opt. Spectros. (USSR) (Engl. Transl.), 19: 248-51(Sept. 1965).

Translated from Opt. Spektros., 19: 446-8(Sept. 1965).

The spectral composition of the radioluminescence of NaI(Tl) and CsI(Tl) was investigated. The spectral distribution depended on the density of the x-ray excitation. As the intensity of x radiation increased, the fraction of pure lattice emission in the total radioluminescence increased. In Tl-activated NaI the fraction of pure lattice luminescence at low excitation density was 12% of the total radioluminescence of the crystal. At high excitation density it was 22%. The corresponding figures for CsI(Tl) crystals were 28% and 45%. It was concluded that hard radiation produces Compton electrons and photoelectrons and that they give rise to cascades of secondary electrons. After certain intermediate processes, fundamental excitations (electrons, holes, and excitons) are produced as the end result. As a result of this, the luminescence of an activation center is described by the following reaction: $Tl^+ + e + p \rightarrow Tl_2^+ + p \rightarrow Tl^+ \rightarrow Tl^+ + h\nu$. The yield of activation luminescence was dependent on temperature. (F.J.H.)

14612 OXIDATION OF TECHNICAL PARAFFIN WAX WITH OXYGEN UNDER THE ACTION OF γ-IRRADIATION. Khmel'nitskii, Yu. L.; Melekhonova, I. I.; Nesterovskii, V. V. (All-Union Scientific Research Inst. for the Processing of Petroleum and Gas, USSR). Petrol. Chem. (USSR) (English Transl.), 2: 245-9(1963).

The effects of temperature on the radioinduced oxidation of the liquid phase of technical paraffin wax with a melting point of 58°C were studied. The experiments were carried out using specially arranged sources containing ^{60}Co. Analyses were made of oxidized paraffin wax from experiments at two dose rates (215 and 455 R/sec) and at temperatures from 120 to 160°C. At both dose rates the rate of formation of nonvolatile carboxylic acids (characterized by acid number) passed through a maximum at about 150°C. This was due to the acceleration of secondary reactions when the temperature was raised above this point. Under the conditions investigated, where the oxidation took place by a chain mechanism, the rate of oxidation within the range of integral doses from 2000 to 8000 kR did not depend on the integral dose. Increasing the dose rate of γ-irradiation led to a marked increase in the rate of accumulation of nonvolatile carboxylic acids and also of compounds with hydroxyl and carbonyl groups, while the content of peroxides passed through a maximum at a dose rate of about 200 R/sec. The increase in the rate of accumulation of oxidation products was a function of the square root of dose rate. (BBB)

14613 PHOTOLYSIS AND RADIOLYSIS OF NITROMETHANE AND NITROETHANE. Paszyc, S. (Univ. of Poznan, Poland). Photochem. Photobiol., 4: 841-8(Oct. 1965).

Decomposition of nitroalkanes under the action of uv light and ^{60}Co γ rays was investigated. Prolonged photolysis of nitromethane and nitroethane in liquid and vapor phases, with simultaneous photolysis of the nitrogen dioxide formed, was studied in the absence and presence of cupric oxide. A high-pressure quartz immersion lamp providing the full range of visible and uv spectrum, with a high output of radiation at 366 and 313 mμ, was employed as light source. The photolysis products were detected by microanalytical methods, absorption spectrum analysis, and gas chromatography. Photolysis of liquid nitroalkanes yielded many compounds; saturated hydrocarbons, and in the case of nitroethane, ethylene, were submitted to detailed examination. Photolysis in the vapor phase was carried out in a specially designed glass apparatus. The main products were nitrogen dioxide, aldehydes, and polyaldehydes; hydrocarbons were not estimated. Liquid nitromethane and nitroethane were also irradiated with γ rays from a ^{60}Co source. The radiolysis products were similar to those obtained on photolysis. A mechanism of photolytic decomposition of nitroalkanes is proposed and discussed. (BBB)

14614 TRANSIENT SPECIES PRODUCED IN IRRADIATED WATER AND AQUEOUS SOLUTIONS CONTAINING OXYGEN. Adams, G. E.; Boag, J. W.; Michael, B. D. (Mount Vernon Hospital, Northwood, Middlesex, Eng.). Proc. Roy. Soc. (London), Ser. A, 289: 321-41(Jan. 25, 1966).

Transient spectra of a number of radicals and radical ions were observed in aqueous solutions saturated with oxygen and irradiated by a short, intense pulse of fast electrons. Depending upon the conditions of pH and upon solute concentrations, absorption maxima are produced in both the visible and u-v regions of the spectrum. In oxygenated alkaline solutions, the u-v absorption contains four components which decay at different rates. One of these is the second absorption band of O_3^-, and it is concluded that the others are due to the species O_2^-, HO_3^-, and HO_2^-. It is suggested that the short-lived u-v absorption observed in alkaline N_2O saturated solution is due to the species O^-. Absolute rate constants were made for several of the reactions involved, and a comprehensive mechanism for the radiolysis is proposed. (auth)

14615 THE TIME DEPENDENCE OF SCINTILLATION INTENSITY IN AROMATIC MATERIALS. King, T. A.; Voltz, R. (The Univ., Manchester, Eng.). Proc. Roy. Soc. (London), Ser. A, 289: 424-39(Jan. 25, 1966).

A description is given of the kinetics of the prompt and delayed luminescence components from aromatic materials excited by ionizing radiation. A theoretical model was developed to describe the origin of the delayed scintillation component. From initial assumptions of molecular triplet state diffusion and triplet-triplet annihilation to form delayed singlet states, equations are obtained defining the intensity of the delayed component with time. These equations are shown to agree well with existing experimental results. From the comparison the following parameters for triplet excitations in anthracene and stilbene crystals were calculated: diffusion constant, 6×10^{-6} cm^2 s^{-1} (anthracene) and 3×10^{-6} cm^2 s^{-1} (stilbene); triplet-triplet interaction rate constant, 1.3×10^{-11} cm^3 s^{-1} (anthracene) and 7.5×10^{-12} cm^3 s^{-1} (stilbene); and diffusion length, 3.5×10^{-4} cm (anthracene). (auth)

14616 RADIATION CHEMICAL REACTIONS IN AQUEOUS OXYGENATED AND OXYGEN-FREE SOLUTIONS OF ALIPHATIC DIPEPTIDES AND TRIPEPTIDES. Liebster, J.; Kopoldova, J. (Czechoslovak Academy of Science, Prague). Radiat. Res, 27: 162-73(Feb. 1966).

The products of radiolysis of 11 dipeptides and tripeptides

were determined before and after hydrolysis of the solutions by exposure to γ radiation in the presence and in the absence of oxygen. The results show that there is no essential difference in the radiation chemical reactions in oxygenated and in oxygen-free solutions. An attempt is made to elucidate the effects of the peptide bond on the radiolysis of amino acids. (C.H.)

14617 A SPECTROSCOPIC STUDY OF ALPHA-RAY-INDUCED LUMINESCENCE IN GASES. PART I. Dondes, S.; Harteck, P.; Kunz, C. (Rensselaer Polytechnic Inst., Troy, N. Y.). Contract AT(30-3)-321. Radiat. Res., 27: 174-210(Feb. 1966).

A spectroscopic study was made at 1 atmosphere pressure of the luminescence produced by polonium-210 α-irradiation of purified noble gases, noble gas–nitrogen mixtures, purified nitrogen, and nitrogen–oxygen mixtures. Spectrograms were taken covering the range from 2400 A to 12,000 A, with and without the application of an electric field to the luminescent gas, and at liquid nitrogen as well as room temperatures. A major observation was that very small concentrations of impurities or additives often made a predominant contribution to the luminescence, and that ion mechanisms are often involved in the light-emitting processes. Mechanisms that give rise to the observed luminescence are discussed. (C.H.)

14618 GRAFT COPOLYMERIZATION OF POLYMER, INITIATED BY ELECTRON IRRADIATION, IN THE PRESENCE OF MONOMER VAPOR. IV. EFFECT OF THE DEGREE OF CRYSTALLINITY ON GRAFTING. Takamatsu, Toshiaki; Shinohara, Kenichi (Inst. of Physical and Chemical Research, Tokyo). Rika Gaku Kenkyusho Hokoku, 38: 1-5(1962). (In Japanese).

Studies were made on the graft copolymerization of polyethylene and polyvinyl chloride films with styrene initiated by electron irradiation of monomer vapor. Two series of experiments were carried out, in one the polymers were irradiated in styrene vapor and were then kept at room temperature for various lengths of time in the same monomer vapor. In the other series, the polymers were immersed, immediately after irradiation in styrene vapor, in the monomer liquid and were kept in that state for the same length of time. No marked difference was observed in two cases in the results of grafting efficiency. There was a difference due to changes in the degree of crystallinity, however. High-density polyethylene gave a much higher degree of grafting than a low-density sample. This result was compared with the results of gamma-initiated grafting in monomer vapor, which gave a smaller degree of grafting for high-density polyethylene. The system of polyvinyl chloride and styrene gave a much lower efficiency, and only a low degree of grafting was obtained even with fairly high radiation doses. (BBB)

14619 REDISTRIBUTION OF THE INITIALLY ABSORBED ENERGY IN THE RADIOLYSIS AND PHOTOLYSIS OF ACYL PEROXIDE SOLUTIONS. Kardash, N. S.; Krongauz, V. A. (Karpov Inst. of Physics and Chemistry, Moscow). Teor. Eksp. Khim., 6: 796-800(1965) (In Russian).

The direct and sensitizing photochemical and radiolytic decomposition of a series of diacyl peroxides in solution was investigated. On the basis of the results obtained, a series of conclusions were made on the intermolecular and intramolecular reactions in the excited molecules. (tr-auth)

14620 MECHANISM OF ELEMENTARY HOT REACTIONS. Filatov, E. S. (Moscow State Univ.). Usp. Khim., 34: 1607-47(Sept. 1965). (In Russian).

The mechanism of hot reactions due to the transfer of excess energy from a recoil atom to a molecule is reviewed. Special attention is given to the theoretical interpretation of experimental results. Eyring's theory of an intermediate, activated complex is shown not to give a satisfactory explanation of the facts because of the absence of an equilibrium state in hot reactions, and because a hot atom approaches its energy region of chemical reactivity from above, that is, from the high-energy side. The slowing down of hot atoms can be described by the use of equations employed in the thermalization of neutrons by elastic collision. The probability of the reaction of hot tritium atoms with various compounds is discussed. The reactions of hot halide atoms are systematically expounded. The conversion of soft, captive gamma rays with subsequent formation of a charge on the atom plays a part in the reactivity of hot halide atoms. A kinetic theory of the reactions of recoil halide atoms is presented with the assumption of elastic collisions. Predicting the reactivity of recoil carbon atoms from $^{14}N(n,p)^{14}C$ or from $^{12}C(p,pn)^{11}C$ reactions is more complex because of the uncertainty of the state of the carbon atom which can exist in a triplet ground state (^3P) or in a sp^3 hybrid state. The deviation in yields of tagged tritium products from additivity in a binary mixture of organic compounds can be explained by a difference in chemical reaction probabilities, in steric hindrance, and in collision cross sections. (109 references). (TTT)

14621 THE STRUCTURE OF RADIATION CHLORINATED AND SULFOCHLORINATED POLYETHYLENE. Dzhagatspanyan, R. V.; Kolbasov, V. L.; Bardenshtein, S. B.; Korolev, B. M.; Romanskii, L. A.; Zetkin, V. I. Vysokomol. Soedin., 7: 1959-63(1965). (In Russian).

The infrared spectra of polyethylene, radiation chlorinated and sulfochlorinated in the solid phase and containing up to 40% chlorine and up to 8% sulfur were investigated. A slight fall in the crystallinity of the specimens as compared with polyethylene was observed. Block radiation-chlorinated polyethylene containing 38.4% chlorine consists mainly of $-CH_2-CHCl-CH_2-$ groups with some $-CHCl-CH_2-CHCl-$ and $-CHCl-CHCl-$ groups. This indicates a certain nonuniformity of chlorination in the solid phase and is explained by the fact that chlorination occurs more readily in the amorphous phase than in the crystalline phase of the polymer. (auth)

14622 STUDIES ON X-AGENT. XLIV. PROGRESSING DIRECTION OF X-AGENT. Moriyama, Hideo (Shonan Hygiene Inst., Kamakura, Japan). Yokohama Med. Bull., 16: 123-34(June 1965).

The secondary X-agent present around a spherical glass bottle containing water was examined using alkaline, aqueous solutions of neutral red. The patterns yielded around the bottle of water by the soft X-agent show a most pronounced peak on the side of the bottle opposite the sunlight. The patterns produced by the X-agent during night-time show a similar peak on the north side, indicating that the night-agent is likewise coming from south. In most cases, distinguished indications of a peak or a valley are revealed in the patterns on the north side of a water bottle enclosed by lead blocks, whose thickness being 5-cm, showing that the hard X-agent that is penetrable through the lead is likewise tending to progress from south to north. In respect of the distinguished indications of the north side, no difference was found between day and night concerning patterns produced around a water bottle placed in a tin box. This indicates that the hard X-agent that can penetrate the tin plate is progressing from south to north whether it be day or night. It is suggested that the migratory movement of birds and other animals can be established by perceiving the X-agent running in a north-south direction, whereby the movement is influenced also by the secondary agent produced by various substances. (auth)

14623 STRUCTURAL INFORMATION AND IDENTIFICATION OF ORGANIC SUBSTANCES BY MEANS OF "ELECTRON PYROLYSIS". PART I. ELECTRON PYROLYSIS OF CARBOXYLIC ACIDS, ALCOHOLS, OLEFINS, AND AMINO ACIDS. Schildknecht, H.; Volkert, O. (Univ., Erlangen, Ger.). Z. Anal. Chem., 216: 97-117(1966). (In German).

The effect of electrons in water on organic substances was studied in theory and practice. The electron source was tritium in the form of tritium-water. Carboxylic acids were decarboxylated; resorcylic acid yielded resorcinol as in simple pyrolysis. The fragments formed by this process were labeled with tritium and hence even traces could be readily detected. The alcohols, hexanol and cyclohexanol,

were oxidized in this way to the carbonyl compounds; the cyclic alcohol reacted more readily. Double bonds became hydroxylated, and the resultant glycols suffered oxidation to the corresponding carbonyl compounds. Amino acids were cleaved preferentially at the C–N bond to give ammonia and the corresponding carboxylic and hydroxycarboxylic acids. Small amounts of keto acids, formed by oxidation of the hydroxy acids, were obtained. Hydroxydicarboxylic and aminodicarboxylic acids, derived from the reaction of two acidic fragments, were also found. The possible use of this method as an analytical tool and the limiting concentrations of compounds to be analyzed are discussed from the theoretical standpoint. Experimental examples proved that satisfactory results can be obtained using this method. (auth)

14624 DETERMINATION OF THE RADICAL LIFETIME FOR THE GAMMA RADIATION INDUCED GRAFT COPOLYMERIZATION OF STYRENE AND POLYETHYLENE [Thesis]. **Steinberg, Neil Ira.** Hoboken, N. J., Stevens Inst. of Tech., 1965. 132p.

The overall reaction rate for the radiation-induced graft copolymerization of styrene and polyethylene was measured under constant and intermittent irradiation. The system equation was solved with the dose rate represented as a periodic function of time for a number of frequencies. These results were used to evaluate the radical lifetime for the above system using the technique employed in flash photolysis experiments. The mathematical results of a frequency response analysis for a sinusoidal driving function were compared with similar results for a square wave driving function of the same average value. The results showed that the assumption of a square wave for driving function that deviated even slightly, introduced a large error. For the range of dose rates studied (20 krads/hr to 220 krads/hr), the reaction rate was not subject to any observed transient period. For dose rates below 22 krads/hr the reaction rate was proportional to the square root of the dose rate. For higher dose rates, the reaction rate increased more gradually and showed tendencies to level off in the region of 200 krads/hr. The radical lifetime at a dose rate of 49.8 krads/hr was found to be 34 seconds. The propagation constant was 55 $(\text{moles/liter})^{-1}$ $(\text{seconds})^{-1}$ and the termination constant was 1.1×10^4 $(\text{moles/liter})^{-1}$ $(\text{second})^{-1}$. These values were compared to values for the homopolymerization of styrene. The results of the intermittent irradiation experiments combined with the rate constants indicated that the gel effect was not a significant factor. An attempt was made to fit a simple steady-state diffusion model to the data. Although there were some discrepancies, diffusion was shown to be the rate controlling process at high dose rates. (Dissertation Abstr.).

14625 THE AQUEOUS PHASE OXIDATION OF CYCLOHEXANE USING GAMMA RADIATION [Thesis]. **Ashline, Ronald Clive.** Ithaca, N. Y., Cornell Univ., 1965. 155p.

A study was made of the radiolytic oxidation of cyclohexane in aqueous solution using cobalt-60 gamma radiation. The effect of oxygen pressure was examined over the pressure range 15.7 to 64.7 psia and the effect of temperature studied over the range 25 to 200°C. Dose rates ranging between 7.7×10^4 and 38.9×10^4 rads per hour were employed. The course of the reaction was followed up to a total dose of 3.0×10^6 rads. In the presence of oxygen gas the reaction proceeds irreversibly with the formation of a number of oxidation products. Those identified were cyclohexanol, cyclohexanone, and hydrogen peroxide. G-values for the formation of these individual products ranged between 0.49 and 1.2. Trace quantities of carbon dioxide were also detected in the aqueous phase. The cyclohexanol and cyclohexanone formed by the reaction account for 16 per cent of the cyclohexane that reacted. When molecular oxygen was excluded from the system, neither cyclohexanol nor cyclohexanone was formed on irradiation. The maximum steady-state concentration of cyclohexanol and cyclohexanone obtained during irradiation of a continuously saturated aqueous solution of cyclohexane was approximately 0.11 and 0.54 millimole per liter, respectively. This maximum occurred at 18.7 psia oxygen pressure and 15×10^4 rads per hour dose rate. Experimental results indicate that higher concentrations may be possible at an oxygen pressure less than 18.7 psia. The effect of increasing the temperature of the system from 25 to 110°C was to increase the ratio of cyclohexanol to cyclohexanone. At temperatures exceeding 110°C the thermal oxidation of cyclohexane became significant. A mathematical model based on competition among the various components of the system for a single primary radical species was presented. The various parameters in the kinetic equations were evaluated at 25°C, 18.7 psia oxygen pressure, and a dose rate of 15.2×10^4 rads per hour. (Dissertation Abstr.).

Radiochemistry

See also Separation Processes and Procedures

Refer also to abstracts 14501, 14542, 14787, and 16061.

14626 (ORNL-P–1944) PREPARATION OF MEGACURIE QUANTITIES OF ^{137}Cs SALTS AND SOURCE COMPOUNDS AT OAK RIDGE NATIONAL LABORATORY. Lewis, R. E.; Ottinger, C. L. (Oak Ridge National Lab., Tenn.). [1965]. Contract W-7405-eng-26. 13p. (CONF-660305–4). Dep. mn. CFSTI $1.00 cy, $0.50 mn.

From American Nuclear Society Topical Meeting, Augusta, Ga.

Processes used for recovery, purification, and conversion of megacurie quantities of ^{137}Cs to salts and source compounds are reviewed with special emphasis on the conversion of cesium alum to cesium carbonate by the cesium tetraoxalate process. Subsequent conversion of cesium carbonate to source compounds is discussed. (auth)

14627 (PAEC(D)IS–651) TEST PRODUCTION OF COLLOIDAL ^{198}Au AT THE PHILIPPINE ATOMIC RESEARCH CENTER. Davila, A. T.; Gregorio, E. G.; Lumba, L. G. (Philippine Atomic Energy Commission, Manila). May 1965. 16p. Dep. mn.

Procedures are described for the preparation of colloidal ^{198}Au. (C.H.)

14628 TRITIUM-HYDROGEN EXCHANGE OF POLY-L-GLUTAMIC ACID IN AQUEOUS SOLUTIONS. **Ikegami, Akira; Yamamoto, Sadaaki; Oosawa, Fumio** (Nagoya Univ., Japan). Biopolymers, 3: 555-66(1965).

Tritium-proton exchange was applied to the simplest model molecule of proteins, poly-L-glutamic acid, which undergoes the coil-helix transition, a kind of one-dimensional crystallization phenomena, depending on pH. The exchange was followed at various pH values. The results showed that all peptide protons (or isotopes) attached to nitrogens are exchanged in a simple first-order reaction and the rate is proportional to the fraction of random coil conformation. This is interpreted to be due to the following situations. Only the protons (or isotopes) in the random coil conformation are exchangeable with them in water. The average conformation or the helical content of the molecule is determined by pH and other conditions of the medium, but the interchange between helical and random coil conformations takes place at very high frequency in each molecule. This result is reasonable and consistent with other reports. Although only the simplest example was treated, the results suggest the usefulness of this type of work on more complex systems such as copolymers of amino acids and natural proteins. (J.B.)

14629 SEPARATION OF ISOTOPE ^{10}B BY EXCHANGE DISTILLATION. **Riedel, J. T.** (Inst. of Nuclear Research, Warsaw). Bull. Acad. Pol. Sci., Ser. Sci. Chim., 13: 741-5(1965).

Investigations on enrichment of the ^{10}B isotope by exchange distillation are reported. A separating column was developed in which ^{10}B was enriched by using the BF_3-dimethyl ether addition compound. The over-all enrichment factor obtained, A = 3.2, corresponded to a ^{10}B proportion of 60.2% in the enriched product. Efficiencies of 89 to 92% were obtained. (M.C.G.)

14630 PRODUCTION OF ^{75}Se-SELENOCYSTINE BY NEUTRON ACTIVATION. Spencer, Richard P.; Brody, Kenneth R.; Gunther, Wolfgang H. H.; Mautner, Henry G. (Yale Univ., New Haven). J. Chromatog., 21: 342-3 (Feb. 1966).

One hundred milligrams of selenocystine were irradiated for 30 hr at a flux of 10^{13} neutrons/cm^2/sec. The original amino acid was a light yellow, while the post-irradiation sample was red. The sample was purified by thin-layer chromatography. The radioactive substance formed was indistinguishable from nonradioactive selenocystine in 6 chromatographic systems. The specific activity of the ^{75}Se-selenocystine was about 2.9 μC/mg. (M.C.G.)

14631 PREPARATION OF ^{242}Pu AND ^{242}Cm FROM NEUTRON-IRRADIATED ^{241}Am. Dedov, V. B.; Volkov, V. V.; Gvozdev, B. A.; Ermakov, V. A.; Lebedev, I. A.; Razbitnoi, V. M.; Trukhlyaev, P. S.; Chuburkov, Yu. T.; Yakovlev, G. N. Radiokhimiya, 7: 453-61(1965). (In Russian).

Irradiation of ^{241}Am with thermal neutrons produces ^{242}Pu, ^{242}Cm, and ^{243}Am. The thermal neutron cross section of ^{241}Am is 900 barn, thus even on short irradiation with a high density thermal-neutron beam a significant amount of the isotopes may be produced. The yield of fission products is small since they are produced mainly during fission of ^{242}Am. This facilitates the chemical processing of irradiated substances. Production of ^{242}Pu by this process requires less time than the method that uses ^{239}Pu as the starting material. The chemical separation of ^{242}Pu, ^{242}Cm, and ^{243}Am from irradiated ^{241}Am is described. The scheme for chemical processing was selected to be such that it would produce rapid separation of the products. The main separation steps involve chromatographic and chemical extraction methods. Chemical processing was carried out in a shielded area on a special stand with remote control of all operations. Some properties of curium oxalate, potassium curium sulfate, curium hydroxide, and curium carbonate are indicated. (CFSTI)

14632 SOME OBSERVATIONS CONCERNING THE ISOTOPIC EXCHANGE BETWEEN IODO AMINO ACIDS AND ^{131}I ON CHROMATOGRAPHIC PAPER. Szantai, Ianos; Uray, Zoltan; Kovacs, Valeria (Service de Medecine Nucleaire, Cluj). Rev. Roum. Biochim., 2: 75-7(1965). (In French).

A study was made on the exchange of ^{131}I between iodine and tyrosine, diiodotyrosine, triiodotyrosine, and histidine, directly on chromatographic paper, when these compounds are used as radioactive standards in the identification of labeled compounds. Studies were carried out with n-butanol: 2N NH_4OH (40:40) and n-butanol: formic acid: water: ethyl alcohol (40:10:40:2). Unlabeled acids were placed on the paper; and, after drying, radioiodine. After two hours of saturation and 16 to 20 hr of development, the chromatograms were dried and radiochromatograms obtained. In the acid system five labeled fractions were found when the histidine chromatogram was developed. The system provides a labeling route for these amino acids. The possibility of labeling thyroid compounds because of the isotope dissolved in butanolic extract was considered. (BBB)

14633 PROCESS FOR PRODUCING TRITIATED ORGANIC COMPOUNDS. Yavorsky, P. M.; Gorin, E. (to U. S. Atomic Energy Commission). U. S. Patent 3,230,261. Jan. 18, 1966.

A method of tritiating organic compounds comprising contacting neutral and acidic organic compounds having active hydrogens with boron trifluoride–tritiated phosphoric acid at temperatures below 100°C in the absence of water to yield a tritiated organic compound is presented. (AEC)

14634 RADIOACTIVE RADIATION EMITTING SOURCES. Jones, L. V.; Tucker, P. A.; Wittenberg, L. J. (to U. S. Atomic Energy Commission). U. S. Patent 3,230,374. Jan. 18, 1966.

The production of radiation sources by embedding controlled amounts of radioactive substances to controlled depths in glass is described. The radioactive substances, which may initially be in the form of beads, microspheres, fibers, or the like, are fused into glass containers by raising the temperature of the glass above the melting point and by allowing the substances to settle into the molten glass. (AEC)

Separation Processes and Procedures

See also Analytical Procedures
ISOTOPE TECHNOLOGY — Separation and Production

Refer also to abstracts 14788 and 15722.

14635 (CONF-660305–5) RECOVERY AND PURIFICATION OF ^{147}Pm. Lowe, J. T. (Du Pont de Nemours (E. I.) and Co., Aiken, S. C. Savannah River Lab.). Jan. 1966. Contract AT(07-2)-1. 5p. Dep. mn. CFSTI $1.00 cy, $0.50 mn.

From American Nuclear Society Topical Meeting, Augusta, Ga.

A process to reclaim the rare earth fission products as a potential source of ^{147}Pm is described. The process is designed to have no significant interference to present plant operation. The rare earth fission products are extracted from Savannah River Plant wastes with 50% tributyl phosphate (TBP) in dodecane. Most of the fission product cerium is oxidized to Ce(IV) through isotopic exchange with inactive Ce(IV), and is retained in the 50% TBP while the trivalent rare earths (including the ^{147}Pm) are back-extracted into the aqueous phase. Removal of ^{144}Ce eliminates the major source of heat in the rare earth fraction and permits easier storage of the ^{147}Pm fraction. After a suitable storage period to permit decay of the undesirable ^{148}Pm, the ^{147}Pm can be purified by ion exchange. (auth)

14636 (CONF-660305–7) CHEMICAL PROCESSING OF CURIUM—STATUS OF THE PILOT PRODUCTION PROGRAM AT SAVANNAH RIVER. Neel, R. B.; Eubanks, I. D.; Thompson, M. C.; Burney, G. A. (Du Pont de Nemours (E. I.) and Co., Aiken, S. C. Savannah River Lab.). Jan. 1966. Contract AT(07-2)-1. 9p. Dep. mn. CFSTI $1.00 cy, $0.50 mn.

From American Nuclear Society Topical Meeting, Augusta, Ga.

A process for purifying ^{244}Cm produced in Savannah River reactors was successfully demonstrated in the laboratory. Radiochemically pure curium was produced in pilot demonstrations that are adaptable to large-scale production. Improvements were made in the processing scheme that simplify chemical processing without sacrificing product quality. Actinide-lanthanide partitioning by solvent extraction with tertiary amines in a chloride system was successfully demonstrated. Recent improvements permit extended reuse of the solvent and removal of californium from the curium product. Several methods for minimizing radiation effects in process solutions were developed. Thermogravimetric studies defined the calcination temperatures for producing curium dioxide as the final product. (P.C.H.)

14637 (DP–1034) EVALUATION OF COMMERCIAL n-PARAFFIN MIXTURES FOR PUREX DILUENT. Wilhite, Richard N. (Du Pont de Nemours (E. I.) and Co., Aiken, S. C. Savannah River Lab.). Feb. 1966. Contract AT (07-2)-1. 7p. Dep. mn. CFSTI $1.00 cy, $0.50 mn.

Commercially available mixtures of n-paraffins produced by molecular sieve processes were found by detailed analysis of composition to be of the high quality necessary for use as diluent in the Purex process. Analyses for aromatic and branched or cyclic paraffin content correlate with measurements of chemical degradation, and serve as a satisfactory test for evaluation of quality of bulk shipments. (auth)

14638 (NP–15753) SOME POSSIBILITIES OF AQUEOUS PROCESSING OF GRAPHITE–CARBIDE FUEL ELE-

MENTS. Lopez-Menchero, E.; Vermeulen, G.; Detilleux, E. (European Company for the Chemical Processing of Irradiated Fuels, Mol (Belgium)). June 1965. 59p. (ETR-172; CONF-650606-10). Dep. mn. CFSTI $3.00 cy, $0.75 mn.

From EURATOM Symposium on Fuel Cycles of High-Temperature Gas-Cooled Reactors, Brussels.

In order to find a suitable head-end process permitting the treatment of graphite-carbide fuel elements in the aqueous processing cycle, a number of alternative methods for attacking graphite, pyrolytic carbon coatings, and silicon carbide layers were tested. For practical reasons, the study was restricted to fuels of two European reactors, namely, the Dragon and the Schülten reactors. Two conceptual head-end flow sheets are presented: for the Schülten type fuel, combustion of the carbon is followed by fluoride catalyzed nitric acid leaching of the ashes; and, for the Dragon type fuel, carbon combustion is followed by combustion of the silicon carbide under the eutectic of the carbonates of lithium, sodium, and potassium at 600°C, and by an aqueous leaching, similar to the one described for the Schülten type fuel. (auth)

14639 (ORNL-P-1968) CURIUM PROCESSING EXPERIENCE. Vaughen, V. C. A.; Baybarz, R. D. (Oak Ridge National Lab., Tenn.). [nd]. Contract W-7405-eng-26. 18p. (CONF-660305-13). Dep. mn. CFSTI $1.00 cy, $0.50 mn.

From American Nuclear Society Topical Meeting, Augusta, Ga.

About 35 g each of curium-244 and americium-243 were prepared in pure form, and about 12 g of curium-242 were also prepared. Processes were demonstrated to yield recoveries of about 95% across the two-cycle (Clanex-Tramex) process, with demonstrated decontamination factors of up to 500 for gross gamma, 2000 for ruthenium-106 and europium-154, and 3000 for cerium-144. Ionic purity was suitable for source fabrication. Final purification and separation of curium-244 from americium-243 yielded an americium product of better than 99.9% purity and a curium product containing about 0.5 wt % americium. Beta-gamma emitting contaminants were below detectable limits. (auth)

14640 (ORNL-TM-1411) SURVEY OF HEAD-END PROCESSES FOR THE RECOVERY OF URANIUM AND THORIUM FROM GRAPHITE-BASE REACTOR FUELS. Witte, H. O. (Oak Ridge National Lab., Tenn.). Feb. 3, 1966. Contract W-7405-eng-26. 15p. Dep. mn. CFSTI $1.00 cy, $0.50 mn.

The literature on development of head-end processes for graphite-base reactor fuels was surveyed. For the coated-particle fuels that are currently receiving the most attention, only two of the processing methods considered appear to be feasible on a technical scale. Work on these methods, the burn-leach and grind-leach processes, is summarized in detail. (auth)

14641 (RL-SA-59) LARGE-SCALE PROCESSING AND SOURCE PREPARATION OF SEPARATED FISSION PRODUCTS. Beard, S. J.; Smith, P. W. (General Electric Co., Richland, Wash. Hanford Atomic Products Operation); Cochran, J. S. (Isochem Inc., Richland, Wash). Dec. 6, 1965. Contract AT(45-1)-1851. 22p. (CONF-660305-3). Dep. mn. CFSTI $1.00 cy, $0.50 mn.

For Presentation at American Nuclear Society Topical Meeting, Augusta, Ga.

Fission product recovery activities currently being conducted at Hanford are discussed, and the processes used are described, and future plans for encapsulation of fission products in the commercial FPCE to be built at Hanford are outlined. Production plant flowsheet performance is discussed for the individual fission product recovery processes. Full level plant tests of improved fission product recovery and purification flow sheets are reviewed. (P.C.H.)

14642 URANIUM EXTRACTION FROM AQUEOUS SOLUTIONS WITH NAPHTHENIC ACID. Efendieva, N. G.; Alekperov, R. A. (Inst. of Chemistry, Academy of Sciences, Azerbaidzhan SSR, Baku). Azerbaidzh. Khim. Zh., 2: 110-14(1965). (In Russian).

The extraction of small quantities of uranyl ions from aqueous solutions was investigated. It was established that naphthenic acid is an effective extraction agent for uranium from aqueous solutions containing large quantities of dissolved salts of the alkali metals; the pH of the extraction was dependent on the anion composition of the salt and its concentration was significantly displaced to the acid range in the presence of chlorides and to the alkali range in the presence of sulfates, which made it possible to increase the selectivity of the uranium extraction. The effectiveness of the extraction of uranium was significantly increased, $K_p = 10^4$ to 10^5, in the presence of the organic phase at minimum concentrations of aniline and other low amines. The high efficiency of the extraction of uranium in the presence of aniline and the comparative stability of extraction in a wide interval of the acidity of the aqueous phase served as the basis for the development of a method for the determination of small quantities of uranium and, indirectly, naphthenic acid by the extraction-photometric method. (tr-auth)

14643 KINETIC INVESTIGATIONS ON ION EXCHANGE PROCESSES WITH REGARD TO URANIUM FISSION-PRODUCT SEPARATION. Bobleter, O. (Oesterreichische Hochschule, Vienna). Ber. Bunsenges. Phys. Chem., 69: 874-84(1965). (In German).

A linear dependence of the break-through volume on flow rate was established with the aid of break-through curves obtained by loading anion exchangers with mineral acids. The exchange behavior at the front and in a larger region near the front of the electrolyte are mathematically described on the basis of a diffusion model. The equations permit the determination of layer thickness and diffusion coefficients in exchanging systems. Up to a maximum permissible flow rate (v_{max}), which could be theoretically and experimentally demonstrated, it is possible to obtain quantitative adsorption of exchangeable ions. The v_{max} values were determined for a separation process of uranium fission products using aluminum nitrate elution. It is thus shown that the highly active wastes from power reactors can be processed without noticeable radiation damage to the material of the organic exchanger. (auth)

14644 EQUIPMENT OF A PLANT ROOM FOR PILOT PLANT REPROCESSING COLD TESTS AT CASACCIA CENTER—TESTS ON COMPONENTS FOR THE EUREX 2AW PLANT. Moccia, Achille; Loiacono, Raffaele. Comit. Naz. Energ. Nucl., Notiz., 11: 29-38(Dec. 1965). (In Italian).

The equipment of a plant room for pilot-scale reprocessing cold tests in operation at the Casaccia Center for Nuclear Studies and the tests conducted on components for the Eurex 2AW Plant are described. (auth)

14645 CLEANING OF FILTERS IN FLUIDIZED BEDS. PART II. APPLICATION OF EJECTOR NOZZLES. Otero, Alberto Rodrigo; Rof, Juan Sancho (Junta de Energia Nuclear, Madrid). Energia Nucl. (Madrid), 9: 334-42(Sept.-Oct. 1965). (In Spanish).

The possibility of using ejector nozzles for cleaning metallic filters for countercurrent flow was studied. From the laboratory tests, optimum dimensions for an ejector whose diffusor does not introduce excessive charge loss to the filtered gas were obtained. A systematic study of the cleaning of filters was carried out with a study of the variables such as the duration of cleaning, filter volume, and filter capacity. The possibility of simultaneously cleaning various filters with the ejector system was also examined. Some practical examples of the use of the filter chamber are presented. (tr-auth)

14646 REPROCESSING TECHNIQUES AND PROGRESS. [PART] II. EuroNuclear, 2: 604-5(Dec. 1965).

Reprocessing techniques and progress are reviewed for Belgium, Italy, the United Kingdom, and the Netherlands. Also the transportation of irradiated fuel is considered. The Eurochemic plant at Mol in Belgium is expected to provide a large percentage of the reprocessing capacity required during the next few years, but several other nuclear-developed countries have their own smaller plants

which may also contribute to the total European requirement. (J.F.P.)

14647 FLUIDIZED BED REPROCESSING OF GRAPHITE MATRIX NUCLEAR FUEL. Reilly, J. J.; Wachtel, S. J.; Johnson, Richard; Wirsing, Edward Jr.; Hatch, L. P. (Brookhaven National Lab., Upton, N. Y.). Ind. Eng. Chem., Process Design Develop., 5: 51-9(Jan. 1966). (BNL-9415).

An oxidation-fluorination process for the recovery of uranium from graphite-base nuclear reactor fuels was studied on a pilot plant scale. The graphite fuel was burned with oxygen, and the residue, containing U_3O_8, was made to react with fluorine to form volatile UF_6. These exothermic reactions were carried out within a fluidized bed of refractory alumina particles, which served as an inert heat transfer medium for control of temperature. In the oxidation step the oxygen was fed continuously to the reactor, while the graphite fuel was added intermittently at intervals of approximately 1 hr. Under these conditions and at 700 to 750°C, an oxidation rate equivalent to 13.6 kg of carbon/hr/ft^2 of reactor cross section could be readily maintained. In the fluorination step the bed material containing the nonvolatile oxidation products was introduced as a single charge into a separate reactor and brought in contact with fluorine at 450 to 550°C. Overall uranium recoveries of >99% were obtained. (auth)

14648 DENSITY AND VISCOSITY OF SOLUTIONS OF A SYSTEM: ORGANIC SOLVENT-RARE EARTH NITRATE SOLUTIONS. Tsylov, Yu. A.; Korpusov, G. V.; Pustyl'nik, A. I. Izv. Akad. Nauk SSSR, Metal., No. 3, 59-64(May-June 1965). (In Russian).

Liquid extraction is the most widely used of the methods for separating materials with similar properties. The value of the accurate determination of the dimensions of the apparatus increases with increasing scale of production. Results are presented of measurements of the density and viscosity of several systems important in calculating the processes of mixing and stratification in mixer-settler extraction devices. Systems studied include various combinations of solutions of $Nd(NO_3)_3$, $La(NO_3)_3$, $Al(NO_3)_3$, TBP, and m-xylene. (M.J.T.)

14649 SOME NOTES ON A PLANT FOR THE REMOVAL OF RADON BY AERATION. Raffety, J. C. J. Inst. Water Eng., 17: 23-35(Feb. 1963).

Problems encountered in developing a system to remove radon from a river water supply in Devon, England, are described. A small pilot plant was erected near the treatment works under construction, and on this basis a plant was designed to provide an air/water ratio of 8/1 when dealing with a maximum rate of abstraction of 2½ Mgal/day. Design of the radon removal plant is described in detail. Laboratory experiments, carried out to ascertain the optimum depth of water required for most efficient aeration, indicated that it might vary between 2 and 4 ft. Thus the tanks were designed initially to provide for 4-ft depth of water. Each diffuser consists of a 7-in. dia dome constructed in Alundum fused with silica. It is necessary to apply air at the rate of 2250 ft^3/min when dealing with the maximum rate of abstraction. To provide fine bubbles the volume of air passing through each diffuser should not exceed 0.8 ft^3/min and, therefore, it is necessary to provide 2800 diffusers to use the maximum rate of flow. It is proposed to install four air-blowers, each driven by electric motors, and capable, when two units are operating together, of delivering 2250 ft^3 of air per min against a 4-ft head of water. The other two units would be for standby purposes. Adequate ventilation is provided in the roof of the compressor room, and also over the tanks, to allow for the dispersal of the diffused radon into the atmosphere. (BBB)

14650 AMINE EXTRACTION OF RADIORUTHENIUM AS THE CHLOROCOMPLEX. Oka, Yoshinaga; Kato, Toyoaki (Tohoku Univ., Sendai). Nippon Kagaku Zasshi, 86: 1153-8(Nov. 1965). (In Japanese).

The distribution of ^{106}Ru between aqueous hydrochloric acid solution and various alkyl amines in organic solvents was investigated in order to establish the successful procedure for the extraction of radioruthenium and to elucidate the chemical forms of the extractable anionic complex species presented in a system. Spectrophotometric observations were also made on the chlororuthenium species. When an aqueous sodium hydroxide solution of $^{106}RuO_4^{2-}$ was acidified to 6 mol/l in HCl by the addition of concentrated HCl, the chlorocomplex species of ^{106}Ru(VI) was formed and was gradually converted to that of ^{106}Ru(IV) by reduction with excess chloride ion to the quadrivalent state in this complexing medium. The extractability of the ^{106}Ru (VI)-chlorocomplex was relatively greater than that of the ^{106}Ru(IV) and ^{106}Ru(III)-chlorocomplexes; extraction with 4% tri-n-octylamine(TNOA) in xylene solution from a 2 mol/l HCl solution of ^{106}Ru(VI) by shaking for 1 min in 98% extraction of original radioruthenium. The TNOA-xylene solvent system was most effective in extracting radioruthenium as its chlorocomplex. (auth)

14651 ION ADSORPTIVE PROPERTIES OF INSOLUBLE TETRA-, PENTA-, HEXA-VALENT METAL HYDROUS OXIDES. Abe, Mitsuo; Ito, Takuji (Tokyo Inst. of Tech.). Nippon Kagaku Zasshi, 86: 1259-66(Dec. 1965). (In Japanese).

Adsorptive properties of K^+ and Cl^- from solutions of varying pH values by the hydrous oxides of tetra-, penta-, and hexavalent metals such as, Si, Mn(IV), Ti(IV), Sn(IV), Zr, Ce(IV), Th, Nb, Ta, Sb(V), Bi(V), Mo(VI), and W(VI) are described. These oxides were prepared mainly in granular form suitable for use in a column. The pH-titration curves and uptake of K^+ and Cl^- were measured at essentially constant ionic strength (0.1 mol/l) using KOH-KCl and KCl-HCl mixed solutions. The adsorptive ability of the hydrous oxides changed with changing acidity of the oxide itself and changes in the pH values of the solution. The hydrous oxides of Ti, Zr, Sn, Th, and Ca behaved as amphoteric adsorbents, and the uptake of Cl^- decreased continuously with increasing pH, becoming essentially negligible in alkaline solutions. Conversely, the uptake of K^+ by the oxides was negligible in acid solutions and increased continuously with pH. In some intermediate pH regions, the oxides showed both cation and anion adsorptive properties. The hydrous oxides of Si, Mn, Nb, Ta, Sb, Mo, and W behaved only as cation adsorbents and the adsorptive capacities increased with increasing pH. Relatively high capacity and stability were observed for the hydrous oxides of pentavalent metals (such as Nb, Ta, and Sb) in dilute acid and alkaline solutions. (auth)

14652 SELECTIVE SORPTION REACTIONS OF STRONTIUM WITH SOIL MINERALS. Tamura, Tsuneo. Nucl. Safety, 7: 99-103(Fall 1965).

The reactions of radiostrontium with soils and clay minerals and with chemical solutions of soils and clay minerals containing microconcentrations of the radionuclide and macroconcentrations of dissolved stable ions are reviewed. In the reactions of strontium in soil-related systems, it is important not only to consider the clay minerals with their ion-exchange properties but also to remember that these systems may contain limestone and the hydrous iron and aluminum oxides. The presence of the latter components appears to have little direct influence on cesium sorption, but these components can play an important role in strontium sorption. (auth)

14653 SOLVENT EXTRACTION OF MOLYBDENUM AND URANIUM FROM SULFATE SOLUTIONS WITH TRI-N-OCTYLAMINE. Golinski, M.; Korpak, W. (Instytut Badan Jadrowych, Warsaw). Nukleonika, 10: 705-14 (1965). (In Polish).

Extraction of Mo and U from sulfate solutions with tri-n-octylamine was investigated. It was demonstrated that the extraction coefficient of Mo (D^0_w), decreased when the U and Fe concentrations were increased. When the pH of the solution was increased D^0_w also increased. The influence of the Mo concentration and pH value on the extraction coefficient of U (E^0_w) was determined. Mo in the aqueous phase decreased the E^0_w value. In the presence of Mo, the changing of pH had no influence on the value of E^0_W. (auth)

14654 EXTRACTION OF CURIUM AND FERMIUM WITH THENOYLTRIFLUOROACETONE. Gvozdev, B. A.; Chuburkov, Yu. T. Radiokhimiya, 7: 419-23(1965). (In Russian).

The quantitative extraction of curium and fermium by solutions of thenoyltrifluoroacetone in toluene from acetate solution and solutions of α-hydroxyisobutyric acid at different concentrations and pH values was studied and the stability constants of the complexes formed were determined. The distribution of fermium and curium between the organic and the aqueous phase was investigated using ^{242}Cm and ^{252}Fm isotopes. Cm and Fm were simultaneously extracted from a 0.1M solution of acetate buffer at different pH values. After extraction phases were separated and dried on gold planchets for measurement of the α activity. In another series of experiments curium was extracted with a 0.2M solution of thenoyltrifluoroacetone from 0.1 and 0.4M solutions of α-hydroxyisobutyric acid. The extraction constants were calculated along with the two phase stability constant ($\beta_z Q_z$) of curium and fermium complexes with thenoyltrifluoroacetone: $K_{Cm} = (2.2 \pm 0.3) \times 10^{-9}$; $K_{Fm} = (2.6 \pm 1.1) \times 10^{-6}$; $(\beta_z Q_z)_{Cm} = (2.1 \pm 0.3) \times 10^{15}$; and $(\beta_z Q_z)_{Fm} = (2.3 \pm 1.0) \times 10^{16}$. Assuming that, in the investigated concentration and pH range, the curium complex with α-hydroxyisobutyric acid is of the CmB form, a complete stability constant was calculated for this complex, equal to $(2.3 \pm 0.6) \times 10^{-6}$. (CFSTI)

14655 KINETICS OF RE-EXTRACTION OF URANYL NITRATE FROM ALKYLPHOSPHATE SOLUTIONS INTO WATER. I. SYSTEM $UO_2(NO_3)_2$.TBP–DILUENT. Pushlenkov, M. F.; Fedorov, V. S. Radiokhimiya, 7: 424-30 (1965). (In Russian).

The reextraction reaction in the systems investigated is represented in the form $UO_2(NO_3)_2 \cdot 2TBP + mH_2O \rightarrow UO_2^{2+}{}_{(aq)} + 2NO_{3(aq)}^{-} + 2TBP$. The rate of re-extraction and the rate constant are defined by the expression $\rho = dC_s/dt = -KC_s$, where ρ is the rate of the re-extraction reaction, C_s is the surface concentration of the extracted compound, and K is the rate constant. The purpose of the investigation was to measure ρ and K and to determine the temperature coefficients in systems with diluents chloroform, dichloroethane, carbon tetrachloride, tri-n-butylphosphate, benzene, and mesitylene. The relation of the rates of the re-extraction reaction to the nature of the diluent are shown. On the basis of these data the experimental and free energy and entropy of activation for the re-extraction reactions of uranyl nitrate from the diluents listed were calculated. The calculations were in accordance with the activated complex theory, which correlates the reaction rate constant with thermodynamic activation quantities. It was proposed that the activation energy consists of the energy necessary for splitting off the diluent molecules and solvating molecules of the disolvate and the energy of transition of disolvate into an activated complex. The mechanism and the influence of these three factors is elucidated. (CFSTI)

14656 RAPID EXTRACTION BY QUASI-SOLID EXTRACTION AGENT. Denig, Richard; Trautmann, Norbert; Herrmann, Guenter (Univ., Mainz). Z. Anal. Chem., 216: 41-50(1966). (In German).

Solvent extractions can be accelerated considerably by absorbing the extracting agent on a fine-grained carrier and quickly sucking the solution to be extracted through a thin layer of this material. Pentavalent antimony and protactinium are extracted almost quantitatively by using di-(2-ethylhexyl-)-orthophosphoric acid and di-isobutylcarbinol adsorbed on poly-trifluoro-monochloro-ethylene, even at a maximum suction rate of 2 to 3 ml/sec. Application of this technique to studies in nuclear chemistry was demonstrated by the following fast separations: protactinium-234m from uranium, antimony from tellurium after a (n,p) reaction, antimony from fission products, and repeated milking of tellurium from fission antimony. (auth)

14657 ION EXCHANGE METHODS OF SEPARATING ZIRCONIUM AND HAFNIUM Charlot, Gaston; Hure, Jacques; Tremillon, Bernard; Saint-James, Rose (to Commissariat a l'Energie Atomique). Canadian Patent 724,080. Dec. 21, 1965.

Compounds of zirconium and hafnium were separated by anion exchange resins using continuous countercurrent methods in which the resin was also movable. Zirconium ions were adsorbed preferentially in a rather complex zone pattern and then the resin was regenerated by elution. The concentration of the sulfuric acid solutions must be carefully controlled to avoid the formation of colloidal dispersions, which cannot be fixed on the resin. The method was adapted for industrial use to yield a product containing less than 200 ppM of hafnium. (F.S.A.)

14658 METHOD FOR THE LIQUID-LIQUID EXTRACTION OF BERYLLIUM. Bourat, Guy (to Commissariat a l'Energie Atomique). German Patent 1,203,745. Oct. 28, 1965. Priority date Aug. 30, 1963, France.

A sulfuric beryllium solution having a pH value between 0 and 5.5 is mixed homogeneously with an organic liquid immiscible with water and which consists of a solution of amines with the formula $RCH_2CH_2CH_2NH_2CH_2R'$. The organic phase is separated with the extracted beryllium. (Gmelin Inst.).

14659 METHOD FOR SEPARATING AMERICIUM AND CURIUM FROM THE LANTHANIDE RARE EARTHS AND YTTRIUM. Kappelmann, F. A.; Weaver, B. S. (to U. S. Atomic Energy commission). U. S. Patent 3,230,036. Jan. 18, 1966.

A method of separating americium and curium from the rare earth fission products by extracting these fission products from an aqueous mixture of an aminopolycarboxylic acid and a water-soluble organic acid with an organic solution of a monoacidic alkyl phosphoric acid, leaving americium and curium in the aqueous phase is presented. (AEC)

ENGINEERING

General

Refer to abstracts 14729 and 15129.

Applications of Nuclear Explosions

14660 (AD–620468) MONO LAKE WAVE EXPERIMENT: FEASIBILITY STUDY. Final Report. (National Marine Consultants, Anaheim, Calif.). June 1965. Contract Nonr-448800. 79p. (NMC-ONR–65). CFSTI $3.00 cy, $0.75 mn.

The results are presented of a study of the feasibility of conducting experiments during which bomb-wave runup mechanics could be observed and measured. The results indicate that the program could be carried out at Mono Lake. Site selection, range instrumentation and operation, and program costs are discussed. (D.C.W.)

14661 (NP–15867) ESPLOSIONI NUCLEARI SOTTERRANEE. (Bibliography on Underground Nuclear Explosions). (Comitato Nazionale per l'Energia Nucleare, Casaccia (Italy). Centro di Studi Nucleari). [1963]. 52p. Dep. mn.

References (307) are given to reports and journals published from 1950 through 1962. Report number indexes are included. (P.C.H.)

14662 (ORNL-TM–1394) CHEMICAL APPLICATIONS OF NUCLEAR EXPLOSIONS (CANE). Progress Report, October 1–December 31, 1965. Blake, C. A. Jr.; Brown, K. B.; Crouse, D. J. (comps.) (Oak Ridge National Lab., Tenn.). Jan. 21, 1966. Contract W-7405-eng-26. 21p. Dep. mn. CFSTI $1.00 cy, $0.50 mn.

Developments are reported for studies on: distribution and possible fate of radionuclides formed during the use of nuclear devices to aid in the recovery of copper ore deposits; measurement of rates of exchange of tritium and hydrogen in water and natural gas under conditions which will aid the feasibility studies of the stimulation of gas production from wells by nuclear explosives (Project Gasbuggy); hypervelocity jet sampling as a means of removing a specimen after irradiation in the neutron flux of a detonation, but ahead of the shock wave; and thermal analysis of actinide compounds. In a column leaching test, tritium (in the form of tritiated water) was readily washed from the copper ore with a relatively small volume of leach solution and most of it could be eliminated from the system before an appreciable amount of copper is dissolved. A leaching test with reactor-irradiated copper ore indicated that radionuclides formed by neutron activation should not represent an important problem, since they are not efficiently leached from the ore and do not follow the copper in the cementation step. Thus, results showed that radio-induced tritium-hydrogen exchange will not be a factor in determining product quality, providing there is no catalytic effect in the presence of the cavity medium. The Frankford Arsenal successfully conducted tests of the jet sampler concept. The velocity with which the jet traveled the 55-ft-long flight chamber was equal to or faster than the estimated velocity that the shock front travels in rock surrounding a nuclear detonation. These tests showed that the techniques of construction and alignment of the explosive charge, target, and flight chamber are now sufficiently precise to ensure good recovery of future test targets. (P.C.H.)

14663 (UCRL–14463(Rev.1)) FREE FIELD MOTION NEAR A NUCLEAR EXPLOSION IN SALT: PROJECT SALMON. Rogers, Leo A. (Lawrence Radiation Lab., Univ. of California, Livermore). Feb. 1, 1966. Contract W-7405-eng-48. 36p. Dep. mn. CFSTI $2.00 cy, $0.50 mn.

Calculations (SOC Computer Code) of shock pressure, position, velocity, and material displacement were made for the Salmon detonation (design yield of 5 kt) based both on results from the Gnome event (3.1 kt in salt) and physical properties measurements of the material in the shot region. Comparison of the calculations with experimental data gives agreement for peak pressure and peak velocity within 20% to 50% over the range calculated (1-600m). The calculated time-of-arrival of the shock front was within 1% to 10% of the experimental data. Calculated displacements of the salt at 300 m were within 25% of the experimental data, and the ground surface motion directly above the shot was within 10% to 50% of the preliminary experimental data. The calculations based on physical property measurements from the shot region generally gave better agreement with the data than those extrapolated from the Gnome event. The central cavity apparently grew to a radius of 24 m during the initial dynamic stage and then contracted back to a radius of 17 m after the shot. (auth)

14664 (UCRL–14487(Rev.1)) THE SALMON SEISMIC EXPERIMENT. Werth, Glenn; Randolph, Philip (Lawrence Radiation Lab., Univ. of California, Livermore). Nov. 15, 1965. Contract W-7405-eng-48. 17p. Dep. mn. CFSTI $1.00 cy, $0.50 mn.

The Salmon nuclear detonation of October 22, 1964, had a nuclear yield of 5.3 ± 0.5 kt. The teleseismic magnitude was 4.35. P-waves observed out to 2500 km show asymmetries in the propagation, with high amplitudes (mμ/sec), faster apparent velocities, and higher signal frequencies to the north and northeast as compared to the west. At teleseismic distances, many of the signals were very weak and could only be identified with Salmon by knowing the time of detonation and expected arrival time. If a cavity were built of a size to fully decouple 5 kt at the Salmon site, theoretical calculations which include the nuclear spike or shock predict a decoupling factor of about 170 or a magnitude of 2.1. If such a cavity were used for partially decoupling a 25-kt shot, the magnitude is predicted to be 3.1. Drilling back into the Salmon shot region revealed a standing shot cavity of 20,000 m^3, corresponding to a sphere with radius of 17 meters. (auth)

14665 NEW APPLICATIONS FOR NUCLEAR ENERGY. Mark, Hans (Univ. of California, Berkeley). 12p. (CONF-650827–1). ORINS. Gmelin, AED-CONF-65-213-1.

From Western Electronics Show and Conference, San Francisco.

One of the important new applications of nuclear energy is the nonmilitary use of nuclear explosives. Some of the ideas which have been considered are discussed. These include large scale excavation and mining operations. Special mention is made of cost estimates and safety considerations for some of the proposed projects. In addition some of the possible scientific experiments performed with nuclear explosives are described. (auth)

Facilities and Equipment

Refer also to abstracts 14964, 15112, and 15178.

14666 (ORNL–P–1946) HOT PRESSES FOR GLOVE BOX AND MANIPULATOR CELL. Quinby, T. C.; Pierce, E. E.; McHenry, R. E. (Oak Ridge National Lab., Tenn.). [nd]. Contract W-7405-eng-26. 12p. (CONF-660305–10). Dep. mn. CFSTI $1.00 cy, $0.50 mn.

From American Nuclear Society Topical Meeting, Augusta, Ga.

A miniature hot press, intended for research and development and for glove-box operation, consists of three components: the heater, which includes a carbon resistance element and variable-voltage, high-amperage power supply; the die column, which includes the die assembly and the hydraulic cylinder for applying pressure to the die plunger;

and the containment shell, which confines the heated zone and contains the vacuum or other atmosphere. The production hot press was designed for fabrication of sources up to 3-in. in dia in a manipulator cell. The press consists of the frame assembly, which allows the furnace to be tilted for loading and contains the hydraulic ram; the furnace, which includes the r-f work coil, the graphite susceptor, and the furnace insulation and shell; and the die column including the die assembly, plungers, and push rods. (W.L.G.)

14667 (ORNL-TM-1312(Vol.1)) STRUCTURAL ANALYSIS OF SHIPPING CASKS. VOLUME 1. ANALYSIS OF A SHIPPING CASK SUBJECTED TO INTERNAL PRESSURE. Spaller, A. E.; Shobe, L. R. (Oak Ridge National Lab., Tenn.). Mar. 1966. Contract W-7405-eng-26. 61p. Dep. mn. CFSTI $3.00 cy, $0.75 mn.

Formulas to be used by the design engineer to calculate the maximum stress produced in a cask used to ship radioactive materials when it is subjected to internal pressure are presented in this report. These formulas were developed for use as a guide to indicate compliance with the proposed AEC regulation pertaining to the design requirement for resistance to internal pressure; however, use of these formulas does not guarantee compliance with this regulation. Formulas, which take into account the elastic nature of the lead shielding, are derived to determine the thickness of the cavity wall for casks of both prismatic and cylindrical configuration, the formulas are tabulated, and example problems are given. Creep of the lead shield is evaluated, and it is concluded from this evaluation that the creep problem tends to be self-alleviating. (auth)

14668 (ORNL-TM-1397) A MACHINE TO TRANSFER POWDERED RADIOACTIVE FUEL REMOTELY. Davis, F. C.; Pate, W. A. (Oak Ridge National Lab., Tenn.). Jan. 28, 1966. Contract W-7405-eng-26. 17p. Dep. mn. CFSTI $1.00 cy, $0.50 mn.

A fuel transfer machine was designed for use as one of the machines in an assembly line that will constitute the Oxide Fabrication Process planned for the Thorium–Uranium Fuel Cycle Development Facility being constructed at Oak Ridge National Laboratory. The fuel transfer machine will receive the thorium–uranium oxide powder from the weighing machines, blend the fuel while transporting it to the fill-compact machine, and empty the blended fuel material into the fill-compact machine. The requirements, problems, and solution of those problems encountered in the design for the fuel transfer machine are discussed. (auth)

14669 (RL-SEP-414) STIRRED-BED GAS-SOLIDS REACTOR FOR PREPARING PLUTONIUM TRICHLORIDE. Soine, T. S. (General Electric Co., Cincinnati, Ohio. Nuclear Materials and Propulsion Operation). Aug. 1965. Contract AT(45-1)-1350. 13p. Dep. mn. CFSTI $1.00 cy, $0.50 mn.

A glass stirred-bed reactor was developed. The reactor was capable of processing batches up to about 500 g of plutonium oxide. The reactor was used to study the chlorination characteristics of plutonium dioxide produced via the direct calcination route. This, in turn, furnished data for studying the variables associated with the direct calciner. The reactor was also used to produce plutonium trichloride. Conversion was routinely 90% or higher, depending on the nature of the plutonium oxide. Chlorination rates were approximately 200 g/hr. Heating and cooling provided cycles of 8 hr for 500 g of plutonium. Purification was good although some reactor design changes could have improved it. Both liquid and gaseous chlorinating agents can be fed to the reactor. (auth)

14670 (SC-R-65-997) DESIGN CONSIDERATIONS FOR ION PLATING. Mattox, D. M. (Sandia Corp., Albuquerque, N. Mex.). Jan. 1966. Contract AT(29-1)-789. 53p. Dep. mn. CFSTI $3.00 cy, $0.50 mn.

A discussion is given of the important design considerations useful in setting up and using apparatus for ion plating. Apparatus and techniques which have proven to be reliable are presented and discussed. Reviews of sputtering and gaseous electronics as applied to ion plating are given in the Appendices. (auth)

14671 (TID–22394) HIGH-TEMPERATURE ENERGY SYSTEMS. Quarterly Progress Report, August 1–October 31, 1965. (Bureau of Mines, Morgantown, W. Va. Morgantown Coal Research Center). 20p. Dep. mn; CFSTI $1.00 cy, $0.50 mn.

Tests are conducted of a turbocompressor equipped with gas-lubricated bearings. After the diffuser vanes are modified to eliminate compressor surge, tests are begun to define gas flow-pressure rise relationships. Design work is reported on a system for testing the high-temperature turbine. Also, a 15 lb/hr combustor is constructed to evaluate the practicability of fluidized-bed combustion of coal in the primary gas heater. Installation of auxiliary equipment for the combustor is started. A series of tests is completed to determine the film coefficients of heat transfer for suspensions of glass beads in inert gas (88 percent N_2, 12 percent CO_2). The results are inconsistent. Observation of flow through a heat-transfer loop and suspension flowmeter simulated in glass reveals the flow to be nonuniform, so both the loop and the meter are modified to eliminate this problem. (auth)

14672 APPLICATION OF MOTOR-CAR ENGINE FOR CONTROL OF AIR POLLUTION WITH RADIOACTIVE AEROSOLS. Merta, Andrzej; Zarnowiecki, Krzysztof. Nukleonika, 10: 457-8(1965). (In Polish).

The carburetor of a running automobile engine is used to provide a negative differential air pressure to pass atmospheric air through a particulate filter. In series with the filter, and ahead of the carburetor suction chamber is a gas-flow meter, which gives a measure of the volume of air passing through a given filter so that the radioactivity count of the filter can be related to the air volume. The advantages of this system and the variations in the methods and the conditions of measurement are discussed. Some yields in terms of volume of air filtered per unit time are given for two different arrangements. (TTT)

14673 BAND RECOVERY APPARATUS (Engineering Materials). (Oak Ridge Gaseous Diffusion Plant, Tenn.). (CAPE–1312).

5 drawings.

The motor-driven, syringe-type liquid withdrawal unit is used to slowly remove thin layers of isopycnically banded materials from density gradients in ultracentrifuge tubes. It is designed for semiautomatic operation and will withdraw 2.5 ml of gradient solution from the tube at a rate of 0.2 ml/min. It may also be used to feed a solution into a system at the same rate. A built-in, collimated light beam can be directed vertically along the axis of the tube to assist in band location by particulate light scattering. The instrument uses a 2.5 ml disposable syringe and a 3.5 in. spinal, square tip needle to remove the liquid. Three centrifuge tubes of different sizes may be accommodated by means of a turret tube holder. An iris is provided to adjust the light beam diam. for each size tube; light intensity is varied by a selector switch on the lamp supply transformer. (M.J.T.)

14674 COLD TRAP ASSEMBLY, 10 IN. (Engineering Materials). (Lawrence Radiation Lab., Univ. of California, Livermore). (CAPE–1329).

1 drawing.

A bakeable cold trap is described, which is used with a 10-in. diffusion pump where an "elbow" design is required. The entire conductance path boundary is at liquid N temperature and, with normal liquid level fluctuations, all thermal gradients are eliminated on the trap walls. The trap operates unattended for at least 8 hr. Minimum liquid consumption is achieved by preventing direct radiation contact between the hot pump and the bottom of the liquid reservoir by using an expanded metal screen. The welded trap construction makes the trap light in weight and dispenses with metallic gaskets. (For details, see TID-4100). (auth)

14675 TELEPERISCOPE (Engineering Materials). (Du Pont de Nemours (E. I.) and Co., Aiken, S. C. Savannah River Lab.). (CAPE–1321).

30 drawings.

The teleperiscope is used for visual examination of irradiated reactor fuel elements in the Receiving Basin for Off-Site Fuel (RBOF). Cell precision optical components are located at the top of the instrument where they are not susceptible to damage by water or radiation. Underwater components are inexpensive and easily replaced. Dismantling and mounting can be accomplished without special handling procedure. The system functions under normal atmospheric conditions. At the normal subject-to-eyepiece distance of ~20 ft, the depth of field is about 1 in. for all magnification. The instrument is rigidly mounted to eliminate vibration. Photographic exposures from five to ten seconds produce clear, sharply defined images on either negative or Polaroid type photographic materials with an emulsion speed rating of ASA 200. The periscope consists of a vertical view tube welded perpendicularly to a short horizontal tube, on the front of which is a sealed glass window. A first-surface mirror, placed at the intersection of the two tubes, reflects light from the window to a telescope and camera mounted at the upper end of the vertical tube. The periscope can be raised, lowered, and rotated manually to provide a large viewing area. Four 500-w lamps are attached to the lower end of the vertical tube for spot illumination of the viewing area. (For details, see TID-4100). (M.C.G.)

14676 IMPROVEMENTS IN FLUID FLOW CONTROL VALVES. Dickie, Alan Bain (to Sydney Smith and Sons, Ltd.). British Patent 1,018,471. Jan. 26, 1966. Filed Feb. 14, 1961.

A fluid flow valve of the lift and non-rotatable spindle type for use in nuclear work is designed to have a minimum of crevices to trap radioactivity. The valve spindle is adapted for non-rotation by having a portion of substantially triangular cross section formed by arcs of circles and mating with a corresponding sectioned slide bearing portion in the valve housing. The portions are formed for accurate coaxial relationship by machine turning while machine turning the valve spindle and valve cover. The valve spindle is slidable for operating the valve through the intermediary of differentially screw threaded means. Preferably, the triangular-sectioned slide bearing portion is formed in the screwed-in part of the cover, and the valve cover has a bonnet secured onto it when the valve is not required to be adjusted. (B.L.M.)

14677 METHOD AND APPARATUS FOR ROENTGENOGRAPHY. (to Rontgenaktiebolaget Iso-X). British Patent 1,018,723. Feb. 2, 1966. Priority date Nov. 8, 1961, Sweden.

A method and apparatus are described for the radiographic examination of a body in which a substantially monochromatic x-ray radiation derived from ^{125}I is used as the principal examining radiation. The x-ray device includes a source of area not greater than a few square millimeters and a shield. The shield and source are relatively movable to and from a position in which the x radiation from the iodine isotope in the form of a metal iodide carried on a support of the same metal is allowed to pass out of the device. The source may also take the form of radioactive ^{125}I absorbed on an ion exchanger. (B.L.M.)

14678 SHIPPING CONTAINER FOR SPENT NUCLEAR REACTOR FUEL ELEMENTS. Bonilla, Charles F.; Brown, Karl P. Jr.; Brown, Steven H. (to National Lead Co.). U. S. Patent 3,229,096. Jan. 11, 1966. Filed Apr. 3, 1963.

In a shipping container for spent fuel elements, a nesting type arrangement of the fuel elements permits the storing of more elements in a given shielded space to reduce shipping costs. The elements are either gas or water cooled within the container and are supported in proper position to prevent criticality and yet to ensure proper cooling. Special provision is made for storing elements that have failed or ruptured in a closed container having its own vent and particulate filter. (B.L.M.)

14679 DEVICE FOR THE STORAGE OF A HEAT EVOLVING MATERIAL. Montgomery, Donald W. (to Babcock and Wilcox Co.). U. S. Patent 3,230,373. Jan. 18, 1966. Filed Apr. 17, 1962.

A spent fuel storage and shipping cask includes a cylindrical steel pressure vessel embedded in a rectangular cask of radiation shielding material in conjunction with an exterior heat exchanger for the removal of heat produced by the decay of fission products in the elements. A radiation shielding lining is provided inside the pressure vessel. The cask is sufficiently large to contain enough fuel elements to lower the shipping costs but small enough to be shipped on any standard railroad car. (B.L.M.)

14680 LAMINATED RADIATION RESISTANT PANELS. Van Wagoner, Mark B.; Testaguzza, Gino U. S. Patent 3,230,375. Jan. 18, 1966. Filed Dec. 4, 1961.

Radiation resistant panels can be formed by molding a combination in varying proportions of a resin, fine washed sand, asbestos cement and powdered lead. If a thicker laminated panel is desired, one or more layup layers of fiberglass fabric impregnated with a liquid mixture of the components can be applied to the surface of the layer in the mold when it becomes tacky. Various other combinations such as two panels with either an air space or a sand-filled space or a lead sheet between the panels are described. The panel may be rendered heat and fire resistant by the addition of a heat- and fire-resistant material such as Sb_2O_3 to the mixture. The liquid mixture may also be used as a paint or caulking material. (B.L.M.)

14681 REMOTE-CONTROL MANIPULATORS. Ainsworth, Alan (to United Kingdom Atomic Energy Authority). U. S. Patent 3,231,098. Jan. 25, 1966. Filed May 1, 1963.

A remote-control manipulator comprises a transverse beam with master and slave arms connected to the beam at shoulder joints spaced axially on the beam. The master arm carries a handgrip, and the slave arm a work handler. Relatively rotatable rods extend axially along the arms and the beam and mechanically interconnect the handgrip and the handler to cause movements of the handgrip to be reproduced by the handler. A compensating mechanism at each shoulder joint applies compensating rotary movement to the connecting rods when arm movements are made relative to the beam. This compensating mechanism includes epicyclic gearing having planetary gears through which rotary movements of the connecting rods are transmitted, a rotary carrier on which the planetary gears are carried, and gearing carried by the arm and the beam. The mechanism includes also some additional planetary gears carried by the carrier that mesh with the gearing carried by the arm and the beam so that relative moment of the arm and the beam about the shoulder joint is reflected by rotation of the carrier in the compensating mechanism. (B.L.M.)

14682 RADIATION BARRIER PANELS. Gazelle, Rolland J. U. S. Patent 3,231,451. Jan. 25, 1966. Filed Nov. 1, 1961.

A radiation, heat, and fire protective panel is patented for installation in existing or new structures to limit the effect of nuclear explosions. The panel consists of a sandwich type arrangement having a central core including a sheet of Al at least $\frac{1}{16}$ in. in thickness and corrugated to a gross thickness of one inch at the center. The Al is embedded in loose or woven fiber glass to yield an overall core thickness of about 3 in. On the outside of the core is mounted a flat plate of Al at least $\frac{1}{16}$ in. in thickness and outside that a sheet of asbestos board to function with the fiber glass as a heat barrier. A sheet of neoprene is mounted on the rear face of the core and functions with the Al plates to reduce the hazards of radiation. The entire panel is surrounded with tar paper to protect the components from moisture. A facing of plywood, sheetrock, Masonite or the like may be provided inwardly of the plate to make it more attractive. (B.L.M.)

14683 VARIABLE SPECIFIC GRAVITY RADIOACTIVE SOURCE HOLDER. Danforth, John P.; Kerwick, Walter (to General Motors Corp.). U. S. Patent 3,231,739. Jan. 25, 1966. Filed Oct. 12, 1960.

A radioactive source assembly for immersion in a fluid, as in a conduit for leak detection, includes a ball having a radioactive source contained within a cavity in the ball, an access port in communication with the cavity, a closure member in the access port, and temperature responsive

means associated with the ball for compensating for the relative change in density of the assembly and the immersion fluid due to temperature changes. The compensating means include a cylindrical opening within the ball, a piston member cooperating with the opening, and a bimetallic spring connected to the piston and adapted to move the piston in response to temperature changes. A fin-like protuberance can be provided on the ball to slightly increase the resistance of the container to relative motion with respect to the fluid to ensure that the container is carried along in the conduit. (B.L.M.)

Heat Transfer and Fluid Flow

See also PHYSICS — Fluid Physics and Thermodynamics

Refer also to abstracts 14671, 14975, 16000, 16086, and 16101.

14684 (ANL–7073) SELF-SUSTAINED HYDRODYNAMIC OSCILLATIONS IN A NATURAL-CIRCULATION TWO-PHASE-FLOW BOILING LOOP. Jain, Kamal C. (Argonne National Lab., Ill.). Aug. 1965. Contract W-31-109-eng-38. 122p. Dep. mn. CFSTI $4.00 cy, $0.75 mn.

The effects of geometry, subcooling, and pressure on the inception and development of oscillatory behavior in a natural-circulation boiling-water loop were studied. The critical power density was determined by an arbitrary criterion, since the steady-oscillation amplitude increases continuously with power. For large oscillations, periodic inlet-flow reversals were found, which could be large compared to the steady inlet-flow velocities. These phenomena are emphasized by lower system pressure and small-diameter test section and riser. Other parameters did not affect these phenomena in a distinct fashion. The frequencies of the oscillations varied from 0.24 to 0.76 cps and, in general, increased with increasing power, as did the flow amplitudes. Two theoretical models were investigated, one linear and one non-linear. The linear analysis in frequency domain due to Jones showed good ability to predict the oscillation threshold and the frequency associated with the initial oscillations. The predictions of the threshold power were correct within ±5% for over 60%, and within ±10% for over 80%, of the tested cases. The nonlinear model of Jahnberg had to be modified to provide a satisfactory prediction of the steady inlet-flow velocities. However, this modification and the original model failed to give reasonable predictions of the oscillation thresholds and frequencies. Neither form of the model provided a satisfactory prediction of the amplitudes. It is thought that the one-dimensional formulation fails to take into account vaporization, which acts as a periodic forcing function, of superheated liquid near the leading edge of the two-phase region: The introduction of such a forcing function allows the computation of periodic bounded oscillations similar to those observed experimentally, and also explains qualitatively the observed trends with parameter variation. (auth)

14685 (CEA-R-2471) ETUDES THEORIQUE ET EXPERIMENTALE DU TRANSFERT DE CHALEUR ET DES PERTES DE CHARGE DE SURFACES MUNIES D'AILETTES DISPOSEES EN CHEVRON. CORRELATION ENTRE PARAMETRES GEOMETRIQUES ET AEROTHERMIQUES. (Theoretical and Experimental Studies of Heat Transfer and Pressure Drops Along Surfaces Fitted with Herringbone Fins. Correlation Between Geometric and Aerothermal Parameters). Pelce, Jacques; Malherbe, Jean; Pierre, Bernard (Commissariat a l'Energie Atomique, Saclay (France). Centre d'Etudes Nucleaires). Oct. 1965. 76p. Dep. mn.

Principal results are given of experimental research which was carried out on the flow of a fluid along a surface fitted with herring-bone fins. Aerothermal tests were effected on a large number of these surfaces whose geometrical parameters were made to vary systematically. In particular, work on a large scale model has made it possible to analyze the mechanisms of heat transfer and of pressure drops. On this basis a theoretical study has led to the establishment of a correlation between the geometric configuration and the aerothermal performances of these surfaces. Experimental results are in good agreement with the theoretical relationships. An expression was derived applicable to this type of herring-boned surface in a wide zone. (auth)

14686 (EURAEC–1448) RESEARCH INTO THE CRITICAL HEAT FLUX (BURNOUT) IN BOILING WATER. Quarterly Progress Report No. 15, April 1–June 30, 1965. Report No. 09.02.07. Henkel, D.; Mayinger, F.; Schad, O.; Weiss, E. (Maschinenfabrik Augsburg-Nuernberg A. G., Nuremberg (West Germany)). July 1965. Contract 057-61-RDD. 73p. (EUR–2382). ORAU.

Work Performed under United States–Euratom Joint Research and Development Program.

A first series of extensive tests was carried out to determine the maximum heat flux vs various inlet conditions. The inlet flow was varied by twisted-tape vortex generators and orifices which were located directly at the beginning of the heated length. A second test series was carried out to obtain more exact information on the effects of the loop characteristics on the occurrence and the influence of pulsating burnout. For this purpose, the location of the throttling points and the connection to the pressurizer on the test rig were varied. (auth)

14687 (GEAP–4785) EXPERIMENTAL RESULTS ON THE DEPENDENCE OF TRANSITION BOILING HEAT TRANSFER ON LOOP FLOW DISTURBANCES. Gaudiosi, G. (General Electric Co., San Jose, Calif. Atomic Power Equipment Dept.). July 1, 1965. Contract AT(04-3)-189. 69p. (EURAEC–1540). Dep. mn. CFSTI $3.00 cy, $0.75 mn.

Work Performed under United States–Euratom Joint Research and Development Program.

Heat transfer results for transition boiling are presented for forced-circulation in a single rod annular test section at 1000 psia and mass velocities of 0.5×10^6 and 1.0×10^6 lb/hr ft^2 over a quality range of 0.20 to 0.50. Measurements of two phase pressure drop indicated a low flow perturbation level for these tests. Results were compared with previous heat transfer data for which pressure drop perturbations were larger. Transition boiling behavior was found to depend strongly on the magnitude of pressure drop perturbations, which in turn are related to the overall flow loop characteristics. The two different levels of flow perturbation behavior were evaluated analyzing the flow pattern by the Griffith and Baker correlations. The flow pattern for the larger flow perturbation data was interpreted to be an interaction between liquid slugs and a steady annular pattern. Based on this assumption, calculated variations in two phase pressure drop were found to be comparable with measured values. The size of the transition boiling region was estimated from the effect of calculated steam quality and mass flow variations on the critical heat flux. It was found to have the same order of magnitude as the experimental data. Evaluation of the present data for which flow perturbations were small indicated that the flow pattern was steady dispersed flow. (auth)

14688 (N65–20692) A CHECK ON THE WEIGHT OF SPACE RADIATORS FOR STEAM SYSTEMS. Kroeger, Henry R. (ASTRA, Inc., Raleigh, N. C.). Feb. 25, 1965. 12p. (ASTRA-G–71).

Calculations are illustrated for a near-optimum aluminum radiator designed for a 1000-kw(e) steam system. The radiator-condenser, a simple, all-aluminum, fin and tube construction, is described in detail. Input and output values for the aluminum radiator parameters are included. The weight per square foot of radiating surface was 0.31 lb/ft^2; the heat radiated per square foot of radiator surface was 0.15 kw(t)/ft^2; the specific weight of the effective radiating area was 2.07 lb/kw(t); the total radiating surface weight was 2.59/kw(t); and the specific weight of the radiator fin and tube section was 11.0 lb/kw(e). Total weight estimates for other types of radiators for 1000-kw(e) steam space power systems are included. (STAR)

14689 (NLCO-970, pp 5.1-7) THERMOELECTRIC COOLING OF CUTTING TOOLS. McCright, R. D. (National Lead Co. of Ohio, Cincinnati).

The effect of thermoelectric, or Peltier, cooling on the tool life of carbide cutting tips when machining uranium was evaluated. The test results showed no significant improvement in tool life when thermoelectric cooling was used. (auth)

14690 (SC-DC-66-1293) A STUDY OF HEAT-GENERATED PRESSURE OSCILLATIONS IN A CLOSED END PIPE [Thesis]. Feldman, Karl Thomas Jr. (New Mexico Univ., Albuquerque. Bureau of Engineering Research). Nov. 1965. Contract AT(29-1)-789. 219p. Dep. mn. CFSTI $6.00 cy, $1.25 mn.

Submitted to Univ. of Missouri, Columbia.

The phenomena investigated is the heat generated pressure oscillation known as the Sondhauss thermoacoustic oscillation. Sondhauss oscillations occur when heat is added steadily to the gas in a pipe having one closed end. The available published references on the Sondhauss oscillation and a related thermoacoustic phenomenon known as the Rijke oscillation are listed and reviewed. A physical analysis of the heat exchange mechanism driving the Sondhauss oscillation is presented. The Sondhauss oscillator is treated as a heat engine operating on a specified thermodynamic engine cycle. The factors which initiate and maintain thermoacoustic oscillations are analyzed. The fundamental driving mechanism is shown to be a combination of simple thermal expansion and a mixing expansion resulting from the difference of molar specific heats of the hot and cold gas which is mixed during the cycle. A mathematical model for the Sondhauss oscillation is also presented. An experimental study of the Sondhauss oscillation is presented where sound pressure level and frequency distribution were measured for variations in pipe length, probe position along the pipe, heater power, heater position, tube bundle position, tube-bundle tube diameter and length and operating gas. The experimental results are presented in dimensional and dimensionless form. A theoretical model of the Sondhauss oscillator is derived from the fundamental hydrodynamic equations and from the heat engine analogy. The solution of the theoretical model was obtained by an analog computer using a finite difference approximation. By scaling the results of the analog computer solution to coincide with the experimental results, the characteristics of the heat addition term were analyzed. The results of the theoretical analog solution were the same as the experimental results to within 5% for both sound pressure magnitude and frequency. The heat engine aspects of the Sondhauss oscillator hypothesized in the physical analysis were verified by the experimental results and the analog computer results. (M.O.W.)

14691 (UCRL-10696(Rev.)(Pt.2)) LONGITUDINAL DISPERSION IN SINGLE-PHASE LIQUID FLOW THROUGH ORDERED AND RANDOM PACKINGS. Jacques, Gabriel L.; Hennico, Alphonse; Moon, Joon Sang; Vermeulen, Theodore (Lawrence Radiation Lab., Univ. of California, Berkeley). Nov. 16, 1964. Contract W-7405-eng-48. 50p. Dep. mn. CFSTI $1.00 cy, $0.50 mn.

Step-function injection and purging of a salt tracer in water was used to measure axial dispersion in sphere- and ring-packed columns. The product of packing Péclet number and void fraction was found to be 0.8 to 0.9 at Reynolds numbers corresponding to the turbulent (eddy) flow range, but only 0.20 in the laminar (filamental) range. For spheres, similar results were given for random packing and for ordered arrangements. It is believed that multiparticle dispersion, or channeling, was largely absent. The higher laminar-range Péclet number observed by others for gases is perhaps explained by the difference in Schmidt numbers. (auth)

14692 (UCRL-16656) BEHAVIOR OF DROPLETS EVAPORATING IN HIGH TEMPERATURE CONVECTIVE ENVIRONMENTS [Thesis]. Wijffels, Joannes Baptists (Lawrence Radiation Lab., Univ. of California, Berkeley). Sept. 1965. Contract W-7405-eng-48. 87p. Dep. mn. CFSTI $3.00 cy, $0.75 mn.

The behavior of small droplets in a high temperature convective environment of their own vapor at low Reynolds numbers was investigated. The behavior of large droplets evaporating in a stagnant environment at quasi steady state is well known. This solution is used as a basis, to which corrections are applied, for the evaporation of very small droplets and for the evaporation in convective flow. An expression was obtained for the drag exerted on the droplet by the convective environment. Approximate analytic and numerical solutions were obtained for the problem although the presence of the convective flow field does not alter the total evaporation rate, the drag exerted and rapidly evaporating drop is lowered appreciably, compared to the case of Stokes flow. (auth)

14693 (AD-625791) ON THE MECHANISM OF BOILING OF LIQUID SODIUM ON A HEATING SURFACE AT FREE CONVECTION. Deyev, V. I.; Solov'ev, A. N. Translated from Inzh. Fiz. Zh., 7: No. 6, 8-12(1964). 11p. (FTD-TT-65-907). CFSTI $1.00 cy, $0.50 mn.

The process of boiling of liquid sodium on a surface of heating during bubbling condition is discussed. Evaluations were made of characteristics for the boiling process of values, such, as the number of vapor formation centers, rate of growth, and break away diameter of the blister. (M.O.W.)

14694 A NEW METHOD OF BURNOUT DETECTION. Afgan, N.; Novakovic, M.; Anastasijevic, P. (Boris Kidrich Inst. of Nuclear Sciences, Belgrade). New York, American Society of Mechanical Engineers, 1965, Preprint No. 65-WA/HT-46, 6p., $1.50. (CONF-651110-16). ORINS.

From American Society of Mechanical Engineers, Annual Winter Meeting, Chicago.

A new method of burnout detection in a large volume of boiling water is described. The method is based on temperature measurement of a test-section inner surface by a gas thermometer. The test section as a measuring part of the gas thermometer was filled with a liquid-vapor mixture. The temperature of the inner wall of the tube was determined by measuring the pressure of the mixture. The measurements were taken with two liquids subsequently. The values of the heat fluxes during burnout conditions for the water temperature nearing saturation are also given. (auth)

14695 CRITICAL HEAT FLUX IN LONG TUBES AT 1000 psi WITH AND WITHOUT SWIRL PROMOTERS. Matzner, B. (Columbia Univ., New York); Moeck, E. O.; Casterline, J. E.; Wikhammer, G. A. New York, American Society of Mechanical Engineers, 1965, Preprint No. 65-WA/HT-30, 16p., $1.50. (CONF-651110-13). ORINS.

From American Society of Mechanical Engineers, Annual Winter Meeting, Chicago.

Presented are 200 critical heat fluxes obtained with boiling water flow in 0.400-in.-ID tubes, uniformly heated over lengths of 8, 12, and 16 ft, at mass velocities between 0.9 and 7.2×10^6 lb/hr-sq ft. Swirl flow, induced by a full-length tape or by two tape inserts, 2 in. long and 8 ft apart, and axial flow were studied. The full-length tape increased the critical heat flux by 30 to 50 percent, while the tape inserts gave 0 to 35 percent improvements, depending on the mass velocity and quality at the second swirl piece. The Winfrith Correlation predicted the critical heat fluxes for the 104 axial-flow points on an RMS deviation of 11.8 percent. (auth)

14696 BURNOUT IN STEAM-WATER FLOWS WITH AXIALLY NONUNIFORM HEAT FLUX. Smith, O. Glenn (Westinghouse Electric Corp., Lima, Ohio); Rohrer, W. M. Jr.; Tong, L. S. New York, American Society of Mechanical Engineers, 1965, Preprint No. 65-WA/HT-33, 9p., $1.50. (CONF-651110-15). ORINS.

From American Society of Mechanical Engineers, Annual Winter Meeting, Chicago.

The question of whether burnout can be predicted from local parameters at the burnout location or whether it depends on inlet enthalpy and axial heat-flux distribution was resolved experimentally. Futhermore, the implicit effect of inlet enthalpy and axial heat-flux distribution upon the burnout heat flux in circular tubes was evaluated

quantitatively. Both uniform and nonuniform heat-flux burnout tests were performed with subcooled inlet and net steam quality at burnout. Ranges of parameters tested were: pressure 515 psia; burnout quality 0.2 to 0.8; burnout heat flux 1.2×10^6 to 2.2×10^6 Btu/hr-sq ft and mass flow rate 0.55×10^6 and 1.10×10^6 lb/hr-sq ft. An analysis was performed considering an annular flow pattern and a simplified rate equation for liquid transfer to the film. A concise expression for evaluating the implicit effect of axially nonuniform heating upon the burnout heat flux was developed. (auth)

14697 SLUG FLOW AND FILM BOILING OF HYDROGEN. Chi, J. W. H. (Westinghouse Electric Corp., Pittsburgh). New York, American Society of Mechanical Engineers, 1965, Preprint No. 65-WA/HT-32, 12p., $1.50. (CONF-651110–14). ORINS.

From American Society of Mechanical Engineers, Annual Winter Meeting, Chicago.

Forced-convective, transient boiling heat transfer was studied by the cooldown of a copper test section by liquid hydrogen. From the slopes of the wall-temperature histories, local forced-convective boiling heat flux was obtained for a wide range of conditions. The bulk-fluid temperature traces showed well-behaved oscillations with two distinct frequencies: A high-frequency, low-amplitude oscillation attributed to mist flow was seen to be superimposed on a low-frequency, high-amplitude oscillation due to slug flow. Based on the bulk-stream temperature traces and the apparent mechanisms of two-phase flow, a general equation was derived for forced-convective film boiling heat flux. It was shown that the correlations are applicable to single-phase gas, mist flow, slug flow, and annular flow. (auth)

14698 STAYING DEVICE FOR TUBES, RODS AND THE LIKE IN STEAM GENERATORS, HEAT EXCHANGERS AND THE LIKE. (to Aktiebolaget Motala Verkstad). British Patent 1,017,455. Jan. 19, 1966. Priority date June 8, 1962, Sweden.

A staying device for tubes, rods, or the like arranged in at least two parallel rows in steam generators, tube heat exchangers, or the like is characterized by two resilient steel strips between two adjacent rows of tubes and a third strip so shaped that the first two strips are resiliently forced against the respective row of tubes to fix them in their positions. The third strip is pleated or corrugated angularly or in wave-shaped form; and these corrugations, pleats, or waves have a pitch equal to the pitch of the tubes. (B.L.M.)

14699 EVAPORATION-CONDENSATION HEAT TRANSFER DEVICE. Grover, George M. (to U. S. Atomic Energy Commission). U. S. Patent 3,229,759. Jan. 18, 1966.

A heat transfer device comprising a sealed tube of niobium-1% zirconium alloy, the inside surface of the tube being, for the most part, covered by capillary means and a small amount of lithium wetting the capillary means is described. (AEC)

Materials Testing

14700 (NYO–3622-1) APPLICATIONS OF ULTRASONIC ENERGY: ULTRASONIC INSTRUMENTATION FOR NUCLEAR APPLICATIONS. Bimonthly Progress Report No. 26, December 1, 1965–January 31, 1966. (Aeroprojects, Inc., West Chester, Pa.). Feb. 1966. Contract AT(30-1)-3622. 13p. Dep. mn. CFSTI $1.00 cy, $0.50 mn.

Ultrasonic instrumentation for the detection of incipient boiling in molten metal is discussed. Preliminary designs for feasibility testing of an acoustic flowmeter are discussed. The method for making preliminary measurements under conditions approximating end-use is outlined. (M.O.W.)

14701 (STI/PUB/105(Vol. 1)) NON–DESTRUCTIVE TESTING IN NUCLEAR TECHNOLOGY. VOL. 1. Proceedings Series. Proceedings of a Symposium held in Bucharest, 17–21 May 1965. (International Atomic Energy Agency, Vienna (Austria)). 1965. 396p. (CONF-650509(Vol. 1)). IAEC: $8.00; S 168,-; £ 2.8.0; F Fr 32,-; DM 28,-.

Twenty articles and one abstract are included; separate abstracts were prepared for 18. Two articles were previously abstracted in NSA as 20: 3890 and 6632. (P.C.H.)

For abstracts of individual papers see: 14703–14720.

14702 (Y–1490) PENETRATION TESTS. Carey, W. T. (Union Carbide Corp., Oak Ridge, Tenn. Y-12 Plant). Mar. 4, 1966. Contract W-7405-eng-26. 17p. Dep. mn. CFSTI $1.00 cy, $0.50 mn.

A test was developed to evaluate the ability of materials to resist penetration by a small-diameter penetrator. The test was developed for use in evaluating high-strength materials. The test results and limitations of the test are presented. (auth)

14703 EDDY-CURRENT TESTING OF FINNED FUEL CLADDING. Otter, A. J. (Atomic Energy of Canada Ltd., Chalk River, Ont.). pp 3-16 of STI/PUB/105(Vol. I).

The application of eddy-current techniques to finned designs is described. The function and geometry of the fins must be considered in the selection of the optimum test parameters and the most suitable test coil geometry. Thus, the presence of fins may limit or restrict the test but they will not prevent a successful test. Where the fin geometry is complex, eddy currents may well be the most suitable of the non-destructive methods which can be used for flaw detection. The thickness of aluminum cladding over a uranium core was measured with a small probe coil placed between the fins and shielded from them. Two flaw detection tests are described, one on sintered aluminum product (SAP) tubing using an internal bobbin coil and the other on an aluminum-clad uranium-aluminum alloy rod with an external encircling coil. The instrumentation described is relatively simple. A small portable instrument was designed for the cladding thickness measurement. For flaw detection a standard oscilloscope with a plug-in carrier-amplifier module provides a means of sensing and displaying the test coil impedance variations. This equipment is adequate for a variety of testing applications and has been specified for routine fuel testing on a production basis. (P.C.H.)

14704 MICRORADIOGRAPHIC FUEL INVESTIGATION IN THIN LAYERS. Neider, R.; De Meester, P. (Studiecentrum voor Kernenergie, Mol, Belg.). pp 17-33 of STI/PUB/105(Vol. I).

A contact microradiographic method was developed, which yields a maximum resolution of about 30 μm. Plates or tubes are radiographed with 60-kev x rays while fine-grained photographic emulsion is in intimate contact with the investigated area. The fuel distribution is checked qualitatively by 10- to 30-fold enlargements of the film on paper and quantitatively by photometric density measurements. For calibration purposes a wedge step of clad Al–U24% alloy was radiographed under the same conditions as the test pieces and developed simultaneously. Exposure data for the used fine-grained emulsions as well as qualitative and quantitative test results are given for rolled plates and coextruded tubes. (P.C.H.)

14705 LIMITATIONS OF ^{192}Ir AS A RADIOGRAPHIC SOURCE FOR THE CONTROL OF REACTOR PRESSURE-VESSELS. Horvat, D. (Nuclear Inst. Josef Stefan, Ljubljana, Yugoslavia). pp 61-73 of STI/PUB/105(Vol. I).

Results of our own investigations have shown that the advantage of ^{192}Ir with regard to the quality of radiographs is obvious when comparing it with ^{60}Co even with thicknesses over 80 mm of irradiated steel. The application of ^{192}Ir in practice is limited by the alternative: either a very long exposure time or a source of very high activity. Possibilities of improvement due to a new shape of radiographic sources are discussed. In the case of narrow primary beams these new sources give smaller effective dimensions and allow shorter source-to-film distances. A further advantage of ^{192}Ir is obvious from the diagrams of the weight of the exposure equipment for ^{192}Ir and ^{60}Co taking into account equivalent activities of both sources re-

garding the same exposure time. The economic disadvantages, because of the short half life, of ^{192}Ir are discussed and a rough economical comparison between ^{60}Co and ^{192}Ir at different extensiveness and densities of the radiographic control is given. (P.C.H.)

14706 USE OF LOW-VOLTAGE RADIOGRAPHY IN DETECTING FLAWS IN THIN-WALLED SINTERED ALUMINIUM POWDER (SAP) TUBES. Bonnet, P.; Jansen, J. (EURATOM-CCR, Ispra, Italy). pp 75-99 of STI/PUB/105(Vol. I). (In French).

To overcome the certain drawbacks in detecting flaws in thin-walled tubes, two radiographic techniques were developed: the rotative technique, more suitable for tubes of fairly wide diameter; and the rolling technique, particularly suitable for fuel-element cans, having been developed principally for testing finned tubes, which present considerable technological obstacles to testing by the normal methods. In the rotative technique, the tube is irradiated through a slit of variable width. The film is placed inside the tube held by a chuck of opaque material, usually lead. The tube, film, and chuck are then rotated together. Results on the effects of various parameters on the degree of geometric sharpness are given: source-slit distance; slit width; radiation characteristics; and speed of rotation. A suitable expanding chuck is also illustrated. The principle of the rolling technique likewise stems from the requirement that only one tube wall shall be radiographed. Irradiation is again carried out through a slit but, while the tube is being rotated, the film is moved in such a way that its linear speed matches the rotational speed of the tube at its external face. Preliminary tests showed that this is a perfectly sound technique. Optimum conditions pertaining to the techniques, including speed of film transport, width of slit, etc., are discussed. Results obtained with tubes containing real or artificial flaws are also presented. The semi-industrial use of these techniques, including advantages and disadvantages, is also considered. (P.C.H.)

14707 NON-DESTRUCTIVE TESTING OF PLUTONIUM-ENRICHED FUEL RODS. Libotte, P.; Inniger, H.; Leblanc, J. M. (Centre d'Etude de l'Energie Nucleaire, Mol, Belg.). pp 101-14 of STI/PUB/105(Vol. I). (In French).

Non-destructive testing techniques developed for assessing the quality of Pu-enriched fuel rods are described. The methods are used primarily for checking the dimensions and quality of fuel-element cladding tubes, the integrity of welds, the leak-tightness of the rods, the density and distribution of the fuel, and plutonium enrichment and radial and axial distribution in the fuel rod. The principal non-destructive testing methods used are radiography, autoradiography, gamma radiography, and ultrasonics. The principles underlying each procedure and equipment used, together with the techniques applied in each case to obtain the required sensitivity and accuracy, are discussed. With the radiography technique, flaws of the order of 50–60 μm in the end-cap welds of fuel elements can be detected. Since the fuel consists of three high-density powder fractions compacted by vibration, with only the fine fraction comprising the plutonium enrichment, it is essential to measure accurately the distribution of plutonium and the density distribution. By counting the gamma radiation emitted by the plutonium it is possible to find the longitudinal distribution of the latter with an accuracy of better than ±2% in the case of perfect radial distribution; the last-named is usually determined by exposure on photographic emulsion. The axial distribution of the fuel density is determined with an accuracy of better than ±1% by measuring the non-absorbed fraction of gamma radiation emitted by an external source, either ^{137}Cs or ^{192}Ir. Cracks of around 10 μm can be detected ultrasonically by the pulse-echo technique. The respective advantages of the various non-destructive techniques were studied in relation to the required accuracy and to their possible application to the automated inspection of plutonium fuel rods fabricated on an industrial scale. (auth)

14708 SOME POSSIBILITIES OF THE EDDY-CURRENT METHOD FOR MULTI-PARAMETER TESTING OF STRUCTURAL COMPONENTS. Vyakhorev, V. G.; Gerasimov, V. G.; Deniskin, V. P.; Trakhtenbert, L. I.; Shkarlet, Yu. M. (State Committee for the Use of Atomic Energy, Moscow). pp 115-36 of STI/PUB/105(Vol. I). (In Russian).

The pattern of occurrence of problems of non-destructive multiparameter testing in nuclear technology and the advisability of approaching these problems by the eddy-current method are discussed. The application of electric models is justified for solving testing problems using a long follow-through coil. Design formulas are given and the principles of designing applied eddy-current probes are explained. An arrangement for testing tube-wall thickness is described: in this apparatus the effect of movement of the tube under testing on the measurement results is eliminated with the aid of a servo-system controlled by a signal depending on the probe voltage phase. Use of a self-oscillating circuit containing a test-coil as the probe of an apparatus for testing tubes is described. On the basis of calculated and experimental data various possibilities are indicated for the construction of single-frequency applied eddy-current testing probes for simultaneous measurement of more than two parameters. (auth)

14709 THE PROBLEMS OF CONTROLLING DEFECTS IN THE MATERIALS USED FOR THE FIRST CZECHOSLOVAK NUCLEAR-POWER STATION. Filipp, Radislav. pp 139-50 of STI/PUB/105(Vol. I). (In Russian).

The reactor vessel of the first Czechoslovak nuclear-power station is briefly described. In order to meet the stringent design and structural requirements involved in fabricating the reactor vessel, which consists of low-alloy, non-aging steel of considerable thickness (650 mm), it was necessary to devise a control method for non-destructive testing of the basic material and welded joints. The ultrasonic pulse method, using one probe, was used extensively in testing the quality of the basic material and welded joints. The methods used for carrying out tests and interpreting the results during the investigation of the basic material, and the methods for testing the quality of molten-slag arcless electric welds, carbon-dioxide welds, and manual arc welds are described. An automatic flaw-detection apparatus was used to test flat forgings and rolled products. The apparatus consists of two parts: a travelling mechanism and an ultrasonic flaw-detector. The apparatus incorporates a number of new features. The effects of distance on the height of the defect signal pulse is compensated and the height remains constant. The effect of irregularity of the acoustic link is also compensated since the data-unit conveys pulses to the remote recording device. An attenuator is used to determine the size of the flaw. An automatic apparatus is now being developed for testing on a vertical cylindrical surface. Since, assembly welds on circumferences must be tested at a high temperature, a special data-unit was developed, which makes it possible to carry out tests at elevated temperatures with a high degree of accuracy. Non-destructive tests of welded structures were also carried out using radiography. The testing of thin longitudinal seam welds and their roots at a high temperature was carried out with an x-ray unit with circular radiation characteristics, using special cassettes. (auth)

14710 NON-DESTRUCTIVE TESTING IN REACTOR PRESSURE-VESSEL FABRICATION. McGonnagle, W. J. (Illinois Inst. of Tech., Chicago). pp 151-66 of STI/PUB/105(Vol. I).

A quality control program for the design and fabrication of a reactor pressure-vessel which will meet all nuclear and safety requirements is outlined, the place and importance of non-destructive testing in achieving that objective are discussed. The non-destructive testing program includes the inspection of plate material, forging, casting, cladding, and welds. The particular non-destructive testing problems met in nuclear pressure-vessels are discussed. The specialized techniques peculiar to the non-destructive testing of pressure vessels and their components are illustrated and discussed. Applicable codes and specifications, such as the Boiler and Pressure Vessel Code of the American Society for Mechanical Engineers and other regulatory

bodies, are outlined. How non-destructive testing can help to comply with the specifications and requirements of various regulatory bodies, and the adequacy and applicability of standards used in such an application are discussed. Realistic but adequate acceptance and rejection criteria are suggested. A procedure is outlined which will help non-destructive personnel to perform adequately their functions at the proper time in the fabrication cycle. (P.C.H.)

14711 CONTROL METHODS USED IN THE DEPARTMENT OF METALLURGY FOR STRUCTURAL AND FUEL ELEMENTS. Destribats, Marie-Therese; Allain, C.; Prot, A.; Thome, P. (CEN, Saclay, France). pp 167-89 of STI/PUB/105(Vol.I). (In French).

Studies of various reactor types undertaken by the Commissariat à l'Énergie Atomique led to the use and development of many non-destructive methods of testing the various materials employed in their construction, and especially methods involving the use of x and γ rays, ultrasonic waves, and eddy currents. A summary is given of the tests carried out during the construction of EDF (graphite gas) and EL 4 (heavy water) reactor types and of co-laminated elements. Emphasis is laid on certain typical aspects of these various methods, some of which are well known. EDF type: ultrasonic measurement of the wall thicknesses of uranium or uranium alloy tubes; gamma-radiographic detection of voids in the tubes; ultrasonic inspection following heat treatment of the tubes; ultrasonic flaw detection (inclusions, pipes) in billets and rough casts for MgZr cladding; leak-tightness testing of slugs by helium eliquation. EL 4 type: ultrasonic and eddy-current measurements of the wall thicknesses of Zircaloy-2 pressure and guide tubes; ultrasonic inspection of Zircaloy-2 pressure tubes and stainless steel cladding tubes; in vacuo radiography of Be claddings; leak-tightness testing of pencils by helium eliquation. Co-laminated elements: cladding thickness measurements by pulsed eddy currents; determination of core position in tubes and plates, using x rays, gamma counting, and pulsed eddy currents; checking of fuel homogeneity by gamma counting; ultrasonic and gamma-radiographic flaw detection in ZrU billets; detection of unbonded areas in plates, using ultrasonic waves, pulsed eddy currents, and resistivity measurements. The methods were developed for industrial use. Several of the inspections already constitute routine manufacturing procedures, others will be introduced shortly, and a further number are likely to come into use at a later date. (auth)

14712 NON-DESTRUCTIVE TESTING METHODS APPLIED TO MULTI-FINNED SAP TUBING FOR NUCLEAR-FUEL ELEMENTS. Lund, S. A. (Danish Central Welding Institution, Copenhagen); Knudsen, P. pp 191-204 of STI/PUB/105(Vol. I).

An account is presented of the non-destructive techniques developed for measuring wall thickness and diameters and for detecting defects in multi-finned SAP tubing for reactor fuel elements. The complex 24-finned cross-section prevents the application of ultrasonic or eddy-current methods for wall-thickness measurements. Therefore, a special recording beta-gauge was developed, based upon the attenuation of beta radiation from a ^{90}Sr source placed inside the tube. An ultrasonic immersion resonance method is used for the continuous recording of the wall thickness of the more simple 12-finned tube design. Inner and outer (across fin tips) diameters are continuously recorded by rapid air-gauge systems. Flaw detection is carried out by the ultrasonic pulse-echo immersion technique and by eddy-current inspection. Transverse cracks can easily be detected by the ultrasonic method whereas inspection for longitudinal flaws has not appeared feasible with this method. Therefore, eddy-current inspection is applied in addition to the ultrasonic testing. (P.C.H.)

14713 FLAW DETECTION IN THIN-WALLED TUBES. Gorskii, V. V.; Zakharov, V. M.; Nikitin, G. A.; Popov, V. K.; Pronyakin, V. T.; Khodulev, B. S. (State Committee for the Use of Atomic Energy, Moscow). pp 233-55 of STI/PUB/105(Vol. I). (In Russian).

Special features and advantages of ultrasonic methods of detecting flaws in thin-walled tubes by means of Lamb's waves are discussed, and the apparatus used is described. The effects of non-uniform thickness and ovalness of tubes on signal fluctuations in inspection by the shadow method are given. Metal structure is tested by the ratio method based on a comparison between signals of different frequency which are reflected by or which pass through the materials. In smooth and finned thin-walled tubes with diameters of 3 to 60 mm and wall thicknesses of 0.2 mm or more, defects are detected with ultrasonic apparatus. Inspection is carried out by the immersion technique, the shadow method, and the reflection method with working frequencies up to 10 MHz. Positive detection is achieved of defects over 0.5 mm in length and with a depth of 5% of the wall thickness. Grain size is controlled by structure analyzers. Eddy-current apparatus is used for measuring the wall thickness of tubes made of non-magnetic materials. (P.C.H.)

14714 QUALITY SELECTION OF ZIRCALOY-2 CANNING TUBES BY ULTRASONIC TESTING ON SMALL DEFECTS. Van Der Linde, A. (Reactor Centrum Nederland, Petten, Netherlands); De Raad, J. A. pp 259-73 of STI/PUB/105(Vol. I).

Zircaloy-2 canning tubes, 10.20 mm I.D. × 0.90 mm wall × 1500 mm length, destined for testing as fuel-rod cladding in a high temperature, 330°C, in-pile pressurized water loop, were tested ultrasonically for defects to get an impression of the tubes' quality. Because only two of the 93 tested tubes had defects with a depth greater than 50 μm it was decided to apply a more severe test by which defects with a depth in the range 10–50 μm could be detected. To detect and record such small defects, longitudinal as well as transverse, a semi-automatic ultrasonic pulse equipment was used in combination with gating systems and a multiple-channel recorder. The adjustment of the scanning system was such that inner and outer defects of the same size were indicated with equal amplitudes. Calibration of the equipment was made on artificial defects. Longitudinal defects were detected with a separated transmitter-receiver system using a focused beam. Transverse defects were scanned by a single probe acting as transceiver. To obtain the sensitivity required the tests were carried out in immersion at a frequency of 4 MHz whereby the tubes were rotated with 120 rpm. Description is given of the mechanical device, the general set-up, and the difficulties encountered. The result was that from the 93 tested tubes 21 had defects in the transverse direction with a depth between 10 and 50 μm. Thus a relative qualification of the tubes was obtained. (P.C.H.)

14715 AUTOMATIC INSPECTION OF CO-LAMINATED ELEMENTS. Destribats, Marie-Therese (CEN, Saclay, France); Dory, J. pp 275-83 of STI/PUB/105(Vol. I). (In French).

An automatic device for the ultrasonic inspection of co-laminated fuel element claddings is described. The elements are placed in a stainless-steel tank filled with water and are carried under the ultrasonic beam by rollers. An auxiliary reflector makes it possible to use the same transducer for both emission and reception. The plates are scanned by six transducers fixed around the edge of a rotating disc, each transducer being brought into action every one-sixth turn by relays triggered by magnetized sectors, so that the ultrasonic pencil traces a series of linked arcs on the surface of the plate. The amount of energy passing through the plate is measured accurately at each point. The measured value is fed into a special recorder which traces a full-scale image of the element inspected (the instrument uses ordinary paper and records by means of carbon paper). Flaws appear as dark patches on the recording. The apparatus can operate either at all-or-nothing response with a pre-determined marking threshold, or at half-tone response. The transducers, which work on a variable frequency between 3 and 15 MHz, are excited by short pulses: they are of barium titanate and 3 mm in dia. The scanning track can be varied from 0.3 to 0.6 mm, with a linear speed of 5–20 mm/s. The apparatus can accept elements of the following maximum dimensions: width–150 mm, length–2000 mm, thickness–

25 mm. Trials already carried disclosed unbonded areas of 0.5 mm dia in elements 2 mm thick. (auth)

14716 ULTRASONIC DETECTION OF LONGITUDINAL DEFECTS IN THIN-WALL CLADDING TUBES. Nystroem, U. (Aktiebolaget Atomenergi, Stockholm). pp 285-301 of STI/PUB/105(Vol. I).

A general description of the ultrasonic methods and waves that can be used for the detection of longitudinal defects in cladding tubes is given. Results are also given of current development work. This includes a study of the multiple indications obtained from longitudinal defects in Zircaloy-2 cladding tubes (OD 13.8 × 0.65 mm) at an incident angle in water of about 36° and using a line-focused transducer with a frequency of 4 MHz. To avoid variations in sensitivity, a method was developed, whereby the sound transmission in the tube wall is controlled simultaneously with the detection of defects. The advantage of this method is that equipment functions can be checked during the tests. Factors that limit the maximum speed of rotation and feed that can be used for such tests are listed. Standardization of methods and equipment for the detection of defects as well as techniques for making standard defects in tubes are recommended. (P.C.H.)

14717 INDUSTRIAL ULTRASONIC INSPECTION OF STAINLESS-STEEL CLADDINGS FOR THE EL4 REACTOR. Prot, A. C.; Foulquier, H. E.; Peyrot, J. P. (CEN, Saclay, France). pp 303-20 of STI/PUB/105(Vol. I). (In French).

An automatic ultrasonic device was designed for inspection of stainless steel cladding tubes for the EL 4 reactor. The device can easily meet the requirements of a fuel-element production line. The potentialities of the device are closely dependent on the characteristics of the inspection equipment used, especially the performances of the electronic part of ultrasonic inspection instruments and of the transducers. (P.C.H.)

14718 AUTOMATION OF THE TUBE-THICKNESS MEASUREMENTS USING ULTRASONICS. Wells, F. H.; Davey, C. N.; Sharpe, C. (Atomic Energy Research Establishment, Harwell, Eng.). pp 321-9 of STI/PUB/105(Vol. I).

Two ultrasonic methods for automatically measuring the wall thickness of thin-walled metal tubing are described and compared for accuracy and measurement rate. The first is a double-probe method using an ultrasonic plane transmitter crystal to irradiate a small area of tube wall and a separate receiving crystal adjusted to receive energy from this same area; the two probes are mounted close to each other. As the transmitter frequency is varied, the receiver output shows an absorption resonance when the ultrasonic wavelength corresponds to twice the tube thickness. The electronic circuits used to automatically adjust the frequency to keep the receiver output at a minimum are described. By measuring this frequency a record in digital form of the thickness of the tube may be obtained. The second is a single-probe method using a focused transmitter probe directing a burst of energy, typically 30 μs duration of 5 MHz frequency, at normal incidence to the tube wall; the same probe acts as a receiver and electronic circuits are used to select the first reflected pulses. Descriptions are given on how the transmitter frequency is varied automatically over a selected range and how the frequency at which a minimum reflected pulse occurs is selected and measured. This minimum occurs at a wavelength of twice the tube wall thickness so that again a direct signal measurement of thickness is achieved. (auth)

14719 NEW METHODS AND FACILITIES FOR THE MEASUREMENT OF PHYSICAL PROPERTIES OF REACTOR COMPONENTS AND IRRADIATED MATERIALS. Foerster, F.; Mueller, P. (Institut Dr. Foerster, Reutlingen, Ger.). pp 331-65 of STI/PUB/105(Vol. I).

An instrument for the fully automatic measurement and recording of Young's modulus and the shear modulus and the damping capacity as a function of temperature and time is illustrated. The measurement of Young's modulus is produced by exciting specimens of various sizes in their natural frequency. The measurement of damping capacity occurs by free decay of the vibration or by the measurement of the half width of the resonance curve. Examples are given for measurements of the recovery after radiation damage and after plastic deformation and for the degree of graphitation. The detection of defects and density variations in graphite bars was proven. Furthermore, a method of investigation of the fastening of UO_2 pellets in thin-walled austenitic tubes is explained. A special oven for the investigation of the elastic and inelastic behavior of hot specimens at temperatures between 20 and 2000°C is described. The quality control of non-ferrous metals by means of eddy-current measurement of the electrical conductivity is discussed. An instrument is shown for the contactless measurement of the electrical conductivity of non-ferrous metals. The correlation between the electrical conductivity and the stress-strain behavior of non-ferrous metals and alloys is explained. Special attention is paid to the measurement of small-size test pieces. A device for remote direct measurement in the hot zone of the reactor is shown. The dependence of the electrical conductivity upon the radiation dose is discussed. An instrument for the measurement of the permeability, the remanence, and the coercive force as a function of the mechanical stress, elastic and plastic strain, and radiation dose is explained. Measurements of the variation of magnetic properties as a function of elastic stress and plastic deformation are shown. The effects of irradiation on the permeability and the coercive force are discussed. An instrument is also shown for the quick measurement and direct reading of the permeability and stainless-steel components. The correlation between permeability and Δ ferrite content is explained. Measurements of the Δ ferrite percentage across welds in stainless-steel tubes and measurements of the Δ ferrite precipitations as a function of the plastic strain are discussed (hammer-forging of reactor fuel-elements). (auth)

14720 AUTOMATIC INSPECTION OF NUCLEAR-REACTOR TUBES DURING PRODUCTION AND PROCESSING, USING EDDY-CURRENT METHODS. Foerster, F.; Mueller, P. (Institut Dr. Foerster, Reutlingen, Ger.). pp 371-92 of STI/PUB/105(Vol. I).

The possibilities of automatic and semi-automatic inspection of tubes using eddy-current methods are described. Modern processes were compared with other non-destructive methods. The methods discussed are ideal for objective automatic inspection. Not only are the known methods described, but certain new methods and their application to the detection of flaws in reactor tubes are discussed. (auth)

14721 RADIOACTIVE COMPOSITION. Farmer, Herbert Edward; Buckley, Arthur Hever (to General Electric Co.). U. S. Patent 3,230,176. Jan. 18, 1966. Filed Oct. 3, 1961.

A magnetic radioactive composition for use in magnetic-particle inspection consists of a paste made from water or kerosene and radioactive iron oxide. The articles to be tested are magnetized and then dipped in the radioactive paste. The articles are then rinsed with an organic solvent to reduce excess radioactivity and to accelerate drying. The article is then subjected to magnetic particle inspection. (B.L.M.)

Protective Structures

14722 AIR INTAKE STACK AND FILTER CARTRIDGE FOR FALLOUT SHELTERS. Zahn, Robert E.; Welty, William H. (to Air Filter Corp.). U. S. Patent 3,228,175. Jan. 11, 1966. Filed Mar. 5, 1962.

An air intake stack for a fallout shelter and a filter assembly for the stack are patented. A detachable hood firmly holds the filter assembly in sealing contact with the upper edge of the stack. The elongated tubular filter includes inner and outer walls of reticulated metal with mats of filtering material between them. The lower end of the cartridge is formed and closed with the filtering material so as to ensure the filtering of all the air entering the cartridge. The hood arrangement ensures that all the

air entering the stack passes through the filter cartridge. (B.L.M.)

14723 PROTECTIVE SHELTER. Garlock, Edward A. Jr. U. S. Patent 3,230,911. Jan. 25, 1966. Filed Feb. 1, 1962.

A prefabricated heat and radiation shelter of the family type comprises a series of hollow sheet steel or Al tapered segments broader at the base than at the top and broader at the outside than at the inside. Each segment bears against a central support member and against the adjacent segment. A waterproofing material is installed between the segments during installation. The segments are filled with a fluid material; water, water containing an anti-freeze material, or another liquid having suitable absorption capacity for penetrating radiation from nuclear explosion. The liquid may be drained from the segments and the shelter easily moved to another location if necessary. For permanent installation the segments may be filled with cement. Air circulation is provided by means of an igloo type door and the hole in the top of the shelter. (B.L.M.)

Space Propulsion

See also ISOTOPE TECHNOLOGY — Power Application
REACTOR TECHNOLOGY — Propulsion and Space

Refer also to abstracts 14692 and 16113.

14724 (65SD5322-A) NAVIGATOR STUDY OF ELECTRIC PROPULSION FOR UNMANNED SCIENTIFIC MISSIONS. CONSTANT POWER MISSION ANALYSIS. Brown, Harold; Taylor, J. R. (General Electric Co.; Philadelphia, Pa. Missile and Space Div.). Mar. 10, 1966. Contract NAS3-2533. 62p.

An analysis of the performance of systems using nuclear-electric propulsion is summarized. Orbiting missions to all of the planets in the solar system were considered, as well as fly-by missions to the four major outer planets. It was assumed that the NAVIGATOR vehicle is boosted beyond earth escape by a multistage Saturn V booster. (D.C.W.)

14725 (N65–15876) DEVELOPMENT OF A CHARGED COLLOID SOURCE FOR ELECTROSTATIC PROPULSION. Report No. 82. Gignoux, D.; Anton, H. F.; Shea, J. J. (Cosmic, Inc., Washington, D. C.). Oct. 1964. Contract NAS3-4106. 78p. (NASA-CR-54176). CFSTI $3.00 cy, $0.75 mn.

A large number of tests were performed with a rotating nozzle source of induction-charged colloid. The geometry was improved, resulting in an increase of the charge-to-mass ratio by one order of magnitude with respect to a previous program. Analytically, the ideal propellant was shown to have high viscosity, low density, low surface tension, low vapor pressure, and high conductivity. The experimental values of the system parameters agreed conclusively with those predicted analytically. The search for a better propellant disclosed several promising avenues. Beam currents up to 1.5 milliamp were obtained. The system has very promising application to high-efficiency electrostatic thrustors. (STAR)

14726 (NASA-CR-54746) INVESTIGATION OF PLASMA ACCELERATOR (CYCLOTRON RESONANCE PROPULSION SYSTEM). Final Report. Miller, David B.; Bethke, George W.; Crimi, Giles F. (General Electric Co., Phladelphia, Pa. Missile and Space Div.). Nov. 1, 1965. Contract NAS3-6266. 158p. (GE–214-252).

Five different electron-cyclotron-resonance plasma accelerators tested. All are of the longitudinal-interaction type, where the r-f propagation vector is parallel to the plasma acceleration direction. Two feature axial injection of the propellant through a hole in the waveguide window; these were shown to have relatively low power efficiency (<0.42), and the window design is apparently weakened by the axial gas injection hole. The other three inject gas through oblique peripheral ports. Solid waveguide walls are used in two of these; the other uses screen waveguide, allowing gas pumping between the window and the injection point. High (up to 0.79) power efficiencies were measured for these peripheral-injection accelerators. A thrust stand was built for these accelerators. Preliminary thrust measurements at 912 w of r-f power indicate thrust efficiencies on the order of 0.4 at 3200 sec. Mapping of the r-f field indicates that most efficient operation occurs when the r-f/plasma coupling takes place in a region removed from the window; an analytical model results in theoretical correlation with these mappings. Potential probes were used to verify and measure the charge-separation electric field profile. A multigrid, retarding-potential probe was used to measure the ion energy distribution. (auth)

14727 (NASA-TM-X-1208) EXPERIMENTAL STUDY OF EFFECT OF SIMULATED REACTOR CORE POSITION ON NOZZLE HEAT TRANSFER. Schmidt, James F.; Boldman, Donald R.; Ehlers, Robert C.; Coats, James W. (National Aeronautics and Space Administration, Cleveland, Ohio. Lewis Research Center). Mar. 1966. 8p. CFSTI $1.00 cy, $0.50 mn.

A simulated reactor core was installed at various positions upstream from a conical nozzle in order to determine the influence of core position on nozzle heat-transfer and boundary-layer characteristics. The tests were conducted in an air facility at a nominal stagnation temperature and pressure of 970° R and 300 lb/in^2, respectively. (auth)

14728 (NASA-TN-D-3328) SIMULATED NUCLEAR HEATING OF LIQUID HYDROGEN IN A PROPELLANT TANK. Huntley, Sidney C.; Gauntner, James W. (National Aeronautics and Space Administration, Cleveland, Ohio. Lewis Research Center). Mar. 1966. 29p. CFSTI $2.00 cy, $0.50 mn.

An experimental study was made to simulate nuclear heating of liquid hydrogen in a propellant tank by using an electrical immersion heater and radiant heaters. Flow tests were made in a 125-gal tank pressurized to 2 atm with a flow rate of about 0.04 pound per second. The test results showed that the inoperative immersion heater did not alter the exit temperature history. Operation of the immersion heater tended to result in a more completely mixed liquid than existed with nuclear heating. A comparison of bottom (radiant) heating with nuclear heating showed a nearly identical generalized exit temperature history with a similar generalized heat input rate distribution and equal heating parameters, although the initial total heat input rates varied by a factor greater than 6. High bottom (or liquid source) heating was observed to consistently result in a liquid disturbance near the surface during the transient development of a temperature gradient. (auth)

14729 INTERNATIONAL COUNCIL OF THE AERONAUTICAL SCIENCES, THIRD CONGRESS, STOCKHOLM, 1962, PROCEEDINGS. Von Karman, Theodore; Roy, Maurice. Washington, D. C., Spartan Books, Inc. London, Macmillan and Co., Ltd., 1964. 1185p. $48.00. (CONF-620804).

A broad and detailed survey of the latest international advances in all phases of aeronautical science is presented. Fifty-two papers are included; the complete texts of question–and–answer discussions that followed the presentation of each paper are given. An extensive discussion is given on speed and safety in civil aviation, covering the entire range of problems encountered in the design, operation, and regulation of supersonic transport planes, sonic booms, and the increased need for flight safety. Other topics covered include experimental and theoretical investigations on: high-atmosphere physics, structural materials, flight testing and simulation techniques, supersonic aircraft, effects on supersonic flows, space flight, spacecraft control systems, digital systems in space communications, fluid flow, magnetohydrodynamics, re-entry configurations, hypersonic ramjets, aeroelasticity, supersonic combustion, and experience with the X-15 airplane in relation to problems of re-entry vehicles. (L.B.S.)

Vacuum Engineering

14730 (AWRE-O-10/66) A VERSATILE AND CHEAP VACUUM LEAK. Jones, P. M. S.; Gibson, R.; Evans, J. A. (Atomic Weapons Research Establishment, Aldermaston (England)). Feb. 1966. 19p. Dep. BIS $0.60. HMSO 3s.0d.

A versatile vacuum leak was developed for use with light gases. Leak rates in the range 10^{-11} to 10^{-8} std ml/s were used but greater variations are readily attainable in principle. The leak rate is proportional to the applied gas pressure and leak area, and the leak can be operated conveniently at room temperature. For high precision work a thermostat would be advantageous since the rate varies by 5% per degree centigrade. The leak was used with deuterium, helium, and tritium. In the latter case radiolytic damage to the membrane produced hydrogen and reduced the permeability so that only ~3 months use is advisable. The effects of radiation on the membrane are discussed. (auth)

GEOLOGY, METEOROLOGY, AND MINERALOGY

General

Refer also to abstract 14661.

14731 (NP–15861) STUDY OF THE PHYSICO-CHEMICAL-BIOLOGICAL PROCESSES AFFECTING THE DISPERSION OF RADIONUCLIDES. Final Report, December 1, 1961–December 31, 1964. Oren, O. H. (Technion-Israel Inst. of Tech., Haifa). Contract 118/RB. 48p. Dep. mn.

Results are reported from a study of oceanographic features of the Israel continental shelf of the Mediterranean Sea that may affect the distribution of radionuclides from waste solutions or other sources. Data are included on the chemical composition of the sea water, with special attention to seasonal changes in nutrient concentrations; sediments of the coastal shelf; biological cycles, with emphasis on the quantity and composition of plankton, macrobenthonic invertebrates, and fish, with emphasis on fish of commercial importance; measurements of primary production in the area at various seasons; and the effects of Nile River floods on upwelling and vertical mixing and the consequences of the interaction of large masses of fresh water containing suspended materials. (46 references.) (C.H.)

Meteorology

See also Site Survey and Selection

14732 (CVNA–172) THE METEOROLOGICAL PROGRAM AT PARR, SOUTH CAROLINA. Allen, R. G.; Courtney, F. E. (Lockheed-Georgia Co., Marietta). Apr. 1, 1963. 97p.

For Carolinas Virginia Nuclear Power Associates, Inc., Parr, S. C.

A summary is presented of meteorological measurements, weather instrumentation, terrain and special effects, on-site weather test results, on-site diffusion climatology, construction and use of atmospheric diffusion overlays, data analysis, projected future meteorological requirements for nuclear sites, and wind and temperature-inversion data. 65 references. (T.F.H.)

Natural Radioactivity and Fallout

See also HEALTH AND SAFETY

Refer also to abstract 14243.

14733 (AD–628982) GAMMA-RAY ENERGY PSEUDOSPECTRA FOR ^{235}U FISSION PRODUCTS AND FOR VARIOUS TIMES AFTER FISSION. Ksanda, C. F.; Laumets, E.; Hogan, M. A. (Naval Radiological Defense Lab., San Francisco, Calif.). Dec. 18, 1965. 95p. (USNRDL-TR–942). CFSTI $3.00 cy, $0.75 mn.

A technique is described for calculating pseudospectra weighting fractions with which to derive simplified spectra consisting of only five representative photon energies. Pseudospectra weighting fractions and pseudospectra for air and iron attenuation are presented. A computer program for the technique is also described. (D.C.W.)

14734 (NP–15844) FALLOUT IN NEW ZEALAND. Quarterly Report, July–September 1965. (National Radiation Lab., Christchurch (New Zealand)). 20p. (NRL–F18). Dep. mn.

Results are reported from fallout monitoring studies in New Zealand during the third quarter of 1965. Data are included on the total γ activity on air filter samples, the total β activity of rain water, the content of ^{90}Sr in rain water, and the content of ^{137}Cs and ^{90}Sr in milk samples collected during the period. (C.H.)

14735 (NP–15853) DATA FROM RADIATION PROTECTION PROGRAMS. Volume 3, Number 11. (Department of National Health and Welfare, Ottawa (Ontario). Radiation Protection Div.). Nov. 1965. 34p. Dep. mn.

Separate abstracts were prepared for the three sections of the report. A list of publications, posters, and information bulletins available from the Division on request is included. (H.G.D.)

For abstracts of individual sections see: 14736–14738.

14736 (NP–15853, pp 3-7) ^{90}Sr IN 1964 CANADIAN HARD RED SPRING WHEAT. Samuels, E. R. (Department of National Health and Welfare, Ottawa (Ontario). Radiation Protection Div.).

Results of stable calcium and ^{90}Sr determinations in 1964 Canadian wheat samples are tabulated. The 1964 values of 77pC/kg wheat and 233 pC/g Ca represent a significant decrease from the 1963 values. Variations of ^{90}Sr levels according to geographical areas are evident, the southern districts showing lower levels than the northern districts. It is suggested that a further decrease is expected for subsequent crop years unless there is a resumption of atmospheric nuclear testing. (H.G.D.)

14737 (NP–15853, pp 8-20) CANADIAN FALLOUT DATA FOR OCTOBER 1965. Samuels, E. R.; Mohindra, V. K. (Department of National Health and Welfare, Ottawa (Ontario). Radiation Protection Div.).

Results of fallout monitoring carried out on air, precipitation, and milk samples collected during October, 1965, are reported. Fallout levels for October, 1965, showed very little change from the September, 1965, values. Total beta activity in air filter samples continued to show negligible levels. Values for ^{90}Sr and ^{137}Cs in precipitation were 0.16 and 0.24 mC/km^2, respectively. Average concentrations of ^{137}Cs and ^{90}Sr in liquid milk remained essentially unchanged from the September values of 65 and 21.9 pC/liter, respectively. (H.G.D.)

14738 (NP–15853, pp 21-33) REACTOR ENVIRONMENT MONITORING FOR OCTOBER 1965. Samuels, E. R.; Mohindra, V. K. (Department of National Health and Welfare, Ottawa (Ontario). Radiation Protection Div.).

Data on environs monitoring are reported for the Chalk River reactors, the Nuclear Power Demonstration (NPD) reactor, the Douglas Point (CANDU) reactor, the Whiteshell Nuclear Research Establishment (WNRE) and the Manitoba (WR-1) reactor. Tables are included for: total α and β activity determinations on the water samples obtained from along the Ottawa River and the shores of Lake Huron; ^{89}Sr, ^{90}Sr, and ^{137}Cs measurements made on selected samples from the same locations; analyses of milk samples collected at the CANDU and WNRE sites; total beta activity determinations on the McMaster University air filter samples; and radioactivity analyses on Winnipeg River water samples. (H.G.D.)

14739 (TID–22655) ^{137}Cs IN PEOPLE AND FOOD IN NORWAY. 1963–1965. Madshus, Kjell (Norsk Hydro's Inst. for Cancer Research, Oslo); Stroemme, Aksel (Norsk Radiumhospital, Oslo); Koren, Kristian (Statens Radiologisk-Fysiske Laboratorium, Oslo (Norway)). Contract AT(30-1)-3364. 90p. Dep. mn. CFSTI $3.00 cy, $0.75 mn.

Data are presented on the content of ^{137}Cs in people and food in Norway during 1963, 1964, and 1965. Emphasis was placed on the population of Lapps in several areas of Norway where unusually high ^{137}Cs body burdens were found. This was attributed to the content of reindeer meat in the diet and to the unusually large deposition of fallout causing a generally high contamination of agricultural foodstuffs consumed in these areas. Data are presented from a correlation between precipitation and ^{137}Cs content in cow's

milk, seasonal variations in the ^{137}Cs content of cow's milk, the ^{137}Cs content of a group of Norwegian school children, the ^{137}Cs content in adults, and the ^{137}Cs content in selected foods such as beef, lamb, carrots, potatoes, and beer. (C.H.)

14740 INVESTIGATION OF THE RADIOACTIVITY OF SNOW LAYERS OF AN ALPINE GLACIER FOR THE ESTABLISHMENT OF DATING BOUNDARIES. Ambach, W.; Eisner, H. (Univ., Innsbruck). Acta Phys. Austr., 20: 58-62(1965). (In German).

It was shown that it is possible in the accumulation range of Alpine glaciers to find dating boundaries by investigation of the radioactivity of the snow layers. The irregular alteration of the radioactivity at the 1961 summer horizon can be assumed as a glaciologically interesting dating boundary. With the use of this dating boundary it is possible to determine the thickness of the snow redepositions since the summer of 1961 over a large snow layer. (J.S.R.)

14741 NEW DATA ON THE ATMOSPHERIC RADIOACTIVITY AND FALLOUT DENSITY NEAR THE BLACK SEA. Kotel'nikov, V. N.; Markelov, V. N.; Nelepo, B. A. At. Energ. (USSR), 19: 469-70(Nov. 1965). (In Russian).

During August and September 1964, at the time of the 16th cruise of the research ship Mikhail Lomonosov the artificial radioactivity of the atmosphere over the Black Sea was determined. The concentration and isotopic composition of the radioactive elements in the lower layers of the atmosphere, the density, and short-lived isotope concentration of the fallout were measured. The aerosols were collected by means of a 225 m^3/hour capacity air filtering system while the fallout samples were obtained from the deposits of trays containing oil-soaked filter paper, placed at a height of 14 meters over the surface of the water. A scintillation spectrometer was used to determine the isotopic composition of the samples. The results indicated a variation of the isotopic composition from 8.9 to 66.6×10^{-4} disintegrations/sec m^3, with an average value of 34.4×10^{-4}. The average density of the long-lived radioactive fallout at sea level ranged from 3.3 to 221×10^{-1} disintegrations/sec m^2, with an average of 46.0×10^{-1}. During the days with precipitation, the concentration of radioactive products in the atmosphere decreased and the activity of the fallout increased. The average concentration of natural radioactive products from the decay of radon and thoron were found to be 9.2×10^{-1} and 17.7×10^{-3} disintegrations/sec m^3, respectively. Thus, the radon daughter concentration was higher by three orders of magnitude than that of aerosols containing long-lived radioactive fission products. The following nuclides were identified in the atmospheric samples: ^{144}Ce, $^{106}Ru + ^{106}Rh$, ^{137}Cs, and ^{54}Mn. The data agreed with other published values but they indicated a slight increase of the concentration and a reduction of the density of the average daily fallout at the Black Sea region in comparison with results obtained during the ninth cruise of the ship in October 1960. (TTT)

14742 ON THE RELATIVE LEVELS OF FISSION FRAGMENT FALLOUT FROM THE STRATOSPHERE. Chalov, P. I.; Tsevelev, M. A. At. Energ. (USSR), 19: 470-2(Nov. 1965). (In Russian).

The concentration of radioactive aerosols in the lowest atmospheric layers increases during the spring and summer, then decreases during the fall and winter. These seasonal variations are due to changes in the exchange rate between the air masses of the stratosphere and the troposphere. The relative level of the stratospheric fallout was determined by comparing the fission-product fallout density of the long-lived isotopes during the summer of 1962 when tropospheric fallout still could occur with the 1963 data when the fallout had to be of stratospheric origin only in view of the nuclear test ban. The fallout density was derived from the average $\beta + \gamma$ activity of the monthly samples. The plot of these data as a function of time revealed that the total activity of ^{137}Cs, ^{144}Ce, and ^{106}Ru in the fallout during 1962 and 1963 exhibited variations usually observed only in the air layer directly above the ground. The 1962 maximum had to be attributed to an overlap of the stratospheric and tropospheric fallout. The 1963 maximum was due primarily to fission products from the stratosphere; it exceeded that 1962 maximum by a factor about 3. This was caused by the introduction of new fission products into the atmosphere during the 1962 tests, which reached the troposphere during the spring and summer of 1963. The cumulative fallout density and the related γ dose during the nuclear test ban period is thus due mostly to the stratospheric fallout. (TTT)

14743 RADIOACTIVITY OF THE AIR OVER THE ATLANTIC OCEAN IN MAY TO JULY, 1964. Gedeonov, L. I.; Dmitriev, V. N.; Nelepo, B. A.; Stepanov, A. V.; Yakovleva, G. V. At. Energ. (USSR), 19: 472-3(Nov. 1965). (In Russian).

The radioactivity of the air and the fallout over the Atlantic Ocean were studied during the 15th cruise of the research ship Mikhail Lomonosov. The samples were collected by filtering the air and allowing the fallout to deposit on a sticky surface. The samples collected south of 8° latitude south, north of 8° latitude north, and between 8° latitude south and 8° latitude north were determined jointly. Comparison of the results with those obtained during the 12th cruise of the ship, at the end of 1962, revealed that, because nuclear testing in the atmosphere was stopped, the specific activity of the aerosols in the lower layer of the atmosphere decreased by about an order of magnitude. Within 38 and 5° latitudes north, the concentration of the aerosols was practically independent of the place of collection, due to the mixing of the atmosphere by the trade winds. No direct correlation could be established between the concentration of radioactive aerosols and the fallout rate, on one hand, and the average daily values of the atmospheric pressure, and temperature, on the other hand. The high fallout rate in the equatorial region was due to the heavy prevailing rainfall. The aerosol concentration was much lower in the equatorial region and the southern hemisphere than in the northern hemisphere. Averaged data of previous cruises indicated that the highest fission product concentrations are distributed between 14 and 40° latitude north; the activity of the air in the southern hemisphere amounted to only about 10% of that in the northern hemisphere. (TTT)

14744 RESULTS OF THE TRITIUM ACTIVITY MEASUREMENT OF SOME WATERS OF THE SOUTHWEST. Leveque, Paul; Vigneaux, Michel (Faculte des Sciences, Bordeaux). Compt. Rend., 261: 4168-71(Nov. 15, 1965). (In French).

Measurements of the tritium activity of rain water, lake water, water levels, and vegetable water furnish, thanks to the distribution of this isotope, information on the seasonal stratification of lakes, the feed mechanism of surface levels, and the effect of the water level on the tritium distribution in several common vegetables. Only the upper fringe of water levels not influenced by pumping seemed actually influenced by the tritium. (tr-auth)

14745 STUDY ON DIFFERENT METHODS FOR DETERMINATION OF RADIOACTIVITY IN AIR. Lindackers, Karl-Heinz; Tscherner, Manfred (Technischer Ueberwachungs-Verein Rheinland e.V., Cologne). Forschungsber. Landes Nordrhein-Westfalen, No. 1518, 1-60(1965). (In German).

Methods published in the last few years on the determination of radioactivity in air were investigated with respect to their utility for routine measurements. It is shown that the measurement of environmental radiation with G-M counters makes possible a sufficiently accurate monitoring of the air with respect to rare gases and fission products when the aerosol activity is measured as a supplement at the site. For measurement of the aerosol activity an enrichment is necessary. For this, suitable measurement installations are available. The installations presently operating for the continuous monitoring of the aerosol activity are suitable for only relative measurements. A method was developed for the routine detection and evaluation of the hot particles released in dust fallout after nuclear weapon testing. A method was also developed for determination of the effect of radioactive materials in the air on film materials. The measurements showed that in

spite of significant variations of the activity concentration in the air, a significant effect on the film material could not be established. On the basis of a large number of measurement results, a relation between the activity concentration in the air and the activity deposited on the ground was investigated. A simple mathematical relation can be given with sufficient statistical safety, that includes both the dry fallout and also the rain-out or wash-out. The determination of long-time averages of the activity concentration in the air from measurement of the activity of the total fallout is possible with sufficient accuracy. In weekly averages the measurements lead to usable results although the deviations are in the order of magnitude of two or three. (tr-auth)

14746 THE INFLUENCE OF ATMOSPHERIC PRECIPITATION ON THE FALLOUT OF RADIOACTIVE SUBSTANCES FROM THE ATMOSPHERE. Zorin, V. M.; Kabishcher, E. I. Gig. Sanit., 11: 114-15(1965). (In Russian).

Measurements of the radioactive fallout at the Vitebsk Sanitation Station were carried out during 1962-3. Fallout on days with atmospheric precipitation (rain and snow) was found to be 6½ times higher than on other days. Radiometric analysis showed that the average monthly density of dry fallout from atmospheric dusts varied from 0.12 to 1.87 mC/km^2/day. The fallout from precipitation varied from 0.84 to 16.03 mC/km^2/day. A direct dependence of the quantity of fallout on the amount of precipitation was not found. The progressively decreasing amount of fallout in the second half of 1963 indicates the beginning of purging of the atmosphere from the products of nuclear explosions after the cessation of nuclear-weapons tests in three media and also the decay of beta-active material found in the atmosphere. (M.J.T.)

14747 THE CONTENT OF SUBMICROSCOPIC AEROSOLS OF SHORT-LIVED DAUGHTER PRODUCTS OF RADON IN MINE AIR. Kirichenko, V. N.; Ogorodnikov, B. I.; Ivanov, V. D.; Kirsh, A. A.; Kachikin, V. I. Gig. Sanit., 11: 115-19(1965). (In Russian).

Measurements of the concentrations of aerosol particles with radii $>10^{-5}$ and $>10^{-7}$ cm in the air of two uranium mines were carried out. The radioactivity of filters of the mine air was measured, and the proportions of atoms of ^{218}Po, ^{214}Pb, and ^{214}Bi were deduced. (M.J.T.)

14748 NUCLEAR ACCIDENTS AND OUR FOOD SUPPLY. Park, A. B. (Dept. of Agriculture, Washington, D. C.). J. Amer. Vet. Med. Ass., 147: 1501-4(Dec. 15, 1965).

Hazards of fission products accidentally released into the environment by reactor accidents are considered in terms of food supply contamination. Recommendations of the Federal Radiation Council (FRC) regarding the problem are cited, and some basic considerations in the development of protective actions and guides are enumerated. FRC recommendations for handling contaminated milk are explained. Major mechanisms of transmission pathways that must be considered in determining what, when, and if protective action is to be taken are discussed. Responsibilities of the veterinary profession in handling these hazards, should they arise, are emphasized. (BBB)

14749 RADIOACTIVE CONTAMINATION OF THE INDO-ANTARCTIC OCEAN WATER IN EARLY PARTS OF 1961 AND 1962. Nagaya, Yutaka; Shiozaki, Masaru; Seto, Yoshio (Maritime Safety Agency, Tokyo). J. Radiat. Res. (Jap.), 5: 206-14(Sept.-Dec. 1964).

Significant increases in ^{144}Ce concentrations detected in the Indo-Antarctic surface sea water collected in early 1962 (mean 0.57 $\mu\mu C/l$), in comparison with those of early 1961 (mean 0.12 $\mu\mu C/l$), were attributed to the stratospheric fallout from the resumption of nuclear explosions by USSR on the northern polar region during September to November, 1961. No increase of ^{90}Sr was noted in these samples (means 0.07 and 0.06 $\mu\mu C/l$) and that of ^{137}Cs was slight (means 0.13 and 0.15 $\mu\mu C/l$). The horizontal distributions of the radionuclides in surface water indicated the decreasing ^{90}Sr and ^{137}Cs concentrations with increasing latitude, but no latitudinal variation of ^{144}Ce was detected. Only 6 months was estimated for the transport time of stratospheric fallout from the northern polar region to the southern hemisphere, a value considerably lower than those reported by other workers. (TCO)

14750 TERRESTRIAL NEUTRINOS. Eder, Gernot (Univ., Giessen, Ger.). Nucl. Phys., 78: 657-62(1966).

Arguments are given for a remarkable abundance of radioactive elements within the earth. Methods are discussed in order to measure this abundance by neutrino experiments. (auth)

14751 VERTICAL DISTRIBUTIONS OF FALLOUT GAMMA-RAY SOURCES IN GROUND SOIL IN EASTERN JAPAN. Yamasaki, Fumio (Inst. Phys. and Chem. Res. (Tokyo); Takeuchi, Masa. Sci. Pap. Inst. Phys. Chem. Res. (Tokyo), 59: 106-11(Sept. 1965).

The amount of fallout gamma-ray sources and their vertical distribution in soil were determined at four typical districts in Japan by chemical analysis and γ-ray spectroscopy. The vertical distribution was exponential with respect to the depth. The natural γ-ray sources were also assayed. (auth)

14752 NATURAL RADIOACTIVITY OF CARBONATE ROCKS. Larionov, V. V.; Shvartsman, M. D. (Gubkin Inst. for the Petrochemical and Gas Industry, Moscow). Vienna, International Atomic Energy Agency, 1965, Preprint No. SM-68/56, 24p. (In Russian). (CONF-651023-36). ORINS.

From Symposium on Radioisotope Instruments in Industry and Geophysics, Warsaw.

Large-scale measurements of the integral and partial (Ra, Th, ^{40}K) radioactivity of limestone, dolomite and other types of carbonate rock with a Clarke content of radioisotopes, were carried out in both laboratory and natural conditions. Both the radioactivity of the rock as a whole and that of its components—the soluble part and the insoluble residue—were investigated. A comprehensive analysis of physico-chemical and lithologo-petrographic properties was made for all the substances subjected to radiometric measurements. (auth)

Techniques and Equipment

14753 (BNWL-47) GEOPHYSICAL SEISMIC EVALUATION STUDY AT HANFORD. Brown, R. E.; Raymond, J. R. (Battelle-Northwest, Richland, Wash. Pacific Northwest Lab.). Dec. 1964. Contract AT(45-1)-1830. 49p. Dep. mn. CFSTI $3.00 cy, $0.50 mn.

A geophysical research program was conducted at Hanford to determine the feasibility and desirability of using seismic methods in geohydrologic studies. Detection and delineation were desired of seven different geological features that in some sites affect the movement of liquid radioactive wastes discharged to the ground. Rotary drilling methods exceeded expectations. They permitted in-well logging methods and produced information not obtainable from cable-tool methods. Results obtained reinforced information received from wells drilled by cable-tool methods and validated concepts from cable-tool well data. By extending the information laterally, the seismic program provided line data where only point data had been available. The reliability and significance of the information and concepts derived from it thus were greatly increased. The importance of seismic methods as an adjunct to other exploration methods used at Hanford was proven. Refraction methods proved the most usable and least expensive seismic techniques for Hanford studies and also minimized drilling needs. Rotary method drilling and in-hole logging provided adequate control on the geology at tie points. The use of fertilizer-grade ammonium nitrate primed with diesel oil was fully adequate and cheaper than other explosives. Surface detonation was completely satisfactory and minimized the drilling of shot holes. (P.C.H.)

14754 (NVO-38-1) MINING ON THE NEVADA TEST SITE. Waltman, F. D. (Fenix and Scisson, Inc., Tulsa,

Okla. Petroleum Consultants, Houston, Tex.). Oct. 25, 1965. Contract AT(26-1)-38. 15p. (CONF-660205-3). Dep. mn. CFSTI $1.00 cy, $0.50 mn.

From Metallurgical Society of the American Institute of Mining, Metallurgical, and Petroleum Engineers, New York.

Mining at the Nevada Test Site consists of rooms at the bottom of drilled and cased 48 in. dia shafts, excavation of drifts and cavities from conventionally sunk shafts, and mining of complexes from tunnels driven into the hills. Information is given on surface plant, downhole installation, geology, groundwater control, ventilation, and lining. (P.C.H.)

14755 (UCRL-7929) NUMERICAL SIMULATION OF SEISMIC DISTURBANCES. Cherry, J. T.; Hurdlow, W. R. (Lawrence Radiation Lab., Univ. of California, Livermore). Jan. 1965. Contract W-7405-eng-48. 31p. Dep. mn. CFSTI $2.00 cy, $0.50 mn.

The results from a Lagrangian numerical scheme of calculating cylindrically symmetric, elastic-plastic, transient disturbances are presented. The numerical technique involves transforming the Eulerian equations of motion containing a cylindrically symmetric stress tensor into Lagrangian coordinates. These transformed equations are then differenced in the Lagrangian coordinate system. Therefore, a given instantaneous stress field determines the accelerations of the points in the Lagrangian mesh. These accelerations are allowed to act over a small time step so that the mesh becomes distorted. This distortion determines the change in strain at a point; the strain change is related to a stress change by Hooke's law. This new stress is used to determine new accelerations. If the material behaves plastically, then the stresses are adjusted so that a Von Mises yield condition is satisfied. Five numerical solutions of various elastic-plastic wave propagation problems are presented and are discussed along with their corresponding analytic and experimental solutions. A shear and tensile failure mechanism is presented that is consistent with the continuum hypothesis. (auth)

14756 MEASUREMENT OF MOISTURE IN ORGANIC SOILS BY NEUTRON METHOD. Churaev, N. V.; Rode, L. G. (Kalinin Leningrad Polytechnic Inst.). Pochvovedenie, 1: 96-100(1966). (In Russian).

Moisture determination in organic soils demands estimation of the soil volume, weight, hydrogen content in the solid phase, and bound water as well as its dispersion capacity. Formulas are presented along with the results of their verification on peats of different moisture and botanical composition. The possible accuracy of organic soil moisture measurement is evaluated. It was concluded that this method should be used only in the case of mass moisture determination in organic soils of the same type and other analogous materials. (auth)

14757 AN HISTORICAL REVIEW OF SEISMOMETER ARRAY DEVELOPMENT. Carpenter, E. W. (Atomic Weapon Research Establishment, Blacknest, Eng.). Proc. IEEE (Inst. Elec. Electron. Eng.), 53: 1816-21(Dec. 1965).

The development of seismometer arrays in the context of nuclear detection is briefly outlined. The original array concept was for ten seismometers distributed in an area of a few square kilometers, but technological progress with magnetic tape recording and subsequent processing led to the construction of crossed linear arrays with dimensions of a few tens of kilometers. The linear arrays, with dimensions such that the delays between arrival at the various elements were of the order of the dominant signal period, demonstrated the usefulness of velocity filtering. Gradually there arose the concept of a few extremely large and powerful arrays replacing the network of many less sophisticated stations. Thus there came into being the LASA, virtually an array of arrays. (auth)

14758 PRINCIPLES OF AN EXPERIMENTAL LARGE APERTURE SEISMIC ARRAY (LASA). Green, P. E. Jr. (Massachusetts Inst. of Tech., Lexington); Frosch, R. A.; Romney, C. F. Proc. IEEE (Inst. Elec. Electron. Eng.), 53: 1821-33(Dec. 1965).

One of the most useful techniques for improving capability to observe small remote seismic events is to connect a large number of seismic sensors distributed in the horizontal plane so as to form an array. This is particularly useful in the monitoring of underground nuclear tests, since the events are of small magnitude and the criteria used to distinguish source type depend on freeing the weak signal as far as possible from additive microseismic noise, reverberation components, and interfering earthquake activity that might chance to occur simultaneously. Results achieved by the use of seismic arrays of several kilometers aperture and several tens of sensors were sufficiently promising to suggest that substantial further improvements might be expected from an even larger array having more than an order of magnitude greater aperture and number of sensors. Such a Large Aperture Seismic Array (LASA) was built and is being evaluated. The number of sensors is 525 and the aperture is 200 km. The notions underlying the LASA development are presented briefly. The principles of array signal processing are reviewed, and a prognosis of LASA capabilities is presented. The extent to which the results obtained to date have confirmed expectations is discussed. (auth)

14759 THE LASA SENSING SYSTEM DESIGN, INSTALLATION, AND OPERATION. Forbes, C. B.; Obenchain, R.; Swain, R. J. (Teledyne, Inc., Pasadena, Calif.). Proc. IEEE (Inst. Elec. Electron. Eng.), 53: 1834-43(Dec. 1965).

The implementation of the LASA sensing system is treated. The design of the sensing system, the establishment of system specifications, and the selection of components are discussed. The installation of the seismograph systems is described in some detail. This includes the drilling and casing of 504 two-hundred foot wells and 21 five-hundred foot wells, the trenching of 3,000,000 feet of cable, and the installation and calibration of the 525 seismometers and amplifiers. To meet the operational requirements the 525 sensing circuits were equalized to the same system sensitivity, 20 millivolts per millimicron of earth motion which corresponds roughly to the saturation of a typical amplifier by the signal generated by a magnitude 7.75 event. The maintenance phase is described. (auth)

14760 LARGE APERTURE SEISMIC ARRAY SIGNAL HANDLING SYSTEM. Wood, R. V. Jr.; Enticknap, R. G.; Lin, C.-S.; Martinson, R. M. (Massachusetts Inst. of Tech., Lexington). Proc. IEEE (Inst. Elec. Electron. Eng.), 53: 1844-51(Dec. 1965).

The location of an array such as LASA is dictated by seismic considerations. Those criteria which affect system design and their implications are discussed with regard to several major components of the system, the signal collection, the communications, the signal recording, and the array control. In the case of the Montana LASA, only a very short time was available for its implementation. This factor had a major influence on component choice and system design, but did not compromise either the performance or reliability of the system. (auth)

14761 DATA RECORDING AND PROCESSING FOR THE EXPERIMENTAL LARGE APERTURE SEISMIC ARRAY. Briscoe, H. W.; Fleck, P. L. (Massachusetts Inst. of Tech., Lexington). Proc. IEEE (Inst. Elec. Electron. Eng.), 53: 1852-9(Dec. 1965).

The high resolution of the Large Aperture Seismic Array (LASA) and the volume of data it produces make many of the recording and processing techniques used for the earlier Vela arrays impractical or obsolete. The history of processing for seismic arrays is briefly reviewed, and the recording and processing requirements of the LASA are summarized. Both the on-line use of the LASA for detection of seismic disturbances and the off-line processing of the data for signal analysis are centered around the use of high-speed digital processing equipment. The on-line processing facilities at the LASA Data Center are described, and the current effort to evaluate processing techniques for use with LASA is discussed. (auth)

14762 DATA PROCESSING TECHNIQUES FOR THE DETECTION AND INTERPRETATION OF TELESEISMIC SIGNALS. Archambeau, C. B.; Bradford, J. C.; Broome, P. W.; Dean, W. C.; Flinn, E. A.; Sax, R. L. (Seismic Data Lab., Teledyne Inc., Alexandria, Va.). Proc. IEEE (Inst. Elec. Electron. Eng.), 53: 1860-84(Dec. 1965).

Six papers are included, describing recent developments in automated detection and identification of teleseismic earthquakes and explosions in a seismic noise background. The assumption is evaluated that the outputs of seismometer arrays can be added since the signals will reinforce while the noise is cancelled. Signal and noise correlations vs distance and frequency are presented for an array of 1600 km in extent. A method is described, utilizing orthogonal expansions of the Kautz type in an effort to determine spectral and temporal differences between both types of signals and noise. Theory and measurements indicate that the seismic noise background is largely composed of fundamental and higher mode Rayleigh waves. A thermal equilibrium analogy is described to estimate the noise energies in each mode to account for the observed depth and frequency behavior. The use of multiple and partial coherence functions for resolving noise backgrounds into their propagation components is considered. It is shown that compressional, shear, and surface wave components of signals can be separated from seismic noise backgrounds by recognizing their differing polarization properties. The source mechanisms can theoretically be identified from their radiation patterns provided instrument and travel path distortions are removed. Means for integrating the various methods of detecting and isolating the signals into an automated signal analysis system are discussed. (auth)

14763 ENGINEERING ASPECTS OF MULTICHANNEL PROCESSING BASED ON MEASURED NOISE CORRELATIONS. Baldwin, Richard (Texas Instruments Inc., Dallas). Proc. IEEE (Inst. Elec. Electron. Eng.), 53: 1884-9(Dec. 1965).

The problem of separating seismic signals from noise on a multichannel basis, by making use of the spatial organization of the noise, is discussed. A brief description of the method used to synthesize the multichannel system on a computer is presented. Results obtained by multichannel processing of the outputs from a 19-seismometer array, including signal response, noise response, and signal-to-noise ratio improvement, are shown. These results are compared with those obtained by performing a simple summation of the array outputs and with those which would be expected from simple summation if the noise were not organized in space. A practical method of applying analog multichannel processing in the field is presented. Finally, examples of teleseismic signals extracted on a multichannel basis are shown. (auth)

14764 AN UNATTENDED SEISMOLOGICAL OBSERVATORY. Reynolds, R. Stanton (Sandia Lab., Albuquerque, N. Mex.). Proc. IEEE (Inst. Elec. Electron. Eng.), 53: 1890-9(Dec. 1965).

Prototype equipment to continuously record outputs from three short-period and three long-period unattended seismometers for up to 120 days is being developed and tested. Timing accuracy will be within 0.1 second throughout the record period. The system will be capable of recording a 70 decibel signal range. As much as 42 decibel attenuation can also be applied to each short-period data channel by an automatic gain control system to compensate for high levels of background noise. Concurrent with the development of the recording system, a playback system is being developed and tested which will convert the recorded data and timing signals to the standard Vela Uniform tape format. According to present schedules, the systems should be fully evaluated in the laboratory and in the field by the beginning of 1967. (auth)

14765 OCEAN-BOTTOM SEISMOGRAPH. Arnett, R. A.; Newhouse, T. W. (Texas Instruments Inc., Dallas). Proc. IEEE (Inst. Elec. Electron. Eng.), 53: 1899-1905(Dec. 1965).

In one program of Project VELA UNIFORM, the ocean-bottom seismograph was developed as a research tool for the study of acoustical wave energy at the solid earth-water interface, generated either by earthquakes or by explosive sources. The seismograph described is a third-generation unit having progressed through more than four years of development, design, and field experiments. The present configuration is spherical, 40 inches in diameter. It was tested successfully in various locations to a depth of 24,000 feet. The primary components, in addition to the three-component seismometer system, are a digital clock having a 40-day capacity, with 0.1 second accuracy, seismic amplifiers capable of detecting noise level of 0.1 microvolt or less, a magnetic tape transport having a 30-day recording capacity for signals of less than 10 cps frequency, and internal battery power supply for all components. In operation, the seismograph descends to the desired depth by free fall, remains unattended and untethered, and is retrieved on sonar code command or preset time by decoupling the anchor base through a cocked spring mechanism, which is triggered by fusion of a small steel wire. Results proved the feasibility of such an ocean-bottom data system, including the important capability to recall the package by sonar code command. (auth)

14766 COHERENCE MEASUREMENTS WITH TIME SAMPLING OCEAN-BOTTOM SEISMOMETERS. Bradner, H.; Dodds, J.; Foulks, R. (Univ. of California, San Diego, La Jolla). Proc. IEEE (Inst. Elec. Electron. Eng.), 53: 1906-8(Dec. 1965).

Instruments for obtaining simultaneous records of ocean-bottom seismic motion are described. Preliminary ocean-bottom seismic data with two simultaneous three-component instruments indicate that instrument noise and water currents may cause small differences in the detailed spectra. The general features of the spectra, however, appear to be the same from proximate instruments. (auth)

14767 OCEAN-BOTTOM SEISMIC OBSERVATORIES. Sutton, G. H.; McDonald, W. G.; Prentiss, D. D.; Thanos, S. N. (Columbia Univ., Palisades, N. Y.). Proc. IEEE (Inst. Elec. Electron. Eng.), 53: 1909-21(Dec. 1965).

Observations of seismic motion and other geophysical parameters on the ocean bottom over extended periods of time and over a wide range of frequencies (periods) provide information on the suitability of the ocean bottom as a site for the detection of seismic events. Instrument systems consisting of long- and short-period seismographs, long- and short-period pressure sensors, a temperature sensor, and a water-current sensor were operated on the ocean bottom. Experience and calculation indicate that these systems can be well coupled to the sediment surface, mechanically stable, and relatively insensitive to water currents. Local and distant earthquakes, tides, microseisms (3–8 seconds period), long-period (2–6 minutes) pressure disturbances, and temperature fluctuations were well recorded from the ocean bottom at depths greater than 2000 fm. Instrument systems were implanted at two locations: south of Bermuda (2400 fm depth, seismic measurements only) and west of San Francisco (2200 fm depth). Data were telemetered acoustically to a ship (Bermuda) and via deep-sea cable to a shore station (California). Results to date indicate that the ocean bottom can be a favorable location for the detection of seismic events. (auth)

14768 THE DETECTION AND RECOGNITION OF UNDERGROUND EXPLOSIONS. A Special Report of the United Kingdom Atomic Energy Authority. United Kingdom Atomic Energy Authority, London. 159p. HMSO $4.20.

The detection and identification of seismic events at long ranges were discussed in terms of the following; teleseismic signals and their transmission paths, ambient noise, seismometer arrays, identification, seismograms and correlograms, explosions and earthquakes in the source window, development and test of criteria, surface waves from underground explosions and the decoupling of explosive shots. (M.O.W.)

14769 THE DETECTION AND RECOGNITION OF UNDERGROUND EXPLOSIONS. APPENDICES. A Spe-

cial Report of the United Kingdom Atomic Energy Authority. United Kingdom Atomic Energy Authority, London. 118p. HMSO $4.20.

Separate sections are presented on the following; (1) array design and processing methods, (2) the design, installation, and operation of seismic array recording and analysis systems, (3) source mechanisms and their implications on identification, (4) decoupling theory, (5) seismometer development, (6) borehole seismometers, and (7) table of selected earthquakes and special events. (M.O.W.)

14770 THE PRESENT STATUS OF NUCLEAR GEOPHYSICS AND PROSPECTS FOR FUTURE DEVELOPMENT. **Alekseev, F. A. (All-Union Scientific Research Inst. for Nuclear Geophysics and Geochemistry, Moscow). Vienna, International Atomic Energy Agency, 1965, Preprint No. SM-68/29, 19p. (In Russian and English). (CONF-651023-1). ORINS.**

From Symposium on Radioisotope Instruments in Industry and Geophysics, Warsaw.

The main developments in nuclear geophysics at the present time are as follows: the widespread practical application of methods derived from nuclear physics in geological prospecting, including the use of compact neutron and gamma-ray sources in borehole logging; intensive prospecting operations and the introduction on an industrial scale of new techniques, based on nuclear physics, for evaluating quantitatively the saturation of gas and petroleum reservoirs and for detecting and recording shifts in the contours of gas and petroleum formations during production; intensive prospecting operations and the introduction on an industrial scale of techniques, based on nuclear physics, for the elementary analysis of rock, especially for the quantitative determination of solid mineral resources in samples, excavations and borings; the intensive development of new and improved apparatus for nuclear geophysics: neutron and gamma-ray generators, nuclear reactors, multichannel analyzers and equipment for the automatic analysis and processing of the materials obtained. The future development of nuclear geophysics will be dictated by the need to devise efficient and accurate techniques and instruments, suitable for field work, for the quantitative determination of mineral resources in samples, excavations and deep borings. This will require the development of compact, portable sources of controlled radiation possessing a wide range of elementary particle energies and high intensity, as well as of automatic multichannel recording equipment and automatic equipment for processing results. Particular importance will attach to the development of techniques and equipment, based on nuclear physics, for investigating deep borings under conditions of high pressure and temperature. Other matters considered are use of isotopes in the elementary analysis of rocks, determinations of absolute age and the basic problems of groundwater age and dynamics. (auth)

14771 THE INFLUENCE OF COMPOSITION AND DENSITY OF SOILS ON READINGS OF NEUTRON MOISTURE METERS. **Majerczyk, J. (Inst. of Nuclear Techniques, Krakow); Zuber, A. Vienna, International Atomic Energy Agency, 1965, Preprint No. SM-68/39, 19p. (CONF-651023-37). ORINS.**

From Symposium on Radioisotope Instruments in Industry and Geophysics, Warsaw.

A proper calibration of neutron moisture probes and the interpretation of field data require the knowledge of how chemical composition and dry bulk density of soils influence the readings of neutron moisture meters. It is known that in the vicinity of a point source the age approximation of the neutron transport equation gives good results even for hydrogen media. On the basis of the age theory there are no difficulties in calculation of the thermal neutron density in homogeneous medium versus its moisture, dry bulk density and concentration of the elements with high absorption cross section, if experimental values of the age are taken into account. Unfortunately, it is rather difficult to calculate the calibration curve, but for neutron moisture meters it is very often assumed that the shape of this curve is the same as the theoretical plot of thermal neutron density. Under the above assumption and on the basis of the age theory it was found how changes in dry bulk density and concentration of elements with high absorption cross section influence the apparent soil moisture. The calculations were done for the wide range of dry bulk densities and for some values of Σ_a. The additional changes of the absorption cross section are mainly caused by presence either of such elements as boron, iron and rare earths in soil or of chlorine in water. Obtained results and graphs given will probably allow improvement of the accuracy of the neutron method, owing to the possibility of prediction of the changes in the apparent moisture caused by soil parameters. (auth)

14772 THE USE OF A PULSED NEUTRON GENERATOR TO DETERMINE NEUTRON DIFFUSION PARAMETERS OF ROCKS AND FLUIDS. **Antonov, A. V.; Granatkin, B. V.; Merkulev, Yu. A.; Miller, V. V.; Shimelevich, Yu. S. (All-Union Research Inst. for Nuclear Geophysics and Geochemistry, Moscow. Lebedev Inst. of Physics, Moscow). Vienna, International Atomic Energy Agency, 1965, Preprint No. SM-68/54, 25p. (In Russian). (CONF-651023-21). ORINS.**

From Symposium on Radioisotope Instruments in Industry and Geophysics, Warsaw.

The use of a pulsed neutron generator is described for determining neutron parameters in samples of rocks and fluids. The method proposed for the experimental determination of the neutron parameters of rocks and fluids is that of non-stationary diffusion, based on the use of a pulsed neutron generator. The method makes it possible to determine three neutron diffusion parameters simultaneously. These are the lifetime of thermal neutrons in an infinite medium, the thermal neutron diffusion coefficient and the diffusion cooling coefficient. A relatively small amount of the substance is needed to carry out the experiment, a feature which may be particularly important when large-scale measurements are undertaken. By taking as an example the determination of neutron diffusion parameters in petroleum and in silicate sand saturated with water, it is shown that it is possible to use this method to determine the neutron parameters of rocks and fluids. (auth)

14773 A PROBE FOR THE COMPLEX STUDY OF THE PHYSICAL PROPERTIES OF SOILS. **Borowczik, M.; Krulikowski, C. (Instytut Geologiczny, Warsaw). Vienna, International Atomic Energy Agency, 1965, Preprint No. SM-68/44, 15p. (In Russian). (CONF-651023-24). ORINS.**

From Symposium on Radioisotope Instruments in Industry and Geophysics, Warsaw.

The increasing demand for rapid and accurate engineering studies of land on which buildings are to be erected makes it necessary to introduce new methods of investigation using the latest scientific and technological developments. The methods used hitherto for the study of building foundations, consisting of drilling test holes, laboratory analysis of soil samples taken during drilling, and various static and dynamic tests, do not always allow reproduction of the actual functioning conditions of the soil in a natural system. The equipment described affords the possibility of simultaneously applying various geophysical methods of determining the physical properties of soil at depths of up to 10 meters. The special construction of the probe makes it possible to determine the resistivity of the soil and its volumetric weight and humidity without carrying out test drills. The first-named parameter is measured in a 3-electrode direct current system, and the volumetric weight and humidity of the soil are determined by isotopic methods. The probe is driven into the ground by a BC-9 pneumatic hammer. In eight hours' work it is possible to drill 2 to 3 holes 10 meters deep. The investigation so performed indicates the change in resistivity and volumetric weight and humidity as a function of depth. The curves obtained supplement the picture of the geological structure derived from test drilling. They may be used as a separate means of investigation, thus reducing the number of test holes requiring to be drilled. The probe data make it possible to draw the cross sections for the physical parameters

mentioned above. The results of some field work are given. This work was carried out both in regions whose geological structure had been extensively studied by test drilling and in regions where the number of holes was limited to the minimum and replaced by the probing described above. From analysis of the results obtained, conclusions can be drawn pointing to the possibility of wide use of the probe for investigating the physical properties of soils under the conditions of their natural occurrence, and also for studying the change in these properties with time. (auth)

14774 OVER-ALL PATTERN AND CHARACTERISTICS OF THE STATIONARY DISTRIBUTION OF NEUTRONS. Kozhevnikov, D. A. (Gubkin Inst. for the Petrochemical and Gas Industry, Moscow). Vienna, International Atomic Energy Agency, 1965, Preprint No. SM-68/58b, 63p. (In Russian). (CONF-651023-34). ORINS.

From Symposium on Radioisotope Instruments in Industry and Geophysics, Warsaw.

Problems of the theory of moderation and diffusion of neutrons, connected with the immediate task of nuclear geophysics are discussed. The spatio-energetic distribution of epithermal and thermal neutrons in homogeneous media is investigated. An explanation is put forward for the existence of a regular connection between the age and area of migration of neutrons from polyenergetic sources and the mean energies of their spectra. Relations are established which make it possible, on the basis of the experimentally determined characteristics of the neutron properties of a certain medium for a polyenergetic source with a given spectrum, to calculate the characteristics of the same medium for other polyenergetic sources with different spectra. The spatial distribution of thermal neutrons from a high-energy neutron point source is described. The nature of the spatial change in the thermal neutron distribution function differs considerably in weak and strong absorbers. A moderator is a weak or a strong absorber depending on the sign relation between the initial free path and the diffusion length of thermal neutrons. The same moderator may be a weak absorber for some sections of the spectrum of a polyenergetic source and a strong one for others, in accordance with the law of change in the neutron free path in the region where the source spectrum is determined. The diffusion characteristics of absorbing media at high temperatures are investigated. (auth)

14775 THEORETICAL AND EXPERIMENTAL MODEL RESULTS IN NEUTRON LIFETIME LOGGING. Caldwell, R. L.; Allen, L. S.; Mills, W. R. Jr. (Socony Mobil Oil Co., Inc., Dallas). Vienna, International Atomic Energy Agency, 1965, Preprint No. SM-68/31, 24p. (CONF-651023-4). ORINS.

From Symposium on Radioisotope Instruments in Industry and Geophysics, Warsaw.

Investigation of borehole and formation parameters in neutron lifetime logging requires controlled experiments in a realistic physical model or a satisfactory theoretical model. A numerical computer code was developed to solve the time-dependent, three-group diffusion equations which apply to the borehole geometry and have built silicate and calcium carbonate models in which formation and borehole parameters are easily changed. Test calculations verifying the computer program are presented for salt water and fresh water (or oil) saturation of a porous sand. The effects of fluid invasion were calculated to estimate the depth of investigation of pulsed neutron logging. Theoretical thermal neutron lifetimes were obtained for two cases of open hole fluid invasion: fresh water filtrate invading a salt-water-saturated formation, and salt water filtrate invading a formation saturated with oil. The formation was a 20 percent porosity sandstone and the diameter of the fluid-filled borehole was 20 cm. It is shown that for any given depth of borehole fluid invasion, up to the point of total masking, it is much easier to detect the presence of oil behind salt water invasion than to detect salt water behind a zone invaded by fresh water. The merits of heterogeneous versus homogeneous simulation of rock formations in a physical model are discussed. A heterogeneous model for simulating sandstone formations of variable porosity was constructed of rods of pure silicate rock. Simulation adequacy is shown by steady-state and pulsed neutron measurements in both homogeneous and heterogeneous models. The steady-state measurements of thermal neutron count rate are 16 percent greater in the heterogeneous model for a source-to-detector spacing of 50 cm; the differences are much smaller for the shorter source-detector spacings typical of commercial logging. Thermal neutron lifetimes were measured in the carbonate and in the heterogeneous and homogeneous silicate models. The lifetimes measured in the two silicate models at a 50 cm source-detector spacing agree within 6 percent. The ease with which parametric studies can be accomplished in the heterogeneous model outweighs the discrepancies inherent in the simulation. (auth)

14776 APPLICATION OF THE SIMILITUDE THEORY TO THE STUDY OF RADIATION TRANSFER PROCESSES. Guberman, Sh. A.; Kozhevnikov, D. A.; Yakubson, K. I. (Gubkin Inst. for the Petrochemical and Gas Industry, Moscow). Vienna, International Atomic Energy Agency, 1965, Preprint No. SM-68/35, 23p. (In Russian). (CONF-651023-30). ORINS.

From Symposium on Radioisotope Instruments in Industry and Geophysics, Warsaw.

For all the many types of radiation used in scientific research and in various branches of industry, the passage of the particles through a substance is described by the same linear integral-differential equation (transport equation). This equation permits of presentation in a dimensionless form. Using the dimensionless complexes involved in the equation and in the boundary conditions, it is possible to derive a set of independent similitude criteria. These allow, firstly, the extension of the results of theoretical calculations and experimental measurements relating to various specific conditions to an entire range of similar conditions, and, secondly, the formulation of a principle for modeling radiation transfer problems. The problems which can be solved if the similitude criteria are accurately fulfilled are discussed. These include investigation of the pattern of change in particle fields as a function of change in the geometry of the medium and its density, and the extent of change with time (for non-stationary fields). The distribution of neutrons and gamma quanta in rock is discussed as an example. The necessary conditions for accurate modeling on the similitude principle are stability of the source spectra, of the energy of the radiation recorded and of the material composition of the media investigated. The range of problems which can be dealt with is thus considerably restricted, but in a number of important practical cases these limitations can be overcome by using approximate modeling. The conditions of approximate similitude for neutrons and gamma quanta in various energy ranges are given. (auth)

14777 THE INFORMATIVENESS OF NUCLEAR GEOPHYSICAL METHODS APPLIED TO GEOPHYSICAL RESEARCH DATA IN IDENTIFYING OIL-BEARING STRATA USING A LEARNING PROGRAMME. Guberman, Sh. A.; Izvekova, M. L.; Ryabykh, O. I. (Gubkin Inst. for the Petrochemical and Gas Industry, Moscow). Vienna, International Atomic Energy Agency, 1965, Preprint No. SM-68/51, 17p. (In Russian). (CONF-651023-31). ORINS.

From Symposium on Radioisotope Instruments in Industry and Geophysics, Warsaw.

Oil-bearing strata in borehole cross sections were identified from a set of industrial geophysical data using a computer with a learning program for sample discrimination. The special feature of the program is that indications of oil-bearing strata previously developed by working were not fed into the machine; the program itself works out indications of oil-bearing or water-bearing strata on the basis of the geophysical data available to it on a number of strata known to belong to these categories. This is the "learning" process. Using the indications thus worked out, the program can interpret fresh strata in the light of the entire compendium of geophysical data, and the number of errors in interpretation is approximately one third of that which occurs when geophysicists interpret data

under production conditions. Such programs permit objective assessment of the informativeness of the various methods of industrial geophysics, including radiometry. For this purpose the number of errors made by the program on certain material is compared using the entire standard set of measurements with those made when one method was excluded from the set. If the number of errors did not increase, this meant that the method in question introduced no new information into the set methods used (when solving the problem in question). If, on the other hand, the number of errors increased, this meant that the informativeness of the method differed from zero; the higher the increase in errors, the more informative the method in question may be regarded. Each of the indications worked out by the program contains values for a number of geophysical parameters. It is possible to assess how often one or another specific parameter appears in the indication, and this assessment can serve as an index of the relative informativeness of the parameter concerned. Specific data are given on the informativeness and relative informativeness of the gamma method and the neutron-gamma method of differentiating between oil-bearing and water-bearing strata by reference to a set of geophysical data on various sites in the USSR, in both carbonate and sandy-clay deposits. The data obtained testify to the high informativeness of the standard methods of borehole radiometry. Data are given which show the effect of calibrating neutron-gamma borehole-logging equipment on the informativeness of the method. The use of statistical calibration methods makes it possible to extract from neutron-gamma logging data more information than can be obtained when separate reference strata in the borehold cross section are used for calibration. (auth)

14778 A LOGGING SYSTEM AND COMPUTER PROGRAM TO DETERMINE ROCK DENSITY OF URANIUM DEPOSITS. Dodd, P. H.; Droullard, R. F. (Atomic Energy Commission, Grand Junction, Colo.). Vienna, International Atomic Energy Agency, 1965, Preprint No. SM-68/33, 21p. (CONF-651023-28). ORINS.

From Symposium on Radioisotope Instruments in Industry and Geophysics, Warsaw.

Bulk density of uranium ores and associated rocks are determined from boreholes using a slim-hole nuclear logging system and computer interpretation program. For density measurements, the system consists of a gamma-gamma density probe employing two scintillation detectors spaced at unequal distances from a cobalt-60 source, conventional amplifier, discriminator and ratemeter combination having digital and analog output for nuclear data. A caliper probe and associated system following conventional methods provides digital and analog records of hole size. An integrating digital voltmeter serves as a BCD conversion unit for nuclear pulse data and analog caliper data. Data are recorded in decimal form on paper and/or perforated tapes and supplemented by analog records. Identification and control data are manually entered. Output data on perforated tape are converted to cards, control cards containing calibration and correction constants are added, and the carded data are edited and submitted for interpretation by computer. Spacings of detectors from the source were selected to minimize non-standard hole conditions and yet obtain an adequate intensity of gamma-rays and favorable response to density change. Bulk density is determined from a second order polynomial equation relating the difference in countrate between the long- and short-spaced detectors to bulk density which minimizes borehole effects and the problem of anomalous natural gamma radiation. Calibration and correction factors for non-standard conditions are derived from full-scale model holes. RHOLOG, a FORTRAN language program written for the IBM 7090 computer, correlates logging, calibration and correction data and calculates bulk densities. Subroutines provide for correcting input data for instrument deadtime, non-standard borehole effects, source decay, and for accepting additional data and constants to calculate dry density, estimated porosity, moisture, and for obtaining averages of these parameters for selectable intervals. Output is in printed tabular form. Density and porosity measurements are used to estimate ore reserves, evaluate water, and rock competence problems in mining and for ore control and genetic studies. (auth)

Thorium and Uranium Minerals

Refer also to abstracts 14491 and 14750.

14779 (RME-4569(Rev.)) URANIUM EXPLORATION IN CHILE. Knowles, Paul H.; Bowes, William A.; Serrano C., Mario; Kolhn H., Erik; Moraga B., Aldo; Gruenwald S., Rodolfo (Division of Raw Materials (AEC), Washington, D. C. Instituto de Investigaciones Geologicas, Santiago (Chile)). Dec. 1962. 45p. Dep. mn. CFSTI $2.00 cy, $0.50 mn.

Uranium reconnaissance was conducted in Chile from March 1958 through December 1960. In the coastal region of northern Chile small pods of uranium were associated with medium- or predominantly high-temperature copper veins in a host of granitic rocks. Other medium- to high-temperature veins with associated uranium occurred in tourmaline-quartz zones or breccia pipes on the western flank of the Andes. In these occurrences the quantity of uranium generally was small but appeared to be proportional to the intensity and the quantity of the copper metallization. In the Andes also were spotty disseminations of uraninite in primary low- to medium-temperature veins associated with various metallic minerals. Minor uranium and thorium minerals also were noted in a granodiorite host in southern Chile and in a pegmatitic zone along the central coast. The sedimentary rocks examined in several provinces of Chile were not significantly anomalous except at one place in Atacama Province where uranium and copper minerals occur in carbonaceous layers in stream-terrace gravels. It is believed that hydrothermal solutions related to Andean volcanism are still concentrating copper and uranium minerals in these sediments. Exploration thus far has revealed no uranium deposits in Chile that are economically minable under present market conditions. (P.C.H.)

14780 (AEC-tr-6579) URANIUM AND CERTAIN OTHER ELEMENTS IN THE RED-COLORED PALEOZOIC DEPOSITS OF THE NORTHERN TIEN SHAN. Grigor'ev, K. A.; Kozyrev, V. I.; Leskov, S. A.; Fedotov, D. N. Translated from Tr. Vses., Nauchn.-Issled, Geol. Inst., 95: 141-8(1963). 13p. Dep. mn. CFSTI $1.00 cy, $0.50 mn. JCL $1.60 fs, $0.80 mf.

The red-colored Paleozoic deposits in Northern Tien Shan were analyzed for uranium and other elements. Uranium was determined by the fluorescent method with a relative error in 80% of the cases not exceeding 20%. Other elements were determined by semi-quantitative spectral analysis. The sensitivity threshold amounted to: Mn, Ni, Co, V, Pb, Sn, Ca, Mo, and Cu 0.001%; Ti, Y, and Cr 0.003%; Zn 0.01%; and Ba and Sr 0.03%. Thus, with respect to the distribution of U and other elements in rocks it was established that the red-colored deposits generally refer to a transitional modification of the variegated type. The effects of sediment accumulation for various transformations was also confirmed. (P.C.H.)

14781 SINGULARITIES IN URANIUM–RADIUM SERIES EQUILIBRIUM SHIFT IN URANIUM DEPOSITS WITH SOLID BITUMENS. Kotel'nikov, G. N. At. Energ. (USSR), 19: 474-5(Nov. 1965). (In Russian).

Changes in the radioactive equilibrium coefficients of uranium were determined in 3 solid bitumen deposits located at distances of hundreds and thousands of miles from each other, in areas of different geological features and climatic conditions. The anomalies in the equilibrium were determined on the basis of samples taken in horizontal and vertical directions, in an attempt to establish the laws governing the changes in the equilibrium. At increasing depths the equilibrium coefficient was found to shift toward the Ra, up to 600% or more. At greater depths this was reversed and the ores were found to be in an equilibrium state. The

lowest diluvial layer was characterized by a depletion of the Ra content. Horizontally, in a direction away from the original deposit, the radioactive equilibrium in the diluvial minerals gradually changed toward Ra but this shift could be followed only if the slope of the area was slight. This regular behavior may be used to establish the location of the primary deposit within a field of well-formed radioactive diluvium. (TTT)

HEALTH AND SAFETY

See also BIOLOGY AND MEDICINE — Radiation Hazards and Protection
GEOLOGY, METEOROLOGY, AND MINERALOGY — Natural Radioactivity and Fallout

Refer also to abstracts 14314, 14467, 14815, 14864, 14944, 15036, 15858, 16001, 16031, 16032, 16114, and 16137.

14782 (AE–211) REPORT ON THE PERSONNEL DOSIMETRY AT AB ATOMENERGI DURING 1964. Edvardsson, K. A. (Aktiebolaget Atomenergi, Studsvik (Sweden)). Jan. 1966. 16p. Dep. mn.

Results are reported from the radiation monitoring of personnel at AB Atomenergi during 1964. No doses exceeding the recommendations of ICRP were reported. (auth)

14783 (AECD/HP/2) RADIATION SAFETY REGULATIONS FOR ATOMIC ENERGY CENTRE, DACCA. Siddiqi, Aziz Ahmad (Atomic Energy Centre, Dacca (Pakistan). Health Physics Div.). Sept. 1965. 40p. Dep. mn.

Definitions, maximum permissible levels of radiation, and regulations are given for safety in working with radioactive materials. (P.C.H.)

14784 (AERE-R–5015) DISTRICT BIOLOGICAL MONITORING AT A.E.R.E., HARWELL. RESULTS FOR 1963 AND 1964. Morgan, A.; Homes, A.; Vandervell, H. D.; Brooks, W. L. (Atomic Energy Research Establishment, Harwell (England)). Nov. 1965. 19p. Dep. BIS $0.60. HMSO 3s.

The results of measurements made during 1963 and 1964 on samples of milk, soil, grass and herbage collected in the vicinity of the Atomic Energy Research Establishment are described. Levels of strontium-90 and cesium-137 in milk, sampled at six farms within three miles of AERE, were no greater than would be expected from world-wide fallout and, at most, only correspond to about 5 and 3% of the respective derived working limits, appropriate for members of the public living in the neighborhood of controlled areas. Levels of iodine-131 in milk remained below the limit of detection (20 pC/litre) throughout this period. Measurements of strontium-90 and cesium-137 in soil, grass, and herbage, collected at a number of sites within three miles of AERE, showed that the total deposition of these fission products could be accounted for by fallout from the testing of nuclear weapons. It was concluded that operations at AERE have not affected significantly the levels of radioactive contamination in its immediate neighborhood. (auth)

14785 (BNWL–182) SNPO AND SNAP BIOLOGICAL STUDIES. Summary Technical Report. Thompson, R. C. (Battelle-Northwest, Richland, Wash. Pacific Northwest Lab.). Jan. 3, 1966. Contract AT(45-1)-1830. 17p. Dep. mn. CFSTI $1.00 cy, $0.50 mn.

Preliminary results are reported from a series of studies related to the biological effects of inhaled or ingested ^{238}Pu SNAP fuel particles. Dogs were exposed to aerosols of ^{59}Fe-labeled ceramic microspheres ranging in diameter from 6.2 to 20μ. Whole-body scanning was used to follow the distribution of inhaled or swallowed particles over a 2 mo. period. Simulated reactor fuel particles, about 1 mm in diameter and consisting of depleted U in a graphite matrix spiked with ^{89}Sr, and ^{90}Sr-^{90}Y, were used to study the effects of dose rates of 13,000 rad/hr at the surface and 4000 rad/hr at a tissue depth of 50 mg/cm^2 on the skin and gastric mucosa of miniature swine and the radiation dose from ingested particles in rats. A single swine was fed massive doses (approximately 1 C) of ^{238}Pu SNAP fuel particles and the α activity of blood, feces, and urine was followed for 14 days before the animal was sacrificed and various tissues were analyzed for ^{238}Pu content. A simulant for gastric juice was prepared for use in studies of the solubility of SNAP fuel element materials. (C.H.)

14786 (BNWL-SA–465) ENVIRONMENTAL MONITORING. Honstead, J. F.; Soldat, J. K. (Battelle-Northwest, Richland, Wash. Pacific Northwest Lab.). Mar. 25, 1965. Contract AT(45-1)-1830. 73p. Dep. mn. CFSTI $3.00 cy, $0.75 mn.

The environmental radiation monitoring program at the Battelle Memorial Institute Pacific Northwest Laboratory, Richland, Washington is described in detail. Criteria for environmental monitoring programs are reviewed and methods used for pre-operational surveys, emergency surveys, operational surveys, radiological monitoring of the Columbia River and the atmosphere are described. Exposure pathways that must be combined to assess the total exposure of employees and the public are discussed. (C.H.)

14787 (CEA-Bib–64) DEGAGEMENT, PROPRIETES ET PIEGEAGE DES IODES RADIOACTIFS DANS LES EFFLUENTS GAZEUX. (Release, Properties, and Trapping of Radioactive Iodines in Waste Gases). Thal, Marie-Florence; Chevalier, Gerard (Commissariat a l'Energie Atomique, Saclay (France). Centre d'Etudes Nucleaires). June 1965. 80p. Dep. mn.

The amounts of stable and radioactive iodines formed in a reactor are large and depend on the power of the reactor, on the fuel, and on the time of irradiation of the fuel. According to the conditions of release they are found in various forms. A study of the various compounds can be carried out using chemical methods (analysis in solution, gas chromatography, etc.), physical methods (mass spectrography, diffusion coefficient measurement, study of ionized particles, etc.) and radiometric methods (γ-spectrography, activation analysis). The methods involving traps depend on the physico-chemical forms in which the iodine is present in waste gases: conventional dust filters stop the majority of the particles, adsorbents such as copper and silver–copper fix 90 to 99 percent of the molecular iodine by chemisorption, whereas carbons trap molecular iodine and iodine-containing compounds in the vapor form by physical adsorption with cleansing coefficients of up to 10^4. It appears that the iodine concentration and the water-content of the carrier gas play a very important role. For waste-gas temperatures of above 350°, special adsorbents are used which operate up to 500°C approximately (special carbons, potassium iodide, etc.). (194 references). (P.C.H.)

14788 (JAERI–1089) RADIATION LEAK TEST OF SHIELDED CELLS AT REPROCESSING ANALYTICAL FACILITY. Emura, Satoru; Onuki, Mamoru; Nakahara, Yoshinori; Suyama, Naohiro (Japan Atomic Energy Research Inst., Tokyo). 1965. 52p. (In Japanese). Dep. mn.

For an analytical cell and sampling blister cell having 15-cm lead shields at the Reprocessing Analytical Facility, radiation leak tests were carried out using approximately 1.5 Curies cobalt-60 as the point source. Radiation levels and surface dose rates were measured by G-M counters and ionization survey meters. As a result of the measurements, some radiation leak was found where ball socket assemblies were located, for both the cells. However, this would be no problem in the normal operation of cells. Leaks were also detected at places where shielding was not sufficient, e.g., close to the duct on the analytical cell roof, the shield between the E and M cells, around the transfer tunnel, and the joint of the sampling blister cell and the concrete wall. It was concluded that, by reinforcing these places in the radiation shielding, up to about 30 Curies of F.P. could be safely handled in the analytical cell and up to about 20 Curies in the sampling blister cells. (P.C.H.)

14789 (ORNL–P–1910) RADIOISOTOPE SOURCES AND SOURCE TESTING. Niemeyer, R. G. (Oak Ridge

National Lab., Tenn.). [1965]. Contract W-7405-eng-26. 17p. (CONF-660207-1). Dep. mn. CFSTI $1.00 cy, $0.50 mn.

From Radioisotope Applications in Aerospace Symposium, Dayton, Ohio.

The excellent safety record of domestically manufactured sealed sources together with information acquired in the ORNL Source Testing Program served as a basis for the ORNL Source Capsule Classification System which is proposed. This system permits classification of source capsules according to structural and temperature characteristics as these relate to the overall objective of ensuring containment of the radioisotope. (P.C.H.)

14790 (RL-SA-43A) ADMINISTERING CRITICALITY CONTROL IN THE HANFORD ATOMIC PRODUCTS OPERATION NON-REACTOR ENVIRONMENT. Isaacson, R. E.; Kiel, G. R.; Ridgway, K. R.; Carter, R. D. (General Electric Co., Richland, Wash. Hanford Atomic Products Operation). June 18, 1965. Contract AT(45-1)-1350. 4p. (CONF-651103-1). Dep. mn; CFSTI $1.00 cy, $0.50 mn.

From IAEA Symposium on Criticality Control of Fissile Materials, Stockholm.

The organizational structures and operational functions for administration of criticality control in ex-reactor environments at Hanford are outlined. (T.F.H.)

14791 (Y-1501) AUTOMATED AIR SAMPLING BY THE USE OF APERTURE CARDS. Sanders, Merwyn (Union Carbide Corp., Oak Ridge, Tenn. Y-12 Plant). Mar. 3, 1966. Contract W-7405-eng-26. 13p. Dep. mn. CFSTI $1.00 cy, $0.50 mn.

A device was constructed which permits successful air monitoring on IBM aperture cards equipped with Whatman 41 filter paper. The cards are passed through a scintillation detector. This technique has been proven to be a highly successful air-monitoring program for buildings compared to the more conventional programs. (C.H.)

14792 BALANCING BENEFIT VERSUS RISK IN THE CONTROL OF CONSUMER ITEMS CONTAINING RADIOACTIVE MATERIAL. Brodsky, Allen (Univ. of Pittsburgh). Amer. J. Public Health, 55: 1971-92(Dec. 1965).

A systematic procedure was developed for determining whether or not a product containing radioactive material should be permitted general distribution to the public. Attempts were also made to illustrate how the available knowledge of radiobiologic effects, together with available population statistics, may be applied in balancing the human benefits vs the human risks (or costs) of particular uses of radioactive material. The guidelines developed here are limited to consumer items containing radioactive material distributed in the United States. Human risks of low-level radiation exposure are outlined, with data provided on radiation-produced chronic disease incidence, ratios between mortality from certain diseases, and total mortality and morbidity. An interim index of human risk from radiation exposure was derived. (TCO)

14793 RADIOLOGICAL PROTECTION SERVICE OF THE JCEA. Bol. Junta Contr. Energ. At. (Peru), 10: 1-152(Jan.-June 1965). (In Spanish).

Plans of the Peruvian Atomic Energy Commission (JCEA) for radiation control on the national level are presented. Site, equipment, and personnel requirements of a radiation protection service are summarized. Health physics terminology is defined in an appendix. (H.G.D.)

14794 A REVIEW OF THE PHYSIOLOGY OF THE GASTROINTESTINAL TRACT IN RELATION TO RADIATION DOSES FROM RADIOACTIVE MATERIALS. Eve, I. S. (United Kingdom Atomic Energy Authority, Harwell, Eng.). Health Phys., 12: 131-61(Feb. 1966).

A table is proposed for the GI tract mass and food retention time of Standard Man. For some methods of calculation, the fraction of the 24 hr during which a section of the GI tract is full of food residues is required (occupancy factor). Suggested values for this factor are as follows: stomach $^{6}/_{24}$, small intestine $^{14}/_{24}$, upper large intestine $^{10}/_{24}$, and lower large intestine $^{22}/_{24}$. It is suggested that the effective radius of the GI tract as a whole be taken as 10 cm: that the radius of the stomach be taken as 10 cm, and of the small intestine also as 10 cm; that the upper and lower large intestine each be taken as 5 cm in radius. The geometrical factors in irradiation of the GI tract by its contents, sites of absorption of different substances in the GI tract, distances of food residues in the GI tract from mitosing cells, and radiation dose to the ovary from the contents of the GI tract are discussed. (C.H.)

14795 DOSIMETRY OF THE GASTROINTESTINAL TRACT. Dolphin, G. W.; Eve, I. S. (United Kingdom Atomic Energy Authority, Harwell, Eng.). Health Phys., 12: 163-72(Feb. 1966).

The dosimetry of the GI tract given in ICRP Publication 2 is reviewed. New equations are derived for calculations of $(MPC)_w$ for the four sections of the GI tract. Values for $(MPC)_w$ are calculated from these equations using values for the parameters obtained from Eve. These $(MPC)_w$ values are compared with the appropriate values from the current recommendations. (auth)

14796 DEPOSITION AND RETENTION MODELS FOR INTERNAL DOSIMETRY OF THE HUMAN RESPIRATORY TRACT. Bates, David V.; Fish, Birney R.; Hatch, Theodore F.; Mercer, Thomas T.; Morrow, Paul E. Health Phys., 12: 173-207(Feb. 1966).

A dust deposition model was developed that is based on dust sampling data. The dust deposited in each respiratory component was considered quantitatively, kinetically, and by pathways. An attempt was made to classify many chemical compounds as to their retention in the respiratory tract. Normal respiratory values were compiled based on anatomical and physiological data, with emphasis on human measurements of males, females, and children. The hazards from the inhalation of radioactive dusts and aerosols is considered and the special problem involved in the dosimetry of Ra and its decay products is reviewed. An attempt was made to organize published data on quantitative lung clearance of inhaled materials. (108 references.) (C.H.)

14797 RADIOBIOLOGICAL ASPECTS OF THE SUPERSONIC TRANSPORT. Upton, A. C. (Oak Ridge National Lab., Tenn.); Chase, H. B.; Hekhuis, G. L.; Mole, R. H.; Newcombe, H. B.; Robertson, J. S.; Schaefer, H. J.; Snyder, W. S.; Sondhaus, C.; Wallace, R. Health Phys., 12: 209-26(Feb. 1966).

The biological aspects of supersonic transport are reviewed with reference to radiation exposure at altitudes of 60,000 to 80,000 ft. Radiation at these altitudes includes that attributable to galactic cosmic rays and that attributable to solar flares. Galactic cosmic radiation varies with geomagnetic latitude, as well as with altitude, is maximal at polar regions, and varies inversely in relation to solar radiation. Under pessimistic assumptions, radiation from this source is estimated not to exceed 1 to 2 mrem/hr at altitudes up to 80,000 ft. Solar flare radiations are produced intermittently in outbursts associated with sun spots and are composed of protons and secondaries. On rare occasions, perhaps once or twice during an 11-year period, a giant relativistic particle event may be expected to deliver a dose equivalent to 1 to 10 rem/hr at an altitude of 80,000 ft on polar flights, with 0.5 to 5 rem in the first hour and decreasing amounts in the succeeding 12 to 48 hr period. Measures which can detect such events in time to warn the craft to descend to lower altitudes when necessary are discussed. It is concluded that, if major solar flares are avoided, the cumulative radiation exposure of the crew and passengers will be within permissible limits. (C.H.)

14798 DISTRIBUTION OF ^{210}Po IN PULMONARY TISSUES OF CIGARETTE SMOKERS. Little, John B.; Radford, Edward P. Jr.; McCombs, H. Louis; Hunt, Vilma R. (Harvard School of Public Health, Boston). New Engl. J. Med., 273: 1343-51(Dec. 16, 1965).

An attempt was made to show that pulmonary tissues of smokers, particularly certain regions of the bronchial epithelium, contain more ^{210}Po than those of nonsmokers. Results showed that ^{210}Po was in higher concentrations in lung parenchyma, peribronchial lymph nodes, and

bronchial epithelium of 25 persons currently smoking cigarettes than in those of 8 nonsmokers. By far the highest local concentrations of ^{210}Po were found in bronchial epithelium from segmental bifurcations, and with continual exposure to the isotope, as experienced by cigarette smokers, the cumulative local radiation dose to these small regions of bronchial tissue may be quite high. On the basis of these results, it is suggested that ^{210}Po may be an important factor in the initiation of bronchial carcinoma in man. (TCO)

14799 ESTIMATION OF GENETICALLY SIGNIFICANT DOSE DUE TO THERAPEUTIC RADIATION IN JAPAN. Hashizume, Tadashi (National Inst. Radiol. Scis., Chiba, Japan); Maruyama, Shizuo (and others). Nippon Acta Radiol., 25: 192-9(June 1965). (In Japanese).

The genetically significant dose to the Japanese contributed by diagnostic x-radiation was estimated to be 38.6 Mrad/yr/newborn child. Determinations were made by use of phantoms and a colonial dosemeter equipped with a chamber that has small energy response. The number of expected children for patients was calculated on the basis of 5 year survival rate. The contribution of genetically significant dose due to therapy was found to be about 2.2% of that due to diagnosis or 0.87 Mrad per person per year. Eighty % of the whole was due to x rays and 20% was due to radioisotopes. Males contributed 62% of the whole, while that by females was 38%. The contribution by children (persons under 15 years) was 40% of the whole. (TCO)

14800 ADMINISTRATION OF NUCLEAR SAFETY AT ANL. Levenson, M.; Adams, R. M. (Argonne National Lab., Ill.). Nucl. Safety, 7: 1-6; 18(Fall 1965).

The nuclear safety program of Argonne National Laboratory and its administration are considered. An attempt was made to establish a system of checks and balances that will ensure that no significant facts are overlooked in analyzing the safety of proposed operations by requiring review by experienced but disinterested experts. To assist in discharging nuclear safety responsibilities, two advisory committees were constituted formally: the Reactor Safety Review Committee, and the Criticality Hazards Control Committee. Neither Committee is intended to be a compliance committee but rather is intended to provide competent technical review at all stages of all operations to ensure the safest possible operation. The functions of these committees and the policies under which they were established are described. (auth)

14801 LEGAL ASPECTS OF A RADIATION-SAFETY PROGRAM. Smith, J. Lloyd. Nucl. Safety, 7: 6-11; 18 (Fall 1965).

Some of the legal benefits of making and keeping good radiation-exposure records are considered. Three lawsuits are referenced and discussed in which such records were of value. The information that should be recorded, the type records that are admissible in a court action, and how long radiation records should be kept are discussed. (auth)

14802 ATOMIC ENERGY FOR SOCIETY AND THE BALANCE BETWEEN HAZARD AND GAIN. Sterner, J. H. (Eastman Kodak Co., Rochester, N. Y.). Nucl. Safety, 7: 14-18(Fall 1965).

Health problems created by the peaceful uses of atomic energy are considered. The experience of some thousand nuclear reactor years is reviewed. No injury was identified in individuals or groups exposed to allowable operational levels of radiation, based on the same kind of risk assessment as was applied in the evaluation of other occupational and environmental health hazards. (M.C.G.)

14803 STORAGE OF IRRADIATED FUEL ELEMENTS AT REACTOR PLANTS. Nichols, J. P. Nucl. Safety, 7: 67-72; 86(Fall 1965).

A survey was made of the methods of storage of irradiated fuel at typical U.S. reactor plants. The use of water-filled pools for storage of metal-clad inert fuels appears to be universally accepted as a safe practice. The appropriate type of confinement for the fuel-storage area and the choice of methods for fuel handling, inspection, monitoring, and criticality assessment are discussed. (auth)

14804 RELEASE AND TRANSPORT OF FISSION-PRODUCT IODINE AND ITS REMOVAL FROM REACTOR CONTAINMENT SYSTEMS. Keilholtz, G. W. Nucl. Safety, 7: 72-81; 86-8(Fall 1965).

The properties of radioactive iodine are described through the stages of generation, release, transport, and deposition in a reactor-containment system. Trapping systems for different forms of airborne iodine are discussed, and methods of evaluating their efficiency are described. The adsorption of iodine on particulate matter, the rate of deposition of iodine under various possible reactor-accident conditions, and the formation of organic iodine compounds are aspects of iodine behavior considered important in evaluating the hazards of nuclear reactor accidents and in establishing reactor-site criteria. Methods of characterizing the forms of iodine and of reducing their removal from aerosols are compared and evaluated. (auth)

14805 THRESHOLD-LIMIT VALUES IN INDUSTRIAL HYGIENE. Clayton, George D. (George D. Clayton and Associates, Inc., Detroit, Mich.). Nucl. Safety, 7: 89-92; 102(Fall 1965).

Threshold-limit values for atmospheric contaminants are used by industrial hygienists. The experience gained shows that these values are beneficial; however, misuse has occurred. Precise terminology and proper usage are shown to be important because the limiting values are frequently enforced by regulatory agencies. (auth)

14806 GAMMA-RAY EXPOSURE MEASUREMENTS IN A MAN PHANTOM RELATED TO PERSONNEL FILM DOSIMETRY. Delafield, H. J. (Atomic Energy Research Establishment, Harwell, Eng.). Phys. Med. Biol., 11: 63-73(Jan. 1966).

The variation of exposure with depth in a man phantom, together with the performance of film dosemeters on the surface, was determined for uncollimated photons of energies from 48 kev to 2.8 Mev. To simulate radiation exposure conditions in the atomic energy industry, measurements were made with the phantom both stationary and rotating. The front to back attenuation factor for the static phantom of thickness 21.8 cm varied from 0.6 to 0.07 for photons of energies from 2.8 Mev to 48 kev in general agreement with published radiotherapy data. The measurements enable an improved estimate of the dose to an organ in the body to be made from a film dosemeter reading, provided that an indication of both the energy and direction of the incident radiation is available. (auth)

14807 RADIATION CONTROL IN MISSISSIPPI. Rester, Robert R. (Mississippi State Board of Health, Jackson). S. Med. J., 58: 346-9(Mar. 1965).

The program of the Mississippi State Board of Health designed to cope with problems arising through the use of radioactive materials and radiation-producing devices is considered in terms of three main features: environmental monitoring, x-ray evaluation, and control of radioactive materials. Another aspect of Mississippi's Radiological Health Program that is described is an x-ray evaluation project. It was found that a significant percentage of the machines inspected did not meet the simple criteria established by the Mississippi State Board of Health. Follow-up surveys in all hospitals and clinics have indicated that the recommendations made during the initial survey were in most instances followed up by the owner, and appropriate modifications in equipment accomplished. (TCO)

14808 OPERATION RED DOG. Anderson, Kenneth N. Todays Health, 43: 64-9(Jan. 1965).

The organization and function of Radiological Assistance Teams of the Atomic Energy Commission that protect the public from the threat of nuclear contamination are briefly reviewed. Several incidents in which they have played a role are described to illustrate their duties. The code name "Red Dog" signifies a nuclear accident situation not involving military weapons. The Atomic Energy Commis-

sion has Radiological Assistance teams stationed at eight offices throughout the United States. Each team is trained and equipped to handle various kinds of emergency that may develop on a highway or railroad siding or in a hospital or industrial plant. Recommended steps to be taken in a nuclear accident are outlined. (TCO)

14809 ALPHA HAND AND FOOT COUNTER (Engineering Materials). (Du Pont de Nemours (E. I.) and Co., Aiken, S. C. Savannah River Lab.). (CAPE–1326). 16 drawings.

Equipment was designed to monitor hands and feet for α particles. Feet are monitored on a pedestal 30 by 24 in. An upright cabinet rack houses the power supplies, hand monitoring assembly, and the display panels. Electronic equipment includes: photomultipliers, silicon diodes, and decade cold cathode counters. The h-v power supplies consist of a relay, signal, and pulser. (For details, see TID-4100.) (M.C.G.)

14810 RADIOLOGICAL MONITORING OF THE ENVIRONMENT. Proceedings of a Symposium held at Berkeley, Gloucestershire, October 1963. Godbold, B. C.; Jones, J. K. (eds.). Oxford, Pergamon Press, 1965. 440p. $17.50. (CONF-365).

Separate abstracts were prepared on two papers. Abstracts of 27 papers were prepared previously and appeared in NSA Vol. 18 as numbers 6775; 7086; 8248; 8249; 8250; 8251; 8586; 8587; 8588; 8589; 8590; 8591; 8593; 8594; 8595; 8596; 8597; 8598; 8599; 8600; 8601; 8602; 8603; 8604; 8689; 8690; and 8698. (C.H.)

For abstracts of individual papers see: 14811 and 14812.

14811 RECENT ADVANCES IN MONITORING FOR AIRBORNE RADIOACTIVITY. Lister, B. A. J. pp 375-84 of Radiological Monitoring of the Environment. Godbold, B. C.; Jones, J. K. (eds.). Oxford, Pergamon Press, 1965.

Recent advances in the collection and analysis of radioactivity in the air are reviewed and the interpretation of data in terms of hazards to man are discussed. Emphasis is placed on the development of sampling equipment for use in operating areas in plants using Pu and U in the environs of reactors, and in stock sampling. (C.H.)

14812 CURRENT PRACTICE IN THE SURVEY OF WORKING ENVIRONMENTS. Greening, J. R. pp 395-403 of Radiological Monitoring of the Environment. Godbold, B. C.; Jones, J. K. (eds.). Oxford, Pergamon Press, 1965.

The measurement of stray x or γ rays resulting from the deliberate irradiation of such varied materials as patients, plastics, chemicals, castings, foods, pharmaceuticals, crystals, and chrysanthemums is discussed. In all cases the radiation source is contained as far as possible and the irradiated object is enclosed to protect the operator. Usually interlocks are provided to prevent inadvertent entry into the radiation area. The examination of the integrity of the shielding of such installations is the duty of a specialized health physics team rather than of the user and special attention should be paid to points where leakage can occur. (C.H.)

14813 SYSTEMATIC OBSERVATION OF THE LONG LIVED RADIOACTIVITY IN THE PILSEN REGION. Matousek, J.; Mertl, F.; Patocka, S. (Karlovy Univ., Pilsen, Czech.). pp 250-61 of Proceedings of 3rd National Bioclimatology Conference, Prague, Oct. 1961. Prague, Czechoslovak Academy of Science, 1963. (In Czech).

The long-lasting radioactivity contained in the atmosphere has been continuously monitored and recorded by the Physical Institute of the Charles University Medical School since 1957. In addition, during 1959 and 1960 the radioactive fallout observed in this area was collected and measured at weekly and monthly intervals. The methods used for collection, measurement, and evaluation of the fallout material and the test studies are described. The relation between the observance of increased radioactivity and the known occurrence of thermonuclear explosions carried out for test purposes was demonstrated. The measurements obtained were compared with those obtained by other measurement centers. At present, the sample collection method is being revised so that the radioactive aerosols will be filtered through membrane filters rather than through filter paper. The network of sample collection stations is being extended. A device for automatic measurement of radioactive samples was completed. (55 references). (BBB)

14814 PROBLEMS INVOLVED IN DELIVERING ADEQUATE RADIATION DOSE TO COMPLEX SAMPLES. Boag, J. pp 75-84 of Ionising Radiation for the Sterilization of Medical Products. London, Panel on Gamma and Electron Irradiation, 1965.

Physical variables that determine uniformity of absorbed dose to complex samples is considered in view of the nature of the survival curve of microorganisms. The criterion of adequacy is not strictly the physical one of maximum uniformity of dose, but is further the maintenance of an adequate margin of safety in sterilization. Therefore, dose fluctuations that do not infringe upon the safety margin are permissible. (H.G.D.)

INSTRUMENTATION

General

Refer also to abstracts 14719, 15061, and 15588.

14815 (COO–401-139) LARGE VOLUME IMPACTOR COLLECTOR. Report No. 2893. Zeller, H. (Litton Systems, Inc., St. Paul, Minn. Applied Science Div.). Dec. 20, 1965. Contract AT(11-1)-401. 70p. Dep. mn. CFSTI $3.00 cy, $0.75 mn.

Development of the Large Volume Impactor Collector (LVIC) is reported. The system uses an air-ejector pump as the prime air mover. The ejector is an uncomplicated device and uses no moving parts. Thus, there is nothing to wear out or burn. The LVIC was successfully flight tested at two altitudes — 33.8 and 32 km. The samples obtained from the two flights were suitable for both radiochemical and electron microscope analysis. (P.C.H.)

14816 (EUR–2512,n) METING VAN VARIATIES IN WANDDIKTE BIJ LANGE RECHTE BUIZEN. BESCHRIJVING EN BEPROEVING VAN DE DEFINITIEVE MEETOPSTELLING. (Measurements of Wall-Thickness Variations in Long Straight Tubes. Description and Approvements of Definite Measuring Device). Meijer, A. C., Platzek, P. (Nederlandse Organisatie voor Toegepast Natuurwetenschappelijk Onderzoek, Delft. Centraal Laboratorium). Sept. 1965. 36p. Dep. mn.

A semi-automatic device for measuring wall-thickness variations in 76 cm long straight tubes, with internal diameters ranging from 5 to 40 mm is described. A radiation source of 25 mC Sr-90 is mounted in the tube with the window of the ionization chamber at a distance of 61 mm from the source. Automatic scanning at a speed of 2-40mm/sec^{-1} is possible along the tube and can be repeated after manual rotation of the angle. The scanning of 5-8 descriptive lines is regarded as sufficient, so that a complete check of 1 m of tubing can be carried out within 10-20 min, depending on the diameter and the desired accuracy. The wall-thickness can be 0.2-0.6 mm in the case of brass and steel and 0.6-1.8 mm in that of aluminium tubes. (auth)

14817 (N65–20421) LOW–LEVEL RADIATION ALTIMETER SYSTEM STUDY. Bird, L. L.; Ziegler, C. A. (Parametrics, Inc., Waltham, Mass.). Oct. 15, 1963. Contract NAS9-1490. 81p. (NASA-CR–57637). CFSTI $3.00 cy, $0.75 mn.

Several radiation techniques were studied as possible means for altitude measurement above the lunar surface in the range of 0 to 50 ft. Both direct (sources ejected and located on the surface during measurement) and indirect (source aboard the vehicle) systems were considered. Indirect charged-particle systems were rejected because of attenuation effects in the rocket exhaust gas, while neutron systems were rejected because of the large amount of hardware required. A gamma backscatter system using photons of moderate energy (60 kev) was found to be very promising since the source-strength requirement (~12 curies) is practical and the weight of the source and detector could be small (~5 lbs.) (STAR)

14818 (ORNL-TM-1391) ±32 VOLT POWER SUPPLY, ORNL MODEL RC11-4-2E. DeLorenzo, J. T. (Oak Ridge National Lab., Tenn.). Dec. 10, 1965. Contract W-7405-eng-26. 7p. Dep. mn. CFSTI $1.00 cy, $0.50 mn.

A power supply that consists of two independent supplies with outputs of +32 v and −32 v, respectively, is described. (D.C.W.)

14819 (RFP–602) THIN FILM EVAPORATION RATE MONITOR. Van Vorous, T.; Hart, G. E.; Martinez, J. L.; Beno, R. L. (Rocky Flats Div., Dow Chemical Co., Golden, Colo.). Feb. 17, 1966. Contract AT(29-1)-1106. 21p. Dep. mn. CFSTI $2.00 cy, $0.50 mn.

A device is described with which the rate of evaporation of metals can be monitored and the final thickness deposited upon a substrate can be measured. (D.C.W.)

14820 (RFP–636) A PRECISION BACK-REFLECTION LAUE CAMERA. Brewer, A. W.; McDonald, R. R. (Rocky Flats Div., Dow Chemical Co., Golden, Colo.). Jan. 19, 1966. Contract AT(29-1)-1106. 7p. Dep. mn. CFSTI $1.00 cy, $0.50 mn.

A precision back-reflection Laue camera is described, which utilizes an optical attachment and micrometer stage to align precisely a small area of specimen to the x ray beam. The beam can be confined to one particular crystal grain or an isolated single crystal as small as 0.5 mm in diameter. The need for such accurate alignment is generated by grain perfection and orientation studies on relatively small-grained polycrystalline specimens. (auth)

14821 (RFP–668) AN AUTOMATIC RECORDING, LOW-TEMPERATURE DILATOMETER. McDonald, R. R.; Pinkney, R. J. (Rocky Flats Div., Dow Chemical Co., Golden, Colo.). Feb. 1, 1966. Contract AT(29-1)-1106. 7p. Dep. mn. CFSTI $1.00 cy, $0.50 mn.

A dilatometer, having the temperature range of 50 to 500°K, is described. Temperature is recorded directly in millivolts on the X axis of a direct-reading, X-Y, fixed-chart recorder while the change in length is simultaneously recorded on the Y axis. The result is a complete graph of the temperature and dilatation, which needs only the translation of the recorded voltage readings to useful values of length and temperature. Control of the cooling cycle can be easily maintained at any rate (within desirable limits) between 0.5 and 100°K/min. Similar control of the heating cycle can be attained by conventional Variac control of the furnace element. (P.C.H.)

14822 (RHEL/R–112, pp 99-128) EXPERIMENTAL TECHNIQUES AND APPARATUS. (National Inst. for Research Nuclear Science, Chilton (England). Rutherford High Energy Lab.).

Engineering studies are reported on: pulse transmission through coaxial cables; the design of synchronizing discriminators, fast discriminators, pedestal generators, a differential amplifier with high common-mode rejection, an adapter for the selective storage unit of a pulse-height analyzer, timing systems for digital voltmeter readout, a high-stability Hall-effect magnetic field probe, temperature-stabilized enclosures for photomultiplier detectors, wedge-shaped scintillation detectors, momentum-analyzing magnets for charged-particle beams, and a charged-particle-beam backscattering chamber; development of components and techniques for use in the $n^1/_2$ spectrometer; development of systems for analog pulse ratio measurements; analysis of the response of analog circuits to Darlington compound-transistor common-base amplifiers; analysis of ion optics in the $n^1/_2$ spectrometer; and floating-wire beam monitoring techniques for the $n^1/_2$ spectrometer. (T.F.H.)

14823 (RL-REA–2595, pp 73-9) A COMPARISON OF A DOUBLE DIFFRACTING X-RAY UNIT WITH A STANDARD X-RAY DIFFRACTION UNIT. Clark, W. I. (Battelle-Northwest, Richland, Wash. Pacific Northwest Lab.).

A sample of unirradiated uranium with a random orientation was run on a standard x-ray diffraction unit, then in a double-diffraction unit. The relative intensity of the diffraction patterns for the 18 planes was calculated by setting the 021 plane equal to 100. The difference between the experimental values and the standard intensity values was determined, and this difference plotted as a function of the 2 θ values. The set of data from the standard unit had a random distribution, whereas the data points from the double-diffracting unit seemed to form an inverted parabola. A curve of the general form, $a + bx + cx^2 - y = 0$, was calculated using the least-squares method. The standard intensity ratios were modified to reflect the difference between the double diffracting and standard unit. This difference was caused by a slight misalignment of the single crystal. This curve would hold true only for those data run under these instrumental conditions. (auth)

14824 (SC-TM-65-523) A COMPUTER PROGRAM FOR PERFORMING RELIABILITY ANALYSES. Breipohl, A. M.; Hernquist, R. A. (Sandia Corp., Albuquerque, N. Mex.). Dec. 1965. Contract AT(29-1)-789. 39p. Dep. mn. CFSTI $2.00 cy, $0.50 mn.

A computer program which will perform system reliability analyses is discussed. The program, after receiving component and wiring diagram information, constructs the dud and premature equations which relate the probabilities of system behavior with the probabilities of the various subsystem (component) behaviors. The ability to evaluate the consequences of electrical shorts in both dud and premature studies, and the ability to obtain component information from such tests as QEST and NMST, were included in the program's logic. The modeling scheme used by a reliability analyst in describing component information for the computer is discussed. Some general comments concerning the treatment of electrical shorts are also included. (auth)

14825 (CEA-tr-X-356) PROCEDE POUR LA FABRICATION D'UN TUBE ELECTRIQUE A DECHARGE DANS UN GAZ CONTENANT UNE CERTAINE QUANTITE DE TRITIUM ET TUBE ELECTRIQUE A DECHARGE DANS UN GAZ OBTENU SELON CE PROCEDE. (Process for the Fabrication of an Electric Discharge Tube in a Gas Containing a Certain Quantity of Tritium and an Electric Discharge Tube in a Gas Obtained According to this Process). Philips, S. A. Translated into French from Dutch Patent No. 97478. 11p. Dep. mn. JCL $1.60 fs, $0.80 mn.

A procedure for the fabrication of a discharge electric tube in a gas containing some tritium, absorbed by a thin layer of titanium, zirconium, or a similar hydrogen absorber, is described. The titanium, zirconium, or analogous metal is deposited as a very finely divided powder in a tube by pulverization in an electric discharge in a rare gas or by vaporization. The tritium is then emitted in contact with the powder in such a quantity that the metallic powder is only incompletely saturated. The most external layers of the grains are inactivated to such a measure that heating at the temperature created by pumping at a long time does not release the tritium. The metallic powder is then placed in suspension and a measured quantity of this suspension is applied to the site in the discharge tube. The customary procedure for tube fabrication is then followed. (J.S.R.)

14826 USE OF α-PARTICLES FOR MEASUREMENT OF MICA THICKNESS IN END WINDOW COUNTER. Zarnowiecki, Krzysztof. Nukleonika, 10: 453-4(1965). (In Polish).

A ^{239}Pu alpha source was collimated to irradiate an area corresponding to 1 mm or less in diameter. The counter was placed in operation and the count rate was plotted as a function of distance in air of the alpha source from the mica window. The straight-line extrapolated end point, R (in cm), of this plot is related to the thickness d in mg/cm^2 by the relation: $d = 1.45/1.23\ [3.72 - (Rp/760) \times (288/273 + t)]$, where p is the atmospheric pressure in mm Hg and t is the air temperature in °C. Thicknesses of 0 to 3.5 mg/cm^2 can be measured with a ^{239}Pu source, and the range of measurement can be extended with the use of higher energy alpha particles. Typical accuracies are 0.1 mg/cm^2 for uncertainties of ±0.5 mm in R. Accuracies of 0.05 mg/cm^2 are feasible with this method. (TTT)

14827 ULTRASTABLE TRIANGLE AND SQUARE WAVE GENERATOR. Cohen, R. L. (Bell Telephone Labs., Inc., Murray Hill, N. J.). Rev. Sci. Instrum., 37: 260-1(Mar. 1966).

A triangle and square wave generator designed to excite Mössbauer velocity drives is described. The version shown runs from 1 to 25 cps, and has frequency and amplitude stability and linearity substantially better than 0.1%. (auth)

14828 DETECTION OF PULSE PILE-UPS WITH PULSE OVERLAP TO PULSE HEIGHT CONVERTER. Monier, L. F.; Tripard, G. E. (Univ. of British Columbia, Vancouver). Rev. Sci. Instrum., 37: 316-18(Mar. 1966).

A new type of pile-up rejector, using a pulse overlap to pulse height converter, is described. It is operated at the output of a double delay line clipped amplifier and has a resolving time better than 20 nsec. (auth)

14829 RELIABLE SAMPLE CHANGER FOR MASS SPECTROMETER. Christie, W. H.; Cameron, A. E. (Oak Ridge National Lab., Tenn.). Rev. Sci. Instrum., 37: 336-7(Mar. 1966). (ORNL-P-1726).

A sample changing device for a mass spectrometer is described. Five filaments are mounted on a wheel which is adapted to be rotated by suitable drive mechanism through the vacuum wall. Reliable wiping electrical contact is made to the filament lugs by means of stationary blades, spring loaded with tungsten wire helices. (auth)

14830 REVERSIBLE INTERREFERENCED POWER SUPPLY FOR DOUBLE FOCUSING MASS SPECTROMETERS. Hanrahan, Leo R. (Knolls Atomic Power Lab., Schenectady, N. Y.). Rev. Sci. Instrum., 37: 369-70(Mar. 1966). (KAPL-P-3129).

A simplified design for a reversible interferenced high-voltage power supply suitable for use in double-focusing mass spectrometers is described, which uses two tracking power supplies instead of the usual three. The circuit operation and test results are discussed. (L.B.S.)

14831 MAGNETOMETER VOLTMETER /Q-2276/ (Engineering Materials). (Oak Ridge National Lab., Tenn.). (CAPE-1287).

1 drawing.

The circuit, which is used in the Oak Ridge Isochronous Cyclotron, consists of a Schnitt Trigger, 3 EECO T-101A flip flops, EECO T-135 delay driver, EECO T-405 "And" Gate, 120 v power supply, and a EECO T-113 emitter follower. (For details, see TID-4100). (M.J.T.)

14832 RADIATION DETECTOR POSITIONER /Q-2258/ (Engineering Materials). (Oak Ridge National Lab., Tenn.). (CAPE-1300).

8 drawings.

This equipment is used to position thin-walled, halogen quenched, geiger tubes (Lionel Electric Laboratories 106C) at two resin-filled ion exchange columns which are used to remove radioactive contamination from waste in the low level waste pilot plant. (For details, see TID-4100). (M.J.T.)

14833 TWIN ISOTHERMAL CALORIMETER (Engineering Materials). (Rocky Flats Plant, Dow Chemical Co., Denver, Colo.). (CAPE-1308).

10 drawings.

The calorimeter described consists of two identical units that house opposite arms of a Wheatstone bridge, which serves as the heat-flux sensing device. The heat flux produced by the sample is compared with that produced by electrical heating. (For details, see TID-4100). (M.C.G.)

14834 SOLUTION OUTPUT PROCESSOR (Engineering Materials). (Los Alamos Scientific Lab., Univ. of California, N. Mex.). (CAPE-1316).

8 drawings.

The solution output processor (SOP) accepts one or more NET Solution Output Tapes as input and produces printouts and graphs of signal source voltages, node voltages, and inductor, transistor, and diode currents. It also produces printouts and graphs of functions of these variables, messages produced by NET during transient analysis, and consolidations of several solution output tapes into a single composite solution output tape. (For details, see TID-4100). (M.J.T.)

14835 A REVIEW OF THE DESIGN AND APPLICATION OF RADIOISOTOPE INSTRUMENTS IN INDUSTRY. Cameron, J. F.; Clayton, C. G. (Atomic Energy Research Establishment, Wantage, Eng.). Vienna, International Atomic Energy Agency, 1965, Preprint No. SM-68/2, 63p. (CONF-651023-5). ORINS.

From Symposium on Radioisotope Instruments in Industry and Geophysics, Warsaw.

A review is given of the history, development and present position of the design and application of radioisotope instruments in industry. Technical advantages of these

instruments and the design of sources, detectors and electronic units are discussed. Health and safety regulations relating to industrial application of radioisotope instruments are outlined. The physical principles of instruments such as thickness and density gages, level gages and analytical measuring instruments and their applications in different industries are summarized. Comments are made on probable future trends in this field of radioisotope applications. (auth)

14836 MEASUREMENT METHODS TO IMPART LINEARITY OF SCALE TO RADIOISOTOPE INSTRUMENTS. Czarnecki, E.; Demus, S.; Kowalik, S. (Wojskowa Akademia Techniczna, Bemowo, Poland). Vienna, International Atomic Energy Agency, 1965, Preprint No. SM-68/50, 25p. (In Russian). (CONF-651023-25). ORINS.

From Symposium on Radioisotope Instruments in Industry and Geophysics, Warsaw.

Linearity of scale in radioisotope instruments is an important matter, since it ensures the required accuracy throughout the whole range of measurement. Three methods of obtaining linear scales in radioisotope instruments are described. They can all be used for measuring levels by radioisotopic methods, and are particularly suitable for measuring high linear displacements, where considerations of safety make it necessary to use radiation sources of low activity. The first method uses this type of movement—of detectors connected in parallel—along the vertical axis of the object to be measured. The linear dependence of the measured or total intensity of the radiation is acceptable for practical purposes. Computer calculations have yielded tables of the optimum dose rate distribution from a point source for various cases which may occur in measuring practice. The theoretical assumptions were checked on a model system. The second method is based on the effect of an increase in the effective surface area of the radiation detector. The method consists, substantially, of using equipment in which the effective surface area "seen" by the radiation source at different distances from the detector increases with an increase in distance between source and detector. Graphs derived from calculations are given for a number of specific cases, and also graphs obtained experimentally using a laboratory model; these confirm the possibility of using the method in practice. The third method is based on using, with the required accuracy, the linear section of the function describing the dependence of the readings of the apparatus measuring the voltage at the output of the integrating circuit (diode pump) on the magnitude of the parameter measured, for example on liquid level. This function consists of two nonlinear components, the dependence of voltage at the integrating circuit output on pulse frequency and the dependence of that frequency on the distance between the radiation source and the detector. These give, in fact, an almost linear dependence over a fixed range of changes in the value to be measured. A theoretical analysis based on expansion of this function into Taylor's series, which makes it possible to determine the linear range for given parameters of the circuit and a given maximum value of the permissible coefficient of non-linearity is presented. Formulas are also quoted for designing a measuring layout adapted to specific conditions of measurement. (auth)

14837 ERRORS OF GAMMA-SCATTERING DENSITY METER AND ITS DESIGN FOR LOW DENSITY MEASUREMENT. Ono, H.; Machida, T. (Central Research Inst. of Electric Power Industry, Tokyo). Vienna, International Atomic Energy Agency, 1965, Preprint No. SM-68/38, 21p. (CONF-651023-38). ORINS.

From Symposium on Radioisotope Instruments in Industry and Geophysics, Warsaw.

Sources of error in density determination of coal and soil by gamma-scattering density meters of depth type are classified into seven types. These are as follows: statistical fluctuation of the radioactivity, variation of electrical characteristics of elements which compose the counting circuit, eccentricity of the density probe in the access tube, wall thickness variation of the access tube, uncertainty of the calibration curve, voids next to the access tube, deformation of the density meter output for nonuniformity of density distribution in the media. It is not always difficult to eliminate these sources or make them negligible, while voids near the source-detector region may cause seriously large negative errors. Experimental results show that the error due to the void with uniform gap along the access tube becomes −2.0% per 1 mm gap length. The density determined by the meter does not always agree with the mean density in the sensitive volume of the media, because of non-uniformity of density distribution. It is impossible to correct errors of this kind. The availability of the density meter which has the calibration curve of positive slope is in the density range from 0.8 to 3.0 g/cm^3. The error due to statistical fluctuation of the radioactivity becomes rapidly large with lowering of density. Then, it is necessary to utilize positive slope characteristic for lower density materials, such as light, liquid, powder and snow. In order to extend measuring range of the density meter for low density, it becomes necessary to make the source-detector separation and the detector length as small as possible, respectively. When the G-M counter of effective length of about 4 cm and ^{137}Cs gamma source of 1 mc are used, it will be possible to measure the density less than 1.2 g/cm^3 within the accuracy of 2% for three minutes' counting time under the optimum design. (auth)

14838 RADIOMETRIC METHOD FOR CONTINUOUS CROSS-SECTION MEASUREMENT OF HOT ROLLED WIRES. Kuehn, W.; Wiesner, L. (Isotopen-Studiengesellschaft e. V.; Karlsruhe, Ger.). Vienna, International Atomic Energy Agency, 1965, Preprint No. SM-68/48, 22p. (CONF-651023-35). ORINS.

From Symposium on Radioisotope Instruments in Industry and Geophysics, Warsaw.

To improve the accuracy and to increase the production speed of the drawing process for wires with diameters between 8–20 mm a continuous cross-section measurement is required, allowing the determination of thickness variation of ±2%. First it will be proved theoretically that variations of the cross-sections of wires may be determined with the required sensitivity by means of the absorption of bremsstrahlung emitted by a laminar source on condition that suitable apertures of diaphragms are applied. The calibration curves obtained by purely static measurements confirm the results of the theoretical investigations. The sensitivity for the detection of cross-section variations is primarily a function of the ratio of cross sections and apertures. Moreover, it depends slightly on the radiation energy. In subsequent tests with an experimental set-up described in detail, the working conditions of a rolling mill were imitated by heating the wires up to about 800°C, and oscillating them in parallel and perpendicular direction to the bremsstrahlung beam. While parallel oscillations do not disturb the measurements, perpendicular ones result in largely reduced accuracy. This difficulty can be overcome, for example, by applying snatch blocks. A 10 mC thallium-204 bremsstrahlung source with silver target was used throughout the experiments. The application of the proposed device in rolling mills requires bremsstrahlung sources containing 200 mC thallium-204 in order to reduce the triple statistic error to ±1.5%, giving an accuracy of about ±0.6%. (auth)

14839 BETA-RAY BACK-SCATTERED TYPE THICKNESS GAGE FOR GALVANIZING PROCESS. Miwa, H.; Mizukoshi, T.; Shimizu, M. (Kobe Kogyo Corp., Akashi, Japan). Vienna, International Atomic Energy Agency, 1965, Preprint No. SM-68/12, 27p. (CONF-651023-9). ORINS.

From Symposium on Radioisotope Instruments in Industry and Geophysics, Warsaw.

The β-ray backscattered type thickness gage was developed which continuously measures the thickness of zinc coating of galvanized steel strip. The gage consists of a β-ray source (85 Kr 1000 mc), two ionization chambers, a d-c amplifier, a self-standardization system, measuring head and a scanner which makes the head traverse on the

strip to be measured keeping a constant distance between them. (auth)

14840 AN ALPHA PARTICLE HYGROMETER. Hallowes, K. H.; Hodgson, A. E. M. (Atomic Energy Research Establishment, Wantage, Eng.). Vienna, International Atomic Energy Agency, 1965, Preprint No. SM-68/19, 10p. (CONF-651023-8). ORINS.

From Symposium on Radioisotope Instruments in Industry and Geophysics, Warsaw.

A method of measuring the relative humidity of air by the transmission of alpha particles through a very thin film containing an equilibrium proportion of moisture is described. The scope of application is similar to that of electrical hygrometers in which the conductivity of a hygroscopic surface layer is measured. However, the employment of the alpha particle technique greatly reduces the dependence of the readings upon traces of sulphur dioxide and the like, in the air. The method provides a rapid response and covers the full range of relative humidities at normal atmospheric temperatures. The radioactive source is americium-241 in a glass bead, providing effectively infinite thickness for alpha particle self-absorption, and with negligible contamination hazard. The use of an infinitely thick source provides a good sensitivity to changes of relative humidity over the whole working range. The detector is a small surface-barrier semiconductor, thus allowing the construction of a compact probe to facilitate measurements in confined places, e.g., in connection with warehouse ventilation problems. The hygroscopic film is specially made from sulphonated cross-linked polystyrene, and mounted on a vane rotated by a miniature electric motor. Rotation of the vane alternates the hygroscopic film with an otherwise similar non-hygroscopic one in the source-detector gap, thus providing a means of compensating for changes in temperature and pressure of the air in the gap, and for detector temperature. The rotation also ensures the necessary circulation of air in the immediate proximity of the hygroscopic film. The output provides for continuous direct or remote indication, servo control, or recording. Details of the performance of the hygrometer, the preparation of the hygroscopic film, and the associated circuit design are included. (auth)

14841 EXPERIMENTAL TECHNIQUES. Panofsky, W. K. H. (Stanford Univ., Calif.). pp 138-54 of Proceedings of the International Symposium on Electron and Photon Interactions at High Energies. Vol. I. Plenary Sessions. Hoehler, G. (ed.). Hamburg, Deutsche Physikalische Gesellschaft e.V., 1965.

Methods of producing monochromatic photon beams are briefly discussed, together with the design and use of magnetic spectrometers. (D.C.W.)

14842 IMPROVEMENTS RELATING TO CO-OPERATING CONTACT ASSEMBLIES. Oram, Derek William (to English Electric Co., Ltd.). British Patent 1,018,783. Feb. 2, 1966. Filed Mar. 24, 1961.

Electrical contact means for providing two electrical connections between two bodies applicable for providing connections between thermocouple leads attached to two adjacent stacked fuel elements includes a first and second pair of contact members. Each pair comprises a cooperating male and female contact member. The contacts of the first pair are frusto-conical and those of the second pair comprise a frusto-conical female member and a frusto-conical or conical male member. One member of each pair is connected to one body and the other member of each pair to the other body; and the axis of one of the contact members of each pair is offset radially from the axis of the other. (B.L.M.)

14843 MEANS FOR PRODUCING FOCUSED HIGH DENSITY ELECTRON STREAMS. Bennett, Willard H. U. S. Patent 3,230,419. Jan. 18, 1966. Filed Oct. 30, 1961.

A system for producing high density electron beams comprises a cylindrical envelope having a longitudinal axis with a cathode positioned at one end of the axis and an anode spaced a short distance from the cathode along the axis. The cathode and anode provide a flow of electrons emitted by the cathode through an aperture in the anode along the axis of the envelope. Another electrode positioned outwardly of the cathode about the axis of the envelope and extending toward the anode about the space between the anode and cathode aids in collimating the electrons and directing them through the aperture in the anode. A number of axially aligned electrodes are spaced along the axis of the envelope to collect the electrons detached from the electron beam. Inlet and outlet at opposite ends of the envelope permit the flow of ionizable gas through the envelope along the electrodes. (B.L.M.)

Radiation Detection

Refer also to abstracts 14444, 14451, 14615, 14806, 15187, 15259, 15710, 15747, 15858, and 16125.

14844 (AD-620395) PULSE SHAPE DISCRIMINATION CONSIDERATIONS IN A DUAL CRYSTAL GAMMA-RAY SCINTILLATION DETECTOR [Thesis]. Lam, Carroll F. (Texas Agricultural and Mechanical Univ., College Station). Aug. 1965. Contract AF33(608)-1120. 80p. CFSTI $3.00 cy, $0.75 mn.

It is shown that a dual-crystal, single-photomultiplier scintillation detector system in conjunction with a pulse-shape discrimination technique can reduce the entire Compton contribution to a gamma spectrum up to 40%. (TAB)

14845 (AD-620434) THE CONSTRUCTION OF A LITHIUM DRIFTED GERMANIUM SOLID STATE DETECTOR SYSTEM WITH SPECIAL ATTENTION TO ^{105}Ag AND ^{192}Ir [Thesis]. Dessert, Robert Allen (Ohio State Univ., Columbus). 1965. Contract AF33(608)-1095. 72p. CFSTI $3.00 cy, $0.75 mn.

A relatively inexpensive cryostat was constructed for operation of Li-drifted Ge gamma detectors at pressures below 0.0000001 mm of Hg and at 77°K. Fundamental data were obtained on a Li-drifted Ge detector, including relative counting efficiency, resolution and peak-to-total ratio. The spectra of ^{192}Ir and ^{105}Ag were investigated using the solid-state detector. A technique of segmentation and expansion of energy subgroups with a multichannel analyzer is proposed as a means to provide more points in a given peak of a spectrum taken on the detector. (TAB)

14846 (AECL-2517) AUTOMATIC SAMPLE CHANGING SYSTEMS UTILIZING THE AECL-2041 DIGITAL READ-OUT SYSTEM. Howell, W. D.; Shorey, W. R. J. (Atomic Energy of Canada Ltd., Chalk River (Ontario)). Nov. 1965. 40p. Dep. AECL $1.00.

AECL automatic sample changing and counting systems using the general purpose read-out system are described. Special attention is given to the control and sample changing mechanisms and the details of modifications to the read-out system for satisfying user requirements. (P.C.H.)

14847 (BMwF-FBK-65-01) VORSTUDIE ZUM AUFFINDEN EINES DETEKTORS, DER IM STRAHLENFELD EINES REAKTORCORES BETRIEBSMAESSIG SPLATPRODUKTE IM KUEHIMITTEL ANZEIGT. (Preliminary Study to Find a Detector Situated within the Radiation Field of a Reactor Core which will Indicate Fission Products in the Coolant under Operating Conditions). Terfloth, H. P. (Battelle Institut E. V., Frankfurt am Main (West Germany)). Aug. 1965. 91p. Dep. mn. Gmelin DM 17,80.

Theoretical investigations regarding the possibilities of locating failed fuel element cans without utilization of nuclear radiation detection methods are studied. Using the Shippingport reactor as an example, the quantities of chemical elements present as contaminants in the coolant are calculated and compared with the expected concentrations of fission product elements in the coolant in case of a defective can. In both cases the concentration of each element at the location of the detector is estimated to be approximately 10^8 atoms per cubic centimeter of coolant. It is deemed impractical to detect concentrations of such an order of magnitude without using nuclear radiation measuring techniques. (auth)

14848 (BMwF-FBK-65-02) STUDIE UEBER DIE ANWENDUNG VON TRACERSYSTEMEN ZUR LOKALISIERUNG VON BRENNELEMENTDEFEKTEN. (Study on the Application of Tracer Systems to Localize Failed Fuel Elements). Henzel, N.; Kadner, M.; Kalix, E. (Battelle Institut E. V., Frankfurt am Main (West Germany)). Sept. 1965. 96p. Dep. mn, Gmelin DM 18,80.

Conventional methods for locating failed fuel element cans, based on the measurement of fission product activities, are compared with the radiotracer method. The latter method consists of labeling the individual fuel elements of a reactor with appropriate tracers, which can be activated within the core by n,γ reaction and identified in the coolant by means of radiation detectors in case of a defective can. Theoretical considerations show that the amount of possible tracer combinations is not sufficient to definitely label the fuel elements of gas and liquid metal cooled reactors. Of the 14 tracer compounds appropriate for water cooled reactors, only about seven can be determined by directly measuring their activities due to the presence of fission products and contaminants. Thus, in water cooled reactors a definite labeling can be achieved only by using enrichment techniques. (auth)

14849 (BNL-9720) GROWTH OF TRACKS FROM SEGMENTS. Stonehill, D. L. (Brookhaven National Lab., Upton, N. Y.). [nd]. Contract AT-30-2-GEN-16. 11p. (CONF-651044-5). Dep. mn; CFSTI $1.00 cy, $0.50 mn.

From Conference on Programming for Flying Spot Devices, New York.

The FILTER program generates track segments from flying-spot-digitizer data taken from particle-track photographs. The methods by which FILTER associates these segments into "strings," and these strings into complete tracks, are discussed. (T.F.H.)

14850 (BNL-9763) STRUCTURE OF THE BROOKHAVEN FSD SYSTEM FOR THE ANALYSIS OF BUBBLE CHAMBER FILM. Hough, Paul V. C. (Brookhaven National Lab., Upton, N. Y.). [1963]. Contract AT-30-2-GEN-16. 7p. (CONF-651044-4). Dep. mn; CFSTI $1.00 cy, $0.50 mn.

From Conference on Programming for Flying Spot Devices, New York.

The operation of the Brookhaven flying-spot digitizer system for the analysis of bubble-chamber photographs is outlined. The advantages of the system are discussed. The discussion is restricted to the case of road-guidance. (T.F.H.)

14851 (BNL-9980) A PARAMETRIC RADIATION DETECTOR PREAMPLIFIER. Radeka, V.; Chase, R. L. (Brookhaven National Lab., Upton, N. Y.). [nd]. Contract AT-30-2-GEN-16. 21p. (CONF-660304-2). Dep. mn. CFSTI $1.00 cy, $0.50 mn.

From Institute of Electrical and Electronics Engineers, Scintillation and Semiconductor Counter Symposium, Washington, D. C.

A charge-sensitive preamplifier is described, in which a pair of varactor diodes is used in a parametric configuration as the first amplifying element. (D.C.W.)

14852 (CEA-R-2862) DETECTION DES FRAGMENTS DE FISSION PAR EMISSION SECONDAIRE. (Detection of Fission Fragments by Secondary Emission). Audias, Arlette (Commissariat a l'Energie Atomique, Saclay (France). Centre d'Etudes Nucleaires). Oct. 1965. 140p. Dep. mn.

A fission fragment detecting apparatus based on the principle that fragments traversing a thin foil will cause emission of secondary electrons was investigated. The electrons are then accelerated (10 kev) and directly detected by means of a plastic scintillator and associated photomultiplier. The theoretical aspects and construction details of the apparatus are included. (M.O.W.)

14853 (CNEA-159) DETECTOR PARA CELDA DE REPROCESAMIENTO. (Detector for Reprocessing Cells). Picard, Horacio; Costigliolo, Furio (Comision Nacional de Energia Atomica, Buenos Aires (Argentina)). 1965. 16p. Dep. mn.

A detector consisting of three miniature G-M tubes is used in the described processing cell alarm system. System performance and detector operation and adjustment are described. (J.S.R.)

14854 (CONF-660304-3) NEUTRON MEASUREMENT BY TRACK IMAGING IN INSULATING MATERIALS. Schultz, Warner W. (Knolls Atomic Power Lab., Schenectady, N. Y.). [nd]. Contract W-31-109-eng-52. 32p. Dep. mn. CFSTI $2.00 cy, $0.50 mn.

From Institute of Electrical and Electronics Engineers, Scintillation and Semiconductor Counter Symposium, Washington, D. C.

The imaging of the tracks of heavy charged particles, particularly those from neutron reactions, is discussed. An application of the technique to the determination of the homogeneity of nuclear fuel is outlined. (D.C.W.)

14855 (JAERI-1090) CENTRALIZED FIELD RADIOLOGICAL MONITORING SYSTEM AT NUCLEAR INSTALLATION. Ishihara, Toyohide (Japan Atomic Energy Research Inst., Tokyo). June 1965. 46p. (In Japanese). Dep. mn.

In the normal operations, radioactive gases and liquids are released from nuclear installations, considering the environmental conditions in the dispersion and dilution of the radioactive substances. There is also the possibility that the populace around are exposed to the radiation at the time of an accident of such nuclear installations. In both cases of the above, the field radiological monitorings are required. The evaluation of the reactor hazards shows that, in the case of major accidents, adequate procedures must be taken within a few hours of the accident in order to minimize the radiation exposures. In this connection, it is desirable to maintain an effective radiological monitoring system, which detects the unusual conditions of radioactivity and permits the adequate steps of radiation control, thus minimizing the radiation hazard from the accident and also compensating for the unfavorable site conditions. Included are the requirements of such field monitoring, theoretical analysis of the monitoring system used when the radioactive substances are released into the atmosphere, detailed design of the system, and the development of the centralized field monitoring system and required equipment. (auth)

14856 (KFK-345) DER AUFBAU UND DIE EIGENSCHAFTEN EINES ANALYSATORS ZUR MESSUNG DER NEUTRONENPOLARISATION. (The Construction and Properties of Analyzer for Measurement of Neutron Polarization). Staudenmaier, H.-M. (Kernforschungszentrum, Karlsruhe (West Germany). Institut fuer Experimentelle Kernphysik). July 1965. 28p. Dep. mn.

A neutron analyzer is described which possesses the advantages of the Levintov analyzers but can be used in a broad energy distribution range. The physical principles of the instrument are described and its construction is given. Measurements made with α particles and neutrons are reported. (J.S.R.)

14857 (NP-15448) IONIZATSIONNYI SPEKTROMETR AL'FA-IZLUCHENIYA TIPA 9014-01 I EGO PRIMENENIE DLYA IZMERENIYA MALYKH KONTSENTRATSII AEROZOLEI AL'FA-AKTIVNYKH IZOTOPOV. (Type 9014-01 Alpha-Radiation Ionization Spectrometer and its Uses for Measuring Small Concentrations of Aerosols of Alpha-Active Isotopes). Report No. 1. Bolotin, V. F.; Chutkin, O. A. (Gosudarstvennyi Komitet po Ispol'zovaniyu Atomnoi Energii SSSR, Moscow. Soyuznyi Nauchno-Issledovatel'skii Institut Priborostroeniya). 1965. 11p. Dep. mn.

The design and construction of the spectrometer, consisting of a pulse ionization chamber with preamplifier and a framework containing the electronic units, pump, and manometer, are described. The use of the apparatus for carrying out fast measurements of small concentrations of aerosols of long-lived alpha emitters is discussed. The apparatus also permits careful radiometric analyses of alpha-active solutions and dry materials to be performed. (M.J.T.)

14858 (NYO–3246-5) STUDY OF SURFACE CONTOURING AS APPLIED TO SEMICONDUCTOR RADIATION DETECTORS. Semiannual Report, January 1965–June 1965. (General Electric Co., Philadelphia, Pa. Missile and Space Div.). July 1965. Contract AT(30-1)-3246. 36p. Dep. mn. CFSTI $3.00 cy, $0.50 mn.

The application of geometrical surface field control (termed "surface contouring") to semiconductor p-n junctions of use in radiation detection and spectroscopy was investigated. Efforts during this period have dwelled on the junctions themselves with particular emphasis on study of the window or energy defect at the particle entrance face. This would seem to be of importance in realizing the potential for very low energy particle detection. Other experimentation was in the areas of attempts to arrive at the inherent speed or pulse risetime of the structures and measurements of uniformity of amplification laterally across the junction. Additional effort went into the development of a stable, low resistance base (n-type) junction contact. In this regard, a gold-antimony alloy contact applied by the thermal compression method was found to work well. (M.O.W.)

14859 (ORNL-TM–1390) CHARGE-SENSITIVE PREAMPLIFIER, ORNL MODEL RC11-4-2X. DeLorenzo, J. T. (Oak Ridge National Lab., Tenn.). Dec. 14, 1965. Contract W-7405-eng-26. 9p. Dep. mn. CFSTI $1.00 cy, $0.50 mn.

The Charge-Sensitive Preamplifier, ORNL model RC11-4-2X, was designed to amplify pulses from a Reuter-Stokes BF_3 detector (RSN 42A). The pre-amplifier output drives a Pulse Amplifier and Count-Rate Meter module, ORNL model Q-2614. The preamplifier and acceptance test procedures are described. (auth)

14860 (RT/FI(65)33) SOPRA UN METODO PER LA DETERMINAZIONE DELLO SPETTRO DEI NEUTRONI INTERMEDI IN UN REATTORE. (Method for the Determination of Intermediate Neutron Spectrum in a Reactor). Pozzo, S. (Comitato Nazionale per l'Energia Nucleare, Rome (Italy)). Sept. 1965. 28p. Dep. mn.

A simple method using activation detectors and gamma spectrometry is suggested for intermediate neutron-spectrum determination in reactors. By an IBM 7090 program, diagrams are obtained by which activation measurements can be interpreted as measurements of parameters that characterize the intermediate neutron spectrum. (auth)

14861 (UCRL–16555) SPIRAL READER CONTROL AND DATA ACQUISITION WITH PDP-4. Stedman, Jon D. (Lawrence Radiation Lab., Univ. of California, Berkeley). Nov. 29, 1965. Contract W-7405-eng-48. 30p. (CONF-651130–2). Dep. mn. CFSTI $2.00 cy, $0.50 mn.

From DECUS Symposium, Stanford, Calif.

A semi-automatic, film digitizing machine that is used to measure photographs of interactions in a hydrogen bubble chamber is described, together with the on-line use of a PDP-4 computer to control the machine and to convert and display data. (D.C.W.)

14862 EXPERIMENTS IN THE DEVELOPMENT OF A NEUTRON DOSIMETER. Tschirf, E. (Oesterreichische Hochschule, Vienna). Acta Phys. Austr., 20: 63-70(1965). (In German).

Experiments made in the development of activation dosimeters are reported. The principle of the activation dosimeter is given and the selection of the material and shape of the partial flux detectors are described. A dosimeter for thermal and epithermal neutrons and a warning dosimeter developed for the measurement of a partial flux are described. (J.S.R.)

14863 COUNTING OF NEUTRONS AT SMALL COUNTING RATES: ELIMINATION OF THE γ BACKGROUND AND ELECTRONIC DISTURBANCES. May, F.; Semturs, F. (Oesterreichische Studiengesellschaft fuer Atomenergie, Siebersdorf, Austria). Acta Phys. Austr., 20: 155-9(1965). (In German).

In the use of BF_3 counters as detectors, the γ background can be eliminated by simple amplitude discrimination. High counting voltages and bad ground connections can, however, lead to significant disturbances in the counting system. A preamplifier is described which is constructed especially to be disturbance-free and which permits the counting of very small pulse rates at small pulse levels (0.2 to 0.3 mv at the counter output). (tr-auth)

14864 RADIATION TRANSMITTER. Beck, Juergen; Leiter, Edgar; Nottelmann, Werner. A E G Mitt., 55: 512-23(1965). (In German).

The multiplicity of measurement problems occurring in radiation monitoring requires installations so constructed that suitable devices can be assembled from individual building components for special application purposes. A system of radiation monitoring installations is described, which is constructed on the pulse basis with pulse detectors and on the direct current basis with ionization chambers. The electronic constituents with which the installations corresponding to particular requirements can be constructed are discussed. A typical installation for a nuclear power plant is described. (tr-auth)

14865 ANTICOINCIDENCE SPECTROMETERS FOR NUCLEAR REACTION STUDIES. Arnell, S. E.; Hasselgren, A. (Chalmers Univ. of Tech., Goeteborg). Arkiv Fys., 30: 397-409(1965).

An anticoincidence spectrometer was constructed, in which the main detector consists of a 5 in. diameter by 6 in. long NaI crystal enveloped by a large cylinder of NE 102A plastic scintillator. The intended use of the spectrometer is to simplify the response of the NaI crystal to high energy gamma radiation resulting from nuclear capture reactions without greatly reducing the detector efficiency. The behavior of the arrangement was tested with some (p,γ) reactions. The other type of anticoincidence spectrometer consists of a 2 mm thick Ge(Li) detector surrounded by the plastic scintillator. The intended use of this arrangement is to simplify the response of the Ge(Li) detector to low energy gammas by reducing the Compton distribution. The arrangement was tested with radioactive sources. (auth)

14866 PORTABLE BETA-GAMMA HAND AND SHOE MONITOR. Hardison, H. V. (E. I. du Pont de Nemours and Co., Aiken, S. C.). Health Phys., 11: 314-16(Apr. 1965). (TID–20987).

A portable beta-gamma hand and shoe monitor was built to supplement the conventional scalar monitors used in permanent locations. This instrument can simultaneously monitor for contamination on both palm and back hand surfaces and on shoes, and will indicate alarm-level detection by buzzer and lights. The prototype provides five-second monitoring in an instrument that may be carried by one person, set up in a small space, and operated immediately and continuously after relocation without adjustment or other service. (J.F.P.)

14867 NEUTRON FLUX MEASUREMENTS WITH COBALT. Eastwood, T. A. (Atomic Energy of Canada Ltd., Chalk River, Ont). Int. J. Appl. Radiat. Isotop., 17: 17-28(Jan. 1966).

A method for accurately measuring the neutron flux in reactor experiments on a routine basis is summarized. Cobalt or cobalt-aluminum alloy wire monitors were prepared with a wire cutting device. After irradiation, the ^{60}Co activity in each was measured with an ionization chamber or well-type NaI crystal scintillation counter. Correction factors for neutron self-shielding, γ self-absorption in the ^{60}Co measurement, and for neutron leakage through cadmium in cadmium ratio measurements are presented graphically. The results, with appropriate corrections, were interpreted using the Westcott convention to give the thermal neutron flux and the epithermal index, a measure of epithermal flux related to the cadmium ratio. Sources of experimental error and uncertainties in the input data are reviewed and it was concluded that the method is accurate to a few percent. The accuracy will improve as more accurate input data become available. (auth)

14868 DEFLECTING PROPERTIES AND DISPERSION OF AN ELECTROSTATIC PRISM SPECTROMETER. Bobykin, B. V.; Kel'man, V. M.; Mednikova, L. S. (Nuclear Physics Inst., Academy of Sciences, Kazakh SSR). Izv. Akad. Nauk SSSR, Ser. Fiz., 29: 808-14(May 1965). (In Russian).

Calculations concerning a previously proposed electrostatic prism spectrometer are presented. Formulas are derived for the dispersion, the deviation, and the condition for minimum deviation with relativistic effects taken into account. Families of curves relating certain of the parameters are presented to facilitate preliminary design calculations. At nonrelativistic energies the dispersion Edx/dE (E is the particle energy and x is the image position) becomes infinite for certain parameter values, and dispersions of several meters can be realized without difficulty. At relativistic energies it is advantageous to design the prism so that the electrons are decelerated rather than accelerated in it. (ATD)

14869 ON THE PROBLEM OF ANALYZING SPECTRA OF γ QUANTA AND FAST NEUTRONS MEASURED BY MEANS OF SINGLE-CRYSTAL SCINTILLATION SPECTROMETERS. Tikhonov, A. N.; Arsenin, V. Ya.; Vladimirov, L. A.; Doroshenko, G. G.; Dumova, A. A. Izv. Akad. Nauk SSSR, Ser. Fiz., 29: 815-18(May 1965). (In Russian).

Methods are discussed for treating the spectra recorded with high-efficiency single-crystal fast-neutron and gamma scintillation spectrometers, in which the recorded line shape differs substantially from the δ shape. An integral Fredholm equation of the first order is given, expressing the measured spectrum in terms of the unknown spectrum and a kernel characterizing the line shape of the spectrometer. Results of previous measurements of the spectrum from a Po-Be neutron source, using a single-crystal scintillation spectrometer, are restored by the method of regularization using rectangular, triangular, and nearly rectangular kernels. The original spectrum and the results from the restorations are compared with a previous restoration by the matrix method and previous measurements using photographic plates. (M.J.T.)

14870 A PRACTICAL COMPARISON BETWEEN NITROUS OXIDE DOSIMETRY AND FRICKE DOSIMETRY FOR THE ESTIMATION OF γ-RAY ENERGY ABSORBED IN GASEOUS MEDIA. Furukawa, Kiyoshi; Shida, Shoji (Japan Atomic Energy Research Inst., Tokyo). J. Nucl. Sci. Technol. (Tokyo), 3: 41-2(Jan. 1966).

A comparison was made between Fricke and nitrons oxide dosimetry by measuring the dose rate of ^{60}Co gamma rays in three types of irradiation cells. One of the cells was a cylindrical vessel 21 cm long and with a 5 cm OD, while the other two cells were packed with sections of tubular glass of 10- and 6-m OD, respectively. Fricke dosimetry gave almost the same dose rates with the three different types of cells. In N_2O dosimetry the yields of nitrogen plus oxygen were reduced to almost $^3/_4$ by the presence of the glass packing material. Variations in pressure also reduced the yields. (M.C.G.)

14871 DEVICE FOR MEASURING CONTINUOUSLY THE ALPHA ACTIVITY OF FLOWING SOLUTIONS. Markl-Musyl, I.; Bobleter, O.; Grass, F. (Oesterreichische Hochschule, Vienna. Univ., Vienna). Kerntechnik, 8: 120-1(Mar. 1966). (In German).

Modification of a methane gas flow counter for continuous measurement of α activity of flowing solutions is described. With the device ^{233}U at a concentration of 3 μg/ml could be detected. (J.S.R.)

14872 UNIVERSAL LABORATORY MONITOR MODEL MSP-2. Kunicki, Adam; Scharf, Waldemar. Nukleonika, 10: 463-8(1965). (In Polish).

The monitor system, designed mostly for measurement of low-level and medium-level contamination of laboratory table tops and floors, consists of a portable counting-control and power supply-chassis with provisions for attaching three different types of probes. For hard beta and for gamma radiation, 3 G-M counters with a wall thickness of 45 mg/cm^2 and a total area of 72 cm^2 are used. For alpha-radiation, a ZnS (Ag) scintillator with a 1.1 mg/cm^2 "Melinex" window and an area of 100 cm^2 is used. It is 20% efficient for a ^{239}Pu source over a solid angle of 2π. For soft beta radiation, G-M counters with 2- and 4-mg/cm^2 mica windows and a sensitive area of 14 cm^2 are used. The counting circuitry employs a count-rate meter designed for three ranges of count-rate; 15 to 600, 150 to 6000, and 1500 to 60,000 counts per minute. Straightforward counting is possible with the use of mechanical scalars having a maximum counting speed of 50/sec and a maximum storage capacity of about 10^4 counts. The count-rate meter has a pulse-forming network in which a univibrator is turned on by a random event (count) and turned off by a multivibrator pulse running at a fixed frequency, N_0. The resultant average current measured by an ammeter gives a (nonlinear) measure of the count rate with the use of a calibrated scale. The accuracy of this scale is about 10% for count rates N of 0.2 to 10 times N_0. (TTT)

14873 A LOW-BACKGROUND BETA SCINTILLATION COUNTING WITHOUT SHIELDING. Dimczew, Todor (Instytut Fizyki Bulgarskiej Akademii Nauk, Sofia). Nukleonika, 10: 585-94(1965). (In Polish).

The spectrum analysis of the beta background for a thin plastic scintillation counter is presented. The background spectrum was measured with an old lead shield and without it. The possibility of the application of the scintillation counter for low-level beta counting without the lead shield is discussed. A plastic scintillator, 13.5 mg/cm^2 thick and a photomultiplier were used as a detector. The apparatus allows measurement of low-level beta background in the laboratory as well as under field conditions. (auth)

14874 SOME SPECTROMETER PROPERTIES OF COUNTER WITH THIN PLASTIC PHOSPHOR USED FOR MEASURING β-PARTICLES OF $^{90}Sr + ^{90}Y$. Dimczew, Todor (Instytut Fizyki Bulgarskiej Akademii Nauk, Sofia). Nukleonika, 10: 595-604(1965). (In Polish).

The differential spectrum $^{90}Sr + ^{90}Y$ obtained by means of a plastic beta scintillator are shown. The thickness of the scintillator was 13.5 mg/cm^2; the parameters of the counter included voltage of the photomultiplier, gain of the preamplifier, and thickness of the scintillator. The purpose of measurement was to establish the best conditions for using very thin plastic scintillators as a counter for $^{90}Sr + ^{90}Y$ detection. (auth)

14875 SEMICONDUCTOR P-N JUNCTION DETECTOR FOR NUCLEAR RADIATION AS ELECTRIC SIGNAL SOURCE. Szawlowski, Marek (Univ., Warsaw). Nukleonika, 10: 613-18(1965). (In Polish).

An equation describing the voltage pulse, arising at the preamplifier input, for a p-n junction detector from an equivalent circuit was derived. The analysis may be used for detector preamplifier system optimization, when high resolution of energy is involved. (auth)

14876 DETECTING PROBES OPERATING IN A SINGLE-CABLE SYSTEM OF PULSE TRANSMISSION AND POWER SUPPLY. Dabek, Tadeusz (Biuro Urzadzen Techniki Jadrowej, Krakow); Korbel, Kazimierz. Nukleonika, 10: 619-22(1965). (In Polish).

The problem of pulse transmission from nuclear detectors for long distances by means of a single cable supplying the high voltage to the counter is considered. Many circuits discussed in the literature are described as well as two types of probes (with scintillation and proportional counters) operating in a single-cable system of pulse transmission and power supply. This system is advantageous for use under field-conditions, especially in a bore hole logging. (auth)

14877 ESTIMATION OF THE MAXIMAL CONCENTRATION OF THORIUM AND URANIUM WHICH CAN BE INTRODUCED INTO NUCLEAR EMULSION. Benisz, Jerzy; Orkisz, Zuzanna (Higher Pedagogical Coll., Katowice, Poland). Nukleonika, 10: 623-5(1965).

The maximum quantity of uranium and thorium that may be introduced into a nuclear emulsion was estimated. The maximum was found at 9% for $UO(NO_3)_2 \times 6H_2$ and at 6% for $ThCl_4 \cdot 4H_2O$. (M.C.G.)

14878 METHOD FOR SIMULTANEOUS COUNTING OF SOURCE AND BACKGROUND FOR SHORT-LIVED RADIOISOTOPES NEAR THE DETERMINATION LIMIT. Sterlinski, Slawomir (Inst. of Nuclear Research, Warsaw). Nukleonika, 10: 641-59(1965).

The problem of simultaneously counting source and background radiations, when determining trace amounts of short-lived radioisotopes by gamma scintillation spectrometry, is discussed. In the case of time-consuming measurements (of the order of hours) the evaluation of the background on the basis of its counting in another time interval may prove to be false, because of daily fluctuations. The error due to this may be in many cases eliminated by estimating background under a given photoelectric peak on the basis of the number of counts measured within another energy range of the spectrum. A method of estimating background within a measuring range is presented, the variance of the estimation is calculated, and a condition is pointed out under which the optimum (the minimum) relative accuracy is attained. (auth)

14879 PROPORTIONAL COUNTER AS A SPECTROMETER FOR LOW-ENERGY γ AND β RAYS. Kownacki, Jan; Marcinkowski, Andrzej (Inst. of Nuclear Research, Warsaw). Nukleonika, 10: 669-73(1965).

A proportional counter for nuclear spectroscopy was built. The counter will be used for the investigations of low energy γ and β radiation and particularly for the measurements of x radiation accompanying electron capture and isomeric transition. The energy resolution of the counter is 10.5% for x radiation of 22.2 kev from the ^{109}Ag nucleus. (auth)

14880 FAST MULTIPLE COINCIDENCE CIRCUIT USING AVALANCHE TRANSISTORS. Kalisz, Jozef (Inst. of Nuclear Research, Warsaw). Nukleonika, 10: 681-92(1965).

A simple and reliable coincidence circuit using transistors working in the avalanche mode is described. Using 56 AVP photomultiplier, NE 102 plastic scintillator, and a ^{210}Po α source, the minimum resolving time is 0.7 ns with 80% efficiency and maximum 15 ns with 100% efficiency. Both the number of coincidence channels and the resolving time of the circuit can be selected independently. (auth)

14881 SCINTILLATION CELL FOR THE DETERMINATION OF ^{222}Rn. Kostyrko, Andrzej; Jaworowski, Zbigniew (Inst. of Nuclear Research, Warsaw). Nukleonika, 10: 738(1965).

A method was developed for preparing scintillation cells, which consists of dry deposition of Zn(Ag) phosphors on wetted inner surfaces of methyl-polymethacrylate plates, and fixation by the action of chloroform vapors. The parameters of the cells show the possibility of efficient determination of ^{222}Rn in samples containing less than one picocurie. (L.B.S.)

14882 ANALYSIS OF BETA SPECTRA BY MEASUREMENTS IN CROSSED ELECTRIC AND MAGNETIC FIELDS. Bosi, G. (Univ., Rome). Nuovo Cimento, (10), 41B: 225-38(Feb. 11, 1966). (In Italian).

An investigation is carried out about crossed magnetic and electric fields. Axially symmetric fields are considered and their optical performances are discussed when applied to mass and β-ray spectroscopy. In the latter case facilities of cancelling any first-order term in the image spread are underlined. Chances of cancelling several second-order terms are also investigated. (auth)

14883 NEUTRON FLUX AND ENERGY MEASUREMENTS. Dennis, J. A. (Atomic Energy Research Establishment, Harwell, Eng.). Phys. Med. Biol., 11: 1-14 (Jan. 1966). (AERE-R-4831).

The problem of neutron energy measurement is considered in the energy ranges, thermal (<0.5 ev), intermediate (0.5 ev–10 kev), fast (10 kev–15 Mev) and relativistic (>15 Mev), together with the general problem of neutron flux measurement. Sensitivities and resolutions obtainable are given for a variety of methods. It is concluded that for thermal and intermediate energy measurements in radiological applications it is best to use BF^3 counters, fission chambers, moderated detectors, together with gold or manganese foils, in conjunction with the Westcott flux convention; at higher energies methods based on proton recoil detectors are preferred for high sensitivity and accuracy, while threshold detectors are suggested if multichannel pulse-height analyzers and computers are not available, or if there is a limitation on the size of the detectors. (auth)

14884 THE SATURATION CURVE IN CYLINDRICAL AND SPHERICAL IONIZATION CHAMBERS. Sprinkle, Ellen A.; Tate, P. A. (Defence Chemical Bilogical and Radiation Labs., Ottawa). Phys. Med. Biol., 11: 31-46(Jan. 1966).

Uniformly irradiated ionization chambers bounded by coaxial cylinders and concentric spheres were studied. The effects of recombination and space charge, but not diffusion, were considered. Approximate expressions were derived for the general saturation curves, valid at degrees of saturation $i/i_s < 0.6$. Exact numerical results in the range $0.25 < i/i_s < 0.6$ were obtained for air-filled chambers using a computer and confirm the validity of these expressions. Experimental work with practical chambers showed good agreement with theory when values of mobilities and recombination coefficient were used which are not far from those commonly accepted for air. (auth)

14885 A COINCIDENT GAMMA-RAY SPECTROMETER AND ITS APPLICATION TO MEASUREMENTS OF LOW-LEVEL RADIOACTIVITY. Overton, T. R.; Burch, P. R. J. (Univ. of Leeds, Eng.). Phys. Med. Biol., 11: 47-61(Jan. 1966).

The construction and performance of a coincidence–anticoincidence low-level gamma-ray spectrometer is described. The radioactive source (in a sealed, cylindrical, stainless steel container) fits into the well of a large plastic scintillator; a NaI(Tl) crystal (6 in. diameter × 4 in.) rests on top of the source inside the well. Electrical pulses from the photomultiplier of the crystal unit are routed via a coincidence–anticoincidence circuit to a multichannel analyzer. Only those pulses are analyzed that are in coincidence–anticoincidence with selected pulses from the plastic scintillator. The flexibility of the system permits optimum discrimination in favor of, or against, particular radionuclides. In measurements of natural radioactivity, potassium and the uranium and thorium series can be separately assayed even at very low levels. Background, calibration and sensitivity data are given, together with the results of measurements of soil samples and cremated human remains. (auth)

14886 THE RESPONSE OF P-I-N JUNCTIONS TO BETA RAYS. II. COUNT RATE VERSUS SURFACE ABSORBED DOSE RATE FOR ^{32}P AND ^{204}Tl. Baily, N. A.; Hilbert, J. W. (Hughes Research Labs., Malibu, Calif.). Phys. Med. Biol., 11: 75-81(Jan. 1966).

The use of lithium-drifted silicon p-i-n junctions as pulse counters for β dosimetry was investigated using the β particles emitted by ^{32}P and ^{204}Tl. The counting rate is directly compared with the surface absorbed dose rate as measured at the polystyrene electrode of a thin window extrapolation chamber. The rate of change of the detector response is compared with the rate of change of absorbed dose rate as a function of source-to-detector distance, source geometry and detector area. It was found that the ratio of these quantities remains constant after a certain minimum source-to-detector distance is achieved. In all cases investigated this distance did not exceed 10 cm. The absolute sensitivity of these devices is such that dose rates as low as 0.1 mrad/hr can be measured. (auth)

14887 ENERGY DEPENDENCE OF LITHIUM FLUORIDE DOSEMETERS AND HIGH ELECTRON ENERGIES. Pinkerton, Arthur P. (Sloan-Kettering Inst., New York); Holt, J. Garrett; Laughlin, John S. Phys. Med. Biol., 11: 129-30(Jan. 1966).

A comparison is made of the response of LiF thermoluminescent detectors to ^{137}Cs and ^{60}Co gamma rays, 6- to 8-Mev electron beams, and 22-Mev x rays. (L.B.S.)

14888 ENERGY DEPENDENCE OF LITHIUM FLUORIDE DOSEMETERS AT HIGH ENERGIES. Crosby, E. H.; Almond, P. R.; Shalek, R. J. (Univ. of Texas, Houston). Phys. Med. Biol., 11: 131-2(Jan. 1966).

A comparison was made of the thermoluminescent response per rad of LiF phosphors to ^{60}Co γ radiation and 10 and 15 Mev electrons. The results obtained at a dose of 200 rads were found not to be significantly different from one another. Additional glow curves obtained as a function of temperature also showed no qualitative difference. (L.B.S.)

14889 A SUPPLEMENT TO CONFIDENCE TEST OF RADIATION COUNTER BY STATISTICAL METHOD NUMERICAL CALCULATION OF NON-CENTRAL χ^2 DISTRIBUTION. Koyanagi, Takami (Niigata Univ., Nagaoka, Japan). Radioisotopes (Tokyo), 15: 1-3(1966). (In Japanese).

In a previous paper (Radioisotopes, 14: 279-85(1965)) under the title "Confidence Test of Radiation Counter by Statistical Method," the result of the power curves of the confidence test calculated by means of the Patnaik's approximation was reported. Later it was found that the probability density function of the non-central χ^2 distribution can be represented by hyperbolic function in the case that the degree of freedom is unity. Namely, the probability density function is represented as follows:

$$y = \frac{1}{2} e^{-(\gamma+x)/2} \left(\frac{x}{2}\right)^{n/2-1} \sum_{k=0}^{\infty} \frac{\left(\frac{\gamma x}{4}\right)^k}{k!\ \Gamma_{(n/2+k)}}$$

where γ = non-centrality; n = degree of freedom. In this case n = 1, and since $\Gamma_{(\frac{1}{2}+k)} = (2k)!\ \sqrt{\pi}/2^{2k}\ k!$ the equation becomes: $y = (1/2\ \sqrt{\pi})\ e^{-(\gamma+x)/2}\ (x/2)^{-\frac{1}{2}} \cosh(\sqrt{\gamma x})$. By means of this equation and by the aid of digital computer, the probability density curves and power curves of the confidence test are calculated and depicted. (auth)

14890 ON THE STATISTICS OF SCALED PULSES. Nistor, C.; Andreescu, M.; Rusu, M. (Univ. of Bucharest). Rev. Roum. Phys., 10: 723-31(1965).

It is shown that the average number of pulses recorded after a K-fold scaling when the scaling remainders are not cancelled is always equal to 1/K of the mean value of the number of the non-scaled pulses; in the case of Poisson distribution, the ratio of the corresponding standard errors is computed. These results may be useful in operations with multichannel analyzers in which time-modulated impulses are analyzed, and in the case of successive recordings of impulse groups by means of automatic instruments. (auth)

14891 METHOD FOR MEASUREMENT OF IONIZATION CURVES BY MEANS OF SCINTILLATION COUNTERS. Tisljar-Lentulis, G. M. (Brookhaven National Lab., Upton, N. Y.). Rev. Sci. Instrum., 37: 291-3(Mar. 1966). (BNL-9582).

A technique is described for measuring the Bragg ionization curve of a certain kind of particle in the presence of a disturbing beam contamination. The pulses of the undesired particles are eliminated electronically by the applied counter telescope. The ionization values are gained from the pulse height spectra which the beam produces in a NaI (Tl) scintillator. The pulse train of the multichannel analyzer used and a program written in FORTRAN II supply the data for the ionization curve. Measurements with 150 Mev protons are compared with curves in the literature. (auth)

14892 DESIGN CALCULATIONS FOR IONIZATION SPECTROMETERS: CASCADE DEVELOPMENT. Pinkau, Klaus; Thomson, Karl V. (Louisiana State Univ., Baton Rouge). Rev. Sci. Instrum., 37: 302-8(Mar. 1966).

The total number of electrons was calculated as a function of depth in air, glass, and iron absorbers. The nuclear interactions were described by the model of Cocconi, Koester, and Perkins. The results were used in the design of ionization spectrometers for the measurement of the total energy of ultrahigh-energy particles. In particular, a correlation is established between the maximum number of electrons and the primary energy. Also, the amount of energy lost from ionization spectrometers due to limited depth can be derived from the results. (auth)

14893 OPTICAL REFLECTORS FOR USE IN INTERNAL SAMPLE AQUEOUS CHERENKOV COUNTERS. Strindehag, Ove M. (Aktiebolaget Atomenergi, Studsvik, Sweden). Rev. Sci. Instrum., 37: 344-9(Mar. 1966).

Properties such as reflectance, deterioration in water, and deposition of activities are investigated for several types of optical reflectors. Reflectance values for both visible and ultraviolet light are included and the deterioration tests extend up to water temperatures of 150°C. The influence of reflector properties on detector efficiency is also studied. (auth)

14894 ON THE MEASUREMENT OF STANDARD ION DOSES IN SOLID AND FLUID MEDIA IN THE CASE OF X AND GAMMA RADIATION WITH ENERGIES BETWEEN 50 kev AND 3 Mev. PART I. ERRORS IN THE MEASUREMENT OF STANDARD ION DOSES IN PHANTOMS WITH DIFFERENT COMMERCIALLY PREPARED IONIZATION CHAMBERS. Will, Wolfram; Rakow, Adalbert (Medizinisch-Biologische Forschungszentrum, Deutsche Akademie der Wissenschaften, Berlin). Strahlentherapie, 128: 532-48(Dec. 1965). (In German).

In general, the standard ion dose, measured with ionization chambers, is multiplied with a certain factor in order to determine the absorbed dose. The technique usually used for measuring the standard ion dose in solid or liquid media applies ionization chambers calibrated in air. Due to different radiation-physical conditions in the chamber environment, incorrect results can be obtained in this way. These results influence directly numerous quantitative investigations in radiation effect and radiotherapeutic studies. Testing the depth dose curves in water phantoms with 14 different ionization chambers for 4 radiation qualities between 120-kv x rays and ^{60}Co γ rays, maximum deviations of about 40% were found. Reasons for these deviations are discussed. (tr-auth)

14895 THE LIGHT YIELD OF PLASTIC SCINTILLATOR NE 102A FOR ELECTRONS OF 3 TO 11 kev. Pleitz, Wolfgang (Univ., Goettingen, Ger.). Z. Phys., 190: 446-54(1966). (In German).

The light yield of the plastic scintillator NE 102A for electrons was measured as a function of electron energy between 3 and 11 kev and scintillator thickness between 0.1 and 50 mm. The scintillation response is a linear function of the electron energy down to energies of 4 to 8 kev, these values depending on the scintillator thickness. The light yield of thin scintillation sheets for low energies was observed to be considerably larger than for thicker sheets. Two possible explanations are discussed. (auth)

14896 INVESTIGATION OF THE ABSOLUTE ACTIVITY MEASUREMENT OF WEAKLY RADIOACTIVE PREPARATIONS USING A DIFFUSION CHAMBER. Sobczynski, Zbigniew; Kolankowski, Stanislaw; Kaminska, Urszula; Kaczor, Krystyna (Zaklad Fizyki Doswiadczalnej Wyzszej Szkoly Pedagogicznej, Gdansk, Poland). Zesz. Nauk. Wyzszej Szkoly Pedagog. Gdansku, Mat., Fiz., Chem., 3: 33-4(1963). (In Polish).

A simple diffusion chamber was developed for absolute activity measurements on ^{210}Pb. With the help of this diffusion chanber a value of 0.46×10^{-6} μC was obtained, whereas measurements with a scintillation counter gave a value of 0.48×10^{-3} μC. (tr-auth)

14897 CALCULATION OF GAMMA RAY SCINTILLATION DETECTOR EFFICIENCIES AND PHOTOFRACTIONS BY MONTE CARLO METHODS [Thesis]. Snyder, Bernard Joseph. Ann Arbor, Univ. of Michigan, 1965. 242p.

The efficiency for detection of gamma rays by scintillation crystals was determined. Calculated results are obtained for both absolute peak and absolute total efficiencies as well as photofractions of gamma-ray scintillation crystals. The absolute peak efficiency is defined as the probability for total absorption in the crystal of gamma rays from the source and is written as the product of two terms. The absolute total efficiency, the probability for

source gammas to interact at least once in the crystal, is determined by numerical integration of analytical expressions for various isotropic source geometries. The photofraction, the fraction of incident gamma rays that are totally absorbed in the crystal, is determined by Monte Carlo simulation of the transport and generation of particles throughout the crystal. The Monte Carlo calculations consider gamma interactions by photoelectric, Compton scattering, or pair production events. Subsequent electron and bremsstrahlung generation are included in the simulation procedure. Two crystal geometries are considered: solid cylinders and cylinders with a coaxial cylindrical well. Calculated absolute total efficiency and photofraction values are tabulated for commonly used sodium iodide crystal sizes, with a limited amount of data given for cesium iodide and calcium iodide crystals. The present calculations include a more rigorous treatment of secondary electrons and bremsstrahlung than used in previous analyses. Calculations were also made for the widely used well-type crystal geometry. (Dissertation Abstr.)

14898 SCANNING PROJECTOR 5 (Engineering Materials). (Lawrence Radiation Lab., Univ. of California, Berkeley). (CAPE–1060).

332 drawings.

The scanning and measuring projector (SMP) is used to perform rapid measurements of interactions and decays of elementary particles that take place in the 72-in. liquid H bubble chamber. An on-line computer swiftly processes large quantities of data. The speed of the computer makes it possible to evaluate the tracks as they are measured. An unacceptable track measurement is immediately rejected and is then remeasured. An IBM typewriter is used for communication with the computer. Modern data processing equipment used with the SMP is easy to operate and simple to maintain. Several sizes of film may be used including 35, 46, and 70 mm. Film is advanced by a d-c servo system driving a capstan. Operator control is through a "joystick." (For details, see TID-4100). (M.C.G.)

14899 VERSATILE SCALER AND READ-OUT SYSTEM (Engineering Materials). (Lawrence Radiation Lab., Univ. of California, Berkeley). (CAPE–1263).

308 drawings.

The scaler system has facilities for visual, typewritten, and computer-oriented readout. The system can operate with any number of scalers and is particularly useful for experiments where automatic counting and recording of large amounts of data are required. The scalers in a single chassis may be used separately with manual control. Each scaler chassis contains two six-decade scalers capable of counting at rates up to 10 Mc. Visual readout is provided by six Nixie tubes. The scaler has a dead time per count of less than 100 nsec. The readout system normally controls a paper-tape punch at 60 characters per sec or a typewriter at 15 characters per sec, but magnetic-tape output can also be used. Planar silocon transistors and diodes are used exclusively in the scaler and readout. (For details, see TID-4100). (M.J.T.)

14900 NEUTRON SCINTILLATION DETECTOR /Q-2230/ (Engineering Materials). (Oak Ridge National Lab., Tenn.). (CAPE–1282).

1 drawing.

This neutron detector employs a stilbene crystal, $1\frac{5}{8}$ in. in diam. and $\frac{1}{2}$ in. thick, and an RCA 6810-A multiplier phototube. The Al crystal can is $2\frac{3}{16}$ in. OD, $2\frac{1}{16}$ in. ID, and is $2\frac{3}{4}$ in. deep with a 0.005 in. thick foil end. The Al cover of the phototube is $3\frac{1}{2}$ in. OD, $3\frac{1}{4}$ in. ID, $7\frac{11}{16}$ in. long, and also has a 0.005 in. thick foil end. (For details, see TID-4100). (M.J.T.)

14901 SPECTROPHOTOMETER PUNCH - IBM /Q-2231/ (Engineering Materials). (Oak Ridge National Lab., Tenn.). (CAPE–1283).

8 drawings.

This automatic, digital data-readout system prepares data from a spectrophotometer continuous chart recording for computer use. The chart records absorbancy vs wavelength. The wavelength output is obtained from a photocell circuit which provides a pulse for each angstrom traversed. The pulses are accumulated in a five-decimal-digit preset counter. The digitized absorbancy information is obtained from a slide-wire potentiometer coupled to the drive mechanism of the spectrophotometer strip chart recorder. The transmitting potentiometer is energized with a precision voltage source (1000 v); the sliding tap feeds a digital voltmeter. The digital information from the wavelength counter and the digital voltmeter is punched serially in accordance with a prepared program in the IBM printing punch. The recording interval can be adjusted in wavelength intervals of 1 to 1000 Å in a 1-2-5 series. The maximum traversing speed is determined by the wavelength interval. This speed in Å/sec is equal to the recording interval. (For details, see TID-4100). (M.J.T.)

14902 AERIAL SURVEY METER /Q-2281/ (Engineering Materials). (Oak Ridge National Lab., Tenn.). (CAPE–1288).

6 drawings.

The monitor described is used to rapidly scan high-intensity radiation from fallout over wide areas. Fast response with good statistics is obtained by using a halogen-filled G-M tube. Ground level intensities of 30 mr/hr to 400 r/h can be measured from an airplane flying 100 mph at altitudes between 300 and 900 ft. The meter is simple to operate, lightweight, and has low battery drain. It operates on either a 12-v battery or 2 self-contained 6-v lantern batteries. (For details, see TID-4100). (M.C.G.)

14903 MONITOR FOR CIVIL DEFENSE (Engineering Materials). (Oak Ridge National Lab., Tenn.). (CAPE–1293).

3 drawings.

The shelter monitor consists of an electrometer and an ion chamber. The electrometer has full scale ranges of 1, 10, 100, and 1000 R/hr when used with the explosive-proof chamber. It is powered by two 6 v lantern batteries that are capable of supplying power for several months. A built-in source checks the electrometer calibration on all ranges, and the cable and ion chamber for leakage. A transistorized d-c to a-c converter supplies a well regulated 500 v potential for the ion chamber. The γ ion chamber, in its housing, is located outside of the shelter through a hole in the shelter room. The housing is constructed of $3\frac{1}{2}$ in. in diam. stainless steel pipe $\frac{9}{32}$ in. thick An Al case, $3\frac{1}{4}$ in. OD, $4\frac{3}{16}$ in. long, and 0.048 in. thick located in the housing holds the 400 cc chamber. The chamber consists of an Al case $1\frac{1}{2}$ in. OD and $4\frac{1}{2}$ in. long with a wall thickness of 0.019 in. The ion chamber is filled with dry N to one atmosphere pressure absolute. (For details, see TID-4100). (M.J.T.)

14904 LITHIUM DRIFTED GERMANIUM DETECTORS (Engineering Materials). (Lawrence Radiation Lab., Univ. of California, Livermore). (CAPE–1317).

18 drawings.

The Li-drifted Ge detectors are used in high resolution β and γ spectroscopy, in nuclear decay scheme determinations, and in identifying the isotopic content of samples containing many isotopes. One of the detectors, with an active volume in excess of 6 cm^3, is primarily intended for high energy (>1.0 Mev) γ spectroscopy. The second type is a large-area, low-capacity, windowless detector intended for very high resolution β and low-energy γ spectroscopy. Both operate in a vacuum at liquid nitrogen temperature (77°K). (For details, see TID-4100). (M.C.G.)

14905 KANNE IONIZATION CHAMBERS (Engineering Materials). (Du Pont de Nemours (E. I.) and Co., Aiken, S. C. Savannah River Lab.). (CAPE–1330).

13 drawings.

Kanne ionization chambers are used in measuring radioisotope, tritium, or other weak β emitters in air. A Kanne system consists of an intake or sample line, filter, flowmeter, chamber, air pump, and exhaust line. The current produced by ionization is measured by a micro-microammeter and recorded continuously. One chamber is constructed of Al and has an active volume of 51.5 liters; the smaller chamber is constructed of stainless steel and

has an active volume of 18.5 liters. The average response of the 51.5 liter chamber is 2×10^7 $\mu C/cm^3/A$ and the response for the 18.5 liter chamber is 6.85×10^7 $\mu C/cm^3/A$ for tritium concentrations. (For details, see TID-4100). (M.C.G.)

14906 E AND ΔE PARTICLE IDENTIFIER (Engineering Materials). (Lawrence Radiation Lab., Univ. of California, Berkeley). (CAPE–1311).

197 drawings.

An apparatus is described, which is used to identify protons, deuterons, tritons, ^3He, and α particles produced by the bombardment of target materials with high-energy particles produced by machines such as cyclotrons and Van de Graaffs. Using an empirical relationship, the identifier employs logarithmic elements to produce an output that has a fixed value for each type of particle. Since the thickness is not limited to a very small value, the identifier can cope with mixtures of all five types of particles, each covering a fairly wide energy range. (For details, see TID-4100). (M.C.G.)

14907 PHOTOGRAPHIC, GLASS OR THERMOLUMINESCENCE DOSIMETRY. Becker, K. (Nuclear Research Establishment, Juelich, Ger.). 30p. (CONF-650616–15). ORINS.

From Health Physics Society Annual Meeting, Los Angeles.

An attempt is made to compare advantages and disadvantages of "classical" photographic and modern solid-state detectors. Both advanced thermoluminescent detectors (TLD), in particular LiF and similar materials, and more recent radiophotoluminescent glasses are superior to photographic systems with regard to reliability and accuracy of the dose indication, sensitivity, dose range, energy and directional dependence of sensitivity, fading and "fogging" stability, reusability, fast and cheap evaluation, etc. LiF seems to be superior for certain radiobiological and medical purposes because of its flat response. For routine and accident (military or civil defense) personnel dosimetry, however, a properly designed glass badge gives more information and is a remeasurable "document" of the exposure similar to the photographic film because the radiation effect is integrated in spite of an unlimited number of interval measurements. As an example of a possible next generation personnel dosimeter proposals for a multiglass badge are briefly described. It is capable of giving instant information about the gamma and beta dose, the average gamma energy and the presence of neutrons. Fast neutrons can be measured by automatic counting of the number of fission fragment tracks in glass or other nonphotographic nuclear track detectors. Some practical aspects of this system are discussed. (auth)

14908 TOTAL ABSORPTION X-RAY CALORIMETER. Paraskevoudakis, P.; Wegst, M.; Gordus, A.; Gomberg, H. J.; Clendinning, W.; Atkins, M.; Siemon, R. (Univ. of Michigan, Ann Arbor). 21p. (CONF-650825–1). ORINS. Gmelin, AED-CONF-65-196-2.

From 20th Annual Calorimetry Conference, Ames, Iowa.

A description is given of a total-absorption thermal x-ray calorimeter for use with photons of energies less than about 10 kev. Photons enter through a thin aluminum-coated polyethylene window, penetrate a thin beryllium heat shield, and are absorbed in a 2 mil thick, 3 cm diameter gold plate to which two thermistors are attached. The gold plate is contained in a high-vacuum chamber cooled by liquid nitrogen. Heating wires attached to the gold plate permit calibration of the unit. A minimum intensity of about 0.6 $\mu watts\text{-}cm^{-2}$ can be measured. The overall measurement error is about ±2.5% and is due principally to the relative lack of sensitivity of the $\mu\mu$ ammeter used in the measurement. The calorimeter was used as a primary standard in determining the fluorescent x-ray flux from a XRD-5 x-ray spectrometer. (auth)

14909 IMPROVEMENTS RELATING TO RADIATION DETECTORS. Freck, David Vernon (to Associated Electrical Industries, Ltd.). British Patent 1,018,402. Jan. 26, 1966. Filed May 9, 1961.

A radiation detector made up of several semi-conductor surface barriers or p-n junction devices stacked as slices, one over the other but electrically insulated from one another by insulating material or air spaces, is proposed for the detection of high energy radiation. A reverse potential bias can be applied to the surface barriers or junctions, and all the separate slices are connected to a common amplifier and detector. (B.L.M.)

14910 IMPROVEMENTS RELATING TO RADIATION DETECTORS. Freck, David Vernon (to Associated Electrical Industries, Ltd.). British Patent 1,018,493. Jan. 26, 1966. Filed June 8, 1961.

A radiation detection apparatus for low energy radiation, such as x rays, includes a solid state detector having a p-n junction and an electrical output circuit including an amplifier and a counter. Biasing means for the detector is so arranged that the detector operates under conditions in which electron-ion pair multiplication will occur. (B.L.M.)

14911 HIGH LEVEL REMOTE RADIATION MONITOR. Eberline, Howard C. (to Eberline Instrument Corp.). U. S. Patent 3,229,090. Jan. 11, 1966. Filed June 1, 1961.

A high level radiation monitor includes a central recorder station to which is connected a multiplicity of detector heads for indicating the radiation levels in a multiplicity of spaced areas. The circuitry includes a high voltage power supply, range varying resistors, a photomultiplier with operatively mounted scintillation crystal, a thermostatically operated heater, and a known radiation source mounted for exposure to the detector at the will of a remote operator. The central recorder station is arranged to briefly and periodically connect with each of the detectors to reduce the fatigue effect exhibited by the photomultipliers when operated at relatively high anode current. (B.L.M.)

14912 SCINTILLATION SELECTOR FOR LOW ENERGY CHARGED PARTICLES. Sinclair, Kenneth F. (to United States Navy). U. S. Patent 3,229,091. Jan. 11, 1966. Filed May 21, 1963.

A detector for low-energy beta particles in a radioactive gas combines a proportional multiplier with a scintillation counting device. Each subatomic particle collides with atoms/molecules of the radioactive gas to produce primary ions that are accelerated by an electric field to produce secondary ions. This large number of ions proportional to the original number of particles is collected at a scintillant positioned near the photocathode of a photomultiplier tube, which detects the light pulses. The signals from the photomultiplier are passed to a conventional counting system for counting. (B.L.M.)

14913 FAST AND SLOW NEUTRON COUNTER. Eberline, Howard C. (to Eberline Instrument Corp.). U. S. Patent 3,229,092. Jan. 11, 1966. Filed Sept. 8, 1961.

A simple, lightweight, portable instrument for the detection of either fast or slow neutrons includes a two-section housing. The upper section contains the source of power and the detecting and amplifying circuitry. The lower section has an outer housing with a thermal neutron shield and a moderator for fast neutrons and an inner recess for a removable probe of the gas proportional type with high efficiency for detecting slow neutrons. The probe is constructed for reception within the recess and has an electrical connection for feeding its output to the electrical components in the upper section. (B.L.M.)

14914 THERMOLUMINESCENT DOSIMETER SHIELD. Durkee, Robin K.; Lucas, Arthur C. (to Edgerton, Germeshausen and Grier, Inc.). U. S. Patent 3,229,097. Jan. 11, 1966. Filed Apr. 24, 1963.

A radiation shield is provided for a thermoluminescent dosimeter comprising a detector of thermoluminescent Mn-activated CaF_2 enclosed in a glass envelope. The shield consists of two thin layers of metal encompassing the envelope except for the base, one within and in contact with the other and having common voids to permit ionizing radiation to impinge without attenuation upon approximately 10% of the exterior area of the detector. The inner envelope is lead and the outer one is tin. (B.L.M.)

14915 RADIATION DOSIMETER SYSTEM USING CADMIUM-BACKED COPPER FOIL. Ballinger, Edward R.; Carr, Leo J.; Harris, Payne S.; Hiebert, Richard D.; Larkins, John H. (to U. S. Atomic Energy Commission). U. S. Patent 3,230,369. Jan. 18, 1966.

A neutron dosimeter system having in combination a portable battery-powered sodium 24-copper 64 detector unit and a thin cadmium-backed copper foil which is placed at the waistline in the person's clothing is described. (AEC)

14916 NUCLEAR RADIATION DETECTION SYSTEM USING A PLURALITY OF DETECTORS. Wolicki, Eligius A.; Knudson, Alvin R. U. S. Patent 3,230,371. Jan. 18, 1966. Filed Apr. 25, 1963.

A radiation detection system includes a number of separately operated nuclear radiation responsive detectors all of which are associated with a single amplifier and multichannel pulse height analyzer. Each detector is connected between a resistor and a number of resistors connected in series, and a bias voltage is connected to the detectors and the series resistors. (B.L.M.)

14917 NUCLEAR RADIATION DETECTOR WITH CONTROL GRID. Spracklen, Howard P. (to U. S. Atomic Energy Commission). U. S. Patent 3,230,372. Jan. 18, 1966.

An ionization chamber radiation detector having an anode, a cathode, and one or more auxiliary collector electrodes which intercept a variable fraction of the ion current, thus preventing the occurrence of saturation conditions at the primary collecting electrodes is described. The effective range over which measurements can be made is thereby extended by several decades. (AEC)

Radiation Effects

14918 (ECOM-01313-1) RADIATION EFFECTS ON MICROELECTRONIC CIRCUITS (SEMICONDUCTOR). First Quarterly Report, May 1, 1965–July 31, 1965. Perkins, C. W.; Marshall, R. W.; Mitchell, E. P.; Liebschutz, A. M. (Hughes Aircraft Co., Fullerton, Calif.). Nov. 1965. Contract DA-28-043-AMC-01313(E). 55p. (ER-65-10-182). CFSTI $3.00 cy, $0.50 mn.

The effects of high-intensity nuclear radiation (both transient and permanent) on semiconductor integrated microelectronic circuits are to be studied, in order to minimize or eliminate any intolerable effects in circuits designed for reliability in specified nuclear environments. The preparation of devices and instrumentation for radiation tests is reported. The circuits are subjected to a pre-irradiation test. The circuits chosen for study and the measurements made in bench tests are described. All of the instrumentation to be used in this study is described. This includes instrumentation for laboratory bench tests, Linac transient radiation effects tests, and pulsed-reactor permanent damage tests. (auth)

14919 (N65-20653) [EFFECTS OF LOW ENERGY PROTON IRRADIATION ON SOLAR CELLS.] Monthly Progress Report, January 1965. Denney, J. M. (Space Technology Labs., Inc., Redondo Beach, Calif. Solid State Physics Lab.). Feb. 19, 1965. Contract NAS-5-3805. 2p. (NASA-CR-57558). CFSTI $1.00 cy, $0.50 mn.

The current-voltage characteristics of solar cells that were exposed to low-energy protons in a solar simulator were measured. Subsequent measurements indicated that considerable annealing had occurred in both the n-p and p-n specimens. The annealing was more extensive than any that had previously been observed in short-time measurements on electron- or proton-irradiated cells. (D.C.W.)

14920 (TID-22664) EFFECT OF NEUTRON IRRADIATED ON TRANSISTOR CURRENT GAIN [Thesis]. Borookhim, Manouchehr (Kansas Engineering Experiment Station, Manhattan). 1966. 190p. Dep. mn. CFSTI $5.00 cy, $1.00 mn.

Kans. State Univ. Eng. Exp. Sta., Spec. Rep. No. 62.

The effects of neutron irradiation on Ge and Si were studied, and the effects of 14.1-Mev neutrons on the performance of several commonly used transistors were investigated. The known effects of neutron irradiation on the minority carriers and conductivity of the semiconductor materials were used to derive a theoretical expression for the variation of transistor current gain with neutron irradiation. To check the validity of this relation, a set of transistors was irradiated with fast neutrons, and collector characteristic curves were obtained. A computer program was developed to analyze the data and to calculate a lifetime damage constant. (D.C.W.)

14921 NUCLEAR BLAST EFFECTS ON COMPONENTS AND EQUIPMENT. Kaplan, Louis L.; Saelens, Richard G. (Army Signal R. and D. Lab., Fort Monmouth, N. J.) Electron. Ind., 21: 94-101(Oct. 1962).

Problems in the design and development of military electronic equipment, the performance of which, under field use, will not be affected deleteriously by nuclear radiation, are considered. In general, electron tubes exhibited, radiation tolerances superior to those of other piece parts. Effects such as discoloration of glass, fractures of glass, and failure of glass-to-metal seals are major factors in tube malfunctions in a steady-state radiation environment. Use of metal-ceramic seals and the elimination of glasses containing boron offer the possibility of raising the radiation tolerance levels to 10^{17} to 10^{18} n/cm^2. In contrast to the permanent damage observed in electron tubes at steady-state reactors, only transient changes were recorded during pulse-type exposures. Permanent radiation damage in semiconductors resulted from defects caused by fast-neutron interaction in the crystalline lattice structure. Impurity atoms are formed and vacancies and interstitials thus created change the electronic equilibrium in transistor operation. In general, h-f germanium devices were more radiation resistant than low-frequency or power silicon devices. A chart depicting this range in devices is shown, illustrating the radiation dosage at which a pertinent parameter will fall to one-half its original value. Some typical results of transient effects in semiconductor devices are also shown. Data on the effects of steady-state nuclear radiation on resistors showed that the ranking of tolerance is as follows: wire wound, metal film, carbon film, and carbon composition. A summary of the effects of nuclear radiation on resistors and capacitors, and their tolerance, is given. A brief review and description of the pulse radiation projects and facilities to investigate these phenomena which are being used are provided. (BBB)

14922 RADIATION DAMAGE OF CARRIER LIFE TIME IN P TYPE Si. Nakano, Takao; Nakasima, Kenshiro; Inuishi, Yoshio (Osaka Univ.). J. Phys. Soc. Jap., 20: 2140-6(Dec. 12, 1965).

The annealing of changes in the electric properties of silicon caused by ^{60}Co gamma irradiation at room temperature was investigated by isochronal annealing and lifetime techniques. For recombination centers introduced by ^{60}Co gamma rays, the recombination energy level position was placed at 0.21 and 0.27 ev above the valence band for the p-type pulled and floating zoned silicon, respectively. The annealing activation energies of the recombination centers were 0.75 and 1.4 ev for the p-type pulled and floating zoned silicon, respectively. In p-type silicon there is a remarkable process of annealing of the recombination centers at about 300°C. The interaction between defects and dislocations were considered from the introduction rates and the annealing characteristics. (auth)

14923 RADIATION-INDUCED NOISE IN SEMICONDUCTOR COUNTERS. Bertin, A.; Gondi, P.; Scandola, G. (Univ., Bologna). Nuovo Cimento, (10), 41B: 198-207 (Feb. 11, 1966).

The effects of electromagnetic radiations of various energies, ranging from 7 to ~10^6 ev, on silicon surface-barrier detectors were examined. Induced shot noise resulted; the noise amount, for equal induced currents, increases with the number of electron-hole pairs per primary electron, with departures from the law of proportionality that depend on the root mean square deviations specific of each

radiation. The most energetical photons give rise to exceptionally high rms deviations whose origin was considered by examining the thickness and bias voltage effects. (auth)

14924 EFFECT OF ELECTRON IRRADIATION ON N-CHANNEL MOS TRANSISTORS. **Stanley, Alan G. (Massachusetts Inst. of Tech., Lexington). Proc. IEEE (Inst. Elec. Electron. Eng.), 53: 2150(Dec. 1965).**

Results of measurements of the source-to-drain leakage current and the turn-on voltage as functions of total electron dose up to 10^{15} e/cm^2 are given for n-channel MOS transistors irradiated with 1.5-Mev electrons. The changes produced in the transfer characteristics by the total dose are shown. The mechanism for the observed effects is discussed. The occurrence of a gate-to-body short after storage of the irradiated devices with all terminals shorted is described. (M.J.T.)

14925 EFFECT OF ELECTRON ENERGY ON DEFECT INTRODUCTION IN SILICON. **Carter, J. R. Jr. (TRW Space Tech. Labs., Redondo Beach, Calif.). 25p. (CONF-650707-8). ORINS. Gmelin, AED-CONF-65-152-16.**

From IEEE Annual Conference on Nuclear and Space Radiation Effects, Ann Arbor, Mich.

Using Hall effects measurements, the electron energy dependence of the defect introduction rates of the $E_c - 0.17$, -0.4, and $E_v + 0.3$ ev levels was determined. The two levels at $E_c - 0.17$ and -0.4 ev are found to be relatively insensitive to incident electron energy as predicted by simple displacement theory. The defect introduction rate for the $E_v + 0.3$ ev level is found to increase rapidly with increasing electron energy. It is also observed that the energy dependence of the $E_v + 0.3$ ev level appears to be a function of material resistivity in that the dependence becomes steeper at lower resistivities. At resistivities of the order of 15 ohm-cm the energy dependence of the defect introduction rate of the $E_v + 0.3$ ev level is identical to the observed energy dependence of the degradation of minority carrier lifetime in 10 ohm-cm n on p silicon solar cells. Empirically it is observed that this energy dependence appears to be proportional to the second power of the simple displacement theory, suggesting that these defects may be associated with a divacancy or other double displacement type defect. (auth)

ISOTOPE TECHNOLOGY

General

14926 PRODUCTION AND CONSUMPTION OF RADIOISOTOPES IN SPAIN IN 1964. Energia Nucl. (Madrid), 9: 377-89(Sept.-Oct. 1965). (In Spanish).

The production and use of radioisotopes in Spain in 1964 is summarized briefly. The organization devoted to the development of increased uses of radioisotopes and to their production is described. The evolution of the use of radioisotopes in Spain since 1957 is shown by tables. (J.S.R.)

14927 CALIBRATION OF A ^{60}Co SOURCE BY COMPARISON WITH A WEAK RADIUM STANDARD. Bierman, A.; Feige, Y. (Israel Atomic Energy Commission, Yavneh). Int. J. Appl. Radiat. Isotop., 17: 79-80(Jan. 1966).

A ^{60}Co source of ~6C was calibrated by comparing its output to that of a 5 mC radium standard. Both sources were measured with a rate meter using the same ionization chamber (range 2.5 R). Since the exposure and distance were the same for both sources, their dose rates were in inverse ratio to the exposure times. The dose rate in the irradiation room at 50 cm from the cobalt source was 33.6 R/hr at the time of measurement with a maximum error of 6%. (F.J.H.)

14928 IMITATORS OF SHORT-LIVING ISOTOPES OF IODINE. Lvova, M. A.; Bochkarev, V. V. Med. Radiol., 10: 90-1(Sept. 1965). (In Russian).

A method is described for preparing emitters from long-lived isotopes that in certain conditions imitate the energetic distribution of beta emissions from ^{131}I and ^{132}I. The imitators may be utilized in clinical practice as a standard in relative measurements of the activity of iodine preparations. (auth)

Industrial Applications

Refer also to abstract 14835.

14929 (CONF-651132-1) NEW DEVELOPMENTS AND TRENDS IN THE ISOTOPE INDUSTRY. Fowler, E. E. (Division of Isotopes Development (AEC), Washington, D. C.). [1965]. 30p. Dep. mn. CFSTI $2.00 cy, $0.50 mn.

From Atomic Industrial Forum, 12th Annual Conference, Washington, D. C.

A review is presented on industrial uses of isotopes and radiation and factors limiting the use of isotopes. Recommendations are made concerning future development of industrial applications. (P.C.H.)

14930 (NP-15676) RESEARCH TEST OF IRRADIATED BEEF, PORK SAUSAGE, AND SHRIMP. Final Report. Paschall, Hunter H. (Army Quartermaster Research and Engineering Field Evaluation Agency, Fort Lee, Va.). May 1964. 21p.

A research test of irradiated beef, pork sausage, and shrimp was conducted by the Field Evaluation Agency. The purpose of the test was to determine the relative consumer preference for irradiated and non-irradiated beef, pork sausage, and shrimp when served as part of a normal meal under garrison feeding conditions. Test results showed that non-irradiated beef, pork sausage, and shrimp are preferred to their irradiated counterparts. The irradiated beef is considered acceptable as a component of standard meals, whereas the acceptability of the irradiated pork sausage and shrimp as components of standard meals is questionable. It is recommended that consideration be given to the improvement of the sensory characteristics of irradiated pork sausage and shrimp. (TCO)

14931 (NP-15677) RESEARCH TEST OF IRRADIATED BEEF, HAM, AND SHRIMP. Final Report. Paschall, Hunter H. (Army General Equipment Test Activity, Fort Lee, Va.). July 1964. 23p.

Research was conducted to determine the relative consumer preference for irradiated and nonirradiated beef, ham, and shrimp when served as a part of a normal meal under garrison feeding conditions. Previous tests of irradiated foods indicated, in most instances, a generally satisfactory level of acceptance of such foods. Analysis of data obtained during this test shows that: the nonirradiated beef, ham, and shrimp are preferred to their irradiated counterparts when served as a part of a normal meal under garrison feeding conditions; the relative consumer preference for irradiated shrimp is not adversely affected by increasing the storage period from 7 to 14 days; and the average preference ratings for irradiated beef, ham, and shrimp are sufficiently high for all items to be considered acceptable as components of standard meals. (TCO)

14932 COMPARATIVE STUDIES OF THE EFFECT OF METHODS OF STERILIZATION ON THE ABSORPTION OF CHROMIC CATGUT. Hufnagel, Charles A.; Zellos, Spyridon; Gillespie, John F. (Georgetown Univ., Washington, D. C.). Amer. J. Surg., 109: 424-6(Apr. 1965).

The comparative rates of absorption of commercially available chromic gut sterilized by irradiation and that sterilized by heat and ethylene oxide were determined. The subcutaneous fascia of rabbits was incised in the direction of the skin incision exposing the anterior rectus fascia. Six sutures were placed in the anterior rectus fascia on each side. On the left side, six ties of heat-ethylene oxide sterilized No. 3-0 chromic catgut were placed using three separate strands of suture material, two ties per strand. On the right side, the same procedure was used, but an irradiation-sterilized suture of No. 3-0 chromic catgut was implanted. After a period of observation, ranging from 60 to 150 days, the rabbits were sacrificed and the sutures removed for examination of: the number of suture remnants present; those which were still intact; those which had knots only; and those in which the loops and knots remained intact with tension on the suture. The loops and knots were analyzed and classified as strong or weak. Of the 168 sutures of each type examined at intervals of from 60 to 150 days, five heat-ethylene oxide sterilized sutures were classed as strong, and all of these were in the 60- to 90-day interval. None were present after this period. In the irradiation-sterilized group, 35 sutures were classified as strong, intact irradiated sutures were seen through the entire 150-day period of observation. This indicates that there is a failure of reabsorption of the irradiated chromic catgut of ~10% at the end of 100 to 150 days. These experiments consistently showed the prolonged persistence of the irradiated sutures in which the only known difference was the method of sterilization. (BBB)

14933 DOSE-RANGE-FINDING TESTS FOR THE ELIMINATION OF SALMONELLAE FROM PROTEINACEOUS FOODS WITH A LOW a_w BY IRRADIATION WITH ^{60}Co GAMMA RAYS. Mossel, D. A. A.; Buechli, K.; De Waart, J. (Central Inst. for Nutrition and Food Research, Zeist, Netherlands). Antonie Van Leeuwenhoek, J. Microbiol. Serol., 31: 220(1965).

In experiments with frozen chickens and ducks all Enterobacteriaceae naturally contaminating such carcasses were studied for the calculation of the most probable safe dose (MPSD) of γ radiation. Initial and surviving numbers of Enterobacteriaceae were determined by swabbing the entire outer and inner body surfaces of the birds with plugs of calcium alginate. The MPSD was found to be 0.5 Mrad for five overall decimal reductions. No organoleptically detectable side-effects were observed by an expert taste-panel with birds exposed to such radiation treatment. (BBB)

14934 INDUSTRIAL APPLICATIONS OF RADIOACTIVE TRACERS. Robin, Gerard. Energie Nucl., 7: 428-36(Nov. 1965). (In French).

The principles and methods which govern the industrial application of radioactive tracers are described. Some

examples are intentionally chosen in the most varied fields and illustrate the vast possibilities offered by these technics. These examples are not meant to provide a complete list of the technics, but are simply listed to give the engineer an idea of their use. (auth)

14935 DIFFERENTIAL EFFECT OF GAMMA RADIATION ON FRUIT FLIES AND FRUIT FLY PARASITES. Balock, J. W. (Laboratorio Entomologico, Mexico City, Mex.). J. Econ. Entomol., 58: 1169(Dec. 1965).

Observations made during experiments in Hawaii to determine the use of γ radiation as a quarantine treatment for destroying infestations of the oriental fruit fly, Dacus dorsalis, and the Mediterranean fruit fly, Ceratitis capitata, in fresh fruits and vegetables, showed that parasitic infestation was high in many of the fruit flies treated. Flies and parasites were counted in treated and nontreated false kamani (Terminalia catappa), T. chebula, ball kamani (Calophyllum inophyllum), hog plum (Spondias mombin), guava (Psidium guajava), strawberry guava (Psidium cattleianum), and acerola or Barbados cherry (Malpighia glabra). Parasites appeared to be more resistant to radiation than their fruit fly hosts. Higher parasite survival occurred at all doses tested (1000 to 8000 R) but differences were most apparent at the lowest doses (1000 or 2000 R). At these doses, higher parasite survival than in nonirradiated controls suggested a beneficial rather than harmful effect, although the effect may have been due to errors in estimating populations. (BBB)

14936 POST-IRRADIATION SURVIVAL OF STAPHYLOCOCCUS AUREUS IN SEA FOODS. Salbyj, Bohdan M. (Univ. of Washington, Seattle). J. of Food Sci., 30: 344-50(Mar.-Apr. 1965).

The ability of Staphylococcus aureus to survive the grow out in brain-heart-infusion broth, heat-sterilized crab meat, and unsterilized crab meat before and after irradiation was tested at various temperatures. The organism died out when stored at 1 and 8°C, regardless of treatment. At 12°C, S. aureus grew well in sterilized crab meat, reaching a count of 10^8 cells per gram after 14 days, but was greatly inhibited in nonsterile crab meat, whether irradiated or not. At 22°C (room temperature), S. aureus grew well and rapidly in sterilized crab meat, reaching a count of 10^9 cells per gram within 3 days, but was inhibited or grew poorly in untreated (non-sterile) crab meat. Apparently the inhibition of growth was due to competition by saprophytic bacteria naturally present in crab meat. The effect of such competition was largely eliminated when crab meat was irradiated at 100 and 200 krad, and S. aureus grew out well in such material when incubated at 22°C. Some evidence indicated that the ratio of staphylococci to saprophytic bacteria influenced outgrowth, but the major effect seemed to be due to the creation of inhibiting conditions in crab meat by competing bacteria, since staphylococci were completely inhibited in spoiling crab meat samples even after irradiation. (TCO)

14937 IRRADIATION OF FOOD. Sheard, Harold. New Sci., 28: 351-2(Nov. 4, 1965).

Fulfillment of the hopes that were originally held for the widespread use of ionizing radiation for food preservation now seems unlikely. The use of large radiation doses for complete sterilization seems to have very limited possible applications, but there are a number of medium and low dose processes that can be very useful. The rate at which these processes are used commercially will depend mainly on economic considerations. But in the last analysis the determining factor may be acceptance by the public that irradiated foods are wholesome and safe. (auth)

14938 RADIATION PRESERVATION OF FOOD. Goldblith, S. A. (Massachusetts Inst. of Tech., Cambridge). Sci. J., 2: 38-42(Jan. 1966).

Uses of radiation in the sterilization of food and in radiation sanitation are discussed. These uses are based largely on the ability of ionizing radiations to destroy microbes. Accelerators and isotopes are used as sources of radiation. To achieve complete sterilization of food dosages greater than 2 Mrad are required. Regulations were issued in the United States permitting sterilization of bacon, disinfestation of flour, and treatment of potatoes to prevent sprouting. The problem of undesirable side reactions occurring when the free radicals and activated molecules produced by radiation react with those components of foodstuffs important in flavor, odor, texture, and color is discussed. (M.C.G.)

14939 RADIOISOTOPE STUDY OF THE OPEN-HEARTH PROCESS. Skrebtsov, A. N. London, Edward Arnold, Ltd., 1965. 165p. 42s.

Originally published in Russian as Radioaktivnye Izotopy pri Issledovanii Martenovskogo Protsessa.

Applications of radioisotopes in the study of steel production processes are discussed. Topics covered include: kinetics of slag formation, kinetics of scrap melting in open-hearth furnaces using the scrap-ore process, hydrodynamics of metal and slag in open-hearth furnaces, behavior of sulfur in open-hearth furnaces, conversion of phosphorus-containing pig iron in the scrap-ore process, solidification of steel, sources of nonmetallic inclusions in steel, refractory wear, and other steel production processes. (149 references.) (M.C.G.)

14940 PROCEEDINGS OF THE FIRST INTERNATIONAL SYMPOSIUM ON THE USE OF IONIZING RADIATION FOR THE STERILIZATION OF MEDICAL PRODUCTS, AT RISO, ROSKILDE DECEMBER 6–9, 1964. London, Panel on Gamma and Electron Irradiation, 1965. 122p. 25s. (CONF-641222).

Eleven papers were presented on: effects of radiation on medical products; practical problems of radiosterilization; and industrial practices for radiosterilization. Separate abstracts were prepared for 10 of the papers presented. The remaining paper was a discussion of international cooperation in instituting a code of practice for manufacturers. (H.G.D.)

For abstracts of individual papers see: 14234, 14387–14390, 14814, and 14941–14944.

14941 PROBLEMS OF MICROBIAL CONTAMINATION IN PREPACKED PREPARATIONS. Tattersall, K. pp 15-24 of Ionising Radiation for the Sterilization of Medical Products. London, Panel on Gamma and Electron Irradiation, 1965.

Sterilization of prepacked plastic and cellulosic medical supplies is discussed in view of requirements for packaging sterilized materials. In the case of certain prepacked items such as disposable plastic instruments, fabrication produces a virtually microbe-free condition. If subsequent handling is conducted properly, recontamination is minimized and low bacterial counts are associated with status of the articles prior to sterilization. When bacterial contaminants on disposable syringes sterilized by a conventional method were compared to the same parameter on syringes sterilized with a 4 Mev Van de Graaff generator, the latter procedure was found more efficient. Data for determining the minimum sterilization dose for production of disposable syringes are tabulated. Rolls of bleached cotton wool given 0.2 to 1.4 Mrad doses of electrons were sterilized. It is suggested that anoxic conditions produced in the cotton rolls during irradiation are responsible for enhancement of sterilization in these products as compared to plastics. (H.G.D.)

14942 PACKAGING REQUIREMENTS FOR RADIATION-STERILIZED ITEMS. Powell, D. B. pp 95-103 of Ionising Radiation for the Sterilization of Medical Products. London, Panel on Gamma and Electron Irradiation, 1965.

Sterility of a packaged product is dependent on the integrity of the package in which the item is contained and packaging is, therefore, an extremely important aspect to be considered in marketing a presterilized product. One of the most important factors affecting bacterial permeability of packaging materials is the occurrence of pinholes. Ordinarily two or more plies of material are used as coatings or laminations to avert this hazard. When materials are converted into a package, the most important problem is to produce efficient heat seals. Methods for packaging surgical items are illustrated by presenting

four ways of packaging a plastic disposable hypodermic syringe and studying the problems encountered. Opening of a sterilized package and the development of printing inks that may be used as indicators in radiosterilized articles are discussed. It is suggested that packaging requirements for various items be considered individually and that the package must be subjected to thorough examination both during production and after marketing. (H.G.D.)

14943 THE VALUE OF RADIATION STERILIZATION IN HOSPITAL PRACTICE. Kelsey, J. C. pp 104-8 of Ionising Radiation for the Sterilization of Medical Products. London, Panel on Gamma and Electron Irradiation, 1965.

The use of radiosterilization in hospitals for items too expensive to be considered disposable or those not subject to conventional means of sterilization is considered. (H.G.D.)

14944 COMMISSIONING A GAMMA RADIATION PROCESSING PLANT. Jefferson, S. pp 109-11 of Ionising Radiation for the Sterilization of Medical Products. London, Panel on Gamma and Electron Irradiation, 1965.

Licensing of gamma radiation processing plants is discussed. The purpose of the inspection procedures is to ensure that all design features are functioning properly, including shielding and process control. (H.G.D.)

Power Application

See also ENGINEERING — Space Propulsion

Refer also to abstract 15038.

14945 (CONF-660305-14) LARGE-SCALE ^{60}Co HEAT SOURCES. King, F. D. R.; Angerman, C. L. (Du Pont de Nemours (E. I.) and Co., Aiken, S. C. Savannah River Lab.). Feb. 1966. Contract AT(07-2)-1. 16p. Dep. mn. CFSTI $1.00 cy, $0.50 mn.

From American Nuclear Society Topical Meeting, Augusta, Ga.

The production and handling of ^{60}Co at the Savannah River Laboratory is discussed, and the development and design requirements for practical ^{60}Co heat sources are summarized. (D.C.W.)

Separation and Production

See also CHEMISTRY — Separation Processes and Procedures

14946 (DP-1015) RADIOISOTOPE PRODUCTION CAPABILITIES OF U. S. POWER REACTORS. Hennelly, Edward J.; Hood, Ramon (Du Pont de Nemours (E. I.) and Co., Aiken, S. C. Savannah River Lab.). Nov. 1965. Contract AT(07-2)-1. 23p. Dep. mn. CFSTI $2.00 cy, $0.50 mn.

The future production capability of the U. S. nuclear power complex is estimated for four radioisotopes that are of interest as heat sources, namely, ^{147}Pm, ^{210}Po, ^{238}Pu, and ^{244}Cm. Production estimates for the next 15 years were derived from forecasts of the growth rate of nuclear power and published data on isotopic yields. The estimated total possible production by power reactors in the decade 1971–1980 ranges from 100 kwt (thermal kilowatts) of ^{244}Cm to 240 kwt of ^{210}Po; the estimated possible annual rates in 1980 range from 30 to 50 kwt. Substantial increases in the production of ^{238}Pu and ^{244}Cm can be achieved by irradiating ^{237}Np and ^{243}Am from power reactors in special reactors that operate at a neutron flux of 10^{14} n/(cm^2) (sec) or higher. Recycling of plutonium in power reactors will also increase production of ^{244}Cm. (auth)

14947 ATTEMPTS AT MATERIAL SEPARATION IN AN ELECTROLYTIC COUNTERCURRENT EXCHANGE PROCESS. VI. REPORT ON COUNTERCURRENT ELECTROLYSIS. Behne, D.; Freyer, H. D.; Wagener, K. (Hahn-Meitner-Institut fuer Kernforschung, Berlin). Ber. Bunsenges. Phys. Chem., 69: 893-5(1965). (In German).

Isotope separations can be based on differences in ionic mobilities in aqueous solution. Electrolytic countercurrent arrangements, which allow the achievement of several thousand plates per meter of column length, are advantageous. Since the isotope effects concerned are only of the order of magnitude $\Delta u/u = 10^{-3}$, it is possible to achieve separation factors of only about 10 for columns of ordinary length. In chemical exchange equilibria the isotope effects are of the order of 10^{-2} (given by the relative difference of equilibrium constants $\Delta K/K$). For the special case of homogeneous ion exchange equilibria (complex formation) it is possible to multiply these elementary effects by countercurrent electrolysis. With a relatively large elementary effect it is then possible to achieve a very large multiplication in a convenient and very advantageous fashion. (auth)

14948 PRODUCTION OF THE HEAVY ISOTOPES OF HYDROGEN AND OF THEIR COMPOUNDS. Kiss, Istvan. Fiz. Szemle, 15: 311-15(Oct. 1965). (In Hungarian).

Natural water contains 0.014 atomic % of deuterium; however, a study of the enrichment methods reveals that preparation of D-rich compounds are costly and require great expenditures of energy. Since 1940, when industrial-scale production was started, the process in use was changed about every five years. The first practical method was based on the electrolysis of water or of an aqueous solution; the H/D ratio in the gas formed at the cathode is higher than the ratio in the liquid. The gas is burned to water and is subjected repeatedly to electrolysis in a cascade process. A later method is based on the slight difference between the vapor pressure of H_2O and D_2O; it was operated economically by evaporating natural thermal waters. Further improvements were made by replacing the distillation methods by a chemical exchange reaction, bubbling H_2S through water; in that case, at 25°C, an enrichment factor of $\alpha = [(H/D)_{H_2O}/(H/D)_{H_2S}] \cong 2.3$ is obtained. A countercurrent technique makes it possible to apply this technique to industrial production of deuterium. During the early 1950's the method was further improved by the use of a dual temperature exchange process. Refinements of the low-temperature technology lead to the development of a process based on the difference of the volatility of H_2 and D_2, burning the D_2 to form heavy water. These methods are often used in combination. Tritium is present only in a very low concentration, representing only 10^{-18} of the hydrogen atoms on earth. Its industrial preparation is based on the ^{6}Li(n,α)T reaction, originating by the irradiation of LiF or Li_2CO_3 in a reactor. The tritium may be purified by adsorption and desorption by metallic uranium. Labeling of compounds may be carried out by hydrolyzing the suitable compounds in heavy water. The preparation of T and D targets is also described. (TTT)

MATHEMATICS AND COMPUTERS

Refer also to abstract 15542.

14949 (ANL–7109) A CHECKER-PLAYING PROGRAM FOR THE IPL-VC COMPUTER. Cowell, W. R.; Reed, M. C. (Argonne National Lab., Ill.). Oct. 1965. Contract W-31-109-eng-38. 14p. Dep. mn. CFSTI $1.00 cy, $0.50 mn.

A computer program was written in the IPL-V language for playing checkers. The program is described. (M.O.W.)

14950 (COO–614-41) ICR QUARTERLY REPORT NO. 7. Miller, Richard H. (Chicago Univ., Ill. Inst. for Computer Research). Nov. 1, 1965. Contract AT(11-1)-614. 157p. Dep. mn; CFSTI $5.00 cy, $1.00 mn.

A summary is presented of Maniac III engineering and operations; the development of integrated circuits for digital-computer uses; operation of error-function and gamma-function library subroutines; the operation of the instruction "Switch State of Computer" in Maniac III; bit and character addressing in Maniac III; the generation of input matrices for numerical calculations in Maniac III; theoretical investigations of a theorem in switching theory; the uses of Banach-space operators in fixed-point theorems; the decomposition of integer programming problems; and computer uses for chromosome Karyotyping and studies of the adiabatic invariants of stars in the galactic field. (T.F.H.)

14951 ON THE UNITARY REPRESENTATIONS OF A CLASS OF PSEUDO-ORTHOGONAL GROUPS. Kihlberg, Arne (Chalmers Univ. of Tech., Gothenburg, Sweden). Arkiv Fys., 30: 121-40(1965).

A method for explicit construction of the unitary, irreducible representations of the pseudo-orthogonal groups L(p,q) is presented. It is based on a realization of the elements of the Lie algebra as differential operators on a carrier space. This space is the product space of the group spaces of the maximal compact subgroup K and an Abelian subgroup A both in L(p,q). The Hilbert space is constructed as a function space on the carrier space. In an irreducible representation the vectors in the Hilbert space have a fixed dependence on the parameters of A, and the scalar product is defined in terms of integration over the parameters of K. The method is particularly simple to apply when q − p is 0, 1, or 2, since then the number of parameters of the carrier space is equal to the number of labels required to characterize a vector. (auth)

14952 A HYPERGEOMETRIC FUNCTION OF TWO VARIABLES OF IMPORTANCE IN PERTURBATION THEORY. I. Olsson, P. O. M. (Royal Inst. of Tech., Stockholm). Arkiv Fys., 30: 187-91(1965).

A hypergeometric function of two variables is introduced. The function is associated with Appell's hypergeometric function F_2 in the sense that it is a solution of the partial differential equations associated with the function F_2. The Laplace transform of a product of a confluent hypergeometric function and a Whittaker function can be expressed in terms of this function, indicating its importance in perturbation theory. (auth)

14953 ON THE CONTRACTION OF REPRESENTATIONS OF THE LORENTZ GROUP TO REPRESENTATIONS OF THE EUCLIDEAN GROUP. Stroem, Staffan (Chalmers Univ. of Tech., Gothenburg, Sweden). Arkiv Fys., 30: 267-81(1965).

If the Lie algebra of the homogeneous Lorentz group L(1,3) is contracted with respect to the Lie algebra of the rotation group, the resulting algebra is the Lie algebra of the three-dimensional Euclidean group E(3). The corresponding process of contraction in the unitary representations of the two groups is studied. Since there is no general theory for contraction of representations, explicit expressions are used for the matrix elements of the unitary representations of L(1,3) and of E(3) respectively. The latter are derived, while the former are known from earlier works. Explicit realizations of the unitary representations of E(3), suggested by the contraction are given. (auth)

14954 CONSTRUCTION OF REPRESENTATIONS OF THE INHOMOGENEOUS LORENTZ GROUP BY MEANS OF CONTRACTION OF REPRESENTATIONS OF THE (1 + 4) de SITTER GROUP. Stroem, Staffan (Inst. of Theoretical Physics, Goeteborg). Arkiv Fys., 30: 455-72 (1965).

If the Lie algebra of the (1 + 4) de Sitter group is contracted, in the sense of Inönü and Wigner, with respect to the Lie algebra of the homogeneous Lorentz group, the resulting algebra is the Lie algebra of the inhomogeneous Lorentz group. The corresponding process of contraction in the representations of the Lie algebra of the de Sitter group is studied. It is shown that the infinitesimal generators of all the unitary irreducible representations of the inhomogeneous Lorentz group can be constructed in this way, in terms of an angular momentum basis. (auth)

14955 LIE GROUPS FOR PHYSICISTS. Hermann, Robert. The Mathematical Physics Monograph Series. New York, W. A. Benjamin, Inc., 1966. 200p. $12.50 Domestic; $13.75 Foreign.

A survey of recently developed parts of the theory of Lie groups is presented. The theory of homogeneous spaces of Lie groups, particularly the theory of symmetric spaces, is emphasized. Discussions are given of transformation groups, subgroups and subalgebras, compact and noncompact semisimple Lie algebras, decompositions, vector bundles and induced representations, and the Fourier transform. Applications to particle quantum mechanics (the hydrogen atom) and to elementary-particle physics are considered. (M.J.T.)

METALS, CERAMICS, AND OTHER MATERIALS

General

Refer also to abstracts 14668 and 16060.

14956 (BM-RI-6734) ELECTRIC-ARC FURNACE REDUCTION OF TIN SLAG FOR PRODUCTION OF COLUMBIUM-TANTALUM-BEARING ALLOY. Hunter, Willard L.; Fursman, Oliver C. (Bureau of Mines, Albany, Oreg. Albany Metallurgy Research Center). June 1965. 19p. Bureau of Mines Free.

The smelting of tin slags was undertaken to produce crude Nb–Ta–Fe alloy as a unit operation in the production of pure Nb and Ta oxides or chlorides. Tin slags from Malaya and the Congo (Geomines) were smelted. These slags were reduced by C in a small, single-phase, steel-making furnace, a larger three-phase, steelmaking furnace, and a three-phase, submerged-arc furnace. In all cases depleted slags were fluid and easily tapped from the furnace. However, unless diluted by Fe additions, the metal product was a viscous, high-melting, heterogeneous mixture that could be removed from the furnace only by hand rabbling. In batch operations in the steel-making furnaces, 90% of the Nb and 85% of the Ta were recovered in the alloy. Although more than 90% of the Nb and Ta were recovered by smelting tin slag in a submerged-arc, ferroalloy furnace, removal of alloy from the furnace hearth was extremely difficult. Alloy produced when smelting tin slag in either type of furnace, without Fe addition, possessed both physical and chemical properties required for further processing. (auth)

14957 (BMI–1754) PROGRESS RELATING TO CIVILIAN APPLICATIONS DURING DECEMBER 1965. Dayton, Russell W.; Paprocki, Stan J. (Battelle Memorial Inst., Columbus, Ohio). Jan. 1, 1966. Contract W-7405-eng-92. 25p. Dep. mn. CFSTI $2.00 cy, $0.50 mn.

Progress in studies on fuels, reactor materials and components, uranium plutonium mononitride fuel materials, coated-particle fuel materials, and corrosion of materials used in the fluidized-bed fluoride-volatility process is reported. (W.L.G.)

14958 (BNL–972) HIGH-TEMPERATURE LIQUID-METAL TECHNOLOGY REVIEW. A Bimonthly Technical Progress Review. Volume 3, Number 6. (Brookhaven National Lab., Upton, N. Y.). Dec. 1965. Contract AT(30-2)-Gen-16. 40p. Dep. mn. CFSTI $2.00 cy, $0.50 mn.

Twenty-one reviews of current topical and progress reports on research and development programs concerned with liquid metals are presented. Subjects covered include: physical properties and thermodynamics, fluid dynamics, heat transfer, material development and corrosion, instrumentation, component development, and chemistry and chemical analysis. (W.L.G.)

14959 (N65–20797) STUDIES OF THERMIONIC MATERIALS FOR SPACE POWER APPLICATIONS. Informal Monthly Report, October 1–October 31, 1963. Yang, L.; Carpenter, F. D.; Holland, W.; Horner, M. H.; Hudson, R. G.; (and others) (General Atomic, San Diego, Calif. John Jay Hopkins Lab. for Pure and Applied Science). [1963]. Contract NAS3-4165. 28p. (NASA-CR-57655; GACD-4768). CFSTI $2.00 cy, $0.50 mn.

Developments in the fabrication of UC-ZrC fuels and the vapor deposition of tungsten are reported. Measurements of the high-temperature properties of UC-ZrC, life tests of Cs thermionic cells, and the results of irradiation studies are also summarized. The fractional fission-product release from UC-ZrC and the fuel temperature as a function of position from the Al wall are tabulated. The results of studies of fission-product diffusion through cladding and of diffusion-emission studies on cladding are also included. (D.C.W.)

14960 (N65–20798) STUDIES OF THERMIONIC MATERIALS FOR SPACE POWER APPLICATIONS. Informal Monthly Report, September 1–September 30, 1963. Yang, L.; Carpenter, F. D.; Horner, M. H.; Hudson, R. G.; Lindgren, J. R.; (and others) (General Atomic, San Diego, Calif. John Jay Hopkins Lab. for Pure and Applied Science). [1963]. Contract NAS3-4165. 9p. (NASA-CR-57657; GACD-4730). CFSTI $1.00 cy, $0.50 mn.

The fabrication and high-temperature properties of UC–ZrC for use in thermionic space power plants were investigated. Diffusion-emission studies were performed on clad fuel materials, and cesium thermionic cells were tested. (D.C.W.)

14961 (N65–20801) STUDIES OF THERMIONIC MATERIALS FOR SPACE POWER APPLICATIONS. Informal Monthly Report, December 1–December 31, 1963. Yang, L. (General Atomic, San Diego, Calif. John Jay Hopkins Lab. for Pure and Applied Science). [1963]. Contract NAS3-4165. 29p. (NASA-CR-57653; GACD-4923). CFSTI $2.00 cy, $0.50 mn.

Isostatic pressing and pore control in UC–ZrC fuel specimens are reported. The status of the work on vaporization rate of UC–ZrC as a function of pore structure is summarized. Measurements on the release of ^{133}Xe, ^{131}I, ^{132}Te, and ^{140}Ba were made at 1800°C on a cold-pressed and sintered 30UC–70ZrC sample of 77.6% theoretical density. The sample was thermally stabilized at 2000°C for a period of 40 hr and had a specific surface area of 4025 cm^2/cc and a surface roughness factor of 236. Diffusion-emission studies were carried out at 2073°K on vapor-deposited W-clad hyperstoichiometric and hypostoichiometric UC. Re-clad metal-rich UC was also studied at 2073°K. A large change in emission was observed. (STAR)

14962 (N65–20803) STUDIES OF THERMIONIC MATERIALS FOR SPACE POWER APPLICATIONS. Information Monthly Report, January 1–31, 1964. Yang, L. (General Atomic, San Diego, Calif. John Jay Hopkins Lab. for Pure and Applied Science). [1964]. Contract NAS3-4165. 44p. (NASA-CR-57654; GACD-4990). CFSTI $2.00 cy, $0.50 mn.

Techniques for the fabrication of UC–ZrC and UO_2 fuels were studied, together with the properties of high-temperature thermionic materials. Measurements were made of the rate of vaporization of fuels and of fission-product release. Fuel-cladding diffusion was also studied, and the development of a cylindrical fueled emitter structure and of testing equipment continued. (D.C.W.)

14963 (NLCO–970) SUMMARY TECHNICAL REPORT FOR THE PERIOD OCTOBER 1–DECEMBER 31, 1965. Burgett, R. (ed.) (National Lead Co. of Ohio, Cincinnati). Feb. 1966. Contract AT(30-1)-1156. 61p. Dep. mn. CFSTI $3.00 cy, $0.75 mn.

Eight articles are included; separate abstracts were prepared for each. (P.C.H.)

For abstracts of individual papers see: 14448–14450, 14689, 14964, 14982, 15006, and 15050.

14964 (NLCO-970, pp 2.1-7) EFFECT OF FURNACE HEATING ELEMENT ARRANGEMENT ON URANIUM METAL QUALITY. Mautz, E. W.; Bonfer, D. C. (National Lead Co. of Ohio, Cincinnati).

The quality of uranium reguli (derbies) was improved in production operations by use of reduction furnaces operating with three resistance heating elements instead of only two elements. Some improvement was also noted at the higher of two magnesium excesses studied. (auth)

14965 (NUMEC–3524-12) DEVELOPMENT AND TESTING OF UO_2–PuO_2 FAST REACTOR FUELS. Progress Report, October 1–December 31, 1965. (Nuclear Materials and Equipment Corp., Apollo, Pa.). Contract AT(30-1)-3524. 32p. Dep. mn. CFSTI $2.00 cy, $0.50 mn.

A production run of coprecipitated UO_2–20 wt % PuO_2 was completed with the powder being of good quality. Coprecipitated UO_2–50 wt % PuO_2 was also produced. Trial sintering runs indicate a powder of good quality. The first lot of mechanically mixed UO_2–20 wt % PuO_2 was rejected as nonrepresentative material due to excessive grain growth. The replacement PuO_2 for this material was also produced and sintering trials are underway. Density control through the use of additions, time at temperature, and pressed density was evaluated. The lower densities required in fast reactor fuels make such a study mandatory. The use of methyl cellulose as an addition appears to effect satisfactory control of fired density. The pellet characteristics for the smear densities required in the EBR-II fuel rods for this program are presented in graphical form. The prototype pellets using UO_2 and cladding material powders of type 316L stainless steel and Hastelloy X were compacted and sintered. Discs of the cladding material were compacted in the center of the UO_2–50 vol % metal powder to provide a low contact surface area for comparing reaction rates with the powder-to-powder high contact surface area. Studies of the possible reactions between PuO_2 and the components of type 316L stainless steel and Hastelloy X with their standard free energies are presented in graphical form. The liquid-binder evaluation has concentrated on the mixing cycle. The effect of wetting agents in shortening the mixing cycle are currently being studied. The first results would appear to indicate Aerosol can shorten the mixing cycle while yielding normal fired density extrusions. (W.L.G.)

14966 (RFP-673) OPTICAL DETERMINATION OF DEPTH OF DEFECTS BY REPLICATION TECHNIQUES. Miley, D. V.; Grotzky, V. K. (Rocky Flats Div., Dow Chemical Co., Golden, Colo.). Jan. 14, 1966. Contract AT(29-1)-1106. 7p. Dep. mn. CFSTI $1.00 cy, $0.50 mn.

Replication of defects was accomplished by a variety of techniques and produced accurate depth determinations. Of the replicating materials tested, General Electric RTV20 was most suitable for this application. A microscope is required for depth determinations on replicated surface defects. Basically, this should be a binocular unit employing vertical illumination, with a fine focus mechanism graduated in microns. Examination is best accomplished at magnifications of 150–200×. (auth)

14967 (RL-SEP-503-1) BATCH ELECTROREFINING OF PLUTONIUM METAL. Progress Report. Soine, T. S. (General Electric Co., Richland, Wash. Hanford Atomic Products Operation). May 1965. Contract AT(45-1)-1350. 32p. Dep. mn. CFSTI $2.00 cy, $0.50 mn.

A batch electrorefining process was developed that reduced the processing time of a 3.5 kg batch of Pu metal from about 80 to 38 hr. This was done by increasing the electrolysis rate from about 70 to 125 g/hr, and decreasing the time required for heatup and cooldown from 30 to about 8 hr. The increased electrolysis rate was realized by designing a new stirrer; a new two-piece cell provided the capability of shorter heatup and cooling-off periods. Purification resulted in nonvolatile impurities usually being less than 100 ppM. The process was completely instrumented so that it did not require attendance once the electrolysis current was started. Some difficulties with the ceramic cell were experienced but were solved; and, therefore, the ceramic reliability should be 90% or greater. (auth)

14968 (USBM-RC-1220) QUARTERLY METALLURGY PROGRESS REPORT NUMBER 29, OCTOBER 1–DECEMBER 31, 1965. (Bureau of Mines, Albany, Oreg. Albany Metallurgy Research Center). Contract AT(11-1)-599. 19p. Dep. mn. CFSTI $2.00 cy, $0.50 mn.

Evaluation of HfC castings disclosed that the practice of bottom-gating the molds eliminated the problem of porosity, which heretofore was a major problem. Tensile strength and and hot hardness data were obtained. Microprobe analysis of the ring surrounding each oxide particle in thorium–thoria cermets showed the ring to be ThO_2. Its different appearance was due to a slight variation in stoichiometry and not to the alloying procedure. Progress in the investigation of the solid-solution region involving the monocarbide of uranium and oxygen in the ternary system U–C–O at 1700°C is reported. A quotation of costs to reprocess about 80 kg of W–Re scrap into prealloyed powder revealed the cost of reprocessing would be 40% greater than the outright purchase of an equivalent amount of elemental powders. Suitability of extruded bars for fabrication to sheets was evaluated by chemical analysis, metallographic examination, and ultrasonic inspection. Samples of test specimens for tensile and creep testing were prepared for evaluation. (W.L.G.)

14969 SEGREGATION OF TANTALUM AT VERY LOW CONCENTRATIONS IN NIOBIUM BY CONTROLLED SOLIDIFICATION: A NEUTRON-ACTIVATION STUDY. Cocks, F. H.; Rose, R. M. Wulff, J. (Massachusetts Inst. of Tech., Cambridge). J. Less-Common Metals, 10: 157-68(Mar. 1966).

The segregation by controlled solidification of small quantities (of the order of 100 ppM) of dissolved tantalum in relatively pure niobium was investigated. Tantalum concentrations were determined by neutron-activation analysis. The equilibrium distribution coefficient for tantalum dissolved in niobium was found to be 1.4 in the limit of pure niobium. With the addition of approximately 1½% titanium to the solid solution, this distribution coefficient was decreased to slightly less than unity. The effect of ingot geometry on segregation in normal freezing was analyzed. The diffusion coefficient for tantalum in liquid niobium at the melting point (slightly above 2468°C) was estimated from the data to be of the order of 4×10^{-4} mm^2/sec. (auth)

14970 SCIENCE OF CERAMICS. Proceedings of the Second Conference held at Noordwijk aan Zee, 13–17 May 1963. Volume 2. Stewart, G. H. (ed.). London, Academic Press Inc., 1965. 434p. $13.50. (CONF-630506-B).

Twenty-eight papers presented at the Second Conference on the Science of Ceramics are given. Topics covered include: properties of raw materials, processing of materials, behavior during firing, structures and properties of products, powder characteristics, milling, powder compaction, diffusion, sintering, microstructural changes at high temperature, properties of clays, ceramic seals, solid oxide electrolytes, and glass ceramics. (M.C.G.)

14971 PROCEDURE AND APPARATUS FOR THE MANUFACTURE OF SPHERICAL PARTICLES. (to United Kingdom Atomic Energy Authority). British Patent 1,018,874. Feb. 2, 1966. Priority date Oct. 9, 1961, Austria.

A procedure and apparatus are described for the production of spherical particles from a refractory particulate material. The powdered metal oxide or carbide of the metal is passed in an inert atmosphere at superatmospheric pressure through a localized region of intense heat produced by a high-current electric discharge to a cool region. The particles are thus heated to a temperature above their melting point and immediately cooled before they adhere to each other. The process is applicable to the production of spherical particles of carbides or oxides of Mo, W, U, Th, Ti, Zr, Hf, Ta, or B. (B.L.M.)

14972 METHOD OF TREATING COLUMBIUM-BASE ALLOY. Gemmell, Gordon D.; McNutt, James E. (to E. I. du Pont de Nemours and Co.). U. S. Patent 3,230,119. Jan. 18, 1966. Filed Sept. 17, 1963.

A process is patented for improving the tensile strength of a Nb-base alloy consisting essentially of from about 0.5 to 12 wt % Zr; from 0.02 to 0.5 wt % of at least one of the interstitial elements selected from the group consisting of O, C, and N; at least one element selected from the group consisting of up to 35 wt % W, up to 10 wt % Ti, up to 25 wt % Mo, up to 25 wt % Ta, and up to 10 wt % V; and the balance Nb. The alloy is solution heat treated at a temperature ranging from about 1600 to 2100°C for a period of from 5 min to 9 hr. The solution heat-treated alloy is then age hardened at a temperature above recrystallization and from about 1000 to 1500°C for a period ranging from ½ hr to 40 hr. (B.L.M.)

14973 SURFACE AREA MEASUREMENTS. Clarke, J. T. (to U. S. Atomic Energy Commission). U. S. Patent 3,230,364. Jan. 18, 1966.

A method for determining the surface areas of powders by adsorbing sequential increments of a gamma ray emitting gas on the surface of the powder in a chamber at low temperatures measuring after each addition of gas the pressure in the chamber and ascertaining by radiolytic measurement the amount of gas adsorbed on the surface of the powder, thereafter calculating the surface area from the data gained is given. (AEC)

14974 REFRACTORY COMPOSITION. Price, Clair E.; Walworth, Claire B. (to Carborundum Co.). U. S. Patent 3,231,401. Jan. 25, 1966. Filed June 22, 1964.

A refractory composition is formed from a substantially homogeneous mixture consisting of from 60 to 97 wt % of ground inorganic ceramic fibrous material and a dispersion of a colloidal inorganic oxide selected from the group consisting of silica, zirconia, and alumina in sufficient amount that the oxide constitutes from 3 to 40 wt % of the mixture. The ground fibrous material consists of short fibers having a mean diameter in the range of from 2.5 to about 20 μ and a length to diameter ratio in the range of from about 10:1 to about 50:1. The composition is suitable for use as a coating cement on a wide variety of porous and non-porous materials including metals, graphite, and refractories to provide a thermal shock-resistant, insulating coating capable of withstanding continuous exposure to temperatures of 2300°F or higher or for casting into bodies that are cured at high temperatures. At temperatures of 1600°F and higher, the coating increases unexpectedly in strength and develops a ceramic bond. (B.L.M.)

Corrosion

14975 (ANL–7091) THE MASS TRANSFER OF SINGLE, SOLID URANIUM SPHERES TO FLOWING MOLTEN CADMIUM IN LAMINAR AND TURBULENT FLOW. Traylor, E. Dean (Argonne National Lab., Ill.). Sept. 1965. Contract W-31-109-eng-38. 166p. Dep. mn. CFSTI $5.00 cy, $1.00 mn.

A $\frac{1}{2}$-in. dia U sphere was used and molten Cd was pumped past the test spheres at different flow rates. Mass transfer coefficients were determined from weight losses of the test spheres. The Cd–U system was chosen because it was possible to operate in a temperature range in which U was the solid phase in equilibrium with the molten Cd solution. The J_d data and other derived correlations were compared with previous correlations and data for different systems. The experimental curves for mass transfer have the same general shape as those found previously by Geankoplis and Steele for the mass transfer from 2-naphthol, benzoic acid, and cinnamic acid in water. An exception to this similarity is that a pronounced hump in the J_d factor vs Reynolds number correlation occurs in the region where turbulence penetrates to the surface of the sphere, and associated pressure changes occur in the vicinity of the sphere. The driving force for mass transfer was varied and the mass fluxes were obtained and plotted vs the concentration and activity driving forces. Extrapolation of these curves to zero driving force yielded finite mass flux rates that were different from the zero value expected at the saturated condition. It was shown that neither attrition nor the activity data and activity driving force could account for the finite flux at zero driving force. U spheres that were heat-treated showed random grain structures and yielded J_d values about 2 to 5 times higher than spheres not heat-treated to give nonrandom structures. The skin friction, f/2, for spheres in organic liquids from Reynolds numbers of 10^2 to 10^3 and at a separate Reynolds number of 1.56×10^5 was 2 to 3 times greater than the J_d for U–Cd. The results of runs with artificially roughened spheres showed that the roughening produced no effect at a Reynolds number of 330. At a Reynolds number of 8.8×10^3 the J_d for the roughened sphere was about 80% higher than for the smooth sphere. This could be attributed to the early onset of the tripping of the boundary layer. The exponent of the Schmidt number was determined at Reynolds numbers of 735 and 115 to be approximately 0.60. However, the range of variation of the Schmidt number was only 60%. (W.L.G.)

14976 (AWRE–O–16/66) THE PERMEATION AND DIFFUSION OF HYDROGEN IN MOLYBDENUM. Jones, P. M. S.; Gibson, R.; Evans, J. A. (Atomic Weapons Research Establishment, Aldermaston (England)). Feb. 1966. 14p. Dep. BIS $0.50, HMSO 2s.6d.

Permeation and diffusion constants determined for H_2 in Mo: $P = 0.17 \exp(-19200/RT)$ std ml s^{-1} $atm^{-0.5}$ $cm^2 mm^{-1}$, $D = 7.6 \times 10^{-5} \exp(-8400/RT)$ cm^2 s^{-1}, and the solubility constant calculated: $S = 220 \exp(-10800/RT)$ std ml cc^{-1} $atm^{-0.5}$. The solution of H_2 in Mo is more endothermic than other systems for which the heat of solution is known. (auth)

14977 (EURAEC–1500) STUDIES OF STEEL CORROSION IN HIGH TEMPERATURE WATER AND STEAM. Quarterly Report No. 13, July 1–October 31, 1965. (Societe d'Etudes, de Recherches et d'Applications pour l'Industrie, Brussels (Belgium)). Nov. 26, 1965. Contract 089-62-7-RDB. 80p. (EUR–2658). Dep. mn. CFSTI $3.00 cy, $0.75 mn.

Work Performed under United States–Euratom Joint Research and Development Program.

The study of surface work-hardened stainless steels oxidized in steam at 400°C and above was continued. Morphological examination of the work-hardened metal zone under the fine oxide skin, formed by lengthy residence in superheated steam, showed the presence of precipitates, even where precipitation of chromium carbides is ruled out. It was previously supposed that this might be an internal oxidation phenomenon. Use of an electron microprobe did not reveal a regular oxygen-enriched zone. However, local oxygen concentrations were observed that may be attributed to discontinuous oxide penetrations which are, undoubtedly, connected with surface tearing by rough machining. The hypothesis identifying the precipitates seen under the microscope with internal oxides, must therefore be rejected. X-ray diffraction examinations, with the grazing emergence of the diffracted rays corresponding to interreticular distances of close to 2 Å, showed the presence of σ-phase in the work-hardened zone of a milled sample of type 304 stainless steel oxidized for 1000 hr in steam at 500°C. This alteration in the work-hardened zone is the result of lengthy heat treatment in the 400 to 500°C temperature zone. When the precipitates were identified, the factor responsible for behavior on re-oxidation after scaling the initial oxide skin had still to be determined. Prior studies showed that the benefit of work-hardening treatment is partly preserved after initial oxidation for 1000 hr at 500°C, whereas it disappears after initial oxidation for 1000 hr at 600°C. It was established that, with type 410 stainless steel, 1000 hr at 500°C are enough to remove all benefits of surface work-hardening. The x-ray diffraction examinations, which identified the σ-phase, revealed that the work-hardened zone underwent partial or complete recrystallization according to the type of steel and the temperature of the initial 1000-hr oxidation treatment. The degree of recrystallization revealed in this way is in complete agreement with the relatively degraded behavior on re-oxidation. (auth)

14978 (EURAEC–1546) DYNAMIC CORROSION TESTS ON CARBON AND STAINLESS STEELS IN PRESSURIZED WATER. Special Report No. 4. Warzee, M.; de Dorlodot, P.; Waty, J. (Societe d'Etudes, de Recherches et d'Applications pour l'Industrie, Brussels (Belgium)). Dec. 6, 1965. Contract 089-62-7-RDB. 28p. (EUR–2688). Dep. mn. CFSTI $2.00 cy, $0.50 mn.

Work Performed under United States–Euratom Joint Research and Development Program.

Type 304 stainless steel with 0.04% C and Creusot 1.2 MDO7 steel were used as the basic materials for the tests. Four quite different surface treatments were compared: milling, grinding, mechanical polishing up to grade

600, and electrolytic polishing. The research was designed to determine whether the influence of the surface state on corrosion at 300°C, which had appeared under static conditions, persisted under dynamic conditions at flow rates between 2 and 18 m/sec. In the case of AISI 304 steel, it appears that the advantage gained with electrolytic polishing remained, provided the water flow rate did not exceed 5 m/sec. At higher flow rates (10 and 18 m/sec.), a leveling of corrosion results for all surface states appears, together with an appreciable lowering of corrosion at 18 m/sec. As regards Creusot 1.2 MDO7 steel, it is noted that the advantage gained by electrolytic polishing, which appeared under static conditions, disappeared in dynamic tests, even at 2 m/sec. This is undoubtedly due to the intense oxidation-erosion phenomena characterizing the behavior of this type of steel under dynamic conditions. A proportion of 90 to 99% of total erosion is due to the release of oxide to the system, which follows almost linear kinetics at the rate of 150 to 400 mg/dm^2/month, depending on whether the rate is 2 or 10 m/sec. (auth)

14979 (GEAP–4835) SODIUM MASS TRANSFER. XIX. LONG-TERM EXPOSURE EFFECTS IN A BIMETALLIC 316SS-2 1/4 Cr TEST LOOP. Rowland, M. C.; Plumlee, D. E.; Pohl, L. E.; Lockhart, R. W. (General Electric Co., San Jose, Calif. Advanced Products Operation). Apr. 1965. Contract AT(04-3)-189. 125p. Dep. mn. CFSTI $4.00 cy, $0.75 mn.

Measurements of the corrosion and mass transfer in a sodium corrosion loop consisting of a type 316 stainless steel hot leg and a 2¼ Cr–1 Mo steel cold leg and operated at 1200°F with a 500°F temperature drop are reported. (W.L.G.)

14980 (GEAP–5065) SPECIFIC ZIRCONIUM ALLOY DESIGN PROGRAM. Quarterly Progress Report No. 11. Klepfer, H. H.; Blood, R. E.; Jaech, J. L. (General Electric Co., San Jose, Calif. Atomic Power Equipment Dept.). Jan. 1966. Contract AT(04-3)-189. 22p. (EURAEC–1574). Dep. mn. CFSTI $1.00 cy, $0.50 mn.

Work Performed under United States–Euratom Joint Research and Development Program.

A Zr–2.0 at. % Cr–0.16 at. % Fe alloy is being evaluated as nuclear fuel cladding. A fuel irradiation was delayed by variable corrosion performance of the first full-scale vendor batch of alloy tubing and bar stock. The difference between the variable performance by material from the large vendor ingot and the reproducibly excellent performance in the same tests by material from small laboratory melts was caused by nonuniform distribution of coarse intermetallic compounds in the vendor material. Laboratory studies resulted in a proposed process for ensuring fine uniform intermetallics under vendor conditions. A slab of the actual vendor ingot to be used for a second batch of tubing was fabricated in the laboratory by three alternate schedules including that proposed to ensure fine uniform intermetallics. Cooling rates, reductions in area, and process times were controlled to simulate vendor conditions. Metallographic, tensile, and corrosion tests are in progress on the resulting material. The effect nitrogen content on the corrosion of Zr–2.0 at. % Cr–0.16 at. % Fe alloy was determined. (auth)

14981 (MSAR–66–09) EFFECT OF HIGH-TEMPERATURE SODIUM ON AUSTENITIC AND FERRITIC STEELS. Quarterly Progress Report, October–December 1965. (MSA Research Corp., Evans City, Pa.). Jan. 17, 1966. Contract AT(11-1)-765. 30p. Dep. mn. CFSTI $2.00 cy, $0.50 mn.

Results of creep-rupture tests and fatigue tests at high cyclic strain levels for type 304 stainless steel exposed to high-carbon and high-oxygen sodium at 1200°F are given.

14982 (NLCO–970, pp 6.1-4) INHIBITION OF CORROSION OF TYPE-304L STAINLESS STEEL FROM FLUORIDES IN NITRIC ACID SOLUTIONS. Kato, T. R. (National Lead Co. of Ohio, Cincinnati).

The inhibiting effects of Fe^{3+}, Al^{3+}, and Th^{4+} ions on the corrosion rate of type-304L stainless steel in nitric acid solutions containing 0.1M HF were investigated over a temperature range of 80 to 190°F. Corrosion data obtained show that all three types of ions are capable of reducing the corrosion rate to a tolerable level, depending upon the cation-fluoride ratio, acid normality, and temperature. (auth)

14983 (NP–15875) CORROSION BEHAVIOUR OF URANIUM-BEARING RESULPHURIZED CHROMIUM STAINLESS STEELS. Biefer, G. J.; Crawford, W. M. (Department of Mines and Technical Surveys (Canada). Mines Branch). July 1965. 42p. (R–166). Dept. of Mines and Technical Surveys, Ottawa $0.75.

In keeping with their much higher sulfur contents, conventional AISI Type 416 and 430F resulfurized chromium stainless steels showed markedly higher aqueous corrosion rates than did AISI Type 430 chromium stainless steel, which has a low sulfur content. Uranium alloying additions to the resulfurized steels improved corrosion resistance in nitric acid solutions at room temperature when U/S ratios were 3.5/1 or more. The performance of such steels approached or equalled that of AISI Type 430 stainless steel. However, the uranium alloying additions had only a slight effect upon corrosion behavior of the resulfurized stainless steels in sulfuric acid, hydrochloric acid and ferric chloride solutions. Metallographic examinations showed that resulfurized steels with U/S ratios of 3.5/1 or more had predominantly globular sulfide inclusions of undetermined chemistry that had sufficiently high melting points to retain their shapes subsequent to hot-rolling. In contrast, the uranium-free resulfurized steels, subsequent to hot-rolling, showed characteristic sulfide stringers. Electrochemical measurements indicated that the uranium additions brought about decreased corrosion in nitric acid solutions because of their effect upon anodic polarization behavior. (auth)

14984 (RFP–511) THE EFFECT OF COMPOSITION ON THE CORROSION OF PLUTONIUM METAL. Thompson, M. A. (Rocky Flats Div., Dow Chemical Co., Golden, Colo.). Feb. 3, 1965. Contract AT(29-1)-1106. 5p. Dep. mn. CFSTI $1.00 cy, $0.50 mn.

Detailed spectrographic analysis, metallography, and electron microscopic examinations were conducted on a large number of plutonium samples that had been stored under approximately the same conditions for periods up to several years. The samples were stored in 1 atm of helium and generally outgassed 1 to 2 mm of gas, primarily hydrogen. Storage time was up to 2 yr. The results for allowed delta phase plutonium showed that Cr, Fe, Mn and the total impurity contents were significantly higher in the corroded samples. Just the opposite was found to be true for the unalloyed metal. (P.C.H.)

14985 ORIENTED GROWTH OF OXIDATION PRODUCTS ON SINGLE CRYSTALS OF URANIUM MONOCARBIDE. Ervin, G. Jr.; Miller, K. T. (North American Aviation, Inc., Canoga Park, Calif.). Acta Met., 14: 222-8(Feb. 1966).

UC monocrystals were oxidized in a vacuum containing O_2 at a partial pressure of 10^{-4} torr or less at temperatures of 900 to 1000°C and at 1800°C. At 900 to 1000°C, a layered epitaxial growth of UC_2 and UO_2 occurred on the surface. At a thickness of 150 μ, the UO_2 layer was randomly oriented. The linear kinetics obtained for the reaction indicates that the rate-controlling process is one occurring at a surface rather than a solid-state diffusion process. The surface features of the original UC were preserved on the UO_2 surface showing that the reaction occurred at an inner surface by O_2 diffusing inward. At 1800°C, the reaction is pictured as the oxidation of UC to form CO and the simultaneous vaporization of U or UO_2. (W.L.G.)

14986 STABILITY OF ALUMINA AND ZIRCONIA IN HYDROGEN. Trostel, Louis J. Jr. (Norton Co., Worcester, Mass.). Amer. Ceram. Soc. Bull., 44: 950-2(Dec. 1965).

Samples of alumina and zirconia refractories were exposed to dry hydrogen atmospheres at temperatures up to

2000°C. Effects of these atmospheres on the alumina, the zirconia, and the other constituents of these refractories were measured and correlated with dew point of the atmospheres and existing thermodynamic data. Results are presented which suggest stability limits for the oxides in these atmospheres. (auth)

14987 PERMEABILITY TO HYDROGEN OF METALS WITH METALLIC COATINGS. Steigerwald, E. A. (Thompson Ramo Wooldridge, Inc., Cleveland). Corrosion, 20: 371t-8t(Dec. 1964).

The ability of hydrogen to permeate through composite systems consisting of metallic coatings on type 304 stainless steel and Haynes 25 alloy as base metals was evaluated. Results indicate that the effectiveness of a particular coating-base metal system in retarding hydrogen passage can often be predicted qualitatively from knowledge of the metallurgical interaction between the coating and base metal. In systems where virtually no interaction or extensive solid solution effects occur, the coating produces a relatively small change in permeability. In systems where a continuous intermetallic layer is formed between the coating and base metal, e.g., aluminum, silicon, or metal-silicide coatings on Haynes 25 alloy, a significant decrease in permeability to hydrogen takes place. (auth)

14988 STRESS CORROSION CRACKING OF Ti AND Zr IN HCl-METHANOL SOLUTIONS. Mori, Kenji; Takamura, Akira; Shimose, Takaaki (Kobe Steel, Ltd., Japan). Corrosion, 22: 29-31(Feb. 1966).

It was discovered that Ti is easily attacked by stress corrosion cracking in methanol containing HCl. A study was made to assess quantitatively stress corrosion cracking of Ti in alcohol solutions. At the same time stress corrosion cracking of Zr was studied because of its similarity in chemical behavior to Ti. Stress corrosion cracking of Ti occurred in methanol solutions containing HCl or H_2SO_4 and that of Zr was observed in methanol containing HCl or H_2SO_4 or HCOOH and in ethanol containing HCl. In HCl–alcohol solutions it was observed, also, that the larger the molecular weight of the alcohol, the longer life the metals have. Addition of water to HCl–methanol solution prevented stress corrosion cracking of Ti and Zr. The critical concentration of water in 0.4% HCl–methanol solution was about 1.5% for Ti and about 3% for Zr. To prevent stress corrosion cracking by stress relief, annealing temperatures should be higher than 500°C (932°F) for Ti and 450°C (842°F) for Zr. (auth)

14989 STUDIES OF THE BEHAVIOR OF NEW MATERIALS WORKING IN CONTACT WITH SOLID METALS, COMPOUNDS, AND MELTS. Burykina, A. L.; Strashinskaya, L. V. (Inst. of Problems in Metallography, Kiev). Fiz.-Khim. Mekh. Mater., 1: 557-62(1965). (In Russian).

The solid-state interaction of refractory compounds and metals and their resistance against attack by copper and nickel mattes, slags, and molten salts were studied by bringing in contact refractory carbides, nitrides, borides and hot-pressed oxides with Nb, Ta, Mo, W, and graphite. Previous studies revealed that intermediate compounds possessing very high microhardness are formed at the metal-refractory compound interface, consisting primarily of chemical compounds or solid solutions. X-ray diffraction analysis and microhardness measurements did not indicate any interaction between graphite and the carbides of Ti, Zr, Hf, Nb, Ta, Mo, and W and the borides of Hf, Nb, Ta and W at temperatures up to 2200°C, and Mo boride up to its melting point. At 2200°C Ti boride was found to react slightly and Zr boride somewhat more strongly with graphite. There are no sufficient data concerning the resistance of refractories against molten salts, glasses, and slags. The behavior of Ti, Zr, Nb, Cr, and W carbides, Ti, Zr, Cr, Mo borides, Al, Zr, and Si nitrides in copper matte, copper and nickel slags, basalt, and molten mixtures containing NaCl–$CaCl_2$ with atomic Cl and metallic Na, and NaCl–$BaCl_2$ at temperatures up to 1400°C for periods from 2 to 5 hours was also investigated. The degree of attack was identified metallographically as active interaction (AlN–basalt), interaction (WSi_2–Ni matte), weak interaction (Cr_3C_2) and no interaction ($MoSi_2$–Ni matte). In a few cases, the refractory compound was not even wetted by the corrosive melt. (TTT)

14990 X-RAY STUDIES OF OXIDATION OF Ni_3Al–Ni_3Nb ALLOYS. Arbuzov, M. P.; Chuprina, V. G. (Inst. of Problems in Metallography, Academy of Sciences, Ukrainian SSR). Izv. Akad. Nauk SSSR, Neorg. Mater., 1: 1121-7(July 1965). (In Russian).

The phase composition of sinters produced during the oxidation of the alloy system Ni_3Al–Ni_3Nb was investigated by x-ray layer analysis in the temperature range from 600 to 1000°C. In the sinters of the alloys the oxides NiO, NiO·Al_2O_3, NiO·Nb_2O_5, γ-Al_2O_3, α-Nb_2O_5, and β-Nb_2O_5, as well as Ni, were found. The crystal structures of these oxides were investigated and the scheme of their distribution in the sinter layers is given. (tr-auth)

14991 REACTIONS OF URANIUM CARBIDE IN A KCl–LiCl/ZINC SYSTEM. Robinson, W. C.; Chiotti, P. (Iowa State Univ., Ames). J. Less-Common Metals, 10: 190-9 (Mar. 1966). (IS-1250).

The reactions of uranium monocarbide with liquid zinc and in a KCl–LiCl–$ZnCl_2$/zinc system were investigated for the temperature range 500–800°C. At temperatures above 725°C there is no noticeable reaction between zinc and UC. At temperatures below 725°C only partial conversion of the carbide to U_2Zn_{17} was observed and a monocarbide residue remained at temperatures down to 500°C. The residue was shown to be an oxygen-stabilized phase, UO_xC_{1-x}. The oxycarbide was found to exist in equilibrium with graphite and no evidence was observed for either U_2C_3 or UC_2 as a reaction- or equilibrium product. Equilibrations carried out in a KCl–LiCl–$ZnCl_2$/zinc system showed that the oxidation of the carbide resulted in the formation of an oxycarbide in equilibrium with UO_2. The relative, partial molal free energy of UC at 700°C in this oxycarbide was estimated to be −18.0 kcal/mole. (auth)

14992 DIFFUSIVITY DATA ON THE FORMATION OF NIOBIUM CARBIDE SURFACE FILMS. Bornstein, N. S.; Hirakis, E. C.; Friedrich, L. A. (Pratt and Whitney Aircraft, Middletown, Conn.). J. Less-Common Metals, 10: 200-5(Mar. 1966).

Activation energies for the growth of the compounds NbC and Nb_2C were determined to be -72.7 ± 3 kcal/mole and -68.8 ± 3 kcal/mole respectively. A value of 2.1×10^{-11} cm^2/sec was obtained for the diffusivity of carbon in NbC at 1700°K. (auth)

14993 THE HYDROGEN EMBRITTLEMENT OF ZIRCONIUM IN SLOW-BEND TESTS. Coleman, C. E.; Hardie, D. (Univ., Newcastle upon Tyne, Eng.). J. Nucl. Mater., 19: 1-8(Apr. 1966).

Zirconium in the vacuum-annealed and hydrided conditions was examined in slow-bending at various strain rates and different temperatures. The load-displacement curves produced prove more useful than standard impact tests for assessing ability to withstand high speed brittle cracks. The maximum load attained in the test appears to be related to temperature, strain rate, and grain size in the same way as the fracture stress in a tensile test. Although a high strain rate is not essential for brittle fracture of hydrided zirconium, increase in either strain rate or hydrogen content has the effect of moving the brittle-ductile transition to higher temperatures. The susceptibility to brittle fracture is also found to be very dependent on the actual distribution of hydride. (auth)

14994 THE REACTION OF URANIUM CARBIDE WITH NITROGEN. Hanson, L. A. (Atomics International, Div. of North American Aviation, Canoga Park, Calif.). J. Nucl. Mater., 19: 15-28(Apr. 1966).

The reaction of uranium carbide with nitrogen was investigated using a thermogravimetric balance to determine the effects of temperature, nitrogen pressure, carbide composition, UC particle size and UC "age" (time of UC exposure to air saturated with water vapor at room temperature). This reaction converts uranium carbide to a powder consisting of a mixture of carbon

and uranium nitrides; the principal nitride phase was identified as U_2N_3. The reaction rate of aged UC is higher by a factor of 28 over freshly melted UC. The reaction rate varies with UC particles size, having a maximum rate for —400 mesh powder and a minimum for the 100–200 mesh size fraction. The reaction rate varies with uranium carbide composition and is a minimum for slightly hypostoichiometric UC. The reaction rate varies as the $^3/_4$ power of the nitrogen pressure. The reaction rate is postulated as being controlled by the formation of the U_2N_3 phase below 650°C; whereas, above 650°C, the observed reaction rate is a combination of a primary process, U_2N_3 formation and a secondary inhibiting effect probably caused by the decomposition of the U_2N_3 phase. Activation energies of 31.8 ± 1.3 kcal/mole for the primary reaction and 37.4 ± 2.2 kcal/mole for the secondary reaction were determined. (auth)

14995 GROWTH CONDITIONS AND PROPERTIES OF THICK ANODIC PRODUCED OXIDE LAYERS ON ZIRCONIUM. Elze, J. Metall, 20: 43-6(Jan. 1966). (In German).

The anodic oxidation of zirconium in 13M thiocyanic acid at 25°C led to a dark green or black oxide layer whose thickness increased constantly with increasing oxidation length. If the oxidation was continued long enough, the zirconium sample was oxidized completely. In contrast to the oxidation of zirconium in strongly diluted acid or salt solutions, the electrode potential at the given acid concentration under a constant anode density (for example 0.5 mamp/cm²) did not increase to high contributions, but amounted to approximately +2 to +3 v after passage through an initial maximum. At a potential static load of around 1 v, an anodic current density of about 0.3 up to 0.4 mamp/cm² was obtained. The oxide layer had relatively low resistance. The time growth pattern of this layer and its porosity pointed to parallels with the oxide layer formation on Al in engineering electrolytes. (tr-auth)

14996 METAL-WATER REACTIONS. Baker, L. Jr. (Argonne National Lab., Ill.). Nucl. Safety, 7: 25-34; 42-3 (Fall 1965).

Recent advances in metal-water investigations are reported for the following reactor metals: uranium, zirconium, stainless steel, and aluminum. Heating these metals in a water or steam environment has involved induction and levitation coils, discharging condensers, laser impulses, resistance furnaces, and reactor transients in TREAT. Mechanisms of reaction with water or steam for the several metals under various conditions were postulated. The information gathered from these studies was used for analyses of two principal types of maximum accidents that could possibly occur in water-cooled reactors. For reactor-excursion accidents, there was good agreement between the theoretical and observed reaction energies for both the SL-1 accident and the final destructive test of the SPERT-ID core. For loss-of-coolant accidents, detailed calculations predicted the nature and timing of failure of Zircaloy-clad fuel elements in the proposed LOFT reactor following blowdown. (auth)

14997 CORROSION RESISTANCE OF BINARY NIOBIUM ALLOYS. Gulyaév, A. P.; Georgieva, I. Ya. (Moscow Inst. of Chemical Engineering). Zashchita Metal., 1: 652-7(1965). (In Russian).

Nb alloys were prepared with contents of 5, 10, 15, and 25 at. % of Ta, Ti, Zr, V or Mo. These alloys were subjected to corrosion testing by boiling for 24 hours in 5, 10, 15, and 20% HCl, in 20, 40, 50, 70, and 90% H_2SO_4, and in 20, 40, 60 and 80% H_3PO_4. A number of alloys were tested at 185°C and a pressure of 15 atm. The corrosion rate increased with increasing acid strength in HCl, but did not exceed 1 mm/yr in any case. Ti, Zr and V increased the corrosion rate of Nb, but additions of Ta and Mo lowered the corrosion rate in HCl. The corrosion rate in HCl increased at a temperature of 185°C as compared to the rate observed at the boiling point of the acid. The corrosion rate of the binary Nb alloys increased sharply with increasing acid concentration in sulfuric acid. Ta and Mo showed a protective effect. Thus, pure Nb is resistant in sulfuric acid up to 40% hot H_2SO_4, while the Nb–25 Ta alloy is resistant to 70% hot H_2SO_4. The behavior of the binary Nb alloys in boiling phosphoric acid is similar to their behavior in hydrochloric and sulfuric acids. The data indicate that Nb alloys containing 15 to 25 at. % Ta can replace pure Ta for use in corrosive acid media. (TTT)

14998 8e COLLOQUE DE METALLURGIE. CORROSION SOUS CONTRAINTE, RUPTURES DIFFEREES, FATIGUE-CORROSION ET RELATIONS ENTRE CES PHENOMENES, ORGANISE A CADARACHE LES 25 ET 26 JUIN 1964. (8th Symposium on Metallurgy. Stress-Corrosion, Delayed Failures, Fatigue-Corrosion and Relations between these Phenomena, Cadarache, June 25–26, 1964). Gif-sur-Yvette, France, Centre d'Etudes Nucleaires de Saclay. Paris, Presses Universitaires de France, 1965. 150p. (CONF-640626).

Proceedings of the Eighth Symposium on Metallurgy are presented. Topics covered in the 10 papers include: delayed failure of steels under the effect of hydrogen, embrittlement of tantalum by hydrogen, delayed failures of stainless steel bolts, role of adsorbed CN growth in hydrogen embrittlement of steels, stress corrosion of high-strength steel wires, fatigue corrosion in metals, dislocation distribution and initiation of stress corrosion cracks, effects of purity and structure of 18–10 type stainless steels on their susceptibility to stress corrosion, stress corrosion resistant stainless steels, and stress corrosion of Cr–Ni–Fe austenites in alkaline media at high temperature. A separate abstract was prepared for one paper. (M.C.G.)

For an abstract of the individual paper see: 15130.

Fabrication

Refer also to abstract 14689.

14999 (EURAEC–1466) FABRICATION OF UO_2 POWDERS OF HIGH BULK DENSITY BY MELTING AND GRINDING AND THEIR PROCESSING INTO FUEL ELEMENTS. Quarterly Report No. 20, April 1–June 30, 1965. Christ, R.; Duerrschnabel, W.; Liebmann, B.; Mueller, N.; Schikarski, L. (Nuklear-Chemie und-Metallurgie G.m.b.H., Wolfgang am Main (West Germany)). Contract 013-63-7-TEED. 23p. (EUR–2390). Dep. mn. CFSTI $1.00 cy, $0.50 mn.

Work Performed under United States–Euratom Joint Research and Development Program.

The number of man-hours per kg of UO_2 melted was reduced by melting powders instead of pellets. The quantity of material melted in the crucible was reduced from 54 to 29% by using powders, but time was saved as material that had sintered could be used after a rough grinding operation instead of regrinding and pelletizing. Densities 88% of theoretical were obtained for vibratory compacted powders in Zircaloy-2 fuel cans having the dimensions of 12 × 0.4 × 2000 and 12 × 0.54 × 1650 mm. All other tube dimensions yielded lower powder densities. Swaging the fuel cans to a 13% reduction in cross section yielded densities 92% of theoretical. Density variations of the compacted powder with length of the fuel cans were decreased by swaging. (W.L.G.)

15000 (EURAEC–1517) EXECUTION AND RESULTS OF WELDING TESTS ON SAMPLE SECTION TAKEN FROM HEAVY-GAGE PLATES OF ROLLED STEEL. Final Report No. 1. Granjon, H.; Gaillard, R. (Institut de Soudure, Paris (France)). Nov. 1965. Contract 090-62-12RDF. 90p. (EUR–2669). Dep. mn. CFSTI $3.00 cy, $0.75 mn.

Work Performed under United States–Euratom Joint Research and Development Program.

Specimens were cut from 200 mm thick LMS2V Mn–Mo steel plate with their axes parallel and perpendicular to the rolling direction. Weld beads were applied by arc welding with coated electrodes, submerged arc welding, and gas metal-arc welding. The thermal cycles during the welding processes were measured and correlated with the hardness of the heat affected zones and the underbead cracking due to the H_2 diffusion from the weld metal to the base metal.

Pellini tests were also made on sections of welded or unwelded plates. (W.L.G.)

15001 (HW–66930) RECENT ZIRCONIUM FIRE EXPERIENCE AT HANFORD AND THE GENERAL ZIRCONIUM FIRE PROBLEM. Zima, G. E. (General Electric Co., Richland, Wash. Hanford Atomic Products Operation). Sept. 29, 1960. Contract AT(45-1)-1350. 9p. ORAU.

Test work indicated that ignition and propagation of ignition in massive Zircaloy-2 components, such as process tubes, is extremely improbable under conceivable environmental conditions presented by Hanford reactors. Small particles of Zircaloy-2 are readily ignited. The fire and explosion hazard increases with the quantity of finely divided material allowed to accumulate. Close inventory must be kept on wastes from machining operations. Large accumulations of Zircaloy-2 fines should not be permitted to develop in working or disposal areas. Particular care should be exercised around operations, such as sawing, which generate powdered Zircaloy-2. Incineration is believed to be the best method of disposing of waste Zircaloy-2. Fires involving small aggregates of Zircaloy-2 fines can be extinguished by water, preferably applied in a spray. The control of fires involving a large quantity of Zircaloy-2 fines can be a difficult, and hazardous, undertaking. Reasonable housekeeping and disposal precautions can prevent such a situation. (auth)

15002 (LA–3378) COATED PARTICLE FUEL ELEMENTS FOR UHTREX. Taub, J. M.; Bard, R. J. (Los Alamos Scientific Lab., Univ. of California, N. Mex.). July 1965. Contract W-7405-eng-36. 49p. Dep. mn. CFSTI $2.00 cy, $0.50 mn.

Fuel elements for the start-up and early operation of UHTREX contain coated UC_2 particles in a graphite matrix. The fuel particles have triplex (three-layer) pyrocarbon coatings. The fuel element shock, 1 in. OD × 0.5 in. ID, is fabricated by extruding a mixture of fuel particles, graphite flour, carbon black (Thermax), and resin binder (Varcum). The extruded stock is successively cured in air to 250°C, baked in vacuum to 800°C, heated in helium to 1700°C, and cut into 5.5-in.-long fuel elements. The fuel elements are then leached with 20% HCl in helium at 1600°C to remove uranium exposed by the slight amount of damage to fuel particles that occurs during the mixing and extrusion steps and by the cutting operation. The coated fuel particles, other fuel element ingredients, fabrication equipment and procedures, and properties of the finished fuel elements are described. (auth)

15003 (LA-DC–7510) HIGH YIELD ^{233}U CASTING OPERATIONS. Gilmore, R. R.; Harbur, D. R. (Los Alamos Scientific Lab., Univ. of California, N. Mex.). Nov. 1965. Contract W-7405-eng-36. 22p. (CONF-660501–1). Dep. mn. CFSTI $1.00 cy, $0.50 mn.

For presentation at American Foundrymen's Society Convention, Cleveland.

One of the fissionable isotopes of uranium (U-233) has a low critical mass, thus making high-yield castings a necessity. Since uranium has a 5% volume change on freezing, there is a serious piping problem. A method of directionally cooling the casting during solidification, has essentially eliminated the piping problem and the need for excess material in a riser-sprue type mold which would normally be used. The equipment and procedures used for casting uranium-233, together with the nuclear safety precautions needed are described. (auth)

15004 (N65–20790) HIGH-TEMPERATURE PROTECTIVE COATINGS FOR REFRACTORY METALS. Progress Report No. 1, October 23, 1964–January 23, 1965. Bitzer, E. B.; Rexer, J.; Fenish, R. G. (Union Carbide Corp., Parma, Ohio. Carbon Products Div.). [1965]. Contract NASw-1030. 29p. (NASA-CR–57768). CFSTI $2.00 cy, $0.50 mn.

A program was initiated to establish the feasibility of using iridium as a protective coating for unalloyed Nb and Ta. The program encompassed a study of methods of applying iridium to the refractory metal substrate, investigation of the chemical and mechanical compatibility of the coating-substrate system, and limited oxidation studies. Electrodeposition of iridium on the substrate appeared to be the most promising method of sample preparation. The effects of chemical interaction on the mechanical behavior of the coating-substrate systems were studied using roll bonded, pressure bonded, and refractory metal plated samples of iridium. A microbend test was used to observe continuously the microstructure of coated samples loaded to fracture. (STAR)

15005 (NASA-SP–5024) BIBLIOGRAPHY ON WELDING METHODS WITH INDEXES. (National Aeronautics and Space Administration, Washington, D. C.). Feb. 1966. 58p. CFSTI $1.00 cy, $0.50 mn.

One hundred ninety five entries taken from the Scientific and Technical Aerospace Reports, its predecessor Technical Publication Announcements, and International Aerospace Abstracts for the years 1962 through 1965 are given. The abstracts are arranged according to year and abstract journal. Subject and personal author indexes are included. (W.L.G.)

15006 (NLCO–970, pp 4.1-5) CONTROLLING FURNACE CYCLE WITH INFRARED PYROMETERS IN THE CASTING OF LARGE URANIUM INGOTS. Brodi, G.; Abbott, A. E.; Koch, J. C. (National Lead Co. of Ohio, Cincinnati).

Two-thousand-pound ingots were cast in a plant test to determine the feasibility of controlling the melting cycle of NPR furnaces with infrared radiation pyrometers sighted on the crucible pour plug. The ingots cast were compared in a statistical test with control ingots cast by the conventional time-power cycle. (auth)

15007 (NP–15881) PROCESS DEVELOPMENT OF SHAPED MAGNESIUM–LITHIUM CASTINGS. Saia, Anthony; Edelman, Ralph E. (Pitman-Dunn Research Inst., Frankford Arsenal, Philadelphia, Pa.). Nov. 1965. 24p. (R–1785). CFSTI $1.00 cy, $0.50 mn.

A process was developed for successfully casting a number of prototype aerospace components using the ternary magnesium-lithium-silicon alloy. These components contained many of the design elements anticipated in aerospace hardware of this type. Since conventional magnesium sand foundry practice was not satisfactory, a new molding material, based upon bentonite-bonded graphite powder, was employed. Melting and pouring practice was also modified to cope with the reactive nature of the alloy. The radiographic quality of the castings and mechanical properties of test bars sectioned from the castings were evaluated and found to be satisfactory and to correspond with earlier experience on separately cast test bars. (auth)

15008 (ORNL–3874) PREPARATION OF UO_2 MICROSPHERES BY A SOL-GEL TECHNIQUE. McBride, J. P. (comp.) (Oak Ridge National Lab., Tenn.). Feb. 1966. Contract W-7405-eng-26. 57p. Dep. mn. CFSTI $3.00 cy, $0.75 mn.

Uranium oxide microspheres were prepared from both natural and enriched uranium by a sol-gel technique. The urania sols were prepared by precipitating hydrous uranium dioxide from uranous nitrate or nitrate-formate solutions, washing the precipitate to the point of incipient peptization, and heating the washed filter cake at 60 to 65°C to form a sol. Gelled microspheres were formed by dispersing the sol as drops in a column of drying solvent and fluidizing the drops during drying and gellation. The gelled microspheres were then fired to strong, dense UO_2 microspheres. Gelled microspheres and fired products were characterized by means of chemical analysis and physical methods which included thermogravimetric analysis, density measurements, crush strength determinations, x-ray diffraction, and metallographic examination. The preferred method of sol preparation was from nitrate-formate solution. Completely satisfactory sphere drying and firing conditions are still under development. (auth)

15009 (TID–22491) DENSIFICATION AND SINTERING OF THORIA AND THORIA GELS. Technical Report

No. XXVIII. Daniels, A. U.; Wadsworth, M. E. (Utah Univ., Salt Lake City. Inst. of Metals and Explosives Research). Dec. 15, 1965. Contract W-7405-eng-26, Subcontract 2176. 163p. Dep. mn. CFSTI $5.00 cy, $1.00 mn.

For Oak Ridge National Lab., Tenn.

The initial densification of thorium oxide prepared as a solid gel from steam-denitrated thoria, and prepared as compacts of crushed gel, and compacts of calcined thorium oxalate powder was studied by continuous isothermal shrinkage measurements made with a recording dilatometer. The gel material exhibited shrinkage due to water loss at temperatures below 600°C and shrinkage due to plastic flow and grain boundary diffusion sintering in the region from 600 to 1000°C. The sintering process was studied in detail. Because of the small thoria particle size (70 to 140 Å) in the solid gel, the material sintered to 98.2% of thoria's theoretical density in 200 minutes at 1000°C. Linear isothermal shrinkage measurements on crushed gel compacts showed rapid initial shrinkage of up to 5%, probably due to surface diffusion and plastic flow, which was activated by temperature increase and by adsorbed water vapor. A general equation for one-mechanism diffusion sintering was derived giving the time dependence of isothermal shrinkage. A method for the calculation of initial sintering boundary conditions from an arbitrary portion of the shrinkage data was developed and used in the form of a Fortran IV computer program. Application of this equation to crushed gel compacts showed that after the rapid initial shrinkage, at least 6% shrinkage occurred by grain boundary diffusion sintering. Measurements in N_2-H_2O and $Ar-H_2$ atmospheres identified O^{2-} vacancies as the diffusion controlling species. The activation energy for diffusion sintering in air was 39.0 kcal/mole. Calcined thorium oxalate compacts also showed isothermal grain boundary diffusion shrinkage, but the activation energy was only 18.9 kcal/mole. This may have been due to a high vacancy concentration in the relic structure left after calcination. (auth)

15010 (UCRL-16534) EFFECT OF LITHIUM FLUORIDE ON THE DENSIFICATION OF MAGNESIUM OXIDE [Thesis]. Benecke, Mark William (Lawrence Radiation Lab., Univ. of California, Berkeley). Dec. 20, 1965. Contract W-7405-eng-48. 33p. Dep. mn. CFSTI $2.00 cy, $0.50 mn.

Compaction-vs-temperature studies were made on magnesium oxide and magnesium oxide + 2 wt % lithium fluoride up to 1000°C using pressures up to 4000 psi. The lithium fluoride addition allows magnesium oxide to be hot-pressed to near theoretical density at reduced temperatures and stress. The hot-pressed density must be at least 99.5% of the theoretical density of magnesium oxide for the subsequent heat treatment to yield a transparent specimen. Because the densification kinetics vary with the temperature and pressure, the hot-pressing process must be designed to yield this critical density. (P.C.H.)

15011 PREPARATION AND PROPERTIES OF URANIUM CARBIDES. Prins, G. Atoomenergie Haar Toepass., 7: 219-24(Nov. 1965). (In Dutch).

Both uranium metal and uranium dioxide have disadvantages in use as fuel elements; therefore, uranium carbide is being investigated. A description is given of the general properties, the fabrication processes, and the chemical properties of uranium carbides. (tr-auth)

15012 ELECTRON-BEAM WELDING OF MOLYBDENUM. Pan, Tsziluan; Wang, Chzhi-lunm; Pan, Mao-lyan (and others). Ch'ing Hua Ta Hsueh Hsueh Pao, 11: No. 2, 15-34(1964).

Optimum parameters were determined for electron-beam welding of Mo, 1.5 mm thick. Welding was carried out on an LD-30C apparatus of Chinese manufacture. A study was made of the effect of vacuum level and welding technology on the properties (especially ductility) of weld joints on Mo and an analysis made of reasons for brittleness. The following conclusions are drawn. During welding, regardless of the parameters, there is a reduction in local vacuum in the weld pool zone due to dissociation and metallurgical reactions in the pool. The vacuum can be made higher by introducing Ti or Ce as getters into the weld metal zone. Treatment of the workpiece surfaces prior to welding has some effect on the local vacuum, but does not improve the ductility of the joints; beam energy concentration has a very marked effect on weld ductility. Before welding, the surfaces of the workpieces must be cleaned by appropriate chemicals; welding should proceed at speeds, power and vacuum specified. The brittle transition temperature of the weldments for these parameters will be 0-100°C. Brittleness in the joints is related to the grain size and presence of impurities on their boundaries. (Rev. Metal Lit.)

15013 THE PREPARATION BY LEVITATION MELTING IN ARGON OF HOMOGENEOUS ALUMINUM ALLOYS FOR NEUTRON MEASUREMENTS. Van Audenhove, J.; Joyeux, J. (EURATOM, Geel, Belg.). J. Nucl. Mater., 19: 97-102(Apr. 1966).

The levitation melting and casting arrangement and the molds are described. The preparation techniques and results of metallographic examinations illustrating the high degree of homogeneity obtained within the alloys are given. (W.L.G.)

15014 MACHINING DIFFICULT MATERIALS—MOLYBDENUM ALLOYS. Field, Michael (Metcut Research Associates, Inc., Cincinnati); Zlatin, Norman; Jameson, Robert T. Metal Progr., 89: 84-9(Feb. 1966).

Machining properties are given for two molybdenum alloys: TZM, which contains 0.5% Ti, 0.015% C, and 0.08% Zr, and Mo-0.5 Ti, which has 0.5% Ti and 0.02% C. Procedures for turning, milling, drilling, tapping, reaming, and grinding are described. (M.C.G.)

15015 OBSERVATIONS ON THE MILLING OF HARD METAL POWDERS. Fischmeister, H. F.; Exner, H. E. (Institut fuer Metallforschung, Stockholm). Planseeber. Pulvermet., 13: 178-98(Dec. 1965). (In German).

Milling of cobalt, tungsten carbide, and 90% WC-10% Co mixtures in alcohol was investigated by means of particle size analysis, x-ray, and magnetic methods. Decarburization was a function of milling time. The milling of pure tungsten carbide could be described by the equation $s = k \cdot t^{\frac{1}{2}}$. In the semilogarithmic diagram, the particle size distribution was shifted to finer particle diameters during milling, with the particle size range remaining the same. The cobalt formed agglomerates whose shapes were modified by milling, while their dimensions remained essentially unchanged. The size of the building units of these agglomerates, however, decreased greatly with increasing milling time, with a simultaneous increase in the coercive force and the proportion of β-phase. The interaction between cobalt and tungsten carbide during milling was found to be less than was assumed. The main effect of prolonged milling was a uniform distribution of the cobalt by purely mechanical mixing and a penetration of WC particles into the cobalt agglomerates. A coating of the tungsten carbide surfaces by cobalt could not be confirmed. The importance of intense milling for the sintering process could not be confirmed. On the contrary, it was found that milling had no effect on sintering. The shrinkage rate was affected only by the particle size of the carbide powder and the activity of the tungsten carbide surface, which varied with carbon content and surface treatment of the carbide powder. Shrinkage began at temperatures of 800 to 1000°C. The particle size and size distribution of the tungsten carbide powder had a quantitative effect on the structure and properties of the sintered alloys. Increasing milling intensity was reflected mainly in a higher density and more uniform distribution of the cobalt. (auth)

15016 RECENT DEVELOPMENTS IN THE APPLICATION AND ELECTROPLATING OF RHENIUM. Camp, Eldridge K. Plating, 52: No. 5, 413-16(May 1965).

Deposits from various aqueous electrolytes with pH values between 0.9 and 5.7 are discussed. Various ferrous

and nonferrous substrate metals, plating bath operating conditions, effects of Pt, Au, and Cu impurities on deposit color and finish, VHN values from 300 to 1200 as a function of current density wear, brightness, microstructure, and corrosion characteristics are described. Ultrasonics applied to the phosphate bath increased electrolyte conductivity 50%, but did not improve current efficiency or corrosion and tarnish resistance. X-ray diffraction patterns indicate deposits on C and bronze are essentially noncrystalline. Applications as electrical contacts, plating of lamp filaments, heat shields, and catalysts are described. Various physical properties of Re are given. (Rev. Metal Lit.)

15017 PREPARATION OF COMPLEX CARBIDE ALLOYS CONTAINING SCANDIUM CARBIDE. Krushinskii, A. N. Porosh. Met., Akad. Nauk Ukr. SSR, 11: 45-51 (1965). (In Russian).

The possibility of using scandium carbide in the preparation of hard carbide alloys of tungsten, scandium, and titanium with increased hardness is discussed. (auth)

15018 THE GAINES FABRICATION PLANT FOR NUCLEAR FUEL AT TREFIMETAUX. Herenguel, J.; Scheidecker, M. Rev. Alumin., No. 331, 623-6(May 1965). (In French).

EdF2, a Mg alloy sheathing for natural uranium metal, was developed for use as a nuclear fuel. The alloy, with 0.45% Zr content, was selected as sheath material for its thermal and long service properties. A special workshop was designed with casting, drawing and machining and surface treatment equipment solely for the production of this sheathing. Service conditions include temperatures from 450 to 500°C over more than 10,000 hr. Production methods and controls are set forth. (Rev. Metal Lit.)

15019 PROBLEMS OF ASSEMBLING HETEROGENEOUS PARTS AND APPLICATIONS OF REMOTE-CONTROLLED AUTOMATIC WELDING IN CONSTRUCTION OF A NUCLEAR REACTOR. Thome, P.; Foulquier, H. Soudage Tech. Connexes, 19: 100-6(Mar.-Apr. 1965). (In French).

In a planned, cold moderator reactor, 216 closed-spaced Zircaloy-2 process pipes, which will contain fuel elements, are to pass through a tank of heavy water. These pipes, each of which will have individual supply of CO_2 at 60 kg/cm^2 for cooling purposes, will also serve as tie-bars in the reactor structure. Specifications require that process pipes be accessible at both ends, that fuel circulation be alternated and that it be possible to replace pipes during life of reactor. Procedures tested and planned for obtaining tight joints with strengths of 50 to 70 tons are: fabrication of Zircaloy-stainless steel tubular joints involving use of a special tapered thread plus brazing from inside with an Ag–Al alloy, components first receiving an electrolytic coating of Cu; welding of Zircaloy ends of these joints to process pipes in one pass, without filler metal, by vacuum electron beam welding; welding of process pipes, with transition joints installed, to double ends of tank by a specially designed, remote-controlled welding machine in a first TIG pass followed by two MIG half-passes (TIG-MIG welding machine, which features a visual weld inspection device and a television circuit, is described); alternate method of joining tubes to tank ends by means of an expanded joint; and joining of extensions of pipes through concrete shield of reactor by threaded connections and internal welds forming overlapping joints, using another remote-controlled welding machine. Details of edge preparation and welding parameters are given. (Rev. Metal Lit.)

15020 RAPID QUENCHING OF REACTIVE AND REFRACTORY ALLOYS FROM THE LIQUID STATE. Willens, R. H.; Buehler, E. (Bell Telephone Labs., Murray Hill, N. J.). Trans. Met. Soc. AIME, 236: 171-4(Feb. 1966).

A melting technique was adapted to the rapid quenching of alloys from the liquid state. The melting method has no limitations on the alloys investigated for there is no reaction with crucible materials and the most refractory materials are easily melted. The rate of heating is so rapid that alloys that have a high vapor pressure constituent can be melted with a minimal loss in material. Several superconductors were discovered by rapid quenching of molten alloys. (auth)

15021 STUDY OF A HOMOGENEOUS SINTERED TUNGSTEN–HAFNIUM ALLOY. Tsukerman, S. A.; Kvin, V. E. pp 277-9 of Tr. VII Vses. Nauch. Tekh. Konf. por Met., Erevan, 1964. (In Russian).

A powdered W–6% Hf alloy compacted at 5 ton/cm^2 and sintered in vacuum of 10^{-3} mm Hg at 2100°C for 50 hr produced an equilibrium solid solution for cathode manufacture. The sintered briquettes, with an $Al(NO_3)_3 \cdot 9H_2O$ activator, are ground in a planetary mill to a fineness of 10 μ, washed to remove impurities, and vacuum annealed at 1500°C. Decomposition of the solid solution renders plasma atomization unsuitable for producing the powder alloy. (Rev. Metal Lit.)

15022 IMPROVEMENTS IN OR RELATING TO NUCLEAR FUEL MATERIALS. Bellamy, Roy Graham; Bourne, Leonard (to United Kingdom Atomic Energy Authority). British Patent 1,017,539. Jan. 19, 1966. Filed Dec. 17, 1963.

An alloy of U containing at least 100 ppM but less than 200 ppM of Fe and 150–1500 ppM of Al with the minimum total alloying addition being 350 ppM is β-quenched and α-annealed to produce a U alloy that is suitable for use as a nuclear fuel material. The resulting alloy has a fine grain size and good swelling resistance. (B.L.M.)

15023 IMPROVEMENTS IN OR RELATING TO NUCLEAR FUEL MATERIALS. Bellamy, Roy Graham; Bourne, Leonard (to United Kingdom Atomic Energy Authority). British Patent 1,017,540. Jan. 19, 1966. Filed Dec. 17, 1963.

A uranium alloy for use as a reactor fuel consists of 200 to 650 ppM of Fe and at least 100 ppM but less than 500 ppM of Al with the minimum total alloying addition being 350 ppM. The metals are melted by high frequency induction heating under vacuum and the alloy is cast into bars that are allowed to cool. The bars are heated to a temperature on the β-phase region and water quenched. After quenching, the bars are annealed at a temperature in the α-phase region. (B.L.M.)

15024 IMPROVEMENTS IN OR RELATING TO NUCLEAR FUEL MATERIALS. Bellamy, Roy Graham; Bourne, Leonard (to United Kingdom Atomic Energy Authority). British Patent 1,017,981. Jan. 26, 1966. Filed Dec. 17, 1963.

An alloy of U containing more than 1200 ppM but not more than 1500 ppM of Al and 200 to 650 ppM of Fe and the rest being U and incidental impurities is β-quenched and α-annealed to produce an alloy that is suitable for use as a nuclear fuel material. The resulting alloy has a smaller volume increase and swelling index than unalloyed U that has been subjected to the same heat treatment and conditions of irradiation. (B.L.M.)

15025 METHOD OF PREPARING COMPACTIBLE THORIUM OXIDE–PLUTONIUM OXIDE PARTICLES. Lloyd, M. H. (to U. S. Atomic Energy Commission). U. S. Patent 3,228,886. Jan. 11, 1966.

A method of making thorium oxide–plutonium oxide particles by mixing plutonyl nitrate with an aqueous phase containing thorium oxide, forming a sol from this mixture, evaporating the sol to form dried gel fragments, and then firing the dried fragments is presented. (AEC)

15026 SINTERED INTERMETALLIC BODIES COMPOSED OF ALUMINUM AND NIOBIUM OR TANTALUM. Beaver, Wallace W.; Paine, Robert M.; Stonehouse, Albert James (to Brush Beryllium Co.). U. S. Patent 3,231,344. Jan. 25, 1966. Filed Dec. 14, 1964.

A process is described for the fabrication of bodies composed of binary intermetallic compound-compositions consisting of Al and another metal M selected from the group consisting of Nb and Ta. The aluminum is present in the sintered body up to about, but not exceeding, its stoichiometric proportion corresponding the MAl_3. The sintered body formed by compacting and sintering the metal powders in a graphite has high strength and oxidation resistance at temperatures ranging from about 2000°F to about 2700°F. (B.L.M.)

15027 NEUTRON SHIELDING USING A COMPOSITION COMPRISING GRAPHITE, BORON CARBIDE AND CARBONIZED RESIDUE. Sturges, Donald G.; Bartholomew, George L. (to Carborundum Co.). U. S. Patent 3,231,521. Jan. 25, 1966. Filed May 24, 1961.

A relatively high density (1.5 to 2.0 g/cc) borated graphite body consisting essentially of graphite, finely divided B_4C, and the carbonized residue of a carbonaceous binder is patented for use as a neutron shielding material or in other applications in which refractoriness, good thermal insulating characteristics, structural strength, and controlled density are of importance. Crushed graphitic solids, finely divided B_4C, and a carbonaceous binder are mixed together; the mixture is cold pressed in a mold at pressures designed to give the desired density; and the green body is baked in a reducing atmosphere at a temperature sufficient to carbonize the binder. (B.L.M.)

Properties and Structure

See also CHEMISTRY — Inorganic and Physical Chemistry
PHYSICS — Solid State Physics

Refer also to abstracts 14506, 14693, 14823, 15004, 15297, 15943–15945, and 15998.

15028 (AGN–8166) ALKALI METALS EVALUATION PROGRAM. Quarterly Progress Report, July 1–September 30, 1965. Achener, P. Y.; Parr, E. E.; Melaika, E. A. (Aerojet-General Nucleonics, San Ramon, Calif.). Oct. 1965. Contract AT(04-3)-368. 23p. Dep. mn. CFSTI $1.00 cy, $0.50 mn.

Progress in the measurement of the thermodynamic and transport properties of the alkali metals is reported. (W.L.G.)

15029 (ANL–7070) MECHANICAL PROPERTIES OF URANIUM COMPOUNDS. Tottle, C. R. (Argonne National Lab., Ill.). Nov. 1965. Contract W-31-109-eng-38. 31p. Dep. mn. CFSTI $2.00 cy, $0.50 mn.

Mechanical tests, in which four-point loading was employed in bending, were performed at temperatures from room temperature to 2000°C, mainly in vacuo, on U compounds with O_2, S, and P. A brittle-ductile transition in UO_2 was shown to exist between 1250 and 1500°C. The effect of strain rate, atmosphere, density, and surface condition was outlined. US was tested in forms incorporating UOS and/or UO_2 as impurities. The ductile transition occurred around 1000°C for UOS-bearing material, and around 1250°C for US containing UO_2. UP containing about 1% UO_2 was shown to have a transition around 1250°C. UO_2 remained stronger than the others at all temperatures except 1000°C, but was less plastic. US containing UOS was consistently the weakest material. The temperature dependence of stress was remarkably similar in all the materials between 1250 and 1750°C. Specimens of all three compounds were (under appropriate conditions) bent to deflections exceeding 2.5 mm around the inner knife edges 6 mm apart and around the outer knife edges 30 mm apart. (auth)

15030 (ANL–7102) GROWTH AND ANNEALING OF EVAPORATED ALUMINUM–SILICON FILMS. Hart, R. K.; Pilney, D. G. (Argonne National Lab., Ill.). Nov. 1965. Contract W-31-109-eng-38. 13p. Dep. mn. CFSTI $1.00 cy, $0.50 mn.

The growth and annealing of aluminum films containing up to 3% silicon were studied by electron-microscope and electron-diffraction methods. The films were prepared by condensing the vapors from heated aluminum-silicon alloys onto rock-salt substrates. The textures and defect structures observed in these films, both before and after annealing, are discussed. (auth)

15031 (ANL–7116) A NEW TECHNIQUE FOR EXPERIMENTAL INVESTIGATION OF HIGH-TEMPERATURE THERMAL DIFFUSIVITY OF URANIUM DIOXIDE UNDER TRANSIENT CONDITIONS. Montgomery, Leslie D. (Argonne National Lab., Ill.). Nov. 1965. Contract W-31-109-eng-38. 43p. Dep. mn. CFSTI $2.00 cy, $0.50 mn.

Two UO_2 rods of different ^{235}U enrichment are bonded end to end. The combined rod is then exposed to a uniform, intense burst of neutron radiation, causing a temperature rise in each portion that is approximately proportional to its respective enrichment. The heat within the sample is generated internally by the fission process. By means of two thermocouples embedded within the rod a certain distance from the interface, the temperature difference between the two thermocouple positions can be measured as a function of time. If the temperature difference at a certain time is known, the thermal diffusivity of the sample may be determined by means of a formula. Another method from the same experiment involves measuring the slope of the photographic data trace. (W.L.G.)

15032 (ANL–7152, pp 50–72) GENERAL REACTOR TECHNOLOGY. (Argonne National Lab., Ill.).

Various results are presented on experimental and theoretical reactor physics, high temperature materials studies, reactor fuels and materials development, engineering development, chemical separations, sodium coolant chemistry, and the plutonium recycle program. (M.O.W.)

15033 (ANL–7152, pp 87–96) NUCLEAR SAFETY. (Argonne National Lab., Ill.).

A brief discussion of the experiments being performed in TREAT is presented. Various molten metals were dropped into 250°C sodium and their fragmentation temperatures were determined. Results are presented. (M.O.W.)

15034 (BNWL–49) THE LOW-TEMPERATURE ALLOTROPIC TRANSFORMATIONS IN PLUTONIUM. Nelson, R. D. (Battelle-Northwest, Richland, Wash. Pacific Northwest Lab.). Apr. 1965. Contract AT(45-1)-1830. 203p. Dep. mn. CFSTI $6.00 cy, $1.25 mn.

Transformation kinetics, phase transformation damage, steady-state creep, and effects of applied stress on phase transformations of Pu were investigated. These related phenomena are discussed and are correlated with similar information about more common metals. There are several characteristics of these phase changes that are consistent with either diffusional or martensitic transformations, but these data alone are insufficient to characterize them. Data for the $\beta \rightarrow \alpha$ and $\alpha \rightarrow \beta$ phase changes indicate martensitic transformations; data for the $\beta \rightarrow \gamma$ and $\gamma \rightarrow \beta$ phase changes are consistent with diffusional transformations. (auth)

15035 (BNWL–196) A STUDY OF TUNGSTEN–TECHNETIUM ALLOYS. Quarterly Progress Report, October 1, 1965–January 1, 1966. (Battelle-Northwest, Richland, Wash. Pacific Northwest Lab.). Jan. 3, 1966. Contract AT(45-1)-1830. 11p. Dep. mn. CFSTI $1.00 cy, $0.50 mn.

Illustrations of the fracture surfaces of Tc–W alloys revealing the effects of Tc content on the cast grain structures, results of density measurements of Tc–W alloys of different compositions, and a description of the technique used to hot roll pure Tc are presented. (W.L.G.)

15036 (BNWL–205) PLUTONIUM RELEASE STUDIES. I. RELEASE FROM THE IGNITED METAL. Mishima, J. (Battelle-Northwest, Richland, Wash. Pacific Northwest Lab.). Dec. 13, 1965. Contract AT(45-1)-1830. 26p. Dep. mn. CFSTI $2.00 cy, $0.50 mn.

Six plutonium rods, ¼-inch in diameter and ¾-inch in length, were ignited in dry air at temperatures ranging from 410 to 650°C. Air drawn over the specimens at velocities ranging from 3.3 to 50 cm/sec was examined for particulate plutonium oxide. Plutonium oxide entrained ranged from 3×10^{-6} to 5×10^{-5} wt. %. The entire oxide produced was subsequently sized using an elutriation-sieving technique. The quantity of particulate material less than 15 microns was found to depend upon the mechanical work used in sizing the particles. Particles equivalent to less than 15 microns in diameter represented as much as

0.03 wt. % of the total oxide and 70–80 per cent of this material was less than 0.1 micron in size. Oxidation conditions producing internal stresses in the oxide increased friability. Less friable oxides were produced by high oxidation temperatures. Increasing particle size was found with increasing oxidation temperatures. The amount and rate of release under any stated conditions was dependent on friability and the forces to which the oxide mass was subjected. Results were compared with other data available relating to particle size and fractional release from ignited plutonium. Reasonable agreement was noted. (auth)

15037 (CEA-R-2621) ETUDE DE LA DIFFUSION DU FER, DE L'ARGENT ET DU CARBONE DANS LE BERYLLIUM AU MOYEN DES TRACEURS RADIOACTIFS [Theses]. (Study of the Diffusion of Iron, of Silver and of Carbon in Beryllium Using Radioactive Tracers [Thesis]). Naik, Mool Chandra (Commissariat a l'Energie Atomique, Saclay (France). Centre d'Etudes Nucleaires). 1965. 50p. Dep. mn.

Submitted to Paris Univ. (France). Faculte des Sciences.

A study was made on the diffusion of radioactive iron and silver tracers in beryllium. The following values were found: $D_{Fe} = 0.53 \exp - (51{,}800/RT)$, $D_{Ag} = 6.2 \exp - (46{,}100/RT)$. A comparison of the diffusion coefficients for iron, silver, and nickel showed that the diffusion rate increased with increasing solute atom radius. The existence of diffusion anisotropy for silver was indicated and studied quantitatively on monocrystals. The anisotropy decreased as the temperature increased. The silver diffused more rapidly along the C axis than in the base plane. This result cannot be explained in terms of the model proposed for the diffusion of foreign atoms in solution in zinc. A greater number of experiments is required before a model can be put forward. An attempt was made to determine the diffusion coefficients of carbon in beryllium by treatment in an atmosphere of acetylene marked with C-14. Diffusion coefficients were obtained but these should not be considered to be significant since a chemical reaction occurred at the surface of the samples. (J.B.)

15038 (CONF-660305-12) ^{244}Cm FOR RADIOISOTOPIC HEAT SOURCES WORK AT THE SAVANNAH RIVER LABORATORY. McDonell, W. R.; Smith, P. K.; Shurcken, E. F.; Livingston, J. T.; Thompson, M. C.; Mosley, W. C. Jr. (Du Pont de Nemours (E. I.) and Co., Aiken, S. C. Savannah River Lab.). Feb. 1966. Contract AT(07-2)-1. 17p. Dep. mn. CFSTI $1.00 cy, $0.50 mn.

From American Nuclear Society Topical Meeting, Augusta, Ga.

Preliminary studies of the curium-oxygen system have demonstrated the existence of five compounds of lower oxygen content than CmO_2. One or two of these oxides appear to be sufficiently refractory to fuel a high-temperature heat source. Thermal and physical properties of these and other compounds of curium and their compatibility with refractory containment metals are being determined. A facility specifically designed for studying properties of small quantities of curium-244 and other alpha-emitting compounds is nearing completion, and shielded facilities for handling larger quantities are being designed. (P.C.H.)

15039 (EURAEC-1475) A STUDY ON PLASTIC FATIGUE EMBRITTLEMENT OF REACTOR VESSEL STEELS. Quarterly Report No. 7, July 1–September 30, 1965. (Centre National de Recherches Metallurgiques, Liege (Belgium)). Oct. 1965. Contract 005-63-12TEEB. 49p. (EUR-2396). Dep. mn. CFSTI $2.00 cy, $0.50 mn.

Work Performed under United States–Euratom Joint Research and Development Program.

The Charpy-V-notch impact strength properties of A 302 B, Ducol W30, and Soudotenax 56 steels after various types of damage by plastic fatigue under compression-tension were studied. An investigation was made on the effects of alternate plastic deformation cycles according to various cycle rates at a temperature of 300°C. A few Charpy-V-notch embrittlement tests were also carried out on one of the steels that had undergone artificial aging at 300°C after fatigue at ambient temperature. The results obtained confirm some of the observations made previously, namely, that the impact strength, after plastic fatigue at 20°C, seems to increase in the low temperature region. On the other hand, plastic fatigue at 300°C seems to cause a noticeable embrittlement, which is evidenced by a slip in the transition curve. Such a slip is of the same order of magnitude as that produced by strain-hardening and aging, though slightly above it for two of the steels under examination. (auth)

15040 (GA-6721) A PROGRAM OF BASIC RESEARCH ON MECHANICAL PROPERTIES OF REACTOR MATERIALS. Annual Summary Report, November 1, 1964–October 31, 1965. Trozera, T. A.; Appel, J. C.; Chambers, R. H. (General Atomic, San Diego, Calif. John Jay Hopkins Lab. for Pure and Applied Science). Dec. 22, 1965. Contract AT(04-3)-167. 68p. Dep. mn. CFSTI $3.00 cy, $0.75 mn.

Work was performed on resistivity and mechanical property measurements of bcc metals; several source materials of Mo were evaluated; and preliminary irradiations were performed on W single crystals. Emphasis was placed on obtaining good resistivity measurements by means of the potential-drop method. This method was chosen as the most suitable for evaluating the purity of the W crystals and for following the changes in a crystal during annealing after both cold work and neutron irradiation. Annealing methods were developed first on a cold-worked W single crystal and extended to include measurements performed on an irradiated W crystal. Measurements on the irradiated crystal called for the development of specialized equipment so that the work could be safely performed in the laboratory without undue complication. Isochronal annealing data were obtained on both an ~20% cold-worked W single crystal and a crystal irradiated with fast neutrons to a dose of $\sim 2 \times 10^{19}$ nvt. Several important experimental features discovered in the oscillating-stress amplitude-dependent internal friction and modulus of very high purity bcc transition metals were explained by the use of a very simple dislocation model. The model is based on the assumption of the existence of sizable Peierls-Nabarro stresses and Peierls potentials, and the existence of significant dislocation-dislocation interactions, resulting in long-range stress fields and static hysteresis phenomena (frequency-independent internal friction). It was shown that the superposition of a static bias stress leads to useful observations concerning the nature of the model of oscillating-stress amplitude dependence. The long-range stress-center model for internal friction should represent the effect of sources of stress centers other than those due to dislocation-dislocation interaction; e.g., neutron irradiation zones should be revealed as a modification of the existing internal stress fields and thus should be measurable via amplitude dependence in high-purity crystals. It is very important to note, however, that only in very high purity crystals were the details of the internal stress contributions to the internal friction observable. (W.L.G.)

15041 (GEMP-397) PROPERTIES OF SOME REFRACTORY METALS. V. NUMERICAL METHODS FOR CREEP AND RUPTURE ANALYSES. Conway, J. B. (General Electric Co., Cincinnati, Ohio. Nuclear Materials and Propulsion Operation). Jan. 31, 1966. Contract AT(40-1)-2847. 277p. Dep. mn. CFSTI $6.00 cy, $1.50 mn.

The commonly employed equations used to express strain-time behavior are discussed. In addition to considering those equations applicable to the transient creep process, several expressions capable of representing combined first- and second-stage creep data are discussed. Special least squares techniques developed for calculating creep equation constants are described in detail and are applied to the analysis of various strain-time measurements. Also, numerical techniques employed in the correlation of steady-state creep rates are considered. And finally, the numerical methods more commonly employed for use in the analysis of rupture data are reviewed to the extent that the basic mathematical procedures are outlined. (auth)

15042 (IITRI-578-P27-14) YIELD PHENOMENA AND FRACTURE OF HYDRIDED ZIRCONIUM. Quarterly Report, October 1–December 31, 1965. Weinstein, D.; Broverman, I. (IIT Research Inst., Chicago, Ill.). Feb. 3, 1966. Contract AT(11-1)-578. 13p. (EURAEC-1576). Dep. mn. CFSTI $1.00 cy, $0.50 mn.

Work Performed under United States–Euratom Joint Research and Development Program.

Previous work showed that the yield point in fine-grained (0.0037-mm grain dia) Zr disappeared as the temperature was lowered from 23 to −196°C. The strain hardening coefficient concomitantly increased progressively. The yield point and strain hardening behavior were consistent with the model developed by Johnston and Hahn. The results suggest that a dynamic dislocation mechanism controlled the observed yield point phenomena. An attempt was made to reproduce and explain the reversal in the temperature dependence of yield point that Keeler found in relatively coarse-grained Zr. Following from the Johnston-Hahn model, it was logical to expect that such a reversal should be accompanied by a reversal of strain hardening coefficient, i.e., decreased strain hardening rate at lower temperatures (−196°C) at which a yield point appeared. For materials annealed so as to produce 0.005- and 0.009-mm grain sizes, no yield point reversal was observed. Since grain size is especially critical, another series of tests is proposed (based on 0.007-mm grain size) before a definite conclusion concerning yield point and strain hardening reversal can be reached. (auth)

15043 (LA-3436) THE SOLUBILITIES OF SELECTED ELEMENTS IN LIQUID PLUTONIUM. VII. NIOBIUM. Bowersox, D. F.; Leary, J. A. (Los Alamos Scientific Lab., Univ. of California, N. Mex.). Nov. 1, 1965. Contract W-7405-eng-36. 13p. Dep. mn. CFSTI $1.00 cy, $0.50 mn.

The solubility of Nb in liquid Pu was measured over the temperature range 700 to 1000°C. The solubility increased from 0.43% (by weight) Nb at 700°C to 1.48% Nb at 1000°C. The data fit the equation $\log N_{Nb} = 0.2771 - 2.183 \times 10^3\ T^{-1}$, where N_{Nb} is the solubility expressed as the mole fraction and T is the temperature in degrees Kelvin. The solubility of Nb in liquid alloy, which initially was 49.3% (by weight) Pu, 40.8% Ce, and 9.9% Co, was measured from 500 to 900°C. The solubility increased from 0.053% (by weight) Nb at 500°C to 0.55% Nb at 900°C. The data fit the equation $\log X_{Nb} = -0.152 - 2.243 \times 10^3\ T^{-1}$, where X_{Nb} is the solubility expressed as the mole fraction and T is the temperature in degrees Kelvin. (auth)

15044 (MCW-1493, pp 15-25) X-RAY DETERMINATION OF THE CRYSTALLITE SIZE OF THORIA. Stoecker, W. C.; Starbuck, J. W. (Mallinckrodt Chemical Works, Weldon Spring, Mo. Uranium Div.).

The effects of several sample preparation variables on the determination of crystallite size are discussed. A method is described for determining crystallite size directly on a sol. A revised method of calculating crystallite size was observed to give values that correlate better with denitration temperatures and other variables than the values calculated normally. Crystallite sizes calculated by the revised method were unchanged when the samples were milled or converted to sols. (auth)

15045 (N65-15534) MAGNETIC SUSCEPTIBILITIES OF COMPOSITIONS IN TANTALUM-TANTALUM CARBIDE SYSTEM. Santoro, Gilbert J. (National Aeronautics and Space Administration, Cleveland, Ohio. Lewis Research Center). Jan. 1965. 13p. (NASA-TN-D-2638). CFSTI $1.00 cy, $0.50 mn.

In the Ta−TaC system, magnetic susceptibility measurements were performed on powder samples; and lattice parameter determinations were conducted on powder and filament specimens. A maximum diamagnetism was observed at $TaC_{0.8}$. The entire Ta_2C phase proved to be paramagnetic, and the results indicated that the zeta phase is diamagnetic. The dissolution of C in Ta reduced its paramagnetism. The minimum in the susceptibility at $TaC_{0.8}$ could be accounted for by applying the bonding concepts of either Bilz or Dempsey, although their approaches are basically different. Lattice parameters were determined on the powder samples throughout the entire Ta−TaC system and on the filament samples in the TaC phase. The variation in the lattice parameter was nonlinear in the high-C end of the fcc phase region. The x-ray data from the carbide filament specimens agreed with those from the powder specimens and with the previously reported data from filaments. (STAR)

15046 (N65-15820) INVESTIGATIONS OF CARBIDES AS CATHODES FOR THERMIONIC SPACE REACTORS. Informal Monthly Report, April 1963. Yang, L.; Weinberg, A. F.; Carpenter, F. D.; Horner, M. H.; Hudson, R. G. (General Atomic, San Diego, Calif. John Jay Hopkins Lab. for Pure and Applied Science). June 6, 1963. Contract NAS3-2532. 29p. (NASA-CR-60404; GACD-43-12). CFSTI $2.00 cy, $0.50 mn.

The rate of vaporization of UC−ZrC cells for 1000-hr runs was established. The two cells were outgassed. The 30 UC−70 ZrC and the 90 UC−ZrC samples were prepared. The 90 UC−10ZrC sample is being outgassed. The second metallurgical life and performance test cell (MLP-B) containing a vapor-deposited W-clad UC emitter was operated for 110 hr. Studies of the controlling factors of vaporization, emission, and the mechanical properties of the UC−ZrC systems were made in relation to high-temperature properties. Studies of the irradiation properties were made for the unclad carbide and the clad capsules. Studies of new cathode materials, 30 UC−70 NbC, 90 UC−10 NbC, 30 UC−70 TaC, and 90 UC−10 TaC, were made for vacuum emission and vaporization. The diffusion and diffusion-emission samples were prepared. (STAR)

15047 (N65-15919) STUDY OF GROWTH PARAMETERS FOR REFRACTORY CARBIDE SINGLE CRYSTALS. Quarterly Status Report No. 3, September 1–December 1, 1964. Halden, F. A.; Eding, H. J. (Stanford Research Inst., Menlo Park, Calif.). Jan. 29, 1965. Contract NASr-49(19). 31p. (NASA-CR-60437). CFSTI $2.00 cy, $0.50 mn.

A theoretical analysis of high-temperature behavior of carbides during fusion crystal growth indicated that it should be possible to maintain single-phase compositions at the melting point. Polished sections and x-ray lattice constant measurements confirmed that, under suitable conditions, carbides can be arc melted without significant shifts in stoichiometry. It appeared that control of the composition of the gaseous environment may permit significant variations in carbide stoichiometry within the single-phase region. Melting of the carbides in the r-f plasma was not attained. Initial carbon solubility runs were completed on germanium, germanium-10 at.% hafnium, aluminum-10 at.% hafnium, and iron-10 at.% hafnium alloys. As a result of these runs, germanium was eliminated from consideration because it was not possible to separate the carbide crystals from the solvent at the completion of a run. Carbon solubilities in the aluminum–hafnium alloy appeared very close to those for silicon, which is employed for the growth of silicon carbide crystals. (STAR)

15048 (N65-16231) AN EVALUATION OF VAPOR-DEPOSITED TUNGSTEN TUBING. Mills, R. G.; Lindgren, J. R.; Weinberg, A. F. (General Atomic, San Diego, Calif. John Jay Hopkins Lab. for Pure and Applied Science). Oct. 19, 1964. Contract NAS3-4165. 39p. (NASA-CR-54277; GA-5721). CFSTI $2.00 cy, $0.50 mn.

Tests were performed on 17 samples of vapor-deposited tungsten tubing. It was concluded that: the chemical impurity content was comparable; the metallic impurities were at a low level; a positive correlation existed between the residual fluorine content and the ductile-to-brittle transition temperature; extruded tungsten tubing had a low fluorine content; the lowest fluorine content of vapor-deposited tubing was comparable to that of the extruded tubing; tubes of stable structure showed little grain growth; highly oriented deposited columnar structures showed less grain growth than the less oriented deposited structure; grain growth of vapor-deposited tubing was not primarily related to the chemical impurity content; extensive grain growth

took place in extruded tubing during heat treatment; and the ductile-to-brittle transition temperatures of extruded tubing and of vapor-deposited tubing were comparable. There was no correlation between hardness and any other variable. (STAR)

15049 (N65-16256) IMPROVEMENT OF CREEP STRENGTH AND LOW-TEMPERATURE DUCTILITY OF REFRACTORY METALS BY MEANS OF MECHANICAL TWINNING. Quarterly Progress Report No. 1, September 1–November 30, 1964. Edington, J. W. (Battelle Memorial Inst., Columbus, Ohio). Contract NASr-100(05). 14p. (NASA-CR-60540). CFSTI $1.00 cy, $0.50 mn.

Three metals were investigated: niobium, tungsten, and niobium–40 wt % vanadium alloy. The niobium alloy was chosen for an evaluation of the high-temperature strengthening mechanism. Niobium and tungsten were used to evaluate the possible improvement of ductility at low temperatures, because a comparison of the behavior of materials known to behave in a ductile and in a brittle manner was considered important. The niobium alloy was produced as a drop casting after melting niobium and vanadium in a nonconsumable-electrode electric-arc furnace. The niobium and tungsten were produced industrially in rod form. Each metal or constituent was originally commercially pure. The results are presented graphically and are discussed for high-temperature strengthening, for twin stability at high temperatures, and for ductility improvement at low temperatures. (STAR)

15050 (NLCO-970, pp 3.1-4) COMPARISON OF ELECTROLYTIC AND FERROSILICON-PROCESS MAGNESIUMS FOR URANIUM PRODUCTION. Mautz, E. W.; Bonfer, D. C. (National Lead Co. of Ohio, Cincinnati).

Electrolytic magnesium (Dow Grade 6) was found to be equivalent to ferrosilicon-process magnesium (Nelco cutcrown) for uranium production operations. Uranium derby and ingot yields, as well as ingot analyses, showed equivalent results between the two magnesium types. A specification range for iron in magnesium of 250 to 350 ppM is needed to meet the present uranium specifications. (P.C.H.)

15051 (NP-15876) HEAT RESISTANCE OF CONCRETE SUBJECT TO LASTING TEMPERATURES OF 300-350 DEG C. Summary of Literature, and a Proposed Experimental Study. Martna, J. (Swedish State Power Board, Stockholm). Dec. 11, 1964. 11p. Dep. mn.

The phenomena that occur in concrete subjected to elevated temperatures are: Hydrated portland cement changes its structure owing to a successive recrystallization of cement minerals. This results in loss of water, shrinkage, loss of strength, and formation of potentially deleterious substances, particularly calcium hydroxide. Hydrated portland cement shrinks during the first heating cycle, whilst the aggregate expands. This results in internal stresses and weakening of the bond between cement and aggregate. Because of these phenomena, the usability of normal concrete at elevated temperatures is limited. There are, however, possibilities to improve the heat resistance of concrete by using suitable aggregates and finely ground admixtures. An experimental study of these problems is proposed. (auth)

15052 (NP-15880) DISSOCIATION AND EVAPORATION OF TaC, HfC, AND ZrC AT ELEVATED TEMPERATURES. Technical Memorandum 62-475.2. Seigle, L.; Resnick, R.; Steinitz, R. (General Telephone and Electronics Labs. Inc., Bayside, N. Y.). Nov. 9, 1962. 24p.

The composition dependence of the thermodynamic activities and vapor pressures of metal and carbon in TaC, HfC, and ZrC at elevated temperatures were calculated on the basis of Wagner's equations of state for solutions with substantially ordered atomic distribution. At the stoichiometric composition the activity of carbon in these compounds is unity, and the vapor pressure equal to that over pure graphite. The activity and vapor pressure of carbon decrease very rapidly with decreasing carbon content, while those of the metal increase. For ZrC and probably also HfC, the molar evaporation rates of metal and carbon in vacuum become identical at a specific composition within the homogeneity range of the carbides and this represents a constant evaporating composition. For TaC, at similar temperatures, the molar rate of evaporation of carbon is considerably above that of the metal at all compositions within the homogeneity range, and therefore a progressive decarburization of this material in vacuum will occur leading to its ultimate decomposition to the lower carbide. (auth)

15053 (NUMEC-3428-17) GROWTH OF SINGLE CRYSTALS OF PLUTONIUM. Progress Report, October 1–December 31, 1965. (Nuclear Materials and Equipment Corp., Apollo, Pa.). Feb. 1, 1966. Contract AT(30-1)-3428. 9p. Dep. mn. CFSTI $1.00 cy, $0.50 mn.

High-purity alpha-Pu was subjected to pressures of 31 to 78 kilobars for 1 hr at temperatures from 350 to 475°C and examined metallographically. The resultant grain sizes did not appear to be a function of the varied parameters. (W.L.G.)

15054 (NUMEC-3505-11) UO_2–PuO_2–ZrO_2 FUEL DEVELOPMENT PROGRAM. Progress Report, October 1, 1965–December 31, 1965. (Nuclear Materials and Equipment Corp., Apollo, Pa.). Jan. 25, 1966. Contract AT (30-1)-3505. 41p. (EURAEC-1563). Dep. mn. CFSTI $2.00 cy, $0.50 mn.

Work Performed under United States–Euratom Joint Research and Development Program.

Studies to develop the $UO_2-PuO_2-ZrO_2$ fuel system were continued. The fuel compositions investigated include 4, 6, 10, and 12 vol % PuO_2 and 25, 50, and 75 vol % ZrO_2, the remainder being UO_2. The enriched-uranium ceramic powders were prepared by coprecipitation. Test pellets of these were sintered to densities in excess of 90% of theoretical. Production pellets were prepared for most of the compositions. Thermophysical studies of the $UO_2-PuO_2-ZrO_2$ system were continued. X-ray crystallographic data were obtained as part of the phase diagram studies. Preliminary data were obtained for melting points, thermal expansion, thermal cycling stabilities, and air oxidation stabilities. (W.L.G.)

15055 (NYO-2394-19) A COMBINED MACROSCOPIC AND MICROSCOPIC APPROACH TO THE MECHANICAL PROPERTIES OF METALS. Progress Report, February 1965–January 1966. Drucker, D. C.; Gurland, J. (Brown Univ., Providence, R. I. Div. of Engineering). Contract AT(30-1)-2394. 9p. Dep. mn. CFSTI $1.00 cy, $0.50 mn.

A method of sample preparation of the two-phase alloy Al–Si for electron transmission studies was developed and the flow strength and fracture strength as function of particle size and concentration of the two-phase alloys Al–Si and Fe–Fe_3C (spheroidized steel) was determined. A theoretical analysis concerned itself with the role of inclusions as sources of plastic deformation both from the dislocation and continuum points of view. It was shown that the increased resistance to additional slip of particle strengthened metals is due, not to the particle strength itself, but mainly to the expanding network of intersecting slip triggered by the particles. A significant advance was achieved also on the problem of characterizing the long range continuity of a particulate phase randomly distributed. (auth)

15056 (NYO-2916-10) A STUDY OF THE THERMODYNAMIC PROPERTIES OF INTERMETALLIC COMPOUNDS. Technical Progress Report. (New York Univ., N. Y. Dept. of Metallurgy and Materials Sciences). Oct. 1965. Contract AT(30-1)-2916. 23p. Dep. mn. CFSTI $1.00 cy, $0.50 mn.

The activity and partial molar enthalpy of solution of Mg in liquid Mg–Ge alloys was determined by an improved isopiestic method and the results given. A theory of retrograde solubility for semiconducting AB compounds is discussed, and the growth and equilibration experiments performed on magnesium stannide monocrystals are described. (W.L.G.)

15057 (PWA-2750) DETERMINATION OF THE EMISSIVITY OF MATERIALS. Semiannual Progress Report, May 15–November 14, 1965. Luoma, W. (Pratt and Whitney Aircraft, East Hartford, Conn.). Dec. 20, 1965. Contract NAS3-4174. 41p. (NASA-CR-54891).

On the basis of at least 10,000 hrs of emittance testing and related adherence testing, it is concluded that iron titanate on either AISI-310 stainless steel or on Nb–1 Zr and calcium titanate on AISI-310 stainless steel are suitable for space radiator use at 1350°F (with a stainless steel substrate) or 1700°F (with a Nb–1 Zr substrate). All of these material combinations are unaffected by thermal cycling and have demonstrated good adherence properties during fatigue testing. Iron titanate applied to Nb–1 Zr has an emittance between 0.88 and 0.84. When applied to AISI-310 stainless steel, it has an emittance between 0.89 and 0.88. Calcium titanate on AISI-310 stainless steel has an emittance between 0.91 and 0.89. Aluminum oxide–aluminum titanate on Nb–1 Zr does not appear to be suitable for space radiator applications at 1700°F. After 5300 hrs of testing at this temperature, the emittance dropped from 0.87 to 0.82. The aging of Be plates coated with calcium titanate for 500 hrs at 800°F does not appear to produce any significant changes in either the coating or the substrate. Aging Be plates coated with iron titanate for 100 hrs at 800°F also produces no significant changes. The emittance of a Be strip coated with iron titanate was found to be between 0.89 and 0.90 over a temperature range from 800 to 1100°F during 670 hrs of testing. (auth)

15058 (SC-DC-66-1130) IMPROVING THE MECHANICAL PROPERTIES OF SLIP-CAST FUSED SILICA BY FIBROUS REINFORCEMENT. Final Report, July 1, 1964–June 30, 1965. Corbett, W. J.; Sales, A. T.; Walton, J. D. Jr. (Georgia Inst. of Tech., Atlanta. Engineering Experiment Station). Contract AT(29-1)-789, Subcontract 16-2082. 42p. Dep. mn. CFSTI $2.00 cy, $0.50 mn.

For Sandia Corp., Albuquerque, N. Mex.

The mechanical properties of slip-cast fused silica containing discontinuous, randomly-oriented, ceramic fibers were investigated. The reinforcements investigated were an amorphous aluminosilicate fiber, a zirconia fiber, a synthetic mullite fiber, and silicon carbide whiskers. Three techniques were developed for producing slips containing fiber and finely-divided silica. These were: ball milling of fiber and fused silica slip, blending of dried and reground fused silica slip with chopped fiber and water, and direct incorporation of whiskers into fused silica slip. Casting slips with fiber concentrations as high as 50 vol % were obtained using the ball milling technique. The percent solids content of the fiber slips was dependent on the volume percent fiber and was in the 70 to 82% range. The slips were cast, using plaster molds, as flat plates, cylinders, and a small radome shape. Good fiber dispersion was obtained with a random orientation of the fiber. The sintering parameter that most influenced the mechanical properties of these composites was the cristobalite content. This parameter was established for a firing temperature of 2200°F. Sintering time was varied to control the cristobalite formation for a particular volume percent fiber in the slip. The variation of elastic modulus with percent cristobalite and percent of theoretical density, modulus of rupture, tensile strength, and impact strength for fused silica were used as standards to determine any degree of fiber reinforcement. Although no reinforcement was detected, volumes of 2½ and 5% synthetic mullite and 2½% zirconia fibers were not detrimental to the mechanical properties of fused silica when evaluated on the basis of percent of theoretical density for fused silica. The elastic moduli of 5% zirconia fiber and 7½% silicon carbide whiskers were respectively 50 and 25% greater than fused silica at the same porosity. When used to determine the strength of composites that are dependent on short fibers for reinforcement, the value of the modulus of rupture test was challenged since the geometric computations are based on the strength of the outer surfaces. Since the surfaces of these composites did not contain appreciable amounts of fiber, this critique seemed confirmed by the test results. Similarly the significance of the Izod impact strength and tensile strength, using the diametral compression test, were critically analyzed. The value of Weibull statistics in the analysis of these data for brittle materials demonstrated the value of the tensile strength test. It was demonstrated that the incorporation of discontinuous, randomly-oriented, ceramic fibers into slip-cast fused silica is possible, without sacrificing the fabrication advantages of the slip-casting process. The feasibility of obtaining significant improvements in the physical properties of slip-cast fused silica by the incorporation of discontinuous, randomly-oriented, ceramic fibers was not conclusively demonstrated. (auth)

15059 (SWRI-1228-1-20) STUDIES OF THE FATIGUE STRENGTH OF PRESSURE VESSELS. 1. CYCLIC PRESSURE TESTS OF LARGE SIZE PRESSURE VESSELS. 2. LOW CYCLE FATIGUE TESTING OF ONE-HALF SCALE MODEL PRESSURE VESSELS. 3. EFFECT OF WELD DEFECTS ON THE FATIGUE STRENGTH OF A302B STEEL. Progress Report No. 17. Pickett, A. G.; Grigory, S. C.; Robinson, C. G. (Southwest Research Inst., San Antonio, Tex.). Jan. 1, 1966. Contract AT(11-1)-1228. 37p. (SWRI-1228-2-20; SWRI-1228-5-20). Dep. mn. CFSTI $2.00 cy, $0.50 mn.

Test specimens were fabricated from a ring cut from the shell of the PM-2A model and the mechanical properties measured. Data on the effects of weld defects on the fatigue strength of A302B steel obtained during the current and prior report periods are summarized, but no conclusions given. (W.L.G.)

15060 (UCRL-7771) MECHANICAL PROPERTIES OF SOME URANIUM ALLOYS. Peterson, C. A. W.; Vandervoort, R. R. (Lawrence Radiation Lab., Univ. of California, Livermore). Mar. 18, 1964. Contract W-7405-eng-48. 6p. (CONF-640416-1). Dep. mn. CFSTI $1.00 cy, $0.50 mn.

From Joint Working Group Meeting, Aldermaston, Berks, Eng.

Mo, Nb, and Zr were added separately and in combination to U and the properties of the gamma-phase alloys measured at room and elevated temperatures. (W.L.G.)

15061 (UCRL-11580) APPARATUS FOR HEAT CAPACITY MEASUREMENTS IN THE RANGE 0.24 TO 20 DEG K; APPLICATIONS TO SOME TRANSITION-METAL SUPERCONDUCTORS AND FERROMAGNETIC-SUPERCONDUCTORS [Thesis]. Batt, Russell Howard (Lawrence Radiation Lab., Univ. of California, Berkeley). Sept. 1964. Contract W-7405-eng-48. 68p. Dep. mn. CFSTI $3.00 cy, $0.75 mn.

An apparatus (described) was developed for the measurement of heat capacities in the temperature range from 0.24 to 20.0°K. The heat capacity of Ru was measured from 0.27 to 1.20°K, and the heat capacities of Ti and Fe–Ti (0.05, 0.25, and 1.00% Fe) were measured from 0.24 to 4.20°K. The heat capacities of two solid solutions of $GdOs_2$–YOs_2 were measured in the temperature range from 0.25 to 20.0°K. The superconducting properties of the materials were studied on the basis of the results. (D.C.W.)

15062 (UCRL-16514) VAPOR PRESSURE OF LEAD AND ACTIVITY MEASUREMENTS ON LIQUID LEAD–TIN ALLOYS BY THE TORSION EFFUSION METHOD [Thesis]. Hawkins, Donald Thomson (Lawrence Radiation Lab., Univ. of California, Berkeley). Jan. 1966. Contract W-7405-eng-48. 30p. Dep. mn. CFSTI $2.00 cy, $0.50 mn.

The vapor pressure of pure lead was measured in the temperature range between 950 and 1105°K. The selected $\Delta H^0_{v,298} = 46620 \pm 170$ cal/gm-atom agrees very well with previous measurements. Vapor pressures of lead over liquid lead–tin alloys were determined over the entire composition range. From these measurements and the Gibbs-Duhem relation, Gibbs energy values for both components were calculated. Correlation with existing heat of formation data allowed determination of entropy values. No surface depletion was found for these liquid alloys. (auth)

15063 (UCRL-16585) STRAIN AGING OF IRON ALLOYS [Thesis]. Busch, Raymond Andrew (Lawrence Radiation Lab., Univ. of California, Berkeley). Jan. 1966. Contract W-7405-eng-48. 53p. Dep. mn. CFSTI $3.00 cy, $0.50 mn.

The strain aging of Fe–Mo and Fe–Cr–Mo alloys was investigated. Large strengthening effects are observed

in both alloys during strain in the 400–500°C range, and in the room temperature properties after this strain. The variation of these effects with impurity content in the Fe–Mo alloy indicates that interstitial solutes are not responsible for the strengthening. The aging of specimens strained at room temperature obeys an activation energy of 42 kcal/mole and $t^{\frac{1}{3}}$ kinetics. This behavior is interpreted according to the Cottrell-Bilby model for strain aging. The data indicate that a similar process occurs during strain at higher temperatures, which requires the existence of strain enhanced diffusion. The magnitude of this enhancement is estimated as ~100, i.e., the diffusivity during deformation under these conditions is about 100 times greater than the normal diffusivity at the same temperature. (auth)

15064 (AD–625748) DEVICE FOR X-RAY STRUCTURAL ANALYSIS OF RADIOACTIVE MATERIALS. Gribanov, Yu. I.; Karmilov, A. G.; Lednev, I. A. Translation of Russian Patent 155318. Mar. 23, 1962. 5p. (FTD-TT-65-977). CFSTI $1.00 cy, $0.50 mn.

The design of a diffractometer was modified to include a modulator between the x-ray tube and the sample. The design of the modulator is included. (W.L.G.)

15065 (ORNL-tr-1018) STUDIES OF THE ADSORPTION OF IODINE ON ACTIVATED CARBON. II. POTENTIOMETRIC STUDIES AT DIFFERENT TEMPERATURES. Jankowska, Helena. Translated for Oak Ridge National Lab., Tenn., from Prezem. Chem., 44: 235-9(1965). 13p. Dep. mn. JCL $1.60 fs, $0.80 mf.

Continuation of previous work on the adsorption of iodine on activated carbon is described. Adsorption and Langmuir isotherms were determined potentiometrically at two temperatures: 50 ± 0.5 and 0 ± 0.5°C. The results of previous work at 25 ± 0.5°C were also used in calculations. For a given equilibrium concentration the greatest surface concentration of iodine on carbon was obtained at the lowest temperature, 0°C, and the smallest at 50°C. An investigation was made on the influence of the potassium iodide concentration in solution on the course of the potentiometric adsorption isotherm. It was found that the lower the concentration, the higher the surface concentration obtained for the same concentrations in a state of equilibrium. (J.B.)

15066 ANNEALING OF URANIUM QUENCHED FROM 100 TO 4.2 DEG K. Jousset, J. C. (Centre d'Etudes Nucleaires, Fontenay-aux-Roses, France). Acta Met., 14: 193-200(Feb. 1966). (In French).

Zone melted uranium quenched from 100°K in liquid helium shows important increases in resistivity that disappear after annealings at very low temperatures (5 to 30°K). This phenomenon is explained by the existence of a very mobile defect of interstitial nature, as this is confirmed by neutron irradiations at 4.5°K and electron irradiations at 6°K. After quench, isochronal and isothermal annealings were made on samples with different crystalline state and purities. The defect migration energy by the tangents method was also calculated. (auth)

15067 THE FRICTION STRESS AND MICRO-YIELDING OF BERYLLIUM. Lawley, A.; Meakin, J. D. (Franklin Inst. Research Labs., Philadelphia). Acta Met., 14: 236-8(Feb. 1966).

Comments are made on a paper on the microstrain behavior of polycrystalline Be by Bonfield and Li (Acta Met. 13: 317(1965)). The derivation and techniques used to obtain the friction stress (σ_F) from the results on hot pressed Be and annealed and prestrained Be samples are questioned. The friction stress is related to the energy dissipated in generating a closed hysteresis loop (ΔW) and the maximum forward plastic strain ($\Delta\gamma$) by the relation: $\Delta W = 2\sigma_F\Delta\gamma$. It is proposed that there are two independent plastic flow processes with different frictional stresses. A reply to the comments is included. (W.L.G.)

15068 COLUMBIUM D43 (HIGH TEMPERATURE ALLOYS). Alloy Dig., Cb-9, 2p.(June 1965).

D-43 is a Nb-base alloy with inhibited grain growth during prolonged exposure at high temperature. The alloy contains 9.0 to 11.0% W, 0.75 to 1.25% Zr and 0.12% C and is recommended for high-temperature service. The tensile strength and yield strength of a 0.030-in. thick sheet are 92,000 and 78,000 psi at room temperature 8000 and 5000 psi at 3000°F. Curves of variation of static modulus vs temperature and of life vs stress are given. (Rev Metal Lit.)

15069 OREMET HPC 85W–15Mo (HIGH TEMPERATURE REFRACTORY ALLOY). Alloy Dig., W-9, 2p. (Aug. 1965).

OREMET HPC Alloy Dig. is a vacuum consumable electrode melted and centrifugally cast refractory W alloy having 100% density. Mo content ranges from 14 to 16%, C, O_2, Fe, and Si levels are less than 0.010%. Room temperature mechanical properties for a 0.105 in. round bar are: tensile strength—164,000 to 181,000 psi; 0.2% yield strength—158,000 to 175,000 psi; elongation—2.6 to 4.7%; reduction in area—1.9% (longitudinal) and 3.9% (transversal); Rockwell hardness—C26 to C34. (Rev. Metal Lit.)

15070 INFLUENCE OF THE CARBON CONCENTRATION ON THE MORPHOLOGY OF URANIUM–MOLYBDENUM. Decours, Jacques; Rouanet, Pierre; Colombie, Michel (CEN de Saclay, Gif-sur-Yvette, France). Compt. Rend., 261: 3601-4(Nov. 3, 1965). (In French).

In uranium–molybdenum alloys with low concentrations of molybdenum the carbon concentration has an effect on the microstructure. This influence is shown by a refining of the γ grain on solidification, by the decrease of the importance of the nucleation and by refining of an α pseudograin when the carbon concentration increases. (tr-auth)

15071 HALL EFFECT IN TERBIUM AND THULIUM. Volkenshtein, N. V.; Fedorov, G. V. (Inst. of Metal Physics, Academy of Sciences, USSR). Fiz. Metal. Metalloved., 20: 508-11(Oct. 1965). (In Russian).

Measurements of the Hall effect in 99.9% pure Tb and Tm in the temperature interval in the range of magnetic conversions are reported. The characteristics of the temperature dependence of the Hall effect in the region of magneto-regulated states is shown. From calculations in the paramagnetic range, the number of carrier currents was found to equal 0.46 el/atom for Tb and 0.80 el/atom for Tm. (tr-auth)

15072 STUDIES OF CARBIDIZATION OF TITANIUM AND ZIRCONIUM NITRATES. Levinskii, Yu. V.; Salibekov, S. E.; Levinskaya, M. Kh.; Strogonov, Yu. D. Fiz. Metal. Metalloved., 20: 519-23(Oct. 1965). (In Russian).

The diffusion of carbon into the nitrates of titanium and zirconium was studied by microstructure and x-ray structure analysis and by measurement of the microhardness. The dependence of the thickness of the carbide film on the temperature and the duration of carburization in the temperature range from 1900 to 2480°C was determined. (tr-auth)

15073 REGULAR CHANGES IN THE HARDNESS OF BINARY NIOBIUM ALLOYS. Georgieva, I. Ya.; Gulyaev, A. P. (Moscow Inst. of Chemical Engineering). Fiz. Metal. Metalloved., 20: 592-6(Oct. 1965). (In Russian).

The hardness of binary alloys of niobium with V, Ta, Ti, Zr, Mo, and W was studied as a function of the degree of alloying, the nature of the alloying elements, heat treatment, and the purity of the alloys with respect to the introduction of inclusions. (tr-auth)

15074 DIFFUSE SCATTERING OF X RAYS BY HfC–ZrC SOLID SOLUTIONS. Umanskii, Ya. S.; Fadeeva, V. I. (Moscow Inst. of Steel and Alloys). Fiz. Metal. Metalloved., 20: 719-22(Nov. 1965). (In Russian).

The distribution of the diffuse scattering of x rays, related to the adjacent order in the single-phase solid solution of 50:50 molar ratio HfC–ZrC was investigated. It was established that in the alloy the ordering of the adjacent type of stratification appears and is enhanced with lower temperatures of treatment. The coefficients of the adjacent orders for the first three coordination areas were determined. (tr-auth)

15075 INFLUENCE OF La_2O_3 AND ThO_2 ON THE CRYSTALLIZATION BEHAVIOR OF OPTICAL GLASSES. Katzschmann, R. Glass Technol., 6: 156-60(Oct. 1965).

To determine the influence of La_2O_3, ThO_2, and Al_2O_3 on the crystallization behavior of optical glasses, some glasses were melted and the rates of crystal growth and the liquidus temperatures were measured. The base glass was of the composition BaO, SiO_2, B_2O_3 (60 : 20 : 20). To study the influence of La_2O_3 and ThO_2, BaO was replaced by La_2O_3 or ThO_2 or both. When La_2O_3 or ThO_2 alone were incorporated into the base glass, a distinct minimum in the maximum rate of crystal growth occurred with a substitution of BaO. Maximum rates of crystal growth of all glasses with La_2O_3 and ThO_2 were lower than those in the base glass. When 1.4% Al_2O_3 was introduced into the base glass, the maximum rate of crystal growth increased from 660 to 840 μm/hr. If, however, the alumina content was increased to 3.4%, the maximum rate of crystal growth decreased to 270 μm/hr. An addition of alumina decreased the maximum rate of crystal growth of the glass containing 10% La_2O_3 and increased it in the glass containing 20% La_2O_3, whereas it always decreased it in glasses that contained ThO_2. For glasses containing La_2O_3, La_2O_3 + ThO_2, and ThO_2 the liquidus temperatures rose with increasing substitution of BaO. The rise of the liquidus temperature was highest with the ThO_2 glasses, next with La_2O_3 glasses, and then with La_2O_3 and ThO_2 glasses. The addition of alumina decreased the liquidus temperature for the base glass and increased it for glass which contained 20% ThO_2. The glasses with La_2O_3 and ThO_2 in a 1 : 1 ratio showed the lowest rates of crystal growth and liquidus temperatures. To obtain La crown stable to crystallization based on barium borosilicate glasses, it is advisable to incorporate both La_2O_3 and ThO_2. (TCO)

15076 SURFACE DUCTILITY AND DENSITY OF OXIDE MELTS CONTAINING VANADIUM OR NIOBIUM PENTOXIDES. Manakov, A. I.; Lepinskikh, B. M. Izv. Akad. Nauk SSSR, Metal., No. 4, 68-71(July-Aug. 1965). (In Russian).

The surface ductility and density of the fused systems $K_2O-Nb_2O_5$, $Cr_2O_3-Nb_2O_5$, $CaO-Nb_2O_5$, $Fe_2O_3-Nb_2O_5$, $CaO-V_2O_5$, $Fe_2O_3-V_2O_5$, and $Cr_2O_3-V_2O_5$ were investigated at 1200 to 1650°C. In the fused niobates of K^+ and Cs^+, in contrast to Ca^{2+} and Fe^{3+}, capillary activity appeared. In systems containing V_2O_5 the addition of oxides, in the composition interval studied, increased ductility. The change of the molar exchange of the fused system with composition is shown. The thermal coefficients $\gamma = d\sigma/dT$ and $\beta = dV/dT$ were found for the liquid pentoxides of V and Nb. The results are based on quasi-molecular structures of fused oxides of the fifth group. (tr-auth)

15077 X-RAY STRUCTURE AND METALLOGRAPHIC STUDIES OF Nb–Co–C SYSTEMS. Borusevich, L. K.; Fedorov, T. F.; Popova, N. M. Izv. Akad. Nauk SSSR, Metal., No. 4, 159-62(July-Aug. 1965). (In Russian).

The phase compositions of the Nb–Co–C system were investigated. It was discovered that no ternary compounds were present. Solid solutions of Co and the binary compounds $NbCo_2$ and NbCo formed biphase alloys with the carbide NbC and the compound NbCo with the carbide Nb_2C. The phase equilibrium diagram of the Nb–Co–C system was constructed for 1000°C. In the vicinity of the composition of Nb_3Co_3C, the existence of previously unknown ternary compounds (η phase) was detected. The compounds found occurred in equilibrium with NbC, Nb_2C, Nb, NbCo, and $NbCo_2$; NbC appeared in equilibrium with Co and $NbCo_2$. (tr-auth)

15078 CONSTITUTION DIAGRAM OF THE Ti–Nb–Cr SYSTEM. Kornilov, I. I.; Shakhova, K. I.; Budberg, P. B. Izv. Akad. Nauk SSSR, Metal., No. 4, 168-75(July-Aug. 1965). (In Russian).

The isothermal profile at 1300°C of parts of the Ti–Nb–Cr system was constructed, bounded by the Ti–Nb side and by the profile passing through the compound $TiCr_2-NbCr_2$. Four of the polythermal profiles of the system with Ti and Nb ratios equal to 4 : 1, 3 : 2, 2 : 3, and 1 : 4 were constructed. From the polythermal profile, phase diagrams of the binary system, formation of the actual ternary, and the general conditions of physicochemical analysis on the phase equilibrium, the high-temperature part of the diagram is presented in the form of isothermal profiles at 1900, 1800, 1700, 1600, 1500, and 1400°C. (tr-auth)

15079 ON THE BINARY OXIDES IN THE $ZrO_2-Nb_2O_5$ SYSTEMS. Trunov, V. K.; Vladimirova, Z. A.; Kovba, L. M.; Komissarova, L. N. (Moscow State Univ.). Izv. Akad. Nauk SSSR, Neorg. Mater., 1: 1152-4(July 1965). (In Russian).

The phase transformations in the system $ZrO_2-Nb_2O_5$ were investigated by x-ray phase analysis. The formation of phases of the variable composition $Zr_{1-n}Nb_nO_{2+n/2}$ was detected and the lattice parameters for the different compositions were determined. The binary oxides $ZrO_2 \cdot nNb_2O_5$, $ZrO_2 \cdot 7Nb_2O_5$, and $ZrO_2 \cdot 5Nb_2O_5$ were produced. It is shown that the phase $ZrO_2 \cdot \underline{n}Nb_2O_5$ is formed only during annealing of the coprecipitated hydroxides of Nb and Zr. (tr-auth)

15080 ATOMIC STRUCTURE AND CORRELATION IN LIQUID BINARIES BY X-RAY AND NEUTRON DIFFRACTION WITH APPLICATION TO NaK. Henninger, E. H. (Purdue Univ., Lafayette, Ind.); Buschert, R. C.; Heaton, Leroy. J. Chem. Phys., 44: 1758-69(Mar. 1, 1966).

For a liquid or amorphous binary three independent diffraction patterns are required to completely characterize the atomic structure, including the correlation of the two atom types. However if the distribution of atomic density is the same about either atom type only two patterns are required. This two-pattern method was applied to 50 at. % liquid sodium–potassium using x ray and neutron diffraction. The results indicated a very nearly random mixing of atom types, but further analysis of the data showed that the assumption of identical distributions about the Na and K atoms is invalid. Indeed, consideration of the factors that may determine the liquid structure makes this assumption highly questionable for most binaries. A method of combining the x-ray- and neutron-diffraction patterns was developed, which can yield qualitative information on the correlation and serve as a test for theoretical structural models. The approach utilized the ratio of the two weighted atomic distributions obtained separately from x-ray and neutron patterns. For the 50% NaK system the neutron pattern alone gave the true atomic distribution with nearest-neighbor concentrations at 4.4, 7.7, and 11.2 Å. Comparison with the x-ray distribution indicated that at the first three nearest-neighbor distances a given atom tends to be paired with atoms of the opposite type, with some concentration of Na–Na pairs at 5.0 Å and K–K pairs at 6 to 7 Å. (auth)

15081 SOME MECHANICAL PROPERTIES OF URANIUM AT INTERMEDIATE STRAIN RATES AND TEMPERATURES. Sykes, E. C. (Central Electricity Generating Board, Berkeley, Eng.). J. Inst. Metals, 93: 485(Sept. 1965).

Mechanical properties of uranium alloyed with carbon, iron, and aluminum were studied at 325 to 625°C with cross-head motions equivalent to initial strain rates ranging from 10^{-1} to 10^{-4} min^{-1}. The variation with temperature of the flow stress (which, particularly at the faster strain rates and lower temperatures, has the characteristics of a tensile strength) is listed. These results indicate that extrapolation of the creep data of Gardiner and Miller to higher strain rates overestimates the stress levels reached. The new data correspond fairly well with an equation of the type $\dot{E} = A \exp \beta\sigma$. The value of A does not vary exponentially with temperature, so that an activation energy for the deformation process cannot be deduced. (J.F.P.)

15082 KINETICS OF URANIUM-DIOXIDE SINTERING BETWEEN 950 DEG C AND 1500 DEG C IN DRY HYDROGEN ATMOSPHERE. Ram, Paras; Gadiyar, H. S.; Jena, P. K. (Atomic Energy Establishment, Trombay, India). J. Less-Common Metals, 10: 185-9(Mar. 1966).

The kinetics of sintering of UO_2 compacts prepared from ammonium diuranate and calcined at 800°C was studied in the temperature range 950 to 1500°C in dry hydrogen atmosphere. The bulk density D_s achieved at a desired period was determined by measuring the change in the volume of

the pellets. At all temperatures studied, the bulk density and the sintering period t were related by the expression $D_s = C \log t + X$, where C and X are constants. From these results the activation energy of the process was evaluated and the mean value was found to be 102 ± 10 kcal/mole. (auth)

15083 A SEARCH FOR LOW-TEMPERATURE ANOMALIES IN THE ELECTRICAL RESISTIVITY OF DILUTE GOLD-ERBIUM ALLOYS. Arajs, S.; Dunmyre, G. R. (United States Steel Corp., Monroeville, Pa.). J. Less-Common Metals, 10: 220-4(Mar. 1966).

Electrical resistivity of gold–erbium alloys containing 0.05, 0.60, and 1.88 at. % erbium was measured from liquid helium temperatures to 300°K. It is concluded that erbium in gold produces neither an electrical resistivity minimum nor a maximum. The resistivity contribution of 1 at. % erbium in gold at 4.2°K is 6.7 $\mu\Omega$ cm. (auth)

15084 THE THERMAL CONDUCTIVITY OF SPRINGFIELDS ADJUSTED URANIUM IN THE TEMPERATURE RANGE 160-620 DEG C. Howl, D. A. (United Kingdom Atomic Energy Authority, Springfields, Eng.). J. Nucl. Mater., 19: 9-14(Apr. 1966).

Results of 150 determinations of thermal conductivity on 15 specimens of Springfields adjusted uranium are discussed. The determinations were made within the range 160–620°C, and the results were found to fit the equation $K = 0.0585 + 6.550 \times 10^{-5}$ T, where K is the conductivity in cal/cm · sec · °C and T is the temperature in °C. This equation gives a substantially higher conductivity above 300°C than that given by a previous equation for Springfields uranium, but agrees well with American data. The specimens were selected to cover a range of iron contents. No correlation was found between the conductivity and any one of the variables: iron, aluminum, or carbon contents. A relationship between the uranium conductivity and the ratio of the carbon-to-iron contents was revealed, but this is of doubtful significance. (auth)

15085 PHASE RELATIONS AND STRUCTURES IN URANIUM–PLUTONIUM–FISSIUM ALLOYS. Kruger, O. L. (Argonne National Lab., Ill.). J. Nucl. Mater., 19: 29-41 (Apr. 1966).

Alloys of U with 20 wt % Pu and various additions of a group of fission product elements were investigated and their transformations, structures and melting points are reported. Additions of fissium, which was composed of the elements Ru, Mo, Pd, Te, Rh, and Zr stabilized the gamma and beta U phases down to 555°C. At high fissium contents the beta transformation was entirely suppressed. Alpha U gamma-prime, and zeta were the stable phases at temperatures below 400°C. A primary phase theta with an unknown crystal structure was present in all the compositions studied. Lattice constants are given for alpha and gamma U and some intermetallic phases. (auth)

15086 CREEP OF SINGLE-CRYSTAL UO_2. Armstrong, W. M.; Causey, A. R.; Sturrock, W. R. (Univ. of British Columbia, Vancouver, Can.). J. Nucl. Mater., 19: 42-9(Apr. 1966).

The initial stages of creep in single-crystal UO_2 were investigated by four-point loading creep-in-bend testing. The temperature and stress dependence of the stationary creep region of the S-shaped deflection-time curve was determined over the temperature range 1340–1685°C and stress range 3600–8000 psi. The data were fitted to an expression of the form $\dot{d}_s = K\sigma^{3.3} \exp(-5.1/kT)$ with a deviation of approximately ±3% and ±8% respectively for the exponents. On the basis of this activation energy it was not possible to establish which activated process was rate controlling, although the stress exponent is in agreement with that of the quasi-viscous movement of dislocations through the lattice. (auth)

15087 DIFFUSION OF URANIUM IN GRAPHITE. Hrovat, M.; Spener, G. J. Nucl. Mater., 19: 53-8(Apr. 1966). (In German).

Measurements of the diffusion of uranium out of uranium carbide pellets in porous graphite at 1400–2000°C surprisingly revealed a strong dependence of the rate on previous treatment of the uranium carbide. Experiments with a 0.5 mm slit between the carbide and graphite proved that uranium is transferred via the gas phase. The results indicate that transport is considerably affected by traces of a uranium–oxygen compound present on the uranium carbide surface. (auth)

15088 THE TOTAL HEMISPHERICAL EMITTANCE OF PLUTONIUM AT 89 DEG C. Karlsson, R. H. (Dow Chemical Co., Golden, Colo.). J. Nucl. Mater., 19: 79-80(Apr. 1966).

The total hemispherical emittance of polished, alpha-phase Pu was found to be 0.37 at 88.7°C. The method used consisted of suspending a heated spherical sample within an evacuated larger hollow sphere of known emissivity. The self-heating property of Pu eliminated the need for internal heating coil leads and provides a means of measuring the emittance of many materials by coating or plating the Pu sphere with the material whose emittance is to be determined. (W.L.G.)

15089 POLARIZED LIGHT MICROSCOPY OF PYROLYTIC CARBON DEPOSITS. Gray, R. J.; Cathcart, J. V. (Oak Ridge National Lab., Tenn.). J. Nucl. Mater., 19: 81-9(Apr. 1966). (ORNL-P-1403).

The optical features frequently encountered in the study of pyrolytic carbon coatings on fuel particles are described and an explanation is proposed for the Maltese cross effect. (W.L.G.)

15090 DIFFUSION OF XENON IN METALS. Nagasaki, R.; Kawasaki, S. (Japan Atomic Energy Research Inst., Tokyo). J. Nucl. Mater., 19: 90-2(Apr. 1966).

The diffusion coefficient for Xe in U was obtained by measuring the concentration distribution of Xe in the U. The specimens were irradiated to a total dose of 2×10^{18} n/cm^2 and heated at 950 and 1000°C for 100 hr. At 950°C, the diffusion coefficient was about 3×10^{-15} cm^2/sec and at 1000°C, about 1×10^{-14} cm^2/sec. (W.L.G.)

15091 SELF-DIFFUSION OF URANIUM IN UO_2. Lidiard, A. B. (Atomic Energy Research Establishment, Harwell, Eng.). J. Nucl. Mater., 19: 106-8(Apr. 1966).

A model is proposed for U^{4+} diffusion via vacancies and interstitials. This model is intended to help predict the influences of impurities and of slight departures from stoichiometric composition upon volume diffusion and to account for the variation in results obtained by different investigators. (W.L.G.)

15092 THE $\beta \rightarrow \alpha$ PHASE CHANGE IN PURE URANIUM. Pickwick, K. M.; Kitchingman, W. J. (Univ. of Manchester, Eng.). J. Nucl. Mater., 19: 109-10 (Apr. 1966).

The combined resistivity and metallographic results support the view that there is a change in the mechanism of the beta-to-alpha phase transformation in pure U below 620°C. (W.L.G.)

15093 THERMAL EXPANSION OF URANIUM DICARBIDE AND URANIUM SESQUICARBIDE. Bowman, A. L.; Arnold, G. P.; Witteman, W. G.; Wallace, T. C. (Los Alamos Scientific Lab., N. Mex.). J. Nucl. Mater., 19: 111-12(Apr. 1966). (LA-DC-7543).

Data were obtained from high-temperature neutron diffraction experiments and a least-squares analysis used to calculate the coefficients of thermal expansion. The coefficient for the sesquicarbide from 1100 to 1730°C was 13.53 (±0.98) $\times 10^{-6}$; for the tetragonal form of the dicarbide from 1000 to 1765°C, 18.1 (± 1.6) $\times 10^{-6}$; and for the cubic form of the dicarbide from 1765 to 2300°C, 25.2 (± 2.1) $\times 10^{-6}$. (W.L.G.)

15094 THE MIGRATION OF PORES IN URANIUM DIOXIDE. Rose, R. G.; Ferrari, H. M. (Westinghouse Electric Corp., Pittsburgh). J. Nucl. Mater., 19: 113-14 (Apr. 1966).

Exploratory experiments were performed to measure the surface diffusion coefficient. The pore migration rates for the mechanisms of surface diffusion and evaporation

and condensation were compared using the coefficient obtained for surface diffusion. (W.L.G.)

15095 COMPRESSIBILITY OF ORIENTED ALPHA PLUTONIUM. Andrew, J. F.; Morgan, J. R. (Los Alamos Scientific Lab., N. Mex.). J. Nucl. Mater., 19: 115-16 (Apr. 1966). (LA-DC-7447).

The calculated volume compressibilities are 19.0×10^{-7}/bar for the preferentially oriented material and 21.9×10^{-7}/bar for the randomly oriented specimen. The preferentially oriented material had the (020) plane aligned perpendicular to the direction of applied stress. (W.L.G.)

15096 LITHIUM METAL: AN EXPERIMENTAL EQUATION OF STATE. Swenson, C. A. (Ames Lab., Ames, Iowa). J. Phys. Chem. Solids, 27: 33-8(Jan. 1966).

The piston-displacement technique was used to obtain pressure-volume-temperature data for lithium metal over the temperature range from 350 to 20°K at pressures up to 20 kbars. The data may be represented by a temperature-independent isothermal bulk modulus B_T, which varies linearly with the pressure with a slope $dB_T/dP = 3.6(\pm 0.25)$. The bulk modulus at the equilibrium molar volume at absolute zero (12.69 cm^3/mole) is 123(±3) kbars. The experimental details as well as the general conclusions are identical with those described in earlier work on potassium metal (J. Phys. Chem. Solids, 26: 291(1965)). The similarity between the experimental results for sodium, potassium, and lithium suggested that to a first approximation the cohesive energies for these three metals can be represented as $U_0(V) = \epsilon f(V/\sigma^3) + E_0$, where the function f and the energy ϵ are the same for all three and the characteristic distance σ and the additive constant E_0 are characteristic of the individual metal. (auth)

15097 HEAT CAPACITIES OF $NbC_{0.702}$, $NbC_{0.825}$, $NbC_{0.980}$, AND Nb_2C BELOW 320 DEG K. Sandenaw, T. A.; Storms, E. K. (Los Alamos Scientific Lab., N. Mex.). J. Phys. Chem. Solids, 27: 217-18(Jan. 1966).

The thermodynamic data for the NbC system as a function of composition are discussed. The NbC phase extends from about $NbC_{0.71}$ to $NbC_{0.99}$ and has a fcc structure over this range. The experimentally determined low temperature heat-capacity curves are shown for the $NbC_{0.825}$, $NbC_{0.98}$, $NbC_{0.702}$, and $NbC_{0.5}$ phases. Entropy at 298°K as a function of mole ratio is shown. The $C_p - T$ curve for $NbC_{0.702}$ below 120°K did not parallel the similar curves for $NbC_{0.825}$ and $NbC_{0.98}$ but crossed over the curve for $NbC_{0.825}$ at 55°K. (F.J.H.)

15098 LOW TEMPERATURE RESISTIVITY OF YTTRIUM-BASED ALLOYS CONTAINING SMALL AMOUNTS OF RARE EARTH METALS. Sugawara, Tadashi (Tokyo Univ.). J. Phys. Soc. Jap., 20: 2252-9(Dec. 12, 1965).

The resistivity of the dilute alloys of rare earth metals with yttrium was measured at low temperatures. The result is in qualitative agreement with the recent theories due to Kondo and others on the s-d or s-f scattering. The effective s-f exchange integrals for various rare-earth solutes were derived from the analysis of the resistivity data and compared with the reported values in other matrices. The integral for Ce is negative, leading to a resistance minimum, while those for heavier rare earths are positive. The sign of the integral was discussed in terms of the mixing of conduction electrons with localized 4f electrons. The increase of the residual resistivity due to added rare earths depends upon the number of 4f electrons of the solute in a complicated way and is anomalously large for lighter rare earths such as La, Ce, and Pr. (auth)

15099 PREFERRED ORIENTATION IN WROUGHT AND ANNEALED METALS. Dillamore, I. L.; Roberts, W. T. (Univ. of Birmingham, Eng.). Met. Rev., 10: 271-380(1965).

Data on preferred orientation in metals are presented. Topics discussed include: pole-figure representation and determination, deformation textures, theories of texture development, recrystallization textures, and theories of the formation of recrystallization textures. Results obtained by modern quantitative methods are presented with emphasis on texture development in the normal processing of metals by deformation and heat treatment. (407 references). (M.C.G.)

15100 THE COBALT CORNER IN THE TRI-COMPONENT SYSTEM COBALT-NIOBIUM-BORON. Stadelmaier, H. H.; Schoebel, J.-D. Metall, 20: 31-2(Jan. 1966). (In German).

The cobalt corner in the tri-component system Co–Nb–B shows, in addition to the binary boundary phases, the incongruently melting ternary phase with the approximate composition Co_2NbB, the almost congruent ternary τ phase with the $Cr_{23}C_6$ structure, and a B-rich phase indicated by λ whose composition is not accurately known. The τ phase has a narrow homogeneity range at 800°C, which contains, at 21.5 at. % B, from 6 to 8.5 at. % Nb. The approximate composition of τ is represented by $Co_{21}Nb_2B_6$. The lattice constant of τ lies between 10.540 and 10.574 Å and increases with increasing Nb content. (tr-auth)

15101 DEVELOPMENT OF TUNGSTEN-BASE ALLOYS FOR HIGH TEMPERATURE SERVICE. Metallurgia, 73: 8-10(Jan. 1966).

The research program on tungsten-base alloys for high-temperature uses consisted of two phases. Thirteen alloys were screened on the basis of castability, tensile strength, and workability in the as-extruded condition. Six of the most promising alloys were prepared for reduction to bar stock by extrusion and swaging. The recrystallization behavior, tensile properties, creep-rupture strengths, and tensile transition temperatures of three tungsten alloys are reported. The alloys were extruded at 3800 to 4000°F. The bars were then swaged at temperatures between 2700 and 3500°F. Data are presented in graphs. (F.J.H.)

15102 THE CRYSTAL STRUCTURES OF YAg_2, YAu_2, AND YZn_{12}. Kusma, J. B.; Laube, E. (Univ., Vienna). Monatsh. Chem., 96: 1496-1502(1965). (In German).

Mixtures of Y and Ag, Au, or Zn powders were sealed in quartz ampoules and heated to reaction; the Au and Ag samples were held 100 hr at 900°C and the samples of YZn_{12} were maintained 50 hr at 450°C. The phases YAg_2 and YAu_2 crystallize with the $MoSi_2$ type with the following lattice parameters: YAg_2: a = 3.69_1; c = 9.24_1Å, c/a = 2.50_4; YAu_2: a = 3.66_7, c = 9.00_5Å, c/a = 2.45_8. An evaluation and intensity comparison of a Debye-Scherrer pattern with calculated values for YAu_2 (CuKα radiation) is tabulated. The compound YZn_{12} exhibits isotropy with the tetragonal $ThMn_{12}$ and therefore crystallizes in the space group D_{4h}^{17}-I4/mmm with the lattice parameters a = 8.87_5, c = 5.19_2Å, c/a = 0.585. Point positions are 2Y in (a), 8 Zn in (f), 8 Zn in (i) with x = 0.353, and 8 Zn in j with x = 0.285. An evaluation of the Debye-Scherrer pattern of YZn_{12} is tabulated. Atomic distances are given: Y–Zn, 3.13 (4x), 3.22 (8x), 3.40 (8x): Zn–Zn, 2.59 (4x), 2.60 (2x), 2.61 (1x), 2.70 (2x), 2.73 (4x), 2.84 (2x), 2.87 (2x), all in Å. (BBB)

15103 SOME NEW η CARBIDES. Reiffenstein, E.; Nowotny, H.; Benesovsky, F. (Univ., Vienna). Monatsh. Chem., 96: 1543-6(1965). (In German).

Ternary carbides, nitrides, and oxides based on a metallic host lattice have been observed in several combinations. In addition to the complex carbides of Nb and Ta already reported, such as $(V,Ni)_3Nb_3C$ and $Co_2(Ti,Ta)_4C$, metals of the 1B group and meta metals also are capable of forming similar phases with the Ti_2Ni type or filled Ti_2Ni type. In the ternary systems Nb–Al–C and Ta–Al–C the tendency is to form H phases or β–Mn carbides; the influence of another transition metal or a meta metal was examined. Samples of the atom % composition 44% Nb or Ta, 42% Al + (V, Cr, Mn, Fe, Co, Ni, Cu, Zn), 14% C were prepared by cold pressing and homogenized 10 hr at 1350°C. An intensity calculation for Ta_3CrAl_2C as an example demonstrates the existence of an η carbide; fairly extensive homogeneous regions were found for each of the added transition metals. Al is an important partner for formation of these carbides, and in the Nb–Fe–Al–C system, for example, the structure is not derived from a Nb–Fe phase as host. In some instances two related η phases exist together. (BBB)

15104 THE CORRELATION AMONG PORE-SIZE DISTRIBUTION, PERMEABILITY, AND DIFFUSION IN GRAPHITE. Schloesser, J. Nucl. Sci. Eng., 24: 123-32(1966).

A model of parallel capillaries with different diameters was developed to explain back-diffusion experiments on four rather different graphites both impregnated and unimpregnated. The transport phenomenon was taken as an interaction between diffusional and molecular flow on one hand, and viscous and slip flow on the other, to cover the whole range of diameter to mean-free-path ratios possible in graphite. It can be shown that only by assuming at least three bundles of capillaries with different diameters can these experiments be adequately explained. It is further possible to relate the material constants, the viscous flow component B_0, and the slip flow component K_0 to the pore-size distribution obtained. When the complexity of porous capillaries in graphite is considered, the agreement is found to be good, about 30%. (auth)

15105 THE CRITICAL FIELD OF SUPERCONDUCTING INDIUM–LEAD ALLOYS. Gygax, Suso (Univ. of California, San Diego, La Jolla). Phys. Kondens. Mater., 4: 207-29(1965). (In German).

Resistance and magnetization measurements were made on α-phase-indium–lead alloys in a longitudinal magnetic field. The results were analyzed in terms of the Ginzburg-Landau-Abrikosov-Gorkov theory and the parameter $\varkappa$ of the alloys was determined. Alloys with concentrations greater than 4.2 at. % Pb were superconductors of the second kind. The temperature variation of $\varkappa$ depended on the mean free path and was somewhat less pronounced for the more dilute alloys. This behavior is not adequately described by recent theories. The phenomena of surface superconductivity and its critical field H_{c3} are in good agreement with the theory of Saint-James and de Gennes except for the constant $C_0 = H_{c3}/H_{c2}$ which for all the alloys studied is about 10% higher than the theoretical value 1.694. Electrolytic deposition of Cu on the surface reduces H_{c3} and gives $C_{cu} = 1.15$ and excludes the alternative explanation of surface filaments. The concentration dependencies of T_c and γ showed irregularities at 7 at.% Pb. They can be explained by the touching of the Fermi surface with the Brillouin zone boundary. (auth)

15106 ANOMALY IN THE BAND STRUCTURE OF TERBIUM METAL. Bergwall, S. (Univ. of Uppsala). Phys. Lett., 19: 539-41(Dec. 15, 1965).

The density of unoccupied states near the Fermi level of heavy rare-earth metals was determined qualitatively from the x-ray isochromat curves of ^{66}Dy, ^{68}Er, ^{64}Gd, ^{67}Ho, ^{71}Lu, ^{65}Tb, ^{69}Tm, and ^{70}Yb. An anomaly in the band structure of Tb was noted. (D.C.W.)

15107 THERMAL CONDUCTIVITY, ELECTRICAL RESISTIVITY, AND LORENZ FUNCTION OF POLYCRYSTALLINE ERBIUM BETWEEN 5 AND 300 deg K. Arajs, S.; Dunmyre, G. R. (U. S. Steel Corp. Research Center, Monroeville, Pa.). Physica, 31: 1466-72(Oct. 1965).

The thermal conductivity and electric resistivity of polycrystalline erbium were studied as a function of temperature between 5 and 300°K. The ferromagnetic-antiferromagnetic and antiferromagnetic-paramagnetic transitions, occurring at 19 and 86°K, respectively, have noticeable influence on the thermal conductivity and electric resistivity. The Lorentz function at any temperature is considerably larger than that expected for pure electronic thermal conductivity, indicating sizable phonon and possibly some magnon contributions to the total heat transport. (auth)

15108 STUDY OF THE SYSTEMS NIOBIUM–CHROMIUM–CARBON AND TANTALUM–CHROMIUM–CARBON. Rassaerts, H.; Benesovsky, F.; Nowotny, H. (Univ., Vienna). Planseeber. Pulvermet., 13: 199-206(Dec. 1965). (In German).

The equilibria of the systems Nb–Cr–C and Ta–Cr–C were determined by x ray methods on the base of sintered specimens at 1350°C. The dominating phase was always the monocarbide solid solution, which dissolved only little chromium carbide; the monocarbide was in equilibrium with the metallic solid solution, the Laves phase, and the chromium carbides. The subcarbides dissolved even less chromium carbide, while the chromium carbides dissolved almost no Nb(Ta) carbide. The η-phase Nb_3Cr_3C indicated in the literature could not be observed. (auth)

15109 MEASUREMENT OF THE ABRASIVE CAPACITY OF POWDERS OF CARBIDES AND BORIDES OF REFRACTORY METALS. Stasovskaya, V. V. (All-Union Scientific-Research Inst. of Abrasive Materials, USSR). Porosh. Met., Akad. Nauk Ukr. SSR, 11: 52-4(1965). (In Russian).

The abrasive capacities of the carbides and borides of titanium, zirconium, hafnium, vanadium, chromium, tantalum, molybdenum, and tungsten, were studied. (auth)

15110 COMPOUNDS WITH STRUCTURES OF THE Th_6Mn_{23} TYPE IN ALLOYS OF RARE EARTH METALS WITH MANGANESE AND IRON. Kripyakevich, P. I.; Frankevich, D. P.; Voroshilov, Y. V. (Lvov State Univ.). Porosh. Met., Akad. Nauk Ukr. SSR, 11: 55-61(1965). (In Russian).

By means of powder metallurgy methods alloys of rare earth metals (R) with manganese or iron were prepared, containing 79.2 at. % Mn (Fe). The existence of the compounds R_6Mn_{23} (R = Pr, Nd, Sm, Gd, Tb, Dy, Ho, Er, Tm, Lu, and Y) and R_6Fe_{23} (R = Gd, Tb, Dy, Ho, Er, Tm, Yb, Lu, and Y) with a structure of the Th_6Mn_{23} type was established or confirmed. Lattice constants are given. (auth)

15111 PHASE EQUILIBRIA IN THE SYSTEM MOLYBDENUM–CHROMIUM–CARBON. Kuzma, Y. B.; Fedorov, T. F. (Lvov State Univ.). Porosh. Met., Akad. Nauk Ukr. SSR, 11: 62-5(1965). (In Russian).

The system Mo–Cr–C was investigated by means of x-ray and microstructural analyses. Phase equilibria were established for the cast alloys and at 1350°C. The compound Mo_2C dissolved 46 at. % Cr and the compound $Cr_{23}C_6$ approximately 15 at. % Mo. The solid solution on a base of $Cr_{23}C_6$ had an ordering arrangement of the atoms. (auth)

15112 HIGH-TEMPERATURE HEATERS MADE WITH NIOBIUM AND ZIRCONIUM CARBIDES. Maltseva, L. F.; Lapshov, Y. K.; Marmer, E. N.; Samsonov, G. V. (Inst. of Problems in Metallography, Academy of Sciences, Ukrainian SSR. All-Union Scientific-Research Inst. of Power Equipment, USSR). Porosh. Met., Akad. Nauk Ukr. SSR, 11: 87-93(1965). (In Russian).

A technology is described for obtaining experimental samples of heaters in the form of NbC tubes and rods. A procedure was developed for testing the rod and tube heaters made of NbC showed that their use in electric resistance furnaces is promising. (auth)

15113 INVESTIGATION OF THE RECRYSTALLIZATION OF Cb_3Sn PREPARED BY GAS-PHASE REACTION WITH A HIGH-TEMPERATURE MICROSCOPE. Hoffmann, Marga; Maier, Richard Georg. Prakt. Metallog., 2: No. 1, 31-4(Feb. 1965). (In German).

A Nb_3Sn crystal, prepared by the reduction of chlorides by H_2 at 1000°C, was embedded in a mixture of 10% Sn and 90% Nb under a pressure of 5 ton/cm^2 and heated in a high-temperature microscope equipped with an interference contrast device. Micrographs showed no change to 1200°C. Recrystallization began at 1350°C with the formation of grains, followed by grain growth to 1450°C. After 15 min at 1600°C, unidentified precipitates were observed both within the grains and at grain boundaries. It is concluded that Nb_3Sn prepared by gaseous reactions contains growth disturbances which, upon suitable heat treatment, may lead to recrystallization. It is assumed that the disturbances consist primarily of point defects, such as voids and foreign atoms, in substitutional positions. The recrystallization resulted in a reduction of the microhardness from 1090 to 840 kp/mm^2 and of the lattice constant from 5.2892 to 5.2826 Å. The (210) x-ray half-width value was reduced from 4 to 2.6 in. (Rev. Metal Lit.)

15114 DIFFUSION OF FISSION PRODUCT ACTIVITY THROUGH FUEL COATINGS. Popescu, Fl. G. (Inst. for

Atomic Physics, Bucharest). Rev. Roum. Phys., 10: 609-22(1965).

A procedure to evaluate the thickness of a coating of nuclear fuel elements for a given set of coefficients of the fission product diffusion in coating, so that only an admissible activity may pass into the cooling fluid of the reactor, is developed. The equation of diffusion for a sandwich composed of a fuel plate and two coatings deposed on its surfaces is solved both for the nonstationary and for the steady case with appropriate boundary conditions. The decay of products during the diffusion through the coating is taken into account directly by writing the equation (steady state) or by integrating the solution of the second Fick's law (nonstationary state). The change in the coefficient of diffusion due to temperature variation along the reactor height is considered while the same change inside the coating thickness is found negligible. (auth)

15115 PHASE DIAGRAM OF THE COLUMBIUM–NICKEL SYSTEM. Svechnikov, V. N.; Pan, V. M.; Korobeinikova, V. G. Sb. Nauch. Tr. Inst. Metallofiz., Akad. Nauk Ukr. SSR, No. 19, 196-205(1964). (In Russian).

The phase diagram of the Nb–Ni system was studied and plotted by microscopic, x-ray, and differential thermal analyses and by measuring hardness and high-temperature oxidation resistance. The maximum solubility of Ni in Nb (alpha-solid solution) was about 4.5% at 1320°C, 1.2% at 1100°C, and 0.6% at 800°C. The maximum solubility of Nb in Ni (gamma-solid solution) was about 13.5% at 1285°C, and 12% at 1100°C. The compound Ni_3Nb (delta phase) had a melting point of 1430°C and a homogeneity region within limits of 1% Nb. The compound NiNb (eta phase) existed within limits of 6.4, 8.4, and 12.8% Nb at 800, 1000, and 1700°C, respectively. Eutectics were formed at 1285°C and 15.2% Nb and 1170°C and 40.5% Nb, respectively. The peritectic transformation took place at 1320°C and 63% Nb in the eta phase. When Ni was added, the hardness of Nb decreased at 800 to 1000°C and when 4% Ni was added, the high-temperature oxidation resistance in air for 5 hr at 1000°C increased five times. (Rev. Metal Lit.).

15116 INVESTIGATION OF ELECTRIC TRANSPORT OF COMPONENTS IN THE MOLYBDENUM–TUNGSTEN SYSTEM IN A WIDE RANGE OF TEMPERATURES. Smolin, M. D. (Inst. of Problems in Material Handling, Kiev). Soviet Phys.-Solid State (Engl. Transl.), 7: 1758-61(Jan. 1966).

Translated from Fiz. Tverd. Tela, 7: 2186-9(July 1965).

Radioactive traces were used in the 1400–2800°C temperature range to investigate electric transport of components in the alloys $xMo-(1-x)W$ $(0.001 \leq x \leq 0.999)$. The effective charge z^* of the ions was determined. (auth)

15117 THERMAL CONDUCTIVITY OF HOLMIUM AND ERBIUM FROM 2 TO 100 deg K. Aliev, N. G.; Volkenshtein, N. V. (Academy of Sciences, Sverdlovsk, USSR). Soviet Phys.-Solid State (Engl. Transl.), 7: 2068-9(Feb. 1966).

Translated from Fiz. Tverd. Tela, 7: 2560-2(Aug. 1965).

The temperature dependence of the thermal conductivity of polycrystalline holmium and erbium of about 99.9% purity were measured in the temperature range 2 to 100°K. To compare the purity of the samples and to calculate their Lorentz number the electric conductivity of the samples was also measured at room temperature and 4.2°K. The temperature dependence of the thermal conductivities of holmium and erbium are each plotted, and the Lorentz numbers are given. It was concluded that at low temperatures there was, in addition to the electronic thermal conductivity, a further mechanism of heat transfer. The phonon and magnon thermal conductivities, which appeared at these temperatures, were likely to be the cause of the higher values of the Lorentz number of Ho and Er. (J.F.P.)

15118 SOME PRELIMINARY TESTS ON THE BERYLLIUM INGOT, PRODUCED BY ARC-MELTING. Mishima, Yoshitsugu. Tokyo Univ. Fac. Eng. J. (A), No. 2, 40-1 (1964). (In Japanese).

As the first step toward the study on the production of sufficient ductile Be tubing to be used for fuel cladding of gas-cooled reactors by working melted ingot instead of hot pressed block, some small ingots of metal Be produced by consumable electrode arc-melting both of compacted electrolytic flake and of induction-melted bar were tested, with special emphasis on ductility during hot or warm working and the latter was found to be preferred. Orientation of the columnar crystals in the ingots was also determined. (Rev. Metal Lit.)

15119 PROPERTIES OF AN YTTRIUM-CONTAINING COLUMBIUM ALLOY. Torgerson, R. T.; Baginski, W. A. (Boeing Co., Seattle). Trans. Met. Soc. AIME, 236: 158-64(Feb. 1966).

Alloying studies were conducted on modifications of a Nb–10W–10Hf (C-129) alloy. The purpose of these studies was to develop a fabricable, high-strength niobium alloy with superior welding properties. The initial investigations of alloy modifications were conducted using laboratory-melted button ingots. An alloy with the composition Nb–10W–10Hf–0.1Y exhibited excellent weld ductility, high-temperature strength, and fabricability. The yttrium-modified alloy was designated C-129Y and was selected for further development. Three production heats of C-129Y were processed into sheet. Welding, forming, and tensile properties are presented for this material. Tungsten-arc welds of C-129Y exhibited a minimum bend radius of $\frac{1}{2}T$ in the as-welded condition compared to 8T for C-129 alloy. An investigation was conducted on Disil coating of C-129Y and test data are presented on oxidation resistance and effects of reentry environments. The excellent combination of strength, fabricability, weldability, and low transition temperature of C-129Y alloy offers potential design advantages for use of this alloy in structures of aerospace vehicles. (auth)

15120 THE INFLUENCE OF STRESS ON THE HYDRIDE HABIT PLANE IN ZIRCALOY-2. Louthan, M. R. Jr.; Angerman, C. L. (E. I. du Pont de Nemours and Co., Aiken, S. C.). Contract AT(07-2)-1. Trans. Met. Soc. AIME, 236: 221-2(Feb. 1966). (TID–22237).

Investigations using polycrystalline Zircaloy-2 samples confirmed the $\{10\bar{1}1\}$ and $\{11\bar{2}1\}$ habit planes and showed that the prism planes are active hydride habit planes. Using single-surface stereographic analysis and back-reflection Laue techniques, most of the previously reported habit planes were observed and one additional plane, the $(10\bar{1}3)$ plane, was noted. All the planes were the habit planes for hydride precipitation in polycrystalline Zircaloy-2. The observed stress orientation effects require that multiple habit planes exist in Zircaloy-2. (M.C.G.)

15121 INTERMEDIATE PHASES IN THE TERNARY SYSTEM Nb(Cb)-Ni-Al AT 1140 DEG C. Benjamin, John S.; Giessen, Bill C.; Grant, Nicholas J. (Massachusetts Inst. of Tech., Cambridge). Trans. Met. Soc. AIME, 236: 224-6(Feb. 1966).

An isothermal section in the Nb–Ni–Al system was determined at 1140°C. There was no Nb_2Ni phase analogous to Ta_2Ni at 1140°C. The μ phase extended from about Nb + 50 at. % Ni down to Nb + 43 ± 2 at. % Ni. The ternary system is characterized by a large extension of the binary μ phase and the occurrence of three ternary intermetallic phases. Crystallographic data are given for the ternary phases. (M.C.G.)

15122 DISLOCATION-RELAXATION INTERNAL-FRICTION PEAK IN COLUMBIUM AND Cb-5Pct Zr. Hanlon, J. E.; Wolf, J. D. (E. I. du Pont de Nemours and Co., Wilmington, Del.). Trans. Met. Soc. AIME, 236: 231 (Feb. 1966).

The lower-temperature dislocation-relaxation peak in Nb and Nb–5% Zr was studied on specimens machined into rods from bars hot-extruded at 1200°C. The internal friction and resonant frequency were measured in torsion at kilocycle frequencies at a maximum strain amplitude of $\sim 10^{-6}$. The dislocation-relaxation peaks in niobium are not characteristic of a single relaxation time. The zirconium addition further broadens the spectrum of relaxation times. A decrease in the average dislocation mobility for the alloy was suggested by the results. (M.C.G.)

15123 THE SUPERCONDUCTIVITY OF FUSION SAMPLES OF THE SYSTEMS Nb–Sn, Nb–Al, Nb–Ga, V–Si, AND V–Ga. **Kunz, W.; Saur, E. (Univ. Giessen, Ger.).** Z. Phys., 189: 401-16(1966). (In German).

Samples of the binary systems Nb–Sn, Nb–Al, Nb–Ga, V–Si, and V–Ga and ternary samples of Nb_3Sn with partial substitution of the Nb by Ti, Zr, V, and Ta were fused in an arc fusion furnace. Induction and resistance measurements gave transition temperatures and widths of these fusion samples in the annealed and unannealed state. By structure investigations, an assignment of the binary samples and their superconductivity properties to known constitution diagrams of the systems were made. (tr-auth)

15124 CRYSTAL STRUCTURE OF GADOLINIUM AT 120 TO 370 DEG K. **Vorob'ev, V. V.; Smirnov, Yu. N.; Finkel, V. A. (Inst. of Physics and Tech., Academy of Sciences, Ukrainian SSR).** Zh. Eksp. Teor. Fiz., 49: 1774-8(Dec. 1965). (In Russian).

The crystal structure of polycrystalline gadolinium was measured by x-ray diffraction in the 120–370°K temperature range. The temperature dependences of the crystal lattice constants, atomic volume and volume and linear expansion coefficients are obtained. A negative λ-anomaly of the thermal expansion coefficient is observed at 293°K due to transition of ferromagnetic Gd to the paramagnetic state. On the change of the character of the temperature dependence of the angle between the direction of the magnetic moment and [001] axis a maximum is observed on the temperature dependence curve of the atomic volume. (auth)

15125 BERYLLIUM, ITS METALLURGY AND PROPERTIES. **Hausner, Henry H. (ed.).** Berkeley, Calif., Univ. of California Press, 1965. 327p. $9.00.

Beryllium metallurgy from ore processing to the finished product is discussed. Topics covered include: extraction of BeO; reduction of BeO to metal; powder metallurgy of Be; melting and casting; rolling and sheet metal fabrication; extrusion of Be structural shapes; powder forging; forging of solid billets; joining processes; and surface treatment and coatings; beryllium alloys; physical properties; mechanical properties; nuclear properties; ductility problems; beryllia; future trends in Be metallurgy research; and health hazards in handling beryllium. Appendixes give information on electron-probe microanalysis and metallography of beryllium. (F.J.H.)

15126 VOLUME AND BOUNDARY DIFFUSION OF TUNGSTEN IN MOLYBDENUM. **Bokshtein, S. Z.; Bronfin, M. B.; Kishkin, S. T.** pp 16-23 of Diffusion Processes, Structure, and Properties of Metals. New York, Consultants Bureau Enterprises, Inc., 1965.

The coefficients of volume and boundary diffusion were measured by either the activity curve shift method or the autoradiographic method for samples prepared by diffusional annealing at temperatures from 1700 to 2100°C. The diffusion coefficient varied from 9.9×10^{-13} to 1.25×10^{-10} cm^2/sec over this range. A summary of existing data indicated the activation energy for diffusion of elements with similar properties in the same solvent are the same, regardless of the solvent lattice. The rate of boundary diffusion exceeded volume diffusion by 2100 times at 1850°C and 1200 times at 1900°C. The increase with temperature was attributed to the activation energy of volume diffusion being greater than boundary diffusion. (24 ref.) (Rev. Metal Lit.).

15127 DIFFUSION OF RHENIUM IN MOLYBDENUM. **Bronfin, M. B.** pp 24-6 of Diffusion Processes, Structure, and Properties of Metals. New York, Consultants Bureau Enterprises, Inc., 1965.

Diffusion annealing gave values for the coefficient of diffusion for ^{186}Re in Mo ranging from 2.8×10^{-12} cm^2/sec at 1700°C to 1.7×10^{-10} at 2100°C. The diffusion rate of Re was much higher than the diffusion rate of Mo atoms; the ratio was 2.5 at 1700°C and decreased to 1.7 at 1900°C. The greater the difference between physical and chemical properties of impurity and solvent atoms, the greater the rate of heterodiffusion. (Rev. Metal Lit.).

15128 INVESTIGATION OF THE STRUCTURE OF GRAIN BOUNDARIES IN MOLYBDENUM AND ITS ALLOYS WITH ZIRCONIUM AND RHENIUM BY THE INTERNAL FRICTION METHOD. **Bokshtein, S. Z.; Bronfin, M. B.; Kishkin, S. T.; Marischev, V. A.** pp 27-34 of Diffusion of Processes, Structure, and Properties of Metals. New York, Consultants Bureau Enterprises, Inc., 1965.

Values obtained for internal friction showed that boundary relaxation increased at different temperatures in different materials (Mo–Re alloy, 700°C; Mo, 600°C; and Mo–Zr alloy, 600°C). This indicated that the mechanism of boundary relaxation is related to the migration of impurities, which penetrate this intercrystalline zone as a result of temperature and cyclic stress. This explains the relatively low value found for the activation energy of the boundary internal friction. (Rev. Metal Lit.).

15129 HIGH TEMPERATURE STRUCTURES AND MATERIALS. Proceedings of the Third Symposium on Naval Structural Mechanics held at Columbia University, New York, January 23–25, 1963. **Freudenthal, A.M.; Boley, B. A.; Liebowitz, H. (eds.).** Office of Naval Research Structural Mechanics Series. Oxford; London; New York; Paris; Pergamon Press, 1964. 478p. 5£; $15.00. (CONF-630101).

The 13 papers presented at the Third Symposium on Naval Structural Mechanics are given. Topics covered include: temperature dependence of elastic and anelastic properties in solids, thermo-mechanical behavior of ceramics, physical aspects of creep, thermal fatigue and its relation to creep rupture and mechanical fatigue, behavior of materials in a high-speed environment, materials aspects of the re-entry problem, analysis of problems of heat conduction and melting, solution of thermoelastic boundary value problems, analysis of thermal stresses in viscoelastic solids, analytical methods of creep design, aspects of reliability under conditions of elevated temperature creep and fatigue, and aspects of elevated temperature design and design criteria for supersonic aircraft structures. A panel discussion on design criteria is also included. (M.C.G.)

15130 EMBRITTLEMENT OF TANTALUM BY HYDROGEN, AT ROOM TEMPERATURE. **Clauss, M. A.** pp 29-39 of 8e Colloque de Metallurgie. Gif-sur-Yvette, France, Centre d'Etudes Nucleaires de Saclay. Paris, Presses Universitaires de France, 1965. (In French).

Tantalum may show, under given conditions, an abnormal brittleness, when it is deformed in the presence of hydrogen. Study of the conditions of the appearance of brittleness, characterized by the decrease of the deformation capacity of the metal, showed that this property depends on the presence of oxygen dissolved in the tantalum lattice. The influence of the deformation rate and of the dissolved oxygen content was the same: each increase of these parameters caused greater brittleness. The appearance of brittleness coincided with a modification of the fracture type as shown by microfractography. An equivalent brittleness was observed when nitrogen was substituted for oxygen in the tantalum lattice. (auth)

15131 AN INSULATING VITREOUS MATERIAL. **Earl, John Alfred (to Physical Sciences Corp.).** British Patent 1,018,021. Jan. 26, 1966. Filed Apr. 24, 1964.

An insulating vitreous material for use as a metal coating or as a high temperature compression seal that does not lose its insulating properties on exposure to radiation is composed of 20 to 34% SiO_2; 5 to 13% Bi_2O_3; 31 to 58% PbO; 0 to 14% of one or more of the glass modifiers from the group BaO, CaO, MgO, ZnO, and SrO; 0 to 9% of one or more of the oxides of the group CeO_2, ZrO_2, TiO_2, and MoO_3, and 0 to 10% in total of Al_2O_3 and/or La_2O_3. The material must be completely free of B_2O_3. The oxides are homogeneously mixed, smelted at a temperature of the order of 2100°F, quenched in water, wet ground to pass through a 400-mesh screen, and sprayed on the metal to be coated. When used as an electrical coating, the material has a resistivity approaching 2×10^{14} Ω at room temperature and 8×10^{7} Ω at 1200°F. (B.L.M.)

Radiation Effects

See also CHEMISTRY — Radiation Chemistry

Refer also to abstract 16989.

15132 (ANL–7079) ON THE THEORY OF MIGRATION AND COALESCENCE OF BUBBLES IN SOLIDS. Gruber, E. E. (Argonne National Lab., Ill.). Nov. 1965. Contract W-31-109-eng-38. 22p. Dep. mn. CFSTI $1.00 cy, $0.50 mn.

The surface-diffusion migration of an isolated pore in a solid is analyzed in detail. The results, which are similar to earlier results, are applied in analyses of bubble coalescence during postirradiation annealing. Coalescence is considered, first, as a result of random migration of bubbles, in which case the results confirm earlier results that the mean bubble radius should be proportional to $(\text{time})^{1/4}$, and second, as a result of biased migration of bubbles. In the latter case, the predicted mean radius increases linearly with time. In both cases, the bubble-size distribution is calculated and used to predict the swelling of the solid, which is about 15% greater in the first case and up to 65% greater in the second case than predicted by approximate treatments based on change in the mean bubble radius with time. (auth)

15133 (GEAP–4893) ACCURATE NUCLEAR FUEL BURNUP ANALYSES. Quarterly Progress Report No. 14, February–May 1965. Rider, B. F.; Ruiz, C. P.; Peterson, J. P. Jr.; Smith, F. R. (General Electric Co., San Jose, Calif. Atomic Power Equipment Dept.). June 1, 1965. Contract AT(04-3)-189. 29p. Dep. mn. CFSTI $2.00 cy, $0.50 mn.

The fabrication and testing of a system for the quantitative recovery of Kr and Xe gas released during the dissolution of irradiated fuel continued. The contents of ^{236}Pu and ^{238}Pu in irradiated UO_2 fuel for boiling-water reactors were measured and were compared with theoretical predictions. The yields of ^{133}Cs, ^{137}Cs, ^{143}Nd, ^{144}Nd, ^{145}Nd, ^{146}Nd, and ^{150}Nd in neutron fission of ^{239}Pu, ^{233}U, and ^{235}U were also measured. Derivations of equations for the determination of burnup from $^{236}U/^{235}U$ ratios were repeated. (D.C.W.)

15134 (N65–15819) A BIBLIOGRAPHY ON THE EFFECTS OF SHORT-WAVE AND PARTICLE RADIATION ON GLASSES. Astrogeophysical Memorandum No. 164. Avery, Lorne (High Altitude Observatory, Boulder, Colo.). July 30, 1964. 9p. (NASA-CR-60407). CFSTI $1.00 cy, $0.50 mn.

References are given to literature available in the High Altitude Observatory. Material pertinent to studies on the extent to which the presence of ultraviolet radiation, x rays, and cosmic rays induces fluorescence, thermoluminescence, scintillation, and solarization of the optical elements of an orbital coronagraph is covered. (STAR)

15135 (NUMEC–3432-18) IRRADIATION TESTING OF UO_2–PuO_2 FUELS. Quarterly Progress Report, October–December 1965. (Nuclear Materials and Equipment Corp., Apollo, Pa.). Jan. 15, 1965. Contract AT(30-1)-3432. 9p. Dep. mn. CFSTI $1.00 cy, $0.50 mn.

The postirradiation examination of fuel elements in two plutonium recycle fuel capsules is described. (W.L.G.)

15136 (RL-REA–2595, pp 51-62) LINE BROADENING IN IRRADIATED MOLYBDENUM. Kissinger, H. E. (Battelle-Northwest, Richland, Wash. Pacific Northwest Lab.).

Molybdenum samples irradiated to a sufficiently high exposure show a change in the damage accumulation mechanism. This change is accompanied by an increase in line breadth and a decrease in lattice parameter, while electron micrographs show a clumping of previously homogeneously distributed defects. The line broadening is analyzed in terms of crystallite size and distortion effects, and the results are correlated with other observations. (auth)

15137 (VDIT–16(5.4)) RADIATION EFFECTS ON SOLID, URANIUM BASED NUCLEAR FUEL MATERIALS. Vol. 5, No. 4. A Bibliography. Uhlmann, W. (Aktiebolaget Atomenergi, Stockholm (Sweden)). Dec. 1965. 96p. Dep. mn.

Fifty-one references with abstracts are given to various journals, progress reports, and conference papers published during 1964 and 1965. Report number and corporate author indexes are included. (J.B.)

15138 (WAPD–292) EVALUATION OF LOW-DENSITY SINGLE-PHASE CUBIC $ZrO_2 + UO_2$ FUELS STABILIZED WITH CaO. Warner, H. R. (Bettis Atomic Power Lab., Pittsburgh, Pa.). Jan. 1966. Contract AT-11-1-GEN-14. 51p. Dep. mn. CFSTI $3.00 cy, $0.50 mn.

The addition of CaO to stabilize the crystal structure of ZrO_2-UO_2 fuels was shown to improve significantly the in-pile characteristics of ZrO_2-base fuels from a plate stability viewpoint, and from retention of porosity, which is necessary to accommodate fuel swelling to exposures of approximately 30×10^{20} fissions/cm^3. The $ZrO_2-41.1$ wt % $UO_2-6.1$ wt % CaO fuel exhibited a substantial reduction in the amount of permanent clad depression over that of the $ZrO_2-37.2$ wt % UO_2 fuel. Experimental techniques were developed for metallographic determination of the total clad depression under in-pile operating conditions, and the fuel thickness decreases measured. Results indicate that the highly plastic two-phase tetragonal ZrO_2-UO_2 fuels are significantly strengthened by the addition of CaO. This strengthening is attributed to the initial single-phase cubic crystal structure imparted by the CaO addition. The minimum flow stress for 90% dense UO_2 and ZrO_2-UO_2-CaO was estimated to be at least 1400 psi, while the apparent flow stress of the 90% dense two-phase tetragonal ZrO_2-UO_2 was 800 to 1000 psi. Lineal analysis of the retained fine porosity indicates that for ZrO_2-UO_2 fuels, the fine porosity was eliminated prior to 1.23×10^{20} fissions/cm^3, while at an exposure of 1.55×10^{20} fissions/cm^3, the addition of CaO to ZrO_2-UO_2 substantially reduces the rate of closure of the fine porosity, with approximately one-third of the initial fine porosity retained. The reduction in the amount of fine porosity is attributed to an in-pile sintering phenomenon, although the exact mechanism is undiscernible in this particular test. Lineal analysis of retained coarse porosity indicates that the closure of coarse porosity of the ZrO_2-UO_2 fuels is strongly dependent on the force transmitted by the cladding to the fuel from the system pressure, whereas for the CaO-stabilized ZrO_2-UO_2, no closure of the coarse porosity was observed. This is attributed to the initial crystal structure of the two materials. The anisotropic ZrO_2-UO_2 crystal structure is affected by fission spikes in-pile such that internal stresses are continuously produced between grains, and then relieved by enhanced creep. The CaO-stabilized ZrO_2-UO_2 cubic structure, as well as the single-phase cubic UO_2 structure, although having enhanced plasticity due to stress relaxation within the thermal spikes generated in-pile, exhibits a smaller enhancement of the creep rate since this latter phenomenon is less effective. The small dimensional change observed in both the UO_2 and ZrO_2-UO_2-CaO fuels observed in the test are attributed to an in-pile sintering phenomenon. (W.L.G.)

15139 RADIATION DAMAGE IN SOLIDS: A SURVEY. Crawford, J. H. Jr. (Oak Ridge National Lab., Tenn.). Amer. Ceram. Soc. Bull., 44: 963-70 (Dec. 1965). (ORNL-P–1101).

Basic mechanisms of radiation damage to crystalline lattices by energetic particles are reviewed and consequences of this damage for the physical behavior of solids are discussed. The effect of special processes occurring in the displacement cascade such as focusing events and channeling of recoils are described. Attention was confined largely to nonmetallic solids for which radiation effects on both electronic and mechanical behavior are extensive. (28 references). (auth)

15140 ALTERATION OF ANTI-FRICTION AND STRENGTH CHARACTERISTICS OF ENGINEERING MATERIALS, SUBJECTED TO NEUTRON IRRADIATION. Markovskii, E.; Krasnoshchekov, M.; Kochegura, N.

(Inst. of Problems in Casting, Kiev). Fiz.-Khim. Mekh. Mater., 1: 552-6(1965). (In Russian).

In view of the lack of knowledge concerning the effect of radiation on the wear resistance, friction coefficient and similar properties of structural materials, experiments were carried out to determine changes in the antifriction characteristics of several structural materials, such as steel, red copper, cast and wrought iron, and lead bronze, exposed to radiation. The specimens were tested for wear resistance, hardness, and fracture strength before and after the exposure, subjecting them also to metallographic and x-ray examinations. The irradiation was carried out in the vertical beamhole of the reactor of the Ukrainian Academy of Sciences, using integral doses of 10^{16}, 10^{17}, 10^{18}, 10^{19}, and 10^{20} n/cm^2. The proportion of fast neutrons in the beam amounted to 1% and 10% for the E > 3.5 Mev and E > 1 Mev, respectively. The results indicated that the radiation induces two states in the materials: weakening, followed by hardening upon supplementary exposure beyond a total dose of 10^{18} n/cm^2. The weakening phase was more pronounced in the wrought than in the annealed specimens. Reduction of the hardness and wear resistance of wrought iron is probably due in part to the thermal effect. Radiation appears to accelerate the stress release in both stressed and metastable hardened metals. Changes in the microhardness with exposure of the perlite phase of steel were found to be similar to changes in macrohardness. Weakening of hardness of steel is probably caused by grain boundary phenomena arising from the migration of defects and their accumulation at the boundary. It was concluded that after the initial weakening, all the tested material acquired after a sufficiently long exposure to neutron radiation satisfactory antifriction properties and mechanical strength. (TTT)

15141 STUDY ON THE HIGH-TEMPERATURE EMBRITTLEMENT OF AUSTENITIC CHROMIUM–NICKEL STEEL AND NICKEL ALLOYS BY NEUTRON IRRADIATION. Boehm, H.; Dienst, W.; Hauck, H.-J. (Kernforschungszentrum, Karlsruhe, Ger.). J. Nucl. Mater., 19: 59-69(Apr. 1966). (In German).

In order to study the high temperature embrittlement due to neutron irradiation, tensile specimens of different austenitic steels and Ni-alloys (16/13 Cr–Ni, 20/25 Cr–Ni, Inconel 600, Inconel 625, Inconel X750) were subjected to a thermal neutron dose of 3×10^{15} to 2.5×10^{20} n/cm^2. The experimental program was based on the assumption that high temperature embrittlement is caused by the formation of helium in the reaction $^{10}B(n,\alpha)^7Li$. The yield strength and the ultimate tensile strength showed no systematic changes due to neutron irradiation. On the other hand, the elongation to fracture was lowered by considerable amount up a certain threshold-neutron dose. The threshold neutron doses depend on the materials; they lie between 10^{16} and 10^{18} n/cm^2 and tend to indicate a relationship with the tensile strength of the materials. The observed saturation of the embrittlement effect above about 3×10^{20} n/cm^2 could be explained by the far advanced ^{10}B burnup in the specimen. By means of a 2 mm Cd shield, the decrease in ductility was reduced to values which correspond to the amount of epithermal neutrons. Metallographs of the fracture-area of tensile specimens which were subjected to tensile tests at temperatures of 500–750°C after irradiation with 1.3×10^{21} thermal neutrons/cm^2, showed a stronger grain boundary crack formation starting at lower temperatures after neutron irradiation. (auth)

15142 STORED ENERGY IN NEUTRON-IRRADIATED BERYLLIUM OXIDE. Heuer, P. M.; Stolarski, G. Z. A. (Research Establishment, Lucas Heights, Australia). J. Nucl. Mater., 19: 70-8(Apr. 1966).

Results are given of measurements, using a differential thermal analysis technique, of the release of stored energy from irradiated beryllium oxide at temperatures up to 1150°C. The energy release was found to increase in a linear manner with dose up to 88 cal/g after a dose of 4×10^{20} nvt at 75–100°C. The energy released per displaced atom was found to be 2.4 ± 0.8 ev. It is concluded that stored energy release should not present a major problem in the utilization of beryllium oxide in nuclear reactors. (auth)

15143 THE SIZE EFFECT OF RADIATION-INDUCED DIMENSIONAL CHANGES OF GRAPHITE. Horner, P.; Phelps, B. A.; Uglow, A. G. (Berkeley Nuclear Labs., Eng.). J. Nucl. Mater., 19: 93-6(Apr. 1966).

No specimen size effect on the radioinduced dimensional changes of graphite struts obtained from a routine discharge of elements from the Berkeley No. 1 reactor was measured. (W.L.G.)

15144 FISSION-PRODUCT RELEASE FROM FUELS. Carroll, R. M. Nucl. Safety, 7: 34-44(Fall 1965).

The behavior of fission gas in UO_2 is used to illustrate the effects of irradiation on fission-product release from fuel materials. Fission gas is released from UO_2 by a temperature-dependent process, which was formerly assumed to be diffusion. However, it was discovered that burnup and fission rate have effects on a measured diffusion coefficient. Earlier diffusion-coefficient values were obtained with a model in which irradiation would not affect the diffusion coefficient; these values are therefore no longer the most accurate for predictive calculations. A defect-trap model for fission-gas release was developed from these observations. According to the defect-trap theory, the rate of escape of fission gas from UO_2 is inversely proportional to the number of defects in the UO_2 structure. Some defects are created by fission, whereas others may be inherent flaws such as grain boundaries and pores. At a given temperature the number of radiation-produced traps will be roughly proportional to the fission rate. Increasing temperatures, however, result in annealing of defects and consequent release of previously trapped fission gas. (auth)

15145 THE EFFECT OF SOLUTE CONCENTRATION ON THE FORMATION OF LOOPS IN ALUMINUM–MAGNESIUM ALLOYS DURING FISSION FRAGMENT IRRADIATION. Vigeholm, B.; Makin, M. J. (Atomic Energy Research Establishment, Harwell, Eng.). Phys. Status Solidi, 12: 877-90(1965). (AERE-R-5035).

A study was made of the effect of magnesium concentration (up to 0.5 at. %) on the formation of dislocation loops in aluminum during fission fragment bombardment at 60°C. Increasing the magnesium content reduces the initial rate of increase of the total loop area with dose, but the loop area saturates at a higher level in more concentrated alloys. A concentration as low as 0.02% reduces the initial rate of loop growth by a factor of 4 to 5. Considerable attention was given to the problems of obtaining accurate measurements of the loop area per unit volume in foils irradiated in the pre-thinned state, and a number of corrections were applied. An unusual surface denudation effect was observed. The results are explained in terms of the effect of trapping on the mobility of both the interstitial atoms and the vacancies. (auth)

15146 VACANCY CLUSTERS AND LOOPS IN ION-BOMBARDED COPPER. Hesketh, R. V.; Rickards, G. K. (Berkeley Nuclear Labs., Eng.). Proc. Roy. Soc. (London), Ser. A, 289: 353-65(Jan. 25, 1966).

Copper foils of 1000-Å thickness were bombarded with 150-kev zinc ions, in the [011] direction, at 300°K, and were examined by quantitative electron microscopy. The damage has an attenuation length of 3000 Å. Each stopped ion creates, on average, three vacancy clusters or loops, the interstitials either reaching the foil surfaces or remaining invisible. Of the created vacancies 80 to 100% survive. Ions create, on average, three secondary knockons in each cascade, and those of energy greater than 20 kev escape to form further cascades. The largest loops (about 1200 vacancies) correspond to a single cascade from a 65-kev ion. The smallest clusters (250 to 300 vacancies) correspond to the hard-sphere radius at which further knockons are too large to escape from the cascade. These clusters are well above the visibility limit. Clusters and loops are formed at their final size, and there is no general growth during subsequent irradiation. The cluster configuration is relevant to irradiation creep and irradi-

ation hardening; the lattice strain at the edge of a cluster is about 5%, within a cluster only one lattice site in four is vacant, and each vacancy is bound to the cluster with an energy of about 0.15 ev. This is the minimum energy configuration for up to 600 vacancies. A cluster is not a void (it does not possess a free surface) nor is it a tetrahedron of stacking faults. Experiment and theory agree that these require higher energies. Clusters of between 600 and 900 vacancies collapse to sessile loops, thereby lowering the strain energy in the surrounding lattice. Larger clusters collapse to prismatic loops. This collapse does not require the nucleation of a Shockley partial dislocation. (auth)

15147 MEASUREMENT OF LENGTH CHANGES TO 0.1 A IN IRRADIATED GERMANIUM AT LOW TEMPERATURE. North, J. C.; Buschert, R. C. (Purdue Univ., Lafayette, Ind.). Rev. Sci. Instrum., 37: 325-9(Mar. 1966).

The apparatus described was developed to measure length changes in germanium due to electron irradiation and subsequent isochronal annealing at low temperatures. Similar techniques would be applicable to other experiments. Length changes of the sample produced changes in spacing of a system of three-terminal capacitors. These capacitors were measured by an a-c ratio bridge capable of detecting changes in capacitance of 4 parts in 10^7. The irradiated portion of the sample, the surrounding framework, and one plate of each of the parallel plate capacitors were all part of the same monolithic germanium single crystal. A system of six capacitors was used to eliminate extraneous effects. The sensitivity and long term stability was on the order of 0.1 Å which corresponds to 2 parts in 10^9 for an irradiated sample length of $\frac{1}{2}$ cm. (auth)

PHYSICS

General

15148 (N65–20165) LIOUVILLE'S EQUATION AND THE n-BODY PROBLEM. Langebartel, R. G. (National Aeronautics and Space Administration, Greenbelt, Md. Goddard Space Flight Center). Apr. 1965. 60p. (NASA-TR-R-217). CFSTI $3.00 cy, $0.50 mn.

The motion of systems of particles is studied using the fundamental equation of statistical mechanics. The Dirac delta function is used to describe systems that are discrete in position space, velocity space, or both position and velocity space as degenerate cases of continuous systems. The approximation procedure, required by the nonlinearity of the problems, is based on the use of expansions in successive derivatives of the delta function. (D.C.W.)

15149 (JPRS–33458) THIRD ALL-UNION SYMPOSIUM ON WAVE DIFFRACTION, TBILISI, 24–30 SEPTEMBER 1964. Abstracts of Reports. Translation of pp 3-245 from Tretii Vsesoyuznyi Simpozium po Difraktsii Voln, Referativy Dokladov, Nauka Publishing House, Moscow, 1964. 350p. (TT–65-45032; CONF-640926(Absts.)). CFSTI $7.00 cy, $1.75 mn.

Abstracts are included for papers (174) on wave diffraction. The papers deal primarily with the propagation of electromagnetic waves; but papers dealing with wind wave reflection, wave diffraction in the ocean, and wave propagation in various media are also covered. (D.C.W.)

15150 A NEW CLASS OF INVARIANCE TRANSFORMATIONS IN CLASSICAL HAMILTONIAN PARTICLE DYNAMICS. Currie, Douglas G. (Northeastern Univ., Boston). Ann. Phys. (N. Y.), 36: 104-29(Jan. 1966).

The relation between hamiltonian dynamics and the representation of relativity groups is explored. The implications of relativistic invariance are first explored for classical particle systems. The relation to representations of the relativity transformations is then considered, in particular showing that the preservation of canonical Poisson bracket relations (the analog to canonical commutation relations) is a strong additional requirement on some types of relativity transformations (like the Lorentz rotation). In this discussion, a system is said to be relativistically invariant if a solution to the second order equation of the position transforms into a solution to an equation of motion of the same functional form. The formalism is developed from a hamiltonian point of view, and in a form which is analogous to the equivalent quantum theory. For a concrete illustration of the discussion, the representation of dilation for simple harmonic motion is developed. (auth)

15151 THE STABILITY OF MANY-PARTICLE SYSTEMS. Fisher, Michael E.; Ruelle, David (Institut des Hautes Etudes Scientifiques, Bures-sur-Yvette, France). J. Math. Phys. (N. Y.), 7: 260-70(Feb. 1966).

It is shown that a quantal or classical system of N particles of distinct species α, $\beta = 1, 2, \ldots \mu$ interacting through pair potentials $\varphi_{\alpha\beta}(r)$ are stable, in the sense that the total energy is always bounded below by $-NB$, provided $\varphi_{\alpha\beta}(r)$ exceeds some $\varphi_{\alpha\beta}^{(2)}(r)$ whose Fourier transform $\varphi_{\alpha\beta}(p)$ corresponds to a positive semidefinite $\mu \times \mu$ matrix for all p. This result is applied to discuss charged systems, and stability is proved for Coulomb interactions if the charges are somewhat smeared rather than concentrated at points. For a large class of potentials it is shown that classical instability implies quantum instability in the case of bosons and, in three or more dimensions, also of fermions. Quantum systems with Coulomb interactions (point charges) are discussed and it is shown in particular that their stability cannot depend on the ratios between the masses of the particles. (auth)

15152 A CLASSICAL TREATMENT OF DISPERSION FORCES. Henry, L. L.; Marshall, T. W. (Manchester Univ., Eng.). Nuovo Cimento, (10), 41B: 188-97(Feb. 11, 1966).

A heuristic connection was obtained between classical radiative reaction, calculated according to the Lorentz electron theory, and the vacuum field of quantum electrodynamics. In this treatment the electromagnetic field quantities, instead of being treated as operators in Hilbert space, are considered as a multivariate stochastic process. It was shown previously that such a field gives a correct result for the attraction between two perfectly conducting plates due to dispersion forces (Casimir effect). The calculation is now extended to treat the attraction between two dielectric plates. In agreement with Lifshitz' quantum-mechanical calculation, this attraction is obtained in terms of an integral over frequency involving the complex dielectric constants of the plate materials. (auth)

15153 POINCARE-INVARIANT EQUATIONS OF MOTION FOR CLASSICAL PARTICLES. Currie, D. G. (Univ. of Wisconsin, Madison). Phys. Rev., 142: 817-24 (Feb. 25, 1966).

Classical particles, and interaction among them governed by second-order equations of motion for the positions of the particles, are considered. Equations of motion, defined for one instant in an arbitrary frame, are derived which are invariant under the Poincaré group. The equations of motion are considered invariant if, when the world-line solutions to the equations of motion are transformed, point by point, into a new frame, the new world lines obey the same second-order equation of motion. The existence of a wide class of such invariant equations of motion is illustrated. The further questions of causality and separability are mentioned. (auth)

15154 INSTANTANEOUS AND ASYMPTOTIC CONSERVATION LAWS FOR CLASSICAL RELATIVISTIC MECHANICS OF INTERACTING POINT PARTICLES. Van Dam, H. (Univ. of North Carolina, Chapel Hill); Wigner, E. P. Phys. Rev., 142: 838-43(Feb. 25, 1966).

It is assumed that the conservation laws for energy and linear momentum are valid and that these quantities are the sums of the energies and linear momenta of the individual particles, i.e., that there is no interaction energy and no interaction momentum. A familiar argument is repeated, and it is shown that there can then be no interaction between the particles, that is, their world lines are straight. The interaction quantities for energy, linear and angular momenta, and the center-of-mass law are derived for the equations of motion proposed in an earlier paper. These interaction quantities in the asymptotic region of collision processes are then studied in order to arrive at asymptotic conservation laws. It is found, in agreement with the earlier paper, that the interaction energy and the linear interaction momenta vanish asymptotically. This, however, is not true in general for the interaction angular momenta and center-of-mass motion. Asymptotic interaction angular momentum is present in all theories, such as classical electrodynamics, which lead to inverse-square-law forces. (auth)

15155 AN EXACT SOLUTION OF THE EINSTEIN-MAXWELL EQUATIONS REFERRING TO A MAGNETIC DIPOLE. Bonnor, W. B. (London Univ.). Z. Phys., 190: 444-5(1966).

A formal similarity exists between stationary exterior solutions of the Einstein equations and static magnetic solutions of the Einstein-Maxwell theory. This is particularly evident for axially symmetric fields, and it is found that the sets of equations governing the two cases can be transformed one into the other by simple transformations of the dependent variables. (auth)

Accelerators

Refer also to abstracts 14841, 15306, 15311, 15731, and 15919.

15156 (BNL-741(Rev.)) ACCELERATORS OF THE FUTURE. Blewett, John P. (Brookhaven National Lab., Upton, N. Y.). Sept. 1965. Contract AT(30-2)-Gen-16. 12p. Dep. mn. CFSTI $1.00 cy, $0.50 mn.

The future development of accelerators is discussed in terms of high intensity, colliding beams, and super-high energies. (M.O.W.)

15157 (CERN-66-1) EXCITATION OF DELAY-TYPE MAGNETS BY SHORT PULSES. Fischer, H. (European Organization for Nuclear Research, Geneva (Switzerland)). Jan. 17, 1966. 12p. Dep. mn.

An excitation method for delay-type magnets is described which has the following major advantages; the voltage is across the magnet for a time which is an order of magnitude less; and the energy to be stored and dissipated is reduced by a factor of two. (auth)

15158 (CERN-542) REPORT ON THE DESIGN STUDY OF INTERSECTING STORAGE RINGS (ISR) FOR THE CERN PROTON SYNCHROTRON. (European Organization for Nuclear Research, Geneva (Switzerland)). May 12, 1964. 283p. Dep. mn.

The experimental program on intersecting storage rings is discussed. Separate detailed discussions are presented on orbit parameters, magnet system, power supply and cooling, r-f system, beam transfer and injection, vacuum, shielding, controls, and other miscellaneous topics. (M.O.W.)

15159 (LNF-65/36) THE EXTERNAL BEAM OF THE FRASCATI ELECTRON SYNCHROTRON. Note No. 292. Bizzarri, U.; Conte, M.; Quercia, I. F.; Turrin, A. (Laboratori Nazionali di Frascati, Comitato Nazionale per l'Energia Nucleare (Italy)). Oct. 27, 1965. 12p. (CONF-650923-26). Dep. mn.

From 5th International Conference on High Energy Accelerators, Frascati, Italy.

The extraction of the beam from the Frascati synchrotron is described, and the preliminary characteristics of the external beam are given. The results of measurements of the extraction efficiency and the spill-out times obtained are presented. (D.C.W.)

15160 (LNF-65/44) AN INSTRUMENT FOR MEASURING MAGNETIC FIELDS IN THE RANGE 0.01 TO 20 GAUSS WITH PEAKING-STRIPS. Note No. 296. Placidi, M.; Renzler, G.; Tazzari, S. (Laboratori Nazionali di Frascati, Comitato Nazionale per l'Energia Nuclear (Italy)). Dec. 16, 1965. 10p. Dep. mn.

An instrument for magnetic field measurements is described. Its performance is discussed in connection with the measurement it was designed for, and namely the determination of the magnetic axis and asymptotes of the quadrupole magnets for Adone. However, the instrument can measure any kind of magnetic field within its range. (M.O.W.)

15161 (NP-15273) ENTWICKLUNG EINES 100 Mev FFAG-ELEKTRONENSYNCHROTRONS. (Development of a 100-Mev FFAG Electron Synchrotron: Broad-Band Adaptation of Accelerator Electrodes). Moehl, D. (Freie Universitaet, Berlin (West Germany). I. Physikalisches Institut). Feb. 20, 1965. 10p. Dep. mn.

On the study of broad-band adaption of the accelerator electrodes by the use of simple coupling networks, additional broad-band systems and other possibilities for the production of accelerated fields were compared with each other in order to determine a h-f system with the best power balance for the 100-Mev FFAG electron synchrotron. On the basis of the parameters proposed for the device, a fixed modulated broad-band system with an additional extended adaptation network on a ferritic controlled system appears suitable. In addition to the fixed modulated broad-band system and the ferritic control system, a mechanical demodulation of the h-f electrodes, a phase displacement system, a cyclic traveling wave system, a modifications of the tank circuit resonators, and modifications of the installed $\lambda/4$ system were considered. (J.S.R.)

15162 (NP-15785) EKSPERIMENTAL'NOE ISSLEDOVANIE PEREZARYADNOI INZHEKTSII PROTONOV V KOL'TSEVYE USKORITELI I NAKOPITELI. (Experimental Investigation of Charge-Transfer Proton Injection into Cyclic Accelerators and Storage Rings). Budker, G. I.; Dimov, G. I.; Popov, A. G.; Sviridov, Yu. K.; Sukhina, B. N.; Timoshin, I. Ya. (Akademiya Nauk SSSR, Novosibirsk. Institut Yadernoi Fiziki). 1965. 15p. Dep. mn.

In experiments on accumulation of protons on a ring, 10^{12} protons were accumulated on a betatron coil cavity (1 amp current). At first a positive hydrogen ion source was used with a current of 21 μamp (400 w, extraction potential 12 kv). A special feature of the system was the confining of the secondary electrons in the supercharged channel of the extracting electrode (250 to 300 volts). In mounting the source in the Van de Graaff accelerator the atom beam was not cut off, which significantly increased the electron charge in the accelerator tube, and a positive hydrogen ion beam of up to 12 μamp was obtained. In the accumulator the pulses were 1 to 300 μsec. The quadrupole beam of negative hydrogen ions was focused at the accumulator entrance (3 to 4 mm, angular aperture 2×10^{-3}), and here the beam passed through the gaseous target, a flow-through tube 5 cm long and 1 cm dia. Subsequently the current was increased to 1.5 mamp. Along the 2000-gauss magnetic field in the anode channel was formed an arc (4 to 5 amp, 300 volts) with the tantalum thermocathode (160 watts), which was a strong electron emitter and formed positive hydrogen ions in the neutral gas. The electron current to the extracting electrode was limited to 100 mamp by the magnetic field. (TTT)

15163 (PPAD-279D(Rev.)) PRINCETON-PENNSYLVANIA 3 Bev PROTON SYNCHROTRON PARAMETERS. Kitagaki, T.; Shoemaker, F. C.; Kirchgessner, J. (Princeton-Pennsylvania Accelerator, Princeton, N. J.). Aug. 1959. Revised Jan. 1966. Contract AT(30-1)-2137. 12p. Dep. mn. CFSTI $1.00 cy, $0.50 mn.

Revised by J. Kirchgessner.

Various design parameters are presented in tabular form. Among these include; orbit geometry, ion optical quantities, magnetic field, magnet, magnetic force, power, injection, capture, r-f acceleration, injection accuracy, and targeting and ejection. (M.O.W.)

15164 (RHEL/R-112) P.L.A. PROGRESS REPORT, 1965. Hanna, R. C.; Dickson, J. M. (eds.) (National Inst. for Research in Nuclear Science, Chilton (England). Rutherford High Energy Lab.). Dec. 1965. 146p. Dep. mn.

Seven sections are included; separate abstracts have been prepared for 5. The remaining two sections are concerned with the operations and design modifications carried out during 1965 on the proton linac of the Rutherford High Energy Laboratory. (T.F.H.)

For abstracts of individual sections see: 14822, 15165, and 15728–15730.

15165 (RHEL/R-112, pp 12-22) ACCELERATOR PHYSICS MEASUREMENTS. (National Inst. for Research in Nuclear Science, Chilton (England). Rutherford High Energy Lab.).

Various developments and measurements at the proton linac of the Rutherford High Energy Laboratory are reported, including: development of an ionizer for a polarized proton source; development of accelerating structures; alignment of drift tubes; perturbation measurements in tanks 2 and 3; deuteron acceleration; beam energy measurements; and the development of grounded-grid triodes for use as valves in the accelerator. (T.F.H.)

15166 (SLAC-49) STORAGE RING SUMMER STUDY, 1965, ON INSTABILITIES IN STORED PARTICLE BEAMS. A Summary Report. Richter, Burton; Sands, Matthew; Sessler, A. M. (eds.) (Stanford Linear Accelerator Center, Stanford Univ., Calif.). Aug. 1965. Contract AT(04-3)-515. 80p. Dep. mn; CFSTI $3.00 cy, $0.75 mn.

Eleven papers are included; separate abstracts have been prepared for 8. The remaining 3 very short papers are concerned with media effects on beams in straight circular pipes, longitudinal resistive instabilities of azimuthally bunched beams, and one-dimensional calculations of particle trajectories in colliding beams. (T.F.H.)

For abstracts of individual papers see: 15167–15174.

15167 (SLAC–49, pp 18-22) THE LONGITUDINAL WAKE FIELDS OF A PULSE OF CHARGE MOVING DOWN A STRAIGHT PIPE OF CIRCULAR CROSS SECTION WITH FINITE CONDUCTIVITY. Morton, P. L.; Sessler, A. M. (Lawrence Radiation Lab., Univ. of California, Berkeley).

The electromagnetic fields of longitudinally bunched charged-particle beams moving in straight circular pipes of finite conductivity are studied, for the case in which the distance between bunches is large compared with the pipe diameter. The effects of pipe thickness are studied. Asymptotic field limits are approximated for various geometries. (T.F.H.)

15168 (SLAC–49, pp 23-31) THE ASYMPTOTIC PERTURBATION FIELDS OF A LONGITUDINALLY BUNCHED BEAM WITHIN A RECTANGULAR PIPE WITH RESISTIVE WALLS. Laslett, L. Jackson; Sessler, Andrew M. (Lawrence Radiation Lab., Univ. of California, Berkeley).

The electromagnetic fields of a bunched charged-particle beam that is oscillating transversely in a rectangular duct whose walls have finite conductivity are studied by asymptotic synthesis of the Fourier components. The method is first used to find the (continuous) components of the perturbation fields, and these components are then used to approximate the "wake" fields. (T.F.H.)

15169 (SLAC–49, pp 32-5) THE WAKE FIELDS OF A CHARGED PARTICLE TRAVELING IN A VACUUM CHAMBER WITH RESISTIVE WALLS. Robinson, K. W. (Cambridge Electron Accelerator, Mass.).

The "wake" electromagnetic fields produced in circular vacuum chambers by the passage of charged-particle bunches are calculated by application of the Maxwell equations to the wall currents induced by these fields. Both the longitudinal and transverse wake fields are calculated. Finite electric conductivity of the chamber walls is assumed. (T.F.H.)

15170 (SLAC–49, pp 36-48) TRANSVERSE COHERENT INSTABILITY OF BUNCHED BEAMS. Courant, E. D. (Brookhaven National Lab., Upton, N. Y.); Sessler, A. M. (Lawrence Radiation Lab., Univ. of California, Berkeley).

Transverse coherent instabilities in bunched charged-particle beams traveling in circles inside toroidal vacuum chambers are studied. (T.F.H.)

15171 (SLAC–49, pp 49-51) THE TRANSVERSE STABILITY OF ULTRA-RELATIVISTIC MULTIPLE-BUNCHED BEAMS. Allen, M.; Lee, M.; Rees, J. (Stanford Linear Accelerator Center, Stanford Univ., Calif.).

A computer program is discussed that solves the normal-mode instability problems for an ultrarelativistic charged-particle beam consisting of bunches. (T.F.H.)

15172 (SLAC–49, pp 52-8) THE INFLUENCE OF DIELECTRIC MEDIA ON THE ELECTROMAGNETIC FIELDS OF A COASTING BEAM IN A STRAIGHT RECTANGULAR PIPE. Laslett, L. Jackson (Lawrence Radiation Lab., Univ. of California, Berkeley).

The effects of dielectric coatings on the electromagnetic fields of an intense coasting beam in a cylindrical pipe are studied. The effects of filling the entire pipe volume with a homogeneous dielectric medium are also studied. The perturbation fields produced by the presence of the dielectrics are formulated. (T.F.H.)

15173 (SLAC–49, pp 61-8) THEORY OF COHERENT BUNCH MOTION IN ELECTRON-POSITRON STORAGE RINGS. Pellegrini, C. (Laboratori Nazionali di Frascati, [Comitato Nazionale per l'Energia Nucleare] (Italy)); Sessler, A. M. (Lawrence Radiation Lab., Univ. of California, Berkeley).

A general theory is developed to describe the coherent motion of bunches of particles in electron-positron storage rings. The bunches are taken to be internally rigid, and to interact with each other through direct fields as well as through fields associated with resistive vacuum tank walls; thus each bunch is affected by its own local fields (including images), its own wake field as encountered on subsequent traversals, the wave fields of other bunches in the same beam, and by the bunches of the other beam through direct fields encountered at crossing as well as wake fields. It is assumed that the storage ring is so designed and operated that each bunch of one beam encounters all bunches of the other beam; in fact, one bunch collides with a given bunch of the other beam twice per revolution. (auth)

15174 (SLAC–49, pp 71-3) INCOHERENT BEAMS BLOW-UP IN COLLIDING BEAMS. Keil, E. (European Organization for Nuclear Research, Geneva (Switzerland)).

A discussion is presented of incoherent proton-beam instabilities in cases of interest in the operation of the CERN intersecting storage rings. Theoretical predictions are compared with experimental results. (T.F.H.)

15175 (UCRL–16312) THRESHOLD DETECTOR APPLICATIONS TO NEUTRON SPECTROSCOPY AT THE BERKELEY ACCELERATORS. Smith, Alan R. (Lawrence Radiation Lab., Univ. of California, Berkeley). Nov. 19, 1965. Contract W-7405-eng-48. 66p. (CONF-651109–19). Dep. mn. CFSTI $3.00 cy, $0.75 mn.

From 1st Symposium on Accelerator Radiation Dosimetry and Experience, Upton, N. Y.

Two systems of these detectors are described. The first system consists of activation elements only, and provides neutron spectral information over the energy range 2 to 30 Mev. Among the activation elements are aluminum, carbon, cobalt, copper, iodine, iron, magnesium, nickel, and titanium. Induced activities are observed by γ-ray scintillation spectrometry, the only reasonable analysis method that permits extension of this technique to low intensities of neutron flux. Digital computer programs are used for γ-ray spectral analysis, and are also used in calculation of the neutron spectra one seeks to determine. Some results obtained at the Bevatron are discussed, in terms of the spectra themselves, and in terms of the unsolved problems attendant on this technique. Among these problems are complexities of γ-ray spectra, lack of neutron cross section data at energies higher than about 15 Mev, and production of desired activities by particles other than neutrons. The second threshold detector set consists of a mixed system of both pulse counters and activation elements, including moderated foil or BF_3 counters, aluminum disc, carbon (in the form of plastic scintillator), and bismuth fission counter. Detector information is related to the neutron spectrum over an energy range extending from about 0.02 Mev up to the primary particle energy. Data analysis involves use of a simple digital computer program, which incorporates detector calibrations, reaction cross sections, and trial neutron spectra as input parameters. The objective of this program is to compute a detector response that matches the observed detector response; attainment of this goal defines the neutron spectrum "measured" by the detectors. The effects of reasonable variations of input parameters on calculated detector response are described, and an example of a neutron spectrum that fits data obtained at the Bevatron is discussed. (M.O.W.)

15176 HIGH-CURRENT POSITRON SOURCE. Budker, G. I. At. Energ. (USSR), 19: 505-7(Dec. 1965). (In Russian).

It is proposed that positrons obtained from a 5- to 10-Mev electron beam be slowed down in a special gaseous target to thermal or near-thermal velocities, be extracted by an electric field from the target, and then be accelerated again to injection energies. Since all the positrons approach the edge of the target with almost zero energy, a parallel monochromatic beam of positrons can be obtained with subsequent acceleration in a homogeneous electric field. It is roughly estimated that the positrons can be slowed down in a trap ~1 m long with a gas pressure of 100 torr (argon or xenon). An electron conversion factor

of about 3×10^{-5} is assumed. This factor increases sharply with increased initial electron energy. The slow positrons are accelerated to 10 kev and enter a second magnetic and electric trap having a length of ~1 m and a gas pressure of <1 torr. At this pressure the time of accumulation is 1 msec. Thus with a synchrotron injection time of 3×10^{-8} sec the time ratio is 3×10^{4}, and 3 Mev positrons can be injected with a current of 1 amp. A model converting electrons to positrons was designed, and experiments will be started in the near future. (TTT)

15177 EXPERIMENTS WITH CHARGE EXCHANGE INJECTION OF PROTONS IN A STORAGE RING. Budker, G. I.; Dimov, G. L.; Popov, A. G.; Sviridov, Yu. K.; Sukhina, B. N.; Timoshin, I. Ya. At. Energ. (USSR), 19: 507-10 (Dec. 1965). (In Russian).

Negative hydrogen ions were extracted from a high-frequency source and were accelerated in a Van de Graaff machine to 12 μamp. This beam then struck a neutralizing gas target of hydrogen or carbon dioxide having an optimum thickness of 2.5×10^{16} or 3×10^{15} molecules/cm^2 respectively. The resulting beam of neutral hydrogen atoms then struck a jet of hydrogen having a thickness of ~10^{17} atoms/cm^2. The hydrogen jet was directed along a radius from the center of a storage ring with an aperture of 8×4 cm and an orbital radius of 42 cm. The particle losses did not exceed a few percent with injections up to 1500 revolutions. The orbital current increased linearly for the first 100 revolutions and remained constant for ~150 revolutions. During this period the orbital radius of the beam decreased and then struck the internal hydrogen stream. Thus the injection efficiency was close to 100%. These preliminary results indicate that it is possible to accumulate a proton current that is limited only by the space charge. (TTT)

15178 ON UNIFORM IRRADIATION OF SURFACES BY PULSED ELECTRON BEAMS. Ryabukhin, Yu. S.; Vasil'ev, A. G.; Belyakov, A. N. At. Energ. (USSR), 19: 535-7(Dec. 1965). (In Russian).

The dose D(x,y) depends on the distribution of current over the cross section of the electron beam and the irradiation lattice parameters a and b. If the deflection of electrons from the beam axis follows a normal distribution, then $I = I_{max} \exp(-r^2/2\sigma^2)$. Here I_{max} is the current density along the beam axis, I is the current density at a distance r from the beam axis, and σ is the standard electron deflection from the beam axis. An expression is derived for D(x,y) in terms of I_{max}, σ, a and b. The ratio ϵ of the minimum dose to the maximum dose is taken to characterize the nonuniformity of irradiation. The minimum dose occurs at x = 0.5 a and y = 0.5 b, while the maximum dose is at x = y = 0. An expression for ϵ is given, which shows that the uniformity of irradiation is best at a = b. The value of ϵ is plotted as a function of a/σ for various ratios of a and b. It is recommended that $a/\sigma < 2$ in order to obtain 90 to 95% irradiation uniformity. On introducing the value for the mass attenuation coefficient of the electrons in the irradiated material, an expression for calculating the average absorbed dose is derived. (TTT)

15179 MEASUREMENTS OF MEAN ENERGY OF ELECTRON BEAMS IN LOW-ENERGY LINEAR ACCELERATORS. Armenskii, E. V.; Borodulin, A. I.; Rybin, V. M.; Smirnov, V. N. Izmeritel. Tekh., 11: 44-5(1965). (In Russian).

A method for determining the mean electron energy in accelerators operating up to 10 Mev was developed. The electron kinetic energy is a function of the angle of deviation of the beam in a magnetic field and of the magnetic-field intensity. A measuring device was built on the basis of the stabilization of the beam after a slight deviation caused by passage through a magnetic field. Measurements were carried out with an accelerator operating with pulse duration 3 μsec, frequency 400 cps, current 30 to 100 mamp, beam diameter 6 mm, mean electron energy less than 10 Mev, and energy variation less than 50 kev/sec. Measurement errors resulted primarily from inhomogeneity in the magnetic field, hysteresis, instability of the electronic-system transfer coefficient, and inaccuracies in the device determining the position. (TTT)

15180 ACCELERATION OF NEGATIVE IONS IN THE MILAN AVF CYCLOTRON. Castiglioni, M.; Dutto, G.; Fois, M.; Resmini, F.; Strini, G.; Succi, C.; Tagliaferri, G. (Univ., Milan. Istituto Nazionale di Fisica Nucleare, Milan). Nuovo Cimento, (10), 41B: 244-6(Feb. 11, 1966).

The AVF Cyclotron was modified in order to accelerate negative hydrogen ions which are then stripped to protons by a very thin target. It is concluded that the acceleration of the H^- can be accomplished effortlessly in this cyclotron, and that this method offers a convenient means of obtaining useful external proton beams. (J.F.P.)

15181 30 Mev FLUX-FORCED FIELD-BIASED BETATRON. Tanaka, Osamu; Hiro, Sanju; Ikeda, Hiroshi (Mitsubishi Electric Corp., Japan). Radioisotopes (Tokyo), 15: 40-6(1966). (In Japanese).

A flux-forced field-biased betatron differs from the conventional type in a point of having two magnetic circuits termed flux forcing. An increase in the acceleration energy by almost a factor of two can be obtained by adding a d-c magnetic field to the orbit field. Therefore it possesses feature of permitting the increase of energy in a high degree for its size. However, phase shift between the central flux and the orbital field places a limitation to the bias angle and the x-ray output was obtained only up to a bias angle of 45°. Nevertheless, from "self-expansion" phenomena due to the phase shift and continuous variation of the stable orbit radius peculiar to the betatron, information of interest about the electronic orbits of the betatron was made available. Characteristics of the x-ray output as a function of d-c bias are complicated. As a typical application of it, the technique of radiography was developed with the high energy x-ray generated by the betatron and its use was extended to the detection of faults by radiographic operation on heavy metal objects. (auth)

15182 INCREASING SYNCHROCYCLOTRON CURRENTS AND THE SPACE CHARGE LIMIT. Rainwater, James (Columbia Univ., New York). Rev. Sci. Instrum., 37: 262-7(Mar. 1966).

Until MacKenzie recently emphasized the dominating role of space charge beam blowup at small radii in synchrocyclotrons, the importance of this factor was not appreciated. Much largely futile effort had been expended on attempts to increase average beam currents by improving other factors. Lawson's extension of MacKenzie's treatment for ordinary cyclotrons is considered in more detail, with numerical examples and a detailed discussion of the extension of the theory to synchrocyclotrons. In addition, a simpler semi-empirical formula is obtained which gives a good match to existing currents in all present synchrocyclotrons. Current gains up to a factor ~100 should be feasible, and a discussion is given as to how such an improvement might be gained by modifications of existing synchrocyclotrons. (auth)

15183 THREE-PHASE, 1.5-Mw, ELECTRONIC LINE REGULATOR FOR THE BERKELEY 88-INCH CYCLOTRON. Smith, Bob H.; Harris, Everett L. Jr. (Univ. of California, Berkeley). Rev. Sci. Instrum., 37: 279-83(Mar. 1966). (UCRL-16062).

Six hundred power transistors on water-cooled heatsinks are connected in a Kerns actuator circuit to modulate the power line feeding the Berkeley 88-inch cyclotron. The regulator senses the rectified three phase line voltage and attenuates the frequency components between 0.001 and 200 Hz to 0.03% of the average value. Elimination of these components from the main power line removes the need for expensive wide band regulators for each of the many critical high power loads in the building. The design considerations and construction techniques of this regulator are discussed. (auth)

15184 ENERGY MONITOR FOR ELECTRON BEAMS. Okabe, Shigeru; Tabata, Tatsuo; Tsumori, Kunihiko (Radiation Center of Osaka Prefecture). Rev. Sci. Instrum., 37: 309-10(Mar. 1966).

An energy monitor for electron beams was developed, which makes use of the elastic scattering of electrons caused by a foil placed in the beam path. The scattered

electrons are magnetically analyzed and detected by measuring the direct current from a plastic scintillator. During use of the beam the sweep of the magnetic field is repeated automatically, and the energy spectrum is displayed on a storage oscilloscope. Performance of the monitor constructed for a 15 Mev linear electron accelerator is presented. (auth)

15185 BEVATRON BEAM SPILL BY AMPLITUDE MODULATION. **Lothrop, Fred H. G. (Univ. of California, Berkeley). Rev. Sci. Instrum., 37: 358-61(Mar. 1966). (UCRL-16219).**

A more efficient method for the delivery of protons onto Bevatron targets was devised. This method involves amplitude modulation of the r-f accelerating voltage by a closed loop system that regulates the rate of loss of circulating beam, as observed on a pickup electrode. The efficiency and reliability of this new method are considerably greater than those of previous methods, and the flexibility of proton delivery control was enhanced. (auth)

15186 NONISOCHRONOUS PHENOMENON IN AN ISOCHRONOUS CYCLOTRON. **Fang, Shou-sien; Chai, Kai-yung. Sci. Sinica (Peking), 15: 1729-44(Dec. 1965). (In Russian).**

The effect of radial betatron oscillations on the frequency of rotation of particles in an isochronous cyclotron is studied. A formula is obtained for the dependence of the rotation frequency on the amplitude of the radial betatron oscillations. Analysis using the results of computer calculations shows that the growth of the average magnetic field along the radius is the main cause of this nonisochronous phenomenon. The effect of the azimuthally varied magnetic field can be neglected. It is also noted that it is necessary to increase the lowest voltage between the dees because of this effect. (tr-auth)

15187 THE USE OF BUBBLE CHAMBERS AND SPARK CHAMBERS AT ELECTRON ACCELERATORS. **Strauch, Karl (Harvard Univ., Cambridge, Mass.). pp 155-68 of Proceedings of the International Symposium on Electron and Photon Interactions at High Energies. Vol. I. Plenary Sessions. Hoehler, G. (ed.). Hamburg, Deutsche Physikalische Gesellschaft e.V., 1965.**

Those aspects in the use of bubble chambers that differ at electron and proton accelerators are discussed. Similar problems that arise in the use of spark chambers are also discussed, and the use of spark-track chambers is described. (G.O.Y.)

15188 METHOD OF IRRADIATING OBJECTS WITH HIGH ENERGY ELECTRONS. **Brynjolfsson, Ari (to Atomenergikommissionen). British Patent 1,017,713. Jan. 19, 1966. Priority date Dec. 19, 1962, Denmark.**

A method of evenly irradiating objects with high energy electrons consists of surrounding the object with a container or otherwise with a material having substantially the same specific gravity as the object and having substantially the same average atomic number as that of the object while the material is placed in the path of the irradiating beam. The material may be surrounded by water, or an electron reflecting material may be placed across the direction of the beam next to the end of the object opposite to where the beam hits the object. (B.L.M.)

15189 ROTATABLE CHARGED PARTICLE BEAM DEFLECTOR. **Farrell, Sherman R. (to High Voltage Engineering Corp.). U. S. Patent 3,230,409. Jan. 18, 1966. Filed Jan. 3, 1962.**

In a particle accelerator for generating a high energy electron beam along the longitudinal axis of the accelerator, an apparatus adapted to provided 90° deflection and 360° rotation of the beam comprises a flexible electrically conductive bellows attached to the output end of the accelerator and arranged to provide an extension of the vacuum system of the accelerator. A bellows restraining member is rotatably affixed to the output end of the accelerator and operably engages the bellows to provide a 90° bend in it and to impart rotation of the bellows about the longitudinal axis of the accelerator. The output end of the bellows is free to precess on its own axis during the rotation. A uniform magnetic field is provided in transverse relationship with the bellows to confine the electron beam within the bellows. (B.L.M.)

Astrophysics and Cosmology

Refer also to abstracts 14950 and 15435.

15190 (AD-620407) REPRESENTATIVE MODELS OF THE OBSERVED SOLAR WIND [Thesis]. **Anderson, Charles Keller (Colorado Univ., Boulder). 1965. Contract AF33(608)-1054. 264p. CFSTI $6.00 cy, $1.25 mn.**

Observed values of the physical parameters that define the solar wind are available from radar and spectral measurements of the lower corona and from space-vehicle measurements of the interplanetary plasma. The problem is to reconcile these observations with the theory of the solar wind and to construct models which are consistent with both. Parker's hydrodynamical equations are solved by numerical methods with observed values used as constraints. With single-index polytropic models, about 10% of the temperature-velocity pairs observed by Mariner II can be matched with density-velocity pairs in the lower corona observed by radar. The other 90% require dual-index models: a low index in the lower corona to accelerate the solar plasma rapidly to supercritical velocities and a high index farther out to reduce temperatures to the values observed. Conclusions derived from the analysis include the following: the observed solar wind can be represented by dual-index polytropic models; the solar plasma in the plane of the ecliptic is diverging more rapidly than it would for precisely radial flow; most of the plasma emanates from low heliographic latitudes; and the solar plasma co-rotates with the Sun for several solar radii beyond the photosphere. (TAB)

15191 (N65-20996) MODEL SOLAR PROTON ENVIRONMENTS FOR MANNED SPACECRAFT DESIGN. **Modisette, Jerry L.; Vinson, Terence M.; Hardy, Alva C. (National Aeronautics and Space Administration, Houston, Tex. Manned Spacecraft Center). Apr. 1965. 25p. (NASA-TN-D-2746). CFSTI $1.00 cy, $0.50 mn.**

A statistical analysis of the solar proton events occurring during the upper half (1956 to 1961) of the last solar cycle was made to determine the radiation environment which may be expected for flights outside the protection of the earth's magnetic field. Distribution functions were derived for both the event size (number of protons) and the spectral parameters for mission durations of 1 to 104 weeks. From these distribution functions, model environments are given, corresponding to various probabilities of occurrence. (STAR)

15192 (N65-21000) THE SOLAR FLARE ENVIRONMENT. **Roberts, W. T. (National Aeronautics and Space Administration, Huntsville, Ala. George C. Marshall Space Flight Center). Mar. 12, 1965. 38p. (NASA-TM-X-53216). CFSTI $2.00 cy, $0.50 mn.**

The solar atmosphere is discussed including the photosphere, chromosphere, and corona. Most of the main structures found within these areas are mentioned. The various types of solar flares which have been observed are then described. The problem of constructing a solar flare model is discussed, and percentile curves based on presently available data are suggested as a solution. These curves are drawn for the 99.9, 90, 67, and 50 percentile groups. Probabilities of solar-flare occurrence and methods now being used as a basis for studies on flare prediction are considered. It is concluded that even accurate solar-flare predictions can not alleviate the amount of shielding required for a long-duration extraterrestrial mission. A few of the complications involved in solar shielding calculations are covered, and a possible means of approach to these problems is suggested for future extraterrestrial missions. (STAR)

15193 (NP-15654) RARE GAS MEASUREMENTS IN 30 STONE METEORITES. Eberhardt, P.; Eugster, O.; Geiss, J.; Marti, K. (Berne Univ. (Switzerland). Physikaliches Institut). Nov. 1965. 36p. Dep. mn.

The concentrations and isotopic composition of He, Ne and Ar in 29 chondrites and 1 achondrite were determined. Detailed accounts of the experimental technique used and the reproducibility and accuracy obtained are given. The U, Th–^{4}He, and K–Ar ages derived from the results are in agreement with the already known age distributions of the different chondrite classes. Measurements revealed a linear correlation between the $(^3He/^{21}Ne)_{spall}$ and the $(^{22}Ne/^{21}Ne)_{spall}$ ratios, following the equation (constants for chondrites): $^3He/^{21}Ne = 2.40 + 23.4\ (^{22}Ne/^{21}Ne - 1)$. The significance of this correlation and its possible application in detecting diffusion losses are discussed. The radiation ages derived confirm the salient features observed in the radiation age distributions of the different chondrite classes. Five new meteorites with trapped gases were found (2 solar type, 3 planetary type). (auth)

15194 MODELS FOR CARBON-BURNING STARS. Deinzer, W. (Heidelberg Univ.); Salpeter, E. E. Astrophys. J., 142: 813-23(Oct. 1, 1965).

Equilibrium models are constructed for homogeneous stars containing only ^{12}C and heavier elements. An "initial carbon-burning main sequence" is found both with and without neutrino energy loss mechanisms. The neutrinos raise the central temperature T_c about 25 per cent, decrease the lifetime by a factor of more than 100, increase the extent of the convective core, decrease the optical luminosity slightly, and raise the mimimum mass for carbon burning from 0.7 M⊙ to about 0.8 M⊙. For gravitationally contracting stars, neutrino processes become important when T_c exceeds 0.3 or 0.5×10^9°K; they lower the temperature gradient (or even reverse its sign) in the deep interior and the contraction is not homologous. (auth)

15195 STRUCTURE AND EVOLUTION OF MODEL HELIUM STARS. Divine, Neil (California Inst. of Tech., Pasadena. Carnegie Institution of Washington, D. C.). Astrophys. J., 142: 824-40(Oct. 1, 1965).

Numerical models were constructed that describe the evolution of stars that are initially pure helium. The iterative technique, programmed for a large computer, permits the inclusion of radiation pressure, electron degeneracy, electron-scattering opacity, gravitational contraction, and detailed composition changing brought about by triple-alpha and (α,γ) reactions. The twenty homogeneous (pure helium) models, which range in mass from 0.4 to 60 M⊙, form a "main sequence" on the left of the H-R diagram. Evolutionary sequences of models at 0.5, 1, and 6 M⊙ exhaust their central helium supply in times of 80, 12, and 0.8 million years. Thereafter the convective core models, which have remained near their main-sequence positions, are replaced by shell-source models of increasing luminosity. At all three masses the final composition of the helium-exhausted core is almost exclusively oxygen, although a reduced rate for $^{12}C(\alpha,\gamma)^{16}O$ can lead to moderate fractions of carbon. Early stages of the computed evolutionary tracks agree with other calculated sequences of fitted models. Massive helium-star models may resemble Wolf-Rayet stars in mass, luminosity, and effective temperature. (auth)

15196 STUDIES IN STELLAR EVOLUTION. III. THE CALCULATION OF MODEL ENVELOPES. Henyey, Louis; Vardya, M. S.; Bodenheimer, Peter (Univ. of California, Berkeley). Astrophys. J., 142: 841-54(Oct. 1, 1965).

The formal theory underlying existing techniques for representing the superadiabatic layers in convective envelopes is re-examined. Particular emphasis is placed on the discussion of points of uncertainty and possible controversy. The analysis was carried out in a form which permits the formulation of certain constants, the arbitrariness of whose values represents the inherent uncertainty in the theory. Parallel calculations based on different values of these constants lead to a quantitative evaluation of their effect upon evolutionary tracks in the Hertzsprung-Russell diagram. Marked effects result from uncertainties in the ratio of mixing length to scale height and possibly from inadequate knowledge concerning opacities at low temperatures. (auth)

15197 A SEARCH FOR DEUTERIUM IN STELLAR SPECTRA. II. NORMAL STARS OF TYPES B, A, AND F. Peimbert, Manuel; Wallerstein, George (Univ. of California, Berkeley). Astrophys. J., 142: 1024-7(Oct. 1, 1965).

Upper limits for the abundance of deuterium were established for nine stars. The search was made primarily in stars that should not have destroyed their original deuterium during contraction. For five of them the deuterium upper limit is lower than the terrestrial value, in two cases by a factor of 4–5. This result tends to support the idea that the terrestrial deuterium is not of cosmic origin. (auth)

15198 SUPRATHERMAL HYDROMAGNETIC WAVES. Parker, E. N. (Univ. of Chicago). Astrophys. J., 142: 1086-92(Oct. 1, 1965).

The linearized equations of motion of a thermal gas and some very hot suprathermal gas, such as interstellar cosmic rays, in a uniform magnetic field are presented for plane waves in the low-frequency limit. The dispersion relation shows that there are three modes altogether. The conventional slow and fast hydromagnetic waves in the thermal gas are unaffected, except that there is a "hole" in the fast mode in the direction perpendicular to the magnetic field. The third mode is the suprathermal mode, representing waves in the suprathermal gas with essentially the velocity of sound in the suprathermal gas alone. The suprathermal mode fills the "hole" in the fast mode and is obviously the first disturbance to reach distant points following a supernova explosion. (auth)

15199 THE TIME EVOLUTION OF AN H II REGION. Mathews, William G. (Univ. of California, Berkeley). Astrophys. J., 142: 1120-40(Oct. 1, 1965).

The dimensions of Strömgren spheres when stellar black-body radiation is first saturated by recombinations are compared to the dimensions of Strömgren spheres in pressure equilibrium. The time scales for the formation of these spheres are compared with the turn-on time for the stellar ultraviolet luminosities and the lifetimes of various stars on the main sequence. The mean absorption coefficient for ionizing hydrogen and the mean photon energy are evaluated as functions of optical depth at the Lyman limit. The equations of hydrodynamics with radiative transfer and cooling by [O II] radiation are differenced. A detailed numerical solution is made for a 30 M⊙ star that moves onto the main sequence with the effective temperature and ultraviolet photon luminosity determined from accurate pre-main-sequence evolution tracks of Bodenheimer. On the main sequence $T_* = 41958$°K and $L = 8.75 \times 10^{48}$ ultraviolet photons/sec. The star is assumed to form in an infinite medium of neutral hydrogen at rest at 100°K. The complete run of gas velocity, density, temperature, pressure, degree of ionization, photon flux, and optical depths are given at times $t = 0.919 \times 10^4$, 3.07×10^4, and 6.16×10^4 years. It is found that a sharp maximum in the gas temperature follows the ionization front. The cooling by [O II] radiation immediately behind the front and the gradual rise in the equilibrium temperature outward from the star keep the velocity of most of the ionized gas in the H II region < 0.1 km/sec. At $t = 6.16 \times 10^4$ years a strong shock is moving ahead of the ionization front into the neutral gas. Allowances for cooling in the neutral gas and magnetic fields are not made. (auth)

15200 EVOLUTION OF EXTENDED RADIO SOURCES. Pacholczyk, A. G. (Joint Inst. for Laboratory Astrophysics, Boulder, Colo.). Astrophys. J., 142: 1141-8(Oct. 1, 1965).

Examined here are the dynamics and radiation of an expanding cloud containing relativistic particles and a magnetic field. The evolution of an extended radio source located outside the parent galaxy, approximated by the expanding cloud, is considered. Physical properties of

extended radio sources are calculated for the evolutionary stage in which the production of relativistic particles was terminated. In this stage the dimension of a typical source is 1 kpc (0.1–10 kpc), the total energy is 10^{60} ergs (10^{59}–10^{62} ergs), and the magnetic field is 10^{-1} G (10^{-2}–10 G). It is shown that the assumption that production of relativistic particles stopped at some earlier stage of expansion is compatible with the observational data concerning extended radio sources. (auth)

15201 AN OBSERVATIONAL TEST OF THEORIES OF NEUTRON-STAR COOLING. Bahcall, John N.; Wolf, Richard A. (California Inst. of Tech., Pasadena). Astrophys. J., 142: 1254-6(Oct. 1, 1965).

It is pointed out that the theories describing the cooling of neutron stars can be tested if such a star is detected. The basic idea of the test is that the photon luminosity of a neutron star should decrease more rapidly if neutrino-energy losses are present than if the only cooling mechanism were photon emission. In particular, the time derivative of the logarithm of the photon flux should be sufficient to determine whether or not the rate of cooling by neutrino emission is large, as predicted, compared to the rate of photon emission. In order to determine the order of magnitude of the effects due to neutrino emission, the cooling times of a typical neutron star were computed assuming the existence of two different mechanisms for neutrino emission and a degenerate Fermi-Dirac spectrum of energies for each of the relevant kinds of particles present. The test proposed is to measure the photon flux in two or more wavelength regions at two or more different times. One can then form the logarithmic derivative of the total photon flux with respect to time. (J.F.P.)

15202 ON THE INTERNAL EVOLUTION OF HELIUM STARS. Wallerstein, George (Univ. of California, San Diego, California Inst. of Tech., Pasadena). Astrophys. J., 142: 1260-2(Oct. 1, 1965).

It is pointed out that the compositions of four-B stars that are deficient in hydrogen can be explained in terms of expected evolution as far as interior helium burning, combined with the loss of any outer envelope that had the same composition as that of normal stars. Following the method of Wallerstein and Greenstein the relative abundances in the stellar cores in successive stages of evolution are traced, starting with hydrogen burning in material of initially normal composition. The composition of four stars and the changes that reproduce these abundances in the various stages of evolution are given. (J.F.P.)

15203 SOLAR X-RAY IMAGES OBTAINED USING GRAZING INCIDENCE OPTICS. Giacconi, R.; Reidy, W. P.; Zehnpfennig, T.; Lindsay, J. C.; Muney, W. S. (American Science and Engineering, Inc., Cambridge, Mass. Goddard Space Flight Center, Greenbelt, Md.). Astrophys. J., 142: 1274-8(Oct. 1, 1965).

X-ray photographs of the sun were obtained using a grazing incidence imaging telescope. The use of such a telescope greatly increases the sensitivity of the experiment. Because of the increased sensitivity, thicker filters and shorter exposure times can be used resulting in a more accurate determination of the instrumental response and an increase in angular resolution. Useful solar photographs were obtained with a spectral response limited to the wavelength interval between 8 and 12 Å. Based on a preliminary orientation a plage-associated x-ray region with a spectral distribution significantly harder than that associated with the coronal x-ray emission and a significant latitude dependence in the coronal x-ray emission were found. Also these photographs show large regions of low x-ray intensity distributed across the solar disk. (J.F.P.)

15204 THE BLACK-BODY RADIATION CONTENT OF THE UNIVERSE AND THE FORMATION OF GALAXIES. Peebles, P. J. E. (Princeton Univ., N. J.). Astrophys. J., 142: 1317-26(Nov. 15, 1965).

A critical factor in the formation of galaxies may be the presence of a black-body radiation content of the universe. An important property of this radiation is that it would serve to prevent the formation of gravitationally bound systems, whether galaxies or stars, until the universe has expanded to a critical epoch. There is good reason to expect the presence of black-body radiation in an evolutionary cosmology, and it may be possible to observe such radiation directly. (auth)

15205 OPTICAL EVIDENCE SUGGESTING THE OCCURRENCE OF A VIOLENT OUTBURST IN NGC 1275. Burbidge, E. Margaret; Burbidge, G. R. (Univ. of California, San Diego, La Jolla). Astrophys. J., 142: 1351-63(Nov. 15, 1965).

A spectroscopic study of the velocity field in the radio and Seyfert galaxy NGC 1275 was carried out, using the Lick 120-inch and McDonald 82-inch prime-focus spectrographs. The results suggest that the after-effects of an outburst in which large amounts of gas have been ejected from the nuclear region are seen in this galaxy. The gas with recession velocities ~ +3000 km/sec with respect to the center of the galaxy has probably been ejected either intermittently or continuously over a time scale of more than 5×10^6 years. Approach velocities of up to –540 km/sec relative to the center of the galaxy were detected. The velocity field in the gas associated with the main body and the appearance of the galaxy in the light of Hα plus neighboring red continuum suggest a continuing activity in the form of ejection in narrow jets from the center with velocities of up to 100–200 km/sec. An attempt was made to relate the radio source with the optical data. The object is apparently a triple radio source and the central small component is concentrated on the Seyfert nucleus. The two components which lie at distances of several hundred kiloparsecs from the nucleus are seen from the polar diagram to lie roughly in the directions of the axes of the two approximate cones of ejected gas, and this suggests that these sources are due to relativistic plasma ejected in the same outbursts which give rise to the optical phenomena. This idea casts doubt on the suggestion that one of the sources originated in the galaxy NGC 1265. It appears that the energy emitted in the outburst, much of which is in the form of kinetic energy of fast-moving but non-relativistic gas, is $\sim 10^{59}$ ergs. Thus the outburst as manifested by the Seyfert nucleus, the ejected gas, and the triple radio source is considerably more powerful than that which occurred in M82. (auth)

15206 THE GRAVITATIONAL COLLAPSE OF A UNIFORM SPHEROID. Lin, C. C.; Mestel, L.; Shu, F. H. (Massachusetts Inst. of Technology, Cambridge). Astrophys. J., 142: 1431-46(Nov. 15, 1965).

A uniform, non-rotating, pressure-free spheroid is supposed to collapse gravitationally from rest. It is shown that the initial eccentricity is steadily increased by the anisotropic gravitational field: an initially oblate spheroid tends toward a disk, and an initially prolate spheroid toward a spindle. Numerical results are computed for a series of initial eccentricities. (auth)

15207 STELLAR EVOLUTION. II. THE EVOLUTION OF A 3 M⊙ STAR FROM THE MAIN SEQUENCE THROUGH CORE HELIUM BURNING. Iben, Icko Jr. (California Inst. of Tech., Pasadena). Astrophys. J., 142: 1447-67 (Nov. 15, 1965).

A 3-M⊙ stellar model of population I initial composition is evolved from the main sequence to the stage of helium exhaustion in the core. Out of the total time elapsed, two-thirds is spent near the main sequence with hydrogen burning in the core and one-fourth is spent in the red-giant region with helium burning in the core combined with hydrogen burning in a shell. During the hydrogen-burning phase near the main sequence, ^{12}C is converted into ^{14}N and Li is destroyed over a large fraction of the stellar interior. ^{16}O is slowly converted into ^{14}N in the core. During the rise toward the red-giant tip immediately preceding the ignition of helium in the core, the extension of a convection envelope almost to the hydrogen-burning shell then leads to an increase in the surface ratio of ^{14}N to ^{12}C by a factor of 3.2 and to a decrease in the surface abundance of Li by a factor of 60. Surface abundances do

not change further during core helium burning. Comparison with the surface Li abundance of Capella F and G permits an inference concerning the average rate of mass loss from the surface of a 3 M⊙ star. (auth)

15208 OVERSHOOTING FROM STELLAR CONVECTIVE CORES. Saslaw, W. C.; Schwarzschild, M. (Princeton Univ., N. J.). Astrophys. J., 142: 1468-80(Nov. 15, 1965).

The possible extent by which the motions in a convective core might overshoot into the surrounding stable layers was investigated by a fundamental mode analysis as well as by the method of following the entropy excess of a rising element. The fact that a great number of convective motions occur consecutively in a relevant evolution time was also taken into account. The results indicate that the usual procedure of neglecting all overshooting from convective cores will generally be a good approximation. (auth)

15209 THE OPACITY DUE TO COMPTON SCATTERING AT RELATIVISTIC TEMPERATURES IN A SEMIDEGENERATE ELECTRON GAS. Chin, Chao-wen (Columbia Univ., New York. Goddard Space Flight Center, New York). Astrophys. J., 142: 1481-7(Nov. 15, 1965).

The Rosseland mean due to Compton scattering at temperatures ranging from $kT = 0.01\ mc^2$ to $kT = 0.35\ mc^2$ and for densities ranging from $\rho = 10^3$ to $10^6\ gm/cm^3$ is calculated. In most of this semidegenerate region, Compton scattering dominates over electron conduction, bound-free transitions, and free-free transitions. The results are compared with Sampson's results in the non-degenerate case and his estimates in the semidegenerate case. Upon comparison, his estimates are smaller by approximately 5–15% in most cases. (auth)

15210 THE STABILITY OF GASEOUS MASSES FOR RADIAL AND NON-RADIAL OSCILLATIONS IN THE POST-NEWTONIAN APPROXIMATION OF GENERAL RELATIVITY. Chandrasekhar, S. (Univ. of Chicago). Astrophys. J., 142: 1519-40(Nov. 15, 1965).

The stability of gaseous masses with respect to radial as well as non-radial oscillations is considered in the framework of the post-Newtonian equations of hydrodynamics. The onset of dynamical instability at a radius R determined by a formula of the type $R = (2GM/c^2)/(K/\gamma - 4/3)$ (where K is a constant) is confirmed in case the "ratio of the specific heats" $\gamma = (\partial \log p/\partial \log \rho)_s$ (where the subs denotes that the derivative is with respect to constant entropy) is a constant. An expression for K is derived which does not involve any knowledge of the equilibrium configuration beyond the Newtonian framework; and the values of K appropriate to the polytropes are also listed. With respect to the onset of instability for non-radial oscillations, it is shown that the classical criterion of Schwarzschild based on the discriminant $S(r) = (dp/dr) - \gamma(p/\rho)(d\rho/dr)$ is replaced by one based on the discriminant

$$G(r) = S(r) + \frac{\Pi}{c^2}\frac{dp}{dr}\left(\Gamma - \gamma + \frac{1}{\Gamma - 1}\frac{d\Gamma/dr}{d\rho/\rho dr}\right)$$

where Π is the internal energy (per unit volume) and Γ is a ratio defined by the relation $\rho\Pi = p/(\Gamma - 1)$. An alternative form for G(r), namely,

$$G(r) = S(r)\left[1 + \frac{\Pi}{c^2}\frac{\Gamma_3 - \Gamma}{\Gamma_3 - 1}\frac{d(\log p)/dr}{d(\log \rho)/dr}\right]$$

where $\Gamma_3 = 1 + (\partial \log T/\partial \log \rho)_s$, shows that the condition for the occurrence of convective instability is unaltered in the post-Newtonian approximation. (auth)

15211 ADIABATIC FLUID SPHERES IN GENERAL RELATIVITY. Tooper, Robert F. (Illinois Inst. of Tech., Chicago). Astrophys. J., 142: 1541-62(Nov. 15, 1965).

Solutions of the spherically symmetric hydrostatic equations of general relativity for a compressible fluid obeying a pressure-energy density relation of the form $P = K\rho_g^{1+1/n}$, $\epsilon = \rho_g c^2 + nP$ are described. This equation is satisfied by an ideal gas undergoing an adiabatic process. Relations of this form are also obtained for degenerate gases in which the constituent particles are non-relativistic or extremely relativistic (in the sense of special relativity). Equations of equilibrium analogous to the Lane-Emden equation in the Newtonian theory of polytropes are derived. Numerical solutions of these equations were obtained in terms of the ratio α of pressure to rest energy density at the center of the configuration. The mass and radius are found in terms of α and the adiabatic constant K. The metric components, pressure, density, and speed of sound are expressed in terms of the solutions to the hydrostatic equations. Integrals for the gravitational potential energy and binding energy are derived and evaluated numerically. The values of α at which instability against radial perturbations sets in are found using Chandrasekhar's variational principle. For $n \leq 3$, the mass as a function of α rises to a first maximum and then oscillates with diminishing amplitude about an asymptotic value. The objects become unstable at the first maximum in the mass. For $n = 3$, the configurations are unstable for all values of α. The binding energy also reaches a maximum at the point of instability. As α increases, the binding energy eventually becomes negative, but there are unstable configurations with positive binding energy. For $n = 3$, the binding energy is always negative. A graphical method is given for determining the parameter α, and hence the internal structure, of a configuration of specified mass and radius. No more than one characteristic value of α yielding a stable configuration can be found, and for some combinations of mass and radius this boundary-value problem is shown to have no solution. Applications are made to degenerate stars, including white dwarfs in which the electron gas is extremely relativistic ($n = 3$), and neutron stars in which the neutrons are non-relativistic ($n = 3/2$). The essential features of the neutron stars described by Oppenheimer and Volkoff are obtained with $n = 3/2$, using the appropriate value for K. Objects composed of baryons interacting with each other through a vector meson field, as described by Zel'dovich, are considered under the case $n = 1$. Using reasonable estimates for the baryon charge and the mass of the vector meson, the maximum mass attained by a Zel'dovich baryon star is ~3 M⊙. Finally, an appendix gives a post-Newtonian approximation that adequately describes configurations for which $\alpha \lesssim 10^{-2}$. (auth)

15212 EQUATION OF STATE OF MATTER AT SUPERNUCLEAR DENSITY. Harrison, E. R. (Goddard Space Flight Center, Greenbelt, Md.). Astrophys. J., 142: 1643-5(Nov. 15, 1965).

The nature of the equation of state is considered at a density exceeding that of ordinary matter. The equation of state can be expressed in the form $p = (\nu - 1)\epsilon$ where p is the pressure and $\epsilon = pc^2$ is the energy density. Classical physics shows that $\nu \leq f + 1/f$, where $f = 1$, 2, or 3 is the number of spatial degrees of freedom, and the equality sign holds for a photon or a neutrino gas. Zel'dovich proposed a model in which stationary baryons interact through a vector meson field. This model suggests that in the limit of high density in an isotropic fluid strong interactions increase the value of ν, such that $\nu = 2$ and, therefore $p = \epsilon$. Using the same model it is shown by plausible arguments that a more realistic interpretation leads to $\nu \leq 4/3$. It is concluded that despite the complexity of interactions in matter at supernuclear density, it is unlikely that the classical equations concerning the maximum possible value of ν are in error. (J.F.P.)

15213 NUMERICAL EVALUATION OF THE DEGENERATE EQUATION OF STATE. Divine, Neil (Carnegie Institution of Washington, D. C. California Inst. of Tech., Pasadena). Astrophys. J., 142: 1652-5(Nov. 15, 1965).

A method is presented for numerical evaluation of equations relating the temperature, pressure, density, and internal energy of an electron gas obeying Fermi-Dirac statistics, when the electrons are both partially degenerate and semi-relativistic. The method is suitable for machine calculation of the state relations required in stellar interior computations. (J.F.P.)

15214 A NEW MODEL OF SOLAR FLARES. Sturrock, P. A.; Coppi, B. (Stanford Univ., Calif.). Astrophys. J., 142: 3-22(Jan. 1966).

Observational data concerning solar flares are reviewed briefly in order to list the salient requirements of a model of solar flares. The requirements of a theory of the flash phase are discussed in more detail, and previous flare theories are reviewed to determine the extent to which they meet these requirements. It is submitted that no theory meets enough of the requirements to be acceptable. A new model is proposed in which the preflare state consists of a mass of gas supported by a sheared magnetic field. This field configuration is likely to be met in the neighborhood of a fault line, across which there has been a shear displacement of the photosphere, since such a fault line tends to coincide with the dividing line between regions of opposite magnetic polarity. Such a configuration of gas and magnetic field is believed to be responsible for quiescent prominences, but the energy released in a flare is believed to come from lower parts of such a system, involving stronger fields and greater mass. This model therefore explains the close relation between flares and quiescent filaments. The flash phase of a solar flare is identified with a gravitational resistive instability of the above plasma-field configuration. It is shown that the rise time of this instability is sufficiently rapid to explain the very rapid development of the flash phase. The instability tends to break up the plasma into filaments with dimensions of a kilometer or less, in agreement with certain inferences which were drawn from flare spectra. The development of fine-scale structure provides conditions for subsequent slower release of stored energy; this subsequent release is identified with the main or decay phase of flares. The flash-phase instability develops high current parallel to the magnetic field, which must be driven by an electric field parallel to the magnetic field. This permits one to identify the acceleration process in solar flares as runaway acceleration, and it is shown that this interpretation enables one to explain the observed energies of protons produced by solar flares. There is a brief discussion of the possibility of interpreting certain secondary flare phenomena, such as surges and loop prominences, by means of the proposed model. (auth)

15215 EXTENSION OF THE PHOTOSPHERIC MAGNETIC FIELD INTO INTERPLANETARY SPACE. Ness, Norman F. (Goddard Space Flight Center, Greenbelt, Md.); Wilcox, John M. Astrophys. J., 143: 23-31(Jan. 1966).

Observations of the nearby interplanetary magnetic field by the magnetometer experiment on the artificial earth satellite IMP-1 were compared with observations of the photospheric magnetic field obtained with the solar magnetograph at the Mount Wilson Observatory. A good correlation was found between the large-scale pattern of the direction (into or out of the sun) of the photospheric field and the pattern of the direction (toward or away from the sun) of the nearby interplanetary field. This substantiates the theoretical model of the transport of solar magnetic fields into interplanetary space by the magnetohydrodynamic expansion of the solar corona. (auth)

15216 DYNAMICAL PROPERTIES OF STELLAR CORONAS AND STELLAR WINDS. V. STABILITY AND WAVE PROPAGATION. Parker, E. N. (Univ. of Chicago). Astrophys. J., 143: 32-7(Jan. 1966).

The stability of an expanding corona against radial compressional waves is considered. It is shown that the linearized equations of motion are hyperbolic and the expanding corona is stable to the same general degree as a static atmosphere. Examples of wave propagation are worked out to illustrate the variation of amplitude of the waves with radial distance from the sun. (auth)

15217 THE PROPAGATION OF SHOCKS IN EXPONENTIALLY DECREASING ATMOSPHERES. Grover, R.; Hardy, J. W. (Univ. of California, Livermore). Astrophys. J., 143: 48-60(Jan. 1966).

An exposition of a similarity solution to the hydrodynamic equations in planar symmetry is presented. The solution describes an explosion in an atmosphere whose density is exponentially decreasing. Comparisons are made between the properties of this solution and those of a calculated explosion. The similarity solution was actually suggested by an examination of the asymptotic behavior of a calculated explosion and agrees excellently with it. A number of numerical results pertinent to these solutions are presented. Stability of the asymptotic behavior of the explosion to boundary conditions (structure of the source) is presented, both through examination of similarity solutions and the explosion calculations for different types of sources. The asymptotic behavior of the shock wave is found to be virtually independent of the source for a large class of them. A comparison of the results for shock acceleration to those predicted by the Chisnell formula is given. Also presented are numerical results for explosions in cylindrical and spherical symmetries. Comments are given concerning the convergence of these solutions to those of planar symmetry. (auth)

15218 EVOLUTION OF O STARS. III. HELIUM BURNING. Stothers, Richard (Goddard Space Flight Center, New York). Astrophys. J., 143: 91-110(Jan. 1966).

The evolution of a star of 30 $M_\odot$ is considered during the phases of helium ignition (I), depletion (He), and exhaustion (X). After the brief I-phase (1.5×10^4 years) during which the onset of helium burning halts the gravitational contraction in the core, helium is depleted in a large convective region growing outward in mass fraction until it nearly overtakes the hydrogen-burning shell. Helium depletion causes a radius shrinkage until $Y_c = 0.3$, whereupon the radius re-expands. The final $^{12}C/^{16}O$ ratio in the core is uncertain, but will be zero if the critical reduced alpha width in ^{16}O is greater than 0.3. The luminosity of the hydrogen shell source is low and monotonically decreases, even though the shell finally reaches the hydrogen-rich semiconvective zone ($\Delta X = 0.15$) when $Y_c = 0.01$. The star covers the spectral range from B1 to B8, while semiconvection maintains the total luminosity at a nearly constant value. The lifetime of the He-phase is 5.2×10^5 years. During the X-phase (1.3×10^4 years), the carbon-alpha reaction is able to sustain the luminosity in the shrinking convective core until $Y_c = 10^{-4}$. Thereupon the gravitational contraction in the core dominates the nuclear sources, and rapidly (10^3 years) brings the star into the region of late-type super-giants. The weak shell burning, prolonged by hydrogen enrichment due to full convective mixing at the inner boundary of the semiconvective zone, will then be extinguished by the envelope expansion. Since the new convective zone (along with the semiconvective zone) eventually retreats toward the surface, leaving behind a radiative zone of frozen composition, two major fixed composition discontinuities occur in the star: hydrogen-helium ($q = 0.44$) and helium-oxygen ($q = 0.37$). The evolutionary features of very massive stars are discussed generally, and a time scale computed for the very late phases with and without neutrino emission. In either case, the total lifetime to iron-core formation will be slightly less than 6 million years. (auth)

15219 ON THE FISSION THEORY OF THE ORIGIN OF BINARY STARS. Roxburgh, Ian W. (High Altitude Observatory, Boulder, Colo.). Astrophys. J., 143: 111-20 (Jan. 1966).

The pre-main-sequence evolution of a rotating non-magnetic star is investigated. Stars forming out of interstellar gas clouds are shown to have sufficient angular momentum to cause centrifugal force to balance gravity before reaching the stable Hayashi phase, so that during subsequent evolution matter must be left behind from the equatorial regions. During contraction through the fully convective Hayashi phase the coupling of central and surface regions by convection determines a definite rotation law which is taken to be uniform rotation. With continued contraction the star develops a radiative core and the "viscosity" effect of the turbulence is no longer operative; each element of the growing core therefore conserves its angular momentum causing an inward increase in angular velocity. It is shown that the ratio of centrifugal force to gravity in-

creases in the central regions and that for stars with mass >0.8 M⊙ rotational instability is likely to occur. This is imagined to cause the splitting of the original star into two components and so form a binary system. Assuming conservation of angular momentum on fission it is shown that stars with mass <4 M⊙ can form a contact binary system whereas more massive stars will produce separated binaries. The theoretical limits of 0.8 M⊙ and 4 M⊙ for the total mass of contact binaries are in good agreement with observations of W Ursae Majoris systems, as is the distribution of total angular momentum with mass. (auth)

15220 OBSERVATIONS OF COSMIC X-RAYS. Fisher, Philip C.; Johnson, Hugh M; Jordan, Willard C.; Meyerott, Arthur J.; Acton, Loren W. (Lockheed Missiles and Space Co., Palo Alto, Calif.). Astrophys. J., 143: 203-17(Jan. 1966).

Results are presented for eight x-ray sources observed on an October 1, 1964, rocket flight. The most detailed information is for the brightest source in Scorpius which has been located at $\alpha = 16^h14^m \pm 1^m$, $\delta = -15°36' \pm 15'$. Although seven of the eight sources lie inside the longitude interval $344° < l^{II} < 16°$, no measurable quantity of 4–8-kev x-rays is associated with the positions of Kepler's supernova or the galactic center. The spectrum of the brightest Scorpius source is peaked in the 4–8-kev range. For all sources, more flux is observed in the 4–8-kev interval than in the 8–12-kev interval. The results are compared with measurements of others. (auth)

15221 NON-RESONANT NUCLEAR REACTIONS AT STELLAR TEMPERATURES. Bahcall, John N. (California Inst. of Tech., Pasadena). Astrophys. J., 143: 259-61(Jan. 1966).

A systematic and accurate procedure is described for calculating the rates of nonresonant nuclear reactions at stellar temperatures. The approximations that are involved and the corrections that are necessary when using current formulas are indicated. (J.F.P.)

15222 CHEMICAL COMPOSITION OF THE PHOTOSPHERE AND CORONA AS INFLUENCED BY THE SOLAR WIND. Brandt, John C. (Kitt Peak National Observatory, Tucson, Ariz.). Astrophys. J., 143: 265-6(Jan. 1966).

It is suggested that the difference in abundances between the solar corona, which is thought to show an enhancement of heavy elements, and the photosphere naturally results from the ability of the lighter elements to escape more readily from the sun in the solar wind. It is concluded that the abundance differences between the photosphere and corona may be the result of the mass-dependent nature of the processes producing the solar wind. Also abundances in the solar wind should reflect the photospheric and not the coronal abundances. Accurate observations of the helium in the solar wind should provide the first accurate determination of the photospheric helium abundance. (J.F.P.)

15223 EVOLUTION OF THE SOLAR MAGNETIC FIELD. Pneuman, G. W.; Mitchell, Thomas P. (General Motors Defense Research Labs., Santa Barbara, Calif.). Icarus, 4: 494-505(Dec. 1965).

The possibility is demonstrated that the solar magnetic field, rather than being of internal origin, may have originated, during the process of the sun's formation, from a galactic magnetic field which pervaded the interstellar gas out of which the sun condensed. The magnetic field in the condensing gas cloud is maintained at approximately the galactic level until a temperature of about 1500°K is reached. At this time the field becomes frozen to the gas. Equations governing its subsequent evolution and which determine its final magnitude and geometry are derived. In particular the effects of disc formation and the Hayashi phase of solar evolution upon the magnetic field are discussed. It is found that, if these effects do not grossly change the net flux of field through the cloud, the magnitude of the surface field predicted for the present day sun compares not unfavorably with the observed 1-2 gauss field. (auth)

15224 STATIC COSMOLOGICAL MODEL AND REDSHIFT FOR RADIO GALAXIES. Gomide, F. M. (Comissao Nacional de Atividades Espaciais, Sao Paulo). Nuovo Cimento, (10), 41B: 156-63(Feb. 11, 1966).

Forty-four strong radio sources optically identified with peculiar galaxies were used in a plot of the radio magnitudes with the logarithm of the red-shifts. A (m_r, log $c\delta$) plot was established also for weak radio sources in 9 groups and clusters. These plots were compared with the photographic magnitude red-shift relation analysis of 15 groups and clusters with log $c\delta$ smaller than 3.74. The coefficients of the three straight lines obtained were not essentially different from the 2.5 value predicted for an Einstein-de Sitter static universe. These results are not inconsistent with that obtained by Hawkins for the (m_p, log $c\delta$) relation of field galaxies brighter than 14 mag. (auth)

15225 POSSIBLE MECHANISM FOR PRODUCING STRONG RADIO SOURCES. Wagoner, Robert V. (California Inst. of Tech., Pasadena). Phys. Rev. Lett., 16: 249-52(Feb. 7, 1966).

A theory of strong radio sources is proposed, which can account for many of the properties of these objects. (D.C.W.)

15226 OPACITY OF THE UNIVERSE TO HIGH-ENERGY PHOTONS. Gould, Robert Schreder, Gerald (Univ. of California, San Diego, La Jolla). Phys. Rev. Lett., 16: 252-4(Feb. 7, 1966).

The effect of the absorption of high-energy photons ($E \gtrsim 3 \times 10^{14}$ ev) traversing cosmic distances due to electron-positron pair production in photon-photon collisions with low-energy ($E \approx 10^{-3}$ ev) cosmic photons is discussed. The implications for observations on cosmic showers are considered. (G.O.Y.)

15227 ADVANCED PHASES OF EVOLUTION OF POPULATION II STARS. GROWTH OF THE CARBON CORE AND SHELL HELIUM FLASHES. Hayashi, Chushiro; Hoshi, Reiun; Sugimoto, Daiichiro (Kyoto Univ.). Progr. Theoret. Phys. (Kyoto), 34: 885-911(Dec. 1965).

Calculations were made of the evolution of a population II star after the formation of a carbon core. At the starting point the star has an inactive hydrogen shell-source, a helium-burning shell-source and a partially-degenerate isothermal carbon core. The luminosity due to shell helium-burning attains a maximum value, 1.6×10^3 $L_\odot$, when the core mass grows to 0.47 $M_\odot$. After this stage, helium-burning decays rapidly while the hydrogen shell-source becomes active. In the next phase the mass of the helium zone grows through shell hydrogen-burning and the inner layers of the helium zone begin to be degenerate. The gravitational contraction of the helium zone gives rise to the heating of the helium shell-source, until the second helium flash sets in at the degenerate shell when the mass interior to the hydrogen shell-source becomes 0.61 $M_\odot$. The subsequent evolution is, in general, the repetition of the preceding phases. The third helium flash sets in when the mass interior to the hydrogen shell-source becomes about 0.7 $M_\odot$ and the luminosity is about 8×10^3 $L_\odot$. (auth)

15228 A SIMPLE AND WELL-ADJUSTED EXTERIOR METRIC FOR A COLLAPSING OR ANTI-COLLAPSING STAR. Nariai, Hidekazu; Tomita, Kenji (Hiroshima Univ.). Progr. Theoret. Phys. (Kyoto), 34: 1046(Dec. 1965).

An exterior metric is presented for a collapsing or anti-collapsing star, which is simple and consistent with previous jump conditions. For the case of anticollapse, the formula predicts a remarkable blue shift in an initial stage of the explosion. (J.F.P.)

15229 ELECTRON DEGENERACY AT EXTREMELY HIGH TEMPERATURES, INCLUDING THE EFFECT OF PAIR CREATION. Kaminisi, Keisuke (Kumamoto Univ., Japan). Progr. Theoret. Phys. (Kyoto), 34: 1048-9(Dec. 1965).

From the number density equation for free electrons

and positrons in thermal equilibrium, the intermediate case between degeneracy and nondegeneracy is studied. The degeneracy-criterion locus separating the degeneracy and nondegeneracy regions is plotted. (J.F.P.)

15230 GRAVITATIONAL COLLAPSE AND THE DEATH OF A STAR. Thorne, Kip S. (Princeton Univ., N. J.). Science, 150: 1671-9(Dec. 24, 1965).

The story of the death of a star as predicted by a combination of nuclear theory, elementary particle theory, and general relativity theory is presented. Not taken into account in this analysis are such complications as stellar rotation, deviation from spherical symmetry, and effects of magnetic fields. These unaccounted-for factors undoubtedly have considerable effect on the quantitative results reported, but it is doubtful that, except in extreme cases, they can change the qualitative picture. (auth)

15231 ORIGIN OF CHEMICAL ELEMENTS IN STARS. [PART] VIII. Kuchowicz, Bronislaw. Urania (Krakow), 36: 247-56(Sept. 1965). (In Polish).

The synthesis of elements by converting hydrogen to helium, called process x, is considered. This process stops with helium in the case of a star the order of one solar mass, because the interaction of hydrogen with the heavier elements, through Li, Be, and B, is such that these elements tend to break up into helium nuclei. It was concluded that neutron capture must be the key in the buildup from hydrogen to the heavier elements. Nuclear reactions with cosmic rays are discussed as a possible method of nucleosynthesis. The relationship between the distribution of elements in a star and the nucleosynthesis processes is discussed. The time-temperature relationship for a star of about one solar mass is broken down into specific regions, each corresponding to a different possible process of nucleosynthesis. (TTT)

15232 THE SPACE RADIATION ENVIRONMENT. Vette, James I. (Aerospace Corp., El Segundo, Calif.). 46p. (CONF-650707-15). ORINS. Gmelin, AED-CONF-65-196-83.

From IEEE Annual Conference on Nuclear and Space Radiation Effects, Ann Arbor, Mich.

The particle space radiation environment is reviewed and some of the latest models for the various phenomena are presented. The properties of the solar wind and interplanetary magnetic fields based on recent satellite measurements are given and solar proton events are discussed. The magnetospheric cavity and the character of the boundary between it and the solar wind based on Imp 1 results are shown. Flux maps and energy spectra for the inner and outer radiation zones are given and examples of temporal variations are shown. (auth)

15233 UNEXPECTED TIME DISTRIBUTIONS OF TERRESTRIAL DETECTION OF SOLAR COSMIC-RAY EVENTS. Dodson, Helen W. (Univ. of Michigan, Ann Arbor). 15p. (CONF-650720-1). ORINS. Gmelin, AED-CONF-65-198-1.

From Symposium on Extra-Terrestrial Influence on Atmospheric Circulation, Boulder, Colo.

Data relating to the detection of solar protons in the neighborhood of the earth (1953-1963) and to neutron counts (1958-1963) were distributed on the basis of the mean synodic solar rotation period, 27.3 days, and the approximate synodic month, 29.5 days. In the latter, apparent departures from random distribution are especially marked. For the same time intervals the geomagnetic indices failed to show related patterns when distributed versus 29.5 days. At the present time it is not clear whether the 29.5 day "effect" is related to the sun or the moon or is only a statistical accident. The days on which protons arrive in the neighborhood of the earth avoided the solstices with suggestion of a pattern similar to that of the well known semi-annual wave in geomagnetic data. A more sure understanding of the latter might lead to clearer insight in solar-terrestrial relations. (auth)

15234 THE SOLAR SPECTRUM. Proceedings of the Symposium held at the University of Utrecht, 26–31 August 1963. de Jager, C. (ed.). Astrophysics and Space Science Library. Dordrecht, Holland, D. Reidel Publishing Co., 1965. 431p. (CONF-630806).

Twenty papers are presented under the following topics: the photosphere; the quiet chromosphere; the active photosphere and chromosphere spots, plages, flares, and prominences; the corona; and particle and radio emission from the sun. (L.B.S.)

Atomic Physics

Refer also to abstracts 14955, 15715, 15716, 15785, 15854, 15886, and 15976.

15235 (AD–620289) ELECTRON-IONIZATION CROSS SECTIONS. Semiannual Progress Report No. 4, December 16, 1964–June 15, 1965. Crawford, C. K.; Roddy, F. M. (Massachusetts Inst. of Tech., Cambridge. Lab. for Insulation Research). Contract AF33(657)-10939. 29p. CFSTI $2.00 cy, $0.50 mn.

A crossed-beam ion source (described) was developed, and work continued on the electron monochromators. (D.C.W.)

15236 (CONF–233(Vol.3)) ROLE OF ATOMIC ELECTRONS IN NUCLEAR TRANSFORMATIONS. Proceedings of International Conference. (International Union of Pure and Applied Physics. International Atomic Energy Agency, Vienna (Austria). Nuclear Energy Information Center, Warsaw (Poland). Polish Academy of Sciences, Warsaw). Sept. 1963. 167p. Dep. ORAU.

Separate abstracts were prepared for 12 of the 13 included papers. The remaining paper appeared previously in NSA as 17: 39969. (M.O.W.)

For abstracts of individual papers see: 15237–15246, 15715, and 15716.

15237 (CONF–233(Vol.3), pp 371-97) L AUGER SPECTRA IN j-j COUPLING. Asaad, W. N. (Cairo Univ. (Egypt). Faculty of Engineering).

The L Auger spectra of argon, krypton, and silver were calculated on the basis of extreme j-j coupling, using the Auger transition amplitudes computed by Rubenstein and Snyder. (auth)

15238 (CONF–233(Vol.3), pp 398-418) $L_1L_{2,3}M_{4,5}$ COSTER-KRONIG TRANSITION RATES. Callan, Edwin J. (Aerospace Research Labs., Wright-Patterson AFB, Ohio).

Transition rates are presented for energetically possible $L_1L_{2,3}M_{4,5}$ Coster-Kronig transitions for atoms between Sc and Th. These rates were computed using screened hydrogenic functions for both P and F terms. The total transition rates increase continuously in the region below Z = 50, rather than showing any maxima. Such maxima was surmised from the maxima in satellite/parent line intensities in this region. For the high Z region beyond Z = 73 the rates show the same trend as the data of Shrader, decreasing slowly beyond Ir. The rates for the ^1F and ^3F terms are from one to two orders of magnitude greater than for the P terms for all Z. Comparisons with calculations of Ramberg and Richtmyer, of Pincherle, and of Rubinstein and Snyder show only fair agreement within a factor of two. (auth)

15239 (CONF–233(Vol.3), pp 419-39) ON K-LEVEL WIDTHS. Callan, Edwin J. (Aeronautical Research Labs., Wright-Patterson AFB, Ohio).

Widths for the K levels of atoms in the range $16 \leq Z \leq 83$ were determined. The radiative widths were computed empirically using the equation $\Gamma^R = \Sigma_n A_n Z^4$, with the A_n being empirical coefficients for the ls-np transitions, suitably modified for the normal filling of levels. Total Auger widths were determined from KLL widths corrected for both KXY/KLL ratios and for relativistic effects for heavy atoms. The level widths so determined agree well with those reported by Parratt, to within 5% for all but the lightest atoms where the agreement is to within 0.15 ev. The K fluorescence yields were also computed, and agree well with reported theoretical and experimental curves, with

maximum deviation from the experimental value of about 0.04 in the medium Z region. Using the K widths and the various Kα line widths, L_2 and L_3 level widths were also obtained, but with considerably greater variations being found among the reported data, so that no definitive L shell widths can yet be specified. (auth)

15240 (CONF-233(Vol.3), pp 440-53) THE L,M,N AUGER SPECTRA AND THE COSTER-KROENIG TRANSITIONS OF THE HEAVY ELEMENTS. Dionisio, J. Sant'Ana (Centre National de la Recherche Scientifique, Orsay (France). Centre de Spectrometrie Nucleaire et de Spectrometrie de Masse).

A review of published and unpublished results of Auger spectra and Coster-Krönig transitions in the heavy elements is presented. The available data on the calculated and observed energies and intensities of the low-energy electron lines are described and a few suggestions are given for further development of this research field. (M.O.W.)

15241 (CONF-233(Vol.3), pp 454-64) ATOMIC M-LEVEL WIDTHS IN ^{151}Sm AND THE MULTIPOLARITY OF THE 4.821 kev TRANSITION AS DETERMINED FROM INTERNAL CONVERSION ELECTRON STUDIES. Geiger, J. S.; Graham, R. L; Merritt, Janet S. (Atomic Energy of Canada Ltd., Chalk River (Ontario). Chalk River Nuclear Labs.).

The internal conversion electron lines of the 4.821 ± 0.003-kev ground state transition in ^{151}Sm were investigated in the Chalk River iron-free beta spectrometer. Widths of the atomic levels characterized by an M_I, M_{II}, and an M_{III} vacancy were deduced from the data by line folding. (M.O.W.)

15242 (CONF-233(Vol.3), pp 465-79) K-SHELL FLUORESCENCE YIELDS OF V, Cr, AND Cu. Taylor, J. G. V.; Merritt, Janet S. (Atomic Energy of Canada Ltd., Chalk River (Ontario). Chalk River Nuclear Labs.).

Values of w_k (k-shell fluorescence yield) for V, Cr, and Cu were determined from absolute measurements of disintegration rates and K-x-ray emission rates of the electron-capturing nuclides ^{51}Cr, ^{54}Mn, and ^{65}Zn. The disintegration rates were found by $(e_A,x)\gamma$ coincidence counting using a $4\pi\beta$-γ coincidence arrangement consisting of a 4π flow-type proportional counter placed between two 7.6 × 7.6 cm NaI γ-ray detectors. K-x-ray emission rates were measured in a large 4π proportional counter which could be filled with 90% Ar + 10% CH_4 to a pressure at which essentially all the x rays were stopped in a sensitive volume. (M.O.W.)

15243 (CONF-233(Vol.3), pp 480-6) THE KLL-AUGER SPECTRUM OF MANGANESE. Lui, Yau-Yin; Albridge, R. G. (Vanderbilt Univ., Nashville, Tenn.).

The energies and relative intensities of six lines of the KLL-Auger spectrum of manganese were measured. The radioactive source used was an electroplated source of ^{55}Fe + ^{57}Co. The manganese Auger spectrum is produced in the electron capture decay of ^{55}Fe. The results are presented. (M.O.W.)

15244 (CONF-233(Vol.3), pp 487-93) STUDIES OF THE AUGER EFFECT IN LIGHT ELEMENTS. Erman, Peter (Nobel Inst. of Physics, Stockholm (Sweden)).

Auger line measurements were performed for ^{79}Br and ^{37}Cl. Problems encountered in Auger line measurements for light nuclei are briefly discussed. (M.O.W.)

15245 (CONF-233(Vol.3), pp 494-504) ATOMIC READJUSTMENT FOLLOWING THE FORMATION OF INNER SHELL VACANCIES. Carlson, Thomas A.; Krause, Manfred O. (Oak Ridge National Lab., Tenn.).

A discussion is presented on the processes involved in the atomic readjustment to a vacancy in an inner atomic shell. This discussion is based on measurements with a mass spectrometer of the relative abundances of the differently charged ions that result from the filling of inner shell vacancies. Calculations were made on multiple ionization following K vacancies. These calculations are compared with experimental data on the charge spectra following electron capture of ^{37}Ar and x-ray ionization of neon. Fairly good agreement is obtained by treating the atomic readjustment as a series of separate Auger processes and including consideration of shake off due to sudden changes in the effective charge. There is, however, also evidence for other contributions to ionization. (auth)

15246 (CONF-233(Vol.3), pp 520-8) VACUUM POLARIZATION IN Mu-MESIC ATOMS. Erber, T.; Shih, H. C. (Illinois Inst. of Tech., Chicago).

The theoretical significance of quantum electrodynamical external field corrections in extremely high fields is discussed. Compact formulas for vacuum polarization shifts in mu-mesic atoms, taking into account relativistic and finite nuclear size effects as well as virtual muons, are derived. (auth)

15247 (N65-15530) DISTORTION OF ATOMIC-BEAM VELOCITY DISTRIBUTIONS DUE TO CLASSICAL HARD-SPHERE GAS SCATTERING. Manista, Eugene J. (National Aeronautics and Space Administration, Cleveland, Ohio. Lewis Research Center). Jan. 1965. 22p. (NASA-TN-D-2617). CFSTI $1.00 cy, $0.50 mn.

The concept of the effective scattering cross section that arises primarily in studies of collisions among thermal-energy particles is reviewed. A formulation of the effective scattering cross section is developed from the definition of the collision cross section and is shown to reduce to the appropriate hard-sphere limit for the case of scattering in the center-of-mass system that is independent of relative velocity. The distortion of the Maxwellian velocity distribution of an atomic beam due to its passage through a classical hard-sphere scattering gas is investigated. The effect of the scattering gas is reduced to a generalized hard-sphere scattering probability function P(z) in which the collision radius d for a motionless scattering gas appears along with a function $\theta(z)$ that takes proper account of the motion of the scattering gas atoms. The function P(z) gives the probability that a beam atom of velocity v undergoes no scattering in passing through a region containing a Maxwellian scattering gas. The parameter z is a reduced velocity that correlates the motion of the scattering gas and the incoming beam atom velocity. (STAR)

15248 (ORNL-AMPIC-3) BIBLIOGRAPHY OF ATOMIC AND MOLECULAR PROCESSES FOR 1964. Barnett, C. F.; Griffin, D. A.; Krause, M. O.; Ray, J. A. (comps.) (Oak Ridge National Lab., Tenn.); Hooper, J. W.; Martin, D. W.; McDaniel, E. W.; Thomas, E. W. (comps.) (Georgia Inst. of Tech., Atlanta). Feb. 1966. Contract W-7405-eng-26. 217p. Dep. ORNL Free.

The bibliography contains references of interest to atomic and molecular processes research. Bibliographical sources consisted of fifty-two scientific journals and four abstract journals. The references are classified into fourteen categories and the references in each category are listed alphabetically by author. (auth)

15249 (TID-22648) COINCIDENCE STUDY OF O^+ ON Kr COLLISIONS. Final Report. Kessel, Quentin C.; Everhart, Edgar (Connecticut Univ., Storrs. Dept. of Physics). Feb. 1, 1966. Contract AT(30-1)-2047. 20p. Dep. mn. CFSTI $1.00 cy, $0.50 mn.

For Sandia Corp., Albuquerque, N. Mex.

The reaction $O^+ + Kr \rightarrow O^{m+} + Kr^{n+} + (m + n - 1)e$ was studied in the energy range from 25 to 230 kev. Scattering of the oxygen ion to angles of 10 to 40° was considered. The charge states of the resultant ions were determined, together with the energy losses of the ions. (D.C.W.)

15250 (UCRL-6987(Rev.1)) CHARGE TRANSFER CROSS SECTIONS FOR H^+, H_2^+, OR H_3^+ ON H_2 FROM 2 TO 55 kev. Chambers, E. S. (Lawrence Radiation Lab., Univ. of California, Livermore). Feb. 26, 1965. Contract W-7405-eng-48. 21p. Dep. mn. CFSTI $1.00 cy, $0.50 mn.

Electron capture cross sections for H^+, H_2^+ and H_3^+ ions colliding with H_2 gas were obtained by measuring the fast neutrals produced. Ion energy ranged from 2 to 55 kev. The

H^+ results agree with previous work at all energies. Electron capture cross sections for the molecular ions were obtained after correcting for dissociation. The effect of using vibrationally excited ions was also studied. Such ions gave about 10% more neutrals. With excited H_3^+, a change in source conditions that increased the dissociation to H_2^+ by a factor of 1.7 only caused a ±5% change in the total number of neutrals, while a change of 21% was expected. This suggests that under these conditions the electron capture decreases as the dissociation increases. The electron capture of H_2^+ produced from H_3^+ was studied. The production of negative ions by collision was investigated. (auth)

15251 ON THE SPECTRA OF SnH AND SnD. **Klynning, Lennart; Lindgren, Bo; Aslund, Nils (Univ. of Stockholm). Arkiv Fys., 30: 141-71(1965).**

Absorption spectra of SnH and SnD were produced in a King's furnace and photographed in a large concave grating spectrograph. Two band systems for each molecule were analyzed and interpreted as transitions from a common $^2\Pi$ ground state to a $^4\Sigma^-$ and a $^2\Delta$ state respectively. Energy formulas were fitted to the energy levels of the different states. A method is presented for the optimal determination of the values of the energy levels. It is based on the fundamental relations which express the wave number of each line as the difference between two term values. Different rotational formulas were applied to the term values determined by this method, and the fits of these formulas were evaluated. The constants derived for the v = 0 levels of the three electronic states are given. Additional constants were obtained for the v = 1 levels and are presented. The dissociation energy and rough values of the vibrational constants are also given. It is demonstrated that, although the fit of the model of the $^2\Delta$ state is satisfactory both for SnH and SnD, the spin-orbit coupling constants differ unexpectedly. For all three electronic states it is found that the coupling constants depend on J. (auth)

15252 ANGULAR DISTRIBUTION OF PRODUCTS OF HYDROGEN ATOM-HYDROGEN MOLECULE REACTIONS. **Micha, David A. (Uppsala Univ.). Arkiv Fys., 30: 437-47(1965).**

A previously developed theoretical model is used to describe the reactions $D + H_2 = DH + H$ and $H + D_2 = HD + D$. Analytical expressions for the cross sections are given, and the permutational symmetry problem is briefly discussed. The results show a threshold region of relative kinetic energies, for which the reactions lead most probably to backward scattering in the center of mass system, the partial cross sections with small relative angular momenta being dominant. At larger energies forward scattering is the most probable, and the partial cross sections with the highest relative angular momenta dominate. Comparison with experiments indicate agreement with the measured scattering directions, with the speed of HD product molecules, and with the absolute value of differential cross sections. The calculations predict an undetected forward scattering peak in the case of $H + D_2$ and show that the HD molecules from these reactions are mostly in low excited rotational states. (auth)

15253 SENSITIZED FLUORESCENCE IN VAPORS OF ALKALI METALS. V. ENERGY TRANSFER IN COLLISIONS BETWEEN CESIUM AND INERT GAS ATOMS. **Czajkowski, M.; McGillis, D. A.; Krause, L. (Univ. of Windsor, Ontario). Can. J. Phys., 44: 91-103(Jan. 1966).**

The total cross sections for excitation transfer between the $6\,^2P_{\frac{1}{2}}$ and $6\,^2P_{\frac{3}{2}}$ levels in cesium, induced by collisions of the second kind between cesium and inert gas atoms, were determined using methods of sensitized fluorescence. The experiments were carried out at a cesium vapor pressure of 1×10^{-6} mm Hg, at which there is no trapping of resonance radiation, and over a range of inert gas pressures extending from 1 to 300 mm Hg. The cross sections $Q_1(^2P_{\frac{1}{2}} \rightarrow {}^2P_{\frac{3}{2}})$ and $Q_2(^2P_{\frac{1}{2}} \leftarrow {}^2P_{\frac{3}{2}})$ are as follows: Cs–He: 5.7×10^{-21} and 3.9×10^{-20} cm^2; Cs–Ne: 1.9×10^{-21} and 3.1×10^{-20} cm^2; Cs–Ar: 1.6×10^{-21} and 5.2×10^{-20} cm^2; Cs–Kr: 8.3×10^{-21} and 18.4×10^{-20} cm^2; Cs–Xe: 7.2×10^{-21} and 27.4×10^{-20} cm^2. A mechanism for the excitation transfer is suggested, which involves an interaction between the inert gas atoms and the $6\,^2P$ electron in cesium, behaving as a free particle. (auth)

15254 EXPERIMENTAL AND THEORETICAL HYPERFINE STRUCTURE OF LOW-LYING LEVELS OF TERBIUM $4f^85d6s^2$ CONFIGURATION; QUADRUPOLE MOMENT OF ^{159}Tb. **Arnoult, Claire; Gerstenkorn, Simon (CNRS, Bellevue, France. CEA, Saclay, France). J. Opt. Soc. Amer., 56: 177-81(Feb. 1966).**

The hyperfine-structure splitting of the lowest levels $^8G_{11/2}$, $^8G_{13/2}$, $^8G_{15/2}$ belonging to $4f^85d6s^2$ configuration of TbI was investigated with a Fabry–Perot spectrometer. Calculations of eigenfunctions were carried out on the basis of recent work by Klinkenberg on the Tb classification. Using the magnetic-moment value given by Baker, Chadwick, Garton, and Hurrell, the value obtained for the parameters belonging to the $4f^85d6s^2$ configuration is $\langle a_0^3/r^3\rangle_{4f} = 7.91 \pm 0.08$ au $\langle a_0^3/r^3\rangle_{5d} = 2.7 \pm 0.4$ au, and $Q = +1.32 \pm 0.13$ b for the quadrupole moment of Tb. (auth)

15255 COLLISIONAL EXCITATION TRANSFER BETWEEN ATOMS IN NEAR-RESONANT PROCESSES. **Nakamura, Hiroki (Tokyo Univ.). J. Phys. Soc. Jap., 20: 2272-8(Dec. 12, 1965).**

The cross sections for the excitation transfer between unlike atoms are calculated by the impact parameter method. Approximate formulas for discrete-continuum and discrete-discrete transition probabilities are obtained. The cross section can be obtained by integrating this probability over the impact parameter. The approximate formula is applied to the case of deuterium-hydrogen excitation transfer as one of practical examples. Comparisons are made with two other formulas, i.e., Rosen-Zener (R-Z) and Vanishtein-Presnyakov-Sobelman (V-P-S) formulas. The dependence of the cross section on the resonance defect in the discrete-discrete case is also investigated. The agreements among these three formulas are found not very good. (auth)

15256 EXCITATION OF MOLECULAR VIBRATION BY SLOW ELECTRONS. **Takayanagi, Kazuo (Saitama Univ., Urawa, Japan). J. Phys. Soc. Jap., 20: 2297(Dec. 12, 1965).**

The vibrational excitation of H_2 by slow electrons was studied theoretically by Takayanagi (J. Phys. Soc. Japan 20: 562(1956)). It was supposed that the interaction most important to the process was the polarization force. A mistake found in this paper is corrected, and the importance of the polarization force in the vibration excitation of other molecules besides hydrogen is pointed out. (J.F.P.)

15257 MEASUREMENT OF EXCITATION CROSS SECTIONS FOR K IONIZATION BY IMPACT OF LOW-ENERGY NEGATON AND POSITONS. **Hansen, H.; Flammersfeld, A. (Univ., Goettingen, Ger.). Nucl. Phys., 79: 135-44(1966). (In German).**

Absolute cross sections for K ionization in thin foils of Ag, Sn, W, Au and Pb by negaton and positon impact were measured with the aid of a β-ray spectrometer and a NaI(Tl) scintillation crystal. The negaton and positon energies were varied from about 100 kev to 400 kev in the cases of Ag and Sn and from 200 kev to 550 kev in the cases of W, Au and Pb. Down to the lowest energies no systematic difference has been found between the values measured with negatons and positons, respectively. A brief discussion of the values obtained in comparison with earlier experimental and theoretical results will be given. (auth)

15258 COMPARISON OF RADIOISOTOPE BREMSSTRAHLUNG SOURCES FOR EXCITATION OF THE CHARACTERISTIC RADIATION IN ELEMENTS OF $14 \leq Z \leq 50$. **Florkowski, T.; Kosiara, A.; Wasilewska, M. (Instytut Techniki Jadrowej, Krakow). Nukleonika, 10: 661-8(1965). (In Polish).**

Results of measurements for the determination of the detection efficiency of the characteristic x rays of light elements excited by the three bremsstrahlung sources ^{3}H/Ti, ^{3}H/Zr and ^{147}Pm/Al are described. The detection of

characteristic x rays of elements, which have the atomic number lower than 20 was performed in the hydrogen and helium atmosphere, what appreciably increases the total detection efficiency. (auth)

15259 MEASUREMENT OF THE IONIZATION IN LIQUID ARGON DUE TO X-RAYS. Ullmaier, H. A. (Technische Hochschule, Vienna). Phys. Med. Biol., 11: 95-101(Jan. 1966).

Measurements of the ionization current in liquid argon are described. In contrast to other liquids investigated, it was possible to reach a saturation current. This can be explained by the presence of free electrons instead of negative ions. The degree of saturation depends on the linear energy transfer of the ionizing photoelectrons. This fact agrees with the theory of columnar ionization. Knowing the saturation current and the absorbed energy the mean energy per ion pair can be calculated. The value of 25.7 ev thus obtained agrees to within experimental accuracy, with the values determined for gaseous argon. (auth)

15260 ULTRAHIGH RESOLUTION $\Delta F = 0, \pm 1$ $(^3He)^+$ HFS SPECTRA BY AN ION-STORAGE COLLISION TECHNIQUE. Fortson, E. N.; Major, F. G.; Dehmelt, H. G. (Univ. of Washington, Seattle). Phys. Rev. Lett., 16: 221-5(Feb. 7, 1966).

The hfs spectra of ground-state $^3He^+$ ions was studied by orienting a sample of the ions, contained in an r-f trap, by spin-exchange collisions with a beam of optically pumped Cs atoms and subsequently monitoring changes in the $^3He^+$ orientation by their effect on the rate of $^3He^+$ neutralization. (G.O.Y.)

15261 STRUCTURE IN THE ELECTRON ENERGY SPECTRUM FROM MULTI-kev Ar^+–Au AND Ar^+–Cu COLLISIONS. Snoek, C.; Geballe, R.; v. d. Weg, W. F.; Rol, P. K.; Bierman, D. J. (FOM Laboratorium voor Massascheiding, Amsterdam). Physica, 31: 1553-6 (Oct. 1965).

The study of two-body atomic collisions using solid target materials was applied to an examination of the energy spectrum of electrons ejected from collisions of Ar^+ and Ne^+ ions with energies of 60, 80, and 90 kev on polycrystalline gold and copper. The results of determinations of the most probable energy for Ar^+ bombardment are given. A number of trials were made using Ne^+ ions on the same targets and at the same ion energy values. The energy spectrum from Ne^+ has no structure in the region of interest, at least to the sensitivity of the analyzer. The term values of Ne and Cu lead to the prediction that no energy groups should be expected from these sources in the interval from 50 to at least 700 ev. The target material Au could give many groups in the energy interval examined. (J.F.P.)

15262 THE POLARIZABILITY OF THE HYDROGEN-ISOTOPES AND OF ORTHO AND PARA HYDROGEN. Hermans, L. J. F.; De Groot, J. J.; Knaap, H. F. P.; Beenakker, J. J. M. (Kamerlingh Onnes Laboratorium, Leiden). Physica, 31: 1567-74(Oct. 1965).

Measurements were performed on the differences in static dielectric constant between gaseous H_2, HD, and D_2 at 77.3°K, and between normal H_2 ($^3/_4$ ortho and $^1/_4$ para) and para H_2 at 20.4°K. From these experimental data the differences in electrical polarizability were calculated. The polarizability of H_2 was found to be about 1.3% higher than that of D_2 and 0.6% higher than that of HD. The difference in polarizability between normal H_2 and para H_2 turned out to be 0.15%. These values agree rather well with the results of theoretical calculations. The measurements on normal and para H_2 permitted calculation of the difference in second virial coefficient at 20.4°K; the obtained value corresponds well with the one found by other investigators. (auth)

15263 HYPERFINE STRUCTURE OF Eu I. Bordarier, Y. (C.N.R.S., Bellevue, Eng.); Judd, B. R.; Klapisch, M. Proc. Roy. Soc. (London), Ser. A, 289: 81-96(Dec. 14, 1965). (UCRL-11745).

A theoretical analysis is made of the hyperfine structure of the twelve levels of $Eu(I)4f^7(^8S)6s6p$ using intermediate-coupled eigenfunctions obtained from a least-squares fit of the energies of the levels. Relativistic effects for the 6p electron are calculated throughout by tensor-operator techniques. Good agreement is obtained with the observed A values, treating as parameters the polarization of the core (by the f electrons) and the hyperfine interaction constant of the 6s electron. The magnitude of the core polarization is related to data on $Eu(I)4f^7(^8S)6s^2$, $Eu(II)4f^7(^8S)6s$, and $Eu(III)4f^7(^8S)$. The hyperfine-structure anomalies also fall into a consistent pattern. The observed B values are related to quadrupole moments of ^{151}Eu and ^{153}Eu. (auth)

15264 RELATIVISTIC EFFECTS IN MANY-ELECTRON HYPERFINE STRUCTURE. I. THEORY. Sandars, P. G. H.; Beck, J. (Oxford Univ.). Proc. Roy. Soc. (London), Ser. A, 289: 97-107(Dec. 14, 1965).

A theory is developed which simplifies the calculation and interpretation of relativistic hyperfine structure effects in many electron atoms. This is achieved through the introduction of the concept of an LS coupled relativistic state. By means of a series of effective Hamiltonians acting between these states the relativistic problems is turned into a nonrelativistic one which can be solved more easily. Some qualitative applications are discussed. (auth)

15265 RELATIVISTIC EFFECTS IN MANY-ELECTRON HYPERFINE STRUCTURE. II. RELATIVISTIC QUADRUPOLE INTERACTION IN MANGANESE. Evans, L.; Sandars, P. G. H.; Woodgate, G. K. (Oxford Univ.). Proc. Roy. Soc. (London), Ser. A, 289: 108-13(Dec. 14, 1965).

Theoretical and experimental work was carried out on the quadrupole interaction constant, B, for the ground state of manganese, whose ground configuration is a half filled d shell. In the nonrelativistic limit B = 0. The theory is based on a new relativistic calculation involving the use of an effective operator acting between nonrelativistic states, and a non-vanishing value of B was obtained. To check the theory, the hyperfine structure of the ground state of manganese was remeasured by the method of atomic beams and an experimental value of B was found. The agreement is satisfactory as to sign and order of magnitude, but high precision is not claimed for the theoretical result. (auth)

15266 RELATIVISTIC EFFECTS IN MANY-ELECTRON HYPERFINE STRUCTURE. III. RELATIVISTIC DIPOLE AND QUADRUPOLE INTERACTION IN EUROPIUM AND REMEASUREMENT OF THE NUCLEAR MAGNETIC DIPOLE MOMENTS OF ^{151}Eu AND ^{153}Eu. Evans, L.; Sandars, P. G. H.; Woodgate, G. K. (Oxford Univ.). Proc. Roy. Soc. (London), Ser. A, 289: 114-21(Dec. 14, 1965).

The nuclear magnetic dipole moments of ^{151}Eu and ^{153}Eu were measured. The results were obtained by the method of triple resonance in an atomic beam. The hyperfine structure anomaly in the ground state of the europium atom is zero within limits of error. In this special circumstance it is shown that part of the nuclear magnetic dipole interaction is explained by relativistic effects. The quadrupole interaction is treated by the same theory, and good agreement with experiment is obtained, but high precision is not claimed for the theoretical result. This theory is based on a new relativistic calculation involving the use of an effective operator acting between nonrelativistic states. (auth)

15267 ENERGY LEVELS IN THE THOMAS-FERMI-DIRAC ATOM. Jain, Ashok (Kyoto Univ.); Tomishima, Yasuo; Yonei, Katsumi. Progr. Theoret. Phys. (Kyoto), 34: 1044-5(Dec. 1965).

An improvement is made on Konya's model (Acta Phys. Hung. 18, 39 (1964)) by taking into account the effect of the exchange interaction between electrons. That is, the one-electron energy levels are determined using the TFD potential and the Bohr-Sommerfeld quantization condition. Energies corresponding to various values of the quantum numbers are given for silver. (J.F.P.)

15268 EXPERIMENTAL INVESTIGATION OF TRANSIENT RADIATION. Michalyak, S. (Lodz Univ., USSR). Yadern. Fiz., 3: 89-98(Jan. 1966). (In Russian).

Results of an investigation of radiation created by elec-

trons with energies between 6 and 60 kev, falling perpendicularly on a metallic target (Ag, Al, Ni) are described. The measured quantities were the absolute intensity, polarization, dependence of the radiation yield on the energy of the electrons and the angular distribution of the radiation energy in the optical part of the spectrum. The results proved to be in good agreement with the predictions of the Ginsburg and Frank theory of transient radiation. The influence of various effects accompanying transient radiation is estimated. (auth)

15269 IONIZATION LOSSES OF SPIN-$\frac{3}{2}$ PARTICLES. Dubovik, V. M. (Lebedev Inst. of Physics, Moscow). Yadern. Fiz., 3: 148-53(Jan. 1966). (In Russian).

The energy losses due to the ionization of the medium were calculated for a point particle with spin $\frac{3}{2}$. The limit of the applicability of the perturbation theory in the electrodynamics of particles with spin $\frac{3}{2}$ is established. Invariant form-factors for particles with the spin $\frac{3}{2}$ are introduced and the ionization losses are calculated, taking the characteristics of the electromagnetic structure of the particles into account. (auth)

15270 MODEL FOR ATOMIC EXCITED STATES AND ITS APPLICATION TO PHOTOABSORPTION CALCULATIONS [Thesis]. McGuire, Eugene Joseph. Ithaca, N. Y., Cornell Univ., 1965. 114p.

To treat atomic photoionization processes in the soft x-ray region a model was developed to obtain a one-electron orbital for the electron removed from the core (active electron). This is then used in the dipole length formulation of the photoionization cross section. The model divides the electrons of the residual ion into two groups, the outer shell electrons and the residual ionic core. The charge distribution seen by the active electron is taken as $\rho(r) = Z\delta(r) - (Z-1)\,\delta(r-r_1)$. That is, the residual core electrons are treated as located at the origin and the valence electrons as located in the shell at $r = r_1$. This leads to the potential: $V(r) = -2Z/r + C$ for $r \leq r_1$, and $V(r) = -2/r$ for $r \geq r_1$, where $r_1 = 2(Z-1)/C$. This potential leads to an exactly solvable Schrödinger equation in terms of Whittaker functions. The discrete and continuum solutions are constructed. The continuum solutions are used in the photoionization cross-section calculation. Applying the quantum mechanical boundary conditions to the discrete solutions at r_1 leads to a condition on the discrete energy eigenvalues. These values are chosen to agree with experiment. This fixes the parameter C or equivalently the radius r_1. Calculations are done with the model orbital for the 4d shell absorption in xenon and the adjoining elements. Theory and experiment are in good agreement. The extension of the above model potential to valence photoabsorption processes is discussed. (Dissertation Abstr.)

15271 EXCITATION OF OXYGEN BY 18- TO 102-kev PROTONS [Thesis]. Layton, Richard Gary. Logan, Utah, Utah State Univ., 1965. 142p.

A spectroscopic study was made of the light (3000-5700 Å) emitted when protons with energies from 18 to 102 kev collide with O_2. The dominant emission is from O_2 to O II. No spectral features of O_2 were observed. A few small O I lines and one weak O III line were observed. Since the major O I lines lie outside the spectral range of this study, little can be said regarding these. The absence of strong O III lines indicated that excited O III was not a major product of the collisions. The H_β line was prominent at the lower energies, indicating the capture of electrons by the incident H^+ into excited states. Absolute emission cross sections were determined for all major transitions observed, and absolute excitation cross sections were calculated for several O II states. The variation of intensity with the target gas pressure and beam current was investigated in order to separate primary and secondary excitations. The shape of the cross-section versus energy curves for the different transitions indicated that several different excitation processes occurred. Comparisons were made between the observed spectra and auroral spectra. (Dissertation Abstr.)

15272 HYPERFINE STRUCTURE IN ^{17}OH AND THE OH DIPOLE MOMENT [Thesis]. Ehrenstein, Gerald Marvin. New York, Columbia Univ., 1962. 35p.

A microwave spectrometer for the study of free radicals or other reactive species is described; it can be used with either Stark or Zeeman modulation. This spectrometer was used for the determination of the electric dipole moment of OH by measuring the Stark shift of the $^2\pi_{\frac{1}{2}}$, $J = \frac{1}{2}$, $M = 4$ Λ-doubling line at a known electric field. The OH dipole moment was found to be 1.60 ± 0.12 debyes. The same spectrometer was used to determine the hyperfine structure of $O^{17}H$. Four main lines were definitely observed, and there is evidence that one satellite line was also detected. Quantum number assignments are made for the four main lines, which are divided into two doublets. The experimental doublet splittings that arise from the magnetic hyperfine structure associated with the H nucleus are compared with splittings calculated from hyperfine structure constants obtained from experiments on $O^{16}H$. The separation between doublets is used to determine the hyperfine constant d associated with the O^{17} nucleus. The constant d is also computed theoretically from a simple molecular model of OH in which a single unpaired $p\pi$ electron about the O^{17} nucleus is assumed. The experimental value is found to be about 8 percent greater in magnitude than the theoretical value, and this difference is discussed. The satellite line is tentatively identified, and a parameter, which is a linear combination of hyperfine constants a, b, and c, is determined. This parameter is computed theoretically from a molecular model similar to that used to compute the hyperfine constant d, and differs from the experimental value by less than 8 percent. (Dissertation Abstr.)

15273 MODERATION AND CASCADE TIMES OF NEGATIVE PIONS AND NEGATIVE KAONS IN LIQUID HELIUM [Thesis]. Kopelman, Jay B. Evanston, Ill., Northwestern Univ., 1965. 62p.

The mean moderation times $T_\pi^{He}(v_A)$ and $T_K^{He}(v_A)$, spent by π^- and K^- respectively in atomic orbits before nuclear capture in the Northwestern helium bubble chamber were measured separately. It was necessary to resolve the velocities of π^- (or K^-) down to $v \approx 0.02$ c. The resolution was obtained in the pion case by measuring the μ^- range from π^--μ^--e^- decays and in the kaon case by the kinematic analysis of the τ-decay mode. The following results were obtained: $T_\pi^{He}(0.02c) = (3.19 \pm 0.23) \times 10^{-10}$ sec, and $T_K^{He}(0.02c) = (2.4 \pm 0.4) \times 10^{-10}$ sec. These measured times are two orders of magnitude longer than that predicted by Day assuming dominant Stark effect and thus S-state capture. A recent calculation by Russell reduces the rate of Stark effect yet predicts cascade times still five times shorter than our experimental values. Thus the angular momentum states of K^- capture in liquid helium are still unknown without a detailed understanding of the de-excitation mechanism of the K-mesic atom. (Dissertation Abstr.)

15274 POLARIZATION AND RELAXATION PROCESSES IN ^{3}He GAS [Thesis]. Gamblin, Rodger Lotis. Princeton, N. J., Princeton Univ., 1965. 117p.

Polarization of ^{3}He when used as a buffer gas for optically pumped rubidium vapor was investigated experimentally and theoretically. Experiment shows that the coupling between a rubidium and ^{3}He atom is scalar in form (i.e., I. S) and is about three orders of magnitude greater than would be expected from the direct magnetic interaction of the dipoles associated with each atom. A theoretical explanation of this effect, which depends upon the overlap of the Rb valence electron with the electrons of the ^{3}He atom, is presented and is in agreement with experiment. Experiments concerning the optical pumping of metastable ^{3}He atoms in order to produce ground state polarization are described. Polarizations of 60% in 1 torr samples at room temperature and 56% in 3 torr samples at 77°K were achieved. The process of metastable pumping only works at these lower pressures. Mercury liquid is shown experimentally to present a poor surface for ^{3}He relaxation. This result opens the possibility of achieving high polar-

ization at high pressure using metastable pumping and gas compression. Various wall coatings of ^3He samples are found to have only small effects upon relaxation rates. A 3.1 amagat sample in pyrex but of high purity is found to have a relaxation time of 2×10^4 seconds. This value sets present limits upon the experimental $^3He-^3He$ relaxation cross-section. A new effect that involves relaxation processes of the ^3He polarization in a magnetic field with a gradient is investigated both experimentally and theoretically. The results of theory and experiment are in close agreement with each other. An effect involving enhanced polarization of either sign of spin temperature of a high pressure sample of ^3He in which a gas discharge is struck, and which is in a 10kG field is described experimentally. (Dissertation Abstr.)

15275 THEORETICAL TRANSITION PROBABILITIES. La Paglia, S. R.; Sinanoglu, Oktay (Yale Univ., New Haven). 39p. (CONF-650661-1). ORINS. Gmelin, AED-CONF-65-150-9.

From Symposium on Molecular Structure and Spectroscopy, Columbus, Ohio.

The contribution to the intensity of atomic and molecular electronic transitions beyond the Hartree-Fock, or independent particle model, is examined by means of "many-electron theory" (MET). The contribution is of first order in the wave functions of the combining states. MET analysis of the off-diagonal matrix element for the transition probability in the frozen core approximation yields physically interesting expressions which are applied to atomic and molecular examples. Considerable improvement in calculated atomic (e.g., Be resonance transition) and molecular (e.g., π-π^* transitions) intensities is obtained when analysis shows that ground state "hole-pairs" are strongly scattered into the orbital sea of the excited state. The uses of energies and operators in the calculation of electronic intensities are also examined. The relation between the expectation values of operators ∇ and r which replace the widely used off-diagonal hypervirial theorem in the absence of exact wavefunctions is given. (auth)

15276 MULTIPHOTON IONIZATION OF RARE GAS AND HYDROGEN ATOMS. Bebb, H. Barry; Gold, Albert (Univ. of Rochester, N. Y.). 15p. (CONF-650638-3). ORINS. Gmelin, AED-CONF-65-156-6.

From Physics of Quantum Electronics Conference, San Juan, Puerto Rico.

The cross sections for ionization of Xe, Kr, Ar, Ne, He, and H atoms by simultaneous absorption of 7, 8, 9, 13, 14, and 8 ruby laser photons were calculated from perturbation theory. The rare gases have previously been treated in only the crudest approximation. An extensive treatment of hydrogen was made as a test of these approximations. It is found that the cross-section for dipolar transitions in the simplest approximation (plane wave final state, simplest approximation to the matrix element) is about three orders of magnitude smaller than that for a fairly sophisticated treatment (coulomb final states, good approximate matrix elements). The best value for H is $\sigma = 1.4 \times 10^{-244}$ (flux)^7 cm^2. This result lowers the predicted "initiation thresholds" for this process by a factor of three. Application of the improved model to rare gases indicates that direct multiphoton ionization can provide the starting electron for observed optical breakdown of gases but that other processes subsequently dominate. The effect of finite widths of states on the rates is also discussed. (auth)

Cosmic Radiation

See *also* Elementary Particles and Radiations
Nuclear Properties and Reactions

15277 COSMIC RAY NEUTRON INTENSITY MONITOR. PART A. UNIVERSITY OF CHICAGO. Simpson, John A. (Enrico Fermi Inst. for Nuclear Studies, Chicago). Geophys. Space Data Bull., 2: 15-25(1965).

The cosmic neutron flux intensity hourly counting rates corrected for pressure variations are presented for Chicago, Illinois; Climax, Colorado; and Huancayo, Peru for January to March 1965. The geographic latitude and longitude, mean station pressure, barometric coefficient, altitude, scale factor, and vertical cut-off rigidity are given for each station. (J.F.P.)

15278 COSMIC RAY NEUTRON INTENSITY MONITOR, PART B. UNIVERSITY OF NEW HAMPSHIRE. Lockwood, John A. (Univ. of New Hampshire, Durham). Geophys. Space Data Bull., 2: 27-37(1965).

The cosmic neutron flux intensity hourly counting rate corrected for pressure is presented for the University of New Hampshire from January to March 1965. The mean station pressure, barometric coefficient, scaling factor, vertical cut-off rigidity, elevation, and geographic latitude and longitude are given. (J.F.P.)

15279 COSMIC RAY NEUTRON INTENSITY MONITOR. A. UNIVERSITY OF CHICAGO. Simpson, John A. (Univ. of Chicago). Contract: AF19(628)-2473. Geophys. Space Data Bull., No. 2, 7-25(Oct. 1964).

The scaled hourly count for cosmic neutron flux intensity, corrected for barometric pressure, is presented for April to June, 1964. The stations for which these counts are given are Chicago; Climax, Colorado; and Huancayo, Peru. The geomagnetic latitude and longitude, the elevation, and vertical cut-off rigidity are given. (J.F.P.)

15280 COSMIC RAY NEUTRON INTENSITY MONITOR. B. UNIVERSITY OF NEW HAMPSHIRE. Lockwood, John A. (Univ. of New Hampshire, Durham). Contract: AF19(628)-2352. Geophys. Space Data Bull., No. 2, 26-35 (Oct. 1964).

The hourly counting rate for cosmic neutron flux intensity corrected for pressure is presented for the University of New Hampshire for April to June, 1964. The mean station pressure, barometric coefficient, and scaling factor are given. Also given are the geographic latitude and longitude, elevation, and vertical cut-off rigidity. (J.F.P.)

15281 COSMIC RAY NEUTRON INTENSITY MONITOR. PART A. UNIVERSITY OF CHICAGO. Simpson, John A. (Enrico Fermi Inst. for Nuclear Studies, Chicago). Geophys. Space Data Bull., 2: No. 2, 23-33(1965).

The cosmic neutron flux intensity hourly counting rates corrected for pressure variations are presented for Chicago, Illinois; Climax, Colorado; and Huancayo, Peru from April to June 1965. The geographic latitude and longitude, mean station pressure, barometric coefficient, altitude, and scale factor are given. (J.F.P.)

15282 COSMIC RAY NEUTRON INTENSITY MONITOR. PART B. UNIVERSITY OF NEW HAMPSHIRE. Lockwood, John A. (Univ. of New Hampshire, Durham). Geophys. Space Data Bull., 2: No. 2, 35-45(1965).

The cosmic neutron flux intensity hourly counting rate corrected for pressure is presented for the University of New Hampshire from April to June 1965. The mean station pressure, barometric coefficient, and scaling factor are given. (J.F.P.)

15283 COSMIC RAY NEUTRON INTENSITY MONITOR. PART A. UNIVERSITY OF CHICAGO. Simpson, John A. (Enrico Fermi Inst. for Nuclear Studies, Chicago). Contract: AF19(628)-2473. Geophys. Space Data Bull., No. 3, 7-34(Jan. 1965).

The cosmic neutron hourly counting rates corrected for pressure variations are presented for Chicago, Illinois; Climax, Colorado; and Huancayo, Peru from January to September 1964. The geographic latitude and longitude, the mean station pressure, barometric coefficient, altitude, and scale factor are given. (J.F.P.)

15284 COSMIC RAY NEUTRON INTENSITY MONITOR. B. UNIVERSITY OF NEW HAMPSHIRE. Lockwood, John A. (Univ. of New Hampshire, Durham). Contract: AF19 (628)-2352. Geophys. Space Data Bull., No. 3, 35-44(Jan. 1965).

The cosmic neutron hourly counting rate corrected for pressure is presented for the University of New Hampshire from July to September 1964. The mean station pressure, the barometric coefficient, and scaling factor are given. (J.F.P.)

15285 COSMIC RAY NEUTRON INTENSITY MONITOR. PART A. UNIVERSITY OF CHICAGO. Simpson, John A. (Univ. of Chicago). Contract: AF19(628)-2473. Geophys. Space Data Bull., No. 4, 7-16(Apr. 1965).

The neutron monitoring hourly counting rate corrected for pressure variations is presented for Chicago; Climax, Colorado; and Huancayo, Peru from October to December 1964. The geographic latitude and longitude, mean station pressure, radiometric coefficient, altitude, and scale factor are given. (J.F.P.)

15286 COSMIC RAY NEUTRON INTENSITY MONITOR. PART B. UNIVERSITY OF NEW HAMPSHIRE. Lockwood, John A. (Univ. of New Hampshire, Durham). Contract: AF19(628)-2352. Geophys. Space Data Bull., No. 4, 17-26 (Apr. 1965).

The neutron monitoring hourly counting rate corrected for pressure variations is presented for Mount Washington, New Hampshire, from October to December 1964. The mean station pressure, barometric coefficient, and scaling factor are given. (J.F.P.)

15287 PROBABLE MOMENTUM SPECTRA IN THE ATMOSPHERE OF LONG-LIVED HEAVY TRIPLETS PRODUCED BY PRIMARY COSMIC RAYS. Adair, Robert K.; Price, Nancy J. (Brookhaven National Lab., Upton, N. Y. Yale Univ., New Haven). Phys. Rev., 142: 844-51(Feb. 25, 1966). (BNL-9467).

A model of high-energy collision processes is constructed on the basis that collisions can be described in terms of a four-momentum transfer q, and that the spectrum of four-momentum transfers varies as $\exp(-q/q_0)$ where q_0 is a parameter of the order of magnitude of 500 Mev/c. The model is used for Monte Carlo calculations of the diffusion through the atmosphere of heavy triplets produced by the nucleons of the primary cosmic radiation. The model parameters are established by fitting the attenuation length of the primary protons in their course through the atmosphere. (auth)

15288 RADIATION FROM COSMIC-RAY AIR SHOWERS. Kahn, F. D.; Lerche, I. (Univ. of Manchester, Eng.). Proc. Roy. Soc. (London), Ser. A, 289: 206-13(Jan. 4, 1966).

Cosmic showers passing through the atmosphere produce electromagnetic disturbances. It has been suggested that these can be detected by means of a radio telescope. A simple model for a shower is set up, and it is found that the time-integrated energy flux in its radiation field, at say 45 Mc/s, is of the order of 60,000 flux units × microseconds, when the shower contains 10^6 electrons and 10^6 positrons. The radiation pattern depends on the decay rate of the shower. (auth)

15289 COSMIC RAY INTENSITIES UNDER SEA-WATER AT DEPTHS DOWN TO 1,500 METERS. Higashi, Shigeru (Osaka City Univ.); Kitamura, Takashi; Miyamoto, Shigenori; Mishima, Yasushi; Takahasi, Tamotsu; Watase, Yuzuru Progr. Theoret. Phys. (Kyoto), 34: 1042-3(Dec. 1965).

By the measurement of cosmic ray intensities in deep seas, the theoretical range-energy relation was confirmed up to several hundreds of Bev. An observation down to 1500 meters was carried out with an accuracy of ±2%. The depths at which the meson (μ) fluxes were measured and the measured vertical and oblique intensities at each depth are given. The depth-intensity relation in sea water is converted to the sea-level spectrum considering the average energy loss of mesons (μ) in sea water. Comparisons of the converted spectrum from these data are compared with the Durham energy spectrum and the converted energy spectra from the range measurements in rocks. (J.F.P.)

15290 AZIMUTHAL ANGULAR DISTRIBUTION OF SHOWER PARTICLES AND GRAY TRACKS MADE BY COSMIC-RAY PARTICLES IN PHOTOEMULSION. Azimov, S. A.; Rasulkulov, M. S.; Chudakov, V. M. (Inst. of Nuclear Physics, Uzbek SSR). Yadern. Fiz., 3: 112-15(Jan. 1966). (In Russian).

The azimuthal angular distribution of secondary particles in showers, created by singly charged particles with the average energy ~50 Bev and satisfying the selection rules $n_h + n_g > 15$; $n_s \geq 10$, is investigated. An azimuthal asymmetry shows up both for shower particles and gray tracks. A tendency for these two groups of particles to be emitted in opposite directions is observed. (auth)

15291 UPPER LIMITS OF THE COSMIC GAMMA-RAY FLUX FROM OSO-1. Peterson, Laurence F. (Univ. of California, San Diego, La Jolla). 23p. (CONF-650422-18; CONF-650534-2). ORINS. Gmelin, AED-CONF-65-118-53.

From American Geophysical Union, Program for Section of Seismology Annual Meeting, Washington, D. C. 6th International Space Science Symposium, Buenos Aires.

New upper limits on the cosmic gamma-ray flux between 50 kev and 4.5 Mev have been obtained from a gamma-ray experiment on the OSO-1. The detectors consisted of a NaI scintillator with a lead collimating shield in the 50–150 kev range and a NaI phoswich type scintillation counter with isotropic response and differential channels of 0.5 to 1.5 and 1.5 to 4.5 Mev, respectively. At 600 Km over the geomagnetic equator, the rates were 0.9, 0.36 and 0.18 counts/cm²-sec for the 50–150 kev, the 0.5 to 1.5 Mev, and the 1.5 to 4.5 Mev channels, respectively. Because of the large geomagnetic latitude effect, most of the counts can be attributed to cosmic ray effects in the instrument and in the earth below. This conclusion was confirmed by a series of balloon studies. The measured counting rates provide extreme upper limits on the flux from cosmic sources, averaged over a 2.8 π solid angle, of 9.0, 0.36 and 0.06 counts/cm²-sec-Mev for the 50–150 kev, 0.5–1.5 Mev, and the 1.5–4.5 Mev ranges, respectively. These results are not inconsistent with those of Arnold and his collaborators who measured a flux of 0.12 counts/cm²-sec-Mev at 1 Mev in cislunar space on the Ranger III spacecraft. (auth)

Direct Energy Conversion

Refer also to abstracts 14959–14962, 15046, and 15882.

15292 (AD-620511) THERMIONIC REACTOR RELIABILITY. Holland, J. W. (General Atomic, San Diego, Calif.). June 28, 1965. Contract NObs-90487. 13p. (GA-6373). CFSTI $1.00 cy, $0.50 mn.

Thermionic converter network reliability is determined as a function of the network electrical configuration and the converter reliability. The study shows that the most reliable configuration is the matrix type of network, with series-connected converters cross-connected in parallel between converters so that an alternate path for electric current is provided in the event of an open-circuit failure. It is found that with an optimized cross-connector, the most reliable matrix has about three times as many cells in series as in parallel, which conveniently coincides with the advantage of high voltage production. By supplying a small amount of redundant power to the network at the beginning of operation, matrix reliabilities can be orders of magnitude higher than the reliability of the converters. (TAB)

15293 (CONF-640921) ROUND-TABLE [SYMPOSIUM] ON THERMIONIC CONVERSION, SACLAY, FRANCE, SEPTEMBER 10–11, 1964. (Institut National des Sciences et Techniques Nucleaires, Paris (France)). 169p. Dep. mn.

In English and French.

Seven papers are included; separate abstracts are prepared for 4. The remaining 3 papers were previously abstracted in NSA, see 18: 20852, 37869, and 40806. (T.F.H.)

For abstracts of individual papers see: 15294–15297.

15294 (CONF-640921, pp 9-45) RECENT PROGRESS IN FUNDAMENTAL AND APPLIED THERMIONIC

CONVERTER TECHNOLOGY. Rasor, N. S. (Thermo Electron Engineering Corp., Waltham, Mass.).

The fundamental technological advances in thermionic cells are reviewed. Design, testing, and engineering of solar-heated, nuclear-heated, isotope-heated, and flame-heated thermionic cells are also reviewed. (T.F.H.)

15295 (CONF-640921, pp 47-77) A FRESH LOOK AT THE CHILD-LANGMUIR PROBLEM. Blue, E.; Ingold, J. H. (General Electric Co., Pleasanton, Calif. Vallecitos Atomic Lab.).

In order to gain some insight regarding the effect of electron-electron collisions on the transport of electrons in a vacuum, a model that allows for collisions is used to calculate steady-state potential distributions and the current-voltage characteristic of a planar diode. Conservation equations (mass, momentum, and energy), which are derived by taking moments of the Boltzmann equation, are used. These equations involve macroscopic variables – density, mass velocity, and temperature – as well as the pressure tensor and the heat flux vector. For simplicity, it is assumed that the electron velocity distribution is Maxwellian in the center of mass, which leads to a scalar pressure and zero heat flux. The solution to this set of equations gives a universal curve of reduced potential vs. reduced distance, similar to that of Langmuir's collisionless theory. This universal curve is used to construct current voltage characteristics, which are compared to those of Langmuir. (auth)

15296 (CONF-640921, pp 81-99) UTILISATION DES COMPOSES D'INSERTION DU GRAPHITE EN CONVERSION THERMOIONIQUE. (Utilization of Impregnation Compounds in Graphite in Thermionic Conversion). Alleau, T.; Devin, B.; Lesueur, R. (Institut National des Sciences et Techniques Nucleaires, Paris (France)).

The use of metal-impregnated graphite (the metal being Cs, Na, Li, Ba, or mixtures of Cs with the latter three) as an ion source for use in thermionic diodes is discussed. Optimal operation regimes for thermionic and thermoelectric emission are studied, and the possibilities for operating in these optimal regimes are discussed. Experimental and theoretical results are compared. (T.F.H.)

15297 (CONF-640921, pp 101-9) THE INFLUENCE OF CESIUM FLUORIDE ON THE EMITTER WORK FUNCTION AND THE PERFORMANCE OF CESIUM DIODES. Jester, A.; Langpape, R.; Minor, A. (Brown, Boveri und Cie, A. G., Mannheim (West Germany)).

The effects of CsF vapor on the work functions of W, Ta, Mo and Re emitter electrodes are studied. The effects of CsF additives on the performance of Cs-filled thermionic cells using the above metals as emitters are also studied. It is found that addition of CsF to the Cs in these thermionic cells reduces the vapor pressure required for operation at a given electrode spacing, and thus increases the cell efficiency. (T.F.H.)

15298 (FEI-22) SOSTOYANIE PRIMESEI V TSEZII, ISPOL'ZUEMOM V TERMOIONNOM PREOBRAZOVATELE. (State of Cesium Impurities Utilized in Thermionic Converters). Subbotin, V. I.; Ivanovskii, M. N.; Arnol'dov, M. N. (Gosudarstvennyi Komitet po Ispol'zovaniyu Atomnoi Energii SSSR, Obninsk. Fiziko-Energeticheskii Institut). 1965. 7p. Dep. mn.

Under approach-to-equilibrium conditions in the thermionic converter, oxygen is present in the form of oxides of the elements in the materials from which the cold electrode is made. At complete equilibrium, oxygen is present as the oxide and hydroxide of the cesium in the reservoir and hydrogen as cesium hydroxide and free hydrogen. This is because the cesium in the reservoir, kept at 300°C to maintain 1 mm Hg pressure, contains CsOH, Cs_2O, and CsH from reaction with air. Dissociation of these compounds to release hydrogen and oxygen, plus some water, is not a significant source of impurities in the vapor; the cesium and cesium oxide in the reservoir actually acts as a getter. The vapor in the hot part of the converter, at 1500–2000°C, contains molybdenum, and that in the cold part, at 500–1000°C, contains niobium and stainless steel components. In the molybdenum electrode zone MoO_2 is formed but goes to the volatile MoO_3, which is reduced by the other materials on the "cold" electrode (e.g., Ni, Ti, Fe, Cr). Any free hydrogen or water in the vapor also reduces the molybdenum oxides. (TTT)

15299 (NASA-TN-D-3324) THEORETICAL BACKGROUND FOR THERMIONIC CONVERSION INCLUDING SPACE-CHARGE THEORY, SCHOTTKY THEORY, AND THE ISOTHERMAL DIODE SHEATH THEORY. Nottingham, Wayne B. (Massachusetts Inst. of Tech., Cambridge); Breitwieser, Roland (National Aeronautics and Space Administration, Cleveland, Ohio. Lewis Research Center). Mar. 1966. 47p. CFSTI $0.70 cy, $0.50 mn.

A theoretical framework for the analysis of the performance of thermionic converters is presented. (D.C.W.)

15300 MPD RESEARCH AND DEVELOPMENT IN THE UK. EuroNuclear, 2: 590-4(Dec. 1965).

Research and development for the MPD generator is described. The use of heavy oil or coal as fuel is considered. Three main combination cycles would allow utilization of all presently available sources of energy. The open-cycle MPD generators are considered including combustion, air preheating, the duct, and seed recovery. Closed-cycle MPD generators including reactor development, the operating pressure level, the fired-heat exchanger, scale effects, the helium-cesium closed loop, and the blow-down argon-potassium rig are also considered. (J.F.P.)

15301 CURRENT-VOLTAGE CHARACTERISTICS OF CESIUM THERMIONIC CONVERTERS OPERATED AT RELATIVELY LOW TEMPERATURE. Michiyoshi, Itaru; Sakano, Kosuke (Kyoto Univ.). J. Nucl. Sci. Technol. (Tokyo), 3: 1-9(Jan. 1966).

Current-voltage characteristics were measured on a thermionic converter composed of a stainless steel emitter and of a collector that could be either stainless steel or nickel. The experimental characteristics were determined at emitter temperatures between 860 and 1,320°K and Cs pressures between 1×10^{-4} and 8.5×10^{-3} mm Hg. Data on the work functions of the stainless steel-Cs system are presented in their relation to energy conversion under relatively low temperature operation. (auth)

15302 SILICON SOLAR CELLS PRODUCED BY ION BOMBARDMENT. Gusev, V. M.; Timov, V. V.; Guseva, M. I.; Kurinnyi, V. I. Soviet Phys.-Solid State (Engl. Transl.), 7: 1673-6(Jan. 1966).

Translated from Fiz. Tverd. Tela, 7: 2077-81(July 1965).

The results of experiments aimed at the production of silicon solar cells by injection of high-energy phosphorus ions into p-Si are described. Single-crystal wafers of silicon were irradiated by phosphorus ions of 30-kev energy in a high vacuum. The current-voltage and spectral characteristics of cells obtained in this way are presented. The integrated sensitivity of these photocells amounts to about 190 ma/w. (auth)

15303 NEW METHOD FOR THE MEASUREMENT OF ELECTRON DRIFT VELOCITY BASED UPON A STUDY OF ELECTRICAL CONDUCTION IN GAS FILLED, CYLINDRICAL, THERMIONIC DIODES [Thesis]. Meisel, Lawrence V. Troy, N. Y., Rensselaer Polytechnic Inst., 1963. 113p.

A study of conduction in gas-filled, cylindrical, thermionic diodes was made. An equation relating the anode current and voltage, in terms of the electron drift velocity function of the specific gas filling, was derived, which applies to space-charge-limited, ion-free, high-pressure current flows in cylindrical diodes. The physical significance of each of these conditions is discussed. The form of the anode-current versus emission-current curve for a given plate voltage is predicted. The theory is developed in such a way that the emission current is thought of as a boundary condition. Experimental procedures and equipment developed to test the theory are described. The experimental results are in excellent agreement with the

theoretical predictions. The anode-current versus cathode-temperature curves for fixed plate voltage have the predicted form for cathode temperatures below a critical temperature for the three gases used, i.e., helium, nitrogen, and argon. The existence of a critical temperature is explained. The theoretical expression for the current-voltage relation is treated as an equation relating the electron drift velocity function to the plate voltage and current in space-charge-limited, ion-free, high-pressure, cylindrical diodes. In this way, the electron drift velocity function is deduced from the current-voltage relation in gas diodes. The electron drift velocity functions, measured in this way, are compared with the values obtained by the standard time-of-flight measurements. The agreement is good. Modifications of the experimental techniques, technical applications, and areas requiring more detailed study are suggested and discussed. (Dissertation Abstr.)

15304 MAGNETOHYDRODYNAMIC SQUEEZE FILM ENERGY CONVERTERS. Dodge, F. T. (Southwest Research Inst., San Antonio, Tex.); Osterle, J. F.; Rouleau, W. T. 16p. (CONF-650826-1). ORINS. Gmelin, AED-CONF-65-210-3.

From International Conference on Energetics, Rochester, N. Y.

A theoretical analysis is given for MHD squeeze film devices which are used as energy convertors. It is shown that such convertors can operate in either direction, i.e., they can convert electric energy to mechanical energy, or mechanical energy to electric energy. The maximum efficiency of energy conversion is determined. The efficiency depends on the direction of energy conversion and the "inertia" of the load, as well as the "figure of merit," which is the only parameter that is significant in a steady flow energy convertor. (auth)

15305 PROGRESS IN PHOTOVOLTAIC ENERGY CONVERSION. Smith, Arvin H. (National Aeronautics and Space Administration, Washington, D. C.). 64p. (CONF-650826-26). ORINS. Gmelin, AED-CONF-65-210-1.

From International Conference on Energetics, Rochester, N. Y.

Progress in the photovoltaic conversion of solar energy is reviewed starting with the observation of the photoelectric effect in selenium in 1877, through the revolutionary development of the diffused p-n junction silicon photovoltaic cell in 1953-54, to recent evolutionary improvements of photovoltaic arrays used to provide long-duration on-board electric power for modern space vehicles. (auth)

Elementary Particles and Radiations

See also Field Theory, Scattering Theory, and Symmetries

Refer also to abstracts 15692, 15728, and 15817.

15306 (CEAL-1026) SUMMARY OF RESEARCH OPERATIONS AT THE CAMBRIDGE ELECTRON ACCELERATOR. Livingston, M. Stanley (Harvard Univ., Cambridge, Mass. Cambridge Electron Accelerator, Mass.). Jan. 10, 1966. Contract AT(30-1)-2076. 19p. Dep. mn. CFSTI $1.00 cy, $0.50 mn.

The photoproduction of a number of particles and pairs was investigated; two of the studies were concerned with testing the validity of quantum electrodynamics. The form factors of the deuteron and nucleons were studied by observing e-d and e-p scattering, respectively. The production of polarized photons with a laser was also investigated, as was the use of wide-gap spark chambers. The elastic scattering of high-energy positrons by protons was studied, and the existence of Compton scattering of photons from protons was demonstrated. The beam facilities were improved, and colliding-beam facilities were considered. (D.C.W.)

15307 (COO-1261-22) SUPPORT OF K-MESON EXPERIMENTS AT THE ZGS. Final Report, February 1, 1963-September 30, 1965. Romanowski, T. A.; Reibel, Kurt (Ohio State Univ. Research Foundation, Columbus). Dec. 1965. Contract AT(11-1)-1261. 11p. Dep. mn. CFSTI $1.00 cy, $0.50 mn.

Brief summaries of various activities of the OSU group during this period are presented. The ZGS beam survey and the extracted proton beam studies involved counters, as does the K production cross section experiment. The Ke_2 and $\Lambda\beta$ experiments make use of counters and spark chambers and considerable effort has gone into the instrumentation for these experiments. Also, OSU personnel became involved in the data analysis of the ANL-CERN spark chamber exposure, first at ANL and later, using the spark chamber and bubble chamber data processing system, at OSU. Finally, a development of digitized spark chamber systems with magnetostrictive readout was initiated. Theorists investigated various mechanisms of the breaking of SU_3 symmetry. In particular, a consequence of the symmetry breaking interaction that transforms as the I = Y = 0 member of 27 representation was found, and also some rules among the axial vector coupling constants were derived when symmetry breaking interaction is taken into account. In weak interactions, the universality in the strength of strong coupling of the vector meson K* with all strangeness changing F type vector current was derived, the $\Delta Q = 0$, $\Delta S = 1$ component of unitary spin current combined with symmetry arguments was exploited in rare decay modes of hadrons, and the nonleptonic K° decay was examined on the basis of CPT theorem and unitary symmetry without the requirement of CP invariance. In addition, the decay widths of the radiative decay mode of vector mesons were calculated in SU_6, and equal time commutation relations of currents in SU_2 were applied to pseudoscalar meson states with the conclusion that strong $\pi^-\pi^+$ and π^-K^+ interactions should exist in the low energy region. (auth)

15308 (IC/66/13) EVALUATION OF THE $N^*_{33}N$ WEAK COUPLING CONSTANTS BY MEANS OF CURRENT ALGEBRA. Furlan, G.; Jengo, R.; Remiddi, E. (International Centre for Theoretical Physics, Trieste (Italy)). Feb. 1966. 9p. Dep. mn.

The form factors of the $N^*_{33}N$ weak axial vectors are expressed in terms of the vector and axial vector form factors of the nucleon. A relation between the $N^*_{33}N\pi$ and $NN\pi$ coupling constants and an estimate of the mass of a hypothetical 1^+ meson are also obtained. (auth)

15309 (JINR-E-2563) A POSSIBLE MECHANISM OF CP VIOLATION. Arbuzov, B. A.; Filippov, A. T. (Joint Inst. for Nuclear Research, Dubna (USSR). Lab. of Theoretical Physics). 1966. 7p. Dep. mn.

The mechanism of CP-violation in interaction of particles with photons with the coupling constant G_e is considered. Possible experiments are discussed, which serve to check this mechanism. (auth)

15310 (JINR-P-2508) SECHENIE OBRAZOVANIYA ZARYAZHENNYKH π-MEZONOV V (n,p)-SOUDARENIYAKH PRI EFFEKTIVNOI ENERGII NEITRONOV 585 Mev. (Production Cross Section of Charged Pions in (n,p) Collisions at the Effective Neutron Energy of 585 Mev). Basiladze, S. G.; Ermolov, P. F.; Oganesyan, K. O. (Joint Inst. for Nuclear Research, Dubna (USSR). Lab. of Nuclear Problems). 1965. 7p. Dep. mn.

Using a scintillation telescope and a liquid hydrogen target Dewar vessel, the production cross section of charged pions in neutron-proton collisions was measured at 585 Mev. The value of the cross section was found. (auth)

15311 (LNF-65/47) VECTOR BOSON HUNTING WITH ADONE. Note No. 299. Bernardini, C. (Laboratori Nazionali di Frascati, Comitato Nazionale per l'Energia Nucleare (Italy)). Dec. 27, 1965. 6p. Dep. mn.

A possible method for producing and detecting mesons (V^0) in the Adone storage ring using $e^+ + e^-$ collisions is discussed. (M.O.W.)

15312 (MIT-2098-86) THE ANALYTIC CONTINUATION OF AN S_{11} PION-NUCLEON AMPLITUDE TO THE P_{11}

AMPLITUDE. Goldberg, H. (Brandeis Univ., Waltham, Mass. Dept. of Physics); Lomon, E. L. (Massachusetts Inst. of Tech., Cambridge). Nov. 5, 1964. Contract AT(30-1)-2098. 23p. Dep. mn. CFSTI $1.00 cy, $0.50 mn.

The MacDowell Symmetry is used to obtain the unique P_{11} pion-nucleon amplitude related to the simple analytic form of the S_{11} amplitude derived previously from a two channel boundary condition model. The a posteriori justification for the extension of the too simple S_{11} amplitude over several Bev is the resulting satisfaction of the stringent P state threshold requirement, and a qualitative agreement of the P state amplitude with experimental information. (auth)

15313 (NP-15822) MESURE DE LA POLARISATION DU PROTON DE RECUL DANS LA DIFFUSION ELASTIQUE ELECTRON-PROTON [Theses]. (Measurement of Recoil Protons in the Elastic Electron-Proton Scattering [Thesis]). Buon, Jean (Paris Univ. (France). Faculte des Sciences). Feb. 1965. 114p. Dep. mn.

An experiment was undertaken to verify the validity of the Born approximation in the first order in the elastic scattering of high energy electrons and protons. The experiment consisted of the measurement of the polarization of recoil protons in an elastic scattering of electrons having an energy of 950 Mev and scattering at an angle of 90° in the center-of-mass system. The electron beam from the Orsay linear accelerator was scattered in a liquid hydrogen target with a useful length of 4 cm. A spectrometer analyzes the recoil protons emitted at angle of 40.3° in the laboratory system, which corresponds to a pulse quadritransfer of 15.4 $Fermi^{-2}$. This spectrometer was designed with 2 quadrupoles and a uniform magnetic field. The resolution of motion quantity is approximately 1%. At the out-put of the spectrometer the transverse component of the polarization of the proton beam was measured in a polarimeter. This makes it possible to scatter the protons in a carbon block. The asymmetry of the second diffusion gives a polarization of the protons. The trajectories of each proton before and after this second scattering were determined by an ensemble of 4 spark chambers. These are released with 5 scintillation counters. The directions of the trajectories were measured with the precision of the order of 0.05% to reduce the systematic errors. The transverse component of the polarization was calculated with a method derived from the method of probability maximum. This method was applied to the distribution observed of the angle between the normal to the plane of the second scattering and the vertical direction. The determination of the trajectories and the calculation of the polarization were made on the Univac 1107 computer. This calculation of the polarization gives for the value of the transverse component perpendicular to the plane of the elastic electron-proton scattering a value of 0.040 ± 0.027. The value of the transverse component parallel to the plane of the elastic electron-proton scattering is 0.000 ± 0.028. The error indicated is a square mean of the statistical error 0.021 and of the estimated systematic error 0.017 and 0.018 for the two components. (tr-auth)

15314 (RT/FI(65)35) SMALL ANGLE ELASTIC SCATTERING OF POLARIZED PROTONS IN PHOTOGRAPHIC EMULSIONS. Beltrametti, E.; Boebel, G.; Gigli, A.; Lamborizio, C.; Ortalli, I.; Picasso, E.; Tomasini, G. (Comitato Nazionale per l'Energia Nucleare, Rome (Italy)). Sept. 1965. 13p. Dep. mn.

Elastic scattering experiments of polarized (89%) protons of 215 Mev energy in photographic emulsions were performed. The right-left asymmetry $\epsilon(\theta)$ was measured at small scattering angles (of the order of a few degrees); the results give indications of a sign change of the asymmetry at a scattering angle of about 4°, though the statistics are too poor to give a definite answer for the behavior of the asymmetry around $\theta = 4°$. The theoretical implications of the observed behavior of $\epsilon(\theta)$ at small θ are discussed taking into account coulomb interaction effects. The conclusion is that the coulomb interference could give rise to a large "anomalous" behavior of $\epsilon(\theta)$ at small angles (1° + 5°) of the same kind as the one suggested by the experimental data. However it is to be remarked that the calculated effects are strongly dependent on the approximation used to calculate the scattering amplitudes. (auth)

15315 (STI/PUB/117) HIGH-ENERGY PHYSICS AND ELEMENTARY PARTICLES. Proceedings Series. Proceedings of the Seminar held at the International Center for Theoretical Physics, Trieste, May 3–June 30, 1965. (International Atomic Energy Agency, Vienna (Austria)). 1965. 1008p. (CONF-650553). IAEA: $15.00; S 315,-; £ 4.10.0; F Fr 60,-; DM 52,50.

Separate abstracts were prepared for 52 of the 54 papers included. The other two papers were previously abstracted for NSA (19: 45004 and 19: 45005). (G.O.Y.)

For abstracts of individual papers see: 15431–15435, 15512–15557, and 15642.

15316 (UCRL-16526) PRODUCTION PROPERTIES AND DECAY MODES OF THE ϕ MESON [Thesis]. Lindsey, James Seward (Lawrence Radiation Lab., Univ. of California, Berkeley). Dec. 21, 1965. Contract W-7405-eng-48. 74p. Dep. mn. CFSTI $3.00 cy, $0.75 mn.

The reaction $K^-p \rightarrow \Lambda\phi$ was studied in an exposure of the LRL 72-inch bubble chamber to a separated beam of K^- mesons of 2.1 to 2.7 Bev/c momentum. The decay branching ratios for K^+K^-, $K_1^0K_2^0$, $\rho\pi$, $\eta\gamma$, $\pi^+\pi^-$, $\rho\gamma$, and $\omega\gamma$ were measured, and the ratio $\beta = [\Gamma(\phi \rightarrow K_1^0K_2^0)/\Gamma(\phi \rightarrow K^+K^-)]$ was used as a test of the ϕ's spin. The quantum numbers assigned to the ϕ, $J^{PC} = 1^{2-}$ and I = 0, were verified. An attempt was made to fit decay-angular distributions to several models, in order to further confirm the spin 1 assignment for the ϕ. However, the distributions are consistent with predictions for both spin 1 and spin 3, so that no independent test of spin is possible. Production processes were investigated with the correlation-matrix method of Berman and Oakes. The low-momentum (2.1 Bev/c beam momentum) data fit a model of K and K* exchange, but the high-momentum (2.45 to 2.7 Bev/c) data are inconsistent with the model. Also, other final states involving KK pairs were investigated, and their cross sections measured, but except for the production of the reaction $K^-p \rightarrow Y_1^*(1385)\phi$, no previously unreported effects were observed. (auth)

15317 (ORNL-tr-677) AN INVESTIGATION OF TRANSITION EFFECT [Thesis]. Mikhalyak, S. (Moscow State Univ. (USSR). Scientific Research Inst. of Nuclear Physics). Translated for Oak Ridge National Lab., Tenn., from a report. 1961. 122p. Dep. mn. CFSTI $4.00 cy, $0.75 mn. JCL $10.10 fs, $3.86 mf.

The emission of electromagnetic radiation by a charged particle in passing from one medium to another was investigated. The light emitted in the reaction of an electron beam with the surfaces of Al, Ni, and Ag targets was observed. The results are in good agreement with the predictions of the Frank-Ginzburg theory for electrons in the energy range from 6 to 60 kev. (D.C.W.)

15318 DOUBLE BREMSSTRAHLUNG. Ehlotzky, F. (Univ., Innsbruck). Acta Phys. Austr., 20: 17-24(1965). (In German).

The process of double bremsstrahlung was investigated. By means of a generalized Weizsacker-Williams method, expressions for the differential and total effective cross section can be obtained. The results agree with the results obtained by Gupta. The double bremsstrahlung contributes, at a maximum, several percent to the total energy loss of the scattered electrons. There is, however, a certain uncertainty for the pulse transmitted to the core with respect to the integration limits. It is not impossible that the expression obtained must be revised and that at extreme relativistic energies in the multi-Bev range the double bremsstrahlung can be equal to the simple bremsstrahlung. (tr-auth)

15319 RADIATION CORRECTORS OF e-p SCATTERING. Bartl, A. (Univ., Graz). Acta Phys. Austr., 20: 25-9(1965). (In German).

Expressions are derived for the soft and hard contribution to the radiative corrector and are numerically evalu-

ated for two cases. The differences from the α^3 order amounts to approximately 2%. (tr-auth)

15320 REMARKS ON REGULARIZATION. Latal, H.; Zingl, H. (Univ., Graz). Acta Phys. Austr., 20: 30-3 (1965). (In German).

The regularization of lepton propagators is established in which the regularization is conceived as a result of structure effects. The interpretation is illustrated by simple identities. (J.S.R.)

15321 INTEGRAL REPRESENTATIONS FOR SCATTERING AMPLITUDES. II. APPLICATION. Predazzi, E. (Univ. of Chicago). Contract AT(11-1)-264. Ann. Phys. (N. Y.), 36: 250-66(Feb. 2, 1966). (COO-264-284).

The formalism developed previously is applied to a phenomenological analysis of high energy proton-proton elastic scattering. The general experimental features appear to be satisfactorily reproduced by a simple empirical spectral function. Spin effects are neglected; for this reason the numerical comparison given here has to be taken simply as a qualitative indication and no least squares analysis has been carried on. Restricting ourselves to a potential picture and solving the inversion problem in the W.K.B. approximation, the potential is roughly reconstructed from the empirical scattering amplitude and is found to be an energy dependent generalization of a Yukawa potential whose Fourier transform is exponentially damped for large values of the momentum variable. (auth)

15322 SU(n) CROSSING MATRICES FOR BARYON-MESON SCATTERING. Mani, H. S. (National Physical Lab., New Delhi, India); Mohan, Gyan; Pande, Lalit K.; Singh, Virendra. Ann. Phys. (N. Y.), 36: 285-307(Feb. 2, 1966).

The crossing matrices giving the relation between the crossed baryon-meson scattering channel and the direct baryon-meson scattering channel are given for the SU(n) symmetry case. The mesons and the baryons are assumed to belong respectively to the regular representation of the symmetry group, and to rank three tensor representations. The crossing matrix relevant for the quark-meson scattering is also given. (auth)

15323 THE BINDING ENERGY AND THE QUADRUPOLE MOMENT OF THE DEUTERON ACCORDING TO A THEORY BY H. A. S. ERIKSSON. Thor, Anders J. (Royal Inst. of Tech., Stockholm). Arkiv Fys., 31: 19-32(1965).

The equations deduced by Eriksson for the deuteron in the triplet and the singlet state respectively are investigated as an approximation, where terms of the order of the square of the ratio between the meson mass and the nucleon mass (≈0.02) and smaller terms are disregarded. The pseudoscalar coupling constant, introduced by Eriksson, can be determined in this approximation from the binding energy alone. Different pairs of value of Eriksson's two remaining scalar coupling constants (ps−ps and ps−pv respectively) are then fitted to suit the experimentally measured quadrupole moment in the triplet state. The special case when there is no p-state contribution at all in the wave function is further investigated by taking the terms of the order of the square of the mass ratio into account. The parameters which give the charge dependence are also determined in this case. A 20% deviation from the charge independence given by the usual theory is found. The result of the investigation is seen to be in accordance with the generalized Pauli principle. (auth)

15324 ABSORPTIVE CORRECTIONS TO THE NUCLEON EXCHANGE TERM IN ELASTIC πN SCATTERING. Smrz, Pavel; von Baeyer, Hans C. (McGill Univ., Montreal). Can. J. Phys., 44: 105-8(Jan. 1966).

The absorption model of Gottfried and Jackson is justified in the case of backward elastic scattering. The model is then applied to the nucleon exchange term in π^+p scattering at 4 and 8 Bev. It is found that the data can be fitted only if a phenomenological form factor is introduced. (auth)

15325 A SCALAR PION-NUCLEON INTERACTION. Coombes, Charles A. (Univ. of Alberta, Can.). Can. J. Phys., 44: 285-7(Jan. 1966).

It is pointed out that mesons (π) may behave both as scalars and pseudoscalars with respect to nucleons, and that there is some evidence in favor of this hypothesis. If nucleons are bound states of quarks or mesons(K) or hyperons(Λ), and if the meson(π) interacts with each particle of the bound states individually and behaves as a scalar with respect to one and as a pseudoscalar with respect to another, then the meson(π) must be considered as both a scalar and a pseudoscalar in its nucleon interactions. (J.F.P.)

15326 EFFECTS OF NEUTRINO BACKGROUND IN THE UNIVERSE ON THE SHAPE OF β SPECTRA. Kocharov, G. E. Izv. Akad. Nauk SSSR, Ser. Fiz., 29: 794-9 (May 1965). (In Russian).

Under the hypothesis of a universal neutrino sea, electrons with energies between $(E_{max} - E_0)$ and $(E_{max} + E_0)$, where E_{max} is the maximum beta-particle energy and E_0 is the Fermi boundary of the neutrino sea, can not be emitted in nuclear beta decay, since the energy levels for the antineutrinos accompanying the decay are filled. The experimental possibility of determining the Fermi boundary of the neutrino sea by means of studying its effect on the beta spectrum of tritium is examined. Sensitivity and background effects on the energy resolution of a proportional counter and of a magnetic spectrometer used to study this effect are computed. (M.J.T.)

15327 ON THE EXISTENCE OF WEAKLY INTERACTING CHARGE-RETENTION CURRENTS. Ahrens, T.; Frahm, C. P.; Quang, B. D. (Georgia Inst. of Tech., Atlanta). Nucl. Phys., 78: 641-9(1966).

Cross sections and cross section ratios of strangeness conserving reactions and expressions for ratios and branching ratios of strangeness changing decays are presented, which can serve as tests of the existence of weakly interacting nucleon and lepton currents of the charge-retention variety, and of the selection rules which govern them. The calculations are principally based on two interaction models within the framework of isospace; as to the nucleon-lepton interaction, one model is charge-independent while the other involves only neutral currents in addition to charge-exchange currents. The strangeness changing currents are assumed to obey the $\Delta I = \frac{1}{2}$ rule. (auth)

15328 SOME REMARKS ABOUT THE COHERENCE PROPERTIES OF FERMION BEAMS. Boffi, S. (Univ., Pavia, Italy); Caglioti, G. Nuovo Cimento, (10), 41B: 247-51(Feb. 11, 1966).

Possible uses of intensity correlations of fermion beams are investigated. It is shown that enormous difficulties are met in the problem of detecting coherence phenomena in a beam of Fermi-Dirac particles. These difficulties are lessened in the case of Bose-Einstein statistics. It is found that there are two types of coherence: the first is connected with the wave description and the superposition of the particle states, and the other depends on the degeneracy of the beam and is connected with temporal coherence. Due to both conditions it is concluded that an experiment suitable for detecting coherence phenomena in fermion beams is hopeless with present techniques of spectroscopy. (J.F.P.)

15329 ATTENUATION COEFFICIENT: FINITE OR INFINITESIMAL? Pfalzner, Paul M. (Ontario Cancer Foundation London Clinic, Can.). Phys. Med. Biol., 11: 132-4(Jan. 1966).

In correct definitions of the attenuation coefficient and the errors involved in their use are pointed out. A new definition is proposed, from which the radioactive decay coefficient is also defined. (L.B.S.)

15330 FISSION-ANTINEUTRINO INTERACTION WITH PROTONS. Nezrick, F. A.; Reines, F. (Case Inst. of Tech., Cleveland). Phys. Rev., 142: 852-70(Feb. 25, 1966).

The positron kinetic-energy spectrum from the antineutrino absorption reaction $p(\bar{\nu}_e, \beta^+)n$ was measured by using a 3.2-liter gadolinium-loaded decalin-based liquid-scintillator target placed between two cylindrical NaI crystals 29 cm in diameter and 7.6 cm thick. The crystals were set

to see 0.51-Mev β^+ annihilation radiation. A prompt triple coincidence of all three detectors followed by the delayed capture of the neutron is the signature for the reaction. The experiment was performed at one of the fission reactors of the Savannah River Plant. The data were obtained during 2484 hr of operation at the rate of 0.187 events per hour, with a signal-to-background ratio of approximately 3/1. The antineutrino spectrum from ^{235}U fission gave evidence for a higher energy tail than previously known, implying the presence of half-lives in the several-millisecond range. The cross section per fission antineutrino for the inverse beta decay of the proton was measured to be $(0.94 \pm 0.13) \times 10^{-43}$ cm^2, a value consistent with the two-component theory of the neutrino. The measured antineutrino spectrum indicates an expected cross section for the reaction $d(\bar{\nu}_e, \beta^+)2n$ of $(4.2 \pm 1.4) \times 10^{-45}$ cm^2/(fission $\bar{\nu}_e$) and a cross section of $(8.4 \pm 2.8) \times 10^{-46}$ cm^2/(fission $\bar{\nu}_e$) for the production of >1.5-Mev recoil electrons by the elastic scattering reaction $\bar{\nu}_e + e^-$. (auth)

15331 $K^0_{\mu 3}$ DECAY SPECTRUM. Carpenter, D. W.; Abashian, A.; Abrams, R. J.; Fisher, G. P.; Nefkens, B. M. K.; Smith, J. H. (Univ. of Illinois, Urbana). Phys. Rev., 142: 871-82(Feb. 25, 1966). (COO-1195-43).

An experiment was performed to observe the energy spectrum of the $K^0_{\mu 3}$ decay ($K^0_2 \rightarrow \pi + \mu + \nu$). The observed spectrum indicates that the decay interaction is vector, rather than scalar or tensor, in agreement with the V−A theory of weak interactions. This conclusion is obtained even when energy-dependent form factors are considered. The two form factors (f_+ and f_-) of the vector interaction are found to be consistent with several possible theoretical models for their behavior. Assuming constant form factors their ratio is found to be $\xi \equiv f_-/f_+ = 1.2 \pm 0.8$. Assuming a J = 1 intermediate K-π state to predominate in the decay, its mass is 540^{+140}_{-70} Mev; if J = 0, a mass of 570^{+180}_{-70} Mev is obtained. The data consist of 1371 events obtained from a neutral-beam spark-chamber detection system in which the charged decay products are observed in a magnetic field. The μ is identified by its ability to pass through several interaction lengths of material into a set of range chambers. A branching ratio of $\lesssim 10^{-4}$ is obtained for neutral-current K^0_2 decays. (auth)

15332 π-PAIR PHOTOPRODUCTION BELOW 1 Bev. Allaby, J. V.; Lynch, H. L.; Ritson, D. M. (Stanford Univ., Calif.). Phys. Rev., 142: 887-93(Feb. 25, 1966).

Measurements of the differential cross section for the reaction $\gamma + p \rightarrow \pi^- + \pi^+ + p$ were made at several angles for photon energies in the range 550−1000 Mev, using the Stanford Mark III linear accelerator. The π^- were detected and momentum-analyzed using a 90° magnetic spectrometer. It was found that the reaction was dominated by the quasi-two-body photoproduction $\gamma + p \rightarrow \pi^- + N^*(1238)$ especially near the threshold for this process. At low momenta, the π^- were identified by range. At high momenta (>250 Mev/c), the contaminating electrons were eliminated by using a lead and scintillation-counter sandwich system. The yields of both π^- and π^+ from hydrogen were measured, and the normalization was obtained by comparison with the known cross sections for $\gamma + p \rightarrow \pi^+ + n$. Computer calculations of the shapes of the yield curves expected from two-body and three-body production enabled the data to be separated into the two possible states $\gamma + p \rightarrow \pi^- + N^*(1238)$ and $\gamma + p \rightarrow \pi^- + \pi^+ + p$. Angular distributions and total cross sections are presented. (auth)

15333 SEARCH FOR THE DECAY $\eta \rightarrow \pi^0 + e^+ + e^-$. Berley, D.; Hart, E. L.; Rahm, D. C.; Stonehill, D. L.; Thevenet, B.; Willis, W. J.; Yamamoto, S. S. (Brookhaven National Lab., Upton, N. Y.). Phys. Rev., 142: 893-5(Feb. 25, 1966). (BNL−9571).

A search has been made for the decay $\eta \rightarrow \pi^0 + e^+ + e^-$, which should be very rare if C is conserved in strong and electromagnetic interactions. No events consistent with this decay were found in a sample of η produced in the reaction $K^- + p \rightarrow \Lambda + \eta$. The upper limit for this decay, at the 90% confidence level, is $R = (\eta \rightarrow \pi^0 + e^+ + e^-)/(\eta \rightarrow \gamma + \gamma) < 0.047$. (auth)

15334 INTERACTIONS OF π^+ MESONS WITH PROTONS AT 2.08 Bev/c. James, Frederick E.; Kraybill, Henry L. (Yale Univ., New Haven. Brookhaven National Lab., Upton, N.Y.). Phys. Rev., 142: 896-912(Feb. 25, 1966).

Interactions of 2.08-Bev/c positive pions with protons were studied using the 20 in. hydrogen bubble chamber and the alternating gradient synchrotron at Brookhaven National Laboratory. Using 3000 elastic and 8000 inelastic events, the partial cross sections for elastic scattering and for meson production were measured. The ρ^+, ρ^0, ω^0, and η^0 resonances are produced strongly and emerge predominantly in the forward direction in the center-of-mass system, suggesting a peripheral mechanism for their production. The possibility of explaining these reactions by specific particle exchange models is investigated. More than 75% of the ρ^0, ω^0, and η^0 are produced with the $N^*_{33}(1238)$ isobar. The N* (1688) is produced in about one-third of the $\pi^+\pi^+N$ final states. Cross sections for production of ρ^+p, $\pi^+p\omega$, $N^*_{33}\omega$, $\pi^+p\eta$, $N^*_{33}\eta$, $\pi^+p\rho^0$, $N^*_{33}\rho^0$, $N^*_{15}\pi^+$, and $N^*_{33}\pi^0$, are given. A_1, B, ϕ, and X mesons are not observed. (auth)

15335 SINGLE-PION PRODUCTION BY 1.96-Bev/c K^+ MESONS. Goldhaber, Sulamith; Chinowsky, William; Goldhaber, Gerson; O'Halloran, Thomas (Univ. of California, Berkeley). Phys. Rev., 142: 913-17(Feb. 25, 1966). (UCRL−16276).

Single-pion production by K^+ mesons at a momentum of 1.96 Bev/c is shown to lead predominantly to K*p and N*K final states. Study of the dynamics of the reaction shows that the N*K final state is produced almost entirely via vector exchange, whereas the K*p final state seems to be produced partly via pion exchange and partly via vector exchange. Numerical values in terms of Gottfried and Jackson's parametrization of the spin-density matrix are given for the K*p final state. Comparison with similar analyses at energies below and above this experiment indicates that a strong energy dependence of the vector-meson exchange contributes to the K*p production. It is shown that the form factors used to fit the vector-meson-exchange contribution to these processes at 3 Bev/c do not fit the data at this energy. (auth)

15336 π-MESON PRODUCTION IN p-p COLLISIONS. Reay, N. W. (Univ. of Rochester, N. Y.); Melissinos, A. C.; Reed, J. T.; Yamanouchi, T.; Yuan, L. C. L. Phys. Rev., 142: 918-22(Feb. 25, 1966). (UR−875-92).

A measurement of the momentum spectra of π^+ and π^- mesons produced at 0° and 17° in the laboratory in p-p collisions is reported. Incoming proton energies of 2.85, 2.4, and 2.0 Bev were investigated. From the π^- spectra an upper limit is set on the production of a possible D^{+++} state. (auth)

15337 PROTON FORM FACTORS FROM ELASTIC ELECTRON-PROTON SCATTERING. Janssens, T.; Hofstadter, R.; Hughes, E. B.; Yearian, M. R. (Stanford Univ., Calif.). Phys. Rev., 142: 922-31(Feb. 25, 1966).

Absolute measurements of the elastic electron-proton cross section were made with a precision of about 4% for values of the square of the four-momentum transfer, q^2, in the range 6.0 to 30.0 F^{-2} and for electron scattering angles in the range 45° to 145°. To within the experimental errors, it is found that the charge and magnetic form factors of the proton have a common dependence of q^2 when normalized to unity at $q^2 = 0$, and that an accurate representation of the behavior of the form factor and that of the cross sections themselves can be given in terms of a three-pole approximation to the dispersion theory of nucleon form factors. (auth)

15338 STUDY OF $\bar{p}$-p ANNIHILATIONS INTO K AND π MESONS AT 3.7 Bev/c. Baltay, C. (Yale Univ., New Haven); Lach, J.; Sandweiss, J.; Taft, H. D.; Yeh, N.; Stonehill, D. L.; Stump, R. Phys. Rev., 142: 932-43 (Feb. 25, 1966). (TID-22182).

At 3.66 Bev/c, the total cross section for $\bar{p} + p \rightarrow K + \bar{K} + m\pi$ where m = 1, 2, . . . , is 2.9 ± 0.4 mb. No two-body reactions of the form $\bar{p}p \rightarrow K\bar{K}$, KK*, or K*$\bar{K}$* were observed. The angular distribution of kaons for three-body final states shows striking anisotropy but this effect diminishes with

increasing multiplicity. An enhancement at low $K\bar{K}$ effective mass, with possible assignment of I = 1, was observed, and this is compared with the $K^0_1K^0_1$ effect noted previously by several groups. The K*(888), ρ, and ω are prominent in several channels, but the data are consistent with no production of the ϕ. Upper limits on the ϕ/ω production ratio are presented. A search for resonances in the $K\pi\pi$ system at 1175, 1215, and 1270 Mev, as well as the $K\bar{K}\pi$ at 1280 and 1410 Mev, yielded negative results. (auth)

15339 PHOTON SPLITTING IN A NUCLEAR ELECTRIC FIELD. **Shima, Yaakov (Oak Ridge National Lab., Tenn. Hebrew Univ., Jerusalem). Phys. Rev., 142: 944-56(Feb. 25, 1966). (ORNL-P-1537).**

The cross section for photon splitting in a nuclear electric field is derived, using the Feynman formulation of quantum electrodynamics. A closed form for the cross section is obtained and numerical values for interesting cases are calculated. (auth)

15340 PHOTOPRODUCTION OF POSITIVE PIONS FROM HYDROGEN AT ENERGIES NEAR THE FIRST RESONANCE. Alvarez, R. A. (Stanford Univ., California). Phys. Rev., 142: 957-71(Feb. 25, 1966).

Angular distributions for positive-pions photoproduction from liquid hydrogen were measured at photon energies near 225, 250, 275, 300, and 350 Mev. These have been normalized to an absolute cross section near the peak of the first resonance measured by means of a polyethylene-carbon subtraction using solid targets. The results are compared with results of previous experiments as well as several dispersion-theoretic predictions of the cross sections. The data can be fitted within the experimental and theoretical uncertainties by a theoretical calculation containing only the pion pole term and the transition to the $P_{3,3}$ state due to the first resonance. (auth)

15341 π^+p INTERACTIONS AT T_π = 781 Mev. Tilger, C. A.; Poirier, C. P.; Alyea, E. D. Jr.; Martin, H. J. Jr.; Scandrett, J. H. (Indiana Univ., Bloomington). Phys. Rev., 142: 972-6(Feb. 25, 1966).

Interactions of 781-Mev π^+ mesons with protons were investigated using a 14-in. hydrogen bubble chamber. A total of 2305 events were observed. The data were normalized to a total cross section of 22.2 mb, giving partial cross sections $\sigma(\pi^+p \rightarrow \pi^+p) = 9.5 \pm 0.5$ mb, $\sigma(\pi^+p \rightarrow \pi^+p\pi^0) = 9.3 \pm 0.5$ mb, $\sigma(\pi^+p \rightarrow \pi^+\pi^+n) = 2.15 \pm 0.17$ mb, and a multiple-pion-production cross section of 1.15 ± 0.17 mb. The elastic angular distribution was obtained and is $d\sigma/d\omega = (0.25 \pm 0.03) + (0.90 \pm 0.11)\cos\theta_{c.m.} + (2.57 \pm 0.24)\cos^2\theta_{c.m.} + (0.19 \pm 0.22)\cos^3\theta_{c.m.} - (1.73 \pm 0.34)\cos^4_{c.m.}$. The kinetic-energy and angular distributions of the outgoing particles in single-pion production are given. The data are compared with other experiments in this energy region and their relevance to the shoulder in the π^+p total cross section near 830 Mev is discussed. (auth)

15342 πp CHARGE-EXCHANGE SCATTERING AND A COHERENT DROPLET MODEL OF HIGH-ENERGY EXCHANGE PROCESSES. Byers, N.; Yang, C. N. (Inst. for Advanced Study, Princeton, N. J.). Phys. Rev., 142: 976-81(Feb. 25, 1966).

A model calculation is presented following a simple viewpoint to approach high-energy two-body processes A + B → C + D. πp charge-exchange scattering is discussed in detail. A number of further experiments are suggested. (auth)

15343 APPLICATION OF THE FADDEEV EQUATIONS TO THE THREE-NUCLEON PROBLEM. **Phillips, A. C. (Imperial Coll. of Science and Tech., London). Phys. Rev., 142: 984-9(Feb. 25, 1966).**

The low-energy three-nucleon system is considered using the multiple-scattering formalism of Faddeev and an approximation scheme that preserves bound-state and three particle scattering unitarity. The approximations involve the use of nonlocal separable potentials to describe the low energy nucleon-nucleon interaction and a phenomenological three-body force to represent the effects on the three-nucleon system of the nucleon-nucleon tensor and short-range interactions. The neutron-deuteron scattering problem above and below the three-particle threshold, and the triton binding-energy problem, are solved exactly. The theoretical results are in impressive agreement with the experimental data. (auth)

15344 MASS OF THE MUON AND CHARGED-MESON DECAY RATES. **Shaffer, R. A. (Lehigh Univ., Bethlehem, Pa.). Phys. Rev., 142: 990(Feb. 25, 1966).**

Consideration of the idea that, given the form of the weak interactions, the muon has a mass value which maximizes the decay of the charged pion and kaon is presented. Results indicate that the muon has, within 0.13%, the mass which maximizes the following quantity: $\Gamma_{\pi\mu}/Q_{\pi\mu} + \Gamma_{K\mu}/Q_{K\mu}$, where Γ is the decay rate and Q is the Q value for the indicated two-body decay modes. (auth)

15345 ONE-BOSON-EXCHANGE MODEL OF NN AND $N\bar{N}$ INTERACTION. Ball, J. S. (Univ. of California, Los Angeles); Scotti, A.; Wong, D. Y. Phys. Rev., 142: 1000-12(Feb. 25, 1966).

The elastic nucleon-nucleon scattering, due to the exchange of π, η, ρ, ω, φ, and an effective I = 0 scalar σ meson is calculated using unsubtracted partial-wave dispersion relations with a cutoff. The p, ω, and φ vector coupling constants are related by SU_3 to a single constant assuming pure F coupling. The ratio of the vector to tensor coupling of the ρ meson is determined by the I = 1 charge and anomalous magnetic moment ratio and the tensor couplings of ω and φ are neglected. The η-nucleon axial-vector coupling constant is related to that of the pion by SU_3 with a D/F ratio of $\frac{3}{2}$. The I = 0 and I = 1 phase shifts are calculated using a total of four adjustable parameters: the mass and coupling constant of the effective σ meson, the octet-vector coupling constant, and the cutoff parameter. For each of the cutoff values corresponding to laboratory kinetic energies of 600, 700, and 800 Mev, the remaining three parameters are adjusted to fit the I = 1, $^1S_0$, $^3P_0$, $^3P_1$, and $^3P_2$, and the I = 0, $^3S_1$ phase shifts at 25, 50, 95, 142, 210, and 310 Mev. In each of the three cases, a goodness-of-fit parameter is obtained corresponding to a theory with approximately 10% inherent uncertainty. A deuteron pole appears in the solution for the $^3S_1$ amplitude corresponding to a binding energy of ~10 Mev. All of the calculated higher partial-wave phase shifts are in good agreement with results of phase-shift analyses. Having obtained a fit to the nucleon-nucleon phase shifts, the nucleon-antinucleon scattering amplitudes are calculated after changing the signs of the odd G-parity exchange terms (π, ω, and φ) but keeping the same values for the four parameters. For each of the three cutoff energies, a bound-state pole is found in the I = 0, $^1S_0$, $^3S_1$, and $^3P_0$, and the I = 1, $^1S_0$ and $^3S_1$ amplitudes. These bound states have the same quantum numbers as the η, ω, σ, π, and ρ, respectively. Although the masses of the bound states are not near those of the physical mesons, it is argued that if the important meson channels (annihilation) were included, the bound-state poles would move toward the physical values. These results lend strong support to the conjecture that the observed mesons are composite particles. (auth)

15346 $p\bar{p}$ ANNIHILATIONS INTO TWO MESONS WITHIN A BROKEN INHOMOGENEOUS $\tilde{U}(12)$ SYMMETRY SCHEME. Hussain, F.; Rotelli, P. (Imperial Coll. of Science and Tech., London). Phys. Rev., 142: 1013-17 (Feb. 25, 1966).

A $\tilde{U}(12)$ generalization of the charge-conjugation operator is constructed. It is then found that only one amplitude is charge-conjugate invariant for the annihilation process of proton-antiproton into two mesons. Branching ratios and sum rules are presented explicitly for annihilations from $^3S_1$ and $^1S_0$ states. (auth)

15347 EFFECT OF INTERMEDIATE VECTOR MESONS ON NEUTRINO PRODUCTION OF LEPTON PAIRS. Dooher, J. (Adelphi Univ., Garden City N. Y.); Tausner, M. Phys. Rev., 142: 1018-24(Feb. 25, 1966).

The total cross section for the production of lepton pairs by the scattering of high-energy muon neutrinos and pro-

tons is calculated with an assumed weakly interacting vector meson W, which has an anomalous magnetic moment κ. A modified Weizsacker-Williams approximation is used with added correction terms which change the result about 50%. In addition to these correction terms, t^2, the square of the four-momentum of the exchanged photon is retained in the denominator of the lepton propagators. This results in an additional deviation of 30% from the standard Weizsacker-Williams approximation. The cross sections are calculated as a function of k for meson masses of 2.0, 2.5, and 3.0 Bev, and for neutrino energies above the threshold for W production. Numerical results are presented for κ = 1, 0, −1. The cross sections for muon-pair and muon-electron production are equal, and larger by a factor of approximately 10^4 than the equivalent cross sections in the four-fermion theory. (auth)

15348 RELATIVISTIC CORRECTIONS TO THE IMPULSE APPROXIMATION IN ELASTIC ELECTRON-DEUTERON SCATTERING. **Gross, Franz (Stanford Univ., Calif.).** Phys. Rev., 142: 1025-34(Feb. 25, 1966).

Equations are derived for the deuteron form factor in the impulse approximation, which include corrections to order M^{-2}, where M is the nucleon mass. The corrections are of two types, arising from (1) the expansion of the nucleon current to order M^{-2} and (2) the treatment of the deuteron wave function in a relativistic manner so as to retain terms of order M^{-2}, which describe the distortion of the wave function of a moving deuteron. All of the results are expressed as functionals of the nonrelativistic S- and D-state wave functions, so that numerical results may be calculated for any deuteron model. Numerical estimates of the charge correction term indicate that it is large enough to substantially affect the determination of the neutron-charge form factor from this experiment, making the form factor more positive than results obtained from the uncorrected theory. Corrections to the magnetic moment are also discussed. (auth)

15349 RADIATIVE CORRECTIONS TO K_{l3} ± DECAYS. Ginsberg, Edward S. (Univ. of Pennsylvania, Philadelphia). Phys. Rev., 142: 1035-40(Feb. 25, 1966).

The radiative corrections to the lepton spectrum and decay rate for K_{l3} ± decays are calculated, assuming a phenomenological weak K-π vertex and using perturbation theory. The answer depends logarithmically on a cutoff. The result applied to pion beta decay yields a fractional change in lifetime of −1.2% and is not sensitive to reasonable variations in the cutoff. The radiative correction to the electron spectrum from K_{e3} ± decays at rest is substantial, averaging about 5% in absolute magnitude over most of the measurable energy range, and is insensitive to the cutoff. The correction to the K_{e3} ± lifetime, the $K_{\mu 3}$ ± lifetime and muon spectrum is probably small (a fraction of a percent) although the numerical estimates are sensitive to the cutoff. (auth)

15350 RECIPROCITY, NORMALITY OF K^0-$\bar{K}^0$ MASS MATRIX, AND CP VIOLATION IN WEAK INTERACTIONS. **Patil, Sharashchandra H.; Tomozawa, Yukio; Yao, York-Peng (Inst. for Advanced Study, Princeton, N. J.).** Phys. Rev., 142: 1041-7(Feb. 25, 1966).

It is proposed that the reciprocity principle may be relevant in weak interactions as a replacement for time-reversal invariance. Various forms of this principle are examined and their consequences are noted. When applied to the K^0-$\bar{K}^0$ system, they all imply that the two observed kaon states are orthogonal, and a sum rule emerges, which relates the rates and the CP-violating parameters of different neutral-kaon decay modes. Using the preliminary experimental data, the amount of CP violation in $K_1 \rightarrow 2\pi^0$ is predicted. Finally, the possible implications of reciprocity for various interactions are discussed. (auth)

15351 LINEAR INTEGRAL EQUATIONS FOR RELATIVISTIC MULTICHANNEL SCATTERING. **Blankenbecler, R. (Princeton Univ., N. J.); Sugar, R.** Phys. Rev., 142: 1051-9(Feb. 25, 1966).

A set of three-dimensional coupled linear integral equations is presented for relativistic scattering and production processes. The new equations seem more amenable to numerical analysis than the standard Bethe-Salpeter equations. In addition multiparticle scattering and hence inelastic processes are discussed. As a numerical example low-energy pion-pion scattering is treated in the simplest approximation. It is found that there are no self-consistent values for the mass and width of the ρ meson if only the elastic and π-ω channels are taken into account. (auth)

15352 NUCLEON AS A COMPOSITE PARTICLE STATE. **Doolen, Gary D.; Kanki, Takeshi; Tubis, Arnold (Purdue Univ., Lafayette, Ind.).** Phys. Rev., 142: 1072-81 (Feb. 25, 1966).

A general scheme is presented for approximately determining the mass M and coupling with pions $g^2/4\pi$ of the nucleon, and the position and width of the πN 33 resonance. No cutoffs are required. Contributions from distant left-hand singularities to the I = J = ½, ³⁄₂ p-wave amplitudes are approximated by Balázs-type pole terms, and those from nearby left-hand singularities, by crossing symmetry. Balázs-pole residues are determined by requiring crossing symmetry in a form relating the πN partial-wave amplitude on the nearby left-hand cut to physical πN scattering. As a first step in the investigation of the general scheme, experimental data on πN scattering in the I = J = ³⁄₂ p-wave state are used to determine the nucleon mass and pion-nucleon coupling constant. M = 1.03 in units of the physical-nucleon mass and $g^2/4\pi$ = 18.6. The latter appears to be weakly dependent on the choice of Balázs-pole positions. The calculated nucleon mass, on the other hand, appears to be practically independent of the choice of pole positions. (auth)

15353 SELF-CONSISTENT DETERMINATION OF THE POSITION AND WIDTH OF THE 33 πN RESONANCE. Doolen, Gary D.; Kanki, Takeshi; Tubis, Arnold (Purdue Univ., Lafayette, Ind.). Phys. Rev., 142: 1082-4(Feb. 25, 1966).

Using a procedure previously discussed the approximate position M* and width Γ of the 33 πN resonance are determined. The N/D formalism is used to generate a unitary I = J = ³⁄₂ πN p-wave amplitude. The nucleon pole parameters are taken from experiment and the nearby left-hand-cut contribution is assumed to be accurately given by crossing symmetry with only the 33 physical-scattering contribution to the crossing relation retained. Distant left-hand singularities are accounted for by two Balázs poles whose residues are determined by requiring the crossing relation for the real part of the amplitude to be satisfied on the nearby left-hand cut. The real part crossing relation is also assumed to be dominated by the 33 contribution. Self-consistency between the 33 amplitude determined by the N/D calculation and that used to evaluate the crossing relations is obtained by an iterative procedure. It is found that M* = 1.22 and Γ = 0.11 in units of the physical-nucleon mass, compared with the experimental values of M* = 1.32 and Γ = 0.11, respectively. (auth)

15354 REGGE-POLE CONTRIBUTION TO VECTOR-MESON PRODUCTION. **Barmawi, M. (Univ. of Chicago).** Phys. Rev., 142: 1088-91(Feb. 25, 1966). (COO-264-273).

A Regge-pole model of vector-meson production is considered and applied to ρ and ω production. The Regge-pole contribution is computed explicitly, without use of the asymptotic forms. The residues are related to the well-known coupling constants. The only parameter is the slope of the trajectory, which is estimated to be 0.64/Bev². Good results for the differential cross section are obtained. The question of the decay density matrices is discussed briefly. (auth)

15355 $\eta\pi\pi$ MODEL OF X^0 AND A POSSIBLE η-π RESONANCE. **Mitra, A. N. (Delhi Univ.); Sundaresan, M. K.** Phys. Rev., 142: 1126-31(Feb. 25, 1966).

An $\eta\pi\pi$ model of the X^0 meson at 960 Mev is proposed through factorable π-π and η-π s-wave forces. The overall dynamics is described by a three-body Schrödinger equa-

tion under a nonrelativistic approximation which is justified by the relatively low Q value (~120 Mev) of the particle with respect to decay into an $\eta\pi\pi$ system. The π-π interaction, which is used as input information, is taken to be of two types: (i) a smooth attractive force which falls short of the requirements of a π-π bound state (called ABC-type), and (ii) a force characterized by a long-range barrier surrounding an inner well, which is capable of producing a π-π resonance at several hundred Mev (called σ-type interaction). Using three-body techniques proposed earlier, the nature and strength of the η-π interaction is deduced from a knowledge of the energy of the $\eta\pi\pi$ system at the experimental position of the X^0-mass. It is found that a σ-type π-π interaction, designed to produce a π-π resonance at 400–600 Mev, requires the existence of a bound η-π system. On the other hand, an ABC-type π-π interaction demands an η-π resonance in the Bev region (via a σ-type η-π interaction). The physical implications of these results are discussed. (auth)

15356 DEVIATIONS FROM CHARGE INDEPENDENCE IN n-p AND n-n SCATTERING LENGTHS BY S-MATRIX METHODS. **Biswas, S. N.** (Univ. of Delhi); **Kumar, Aditya; Saxena, R. P.** Phys. Rev., 142: 1141-4(Feb. 25, 1966).

The difference between the zero-energy $^1S_0$ n-p and n-n scattering lengths is calculated, using the dispersion-theoretic method of Dashen and Frautschi, originally employed for calculating electromagnetic mass splittings. It is assumed that the deviation is due to the perturbative effect of (i) magnetic interaction between nucleons, (ii) electromagnetic mass shifts between exchange bosons, and (iii) electromagnetic mass difference between neutron and proton. The calculation predicts $a(np) - a(nn) = 3.58$ F, if the definition $\lim_{q\to 0}(q\cot\delta)^{-1} = 1/a$ is used. The result is in qualitative agreement with the experimental value $a(np) - a(nn) = 7.28 \pm 1.9$ F. The effects of the ρ^+-ρ^0 mass difference and the vertex corrections, which were ignored in the calculation, may, hopefully, account for the remaining deviation. (auth)

15357 B EXCHANGE IN π-ω SCATTERING AND THE SPIN OF THE B MESON. Atkinson III, Reilly (Tufts Univ., Medford, Mass.). Phys. Rev., 142: 1154-5(Feb. 25, 1966).

A study was made of π-ω scattering with forces due to ρ and B exchange. It was found that the ρ-exchange force is much stronger in the 2^- channel than in the 1^+ channel in agreement with Kuo. It was also found that 2^- B exchange is strongly repulsive in the L = 0, J = 1 state, and attractive in the L = 1, J = 2 state. It is concluded that theory suggests the B meson is a 2^- particle. (auth)

15358 S-WAVE π-π SCATTERING AMPLITUDES IN THE NEW FORM OF THE STRIP APPROXIMATION. Collins, P. D. B. (Univ. of California, Berkeley). Phys. Rev., 142: 1156-63(Feb. 25, 1966). (UCRL-16339).

The new form of the strip approximation devised by Chew is applied to the calculation of the S-wave π-π scattering amplitudes, with forces produced by the exchange of ρ, P, and P′ trajectories, and with Regge asymptotic behavior built in. Because of the sensitivity of the S wave to short-range forces not included in the strip approximation, a subtraction is made at the symmetry point, so that an extra free parameter λ is introduced, in addition to the strip width. Self-consistency is imposed on the S waves in the direct and crossed channels; λ is related to the scattering lengths for isospin 0 and 2 (a_0 and a_2), and it is concluded that solutions with $\lambda \approx -0.1$ giving $a_0 \approx 1$ and $a_2 \approx 0.2$ are in the best agreement with experiment. But some discussion is also given to the possibility that a_0 is negative, there being a bound-state pole of vanishing residue, which should correspond to the P′ trajectory's crossing angular momentum zero. (auth)

15359 INADEQUACIES OF THE NEW FORM OF THE STRIP APPROXIMATION FOR THE π-π SCATTERING AMPLITUDE. Collins, P. D. B. (Univ. of California, Berkeley). Phys. Rev., 142: 1163-72(Feb. 25, 1966). (UCRL-16347).

The new form of the strip approximation is used to obtain mutually self-consistent trajectories with isospin I = 0 and I = 1 in the π-π system. However, these trajectories do not correspond to those which are obtained from experiment, and violate unitarity in the asymptotic region. The trajectories obtained from experiment, which satisfy unitarity, are shown not to produce sufficient strength to bootstrap themselves. Also the I = 0 trajectory gives rise to a repulsive potential, and to obtain a solution of the N/D equations it is assumed that this repulsion is completely cancelled by other I = 0 trajectories that do not reach the right-half angular-momentum plane. It is concluded that both these difficulties stem from the fact that the potential is included only in the first Born approximation, and that more satisfactory results would be forthcoming if the potential were iterated in the way proposed by Mandelstam. (auth)

15360 FRONSDAL'S MODEL FOR LEPTONIC INTERACTIONS. **Ferwerda, Hedzer A.** (Cornell Univ., Ithaca, N. Y.). Phys. Rev., 142: 1185-7(Feb. 25, 1966).

Fronsdal's model for leptonic interactions is criticized. It is shown that the electromagnetic corrections to neutron and muon decay give rise to infinite coupling-constant renormalizations, contrary to Fronsdal's statement. (auth)

15361 HIGH-ENERGY DEUTERON CROSS SECTIONS. **Franco, V.** (Massachusetts Inst. of Tech., Cambridge); **Glauber, R. J.** Phys. Rev., 142: 1195-1214(Feb. 25, 1966). (MIT-2098-165).

A theoretical analysis of the collisions of particles with deuterons is carried out in the high-energy approximation. This approximation, which corresponds to a generalized form of diffraction theory, takes explicit account of double collision processes as well as single ones. It is used to express the amplitudes for elastic and inelastic scattering by deuterons in terms of the elastic-scattering amplitudes of the neutron and proton and the deuteron wave functions. The resulting expressions are used to evaluate the differential cross section for elastic scattering, and the angular distribution of inelastic scattering (i.e., the differential cross section for deuteron breakup integrated over final energies of the incident particle). The contributions to these cross sections of the various single and double scattering processes and the terms that represent their interference are exhibited individually. Expressions are derived for the total cross section of the deuteron and for its elastic and inelastic total scattering and absorption cross sections. The difference between the various types of deuteron cross sections and the sum of the corresponding cross sections for the free neutron and proton are explained in some detail. Spin-dependent interactions are treated, and for incident particles of spin $\frac{1}{2}$ an expression is given for the deuteron total cross section in terms of the general spin-dependent scattering amplitudes of the neutron and proton. The theory is applied to antiproton-deuteron collisions in the energy range from 0.13 to 17.1 Bev. The results for the total and absorption cross sections, which are calculated for a variety of models of the deuteron wave function, are found to be in good agreement with the measurements. The magnitudes of such effects as double scattering and the interference of single- and double-scattering amplitudes are seen to be appreciable. (auth)

15362 NONLEPTONIC DECAYS OF THE INTERMEDIATE VECTOR MESON. **Carhart, R.** (Brookhaven National Lab., Upton, N. Y.); **Dooher, J.** Phys. Rev., 142: 1214-18(Feb. 25, 1966).

The nonleptonic decay modes of the intermediate vector meson are discussed using SU_3 symmetry. The decay rates into two pseudoscalar mesons and two baryons are calculated, estimating the effects of the strong interactions. It is found that for a W mass of 2.5 and 3.0 Bev the baryon decay rate is comparable to the leptonic decay rate whereas the meson decays are negligible. (auth)

15363 APPLICATION OF THE PADE APPROXIMANT TO SCATTERING THEORY. **Gammel, J. L.**; **McDonald, F. A.** (Texas A and M Univ., College Station, Tex.). Phys. Rev., 142: 1245-54(Feb. 25, 1966). (UCRL-14260-T).

The Padé approximant is shown to yield exactly unitary

S matrices in scattering theory. The method is used to construct a unitary S matrix for n-d scattering above the threshold for inelastic scattering. Thus the effect of inelastic scattering on elastic-scattering total cross sections and angular distributions is calculated. No cusps are found at the threshold. (auth)

15364 πN CHARGE-EXCHANGE SCATTERING AND THE ρ TRAJECTORY. Desai, Bipin R. (Univ. of California, Riverside). Phys. Rev., 142: 1255-8(Feb. 25, 1966).

πN charge-exchange scattering is considered within the Regge framework. Among meson exchanges only ρ exchange is possible in this reaction. On the basis of the nucleon electromagnetic-structure data it is found that at the momentum-transfer variable $t = m_\rho^2$ the ratio of the spin-flip to non-spin-flip residues is quite large, ~4.5, and arguments are given in favor of an even larger ratio, ~20, at $t = 0$. This latter result helps explain the hump near the forward direction in the charge-exchange differential cross section. With the ρ trajectory and residues consistent with the π^+p total and differential cross-section data, good fits for $-t \leq 0.5$ (Bev/c)^2 are obtained to the recent $\pi^- + p \rightarrow \pi^0 + n$ data between 9 and 18 Bev/c. (auth)

15365 SUM RULES FOR MAGNETIC QUADRUPOLE AND ELECTRIC DIPOLE MOMENTS: AN APPLICATION OF THE ALGEBRA OF CURRENT COMPONENTS. Bietti, A. (California Inst. of Tech., Pasadena). Phys. Rev., 142: 1258-62(Feb. 25, 1966). (CALT-68-55).

Assuming simple commutation relations between the various components of the vector current density, three commutation relations between electric dipole and magnetic quadrupole operators are derived. Taking these commutators between proton states at rest, three sum rules are obtained. Considering only one intermediate state, namely the $I = \frac{1}{2}$, $J = \frac{3}{2}^-$ pion-nucleon resonance N** (1518), a consistency relation between them is found. The sum rules are then used for deriving the ratio between the E_{2-} and M_{2-} amplitudes in single-pion photoproduction, and a result is obtained in good agreement with experiment. (auth)

15366 CURRENT ALGEBRAS AND NONLEPTONIC K-MESON DECAYS. Bose, S. K.; Biswas, S. N. (Univ. of Delhi). Phys. Rev. Lett., 16: 330-3(Feb. 21, 1966).

The Sugawara and Suzuki model was applied to the nonleptonic meson (K) decays. It was assumed that the final 3π state in these decays is completely symmetric with respect to the space coordinates (i.e., each pair of pions is in relative s wave). The Clebsch-Gordan coefficient for eleven decay processes were evaluated. (G.O.Y.)

15367 STUDY OF THE DECAY $\eta^0 \rightarrow \pi^+ + \pi^- + \gamma$. Crawford, Frank S. Jr.; Price, LeRoy R. (Univ. of California, Berkeley). Phys. Rev. Lett., 16: 333-7(Feb. 21, 1966).

The decay process $\eta^0 \rightarrow \pi^+ + \pi^- + \gamma$ was investigated using π^+p interactions at 1170 Mev/c. (D.C.W.)

15368 EXPERIMENTAL STUDY OF π-π INTERACTION IN THE REACTION $\pi^- + p \rightarrow \pi^0 + \pi^0 + n$ AT INCIDENT π^- ENERGY OF 378 Mev. Maung, Tin; Crowe, Kenneth M.; Dairiki, Ned T. (Univ. of California, Berkeley). Phys. Rev. Lett., 16: 374-7(Feb. 28, 1966). (UCRL-16444).

The differential neutron time-of-flight distribution from the interaction $\pi^- + p \rightarrow n + \pi^0 + \pi^0$ at 378 Mev was measured. A lower limit for the magnitude of the $I = 0$, s-wave π-π scattering length was obtained. It was found that at low momentum transfers the data do not agree with a pure one-pion-exchange model. It was concluded that the π-π cross section is 60 mb or larger. (D.C.W.)

15369 NONLEPTONIC DECAYS OF HYPERONS. Hara, Y. (Inst. for Advanced Study, Princeton, N. J.); Nambu, Y.; Schechter, J. Contracts AFOSR Nr 42-65; AT(11-1)-264. Phys. Rev. Lett., 16: 380-3(Feb. 28, 1966).

It is shown that both s- and p-wave decay amplitudes can be determined under the assumption of the quark model and the partial conservation of axial-vector currents, as well as octet dominance. The $K_{2\pi}$ decays are also briefly considered. (D.C.W.)

15370 RELATIVISTIC EXTENSION OF NON-COMPACT SYMMETRY GROUPS. Delbourgo, R.; Salam, A.; Strathdee, J. (International Centre for Theoretical Physics, Trieste, Italy). Proc. Roy. Soc. (London), Ser. A, 289: 177-91(Jan. 4, 1966). (IC/65/72).

The problem of relativistically boosting the unitary representations of a non-compact spin-containing rest-symmetry group is solved by starting with non-unitary infinite-dimensional representations of a relativistic extension of this group, by adjoining to this extension four space-time translations, and by then applying Bargmann-Wigner equations to guarantee a unitary norm. The procedure has similarities to the conventional method of induced representations. The boosting problem considered here is the first step towards the solution of the problem of coupling of such infinite-dimensional representations which is also briefly investigated. Starting from a rest-symmetry like U(6,6) a chain of subgroups GL(6), U(3,3), etc., is exhibited for collinear and coplanar processes, etc. (auth)

15371 INTRODUCTORY REMARKS ON THE STUDY OF THE PION-NUCLEON INTERACTION. Dalitz, R. H. (Oxford Univ.). Proc. Roy. Soc. (London), Ser. A, 289: 442-8(Jan. 25, 1966).

A brief review of information obtained from the pion-nucleon interactions is given. The excited nucleon states with their spins and parities are listed. The unitary multiplets for excited baryons in SU(3) representation are also given. (C.E.S.)

15372 MEASUREMENTS OF DIFFERENTIAL CROSS SECTIONS AND POLARIZATION EFFECTS IN PION-PROTON ELASTIC SCATTERING IN THE MOMENTUM RANGE 875 TO 1579 Mev/c. Atkinson, H. H. (Rutherford High Energy Lab., Chilton, Eng.); Cox, C. R.; Duke, P. J.; Heard, K. S.; Jones, D. P.; Kemp, M. A. R.; Murphy, P. G.; Prentice, J. D.; Thresher, J. J. Proc. Roy. Soc. (London), Ser. A, 289: 449-62(Jan. 25, 1966).

Measurements of differential cross sections and polarization effects in πp elastic scattering are discussed. The measurements were made in an attempt to determine the spins and parities of the $N_{\frac{3}{2}}^*(1688)$ and the $N_{\frac{5}{2}}^*(1920)$ isobars and to examine the behavior of the π^+p elastic scattering cross section at momenta around 950 Mev/c where a shoulder exists in the π^+p total cross sections. (C.E.S.)

15373 RECOIL PROTON POLARIZATION MEASUREMENTS IN PION-NUCLEON ELASTIC SCATTERING. Bareyre, P. (C.E.N., Saclay, France). Proc. Roy. Soc. (London), Ser. A, 289: 463-70(Jan. 25, 1966).

The angular distributions of the recoil proton polarization in π^+p elastic scattering were measured at 410 and 492 Mev incident pion kinetic energy by using a carbon plate spark chamber. (C.E.S.)

15374 CHARGE EXCHANGE SCATTERING NEAR THE N*(1510) AND N*(1690) RESONANCES. Guerriero, L. (Univ. of Padua). Proc. Roy. Soc. (London), Ser. A, 289: 471-88(Jan. 25, 1966).

Preliminary results of an experiment to measure the total cross sections and the angular distributions in the charge exchange reaction $\pi^- + p \rightarrow \pi^0 + n$ at eleven energies between 500 and 1150 Mev are reported. (C.E.S.)

15375 THE REACTION $\pi N \rightarrow \pi N^*$ (1238) NEAR THE N*(1510) AND THE N*(1690) RESONANCES. Merlo, J. P.; Valladas, G. (C.E.N., Saclay, France). Proc. Roy. Soc. (London), Ser. A, 289: 489-99(Jan. 25, 1966).

A brief review of the experimental results relative to the reaction $\pi^-p \rightarrow \pi^-\pi^+n$ below 1 Bev is given. The angular distributions of the π^+ and the π^- in the overall center of mass are expanded in Legendre polynomials. The variation of the coefficients as a function of the kinetic incident energy is examined. (auth)

15376 PION-NUCLEON SCATTERING AT HIGH ENERGIES. Hoehler, G.; Baacke, J.; Giesecke, J.; Zovko, N.

(Technische Hochschule, Karlsruhe, Ger.). Proc. Roy. Soc. (London), Ser. A, 289: 500-8(Jan. 25, 1966).

The charge exchange forward scattering amplitude $F_{ex.} = -\sqrt{2}\,F^{(-)}$ was calculated from the optical theorem and dispersion relations using an interpolation of the total cross sections. From $F^{(-)}$ follows a prediction of the charge exchange forward cross section (c. m. system) which is compared with experimental data. (C.E.S.)

15377 THE ELASTIC SCATTERING OF NEGATIVE PIONS ON PROTONS NEAR 2 Gev/c. Bellamy, E. H. (Westfield Coll., London); Buckley, T. F.; Busza, W.; (and others). Proc. Roy. Soc. (London), Ser. A, 289: 509-12 (Jan. 25, 1966).

Preliminary results on a spark chamber experiment to determine the differential cross section of the reaction $\pi^- + p \rightarrow \pi^- + p$ at a number of pion momenta in the vicinity of the 2.07 Bev/c resonance are reported. (C.E.S.)

15378 PION-PROTON CHARGE-EXCHANGE SCATTERING NEAR 2.0 Gev/c. Carroll, A. S. (Rutherford High Energy Lab., Chilton, Eng.); Clegg, A. B.; Corbett, I. F.; Damerell, C. S. J.; Middlemas, N.; Newton, D.; Quirk, T. W.; Williams, W. S. C. Proc. Roy. Soc. (London), Ser. A, 289: 513-20(Jan. 25, 1966).

Results based on an analysis of 25% of the pictures obtained from a measurement of the charge-exchange reaction $\pi^-p \rightarrow \pi^0n$ with thick-plate spark chambers are given. Differential and total cross sections for charge-exchange scattering were obtained at five momenta centered about the $T = \frac{1}{2}$ resonance found at 2.07 Bev/c in the π^-p total cross section. In the vicinity of the resonance the total cross section is falling smoothly, and the higher coefficients of Legendre polynomial expansions show no significant variation with momentum. From this it is concluded that there is either a complicated interference of several states at the resonance or that the resonance is in a relatively high partial wave and is mainly inelastic. (auth)

15379 PION-NUCLEON RESONANCES AND THEIR EFFECT UPON π^+p TOTAL CROSS SECTIONS. Galbraith, W. (Atomic Energy Research Establishment, Harwell, Eng.). Proc. Roy. Soc. (London), Ser. A, 289: 521-30 (Jan. 25, 1966).

Precise measurements of the total cross sections of positive and negative π mesons on hydrogen have revealed the presence of structure or enhancements in these cross sections at various momenta up to 3 Bev/c. Measurements of this type are discussed and in particular, a recent experiment to search for structure in the region 3 to 7 Bev/c, where previous experiments have shown that, if structure were present, it was likely to reveal itself as an amplitude in the total cross section of 1 mb or less. The recent measurements indicate four regions of structure, two in each of the isotopic spin states $\frac{3}{2}$ and $\frac{1}{2}$. The possible relation of these regions of structure to the formation of pion-nucleon resonances is discussed. (auth)

15380 STUDY OF THE REACTIONS $\pi^- + p \rightarrow \pi^0 + n$ AND $\pi^- + p \rightarrow \eta + n$ AT HIGH ENERGIES. Amblard, B. (Institut du Radium, Orsay, France); Borgeaud, P.; Bruneton, C.; (and others). Proc. Roy. Soc. (London), Ser. A, 289: 531-6(Jan. 15, 1966).

A spark chamber experiment which permits the study of the angular distributions of the all-neutral reactions $\pi^0 + n$ and $\eta + n$ coming from π^-p interactions at high energies. The method consists in detecting in a heavy-plate spark chamber the showers of γ rays coming from the decay of the π^0 or η meson. Experimental results are included. (C.E.S.)

15381 AN ANALYSIS OF PION-NUCLEON SCATTERING AND THE LOWER NUCLEON ISOBARS. Bransden, B. H. (Durham Univ., Eng.); Moorhouse, R. G.; O'Donnell, P. J. Proc. Roy. Soc. (London), Ser. A, 289: 538-46 (Jan. 25, 1966).

Pion-nucleon scattering is analyzed using a parametrization of the partial wave amplitudes as analytic functions of the energy. It is shown that the structure of the "second pion-nucleon resonance" is more complicated than previously thought. (auth)

15382 PION-NUCLEON PHASE SHIFTS AND THEIR IMPLICATIONS. Lovelace, C. (Imperial Coll. of Science and Tech., London). Proc. Roy. Soc. (London), Ser. A, 289: 547-58(Jan. 25, 1966).

Recent πp phase shift analyses and evaluations of dispersion relations are discussed. Besides the D_{13} resonance, which is much narrower than previously thought, they have revealed P_{11}, S_{11} and S_{31} "objects" in the 500 to 800 Mev region, all with strong inelastic decay modes. The P_{11} phase shift reaches 81°. S_{11} and S_{31} objects were predicted by SU(6), but the behavior of P_{11} is difficult to reconcile either with pure SU(6) or with the reciprocal NN* bootstrap. (auth)

15383 ELECTRON INTERACTION AND POSITRON ANNIHILATION IN ELECTRON GASES. Hatano, Akira; Kanazawa, Hideo; Mizuno, Yukio (Tokyo Univ.). Progr. Theoret. Phys. (Kyoto), 34: 875-84(Dec. 1965).

An intuitive many-body treatment is presented for the distribution in the total momentum of two gamma rays emitted in annihilation of positrons in a gas of interacting electrons. This treatment results in a momentum distribution of photon pairs which is very close to that of the ideal Fermi distribution of quasi-electrons in the electron gas. This seems to be supported by Stewart's experiment for sodium metal. (auth)

15384 MULTIPLICITY OF NEUTRAL PIONS PRODUCED IN 9 Gev/c TWO-PRONG π^--p INTERACTIONS. Friedlaender, E. M.; Nitu, R. (Inst. of Atomic Physics, Bucharest). Rev. Roum. Phys., 10: 774-6(1965).

The yield of photons from inelastic two-prong interactions in propane by mesons (π^-) at 9 Bev/c was investigated in order to verify previous results under conditions ensuring a considerably increased efficiency for gamma-ray registration. No evidence was found for an anomalously low photon yield. The results for the mean meson (π^0) multiplicity are given. (J.F.P.)

15385 ON THE DISPERSION-RELATION TREATMENT OF THE LOW-ENERGY PION-NUCLEON SCATTERING. Hu, Ning (Peking Univ.). Sci. Sinica (Peking), 15: 1745-55(Dec. 1965).

The relation between the subtracted dispersion relations for the low-energy pion-nucleon scattering and the usual Lagrangian formulation under the renormalization treatment is discussed. It is shown that the subtraction integrals actually represent the renormalization of the interaction constants. Using the subtracted dispersion relations, the problem of the S-wave pion-nucleon scattering is treated. The result shows that the interaction of the pion with the nucleon should be of the pseudo-vector type rather than the pseudo-scalar type. (auth)

15386 SOLUTION OF THE THREE-NUCLEON INTERACTION PROBLEM. Popova, A. M. (Moscow State Univ.). Yadern. Fiz., 3: 34-42(Jan. 1966). (In Russian).

The problem of inelastic interactions of nucleons with deuterons is solved for the case when two nucleons in the final state interact with a small relative momentum f. It is shown that the amplitude of this reaction can be written accurately within terms proportional to $(f/k_0)^2$ (k_0 is the initial momentum of the nucleons in the deuteron in c.m.s.), as a sum of the impulse approximation amplitude and a function, which is the product of the interaction amplitude of two particles with the relative momentum f and the quantity $C_1(k_0, \vartheta)$, depending on the initial energy and scattering angle ϑ. Integral equations are obtained for $C_1(k_0, \vartheta)$. (auth)

15387 NEUTRINO-NUCLEON INTERACTIONS WITH LEPTON PRODUCTION. Sokolov, A. A.; Kerimov, B. K.; Takvale, R.; Dzhafarov, I. G.; Yakhyaev, R. Sh. (Moscow State Univ.). Yadern. Fiz., 3: 99-107(Jan. 1966). (In Russian).

The spin-dependence of the high energy neutrino–nucleon interactions is investigated in the reactions $\nu_l(\bar{\nu}_l) + N \rightarrow$

$N' + 1(\bar{l})$ taking the nucleon-current form-factors into account. General formulas are derived, describing the angular distribution of longitudinally polarized leptons (antileptons) and arbitrarily polarized recoil nucleons, created in the interactions of neutrinos with a polarized nucleon target. These formulas are used to investigate in detail the influence of the weak vector and axial–vector nucleon form-factors on the angular and polarization correlations of particles. (auth)

15388 PHASE-SHIFT ANALYSIS OF ELASTIC πN SCATTERING AT 240 Mev. Ivanchenko, I. M.; Shchegelskii, V. A. (Ioffe Inst. of Physics and Tech., Leningrad). Yadern. Fiz., 3: 108-11(Jan. 1966). (In Russian).

The phase-shift analysis of $\pi \pm$ p-scattering at 240 Mev was performed, taking the data on recoil proton polarization in π + p-scattering into account. The absence of experiments on the polarization in $\pi -$ p-scattering makes it impossible to obtain a unique set of phase-shifts. A comparison with analyses at other energies indicates that the most probable solution is that with the following nuclear phase-shifts (in degrees): $S_{31} = -15.7 \pm 1.3$; $P_{33} = 112.6 \pm 0.5$; $P_{31} = -3.4 \pm 2.3$; $D_{35} = -2.6 \pm 1.1$; $D_{33} = 2.1 \pm 1.3$; $S_{11} = 6.0 \pm 5.9$; $P_{13} = 0.16 \pm 2.4$; $P_{11} = 19.0 \pm 3.1$. The accuracy of the experiment is not sufficient to determine the D-phase-shift with the isospin $I = \frac{1}{2}$. (auth)

15389 ON $\gamma 3\pi$ AND $\rho\pi\gamma$ INTERACTIONS. Meshcheryakov, V. A.; Solovev, L. D.; Tkebuchava, F. G. (Joint Inst. for Nuclear Research, Dubna, USSR). Yadern. Fiz., 3: 116-29(Jan. 1966). (In Russian).

It is shown that the data on $\rho\pi\gamma$- and $\gamma 3\pi$-interactions near to the threshold are in agreement with the dynamical picture of the $\gamma 3\pi$-interaction, following from dispersion relations, taking high energy contributions into account. The existing data on $\rho\pi\gamma$-interactions are analyzed paying special attention to the normalization of the constant of this interaction, used in the literature. The connection of the $\rho\pi\gamma$-interaction with analogous interactions of other vector and pseudoscalar mesons in the framework of SU(3) and SU(6) symmetries is discussed. (auth)

15390 STRONG INTERACTIONS AND RELATIVIZED SU(6) SYMMETRY ($\tilde{U}(12)$). MESON-BARYON SCATTERING. Marinov, M. S. Yadern. Fiz., 3: 130-4(Jan. 1966). (In Russian)

The $\tilde{U}(12)$ symmetry is used to find the amplitudes of quasi-elastic interactions between pseudoscalar mesons and nucleons. It is shown that the Johnson–Treiman relations for the πN, KN and $\bar{K}$N total cross sections remain to be valid for arbitrary energies. It is shown that in the $\tilde{U}(12)$ framework there is no polarization when Σ^- is created in the reactions $\pi^- p \to K^+\Sigma^-$ and $K^- p \to \pi^+\Sigma^-$, and when Ξ is created in the reaction $K^- p \to K\Xi$. (auth)

15391 ELASTIC ELECTRON-PROTON SCATTERING AT FORWARD ANGLES [Thesis]. Rouse, Gerald Russell. Ithaca, N. Y., Cornell Univ., 1965. 123p.

The elastic scattering of electrons from protons was investigated at forward scattering angles and high incident energy, in order to determine if the form of the Rosenbluth formula was still obeyed in this kinematic region. A synchronously rotating polyethylene target intercepted the circulating electron beam of the Cornell 1.3-Bev synchrotron. A hyperbolic quadrupole magnet was used to momentum-analyze the scattered electrons, which were detected by simultaneous response of two plastic scintillation counters and a lead glass Cherenkov counter. The recoil protons were detected in coincidence with the scattered electrons by a plastic scintillation counter after a sufficient fraction of their initial energy had been lost in copper absorbers placed in front of the counter. Data were taken at electron scattering angles θ of 18°, 30°, 60°, and 90° and at values of q^2 (the square of the four momentum transferred to the proton) of 4 and 10 fermis^{-2}. The Rosenbluth formula states that at fixed momentum transfer the ratio of the differential cross section $d\sigma/d\Omega$ to the Mott cross section σ_{NS} should be linear with $\tan^2 \theta/2$. One expects a departure from linearity at forward scattering angles and high incident energy due to the contribution of two-photon exchange processes. One might also expect a departure from linearity in this kinematic region under the assumption that the photon has a Regge trajectory similar to that of the strongly interacting particles. The data of this experiment show that plots of $(1/\sigma_{NS})/(d\sigma/d\Omega)$ as a function of $\tan^2 \theta/2$ are linear for $q^2 = 4$ and $q^2 = 10$ inverse fermis. No evidence of contribution from two-photon exchange effects or the Regge pole was seen. Thus it was concluded that the Rosenbluth formula is still valid in the kinematic region of this data. (Dissertation Abstr.)

15392 TWO-RESONANCE MODEL FOR Λ-K^0 PRODUCTION [Thesis]. Rush, John Edwin Jr. Nashville, Vanderbilt Univ., 1965. 152p.

The elementary-particle process $\pi^- + p \to \Lambda + K^0$ is examined in a semiphenomenological manner. Various simple models are considered, and a particular one is compared with the cross section and polarization data for a range of the laboratory kinetic energy of the pion from threshold (768 Mev) to 1375 Mev. All of the models considered contain basic constituents of two types: (1) pole terms, or contributions to the S matrix from particles that may be assumed, for practical purposes, to be stable, and (2) resonances in individual partial-wave amplitudes, or contributions from unstable particles that are intermediate states of the reaction. In the model for which a comparison with the data is given, the K*(888 Mev) exchange contribution is the only pole term. A single resonance is shown to be untenable, and the best fit for two resonances is obtained with an $F_{5/2}$ resonance at a total center-of-mass energy of 1680 Mev with a width of 100 Mev, and a $D_{3/2}$ resonance at 1630 Mev, width 100 Mev. Comparisons with the data are given for kinetic-energy values of 829, 871, 890, 905, 990, and 1374 Mev. Brief discussions of S-matrix theory, including unitarity, the substitution rule, and some analyticity properties, and the kinematics of Λ-K^0 production are included. Prior to presentation of the model, a derivation of the K*-pole contribution and a simple discussion of resonance contributions are given. (Dissertation Abstr.)

15393 $K^+\Lambda$ PHOTOPRODUCTION FROM HYDROGEN NEAR 90° IN THE CENTER OF MASS [Thesis]. Marshall III, J. Howard. Pasadena, Calif., California Inst. of Tech., 1965. 114p.

The differential cross section for $\gamma + p \to K^+ + \Lambda$ was measured for a center-of-mass angle of 90° and for photon energies between 1100 and 1300 Mev. Range telescopes detected both the K^+ and the proton from the Λ decay. This experiment was performed in collaboration with D. E. Groom, who measured the polarization of the Λ hyperon in the above reaction. The electronic instrumentation for this experiment is emphasized here. The differential cross section was found to remain nearly constant at 0.14 ± 0.01 μb/sr over the above energy interval. (Dissertation Abstr.)

15394 PHOTOPRODUCTION AT MEDIUM ENERGIES [Thesis]. Knight, Kenneth Douglas. Los Angeles, Univ. of California, 1965. 195p.

The effect of the inelastic channel (pN) in the photoproduction reaction $\gamma + N \to \pi + N$ is studied using the multichannel ND^{-1} method. A solution is obtained by approximating the left hand cuts resulting from particle and resonance exchanges in the cross channels by sums of poles. The elastic differential cross sections at 90° are computed for energy values near the second resonance (1512 Mev) for the reactions $\gamma + p \to p + \pi^0$, $\gamma + p \to n + \pi^+$, $\gamma + n \to n + \pi^0$, and $\gamma + n \to p + \pi^-$ retaining only $D_{3/2}$ partial waves. Values of the coupling constants Λ_p and Λ_ω, which are proportional to the coupling constants for the decays $p \to \pi + \gamma$ and $\omega^0 \to \pi^0 + \gamma$, are determined from the best fit to the data for the (γp) reactions. The magnitude and sign of Λ_p are found to agree with previous determinations made near thresholds. In contrast to the threshold region, the peak height of the second resonance is found to be quite sensitive to the value of Λ_p. (Dissertation Abstr.)

15395 NEUTRAL DECAY MODES OF THE ETA MESON [Thesis]. Kounosu, Shigeru. Philadelphia, Univ. of Pennsylvania, 1965. 85p.

The neutral decay modes of the eta meson were studied by means of spark chambers and neutron time-of-flight measurement in the reaction $\pi^- + p \rightarrow n + \eta$. The eta mesons were produced in a hydrogen target by a negative pion beam of 970 Mev/c at the Princeton Pennsylvania Accelerator. The neutron time of flight was measured over a path length 210 cm at lab angles between 4 and 14 degrees with plastic scintillators. The time of flight information was displayed on a 519 Tektronix oscilloscope and photographed. The spark chambers were arranged to cover a solid angle of almost 4π around the hydrogen target. Each spark chamber had two thin aluminum plates at front and twenty lead plates constituting six radiation lengths. The principal reactions were $\pi^- + p \rightarrow n + X$ where X denotes a neutral system consisting of pions, gamma rays, and the eta meson. Events involving 2, 3, 4, 5, and 6 gamma rays were analyzed, and the 2 gamma-ray decay mode and the $\pi^0 2\gamma$ decay mode of the eta were observed. As to $3\pi^0$ decay mode of the eta, the data were not conclusive and require further investigation with higher statistics. The branching ratio of the $\pi^0 2\gamma$ decay mode to the 2γ decay mode is 1.18 ± 1.06. (Dissertation Abstr.)

15396 CONSEQUENCES OF STRONG PAIR INTERACTIONS OF THE WEAK INTERMEDIATE BOSON WITH HADRONS AND DECAY MODE $K \rightarrow 2\pi + \gamma$ [Thesis]. Pepper, Stephen V. Rochester, N. Y., Univ. of Rochester, 1965. 114p.

In Part I are investigated some consequences of a hypothesis that the intermediate vector boson W supposed to be responsible for the weak interactions may have strong pair interactions with hadrons. The W triplet is assumed to constitute the fundamental representation of the U(3) group and to possess unit triality. Since triality is conserved in strong interactions (but not in semiweak), W may interact strongly only in pairs with the zero-triality hadrons. It is shown that a strong quadratic W-hadron interaction does not contradict present experimental data, provided $m_W > 2.5$ Bev. This strong pair interaction can generate the large W mass and can explain the small discrepancy between the muon-decay constant and the renormalized vector coupling constant in β decay. The search for strong W pair production in a reaction such as $\bar{p} + p \rightarrow W + \overline{W}$ seems justified. The large polarization effects in the decay $W \rightarrow \mu + \nu_\mu$ would be helpful in identifying the above reaction. In Part II the radiative decay $K^+ \rightarrow \pi^+ + \pi^0 + \gamma$ is considered in the light of the $\Delta T = 1/2$ rule. The possibility that the nonradiative and radiative rates are of the same order of magnitude is investigated by constructing mechanisms that obey the $\Delta T = 1/2$ rule in the absence of electromagnetic interactions. We consider a boson pole model and a model involving a two-particle intermediate state and find that neither model can give contributions to the radiative rate that are of the same order of magnitude as the internal bremsstrahlung contribution. The pole model also furnishes an estimate of the rate for $K_2^0 \rightarrow \pi^+ + \pi^- + \gamma$. (Dissertation Abstr.)

15397 $Y_1^*(1660)$—SPIN AND PARITY DETERMINATION [Thesis]. Dockery, John Thomas. Tallahassee, Florida State Univ., 1965. 315p.

A study of K^-d interactions at principal beam settings of 670, 720, and 770 Mev/c in the 30" BNL chamber is reported. The cms energy region from 1580 to 1760 was investigated with particular reference to the $Y_1^*(1660)$ resonance. Utilizing the impulse approximation, 1028 events of the type $K^-d \rightarrow Y^* \rightarrow \Lambda + \pi^- + (p)$ were accepted. The angular distribution in 20-Mev intervals was fit to the form $W = \Sigma A_l P_l^0(\mu) + \alpha\eta\Sigma B_l P_l^1$. A plot of the coefficients' variation with energy was then employed to determine the spin and parity. A spin-parity assessment of $3/2^-$ was made, which is in accord with SU(3) predictions. Two out of three combinations for the reaction $K^-d \rightarrow \Lambda + \pi^- + \pi^0 (p)$ were also examined and revealed the possibility of the cascade decay $Y_1^*(1660) \rightarrow \pi + Y_1^*(1385)$. A brief look at the $\Sigma^0\pi^-$ channel is also included. (Dissertation Abstr.)

15398 RESONANT PARTICLES. Proceedings [of the] Second Topical Conference, Ohio University, Athens, Ohio, June 10–12, 1965. Munir, B. A. (ed.). Contract AT(49-12)-2802. 560p. Fazl-i-Umar Research Inst., Athens, Ohio $12.00.

Separate abstracts were prepared for 37 of the 42 papers included. The other five papers were previously abstracted for NSA (19: 37522, 37539, 43144, 44997; and 20: 9785). (G.O.Y.)

For abstracts of individual papers see: 15399–15430, and 15506–15510.

15399 NEW EVIDENCE FOR A MOLECULAR STRUCTURE OF MESON AND BARYON RESONANCE STATES. Sternglass, E. J. (Westinghouse Research Labs., Pittsburgh, Pa.). pp 33-56 of Resonant Particles. Athens, Ohio, Fazl-i-Umar Research Inst., 1965.

The extent to which the quasi-molecular rotator models have been substantiated by the discovery of higher rotational levels is outlined, and it is shown that the same models account for the observed mass and angular momenta of the excited baryon states. (D.C.W.)

15400 POLES AND RESONANCES IN THE PROCESS $\pi^+ + p \rightarrow \Sigma^+ + K^+$. Holladay, W. G. (Vanderbilt Univ., Nashville). pp 72–102 of Resonant Particles. Athens, Ohio, Fazl-i-Umar Research Inst., 1965.

The angular distribution and polarization of the hyperon (Σ^+) from the interaction $\pi^+ + p \rightarrow \Sigma^+ + K^+$ were calculated using several models involving various combinations of poles and resonances. The results were compared with experimental data. The study was undertaken to determine the extent to which simple pole and resonance contributions constitute an adequate description of two-particle interactions involving strongly interacting particles. (D.C.W.)

15401 POSSIBLE TESTS OF ISOSPIN PURITY OF Σ^0 AND Λ^0 HYPERONS. Chand, Ramesh (Wayne State Univ., Detroit). pp 110–18 of Resonant Particles. Athens, Ohio, Fazl-i-Umar Research Inst., 1965.

A few of the possible methods of determining the isospin mixing angle of hyperons (Λ^0) and hyperons (Σ^0) are discussed. (D.C.W.)

15402 SMALL WAVE-FUNCTION RENORMALIZATION CONSTANTS IMPLIED BY A PARTIALLY CONSERVED AXIAL-VECTOR CURRENT. Ogimoto, Takesi (Univ. of California, Berkeley). pp 119-23 of Resonant Particles. Athens, Ohio, Fazl-i-Umar Research Inst., 1965.

It is shown that the combined use of unsubtracted dispersion relations with the partially conserved axial-vector current (PCAC) hypothesis of Nambu leads to a very small wave-function renormalization constant of the pion field ($Z_3 \ll 1$), where an additional condition for PCAC is necessary to obtain the case $Z_3 = 0$. (D.C.W.)

15403 THE PRODUCTION AND DECAY OF ρ^0 AND ω MESONS IN π^+n AND π^-p INTERACTIONS AT 1.7 Gev/c. Bacon, T. C.; Fickinger, W. J.; Hill, D. G.; Hopkins, H. W. K.; Robinson, D. K.; Salant, E. O. (Brookhaven National Lab., Upton, N. Y.). pp 129-51 of Resonant Particles. Athens, Ohio, Fazl-i-Umar Research Inst., 1965.

The results of an investigation of the production and decay of mesons(ω) and mesons(ρ) in the interactions $\pi^-p \rightarrow \pi^+\pi^-n$, $\pi^+n \rightarrow \pi^+\pi^-p$, and $\pi^+n \rightarrow \pi^+\pi^-\pi^0p$ at 1.7 Bev/c are presented. (D.C.W.)

15404 OBSERVATIONS OF $Y_0^*(1405)$ AND $Y_1^*(1358)$ RESONANCES IN $\pi-N$ COLLISIONS AT 1.68 Bev/c. Engler, A. (Carnegie Inst. of Tech., Pittsburgh); Fisk, H. E.; Kraemer, R. W.; Meltzer, C. M.; Westgard, J. B.; Bacon, T. C.; Hill, D. G.; Hopkins, H. W. K.; Robinson, D. K.; Salant, E. O. pp 152– 61 of Resonant Particles. Athens, Ohio, Fazl-i-Umar Research Inst., 1965.

The production and decay of the $Y_0^*(1405)$ and $Y_1^*(1358)$ resonances in π^-p and π^+d interactions at 1.68 Bev/c were observed, and the spins of the two resonances were studied by applying the method of moments to the data. (D.C.W.)

15405 ENHANCEMENTS IN THE INTERACTIONS OF 3.2 Bev/c-π^- WITH DEUTERIUM. Seidlitz, Leo; Dahl,

Orin I.; Miller, Donald H. (Univ. of California, Berkeley). pp 162-76 of Resonant Particles. Athens, Ohio, Fazl-i-Umar Research Inst., 1965.

An investigation of enhancements in deuteron-meson(π^-) interactions at 3.15 Bev/c is summarized, in which the A_1 and A_2 enhancements were studied in detail. Several possible mechanisms for the structure in the $\pi\rho$ systems were considered. (D.C.W.)

15406 RECENT RESULTS ON π^--p AND K^+-p INTERACTIONS AT HIGH ENERGY. (A) A SEARCH FOR ELECTRON DECAYS OF VECTOR BOSONS. Erwin, A. R.; Garfinkel, A.; Peekna, A.; Thompson, M. A.; Walker, W. D.; Weinberg, A. (Univ. of Wisconsin, Madison). pp 183 of Resonant Particles. Athens, Ohio, Fazl-i-Umar Research Inst., 1965.

An attempt was made to observe the beta decay of vector mesons produced in π^-p interactions at 3.0 and 7.0 Bev. It was concluded that the branching ratio for $\omega^0 \rightarrow e^+ + e^-$ is $<10^{-3}$. An event that is consistent with the decay $\varphi^0 \rightarrow e^+ + e^-$ was observed at 3.0 Bev. (D.C.W.)

15407 RECENT RESULTS ON π^--p AND K^+-p INTERACTIONS AT HIGH ENERGY. (B) A STUDY OF 3- AND 4-BODY FINAL STATES IN K^+p AT 3.6 Bev/c. Bishop, J. M.; Erwin, A. R.; Walker, W. D. (Univ. of Wisconsin, Madison). pp 184-97 of Resonant Particles. Athens, Ohio, Fazl-i-Umar Research Inst., 1965.

Some preliminary results of an investigation of 3- and 4-body final states in K^+p interactions at 3.6 Bev/c are presented. (D.C.W.)

15408 A STUDY OF THE A AND B MESONS. Abolins, M. A.; Carmony, D. D.; Lander, R. L.; Xuong, Nguyen-huu; Yager, P. M. (Univ. of California, La Jolla, San Diego). pp 198-216 of Resonant Particles. Athens, Ohio, Fazl-i-Umar Research Inst., 1965.

The isotopic spin of the A_1 and A_2 resonances was investigated; and the possibility that the A_1 resonance and the meson(B) are kinematic enhancements in the $\rho\pi$ and $\omega\pi$ mass spectra, respectively, according to the Deck hypothesis, was studied. (D.C.W.)

15409 THE REACTION $\pi^-D \rightarrow D\pi^-\pi^+\pi^-$ AT 3.7 Gev/c AND EVIDENCE FOR A D π^- ENHANCEMENT. Abolins, M. A.; Carmony, D. D.; Lander, R. L.; Xuong, Nguyen-huu (Univ. of California, La Jolla, San Diego). pp 217-27 of Resonant Particles. Athens, Ohio, Fazl-i-Umar Research Inst., 1965.

The interaction $\pi^-d \rightarrow d\pi^-\pi^+\pi^-$ was studied at 3.7 Bev/c using a deuterium-filled bubble chamber. Evidence for an enhancement in the region 2040 Mev $< M(d^+\pi^-) <$ 2280 Mev of the histogram of the $d\pi_1^-$ mass vs the $\pi_2^-\pi^+$ mass was noted. An enhancement in the $d\pi^+$ effective mass at ~2170 Mev was observed. (D.C.W.)

15410 AN ANGULAR CORRELATION STUDY OF THE REACTION $\pi^-p \rightarrow \pi^-\pi^+p\pi^-$ AT 2.7 Bev/c. Klein, P. R.; Sahni, R. J.; Johnson, P. B.; Tautfest, G. W. (Purdue Univ., Lafayette, Ind.). pp 228-43 of Resonant Particles. Athens, Ohio, Fazl-i-Umar Research Inst., 1965.

Experimental decay angular correlations for resonances in the interaction $\pi^-p \rightarrow \pi^-\pi^+p\pi^-$ at 2.7 Bev/c were obtained considering seven possible mechanisms of resonance production. An attempt was made to determine the extent to which the separation or enrichment of a subclass of events, purportedly belonging to a particular graph, can be accomplished. The ρ^0 asymmetry was studied from the viewpoint that it may be a kinematical reflection. (D.C.W.)

15411 SINGLE PION PRODUCTION IN π^-p INTERACTIONS BETWEEN 600 AND 900 Mev. Derado, I. (Univ. of Notre Dame, Ind.); Kenney, V. P.; Lamsa, J. W.; Poirier, J. A.; Shephard, W. D.; Stautberg, J. L.; Vittitoe, C. N. pp 244-50 of Resonant Particles. Athens, Ohio, Fazl-i-Umar Research Inst., 1965.

The results of a study of single pion production in π^-p interactions at incident pion kinetic energies of 604, 790, 830, and 870 Mev are prescribed. The analysis of these data in terms of the formation of the $N^*_{3,3}(1238)$ isobar is also discussed. (G.O.Y.)

15412 FINAL-STATE INTERACTION INVOLVING HYPERONS. Smith, Gerald A.; Lindsey, James S. (Univ. of California, Berkeley). pp 251-61 of Resonant Particles. Athens, Ohio, Fazl-i-Umar Research Inst., 1965.

A hydrogen-filled bubble chamber was exposed to a meson(K^-) beam at various momenta in the range from 2.1 to 2.7 Bev/c. All the observed interactions involving B = +1, S = −2 particle groups were analyzed. Copious production of $\Xi^*(1532)$ and K*(890) was observed as well as a resonance (1817 ± 7 Mev) which is coupled strongly to the $\Lambda\overline{K}$ channel. The results for the $\Xi\pi$ system appear to be consistent with a proposed resonance near 1933 Mev. Evidence for a 1705-Mev resonance, coupled to both the $\Lambda\overline{K}$ and $\Xi\pi$ channels, was also obtained. The results also support the view that there is no resonance in the 1600-Mev region. (D.C.W.)

15413 LOW ENERGY HYPERON PROTON REACTIONS. Snow, G. A. (Univ. of Maryland, College Park). pp 262-8 of Resonant Particles. Athens, Ohio, Fazl-i-Umar Research Inst., 1965.

Some predictions of SU(3) and SU(6) for S-wave baryon-baryon scattering were compared with experimental observations. The results show that the $^1S_0$ scattering interaction is very strong in the np or pp channel and probably in the Σ^+p or Σ^-n channels, and is moderately strong in the Λp elastic scattering channel. The S-wave Σ^-p interaction is dominated by very strong absorption processes almost equally divided between Λn and Σ^0n. (D.C.W.)

15414 THE SPIN AND PARITY OF THE Y_1^*(1815) AND THE Y*(1765). Birge, Robert W.; Ely, Robert P.; Kalmus, George E.; Kernan, Anne; Louie, James; Sahouria, Jack S.; Smart, Wesley M. (Univ. of California, Berkeley). pp 296-311 of Resonant Particles. Athens, Ohio, Fazl-i-Umar Research Inst., 1965.

The interactions of mesons (K^-) with neutrons and protons were studied at 825 to 1115 Mev/c in hydrogen and at 920 and 1020 Mev/c in deuterium. The existence of the proposed $Y_1^*(1765)$ resonance was not verified. On the basis of an analysis of the angular distribution of $K^- + p \rightarrow Y_1^*(1385) + \pi$ and $K^- + n \rightarrow Y^*(1385) + \pi$ at center-of-mass energies near 1815 Mev, an assignment of $5/2^+$ was made for the $Y_0^*(1815)$ resonance. (D.C.W.)

15415 K^+p INTERACTIONS AT 3.6 Bev/c. Erwin, A. R.; Bishop, J. M.; Goshaw, A.; Walker, W. D.; Weinberg, A. (Univ. of Wisconsin, Madison). pp 312-24 of Resonant Particles. Athens, Ohio, Fazl-i-Umar Research Inst., 1965.

An attempt was made to observe a K^+K^+ resonance at 1280 Mev and the meson(κ) (730 Mev). Little evidence for the 1280-Mev resonance was obtained, and the meson(κ) was not observed. (D.C.W.)

15416 V-2-PRONG K^-p INTERACTIONS AT 5.5 Gev/c. Derrick, M. (Argonne National Lab., Ill.); Hyman, L.; Loken, J.; Fields, T.; Schweingruber, F.; Ammar, R.; Davis, R.; Mott, J.; Sun, C. pp 325-36 of Resonant Particles. Athens, Ohio, Fazl-i-Umar Research Inst., 1965.

Some preliminary results on 2-prong + V final states of 5.5-Bev/c K^-p interactions are presented. The interactions $K^-p \rightarrow K^{*-}p$ and $K^-p \rightarrow Y^{*+}(1385) + \pi^-$ are discussed in some detail. (D.C.W.)

15417 SEARCH FOR HYPERON RESONANCES WITH SPARK CHAMBERS. Blackall, P.; Dowell, J. D.; Leontic, B.; Lewis, G. M.; Lundby, A.; Meyer-Berkhout, U. (CERN, Geneva). pp 337-42 of Resonant Particles. Athens, Ohio, Fazl-i-Umar Research Inst., 1965.

A study of the interaction $\pi^- + p \rightarrow K^+ + Y^-$ was performed in which the kinematic parameters of the mesons (K^+) were determined by means of a magnet and spark-chamber arrangement. The Y^- mass range between 1 and 1.9 Bev was covered with a mass resolution of 10 Mev. (D.C.W.)

15418 K^-p INTERACTIONS AT 3.8 Bev/c. Carmony, D. D.; Lander, R. L.; Hendricks, T. J.; Xuong, Nguyen-huu (Univ. of California, La Jolla, San Diego). pp 343-50 of

Resonant Particles. Athens, Ohio, Fazl-i-Umar Research Inst., 1965.

Some preliminary results of a study of K^-p interactions at 3.8 Bev/c are presented. Some evidence for $K^{*0}N^{*0}$ production was observed, but no evidence for the production of the meson(η) was obtained. (D.C.W.)

15419 PERIPHERAL MODEL OF MESON-NUCLEON COLLISIONS. Lichtenberg, D. B. (Indiana Univ., Bloomington). pp 351-79 of Resonant Particles. Athens, Ohio, Fazl-i-Umar Research Inst., 1965.

A procedure for modifying the peripheral model to include absorption effects is described using a partial-wave representation. The results of some calculations for π-N elastic scattering and meson(ρ) production are presented. The predictions of some peripheral models are compared with the results of an exact calculation. (D.C.W.)

15420 EXCHANGE MECHANISMS IN K^-p REACTIONS AT 1.8 AND 1.95 Gev/c. Smith, L. T.; Stork, D. H.; Ticho, H. K. (Univ. of California, Los Angles). pp 380-96 of Resonant Particles. Athens, Ohio, Fazl-i-Umar Research Inst., 1965.

Some observations on K^-p interactions that lead to pseudoscalar and vector bosons and to the $\frac{1}{2}^+$ baryon octet and $\frac{3}{2}^+$ decuplet states are discussed in terms of boson exchange mechanisms. (D.C.W.)

15421 VECTOR EXCHANGE IN K-N SCATTERING AS A TEST OF BROKEN M(12) SYMMETRY. Warnock, Robert L. (Illinois Inst. of Tech., Chicago. Argonne National Lab., Ill.). pp 397-404 of Resonant Particles. Athens, Ohio, Fazl-i-Umar Research Inst., 1965.

The predictions of broken M(12) symmetry for the coupling constants involved in K-N scattering were compared with some experimental observations on low-energy K-N scattering. It was found that there is no striking incompatibility between the experimental and theoretical results. (D.C.W.)

15422 SINGLE PARTICLE EXCHANGE IN 3 PARTICLE FINAL STATES OF THE REACTION K^+p AT 2.26 Bev/c. Bomse, F.; Cole, J.; Zdanis, R.; Pevsner, A.; Miller, I.; Singh, R.; Kane, G.; Kraemer, R. (Johns Hopkins Univ., Baltimore). pp 405-20 of Resonant Particles. Athens, Ohio, Fazl-i-Umar Research Inst., 1965.

The results of some studies of the interaction $K^+p \rightarrow K^0\pi^+p$ at 2.26 Bev/c are presented. The decay correlations and production of the K* and N* resonances are analyzed in terms of the single-particle-exchange model. (D.C.W.)

15423 STUDY OF EXCHANGE MECHANISM IN p-p INTERACTIONS AT 2.80 Bev/c. Ijaz, M. A.; Munir, B. A. (Ohio Univ., Athens). pp 442-60 of Resonant Particles. Athens, Ohio, Fazl-i-Umar Research Inst., 1965.

A study of single pion production in p-p interactions at 2.80 Bev/c is summarized. The experimental data were compared with the predictions of the one-pion-exchange model. (D.C.W.)

15424 EVIDENCE FOR HYPERON STATES WITH MASSES GREATER THAN 1900 Mev FROM PHOTOPRODUCTION OF CHARGED K MESONS. Minehart, R. C.; Greenberg, J. S.; Blanpied, W. A.; Hughes, V. W.; Kitching, P.; Lu, D. C. pp 464-75 of Resonant Particles. Athens, Ohio, Fazl-i-Umar Research Inst., 1965.

The photoproduction of mesons($K^\pm$) was investigated at sufficiently high energies to give K momenta of 2.63 and 3.15 Bev/c. Evidence for hyperon states with masses >1900 Mev was obtained. (D.C.W.)

15425 HIGH ENERGY PHOTOPRODUCTION OF NUCLEON AND PIONIC RESONANCES. Crouch, H. R. Jr.; Hargraces, R.; Kendall, G.; (and others) (Brown Univ., Providence). pp 476-98 of Resonant Particles. Athens, Ohio, Fazl-i-Umar Research Inst., 1965.

The photoproduction of resonances in 3-prong γ-p interactions at 4.8 to 6.0 Bev was investigated. The production of the meson(ρ^0) and the N*(1238) resonance were considered in detail. It was concluded that the one-pion-exchange model fails to give a proper interpretation of the data in both channels. (D.C.W.)

15426 PRODUCTION PROCESSES IN LOW ENERGY p-p COLLISION. Melissinos, A. C. (Univ. of Rochester, N. Y.). pp 499-513 of Resonant Particles. Athens, Ohio, Fazl-i-Umar Research Inst., 1965.

Some of the processes that occur in p-p interactions at energies of a few Bev are discussed. (D.C.W.)

15427 SEARCH FOR THE DECAY $\eta^0 \rightarrow \pi^0e^+e^-$. Foster, M. (Univ. of Wisconsin, Madison); Good, M.; Meer, M. pp 514-21 of Resonant Particles. Athens, Ohio, Fazl-i-Umar Research Inst., 1965.

An attempt was made to observe the decay $\eta^0 \rightarrow \pi^0e^+e^-$ using the interaction $\pi^+ + p \rightarrow \pi^+p\eta^0$ at 1225 and 1275 Mev/c. No definite examples of this decay were observed. An upper limit of the branching $R = \eta^0 \rightarrow e^+e^-\pi^0/\eta^0 \rightarrow \gamma\gamma$ was established. (D.C.W.)

15428 AN EXPERIMENTAL VERIFICATION OF THE JOHNSON-TREIMAN RELATIONSHIP. Galbraith, W. (Brookhaven National Lab., Upton, N. Y.); Jenkins, E. W.; Kycia, T. F.; Leontic, B. A.; Phillips, R. H.; Read, A. L.; Rubinstein, R. pp 524-6 of Resonant Particles. Athens, Ohio, Fazl-i-Umar Research Inst., 1965. (BNL-9410).

The total cross sections of $K^\pm$, $\pi^\pm$, p, and $\bar{p}$ on hydrogen and deuterium were previously measured in the momentum interval from 6 to 22 Bev/c. The results for the total cross sections of kaons and pions are consistent with the Johnson-Treiman relation. (D.C.W.)

15429 ANGULAR DISTRIBUTIONS OF THE K*(888) AND N*(1425) FROM K^--p COLLISION AT 1.5 Gev/c. Adelman, Stuart Lee (Univ. of Cambridge, Eng.). pp 527-36 of Resonant Particles. Athens, Ohio, Fazl-i-Umar Research Inst., 1965.

The results of an analysis of the decay angular distributions of the resonances N*(1425) and K*(888) from interactions of the type $K^-p \rightarrow K^*N$ and $K^-p \rightarrow KN^*$ are presented. (D.C.W.)

15430 EXPERIMENTAL EVIDENCE ON C VIOLATION IN η DECAY. Meer, M. (Purdue Univ., Lafayette, Ind.); Foster, M.; Good, M. pp 537-44 of Resonant Particles. Athens, Ohio, Fazl-i-Umar Research Inst., 1965.

The possibility of C violation in the decay of mesons(η) was investigated using π^+p interactions at 1215 and 1265 Mev/c. The results were inconclusive. (D.C.W.)

15431 SPIN AND PARITY DETERMINATION OF RESONANCES. Berman, S. M. (International Center for Theoretical Physics, Trieste, Italy). pp 913-27 of STI/PUB/117.

A method for the determination of the spins and parities of resonances is described. (D.C.W.)

15432 PHENOMENOLOGICAL THEORY OF CP-VIOLATING K^0 DECAYS. Sachs, R. G. (Argonne National Lab., Ill. Univ. of Chicago). pp 929-36 of STI/PUB/117.

The phenomenological parameters of mesons (K^0) are discussed in terms of the parameters that occur in the propagator matrix and in the complex decay amplitudes. (G.O.Y.)

15433 POSSIBLE PROPERTIES OF CP-VIOLATING NON-LEPTONIC INTERACTIONS. Okun, L. B. (Inst. of Theoretical and Experimental Physics, Moscow). pp 939-51 of STI/PUB/117.

The properties of CP-violating non-leptonic interactions are discussed. The selection rules which this interaction may satisfy are investigated. (G.O.Y.)

15434 CP VIOLATION IN K-DECAY. Byers, N.; MacDowell, S. W.; Yang, C. N. (Inst. for Advanced Study, Princeton, N. J.). pp 953-80 of STI/PUB/117.

The effects of CP violation, especially in the $K_{\pi 3}$ and K_{l3} modes, are discussed assuming that TCP invariance holds. A review of the results for $K_{\pi 2}$ is included. (D.C.W.)

15435 THE QUARKS: ASTROPHYSICAL AND PHYSICO-CHEMICAL ASPECTS. Okun, L. B.; Pikelner, S. B.; Zeldovich, Ya. B. (Inst. of Theoretical and Experimental Physics, Moscow). pp 983-95 of STI/PUB/117.

The production, burning, and conservation of quarks in galactic evolution are discussed, and some physicochemical properties of quarks and of some hypothetical particles with integral charge are considered. Possible methods of searching for these particles are discussed. (D.C.W.)

15436 THE EFFECT OF SOME MINOR IMPURITIES ON THE POSITRON ANNIHILATION LIFETIME SPECTRUM IN ARGON. Tao, S. J. (New England Inst. for Medical Research, Ridgefield, Conn.); Bell, J. 14p. (CONF-650721-1). ORINS. Gmelin, AED-CONF-65-211-1.

From Positron Annihilation Conference, Detroit.

The effect of the presence of minor amounts of impurities in argon on the positron annihilation lifetime spectrum is described. (auth)

15437 PROCEEDINGS OF THE INTERNATIONAL SYMPOSIUM ON ELECTRON AND PHOTON INTERACTIONS AT HIGH ENERGIES. VOLUME I. PLENARY SESSIONS. Hamburg, June 8–12, 1965. Hoehler, G.; Kramer, G.; Meyer-Berkhout, U. (eds.). Hamburg, Deutsche Physikalische Gesellschaft e.V., 1965. 182p. (CONF-650636).

Separate abstracts were prepared for eight of the nine papers included. The other paper was previously abstracted for NSA 19: 45024. (D.C.W.)

For abstracts of individual papers see: 14841, 15187, and 15438–15443.

15438 THEORY OF STRONG INTERACTIONS OF ELEMENTARY PARTICLES IN THE Gev REGION. Van Hove, L. (CERN, Geneva). pp 1-19 of Proceedings of the International Symposium on Electron and Photon Interactions at High Energies. Vol. I. Plenary Sessions. Hoehler, G. (ed.). Hamburg, Deutsche Physikalische Gesellschaft e.V., 1965.

The main aspects of strong-interaction processes in the high-energy region where cross sections show a smooth energy dependence that indicates an asymptotic behavior are reviewed. (42 references). (G.O.Y.)

15439 RECENT HIGH ENERGY ELECTRON INVESTIGATIONS AT STANFORD UNIVERSITY. Buchanan, C. D. (Stanford Univ., California); Collard, H.; Crannell, C.; (and others). pp 20-42 of Proceedings of the International Symposium on Electron and Photon Interactions at High Energies. Vol. I. Plenary Sessions. Hoehler, G. (ed.). Hamburg, Deutsche Physikalische Gesellschaft e.V., 1965.

Some investigations are summarized in which the form factors of deuterons and nucleons, the magnetic octupole moments of light nuclei, and the nuclear parameters of ^{40}Ca and ^{44}Ca were studied by electron scattering. Studies of the inelastic continuum in ^{3}He and electron showers in Cu and Pb are also discussed. (D.C.W.)

15440 REVIEW OF NUCLEON FORM FACTORS. Wilson, Richard (Harvard Univ., Cambridge, Mass.). pp 43-54 of Proceedings of the International Symposium on Electron and Photon Interactions at High Energies. Vol. I. Plenary Sessions. Hoehler, G. (ed.). Hamburg, Deutsche Physikalische Gesellschaft e.V., 1965.

A survey of electron-scattering studies of the form factors of nucleons is presented. (D.C.W.)

15441 SPECIAL MODELS AND PREDICTIONS FOR PION PHOTOPRODUCTION (LOW ENERGIES). Hoehler, G. (Technische Hochschule, Karlsruhe, Ger.). pp 55-70 of Proceedings of the International Symposium on Electron and Photon Interactions at High Energies. Vol. I. Plenary Sessions. Hoehler, G. (ed.). Hamburg, Deutsche Physikalische Gesellschaft e.V., 1965.

Some attempts to analyze the photoproduction of pions at low energies using the isobar approximation and the phenomenological approach are reviewed. Experimental data are compared with theoretical predictions. (D.C.W.)

15442 SPECIAL MODELS AND PREDICTIONS FOR PHOTOPRODUCTION ABOVE 1 Gev. Drell, S. D. (Stanford univ., California). pp 71-90 of Proceedings of the International Symposium on Electron and Photon Interactions at High Energies. Vol. I. Plenary Sessions. Hoehler, G. (ed.). Hamburg, Deutsche Physikalische Gesellschaft e.V., 1965.

Some approaches to the analysis of photoproduction at high energies are reviewed. (D.C.W.)

15443 THEORETICAL ASPECTS OF COLLIDING BEAM EXPERIMENTS. Gatto, R. (Univ., Florence. C.N.E.N., Frascati, Rome). pp 106-37 of Proceedings of the International Symposium on Electron and Photon Interactions at High Energies. Vol. I. Plenary Sessions. Hoehler, G. (ed.). Hamburg, Deutsche Physikalische Gesellschaft e.V., 1965.

The basic theoretical aspects of colliding electron-beam experiments are summarized. (G.O.Y.)

Field Theory, Scattering Theory, and Symmetries

See also Elementary Particles and Radiations

Refer also to abstracts 14951, 14953–14955, and 15315.

15444 (IC/66/14) IMPOSSIBILITY OF HAVING THE EXACT U(6) GROUP BASED UPON ALGEBRA OF CURRENTS. Okubo, Susumu (International Centre for Theoretical Physics, Trieste (Italy)). Feb. 1966. 9p. Dep. mn.

It was previously shown by Coleman that if the algebra of the U(6) or W(6) group is a good symmetry according to Dashen and-Gell-Mann, then they must actually be exact symmetries. It is proven that the exact U(6) or W(6) group is in reality impossible, and hence that these groups must be regarded as broken symmetries at best. (M.O.W.)

15445 (RHEL/R-102) AN INTRODUCTION TO THE HIGHER SYMMETRIES. Hendry, Archibald W. (National Inst. for Research in Nuclear Science, Chilton (England). Rutherford High Energy Lab.). June 1965. 96p. Dep. mn.

Symmetry theory is discussed from its early beginnings. The SU(3) and SU(6) groups are then discussed in detail. (M.O.W.)

15446 (UCRL-12380-T) APPARENT CP NON INVARIANCE AND THE NEUTRINO SEA. Csonka, P. L. (Lawrence Radiation Lab., Univ. of California, Livermore). Feb. 4, 1965. Contract W-7405-eng-48. 7p. Dep. mn. CFSTI $1.00 cy, $0.50 mn.

An explanation of $K_2 \rightarrow 2\pi$ events is proposed in which violation of CP invariance, the existence of new fields, violation of the $\Delta S = \Delta Q$ rule, and $\Delta S = 2$ transitions are not assumed. The existence of weak neutral currents and of a neutrino (antineutrino) sea is assumed. (D.C.W.)

15447 (UCRL-14698-T) THE RADIAL WAVE EQUATIONS FOR A VECTOR MESON IN A SPHERICALLY SYMMETRIC POTENTIAL. Fritz, Karl (Lawrence Radiation Lab., Univ. of California, Livermore). Jan. 27, 1966. Contract W-7405-eng-48. 11p. Dep. mn. CFSTI $1.00 cy, $0.50 mn.

The radial wave equations for a spin-one particle are derived in a direct fashion by expanding the angular part in vector spherical harmonics, $e_r\, Y_j^m(\Omega)$, $L\, Y_j^m(\Omega)$, and $e_r \times L\, Y_j^m(\Omega)$. The orthogonality of these functions allows eliminating them to obtain radial wave equations which may be expressed in several different ways. (auth)

15448 A HIGHER SYMMETRY OF LEPTONS. Kuehnelt, H.; Urban, P. (Univ., Graz). Acta Phys. Austr., 20: 34-7(1965). (In German).

With the use of two neutrinos a higher symmetry of leptons was derived. The degree of the symmetry refraction can be estimated with muon or β decay. (J.S.R.)

15449 RESULTS OF ISOSPIN EXCHANGE RELATIONS FOR PION PRODUCTION AMPLITUDES. Stremnitzer, H. (Univ., Vienna). Acta Phys. Austr., 20: 39-42(1965). (In German).

The group properties of the isospin are used in order to derive relations between amplitudes and nucleon form factors. (J.S.R.)

15450 n-PION CONFIGURATIONAL WAVE FUNCTIONS WITH DEFINITE SYMMETRY. Grynberg, M. (Inst. for Nuclear Research, Warsaw). Ann. Phys. (N. Y.), 36: 188-216(Feb. 2, 1966).

A set of n-meson (π) configurational wave functions which should transform under any permutation of mesons (π) according to the irreducible representations of the symmetric group S_n, and possess definite values of the grand angular momentum Λ and the total angular momentum J, is given in the case of $\Lambda \leq 3$. The method of construction of such functions is described. In order to apply this method it is necessary to know the Clebsch-Gordan coefficients for the group S_n; for the products of the representations that enter the problem for $\Lambda \leq 3$. These are given. (auth)

15451 INTEGRAL REPRESENTATIONS FOR SCATTERING AMPLITUDES. I. FORMALISM. Predazzi, E. (Univ. of Chicago). Contract AT(11-1)-264. Ann. Phys. (N. Y.), 36: 228-49(Feb. 2, 1966). (COO-264-282).

The scattering amplitude given by its partial waves expansion is shown to obey an integral representation of the form of a Bessel transform. This integral representation appears to be valid for all energies and in the whole angular domain $(0,\pi)$ and coincides with the expression previously proposed by Blankenbecler and Goldberger for high energy amplitudes. The expression of the spectral function in terms of the partial waves is given together with its inversion. Decomposing the amplitude in its even and odd part (with respect to cos θ), an alternate equivalent integral representation is similarly deduced which exhibits in a simpler way the even/odd character of the amplitude. The connections between the two representations are then discussed. Spin complications are ignored. (auth)

15452 RENORMALIZABILITY IN LSZ PERTURBATION THEORY. Steinmann, O. (New York Univ., New York). Ann. Phys. (N. Y.), 36: 267-84(Feb. 2, 1966).

A divergenceless perturbation expansion for the retarded functions in the LSZ formulation of quantum field theory was derived previously. The ambiguities inherent in this expansion are studied. It is shown that the number of ambiguities is intimately connected with the asymptotic behavior of the retarded functions in p-space, when all variables p_i tend to infinity simultaneously. Upper bounds for this asymptotic behavior are derived for the case of a scalar field in interaction with itself. The number of ambiguities remains finite for all orders of perturbation theory for the two theories corresponding to A^3- and A^4-coupling respectively, i.e., the renormalizable theories of the Lagrangian formalism. (auth)

15453 SIMPLIFIED RENORMALIZATION THEORY IN MESODYNAMICS. Bialynicki-Birula, I. (Univ., Warsaw). Bull. Acad. Pol. Sci., Ser. Sci. Math. Astron. Phys., 13: 585-8(1965).

The new method of renormalization is applied to theories of self-interacting meson fields with $\lambda\Phi^4$ couplings. The necessary changes in an earlier formalism which are needed to cover the case of quartic couplings are presented. An alternative treatment is given based on an equivalence between theories with quartic couplings and certain theories with cubic couplings. The method of renormalization can be easily extended to nucleon-meson interactions. This method not only overcomes the difficulties connected with overlapping divergences, but it provides a set of equations which are logical even in the divergent case Z = 0. (J.F.P.)

15454 BOOTSTRAP MECHANISM AND CHARGE INDEPENDENCE OF STRONG INTERACTIONS. Majewski, W. (Polish Academy of Sciences). Bull. Acad. Pol. Sci., Ser. Sci. Math. Astron. Phys., 13: 829-38(1965).

An example of a specific dynamical model, which leads to isotopic symmetry of some interactions between mesons (π) and baryons is presented. This model constitutes a straightforward generalization of the well-known reciprocal bootstrap between nucleon N and baryonic resonance $\Delta(1238)$. This generalization consists in omitting the usual assumption concerning the charge independence of interactions between particles π, N and Δ. Therefore, the existence of a doublet N of baryons, a quartet Δ, containing baryons, and of a pseudoscalar meson triplet is assumed. Also the dynamical model is assumed, in which six baryons N and Δ are generated simultaneously in P-wave scattering. Only baryon forces are included, and all possible couplings of the Yukawa type between particles belonging to the multiplets π, N, and Δ are left arbitrary. Mass differences between baryons are neglected. (J.F.P.)

15455 APPLICATIONS OF THE GEL'FAND-MOSHINSKY BASES IN UNITARY SYMMETRY AND ITS BREAKING. Castilho Alcaras, J. A.; Aguilera Navarro, V. C.; Ferreira, P. Leal (Instituto de Fisica Teorica, Sao Paulo, Brazil). J. Math. Phys. (N. Y.), 7: 205-14(Feb. 1966).

The Gel'fand-Moshinsky bases for the unitary irreducible representations of the SU_3 group are applied to the unitary scheme for the classification of elementary particles and resonances. A unified method is given for the derivation of the matrix elements of the octet tensor operators in a way which makes transparent its application for other irreducible tensors. The results are given in a remarkably simple form. The systematic use of the basis provides a methodological alternative to the current tensorial methods. (auth)

15456 FADDEEV-TYPE EQUATIONS FOR THE FOUR-BODY PROBLEM. Alessandrini, Victor A. (Univ. of California, Berkeley). J. Math. Phys. (N. Y.), 7: 215-20 (Feb. 1966). (UCRL-16158).

The technique used by Faddeev to obtain connected equations for the nonrelativistic three-body T matrix is generalized for four particles. It is shown that the four-body equations are completely determined by the solutions of all the possible two-body subsystems, as is the case in the three-body problem. This approach can be extended to more complicated multiparticle systems. (auth)

15457 CARTAN FRAMES AND THE GENERAL RELATIVISTIC DIRAC EQUATION. Brill, Dieter R.; Cohen, Jeffrey M. (Yale Univ., New Haven). J. Math. Phys. (N. Y.), 7: 238-43(Feb. 1966).

The Dirac equation for spin-$\frac{1}{2}$ particles in curved spacetime is formulated using Cartan calculus. Unlike previous formulations, this method is easy to use because it expresses the Dirac equation in terms of well known objects like partial derivatives and special relativistic Dirac matrices. It allows a simple and direct treatment of neutrinos in homogeneous nonisotropic universes and in plane-wave geometries. These solutions are compared and contrasted with the corresponding solutions containing electromagnetic radiation. (auth)

15458 ON THE REDUCTION OF DIRECT PRODUCTS OF THE IRREDUCIBLE REPRESENTATIONS OF SU(n). Harari, H. (Israel Atomic Energy Commission, Yavne). J. Math. Phys. (N. Y.), 7: 283-5(Feb. 1966).

Explicit simple formulas are given for the reduction of some direct products of the irreducible representations of SU(n). All the interesting products from the point of view of the various symmetry models in particle physics are included as special cases of our results. In particular, all products of the totally symmetric and the regular representations of SU(n) are evaluated. (auth)

15459 Vθ-BOUND STATE AND UNIQUENESS IN THE THREE-PARTICLE SECTOR OF THE LEE MODEL. Pagnamenta, Antonio (Univ. of Maryland, College Park). Contract AFOSR 500-64. J. Math. Phys. (N. Y.), 7: 356-65(Feb. 1966).

If the coupling constant is large enough, but still smaller than its critical value, there exists a Vθ-bound state in the Lee model. The bound-state wavefunction is found via the solution of the homogeneous Källen-Pauli equation. The condition for the existence of a Vθ-bound state is seen to give a statement about the uniqueness of the scattering solutions of both the Vθ- and N2θ-integral equations. There

exists no N2θ-bound state if the V particle is unstable. (auth)

15460 GAUGE APPROXIMATIONS IN MESODYNAMICS. Rivers, R. J. (International Atomic Energy Agency, Trieste, Italy). J. Math. Phys. (N. Y.), 7: 385-94(Feb. 1966).

In a nonperturbative theory for vector and scalar mesodynamics of the kind proposed by Salam, it is found that the "gauge approximations" introduced in this approach are the most sensible of a set of approximation schemes that preserve the scalar gauge properties of the amplitudes of the theory. The Green's functions used are those suggested by the functional derivative approach. The generalized identities of the Ward-Takahashi kind that these Green's functions satisfy are exhibited, as well as the decomposition of the general n-point function in terms of these Green's functions. (auth)

15461 INTERNAL SYMMETRY AND MASS SPLITTING. Roskies, Ralph (Oak Ridge National Lab., Tenn.). J. Math. Phys. (N. Y.), 7: 395-8(Feb. 1966). (ORNL-P-1328).

Two theorems concerning the possibility of embedding the Lie algebra S of an internal symmetry group $\mathcal{S}$ and the Lie algebra P of the Poincare group $\mathcal{P}$ into a larger algebra G to obtain intrinsic mass splitting among the multiplets belonging to the irreducible representations of $\mathcal{S}$. It is assumed that G is a semi-direct sum of the invariant subalgebra S and of P. First, if $\mathcal{S}$ is a compact Lie group, then G is in fact a direct sum of S and P and there is no mass splitting. Second, if $\mathcal{S}$ is a semi-simple Lie group, with an appropriate definition of the mass operator, there is still no mass splitting. The relation of these results to previous papers is discussed. (auth)

15462 GENERATING RELATIONS OF THE SUB-ALGEBRAS IN THE DUFFIN-KEMMER ALGEBRA. Tokuoka, Zensuke (Univ. of Liverpool). Nucl. Phys., 78: 681-93(1966).

The Duffin-Kemmer algebra is resolved into the three sub-algebras which correspond to the one, five and ten dimensional irreducible representations. The linearly independent basis elements of each subalgebra are listed. The generating algebraic relations specific to the latter two sub-algebras are given. (auth)

15463 DEDUCTION OF POTENTIALS FROM SCATTERING PHASE SHIFTS. I. NEUTRAL PARTICLES. Swan, P.; Pearce, W. A. (Rice Univ., Houston, Tex.). Nucl. Phys., 79: 77-107(1966). (TID-21956).

A summary is given of past attempts to find methods for deducing potential interactions from elastic scattering phase versus energy curves. The distorted plane wave approximation for $tg\eta_l(k)$ is improved by introducing energy dependent terms in the wave function. The phase-potential expression may then be made as accurate as the phase data supplied and is applied to obtain a practical method of deducing potentials from $\eta_l(k)$ curves. The latter need only be over a finite range of k, and $\eta_l(k_{max})$ need not be small. Phase analysis of elastic scattering data provides smooth $\eta_l(k)$ curves for particular l values, which may be least-square fitted by orthogonal polynomial series to give truncated polynomials, in powers of k^2, of $k^{2l+1}\,cotg\eta_l(k)$ or $tg\eta_l(k)/k^{2l+1}$. The scattering parameters (coefficients of k^2) in principle identify the interaction potential, although they are in general functions of the total energy interval $0 - E_{max}$ covered, as the corresponding infinite power series is divergent. The $tg\eta_l(k)$ approximation reduces to the shape-dependent expansion, the scattering parameters being given as linear combinations of moment and weighted moment integrals over the interaction potential. The experimental values of the scattering parameters in these relations are used. If the potential is expanded as a finite series of short range functions, such as the exponential, the series coefficients may be found by solving a corresponding number of simultaneous equations based on the above. The resulting approximate potential has a strength function (first moment integral of the potential) accurate to within several per cent. A simple iterative procedure, based on the distorted plane wave function and equations, is used to improve the potential, the error in the strength function being reduced by a factor of 2–5 per iteration in typical cases. This method may also be used to improve arbitrary approximate potentials, any accuracy being possible. (auth)

15464 SPIN AND PARITY OF THE Ξ^* (1530 Mev). Button-Shafer, Janice; Lindsey, James S.; Murray, Joseph J.; Smith, Gerald A. (Univ. of California, Berkeley). Phys. Rev., 142: 883-7(Feb. 25, 1966). (UCRL-11436 (Rev.)).

Results are presented from the spin-parity analysis of reactions of the type $K^- + p \rightarrow \Xi K\pi\pi$ in which nearly pure samples of the $\Xi^*(1530)$ are produced. Comparison is made with the analysis of randomly generated events. The hypothesis of $P_{\frac{3}{2}}$ fits the data better than that of $D_{\frac{3}{2}}$, the latter having a confidence level of ≤ 0.03. Spin $\frac{5}{2}$ is not required. (auth)

15465 KRONECKER-DELTA-TYPE SINGULARITIES AND REGGEIZATION. Srivastava, Y. N. (Northeastern Univ., Boston); Nath, Pran. Phys. Rev., 142: 982-3 (Feb. 25, 1966).

The question of Kronecker-delta terms in the partial-wave scattering amplitudes is examined when the force is obtained from the exchange of a Regge pole. It is shown that such terms may arise when an approximation to the force from the asymptotic part of the trajectories in the crossed channels is made. (auth)

15466 DYNAMICAL QUESTION BEARING ON CALCULATIONS OF MASS SHIFTS IN S-MATRIX THEORY. Sawyer, R. F. (Univ. of California, Santa Barbara). Phys. Rev., 142: 991-5(Feb. 25, 1966).

It is argued that the ND^{-1} method is inadequate for determination of the basic dynamical inputs, A_I^{exch}, in the Dashen and Frautschi theory of octet enhancement in the reciprocal bootstrap model. Some models are developed which have the properties: a pole in the u channel as a Born term, two- and three-particle unitarity with pole terms for production, a rather general form for an unknown short-range force. In these models it is proved that the A^{exch} coefficients have consistently the opposite signs to those given by the ND^{-1} approximation (with the identical Born term). The qualitative interpretation of the result is that an increase in an attraction gives rise to a greater binding energy, as contrasted with the results of Dashen and Frautschi, which seem to have the opposite interpretation. (auth)

15467 W-SPIN AND THE ROTATION GROUP IN FOUR DIMENSIONS. Ahmed, K.; Dunne, S. A.; Martinis, M.; Poston, J. R. (Imperial Coll. of Science and Tech., London). Phys. Rev., 142: 995-9(Feb. 25, 1966).

The properties of W-spin are derived from the group IU(2,2) and its subgroups. W-S flip for mesons is obtained from consideration of the four-dimensional rotation group contained in U(2,2) and also from the Duffin-Kemmer algebras. Higher representations are considered, and some W-spin selection rules obtained for spin-2 decays. (auth)

15468 EQUIVALENCE OF LOCALITY AND PARA-LOCALITY IN FREE PARAFIELD THEORY. Araki, H.; Greenberg, O. W.; Toll, J. S. (Univ. of Maryland, College Park). Phys. Rev., 142: 1017-18(Feb. 25, 1966).

It is shown that locality, i.e., vanishing of the commutator at space-like separation in the parafield Hilbert space A, implies paralocality, i.e., vanishing of the commutator at space-like separation in the larger Green component Hilbert space B. This demonstration removes an unwanted assumption in a recent derivation of parafield selection rules. The method of demonstration yields the general statement that the vacuum is separating for polynomials of localized free parafields in the representation on the space B. (auth)

15469 VERTEX POLES AND BOUND STATES IN THE LEE MODEL. Gerstein, I. S. (Univ. of Pennsylvania, Philadelphia). Phys. Rev., 142: 1047-51(Feb. 25, 1966).

The Z = 0 limit of a version of the Lee model, recently introduced and solved by Bronzan, is studied from the point

of view of recent work by Gerstein and Deshpande. It is shown how vertex function and inverse propagator poles develop and behave for small vertex renormalization constant, and their connection with the bound-state limit is studied. It is found that the condition of finite mass renormalization in the $Z_U = 0$ limit can be satisfied in this model and leads to bootstrap-type results. (auth)

15470 CONFORMAL GROUP IN SPACE-TIME. **Kastrup, H. A. (Princeton Univ., N. J.). Phys. Rev., 142: 1060-71(Feb. 25, 1966).**

Representations of the conformal group and their physical interpretations are discussed in order to provide a basis for interesting applications of this group in particle physics. The conformal group seems to be of particular interest in connection with the ultraviolet singularities in field theory, for it is associated with test functions which vanish on the light cone and may therefore provide an appropriate regularization of Green's functions in coordinate space. In momentum space this property corresponds to an indefinite metric in Hilbert space with the transformation by reciprocal radii as the metric operator. Two examples of representations are investigated in detail; the first one belongs to the case of spin zero and mass zero, and the second one describes a system with spin zero but nonvanishing mass. Possible physical applications of these representations are illustrated by a simple measuring process which determines the value of the electron mass. (auth)

15471 BHABHA'S IRREDUCIBLE SPIN $(\frac{3}{2},\frac{1}{2})$ EQUATION AS A BASIS OF STRONG-INTERACTION SYMMETRIES. **Acharya, R.; Narayanaswamy, P. (Tata Inst. of Fundamental Research, Bombay). Phys. Rev., 142: 1085-7(Feb. 25, 1966).**

It is demonstrated that Bhabha's irreducible relativistic equation describing a particle with two mass states, one of mass m and spin $\frac{3}{2}$ and another of mass λm and spin $\frac{1}{2}$, where λ is arbitrary, can be used as the basis of a covariant theory of strong-interaction symmetries which incorporates spin splitting in a dynamical fashion. Detailed consequences of the theory were obtained for the nonrelativistic case. Some new mass relations, in addition to the well-known ones, are derived. (auth)

15472 RADIATIVE DECAY OF VECTOR MESONS IN SU(6). **Tanaka, K. (Ohio State Univ., Columbus). Phys. Rev., 142: 1087-8(Feb. 25, 1966). (COO-1261-16).**

The relations among the partial decay widths of a vector meson into two pseudoscalar mesons and a photon are derived in the framework of SU(6) symmetry broken by electromagnetic interactions. The decay widths depend on two independent amplitudes, so that a large number of relations are obtained some of which are directly related to that of $\omega \to \pi^+ + \pi^- + \gamma$. (auth)

15473 BOSONS, A PARITY, AND G_2. **Behrends, R. E.; Landovitz, L. F.; Tunkelang, B. (Yeshiva Univ., New York). Phys. Rev., 142: 1092-4(Feb. 25, 1966).**

The quantum number A is re-examined in the framework of G_2. The only two outstanding difficulties of the A selection rule are shown in this picture to be removed. Further consequences of A invariance and the assignment of bosons to G_2 multiplets are examined. (auth)

15474 WEAK INTERACTIONS AND G_2. **Behrends, R. E. (Yeshiva Univ., New York); Sirlin, A. Phys. Rev., 142: 1095-1101(Feb. 25, 1966).**

A speculative model of the weak interactions constructed in the framework of the G_2 symmetry scheme is discussed. The model leads to the existence of $\Delta Q = -\Delta S$ matrix elements in the vector interaction and their absence in the axial-vector contribution. In particular, it leads in a natural manner to the existence of $\Sigma^+ \to n + e^+ + \nu$ at a rate compatible with the present upper limit, to the existence of $\Delta Q = -\Delta S(K^0)_{e3}$ decays, and to a strong inhibition of the reaction $K^+ \to \pi^+ + \pi^+ + e^- + \bar{\nu}$. It also gives rise to rigorous predictions involving the $(K^+)_{e3}$ and $(K^0)_{e3}$ decays. The scheme allows for the possible violation of CP invariance in the $(K^0)_{e3}$ and is qualitatively compatible with Sach's explanation of the order of magnitude of the CP violation in $K_2^0 \to \pi^+ + \pi^-$. Several qualitative and quantitative predictions, some of which hold to all orders in the symmetry-breaking interactions, are discussed and compared, whenever possible, with experimental information. (auth)

15475 ELECTROMAGNETIC INTERACTIONS AND G_2. **Behrends, R. E. (Yeshiva Univ., New York). Phys. Rev., 142: 1101-3(Feb. 25, 1966).**

The electromagnetic predictions of the particle symmetry G_2 with symmetry breaking are given. Since none of these predictions are in conflict with present experimental results, it is concluded that arguments against G_2 based on its electromagnetic predictions without symmetry breaking are invalid. (auth)

15476 FINAL-STATE INTERACTIONS AMONG THREE PARTICLES. II. EXPLICIT EVALUATION OF THE FIRST RESCATTERING CORRECTION. **Aitchison, I. J. R. (Cavendish Lab., Cambridge, Eng.); Kacser, C. Phys. Rev., 142: 1104-18(Feb. 25, 1966).**

The lowest approximation to the three-body final-state interaction problem is a simple superposition of 3 two-body interaction terms, as given by the Watson final-state formula. The first rescattering correction corresponds to the triangle graph of perturbation and dispersion theory; for example, the process $W \to 2 + (13) \to 1 + (23) \to 1 + 2 + 3$, i.e., where first particles 1 and 3 interact strongly, then separate in such a way that 2 and 3 come together and interact strongly. For the case in which the (13) interaction is dominated by a resonance, the kinematic conditions are discussed under which such a rescattering correction will contribute appreciably to the total transition amplitude. This term is then evaluated exactly in the nonrelativistic (N.R.) case; that is, the N.R. triangle graph is evaluated. An analogous expression is proposed for the relativistic case, with suitable reinterpretation of the variables. The method is generalized to include spin and angular momentum, and to incorporate (23) rescattering to all orders, for the cases in which this can be parametrized either by a scattering length or by a resonance. Specific application is made to the $\pi\pi$N case. (auth)

15477 NONRELATIVISTIC QUARK MODEL FOR BARYONS. **Mitra, A. N. (Delhi Univ.). Phys. Rev., 142: 1119-25(Feb. 25, 1966).**

A nonrelativistic quark model is proposed for baryons, according to which any two quarks are assumed to interact with each other through p-wave forces. Such forces are shown to be capable of producing strong binding in a three-quark system in a spatially antisymmetric state of angular-momentum unity, and making the model compatible with an extension of the [56] representation of SU_6. If the strength of the quark-quark force is adjusted to fit some central baryon mass (m_0), the model predicts a 2-quark bound state at a mass $\sim\frac{1}{2}(M + m_0)$, where M is the central mass of a quark. The validity of the nonrelativistic description is shown to depend on the smallness of a certain "inverse range parameter" β compared with the quark mass M, and this condition is shown to be fully compatible with the present experimental knowledge on baryon sizes, as measured by the charge radius of the proton. Further, using an SU_3-invariant interaction, an "equal interval rule" for the baryon masses is shown to follow dynamically from the assumption of a mass difference between the singlet and doublet quarks, under the same condition, $\beta \ll M$, as above. It is argued that a p-wave quark interaction, which leads more easily to the formation of antisymmetric spatial states than of symmetric ones, gives a sort of "saturated system" at the 3-quark level. This reduces considerably the (undesirable) prospects of very strong binding of a larger number of quarks, compared to the situation with s-wave forces (which facilitate the formation of symmetric states in multiquark systems with stronger and stronger binding as the number of quarks is increased). By ruling out the generally stronger s-wave forces as the main bond between two quarks, the model leaves scope for their action in quark-antiquark systems, which should require stronger binding in order to generate the (less massive) mesons. (auth)

15478 MASS FORMULAS FOR THE 189 MULTIPLET OF SU(6). Chang, Chia-Hwa; Xuong, Nguyen-Huu (Univ. of California, San Diego, La Jolla). Phys. Rev., 142: 1132-4(Feb. 25, 1966).

Mass relations for the 189 multiplet of SU(6) are discussed in detail. They (the masses of the 25 different isomultiplets belonging to 189) are given in terms of six mass-splitting parameters. If the newly discovered mesons are assumed to belong to 189, as soon as the determination of spin and parity of six of them is made, their masses can be used as input and all the masses of the remaining particles belonging to 189 can be predicted. (auth)

15479 KINETIC SUPERMULTIPLETS OF $\tilde{U}(12)$. II. Gatto, R. (Univ., Florence); Maiani, L.; Preparata, G. Phys. Rev., 142: 1135-40(Feb. 25, 1966).

Possible baryon "kinetic supermultiplets" are discussed as candidates for classifying higher baryonic resonances of negative parity. The kinetic supermultiplets had been proposed, in a previous work, as an extension of the supermultiplet scheme of broken $\tilde{U}(12)$. The classification of higher boson resonances in terms of a kinetic supermultiplet has proved remarkably successful and led to correct predictions of quantum numbers and accurately verified mass relations. The baryon kinetic supermultiplet discussed here employs the hitherto unused representation 220 in $\tilde{U}(12)$, which corresponds to the 20 of SU_6, and is tentatively chosen on the basis of its economy. It groups together a baryon nonet with $J^P = \frac{1}{2}^-$, another nonet with $J^P = \frac{3}{2}^-$, and a singlet with $J^P = \frac{5}{2}^-$. The mass formulas are derived up to first order in SU_3 breaking. Based on the quantum-number predictions and the mass formulas, a classification of higher baryon resonances is attempted, and a tentative scheme of assignments and consequent predictions are presented. An alternative scheme employing the representation 364 in $\tilde{U}(12)$, corresponding to the 56 of SU_6, is also examined. (auth)

15480 PERTURBED BOUND-STATE POLES IN POTENTIAL SCATTERING. I. Kim, Y. S. (Univ. of Maryland, College Park). Phys. Rev., 142: 1150-3(Feb. 25, 1966).

The perturbation formula of Dashen and Frautschi is studied in nonrelativistic potential scattering. A formalism based on the Jost function is presented and is shown to be equivalent to the Dashen-Frautschi approach. It is shown for both cases that unless the Born approximation is satisfied for the unperturbed problem, the mass shift cannot be calculated in a simple way. It is pointed out that the Born approximation is not expected to be valid if the bound state is assumed to exist. The formalism is illustrated by the use of a soluble square-well potential. The infrared problem is also discussed. It is pointed out that the infrared divergence is automatically eliminated at the binding energy and is not "spurious." (auth)

15481 CONSISTENT THEORY OF WEAK INTERACTIONS. Pietschmann, Herbert V. R.; Nilsson, Jan S. (Univ. of Virginia, Charlottesville). Phys. Rev., 142: 1173-84(Feb. 25, 1966).

An S-operator theory of weak interactions is presented, which fulfills all requirements of consistency, including unitarity. In an expansion to first order in G the results are identical to those obtained in first-order perturbation theory from the standard Lagrangian formulation of weak interactions, but higher order corrections can be calculated. They are finite apart from a single infinite parameter that can be absorbed in a coupling-constant renormalization. It is shown that the renormalizations of the coupling constants in μ decay and n decay are different. Higher order corrections to e-ν_e scattering are discussed. The complete renormalization of the theory is carried out. One of the main differences from standard Lagrangian theory is that the theory is not crossing symmetric. (auth)

15482 GENERAL METHOD OF CONSTRUCTING HELICITY AMPLITUDES FREE FROM KINEMATIC SINGULARITIES AND ZEROS. Wang, Ling-Lie Chau (Univ. of California, Berkeley). Phys. Rev., 142: 1187-94(Feb. 25, 1966). (UCRL-16240).

A simple and straightforward method to identify and remove the kinematic singularities of helicity amplitudes is constructed from the Trueman-Wick crossing relations. A set of amplitudes free of all kinematic singularities and zeros is obtained for two-particle → two-particle reactions of any spins and masses, except that for boson-fermion interactions with general mass assignments there is still a kinematic $s^{\frac{1}{2}}$ singularity left in the amplitude. (auth)

15483 SOLUTION OF SCATTERING AND BOUND-STATE PROBLEMS BY CONSTRUCTION OF APPROXIMATE DYNAMICAL SYMMETRIES. Fivel, Daniel I. (Univ. of Maryland, College Park). Phys. Rev., 142: 1219-35(Feb. 25, 1966).

A concept of "approximate dynamical symmetry" is formulated by means of which approximate solutions to scattering and bound-state problems can be produced in a purely group-theoretic manner for essentially any isotropic potential and to any desired degree of accuracy. This concept forms a natural generalization to arbitrary potentials of the familiar Runge-Lenz symmetry of the Coulomb problem and the SU_3 symmetry of the harmonic oscillator. The method consists in transforming the dynamical Lie algebra, i.e., the smallest algebra generated by the hamiltonian and a complete set of dynamical variables, which is usually infinite and simple, into a finite, simple Lie algebra as follows. The dynamical algebra is first transformed into another infinite Lie algebra, but one which contains a "large" ideal, by a process similar to Inonu-Wigner contraction, the angular momentum acting as the contraction parameter. The factor algebra modulo ideal turns out to be a finite, simple Lie algebra, which still contains some of the dynamical information. The above two-stage process will be called "truncation." A sequence of such truncations is developed leading to successively higher dimensional simple Lie algebras whereby, successively better approximations to energy levels and phase shifts are obtained. The solutions obtained involve all powers of the coupling constant, and the Nth-order approximation is at least as good as the Nth-order W.K.B. approximation and probably better. The special role of the angular momentum in the contraction process enables the group-theoretic methods to be related to the Regge formalism in a natural way. Exact solutions to dispersion relations for Regge trajectories can be obtained by including an arbitrarily large but finite set of trajectories in the unitarity relation. As an illustration of the methods developed a calculation to the first nontrivial order of energy levels of an anharmonic oscillator and the well-depth parameter and phase shifts for a Yukawa potential is included. (auth)

15484 CLUSTER DECOMPOSITION OF S-MATRIX ELEMENTS. Taylor, John R. (Princeton Univ., N. J.). Phys. Rev., 142: 1236-45(Feb. 25, 1966).

The physical basis for the cluster-decomposition properties of momentum-space S-matrix elements is discussed. The starting point is the proposition that in the limit of wide separation the probability for two separate processes should factor as the product of the individual probabilities. It is shown that factorization of the probabilities implies factorization of the corresponding S-matrix elements; i.e., any phase factors which might appear are at most constants which can be adjusted to unity. This provides the basis for the proof given recently by Wichmann and Crichton of the momentum-space cluster properties. It is shown that the resulting decomposition equations may contain unwanted factors that depend on the phase of the one-particle S-matrix elements. In order to minimize the effect of these factors the decomposition equations can be rewritten so that the unitarity equations for the "connected parts" (which are supposed to be the basis of a dynamical S-matrix theory) take their usual form without spurious phase factors. (auth)

15485 PARTIALLY CONSERVED AXIAL-VECTOR CURRENT AND THE DECAYS OF VECTOR MESONS. Kawarabayashi, Ken; Suzuki, Mahiko (California Inst. of Tech., Pasadena). Phys. Rev. Lett., 16: 255-7(Feb. 7, 1966).

The notion of a partially conserved axial-vector current and the current commutation relations that generate the algebra U(2) ⊗ U(2) are applied to the decays of vector mesons. (G.O.Y.)

15486 GENERALIZED DEFINITION OF P AND C. Chang, N. P. (Univ. of New York, New York). Phys. Rev. Lett., 16: 337-41(Feb. 21, 1966).

A definition of the transformation properties corresponding to space inversion and to antiparticle conjugation is presented. This concept leaves invariant the interaction hamiltonian involving the hadrons, including the strong and electromagnetic interactions as well as the weak interactions of the hadrons. (G.O.Y.)

15487 COROLLARIES OF THE GOLDSTONE THEOREM. Frishman, Yitzhak; Katz, Amnon (Weizmann Inst. of Science, Rehovoth, Israel). Phys. Rev. Lett., 16: 370-1(Feb. 28, 1966).

Some corollaries to the Goldstone theorem on broken symmetries and massless particles are presented. The results are important in the explanation of μ-e splitting by spontaneous symmetry breaking. (G.O.Y.)

15488 RELATION BETWEEN D/F AND G_A/G_V FROM CURRENT ALGEBRA. Gatto, R. (Univ., Florence, Italy); Maiani, L.; Preparata, G. Phys. Rev. Lett., 16: 377-9(Feb. 28, 1966).

The inclusion of higher baryonic resonances in the saturation of the chiral U(3) ⊗ U(3) commutation rules of Gell-Mann's current algebra is investigated. A consistent solution is found if the relation $-G_A/G_V = \frac{1}{3}[(D+F)/(D-F)]$ is verified. (G.O.Y.)

15489 SOME ACTUAL PROBLEMS IN THE QUANTUM THEORY OF FIELDS. Lopuszanski, Jan (Univ., Wroclaw, Poland). Postepy Fiz., 16: 483-503(1965). (In Polish).

A few results are given for the axiomatic quantum theory of fields. After a review of the axiomatic basis, the following areas are covered: Borchers' classes; certain criteria for nondispersive fields; generalized free fields-theorems of Licht and Toll; theorems of Reeh and Schlieder; criteria for free fields resulting from support of fields in momentum space; criteria for free fields resulting from the properties of momentum; weak coupling; Haag's theorem; and strong coupling fields of Haag. (TTT)

15490 MANY-POLE AMPLITUDES AND ELEMENTARITY. II. THE CASE OF TWO NON-COMPOSITE PARTICLES. Kinoshita, Kisei; Yabuki, Haruichi (Tokyo Univ.). Progr. Theoret. Phys. (Kyoto), 34: 981-9(Dec. 1965).

Two non-composite particles with the same quantum numbers are investigated. The types of the pairs of the particles are classified and found to be those obtained by adding an elementary particle to the four types of the one particle case. It is shown that pseudo-particles can be classified in the same way as physical particles. (auth)

15491 PROPERTIES OF NONCOMPOSITE PARTICLES. Ida, Masakuni (Tokyo Univ.). Progr. Theoret. Phys. (Kyoto), 34: 990-9(Dec. 1965).

The connection among elementary, intermediate, and composite particles is investigated. The transition from one type of particle to another is discussed in terms of limits concerning the mass and coupling constant of the particle. They are equivalent to the limits, $Z_1 \to 0$ and $Z_3 \to 0$, in the scalar theory. It is shown how the bootstrap idea fails for particles of elementary or intermediate type. It is also found that such particles do not lie on Regge trajectories. (auth)

15492 MAGNETIC MOMENTS OF BARYONS AND FUNDAMENTAL TRIPLET. Ishida, Shin (Nihon Univ., Tokyo); Otokozawa, Jun; Shimodaira, Hajime Progr. Theoret. Phys. (Kyoto), 34: 1000-6(Dec. 1965).

The electromagnetic form factors of octet baryons are investigated from the standpoint that the baryons are the three body composite system of fundamental triplet. At first it is shown that the magnetic moments of fundamental triplet are proportional to its charge and that the magnitude is understood to be due to the effect of meson cloud. Then the satisfactory results are obtained on the magnetic moments of the baryons, provided that they are produced by the magnetic moment of each constituent triplet. Further the following relations among the form factors of the nucleon: $G_{M,p}/\mu_p = G_{M,n}/\mu_n = G_{E,p}$, $G_{E,n} = 0$ are obtained. (auth)

15493 ELASTIC SPHERE MODEL OF ELEMENTARY PARTICLES AND ITS RELATION TO THE QUADRI-LOCAL FIELD MODEL. Goto, Tetsuo (Nihon Univ., Tokyo). Progr. Theoret. Phys. (Kyoto), 34: 1007-22(Dec. 1965).

The quantum theory of an elastically isotropic and spherically symmetric body is developed both in a non-relativistic and a relativistic way. It can be shown that the model considered is kinematically equivalent to the quadri-local field model proposed by Yukawa et al. and T. Takabayasi. Therefore, in the same way as Takabayasi did, baryonic states are constructed by irreducible representations of SU(3) group. In connection to the relativistic formulation of the model, the relativistic rigid body motion is also studied. (auth)

15494 AN EXTENSION OF INVERSION WITH A NON-ABELIAN GROUP OF PARITY TRIPOD. Okabayashi, Takao (Tokyo Univ.). Progr. Theoret. Phys. (Kyoto), 34: 1023-39(Dec. 1965).

An extension of inversion (and therefore of the full group of inhomogeneous Lorentz transformations) with a non-Abelian group, group of parity tripod, is proposed. It gives a foundation of the equation which was proposed previously and a correlation of the selection rule about hypercharge with the violation of the conservation law of parity. The expectation values of the two generators of the group of parity tripod are identified with hypercharge and K-mesonic charge. The empirical formulas for the strong interactions of mesons(π) and mesons(K) and for the weak interactions of mesons(π) are tentatively expressed by the direct product group of the extended group with the isotopic spin group in the doublet description of baryons. The results are very suggestive of the intimate connection of the group of parity tripod with the isotopic spin group, although they cannot have the final forms. (auth)

15495 UNIFORMIZATION OF THE SCALAR SELF-ENERGY DIAGRAM. Zaganescu, M.; Hegedues, E.; Schiller, D. H. (Univ. of Timisoara, Rumania). Rev. Roum. Phys., 10: 715-21(1965).

The manner in which the methods of the uniformization theory may be applied to the study of the Riemann surface associated with a Feynman diagram is shown by means of an example. (auth)

15496 ON THE ASSIGNMENTS OF HIGHER RESONANCES IN $\tilde{SU}(12)$. Liu, Lian-sou; Ma, Chung-chi (Peking Univ.). Sci. Sinica (Peking), 15: 1877-80(Dec. 1965).

The difficulties associated with the assignment of higher resonances to the higher representation of $\tilde{SU}(12)[SU(6)]$ are pointed out, and it is concluded that as a scheme for the classification of hadrons, $\tilde{SU}(12)$ succeeds only with 143 and 364. It is pointed out that the difficulties result from failure to properly account for the orbital angular momentum. (L.B.S.)

15497 AN INTERMEDIATE BOSON THEORY IN THE SU(6) SYMMETRY. Song, Xing-chang (Peking Univ.). Sci. Sinica (Peking), 15: 1881-4(Dec. 1965).

An intermediate boson theory is proposed, which is based on the following considerations: (i) the weak currents, the intermediate bosons, and their couplings must belong to the lower possible representations; and (ii) the semi-weak couplings between the currents and bosons transform under SU(3) as the neutral components of the irreducible representations $\underline{3}$ to ensure the $|\Delta I| = \frac{1}{2}$ rule for the nonleptonic processes. Relations are obtained among various decay amplitudes, which agree well with experimental data. (L.B.S.)

15498 SYMMETRY GROUP ISL(6): REPRESENTATIONS AND INVARIANTS. Kadyshevskii, V. G.; Todorov, I. T. (Joint Inst. for Nuclear Research, Dubna, USSR). Yadern. Fiz., 3: 135-44(Jan. 1966). (In Russian).

The theory of the ISL(6) group (inhomogeneous SL(6) group), as a symmetry group for elementary particles is expounded systematically. The connection between the adjoint representation and the infinitesimal one is discussed and the transformation law for the matrix of generators is derived. The Casimir operators of ISL(6) are found and the simplest invariant equations are discussed. (auth)

15499 MASS FORMULA PROBLEM IN THE ISL(6) GROUP. Shurani, P. (Joint Inst. for Nuclear Research, Dubna, USSR). Yadern. Fiz., 3: 145-7(Jan. 1966). (In Russian).

It is shown that the so-called intrinsically broken group ISL(6) in the theory of elementary particles cannot lead to nontrivial mass-formulas. (auth)

15500 THRESHOLD BEHAVIOR OF PARTIAL AMPLITUDES OF INELASTIC PROCESSES. Kancheli, O. V.; Matinyan, S. G. (Inst. of Physics, Academy of Sciences, Georgian SSR). Yadern. Fiz., 3: 154-63(Jan. 1966). (In Russian).

The threshold behavior of partial amplitudes in inelastic processes is studied for complex angular momenta, starting from simple assumptions on the analytic properties of inelastic process amplitudes. It is shown that the partial amplitudes contain parts, which have a normal threshold behavior, but cannot be continued in a finite way to complex values of momentum. (auth)

15501 SUMMATION OF LADDER GRAPHS AT HIGH ENERGIES. Ginsburg, I. F.; Serebryakov, V. V. (Inst. of Mathematics, Academy of Sciences, Siberian SSR). Yadern. Fiz., 3: 164-75(Jan. 1966). (In Russian).

A general method for calculating the asymptotic behavior of the scattering amplitude f(s,t) at high energies $|s| \gg |t|$, 1 in the latter approximation is developed for various potentials in renormalizable theories. In the logarithmic theory the problem is reduced to a simple Riccati differential equation. This equation is obtained by two different methods: using only the two-particle unitary condition and by a straightforward summation of the Feynman diagrams. A calculation taking only two-particle unitary terms into account in the corresponding Feynman graphs gives a correct result in the leading logarithmic approximation. (auth)

15502 REDUCTION FORMULAS IN WIGHTMAN AXIOMATICS. Khoruzhii, S. S. (Steklov Inst. of Mathematics, Academy of Sciences, USSR). Yadern. Fiz., 3: 176-87(Jan. 1966). (In Russian).

Matrix elements of the S-matrix are reduced to retarded, chronological, and generalized retarded functions, for the case of a scattering theory, developed in the framework of the Wightman approach to axiomatic quantum field theory. (auth)

15503 DISPERSION SUM RULES AND SU(6) SYMMETRY. Vorob'ev, L. D. (Joint Inst. for Nuclear Research, Dubna, USSR). Yadern. Fiz., 3: 188-9(Jan. 1966). (In Russian).

It is shown that by assuming a certain behavior of physical amplitudes at high energies it is possible to use ordinary dispersion relations for developing sum rules binding magnetic moments and other constants with multiple amplitudes, the sum rules combined with the unitary symmetry are applied in the study of the amplitude of virtual photoproduction of pions on nucleons. (R.V.J.)

15504 NEUTRAL a-PARTICLES. Okun, L. (Inst. of Theoretical and Experimental Physics, State Atomic Energy Commission, USSR). Yadern. Fiz., 3: 189-92(Jan. 1966). (In Russian).

A model with CP nonconservation in which a hypothetical charged a particle ($m_a > 5$ Bev) was considered responsible for nonconservation was previously constructed by T. D. Lee. Examination of a model with neutral a particles in which the $K_2^0 \rightarrow 2\pi$ decay was induced by the superweak interactions with $\Delta Y = 2$ showed that the CP nonconservation is of the order of unity in experiments involving real a particles. (R.V.J.)

15505 ANALYTICAL PROPERTIES OF THE S-MATRIX IN MANY-CHANNEL-SCATTERING. Gloeckle, Walter (Univ., Heidelberg). Z. Phys., 190: 391-413(1966).

An extension of previous work by Newton and Weidenmueller is made to a more realistic case of many-channel scattering: an arbitrary orbital angular momenta and a potential matrix of the Yukawa type are considered. The analytical properties of the modified S-matrix are investigated. The modified S-matrix is meromorphic in certain strips around the real axes of the Riemann surface. This surface is determined solely by the kinematical branchpoints. The region of analyticity can be extended further for the diagonal and the squared nondiagonal elements of the S-matrix to include the entire Riemann surface except cuts on the imaginary axes. These cuts can possibly include part of the real axes. The one-pole approximation of the S-matrix is of a Breit-Wigner form. An exact expression for the partial widths and a sum rule for the partial widths are derived. A generalized Levinson theorem is proved. (auth)

15506 BAND SPECTRA GENERATED BY NON-COMPACT ALGEBRA. Dothan, Yossef; Ne'eman, Yuval (California Inst. of Tech., Pasadena). pp 17-32 of Resonant Particles. Athens, Ohio, Fazl-i-Umar Research Inst., 1965. (CALT-68-41).

An algebraic approach to hadron physics is proposed. The differences between the approximate symmetry algebras, the spectrum-generating algebras, and the transition operators algebras as applied to strong coupling theories are stressed. (G.O.Y.)

15507 ON THE INTERPRETATION OF $\tilde{U}$ SYMMETRIES. O'Raifeartaigh, L. (Syracuse Univ., N. Y.). pp 57–62 of Resonant Particles. Athens, Ohio, Fazl-i-Umar Research Inst., 1965.

An attempt to interpret the $\tilde{U}$ symmetries is summarized. (G.O.Y.)

15508 A POSSIBLE ALTERNATIVE TO SU(6). Joseph, D. W. (Univ. of Nebraska, Lincoln). pp 63-71 of Resonant Particles. Athens, Ohio, Fazl-i-Umar Research Inst., 1965.

The more interesting representations of SU(6), R(11), R(17), and Sp(16) are discussed; and it is shown that R(11), with its relativistic extension L(12), is, at least superficially, a possible alternative to the SU(6) schemes. (D.C.W.)

15509 MASSES AND COUPLINGS OF $P_{\frac{1}{2}}$ OCTET AND $P_{\frac{3}{2}}$ DECUPLET. Ernst, Frederick J. (Illinois Inst. of Tech., Chicago); Wali, K. C.; Warnock, Robert. pp 103-9 of Resonant Particles. Athens, Ohio, Fazl-i-Umar Research Inst., 1965.

The couplings and masses of the $P_{\frac{1}{2}}$ baryon octet and the $P_{\frac{3}{2}}$ baryon resonance decuplet were studied on the basis of a model in which the baryons and resonances are regarded as composites of pseudoscalar mesons and baryons. The symmetry breaking was introduced through the phase-space factor in the dispersion integral. (D.C.W.)

15510 SUMMARY OF SESSION OF PRODUCTION MECHANISMS. Jackson, J. D. (Univ. of Illinois, Urbana). pp 461-3 of Resonant Particles. Athens, Ohio, Fazl-i-Umar Research Inst., 1965.

A survey of the experimental and theoretical observations of production mechanisms is presented. (D.C.W.)

15511 DETERMINATION OF THE NEUTRON-NEUTRON S-WAVE SCATTERING LENGTH FROM THE REACTION $\pi^- + d \rightarrow 2n + \gamma$. Salter, Robert Mundhenk Jr. Los Angeles, Univ. of California, 1965. 231p.

A determination of the S-wave, neutron-neutron scattering length (a_{nn}) from a measurement of the distribution of the products from the reaction $\pi^- + d \rightarrow 2n + \gamma$ is reported. Negative pions from the Berkeley 184 in. cyclotron were stopped in a liquid deuterium target. Times-

of-flight of both neutrons were measured over a ten-foot path using the detection of the γ ray in coincidence with the incoming pion as a timing signal. Fourteen liquid scintillator neutron counters (counting either neutron) and six lead-and-plastic scintillator γ-counters provided a variety of angular combinations of the three particles for analysis purposes. The method for determining a_{nn} followed that recommended by Bander essentially consisting of the effective range (r_o) approximation with an additional transition factor that includes γ-polarization effects. Comparisons of theoretical and experimental neutron time-of-flight (t) spectra for given angular separations of the neutrons (θ) were made using computed phase space factors. Shapes of these spectra were compared employing minimum χ^2 as the criterion. The complementary spectrum for θ for a fixed t interval also was analyzed. A Monte Carlo computer program was needed to find expected phase space distributions. The final result using combined χ^2 Pearson probability distributions yielded $a_{nn} = -16.47\ F \pm 1.27\ F$ (assuming an effective range of $r_{nn} = 2.65\ F$). A computer program was devised that iteratively searched through possible angle and time excursions for the best overall solution of momentum balance and predicted reaction energy. Improvement in signal/background ratios of better than an order of magnitude was attained. Time spectrum fits of events corrected in this fashion were performed under the assumption of zero background and time resolution spread. Results were consistent with the above a_{nn}. (Dissertation Abstr.)

15512 ANALYTIC S-MATRIX THEORY. Stapp, H. P. (International Center for Theoretical Physics, Trieste, Italy). pp 3-54 of STI/PUB/117.

The theoretical bases for generalized, Mandelstam-type calculations are developed from postulates based directly on properties of the physical scattering amplitudes. A mass-shell analyticity postulate, which provides the general theoretical framework of analytic S-matrix theory, is also presented. The role of anti-particles and crossing relations in S-matrix theory is discussed in detail. (G.O.Y.)

15513 TWO, THREE, AND FOUR POINT FUNCTIONS IN QUANTUM FIELD THEORY. Toll, J. S. (Univ. of Maryland, College Park). pp 55-83 of STI/PUB/117.

Some developments in axiomatic quantum field theory are reviewed. Analytic properties and functional representations of the two, three, and four point functions are discussed. Functional representations that summarize the restrictions on scattering amplitudes and Green's functions, which are imposed by the axioms of quantum field theory, are emphasized. (G.O.Y.)

15514 AXIOMATIC FIELD THEORY. Bros, J. (CEN, Saclay, France). pp 85-120 of STI/PUB/117.

Reduction formulas were previously developed which display the scattering amplitudes as the boundary values on the mass shell of some analytic functions ($H_n(k)$) of four-momenta that are primitively defined off the mass shell. Since the primitive domain of analyticity of the $H_n(k)$ is not a natural domain of holomorphy, the function $H_n(k)$ is certainly analytic, at least in the envelope of holomorphy of the primitive domain. The calculation of this envelope of holomorphy—or at least some subdomain of it—is considered, together with the determination of whether this domain has points on the mass shell. Regions of analyticity are obtained for three, four, and n-point functions. (G.O.Y.)

15515 CAUSAL S-MATRIX IN THE AXIOMATIC APPROACH. Polivanov, M. C. (International Center for Theoretical Physics, Trieste, Italy). pp 121-36 of STI/PUB/117.

Some of the results of the formulation of local S-matrix theory that is based on the Bogoliubov causality condition on the s-matrix in terms of variational derivatives are reviewed. The problem of extending the s-matrix off the energy shell is emphasized. (G.O.Y.)

15516 ARBITRARINESS IN THE CHOICE OF FIELD OPERATORS. Nishijima, K. (International Center for Theoretical Physics, Trieste, Italy). pp 137-46 of STI/PUB/117.

The formulation of bound states or composite particles in axiomatic field theory is considered. It is emphasized that the lack of uniqueness of the correspondence between fields and particles in the case of interacting fields permits the introduction of field operators corresponding to composite particles. (D.C.W.)

15517 LOCAL RING AND QUANTUM FIELD THEORY. Borchers, H. J. (Institut des Hautes Etudes Scientifiques, Bures-sur-Yvette, France). pp 147-51 of STI/PUB/117.

Some results of the treatment of quantum field theory in terms of local rings (algebras) are reported. (G.O.Y.)

15518 QUALITATIVE AND QUANTITATIVE CONSEQUENCES OF ANALYTICITY AND UNITARITY. Martin, A. (CERN, Geneva). pp 155-67 of STI/PUB/117.

Asymptotic bounds on the scattering amplitude are briefly reviewed, and the limitations imposed on the π-π scattering amplitude by analyticity and unitarity are studied. (D.C.W.)

15519 UNIVALENT FUNCTIONS AND SCATTERING AMPLITUDES AT HIGH ENERGIES. Khuri, N. N. (Rockefeller Inst., New York); Kinoshita, T. pp 169-77 of STI/PUB/117.

The problem of constructing a univalent (Schlicht) function from the forward scattering amplitude is considered. Since univalent functions satisfy many sharp inequalities, several of these inequalities are used to study the asymptotic properties of the univalent function and to derive inequalities which can in principle be used for an experimental test of the consequences of local field theory with data obtained from a finite range of energies. (G.O.Y.)

15520 CONSEQUENCES OF ANALYTICITY IN ENERGY FOR HIGH-ENERGY SCATTERING. Van Hove, L. (CERN, Geneva). pp 179-94 of STI/PUB/117.

A unified treatment is given of the consequences of analyticity of the scattering amplitude in the energy variable for the asymptotic properties of high-energy scattering. (G.O.Y.)

15521 KRONECKER-DELTA SINGULARITIES IN THE j-PLANE. Mandelstam, S. (Univ. of California, Berkeley). pp 195-208 of STI/PUB/117.

A type of non-Regge behavior that occurs when Lagrangian field theories are solved in conventional approximations is studied. The conditions for the existence of Kronecker-delta terms are derived. It is shown that in the spinor-vector system, no Kronecker-delta term exists in the channel with the quantum numbers of the nucleon and that there is a non-Regge term in the channel with the quantum numbers of the vector meson. (D.C.W.)

15522 DISPERSION DESCRIPTION OF LOW-ENERGY SCATTERING. Shirkov, D. V. (Inst. for Mathematics, Novosibirsk, USSR). pp 209-26 of STI/PUB/117.

The results obtained in recent years in the dispersion theory of low-energy π-π scattering as well as in πN scattering are reviewed. (G.O.Y.)

15523 ANALYTIC PROPERTIES OF FEYNMAN INTEGRALS. Polkinghorne, J. C. (Cambridge Univ., Eng.). pp 229-53 of STI/PUB/117.

A review is presented on the analytic properties of Feynman integrals. (G.O.Y.)

15524 AN INTERPRETATION FOR SINGULARITIES IN THE PHYSICAL REGION. Norton, R. E. (Univ. of California, Los Angeles). pp 255-62 of STI/PUB/117.

It is shown that any singularity which occurs in the physical region is subject to a simple, completely classical, physical interpretation and that no singularity lies in this domain unless the interpretation is applicable. The validity of this conclusion is demonstrated to arbitrary order in perturbation theory. (G.O.Y.)

15525 DIFFERENTIAL PROPERTIES OF FEYNMAN AMPLITUDES. De Alfaro, V. (Univ., Turin); Jaksic, B.; Regge, T. pp 263-72 of STI/PUB/117.

The existence of ordinary differential equations for each variable appearing in each term of the relativistic expan-

sion of the Feynman scattering amplitude was investigated. (G.O.Y.)

15526 S-MATRIX PERTURBATION THEORY. Sharp, D. H. (Princeton Univ., N. J.). pp 273-92 of STI/PUB/117.

The Dashen–Frautschi formulas for the first-order change in the position and residue of the bound-state pole resulting from a small change in the forces that produce the bound state are derived. The relation of the formalism that is used to ordinary Rayleigh–Schroedinger perturbation theory is also discussed. (G.O.Y.)

15527 SOME REMARKS ON NON-RENORMALIZABLE QUANTUM FIELD THEORIES. Schroer, B. (Univ. of Pittsburgh). pp 295-303 of STI/PUB/117.

Nonrenormalizable field theories are studied. It is shown that nonlocalizable (nonrenormalizable) fields can lead to local observables. (D.C.W.)

15528 CALCULATION OF RADIATIVE CORRECTIONS IN NON-RENORMALIZABLE FIELD THEORY. Filippov, A. T. (Joint Inst. for Nuclear Research, Dubna, USSR). pp 305-14 of STI/PUB/117.

The radiative corrections to the vertex function in a nonrenormalizable weak-coupling field theory are calculated using an iteration method. The possibility of applying the method to strong-coupled problems is considered. (D.C.W.)

15529 INTRODUCTION TO SU(3). Lipkin, H. J. (Weizmann Inst. of Science, Rehovoth, Israel). pp 317-23 of STI/PUB/117.

A brief introduction to SU(3) symmetry is presented. (D.C.W.)

15530 SOME PROPERTIES OF MESONS IN SU(3). Lipkin, H. J. (Weizmann Inst. of Science, Rehovoth, Israel). pp 325-30 of STI/PUB/117.

The states of systems of two octet pseudoscalar mesons are studied to demonstrate the manner in which SU(3) couplings are used and their connection with other symmetries. The medium-strong interaction that is responsible for the mass splittings in the SU(3) multiplets is then considered, and the derivation of relations for the charge-conjugation properties of SU(3) multiplets is outlined. (D.C.W.)

15531 FUN WITH SU(3). Coleman, S. (Harvard Univ., Cambridge, Mass.). pp 331-52 of STI/PUB/117.

It is demonstrated that many of the most important properties of SU(3) can be derived using only the elements of group theory. The irreducible representations of SU(3) are treated by simple tensorial methods. Algorithms for the isospin-hypercharge content of an irreducible representation and for the Clebsch–Gordan series are derived. The calculation of invariant couplings (Clebsch–Gordan coefficients) is also considered. (D.C.W.)

15532 REVIEW OF EXPERIMENTAL TESTS OF SU(3) IN SCATTERING REACTIONS. Harari, H. (Israel Atomic Energy Commission, Yavne). pp 353-69 of STI/PUB/117.

Some predictions of the SU(3) symmetry scheme are discussed and are compared with experimental observations. (D.C.W.)

15533 SELECTED TOPICS IN UNITARY SYMMETRY AND WEAK INTERACTIONS. Lee, B. W. (Inst. for Advanced Study, Princeton, N. J.). pp 371-92 of STI/PUB/117.

Some applications of unitary symmetry to weak interactions are discussed assuming that weak interactions have a current × current form and that the currents have definite transformation properties under SU(3). (D.C.W.)

15534 NOW WE ARE SU(6). Lipkin, H. J. (Weizmann Inst. of Science, Rehovoth, Israel). pp 395-422 of STI/PUB/117.

The SU(6) symmetry of elementary particles is discussed using the quark model. (D.C.W.)

15535 ELECTRODYNAMIC MASS FORMULA IN SU(3) AND SU(6). Glashow, S. L.; Socolow, R. (Univ. of California, Berkeley). pp 423-31 of STI/PUB/117.

The predictions of SU(3) symmetry and SU(6) symmetry for the electromagnetic mass splittings and magnetic moments are summarized. A one-parameter description of all the electromagnetic splittings of baryons and mesons in terms of octet dominance is also outlined. (D.C.W.)

15536 THE SL(6,C) MODEL AS A RELATIVISTICALLY INVARIANT FORMULATION OF SU(6) SYMMETRY. Ruehl, W. (CERN, Geneva). pp 435-53 of STI/PUB/117.

The relativistically invariant model of SU(6) symmetry that is based on the group $SL(6,C) \times T_{72}$, where the space of translations (T_{72}) contains the Minkowski space as a subspace, is developed. The relation of the group SL(6,C) to the group $\tilde{U}(12)$ is discussed, together with the role played by some subgroups of SL(6,C). (D.C.W.)

15537 THE $\tilde{U}(12)$ SYMMETRY. Delbourgo, R.; Rashid, M. A.; Salam, Abdus; Strathdee, J. (International Center for Theoretical Physics, Trieste, Italy). pp 455-532 of STI/PUB/117.

The U(6,6) theory is restated incorporating some recent developments. It is shown that the theory has a logical basis; that even though it uses a noncompact group, it employs perfectly unitary representations; and that it does not violate either unitarity or antiparticle conjugation. (D.C.W.)

15538 A LORENTZ COVARIANT SUPERMULTIPLET SCHEME. Oehme, R. (Univ. of Chicago). pp 533-48 of STI/PUB/117.

A Lorentz-covariant scheme for elementary particles, which reproduces the successful features of SU(6) models, is described. (G.O.Y.)

15539 W-SPIN AND SU(12) SUBGROUPS. Lipkin, H. J. (Weizmann Inst. of Science, Rehovoth, Israel). pp 549-60 of STI/PUB/117.

The classification of particles and the treatment of interactions in terms of W-spin and SU(12) subgroups are outlined. B-spin and Z-spin are briefly considered. (D.C.W.)

15540 A SURVEY OF REPRESENTATIONS OF NON-COMPACT GROUPS. Stein, E. M. (Princeton Univ., N. J.). pp 563-84 of STI/PUB/117.

A survey of the theory of unitary representations of non-compact groups is presented. (G.O.Y.)

15541 THE THEORY OF REPRESENTATIONS OF NON-COMPACT LIE ALGEBRAS. Fronsdal, C. (International Center for Theoretical Physics, Trieste, Italy). pp 585-624 of STI/PUB/117.

The theory of unitary representations of non-compact Lie groups is reviewed. (G.O.Y.)

15542 SOME PROPERTIES OF REPRESENTATIONS OF NON-COMPACT GROUPS. Hermann, R. (Argonne National Lab., Ill.). pp 625-39 of STI/PUB/117.

The irreducibility of representations to which the Gell-Mann formula applies is discussed, and some group representation theory is outlined. (D.C.W.)

15543 ON JORDAN ALGEBRA M_3^8. Gamba, A. (Univ., Genoa). pp 641-6 of STI/PUB/117.

The general properties of Jordan algebras are summarized; and the more important properties of the Jordan algebra M_3^8, from the viewpoint of physics, are given. The M_3^8 algebra can not be expressed as a matrix algebra. Its use as a basis for particle symmetries is considered. (D.C.W.)

15544 DYNAMICAL QUANTUM NUMBERS IMPLIED BY THE REPRESENTATION TYPES OF THE POINCARE GROUP INCLUDING SPACE, TIME, AND CHARGE REFLECTIONS. Tarimer, N. (Middle East Technical Univ., Ankara). pp 647-53 of STI/PUB/117.

A theory is considered in which the addition of the generalized charge-conjugation symmetry to the full Poincaré group suffices to determine all the dynamical quantum

numbers, except those implied by the electromagnetic interactions, in a manner that is consistent with the superselection rules. An explicit construction of the additive quantum numbers is given. (D.C.W.)

15545 INTERPRETATIONS OF SPIN AND UNITARY SPIN SYMMETRY. Zumino, B. (New York Univ., New York). pp 657-64 of STI/PUB/117.

It is shown that it is possible to construct field theoretic models which have all the properties required by a local Lagrangian field theory and which provide a unification of spin and unitary spin and also a way of breaking the symmetry. The inherent difficulties of this approach are also described. (G.O.Y.)

15546 REMARKS ON RELATIVISTIC FORMULATIONS OF SU(6). Guersey, F. (Middle East Technical Univ., Ankara). pp 697-706 of STI/PUB/117.

A method of generalizing the SU(6) group to local field theory is discussed, in which the Hilbert space is enlarged by taking the unitary representations of the group L that admits all little groups as subgroups and combining this with SU(3) into a non-compact group G. (G.O.Y.)

15547 INVARIANT AMPLITUDES AND THE INTERPRETATION OF SU(3)- AND SU(6)-TYPE SYMMETRIES. Barut, A. O. (International Center for Theoretical Physics, Trieste, Italy). pp 707-21 of STI/PUB/117.

Different types of representations of the Poincaré group according to the choice of the diagonalized subgroup, and different realizations in each type are reviewed. The construction of invariant and covariant amplitudes is discussed on the basis of a global representation. The two ways in which the spin-orbit effects enter into the amplitude are discussed. Then starting with the amplitudes under the exact invariance group of the strong interactions, $\underline{L} \otimes SU_2(\tilde{I}) \otimes U_1(Y)$, where $\underline{L}$ is the full inhomogeneous Lorentz group, it is shown that one obtains automatically terms in the amplitude which are SU(3), SU(4), and SU(6) invariant, with other terms having definite transformation properties. A criterion is given when these symmetries (especially those of the SU(4) and SU(6) type) are consistent approximate symmetries. (auth)

15548 THEORY OF APPROXIMATE SYMMETRIES. Sudarshan, E. C. G. (Syracuse Univ., N. Y.). pp 723-38 of STI/PUB/117.

Several aspects of the theory of approximate symmetries of strong interactions are discussed from a unified point of view considering approximate symmetries as masked symmetries-exact symmetries among states that are related to the natural (particle) states by a nontrivial unitary transformation. It is also postulated that these unitary transformations are directly related to the structure of strong interactions and are automorphisms of the Lie algebra of currents. The generators of the symmetry group are identified with the coupling vertices in physical processes such as nuclear beta decay. As an application of the method, a new sum rule for the renormalization of the Gamow–Teller coupling constant is derived. (G.O.Y.)

15549 THE USE OF DISPERSION METHODS IN THE STUDY OF SYMMETRIES. Fubini, S. (Univ., Turin. CERN, Geneva); Furlan, G.; Rossetti, C. pp 739-52 of STI/PUB/117.

A method for the evaluation of commutator matrix elements, which preserves covariance at each order of approximation, is developed using a causality condition. The application of the method to dynamical groups that also involve space-time quantum numbers such as spin and parity is discussed. (D.C.W.)

15550 HIGHER SYMMETRIES AND COMPOSITE MODELS OF ELEMENTARY PARTICLES. Tavkhelidze, A. (International Center for Theoretical Physics, Trieste, Italy). pp 753-62 of STI/PUB/117.

A composite, dynamical model for elementary particles is discussed, and the form factors and magnetic moments of baryons and mesons are investigated in the framework of this model. (G.O.Y.)

15551 ELECTROMAGNETIC FORM FACTORS IN COMPOSITE MODELS OF ELEMENTARY PARTICLES (RELATIVISTIC MODELS). Tavkhelidze, A. (International Center for Theoretical Physics, Trieste, Italy). pp 763-79 of STI/PUB/117.

A composite model that satisfies the requirements of $\tilde{U}(12)$ invariance, as well as the relativistic requirements, is described. The form factors, magnetic moments, and decay constants of baryons and mesons are calculated. (D.C.W.)

15552 BROKEN SYMMETRIES AND THE GOLDSTONE THEOREM. Streater, R. F. (Imperial Coll. of Science and Tech., London). pp 781-8 of STI/PUB/117.

It is shown that gauge invariance implies zero-mass particles only in the time-like (indefinite) component. It provides no explanation of the vanishing of the mass of the physical photon. (D.C.W.)

15553 BOOTSTRAPS. Udgaonkar, B. M. (Tata Inst. of Fundamental Research, Bombay). pp 791-822 of STI/PUB/117.

A survey on the bootstrap hypothesis is presented. The approximations used in bootstrap calculations are discussed, together with the insight that is provided by the bootstrap method into the dynamics underlying the symmetries of strong interactions. (D.C.W.)

15554 WHAT, IF ANYTHING, IS THE BOOTSTRAP? Zachariasen, F. (California Inst. of Tech., Pasadena). pp 823-55 of STI/PUB/117.

The bases of the bootstrap hypothesis are reviewed, and the implications of the hypothesis for particle symmetries are discussed. Some possible criteria for distinguishing between dynamical particles and elementary particles are considered. (D.C.W.)

15555 SIMPLE BOOTSTRAP RULES. Cutkosky, R. E. (Carnegie Inst. of Tech., Pittsburgh). pp 857-63 of STI/PUB/117.

A set of rules for bootstrap calculations is discussed, together with some of the results of such calculations. (D.C.W.)

15556 SYMMETRY PROPERTIES OF BOOTSTRAP MODELS. Belinfante, J. G.; Cutkosky, R. E.; Renninger, G. H. (Carnegie Inst. of Tech., Pittsburgh). pp 865-75 of STI/PUB/117.

Some symmetry properties that are inherent in the bootstrap hypothesis are described. The formulation and manifest symmetries of bootstrap models are considered, and the general covariance group of the bootstrap equations is discussed. Perturbations of the bootstrap symmetry are also considered. (D.C.W.)

15557 SELF-CONSISTENT BROKEN SYMMETRIES. Cutkosky, R. E. (Carnegie Inst. of Tech., Pittsburgh). pp 877-81 of STI/PUB/117.

Four intuitively reasonable qualitative properties of self-consistent solutions are presented in the form of assumptions from which five basic results follow. It is found that the assumptions severely restrict the kinds of small dissymmetries that are possible. (D.C.W.)

15558 CHERENKOV AND TRANSITION RADIATION IN A PERIODIC MEDIUM [Thesis]. Casey, Kendall Francis Jr. Los Angeles, Calif., Univ. of Southern California, 1965. 171p.

The radiation emitted when a charged particle traverses a continuous, periodically varying dielectric medium is considered. Both Cherenkov and transition radiation are expected. The propagation of transverse-magnetic waves in a sinusoidally varying medium is discussed in detail, and methods are presented for determining the dispersion relations of these waves from the stability charts for Hill's equation. A formal solution for the fields excited by the passage of the charged particle through the medium is presented, as well as a formal expression for the spectral density of the emitted radiation. A Cherenkov threshold condition is defined for the periodic medium. It is found that although radiation is produced for an arbitrarily low

particle velocity, the Cherenkov threshold must be crossed before a large amount of energy is radiated. The magnitude of the spectral density of the radiation emitted above the Cherenkov threshold is found to be nearly equal to that emitted in a homogeneous medium having a permittivity equal to the average value of the permittivity of the periodic medium. The angular distribution of the bulk of the energy radiated above the Cherenkov threshold is also found to be similar to the angular distribution of Cherenkov radiation in a homogeneous medium except at certain discrete frequencies where the radiation is emitted in the backward direction. This phenomenon may have practical consequences in the generation of radiation at very small wavelengths. (Dissertation Abstr.)

15559 QUASI-CLASSICAL SOLUTION TO THE DIRAC EQUATION AND ITS APPLICATION TO HIGH ENERGY ATTRACTIVE COULOMB SCATTERING [Thesis]. **Spargo, Edward. Hoboken, N. J., Stevens Inst. of Tech., 1965. 107p.**

Previous treatments of the quasi-classical (QC) solution to the Dirac equation are reviewed, and the failure of these treatments to account for high energy attractive Coulomb scattering is demonstrated. A new interpretation of the QC procedure is given, applying concepts from the geometric theory of diffraction. The new QC Dirac wave function is obtained from the solution of the second order Dirac equation, which is taken as the first term in an expansion in powers of Planck's constant, consisting of a phase satisfying the relativistic Hamilton-Jacobi equation for a spinless particle, a scalar amplitude satisfying the equation of continuity, and a constant spinor. The novelty of the procedure lies in the concept of the wave function being the sum of wave functions on all classical trajectories passing through a point. The new QC wave function is applied to high-energy attractive Coulomb scattering. The corresponding classical trajectories are shown to have multiple loops, with many trajectories giving the same scattering angle. The wave function describing the scattering is a sum over these trajectories, and the scattering cross section is a coherent or vector sum of classical cross sections. The failure of the QC method on trajectories with very small angular momenta is discussed, and an analogy with the quantum-mechanical S-wave is used to account for these trajectories. A geometric correction factor is developed for scattering angles in the backward direction. The spin properties and scattering cross section given by the new QC wave function are in good agreement with the exact results. The new QC wave function involves only simple classical quantities and ordinary differential equations, even in a non-separable problem. It should prove useful in other high energy problems requiring the use of the Dirac equation. (Dissertation Abstr.)

15560 THEORY OF MANY-BOSON SYSTEMS [Thesis]. **Etters, Richard David. Ames, Iowa, Iowa State Univ. of Science and Tech., 1965. 70p.**

A many-boson theory is developed that is applicable to systems with intermediate as well as weak-coupling strength. A transformation of basis from the single-particle representation to an independent collection of quasiparticles, which represent the normal modes of the system, is accomplished in an approximate way. The results are in the form of coupled, non-linear, integral equations for the ground state energy, the excitation energy, the quasiparticle excitation operator, and the momentum distribution function. No a priori assumptions concerning the population in any single low-lying momentum state are required nor is any artificial separation of the single-particle zero-momentum state from states of higher momentum necessary. Contact with the results of weak-coupling theories is established by imposing additional restrictions on the interaction potential and on the distribution of particles. It is shown that the weak-coupling equations are valid under more general circumstances than was previously apparent. A general theorem is provided that requires the existence of a zero in the excitation spectrum at zero-momentum. It is also shown that the low-lying excitations follow a dispersion rule that is linear in momentum, independent of the form of the interaction. The theory is applied to the charged boson gas problem, where it is found that the resulting excitation spectrum is not in agreement with previous calculations at low momenta, but is elsewhere. For systems with interaction potentials similar to that of He II, it is shown that the weak-coupling equations may be valid at sufficiently low temperatures provided that depletion effects are completely ignored. (Dissertation Abstr.)

15561 GEOMETRICAL AND GAUGE THEORETICAL INVESTIGATIONS ON ELEMENTARY PARTICLE INTERACTIONS [Thesis]. **Inomata, Akira. Troy, N. Y., Rensselaer Polytechnic Inst., 1964. 148p.**

A theory of neutrinos is constructed within the present scheme of geometrodynamics. Firstly it is mentioned that the only non-vanishing bilinear form of a two-component c-number spinor field is a null vector. This fact makes it possible that a particular class of neutrinos satisfies the Rainich null field conditions. Secondly, a geometry suitable for the special neutrino physics is distinguished from general Rainich-Riemannian null geometries by imposing differential conditions analogous to the Rainich-Misner-Wheeler equations. Finally, it is observed that the gravito-neutrino coupling turns out no longer universal. The geometrical behavior of the two-component c-number neutrino field is investigated. The neutrinos are endowed with the following two comparatively interesting features: they move along the null geodesics and their current is a null vector. If the current flows along the geodesic, the above two statements become equivalent. Under this situation, the parallel displacement of the neutrino spinor is defined. A space-time with torsion is examined. It is recognized that the Finkelstein's neutral space with quasi-teleparallelism and uniform null torsion is equivalent to the Rainich null geometry that has been accepted as a neutrino geometry. The neutrino current is identified with the null torsion. A topological speculation is also presented. A five-dimensional formalism is applied to the gauge theory of a neutral vector meson. The imposition of the supplementary massive condition reduces the theory to the conventional neutral massive vector field theory. Quantization of the five-vector field is also carried out. Some consequences of gauge invariance are explored on the assumption that no experimental measurement determines the phase of mass of an elementary particle if any. At first the concept of the fermion mass gauge is introduced. The mass gauge invariance is used as a selection rule of coupling types in electromagnetic and mesonic interactions. Renormalizability of a pseudo-vector meson generated by the local mass gauge group is discussed. (Dissertation Abstr.)

15562 PRODUCTION PROCESSES IN A NUCLEAR COULOMB FIELD [Thesis]. **Halprin, Arthur. Philadelphia, Univ. of Pennsylvania, 1965. 165p.**

The relationship between the $A \rightarrow B + \gamma$ decay process and the associated "inverse" process: $B + Z \rightarrow B + \gamma' + Z \rightarrow A + Z$ (Z = high-Z nucleus, γ' = virtual Coulomb photon) is studied in some detail for arbitrary particles A,B. In particular, it is found that at sufficiently high incident energies and small production angles, measurement of the nuclear-Coulomb-field $B \rightarrow A$ production cross section is always tantamount to a measurement of the $A \rightarrow B + \gamma$ decay rate. The results are compared with already existing calculations that utilize the most general explicit form of the ABγ vertex function for $(A,B) = (\pi^0,\gamma)$, $(\ ,\gamma)$, and (Σ^0,Λ); calculations of this explicit type for $(A,B) = (\ ,\gamma)$, (f,γ), (V_8,P_8) and $(W^{\pm},\pi^{\pm})$ are performed where V_8 and P_8 represent members of the vector unitary octet and pseudoscalar unitary octet, respectively, and where $W^{\pm}$ is the conjectured intermediate vector-boson. In addition, a priori estimates for all of the above photonic decay rates are obtained, and, after a discussion of the contribution of various strong interaction mechanisms to the $B + Z \rightarrow A + Z$ process, the incident energies required in order that the γ'-exchange dominate the $B \rightarrow A$ production reaction are calculated. (Dissertation Abstr.)

15563 CLASSICAL LIMIT OF RADIATIVE AND DAMPING CORRECTIONS TO MESON SCATTERING [Thesis]. Page, William E. Logan, Utah, Utah State Univ., 1965. 83p.

In an extensive comparison previously carried out by Chatelain, it was found that the classical limit of scattering cross sections calculated on the basis of Heitler's radiation damping theory agreed in all cases with the results of classical action-at-a-distance theory, but not with calssical field theoretical results. The classical limit in the case of meson-nucleon scattering with dipole coupling was found by treating the nucleon spin as a classical unit vector when evaluating sums in which it was involved. The radiation damping calculation was extended to fourth order in the coupling constant in calculating the cross section for meson-nucleon scattering using PS(PV) theory. The nucleon mass M_0 is assumed large; the nucleon is allowed to recoil but treated nonrelativistically, and the calculation is carried to second order in $1/M_0$. The interaction Hamiltonian is determined to this order by means of a Foldy-Wouthuysen transformation. In finding the fourth order matrix element a method given by Heitler is used to account for the nucleon mass self energy. It is found that the resulting matrix element is finite if classical spin summations are used, while in the quantum mechanical case an additional logarithmic divergence occurs. This arises since a complete renormalization of the process is not made. The finite matrix element is used to solve the damping equation and determine the total cross section. These calculations are carried out using both classical and quantum mechanical spin summations. A comparison is made between the classical cross section obtained and the results of classical action-at-a-distance theory and of classical field theory. The differences between the classical limit of radiation damping theory and classical field theory are seen to reside in the lowest order of the calculation. (Dissertation Abstr.)

15564 A STUDY OF MANY-FERMION SYSTEMS [Thesis]. Stoelan, Birger. Providence, Brown Univ., 1965. 115p.

Various cases of many-fermion systems were analyzed with linked-cluster techniques. Although the strong coupling approximation was used, some of the results obtained have a more general validity. The analysis of the diagrams originating in various hamiltonians was emphasized; in particular the cases of the B.C.S. hamiltonian and a single-particle potential are discussed in detail. It is found that the B.C.S. diagrams constitute a topological subset of the general singlet two-body diagrams. A scheme is presented whereby the volume dependence of an arbitrary B.C.S. diagram is easily obtained. The B.C.S. diagrams are seen to be ladder diagrams or diagrams that violate statistics in intermediate states. The contribution from each of the latter type is at most of the order of Ω^{-1}, however their role is very important. This is demonstrated in our discussion of some results that Fukushima and Fukuda obtained by using the ladder approximation to the B.C.S. diagrams. (Dissertation Abstr.)

15565 INTRODUCTION TO DISPERSION TECHNIQUES IN FIELD THEORY. Barton, Gabriel. Lecture Notes and Supplements in Physics. New York, W. A. Benjamin, Inc., 1965. 252p. $5.95 Domestic; $11.00 Foreign.

Dispersion techniques are introduced and developed within the framework of field theory for the general class of problems concerning the calculations of properties and behavior of strongly interacting particles. Emphasis is given primarily to the effects of their strong couplings on their weak and electromagnetic ones. Topics covered include: the field hypothesis in particle physics; contraction scheme and crossing symmetry; kinematics, crossing symmetry, and cross sections; charge and spin; the two-point functions; form factors; subtractions, conserved currents, and asymptotic behavior; the Ömnes equation; approximations to partial waves and to Omnes functions; the second Riemann sheet; anomalous thresholds, electromagnetic structure of nucleons; and axial vector current and Goldberger-Treiman formula. (L.B.S.)

15566 POTENTIAL SCATTERING. de Alfaro, V.; Regge, T. New York, John Wiley and Sons, Inc., 1965. 212p.

A systematic and rigorous treatment is presented of the most recent developments in the theory of potential scattering as the quantum mechanical description of a nonrelativistic system of two interacting particles, where the potential depends on the relative position of the bodies only. Spinless particles and isotropic potentials are assumed. The relevant mathematical methods are first treated, followed by chapters on: partial wave boundary conditions; the Jost function and the S matrix; Yukawian potentials; physical interpretation of the poles of $S(\lambda,k)$ for physical angular momenta; asymptotic behavior of $S(\lambda,k)$ for large λ and fixed k; analytic properties of the scattering amplitude, ordinary dispersion relations, Mandelstam representation, the inverse problem, and the generalization of ordinary potential scattering. (L.B.S.)

15567 ON RELATIVISTIC SCHROEDINGER EQUATIONS FOR PARTICLES OF ARBITRARY SPIN. Mathews, P. M. (Brandeis Univ., Waltham, Mass.). 28p. (CONF-650653-12). ORINS. Gmelin, AED-CONF-65-170-18.

From American Physical Society, Summer Meeting, New York.

Relativistic wave equations in the Schrödinger form $i\partial\psi/\partial t = H\psi$ for particles of nonzero mass and arbitrary spin are investigated. The wave function ψ is taken to transform according to the representation $D(o,s) \oplus D(s,o)$ of the homogeneous Lorentz group, a unique spin s for the particle being thereby assured without the aid of any supplementary condition. It is shown that the requirement that the Schrödinger equation be invariant under the operations of the Poincaré group, as well as under space and time inversions and charge conjugation, restricts the possible choices of H (as a function of the operators representing the above symmetry operations) to a well-defined class which shrinks to a unique possibility (coinciding with the hamiltonian derived by Weaver, Hammer and Good) when a further regularity condition of a physical nature is imposed: namely, that the hamiltonian have a unique finite limit in the rest system of the particle. In this process, an ambiguity which exists initially in the definition of operators representing time reversal and charge conjugation gets eliminated. The hamiltonian itself is obtained in explicit form for particles of any spin. (auth)

Fluid Physics and Thermodynamics

See also Plasma Physics and Thermonuclear Processes

Refer also to abstracts 15626 and 15675.

15568 (AD-620324) THE HALL EFFECT IN THE TWO-DIMENSIONAL FLOW ALONG AN INSULATING PLANE. Hasimoto, H.; Janowitz, G. S. (Johns Hopkins Univ., Baltimore, Md. Dept. of Mechanics). June 1965. Contract AF49(638)-496. 33p. (AFOSR-65-1201). CFSTI $2.00 cy, $0.50 mn.

Two-dimensional flow of a conducting gas interacting weakly with an external inhomogeneous magnetic field is considered. It is proved that for flow over an insulating wall, the total drag force is reduced by the Hall effect, and the total transverse force is zero. General expressions for the Hall current and the induced transverse flow are obtained for the case of flow with small Hall parameter over an infinite insulating plane. Examples are given for the dipole magnetic field. An inversion of the transversal flow, varying with the dipole orientation, is found. This situation also suggests a transverse deflection of the flow behind a magnetized body in the flow of a plasma. (TAB)

15569 (INR-626/IX/R) ON THE APPLICATION OF NOISE TECHNIQUE TO THE DIAGNOSTICS OF MAGNETO-HYDRODYNAMICS. Ciechanowicz, W. (Institute of Nuclear Research, Warsaw (Poland)). Apr. 1965. 20p. Dep.

Two methods of applying the noise technique to the diagnostics of MHD flow are discussed. The determination of the electric conductivity of the ionized gas from the velocity of the gas and the magnetic induction is considered as an example. (D.C.W.)

15570 (N65-21084) MAGNETOHYDRODYNAMIC BOUNDARY LAYER BETWEEN PARALLEL STREAMS OF DIFFERENT MAGNETIC FIELDS AND TEMPERATURES. Pao, H. P.; Chang, C. C. (Catholic Univ. of America, Washington, D. C. Dept. of Space Science and Applied Physics). Dec. 1964. 43p. (NASA-CR-57845). CFSTI $2.00 cy, $0.50 mn.

An analysis and calculations of the free laminar boundary-layer flow between parallel streams of different magnetic fields and temperatures were made for an incompressible, viscous, thermally and electrically conducting fluid. Small perturbation and approximate solutions were given. The approximate solution for $\alpha = 1$ gives quite a satisfactory flow field which only involves a discrepancy of 1% from the exact numerical solution in most cases. The integration of the exact boundary layer equations was carried out. The magnetic field thickens the flow boundary layer and thus provides a stabilizing effect on the flow field. The possibility of an extension to the parallel streams of two fluids is also investigated. (STAR)

15571 (UCRL-14531) THE USE OF ONE- AND TWO-DIMENSIONAL HYDRODYNAMIC MACHINE CALCULATIONS IN HIGH EXPLOSIVE RESEARCH. Wilkins, Mark L. (Lawrence Radiation Lab., Univ. of California, Livermore). Oct. 29, 1965. Contract W-7405-eng-48. 15p. Dep. mn. CFSTI $1.00 cy, $0.50 mn.

Hydrodynamic calculations in conjunction with experiments provide an effective method for obtaining otherwise inaccessible information on high explosives. The credibility of the calculational program (code) is established by comparison with the steady state solutions for certain detonation problems obtained by the method of characteristics. The machine calculation is then applied to specific problems in one and two dimensions to explain some of the difficulties an experimenter would encounter in attempting to measure the pressure at a detonation front. (auth)

15572 AN EXACT SOLUTION OF EQUATIONS OF RADIATIVE TRANSFER FOR LOCAL THERMODYNAMIC EQUILIBRIUM IN THE NONGRAY CASE. PICKET FENCE APPROXIMATION. Siewert, C. E.; Zweifel, P. F. (Middle East Technical Univ., Ankara). Ann. Phys. (N. Y.), 36: 61-85(Jan. 1966).

Case's method of singular normal modes is used to obtain an exact solution to the equations of radiative transfer in the "uniform" or "random" picket fence model assuming local thermodynamic equilibrium. Completeness and orthogonality theorems are proved, and explicit results are obtained for the extrapolated endpoint, the temperature distribution, and law of darkening for the Milne problem. In addition, the method for solving other half-space problems is sketched. The case when the determinant of the "transfer matrix" does not vanish (corresponding to radiative transfer without complete local thermodynamic equilibrium or the neutron transport problem) is also discussed. Full range completeness and orthogonality theorems are presented for this case; however, no convenient form for the half-range case was found. (auth)

15573 CORRELATED ELECTRICAL AND X-RAY MEASUREMENTS IN FLASH X-RAY DISCHARGES. Haendel, S. K.; Berg, J. M. (Univ. of Uppsala). Arkiv Fys., 31: 1-18(1965).

A low-inductance flash x-ray system of new design permitted the simultaneous recording of the voltage across the electrodes together with the current, current derivative, and x-ray output, all as functions of time. The shape of these operating characteristics of the flash x-ray discharge indicates a pinched discharge column, as predicted by the Händel discharge theory. During the pinches x-ray bursts of short duration (about 100 nsec) were emitted. Sausage instabilities in the discharge column caused the emission of single as well as multiple superhard x-ray bursts. The observed discharge phenomena were essentially unaffected by the electrode shape. A new kind of cathode made the discharge time more reproducible. The interpretation of the discharge process, as given, accounts satisfactorily also for the multiple x-ray output, which causes much trouble in flash x-ray photography of high-speed events. (auth)

15574 NUCLEAR SPIN RELAXATION IN GASEOUS H_2 AT LOW DENSITIES. Hardy, Walter N. (Univ. of British Columbia, Vancouver). Can. J. Phys., 44: 265-80(Jan. 1966).

The longitudinal and transverse nuclear relaxation times, T_1 and T_2, were measured in normal H_2 gas at 77.5°K in the pressure range 0.05-2 atm. In this region T_1 goes through a minimum, and T_2 deviates significantly from a linear dependence on the density. Comparison of the experimental data with existing theory establishes the following results for the J = 1 state of orthohydrogen: Autocorrelation functions of the molecular angular momentum operators are exponential or nearly so. The ratio of the correlation times τ_1 and τ_2 that are associated with operators of the form J_z and $3J_z^2 - J(J+1)$, respectively, lies within the limits $0.6 < \tau_1/\tau_2 \lesssim 1$. The splitting of the molecular Zeeman levels cannot be neglected as in the original Schwinger theory. (auth)

15575 KINETIC THEORY OF HIGH-FREQUENCY RESONANCE GAS DISCHARGE BREAKDOWN. Maroli, C. (Univ., Milan). Nuovo Cimento, (10), 41B: 208-24 (Feb. 11, 1966).

The breakdown regime of a diffusion-controlled high-frequency resonance discharge is analyzed from the kinetic point of view. Neglecting space-charge effects, the Boltzmann equation for the electron distribution function is solved by using the small parameter $\epsilon = \sqrt{m/m'}$ (m and m' being, respectively, the electron and neutral mass) as an expansion parameter. The multiple time scale method is applied to find an equation for the dominant term in the expansion of the electron distribution function in terms of ϵ. This equation can be solved, in a relatively simple way, by the same technique, in the limit of large-size container and small rate of ionization inside the discharge cavity. It is possible to deduce for the dominant term of the electron number-density in this double expansion, a diffusionlike equation, which can be ultimately used to obtain the so called breakdown condition. (auth)

15576 MAGNETOHYDRODYNAMIC SHOCKS IN NON-ALIGNED FLOW. Lynn, Y. M. (New York Univ.). Phys. Fluids, 9: 314-35(Feb. 1966).

The transition solution across a plane nonrelativistic magnetohydrodynamic shock of finite strength in nonaligned flow in a perfect gas is investigated. A unified point of view is taken to analyze shocks in both one-dimensional unsteady flow and two-dimensional steady flow for which a set of conversion formulas connecting pertinent parameters in these two cases is given. A convenient parametric representation of the shock solution is presented from which an analytical solution expressed in terms of any desirable shock-strength parameter can be readily obtained by performing a straightforward calculation. Detailed analytical and numerical solutions expressed in terms of the flow deflection angle across the shock, which is most often prescribed in two-dimensional steady flow, are then given, with entire ranges of all upstream parameters being covered. Limiting solutions for several special cases are derived. The connection of the present general solution with several other major results in the literature are illustrated. Dynamical stability criteria associated with general magnetohydrodynamic shocks are discussed. (auth)

15577 ELECTRICAL PRECURSORS OF IONIZING SHOCK WAVES. Appleton, J. P. (General Motors Defense Research Labs., Santa Barbara, Calif.). Phys. Fluids, 9: 336-42(Feb. 1966).

Electrical precursors in the immediate vicinity of ionizing shock waves in argon were examined using a simplified model that describes the mechanism of electron

diffusion through the shock. The solutions demonstrate the existence within the translational shock of a charged double layer where the electric field intensity may rise to peak values of several hundred volts per centimeter. The magnitude of the electron densities obtained at the shock front are not inconsistent with those required by Pipkins' analysis which predicts the main features of experimentally observed electron precursors at relatively large distances ahead of the shock. A discussion of precursors produced by photoionization is included together with a simple demonstration, which shows that an impurity such as oxygen, present in concentrations if only one part per million, could be photoionized and thus explains the electron and ion densities recently observed in the region ahead of moderately strong shocks in argon. (auth)

15578 LINEARIZED RAYLEIGH'S PROBLEM IN MAGNETOGASDYNAMICS. **Cercignani, Carlo; Tironi, Gino (Applicazioni e Ricerche Scientifiche, Milan. Univ., Milan). Phys. Fluids, 9: 343-50(Feb. 1966).**

Rayleigh's problem for a viscous, compressible, conducting fluid is studied. Linearization yields a solution which is equal, in first approximation, to the one for the incompressible, viscous, conducting fluid. Compressibility effects are then taken into account by evaluating the solution of the pressure equation. This equation contains a complicated source term depending upon the previously found expressions for the velocity parallel to the plate and the induced magnetic field. Due to the complicated expression of the source term, an operational solution of the equation is quite intractable. Thus, numerical techniques are used. The equation is solved by a finite-differences method, which is shown to be numerically stable. Comparisons are made between the pressure profile and Hanin's graphs. (auth)

15579 TIME-DEPENDENT CORRELATIONS IN A MAXWELL GAS. **Ranganathan, S.; Yip, Sidney (Cornell Univ., Ithaca, N. Y.). Phys. Fluids, 9: 372-9(Feb. 1966).**

The Fourier transform of the time-dependent density-density correlation function is calculated from the linearized Boltzmann equation for Maxwell molecules. The initial value problem is solved numerically for a small density disturbance. The results are compared with relaxation-time kinetic models, and it is found that the triple-relaxation time model with eigenvalue ordering gives good agreement for all wavelengths and frequencies. Similar macroscopic responses can also be calculated with appropriate changes in the initial conditions. The heat-heat correlation function is considered as a specific example. (auth)

15580 BRILLOUIN SCATTERING BY GASES AS A TEST OF THE BOLTZMANN EQUATION. **Nelkin, Mark; Yip, Sidney (Cornell Univ., Ithaca, N. Y.). Phys. Fluids, 9: 380-1(Feb. 1966).**

The frequency distribution of monochromatic light scattered by a gas is proposed as an experimental test of kinetic theory away from the hydrodynamic regime. The phenomenon is closely analogous to high-frequency sound propagation and is governed by the same linearized Boltzmann equation. The problem can be posed as an initial value problem in an infinite medium. The exact numerical solutions for Maxwell molecules previously obtained give an estimate of the results to be expected. (auth)

15581 ALFVEN WAVE GENERATION IN A SPHERICAL SYSTEM. **Motz, Robin O. (Columbia Univ., New York). Phys. Fluids, 9: 411-12(Feb. 1966).**

Magnetohydrodynamic waves were generated by small amplitude oscillation of a dielectric sphere in a mercury-filled spherical shell in a longitudinal magnetic field. The velocity of the waves was determined by creating a standing wave resonance. The waves were moving with Alfvén velocity. (auth)

15582 EVIDENCE AGAINST AN INTERMEDIATE STATE BETWEEN HeI AND HeII. **Kierstead, Henry A. (Argonne National Lab., Ill.). Phys. Rev. Lett., 16: 343-4 (Feb. 28, 1966).**

It is shown that some experiments have defined the λ line at elevated pressures sufficiently close to rule out the possibility of two transitions a half millidegree apart. (D.C.W.)

15583 THE VISCOSITY AND ACOUSTIC IMPEDANCE OF LIQUID ^{3}He. **Betts, D. S.; Keen, B. E.; Wilks, J. (Oxford Univ.). Proc. Roy. Soc. (London), Ser. A, 289: 34-45(Dec. 14, 1965).**

Previous experiments have shown that at low temperatures the acoustic impedance of liquid ^{3}He under the saturated vapor pressure rises by about 10% below about 0.092°K. This rise is predicted by Landau's theory of a Fermi liquid. It comes about because, at sufficiently low temperatures, sound waves in liquid ^{3}He are propagated as a new mode, the so-called zero sound. The present experiments study the dependence on pressure of the temperature and magnitude of the transition in the impedance. The transition temperature is shifted from 0.092 to about 0.07°K on subjecting the liquid to a pressure of 12.5 atm, and the magnitude of the change considerably reduced. To interpret these results, measurements were also made of the viscosity as a function of pressure. (These give information about the thermal relaxation times in the liquid.) All the results are in accord with the theory of zero sound in a Fermi liquid. (auth)

15584 MASS AND ENERGY TRANSFER BETWEEN A CONFINED PLASMA JET AND A GASEOUS COOLANT [Thesis]. **Smith, Dean Leroy Jr. Ann Arbor, Mich., Univ. of Michigan, 1965. 153p.**

The mass and energy transfer between confined plasma and coolant gas streams was studied experimentally. An 11-millimeter-diameter axially symmetrical plasma jet was introduced into a surrounding concentric, cocurrent flow of coolant gas. The resulting flow system was confined in a 27-millimeter-diameter quartz tube. Argon was used as the plasma gas at flow rates of 40 to 80 grams per minute with a net power input to the gas of approximately 3 kilowatts. Nitrogen was used as the coolant gas at flow rates of 2 to 20 grams per minute. The plasma and coolant mixing took place at atmospheric pressure. The temperature profiles present in the mixing region were determined by optical spectrographic methods. Both the electronic excitation temperature of the argon atoms and the rotational temperatures of the nitrogen molecules were determined. The compositions and axial velocities present in the plasma-coolant mixing region were determined by sampling probe methods. The measured nitrogen temperatures were found to be much lower than the argon temperatures present at the same point in the flow. The difference could be explained on the basis of the inability of argon atoms to give their translational energy directly to the rotational modes of nitrogen molecules. The composition profiles indicated that direct induction of coolant into the high-velocity plasma jet and the formation of a recirculation eddy greatly increased the mixing of plasma and coolant. Mass and energy balances computed at various axial cross sections in the mixing region indicated that from ½ to ¾ of the nitrogen coolant was present in the high-temperature region of the flow but that this coolant fraction contained less than 10% of the total energy present. The solution of the differential equation describing argon-nitrogen diffusion indicated that flow and turbulent diffusion controlled the mixing of the plasma and coolant. From a plasma jet chemical reaction standpoint, the results of this study indicate that the mixing with the plasma of a reactant injected into a plasma jet reaction chamber would be very rapid but that the internal energy modes of the reactant molecule would not be fully excited during the short residence time in the high-velocity flow. (Dissertation Abstr.)

15585 TWO-DIMENSIONAL MAGNETOHYDRODYNAMICS [Thesis]. **Salathe, Eric Paul. Providence, Brown Univ., 1965. 81p.**

The linearized theory of compressible, dissipative magnetohydrodynamic flow is studied. No restriction is placed on viscosity, thermal or electrical conductivity, or the orientation of the applied magnetic field with respect to the

free stream velocity. An asymptotic description of the fundamental solutions is obtained, valid for distance from the origin large compared to mean free path. These fundamental solutions also provide the asymptotic flow field for the flow past a body when the distance from the body is large compared to the body size. Complete solutions for the non-dissipative case are first obtained. Two distinct types of flows occur. These are doubly hyperbolic (four characteristics) and hyperelliptic (two characteristics superimposed on an elliptic field). In each regime the non-dissipative limit of the wake also appears (i.e., particle paths are characteristics). In the dissipative case these characteristics appear as lines of maximum asymptotic behavior—that is lines across which the flow variables change rapidly. The neighborhood of each characteristic is analyzed and a detailed description of the flow in this region is obtained. One feature of the analysis is that these solutions are uniformly valid from the doubly hyperbolic into the hyperelliptic regime, or through "magneto-sonic" conditions, where the characteristic disappears. In the limit as the dissipation approaches zero the non-dissipative solution is obtained. However, the limit is nonuniform, in the sense that no matter how small the dissipation it is possible to go far enough from the origin that the flow is essentially dissipative. (Dissertation Abstr.)

Geophysics

Refer also to abstract 15634.

15586 (AD-620243) A POSSIBLE EXPLANATION OF THE APPLETON ANOMALY OF THE F2 LAYER. II. A MODEL WITH UNEQUAL HORIZONTAL VELOCITIES. Windle, D. W.; Kendall, P. C. (Sheffield Univ. (England). Dept. of Applied Mathematics). 1965. Contract AF-EOAR-6474. 14p. (AFCRL-65-621). CFSTI $1.00 cy, $0.50 mn.

The effects of an assumption that the neutral air in the F2 layer is set in horizontal motion by the ionization are examined. It is assumed that the horizontal velocity of the neutral air is a fixed proportion of the horizontal velocity of the ionization. The model F2 layer discussed is in equilibrium at noon, and there is no electrodynamic drift. The earth's magnetic field is assumed to be that of a geocentric dipole whose axis coincides with the earth's axis of rotation. The sun's radiation is assumed to be symmetrically incident on the earth. It is found that the theoretical enhancement of the equatorial trough in N_m, discovered when the horizontal velocities are the same is only present to a marked degree when the horizontal velocities differ by 2.5% or less. However, although moderate induced horizontal winds may have little effect on the shape of the equatorial trough, they do affect the overall magnitude of N and N_m by a factor which may be as large as three. (TAB)

15587 (AD-620244) ON THE MAGNETOHYDROSTATIC CAVITY FORMED ROUND A SYSTEM OF LINE CURRENTS IN AN INFINITELY CONDUCTING ATMOSPHERE; A TWO DIMENSIONAL CONFIGURATION. Downs, Angela M.; Hewson-Browne, R. C.; Deirmendjiana, Astrik (Sheffield Univ. (England). Dept. of Applied Mathematics). May 1, 1965. Contract AF-EOAR-6474. 27p. (AFCRL-65-622). CFSTI $2.00 cy, $0.50 mn.

A fluid of infinite electric conductivity without an internal magnetic field and at uniform pressure is in equilibrium outside an infinitely long irregular cylindrical cavity. The cavity is prevented from collapsing by the magnetic field of a finite number of line currents parallel to the axis of the cylinder. The systematic method of solution of this problem is given in the case when the trace of the cavity is a single, simply connected region. The character of the solution is governed by the number of magnetic neutral points inside the cavity, as well as the nature of the magnetic singularities. The method is demonstrated by considering the case of two unequal line currents and the case of a dipole with equal and oppositely-directed line currents at equal distances on either side. It is shown that the solution can be extended to cases when the external hydrostatic pressure is nonuniform. As examples, the cases of a line current and a line dipole immersed in an exponential atmosphere are considered. (TAB)

15588 (AD-620682) A ROCKET BORNE AIR DENSITY MEASUREMENT SYSTEM UTILIZING ELECTRON-BREMSSTRAHLUNG: DESIGN AND DEVELOPMENT. Scientific Report No. 1, September 1961-July 1965. Sellers, Bach; Ziegler, Charles A. (Parametrics, Inc., Waltham, Mass.). Contract AF19(628)-5068. 89p. (AFCRL-65-507). CFSTI $3.00 cy, $0.75 mn.

A system that was developed for the measurement of air density at 100 to 200 km is described, in which the bremsstrahlung x rays that are produced by the injection of an electron beam into the atmosphere are detected. An analysis of the system is presented, and some experiments by which the theoretical predictions were verified are summarized. (D.C.W.)

15589 (ASE-1125) MEASUREMENTS OF LOW ENERGY ELECTRON PRECIPITATIONS ASSOCIATED WITH AURORAL DISTURBANCES AND TRAPPED RADIATION BELTS. Final Report, March 1, 1963-September 31, 1965. Reidy, William P.; Sinnamon, Gerald F.; Ruby, Peter R. (American Science and Engineering, Inc., Cambridge, Mass.). Nov. 12, 1965. Contract AF19(628)-2814. 134p. (AFCRL-65-856). CFSTI.

An electrostatic analyzer that is designed to measure the energy and angular distribution of electrons in the regions covered by a satellite in a high elliptical orbit is described. The operation and calibration of the instrument are outlined, together with its integration into the satellite. Integration of an instrument payload into the Astrobee 200 rocket system is described, and some measurements of auroral electron energy spectra are summarized. (D.C.W.)

15590 (NASA-TN-D-3086) SOLAR CYCLE EFFECTS ON INNER ZONE PROTONS. Blanchard, R. C.; Hess, W. N. (National Aeronautics and Space Administration, Greenbelt, Md. Goddard Space Flight Center). Feb. 1966. 34p. CFSTI $2.00 cy, $0.50 mn.

Solar cycle variations of the proton population of the inner radiation belt are calculated. The analysis includes proton energies from 10 to 700 Mev, field lines from 1.2 to 1.6 earth radii, and appropriate values of field strength. An averaged atmospheric model is constructed in terms of B (flux density in gauss) and L (earth radii) coordinates which represents the average proton number density that trapped particles would encounter. The averaging process includes diurnal, longitudinal, north-south, and "bounce" averaging. The time dependence of the atmospheric model is constructed for the current cycle using averaged information of the 10.7-cm solar flux of the recent past. Proton flux spectra for solar minimum and solar maximum are calculated from the particle conservation equation. Transient proton spectra and time histories are presented showing the dynamical behavior of trapped protons when influenced by the fluctuating atmosphere and a variable source. The results indicate that in the region of B-L space corresponding to minimum altitudes of 300 to 800 km, the proton flux is changed appreciably from solar maximum to solar minimum where solar minimum is the larger. Calculations indicate a change in the nature of the proton spectra where the spectra become peaked at some energy level depending on the time in the cycle and position in space. Comparisons are made with available data. (auth)

15591 (RM-4858) EQUATORIAL TRANSMISSION OF GEOMAGNETIC MICROPULSATIONS THROUGH THE IONOSPHERE AND LOWER EXOSPHERE. Field, E. C.; Greifinger, C. (RAND Corp., Santa Monica, Calif.). Feb. 1966. 29p.

The propagation of hydromagnetic waves at altitudes below about 2000 km is considered. The case of plane-wave propagation in the vertical direction, is treated, and the geomagnetic field is assumed to be horizontal (equatorial propagation). The propagation equations are derived and

are discussed in detail. A physically realistic analytic representation of the medium permits a solution of the wave equation in terms of known functions. Analytic expressions for the magnetic transmission coefficients are derived, and numerical results are given and are compared with experiments. The transmission coefficients are shown to exhibit resonances, although for daytime conditions the resonant peaks are much less pronounced than those found earlier for vertical polar propagation. Low and mid-latitude daytime observations seem to exhibit a resonant structure more characteristic of polar than of equatorial propagation. Some possible reasons for this are suggested. Further, due to the relatively greater opacity of the ionosphere at low latitudes, the daytime transmission coefficients fall off with increasing frequency much more rapidly than did those computed for high latitudes. On the other hand, the nighttime equatorial coefficients have many of the strong resonance characteristics of the polar ones. This diurnal behavior is in good agreement with the nocturnal appearance of certain classes of low and mid-latitude geomagnetic fluctuations. (auth)

15592 AXISYMMETRIC PLASMASPHERE RESONANCES: TOROIDAL MODE. Radoski, Henry R. (Boston Coll., Weston, Mass.); Carovillano, Robert L. Phys. Fluids, 9: 285-91(Feb. 1966).

The usual magnetohydromagnetic approach is used to investigate axisymmetric perturbations in a plasma permeated by a static dipole field. The model plasmasphere used has stationary, perfectly reflecting boundaries concentric with the dipole, and the plasma density is assumed to be spherically symmetric. The poloidal wave equation is reduced to a hierarchy of coupled differential equations in the radial variable. The toroidal wave equation is solved exactly using a density law which gives a good order of magnitude fit to recent whistler data. Because the extent of the plasma is finite, the eigenperiods are everywhere finite, including the poles. The stretched string model of vibrating lines of force is derived using the Wentzel-Kramers-Brillouin approximation, which fortuitously gives the exact periods for the density law utilized. Two unusual results are the prediction of shorter peroids in the polar zones than at some high middle latitudes and discontinuous eigenperiods across the line of force which just grazes the outer plasma boundary. A general discussion of the results and the special significance of the toroidal and poloidal modes because of their symmetry is provided. (auth)

15593 ORIGIN OF RADIATION BELTS. Gintzburg, M. A. (Inst. of Terrestrial Magnetism, Moscow). Phys. Rev. Lett., 16: 327-9(Feb. 21, 1966).

The acceleration of solar plasma electrons to energies of 30 to 100 kev is discussed. (D.C.W.)

15594 SYSTEMS FOR THE DETECTION AND IDENTIFICATION OF NUCLEAR EXPLOSIONS IN THE ATMOSPHERE AND IN SPACE. Dickinson, H. (Office of the Secretary of Defense, Washington, D. C.); Tamarkin, P. Proc. IEEE (Inst. Elec. Electron. Eng.), 53: 1921-34(Dec. 1965).

A qualitative perspective is given of problems encountered in designing systems for the detection and identification of nuclear explosions above the earth's surface. Pertinent physical phenomenology is summarized; detection techniques are explained briefly; effects of natural backgrounds are mentioned; system requirements are discussed; a summary comparative table is presented which incorporates these various considerations. (auth)

15595 THE VELA SATELLITE PROGRAM FOR DETECTION OF HIGH-ALTITUDE NUCLEAR DETONATIONS. Singer, Sidney (Los Alamos Scientific Lab., N. Mex.). Proc. IEEE (Inst. Elec. Electron. Eng.), 53: 1935-48(Dec. 1965). (LA-DC-7508).

The Vela satellite high-altitude test detection system contains x-ray, gamma-ray, and neutron detectors which sense the radiations generated by a detonation in space. The satellites also contain background radiation monitors. Problems involved in the design of the system are reviewed, and a description of the instruments is given. Three pairs of spacecraft are currently in orbit, and the detection systems are operating essentially as expected. A survey of the characteristics of the far magnetosphere and its environs, as determined from the background radiation monitors, is also presented. (auth)

15596 VELA SATELLITE SYSTEM DETECTOR ELECTRONICS. Glore, J. P.; Aiello, W. P. (Los Alamos Scientific Lab., N. Mex.). Proc. IEEE (Inst. Elec. Electron. Eng.), 53: 1949-58(Dec. 1965). (LA-DC-7512).

The block diagrams of detector electronics used in the Vela Satellite Program are discussed. The auxiliary ground equipment used in conjunction with these instruments is mentioned along with details on the design of two circuits more commonly used in the Vela Satellite detectors. (auth)

15597 A MODULAR SYSTEM OF LOGIC FOR THE VELA SATELLITE PROGRAM. Goldrick, W. B.; Thompson, F. E.; Myre, W. C. (Sandia Lab., Albuquerque, N. Mex.). Proc. IEEE (Inst. Elec. Electron. Eng.), 53: 1959-69(Dec. 1965).

A description is given of the system of logics used to provide on-board processing of data from a system of nuclear test detection instruments so that only significant information is relayed to earth. Particular emphasis is placed on some of the design techniques used to ensure long life and conserve power and weight. A discussion of the results of these efforts to date is included. (auth)

15598 REDUNDANCY DESIGN FOR THE VELA SPACECRAFT. Noneman, E. M.; Maxey, T. J. (TRW Space Tech. Lab., Redondo Beach, Calif.). Proc. IEEE (Inst. Elec. Electron. Eng.), 53: 1969-81(Dec. 1965).

Various redundancy tradeoffs with respect to weight, power, reliability, and testing ability are discussed for the Vela spacecraft. The types of redundancy considered were complete circuit, standby automatic switchable, standby command switchable, and fully automatic. Complete circuit redundancy was rejected because of weight and power limitations. Standby automatic switchable redundancy was rejected because of possible failure modes and complexity of the automatic detection circuits. Fully automatic redundancy was applied to those portions of the system where a failure would cause loss of the mission. Standby command switchable redundancy was applied to those portions of the system where a failure could be detected and corrected by command switching. The final redundant system is compared with a nonredundant system to indicate the additional weight and power required to accomplish the redundancy design. (auth)

15599 COMPUTER SIMULATION OF SATELLITE SYSTEMS. Lukasik, S. J. (Stevens Inst. of Tech., Hoboken, N. J.); Scholz, L. C. Proc. IEEE (Inst. Elec. Electron. Eng.), 53: 1981-8(Dec. 1965).

A digital computer program is described that simulates the physical characteristics of the Vela satellite system for the detection of nuclear detonations in space. The program consists of a modular set of subroutines that calculate the output of a nuclear device, the transport of the radiation to each sensor, and the contribution of each sensor output response to the transmitted data word from each satellite. Stochastic elements in the system such as the various event-satellite configurations, background radiation conditions, and data word transmission errors are included in the simulation. The ensemble of data words resulting from a number of replications under statistically identical-system-event conditions yields probabilistic information about the detection capability and false alarm rate of the system. The latter measures of system performance can be investigated by means of a flexible set of decision criteria subroutines that enable the user to investigate the effect of applying to the calculated data various criteria to determine when a sensor can be said to have reported an event and when the systems as a whole can be said to have reported an event. (auth)

15600 STATISTICAL ANALYSIS OF SPACECRAFT REPLENISHMENT. Modesitt, G. E. (Rand Corp., Santa Monica, Calif.). Proc. IEEE (Inst. Elec. Electron. Eng.), 53: 1989-93(Dec. 1965).

A statistical analysis of the number of launches required to establish and maintain a system of several spacecraft is made, based on the assumption that replenishment launches can be effected immediately after failure. (auth)

15601 NUCLEAR EXPLOSION PHENOMENA AND THEIR BEARING ON RADIO DETECTION OF THE EXPLOSIONS. Pierce, E. T. (Stanford Research Inst., Menlo Park, Calif.) Proc. IEEE (Inst. Elec. Electron. Eng.), 53: 1994-2008(Dec. 1965).

The characteristics of nuclear explosions are discussed. It is shown that nuclear events can create radio noise signals, change the height distribution of existing ionospheric ionization, and produce fresh ionization; the last effect is the most important in radio detection. The effects of x rays, γ rays, neutrons, and radioactive debris in augmenting ionospheric ionization are considered in turn. The most significant increases are at altitudes of 60 to 100 km, and the consequent modifications to vlf propagation and to the absorption and phase of h-f signals traversing the region of enhanced ionization are examined. (auth)

15602 THE DETECTION OF DAYTIME NUCLEAR BURSTS BELOW 150 km BY PROMPT VLF PHASE ANOMALIES. Field, E. C. (Rand Corp., Santa Monica, Calif.); Engel, R. D. Proc. IEEE (Inst. Elec. Electron. Eng.), 53: 2009-17(Dec. 1965).

The detectability of daytime nuclear bursts via prompt vlf phase anomalies is examined theoretically. Detailed consideration is given to low-fission-yield bursts exploded at altitudes below about 150 km. The distribution of atmospheric ionization due to fission-decay gamma radiation is calculated for times up to a minute after the bursts. It is noted that, at the deposition altitudes of interest for daytime vlf detection, the distribution of ionization computed for a time of one second after the burst is typical of that which persists for some tens of seconds. By using these one-second values of ionization and by applying existing techniques, equivalent, nonuniform, sharply bounded, earth-ionosphere cavities are constructed. Currently used vlf propagation theory is then applied to compute the bomb-induced phase anomalies for various burst-transmission path configurations. Detection criteria, based upon phase changes which should be distinguishable from those caused by natural events, are chosen. The corresponding detection ranges (the smallest great-circle distance from the burst to the transmission path) for long daytime vlf transmission paths are computed. Numerical results, which show the detection ranges as functions of the height and magnetic latitude of a nominal 5-kiloton fission-yield device, are presented. The manner in which these ranges scale with fission yield is indicated. The detection ranges are shown to depend very strongly upon the burst altitude but quite weakly on other parameters. For very low bursts the ranges become extremely small while, for burst heights the order of 100 km or more, they are quite large. (auth)

15603 A COMPARISON BETWEEN SOLAR X-RAY EMISSION AND VLF SUDDEN PHASE ANOMALIES. Chilton, C. J. (National Bureau of Standards, Boulder, Colo.); Conner, J. P.; Steele, F. K. Proc. IEEE (Inst. Elec. Electron. Eng.), 53: 2018-26(Dec. 1965).

Very low frequency (vlf) sudden phase anomaly (SPA) data obtained during 1963 are presented for comparison with solar x-ray emission measurements made by Vela satellites during the same period. From the SPA data an estimate is made, for each of three flares, of the effective wavelength of monochromatic x rays that would have produced the same vlf phase effect as the actual x-ray emission. In addition, by using the x-ray intensity (flux density) measurements of the satellite data and the wavelength functions obtained from the SPA data, estimates are made of the effective recombination coefficients. Furthermore, it is indicated that the vlf phase anomaly produced by x rays from a high-altitude nuclear explosion can possibly be distinguished from that produced by x rays from a solar flare. (auth)

15604 ON THE USE OF VLF MEASUREMENTS FOR OBTAINING INFORMATION ON THE LOWER IONOSPHERE (ESPECIALLY DURING SOLAR FLARES). Crombie, D. D. (Inst. for Telecommunication Sciences and Aeronomy, Boulder, Colo.). Proc. IEEE (Inst. Elec. Electron. Eng.), 53: 2027-34(Dec. 1965).

Three types of vlf propagation measurements which can be used to determine some characteristics of the lower ionosphere are described. These methods are 1) determination of the field strength (and ideally the phase) of a continuous wave transmitter as a function of distance, 2) determination of the relative phase and amplitude of a broadband signal, such as an atmospheric, and 3) observing simultaneously the phase and amplitude of a continuous wave signal at a single point remote from the transmitter. The latter method is discussed in detail. Although it can not alone yield much information about the normal steady-state ionosphere, it can be used to investigate changes in the density distribution. Phase and amplitude variations observed during solar flares are used to deduce the corresponding D-region changes, both for a sharply bounded and for an exponentially varying model of the ionosphere. It is further suggested that the exponential model can be used to explain vlf observations made during polar cap absorption events, as well as the somewhat anomalous diurnal variation of vlf signals observed on equatorial paths. (auth)

15605 EFFECTS OF PROPAGATION ON THE HIGH-FREQUENCY ELECTROMAGNETIC RADIATION FROM LOW-ALTITUDE NUCLEAR EXPLOSIONS. Sollfrey, William (Rand Corp., Santa Monica, Calif.). Proc. IEEE (Inst. Elec. Electron. Eng.), 53: 2035-42(Dec. 1965).

The high-frequency electromagnetic pulse radiation from nuclear explosions presents a possible detection mechanism. The selective attenuation of the higher-frequency components of the pulse when it travels via ground wave is considered, and it is shown how the waveform is modified with distance. Effects of the height of the source are included. Propagation via sky wave is investigated, and it is demonstrated that ionospheric dispersion considerably stretches the pulse for reasonable propagation distances. The receiver bandwidth should be selected to match the ionospheric dispersion at the receiver frequency. (auth)

15606 PROPAGATION OF THE GROUND WAVE ELECTROMAGNETIC SIGNAL, WITH PARTICULAR REFERENCE TO A PULSE OF NUCLEAR ORIGIN. Johler, J. R. (Ionospheric Telecommunications Lab., Boulder, Colo.); Morgenstern, J. C. Proc. IEEE (Inst. Elec. Electron. Eng.), 53: 2043-53(Dec. 1965).

The physical phenomena of the theory of propagation of an electromagnetic pulse at low radiofrequencies are scrutinized from the viewpoint of detection systems. Methods for tagging a point in time on the pulse are described theoretically. The filter action of the propagation medium together with various select receiver filters is considered in the analysis. A particular electromagnetic pulse observed and recorded at a short distance from the source (44.6 km) is propagated theoretically to a great distance (>2000 km) as a ground wave. The behavior of the tagged point in time on the pulse is studied both as a function of distance and as a function of the conductivity of the ground. The computer method is also used to determine the attenuation vs distance function of the pulse. This study provides information of general interest on the subject of low radiofrequency pulse propagation. In addition, the results form a basis for the determination of the effects of ground conductivity on location finding systems. (auth)

15607 UTILIZATION OF RIOMETERS FOR THE DETECTION OF NUCLEAR EXPLOSIONS IN SPACE. Potts, B. C. (Rand Corp., Santa Monica, Calif.). Proc. IEEE (Inst. Elec. Electron. Eng.), 53: 253-8(Dec. 1965).

The detection of nuclear explosions in space by riometer measurement of the effects of explosion-induced ionization on the absorption of high-frequency cosmic noise is considered. The dependence of the riometer response on the

x-ray explosion characteristics, the rate of decay of the ionization, and the integration time constant of the riometer are determined. Maximum detection heights are then tabulated based on a criterion of a 1-db change in riometer response. (auth)

15608 GROUND-BASED OPTICAL DETECTION OF DEEP SPACE NUCLEAR DETONATIONS. Cunningham, S. P. (Rand Corp., Santa Monica, Calif.); Murray, B. C. Proc. IEEE (Inst. Elec. Electron. Eng.), 53: 2058-66(Dec. 1965).

Simple approximate expressions are developed to describe the ring of fluorescent light from x rays impinging on the atmosphere. The relative ranging capability of zenith-oriented detectors is then estimated as a function of effective collecting area, field of view, electronic bandwidth, burst angle, and atmospheric pulse broadening. Narrow fields of view comparable in width to the fluorescent ring are shown to afford greater ranging capability than wide ones for all events more than 10° above local horizon, even under hazy conditions; however, the advantage is at most a factor of two. Both photomultiplier and solid-state detectors are treated. Some consideration is given to the performance of a multistation network, each station of which uses a solid-state detector array fed by a large collecting mirror. Triangulation out to 10^4 or 10^5 km appears feasible and would allow an approximate determination of yield. (auth)

15609 THE LOS ALAMOS AIR FLUORESCENCE DETECTION SYSTEM. Westervelt, D. R.; Hoerlin, H. (Los Alamos Scientific Lab., N. Mex.) Proc. IEEE (Inst. Elec. Electron. Eng.), 53: 2067-72(Dec. 1965).

A nuclear explosion far from the earth is a strong source of thermal x rays that deposit their energy in the upper atmosphere and cause air fluorescence, which provides a method of detecting such explosions by ground instrumentation. Energy deposition occurs in the ionosphere over a region several tens of kilometers thick, but because the x-ray flux and the light emitted travel downward with the same velocity, the time smear along the direct line of sight to the explosion depends only on the x-ray source lifetime and on the stopping time of photoelectrons produced by the x rays. These times are short, and the effective deposition rate is high; along this line of sight, therefore, is observed a bright flash of light whose direction can serve to locate the explosion in space. If the sky is viewed by a wide-angle detector covering π steradians, a pulse rising in <1 microsecond and falling to half intensity in $\frac{1}{4}$ millisecond is obtained. A system for detection of this pulse in the presence of daylight was developed and is described. The range for detection is estimated to be $R = 10^5 \sqrt{Y_x}$ kilometers in daylight where Y_x is the thermal x-ray yield of the explosion in kilotons. At night the range is more than one order of magnitude larger. (auth)

15610 DETECTION OF HIGH-ALTITUDE EXPLOSIONS BY OBSERVATION OF AIR FLUORESCENCE. Donahue, T. M. (Univ. of Pittsburgh). Proc. IEEE (Inst. Elec. Electron. Eng.), 53: 2072-8(Dec. 1965).

X rays radiated from a nuclear explosion in space excite fluorescence of air molecules in the upper atmosphere. The fluorescence has a characteristic space-time signature which can be recognized from the ground even against a bright sky. The criteria determining detectability and range are discussed, along with a number of practical systems of detection. False alarms, caused mainly by lightning flashes, can cause excessive triggering of single-station detectors unless discrimination techniques are employed. They also compel reliance on a net of stations for reliable recognition of true nuclear explosion induced fluorescence. (auth)

15611 SIMPLIFIED NORMAL MODE TREATMENT OF LONG-PERIOD ACOUSTIC-GRAVITY WAVES IN THE ATMOSPHERE. Meecham, W. C. (Univ. of Minnesota, Minneapolis. Rand Corp., Santa Monica, Calif.). Proc. IEEE (Inst. Elec. Electron. Eng.), 53: 2079-87(Dec. 1965).

The effects of geometric dispersion on low-frequency mechanical waves generated by nuclear explosions are studied. This dispersion is the result of the stratification of the atmosphere. It is found that the pressure signal can be divided naturally into an early-arriving acoustic-gravity portion and a later acoustic portion. In general, both portions of the signal are inversely proportional to the range (geometric spreading included), although, at very great ranges, portions of the gravity wave fall off faster by $r^{-\frac{1}{2}}$; the effect of dispersion is to reduce the signal by $r^{-\frac{1}{2}}$. Most of the signal is composed of many propagating modes which, at a given time and range, will each demonstrate a characteristic frequency. A simplified treatment of this complicated model picture is presented. It is argued that a ray treatment for the higher-frequency portion is appropriate. It is shown that the frequency of the long-period signal increases with time. So long as the frequency of the received signal is less than the characteristic frequency of the initiating explosive impulse, it is found that the signal has a universal form for the fundamental mode. Such characteristics as yield, range, and phase velocity merely change the scaling of the signal. It is concluded that attenuation is probably not important for the low-frequency signals usually observed. (auth)

15612 TECHNIQUES FOR DETECTION OF HIGH-ALTITUDE NUCLEAR EXPLOSIONS. Jean, A. G.; Hornback, C. E.; Doherty, R. H.; Winkelman, J. R.; Moore, R. T. (National Bureau of Standards, Boulder, Colo.). Proc. IEEE (Inst. Elec. Electron. Eng.), 53: 2088-98(Dec. 1965).

Project Vela, on ground-based techniques for detecting geophysical effects produced by nuclear explosions at altitudes above about 20 km and in space, has been designated HANDS, for High-Altitude Nuclear Detection Studies. A substantial amount of experimental data exists on effects produced by high-altitude explosions, and theoretical predictions have been made of effects expected from explosions in space. The ability to record and identify these signatures is limited by a lack of knowledge of natural variations, especially those having fractional-second onset times. The objective of the HANDS is to develop methods for detecting nuclear explosion effects in the natural background. The experimental facility for collecting and processing background data from a collection of colocated geophysical sensors is described. (auth)

15613 STATISTICAL STUDIES ON THREE TYPES OF GEOMAGNETIC CONTINUOUS PULSATIONS. PART I. TYPE I pc (5 ~ 40 SEC). Saito, Takao (Tohoku Univ., Sendai). Sci. Rep. Tohoku Univ., Fifth Ser., 14: 81-106 (Dec. 1962).

Continuous and sinusoidal geomagnetic pulsations are classified into the following three types with respect to the period band by analyzing the world-wide IGY data and referring to results of investigations obtained by many researchers. I pc is consistent with the internationally decided so-called pc except for its period range (5 to 40 sec, peak intensity at 20 sec). Amplitude of II pc (40 to 150 sec, peak intensity at about 70 sec) shows first maximum at the auroral zones and second maximum at about ±50 degrees in geomagnetic latitude, while amplitude of III pc (150 to 900 sec, peak intensity at about 7 min) reaches its maximum at the auroral zones. Since II pc and III pc are different from I pc in diurnal and seasonal variation of periods, I pc is separately discussed. High correlation between the activity of I pc with daily solar radio emission at 1,000 Mc and outburst infers possibility of I pc as an indicator for both low and high energetic solar streamers. In accordance with the geographical distribution of I pc periods, altitudinal distribution of hydromagnetic barrier, in other words, the lower boundary of protonosphere around the earth is expected to be rather ruleless in latitudinal sense, though a very indistinct prolonging tendency of the period from the lower latitude to the higher latitude is recognized. The various types in diurnal variation of I pc activity at each station can be attributed to F2 control; the increase of f_0F2 activates the I pc. It is assumed that summer maximal type (S-type) and equinoctical maximal type (E-type) in the seasonal variation of I pc observed at each station every year is caused by the combination of F2

control and hydromagnetic disturbances far above the station by the solar wind which depends on the solar cycle, local time (earth's rotation), and season (inclination of the earth's rotational axis to the sun). (auth)

15614 THE SPIRAL DISTRIBUTION OF THE POLAR Es IONIZATION. Kamiyama, Hiroshi (Tohoku Univ., Sendai). Sci. Rep. Tohoku Univ., Fifth Ser., 14: 120-7 (Dec. 1962).

The IGY and IGC data from a number of ionospheric stations widely distributed over the northern hemisphere are analyzed with special reference to the sporadic E ionization in the polar region. Both from the statistical study and from the analyses of the individual cases, it is concluded that the Es ionization in the high latitudes shows a spiral distribution; the Es activity is maximum at 19^h local geomagnetic time at the geomagnetic colatitude of 20° and at 24^h at the colatitude of 30°. (auth)

15615 POLARIZATION OF THE LONG PERIOD GEOMAGNETIC PULSATION, pc5. Kato, Yoshio; Utsumi, Takeshi (Tohoku Univ., Sendai). Sci. Rep. Tohoku Univ., Fifth Ser., 15: 83-96(Mar. 1964).

The sense of the rotation of the vector diagram of the long period geomagnetic pulsation, pc 5 (the period is 150 sec–600 sec), which is observed in high latitude geomagnetic observatories, is studied. It is found that the sense of the rotation of the vector diagram of these pulsations is counterclockwise when these pulsations occur before the local noon of the station, on the other hand, the sense of the rotation is clockwise when these pulsations occur after the local noon. These characters are very distinct at College and Sitka, while these characters are clear at Point Barrow only when it is magnetically quiet days K = 0, 1 and 2. These long period puslations are considered as the isotropic hydromagnetic oscillation excited at the external boundary of the exosphere by the fluctuation of the solar wind and converted to the transverse mode of the hydromagnetic wave along the line of force of the geomagnetic field. Therefore these characters show the mechanism of the excitation of the hydromagnetic disturbance at the boundary of the exosphere, and they are explained if the isotropic hydromagnetic oscillations caused by the periodic external stress due to the fluctuation of the solar wind are considered. (auth)

15616 ON A POSSIBLE MECHANISM FOR THE RULES OF POLARIZATION OF pc5 GEOMAGNETIC PULSATIONS. Kato, Yoshio; Tamao, Tsutomu (Tohoku Univ., Sendai). Sci. Rep. Tohoku Univ., Fifth Ser., 16: 15-36(Feb. 1965).

With relation to the possible origin of the geomagnetic pulsations, the qualitative consideration on the interaction of the solar wind with the magnetosphere is given. As a possible mechanism for the polarization rules of the observed perturbation vector of pc5 pulsations, which show the counterclockwise rotation of polarization ellipse on the forenoon and clockwise on the afternoon sides in the northern hemisphere, the transverse hydromagnetic waves, caused by the fluctuations of the asymmetric radial stress of the solar wind, acting on the boundary surface of the magnetosphere on the daylight side are discussed. Using the cylindrical model it is shown that the proposed mechanism can explain the above mentioned polarization rules including some other characteristics of these pulsations. (auth)

15617 THE EFFECT ON THE GEOMAGNETIC MICROPULSATION OF THE SOLAR ECLIPSE OF 20 JULY 1963. Kato, Yoshio (Tohoku Univ., Sendai). Sci. Rep. Tohoku Univ., Fifth Ser., 16: 49-62(Mar. 1965).

The effect on the geomagnetic micropulsation of the total solar eclipse of 20 July 1963 was observed very distinctly at Northway, Alaska, in the auroral zone. The continuous geomagnetic micropulsations (pc 3) were observed almost every day at Northway. The direction of the principal axis of the vector diagram of these micropulsations changed very distinctly at the time of solar eclipse. This is due to the decrease of the electrical conductivity in the ionosphere at the time of solar eclipse and a brief estimation was made theoretically. (auth)

15618 THE EFFECT ON THE GEOMAGNETIC FIELD OF THE TOTAL SOLAR ECLIPSE OF 5 FEBRUARY 1962 AND THE CORPUSCULAR ECLIPSE OF THE SOLAR CORPUSCULAR BEAM ON THE SURFACE OF THE BOUNDARY OF GEOMAGNETIC CAVITY. Kato, Yoshio (Tohoku Univ., Sendai). Sci. Rep. Tohoku Univ., Fifth Ser., 16: 63-77(Mar. 1965).

In order to observe the effect on the geomagnetic field of the solar eclipse of February 5, 1962 at Lae, New Guinea, the geomagnetic field was observed using a field magnetometer and the geomagnetic pulsation was also observed using the induction magnetometer. While the magnetic storm with sudden commencement occurred at 19^h30^m, February 4 (150° E.M.T.) this magnetic storm still continued at the time of the solar eclipse of February 5. Therefore it is too complicated to study the effect on the geomagnetic daily variation of this solar eclipse. On the other hand the geomagnetic micropulsation accompanying this magnetic storm could be observed, and it is very interesting that the effect on this magnetic micropulsation of the solar eclipse was observed, that is, the direction of the principal axis of the vector diagrams of these geomagnetic micropulsations changed during the solar eclipse. This character is expected if the electrical conductivity in the ionosphere decreased at the time of eclipse as observed at the same place. On the other hand the zone of the totality of the corpuscular eclipse of the solar corpuscular beam of this storm on the surface of the magnetopause was calculated. It is very interesting that the effect of the corpuscular eclipse on the surface of the boundary of the geomagnetic cavity, whose radius is six earth radii, was observed too, and this effect is expected as the hydromagnetic disturbance excited on the boundary of the magnetic cavity due to the moon's shadow of the solar wind or the lunar hydrodynamic wake staying few hours on the same place on the boundary of the magnetopause. (auth)

15619 EFFECT OF THE ANISOTROPIC IONOSPHERE ON THE HYDROMAGNETIC OSCILLATIONS. Kato, Yoshio; Sato, Yoshiaki (Tohoku Univ., Sendai). Sci. Rep. Tohoku Univ., Fifth Ser., 16: 123-45(Mar. 1965).

The geomagnetic micropulsations with the period from about 120 to 600 sec which are observed in high latitude are considered as the standing oscillation of the geomagnetic field lines which pass through the stations in high latitude. The multiple partial reflections and transmissions of this primary wave can be expected at the boundary of the ionosphere at the high latitude. The power spectrum and polarization of this standing oscillation between the north and the south hemisphere, and the effect of the anisotropic ionosphere on these hydromagnetic oscillations were calculated. It is interesting that only the odd-mode oscillation is predominant if the source force acts symmetrically on the equatorial plane in the outer exosphere. The rotational sense of the primary wave is not influenced by the anisotropy of the ionosphere, and the local dependence of the sense of rotation of the vector of pc5 is not explained by the effect of anisotropy of the ionosphere. The amplitude of the disturbance produced by the primary HM-wave which has counterclockwise sense is larger than that of disturbance, produced by the primary HM-waves which have clockwise sense. (auth)

15620 DISTRIBUTION FUNCTIONS OF PARTICLE TRAJECTORIES IN PLAIN MAGNETIC FIELDS. Pfirsch, D. (Max-Planck-Institut fuer Physik und Astrophysik, Munich). Z. Phys., 190: 238-52(1966). (In German).

Solutions of Vlasov's equations are derived for a class of curved plain magnetic fields. These fields can be made approximately selfconsistent, i.e., they result approximately from the plasma currents. Electric fields are treated in a quasineutral approximation. Such solutions are of interest in the case of the collisionless shockwave observed at the earth's magnetopause. It is speculated in this connection that the shockwave may be explained by a turbulent state, which arises from the instabilities of the laminar flows. (auth)

15621 PROTONS AND ELECTRONS IN THE INNER RADIATION ZONE. Vette, James I. (Aerospace Corp.,

El Segundo, Calif.). 50p. (CONF-650711-54). ORINS. Gmelin, AED-CONF-65-200-1.

From AIAA 2nd Annual Meeting and Technical Demonstration, San Francisco.

The inner-zone proton fluxes have been stable over several years except at low altitudes. A proton model environment based on data extending from 1958–1963 is presented and compared with measurements. Energy spectra as a function of position are given. Recent satellite measurements have shown that Starfish electrons are decaying with apparent lifetimes that are energy dependent. Consequently the distribution and energy spectrum of these particles is considerably different than in 1962. Comparisons will be made with earlier electron maps to demonstrate these changes. Longitudinal variations at low altitudes produced by the loss of particles as they drift through the South Atlantic anomaly are discussed. Several representations of the flux maps are discussed including orbital integrations. (auth)

15622 OBSERVATIONS OF IONOSPHERIC IRREGULARITIES AND PLASMA RESONANCES BY THE FIXED-FREQUENCY TOPSIDE SOUNDER SATELLITE. Calvert, Wynne (National Bureau of Standards, Boulder, Colo.). 30p. (CONF-650422-17). ORINS. Gmelin, AED-CONF-65-118-56.

From American Geophysical Union, Program for Section of Seismology Annual Meeting, Washington, D. C.

The Explorer XX topside sounder is producing unique observations of ionospheric irregularities in electron density and of plasma-wave electrostatic resonances. The pattern of the echoes from the irregularities is consistent with elongation along the earth's field and arise by two mechanisms: scattering and ducting. Scatter irregularities are most often observed in sheets at high latitudes and are probably intimately associated with aurora. Duct irregularities, observed also at lower latitudes, are sometimes continuous between hemispheres and permit radio echoes from the conjugate reflection level. As the result of varying antenna attitude, the pattern of the resonance response is very complicated. While the patterns depend on gross changes in the conditions of observation, they are repeatable from day to day and give some insight into the excitation mechanism. (auth)

Gravitation, Quantum Mechanics, and Relativity Theory

15623 (MPI-PAE/P1.15/65) THE VARIATION OF THE ADIABATIC INVARIANT OF THE HARMONIC OSCILLATOR. Knorr, G.; Pfirsch, D. (Max-Planck-Institut fuer Physik und Astrophysik, Munich (West Germany)). Oct. 1965. 16p. Dep. mn.

The problem of the adiabatic invariant (or magnetic moment) of a harmonic oscillator, or of a gyrating particle in a homogeneous, time-varying magnetic field, is studied. The solution is given as an absolutely converging series, and some asymptotic results are discussed. (T.F.H.)

15624 ELECTROMAGNETISM AS AN ASPECT OF GEOMETRY? ALREADY UNIFIED FIELD THEORY–THE NULL FIELD CASE. Geroch, R. P. (Princeton Univ., N. J.). Ann. Phys. (N. Y.), 36: 147-87(Feb. 2, 1966).

The already unified field theory of Rainich-Misner-Wheeler is extended to include null electromagnetic fields. This generalization involves two difficulties: the imposition of new integrability conditions on the complexion in the nonnull regions, and the actual determination of the electromagnetic field in the null regions. These difficulties are surmounted: a prescription is given for determining in every case whether or not a given geometry (Riemannian manifold) arises from a solution of the Einstein-Maxwell equations. Only in a very special set of solutions containing null regions of four dimensions in space-time does the electromagnetic field not follow uniquely (up to a constant duality rotation) from the geometry. All such solutions are explicitly displayed. Hence, except in these latter very special cases, it is found that the electromagnetic field–even in the null case–leaves such a distinctive imprint on the geometry in which it lies that the electromagnetic field follows from the geometry. This remarkable fact–the basis of already unified field theory–is discussed. (auth)

15625 ON THE JWKB-APPROXIMATION FOR BARRIER TRANSMISSION. Soop, Mattias Arkiv Fys., 30: 217-29(1965).

For two special cases of transmission through a potential barrier the estimates of the matrix appearing in the method of N. Fröman and P. O. Fröman for studying the JWKB approximation are compared with the corresponding exact matrix. Certain formulas (symmetry relations) valid for a symmetric barrier are given. (auth)

15626 THE POST-NEWTONIAN EQUATIONS OF HYDRODYNAMICS IN GENERAL RELATIVITY. Chandrasekhar, S. (Univ. of Chicago). Astrophys. J., 142: 1488-1512(Nov. 15, 1965).

The standard Eulerian equations of hydrodynamics are generalized to take into account, consistently with Einstein's field equations, all effects of order $1/c^2$. It is further shown that these post-Newtonian equations allow integrals of motion which are entirely analogous to the Newtonian integrals that express the conservation of mass, linear momentum, angular momentum, and energy. The continued validity of these conservation laws enables a consistent definition of "mass," "momentum," and "energy" in the framework of the post-Newtonian theory. Besides the equations of motion, an appropriate tensor form of the virial theorem is also derived. (auth)

15627 THE POST-NEWTONIAN EFFECTS OF GENERAL RELATIVITY ON THE EQUILIBRIUM OF UNIFORMLY ROTATING BODIES. I. THE MACLAURIN SPHEROIDS AND THE VIRIAL THEOREM. Chandrasekhar, S. (Univ. of Chicago). Astrophys. J., 142: 1513-18(Nov. 15, 1965).

The post-Newtonian effects of general relativity on the equilibrium of uniformly rotating bodies are considered with the aid of a suitably generalized version of the classical tensor virial theorem. An exact relation exhibiting the relativistic effects is obtained; and it shows that, if the figure of equilibrium is approximated by a spheroid, the effect of general relativity is to attribute to the spheroid a larger angular velocity than the Newtonian value. (auth)

15628 DIRAC'S δ FUNCTION AND THE DISTRIBUTION THEORY. Montvay, Istvan (Lorand Eoetvoes Univ., Budapest). Fiz. Szemle, 15: 339-42(Nov. 1965). (In Hungarian).

Dirac's δ function is often cited in discussions concerning the role of mathematics and physics, being used to support opposite arguments on the imprecise application of exact mathematical concepts. A study of the development of quantum mechanics on the basis of Dirac's contributions seems to indicate that mathematical precision has been sacrificed in order to extend the validity of the concept and to simplify it. However, there are deeper interrelations behind the formal elegance and the simplicity of this expression; it took nearly forty years before it was possible to indicate Dirac's imprecision by an exact mathematical derivation. The distribution theory, developed by Laurent Schwartz, is reviewed, pointing to its application for determining the charge distribution. The Wightman distributions are of special interest to the quantum space theory. It is shown that Dirac did not only find intuitively the most suitable form to express quantum mechanical correlations but by using the δ function, he contributed greatly to the development of the distribution theory. (TTT)

15629 STRUCTURE OF SPACE AND THE FORMALISM OF RELATIVISTIC QUANTUM THEORY. [PART] III. Ahmavaara, Yrjoe (Univ. of Turku, Finland). J. Math. Phys. (N. Y.), 7: 197-201(Feb. 1966).

The elastic scattering of two scalar particles having equal masses is considered in the formalism of relativistic quantum theory over a Galois field GF(q). The scat-

tering function σ determining the cross section is introduced. It is determined by the geometrical relations of Euclidicity, to be imposed on observable 4-momenta in a finite geometry. Thus the requirement of Euclidicity of observable 4-momenta can be considered as the counterpart, in a finite geometry, of the requirement of the analyticity of the invariant amplitude used in conventional S-matrix theory for the determination of the cross section. (auth)

15630 STRUCTURE OF SPACE AND THE FORMALISM OF RELATIVISTIC QUANTUM THEORY. [PART] IV. Ahmavaara, Yrjoe (Univ. of Turku, Finland). J. Math. Phys. (N. Y.), 7: 201-4(Feb. 1966).

The decay functions determining the lifetimes and the stability of particles in finite models of relativistic quantum theory are considered. (auth)

15631 AXIOMATIC FOUNDATIONS OF QUANTUM THEORIES. Guenin, Marcel (Princeton Univ., N. J.). J. Math. Phys. (N. Y.), 7: 271-82(Feb. 1966).

A formalism is developed on an axiomatic basis and is shown to contain as special cases classical mechanics, the usual quantum mechanics, as well as the quantum theory of systems with continuous superselection rules. The structure of the symmetries of a general physical theory is studied and a classification of observables is exhibited. (auth)

15632 ON THE SPACE-TIME BEHAVIOR OF SCHROEDINGER WAVEFUNCTIONS. Hunziker, W. (Princeton Univ., N. J.). J. Math. Phys. (N. Y.), 7: 300-4(Feb. 1966).

For the Schrödinger equation in R^1, with a potential $V(x_1 \ldots x_1)$ of the type considered by Kato, the following problem is solved; Given a monomial $M(x_1 \ldots x_1)$ of degree n in the coordinates, find sufficient conditions on the initial state u such that $Me^{-iHt}u$ is continuous in t and increasing in norm not faster than $|t|^n$ as $|t| \to \infty$. In the special case where $V(x_1 \ldots x_1)$ is a bounded C^∞-function with bounded derivatives, the result implies that $(u,t) \to e^{-iHt}u$ is a continuous mapping of $S(R^1) \times R$ onto $S(R^1)$, $S(R^1)$ being the Schwartz space of rapidly decreasing functions in the usual topology. (auth)

15633 METRICAL LATTICE AND THE PROBLEM OF ELECTRICITY. Lanczos, C. (Dublin Inst. for Advanced Studies. Ford Motor Co., Dearborn, Mich.). J. Math. Phys. (N. Y.), 7: 316-24(Feb. 1966).

A reinterpretation of Einstein's tetrad geometry leads to new results if one abandons the oversimplified picture of the vacuum as an almost empty Minkowskian manifold. The basic tetrad is identified with the four principal axes of the matter tensor which belongs to a strongly curved fourfold periodic Riemannian world. The macroscopic perturbation of the metrical lattice is investigated, corresponding to a mere rotation of the principal axes and assuming the quadratic action principle of general relativity. The perturbation lagrangian yields the scalar $E^2 - H^2$, (and thus the Maxwellian equations), although the basic manifold is strictly Riemannian, with a positive-definite line element. (auth)

15634 ORBITS IN A MAGNETIC UNIVERSE. Melvin, M. A.; Wallingford, J. S. (Florida State Univ., Tallahassee). J. Math. Phys. (N. Y.), 7: 333-40(Feb. 1966).

A cylindrically symmetric parallel bundle of magnetic lines of force, in equilibrium under their mutual gravitational attraction ("magnetic universe"), has recently received attention. While a Newtonian analysis suggests that the equilibrium is unstable, the complete general relativity analysis shows that the equilibrium is stable. This discrepancy may have to do with the unusually slow falloff of the gravitational field at large distances in this geometry. In order to understand the gravitational field of the static magnetic universe somewhat better, its timelike and lightlike geodesics (i.e., the orbits in it of electromagnetically neutral test particles with unit or zero rest mass) are studied. Since the density of magnetic flux—and energy and stress and, therefore, "gravitating mass"—is approximately uniform in the vicinity of the axis, the motion of test particles there is like that in a Newtonian simple harmonic oscillator field. "Vicinity" here means within a small fraction ρ of the range radius $\bar{a} = (6.96/B_0) \times 10^{24}$ cm (B_0 is the magnetic field on the axis measured in gauss). As is to be expected from the universality of the angular frequency ω_0 in the harmonic oscillator field and the relation: orbital velocity $\cong \omega_0\rho$, no motion can get too far from the axis. Otherwise the physical orbital velocity would exceed the speed of light. It is in this way that the strength of the attractive field, though it does not remain strictly of the harmonic oscillator type as one proceeds outward, implies that there is a critical straddling radius $\rho = 1/\sqrt{3}$. Circular or circular helical light tracks occur only at the critical radius, and with $B_0 = 10^5$ G, the time required for light to circumnavigate the critical circle is about 200 years. The cylinder marked out by this radius plays a unique limiting role: All particles, whether of zero or nonzero mass, and no matter what their initial positions and velocities (except in the one singular subcase of light tracks parallel to the cylindrical axis), must have their orbits lying wholly or partially within the cylindrical region $\rho < 1/\sqrt{3}$; hence the use of the adjective "straddling." Constants of motion which correspond closely to ξ-component linear momentum, angular momentum, and energy in Newtonian mechanics are defined. Bounds are placed on these dynamical constants and on the apsidal radii by the requirement that the range of motion be real. Finally, the magnetic universe is complete in the sense that "no news can enter or leave"—all orbits are of infinite duration. (auth)

15635 S-OPERATOR THEORY. II. QUANTUM ELECTRODYNAMICS. Pugh, Robert E. (Univ. of Toronto). J. Math. Phys. (N. Y.), 7: 376-84(Feb. 1966).

The formalism of S-operator theory is generalized to apply to all low-spin particles with particular emphasis on quantum electrodynamics. It is shown that only direct (nongradient) interactions are allowed, when spinor fields are involved. The Pauli interaction is explicitly shown to be forbidden. Problems of gauge invariance are discussed and commutation rules between the interpolating quantum fields and $\partial_\mu A_1^{in}(x)$ are derived. Finite S-matrix elements are easily calculated with complete convergence at each stage of the calculation. (auth)

15636 LIGHT FLUCTUATIONS DUE TO AN INTERGALACTIC FLUX OF GRAVITATIONAL WAVES. Zipoy, David M. (Univ. of Maryland, College Park). Phys. Rev., 142: 825-38(Feb. 25, 1966).

A formula is derived that gives the time dependence of the intensity of a light beam that has passed through an arbitrarily varying gravitational field. The formula is valid to second order in the gravitational field strength and is valid only in the geometrical-optical limit for the light beam. An application of the formula to the case where there is only a single source of gravitational field, such as a binary star system, shows that the effect is exceedingly small. Then the case where space is filled uniformly with gravitational radiation is considered. It is found that for a small light source at a distance of a few billion light years the largest effect that can be expected amounts to an intensity variation of a thousandth of a percent. At larger distances it is conceivable that there would be observable intensity fluctuations; however, the formulas are not valid at such great distances. (auth)

15637 GRAVITATIONAL WAVES FROM ISOLATED SOURCES. Bonnor, W. B.; Rotenberg, M. A. (Univ. of London). Proc. Roy. Soc. (London), Ser. A, 289: 247-74 (Jan. 4, 1966).

Gravitational waves from isolated, axially symmetric sources are studied using the metric proposed by Bondi and the double-series approximation method. (D.C.W.)

15638 RADIATIVE POLARIZATION OF ELECTRONS IN A MAGNETIC FIELD. Baier, V. N.; Katkov, V. M. (Novosibirsk State Univ., USSR). Yadern. Fiz., 3: 81-8 (Jan. 1966). (In Russian).

The electron polarization due to radiation when moving in a magnetic field is considered. (auth)

15639 OBSERVATIONS ON VACUUM POLARIZATION IN EXTERNAL FIELDS. Hasselberg, G. (Univ., Wuerzburg, Ger.). Z. Phys., 190: 110-28(1966). (In German).

The evaluation of the observable part of vacuum polarization for the electron-positron field interacting with an external electromagnetic field is discussed on the basis of a model field in one space dimension. The mathematically ambiguous vacuum expectation value of the charge-current density can be defined by two postulates following from gauge-invariance. In the light of these postulates the applicability of usually employed auxiliary prescriptions (regularization or causal connection between external and induced current) is re-examined. (auth)

15640 THE RELATIVISTIC MOTION OF AN ELECTRON IN EXTERNAL HOMOGENEOUS MAGNETIC FIELDS. Jannussis, A. (Democritus Nuclear Research Center, Athens). Z. Phys., 190: 129-34(1966). (In German).

The solution of the Dirac equation, for a free particle moving in a uniform external magnetic field is obtained by using the Schrauben-functions. In case the magnetic field tends to disappear, all physical quantities tend to the corresponding quantities of the completely free particle. (auth)

15641 MULTIPOLE FORMALISM FOR TEST PARTICLES IN GENERAL RELATIVITY [Thesis]. Porter, John Robert. Austin, Tex., Univ. of Texas, 1965. 50p.

The equations of motion are derived for a pole-dipole test particle from Einstein's gravitational field equations for vacuum. This is done using a modification of the method developed by Infeld and Schild for the derivation of the equations of motion for a single-pole particle. A particle is enclosed with a time-like world tube L and the field is specified only outside this tube. A test particle is defined in terms of a limiting process. The precise formulation of a pole-dipole test particle moving along the world line L in a background metric $g_{\mu\nu}(x^\rho)$ is obtained by considering a one-parameter sequence of metrics $\tilde{g}_{\mu\nu}(x^\rho,\lambda)$ defined on the differentiable manifold on which $g_{\mu\nu}(x^\rho)$ is defined and such that $\tilde{g}_{\mu\nu}(x^\rho,0) = g_{\mu\nu}(x^\rho)$. (A.G.W.)

15642 THE QUANTUM THEORY OF GRAVITATION. Kibble, T. W. B. (International Center for Theoretical Physics, Trieste, Italy). pp 885-910 of STI/PUB/117.

In the course of a review of the various approaches to the theory of gravitation, a field-theoretic framework is developed within which one can describe the phenomena of gravitation. It is pointed out that a quantized approach is needed to explain the case of gravitational collapse. (G.O.Y.)

Low Temperature Physics

Refer also to abstracts 14697, 15105, and 15123.

15643 (NASA-TN-D-3293) CURRENT DISTRIBUTION IN AN ARRAY OF SUPERCONDUCTING THIN FILMS. Skurnick, I. D.; Simmons, J. H.; Sass, A. R. (National Aeronautics and Space Administration, Cleveland, Ohio. Lewis Research Center). Feb. 1966. 15p. CFSTI $1.00 cy, $0.50 mn.

The conservation-of-fluxoid approach is used to derive the integral relations describing the current distribution in a general array of cylindrical London superconductors. This approach highlights properties of the kernel of the integral equation that permit the development of analytic solutions for a 2 by 2 array of closely spaced thin films of rectangular cross section. It was found that the current is distributed across the width of the film in a nonlinear, and nonsymmetric fashion, peaking at both edges. This peaking, in turn, dictates the switching characteristics of the system. It is shown that the dependence of the peaking on the separation distance between coplanar films can cause considerable variations in the critical current of the system I_c as this separation is varied from 1 to 20 times the film thickness. (auth)

15644 ON THE SUPERCONDUCTIVITY WITH PAIRS IN TRIPLET OF SPINS. Czerwonko, J. (Univ., Wroclaw, Poland). Bull. Acad. Pol. Sci., Ser. Sci. Math. Astron. Phys., 13: 681-6(1965).

A model hamiltonian, $H = H_0 - V$, is considered for a system of Fermi particles with momentum k and spin σ in terms of the creation and annihilation operators, $a^+_{k\sigma}$, $a_{k\sigma}$. A method for providing the asymptotic properties of the hamiltonian for the energy and correlation functions is discussed on the basis of the existence of macroscopic number of operators that commute with H, and the selection rule of averages. A simplified form for the gap equation is obtained. (L.B.S.)

15645 LIQUID HELIUM AND THE PROPERTIES OF FINITE BOSE-EINSTEIN ASSEMBLIES. Goble, D. F.; Trainor, L. E. H. (Univ. of Toronto). Can. J. Phys., 44: 27-43(Jan. 1966).

In order to explain certain properties of thin helium films, Ziman has proposed an ideal gas model in which the bulk liquid is treated as a collection of independent, Bose-Einstein assemblies each a few hundred angstroms in extent. An extensive numerical study is made of the thermodynamic properties of such finite assemblies. In particular, the specific heats of thin films were calculated on the basis of the model and the results compared with the experimental data of Frederikse. It is found that the model predicts a shift of the specific-heat maxima to higher temperatures as the film thickness is decreased, rather than to lower temperatures as required by the observations on actual helium films. The nature of the Bose-Einstein condensation in finite assemblies is discussed in some detail and some general conclusions are drawn concerning Ziman's model. (auth)

15646 VISCOSITY COEFFICIENTS AND THE PHONON DENSITY TEMPERATURE DEPENDENCE IN LIQUID ^{4}He. Webeler, R. W. H.; Hammer, D. C. (Lewis Research Center, Cleveland). Phys. Lett., 19: 533-4(Dec. 15, 1965).

The viscosity coefficient (Δ_1) of liquid ^{4}He was measured for temperatures between 0.375 and 1.050°K and was compared to theoretical values. The slope of the logarithmic plot of the smoothed experimental values of Δ_1 below 0.6°K gave a temperature dependence of $T^{4.0\pm1.0}$ for Δ_1 and for the phonon density. The results are in excellent agreement with the Landau expression for phonon density. (G.O.Y.)

15647 QUANTUM THEORY OF VORTEX RING FORMATION IN SUPERFLUID HELIUM. Pollock, F. (Stevens Inst. of Tech., Hoboken, N. J. Columbia Univ., Dobbs Ferry, N. Y.). Phys. Lett., 19: 538-9(Dec. 15, 1965).

A description of vortex ring formation behavior in superfluid helium is proposed. (G.O.Y.)

15648 SUPERCONDUCTIVITY IN FERROMAGNETIC ALLOYS. Bennemann, K. H.; Nakajima, S. (Univ. of Cambridge, Eng.). Phys. Rev. Lett., 16: 243-7(Feb. 7, 1966).

It is shown that the ferromagnetic ordering of the magnetic impurities in a super-conductor is strongly reflected in the density of states of the conduction electrons and thus could be detected by tunneling experiments. (G.O.Y.)

15649 OBSERVATION OF A "PELTIER" EFFECT IN A TYPE-II SUPERCONDUCTOR. Fiory, A. T.; Serin, B. (Rutgers, State Univ., New Brunswick, N. J.). Phys. Rev. Lett., 16: 308-10(Feb. 21, 1966).

The absorption and emission of heat were observed at a junction in superconducting In-Pb between a region in the flux-flow state and a region in which there is no flux flow. The direction of the electric current determined whether heat was emitted or absorbed. (D.C.W.)

15650 ENERGY SPACING OF GEOMETRICAL RESONANCE STRUCTURE IN VERY THICK FILMS OF SUPERCONDUCTING In. Tomasch, W. J. (Atomics International, Canoga Park, Calif.); Wolfram, T. Contract AT-(11-1)-GEN 8. Phys. Rev. Lett., 16: 352-4(Feb. 28, 1966).

The energy dependence of geometrical resonances in thick films of superconducting In was investigated. The

data were interpreted in terms of a standing-wave model involving interference between electron-like (or hole-like) states which are degenerate in energy, but which propagate with different velocities. (D.C.W.)

15651 SUBHARMONIC STRUCTURE IN Pb-Pb SUPERCONDUCTIVE TUNNELING JUNCTIONS. Rochlin, G. I.; Douglass, D. H. Jr. (Univ. of Chicago). Phys. Rev. Lett., 16: 359-61(Feb. 28 1966).

Subharmonic structure was observed in the tunneling characteristics of Pb–Pb junctions at voltages less than $2\Delta_{Pb}$. The structure was interpreted in terms of critical values of the energy gap (a relative maximum, minimum, or saddle point on the gap surface). (D.C.W.)

15652 THE EFFECT OF ISOTOPES ON LATTICE HEAT CONDUCTION. II. SOLID HELIUM. Berman, R.; Bounds, C. L.; Rogers, S. J. (Oxford Univ.). Proc. Roy. Soc. (London), Ser. A, 289: 66-80(Dec. 14, 1965).

The thermal conductivity of solid mixtures of the helium isotopes was determined from 1°K to near the melting temperatures. In the hexagonal close-packed phase, pure ^{4}He and three ^{4}He-rich mixtures were measured at three different pressures of formation (60, 90 and 140 atm) and pure ^{3}He and six ^{3}He-rich mixtures at a single pressure of formation (145 atm). The results are analyzed on the basis of Callaway's relaxation-time theory, and a consistent explanation is obtained if the relaxation rate for three-phonon normal processes is assumed to be proportional to ω^2T^2. Scattering of phonons by the isotopic impurities is greater than corresponds to the mass difference alone and the additional scattering is attributed to the effect of lattice strain around the impurity. Although the magnitude of this effect is considerably less than has been calculated, its variation with pressure is as predicted. These conclusions are supported by consideration of the behavior of the conductivity in the limit of low isotopic concentration, when the calculated conductivity is independent of the form of the relaxation rate for normal processes. (auth)

15653 EXCITATION SPECTRUM OF SUPERIMPOSED NORMAL AND SUPERCONDUCTING FILMS. de Gennes, P. G.; Mauro, S. (Faculte des Sciences, Orsay, France). Solid State Commun., 3: 381-4(Dec. 1965).

The excitations in a binary layer system with one superconducting film and one normal film under O magnetic field are studied. If the normal film is of finite thickness, an expansion of the density of states in powers of the order parameter $\Delta(\underline{r})$ does not converge (this singularity is interpreted as due to the existence of a non-O energy gap at all temperatures). On the other hand, a similar expansion for the tunneling characteristic I(V) does converge at sufficiently high temperatures (the most important excitations being then far above the gap). Results for I(V) are given for some simple situations with "dirty" films. (auth)

15654 GENERAL APPROXIMATION METHOD FOR THE FREE ENERGY FUNCTIONAL OF SUPERCONDUCTING ALLOYS. Eilenberger, Gert (Univ., Cologne). Z. Phys., 190: 142-60(1966).

The free energy of a superconductor in magnetic fields can be expressed in a simple manner by Green's functions, as shown in earlier works. These are functionals of gap parameter $\Delta(r)$ and vector potential $A(r)$; variations of these quantities yield generalized Ginzburg-Landau equations. A gauge invariant method is presented for the explicit calculation of free energy, with the presence of impurities. The method is based on a power expansion of the gauge invariant differential of $\Delta(r)$. Considerable reductions are obtained by the use of partial fraction decomposition of the matrix Green function, which possesses special zero-part characteristics. Vertex corrections can therefore be carried out by a homogeneous operation, which is outlined. The second power of the differential reproduces Tewort's results; furthermore, the summation of all terms quadratic in Δ results. The expression for the term quadratic in Δ of the free energy is given in the fourth power of the differential using the expression given by Tewort, as well as the gap equations used by Gorkow and Maki for the limiting cases of very pure and very impure superconductors. An implicit formula for H_{c2}, valid for arbitrary temperatures and collision times, is given. (tr-auth)

15655 THE THEORY OF NONHOMOGENEOUS SUPERCONDUCTORS [Thesis]. Silvert, William Lawrence. Providence, Brown Univ., 1965. 91p.

A variational principle is derived for calculating the properties of nonhomogeneous superconducting systems at finite temperatures. The quantity varied is the energy gap function occurring in the Gor'kov-Green's function formulation of the Bardeen-Cooper-Schrieffer theory of superconductivity, and it is shown that the correct solution of Gor'kov's equations is obtained by minimizing a form of the energy functional. A simple criterion for the existence of the superconducting state is also given. The procedure is illustrated by evaluating the transition temperatures of thin film systems in the limits of both long and short mean free path. The results are compared with previous experimental and theoretical work on thin films. (Dissertation Abstr.)

15656 A STUDY OF POSITION DEPENDENT SUPERCONDUCTIVITY BY THERMAL AND ELECTRICAL CONDUCTIVITY IN SUPERCONDUCTING FILMS [Thesis]. Seidel, Thomas Edward. Hoboken, N. J., Stevens Inst. of Tech., 1965. 120p.

Measurements of the thermal and electrical conductivity of plain films of Pb, In, and Sn, and multiple films of Au–Sn and Mn–Sn were made in a parallel magnetic field. The data on thick pure Pb expose the nature of surface superconductivity in Pb. By comparison, the lack of this effect in thick and rather pure In is noted. A simple but detailed and self-contained two-fluid analysis is presented to aid in interpreting the results in Pb. The experiment and analysis indicate that in pure Pb, the surface remains superconducting at temperatures below about 5.1°K for a magnetic field value just above the critical field of the thick film. The average width of the superconducting surface layer comes from the analysis and is about twice the BCS coherence distance of pure lead for each surface. The thermal data of Sn and Au–Sn multiple films are compared. The results show that the excitation spectra of the multiple film has considerably more low energy states and fewer high energy states than an ideal BCS superconductor with the same transition temperature. Finally, measurements of the thermal conductivity of Mn–Sn are consistent with the theoretical prediction that superconductors containing paramagnetic impurities have superconducting electronic thermal conductivity less than the normal state. (Dissertation Abstr.)

15657 AMPLITUDE DEPENDENT ULTRASONIC ATTENUATION IN SUPERCONDUCTING LEAD [Thesis]. Tittmann, Bernhard Rainer Michel. Los Angeles, Univ. of California, 1965. 196p.

An anomaly in the absorption of ultrasonic waves was found and investigated in superconducting lead. This anomaly consists of a strong dependence of the absorption on the amplitude of the ultrasonic waves. The amplitude dependence is only weakly present in the normal state. The effect is found to be strongly temperature-dependent, decreases as impurities are added to the crystal, and exhibits little or no change with frequency. Deformation and annealing have a pronounced effect on the anomaly. It appears that these characteristics can be understood in terms of a model, which is proposed here, based on the assumption of a strong interaction between the conduction electrons and the dislocations in the metal crystal. The presence of weakly pinned dislocations and their motion in the field of the sound wave is assumed. In the normal state, this motion is highly damped by the conduction electrons, and therefore the dislocations cannot contribute much to the ultrasonic absorption. In the superconducting region, this damping decreases with the same temperature dependence as the ultrasonic absorption by the electrons. Now the dislocations become free to move and therefore can cause an amplitude-dependent absorption by themselves.

The mechanism for this absorption is thought to be dislocation unpinning similar to that discussed by Granato and Lücke. (Dissertation Abstr.)

15658 MILLIMETER MICROWAVE STUDIES OF THE CRYSTALLINE ANISOTROPY OF THE SUPERCONDUCTING ENERGY GAP IN ALUMINUM [Thesis]. Thompson, William Alexander Jr. Pittsburgh, Univ. of Pittsburgh, 1964. 57p.

Microwave measurements were made of the temperature and frequency dependence of the absorption in superconducting single crystals of pure and silver-doped aluminum. The (100), (110), and (111) crystal faces were irradiated with polarized microwaves, and the absorption was measured calorimetrically. The results for each pure aluminum crystal face — when plotted as isotherms of surface resistance ratio vs photon energy — exhibited two rapid changes in slope, which were interpreted as being two different superconducting energy gaps about 10% different in value. These two gaps have small differences (maximum 4%) among the three crystal faces. The extrapolated pure aluminum gap values for T = 0°K were from 3.04 kT_c to 3.50 kT_c, where T_c was measured to be 1.175 ± .001°K. Two different nonmagnetic impurity levels were used, depressing the transition temperature 15 and 60 millidegrees, respectively. At the intermediate doping level, only one superconducting energy gap was found in the energy region where two gaps existed in the pure material. At the higher doping level, this single gap increases in energy and a second new gap is observed at a value 6% higher in energy. This new gap is interpreted (in the light of Anderson's theory of "dirty" superconductors and the detailed calculation resulting from his theory) as coming down in energy from a position in the pure material above our maximum experimental frequency. The gaps in the pure material were interpreted as belonging to different pieces of the Fermi surface with some small anisotropy with $\underline{k}$ direction within each zone. (Dissertation Abstr.)

15659 ULTRASONIC LONGITUDINAL WAVE ATTENUATION IN SUPERCONDUCTING TIN [Thesis]. Thomas, Robert Leighton. Providence, Brown Univ., 1965. 110p.

The attenuation of longitudinal ultrasonic waves was studied in superconducting tin samples as a function of temperature (2.19°K–1.1°K) and frequency (30–190 Mc/sec). Three single crystals, having resistivity ratios 300, 3000, and 30000 were investigated for propagation along the [001] and the [110] crystallographic directions. The temperature-dependent behavior of the ultrasonic attenuation was found to be consistent qualitatively with the theory of Bardeen, Cooper, and Schrieffer (BCS) for each crystal. Anisotropy in the energy-gap parameter of this theory between the two directions of propagation was demonstrated and was found to be in quantitative agreement with values quoted in the literature for the case $ql \gg 1$. It was found that the anisotropy in the energy gap persisted in the region $ql < 1$, and was nearly constant over a region ($0.25 < ql < 95$), in contradiction with predictions based upon the free electron model. The results suggested the importance of real metal effects upon the selectivity of the electron-phonon interaction for metals having a multiple-connected Fermi surface. (Dissertation Abstr.)

15660 LOW-TEMPERATURE THERMAL EXPANSION OF HOLMIUM AND ERBIUM SESQUIOXIDES FROM 300 deg K TO 94 deg K: CRYOFLASK AND CONTROL SYSTEM DESIGN [Thesis]. Mills, Norman David. Washington, D. C., Howard Univ., 1965. 39p.

Thermal expansion data for Ho_2O_3 and Er_2O_3 are provided; necessary design features, electronic and physical, for the cryoflask and control system are explained; and an effective recently developed method for the determination of lattice parameters, which uses only wavelength as a standard, is described. The thermal expansion characteristics of annealed, polycrystalline Ho_2O_3 and Er_2O_3, better than 99.9% pure, were determined from 300 to 94°K. The Singh x-ray back-reflection techniques were utilized. For the range covered the values of the average and "instantaneous" thermal expansion coefficients along with curves of the lattice parameter versus temperature for the range covered are reported. The lattice constant of Ho_2O_3 at 296°K was found to be 10.6023Å, and at 94°K a value of 10.5974Å was obtained. For Er_2O_3 the corresponding 300°K room temperature value was 10.5469Å, and at 102°K it was 10.5361Å. Both room temperature values agree with those of Dauben and Temple. Temperatures were measured with a thermocouple, (Au, 2.1 at. % Co vs Ag, 0.37% Au), calibrated by the National Bureau of Standards, Washington, D. C. Control of the temperature to better than 0.5°K was maintained by using a control system capable of achieving far closer control. The lattice constants were found to vary drastically over temperature increments small in comparison with increments of 100°K as are often found in expansion work done above room temperature. Ho_2O_3 exhibited negative expansion coefficients at two temperatures. Perhaps one or the other might be the Neel temperature. The Singh method for back-reflection x-ray determination of lattice constants consists essentially of measuring the two radii on the film corresponding to say $CuK\alpha_1$ and $CuK\alpha_2$, ascertaining the quadratic form of the appropriate Miller indices, inserting these values into a six-degree algebraic equation, and using a program for an IBM 1620 computer. (A.G.W.)

15661 AN EXPERIMENTAL TEST OF THE ONSAGER-FEYNMAN QUANTIZED VORTEX LINE THEORY OF ROTATING LIQUID HELIUM II INCLUDING THE MEASUREMENT OF THE MUTUAL FRICTION PARAMETERS B, B′, AND γ' [Thesis]. Linekin, David Maynard. Providence, Brown Univ., 1965. 115p.

The mutual friction parameters B and B′ in the theory of rotating liquid helium II were measured in the temperature range between 1.28° and 2.156°K, and the parameter γ' was measured at various rotational frequencies at 1.63°K. These experimental results support the Onsager-Feynman quantized vortex line hypothesis. The parameters B and γ' are measured by observing the attenuation of a second sound signal in a resonating cavity, opposite sides of which serve as second sound transmitters and receivers. If the resonator is made square in the x-y plane (the z axis being the axis of rotation), a resonant second sound wave in the x direction induces another resonant second sound wave in the y direction. The coupling of the two degenerate normal modes by rotation raises the degeneracy and splits the resonant frequency into two. B′ is measured by observing the amount of separation of the two resonant peaks on the frequency response curve at various rotational frequencies. The value of the mutual friction parameter B′ is measured as 0.4 at 1.28°K. It decreases to 0.2 at 1.63°K, and increases to 5 at 2.156°K. This is in agreement with the theory of Hall and Vinen near the λ-point. Measurements of the mutual friction parameter B reveal that it is 1.6 at 1.28°K, that it decreases to 0.70 at 1.79°K, and that it increases to 6 at 2.170°K. The experimental values are in agreement with the theory of Lifshitz and Pitaevskii at the lower temperatures and are in agreement with the theory of Hall and Vinen throughout the temperature range up to near the λ-point. The value of the mutual friction parameter γ' was found to depend upon the amplitude and the frequency of oscillation but not the frequency of rotation. The conclusion is made that neither the theory of Hall and Vinen nor the theory of Lifshitz and Pitaevskii is acceptable. Each theory includes an undetermined empirical constant in the calculations. Bablidze's hypothesis that the resonant second sound amplitude depends upon the balance between the formation of new vortex lines and the decay of existing vortex lines is strengthened by the similar results obtained at finite frequencies of rotation. (Dissertation Abstr.)

15662 DEPENDENCE OF THE CRITICAL CURRENTS IN SUPERCONDUCTING FILMS ON APPLIED MAGNETIC FIELD AND TEMPERATURE [Thesis]. Mydosh, John A. Hoboken, N. J., Stevens Inst. of Tech., 1965. 130p.

Measurements of critical currents were performed on planar and cylindrical films of tin of 650 to 2500 Å thick-

ness. Both pulsed currents (80 nanoseconds duration) and dc currents with stabilizing network were used. Close agreement was obtained for the dc data in the temperature dependence and approximate agreement in the magnitude of the critical current when compared with Bardeen's calculation as long as the stabilizing network was effective. The pulse measurements deviate from theory and the dc data for temperatures $T/T_c < .9$. Oscilloscope pictures of the transition indicate this deviation towards lower currents is not caused by usual Joule heating. Also eddy current heating in the contacts was ruled out by the use of completely superconducting contacts and the thinness of the films. This and other similar work with pulsed currents and fields would indicate that an entirely new mechanism is responsible for the discrepancy in fast pulsed critical currents. Critical current measurements were also taken with the superposition of external magnetic fields. The whole range from the critical current in zero field to the critical field as measured with a current of 100 μamp was covered. When the data are plotted as log i_c vs H_e, they form a series of similar curves as the temperature is lowered. The shape of these curves resembles that of the theoretical predictions of Ginzburg, but they differ in magnitudes. (Dissertation Abstr.)

15663 ON THE THEORY OF THE ABSORPTION OF SOUND IN SUPERCONDUCTORS OF THE SECOND KIND [Thesis]. Lee, Hyung Joon. Providence, Brown Univ., 1965. 112p.

A formula is derived for ultrasonic attenuation in type II superconductors. The Green's function method is used, and it is shown that the method will give the same result for a type I superconductor as that based on the quasi-particle method. The procedure is further illustrated by calculating the attenuation constant of a compressional wave in a type II superconductor with a spatially varying energy gap. The results are discussed, and some experiments are suggested to obtain information on the structure of type II superconductors. (Dissertation Abstr.)

15664 PHONON EFFECTS IN SUPERCONDUCTORS [Thesis]. Fibich, Moshe. College Park, Md., Univ. of Maryland, 1964. 100p.

Beside the gross features of a superconductor the electron-phonon (el-ph) interaction results in additional structures observed in various experiments. In tunneling experiments structure was observed in dI/dV v.s. V characteristics. Schrieffer et al showed, by solving the gap function for an assumed phonon spectrum (for lead), how the structure in the dI/dV results from the el-ph interaction. The structure is mainly centered around energies that equal multiples of the phonon frequencies above the gap. A similar method was applied to calculate structure on the radiation absorption curve, until now not observed in experiments. Deviations of the order of 2–5% from the Mattis-Bardeen absorption curve were found, at frequencies that are multiples of the phonon characteristic frequencies above the $2\Delta_0$. Since the electron spectrum in a superconductor has an energy gap, many processes are cut off below a certain energy. For example power absorption from radiation fields is zero for frequencies below $2\Delta_0$, where Δ_0 is the energy gap. More generally the superconducting electrons density of states is zero for energies below Δ_0. At finite temperatures, though low, thermally excited phonons are present. The idea of so-called phonon assisted processes in which a thermal phonon is absorbed, thereby enabling a process which otherwise is forbidden is considered. To consider these processes the gap function generalized to finite temperatures was obtained. This yielded a finite density of states for energies below Δ_0. It is strongly temperature-dependent and vanishes as the temperature goes to zero. The tunneling current observed by Taylor and Burstein at voltages smaller than $2\Delta_0$ was then obtained. This current is strongly temperature-dependent ($T^{7/2}$) and is roughly exponential in the voltage. Results are in fair agreement with experiment. (Dissertation Abstr.)

Neutron Physics

See also REACTOR TECHNOLOGY — Criticality Studies

Refer also to abstract 15572.

15665 (AWRE-O-103/65) THE CALCULATION OF GROUP AVERAGED NEUTRON CROSS SECTIONS. THE DEVELOPMENT OF GALAXY 3 FACILITIES IN S2 (FORTRAN) LANGUAGE FOR THE IBM-7030 (STRETCH) COMPUTER DURING 1965. Gately, P.; Parker, K.; Stanley, P.; Williams, D. V. J. (Atomic Weapons Research Establishment, Aldermaston (England)). Feb. 1966. 43p. Dep. BIS $1.20. HMSO 6s.

Some developments in the adaptation of the GALAXY 3 system of programs for use on the IBM 7030 computer are summarized. (D.C.W.)

15666 (CONF-660204-4) VARIATIONAL METHODS IN THE CALCULATION OF SPATIALLY DEPENDENT SPECTRA. Francis, N. C. (Knolls Atomic Power Lab., Schenectady, N. Y.). [1965]. Contract W-31-109-eng-52. 30p. Dep. mn. CFSTI $2.00 cy, $0.50 mn.

From American Nuclear Society Meeting, San Diego, Calif.

A discussion is presented of variational methods for cases in which the quantities studied are stationary with respect to the variable of interest. Resonance capture is not studied. After an introduction of the spatially independent problem, a specific thermal-energy-range spatially dependent neutron problem is discussed. The method is then applied to calculations of group constants for a multigroup Monte Carlo method, multigroup space-energy problems in slab geometry, and the use of overlapping groups in diffusion theory. (T.F.H.)

15667 (EIR-72) EXAKTE UND ANGENAEHERTE LOESUNGEN DER MEHRGRUPPEN-TRANSPORTGLEICHUNG IN EBENER GEOMETRIE [Theses]. (Exact and Approximate Solutions of Many-Group Transport Equations in Plane Geometry [Thesis]). Zumbrunn, Kurt (Eidgenoessische Technische Hochschule, Zurich (Switzerland)). 1965. 92p. Dep. mn.

The transport equations of the multigroup type were investigated using the Case method to determine how exact solutions of the transport equation could be found for simple problems. The methods used by Zelazny and Kuszell was simplified; the problem, to develop a function with respect to the complete system of the eigensolutions of the transport equation, can be solved explicitly because of the limitation to the multigroup equations. Approximate solutions of the same transport equation were derived in the P_n formalism (development of the angular dependent part of the neutron flux by Legendre polynomials) and some analogies to the exact Case method were shown. The solutions were then applied to the numerical solution of the Milne problem. Heavy ideal gases were used as the scattering model. The results found agree quantitatively with previous studies. (tr-auth)

15668 (EUR-2624.e) A ONE-GROUP COLLISION PROBABILITY CODE FOR CYLINDERS AND SLABS. Quiquemelle, B. (European Atomic Energy Community, Ispra (Italy). Joint Nuclear Research Center). Nov. 5, 1965. 38p. Dep. mn.

The code TIJ performs a numerical evaluation of the collision probabilities in concentric cylinders or slabs. For cell calculations several boundary conditions can be imposed, including a black inner region. Escape probabilities and Dancoff coefficients calculations are compared with other methods. The complete list of the FORTRAN program is given. (auth)

15669 (NASA-TN-D-3237) THERMAL NEUTRON FLUX PERTURBATION BY DYSPROSIUM–ALUMINUM FOILS IN WATER AND URANYL FLUORIDE–WATER SOLUTIONS. Shook, Donald F.; Bogart, Donald; Alger,

Donald L.; Mueller, Robert A. (National Aeronautics and Space Administration, Cleveland, Ohio. Lewis Research Center). Mar. 1966. 17p. CFSTI $1.00 cy, $0,50 mn.

Thermal neutron flux perturbation factors were measured for Al-Dy foils in water and uranyl fluoride-water solutions. The foils are representative of a type widely used for thermal neutron flux surveys. The measurements provide additional data for comparison with analytical calculations of foil perturbation factors in water. The experimental perturbation factors are in good agreement with the predictions of published calculational methods, except for the dimensionless generalization of Dalton and Osborn. (auth)

15670 (WAPD-TM-524) SHREW—A FORTRAN CODE FOR COMPUTING ANGULAR DISTRIBUTIONS, POLARIZATIONS AND TRANSPORT CROSS SECTIONS OF NEUTRONS SCATTERED BY SPINLESS TARGETS. Goldsmith, M.; Raspotnik, S. L. (Bettis Atomic Power Lab., Pittsburgh, Pa.). Dec. 1965. Contract AT-11-1-GEN-14. 13p. Dep. mn. CFSTI $1.00 cy, $0,50 mn.

SHREW uses phase shifts to compute elastic scattering cross sections employed in neutron transport codes. Polarizations and angular distributions, essential in checking the accuracy of the input phase shifts, are also calculated as is the modification of the transport cross section caused by neutron polarization. Output may be either printed or punched on cards which are used to prepare a ROC record. (auth)

15671 COHERENT EXTINCTION AND SECOND ORDER NEUTRON SCATTERING ON SINGLE CRYSTALS. Kuich, G.; Rauch, H. (Oesterreichische Hochschule, Vienna). Acta Phys. Austr., 20: 7-16(1965). (In German).

The accuracy of the experimental determination of neutrons scattered in the second order by a single crystal can be improved by the use of a suitable neutron transmission counter and a thick 1/v absorber. The calculation of the coherent extinction was treated using reciprocal lattices. From the calculated curves it is seen that through suitable twisting of the crystals the occurrence of coherent extinction can be prevented; this is essential in the use of crystal spectrometers for energy analysis. The results of measurements in which the crystal at constant Bragg positions was rotated around the plane normal are shown. (tr-auth)

15672 CLUSTER EXPANSION OF THERMAL AVERAGES IN SLOW NEUTRON SCATTERING IN REAL GASES. Sigmar, D. J. (Technische Hochschule, Vienna). Acta Phys. Austr., 20: 180-95(1965).

A special cluster expansion is developed for the inelastic scattering of neutrons in a target of temperature T. The quadrature of the graphs and the convergence of the expansion are briefly discussed. (J.S.R.)

15673 CONDITIONAL SEPARATION OF SPATIAL AND ANGULAR VARIABLES IN SOLVING THE NEUTRON TRANSPORT EQUATION. Khromov, V. V.; Slesarev, I. S. At. Energ. (USSR), 19: 540-2(Dec. 1965). (In Russian).

Separation of variables is used to solve the problem of determining the spatial-angular distribution of neutrons in a plane parallel plate with a single-velocity approximation. The variables are separated by defining the new functions X(x) and M(μ), and introducing these functions into the transport equation. In this manner the transport equation is reduced to a set of two equations, one of which is a simple algebraic equation. These two equations are solved by successive approximations. The percent error in calculating the critical half thickness of the plate is calculated and compared with the error found by other approximate methods of calculation. (TTT)

15674 FIRST-ORDER SOLUTIONS OF THE ONE-SPEED TRANSPORT EQUATION IN PLANE MULTIREGION GEOMETRIES. Mendelson, M. R. (General Electric Co., Schenectady, N. Y.). Contract W-31-109-Eng-52. J. Math. Phys. (N. Y.), 7: 345-55(Feb. 1966). (TID-21655).

Case's method is applied to multiregion problems in plane geometry. Half-range and "two-media" orthogonality relations are used to obtain a system of coupled integral equations for the appropriate expansion coefficients. The system is explicitly solved in a first-order approximation, which is valid for wide regions. Numerical analysis and comparison with transport computer codes indicates that such solutions are essentially exact for region thicknesses of five mean free paths or more. (auth)

15675 ATOMIC MOTIONS IN A RIGID SPHERE GAS AS A PROBLEM IN NEUTRON TRANSPORT. Desai, Rashmi C.; Nelkin, Mark. Nucl. Sci. Eng., 24: 142-52 (1966).

The time-dependent moments equations derived from the linearized Boltzmann equation are solved for the case of an infinite nonabsorbing medium of hard spheres. The distribution function at zero time is chosen to be Maxwellian at origin and zero elsewhere. The solutions can be applied to neutron diffusion in monatomic hydrogen and to the motion of atoms in a dilute monatomic gas. In the latter case, the solutions give the spatial moments of Van Hove's self-correlation function $G_s(r,t)$. Non-Gaussian corrections to $G_s(r,t)$ are studied. It is found that these corrections are very sensitive to the type of anisotropy of the scattering kernel. Various approximations (including synthetic kernel) of the exact kernel for a hard sphere gas are considered. The non-Gaussian corrections obtained from approximate kernels are compared with those obtained from the exact kernel. In particular, a recently published kinetic model calculation, using a separable isotropic kernel with 1/v scattering cross section, overestimates the non-Gaussian corrections by a factor of almost 4. (auth)

15676 NEUTRON DIFFUSION PARAMETERS IN BENZENE. Boffi, V. C.; Marsico, B.; Molinari, V. G.; Scozzafava, R. (EURATOM-CNEN, Frascati, Rome). Nucl. Sci. Eng., 24: 211-12(1966).

Some parameters were previously developed for neutron diffusion parameters in benzene on the basis of a theoretical model, neglecting carbon effects. These data are completed by showing their dependence on temperature, comparing them with more recent experimental results, and taking into account the carbon effects. The contribution of the carbon was evaluated by accounting for the effects of the chemical binding, but ignoring the coherent scattering. The average cosine of the scattering angle the total transport cross section, and the mean energy loss for neutrons in benzene at certain temperatures are each plotted at a function of energy. The thermal diffusion coefficient times the volume density is also given as a function of temperature. (J.F.P.)

15677 NEUTRON THERMALIZATION AND DIFFUSION IN NONISOTHERMAL MEDIA. Sehgal, Bal Raj (Brookhaven National Lab., Upton, N. Y.). Nucl. Sci. Eng., 24: 212-16(1966). (BNL-9292; BNL-9596).

The problem of thermal-neutron diffusion and distributions in a nonisothermal moderator medium is studied. The case of a hydrogen moderator, where the P_1 integral equation was solved by converting it to a differential equation and solving the latter by the Ritz-Galerkin variational method is reported. Also the case of a heavy gas moderator was studied, and the solution of the P_1 integral equation was obtained by the method of successive approximations. The solutions for both of these cases are compared with those of Kladnik. The neutron concentration and thermal diffusion coefficients are evaluated and compared with other results. The moderator medium is supposed to be nonabsorbing and macroscopically isotropic, and the temperature in this medium varies slowly with position. The neutron distribution is considered well within the medium and at energies well below the source energy, where transient effects due to the boundaries and the source are negligible. (J.F.P.)

15678 ON THERMAL-NEUTRON PULSE PROPAGATION. Cheung, K. Y.; Miley, G. H. (Univ. of Illinois, Urbana). Nucl. Sci. Eng., 24: 216-17(1966).

The one-group analysis for the measured propagation velocities and attenuation factors for a reactor-initiated thermal-neutron pulse propagating through graphite is ex-

tended to include thermalization effects. The results are compared with a pulse-dispersion analysis. (J.F.P.)

15679 THE DIFFUSION LENGTH OF THERMAL NEUTRONS IN WATER BETWEEN 18 AND 255 DEG C. Besant, C. B.; Grant, P. J. (Imperial Coll. of Science and Tech., London). Proc. Roy. Soc. (London), Ser. A, 289: 342-52 (Jan. 25, 1966).

The diffusion length of thermal neutrons in water was measured at various temperatures between 18 and 255°C using an $^{124}Sb-Be$ source. Diffusion length measurements were also made in water with three boric acid concentrations and with water poisoned with a cadmium sulphate solution, the measurements being taken over a temperature range of 18 to 200°C. The variation with temperature of the diffusion coefficient of water was determined from the experiments with poisoned water. A value 0.324 ± 0.006 barn was obtained for the 2200 m/s microscopic absorption cross section of hydrogen. Close agreement was found between the experimental results and theoretical predictions based on the Nelkin model for slow-neutron scattering. (auth)

15680 A STUDY ON THE DIFFUSION LENGTH OF THERMAL NEUTRONS IN TERPHENYL (SANTOWAX-R) AT HIGH TEMPERATURES UP TO 400 deg C. Hoki, Shiro; Tsuji, Yoshio; Matsubara, Takeo; Mukaiyama, Takeshi; Tada, Hiromitsu. Sumitomo Elec. Tech. Rev., No. 2, 98-102(July 1963).

The temperature dependence of the thermal diffusion length in Santowax-R was measured at temperatures from 200 to 400°C. The results were compared with the calculated value using the Brugger's cross section. At temperatures above 300°C, the diffusion length deviated considerably from the curve proportional to $(1/\rho)\sqrt{T}$. (auth)

15681 DETERMINATION OF NEUTRON RESONANCE SPINS IN ^{165}Ho NUCLEI BY THE TRANSMISSION OF POLARIZED NEUTRONS THROUGH A POLARIZED TARGET AT THE ENERGY REGION 0 TO 55 ev. Alfimenkov, V. P.; Lushchikov, V. I.; Nikolenko, V. G.; Taran, Yu. V.; Shapiro, F. L. (Joint Inst. for Nuclear Research, Dubna, USSR). Yadern. Fiz., 3: 55-64(Jan. 1966). (In Russian).

Experiments on the transmission of polarized neutrons through a polarized target of polycrystal metallic Ho are described. A polarized proton target on a double lanthan-magnesium nitrate backing with the degree of polarization 44% was used as a polarizer. The Ho nuclei were polarized using the Horter-Rose method at the temperature 0.35°K and magnetic field 15 koe. The spins of eleven excited states of the ^{166}Ho compound nucleus, corresponding to neutron resonances at the energies 3.92; 8.1; 12.6; 18.1; 21.0; 35.3; 37.0; 39.4; 47.3; 51.2 and 54.0 ev, were found to be 4,3, 4, 3, 4, 3, 3(4), 4, 3, 3 and 3(4), respectively. (auth)

15682 MEASUREMENT OF FREE AND INCOHERENT NEUTRON CROSS SECTIONS OF SILICON AND LEAD. Niklaus, J. P.; Simson, R.; Triftshaeuser, W.; Schmatz, W. (Technische Hochschule, Munich. Kernforschungsanlage, Juelich, Ger.). Z. Phys., 190: 295-303(1966). (In German).

The free neutron cross section of silicone and lead was determined to (2.022 ± 0.003) barns and (10.58 ± 0.03) barns respectively and the incoherent cross section of the same elements to $(15 \pm 1.3) \cdot 10^{-3}$ barns and $(15 \pm 15) \cdot 10^{-3}$ barns respectively. From these results the coherent cross sections were calculated under consideration of various correction terms to (2.153 ± 0.005) barns and (10.65 ± 0.05) barns. (auth)

15683 INVESTIGATION OF THE THERMALIZATION PROCESS OF NEUTRONS FROM Po-Be NEUTRON SOURCES IN A PARAFFIN MODERATOR. Bielaczyc, Czeslaw; Flatau, Bogumila; Lewa, Czeslaw; Sobczynski, Zbigniew (Zaklad Fizyki Doswiadczalnej Wyzszej Szkoly Pedagogicznej, Gdansk, Poland). Zesz. Nauk. Wyzszej Szkoly Pedagog. Gdansku, Mat., Fiz., Chem., 3: 39-43(1963). (In Polish).

The geometrical distribution of slow neutrons from Po-Be neutron sources in paraffin was measured in the energy range of E = 0.18, 1.44, and 5.1 ev using the activation method. Neutron spectra were theoretically calculated in the region from 30 to 400 ev and were tested experimentally by activation of ^{79}Br. (tr-auth)

15684 ONE-SPEED NEUTRON TRANSPORT PROBLEMS IN PLANE GEOMETRY [Thesis]. McCormick, Norman Joseph. Ann Arbor, Mich., Univ. of Michigan, 1965. 198p.

The method developed by Case is used to consider several time-independent problems of neutron transport theory for a homogeneous medium in plane geometry. This method utilizes a direct expansion of the neutron angular density in terms of the eigenfunctions of the homogeneous transport equation. The solutions to these problems are greatly facilitated by the use of half-range orthogonality relations (for $0 < \mu < 1$) between the eigenfunctions of the transport equation. Both the half-range orthogonality equations and the previously known full-range equations (for $-1 < \mu < 1$) are shown to be special cases of a more general partial-range orthogonality equation. These orthogonality relations are derived and are used to obtain solutions for the following problems: (1) the half-space Milne, albedo, constant isotropic source, and Green's function problems for linearly anisotropic scattering; (2) the half-space Milne and albedo problems for quadratically anisotropic scattering when there is no absorption; and (3) the albedo problem for isotropic scattering in a slab of finite thickness. In each case, simplified expressions are derived for the emerging angular density and the density and net current on the surface(s). A speculative approach for finding the half-range orthogonality relations for general-order anisotropic scattering is also discussed. Some of the results from the slab albedo problem are used to determine new integral expressions for the X- and Y-functions of Chandrasekhar. These yield convenient asymptotic values valid for large slab thicknesses. Also included is a generalization of the slab albedo boundary conditions to the case of a slab bounded on one side by a vacuum and on the other side by a specularly and diffusely reflecting face. (Dissertation Abstr.)

15685 INVESTIGATION OF TRANSPORT EFFECTS IN THE NEUTRON WAVE EXPERIMENT [Thesis]. Johnson, Robert Lewis. Los Angeles, Univ. of California, 1965. 124p.

The neutron wave experiment and the pulsed neutron source experiment are analyzed using the multivelocity Boltzmann equation by expanding the energy dependence into a series of associated Laguerre polynomials of order one. The matrix elements are evaluated for the case where the scattering cross section is independent of energy and for 1/N absorption. The scattering is assumed to be isotropic in the laboratory system. In the two Laguerre polynomial approximation, a general expression, independent of the scattering model, is obtained for the dispersion function of a non-multiplying medium. The corresponding fundamental mode decay constant for the pulsed neutron source experiment is also calculated. The resulting expression for the diffusion cooling coefficient can be divided into two parts. The first, or transport correction, arises even if the energy distribution of the flux is Maxwellian, and is found to be only 37% of the value calculated using one-velocity transport theory. The second part is the same as the multivelocity diffusion theory result except that it is multiplied by a factor that depends on the scattering kernel. The factor has the value $1-\xi$ when the heavy gas scattering model is used, where ξ is the logarithmic energy decrement. For a more realistic crystal scattering model its value is very close to one. Thus, it is shown that to order B^4 in the buckling or to ω^2 in the frequency, the multivelocity diffusion equation is an excellent approximation to the Boltzmann equation. The diffusion cooling coefficient of graphite is calculated using a modification of Wick's scattering kernel. The value obtained 67×10^5 cm^4sec, is considerably higher than the most recent measurements of this quantity using the pulsed

neutron source experiment but is in good agreement with at least one value reported using the neutron wave experiment. The results suggest, but do not prove, that the value of the diffusion cooling coefficient measured by the pulsed neutron source experiment is still too low. (Dissertation Abstr.)

15686 PULSED SOURCE MEASUREMENT OF NEUTRON DIFFUSION PARAMETERS IN WATER. Gon, Elieser (Columbia Univ., New York). 114p. (CONF-650602-70). ORINS. Gmelin, AED-CONF-65-125-109.

From American Nuclear Society 11th Annual Meeting, Gatlinburg, Tenn.

Neutron diffusion parameters of water were measured by the pulsed neutron source technique. Spherical containers were used whose parameters are easily calculable, and might serve in the future for comparison with theory. For this purpose the decay constant was also measured for smaller samples than hitherto attempted, the smallest sphere having a radius of 1.52 cm. The samples within the range of geometrical buckling $0.08906 < B^2 < 0.9472$ were used to determine the diffusion parameters. The results are $\Sigma_{av} = 4817 \pm 29$ sec^{-1}, $D_0 = 36{,}300 \pm 650$ cm^{2}sec^{-1} and $C = 3{,}700 \pm 615$ cm^{4}sec^{-1} for water at 22°C. Effects of higher spatial modes, especially in the large samples, were calculated, in order to determine the waiting time necessary for a pure exponential decay to prevail. Erroneous results in previous measurements are shown to be caused by underestimation of higher spatial modes. A Cockroft-Walton type accelerator was used as the pulsed neutron source. The beam on/beam off ratio was improved by introducing additional electrostatic deflection plates as well as a deflecting magnet and anti-scattering pockets. The beam on/beam off ratio obtained is about 5×10^5, which is at least one order of magnitude better than formerly obtained with similar accelerators. Special care was taken to suppress time-dependent background, and backscattering by the detector assembly itself. (auth)

15687 A NEUTRON DIFFUSER. Hofman, Walter (to Reactor Centrum Nederland). British Patent 1,017,789. Jan. 19, 1966. Filed Dec. 15, 1964.

A neutron diffuser is made up of a tank containing D_2O in a particular shape and enclosed by concrete walls or some other material that has good neutron-reflecting qualities. The tank consists of two coaxial cylindrical parts connected by a conical part and having convex end walls. The lower wall of the tank is in the form of a detachable cover having flanges for securing it to the rest of the tank and fixing the tank to the surrounding concrete mass. This diffuser yields a neutron beam having a very regular and flat spectrum of a diffuse character. (B.L.M.)

Nuclear Properties and Reactions

Refer also to abstracts 14461, 15236, 15242, 15244, 15245, 15254, 15266, and 15439.

15688 (AD-620384) HALF-LIFE MEASUREMENTS OF SOME NEUTRON INDUCED ISOMERS [Thesis]. Button, Edward J.; Smith, Thomas M. (Naval Postgraduate School, Monterey, Calif.). 1965. 55p. CFSTI $3.00 cy, $0.50 mn.

The half lives of isomers of ^{178}Hf, ^{179}Hf, ^{183}W, and ^{177}Yb that were activated by thermal neutrons were determined by direct decay measurements with a scintillation counter. (D.C.W.)

15689 (CEA-R-2786) CONTRIBUTION A L'ETUDE DE L'INTERACTION ALPHA-ALPHA [THESES]. (Contribution to the Study of the Alpha-Alpha Interaction [Thesis]). Darriulat, Pierre (Commissariat a l'Energie Atomique, Saclay (France). Centre d'Etudes Nucleaires). 1965. 96p. Dep. mn.

Submitted to Paris Univ.

Two sets of measurements of the α-α elastic scattering differential cross section are presented. The first set—angular distributions from 50 to 120 Mev—shows resonances, 6^+ and 8^+, at 25 and 57 Mev. Complex phase shifts are extracted from the data and a phenomenological potential is given. A description of the 3 α-particle 0^+ states in ^{12}C is made with this interaction potential. The second set—excitation curves between 20 and 50 Mev—allows investigation of the ^{8}Be level structure within this energy range. The 16.6 and 16.9 Mev states are identified as 2^+, but the rise of inelastic processes at higher energies makes further identification of spins and parities difficult. (auth)

15690 (CEA-R-2813) CONTRIBUTION A LA MESURE ABSOLUE DE L'ACTIVITE DES ISOTOPES SE DESINTEGRANT PAR CAPTURE ELECTRONIQUE. DETERMINATION DU RENDEMENT DE FLUORESCENCE DE QUELQUES ELEMENTS. (Contribution to the Absolute Measurement of Activity of Electron Capture Nuclides. Determination of the Fluorescence Yield of Some Elements). Legrand, Jean (Commissariat a l'Energie Atomique, Saclay (France). Centre d'Etudes Nucleaires). Sept. 1965. 56p. Dep. mn.

The object of this work is the study of techniques of measurement of the absolute activity of electron capture nuclides. Two methods are specially studied. The first comprises determination of the number of x rays emitted from the k shell due to the reorganization of atomic electrons following electron capture. This measurement is made with a high pressure (5 kg/cm^2) 4 π proportional counter. The absorption in the source and the backing are also studied. To determine the absolute activity it is necessary to know the fluorescence yield and the different capture probabilities P_L and P_K. When the electron capture is followed by γ emission (within the resolution time of the coincidence circuit) the activity is determined by the x-γ coincidence method. In such a case it is not necessary to know the fluorescence yield and the capture probabilities. Various corrections, viz. dead time and chance coincidences, are also studied. This method minimizes the decay scheme corrections. By applying these two methods to ^{51}Cr, ^{54}Mn, and ^{65}Zn, the corresponding fluorescence yields are determined. (auth)

15691 (CEA-R-2840) MESURE DES INTEGRALES DE RESONANCE D'ABSORPTION (Mn, Fe, Co, Ni, Cu, Zr, Mo). (Measurement of Resonance Absorption Integrals (Mn, Fe, Co, Ni, Cu, Zr, Mo)). Vidal, Rene; Cardoso-Martinho, Eduardo (Commissariat a l'Energie Atomique, Saclay (France). Centre d'Etudes Nucleaires). Nov. 1965. 43p. Dep. mn.

The measurements were carried out with the oscillation technique, without a cadmium tube, in a spectrum rich in epithermal neutrons. The samples consist in metal plates or deposits on aluminum. Results are presented. (M.O.W.)

15692 (CERN-66-3) CHOICE OF SUBSTANCES FOR POLARIZED PROTON TARGETS. Borghini, M. (European Organization for Nuclear Research, Geneva (Switzerland)). Jan. 31, 1966. 29p. Dep. mn.

The performance of various inorganic and organic substances for use as polarized-proton targets is surveyed. Both magnetic polarization and "solid-effect" polarization of the target are considered. (T.F.H.)

15693 (CONF-233(Vol.1)) ROLE OF ATOMIC ELECTRONS IN NUCLEAR TRANSFORMATIONS. Proceedings of International Conference. (International Union of Pure and Applied Physics. International Atomic Energy Agency, Vienna (Austria). Nuclear Energy Information Center, Warsaw (Poland). Polish Academy of Sciences, Warsaw). Sept. 1963. 103p. Dep. ORAU.

Separate abstracts were prepared for 3 of the 4 included papers. The remaining paper appeared previously in NSA as 19: 32955. (M.O.W.)

For abstracts of individual papers see: 15694–15696.

15694 (CONF-233(Vol.1), pp 1-29) INTERNAL CONVERSION. Gerholm, T. R.; Pettersson, B. G. (Stockholm Univ. (Sweden). Inst. of Physics).

A review of present knowledge on the M1 and E0 conversion processes is presented. Anomalies were found for

certain strongly retarded E1 transitions. The interpretation of these anomalous E1 transitions in terms of nuclear penetration matrix elements is much more involved and less unambiguous. There was no clear cut evidence for any anomalies in the E2, M2, and higher multipoles. (M.O.W.)

15695 (CONF-233(Vol.1), pp 30-59) ORBITAL ELECTRON CAPTURE BY THE NUCLEUS. Bouchez, R.; Depommier, P. (Grenoble Univ. (France). Laboratoire de Physique Nucleaire).

A review of electron capture investigations is presented. The review surveys data on L/K capture ratios, M/L capture ratios, capture to β^+ emission ratios, and radiative orbital electron capture. (M.O.W.)

15696 (CONF-233(Vol.1), pp 60-86) INTERNAL PAIR FORMATION AND ELECTROEXCITATION OF NUCLEI. Rose, M. E. (Virginia Univ., Charlottesville).

A brief review of internal pair production by electron capture and by electron beam excitation is presented. The possibilities of each method for determining the more useful information is discussed. (M.O.W.)

15697 (CONF-233(Vol.2)) ROLE OF ATOMIC ELECTRONS IN NUCLEAR TRANSFORMATIONS. Proceedings of International Conference. (International Union of Pure and Applied Physics, International Atomic Energy Agency, Vienna (Austria). Nuclear Energy Information Center, Warsaw (Poland). Polish Academy of Sciences, Warsaw). Sept. 1963. 282p. Dep. ORAU.

Separate abstracts were prepared for 17 of the 24 papers. The remaining 7 papers appeared previously in NSA as; 18: 26620, 42711, 44810, and 19: 12517, 23818, 26698, and 34868. (M.O.W.)

For abstracts of individual papers see: 15698—15714.

15698 (CONF-233(Vol.2), pp 109-16) PARTICLE PARAMETER OF THE 2+ → 0+ E2 TRANSITION IN ^{152}Sm. George, T. M.; Hamilton, J. H. (Vanderbilt Univ., Nashville, Tenn.).

The gamma-gamma and gamma-K conversion electron directional correlation of the 245-122 kev, 4+ → 2+ → 0+ cascade transitions was measured. A magnetic lens spectrometer was used in the correlation studies involving the K conversion electrons of the 122-kev transition. The particle parameter, b_2, of the 122-kev transition was determined to be 1.65 ± 0.27 which is in agreement with the theoretical value of 1.89 within limits of error. (auth)

15699 (CONF-233(Vol.2), pp 117-19) EXPERIMENTAL AND THEORETICAL STUDIES OF L-CONVERSION ELECTRON DIRECTIONAL CORRELATIONS. Thun, J. E.; Toernkvist, S.; Falk, F.; Snellman, H. (Uppsala Univ., (Sweden). Inst. of Physics).

A brief description is presented of calculations initiated in order to make possible the use of L conversion electrons in directional correlation experiments. The results of a measurement of the 50-kev (L_I + L_{II} electrons) 158-kev gamma correlation in ^{199}Hg are presented. (M.O.W.)

15700 (CONF-233(Vol.2), pp 120-7) PARTICLE PARAMETER OF THE 2+ → 0+ E2 TRANSITION IN ^{170}Yb. Croft, W. L.; Pettersson, B. G.; Hamilton, J. H. (Vanderbilt Univ., Nashville, Tenn.).

The directional correlations of the 880-kev beta group with the gamma rays and with the K conversion electrons which depopulate the 84-kev level in ^{170}Yb were measured. A magnetic lens spectrometer adapted for electron-gamma and electron-electron directional correlation studies was used. The particle parameter, b_2, was determined from these correlations. The value of b_2 was found to be 2.56 ± 0.4 which includes a correction (0.6%) to the β-γ correlation for β-innerbremsstrahlung correlation. This b_2 value is higher than the theoretical value of 1.92 but does not definitively exclude agreement with theory. (auth)

15701 (CONF-233(Vol.2), pp 128-41) ANGULAR CORRELATION AND INTERNAL CONVERSION STUDIES IN ^{125}I AND ^{127}I AND THEIR ANALYSIS USING CORRECTED FORMULAE. Geiger, J. S.; Brown, F. (Atomic Energy of Canada Ltd., Chalk River (Ontario). Chalk River Nuclear Labs.).

The internal conversion electron spectra resulting from the K-capture decay of ^{127}Xe and ^{125}Xe were studied using the Chalk River $\pi\sqrt{2}$ β-spectrometer. These investigations provide detailed knowledge of the energies, relative intensities, and multipolarities of the transitions in ^{127}I excited in the decay of ^{127}Xe and of the transitions between the lower-lying levels in ^{125}I excited in the ^{125}Xe decay. Gamma-gamma and gamma-conversion electron angular correlation studies were also made in order to experimentally establish the spins of the second and third excited states in these nuclei. (M.O.W.)

15702 (CONF-233(Vol.2), pp 142-7) 30.7-kev ANOMALOUS ELECTRIC DIPOLE TRANSITION. Valentin, Jacques (Paris Univ., Orsay (France). Institut du Radium).

The 30.7-kev transition in the electron-capture decay of ^{179}W was investigated. Internal conversion coefficients were calculated. The decay scheme of ^{176}W was also investigated. (M.O.W.)

15703 (CONF-233(Vol.2), pp 148-57) ANOMALOUS L-SUBSHELL CONVERSION OF SOME HINDERED E1 TRANSITIONS IN THE RARE EARTH REGION. Herrlander, C. J.; Ewan, G. T. (Atomic Energy of Canada Ltd., Chalk River (Ontario). Chalk River Nuclear Labs.).

The relative intensities of the L-subshell conversion lines were investigated for highly retarded E1 transitions in the rare earth region. The conversion electron spectra were studied in the Chalk River high resolution β-ray spectrometer. (M.O.W.)

15704 (CONF-233(Vol.2), pp 164-76) E2 CONVERSION COEFFICIENTS IN ^{110}Cd AND ^{132}Xe. Newbolt, W. B.; Boyd, H. W.; Hamilton, J. H. (Vanderbilt Univ., Nashville, Tenn.).

The K internal conversion coefficients of the 657.7-, 884.3-, 937.3-kev E2 transitions in ^{110}Cd and the 667.8-kev E2 transition in ^{132}Xe were measured by the internal-external conversion method. The following α_K values × 10^3 were found for the above four transitions: 2.64 ± 0.10, 1.26 ± 0.06, 1.12 ± 0.08 and 3.59 ± 0.30 respectively. The α_K results are all in agreement with the theoretical values of Sliv and Band and of Rose. (auth)

15705 (CONF-233(Vol.2), pp 177-90) E2 CONVERSION COEFFICIENTS IN ^{152}Sm, ^{154}Gd AND ^{160}Dy. Jansen, J. F. W.; Hamilton, J. H.; Zganjar, E. F. (Instituut voor Kernphysisch Onderzoek, Amsterdam (Netherlands). Vanderbilt Univ., Nashville, Tenn.).

The K and L internal conversion coefficients of the pure E2 transitions from the lowest excited states in ^{152}Sm, ^{154}Gd, and ^{160}Dy and of two higher energy E2 transitions in ^{160}Dy were measured with the internal-external conversion method. Several parameters such as source sizes and converter thicknesses were varied to test for systematic errors. The α_K for the first three mentioned transitions are about 20% above theory, but a correction for scattering of photoelectrons in the converter must still be applied. The results for the other transitions are in agreement with theory. (auth)

15706 (CONF-233(Vol.2), pp 191-7) K-SHELL CONVERSION COEFFICIENTS FOR PURE E2 TRANSITIONS IN SOME DEFORMED NUCLEI. Thosar, B. V.; Joshi, M. C.; Sharma, R. P.; Prasad, K. G. (Tata Inst. of Fundamental Research, Bombay (India)).

The transitions from the first excited state of ^{166}Er, ^{170}Yb, ^{176}Hf, ^{186}W, ^{186}Os, and ^{188}Os were studied by beta-gamma coincidence methods. In the first three cases the de-excitation energy lies at about 80 kev while in the other three it is 122, 137, and 155 kev. The conversion coefficients were measured and compared with previous work. (M.O.W.)

15707 (CONF-233(Vol.2), pp 198-212) THE K-CONVERSION COEFFICIENT OF THE 412-kev E2 TRANSITION

IN ^{198}Hg. Lewin, W. H. G.; van Nooijen, B.; van Eijk, C. W. E.; Wapstra, A. H. (Technische Hogeschool, Delft (Netherlands)).

The K-conversion coefficient of the 412-kev E2 transition in ^{198}Hg was determined by K-conversion electron-beta coincidence measurements on ^{198}Au. The result is $\alpha_K = (303.5 \pm 4.5) \times 10^{-4}$ or $(298.5 \pm 4.5) \times 10^{-4}$ depending on the adopted experimental shape factor for the 960 kev negaton distribution. Both results are in excellent agreement with the theoretical value of 302×10^{-4} computed by Rose and by Sliv and Band. (auth)

15708 (CONF-233(Vol.2), pp 213-19) AN EXPERIMENTAL STUDY OF THE K-CONVERSION PROCESS OF THE 412-kev E2 TRANSITION IN ^{198}Hg. Pettersson, B.-G.; Holmberg, L. (Stockholm Univ. (Sweden)).

The K-conversion process of the 412-kev E2 transition was analyzed using the R_2 radial matrix element as a free parameter to be determined by experiment. The analysis is based on an experimental determination of the A_4 terms in the Legendre expansion of the gamma-gamma and gamma-Ke^- correlation functions of the 676 kev–412 kev cascade emitted in the decay of ^{198}Au to ^{198}Hg. The experimental results are presented. (M.O.W.)

15709 (CONF-233(Vol.2), pp 247-51) THE REPRESENTATION, IN PHOTOELECTRIC ANGULAR DISTRIBUTIONS, OF PHOTOELECTRON SCATTERING AND THE CONSEQUENCES FOR THE DETERMINATION OF INTERNAL CONVERSION COEFFICIENTS BY THE IEC METHOD. Hultberg, Soelve; Erman, Peter (Nobel Inst. of Physics, Stockholm (Sweden)).

The principal difficulty of the internal-external conversion method is associated with obtaining the correct representation of the photoelectric anisotropy. The solution to this problem is briefly discussed in terms of the photoelectric angular distributions. (M.O.W.)

15710 (CONF-233(Vol.2), pp 252-5) APPLICATION TO THE LENS TYPE SPECTROMETER OF THE INTERNAL-EXTERNAL CONVERSION /IEC/ METHOD FOR THE DETERMINATION OF INTERNAL CONVERSION COEFFICIENTS. Hultberg, S.; Hamilton, J. H.; Sistler, J. (Nobel Inst. of Physics, Stockholm (Sweden). Vanderbilt Univ., Nashville, Tenn.).

The use of a lens type beta spectrometer for internal-external conversion measurements is briefly discussed. The various difficulties involved are outlined. (M.O.W.)

15711 (CONF-233(Vol.2), pp 345-58) SOME ALLOWED K-CAPTURE TO POSITRON RATIOS. Konijn, J.; de Wit, S. A.; Wapstra, A. H. (Instituut voor Kernphysisch Onderzoek, Amsterdam (Netherlands)).

The K/β^+ ratios were determined for ^{52}Mn, ^{22}Na, and ^{48}V. The experimental techniques are described and the results are compared with previous work. (M.O.W.)

15712 (CONF-233(Vol.2), pp 359-64) THE RATIO OF K-CAPTURE TO POSITRON EMISSION IN THE DECAY OF ^{13}N. Ledingham, K. W. D.; Payne, J. A.; Drever, R. W. P. (Glasgow Univ. (Scotland). Dept. of Natural Philosophy).

A flow counter technique was used to measure the K-capture/β^+ ratio for ^{13}N. The arrangement of the gas system and the experimental procedures used are briefly discussed. The obtained results are compared with theoretical ones. (M.O.W.)

15713 (CONF-233(Vol.2), pp 365-8) COMPARISON OF RECENT PRECISION RESULTS OF ORBITAL ELECTRON CAPTURE RATIOS WITH THEORY. Fink, R. W. (Marquette Univ., Milwaukee, Wis.).

A survey was made for the purpose of comparing experimental and theoretical values of the L/K-capture ratios for the following nuclei; ^{36}Cl, ^{37}Ar, ^{51}Cr, ^{54}Mn, ^{55}Fe, ^{57}Co, ^{58}Co, ^{65}Zn, ^{71}Ge, and ^{79}Kr. (M.O.W.)

15714 (CONF-233(Vol.2), pp 369-70) MEASUREMENT OF THE M/L-CAPTURE RATIO IN 30-MILLION-YEAR ^{205}Pb DECAY WITH THE MULTIWIRE PROPORTIONAL COUNTER. Moler, R. B.; Fink, R. W. (Arkansas Univ., Fayetteville. Dept. of Chemistry).

Experimental work being done in an attempt to measure the M/L-capture ratio for ^{205}Pb is briefly discussed. It involves conversion of the lead into gaseous lead tetraethyl for introduction into a multiwire proportional counter gas for direct measurement of the M/L ratio. (M.O.W.)

15715 (CONF-233(Vol.3), pp 505-9) DOUBLE IONIZATION ACCOMPANYING ^{6}He DECAY. Demeur, M.; Meert, M. (Brussels Univ. (Belgium)).

Carlson (Phys. Rev. 129, 2220 (1963)) has measured the charge spectrum of the ^{6}Li ions formed following the β^- decay of ^{6}He as a function of their recoil energy. The interpretation of Carlson's experimental results by means of factorized wave functions was attempted. The theoretical results are in disagreement with experimental ones. (M.O.W.)

15716 (CONF-233(Vol.3), pp 529-37) INFLUENCE OF NUCLEAR CHARGE DISTRIBUTION ON BETA DECAY. Vinduska, M. (Ustav Jaderneho Vyzkumu, Ceskoslovenska Akademie Ved, Rez).

The influence of the Coulomb field on β-decay processes is investigated theoretically. The electron wave functions were calculated from the known form of the electromagnetic field. Calculations were made for Z = 49 and compared with previous results. (M.O.W.)

15717 (GEAP-4950) ACCURATE NUCLEAR FUEL BURNUP ANALYSES. Fifteenth Quarterly Progress Report, June 1965–August 1965. Peterson, J. P. Jr.; Ruiz, C. P.; Rider, B. F.; Jaech, J. L.; Smith, F. R. (General Electric Co., San Jose, Calif. Atomic Power Equipment Dept.). Sept. 1, 1965. Contract AT(04-3)-189. 34p. Dep. mn. CFSTI $2.00 cy, $0.50 mn.

During this quarter, the capture-to-fission ratios of ^{235}U and ^{239}Pu, α_5 and α_9, were calculated as a function of neutron temperature from recently revised cross section data. They are presented graphically for inclusion in the ASTM tentative method for determination of atom percent fission in uranium fuel. Also, a statistical evaluation of the precision of two burnup methods (heavy element and neodymium mass spectroscopy) was completed. (M.O.W.)

15718 (IDO-17083) MEASUREMENT OF THE ABSOLUTE VALUE OF ETA FOR ^{233}U, ^{235}U AND ^{239}Pu USING MONOCHROMATIC NEUTRONS. Smith, J. R.; Reeder, S. D.; Fluharty, R. G. (Phillips Petroleum Co., Idaho Falls, Idaho. Atomic Energy Div.). Feb. 1966. Contract AT(10-1)-205. 51p. Dep. mn. CFSTI $3.00 cy, $0.50 mn.

The absolute value of eta, the number of fission neutrons per absorption, was measured for ^{233}U, ^{235}U, and ^{239}Pu, using monochromatic neutrons from the crystal spectrometer at the Materials Testing Reactor. Measurements were made on all three isotopes at 0.025-ev neutron energy, and on ^{233}U and ^{239}Pu at 0.057 ev. The Bragg beam from Be (0002) was passed through a mechanical monochromator to remove higher-order neutrons and yield a truly monochromatic beam. The neutron detector was a manganous sulphate bath, which absorbed in turn the Bragg beam and then the fission neutrons produced when the beam was completely absorbed in a fissionable sample. The ratio of the levels of ^{56}Mn activities produced in the two types of irradiation yielded the value of eta for the fissionable material of the sample, after the application of a few small corrections. The method of least squares was used to extract the values of eta from the experimental data. (auth)

15719 (INP-431/PL) OCTUPOLE COULOMB EXCITATION OF ^{208}Pb NUCLEUS. Hrynkiewicz, A. Z.; Kopta, S.; Szymczyk, S.; Walczak, T. (Institute of Nuclear Physics, Krakow (Poland); Kuzniecov, I. (Joint Inst. for Nuclear Research, Dubna (USSR). Lab. of Nuclear Reactions). Nov. 1965. 18p. Dep.

The 3^- states of ^{208}Pb was excited using ^{12}C ions with energies of 45.5 to 60.2 Mev. The reduced transition probability B(E3)↑ for the 2615-kev level was determined. (D.C.W.)

15720 (JINR-E-2516) ASYMMETRY IN THE ANGULAR DISTRIBUTION OF THE HIGH-ENERGY NEUTRONS FROM MU⁻ CAPTURE IN SULFUR. Evseev, V. S.; Chernogorova, V. A.; Kilbinger, F.; Roganov, V. S.; Shimchak, M. (Joint Inst. for Nuclear Research, Dubna (USSR). Lab. of Nuclear Problems). 1965. 10p. Dep. mn.

The asymmetry coefficient B in the angular distribution of high energy neutrons from meson (μ^-) capture in sulphur was measured. The value of the asymmetry coefficient reduced to 100% of meson (μ^-) residual polarization is close to −1, which contradicts calculations on the basis of the universal weak interaction theory. (auth)

15721 (JINR-E-2517) ANGULAR DISTRIBUTION OF HIGH-ENERGY NEUTRONS EMITTED IN ABSORBING POLARIZED μ^--MESONS IN CALCIUM. Evseev, V. S.; Chang, Run-hwa; Chernogorova, V. A.; Roganov, V. S.; Shimchak, M. (Joint Inst. for Nuclear Research, Dubna (USSR). Lab. of Nuclear Problems). 1965. 30p. Dep.mn.

The asymmetry coefficient B was measured in the angular distribution of neutrons from mesons (μ^-)-capture in Ca in the E_n energy range from 6.7 to 20.7 Mev. For higher thresholds ($E_n \geq 18$ Mev) the asymmetry coefficient reduced to the 100% residual polarization of mesons (μ^-) is close to −1, which contradicts calculations on the basis of the universal weak interaction theory. (auth)

15722 (KR-76) RADIOCHEMICAL AND NUCLEAR STUDIES OF THE SHORT-LIVED FISSION PRODUCTS ^{145}Ce, ^{146}Ce, AND ^{147}Ce. Hoffman, D. C.; Michelsen, O. B. (Institutt for Atomenergi, Kjeller (Norway)). Dec. 1965. 60p. Dep. mn.

A procedure based on extraction by di-(2-ethylhexyl) orthophosphoric acid (HDEHP) was developed for the rapid separation of Ce from fission products and also (through extraction chromatography) for the continuous separation of Pr activities from their parent activities. The latter procedure permits the observation of radiocerium with a minimum of interference from its daughters. The decay properties of ^{145}Ce, ^{146}Ce, and ^{147}Ce were studied by gamma and beta scintillation spectrometry and by gamma-gamma, gamma-beta, and beta-gamma coincidence measurements. Information was obtained on half lives, gamma and beta energies, and the relative intensities of gamma rays. Decay schemes are proposed for ^{146}Ce and ^{145}Ce. The decay of ^{147}Ce was observed directly for the first time, and its half life was determined by both gamma and beta decay measurements. However, attempts to single out specific gamma or beta energies for this nuclide failed. A search for a possible ^{146m}Pr gave no definite results. (auth)

15723 (MIT-2098-162) THE ENERGY AND ANGULAR DISTRIBUTION OF PHOTONEUTRONS FROM HEAVY ELEMENTS. Bertozzi, W.; Kowalski, S.; Mutchler, G. S.; Sargent, C. P.; Turchinetz, W. (Massachusetts Inst. of Tech., Cambridge. Lab. for Nuclear Science). [1965]. Contract AT(30-1)-2098. 19p. (CONF-650817-2). Dep. mn. CFSTI $1.00 cy, $0.50 mn.

From Gordon Research Conference on Ion Exchange, New London, N. H.

Photoneutron energy spectra are measured using time-of-flight methods at emission angles of 24 to 156°, using bremsstrahlung having a maximum energy of 16 Mev, for 14 elements. Data are also measured for the Pb isotopes having mass numbers of 206, 207, and 208. (T.F.H.)

15724 (MIT-2098-224) THE ANGULAR DISTRIBUTIONS AND ENERGY SPECTRA OF PHOTONEUTRONS FROM HEAVY ELEMENTS [Thesis]. Mutchler, Gordon Sinclair (Massachusetts Inst. of Tech., Cambridge). Feb. 1966. Contract AT(30-1)-2098. 307p. Dep. mn. CFSTI $7.00 cy, $1.50 mn.

The energy spectra of photoneutrons from Bi, ^{208}Pb, ^{207}Pb, ^{206}Pb, Tl, Hg, Au, W, Ta, Er, Ho, Sm, Pr, La, I, Sn, and In were measured at 24, 76, and 156° relative to the photon beam from the MIT Linear Accelerator. Bremsstrahlung spectra were used with endpoints of 15, 14 and 13 Mev. The neutron energies were determined using a time-of-flight spectrometer with 10 meter flight paths and 8 ns resolution. Subtracting the 14-Mev (or 13 Mev) data (properly normalized) from the 15-Mev (or 14 Mev) data yields neutron spectra generated by an equivalent photon spectrum peaked at 14 Mev (or 13 Mev) with a full width at half maximum of 2 Mev. The angular distributions of the photoneutron spectra from these three bremsstrahlung spectra were analyzed in the form $W(\Theta) = a_0 + a_1P_1(\cos\Theta) + a_2P_2(\cos\Theta)$. a_1 was found to be approximately constant with energy for each target and to range from −0.07 to +0.05 with statistical errors of ±0.02 and estimated systematic errors of ±0.09. Therefore, a_1 was assumed to be zero for all targets; and the angular distributions are presented in the form $W(\Theta) = a_0 + a_2P_2(\cos\Theta)$. The anisotropy ($a_2/a_0$) was found to increase with neutron energy. The low energy photoneutrons (<3 Mev) are isotropic ($a_2/a_0 = 0$) and the anisotropy is a maximum at or near the neutron endpoint. This maximum value of the anisotropy shows marked shell effects. It is a maximum ($-a_2/a_0 = 0.6$ to 0.7) near the closed shell nuclei ^{208}Pb and Pr, and it has a minimum ($-a_2/a_0 = 0.15$ to 0.3) between these two closed shells, in the region of the deformed nuclei. The neutron difference spectra are characterized by an isotropic evaporation component which dominates at low neutron energies, and an anisotropic resonance direct component which dominates at high neutron energies. The transition from one component to the other is quite abrupt, typically taking place in an energy interval of about one to two Mev. It was found to be possible to fit the neutron difference spectra with the theoretical curve $dN/dE_n = \text{const}\ E_n\sigma_C\omega(U) + kS(E_n)$, where $\omega(U)$ is the level density of the residual nucleus at an excitation energy U, σ_C is the inverse capture cross section, and $S(E_n)$ is the energy spectrum of the direct component. The data were analyzed using three approximations for the level density, $[\exp 2\sqrt{a_{\frac{1}{2}}U}]/(U+t)^{\frac{1}{2}}$, $[\exp 2\sqrt{a_2U}]/(U+t)^2$, and $\exp(-E_n/T)$, where t is given by the equation $U = a_mt^2 - t$. $S(E_n)$ was calculated using Wilkinson's model of the giant resonance. In the above equations, a_m (or T), and k were the only adjustable parameters. The values of a_2 generally follow the predictions of Newton, $a_2 = K[(\vec{J}_t + \vec{J}_p + 1)A^{\frac{1}{3}}$. K was found to be 0.067. The fraction of directly emitted neutrons, f, defined as the integral of the direct spectrum divided by the integral of the total spectrum, was found to be about 14%, and approximately constant with A, the mass number. (auth)

15725 (NP-14855) KERNDATEN UEBER DIE ERZEUGUNG VON GAMMASTRAHLUNG DURCH WECHSELWIRKUNGEN MIT SCHNELLER NEUTRONEN. (Nuclear Data on the Production of Gamma Rays through Interaction with Fast Neutrons). Krueger, F. Wolfgang (VEB Entwicklung und Projektie ung Kerntechnischer Anlagen, Berlin (East Germany)). Jan. 20, 1963. 232p. Dep. mn.

More than 300 original articles were evaluated in order to compile nuclear data on the production of γ rays by fast neutron reactions. The compilation contains data on the energy of the γ radiation produced in the inelastic neutron scattering, the effective cross section for this production, and the effective cross section for fast neutron induced nuclear reactions which lead to the formation of radioactive nuclides in whose decay γ quanta or positrons are emitted. (tr-auth)

15726 (ORNL-P-1957) INELASTIC SCATTERING AND THE DISTORTED WAVE METHOD. Perey, F. G. (Oak Ridge National Lab., Tenn.). [1965]. Contract W-7405-eng-26. 27p. (CONF-651118-9). Dep. mn. CFSTI $2.00 cy, $0.50 mn.

From American Physical Society, Gatlinburg, Tenn.

The determination of spin and parity of nuclear levels from the analysis of inelastic scattering angular distributions using the distorted wave method is discussed. Applications of the collective and optical models for spin and parity assignments are discussed. Various examples point out the usefulness of these methods. (M.O.W.)

15727 (PPAD-572F) EXPERIMENTAL INVESTIGATION OF SOME NEUTRON-DEFICIENT NUCLEI [Thesis]. Evans, J. S. (Princeton-Pennsylvania Accelerator, Princeton, N. J.). Dec. 1, 1965. Contract AT(30-1)-2137. 217p. Dep. mn. CFSTI $6.00 cy, $1.25 mn.

A windowless flow-type proportional counter was used to detect the 1.5-kev M x rays and Auger electrons emitted following the decay of ^{163}Ho by orbital electron capture from the atomic M shell. A preliminary value of (33 ± 23) yr was obtained for the half life of ^{163}Ho. A six-gap electron spectrometer was adjusted and calibrated for use in beta-ray and conversion electron studies. The spectrometer was used both for recording conversion electron spectra and for obtaining conversion electron–gamma-ray coincidence spectra in studies of some palladium and rhodium isotopes. Using a time-to-amplitude converter, the half life of the 75-kev state in ^{100}Rh was measured to be 235 ± 3 nsec. The g-factor of this same state was determined by the time-differential angular correlation method to be +2.13 ± 0.03. A novel method for rapidly dissolving bulk rhodium metal was devised. The rhodium is fused with molten zinc to form a rhodium-zinc alloy, which is then converted to a water-soluble form by a second fusion with potassium hydrogen sulfate. Carrier-free radiochemical procedures are described for preparing sources of palladium and rhodium species. A general survey of the mass 100 region was made using the spherical shell model as a guide. The systematics of the single-particle proton and neutron states, $39 \leq Z \leq 49$ and $51 \leq N \leq 81$, were used to correlate existing data in odd-A nuclei and to suggest where to look for additional states which have not yet been located. The collective states in both even-even and odd-A nuclei were found to agree fairly well with the model of collective vibrations about a spherical equilibrium shape. The Brennan-Bernstein coupling rules were used to correlate the spins and magnetic moments of levels in odd-odd nuclei with those for levels in adjacent odd-A nuclei. The nuclei near mass 100 were compared with nuclei at the beginning and end of the deformed rare earth region, in order to look for possible nonspherical equilibrium shapes. Several experimental criteria for distinguishing between the spherical and spheroidal shapes are discussed and applied to the ruthenium and palladium isotopes. Although the well-studied nuclides seem to be adequately described by the spherical approximation, it is pointed out that spheroidal shapes might be encountered for ^{106}Ru and ^{114}Pd. (M.O.W.)

15728 (RHEL/R–112, pp 23-36) PROTON SCATTERING. (National Inst. for Research in Nuclear Science, Chilton (England). Rutherford High Energy Lab.).

Measurements are reported on: p-p interaction differential cross sections at 50 Mev; polarization in elastic scattering of 25- to 50-Mev protons by Ca, ^{58}Ni, ^{60}Ni, and ^{208}Pb; polarization in elastic scattering of 20- to 30-Mev protons by ^{12}C; differential scattering cross sections for 50-Mev protons on ^{12}C, ^{16}O, and ^{51}V; polarization and differential scattering cross section for proton scattering by deuterons at a proton energy of 30.2 Mev. (T.F.H.)

15729 (RHEL/R–112, pp 37-66) PROTON INDUCED REACTIONS. (National Inst. for Research in Nuclear Science, Chilton (England). Rutherford High Energy Lab.).

Measurements are reported on the parameters of proton reactions and scattering on nuclei having atomic numbers of 1 to 92, for proton beam energies between 20 and 50 Mev. (T.F.H.)

15730 (RHEL/R–112, pp 67-98) THEORETICAL STUDIES. (National Inst. for Research Nuclear Science, Chilton (England). Rutherford High Energy Lab.).

Optical and shell model analyses are carried out of proton scattering and reactions on nuclei, using phase-shift and distorted-wave techniques. (T.F.H.)

15731 (RPI–328-49) LINEAR ACCELERATOR PROJECT. Progress Report, October 1965–December 1965. (Rensselaer Polytechnic Inst., Troy, N. Y. Dept. of Nuclear Engineering and Science). Contract AT(30-3)-328. 82p. Dep. mn. CFSTI $3.00 cy, $0.75 mn.

Summaries of 7 papers dealing with neutron thermalization are presented. Steady state neutron spectra measurements in borated water and a feasibility study of a new method for measuring resonance absorption are included discussions. Brief discussions on neutron cross section measurements are presented along with resonance capture gamma spectra in iron and manganese. Also brief discussions are presented on the instrumentation development program for neutron cross section measurements. (M.O.W.)

15732 (TID–21654) DOPPLER COEFFICIENT OF THORIUM OXIDE. [Quisenberry, K. S.] (Knolls Atomic Power Lab., Schenectady, N. Y.). [nd]. Contract W-31-109-eng-52. 18p. Dep. mn. CFSTI $1.00 cy, $0.50 mn.

The neutron Doppler coefficient is briefly discussed. The method of measurement for ThO_2 in the KAPL Thermal Test Reactor is briefly reviewed. The results are given. (M.O.W.)

15733 (UCRL–7769) NEUTRON-NEUTRON INTERACTION IN THE T + T REACTION. Lacina, B.; Ingley, J.; Dorn, D. W. (Lawrence Radiation Lab., Univ. of California, Livermore). Jan. 26, 1965. Contract W-7405-eng-48. 29p. Dep. mn. CFSTI $2.00 cy, $0.50 mn.

The effects of a final-state neutron-neutron interaction in the reaction $\tau + \tau \rightarrow {}^4\text{He} + 2n + Q$ (11.33 Mev) are studied. It is shown that the energy spectra peak is near Q/3 if a square-well interaction is assumed. (D.C.W.)

15734 (ZfK-PhA–18) GAMMA-UEBERGAENGE IM ^{153}Eu. (Gamma Transitions in ^{153}Eu). Funke, L.; Graber, H.; Kaun, K.-H.; Sodan, H. (Zentralinstitut fuer Kernforschung, Rossendorf bei Dresden (East Germany); Frana, J.; Rezanka, I. (Ustav Jaderneho Vyzkumu, Ceskoslovenska Akademie Ved, Rez). Dec. 1965. 11p. Dep. mn.

The gamma spectrum of ^{153}Sm was measured using a Li-drifted Ge detector. The gamma energies and intensities were compared with values obtained from an investigation of the external conversion electron spectrum. Previously unreported gamma rays with energies of 509, 617, and 657 kev were observed. It is proposed that the 681.6- and 694.3-kev levels of ^{153}Eu are the beta-vibrational levels corresponding to the one-particle levels $5/2^+[413]$ and $3/2^+(411)$, respectively. (D.C.W.)

15735 (ANL-Trans–265) NEUTRON POLARIZATION IN THE REACTION D(d,n)^{3}He AT LOW DEUTERON ENERGIES. Haensgen, H.; Pose, H.; Schirmer, G.; Seeliger, D. Translated by Elmar K. Wilip (Argonne National Lab., Ill.), from Nucl. Phys., 73: 417-23(1965). 9p. Dep. mn. JCL $1.10 fs, $0.80 mf.

The polarization of neutrons emitted from the reaction D(d,n)^{3}He at an angle of 50° in the laboratory system was measured at eight deuteron energies from 57.3 to 116.8 kev. The neutron polarization was calculated from the measured left-right asymmetry in the elastic scattering of the neutrons from carbon. The polarization exhibits resonance behavior in the energy range covered and attains a maximum at 80 kev. (D.C.W.)

15736 THE NEUTRON COHERENT SCATTERING AMPLITUDE OF CESIUM. Zivadinovic, M. S.; Prelesnik, B. V. (Boris Kidric Inst. of Nuclear Sciences, Belgrade). Acta Crystallogr., 20: 315-16(Feb. 10, 1966).

The neutron coherent scattering amplitude of the cesium atom was investigated. The neutron diffraction measurements were made on a powder sample of CsCl. The neutron wavelength was 1.031 Å. The powder diagram of CsCl is shown. The accuracy of the diffraction peak areas was estimated to 3% or better. The absorption correction was made, and the experimentally determined value of μR for CsCl was 0.17 cm^{-1} and $Q'/Q_0 = 0.645$. The coherent scattering amplitude of cesium was found to be $(0.75 \pm 0.02) \times 10^{-12}$ cm. (F.J.H.)

15737 MOESSBAUER EFFECT OF THE 46.5-Kev LINE OF ^{183}W. Drosg, Manfred (Oesterreichische Studiengesellschaft fuer Atomenergie, Siebersdorf, Austria); Ujlaki, Endre. Acta Phys. Austr., 20: 171-4(1965). (In German).

The principle of the apparatus used for the measurement of the Mössbauer effect is described, and a representation is given. The γ quanta were measured with a Xe-filled proportional counter with the resolution of approximately 10%

and additional measurements were made with a NaI crystal. The transmission curve of the 46.5-kev line was obtained. A resonance absorption constituent of 4.4% was established, but a correcting effect of approximately 26% was necessary. The measurements were made at a temperature of 80°K. (J.S.R.)

15738 THE REACTION $^{16}O(n,\alpha)^{13}C$ AT NEUTRON ENERGIES AROUND 14 Mev. Fuerst-Rauch, M.; Muenzer, H. (Institut fuer Radiumforschung, Vienna). Acta Phys. Austr., 20: 300-3(1965). (In German).

The $^{16}O(n,\alpha)^{13}C$ reaction was studied using vanadium pentoxide foil deposited on gold foils. Photographic plates were used for the detection of the α particles. The horizontal and vertical components of the α paths were measured in order to determine both the angular and energy distributions. The results obtained are graphed. A maximum in the forward direction and in the backward direction was detected. The maximum in the backward direction corresponds to the heavy particle stripping mechanism. For the maximum in the forward direction two reaction mechanisms were proposed: the pick-up process and the knock-on process. (J.S.R.)

15739 DETERMINATION OF THE EFFECTIVE CROSS SECTION FOR THE (n,^{3}He) PROCESS ON ^{55}Mn, ^{59}Co, ^{75}As, AND ^{103}Rh FOR 14.8-Mev NEUTRONS. Frevert, E. (Institut fuer Radiumforschung und Kernphysik, Vienna). Acta Phys. Austr., 20: 304-13(1965). (In German).

The effective cross section for the (n,^{3}He) process on ^{55}Mn, ^{59}Co, ^{75}As, and ^{103}Rh, at neutron energies of 14.8 Mev was determined. The time decay of the total β activity, the time decay of the γ activity, the total γ spectrum, and, in the case of Mn, the Compton spectrum were measured. The results are tabulated. An upper limit was given for the effective cross sections. (J.S.R.)

15740 SYNTHESIS OF TRANSCURIUM ELEMENTS BY NUCLEAR REACTIONS WITH HEAVY IONS. Keller, C. (Technische Hochschule, Karlsruhe, Ger. Kernforschungszentrum, Karlsruhe, Ger.). Angew. Chem. Int. Ed. Engl., 4: 903-14(Nov. 1965).

Experimental techniques are described for the preparation of transcurium elements. Nuclear reactions with heavy ions appear to be most promising for the preparation of new transcurium elements and isotopes. Since these nuclear reactions have extremely small cross sections, only a few atoms will be produced. Because of their short half lives, the heaviest nuclei can presumably be identified only indirectly through the probabilities of their formation and disintegration. (auth)

15741 GENEALOGICAL COEFFICIENTS FOR α-PARTICLES. Rotter, Ingrid (Research Inst. for Nuclear Research, Dubna, USSR). Ann. Phys. (7), 16: 242-9 (1965). (In German).

The fractional parentage coefficients for the separation of four particles from the 1 p-shell are expressed through the coefficients for two particles. For α-particles they are calculated and given. (auth)

15742 VARIATIONAL DERIVATION OF THE PAIRING EQUATION IN A FINITE NUCLEUS. Malik, F. B. (Yale Univ., New Haven). Ann. Phys. (N. Y.), 36: 86-103(Jan. 1966).

For nonsingular two-nucleon forces, the equation of a pair of nucleons embedded in a finite nucleus, assuming other nucleons to be in the well-defined single particle orbitals was derived from the variational principle. The total wave functions of the system are completely antisymmetrized with respect to the interchange of particles, and the boundary condition of the square integrability of the stationary state wave functions is incorporated in the treatment. In Model I which corresponds to the independent pair model the extrapair nucleons are in the well-defined pre-assigned single particle orbitals of any type, e.g., Fermi or Shell model or Hartree-Fock orbitals; the effect of the pair on these single particle orbitals is neglected. In Model II the effect of the pair on the single particle orbitals is considered by extremizing the total energy with respect to the pair as well as the single particle orbitals. The final equation of the pair in both cases is similar and unlike the usual Bethe-Goldstone equation has hermitian operators, which means that this equation defines an eigenvalue problem. In the pair equation of motion of two nucleons additional to a closed shell, the term describing the interaction of these two particles, as derived from the variational analysis, is the full two nucleon potential. (auth)

15743 ANALYTICAL EXPRESSIONS FOR INELASTIC SCATTERING CROSS SECTIONS. Bassichis, W. H.; Dar, A. (Weizmann Inst. of Science, Rehovoth, Israel). Ann. Phys. (N. Y.), 36: 130-41(Jan. 1966).

The Blair-Austern expression for the cross section for inelastic scattering via collective excitation, under strong absorption conditions, is rederived using the W.K.B. approximation. It is then shown that application of a small number of approximations transforms the Blair-Austern formula into a very simple, analytical expression, suitable for comparison with experiment without resorting to lengthy computer calculations. The Blair Phase Rule is obtained from this expression for all angles and the double phase rule is shown to be valid only for large angles. The resulting expression is compared to experimental cross sections to illustrate the validity of the approximations. Satisfactory agreement is obtained. (auth)

15744 CHANNELS PROJECTION OPERATORS AND PAULI PRINCIPLE. Coz, Marcel (Massachusetts Inst. of Tech., Cambridge). Contract AT(30-1)-2098. Ann. Phys. (N. Y.), 36: 217-27(Feb. 2, 1966). (MIT–2098-161).

The problem of constructing projection operators in the antisymmetrized case is now considered. The definition of elementary nonhermitian idempotent operators which are called projectors is used. The nonexistence of these operators implies a functional dependence between the states expressing the channels such that these channels do not look like physical channels. In a special case the coupled equations for the amplitudes are written down. (auth)

15745 ON THE ANOMALIES OF E2 CONVERSION COEFFICIENTS IN THE DEFORMED-NUCLEUS REGION. Erman, Peter; Hultberg, Soelve (Research Inst. for Physics, Stockholm). Arkiv Fys., 30: 101-9(1965).

E2 conversion coefficients for transitions between 2+ and 0+ states are generally known to be in good agreement with the theoretical calculations and are sometimes used as standards for determining conversion coefficients. However, in the deformed-nucleus region $150 < A < 200$, previous experiments systematically give higher values than the theoretical ones, possibly suggesting that the deformation of the nucleus should affect the conversion coefficients. The IEC method recently improved by the introduction of scattering corrections was used. In this way internal conversion coefficients for the $2+ \rightarrow 0+$ E2 transitions to the ground states of ^{160}Dy, ^{166}Er, ^{170}Yb, and ^{182}W were measured. The results are $\alpha_K = 1.56 \pm 0.15$ (1.55), $\alpha_K = 1.68 \pm 0.15$ (1.65), $\alpha_K = 1.37 \pm 0.07$ (1.36), and $\alpha_K = 0.86 \pm 0.05$ (0.86), respectively. These results are in excellent agreement with the corresponding theoretical values given in the brackets. Together with other evidence these data indicate that previously obtained anomalies are probably not real. (auth)

15746 ELECTRIC DIPOLE SUM RULES AND INELASTIC ELECTRON SCATTERING FORM FACTORS OF 1^-, $T = 1$ STATES IN LIGHT NUCLEI. Czyz, W. (Institute of Nuclear Physics, Krakow). Bull. Acad. Pol. Sci., Ser. Sci. Math. Astron. Phys., 13: 823-7(1965).

Some simple relations between certain electric dipole sum rules and recent measurements of the inelastic electron scattering form factors of the 1^-, $T = 1$ excitations in light nuclei are discussed. It is considered to what extent the experimental data can be explained without resorting to any detailed calculations of the particle-hole states and their interactions. (J.F.P.)

15747 THE USE OF A CALIBRATED GAMMA SPECTROMETER FOR PRECISION ACTIVITY MEASUREMENTS

OF GAMMA EMITTERS AND E.C.-NUCLIDES AND FOR PURITY AND SORPTION TESTS OF SOLUTIONS OF RADIONUCLIDES. Vaninbroukx, R.; Grosse, G. (EURATOM, Geel, Belg.). Int. J. Appl. Radiat. Isotop., 17: 41-6 (Jan. 1966).

The experimental intensity calibration of a γ spectrometer as well as the use of the calibrated instrument for standardization of γ emitters and nuclides decaying by electron capture, half-life measurements, determination of branching ratios and purity and sorption tests are described. (auth)

15748 ACTIVATION OF THE NUCLEAR ISOMER ^{113m}In BY GAMMA RAYS OF ^{60}Co. Veres, A.; Pavlicsek, I. (Inst. of Isotopes, Budapest). Int. J. Appl. Radiat. Isotop., 17: 69-73(Jan. 1966).

Evaluation of the effective activation cross section and measurement of the energy and half life of the nuclear isomer ^{113m}In were performed by making use of the ^{113}In$(\gamma,\gamma')^{113m}$In reaction induced by irradiation from a ^{60}Co source. By comparison with data obtained simultaneously on ^{115m}In, as estimation of the cross section for resonance absorption was made, the value of which was found to be in good agreement with that obtained from bremsstrahlung experiments. (auth)

15749 15th ANNUAL CONFERENCE ON NUCLEAR SPECTROSCOPY AND STRUCTURE OF THE ATOMIC NUCLEUS, MINSK, USSR, JANUARY 25–FEBRUARY 2, 1965. Izv. Akad. Nauk SSSR, Ser. Fiz., 29: 714-871(May 1965). (In Russian). (CONF-650119).

Twenty-five papers are included. Separate abstracts were prepared for each paper. (M.J.T.)

For abstracts of individual papers see: 14868, 14869, 15326, and 15750–15771.

15750 NEW DATA ON DECAY OF ^{184*}Re. Dzhelepov, B. S.; Tishkin, P. A.; Shishelov, I. A. (Leningrad State Univ.). Izv. Akad. Nauk SSSR, Ser. Fiz., 29: 714-20(May 1965). (In Russian).

The decay of 167-day ^{184*}Re was studied by the conversion-electron coincidence method using a double toroidal beta spectrometer. Conversion electrons from 25 to 170 kev were observed. Spectra of the ^{184}Re and ^{184}W conversion electrons and various coincidences are shown, and a partial decay scheme is presented. Coincidences between the Re L105 and W K162, the W L111 and Re (M + N)105, and the W L64 and W (M + N)55 conversion electrons are discussed. Coincidences between the W L111 and the W L55, K162, L162, K217, and L217 lines were not observed. These data indicate that ^{184}W has an isomeric state at 1287 kev with a half life greater than 5×10^{-6} sec. (M.J.T.)

15751 ON THE DECAY OF ^{90}Mo. Grigor'ev, E. P.; Egorov, Yu. S.; Zolotavin, A. V.; Sergeev, V. O.; Sovtsov, M. I. Izv. Akad. Nauk SSSR, Ser. Fiz., 29: 721-8(May 1965). (In Russian).

Results of measurements of the conversion-electron spectra of the ^{93m}Mo, ^{99}Mo, and ^{90}Mo source and of the gamma transition energies and K/L conversion-electron intensity ratios for ^{90}Mo and ^{90}Nb decay are given. Multipolarity assignments for the 257.2- and 122.4-kev transitions in ^{90}Nb and the 262.7-kev transition in ^{93}Mo are discussed. A decay scheme for ^{90}Mo is proposed. Results are correlated with previous data. (M.J.T.)

15752 DECAY SCHEME OF ^{109}Sn. Khulelidze, D. E.; Chikhladze, V. L.; Onufriev, V. G. (Physico-Technical Inst., Erevan). Izv. Akad. Nauk SSSR, Ser. Fiz., 29: 729-33(May 1965). (In Russian).

Results of measurements of the β^+ spectrum of ^{109}Sn and the gamma and conversion-electron spectra of ^{109}In are presented. Multipolarity assignments for the ^{109}In gamma transitions are discussed. The branching ratios for positron and electron-capture decays of ^{109}Sn and the spin-parity of various ^{109}In levels are deduced, and a decay scheme is proposed. (M.J.T.)

15753 ISOMERIC TRANSITIONS OF ^{114*}In AND ^{115*}Te. THE β^+ SPECTRUM OF ^{115}Te. Khulelidze, D. E.; Chikhladze, V. L.; Onufriev, V. G.; Kushakevich, Yu. P.; Dyatlov, V. K. (Inst. of Physics and Tech., Erevan). Izv. Akad. Nauk SSSR, Ser. Fiz., 29: 734-8(May 1965). (In Russian).

The experimental scheme for measuring spectra of short-lived ($\approx 10^{-4}$ sec) isotopes and isomers, by recording emitted radiation simultaneously with the target irradiation, is described. The spectra of the K and L conversion electrons of the 310-kev transition of ^{114*}In (42 msec) and the 275-kev transition of ^{115*}Te were measured, and the transitions were deduced to have multipolarity E3 and M3, respectively. The spin and parity of the ^{115}Te levels were deduced. The ^{115}Te positron spectrum was measured, and a decay scheme derived from these and previous data is shown. (M.J.T.)

15754 INVESTIGATION OF THE EXCITED STATES ^{104,104*}Rh BY OBSERVATION OF γ RAYS FROM THE (n,γ) REACTION. Sumbaev, O. I.; Alekseev, V. L.; Kaminker, D. M.; Smirnov, A. I.; Shaburov, V. A. Izv. Akad. Nauk SSSR, Ser. Fiz., 29: 739-59(May 1965). (In Russian).

Gamma rays emitted in the ^{103}Rh(n,γ)^{104}Rh reaction were observed using a bent-crystal scintillation spectrometer. Energies and intensities of 158 gamma rays are tabulated. Measurement errors are discussed, and results are compared with those of previous experiment. A partial level and transition scheme was derived for ^{104}Rh by a general sum-difference method. The fine-structure grouping of the spectral lines is discussed. (M.J.T.)

15755 GAMMA-RAY SPECTRUM PRODUCED BY THERMAL NEUTRON CAPTURE IN PALLADIUM. Groshev, L. V.; Demidov, A. M.; Shadiev, N. Izv. Akad. Nauk SSSR, Ser. Fiz., 29: 760-5(May 1965). (In Russian).

Gamma spectra from thermal-neutron capture in a natural mixture of Pd isotopes were observed. Data on the isotopic abundance in the natural mixture and on the binding energy of the neutron in the product nucleus are reviewed. Measured energies and intensities of gamma rays from 4.5 to 9.6 Mev are presented. Results of identifying specific gamma lines of the measured spectrum with various energy levels of the isotopes ^{105}Pd, ^{106}Pd, ^{107}Pd, and ^{109}Pd are given. Gamma-transition and energy-level schemes are presented for ^{105}Pd and ^{106}Pd. (M.J.T.)

15756 GAMMA-RAY SPECTRUM PRODUCED BY THERMAL NEUTRON CAPTURE IN GOLD. Groshev, L. V.; Demidov, A. M.; Shadiev, N. Izv. Akad. Nauk SSSR, Ser. Fiz., 29: 766-71(May 1965). (In Russian).

The gamma spectrum produced in ^{197}Au thermal-neutron capture was measured from 3.5 to 7.7 Mev. Energies and intensities of the gamma lines of ^{198}Au from 4.4 to 6.6 Mev and the energies of the corresponding excited states are presented. A diagram of the energy levels and radiative transitions of ^{198}Au is shown. (M.J.T.)

15757 NUCLEAR LEVELS OF ^{168}Er EXCITED BY THE (n,γ) REACTION. Groshev, L. V.; Demidov, A. M.; Ivanov, V. A.; Lutsenko, V. N.; Pelekhov, V. I.; Shadiev, N. Izv. Akad. Nauk SSSR, Ser. Fiz., 29: 772-81(May 1965). (In Russian).

The gamma rays between 0.5 and 8 Mev from the ^{167}Er(n,γ) reaction were studied, using a natural isotopic target. Energies and intensities of the gamma rays are tabulated, and their origins are considered. Conversion electron measurements are presented for 21 transitions with energies below 1.4 Mev. Conversion coefficients were obtained for 19 of the transitions, and multipolarities were assigned. A diagram of energy levels and transitions for ^{168}Er is shown, and spin and parity assignments are discussed. (M.J.T.)

15758 NUCLEAR LEVELS OF ^{166}Ho FROM THE (n,γ) REACTION. Groshev, L. V.; Shadiev, N. Izv. Akad. Nauk SSSR, Ser. Fiz., 29: 782-6(May 1965). (In Russian).

The gamma spectrum from the ^{165}Ho(n,γ) reaction was recorded for gamma energies from 4.5 to 6.35 Mev. Energies and intensities of 38 lines are tabulated, and esti-

mated errors are discussed. Relative intensities were converted to absolute intensities by normalizing the total gamma radiation to the neutron binding energy. Level excitation energies were derived and are compared with those obtained from previous measurements of the (d,p) and (n,γ) reactions. Spin-parity assignments for some of the ^{166}Ho levels are considered. (M.J.T.)

15759 STUDY OF POLARIZED γ RADIATION EMITTED DURING COULOMB EXCITATION OF CERTAIN NUCLEI WITH ODD A. Alkhazov, D. G.; Gal'perin, L. N.; Gusinskii, G. M.; Lemberg, I. Kh.; Nabichvrishvili, V. A. Izv. Akad. Nauk SSSR, Ser. Fiz., 29: 787-93(May 1965). (In Russian).

The polarization of gamma radiation is determined as the ratio of the number of gamma quanta polarized in the reaction plane to the number of quanta polarized in a plane perpendicular to it. The angle between the incoming beam and the emitted radiation is taken to be 90°. An expression for the polarization of gamma quanta emitted in Coulomb excitation in terms of the spins of the nuclear states is obtained. The response of the polarimeter was found by measuring polarization of gamma rays emitted during Coulomb excitation of known nuclear levels. Triply charged N ions with energies 16.2 and 17.7 Mev were used for bombarding. Results of polarization measurements of the 440-kev gamma of ^{23}Na, the 350-kev gamma of ^{57}Fe, the 322-kev gamma of ^{69}Ga, and the 457-kev gamma of ^{77}Se are discussed and correlated with previous data. (M.J.T.)

15760 MEASUREMENT OF LINEAR POLARIZATION OF 1.97-Mev GAMMA RAYS IN THE REACTION ^{36}Ar (p,p'γ)^{36}Ar. Val'ter, A. K.; Kopanets, E. G.; Tsytko, S. P. (Physics-Engineering Inst., Academy of Sciences, Ukrainian SSR). Izv. Akad. Nauk SSSR, Ser. Fiz., 29: 800-2 (May 1965). (In Russian).

The linear polarization of the 1.97-Mev gamma rays excited in the reaction ^{36}Ar(p,p'γ) at 3.05 Mev was determined experimentally. The results confirm the assignment of spin-parity 2^+ for the first-excited state of ^{36}Ar and the E2 character of the 1.97-Mev transition to the ground state. (M.J.T.)

15761 NUCLEAR LEVELS OF ^{27}Al AT EXCITATION ENERGIES OF 10.495 AND 3.95 Mev. Val'ter, A. K.; Kopanets, E. G.; Tsytko, S. P. (Physics-Engineering Inst., Academy of Sciences, Ukrainian SSR). Izv. Akad. Nauk SSSR, Ser. Fiz., 29: 803-6(May 1965). (In Russian).

The gamma rays from the reaction ^{26}Mg(p,γ)^{27}Al at 2.298 Mev were studied in detail. The gamma spectrum from 0.8 to 10.5 Mev is shown, and results of analyzing the spectral lines are given, including comparison with the calculated transition energy, angular asymmetry, relative intensity, and corresponding transition in the ^{27}Al level scheme. Decay schemes are presented for the 10.405-Mev resonance state and the low-lying levels of ^{27}Al, including spin-parity assignments. The assignment of spin-parity $^7/_2{}^+$ to both the 10.495- and 3.95-Mev levels, made on the basis of the angular distributions and angular correlations in the ^{26}Mg(p,γ) and ^{26}Mg(p,p'γ) reactions, is discussed. (M.J.T.)

15762 DECAY SCHEME OF ^{119}*Te. Sorokin, A. A.; Shtal', M. Z.; Rybakov, V. P. (Moscow State Univ. Joint Inst. for Nuclear Research, Dubna, USSR). Izv. Akad. Nauk SSSR, Ser. Fiz., 29: 819-22(May 1965). (In Russian).

The source, containing ^{118}Te, ^{119}Te, and ^{119}*Te isotopes, was prepared by proton irradiation of a CsCl target and allowing it to decay a few days. Measurements were made of the γ spectrum, and the γ-γ and β^+-γ coincidence spectra with respect to the ^{119}Sb 0.65-Mev γ, and the relative intensity of the 1.10-Mev γ and the β^+ with respect to the ^{119}Te K-capture intensity. The decay scheme of the ^{119}Te ground state is shown. (M.J.T.)

15763 INELASTIC SCATTERING OF HEAVY PARTICLES WITH EXCITATION OF COLLECTIVE NUCLEAR STATES. Luk'yanov, V. K.; Petkov, I. Zh. (Joint Inst. for Nuclear Research, Dubna, USSR). Izv. Akad. Nauk SSSR, Ser. Fiz., 29: 823-9(May 1965). (In Russian).

A method is presented for calculating the cross sections for inelastic scattering of heavy particles on nuclei at energies above the barrier, taking into account the excitation of collective nuclear states by Coulomb and nuclear interaction potentials. The method can be used in the analysis of experiments with heavy ions and alpha particles when it is impossible to be limited by the first order of perturbation theory. In order to study the mechanism of excitation by the nuclear field, the angular distribution of particles scattered elastically at angles $\theta > \theta_0$, i.e., where nuclear forces play an essential role, is examined. (M.J.T.)

15764 INFLUENCE OF PAIRING CORRELATIONS ON E1 TRANSITIONS IN DEFORMED NUCLEI. Gadetskii, O. G.; Pyatov, N. I. (Joint Inst. for Nuclear Research, Dubna, USSR). Izv. Akad. Nauk SSSR, Ser. Fiz., 29: 830-7(May 1965). (In Russian).

An attempt is made to obtain reliable values of the retardation factors R_γ for E1 transitions in deformed nuclei by the use of modified wave functions. Expressions for the retardation factors are obtained in the superfluid (Bardeen-Cooper-Schrieffer) model of the nucleus. Calculations of the retardation factors are carried out for neutron and proton E1 transitions in rare earth nuclei, using the ordinary Bardeen wave functions and the projected functions, with and without taking the effect of blocking into account. The calculations do not lead to satisfactory agreement of the theoretical values of the E1 transition probability with the experimental values. (M.J.T.)

15765 PECULIARITIES OF ELECTRIC DIPOLE TRANSITIONS IN DEFORMED ODD NUCLEI. Berlovich, E. E. (Ioffe Inst. of Physics and Tech., Leningrad). Izv. Akad. Nauk SSSR, Ser. Fiz., 29: 838-45(May 1965). (In Russian).

The occurrence of a significant number of electric dipole transitions in odd deformed nuclei which are strongly delayed in comparison with results of calculations using the Nilsson formula is examined in detail. The roles of the self-consistent field, effective charge, and pair correlations in this anomaly are considered. Calculations are carried out of the pair-correlation corrections and the delay factors for various E1 transitions in isotopes of Gd, Tb, Dy, Yb, Lu, Hf, and Ta. (M.J.T.)

15766 ON THE APPLICABILITY OF THE IKEGAMI-UDAGAVA METHOD FOR CONSIDERING PAIRING CORRELATIONS IN THE COMPUTATION OF ELECTROMAGNETIC TRANSITION PROBABILITIES IN DEFORMED NUCLEI. Berlovich, E. E.; Meiling, V.; Tarasov, V. K. (Ioffe Inst. of Physics and Tech., Leningrad). Izv. Akad. Nauk SSSR, Ser. Fiz., 29: 846-8(May 1965). (In Russian).

The expression proposed by Ikegami and Udagava for R_γ, the pair-correlation correction factor for the probability of E1 transitions in strongly deformed odd nuclei, is given, in which R_γ is expressed in terms of the levels of the average field for the initial and final states and the corresponding quasiparticle energies. Approximations for the quasiparticle energies in terms of the odd-even mass differences are presented. Results of calculations of R_γ and the resulting delay factors, using various energy-level data, are shown, for neutron and proton transitions in isotopes of Gd, Dy, Yb, Hf, Tb, Lu, and Ta. (M.J.T.)

15767 INFLUENCE OF SECOND-ORDER EFFECTS ON THE ANGULAR CORRELATIONS OF COULOMB-EXCITED NUCLEI. Isakov, V. I. Izv. Akad. Nauk SSSR, Ser. Fiz., 29: 849-52(May 1965). (In Russian).

The angular correlation between the inelastically scattered ion and the gamma quantum emitted after Coulomb excitation of the target nucleus is found; the amplitude of the Coulomb transition is examined in the second order of perturbation theory. The process of Coulomb excitation is considered semiclassically. Expressions are found for the amplitude and probability of the Coulomb transition. The case is considered in which recording of the ions or gamma quanta is carried out in an axially symmetric manner and the radiative transition is represented by a mixture of transitions of the type EL and ML'. As an example, calculations are performed for the angular correlation of

gamma quanta emitted from the second levels of the double-phonon triplet (0^+, 2^+, 4^+) to the first excited state $2'^+$ in even-even nuclei. (M.J.T.)

15768 INTERFERENCE EFFECTS IN COULOMB EXCITATION OF 2^+ LEVELS IN EVEN-EVEN NUCLEI. Gangrskii, Yu. P.; Isakov, V. I.; Lemberg, I. Kh. (Ioffe Inst. of Physics and Tech., Leningrad). Izv. Akad. Nauk SSSR, Ser. Fiz., 29: 853-6(May 1965). (In Russian).

The cross section of interference between processes of the first and second orders, appearing in the formula for the differential cross section of Coulomb excitation in the second order of perturbation theory, is calculated for the case of E2-type transitions in even-even nuclei with spin-0 ground state and spin-2 intermediate and final-excited states. Results of computing the Coulomb excitation function, used in the cross-section calculation, are given for four angles. The relative contribution of the interference cross section to the total cross section is examined; the dependence of this contribution on the intermediate- and final-state energies is shown. Results are presented of numerical calculations of the relative contributions of the interference cross section in the excitation of the first 2^+ and the second $2'^+$ levels of ^{78}Se and ^{152}Sm by ^{14}N ions at 36 and 52 Mev, respectively. (M.J.T.)

15769 ATOMIC MASSES OF STABLE NEODYMIUM, PRASEODYMIUM, CERIUM, AND LANTHANUM ISOTOPES. Demirkhanov, R. A.; Dorokhov, V. V.; Dzkuya, M. I. Izv. Akad. Nauk SSSR, Ser. Fiz., 29: 857-61(May 1965). (In Russian).

Masses of the stable isotopes of Nd, Pr, Ce, and La were measured by means of doublets formed by an organic compound and the measured isotope, using several independent doublets and various organic compounds for each isotope. Measurements were carried out using a double-focusing mass spectrometer. In all, 62 doublets were measured and used to calculate masses of 14 isotopes. Results are presented and compared with previous measurements. (M.J.T.)

15770 ELASTIC SCATTERING OF MEDIUM-ENERGY NEUTRONS AND THE OPTICAL NUCLEAR MODEL. Korzh, I. A.; Kashuba, I. E.; Totskii, I. A. (Inst. of Physics, Academy of Sciences, Ukrainian SSR). Izv. Akad. Nauk SSSR, Ser. Fiz., 29: 862-7(May 1965). (In Russian).

The optical model with diffuse boundary, surface absorption, and spin-orbit potential is used to describe the angular distributions of elastically scattered neutrons at 0.8 Mev on light, medium, and heavy nuclei. Expressions are obtained for the cross sections for compound-nucleus formation and for elastic scattering. Results are given of calculations of the elastic-scattering differential cross sections and the total cross sections at 0.8 Mev for Na, Mg, Al, Si, Cr, Fe, Ni, Cu, Zn, Se, Zr, Mo, Cd, Zn, Sb, Te, Ba, W, Hg, Pb, Bi, and U. Good agreement with previous experimental data is found. (M.J.T.)

15771 ABSOLUTE (REDUCED) AND RELATIVE PROBABILITIES FOR E0 CONVERSION. Borisoglebskii, L. A. (Belorussian State Univ.). Izv. Akad. Nauk SSSR, Ser. Fiz., 29: 868-71(May 1965). (In Russian).

Reduced M- and N-shell E0 conversion probabilities are calculated and tabulated for 55 of the 96 cases of E0 conversion of MI, MII, NI, and NII electrons in Tb, Hg, Tl, and U. Thomas-Fermi-Dirac wave functions were used in all the calculations except those for Hg, in which Hartree wave functions were employed. The finite nuclear radius was taken into account by assuming a uniform charge distribution. It was estimated that the use of Hartree instead of Thomas-Fermi-Dirac wave functions changed the MI conversion probability by 1 or 2%. The MI/MII conversion ratios previously calculated without screening for U differed from the present results by 3 to 6%. The calculated K/(L + M + N) E0 conversion ratios in ^{90}Zr (by extrapolation) and ^{234}U are found to be in good agreement with previous experimental data. (M.J.T.)

15772 ISOMER OF ^{130}I. Wilkey, D. Dennis; Willard, John E. (Univ. of Wisconsin, Madison). J. Chem. Phys., 44: 970-3(Feb. 1, 1966).

The existence of the isomer ^{130m}I (9.2 min) was established by growth of the gamma spectrum of the ^{130}I ground state following neutron irradiation of ^{129}I, and also by the incorporation of ^{130}I into organic combination as a result of the isomeric transition of I_2 (^{130m}I) dissolved in n-hexane. The isomer decays to the ground state by a highly converted isomeric transition with a 0.77 probability and to the 0.54-Mev level of ^{130}Xe by beta emission with 0.23 probability. The cross-section ratio, $\sigma(^{130m}I)/\sigma(^{130}I)$, for production of the isomers from ^{129}I by pile neutrons is about 2.0. The fraction of the isomeric transition events that results in organic incorporation of the ^{130}I daughter in solutions of $I_2(^{130m}I)$ in n-hexane, or in solutions of RI(^{130m}I) in ethyl iodide, is about 0.40. (auth)

15773 ISOMERIC CROSS-SECTION RATIOS FOR 14.6 Mev NEUTRON INDUCED REACTIONS. Kolar, Z.; Strohal, P.; Cindro, N. (Inst. Ruder Boskovic, Zagreb). J. Inorg. Nucl. Chem., 27: 2471-9(Dec. 1965).

The isomeric cross section ratios for the reactions ^{69}Ga(n,p)^{69}Zn, ^{72}Ge(n,α)^{69}Zn, ^{133}Cs(n,p)^{133}Xc, and ^{192}Os(n,2n)^{191}Os were measured. The results were fitted with the compound nucleus theory, using $\frac{1}{2}$ of the rigid body value for the moment of inertia parameter and a rather low value for the number of γ-de-excitations ν. The result for ^{192}Os(n,2n) did not fit very well into the theory. (auth)

15774 MASS SPECTROMETRIC MEASUREMENTS OF THE RATIO OF THERMAL NEUTRON CAPTURE TO FISSION FOR ^{241}Pu. Cabell, M. J.; Wilkins, M. (Atomic Energy Research Establishment, Harwell, Eng.). J. Inorg. Nucl. Chem., 27: 2481-91(Dec. 1965). (AERE-R-4865).

Highly enriched samples of ^{241}Pu were irradiated in five different positions in a flux scanning tube of the PLUTO reactor so that α (the ratio of neutron capture to fission) could be measured for this nuclide. Highly enriched samples of ^{239}Pu and ^{240}Pu were also irradiated at the same time so that allowance could be made for the effects of their destruction. Experimental values of $\hat{\alpha}$ for ^{241}Pu varied from 0.352 to 0.395, with a mean value of 0.371 ± 0.016. Correcting all results to 2200 m/sec neutrons gave a final value for α_0 of 0.390 ± 0.023. Where a comparison was possible with previously published data, good agreement was found. (auth)

15775 QUADRUPOLE SPLITTING OF THE 14.4 kev GAMMA LINE OF ^{57}Fe IN IRON SULPHATES OF THE JAROSITE GROUP. Hrynkiewicz, A. Z. (Inst. of Nuclear Physics, Krakow); Kubisz, J.; Kulgawczuk, D. S. J. Inorg. Nucl. Chem., 27: 2513-17(Dec. 1965).

The Mössbauer effect was used for the investigation of the hyperfine structure of the 14.4-kev γ line of ^{57}Fe in iron compounds belonging to the jarosite group. From the observed quadrupole splittings and isomer shifts some conclusions concerning the interaction of the ferric ion Fe^{3+} with its surroundings and the properties of this ion in these compounds are drawn. (auth)

15776 RUTHENIUM AND RHODIUM ISOTOPES IN SPONTANEOUS FISSION OF ^{238}U. Rao, M. N.; Shahani, C. J. (Atomic Energy Establishment, Trombay, India). J. Inorg. Nucl. Chem., 27: 2679-81(Dec. 1965).

The cumulative fission yields of ^{105}Rh and ^{105}Ru were investigated. ^{105}Rh activity was allowed to grow in the mother uranium solution for 30 hr and ^{105}Ru for 10 days before chemical separation was carried out. The chemical yields were 63.28 and 24.7%, respectively. The ^{105}Rh decay curve yielded an initial activity (at zero time) of 1.75 cpm. The ^{105}Ru decay curve, after correction for background and ^{105}Rh activity, yielded an initial activity (at zero time) of 4.8 cpm. The equilibrium ratios of ^{105}Rh to ^{238}U and ^{105}Ru to ^{238}U were calculated and found to be 15.28 ± 3.06 and 16.86 ± 3.40, respectively. The fission yields for ^{105}Rh and ^{105}Ru were found to be 0.688 ± 0.138 and 0.634 ± 0.127%, respectively. (F.J.H.)

15777 ISOMERIC CROSS-SECTION RATIOS IN THE (n,γ) REACTIONS ON ^{130}Te AND ^{110}Pd. Namboodiri, M. N.; Rajagopalan, M.; Ravindran, N.; Rengan, K.; Ramaniah, M. V. (Atomic Energy Establishment, Trombay, India). J. Inorg. Nucl. Chem., 28: 1-4(Jan. 1966).

Isomeric cross-section ratios, $\sigma m/(\sigma m + \sigma g)$, in the (n,γ) reactions on ^{130}Te and ^{110}Pd were determined using radiochemical techniques and were found to be 0.059 and 0.045, respectively. These results were compared with those of others and those calculated on the basis of Huizenga-Vandenbosch model. (auth)

15778 ISOMERIC CROSS-SECTION RATIOS FOR ^{134m}Cs, ^{134}Cs AND ^{133m}Ba, ^{133}Ba FORMED IN (d,p) AND (d,2n) REACTIONS. Mocoroa, A.; Vignau, H.; Caracoche, M. C.; Nassiff, S. J. (La Plata National Univ., Argentina. Atomic Energy Commission, Argentina). J. Inorg. Nucl. Chem., 28: 5-9(Jan. 1966).

Ratios between the cross sections σ_m/σ_g as a function of deuteron energy were experimentally determined for the isomers ^{134m}Cs, and ^{134}Cs produced by the reaction ^{133}Cs $(d,p)^{134}Cs$ and for the isomers ^{133m}Ba and ^{133}Ba produced by the reaction $^{133}Cs(d,2n)^{133}Ba$. (auth)

15779 THE HALF-LIFE OF ^{149}Nd. Rider, B. F.; Peterson, J. P. Jr.; Ruiz, C. P. (General Electric Co., Pleasanton, Calif.). J. Inorg. Nucl. Chem., 28: 266-8(Jan. 1966).

The half life of ^{149}Nd was measured to be 1.72 ± 0.01 hr. The ^{149}Nd was obtained by neutron activation of natural and ^{148}Nd-enriched neodymium as the oxide. After irradiation the neodymium was purified by reverse-phase chromatography. Gamma pulse-height analysis was used to measure the half life following decay of the 650-kev peak with time. The half life was also determined independently by 4π beta counting to ensure that there was no bias in the measurements. (M.C.G.)

15780 MEASUREMENT OF THE LIFETIMES OF THE FIRST EXCITED STATES OF ^{19}F AND ^{25}Mg. Bougnot, G.; Espi, G.; Poizat, J. C.; Samueli, J. J.; Sarazin, A. (Institut de Physique Nucleaire, Lyon). J. Phys. (Paris), 26: 546-8(Oct. 1965). (In French).

The mean lives of the first excited state of ^{19}F and ^{25}Mg were measured by means of a pulsed beam technique. The values obtained are: 110 kev state of ^{9}F: $\tau_m = 0.84 \pm 0.04 \times 10^{-9}$ s, 580 kev state of ^{25}Mg: $\tau_m = 4.97 \pm 0.15 \times 10^{-9}$ s. (auth)

15781 STUDY OF TRANSITIONS IN ^{189}Pt. Kilcher, Pierrette (Univ. Paris, Orsay, France). J. Phys. (Paris), 26: 591-3(Oct. 1965). (In French).

The decay of isotopically separated ^{189}Au was studied in order to obtain information about the excited levels of the nucleus ^{189}Pt. The measurements were performed with the aid of semiconductor detectors, a semiconductor β spectrograph and scintillations techniques. (auth)

15782 DECAY OF ^{159}Eu. Iwashita, Takeki (Tokyo Univ.). J. Phys. Soc. Jap., 20: 2105-17(Dec. 12, 1965).

The decay scheme of ^{159}Eu was investigated by using beta and gamma ray scintillation spectrometers with a fast-slow coincidence circuit. The half-life of ^{159}Eu was measured as 19.0 ± 0.5 min. Beta rays with end-point energies 2.57 ± 0.05, 2.35 ± 0.05, 1.90 ± 0.05, 1.75 ± 0.05, 1.50 ± 0.05 and 1.0 ± 0.1 Mev, and gamma rays with energies 1500, 1100, 800, 670, 220, 145, 130, 90 and 75 kev were found. On the basis of the experimental results obtained by β-γ, γ-β and γ-γ coincidence measurements, a tentative decay scheme of ^{159}Eu was proposed. The assignments of the excited levels were made based on the Nilsson model and the systematics in neighboring odd-N nuclei. The systematic behavior of low excited levels of gadolinium isotopes and N = 95 isotones are discussed. (auth)

15783 POLARIZATION OF PROTONS SCATTERED BY ^{14}N. Brown, R. I. (Univ. of Wisconsin, Madison). Nucl. Phys., 78: 492-6(1966). (TID-22297).

The polarization of protons elastically scattered by ^{14}N was measured by observing the left-right asymmetry in scattered beam intensity when the polarized proton beam from the Wisconsin tandem accelerator was scattered from a gaseous nitrogen target. Measurements were made at 45° (lab) from 4.9 to 6.9 Mev in 100 kev steps with 120 kev target thickness, and from 7.1 to 10.1 Mev in 200 kev steps with 220 kev target thickness. The polarization is always negative, averages about −0.6 but shows considerable variation with energy. The uncertainties of the measurements are of the order of ±0.02. Measurements of the asymmetry for the inelastic scattering of protons leaving ^{14}N in its first excited state were obtained between 7.1 and 8.3 Mev. (auth)

15784 THE STATISTICS OF THE EIGENVALUES OF RANDOM MATRICES. Cristofori, F; Sona, P. G.; Tonolini, F. (CISE, Segrate, Italy. Univ., Milan). Nucl. Phys., 78: 553-6(1966).

The connection between the single level distribution of the ensembles of the antisymmetric hermitian matrices and of the positive definite hermitian matrices is obtained. The time reversal properties of the statistical matrix ensembles are also discussed. (auth)

15785 ASYMPTOTIC SOLUTION FOR THE BROWNIAN MOTION OF THE EIGENVALUES OF A RANDOM MATRIX. Ullah, Nazakat (Tata Inst. of Fundamental Research, Bombay). Nucl. Phys., 78: 557-60(1966).

It is shown that in the limit $N \to \infty$, each element of the $N \times N$ random orthogonal matrix behaves like a random Gaussian variable. This result can be used in finding the asymptotic distribution of any nuclear or atomic property which is a function of the elements of the random orthogonal matrix. The asymptotic form of the solution for the Brownian motion of a random matrix, which is used to describe the statistical properties of spectra of complex systems which possess approximate constants of the motion, is obtained. (auth)

15786 ^{54}Fe: THE SPINS AND DECAY MODES OF SOME LOW-LYING EXCITED STATES. Thomas, M. F.; Poletti, A. R.; Grace, M. A. (Nuclear Physics Lab., Oxford). Nucl. Phys., 78: 561-75(1966).

The decay schemes of the states below 4 Mev in ^{54}Fe, excited by inelastic proton scattering at bombarding energies between 7.0 and 8.5 Mev were determined by particle-gamma-ray coincidence experiments. The method of particle-gamma-ray angular correlations presented by Litherland and Ferguson was applied to determine unambiguously the spins of the states at 1.41, 2.96, 3.16, and 3.83 Mev as J = 2, 2, 2, and 4, respectively. The spin of the state at 3.34 Mev was limited to the values 2, 3, 4. Information upon radiative mixing ratios in the decay of the states at 2.96, 3.16, and 3.83 Mev was also obtained. The results are compared with spin assignments from inelastic electron, proton and alpha-particle measurements and are discussed in terms of models of nuclear structure. (auth)

15787 THERMAL AND RESONANCE NEUTRON CAPTURE IN Cl, Sc, V, Co, AND Ir. Wasson, O. A.; Draper, J. E. (Yale Univ., New Haven). Contract AT(30-1)2726. Nucl. Phys., 78: 576-92(1966).

The γ-ray spectra emitted following capture of low energy neutrons ($E_n < 10$ kev) were observed as a function of incident neutron energy. The neutron energies were selected by the time-of-flight technique while the γ rays were detected in a NaI(Tl) anticoincidence spectrometer. Significant variations of the γ-ray intensities as a function of neutron energy occur. Two previously unreported resonances at 470 ± 20 and 1080 ± 60 ev neutron energy are observed in scandium. (auth)

15788 EQUILIBRIUM DEFORMATIONS OF THE ODD-MASS NUCLEI IN THE RARE-EARTH REGION. Hassan, M. Y. M. (Univ. of Warsaw); Skladanowski, Z.; Szymanski, Z. Nucl. Phys., 78: 593-608(1966).

Previous calculations of the ground-state equilibrium deformations and quadrupole moments for the even nuclei in the rare earth region were extended to the case of the odd-mass nuclei. These calculations were performed in the framework of the Nilsson model including pairing force. The calculated quadrupole moments are generally found to be in agreement with experiment to better than 10%, with exception of the neighborhood of the Eu and Sm nuclei, where the transition takes place between spherical and de-

formed shapes. The density deformation parameter corresponding to the calculated quadrupole moments overlaps within 10% difference with the deformation of the nuclear potential. The influence of the blocking effect on the equilibrium deformation is also discussed. (auth)

15789 DEUTERON PHOTODISINTEGRATION WITH A SEPARABLE TWO-NUCLEON POTENTIAL. Naqvi, J. H. (Aligarh Muslim Univ., India). Nucl. Phys., 78: 609-12(1966).

The deuteron photodisintegration cross section is calculated using a separable nonlocal two-nucleon potential. There is good agreement between theory and experiments up to γ-ray energies of about 10 Mev. However, the agreement becomes progressively worse as the γ-ray energy is increased. (auth)

15790 REACTION MECHANISM FOR THE $^{11}B(\alpha,n)^{14}N$ REACTION. Mani, G. S.; Dutt, G. C. (The Physical Labs., Manchester, Eng.). Nucl. Phys., 78: 613-24(1966).

The reaction $^{11}B(\alpha,n)^{14}N$ was studied to establish the reaction mechanism and, if this proceeds through the formation of the compound nucleus, to investigate the levels in ^{15}N around 13 Mev excitation. Using a time-of-flight spectrometer, 47 angular distributions were measured of the n_0 group of neutrons leaving ^{14}N in the ground state, between incident alpha particle energies of 2.38 and 3.67 Mev; and 10 angular distributions were obtained of the n_1 group of neutrons, between incident alpha particle energies of 3.46 and 3.67 Mev. The analysis of the angular distributions shows that the reaction $^{11}B(\alpha,n_0)^{14}N$ leaving ^{14}N in the ground state proceeds predominantly through the compound nucleus process, while direct interaction seems to be the main contribution to the reaction $^{11}B(\alpha,n_1)^{14*}N$, leaving ^{14}N at the first excited state. Spins and parities of $3/2^-$, $3/2^-$ and $7/2^-$, respectively, have been assigned to the levels in the compound nucleus, corresponding to the resonances at alpha particle energies of 2.63, 3.23 and 3.57 Mev. (auth)

15791 SHELL MODEL WITH $\sigma \cdot \chi$ POTENTIAL. Araki, Gentaro (Kyoto Univ.). Nucl. Phys., 78: 625-40 (1966).

The one-nucleon state of a definite j-value is constructed as a linear combination of two states which belong to the azimuthal quantum numbers $j - 1/2$ and $j + 1/2$, respectively. The invariance of the state for space inversion is guaranteed by introducing a unit pseudoscalar. The Hartree-Fock equation satisfied by such one-nucleon states and the isospin and spin-angle dependence of the Hartree and exchange fields are discussed on the assumption that the two-nucleon interaction consists of three parts, i.e., the central, the $\sigma \cdot \sigma'$ and the tensor-force type. It is shown that the Hartree-Fock equation reduces to a form of eigenvalue equation of the hamiltonian with central plus $\sigma \cdot \chi$ type potentials. Addition theorems for spin-orbital harmonics are obtained in the ljm scheme. (auth)

15792 DOUBLE EMISSION OF HAMMER TRACKS FROM HEAVY EMULSION NUCLEI IN HIGH-ENERGY INTERACTIONS. Baumann, G. (Centre de Recherches Nucleaires, Strasbourg); Bechdolff, A.; Gerber, J. P.; Braun, H.; Cueer, P.; Harmsen, D. M. Nucl. Phys., 78: 650-6(1966).

Experimental data concerning 46 events involving the emission of two hammer tracks in the same star are given for various high-energy interactions. The emission frequencies for different incident energies of protons, K^- and π^- mesons are compared with those of single hammer tracks. The ^8Li energy spectrum is given. The distribution of the angle between the two fragments seems inconsistent with the hypothesis of an independent emission. (auth)

15793 THE REACTION $(\pi^-,2n)$ IN ^6Li AND ^7Li. Davies, H.; Muirhead, H.; Woulds, J. N. (Univ. of Liverpool). Nucl. Phys., 78: 663-72(1966)

The energy spectra and angular distributions of the two neutrons emitted following meson (π) capture at rest in the isotopes of ^6Li and ^7Li. At time-of-flight technique was used. Data are presented on the binding energies and total momenta of the neutrons in the parent nuclei. In approximately 40% of the meson (π) captures the reactions lead to the ground states of the nuclei ^4He and ^5He from capture in ^6Li and ^7Li, respectively; the characteristic features involving the emission of a pair of neutrons differ considerably in the two isotopes. (auth)

15794 HIGH ENERGY γ RAYS FROM PION CAPTURE. Davies, H.; Muirhead, H.; Woulds, J. N. (Univ. of Liverpool). Nucl. Phys., 78: 673-80(1966).

The yields and energy spectra of the high energy γ radiation arising from meson(π) capture in complex nuclei were measured by means of a sodium iodide crystal. The γ-rays appear to peak strongly in the region of 100–115 Mev for a range of nuclei from ^6Li to natural copper; the yield is about 2% per meson(π) capture and falls slowly with increasing atomic weight. Possible reaction mechanisms are discussed. (auth)

15795 DECAY OF ^{153}Sm(47h) TO ^{153}Eu. Blichert-Toft, P. H.; Funk, E. G.; Mihelich, J. W. (Univ. of Notre Dame, Ind.). Nucl. Phys., 79: 12-26(1966).

The decay of ^{153}Sm(47 h) to excited states in ^{153}Eu was studied with a lithium-drifted germanium detector and a scintillation spectrometer. Singles and coincidence spectra were obtained. The energies and relative photon intensities of the previously reported transitions of 103.18, 151.49, 172.85, 412.1, 424.3, 437.3, 463.6, 521.3, 531.4, 533.2, 539.2, 554.7, 578.5, 596.7, 603.0, 609.1 and 636.2 kev were obtained. The energies and relative photon intensities of hitherto unreported transitions of 481, 485, 509.2, 584.2, 615.9, 657.7, 683, 713 and 760 kev were determined. The present data are consistent with a level scheme with states at 83.37 kev ($7/2^+$), 97.45 kev ($5/2^-$), 103.18 kev ($3/2^+$), 151.5 kev ($7/2^-$), 172.85 kev ($5/2^+$), 585 kev ($3/2^+$), 589 kev ($5/2^-$), 597 kev ($1/2^+$), 604 kev ($5/2^+$), 634.6 kev ($1/2^+$), 636.4 kev ($3/2^+$), 658 kev ($3/2^+$), 683 kev ($5/2^+$), 712 kev ($5/2^-$) and 760 kev ($5/2$). The log ft values for transitions to these levels were obtained. Ratios of experimental gamma-ray transition probabilities from the 712, 683, 658, 636.4 and 172.85 kev states are presented. All gamma-ray transitions were placed into a consistent decay scheme, which may be treated in terms of the Nilsson model. (auth)

15796 P_L/P_K ELECTRON CAPTURE RATIO IN THE DECAY OF ^{204}Tl. Klein, H.; Leutz, H. (Univ., Heidelberg). Nucl. Phys., 79: 27-32(1966).

The P_L/P_K electron capture ratio in the decay of ^{204}Tl was determined to be 0.55 ± 0.05 by using NaI(Tl) scintillation crystals containing ^{204}Tl as a constituent of the crystal lattice. A disintegration energy of 324^{+21}_{-18} kev was calculated from this capture ratio. The branching ratio of electron capture to β^--emission was determined to be $(2.29 \pm 0.06)\%$. (auth)

15797 INELASTIC SCATTERING OF HIGH-ENERGY PROTONS IN THE COLLECTIVE THEORY OF EXCITATIONS. Haybron, R. M. (Michigan State Univ., East Lansing. Oak Ridge National Lab., Tenn.). Nucl. Phys., 79: 33-45(1966). (ORNL-P-1491).

The cross section for the inelastic scattering of 155 Mev protons from several light, even nuclei was calculated for the excitation of some strongly excited low-lying states using the collective theory of excitations. Comparison with experiment produces deformation parameters which are in reasonable agreement with those obtained by other means, provided both the real and imaginary portions of the appropriate volume absorbing optical potential are deformed. Similar treatment of surface absorbing potentials yields cross sections which compare closely in shape to the results for volume potentials, but require unreasonably large deformations. Deformation of only the real part of either type of potential does not yield satisfactory fits. (auth)

15798 DIRECT REACTIONS WITH TWO-NUCLEON TRANSFER. Shapiro, I. S.; Timashev, S. F. (Inst. for Theoretical and Experimental Physics, Moscow). Nucl. Phys., 79: 46-64(1966).

Angular distributions in the direct nuclear reactions

(t,p) and (^{3}He,n) on light nuclei are calculated. Satisfactory agreement with experimental data in the region of small momentum transfers is obtained. (auth)

15799 THE ENERGY LEVELS OF ^{90}Y. **Black, J. L.; Darcey, W.; Islam, M. M. (Nuclear Physics Lab., Oxford). Nucl. Phys., 79: 65-76(1966).**

The energy levels of ^{90}Y were studied from the reactions ^{89}Y(d,p)^{90}Y at E_d = 11.95 Mev and ^{92}Zr(d,α)^{90}Y at E_d = 12.00 Mev. A total of 45 energy levels were observed in the (d,p) reaction up to an excitation of 3.88 Mev. Angular distributions for 18 levels were obtained and reduced widths extracted for them from DWBA analysis. Single-particle states arising from the neutron configurations $2d_{5/2}$, $3s_{1/2}$ and $2d_{3/2}$ were identified at 0/0.202; 1.214/1.374 and 2.479/2.628 Mev, respectively. It is noted that some of the single particle strengths are distributed in a number of weak levels above 1.4 Mev. An l = 4 distribution was observed for the 2.938 Mev state and possibly for the levels at 1.965 and 2.245 Mev; the low-lying l = 4 transitions are expected from the $1g_{7/2}$ neutron configuration. The positive parity states of ^{90}Y arising from the configuration $[(2p_{1/2})^{-2}(1g_{9/2})^1]_p$ $[2d_{5/2}]_n$ could not be observed in the (d,p) reaction. Extra states observed in the (d,α) reaction at 0.68, 0.78 and 0.965 Mev were interpreted as belonging to the above configuration. The results were compared with the theoretical predictions of Kim and Auerbach and Talmi. (auth)

15800 THE EXCITATION FUNCTION OF THE ^{29}Si(n,α_0)^{26}Mg REACTION FOR NEUTRON ENERGIES AROUND 14 Mev. **Jaskola, M.; Turkiewicz, I. M.; Turkiewicz, J.; Gradzki, F. (Inst. of Nuclear Research, Warsaw). Nucl. Phys., 79: 108-12(1966).**

The nuclear reaction ^{29}Si(n,α)^{26}Mg was studied by bombarding a silicon detector with fast neutrons. The excitation function for the ground state transition was measured in the neutron energy range 13.4 to 15.0 Mev. (auth)

15801 CONTINUOUS GAMMA RADIATION ACCOMPANYING NUCLEAR BETA DECAY. **Struzynski, R. E. (Stevens Inst. of Tech., Hoboken, N. J.); Pollock, F. Nucl. Phys., 79: 113-34(1966).**

The photon spectrum associated with the internal bremsstrahlung of the nucleus ^{35}S is computed. Relativistic Coulomb wave functions are used for the final states of the negatron. The Green function for the Dirac equation is computed using a potential based on a finite size nucleus of uniform charge density. The equivalence between the two methods of calculation originally proposed by Knipp and Uhlenbeck is proven. The results agree with those of Mau. Since the calculation includes Coulomb effects completely, the discrepancy between theory and experiment may now be attributed to either the neglecting of screening effects in the calculations or to experimental procedures. (auth)

15802 THE EXCITED LEVELS OF ^{79}Br. **Langhoff, H.; Frevert, L.; Schoett, W.; Flammersfeld, A. (Univ., Goettingen, Ger.). Nucl. Phys., 79: 145-58(1966).**

The resonance fluorescence technique was applied to study the excited levels of ^{79}Br. Using gaseous sources of ^{79}Kr four well-known levels at 834 kev, 606 kev, 398 kev and 307 kev were excited. A fifth level excited at 526 kev was newly established. The cross sections for resonance scattering yield the following mean lifetimes: 834 kev level $\tau = (0.17 \pm 0.05)$ psec, 606 kev level $\tau = 3.7 \pm 0.4$ psec, 526 kev level $\tau = 3.5 \pm 1.0$ psec, 398 kev level $\tau = 45 \pm 15$ psec, and 307 kev level $\tau = 18 \pm 10$ psec. The results were confirmed by a self-absorption experiment. The angular distribution of the resonantly scattered radiation gives further information about the spins of the excited levels. The decay scheme of ^{79}Kr was investigated using a Li-drifted germanium counter and a two-dimensional coincidence spectrometer. In addition to the results of former decay scheme studies γ-transitions of 526 kev, 617 kev, 811 kev, 858 kev and very likely 1165 kev were identified. Coincidence experiments revealed that ^{79}Kr decays by emission of positron to the ground state (7.6%), to the 261 kev level (0.13%), and to the 398 kev level (0.015%). (auth)

15803 A SIMULTANEOUS DETERMINATION OF THE PARAMETERS OF THE CORE-PARTICLE MODEL IN ^{197}Au. **McKinley, John M.; Rinard, Phillip M. (Kansas State Univ., Manhattan). Nucl. Phys., 79: 159-64(1966).**

The parameters of the core-particle model of Lawson and Uretsky were determined for ^{197}Au by fitting simultaneously all the available experimental data and also a part of the data. Those quantities that are known with some precision (energy levels and static moments) were found to be very well described by the model whereas the more difficult to measure transition rates were not so satisfactorily fitted. The values found for the parameters were compared where possible to those found in other investigations. (auth)

15804 EXCITATION OF ISOBARIC ANALOGUE STATES BY (p,n) REACTIONS. **Harchol, M.; Cochavi, S.; Jaffe, A. A.; Drory, Ch. (Hebrew Univ., Jerusalem). Nucl. Phys., 79: 165-76(1966).**

Excitation functions for the (p,n) reactions on targets of ^{65}Cu, ^{76}Ge, ^{93}Nb, ^{116}Sn, ^{118}Sn, ^{119}Sn, ^{122}Sn, ^{124}Sn, ^{121}Sb, ^{123}Sb, ^{125}Te, ^{126}Te, ^{130}Te, and ^{197}Au were studied. Sharp resonances corresponding to isobaric analog states were observed in all cases with the exception of ^{121}Sb and ^{197}Au. A close correspondence of both spacing and strength was observed between the compound resonances and states found in (d,p) reactions on the same targets, where such data are available. The widths of the majority of resonances are presented. Using recently available mass data, accurate Coulomb displacement energies were calculated from the above results and from those of other workers. (auth)

15805 THE ELASTIC AND INELASTIC SCATTERING OF 20-28 Mev POLARIZED PROTONS BY CARBON. **Craig, R. M.; Dore, J.-C.; Greenlees, G. W.; Lowe, J.; Watson, D. L. (Univ. of Birmingham, Eng.). Nucl. Phys., 79: 177-87(1966).**

Measurements are presented of the polarization in proton-carbon scattering at incident energies of 20.2, 21.7, 22.6, 24.1, 26.2, 27.1, and 28.3 Mev (lab). Results cover the angular range 20°–160° (lab) for elastic scattering and inelastic scattering (Q = −4.43 Mev) from ^{12}C. The data show an irregular, non-monotonic variation with energy, which is not characteristic of scattering by a complex potential. The addition of a resonant compound elastic contribution from a few states, which has previously been shown to fit experimental cross sections in this energy range, does not improve the agreement with the present polarization results. (auth)

15806 POLARIZATION OF PROTONS FROM ELASTIC AND INELASTIC SCATTERING ON ^{24}Mg. **Boca, I.; Borsaru, M.; Cenja, M.; Hategan, C.; Iliescu, E.; Martalogu, N. (Inst. for Atomic Physics, Bucharest). Nucl. Phys., 79: 188-92(1966).**

The angular distributions of the polarization of protons from elastic and inelastic scattering on ^{24}Mg were measured at E_p = 5.8 Mev. The polarizations of the elastically and inelastically scattered protons are of opposite sign. The results obtained are explained by a direct interaction mechanism with channel coupling. (auth)

15807 A STUDY OF THE DECAY OF ^{187}W USING A 2 m CURVED-CRYSTAL SPECTROMETER. **Reidy, J. J.; Wiedenbeck, M. L. (Univ. of Michigan, Ann Arbor). Nucl. Phys., 79: 193-202(1966).**

The gamma rays in the decay of ^{187}W were studied using a 2 m curved-crystal spectrometer and a lithium-drifted germanium diode spectrometer. One previously unreported transition was observed and the energies of all observed transitions were determined with the curved-crystal spectrometer. Upper limits were determined for the intensities of possible unobserved gamma rays in the 160–1200 kev region. The relative merits and complementarity of the curved crystal spectrometer and the Ge(Li) spectrometer are discussed. In addition, data are presented concerning the reflectivity of the curved crystal using the germanium ($0\bar{2}2$) planes. (auth)

15808 ABSOLUTE CROSS SECTIONS AND EXCITATION FUNCTIONS FOR DEUTERON INDUCED REACTIONS ON CHROMIUM BETWEEN 2 AND 12 Mev. **Cogneau, M.;**

Gilly, L.; Cara, J. (Univ., Louvain, Belg.). Nucl. Phys., 79: 203-8(1966).

Absolute cross sections and excitation functions between 2 and 12 Mev were measured for the following reactions: $^{52}Cr(d,2n)^{52m}Mn$, 21 min, $^{52}Cr(d,2n)^{52}Mn$, 5.6 d, $^{50}Cr(d,n)^{51}Mn$, 45 min. This was done by activation and stacked foil techniques. The experimental results show that the (d,2n) reactions proceed via the compound nucleus mechanism whereas the (d,n) excitation function shows a mixture of compound nucleus and direct reaction mechanism. Measurements of the cross section ratio $\sigma_{21min}/\sigma_{5.6d}$ show that the ground state (5.6 d) is preferentially formed at low deuteron energies. (auth)

15809 DEFORMATIONS IN PERTURBATION THEORY. Bertsch, George F. (Princeton Univ., N. J.). Nucl. Phys., 79: 209-19(1966). (PUC-937-170).

The Nilsson model for light nuclei is studied from the point of view of perturbation theory. Core wave functions are calculated using realistic two-body interactions. It is found that the Nilsson model describes the core energy and quadrupole polarization quite well, but that the assumption of constant volume upon deformation is poor for calculating electric monopole amplitudes. (auth)

15810 THE BETA DECAY OF ^{147}Nd. Beekhuis, H.; Boskma, P.; van Klinken, J.; de Waard, H. (Rijksuniversiteit Groningen, Netherlands). Nucl. Phys., 79: 220-30 (1966).

The beta components with maximum energies of 806 and 364 kev in the decay of ^{147}Nd were studied. The coefficient a in the expression $C(W) = k(1 + aW)$ for the shape factor is found to be -0.07 ± 0.01 for the 806 kev transition and -0.20 ± 0.15 for the 364 kev transition. The previously reported degree of longitudinal polarization, measured for an electron energy of 261 kev, is $-(1.000 \pm 0.025)\ v/c$ yielding $b = 0.00 \pm 0.05$ for the 806 kev component and $b = 0.00 \pm 0.16$ for the 364 kev component in the expression $P = -(v/c)(1 - b/W)$. The coefficients R and e in the expression $\epsilon = (p^2/W)(R + eW)/C'(W)$ for the $\beta-\gamma$ angular correlation are $R = -0.008 \pm 0.006$, $e = 0.002 \pm 0.003$ for the (806β, 91γ) cascade and $R = +0.06 \pm 0.05$, $e = -0.04 \pm 0.03$ for the (364β, 531γ) cascade. The very low intensity of the beta component to the ground state of ^{147}Pm (<0.2% of the 806 kev component) is briefly discussed. (auth)

15811 ELASTIC AND INELASTIC NEUTRON SCATTERING BY SILICON AND SULPHUR. Petitt, G. A. (Duke Univ., Durham, N. C.); Buccino, S. G.; Hollandsworth, C. E.; Bevington, P. R. Nucl. Phys., 79: 231-40(1966).

The energy spectra of neutrons scattered elastically and inelastically to the first excited states of ^{28}Si and ^{32}S were measured using time-of-flight techniques. Angular distributions were taken for incident neutron energies of 2.45, 2.85, 4.00, 4.90, and 5.80 Mev and an excitation function was measured at 60°. The elastic scattering distributions are fairly well described by the Perey-Buck non-local potential optical model with slightly reduced well depths, corrected for the compound elastic component. The inelastic scattering cross sections show large fluctuations, but the angular distributions are fairly isotropic. For ^{28}Si, the inelastic scattering is fairly well described by the Hauser-Feshbach formula modified by Dresner's "width fluctuation" correction at low energies, but above 2.7 Mev the correction becomes too large. This may be an indication of the inapplicability of the theories in the region where $\langle\Gamma\rangle_{J\pi} \cong D_{J\pi}$. (auth)

15812 HYPERTRITON BINDING ENERGY WITH N.L.S. POTENTIALS. Monga, S. K. (Univ. of Delhi). Nuovo Cimento, (10), 41B: 164-73(Feb. 11, 1966).

The $_{\Lambda}H^3$ binding-energy problem is solved as an exact eigenvalue problem using nonlocal separable (N.L.S.) potentials between pairs of particles, two of which are of unequal masses. All the potentials are taken to operate between pairs in the s-state but with the effects of spins included. The parameters of the N-N potential are well known and those of Λ-N potential are adjusted to fit the experimental low-energy total cross sections for Λ-N scattering. The binding energy obtained for $_{\Lambda}H^3$ is in satisfactory agreement with experiment. (auth)

15813 ON THE THEORY OF DOUBLE-CHARGE-EXCHANGE NUCLEAR REACTIONS WITH π-MESONS. Becker, F.; Maric, Z. (Faculte des Sciences, Orsay, France). Nuovo Cimento, (10), 41B: 174-87(Feb. 11, 1966).

The cross section for double-charge-exchange nuclear reactions with mesons(π) for 1p shell nuclei is calculated in the impulse approximation. The comparison with the other theories is discussed. The numerical results for the measured cross section are given and the expected angular distribution is shown. (auth)

15814 ROTATIONAL LEVELS OF ODD-ODD LIGHT DEFORMED NUCLEI. Picard, J. (CEN, Saclay, France); De Pinho, A. G. Nuovo Cimento, (10), 41B: 239-43 (Feb. 11, 1966).

The low-lying rotational levels of odd-odd light deformed nuclei ^{18}F, ^{20}F, ^{22}Na, ^{24}Na, ^{26}Al, ^{28}Al, and ^{30}P are calculated using the unified model wave functions and taking into account the neutron-proton interaction through a residual two-body force. (J.F.P.)

15815 INTERNAL COMPTON EFFECT AT SMALL ANGLES. Fuschini, E.; Maroni, C.; Veronesi, P. (Univ., Bologna). Nuovo Cimento, (10), 41B: 252-3(Feb. 11, 1966).

The results of a measurement of the internal Compton effect using the M4, 662-kev transition from isomeric to ground state of a ^{137}Cs source are reported. This measurement was performed at small angles from 10 to 37.5°, where the cross section shows its maximum value. (J.F.P.)

15816 DECAY THEORY OF CLOSELY COUPLED UNSTABLE STATES. Mower, Lyman (Joint Inst. for Laboratory Astrophysics, Boulder, Colo.). Phys. Rev., 142: 799-816(Feb. 25, 1966).

A treatment of decay theory is presented which generalizes existing treatments so as to apply to closely coupled unstable states. The treatment is based upon a Green's function formulation for the transition amplitude in which the states of interest are selected by suitable projection operators. As an indication of the practicality of the resulting formulation a number of examples are given involving the stimulated transition between closely coupled unstable states. (auth)

15817 MESON RESONANCES AND NUCLEAR FORCES. Barker, Bruce M.; Gupta, Suraj N.; Haracz, Richard D. (Wayne State Univ., Detroit). Phys. Rev., 142: 1144-9 (Feb. 25, 1966).

The effect of η^-, ω^-, and ρ-meson resonances on nuclear forces is investigated with special attention to the $\eta + \pi$ exchange contribution, which requires extensive calculations. The exact relativistic results are expressed in terms of the W matrix, which was employed earlier for the one- and two-pion-exchange nucleon-nucleon interactions. It is pointed out that the relativistic approach is necessary for the treatment of nucleon-nucleon scattering up to 310 Mev, and an application of the present results to the experimental scattering data should enable us to estimate the coupling constants for the meson resonances. (auth)

15818 LACK OF STRUCTURE IN ^{235}U FISSION CROSS SECTION IN THE NEUTRON ENERGY RANGE FROM 150 TO 335 kev. Macklin, R. L.; Gibbons, J. H. (Oak Ridge National Lab., Tenn.). Phys. Rev. Lett., 16: 248-9(Feb. 7, 1966). (ORNL-P-1865).

The cross section for neutron fission of ^{235}U was studied in the energy range from 150 to 335 kev. No evidence for the detailed structure that was previously reported by Albert was observed. (D.C.W.)

15819 DYNAMIC POLARIZATION OF NUCLEI BY ELECTRON-NUCLEUS DIPOLAR COUPLING ("EFFECT SOLIDE"). Borghini, M. (Centre d'Etudes Nucleaires, Saclay, France). Phys. Rev. Lett., 16: 318-22(Feb. 21, 1966).

A theoretical description of the "solid effect" and of the relaxation of nuclei coupled by dipolar interactions with electron spins is presented. The results are applied to the case of neodymium-doped lanthanum magnesium double nitrate. (D.C.W.)

15820 ISOMER-SHIFT MEASUREMENT IN ^{182}W. Cohen, S. G.; Blum, N. A.; Chow, Y. W.; Frankel, R. B.; Grodzins, L. (Massachusetts Inst. of Tech., Cambridge). Contract AT(30-1)-2098. Phys. Rev. Lett., 16: 322-5 (Feb. 21, 1966). (MIT-2098-207).

The Mössbauer absorption spectra of the 2^+ to 0^+, 100 kev transition were observed at 4.2°K in tungsten metal and tungsten-hexachloride absorbers using a ^{182}Ta source in tantalum metal. The results indicate that the radius of the 2^+ rotational state is different from the radius of the 0^+ ground state. Preliminary results on the shifts of ^{184}W and ^{186}W are also given. (G.O.Y.)

15821 CENTRIFUGAL-STRETCHING AND CORIOLIS-FORCE ANTIPAIRING EFFECTS IN ^{182}W. Udagawa, T.; Sheline, R. K. (Florida State Univ., Tallahassee). Phys. Rev. Lett., 16: 325-7(Feb. 21, 1966).

The centrifugal-stretching and the Coriolis-force antipairing effects were calculated for ^{182}W. The results were compared with the results of Mössbauer measurements of the isomeric shift. (D.C.W.)

15822 CHARGE AND ENERGY DISTRIBUTIONS OF RECOILS FROM ^{226}Th ALPHA DECAY. Gunter, K.; Asaro, F.; Helmholz, A. C. (Univ. of California, Berkeley). Phys. Rev. Lett., 16: 362-4(Feb. 28, 1966).

The charge and energy distributions of recoils from the alpha decay of ^{226}Th were investigated using a high-resolution alpha spectrograph. (G.O.Y.)

15823 NUCLEAR GIANT QUADRUPOLE RESONANCE. Ligensa, R. (Univ., Frankfurt am Main); Greiner, W.; Danos, M. Phys. Rev. Lett., 16: 364-7(Feb. 28, 1966).

The description of the giant quadrupole resonance of the deformed nucleus was extended to include the coupling between the different collective modes in a quantum mechanical treatment. (D.C.W.)

15824 THE MEASUREMENT OF MATRIX ELEMENTS FOR FIRST FORBIDDEN BETA TRANSITIONS. II. EXPERIMENTAL METHODS AND RESULTS. Subotowicz, Mieczyslaw (Marie Curie Sklodowska Univ., Lublin). Postepy Fiz., 16: 413-28(1965). (In Polish).

The methods of measuring the beta-gamma angular correlation and polarization of circularly polarized gammas are reviewed. These measurements, which determine the value of the coefficient of asymmetry, include the forward-scattering of gammas by magnetized iron, the method of Beard and Rose, a backscattering method, and utilization of the Mössbauer effect. The measurement of beta-particle polarization and the angular correlation between polarized betas and circularly polarized gammas are also reviewed. The experimental methods include electron-electron scattering, and scattering of polarized electrons by heavy nuclei. All the experimental methods outlined in this paper have been applied to over a dozen beta emitters. The results are presented in detail for Tm-170, Sb-124, and La-140. (TTT)

15825 EFFECT OF FINAL STATE INTERACTIONS IN $(\alpha,2\alpha)$ REACTIONS. Kudo, Yoshiteru (Tohoku Univ., Sendai). Progr. Theoret. Phys. (Kyoto), 34: 942-55(Dec. 1965).

The effect of final state interaction is examined in detail in the $(\alpha,2\alpha)$ reactions at intermediate energies of an incident α particle. First, the angular correlation distribution is calculated by employing the plane-wave cutoff Born approximation. It is found impossible to explain the angular correlation distributions of the $^{16}O(\alpha,2\alpha)^{12}C$ (ground state) and $^{12}C(\alpha,2\alpha)^{8}Be$ (ground state) reactions by this simple treatment. Next, the angular correlation distribution in the cutoff Born approximation is improved in such a way that the effect of the final state interaction is correctly taken into account through the empirical phase shift of α-α scattering. The result of calculation is compared with the experimental data. It is shown that the experimental angular correlation distributions of the $^{16}O(\alpha,2\alpha)^{12}C$ (ground state), $^{12}C(\alpha,2\alpha)^{8}Be$ (ground state) and $^{9}Be(\alpha,2\alpha)^{5}He$ (ground state) reactions can be well reproduced by the improved treatment. It is concluded that the final state interaction plays an essential role in the angular correlation distribution of the $(\alpha,2\alpha)$ reactions for light nuclei. The relation between the impulse approximation and the formalism is briefly discussed. (auth)

15826 WAVE FUNCTIONS IN HYPERNUCLEI AND NUCLEAR COMPRESSIBILITY. Kohmura, Toshitake (Tokyo Univ.). Progr. Theoret. Phys. (Kyoto), 34: 956-62(Dec. 1965).

The wave functions in hypernuclei are investigated to avoid their uncertainties. It is shown that the nuclear wave function in hypernuclei are contracted by 3 to 5 percent by the Λ-N interaction. The contraction is seriously influenced by the nuclear compressibility. The wave function of the lambda particle is rather independent of it. The effect of the contraction on the decay rate of hypernucleus is discussed. (auth)

15827 NUCLEAR REACTIONS BY A LOW-ENERGY PION. Kohmura, Toshitake (Tokyo Univ.). Progr. Theoret. Phys. (Kyoto), 34: 963-71(Dec. 1965).

The effect of multiple scatterings by a pair of bound nucleons on nuclear reactions induced by a low energy meson (π) is investigated. It is pointed out that in the double charge exchange scattering the energy loss of meson (π) and the decrease of the cross section for the forward scattering with the mass number of the target nucleus result from the multiple scatterings. (auth)

15828 ON A UNIFIED DERIVATION OF THE CRANKING MODEL AND PEIERLS-YOCCOZ METHOD. I. WAVE FUNCTIONS. Shono, Yoshiyuki (Hiroshima Univ.). Progr. Theoret. Phys. (Kyoto), 34: 972-80(Dec. 1965).

The two typical methods describing the nuclear rotational motion, the cranking model and the Peierls-Yoccoz method, are understood in a unified manner, and at the same time a relation between the two methods is established. Discussions are mainly based on Elliott's analysis and the results of previous work in which a harmonic oscillator model with the Q-Q interaction was analyzed. It is emphasized that "a rotation generating operator" introduced previously has two kinds of important functions. The main results are derived from this property of "a rotation generating operator." (auth)

15829 ON THE ENERGY DEPENDENCE AND THE NON-LOCALITY OF THE OPTICAL POTENTIAL. Yazaki, Koichi (Tokyo Univ.). Progr. Theoret. Phys. (Kyoto), 34: 1047-8(Dec. 1965).

Quantitative arguments are given for Austern's interpretation (Phys. Rev., 137: 752(1965)) of the Perey effect and the related problem of flux nonconservation. For clarity restriction is made to the first-order effect of the nonlocality and the energy dependence of the potential. It is also assumed that the potential is hermitian. (J.F.P.)

15830 REDUCED WIDTHS FOR NUCLEON EMISSION IN SHELL MODEL INTERMEDIATE COUPLING. Iosifescu, M. (Inst. for Atomic Physics, Bucharest); Sandulescu, A.; Dumitrescu, O. Rev. Roum. Phys., 10: 623-8 (1965).

Reduced widths for nucleon emission from normal parity states of 1p-shell nuclei were calculated using intermediate coupling shell model wave functions. The intermediate coupling reduced widths are closer to the experimental reduced widths than those calculated using LS coupling wave functions. (auth)

15831 GAMMA RADIATION FROM INTERACTION OF NEUTRONS WITH IODINE NUCLEI. Cristu, M. I.; Popa, M. S. (Inst. for Atomic Physics, Bucharest). Rev. Roum. Phys., 10: 673-98(1965).

By means of a gamma scintillation spectrometer and gamma-gamma coincidence arrangement single spectrum and coincidence spectra of the gamma rays emitted in ^{127}I $(n,\gamma)^{128}$I reaction were investigated with an external target

of pure iodine and with the NaI(Tl) detector crystal used as internal target. Differences between the spectra recorded with the external and internal target were explained. The energies of the gamma rays separated in the single spectrum are given together with their absolute intensities up to about 500 kev. Coincidence measurements revealed the following cascades: 90–154, 134–134, 154–188, 134–285, 154–230, 188–230, 188–297, 240–764, 376–700, and 950–1370 kev. The information from the single and coincidence spectra measurements were used in the building of the scheme of low-lying levels in ^{128}I. The level scheme is discussed in terms of nuclear multiplets due to the coupling of odd nucleons in the odd-odd nucleus ^{128}I. Assignments concerning the spins and parities of the first levels and of the capturing state are made. (auth)

15832 γ RADIATION OF ^{152}Eu IN THE ENERGY RANGE 1380 TO 1900 kev. Voinova, N. A.; Dzhelepov, B. S.; Zhukovskii, N. N.; Kalinichev, Yu. V.; Maloyan, A. G.; Sergeev, A. G. (Ioffe Inst. of Physics and Tech., Leningrad. Radium Inst., Academy of Sciences, USSR). Yadern. Fiz., 3: 3-7(Jan. 1966). (In Russian).

The γ-spectrum of ^{152*}Eu in the energy range 1380 to 1900 kev was investigated using a magnetic compton γ-spectrometer elotron. New γ-lines with the energies 1510, 1557, 1680 and 1758 kev were found and their relative intensities determined. The energy of the 1411.9 ± 0.7 kev γ-line in ^{152}Eu was determined more precisely and this line was separated from the 1407.6 kev χ-line in ^{152}Eu. The levels 1680 kev 1^+ in ^{152}Sm and 1756 kev 1^- in ^{152}Gd are introduced. The decay scheme is discussed. (auth)

15833 COLLECTIVE LEVELS IN ODD-A DEFORMED NUCLEI IN THE RARE EARTH REGION. Gnatovich, V.; Gromov, K. (Joint Inst. for Nuclear Research, Dubna, USSR). Yadern. Fiz., 3: 8-12(Jan. 1966). (In Russian).

Experimental data on collective levels in odd-A deformed nuclei in the rare earth region are reviewed. (auth)

15834 PAIR PRODUCING CONVERSION TRANSITIONS IN ^{72}Ge. Belyaev, B. N.; Vasilenko, S. S.; Gvozdev, V. S.; Grigorev, V. N. (Ioffe Inst. of Physics and Tech., Leningrad). Yadern. Fiz., 3: 13-16(Jan. 1966). (In Russian).

Pair conversion positrons created in the decay of ^{72}Ga, obtained in (n,γ) reactions, were investigated. Positrons corresponding to the following γ-transitions were detected: 2510, 2490, 2465, 2400, 2200, 2120, 1865 kev. Using the pair conversion coefficients the multipolarities of the following γ-transitions were obtained: 2510 kev (E1), 2490 kev (E1), 2200 kev (E1). It follows from the multipolarities of the 2200 kev γ-transition, that the spin of the 3050 kev level is 2^-. The existence of a E0 transition with the energy 2400 kev is assumed. (auth)

15835 NUCLEAR MOMENTS OF INERTIA. Medvedev, B. I.; Khudakov, S. V. Yadern. Fiz., 3: 17-20(Jan. 1966). (In Russian).

The theory of finite Fermi-systems is used to consider nuclear moments of inertia. It is shown that the residual interactions between quasiparticles (besides pairing correlations) are significant only for the momenta of inertia of odd nuclei and for small deformations. This explains the good agreement of numerical calculations, not taking this interaction into account, with the experimental data. (auth)

15836 INFLUENCE OF STRONG INTERACTIONS BETWEEN NUCLEONS IN NUCLEI ON FORBIDDEN β DECAY. Rapoport, L. P.; Kopytin, I. V. (Voronezh State Univ., USSR). Yadern. Fiz., 3: 21-31(Jan. 1966). (In Russian).

General formulas are obtained for the probabilities of transitions of any order of forbiddenness and for various effects measured in β-decay, using the Fermi–liquid theory and techniques of spherical tensor operators. The special case of first-forbidden transitions is studied in detail. The value of lg ft is compared with experiments. (auth)

15837 FIVE-PARTICLE ISOMER STATE IN ^{125}Xe. Peker, L. K. (Leningrad State Univ.). Yadern. Fiz., 3: 32-3(Jan. 1966). (In Russian).

It is shown that a recently discovered many-particle isomer state in ^{125}Xe cannot be a three-particle state, but is more complicated. It is suggested that this is the first example of five-particle isomer states, in which the spin is due to five unpaired nucleons. (auth)

15838 COHERENT EFFECTS IN ASSOCIATION REPLACEMENT REACTIONS. Boyarkina, A. N.; Chiofi, K. (Moscow State Univ.). Yadern. Fiz., 3: 43-7(Jan. 1966). (In Russian).

The association replacement amplitudes are summed for the example of the ^{14}N(^{3}He,α)^{13}N reaction, taking state mixing into account. The calculations are compared with experiments. The most intensive transitions correspond to cases of along-row replacement in the Young schemes of the corresponding associations. The possibility of such a replacement is a necessary, but not sufficient condition for a positive coherent effect in the summation of amplitudes. (auth)

15839 NEUTRON RESONANCES OF Yb ISOTOPES. Wang, Nai-yen; Karzhavina, E. N.; Popov, A. B.; Yazvitskii, Yu. S.; Yao, Chi-chuan (Joint Inst. for Nuclear Research, Dubna, USSR). Yadern. Fiz., 3: 48-54(Jan. 1966). (In Russian).

Measurements concerning the transmission of a natural Yb mixture and the radiative capture of ^{171}Yb, ^{172}Yb, ^{173}Yb, ^{174}Yb and ^{176}Yb isotopes with energies up to 150 ev, were performed on a slow-neutron spectrometer. The resonances were identified for the first time and their parameters were determined. Values of the ^{171}Yb and ^{173}Yb strength function were obtained ($S_0^{171} = (1.1 \pm 0.4) \times 10^{-4}$, $S_0^{173} = (2.4 \pm 0.9) \times 10^{-4}$). The parameter σ in the Bethe formula, determining the dependence of the level density on the excitation energy and spin of the compound nucleus, was determined from the number of observed levels in ^{171}Yb and ^{173}Yb ($\sigma = 2.5$). (auth)

15840 CHARACTERISTICS OF THE DEUTERON FISSION OF ^{232}Th AND THE DEPENDENCE OF THE FRAGMENT KINETIC ENERGY ON THE EXCITATION ENERGY OF THE FISSILE NUCLEUS. Selitskii, Yu. A.; Solovev, S. M.; Eismont, V. P. Yadern. Fiz., 3: 65-72(Jan. 1966). (In Russian).

Various fission properties — the mass distribution of the fragments, mean values and dispersions of the kinetic energy distributions of fragments with equal masses — are determined by measuring the kinetic energies of equal fragments at two deuteron energies and are compared with each other. The results of this investigation and of other analyses, concerning the dependence of the kinetic energies of fragments with given masses on the excitation of the fissile nucleus, are discussed in the framework of the nuclear shells in fragments model for two independent types of fission. This is in agreement with experimental data in the region of medium energies. (auth)

15841 INVESTIGATION OF 9 Gev/c π^- MESON INTERACTIONS WITH XENON NUCLEI ACCOMPANIED BY Λ AND K^0 PARTICLE PRODUCTION. Bogdanovich, E.; Dobrovolskii, T.; Ivanovskaya, I. A.; Maltsev, V. M.; Penchev, G. I.; Filipkovskii, A. (Joint Inst. for Nuclear Research, Dubna, USSR). Yadern. Fiz., 3: 73-80(Jan. 1966). (In Russian).

The cross sections for the creation of Λ- and K^0-particles on Xe by 9 Bev/c π^--mesons were measured: $\sigma_\Lambda = 139 \pm 11$ mb and $\sigma_{K^0} = 168 \pm 17$ mb. The momentum and angular distributions of Λ- and K^0-particles were measured. These results are compared with analogous data obtained on hydrogen nuclei and with calculations performed according to the Monte-Carlo method and it is concluded that the interaction of the particles with the nucleus has a cascade character. (auth)

15842 DIPOLE APPROXIMATION IN NON-LOCAL POTENTIAL. Weigel, M.; Suessmann, G. (Univ., Frankfurt am Main). Z. Phys., 190: 267-77(1966). (In German).

The integrated cross section of photonuclear reactions is considered in the electric-dipole approximation. The nucleon-nucleon potential used is well-behaved and nonlocal. The Tabakin potential is used, which matches S-, P-

and D-wave phase shifts up to 320 Mev without generating strong short-range correlations. (auth)

15843 SELFCONSISTENT CALCULATION OF NUCLEAR EQUILIBRIUM DEFORMATIONS. Dietrich, K.; Mang, H. J.; Pradal, J. (Univ. of California, Berkeley). Z. Phys., 190: 357-77(1966).

The Bogoliubov method of general linear transformations is applied to a self-consistent calculation of deformed shapes of rare earth nuclei and light nuclei around ^{24}Mg. Nucleon-nucleon forces of finite range and different spin-dependence and exchange character are used. The dependence of the deformation on the particle number and the different components of the nuclear interaction is investigated. (auth)

15844 THE γ-SPECTRUM OF ^{214}Po(RaC'). Hultzsch, H.; Luehrs, G. (Univ., Mainz). Z. Phys., 190: 378-86 (1966). (In German).

The γ-ray spectrum arising from $^{214}Bi \rightarrow {}^{214}Po$ β-decay was investigated by means of a three-crystal-pair-spectrometer. In addition to many already known energies and intensities several new lines were found, partly improved values for relative intensities are given. These results were achieved by programming a computer to reproduce the obtained data in a trial and error procedure. (auth)

15845 MEASUREMENT OF TWO β-γ DIRECTIONAL CORRELATIONS IN THE DECAY OF ^{126}I. Schmidlin, P. (Max-Planck-Institut Fuer Kernphysik, Heidelberg). Z. Phys., 190: 387-90(1966). (In German).

In the decay of ^{126}I two β-γ directional correlations were measured. The 0.865 Mev $\beta - 0.386$ Mev γ correlation shows a big anisotropy; the reduced coefficient $\epsilon/(p^2/W)$ has a mean value of 0.0419 ± 0.0005 and is not quite energy independent. The 0.385 Mev $\beta - 0.86$ Mev γ correlation is isotropic within about 2%. Therefore the 0.386 Mev 2^+ state and the 0.86 Mev 2^+ state in ^{126}Xe may not be described by differences in collective properties only. (auth)

15846 MEASUREMENT OF THE ANGULAR DISTRIBUTION OF 440 kev γ-RAYS FROM THE REACTION $^{23}Na(p,p'\gamma)^{23}Na$ IN THE RESONANCES E_p = 1281 kev AND E_p = 1456 kev. Heinemann, K.; Richter, F. W. (Univ., Marburg, Ger.). Z. Phys., 190: 423-6(1966). (In German).

The angular distribution of the 440 kev-γ-radiation following the reaction $^{23}Na(p,p')^{23}Na$ was measured. The experimental results are $W(\Theta) = 1 - (0.147 \pm 0.05)P_2(\cos\Theta)$ in the resonance E_p = 1281 kev, and $W(\Theta) = 1 - (0.099 \pm 0.06)P_2(\cos\Theta)$ in the resonance E_p = 1456 kev. (auth)

15847 ANGULAR DISTRIBUTION OF PROTONS OF THE REACTION $^{11}B(d,p_{0,1})^{12}B$ IN THE ENERGY REGION 0.7 TO 1.7 Mev. Hanke, G.; Kamke, D. (Ruhr-Univ., Bochum, Ger. Univ., Marburg, Ger.). Z. Phys., 190: 468-80(1966). (In German).

Angular distributions of the protons in this low-energy region were measured by only few groups for obvious reasons: the energy of the emitted protons is very low. It is shown that by using non-supported targets of ^{11}B with very little oxygen contamination the angular distributions can be obtained between approximately 5 and 165 degrees (c.m., p_0-group) and between 20 and 165 degrees (c.m., p_1) with high accuracy. The Butler-fits give $l = 1$, $r_B = 5.2$ fm for p_0 and $l = 1$, $r_B = 4.7$ fm for p_1. All angular distributions seem to exhibit strong participation of non-stripping mechanism. (auth)

15848 COULOMB EXCITATION. Biedenharn, L. C.; Brussaard, P. J. Oxford Library of the Physical Sciences. Oxford, Clarendon Press, 1965. 338p.

A comprehensive account of the development of Coulomb excitation is given. The relation of Coulomb excitation to nuclear structure physics is emphasized and its role in the development of the Bohr-Mottelson unified model of the nucleus is discussed in detail. Symmetry techniques are used in particular to eliminate the meaning of the semi-classical approximation. A number of fundamental problems of quantum physics are discussed. The techniques of multiple Coulomb excitation, triple correlation, gamma-ray processes, and polarization are reviewed, and excitation by energetic electrons is treated. (L.B.S.)

15849 THE $^{40}Ca(p,\gamma)^{41}Sc$ REACTION. [Thesis]. Youngblood, Dave Harper. Houston, Tex., Rice Univ., 1965. 164p.

The investigation of the energy levels of ^{41}Sc by means of the $^{40}Ca(p,\gamma)^{41}Sc$ reaction was undertaken in two stages. The first stage consisted of the location of levels in the range of bombarding energy between 600 kev and 5.2 Mev (corresponding to a range of excitation in ^{41}Sc from 1.7 to 6.0 Mev) by measuring the positron activity of ^{41}Sc (E^{β}_{max} = 5.47 Mev, $\tau_{\frac{1}{2}} = 0.6$ sec). Since all excited states of ^{41}Sc are proton unstable, the occurrence of this activity can be taken as the signature of those capture states having transitions directly to the ground state. Forty-six resonances found in the excitation function were identified with states of ^{41}Sc by measuring the associated beta spectra. Total widths were obtained for 6 of the levels, $g\Gamma_{\gamma\,g.\,s.}$ was obtained for all 46, assuming decay principally to the ground state. In the second stage of this investigation, the angular distributions of the gamma decay of 16 capture resonances, located at $E_p < 4.1$ Mev, to the $f_{\frac{7}{2}}$ ground state of ^{41}Sc were measured. J values were assigned to 8 of the levels, while J values for 7 more were limited to two possibilities. The cross section for non-resonant capture was measured and found to agree in magnitude with that calculated by Thomas and Tanner for capture directly into the ground state of ^{41}Sc. The energy dependence observed is greater than predicted. The half life of the ^{41}Sc positron decay was determined to be 0.596 ± 0.006 seconds. The Q value for the $^{40}Ca(p,\gamma)^{41}Sc$ reaction was determined to be 1.083 ± 0.006 Mev, corresponding to a ^{41}Sc mass excess of $-28{,}640 \pm 10$ kev on the ^{12}C mass scale. A value of $5.1 \pm 1.5 \times 10^{13}$ seconds was obtained for the lifetime of the first excited state of ^{41}Sc, an enhancement of a factor of 12 over the single particle value. (Dissertation Abstr.)

15850 ELASTIC AND INELASTIC SCATTERING OF 15 Mev DEUTERONS FROM NUCLEI [Thesis]. Jolly, Rajinder Kumar. Pittsburgh, Univ. of Pittsburgh, 1964. 221p.

Results of measurements and analyses of elastic and inelastic scattering of 15-Mev deuterons from nuclei are reported. To determine the optical potential for 15-Mev deuterons for various nuclei, detailed elastic scattering angular distributions were measured for twenty-three elements selected from throughout the periodic table. The data were analyzed with two sets of potentials called "a" and "b". Set "a" is similar to the nucleon potential while set "b" is like a sum of the neutron and proton potentials. The energy spectra of deuterons inelastically scattered from numerous isotopic and elemental targets were measured using both magnetic analysis and solid state detectors to yield excitation energies, cross sections, and also spins and parities in some cases. Parity assignments to states of some nuclei were made using Blair phase rule. The validity of the rule for 15-Mev deuterons was investigated by intercomparisons of elastic angular distributions and inelastic angular distributions for states of known different parities. It was found that Blair phase rule has greatest validity for comparisons between one-phonon 2^+ and 3^- states. The rule was then applied to cross-section ratios for measurements at two angles that give very different values of the aforesaid ratio for states of opposite parities. Spin and parity assignments to some states of ^{120}Sn, ^{92}Zr, and ^{60}Ni were made by comparing the experimental angular distributions with the DWBA predictions for definite excitation energies and values of the orbital angular momentum transfer in the inelastic collision. It was found that the theoretical predictions agree quite well both in shape and magnitude with the result for some known cases of single excitations so that the theoretical predictions were then used for spin and parity assignments to unknown states for which the experimental data were definite. (A.G.W.)

15851 MICROSCOPIC MODELS FOR VIBRATIONAL STATES IN NUCLEI [Thesis]. Hsu, Loke Soo. Rochester, N. Y., Univ. of Rochester, 1965. 174p.

The formalism was worked out for two microscopic vibrational models, the quasiparticle approximation, and the multishell seniority approximation by second quantized tensorial techniques developed by J. B. French. In the former, both the random-phase RPn and the Tamm-Dancoff TDn approximations for n = 2 and 4 were considered. In the RPn approximation the basis operators are taken to be linear in the creation and destruction tensors involving up to n quasiparticles. The TDn approximation is a special case of RPn in which the destruction operators are not included. In all cases the spurious states were projected out. The part of the TDn wave function with the desired number of particles was also projected out and renormalized and the energies were recalculated using the projected wave functions. This approximation is referred to as PTDn. In the multishell seniority approximation vn, the shell model Hamiltonian is diagonalized in a truncated vector space containing states whose multishell seniority does not exceed n. The even Ni isotopes ^{58}Ni, ^{60}Ni, ^{62}Ni, and ^{64}Ni are considered as examples. The spectra and wave functions in the TD2, TD4, RP2, RP4, PTD2, PTD4, v2, and v4 approximations are calculated using a best fit s-state interaction. The E2 electromagnetic transition probabilities were also calculated using the TD2, TD4, PTD2, PTD4, v2, and v4 wave functions. The spectra and wave functions for the TDN and RPn approximations are very close. The results of the PTDn approximations are closer to the shell-model results than the corresponding TDn. The vn and PTDn results are comparable. The low-lying spectra look like phonon spectra. (A.G.W.)

15852 CORE POLARIZATION IN TRANSFER REACTIONS VIA SHELL MODEL AND SUM-RULE TECHNIQUES [Thesis]. Bansal, Ram Krishan. Rochester, N. Y., Univ. of Rochester, 1965. 136p.

Core polarization effects produced when a nucleon (or nucleon hole) is added to a core were investigated. The weak coupling model for the recently discovered $d_{\frac{3}{2}}$-hole states in Ti and Sc isotopes is considered, and it is shown that, at first sight, anomalous behavior of these states is easily explainable by a calculation involving two parameters, the isoscalar-monopole and the isovector-monopole strengths of the interaction. A satisfactory explanation of the greatly retarded magnetic quadrupole γ-ray lifetimes of the same hole states in the Sc isotopes can be given without any modifications of the electromagnetic transition operator, if the departures from weak coupling due to the excitation of the first 2^+ state in the Ti core are incorporated into the theory. The broadening of the resonances produced by the addition of a proton to a closed neutron shell can be satisfactorily explained using reasonable interactions consistent with the previously calculated weak coupling parameters. A general multipole sum rule technique is introduced to analyze reaction strengths for single-particle transfers. The variations of the energy moments of the reaction strengths with the final state angular momenta and the isobaric spin J and T are considered. From these variations can be deduced multipole moments and correlation moments for the target state and multipole interaction parameters. (A.G.W.)

15853 MASS SPECTROMETRIC DETERMINATION OF THE MASS OF ^{1}H AND THE STABLE ISOTOPIC MASSES AND MASS DIFFERENCES OF CHLORINE, BARIUM, CERIUM AND NEODYMIUM [Thesis]. Benson, Jay Lynn. Minneapolis, Univ. of Minnesota, 1965. 80p.

The sixteen-inch double-focusing mass spectrometer at the University of Minnesota was employed to measure the atomic mass of H^1 and the atomic masses and mass differences of chlorine, barium, cerium, and neodymium. Recent improvements in instrumentation increased the precision of both narrow and wide doublet measurements. The signal detection in the peak-matching technique was improved by employing a 1024 channel digital memory device for detection of mass peak mismatch. A new voltage divider was built to give voltage ratios known to one part per million for use in wide isotopic doublet measurements. The doublet $C_{11}H_{22}-C_{12}H_{10}$ was used to relate the H^1 mass directly to the ^{12}C mass standard with a precision of ±30 ev. The chlorine masses obtained have a precision greater than that of previous measurements. Additional atomic masses are calculated from the stable mass data of barium, cerium, and neodymium, together with alpha-decay, beta-decay, and nuclear reaction energies. The resulting table of masses is used to calculate nuclear systematic energies in the region including the shell closure at 82 neutrons. The separation energies display very smooth characteristics except at the shell closure. The systematics are generally so regular as to be a powerful aid in the evaluation of some possible errors in reaction and decay data used in the calculation of these nuclear separation energies. Other features of the nuclear systematics are discussed in terms of the shell model theory of these nuclei. (Dissertation Abstr.)

15854 EQUILIBRIUM CHARGE STATES OF ^{16}O IONS AND A STUDY OF THE ^{12}C(^{3}He,n)^{14}O REACTION BY PULSED-BEAM TIME-OF-FLIGHT TECHNIQUES. PARTS I AND II [Thesis]. Bernard, Davy Lee. Houston, Tex., Rice Univ., 1965. 111p.

The Rice University tandem accelerator was used to accelerate ^{16}O ions, and the charge state distributions of an O^{4+} ion beam were measured after passage through thin foils of gold and nickel. The average energy in the gold and nickel targets were 4.3 and 3.9 Mev, respectively, and did not change appreciably for the incident bombarding energy range covered. Charge state fractions are calculated as functions of emergent ion velocity. From these fractions, the Z_{rms}/Z is calculated as a function of $V/Z^{\frac{2}{3}}$, where Z_{rms} is the root-mean-square of the charge on the ion, Z is the atomic number of the ion, and V is the emergent ion velocity. These results compare favorably with other data taken with ^{16}O ions at higher and lower ion velocities. There appears to be no indication of a decrease of the degree of ionization with atomic number of the stopping material from these comparisons. A 2.5-Mc/sec beam pulser was incorporated in the terminal of the Rice University 6-Mev Van de Graaff and was used to obtain a pulsed beam of ^{3}He ions. The pulsed ^{3}He beam was used in the study of the ^{12}C(^{3}He,n)^{16}O reaction. The characteristics of the pulsed-beam time-of-flight system is described. Angular distributions of the ^{12}C(^{3}He,n)^{14}O reaction were measured for the angular range of 0 to 80° and the ^{3}He bombarding energy range of 1.97 to 4.70 Mev. The angular distributions were measured at each 200-kev increment of the bombarding energy. Excitation curves were extracted from the angular distributions for the bombarding energy range reported. The results are discussed within the existing theories of direct-interaction and compound nucleus mechanisms. (Dissertation Abstr.)

15855 QUANTITATIVE SPECTROSCOPIC STUDIES USING THE (^{3}He,α) REACTION. Blau, Lawrence Martin. Rochester, N. Y., Univ. of Rochester, 1965. 189p.

The first part of the investigation reported consists of the measurement of the ^{16}O(^{3}He,α_0)^{15}O and ^{40}Ca(^{3}He,α)^{39}Ca reactions and the analysis of the resulting data using the distorted wave Born approximation (DW) code JULIE. The second part consists of the investigation of the ^{39}K(^{3}He,α)^{38}K reaction and the analysis of the data using the DW code JULIE and the renormalization factor found from the analysis in the first part. The DW calculations gave good fits to the shape of the angular distributions for both the ^{16}O(^{3}He,α_0)^{15}O and ^{40}Ca(^{3}He,α)^{39}Ca reactions. The optical model parameters used in the analysis had a small monotonic dependence on incident energy and are only slightly different for the two reactions. However, the DW calculations predicted magnitudes for the cross sections smaller than the measured cross sections by an average factor of 24 ± 5 for the ^{16}O(^{3}He,α_0)^{15}O reaction and an average factor of 25 ± 4 for the ^{40}Ca(^{3}He,α_0)^{39}Ca reaction. The data from the ^{39}K(^{3}He,α)^{38}K reaction leading to the ground and first four excited states in ^{38}K were analyzed by the DW code

JULIE using essentially the same optical model parameters as used for the analysis of the $^{40}Co(^{3}He,\alpha)^{39}Ca$ reaction. The angular distributions calculated by the DW code are in reasonably good agreement with the measured angular distributions for all the levels. The reactions leading to the ground ($J^{\pi} = 3^{+}$, T = 0) state and first excited ($0^{+}1$) state proceed by pure d-wave pick-up as is expected on the basis of the shell model. The reactions leading to the second excited ($1^{+}0$) state, third excited ($1^{+}0$) state, and fourth excited ($2^{+}1$) state proceed primarily by $\ell = 2$ with a small admixture of $\ell = 0$ for the picked-up neutron. When the renormalization factor of 25 found in the analyses of the first part is used, the extracted spectroscopic factors are in reasonably good agreement with the predictions of two theoretical models. (Dissertation Abstr.)

15856 A SURVEY OF ISOMERS WITH HALF-LIVES IN THE RANGE 5-1000 MICROSECONDS OBSERVED IN PULSED 15 Mev DEUTERON BEAM BOMBARDMENTS OF NATURAL ELEMENTS [Thesis]. McCarthy, Arthur Lancelot. Pittsburgh, Univ. of Pittsburgh, 1964. 98p.

The half lives and gamma energies are given for 18 new isomers observed in a pulsed 15-Mev deuteron beam survey of 72 elements. Gamma transitions were observed using time and energy channels in a two-dimensional 4096-channel analyzer. Eleven isomers previously reported were confirmed, and in some cases, new information on them was obtained. (D.E.B.)

15857 THE BETA-NEUTRINO ANGULAR CORRELATION AND THE NUCLEAR MATRIX ELEMENTS IN A FIRST-FORBIDDEN NONUNIQUE BETA DECAY [Thesis]. Palathingal, Jose Chekkorv. Philadelphia, Univ. of Pennsylvania, 1965. 142p.

In measuring the beta-neutrino angular correlation, a new method based on nuclear resonance fluorescence is employed. The gamma rays from a gaseous source of ^{122}Sb in the form of SbH_3 are studied in coincidence with beta rays of selected energy. The γ rays travelling at about 180° relative to the beta rays are scattered from a Te scatterer (2.47% ^{122}Te). When the beta energy is varied, the neutrino direction varies accordingly. Therefore, the variation of the cross section of resonance scattering with beta energy gives the beta-neutrino angular correlation. For first-forbidden nonunique decay, the angular correlation has the form, $1 \lambda\ v/c \cos\theta$, if the ξ-approximation is valid. For ^{122}Sb, λ is found to be $(1.32 \pm 0.48$. From a preliminary experiment involving a study of the resonance effect in ^{122}Te, it was possible to make a measurement of the mean life of the 564-kev state in ^{122}Te. The result, $\tau = (1.05 \pm 0.16) \times 10^{-11}$ sec, is in agreement with previous resonance fluorescence and Coulomb excitation experiments. The experimental value of $\lambda = 1.32 \pm 0.48$ suggests that the ^{122}Sb decay is predominantly axial vector. Vector interaction is small. If any tensor or scalar interaction is present, it must also be small. The most probable values of the nuclear matrix elements are, $\langle\vec{\sigma} \cdot \vec{r}\rangle = (1.9 \pm 0.2) \times 10^{-3}$, $i\langle\gamma_5\rangle = (3.6 = 0.2) \times 10^{-2}$, $\langle\vec{r}\rangle = (-2.9 \pm 1.7) \times 10^{-4}$, $i\langle\vec{\sigma} \times \vec{r}\rangle = (0 \pm 0.8) \times 10^{-4}$, $i\langle\vec{\alpha}\rangle = (5.4 \pm 1.7) \times 10^{-3}$, and $\langle B_{ij}\rangle = (1.47 \pm 0.05) \times 10^{-3}$. Comparing the coordinate matrix elements to the nuclear radius, 1.53×10^{-2} ($\hbar$/mc) and the velocity matrix elements to typical nucleon velocities ($v \sim 0.1$), it is seen that the initial and final nuclear state wave functions do not overlap appreciably. The ratio of the axial vector matrix elements $i\langle\gamma_5\rangle$ and $\langle\vec{\sigma} \cdot \vec{r}\rangle$ lies between the values expected from the estimates of Ahrens and Feenberg on the basis of the shell model and by Pursey using the Hartree type single-particle model of the nucleus. (Dissertation Abstr.)

15858 THE $^{11}B(d,n)^{12}C$ REACTION AND A CALORIMETRIC DOSAGE CALIBRATION AND A DETERMINATION OF ABSORBED DOSE FOR PROTON IRRADIATION [Thesis]. Almond, Peter Richard. Houston, Tex., Rice Univ., 1965. 146p.

A proton recoil telescope spectrometer was used to study the reaction $^{11}B(d,n)^{12}C$. Modifications on a prototype spectrometer, made in order to improve resolution, are described. The excitation functions at zero degrees for the first four neutron groups of the reaction were obtained from 1 to 11 Mev. These groups are separated by 4.433, 3.223, and 1.984 Mev respectively. The excitation curves were compared to the one for the 15.1-Mev gamma ray from the reaction $^{11}B(d,n\gamma_{15.1})^{12*}C$. If the peaks in the neutron curves are assumed to be due to states in the compound nucleus ^{13}C, then levels at 20.0, 21.6, 22.1, 22.3, 22.9, 23.2, 25.2, 26.9, and 27.5 Mev were found. Angular distributions were measured in this region for the ground and first excited state neutrons. Analyses of these distributions were carried out using DWBA theory, heavy particle stripping theory, and single level compound nucleus theory. It was found that the DWBA analysis predicted the shapes of the distributions in the range 2.4 to 10 Mev. A calorimetric method was used to measure absorbed radiation dose in terms of the rad by measuring the temperature rise imparted to a thermally isolated absorber. Three sources were calibrated: the 22-Mev betatron x-ray generator and the Co-60 and Cs-137 γ-ray teletherapy units at M. D. Anderson Hospital. These results were used to check the validity of the ionization chamber dose standardizations. Agreement was within a few per cent. Calculations were made to determine the absorbed dose, in rads, delivered by protons entering a biological solution. Protons with energies from 1 to 5 Mev from the Rice 5.5-Mev Van de Graaff accelerator were used to irradiate a number of such solutions. (Dissertation Abstr.)

15859 STUDY OF ELASTIC AND INELASTIC SCATTERING OF ALPHA PARTICLES BY ^{7}Li [Thesis]. Cusson, Ronald Yvon. Pasadena, Calif., California Inst. of Tech., 1965. 145p.

The absolute cross sections for the reactions $^{7}Li(\alpha,\alpha)^{7}Li$ and $^{7}Li(\alpha,\alpha')^{7*}Li(0.48)$ were measured in the range of energies and angles, $1.6 \leq E_{\alpha L} \leq 12.0$ Mev, $20° \leq \theta_{\alpha L} \leq 150°$, using thin ^{7}Li-bearing targets. Solid state detectors were used to detect the scattered α particles. Nineteen scattering anomalies were observed in this energy range. In the excitation energy range, $9.88 \leq E_{exc.}(^{11}B) \leq 11.27$ Mev, six levels were observed. The measured cross sections were fitted in this energy region using a multilevel R-matrix theory model program for the 7094 computer. The best fits were obtained with the assignments: $9.88(3/2^{+})$, $10.26(3/2^{-})$, $10.32(5/2^{-})$, $10.60(7/2^{+})$, $11.0(5/2^{-})$, $11.27(7/2^{+}, 9/2^{+})$. Some alternatives for these assignments are discussed. The results were found to be consistent with the level structure of the analog nucleus ^{11}C. The applications of the rotator model of the nucleus to the excited states of ^{11}B and ^{11}C are discussed. (Dissertation Abstr.)

15860 THE $^{58}Ni(^{3}He,\alpha)^{57}Ni$ REACTION [Thesis]. Fou, Cheng-Ming. Philadelphia, Univ. of Pennsylvania, 1965. 113p.

A ^{58}Ni target (99.98% enriched) was bombarded with a 15- and 18-Mev ^{3}He beam from the University of Pennsylvania tandem accelerator. Levels in ^{57}Ni were studied by detecting the α particles from the $^{58}Ni(^{3}He,\alpha)^{57}Ni$ reaction in a 24-in. diameter scattering chamber using surface barrier solid state detectors. The Q-value of the reaction was measured to be 8.40 ± 0.05 Mev. Excited levels in ^{57}Ni at 0.75 1.05, 2.55, 3.25, 3.70, 3.85, 4.25, 4.55, 4.95, 5.25, 5.57, 5.85, 6.05, 6.97, 7.15, 7.85 Mev were observed. Angular distributions of elastically scattered ^{3}He, as well as that of α particles leading to ground, 0.75-, 1.05-, 2.55-, 3.25-, 5.25-, 5.57-, and 6.05-Mev states were measured. Gamma rays, in coincidence with the reaction α particles, were also measured with a 3 × 4 in. NaI(Tl) crystal and analyzed by using the 2-dimensional pulse height analyzer to study the decay scheme of the excited states. Distorted wave analysis, using the Oak Ridge National Laboratory's JULIE computer code, yielded the following spin assignments: Ground state $\ell = 1$, 0.75-Mev state $\ell = 3$, 1.05-Mev state $\ell = 1$, 2.55-, 3.25-, 5.25-, 5.57-Mev states all $\ell = 3$, 6.05-Mev state either $\ell = 2$ or $\ell = 3$. Relative spectroscopic factors of these states were also extracted. (Dissertation Abstr.)

15861 PHOTONUCLEAR ACTIVATION OF CARBON OVER THE GIANT RESONANCE [Thesis]. Lochstet, William Albert. Philadelphia, Univ. of Pennsylvania, 1965. 100p.

To obtain some insight about the structure of photonuclear reactions, and the applicability of models over the giant resonance, the reaction $^{12}C(\gamma,n)^{11}C$ was measured over the energy range of 21.7 to 26.7 Mev. Gamma rays were obtained from the $^{3}H(p,\gamma)^{4}He$ reaction and monitored by a 4.5 × 6-inch NaI(Tl) crystal. The yield of ^{11}C in a suitable sample was measured with a coincidence arrangement of two 5 × 2-inch NaI(Tl) crystals. The energy resolution gradually increased from 100 kev to the lowest energy to 200 kev at the highest. The cross section at peak height is 7.8 mb and the integrated cross section from 20 to 27 Mev is 38.5 Mev-mb. Structure was observed at 22.15, 23.0, 23.7, and 25.6 Mev. By comparison with the neutron time-of-flight data, it is shown that the resonance at 23.7 Mev is at least partly due to events that leave the remaining ^{11}C nucleus in its first excited state rather than its ground state. An attempt is made to determine the shell model configuration of this two hole–two particle state. Comparison of the experimental results with theoretical predictions indicates some agreement with the deformed nucleus calculations of Nilsson, Sawicki, and Glendenning. (Dissertation Abstr.)

15862 ALPHA-ALPHA ANGULAR CORRELATION STUDIES OF THE REACTION $^{12}C(\alpha,\alpha')^{12*}C(\alpha_0)^{8}Be$ [Thesis]. LaSalle, Richard Alan. Bloomington, Ind., Indiana Univ., 1965. 119p.

The nuclear polarization produced by inelastic alpha-particle scattering that excites the 9.63-Mev state in ^{12}C was studied by measuring the alpha-alpha angular correlations between the inelastically scattered alpha particles and the decay alpha particles at ten inelastic scattering angles, and by measuring the angular distribution of the inelastically scattered alpha particles. All of the particles in this reaction, except for the excited nucleus, are spinless. The spin of the 9.63-Mev state in ^{12}C is 3^-. Therefore, it was necessary to measure angular correlations out of the reaction plane as well as in the reaction plane in order to determine the parameters describing the nuclear polarization. The analysis of the alpha-alpha angular correlations in terms of nuclear polarization parameters shows that these correlations behave in ways similar to many $(\alpha,\alpha'\gamma)$ angular correlations and very much unlike $(p,p\gamma)$ angular correlations. This behavior is characterized by a smooth variation of the relative substate population amplitudes a_3, a_+, a_- as a function of inelastic scattering angle, and rapid variation of the relative phases δ_3, δ_+, δ_- repeatedly through 360°. At $\theta' = 63.5°$ in the recoil center-of-mass system the correlation function reduces to $W(\phi) \alpha (1-a_3^2) + 4a_3 \sin^2 3(\phi - 1/6\ \delta_3)$; therefore correlation patterns obtained at this angle appear quite similar to those obtained from $(\alpha,\alpha'\gamma)$ angular correlation measurements with $j = 2$ and $\theta' = 90°$. These angular correlations measurements are a critical test of several existing direct reaction models. The semiclassical model of Austern, Butler and McManus, the PWBA model, and the adiabatic diffraction scattering model of Blair grossly fail to predict the experimental results. The variation of the relative phase δ_3 is shown, qualitatively, to result from sharp l-value selection, a property to be a feature of alpha-particle scattering. (Dissertation Abstr.)

15863 (n,2n) EXCITATION FUNCTIONS OF SEVERAL LOW NEUTRON EXCESS NUCLEI [Thesis]. Arnold, Dan McCay. Athens, Ga., Univ. of Georgia, 1965. 117p.

Excitation functions of seven previously unmeasured (n,2n) reactions were measured. Incident neutron energies between 12 and 18 Mev were used. Results are tabulated for ^{27}Al, ^{35}Cl, ^{39}K, ^{40}Ca, ^{28}Si, ^{24}Mg, and ^{32}S. New evaluations of two parameters (the level density parameter and the cross section for the emission of the first neutron) required for computation of theoretical values of the (n,2n) cross section by the compound nucleus model are presented. The (n,2n) cross section calculations using these new values agree better with experimental data than previous calculations. (A.G.W.)

15864 ALPHA DECAY STUDIES OF PROTACTINIUM ISOTOPES [Thesis]. Subrahmanyam, Vishnubhotla. Berkeley, Calif., Univ. of California, 1964. 71p.

The alpha decay of ^{231}Pa, ^{229}Pa, ^{227}Pa, and ^{223}Ac was studied. An alpha–gamma coincidence technique was employed. A 180-deg double-focusing spectrograph or gold-silicon solid-state detectors were used for alpha analysis, and a sodium iodide (Tl-activated) scintillation crystal was used for gamma-ray detection. The ground states of ^{227}Pa and ^{229}Pa are shown to be populated by 5.46- and 5.73-Mev α particles, respectively. The rotational bands populated in the decay of ^{227}Pa are interpreted as being based on octupole vibrational levels predicted by the Bohr-Mottelson strong-coupling model. Modified decay schemes are presented. It is suggested that in odd-proton nuclei, the permanent nuclear deformation starts closer to the closed shell than in the even-even nuclei. A new alpha group at 5.47 Mev is reported in the alpha decay of ^{223}Ac. No rotational structure is observed in the levels populated. Evidence is presented for the presence of two additional levels populated in the alpha decay of ^{231}Pa. (Dissertation Abstr.)

15865 COMPOUND ELASTIC SCATTERING OF 3.15-Mev NEUTRONS BY ^{40}Ca [Thesis]. Singh, Zorawar Khangura. Baton Rouge, La., Louisiana State Univ., 1964. 63p.

An attempt was made to measure the differential compound elastic scattering of neutrons of energy 3.15 Mev by calcium-40 using a method based on the dissimilarity between the energy level schemes of potassium-39 and calcium-40, and based further on the assumption that the shape elastic scattering of neutrons from these two nuclei is essentially the same. Since potassium-39 will exhibit very small compound elastic scattering compared to calcium-40, the difference in differential elastic scattering cross sections of these two nuclei will represent, to a close approximation, differential compound elastic scattering by calcium-40. The measured compound elastic cross section of calcium-40 appears larger at angles below 50° and smaller above 110° than predicted by Hauser-Feshbach theory. The experimental data curve agrees fairly well with theory between 50 and 110°. The measured total compound elastic cross section is 1.0 ± 0.05 barns and that found by theory is 1.0 barn. The detailed fit between the measured and computed differential compound elastic cross section is not good. This may be due in part to the choice of single level parameters used in the theoretical calculations. That the general magnitude of the compound elastic cross sections is correct is supported by the good agreement of the total cross sections. The asymmetry of the differential compound elastic cross section presumably results from a breakdown of the assumption of identical shape elastic scattering in the calcium-40 and potassium-39. (Dissertation Abstr.)

15866 ELASTIC ELECTRON SCATTERING BY ^{6}Li. Lodhi, M. A. K. (Texas Technological Coll., Lubbock). 9p. (CONF-650653-9). ORINS. Gmelin, AED-CONF-65-170-25.

From American Physical Society, Summer Meeting, New York.

It is possible to fit the elastic electron scattering data with a single oscillator parameter as in other 1p-shell nuclei even for large momentum transfer if the residual two-body interaction in the single particle shell model is taken into account. The residual interaction causes the configuration mixing from the states higher than the lowest one including the core excitation. (auth)

Plasma Physics and Thermonuclear Processes

See also Fluid Physics and Thermodynamics

Refer also to abstracts 15592, 15733, and 15941.

15867 (AD-620664) COLLISION FREQUENCY MEASUREMENTS IN OXYGEN AND HELIUM MAGNETO-PLASMA AFTERGLOWS. Veatch, G. E.; Verdeyen, J. T.; Cahn, J. H. (Illinois Univ., Urbana. Gaseous Electronics

Lab.). July 1965. Contract AF19(628)-2391. 44p. (AFCRL-65-453). CFSTI $2.00 cy, $0.50 mn.

Collision-frequency measurements were carried out in helium and oxygen at thermal energies. The helium measurements yield a collision probability of 18.7 at 300°K and 1 torr. This corresponds to a cross section for momentum transfer of 5.29×10^{-16} sq-cm at 300°K. The helium collision frequency (f) is directly proportional to approximately the first power of the velocity at 300°K. The oxygen measurements yield a value of $f = 4.6 \times 10^{-8}\ N(O_2)u$ where u is the electron energy in electron volts and $N(O_2)$ is the number density of oxygen molecules. The measurements were carried out by two independent methods. (TAB)

15868 (AD-628186) THE ADMITTANCE AND RESONANCE PROBE CHARACTERISTICS OF A SPHERICAL PLASMA PROBE. Scientific Report No. 2. Aeronomy Report No. 8. Kostelnicek, R. J. (Illinois Univ., Urbana. Engineering Experiment Station). Nov. 1965. Contract AF19(628)-3900. 73p. (AFCRL-65-858).

A formula for the admittance of a spherical probe in a warm plasma is derived. The equations for the perturbations in sheath voltage and number density at the plasma-sheath interface are related to the resonance-probe phenomenon. Measurements of the resonance-probe and admittance characteristics were found to agree fairly well with the theoretical calculations. (auth)

15869 (AD-628317) THERMODYNAMIC PROPERTIES OF AN ELECTRON PLASMA. Lie, T. J.; Ichikawa, Y. H. (Illinois Univ., Urbana. Coordinated Science Lab.). Feb. 1966. Contract DA28-043AMC-00073(E). 27p. (R-276).

The thermodynamic properties of electron plasma are investigated on the basis of the BBGKY hierarchy equation. The correlation energy was calculated up to the ϵ^2 term (ϵ is the standard plasma parameter) in terms of an exact solution of the binary correlation function, taking into account the short-range collision effect. The contribution of ternary correlation to the correlation energy was determined in lowest order, which turns out to be of the second order in ϵ. The total sum of the corrections due to the short-range collision effect and the ternary correlation effect is found to be in agreement with the result obtained by Abe, Bowers, and Salpeter within the regime of Gibbs' statistical thermodynamics. Although the appearance of the binary correlation function obtained differs from those derived by Bowers-Salpeter and by O'Neil-Rostoker, it is shown that all of these expressions are essentially equivalent. According to the present analysis, however, it is proved that these expressions do not describe correctly the way in which correlation effects diminsh at a large distance; therefore, DeWitt's statement that $g(x) \sim \frac{1}{8}\ (\ln 3)\ \epsilon^2 \exp(-k_D r)$ as $r \to \infty$ is not correct. (auth)

15870 (CEA-R-2881) LE RAYONNEMENT ELECTRONIQUE D'UN PLASMA DANS UN CHAMP MAGNETIQUE. (Electronic Radiation of a Plasma in a Magnetic Field). Canobbio, Ernesto; Consoli, Terenzio; Ichtchenko, Georges; Parlange, Francois (Commissariat a l'Energie Atomique, Saclay (France). Centre d'Etude Nucleaires). Oct. 1965. 45p. Dep. mn.

The influence on the microwave spectrum of the number of fast electrons, density, pressure, and plasma inhomogeneities, was studied in a hot cathode reflex discharge, operating either in a steady state or in a pulsed regime. Under some conditions a strong emission is observed between the harmonics of the electron gyrofrequency. A theoretical interpretation of the results is advanced by extending a model already proposed by CANOBBIO and CROCI. In particular it is indicated that the transition radiation can be responsible for the emission observed between the harmonics. (auth)

15871 (IPP-1/38) RADIALE UND AXIALE ABHAENGIGKEIT DER ELEKTRONENDICHTE ZU VERSCHIEDENEN ZEITPUNKTEN EINER THETA-PINCH ENTLADUNG. (Radial and Axial Distribution of the Electron Density of a Theta Pinch as a Function of Time). Glaser, H. (Institut fuer Plasmaphysik, G.m.b.H., Garching (West Germany)). June 1965. 55p. Dep. mn.

The spatial distribution of the electron density in the main discharge of a 26-K Joule Θ-pinch was investigated as a function of time. The electron density was determined spectroscopically from the continuum radiation. Eight light pipes yielded the radial distribution of the plasma radiation. The radial distribution of the magnetic field was determined by probe measurements. Streak photographs yield additional information on the radial, axial, and temporal behavior of the plasma column. Measurements were carried out with a parallel trapped magnetic field (0.8 KG, $p_{H_2} = 0.15$ Torr) and an antiparallel trapped magnetic field (-2.3 KG, $p_{H_2} = 10$ Torr). For interpreting the experimental results obtained from the main discharge, knowledge of the characteristic data of the preionization is required. Therefore, the electron density, temperature, and magnetic field distribution in the applied preionization close to the medium plane of the coil was measured at the beginning of the main discharge. (auth)

15872 (IPP-1/41) TIME-RESOLVED PROFILE MEASUREMENTS OF IMPURITY LINES IN A THETA PINCH DISCHARGE. Eberhagen, A.; Bernstein, M. J.; Hermansdorfer, H. (Institut fuer Plasmaphysik, G.m.b.H., Garching (West Germany)). Aug. 1965. 28p. Dep. mn.

Line profile measurements were carried out on a small theta pinch experiment in order to get information on the ion motions during the discharge. A Fabry-Perot interferometer combined with a so-called Fafnir arrangement was used for measuring the shape of the investigated N(V) (4603 Å) and O(VI) (3811 Å) lines. The additional use of a polarizer and $\lambda/4$ plate made it possible to eliminate Zeeman splitting caused by a magnetic field present, which effects the line shape, and to measure the magnitude of the magnetic field strength at the site of line emission in the plasma. By means of a combined system comprising image converter and intensifier the emission regions of the investigated lines in the plasma could be identified. The experimentally obtained results are discussed considering the different influences leading to line broadening in the present experiment. (auth)

15873 (IPP-1/42) ENTWICKLUNG EINES LASER-VERSTAERKERS UND SEINE ANWENDUNG IN DER PLASMA-DIAGNOSTIK. (Development of a Laser Amplifier and its Application in Plasma Diagnostics). Zietemann, H. (Institut fuer Plasmaphysik, G.m.b.H., Garching (West Germany)). June 1965. 34p. Dep. mn.

In order to measure the electron temperature and the electron density of a 26 k Joule Θ-pinch by means of light scattering, a high power laser was assembled by combining an oscillator laser and an amplifier laser. The highest possible initial power of the oscillator laser was achieved by finding the most suitable mirror reflection and by reducing the resonance space. The amplification of the oscillator impulse by the ruby of the amplifier laser was calculated and measured. The amplification is expressed as a function of the temperature of the amplifier ruby. Electron temperatures measured had the following properties: during the first maximum compression the maximum temperature was 50 ev, and at the moment of the maximum B-field the maximum temperature was 85 ev. The corresponding electron densities were measured as max. 1.3×10^{17} particles/cm^3 and 1.6×10^{17} particles/cm^3 respectively. The spatial distribution of electron temperature and electron density in the plasma is also stated. (auth)

15874 (IPP-3/31) MESSUNGEN DER ELEKTRONENTEMPERATUR IN EINEM ARGON-KALIUM-PLASMA. (Measurements of Electron Temperature in an Argon-Potassium Plasma). Riedmueller, W. (Institut fuer Plasmaphysik, G.m.b.H., Garching (West Germany)). Oct. 1965. 38p. Dep. mn.

When an electric current is passed through a rare gas alkali plasma the electron temperature is expected to rise above the gas temperature. This effect was investigated in a streaming argon-potassium plasma at atmospheric pressure and a gas temperature of 2000°K. The electron temperature was measured as a function of the current density by means of the line reversal method. The results were

compared with the values calculated from the theory and with the values calculated from the measured conductivities. For temperatures above 2400°K all three methods give the same results. The applicability of the line reversal temperature measurement method was investigated. General conditions under which the electron temperature equals the line reversal temperature were derived. In the case studied, the plasma had to be optically thick to the resonance radiation used. The influence of nitrogen impurities on the electron temperature elevation was also investigated. (auth)

15875 (IPP–3/32) BESETZUNG DER DISKRETEN ENERGIENIVEAUS IN EINEM STATIONAEREN NICHTTHERMISCHEN WASSERSTOFFBOGEN. (Population Densities of the Discrete Energy Levels in a Stationary Nonthermal Hydrogen Arc). Ramer, S. (Institut fuer Plasmaphysik, G.m.b.H., Garching (West Germany)). Aug. 1965. 43p. Dep. mn.

The deviations from local thermal equilibrium are calculated for an inhomogeneous hydrogen plasma with given distributions of n_e and T_e. The calculations are based on a cylindrically symmetric model with electron temperature T_e between ≈5000° and 25000°, and electron density $n_e \leq 2.5 \cdot 10^{16} cm^{-3}$. Practically all processes of interest are taken into account. Since absorption is most important in the resonance lines, absorption terms are considered only for the lines Ly α and Ly β. As these terms contain the radiation intensity, the simultaneous solution of the equation of radiative transfer and the equations for the rate of change of the occupation numbers of the energy levels is required. This was done using an iterative procedure. It is shown that the ground level is nonthermal with a correction factor ≥2. The excited levels are essentially thermal except for the outer zone, where the electron density becomes very low. (auth)

15876 (IPP–6/33) DER EINFLUSS VON ROTATION UND MAGNETFELDERN AUF DIE WAERMEINSTABILITAET EINER FLUESSIGKEITSKUGEL. (The Influence of Rotation and Magnetic Fields on the Thermal Instability of a Fluid Sphere). Kovetz, Attay (Institut fuer Plasmaphysik, G.m.b.H., Garching (West Germany)). Jan. 1965. 73p. Dep. mn.

The effects of rotation and magnetic fields on the thermal instability of a homogeneous fluid sphere are examined. It is assumed that there is a constant distribution of heat sources throughout the sphere, and that the convection pattern possesses axial symmetry. The determination of conditions for the onset of convection leads to a characteristic value problem for the critical Rayleigh number, as a function of other nondimensional parameters (the Taylor, Hartmann, and Prandtl numbers). The solutions are carried out with the aid of variational principles. Stationary convection and overstability are both treated. (auth)

15877 (IPP–6/41) EBENE MAGNETOHYDROSTATISCHE GLEICHGEWICHTE MIT INNENFELD. (Plane Magnetohydrostatic Equilibria with Interior Field). Gorenflo, Rudolf; Schlueter, Arnulf (Institut fuer Plasmaphysik, G.m.b.H., Garching (West Germany)). Aug. 1965. 32p. Dep. mn.

Two-dimensional analogues of toroidal plasma equilibrium configurations with purely meridional electric currents are discussed. The given plane is taken as a cross sectional plane of a doubly connected cylinder (limiting case of a torus) perpendicular to the plane; all currents flow perpendicular to the plane. Two cases are considered: (1) inside the plasma no currents flow and the pressure p is constant, but $\ll B^2$, and (2) currents flow inside the plasma as well, the pressure being variable. In both cases equilibrium is possible when $g(\nu) = \int_{\Gamma(\nu)} (d_s/B)$ has an extremum inside the plasma ($\Gamma(\nu)$ being the field line belonging to the value ν of the flux function of the field $\mathcal{F}$). In case (2) a further condition is that inside the plasma p depends only on g. (auth)

15878 (IPP–6/42) BERECHNUNG DES ZWEIDIMENSIONALEN MAGNETFELDES EINER GERADEN ANZAHL VON IOFFE-STAEBEN MITTELS KOMPLEXER ANALYSIS. (Calculation of the Two-Dimensional Magnetic Field of an Even Number of Ioffe Bars by Complex Analysis). Gorenflo, Rudolf; Welter, Helmut (Institut fuer Plasmaphysik, G.m.b.H., Garching (West Germany)). Sept. 1965. 33p. Dep. mn.

By complex representation of a plane vector field a finite expression (in elementary functions) is derived for the magnetic field produced by an even number of infinitely long Ioffe bars. This expression is valid at all points of a cross sectional plane, in the interior of the conductors as well. For numerical computation an ALGOL program is written which gives the components B_r and B_φ of the field at every point required. The field line plots are then obtained by using a numerical method, which is described. In addition, the behavior of quadrupole and hexapole fields in the vicinity of the axis is dealt with in detail. (auth)

15879 (IPP–6/43) THREE-DIMENSIONAL NORMAL MODES OF A VLASOV PLASMA WITH AND WITHOUT MAGNETIC FIELD. McCune, J. E. (Institut fuer Plasmaphysik, G.m.b.H., Garching (West Germany)). Oct. 1965. 86p. Dep. mn.

The three-dimensional velocity-space eigenmodes of the linearized Vlasov equation for an electron plasma, with and without a uniform applied magnetic field, are derived in the electrostatic limit and are shown to be complete. In general, a continuum of modes exists (except for $k \cdot B_0 = 0$) and, if the plasma is unstable, an additional set of discrete modes appears. For $B_0 = 0$, these modes reduce to the Van Kampen-Case spectrum upon integration over all velocities perpendicular to k. The adjoint modes are also derived and are used to establish certain orthogonality properties which are sufficient to enable one to use essentially standard eigenfunction techniques. It is shown for $B_0 = 0$ that the Balescu-Lenard kinetic equation can readily be derived with the use of the three-dimensional modes. For the case with magnetic field, it is found that a particular functional of the undisturbed function plays a role (for $k \cdot B_0 \neq 0$) analogous to Case's $\eta(\nu)$ in establishing the properties of the modes. For the case $k \cdot B_0 = 0$, which must be treated separately, two discrete sets of modes exist, only one of which contributes to the density and field fluctuations in the electrostatic approximation. (auth)

15880 (ML–1292) INSTABILITY AND AMPLIFICATION IN FINITE BEAM-PLASMA SYSTEMS. I. THEORY. Self, S. A. (Stanford Univ., Calif. Microwave Lab.). Jan. 1965. Contract AT(04-3)-326. 48p. Dep. mn. CFSTI $2.00 cy, $0.50 mn.

A study was made of the stability of, and amplification along, a cylindrical electron beam of finite radius passing through a stationary plasma in the absence of steady magnetic field. In the theory, the dispersion relation is analyzed for two cases, when the plasma is unbounded and when it is bounded by a cylindrical conductor. The general criteria for determining instability and wave types were applied and it is found that, when there are no stabilizing effects such as collisions or temperature, the system is always absolutely (nonconvectively) unstable. The temporal growth rates of the instability are typically sufficiently low that in practical cases the effect of collisions is sufficient to stabilize the system, leaving it supporting an amplifying wave (convective instability) whose spatial growth rate is determined by the collision rate, and which may be very large indeed under conditions that the absolute instability is only just stabilized. A number of representative numerical solutions are presented. (auth)

15881 (MPI-PAE/PL–7/65) DETERMINATION OF ELECTRON DENSITY FROM LINE MERGING. Vidal, C.-R. (Max-Planck-Institut fuer Physik und Astrophysik, Munich (West Germany)). Nov. 1965. 28p. Dep. mn.

The often used Inglis-Teller relation estimates the electron density from the line merging within a factor of two. A new method of evaluation is suggested, which gives the electron density from the ratio of the envelope curves of the merging lines. The achievable accuracy is about 5% as long as the conditions $T < (4.6 \times 10^5 z/n_m)°K$ and $N_e < z^{4.5} \times 10^{16} cm^{-3}$ are fulfilled. (auth)

15882 (NP–15868) ANNUAL REPORT [ON PLASMA PHYSICS], 1964. (Institut fuer Plasmaphysik, G.m.b.H., Garching (West Germany). Max-Planck-Institut fuer Physik und Astrophysik, Munich (West Germany)). 148p. Dep. mn.

The containment, heating, and stability of plasmas were investigated, and techniques of plasma diagnostics were studied. A number of studies were carried out on MHD energy conversion. Equipment was developed for use in various studies. (D.C.W.)

15883 (SU-IPR–31) INSTABILITY OF THE STEADY STATE OF A PLASMA IN A UNIFORM ELECTRIC FIELD. Reiter, G. F. (Stanford Univ., Calif. Inst. for Plasma Research). Dec. 1965. Contract AT(04-3)-326. 35p. Dep. mn. CFSTI $2.00 cy, $0.50 mn.

The BGK equations are used to obtain the steady-state velocity distribution for a uniform, fully ionized plasma in a d-c electric field. The Joule heating of the plasma is assumed to be compensated for by volume heat losses such as bremsstrahlung. The distribution obtained is far from Maxwellian if the drift currents are comparable to the thermal velocity. Longitudinal oscillations with wave vector in the direction of the field are introduced as a perturbation, and their dispersion relation is obtained. The stability of the steady state is investigated numerically, and it is found to be unstable for sufficiently high drift velocities, the instability being due to the familiar electron-ion two-stream interaction. The instability is impeded, but not prevented by collisions. (auth)

15884 (SU-IPR–33) ELECTRON BEAM PROBING OF THE CATHODE SHEATH AND BEAM-PLASMA INTERACTION. Cannara, A. B. (Stanford Univ., Calif. Inst. for Plasma Research). Dec. 1965. Contract AT (04-3)-326. 76p. Dep. mn. CFSTI $3.00 cy, $0.75 mn.

A non-perturbing electron beam probe was used to measure the a-c and r-f electric fields in, and beyond the cathode sheath of an ordinary, hot-cathode discharge. This technique was next applied to the measurement of the axial and radial r-f fields accompanying beam-plasma interaction in cylindrical geometry. Comparisons are made with recent, relevant theories. For the case of beam-plasma interaction, theories for both cold and warm plasmas are reviewed. (auth)

15885 (UCRL–12207(Rev.1)) DISPERSION RELATION FOR RELATIVISTIC STREAMS OF FINITE RADIUS. Landau, Ronald W. (Lawrence Radiation Lab., Univ. of California, Livermore). Dec. 21, 1964. Contract W-7405-eng-48. 10p. Dep. mn. CFSTI $1.00 cy, $0.50 mn.

A dispersion relation that includes relativistic and retardation effects, temperature, and streaming was obtained for longitudinal oscillations of a finite plasma. The equations exhibit a discontinuity when the phase velocity of the plasma wave equals the velocity of light. (D.C.W.)

15886 (UCRL–14285) CONTROLLED THERMONUCLEAR RESEARCH. Semiannual Report, January–June 1965. (Lawrence Radiation Lab., Univ. of California, Livermore). Contract W-7405-eng-48. 128p. Dep. mn; CFSTI $4.00 cy, $1.00 mn.

A summary is presented of thermonuclear studies in magnetic mirror machines, Astron devices, and various other machines having a toroidal configuration; and plasma studies of a theoretical, experimental, and engineering nature. The particular machines studied include Table Top III, Alice, Astron, Levitron, Homopolar Gun I, Homopolar V, and others. (T.F.H.)

15887 (AD–625789) SOURCE OF GAS-DISCHARGE PLASMA. Kubarev, Yu. V. Translation of Russian Patent 166974. Nov. 4, 1963. 4p. (FTD-TT–65-806). CFSTI $1.00 cy, $0.50 mn.

A gas-discharge-plasma source is described which is different from known ones in that on its output there is placed an ionizing chamber the casing of which through cross-over switches is connected to the anode and in which there is an opening for supplying active gas. (M.O.W.)

15888 (SC-T–65-775) KINETIC THEORY OF WEAKLY IONIZED HOMOGENEOUS PLASMA. PART III. THE COLLISION OPERATOR IN THE CASE OF AN IMPERFECT LORENTZ GAS. Bayet, Michel; Delcroix, Jean-Loup; Denisse, Jean-Francois. Translated by Marcel I. Weinreich (Sandia Corp., Albuquerque, N. Mex.), from J. Phys. Radium, 17: 923-30(1956). 22p. Dep. mn. JCL $2.60 fs, $0.86 mf.

The effects of elastic collisions of electrons with molecules are studied assuming that the electron-molecule interaction is described by a law of central force. (D.C.W.)

15889 (SC-T–65-776) KINETIC THEORY OF WEAKLY IONIZED HOMOGENEOUS PLASMA. PART IV. STUDY OF THE EVOLUTION OF THE ISOTROPIC PART OF THE DISTRIBUTION FUNCTION. Bayet, Michel; Delcroix, Jean-Loup; Denisse, Jean-Francois. Translated by Marcel I. Weinreich (Sandia Corp., Albuquerque, N. Mex.), from J. Phys. Radium, 17: 1005-9(1956). 14p. Dep. mn. JCL $1.60 fs, $0.80 mf.

The evolution in time of the isotropic part of the distribution function is studied. The case in which the law of interaction among the electrons and molecules is expressed by r^{-5} is treated in detail. (D.C.W.)

15890 HYDROMAGNETIC OSCILLATIONS OF NON-UNIFORM PLASMA. I. APPROXIMATE SOLUTION. Stepien, K. (Univ., Warsaw). Bull. Acad. Pol. Sci., Ser. Sci. Math. Astron. Phys., 13: 675-9(1965).

Approximate wave solutions are obtained for an isothermic plasma in a uniform gravity field and a uniform magnetic field, using Maxwell equations, equations of motion and continuity, and the adiabatic equation. The effect of the magnetic field on gravity and sound waves (ω_g and ω_s) is investigated. (L.B.S.)

15891 RADIATION FROM A CURRENT STRIP IN A UNIAXIALLY ANISOTROPIC PLASMA MEDIUM. Seshadri, S. R. (Sylvania Electronic Systems, Waltham, Mass.). Can. J. Phys., 44: 207-17(Jan. 1966).

The radiation resistance of a linear current strip of finite width immersed in a uniaxially anisotropic plasma medium is evaluated for the case in which the width of the strip is parallel to the direction of the magnetostatic field. The current on the strip is assumed to be directed along the length of the strip and hence is perpendicular to the direction of the magnetostatic field. It is assumed also that the current is constant along the width of the strip but has a triangular variation along its length. Meaningful values for the radiation resistance are obtained for all frequencies, especially for frequencies below the plasma frequency. The dependence of the radiation resistance on the frequency and the length of the strip is examined. (auth)

15892 MULTISTAGE PLASMA ACCELERATION AND HEATING. Schindler, H. (Siemens-Schuckertwerke, Erlangen, Ger.). EuroNuclear, 2: 587-90(Dec. 1965).

The behavior of plasma in a three-stage acceleration experiment was investigated in order to gain a knowledge of the velocities attainable by this method, of the particle densities, and of the total particle number. In addition, the details of the acceleration process are explored as a basis for further experiments. A view of the axial plasma motion and the radial momentum distribution are given. The experimental results show that the applied principle of step-by-step plasma heating is effective. (J.F.P.)

15893 MICROWAVE RADIATION FROM A BOUNDED PLASMA. Idehara, Toshitaka (Kyoto Univ.); Abe, Haruhiko; Kubo, Hiroshi. J. Phys. Soc. Jap., 20: 2298(Dec. 12, 1965).

Microwave radiation from a plasma column in the region of $\omega_c/\omega > 1$ and $\omega_p/\omega > 1$ (where $\omega_c = eB/m$, and $\omega_p^2 = ne^2/m\epsilon_0$), was studied, and it was found that this radiation exhibits structure consisting of many lines. The characteristics of these lines are given. Then for one possible explanation, standing waves in a bounded plasma column are considered to exist. (J.F.P.)

15894 APPLICATION OF MICROWAVE SCATTERING THEORY TO MEASUREMENT OF UNDERDENSE CYLINDRICAL PLASMAS. **Shiobara, Shinji (Inst. of Physical and Chemical Research, Tokyo). J. Phys. Soc. Jap., 20: 2301(Dec. 12, 1965).**

Comparison is made between the values of phase shift obtained experimentally at 34 Gc on a helium plasma of 27 mm diameter and those calculated based on the Born approximation. The variation of phase shift against distance with discharge current as a parameter for three types of density distribution is shown. The electron density obtained using a Langmuir probe is used for theoretical curves. The result shows that this method of phase-shift analysis is applicable to underdense cylindrical plasmas of small diameter when plasmas can be regarded as uniformly illuminated by microwaves, irrespective of the directivity of antennas, provided the multiple reflection effect is smoothed away. (J.F.P.)

15895 ELECTRICAL CONDUCTIVITY OF A TURBULENT PLASMA. **Kato, Kiyoe; Kiyama, Satoru; Shimahara, Hiroko (Electrotechnical Lab., Tokyo). J. Phys. Soc. Jap., 20: 2308-9(Dec. 12, 1965).**

A method is described for measuring the d-c conductivity of a plasma. The turbulent plasma is prepared by superposing r-f voltage on the discharge d-c voltage. The variation of the effective conductivity is directly displayed on a cathode ray oscilloscope, comparing the turbulent plasma with the quiescent plasma. The typical pattern of the conductivity variation taken with an oscilloscope is reproduced. It is confirmed by this experiment that the effective conductivity of the turbulent plasma is smaller than that of the quiescent plasma. These experimental results are qualitatively consistent with the theoretical prediction. (J.F.P.)

15896 SPECTROSCOPIC STUDIES ON HELIUM PLASMA HEATED BY REFLECTED SHOCK IN T-TUBE. **Fukuda, Kuniya; Ishii, Keishi; Okasaka, Rei; Fujimoto, Takashi (Kyoto Univ.). J. Phys. Soc. Jap., 20: 2309-10 (Dec. 12, 1965).**

The luminous front and preceding shock wave in a T tube are studied. The time-resolved streak picture and corresponding x-t diagram, and typical time-resolved spectra are shown. The space resolved spectrum along the tube axis in front of the reflector is also given and demonstrates the separation of the weak luminous region of the reflected shock from the bright region of the arc plasma containing impurity emissions. From the intensity ratio of He(I) λ 3188 and λ 3889 it is clear that the temperature in the reflected shock region reaches a maximum of 1.7 ± 0.1 ev at 5 μ sec after the arrival of the front and then falls gradually. (J.F.P.)

15897 CONDUCTIVITY MEASUREMENTS CONCERNING LOW-TEMPERATURE PLASMAS USED IN MAGNETOGASDYNAMIC GENERATORS. **Kordus, Aleksander (Univ. of Poznan, Poland). Nukleonika, 10: 605-11(1965).**

Measurement methods are described and results obtained are compared with calculations. A plasma conductivity measurement system in the channel of a magnetogasdynamic generator is proposed. (auth)

15898 VARIATIONAL PRINCIPLE FOR A GUIDING-CENTER PLASMA. **Grad, Harold (New York Univ.). Phys. Fluids, 9: 225-51(Feb. 1966).**

A new variational formulation is presented for the equilibrium and stability of a guiding-center plasma with emphasis on open-ended systems confined by mirrors. In contrast to all earlier formulations, this is a classical one in which equilibria arise as stationary states of a certain potential and stable equilibria minimize the same potential. The formulation is more general than earlier ones in that it includes nonlinear perturbations, a variety of boundary conditions (lines tied or not), multiple turning points, and a correct treatment of electric fields along the lines. In addition, a number of ambiguous procedures and incorrect statements, are found in earlier stability analyses, are corrected. (auth)

15899 KINETIC STRUCTURE OF A PLASMA. **Dawson, John M.; Nakayama, Toshio (Nagoya Univ., Japan). Phys. Fluids, 9: 252-64(Feb. 1966). (MATT-395).**

The kinetics of a plasma is investigated by expanding the motion in terms of the deflection of the particles from their noninteracting orbits. It is shown that this procedure leads to the following results. At the first stage, the dressed-particle picture of Thompson and Hubbard, and of Rostoker for obtaining fluctuations in a plasma is obtained. Rostoker's principle for obtaining two-particle correlations in terms of test particle results is also obtained at this state. At the second stage, encounters between shielded particles appear and the picture of Birmingham, Dawson, and Oberman for computing bremsstrahlung emerges. The usual Fokker–Planck equation may also be obtained at this stage. The treatment applies to the full electromagnetic field. (auth)

15900 ION WAVES IN BOUNDED PLASMA. **Bertotti, B.; Cavaliere, A.; Giupponi, P. (C.N.E.N., Frascati, Rome). Phys. Fluids, 9: 265-70(Feb. 1966).**

The role of the charge sheath at the wall of a discharge in determining the appropriate boundary conditions for a low-frequency wave in a low-pressure discharge is discussed by means of a hydrodynamical model. It is found that Bohm's condition for the mean ion velocity holds even when oscillations are present. The electron dynamics is neglected and the dispersion relation shows the existence of a principal mode which propagates along the tube just as in an infinite medium; all other modes are damped. Analysis of the dynamics of the oscillating sheath shows that it behaves like a battery, transferring the electrostatic oscillation to the wall with no distortion and no impedance. (auth)

15901 ION WAVES ON BOUNDED PLASMAS. **Andersson, Bengt (Royal Inst. of Tech., Stockholm); Weissglas, Peter. Phys. Fluids, 9: 271-4(Feb. 1966).**

Ion acoustic waves propagating along a cylindrical plasma column are studied theoretically. By neglecting the ion temperature, it is possible to derive a simple boundary condition at the plasma surface. In addition to the infinite number of ion wave modes which degenerate into purely longitudinal waves in an infinite plasma, it is found that there exists a surface mode which is the ion equivalent of the electron surface mode of Gould and Trivelpiece. It is also shown that due to interaction between the ion modes and the Gould and Trivelpiece mode the dispersion curves of the ion waves are strongly modified. (auth)

15902 LONGITUDINAL PLASMA WAVES IN THE LOW-FREQUENCY LIMIT. **Parker, Lee W. (Mt. Auburn Research Associates, Inc., Cambridge, Mass.). Phys. Fluids, 9: 274-6(Feb. 1966).**

In a partially ionized gas, two longitudinal wave modes propagate at high frequencies, the ion-acoustic mode and the neutral-acoustic mode. At very low frequencies, there are also two roots of the dispersion relation, one representing a damped wave and one representing an undamped wave. It the roots are traced as a function of frequency from the high-frequency regime to the low-frequencies, the identification of the roots depends on the ratio of concentrations of ionized and neutral particles. In the low-frequency limit, either the ion wave is damped or the neutral wave is damped, depending on the value of this ratio. The critical value is derived. (auth)

15903 STABILITY OF SHEET PINCH. **Hoh, F. C. (Boeing Scientific Research Labs., Seattle, Wash.). Phys. Fluids, 9: 277-84(Feb. 1966).**

The growth rate of the sheet pinch instability is calculated in the small Larmor radius limit using the method of integration along unperturbed orbits. It is found that the instability is driven by a small group of "resonant" electrons which cross and drift about the neutral plane having zero velocity along the field lines. The microinstability is absolute and develops fastest for a critical perturbation wavelength, of the order of several times the thickness of the plasma sheet. (auth)

15904 LOW-FREQUENCY SPATIAL RESPONSE OF A COLLISIONAL ELECTRON PLASMA. Fried, Burton, D.; Kaufman, Allan N.; Sachs, David L. (Univ. of California, Los Angeles). Phys. Fluids, 9: 292-8(Feb. 1966). (UCRL-16374).

A study is made of the linear spatial response of an electron plasma to be localized one-dimensional electric field, whose frequency ω is low compared with the electron-collision frequency ν. For a fully ionized plasma both electron-electron and electron-ion collisions are included in the calculations, the ions being treated as fixed scatterers. It is shown that the neglect of ion dynamics is justified for a suitable choice of parameters. In the hydrodynamic regime, the response function decays exponentially, with decay length equal to a diffusion length $a(\omega\nu)^{-\frac{1}{2}}$, where a is electron thermal speed, and its amplitude is proportional to $\omega^{\frac{1}{2}}$. In the kinetic regime, the amplitude is proportional to ω, and the decay is not exponential, with characteristic distance being the mean free path a/ν. For a weakly ionized gas, only electron-neutral collisions are included; in the hydrodynamic region, the dependence of amplitude and decay length on ω is the same as for the fully ionized gas, but the decay is no longer exponential. (auth)

15905 STEADY-STATE STRUCTURE AND LOW-FREQUENCY OSCILLATIONS OF AN INFINITELY LONG E LAYER. Enoch, Jacob (Univ. of California, Livermore). Phys. Fluids, 9: 299-308(Feb. 1966). (UCRL-14392).

The time-independent self-consistent equilibrium structure of an infinitely long E layer of finite thickness is investigated by expanding the current density and the magnetic field in powers of the ratio of the layer thickness to its radius. Time-dependent perturbations of the equilibrium solution are studied via the linearized Vlasov equation and a dispersion relation for frequencies well below the cyclotron frequency of the electrons in the total magnetic field is obtained. For perturbations of the form $\sim e^{i(\theta-\omega t)}$, two roots of this dispersion relation exist. One of these is equal to the experimentally observed precession frequency of the E layer. (auth)

15906 INVESTIGATION OF THE KELVIN-HELMHOLTZ INSTABILITY IN A CESIUM PLASMA. D'Angelo, N.; Goeler, S. V. (Princeton Univ., N. J.). Phys. Fluids, 9: 309-13(Feb. 1966). (MATT-351).

Experiments were performed in a thermally ionized cesium plasma, in which a relative drift between ions in adjacent layers appears to excite the Kelvin-Helmholtz instability. The relative drifts required are of the order of c_i, the ion thermal velocity, or somewhat smaller. The frequency of the oscillations is generally in the range 1-4 kc/sec. A study was made of the type of waves excited, by means of amplitude and phase measurements. (auth)

15907 CONVECTIVE STABILITY IN A PLASMA WITH HORIZONTAL MAGNETIC FIELDS. Yu, C. P. (State Univ. of New York, Buffalo). Phys. Fluids, 9: 412-14 (Feb. 1966).

Convective instability induced by gravity in a perfectly conducting, inviscid, and compressible plasma permeated by a general horizontal magnetic field is considered. Stability conditions obtained by Tserkornikov and Newcomb are interpreted following the reasoning of Schwarzchild. (auth)

15908 SPECTROSCOPIC DETERMINATION OF ELECTRON TEMPERATURE IN A HELIUM PLASMA. de Vries, R. F.; Mewe, R. (Istituut voor Plasma-Fysica, Jutphaas, Netherlands). Phys. Fluids, 9: 414-15(Feb. 1966).

Optical excitation functions measured in collision chamber experiments should be applied with caution on plasma diagnostics. This is illustrated for the upper level (4^1S) of λ5048 of neutral helium. (auth)

15909 GENERATION OF THE THIRD-HARMONIC CURRENT DENSITY IN A PLASMA. Tang, Ting-wei (Univ. of Connecticut, Storrs). Phys. Fluids, 9: 415-17 (Feb. 1966).

An explicit expression for the third-harmonic current density generated by an alternating electric field is obtained for a velocity-dependent collision frequency by using a perturbation-theoretic approach. (auth)

15910 ON THE PROPAGATION OF ELECTROMAGNETIC WAVES IN A PLASMA WITH HEAVY POSITIVE AND NEGATIVE IONS. Teichmann, J. (Univ., Montreal) Phys. Lett., 19: 534-6(Dec. 15, 1965).

The propagation of electromagnetic waves in a cold, collisionless plasma containing both positive and negative heavy ions was studied using a three-fluid MHD model. (D.C.W.)

15911 OBSERVATION OF COOPERATIVE EFFECTS IN THE SCATTERING OF A LASER BEAM FROM A PLASMA. Ramsden, S. A.; Davies, W. E. R. (National Research Council, Ottawa). Phys. Rev. Lett., 16: 303-6 (Feb. 21, 1966).

The effects of cooperative interactions between ions and electrons were observed in the scattering of a laser beam by a plasma produced in a small theta pinch. The data indicate that the electrons have a thermal velocity distribution. (D.C.W.)

15912 EXTERNAL EXCITATION OF STANDING WAVES IN A RF DISCHARGE. Sato, Noriyoshi; Hatta, Yoshisuke (Tohoku Univ., Sendai, Japan). Phys. Rev. Lett,. 16: 306-8(Feb. 21, 1966).

Standing waves were excited in a Hg plasma produced by an r-f discharge under the application of a weak axial magnetic field. The waves differ from the waves that were previously excited by the same method in a d-c discharge. (D.C.W.)

15913 ON THE GENERALIZED CONSTITUTIVE PARAMETERS AND GOVERNING EQUATIONS FOR COMPRESSIBLE ANISOTROPIC PLASMA. Musal, Henry M. Jr. (General Motors Corp., Santa Barbara, Calif.). Proc. IEEE (Inst. Elec. Electron. Eng.), 53: 2124-5(Dec. 1965).

The equations describing the behavior of anisotropic compressible plasma are reduced to two generalized Maxwell's equations, from which a wave equation for the electric field intensity immediately follows. The generalized wave equation describes the plasma by two dyads (tensors), the dielectric and acoustic constants, which incorporate the intrinsic plasma properties. (M.J.T.)

15914 CYLINDRICALLY SYMMETRIC PLASMA SOURCE. Knopp, C. F.; Cambell, Ali Bulent (Northwestern Univ., Evanston, Ill.). Rev. Sci. Instrum., 37: 332-6(Mar. 1966).

A wall stabilized arc constrained to operate within a transparent tube is described. The device produces a plasma column of true cylindrical symmetry, justifying a one dimensional analysis of energy transfer within the column. Axial temperatures in excess of 12,000°K have been achieved in argon. (auth)

15915 MASS SPECTROMETRIC SAMPLING PROBE FOR DISCHARGE PLASMAS. Boehme, D. K.; Goodings, J. M. (McGill Univ., Montreal). Rev. Sci. Instrum., 37: 362-6(Mar. 1966).

A versatile sampling technique is described which permits a more definitive study of ion extraction and plasma sheath formation in discharge plasma. The ionic species from the plasma are sampled into a quadrupole mass spectrometer through a metal leak arrangement which itself acts as a probe. This behavior is substantiated by sampling probe characteristics, and charge density and electron temperature determinations for a flowing microwave discharge plasma in nitrogen at low pressure. (auth)

15916 USE OF SILICON SOLAR CELLS AS DETECTORS OF ENERGETIC ELECTRONS FROM PLASMAS. Ard, W. B. (Oak Ridge National Lab., Tenn.); Dandl, R. A.; Stetson, R. F. Rev. Sci. Instrum., 37: 380-1(Mar. 1966).

The use of silicon solar cells with fast response time for detecting energetic electron bursts from plasmas is briefly described. (L.B.S.)

15917 RELATION BETWEEN MOMENT EQUATIONS AND KINETIC EQUATION IN A COLLISIONLESS PLASMA [Thesis]. **Bloomberg, Howard Warren. Evanston, Ill., Northwestern Univ., 1965. 64p.**

Use of the moment cut-off method for obtaining description of a collisionless electron plasma perturbed by a longitudinal electric field is studied. Results from the method are compared with those obtained by a direct study of the Vlasov equation. It is found that for cut-off effected at moment order greater than three an "apparent" growing wave instability occurs. No such behavior results from direct analysis of the Vlasov equation. It is concluded that the effect of the moment cut-off method is to yield a correct representation of the Laplace transformed moments for only a limited domain of Laplace space. Subsequent Laplace inversion by the theory of residues leads to the anomalous behavior. (Dissertation Abstr.)

15918 KINETIC EQUATION FOR A WARM PLASMA [Thesis]. **Woollett, Edwin Lee. Manhattan, Kan., Kansas State Univ., 1965. 114p.**

A new kinetic equation is derived for a fully ionized plasma. A calculation is presented which determines a generalization of the Balescu-Lenard equation that includes relativistic corrections through terms of the order of the square of the ratio of the mean thermal speed to the speed of light. The model adopted is a single species of charged particles relaxing in a uniform background of immobile neutralizing charge. Wall effects are neglected, there is no externally imposed force field, and the system is assumed to be homogeneous. A classical description is assumed adequate, the microscopic motion being governed by the Darwin lagrangian. The calculation proceeds by first finding the equation obeyed by the N-particle distribution function, considered as a function of the coordinates and relativistic mechanical momenta. This equation is equivalent to a chain of equations involving reduced distribution functions. The first two members of this chain are studied by means of a new perturbation method devised by E. Frieman and G. Sandri. By requiring the absence of secular behavior, the Frieman-Sandri method allows one to easily write the formal kinetic equation which governs the relaxation of the one particle distribution function for times of the order of $t_{p/\epsilon} \gg t_p$, where t_p is the short natural time scale. The resulting kinetic equation is convergent for distant collisions due to an automatic distribution dependent, shielding of the microscopic Lorentz force. The effects of the three-body Lorentz force, which appear when the acceleration of a source particle is expressed in terms of the coordinates and velocities of all the other particles, disappears in the final result. The kinetic equation has, however, a divergence due to that part of the collision integral corresponding to small impact parameter collisions; this indicates that the method used overemphasizes the importance of the distant collisions. (Dissertation Abstr.)

15919 BEHAVIOR OF RUNAWAY ELECTRONS IN A PLASMA BETATRON [Thesis]. **Ferrari, Lawrence August. Hoboken, N. J., Stevens Inst. of Tech., 1965. 179p.**

Runaway electrons generated by induction acceleration in a plasma betatron with axially symmetric guide field $B_z(r,z,t) = B_0 (r_0/r)^p \times f(z) \sin 2\pi t/\tau$ ($n = 0.6$, $\tau = 16$ μsec, $r_0 = 4.8$ cm) together with auxiliary azimuthal guide field $B_\theta(r) = (k/r)$, ($2\ kG \leq B_\theta(r) \leq kG$) were studied for a wide range of induction electric fields E_θ ($2.5\ v/cm \leq (E)_\theta \leq 26 v/cm$). Experiments were carried out in argon and krypton at ambient pressures of 0.5-2 torr. The ratio of the applied electric field to the critical electrical field for runaway was typically ~500 so that most of the electrons should run away. Runaway currents of ~1 amp were observed immersed in a background conduction current of 25–100 amp. The runaway electrons strike the vacuum chamber walls at a time t_x after betatron acceleration has begun. The resulting x rays are detected with a scintillation counter. The x-ray time t_x was measured as a function of E_θ and B_θ for several half cycles of the guide field. It is found that t_x decreases with E_θ but increases with B_θ. It is also found that t_x depends on the relative orientation of E_θ with respect to B_θ. This is shown to be due to a small transverse magnetic field associated with the B_θ guide field. The small runaway current is consistent with that determined from the self electric field generated by the adiabatic constriction of the runaway stream or the negative-mass-instability. The reason for the beam disruption and subsequent x-ray emission are unexplained but the mechanism of Field and Fried appears to describe the process. The betatron guide field was generated in a low-inductance (50×10^{-9}h) single-turn coil using flux concentrators. Techniques used to construct the flux-concentrators and measure the resulting pulsed magnetic field distribution are also described. (Dissertation Abstr.)

15920 PLASMA PRODUCTION BY KINETIC IMPACT [Thesis]. **Pernick, Benjamin J. Hoboken, N. J., Stevens Inst. of Tech., 1965. 221p.**

High speed photographic and time-resolved spectrographic observations were made of the head-on collision of two hypervelocity copper jets formed from metal-lined explosive charges. Streak camera records show that the jets are moving at about 8 mm/μsec, or equivalently, with a kinetic energy of 21 ev/atom. Framing camera observations of the collision in air and in a low pressure helium atmosphere indicate that a region of intense luminosity is created about the point of impact. Time-integrated spectrograph records show that the composition of the collision light over the visible region is that of a continuum with superposed copper spectral lines. A time-resolved spectral record in the 4400–5300Å region of a collision in helium shows that an intense continuum first appears for about 5 μsec. The continuum intensity then decreases and a copper emission line spectrum emerges, consisting of both neutral and first-ionized copper lines. The ionized copper lines originate from energy levels that are about 25 ev above the neutral atom ground state. Several neutral copper lines are shown to possess combined instrumentation and resonance-broadened profiles. Estimates of the neutral copper atom density in the jet collision plasma are derived from line halfwidth measurements resulting from theoretical profile fits to the observed line shapes. Neutral atom densities are of the order of 4×10^{19} cm^{-3}. An intermolecular electric field created by copper ions and electrons in the plasma result in a Stark shift of the observed CuI 4531 line. The copper ion densities determined from measured wavelength shifts of this line are about 4×10^{17} cm^{-3}. Oscillator strengths for two neutral copper transitions observed in the time-resolved spectrum are also determined. A comparison of the resonance-broadened halfwidths for the CuI 4525 and 4643 lines with that of the CuI 4651 line whose oscillator strength is known results in an estimate of the f-numbers for these transitions. Conclusions derived from existing theoretical models of hypervelocity impact are found to be in good agreement with the observations and detailed measurements obtained from these experiments. Applications of this work to other areas of interest are indicated. (Dissertation Abstr.)

15921 PLASMA GUN (Engineering Materials). (Los Alamos Scientific Lab., Univ. of California, N. Mex.). (CAPE–1328).

15 drawings.

The coaxial plasma gun produces an accelerated plasma having a particle density $\rho \sim 2$ to 3×10^{19}cm^3, a temperature $T \sim 1$ to 3 kev, a time duration $t \sim 0.2$ to 0.3 μsec, a volume ~15 mm^3, and a neutron yield $>10^{10}$/burst. It is a two-gun structure with Cu electrodes, which may be adjusted for length. The discharge chamber is statically filled with deuterium before firing to remove unknown pressure distribution encountered in pulsed injection. The condenser bank for each gun consists of two 45 μF, 20-kv modules each switched by vacuum spark gaps with a current rise time of ~2.2 μsec. The insulator at the breech end of the gun is fabricated from glass into a flat Pyrex plate with a cylindrical extension 5 cm long. The insulator allows a longer breakdown path and produces an initial nonplanar current sheath. The inner and outer diameters of the electrodes are 5 and 9.6 cm with a maximum center electrode length of 25 cm. (For details, see TID-4100.) (M.C.G.)

15922 EVAPORATIVE PUMPS FOR ULTRA HIGH VACUUM SYSTEMS (Engineering Materials). (Lawrence Radiation Lab., Univ. of California, Livermore). (CAPE–1319).

4 drawings.

In evaporative pumping, the metal wire to be evaporated is wound on a tungsten core wire, which is held by the filament holders. Two types of pumps are described. In the water-cooled pump, refrigerated water cooling is provided to the outer vacuum wall. An inner liner, cooled with liquid N, may be added when lower base pressures are needed. This equipment is used with the "ALICE." (For details, see TID-4100). (M.C.G.)

15923 BAKEABLE VALVE, 12 IN. (Engineering Materials). (Lawrence Radiation Lab., Univ. of California, Livermore). (CAPE–1324).

30 drawings.

The valve, used with the "ALICE," consists of a large hydraulic cylinder that operates through a welded bellows and moves the carrier plate and gate in a simple rectilinear path. Closure is accomplished by rollers on ramps encountered near the end of carrier plate travel. The gate carries a copper disk with the seal surface machined at its outer periphery. The seal must be accomplished against a surface provided on a mating member, external to the valve assembly. A rectangular Al foil seal flange permits the removal of all valve components for service or replacement without removing the valve from its system. (For details, see TID-4100). (M.C.G.)

15924 CONVERTABLE TRAPS, 4 IN. (Engineering Materials). (Lawrence Radiation Lab., Univ. of California, Livermore). (CAPE–1320).

64 drawings.

High-conductance traps are described, which are used with oil diffusion pumps to produce vacuums of 1×10^{-10} torr. Copper tubing is used as a reservoir for liquid N or as part of a circulating circuit for N. The drum is a two-bounce baffle with an oil migration barrier at one end. Trap configurations are given for vertical mounting and for horizontal port applications. Both versions have a movable-flapper valve to stop oil splash during start-up of the diffusion pump. The traps are used with "ALICE." (M.C.G.)

15925 VISCOUS EFFECTS IN A HYDROMAGNETIC WAVEGUIDE. Sodek, Benard A. Jr. (General Dynamics, Fort Worth, Tex.). 18p. (CONF-650653–11). ORINS. Gmelin, AED-CONF-65-170-23.

From American Physical Society, Summer Meeting, New York.

The dynamics of a plasma may be described by a model formulated on the bases of Maxwell's equations and the quasi-one-fluid magnetohydrodynamic equations. The description of hydromagnetic wave propagation in a magneto-plasma-filled waveguide is obtained by the calculation of dispersion relations which connect the propagation constant with the wave frequency. In this approximate treatment first order effects of pressure, current inertia, resistivity, viscosity, and heat conduction are included. The influences of diffusion, space charge, and Hall effect are neglected. The plasma is considered fully ionized, uniform and enclosed in a perfectly conducting waveguide. Results show that the addition of viscous effects to the theoretical model accentuate the previously obtained effects due to resistivity. (auth)

15926 VALIDITY CONDITIONS OF TRANSPORT PROPERTY MEASUREMENTS USING ARC COLUMNS. Chen, Michael Ming (Yale Univ., New Haven). New York, American Inst. of Aeronautics and Astronautics, 1965, Preprint No. AIAA 65-541, 33p., $1.00. (CONF-650711–52). ORINS.

From AIAA 2nd Annual Meeting and Technical Demonstration, San Francisco.

A comprehensive investigation of thermal and chemical equilibria and the transport processes occurring in a confined arc column was carried out, with particular emphasis on the validity of the simplifying assumptions usually employed in the measurement of transport properties. It is shown that, in general, thermal and dissociation equilibria are not likely to be satisfied for the neutral gases around columns of 5-millimeter diameter or less, but the equality of electron and heavy particle temperatures can be assumed everywhere except for the weakly ionized regions. Both hydromagnetic and hydrodynamic instabilities may occur in the confined column, and stability criteria estimated from order-of-magnitude analysis indicate that the column may not be stable at moderate pressures and current levels. Some systematic errors in arc column spectroscopy are also discussed. While all estimates are approximate and subject to considerable refinements, any of these suspected mechanisms, either jointly or separately, could be responsible for some of the discrepancies between observed and calculated thermal conductivities. Diagrams showing latitudes of experimental parameters are presented to facilitate minimizing these errors. (auth)

15927 APPARATUS FOR MAGNETICALLY CONFINING A PLASMA. Furth, H. P.; Rosenbluth, M. N. (to U. S. Atomic Energy Commission). U. S. Patent 3,230,145. Jan. 18, 1966.

An apparatus for confining a plasma is described. In particular, the confinement is provided by an annular magnetic field extending along the length of the apparatus. Transverse sections of the constant magnetic field surface vary periodically along the length of the apparatus from an elliptical shape to a circular shape and back to an elliptical shape in which the major and minor axes of any particular ellipse are rotated ninety degrees from those of a succeeding ellipse. (AEC)

15928 DEVICE HAVING HIGH GRADIENT CUSP GEOMETRY. Dandl, R. A.; Kerr, R. J. (to U. S. Atomic Energy Commission). U. S. Patent 3,230,418. Jan. 18, 1966.

Means for providing a magnetic field configuration possessing cusps for containment of plasmas are described. A pair of concentric coils are spaced from another pair of concentric coils. Each outer coil of each pair of coils is energized to provide a magnetic field reinforcing the other, while the inner coils of each pair of coils are energized to provide a magnetic field directed opposite to that of the outer coils. The resultant field has point and line cusps. With adjustment of coil currents, one or more low field regions are provided in the center between the pairs of coils. A plasma is injected into the region for trapping therewithin, or a plasma may be formed in the region by ionizing the background gas with energetic electrons. (AEC)

Shielding

15929 (AD–627890) MONTE CARLO CALCULATIONS OF GAMMA-RAY STREAMING THROUGH COPLANAR AND NONCOPLANAR DUCTS. Gardner, Leonard B.; Mettler, Alan J. (Naval Civil Engineering Lab., Port Hueneme, Calif.). Jan. 1966. 39p. (R–412). CFSTI $2.00 cy, $0.50 mn.

The Monte Carlo technique, using the ADONIS computer code developed by the United Nuclear Corporation, was used to calculate gamma dose rates and energy spectra within two-legged and three-legged rectangular air ducts through concrete. These calculations were performed to intercompare a coplanar and a noncoplanar configuration for ^{60}Co gamma streaming through a three-legged duct. The results of the Monte Carlo calculations are compared with previously obtained experimental findings. The agreement between the Monte Carlo method and previous experiments supports the validity of using the Monte Carlo method to simulate the behavior of gamma rays in ducts. (auth)

15930 (NP–15697(Vol.2)) DATA COMPILATION AND EVALUATION OF SPACE SHIELDING PROBLEMS. VOLUME II. DOSE CALCULATIONS IN SPACE VEHICLES. Hill, C. W.; Ritchie, W. B.; Simpson, K. M. (Lockheed Nuclear Products, Marietta, Ga.). Aug. 1965. Contract NAS-8-11164. 128p. (ER–7777(Vol.2)).

A system of computer programs that provides an estimate of alpha and proton doses within realistic space-vehicle configurations is described. The results of proton-dose calculations for three vehicle configurations are presented. (D.C.W.)

15931 (TO-B-65-27) STRUCTURE SHIELDING FROM SIMULATED FALLOUT GAMMA RADIATION. Final Report—Phase I. Kaplan, A. L.; Waldman, J.; Jones, J. L.; Barch, W. E.; MacNeil, R. L. (Technical Operations Research, Burlington, Mass.). Nov. 1965. Contract N228-(62479)-65776. 114p.

Experiments were performed to evaluate the application of the presently used structure shielding theory to structures of simple geometry. Steel structures with cylindrical configurations and with rectangular configurations of different width-to-length ratios were used in these experiments to verify the theory, to study the effects of interior partitions and outer-wall apertures, and to evaluate theoretical predictions of in-and-down scattering below ground. The shape factor verification experiments yielded results which the theory predicted to within 15%. For the interior partitions experiments, the theory predicted the experimental results to within 10% in most cases and 20% in all cases. For the structures with outer-wall apertures and no interior partitions, theory and experiment agree to within 15%. Introduction of the interior partitions, however, causes theoretical predictions to be up to 50% lower than experimental results at detector locations opposite the aperture, apparently due to the failure of the theory to account for radiation scattering effects by the interior partition. The results of the basement shielding experiments showed agreement within 30% between theory and experiment for structures with no floor. However, the theory was a factor of 3 lower than the experimental results for structures with a 0.5-in. (20 psf) steel floor, indicating the requirement for a change in the floor barrier reduction factor currently used in the theory. (auth)

15932 (ORNL-tr-843) γ-RAY SHIELDING PROPERTY, STRENGTH AND WORKMANSHIP OF A BUILT-UP TYPE LEAD SLAB STRUCTURE. Sakai, Toshio; Tanaka, Mamoru; Hirowatari, Tomoyuki; Nishimaki, Ko; Nagahata, Yasuo; Shindo, Mitsuo; Miyakoshi, Junichi. Translated for Oak Ridge National Lab., Tenn., from Hitachi Zosen Giho, 25: No. 4, 24-32(1960). 33p. Dep. mn. JCL $3.60 fs, $1.19 mf.

The properties of lead plate for use as secondary shielding on nuclear-powered ships were investigated with particular emphasis on gamma leakage around bolt sections. The effects of vibrations on bolt holes and bolt tension were studied. (D.C.W.)

15933 (ORNL-tr-1060) COMPUTATION OF THE THICKNESS OF STEEL SHIELDING WALLS AGAINST GAMMA RADIATION. Hoenig, Arnost. Translated for Oak Ridge National Lab., Tenn., from Inzenyrski Stavby, 8: 351-5(1965). 11p. Dep. mn. JCL $1.60 fs, $0.80 mf.

The results of a calculation of gamma dose buildup factors in steel from an isotropic point source are presented; and the use of the buildup factors in the calculation of the thickness of steel shielding is demonstrated. (D.C.W.)

15934 TRANSFER-MATRIX METHOD FOR GAMMA-RAY AND NEUTRON PENETRATION. Aronson, Raphael (New York Univ., New York); Yarmush, David Leon. Contracts AF 33(616)-3616; AF 33(616)-6081; DA-30-069-AMC-96(R). J. Math. Phys. (N. Y.), 7: 221-37(Feb. 1966).

The problem of radiation transport is formulated in terms of a transfer matrix H which is a 2×2 matrix of operators. H is simply related to the more intuitive transmission and reflection operators T and R. An explicit expression for H is derived in slab geometry for radiation distributions that depend on the angle with the slab normal and on energy. H for a multilayer slab is the matrix product of the transfer matrices for the individual layers. A formal expression for H for a homogeneous slab of finite thickness is found in terms of the T and R appropriate to an infinitesimally thin slab. These in turn are related to the single-scattering distribution and therefore can be computed from the microscopic cross section. For purposes of computation, finite matrix representations for the operators must be introduced corresponding to the finite vectors which approximate the distributions. Expansions of the distributions in the cosine of the angle and group representations in energy were chosen. Some numerical results are presented for gamma rays on aluminum. The extension to problems with internal sources and to nonplanar geometries is outlined. (auth)

15935 A METHOD FOR PREDICTING THE PENETRATION AND SLOWING DOWN OF NEUTRONS IN REACTOR SHIELDS. Hjaerne, L.; Leimdoerfer, M. Nucl. Sci. Eng., 24: 165-74(1966).

A new approach is presented in the formulation of removal-diffusion theory. The removal cross section is redefined and the slowing down between the multigroup diffusion equations is treated with a complete energy-transfer matrix rather than in an age-theory approximation. The method, based on the new approach, contains an adjustable parameter. Examples of neutron spectra and thermal flux penetrations are given in a number of differing shield configurations, and the results compare favorably with experiments and Moments-Method calculations. (auth)

15936 AN ELECTRON SHIELDING ANALYSIS FOR SPACE VEHICLES. Mar, B. W. Nucl. Sci. Eng., 24: 193-9(1966).

A nomograph for electron number transmission and an expression for the differential energy spectra of the penetrating electrons are developed from Monte Carlo calculations of normal incident electrons on slabs of beryllium, aluminum, iron, silver, and lead with energies in the range of 0.4 to 10 Mev. Comparison of the Monte Carlo calculations with experimental data and comparison of nomograph results with Monte Carlo calculations of Berger and Seltzer show the accuracy of the proposed method. A method for calculating the dose from electrons penetrating a space vehicle is developed, based on the nomograph, the predicted energy spectra of penetrating electrons, and a geometric analysis of the vehicle. (auth)

15937 A NEW VARIANT TO THE EXPONENTIAL TRANSFORMATION TECHNIQUE IN MONTE CARLO SHIELDING CALCULATIONS. Chilton, A. B. Nucl. Sci. Eng., 24: 200-8(1966).

Monte Carlo calculations of deeply penetrating radiation fields are improved by use of a transformation involving the factor e^{-cr}. The optimum value of c generally appears to be at or near the value for total attenuation coefficient for the source radiation, but there are some difficulties in choosing such a value of c. An approach is described and illustrated that allows c to be made equal to μ_0, and the resulting transformed equation is handled in a simple fashion. The technique is encoded into a FORTRAN program called FETMOC, and illustrative problems are solved. Results are given in terms of buildup factors. Two-way energy spectrum and directional distribution at arbitrary points are obtained, also. All results are compared with previously reported calculations to the extent possible. (auth)

15938 A STUDY OF ELECTRON-PHOTON SHOWERS BY THE MONTE CARLO METHOD. Tamura, Masami (Kyoto Univ.). Progr. Theoret. Phys. (Kyoto), 34: 912-41 (Dec. 1965).

The detailed structure of electron-photon showers is investigated by simulating the physical processes accurately with the Monte Carlo method. The distributions of characteristic quantities of the showers in aluminum are given for electron- and photon-initiated showers at the incident energy of $400m_e$ (m_e: the electron rest mass). The longitudinal transitions, energy distributions, and radial distributions for the average numbers of electrons and photons in a shower are given, and the interrelations between the distributions of electrons and of photons are discussed. The spatial distributions of energy loss by shower particles

are also presented. Furthermore, fluctuations in the number of electrons at a given depth and the energy loss in a specified volume are given. Some of these distributions are compared with other results. (auth)

Solid State Physics

See also CHEMISTRY — Inorganic and Physical Chemistry
METALS, CERAMICS, AND OTHER MATERIALS — Properties and Structure

Refer also to abstracts 15045, 15302, and 15819.

15939 (AD-620189) ELECTRON-PHONON RENORMALIZATION EFFECTS IN HIGH MAGNETIC FIELDS. THE DE HAAS-VAN ALPHEN EFFECT. Fowler, M.; Prange, R. E. (Maryland Univ., College Park. Dept. of Physics and Astronomy). Mar. 10, 1965. Contract AF-AFOSR-735-65. 26p. (AFOSR-65-1192). CFSTI $2.00 cy, $0.50 mn.

The amplitude dependence of the de Haas-van Alphen effect was calculated as a function of temperature and magnetic field. This amplitude can be interpreted as giving a field-dependent effective mass. The amplitude was calculated numerically for several cases of interest. It is found that the field effects are rather smooth and depend most directly on the electron self-energy function for pure imaginary values of the frequency. (TAB)

15940 (JUL-292-RW) DISPERSIONSKURVEN FUER ROTATIONSSCHWINGUNGEN VON TETRAEDRISCHEN MOLEKUELEN IN EINEM FLAECHENZENTRIERTEN GITTER MIT TETRAGONALER MOLEKUELORIENTIERUNG. (Dispersion Curves for Rotation Oscillations of Tetrahedral Molecules in a Face-Centered Lattice With Tetragonal Molecular Orientation). Stockmeyer, R. (Kernforschungsanlage, Juelich (West Germany). Institut fuer Reaktorwerkstoffe). Sept. 1965. 24p. Dep. mn.

The rotation oscillation spectrum of molecular orientation with tetragonal symmetry was investigated in fcc lattices. Only Cartesian coordinates were used and the dispersion curves are given as a function of the corresponding coupling parameters. The complete motion equation is given and the perturbation calculation for the coupling between translational and rotational motions is described. The symmetry properties of the coupling matrices for rotation oscillations of very small amplitude were derived, and dispersion curves with general coupling parameters were calculated. The octupole interaction in Euler angles was considered along with the approximation of small angles in Euler coordinates. Dispersion curves are given for rotation oscillations with octupole interactions. (J.S.R.)

15941 (NP-15698) ANOMALOUS PROPAGATION IN A QUANTUM PLASMA AND MAGNON-HELICON COUPLING. Technical Report No. 465. Callen, Earl; Heiche, Gerhard (Naval Ordnance Lab., White Oak, Md.); Glick, Arnold J. (Maryland Univ., College Park. Dept. of Physics and Astronomy). July 1965. 8p.

The dielectric function tensor of a free electron gas quantized by a magnetic field was used to study the possibility of the propagation of collective modes (analogous to the helicon) within the semi-classical Doppler-shifted absorption cone in a nonmagnetic metal. The propagation of a coupled helicon-magnon wave within the semi-classical absorption cone in a magnetic metal was also studied. (D.C.W.)

15942 (NYO-2150-11) THE ELECTRON SPIN RESONANCE IDENTIFICATION OF N_2^- IN IRRADIATED SODIUM AZIDE [Thesis]. Gelerinter, Edward (Cornell Univ., Ithaca, N. Y. Materials Science Center). Feb. 1966. Contract AT(30-1)-2150. 69p. Dep. mn. CFSTI $3.00 cy, $0.75 mn.

A radioinduced defect in sodium azide was studied and identified as an N_2^- ion in the azide position. Since the valence electron of the N_2^- ion was in an orbitally degenerate state and the defect was in a site of trigonal symmetry, a Jahn-Teller distortion was expected. ESR spectra are predicted for the cases when the molecular configuration is frozen in one of three static distortions, when tunnelling matrix elements exist between these three distortions and are small compared to the magnetic splittings, and when the tunnelling matrix elements are large compared to the magnetic splittings. The observed data correspond to the first case and a value of 500 cm^{-1} for the Jahn-Teller energy splitting was obtained. Part of the Jahn-Teller distortion consists of a tilt of the internuclear axis of the N_2^- and the amount and direction of this tilt was found from the data. An attempt was made to understand some of the observed hyperfine effects using published data pertaining to N_2^- in potassium azide. (P.C.H.)

15943 (RL-REA-2595) PAPERS AND PROCEEDINGS OF THE MEETING ON APPLICATIONS OF X-RAY DIFFRACTION IN THE ATOMIC ENERGY FIELD, RICHLAND, WASHINGTON, FEBRUARY 25-26, 1965. Jolley, W. G.; Clark, W. I. (eds.) (General Electric Co., Richland, Wash. Hanford Atomic Products Operation). Oct. 1965. Contract AT(45-1)-1350. 79p. (CONF-650210). Dep. mn; CFSTI $3.00 cy, $0.75 mn.

Eight papers are included; separate abstracts have been prepared for 4. The remaining 4 papers were abstracted previously in NSA, see 19: 16065, 16066, and 22991, and 20: 5863. (T.F.H.)

For abstracts of individual papers see: 14823, 15136, 15944, and 15945.

15944 (RL-REA-2595, pp 12-14) TEXTURE STUDIES IN MONOCLINIC PLUTONIUM. Bowman, F. E. (Battelle-Northwest, Richland, Wash. Pacific Northwest Lab.).

An investigation of the texturing introduced in monoclinic plutonium by various treatments is undertaken. An underlying objective is the production and identification of pseudo-single crystals. The fundamental crystallographic characteristics of the monoclinic plutonium are presented, as well as a discussion of the unique problems in their investigation. Despite an inherent lack of ductility, this material has been successfully deformed by rolling. The existence of a resulting texture has been established, and the derivation of the details of this texture is discussed. Other treatments, not necessarily involving plastic deformation, also have been found to produce a textured structure. These treatments, together with the type of texturing produced, are presented and discussed. (auth)

15945 (RL-REA-2595, pp 43-50) DETERMINATION OF RESIDUAL STRESS IN URANIUM WITH AN X-RAY DIFFRACTOMETER. Jolley, W. G. (General Electric Co., Richland, Wash. Hanford Atomic Products Operation).

The technique and limitations of residual stress analysis with an x-ray diffractometer as applied to uranium are discussed. A review of the theory is presented, and the type of equipment and x-ray geometry are discussed. Preparation of the standard uranium plate and the procedure used to standardize the x-ray results are presented in detail. Data showing a linear plot of increasing deflections of a uranium plate versus change in the "d" spacing are given. (auth)

15946 (UCRL-16643) DISLOCATION MECHANISMS OF MOLYBDENUM SINGLE CRYSTALS AT LOW TEMPERATURES [Thesis]. Lau, Silvanus Siu-wai (Lawrence Radiation Lab., Univ. of California, Berkeley). Jan. 1966. Contract W-7405-eng-48. 34p. Dep. mn. CFSTI $2.00 cy, $0.50 mn.

The effects of temperature and strain rate on flow stress of Mo single crystals were investigated. The flow stress increased slightly as the temperature decreased from approximately 600 to 425°K. A rapid increase in flow stress then occurred upon testing at lower temperatures. The strong temperature and strain rate dependence of the flow

stress (below 425°K) were rationalized satisfactorily in terms of the Dorn and Rajnak theory of the Peierls' mechanism of plastic deformation. Above 425°K, the experimental results did not agree exactly with the theory, which indicates that there might be some other, as yet unidentified, thermally activated mechanism operative in this region. (auth)

15947 (UCRL-16645) DISLOCATION MECHANISMS IN THE DEFORMATION OF HIGH PURITY TANTALUM AT LOW TEMPERATURES [Thesis]. Ranji, Sampath (Lawrence Radiation Lab., Univ. of California, Berkeley). Jan. 1966. Contract W-7405-eng-48. 37p. Dep. mn. CFSTI $2.00 cy, $0.50 mn.

The rate controlling mechanism for slip in bcc Ta at low temperatures [$T < 0.2\ T_m$] was investigated. High purity single crystals of Ta, oriented for single slip, were grown by electron beam zone refining. These crystals were tested in an Instron tensile machine to determine the temperature and strain rate dependence of the flow stress. The temperature range studied was 4.2 to 550°K, at two strain rates differing by about a factor of 100. At low temperatures the effect of both the temperature and strain rate could be rationalized satisfactorily in terms of the Peierls' mechanism, when the deformation is controlled by the nucleation of pairs of kinks [the Dorn-Rajnak model]. (auth)

15948 THE POSSIBILITY OF THE APPLICATION OF THE SCATTERING OF γ QUANTA TO THE DETERMINATION OF PHONON PROPERTIES. Hoerl, Erwin M. (Oesterreichische Studiengesellschaft fuer Atomenergie, Siebersdorf, Austria). Acta Phys. Austr., 20: 175-9(1965). (In German).

A way was discussed by which it was possible to determine phonon properties by using the Mössbauer effect in the scattering of γ quanta on single crystals. The measurement of phonon dispersion curves and the determination of the frequency of defect oscillation states appear possible. (tr-auth)

15949 STUDY OF THE UAs_2 BY NEUTRON DIFFRACTION. Oles, A. (CEN, Saclay, France). J. Phys. (Paris), 26: 561-4(Oct. 1965). (In French).

A neutron diffraction study of the tetragonal compound UAs_2 gives an improved crystal structure and establishes the magnetic structure below the Néel point. The latter consists of a piling up of ferromagnetic sheets of uranium along the c axis in the order + + − −. The magnetic moments of uranium are parallel to the c axis; their magnitude is found to be $\mu = (1.61 \pm 0.11)\ \mu_B$. The variation of the magnetic form factor as a function of $\sin\theta/\lambda$ was also obtained. (auth)

15950 MOESSBAUER EFFECT OF FERROMAGNETIC INTERMETALLIC COMPOUNDS IN IRON-GERMANIUM SYSTEM: Fe_3Ge AND Fe_5Ge_3. Yamamoto, Hisao (Tohoku Univ., Sendai). J. Phys. Soc. Jap., 20: 2166-9(Dec. 12, 1965).

The hyperfine fields for an Fe atom in ferromagnetic intermetallic compounds, Fe_3Ge and Fe_5Ge_3, were investigated by using the Mössbauer effect. The hyperfine fields at a given Fe site of ϵ_1 and ϵ phases in Fe_3Ge were nearly equal to each other in spite of the difference in the environment beyond second neighbors which affected their Curie temperatures. The hyperfine field on 2(a) site of Fe_5Ge_3 is 136kOe which is unexpectedly small in comparison with the neutron diffraction data by Katsuraki. The hyperfine field on 2(d) site has two values (214 and 256kOe) which suggests the existence of two magnetic sublattices associated with this site. (auth)

15951 PLASMA OSCILLATION OF ELECTRONS IN Be, Mg, Al, Si, Ge, Sn, Sb AND Bi. Sueoka, Osamu (Tokyo Univ.). J. Phys. Soc. Jap., 20: 2203-11(Dec. 12, 1965).

The plasma oscillation of electrons in Be, Mg, Al, Si, Ge, Sn, Sb, and Bi was studied using the method of energy analysis of electrons passed through thin foil of those solids. The energy loss value ΔE, the dispersion relation, i.e. the dependence of ΔE on the scattering angle θ, the angular dependence of the intensity, the half breadth of ΔE, and the cutoff scattering angle θ_c (corresponding to the cutoff wave number K_c) were measured by the photometric method. The angular distribution of the intensity does not agree with θ^{-2} law given by Ferrell, but shows $\theta^{-1.6}$ to $\sim\theta^{-1.7}$ dependence. The curvature of ΔE vs. θ curve for Be, Mg, Al, and Si agree well with the theoretical values calculated by the free electron theory, but those for Ge, Sn, and Sb are 20 ~ 30% larger than the corresponding theoretical values, and that for Bi is twice as large as the latter. The half breadths of energy loss peak due to the plasma oscillation increase with increase in the scattering angle. Specimens of Ge were studied in the crystalline and in the amorphous states. The half breadth of energy loss peak of crystalline Ge is narrower than that of amorphous Ge, and the total cross section of the excitation of plasmon in both specimens are almost the same. The ratios of the total cross sections of the excitation of the plasmon in Al and in Be, and of that in Al and in Mg were measured. (auth)

15952 PLASMA OSCILLATION OF ELECTRONS IN ALLOY. III. Al-Be, Al-Ge AND Al-Sn EUTECTOIDS. Sueoka, Osamu (Tokyo Univ.). J. Phys. Soc. Jap., 20: 2212-25(Dec. 12, 1965).

The plasma oscillation of electrons in Al−Be, Al−Ge and Al−Sn eutectoids was studied using the method of energy analysis of electrons passed through a thin foil of eutectoid. The energy of the plasma oscillation of electrons in eutectoid depends upon the grain sizes of component elements. In the case of Al−Be, two kinds of the plasma oscillation of Al and Be themselves are excited, if the grain sizes of Al and Be are more than several hundreds angstroms. On the other hand, if the grain sizes are less than about 60Å, only one plasma oscillation due to the bulk plasma oscillation is excited. For an intermediate grain size, two plasma oscillations with energy values each of which shift from that of Al or Be are observed. The grain size dependency of the plasma oscillation is eutectoid is explained phenomenologically. The energy loss value, the dispersion relation, the cutoff scattering angle, θ_c (corresponding to the cutoff wave number, k_c), the angular dependencies of the intensity and the half breadth of energy loss peak of the plasma oscillation in small grain size eutectoid less than 60Å were measured. Those values are compared with the corresponding theoretical values. (auth)

15953 PLASMA OSCILLATION OF VALENCE ELECTRONS AND EXCITON IN ALKALI HALIDES. Sueoka, Osamu (Tokyo Univ.). J. Phys. Soc. Jap., 20: 2226-35 (Dec. 12, 1965).

The characteristic energy losses of electrons passed through a thin foil of alkali halides, LiF, NaCl, KCl, and KBr were studied using the transmission technique. The differential cross section, the dispersion relation and the cutoff scattering angle of the strongest loss peak in a spectrum were measured. It is pointed out that the loss peak comes from the plasma oscillation of valence electrons. For the first loss peak due to the exciton, and for the 2nd (3rd for LiF) loss peak, the same sort of measurements are carried out. These measured values for the plasma oscillation were supported roughly by the free electron theory with 6 electrons per molecule taking part in the oscillation, and especially the value of the plasma energy agrees well with that by Horie's theory. The loss peak located between the exciton and the plasma peak may be due to the tangential (surface) plasma oscillation. The ratio of the total cross section of these loss peaks to that of the loss peak due to the plasma oscillation was measured. (auth)

15954 ON THE NEUTRON DIFFRACTION STUDY OF Cr_2As. Watanabe, Hiroshi; Nakagawa, Yasuaki (Atomic Energy of Canada Ltd., Chalk River, Ont.). J. Phys. Soc. Jap., 20: 2244-8(Dec. 12, 1965).

A powder neutron diffraction study was made of Cr_2As with the spectrometers at the NRX and NRU reactors. Published magnetic and thermal data show this substance

to be an antiferromagnet with a Néel temperature of 393°K. Antiferromagnetic order along the c axis was established in the present study by the presence of the magnetic line [00(1/2)]. The magnetic line (100) was found to be present, which shows another type of antiferromagnetic order developed in the c-plane. None of the antiferromagnetic spin structures which were tried in order to explain the observed peak intensities was completely successful, but the most favorable is that in which Cr(a) moments couple antiferromagnetically within the c-plane. (auth)

15955 PLASMA OSCILLATION OF CONDUCTION ELECTRON IN Na. Sueoka, Osamu (Tokyo Univ.). J. Phys. Soc. Jap., 20: 2249-52(Dec. 12, 1965).

The plasma oscillation of conduction electrons in Na was studied by the energy analysis of electrons passing through the thin foil of Na. Results of the energy, the dispersion relation and the cutoff scattering angle of the plasma oscillation agree well with the calculated values based on the free electron theory. Result of the differential cross section does not agree with the free electron theory, as is in the case of Al. (auth)

15956 AN ELEMENTARY THEORY OF INELASTIC SCATTERING OF FAST ELECTRONS BY THIN CRYSTALS. Kainuma, Yoshiro (Nagoya Univ., Japan). J. Phys. Soc. Jap., 20: 2263-71(Dec. 12, 1965).

This theory deals with a single process of inelastic scattering. It is shown that the superposition of spherical inelastic waves scattered in a thin layer within a crystal forms waves expressed by Bloch functions and the superposition of the inelastic waves scattered in various depths in the crystal forms the inelastic waves observed in vacuum. The result of the present theory agrees with the results of other theories. (auth)

15957 QUADRUPOLE COUPLING CONSTANTS OF DEUTERON IN POLYCRYSTALLINE GLYCINE COMPOUNDS. Vijayaraghavan, R.; Saraswati, V. (Tata Inst. of Fundamental Research, Bombay). J. Phys. Soc. Jap., 20: 2290(Dec. 12, 1965).

The deuteron magnetic resonances were studied in partially deuterated glycine and some glycine compounds to understand the nature of glycine molecules. The deuteron resonance was observed at 5–7 Mcs (about 11.5 kgauss) in the temperature range between 110 and 350°K. The peak separations were field independent but temperature dependent in some samples. Deuteron resonance properties in the various compounds studied are considered. (J.F.P.)

15958 FAR-INFRARED VIBRATION MODE IN $SrCl_2$. Hisano, Kumao; Ohama, Nobuhiko; Matumura, On (Kyusyu Univ., Fukuoka, Japan). J. Phys. Soc. Jap., 20: 2294 (Dec. 12, 1965).

Measurements of spectral reflectance were made for a single crystal of strontium chloride by means of a far infrared spectrometer. The reflectivity of natural light in the range from 100 to 400 cm^{-1} was investigated at room temperature by using an aluminum mirror as a reference. The obtained reflectivity curve is shown. The curves of the index of refraction and the extinction coefficient of $SrCl_2$ are also given. (J.F.P.)

15959 RELATIVISTIC DYNAMICAL THEORY OF ELECTRON DIFFRACTION CONTAINING INELASTIC SCATTERINGS. Ohtsuki, Yoshihiko H.; Yanagawa, Sadaaki (Tokyo Univ.). J. Phys. Soc. Jap., 20: 2295 (Dec. 12, 1965).

In electron microscopes of high voltage relativistic effects cannot be ignored. It is necessary to deduce the absorption coefficient and other quantities in terms of the relativistic dynamical theory taking account of inelastic as well as elastic scattering. Since it seems tedious and hard to solve the Dirac equation in the Shrodinger representation, the Green function method is extended to the relativistic case. Only electronic excitation is considered as the process of inelastic scattering in the crystal. (J.F.P.)

15960 FERROMAGNETIC RESONANCE IN $ZrZn_2$. Ogawa, Shinji (Electrotechnical Lab., Nagatacho, Tokyo). J. Phys. Soc. Jap., 20: 2296(Dec. 12, 1965).

An observation of a ferromagnetic resonance in $ZrZn_2$ is reported. A microwave resonance absorption measurement was made at 24 kMHz on fine powders of this compound. Examples of ferromagnetic resonance absorption lines are shown for powders of approximately 5μ and 100μ in diameter at 4.2°K. For powders of smaller diameter than the skin depth the line shape is nearly Lorentzian. The absorption intensity, line width, and g-factor are shown as a function of temperature. (J.F.P.)

15961 PARAMAGNETISM OF COLOR CENTERS IN SODIUM CHLORATE CRYSTALS. Ramasastry, C.; Sastry, S. B. S. (Indian Inst. of Tech., Madras). J. Phys. Soc. Jap., 20: 2303(Dec. 12, 1965).

The changes in static magnetic susceptibility of the sodium chlorate crystal due to irradiation and subsequent optical bleaching were followed by the Guoy method. After irradiation with a moderate dose of x rays a reduction in diamagnetic force of about 4 milligrams was noticed. This reduction is interpreted as due to the paramagnetism of the color centers formed in irradiated crystals. Destruction or creation of paramagnetic centers as a result of optical bleaching produced corresponding variations ranging from 0.5 to 2 milligrams in the magnetic force. The variation of the paramagnetic force is plotted as a percentage of the diamagnetic force on the x-irradiated crystal due to bleaching with light of different spectral regions. (J.F.P.)

15962 EFFECT OF CRYSTAL SIZE ON MOESSBAUER RECOIL-FREE FRACTION IN ^{197}Au. Marshall, S. W.; Wilenzick, R. M. (Tulane Univ., New Orleans). Phys. Rev. Lett., 16: 219-21(Feb. 7, 1966).

The Mössbauer effect was observed in ^{197}Au microcrystals with mean diameters of 60 and 200Å. The microcrystals were grown in a hydrosol and were bound in gelatin. The results indicate that the crystal surfaces are loosely bound to the gelatin and that the recoil-free fraction is greater in the smaller microcrystals than in the larger microcrystals. (G.O.Y.)

15963 PARAMAGNETIC RESONANCE OF COBALT IN INTERMETALLIC COMPOUNDS. Barnes, R. G.; Cornell, D. A.; Torgeson, D. R. (Iowa State Univ., Ames). Phys. Rev. Lett., 16: 233-4(Feb. 7, 1966). (IS-1302).

Initial results are presented on the paramagnetic resonance of cobalt in Co-rare earth, Co-Sc, and Co-γ intermetallic compounds at 77 to 375°K. (D.C.W.)

15964 SIZABLE PROTON POLARIZATION USING A SPIN REFRIGERATOR. McColl, J. R.; Jeffries, C. D. (Univ. of California, Berkeley). Phys. Rev. Lett., 16: 316-18(Feb. 21, 1966).

Proton polarizations of up to 35% were obtained in ytterbium-doped yttrium ethyl sulfate crystals by subjecting the crystals to both d-c and pulsed magnetic fields at helium temperatures. (D.C.W.)

15965 ELECTRON SPIN RESONANCE OF NO_3 IN IRRADIATED $NaNO_3$. Zdansky, K.; Sroubek, Z. (Inst. of Radio Engineering and Electronics, Prague). Phys. Status Solidi, 12: K85-7(1965).

The ESR of sodium nitrate irradiated by x rays at 77°K was studied. A spectrum with a resolved hyperfine structure due to the nitrogen nucleus was observed. This spectrum was attributed to neutral NO_3. The spectrum obtained with resolved hyperfine structure is shown. The magnitudes of the eigenvalues of the g and A tensor of NO_3 measured in $NaNO_3$ crystals are given and compared with those of nitrate in KNO_3. (J.F.P.)

15966 DIFFUSION AND ISOTOPIC EFFECTS OF ^{22}Na AND ^{24}Na ON SILVER CHLORIDE. Sueptitz, P. (Institut fuer Kristallphysik, Berlin). Phys. Status Solidi, 12: 555-67(1965). (In German).

The transport mechanism of Na^+ ions in AgCl is clarified by measurements of the dependence of the diffusion coefficient on temperature (180 to 450°C) and impurity (Na, Cd),

and also by measurements of the isotope effect (^{22}Na and ^{24}Na). For the temperature dependence, it is found: $D_{22} = 8.81 \times \exp(-1.19\ eV/kT)$; above 300°C, D increases more rapidly. In the Na^+ doped samples D is only weakly influenced, but in the Cd^{++} doped samples the effect is strong. This can be explained by the assumption of a vacancy mechanism. The magnitude of Na diffusion is taken as a measure of the concentration of the cation vacancies. The association of vacancies with Cd^{++} ions is calculated for Cd-doped crystals. The strong increase of D in undoped crystals at high temperatures probably arises from the anomalously strong increase of Frenkel disorder. The isotope effect measurements give no evidence regarding the transport mechanism, since the determined value for $(D_{22}/D_{24}-1)/[(m_{24}/m_{22})^{1/2}-1]$ of 0.9886 ± 0.0187 could arise from several mechanisms. (auth)

15967 PHOTOCONDUCTIVITY AND p-n PHOTOEFFECT IN SiC DURING EXCITATION WITH X RADIATION. Jungk, G.; Keiper, A.; Thiessen, K. (Inst. of Physics and Tech., Berlin). Phys. Status Solidi, 12: 589-93(1965). (In German).

Photoconductivity and the p–n-photoeffect were measured in high resistivity SiC monocrystals during x-ray excitation. At low temperatures the photoconductivity measurements indicate a minority carrier trapping effect. The x-ray photoconductivity was quenched by temperature and/or radiation with photon-energies smaller than the band gap. (auth)

15968 TRANSITION RADIATION FROM THIN SILVER FOILS. Buerker, U.; Steinmann, W. (Univ., Munich). Phys. Status Solidi, 12: 853-63(1965). (In German).

Thin Ag-foils (200 to 2000 Å) are irradiated by electrons with intermediate energy (15, 25, 35 kev), and the radiation produced is investigated. The degree of polarization, the spectrum in the region of the plasma wavelength (3330 Å) and the dependence of the intensity on film thickness and electron energy is measured. The radiation consists primarily of transition radiation and, to a smaller extent, of bremsstrahlung. When the latter is separated out, the results agree with the calculated transition radiation. The results are discussed in terms of the plasma radiation. (auth)

15969 LOCALIZED VIBRATIONS OF H^- AND D^- IONS IN THE ALKALINE EARTH FLUORIDES. Elliott, R. J.; Hayes, W.; Jones, G. D.; Macdonald, H. F.; Sennett, C. T. (Oxford Univ.). Proc. Roy. Soc. (London), Ser. A, 289: 1-33(Dec. 14, 1965).

Measurements of the absorption spectra associated with the vibrations of H^- and D^- ions in CaF_2, SrF_2 and BaF_2 were made in the region 1 to 17 μm. The most detailed investigation was made in CaF_2, where, in addition to the fundamental vibrational frequency, a second harmonic and two third harmonics of the fundamental frequency were observed. The spectra were assigned to the localized vibrations of isolated light ions on fluorine sites. The harmonics are seen because of anharmonic effects; to a good approximation the light ions can be considered to oscillate in an anharmonic tetrahedral potential well produced by a nearly static host lattice. Weak satellite lines are observed in the immediate vicinity of the fundamental vibrational lines due to the presence of small concentrations of H^- and D^- ions in other lattice configurations. Broad bands occur at displacements greater than about 100 cm^{-1} to higher and lower frequencies from the localized vibrational lines due to combined excitation of the localized mode and lattice band modes. The temperature-dependent intensity, shift and width of the localized vibrational lines were measured. The presence of the broad side bands and the temperature-dependent effects arise from anharmonic interactions with the band modes of lattice vibration. A simple model of the band modes leads to very satisfactory agreement between theory and observed anharmonic effects for reasonable values of the anharmonic force constants which are regarded as parameters. (auth)

15970 THE EFFECT OF ISOTOPES ON LATTICE HEAT CONDUCTION. I. LITHIUM FLUORIDE. Berman, R.; Brock, J. C. F. (Oxford Univ.). Proc. Roy. Soc. (London), Ser. A, 289: 46-65(Dec. 14, 1965).

The thermal conductivities of eight lithium fluoride crystals with ^{6}Li contents ranging from 0.01 to 90% were measured between 1 and 300°K. The calculated phonon scattering by isotopes was used throughout, without numerical adjustment, except for the isotopically purest specimens in which the residual chemical impurity is evident. Boundary scattering is in excellent agreement with calculation; dislocation scattering correlates approximately with the measured density of dislocations. Callaway's expression for the conductivity consists of two terms; κ_1, normally the main contribution and κ_2, which may be regarded as a correction term related to the treatment of three-phonon normal processes. In crystals which are both chemically and isotopically pure, κ_2 becomes very large and the conductivity then varies extremely rapidly with point defect concentration. The predictions of the Callaway theory were computed in this limit and the experimental observations on the purer crystals confirm this distinctive behavior. The discrepancies between experimental results and the predictions of both Klemens's and Ziman's theories are discussed. (auth)

15971 RADIATION-INDUCED STRESS RELAXATION AND FLOW IN VITREOUS SILICA. Lungu, S. (Inst. for Atomic Physics, Bucharest). Rev. Roum. Phys., 10: 604-8(1965).

A quantitative description of the processes suggested by the experimental results recently obtained by Primak with proton-beam irradiations is considered. An expression of the stress evolution is developed. This one includes a stress generation term proportional to the specific volume variation and a first order attenuation term. The solution of this differential equation is in agreement with the experimental results. The attenuation term, expressing a radioinduced flow, suggested a corresponding Maxwell-type expression for the radioinduced "fluidity" used afterwards for the total fluidity-temperature plot. This plot accounts for the Mayer-Lecompte observed radioinduced rate of silica glass fiber elongation. Some implications with respect to thermal stress relaxation and flow under load of the uncanned silica fuels are also analyzed. (auth)

15972 THE PARAMAGNETIC CENTERS FORMED BY IRRADIATION IN THE OXYGENATED COMPOUNDS OF SELENIUM. I. E.S.R. SPECTRA OF THE IRRADIATED SeO_4Na_2. Constantinescu, O. (Inst. for Atomic Physics, Bucharest); Pascaru, I.; Constantinescu, M.; Paun, I. Rev. Roum. Phys., 10: 699-708(1965).

The irradiated polycrystalline SeO_4Na_2 by ESR and point out paramagentic species stable at the room temperature, in which the odd electron is found in interaction with the magnetic moment of ^{77}Se(I = 1/2) nucleus. On the basis of data supplied by ESR spectra and by their behavior on heating, a hypothesis is formulated by which SeO_4^- and SeO_3^- are formed by irradition. The recombination kinetics of paramagnetic centers is studied by ESR, and their rate constants are determined. Likewise the influence of water of crystalization on the formation of paramagnetic centers and their dependence on the integral dose are studied. (auth)

15973 USE OF ON-LINE COMPUTER FOR MOESSBAUER EXPERIMENTS. Goodman, R. H.; Richardson, J. E. (Dept. of Mines and Technical Surveys, Ottawa). Rev. Sci. Instrum., 37: 283-6(Mar. 1966).

The application of a small general purpose computer as an "on line" data acquisition device for Mössbauer effect experiments is described. A method of conversion from analog to digital information and an outline of the computer program are given. The performance of the system is demonstrated by a Mössbauer spectrum of iron sulphide (pyrite). The extension of these techniques to other experiments is briefly considered. (auth)

15974 HIGH PRESSURE PHASE TRANSITION OF EUROPIUM TELLURIDE. Rooymans, C. J. M. (Philips' Gloeilampenfabrieken, Eindhoven, Netherlands). Solid State Commun., 3: 421-4(1965).

By means of x-ray diffraction at high pressure conditions it was possible to observe a phase transition in europium telluride. The crystal structure remains fcc also in the high pressure phase. The lattice constant of this phase fits in with the assumption of a trivalent cation, as is the normal situation for the majority of the other monochalcogenides. Resistance measurements at high pressure are in accordance with the x-ray results. (auth)

15975 PARAMAGNETIC RESONANCE OF FREE SILVER ATOMS FORMED IN FROZEN SOLUTIONS OF SILVER SALTS IRRADIATED AT 77 deg K. Zhitnikov, R. A.; Orbeli, A. L. (Ioffe Physicotechnical Inst., Leningrad). Soviet Phys.-Solid State (Engl. Transl.), 7: 1559-71(Jan. 1966).

Translated from Fiz. Tverd. Tela, 7: 1926-43(July 1965).

By x-ray irradiation at 77°K of frozen solutions of various silver salts in H_2O and D_2O, as well as in various normal alcohols, free silver atoms were obtained, stabilized in these media. Paramagnetic resonance spectra of the stabilized atoms were obtained and investigated. Two different types of stabilization locations for the silver atoms in frozen and irradiated aqueous solutions were observed and studied. It was found that the properties of the silver atoms stabilized in a given solvent are practically independent of the nature and concentration of the dissolved salt, but are different in aqueous and alcohol solutions. This evidently shows that the immediate environment of the atom in such a matrix consists solely of solvent molecules, and that the properties of the stabilized atom are completely determined by the nature of the solvent. (auth)

15976 APPLICATION OF THE METHOD OF SECONDARY ION-ION EMISSION TO THE STUDY OF THE INTERACTION OF OXYGEN WITH A NIOBIUM SURFACE. Shvachko, V. I.; Nadykto, B. T.; Fogel', Ya. M.; Vasyutinskii, B. M.; Kartmazov, G. N. (Gor'kii Khar'kov State Univ., USSR). Soviet Phys.-Solid State (Engl. Transl.), 7: 1572-7(Jan. 1966).

Translated from Fiz. Tverd. Tela, 7: 1944-51(July 1965).

An investigation is made by the method of secondary ion-ion emission of the composition of oxides formed on the surface of niobium during interaction with oxygen. It is established that within the 20 to 1200°C temperature range the following oxides are formed on the surface of niobium in an atmosphere of oxygen having a pressure of $\sim 10^{-4}$ mm Hg: NbO, NbO_2, Nb_2O_3, and Nb_2O_5. Within the 1200 to 2000°C temperature range only the oxides NbO and Nb_2O_3 exist on a niobium surface. Corrosion wear of Nb takes place as a consequence of the formation and subsequent evaporation of the oxide NbO. The evaporation of the oxide NbO begins at 1400°C and thereafter grows rapidly with increase of the temperature. Within the 20 to 800°C temperature range a process of decomposition of the oxide NbO_2 takes place according to the scheme $NbO_2 \rightarrow NbO + O$ with desorption of the atomic oxygen to the gaseous phase. (auth)

15977 GENERATION OF VACANCIES IN KBr–Sr IRRADIATED BY A PROTON BEAM. Melik-Gaikazyan, I. Ya.; Lisitsyn, V. M. (Kirov Tomsk Polytechnic Inst., USSR). Soviet Phys.-Solid State (Engl. Transl.), 7: 1610-11(Jan. 1966).

Translated from Fiz. Tverd. Tela, 7: 1994-6(July 1965).

The influence of Sr impurities on the buildup of F-centers in a KBr crystal during irradiation by protons was investigated. It is shown that the rate of formation of F-centers is increased on the introduction of an impurity. Analysis of the results of a calculation carried out on the basis of the Mitchell-Fröhlich kinetic equation for the accumulation of F-centers makes it possible to suppose that an impurity facilitates the generation of anionic vacancies in a crystal during irradiation. (auth)

15978 CONDUCTIVITY INDUCED IN GERMANIUM BY BOMBARDMENT WITH POTASSIUM IONS IN DIFFERENT CRYSTALLOGRAPHIC DIRECTIONS. Abroyan, I. A.; Titov, A. I. (Kalinin Polytechnical Inst., Leningrad). Soviet Phys.-Solid State (Engl. Transl.), 7: 1619-23(Jan. 1966).

Translated from Fiz. Tverd. Tela, 7: 2007-12(July 1965).

Conductivity induced in germanium single crystals by bombardment with 7-kev potassium ions was investigated. It was found that the electric conductivity of germanium which results from the excitation of bound electrons during the deceleration of ions in the crystal, is a nonmonotonic function of the angle of incidence of primary particles on the surface of the sample. The maximum induced conductivity corresponds to the direction of maximum "transparency" of the crystal to ions. (auth)

15979 ENERGY SPECTRUM OF DEFECTS FORMED IN INDIUM ANTIMONIDE BY γ IRRADIATION AT LOW TEMPERATURES. Mashovets, T. V.; Khansevarov, R. Yu. (Ioffe Physicotechnical Inst., Leningrad). Soviet Phys.-Solid State (Engl. Transl.), 7: 1796-7(Jan. 1966).

Translated from Fiz. Tverd. Tela, 7: 2229-31(July 1965).

An investigation of the energy spectrum of defects was made. Gamma rays were used to irradiate n-type indium antimonide, and the resistivity, carrier density, and spectral dependence of the impurity photoconductivity were measured at 77°K before and after irradiation. The dependence of the carrier density on the exposure dose for two samples having different initial donor concentrations, and the spectral dependence of the photoconductivity for a p-type sample are shown. It is seen that during irradiation the type of conduction altered from n-type to p-type and the properties of the samples passed through a region of complete compensation. It is concluded that the Fermi level lies in the lower half of the forbidden band. (J.F.P.)

15980 INFLUENCE OF IMPURITIES AND OF DEFORMATION ON THE KINETICS OF ACCUMULATION OF F-CENTERS IN KCl CRYSTALS. Roshchina, L. I.; Klyukvina, V. P. (Kirov Polytechnical Inst., Tomsk, USSR). Soviet Phys.-Solid State (Engl. Transl.), 7: 1829-30(Jan. 1966).

Translated from Fiz. Tverd. Tela, 7: 2262-4(July 1965).

The intensification of the process of accumulation of F centers in the linear stage in deformed crystals is explained by the effects of redistribution of impurities present even in pure crystals. The effects of deformation on the vacancies generated by irradiation in KCl and KCl · Sr were investigated. The rate of accumulation of F centers in KCl crystals and kinetic curves of the accumulation of F centers in KCl and KCl · Sr are given. The results on the increase of the rate of accumulation of F centers in the second stage of the slow coloration process show that although the degree of deformation of the KCl · Sr crystal was less than that of the KCl crystal, the increase in vacancies generated by regeneration was greater in the former case. (J.F.P.)

15981 TRANSPORT MECHANISM IN SAMARIUM SULFIDE. Golubkov, A. V.; Goncharova, E. V.; Zhuze, V. P.; Manoilova, I. G. (Inst. of Semiconductors, Leningrad). Soviet Phys.-Solid State (Engl. Transl.), 7: 1963-7(Jan. 1966).

Translated from Fiz. Tverd. Tela, 7: 2430-6(Aug. 1965).

The Hall effect, the electric conductivity, and the thermo-emf of SmS at temperatures between 300 and 1000°K were measured. It was shown that the electrons are excited into the conduction band from the local $4f$-levels of samarium ions. Their activation energy, the variation of their mobility with temperature, and the magnitude of the effective mass were determined. (auth)

15982 ELECTRON PARAMAGNETIC RESONANCE OF ATOMIC HYDROGEN IN BERYLLIUM. Koryagin, V. F.; Grechushnikov, B. N. (Inst. of Crystallography, Moscow). Soviet Phys.-Solid State (Engl. Transl.), 7: 2010-12(Feb. 1966).

Translated from Fiz. Tverd. Tela, 7: 2496-8(Aug. 1965).

The electron paramagnetic resonance of atomic hydrogen in irradiated beryllium crystals was investigated. The following values of the constants of the spin hamiltonian: $g = 2.00265 \pm 0.00005$, $B = 1004.7 \pm 0.2$ Oe were found. The hyperfine structure of the spectrum due to Na ions present in the structural channels of beryllium was shown. (auth)

15983 INVESTIGATION OF THE GALVANOMAGNETIC PROPERTIES OF HOLMIUM. **Babushkina, N. A. Soviet Phys.-Solid State (Engl. Transl.), 7: 2048-9(Feb. 1966).**
Translated from Fiz. Tverd. Tela, 7: 2540-1(Aug. 1965).
The results of the measurement of the even galvanomagnetic effect in holmium are described. The critical fields which destroy the antiferromagnetism reach 30,000 Oe, for this reason the measurements were carried out in magnetic fields up to 33,000 Oe in the temperature range from 20 to 300°K. Isotherms of the longitudinal galvanometric effect in holmium are given. Using these isotherms the temperature dependence of the critical magnetic field, which is found to be identical with a similar curve obtained from the magnetization isotherms, is ploted. The change in the resistance of holmium in a magnetic field in the paramagnetic region was also studied. (J.F.P.)

15984 LOW-TEMPERATURE ANNEALING OF GERMANIUM, IRRADIATED WITH FAST ELECTRONS. **Gerasimov, A. B.; Konovalenko, B. M. (Ioffe Physicotechnical Inst., Leningrad). Soviet Phys.-Solid State (Engl. Transl.), 7: 2054-5(Feb. 1966).**
Translated from Fiz. Tverd. Tela, 7: 2545-7(Aug. 1965).
Results of a further investigation of the low-temperature annealing of germanium subjected to bombardment with 3.5-Mev electrons at the temperature of liquid nitrogen are reported. Three annealing stages were detected. At each of these stages the carrier density changed monotonically, tending to revert to the initial value before irradiation. The activation energy was determined for all three annealing stages for n- and p-type samples, annealed isothermally. The temperature dependence for the carrier density and mobility in an n-type sample during isochronous annealing is shown. (J.F.P.)

15985 DIRECT PROOF OF THE EXISTENCE OF POSITIVE CHARGE IN ADSORBED Th ATOMS. **Vedula, Yu. S.; Gavrilyuk, V. M. (Physics Inst., Kiev). Soviet Phys.-Solid State (Engl. Transl.), 7: 2056-7(Feb. 1966).**
Translated from Fiz. Tverd. Tela, 7: 2547-9(Aug. 1965).
In order to prove the existence of positive charge in adsorbed thorium atoms, the surface diffusion of adsorbed thorium atoms under the action of a uniform electric field, which appears due to the drop of the voltage along a conductor through which an electric current is flowing, and of the electron wind force appearing when the conduction electrons are scattered by adsorbed atoms, was investigated. This phenomenon, occurring in the interior of a metal, is known as electric transport. If a surface of a metal has an adsorbed layer of atoms capable of diffusing on the surface, then it is postulated that the electric transport of the substance can be established in the adsorbed layer by passing a constant electric current through the substrate. The Th–W system was investigated, and the variation of the surface coverage along a tungsten crystal is shown. These curves clearly indicate the presence of electric transport in the direction of the negatively charged part of the crystal. (J.F.P.)

15986 SOME CHARACTERISTICS OF THE INTERACTION OF OXYGEN WITH THE SURFACE OF A TUNGSTEN SINGLE CRYSTAL. **Zingerman, Ya. P.; Ishchuk, V. A.; Krutilina, T. A. (Physics Inst., Kiev). Soviet Phys.-Solid State (Engl. Transl.), 7: 2078-9(Feb. 1966).**
Translated from Fiz Tverd. Tela, 7: 2569-71(Aug. 1965).
It is expected that the interaction of molecular oxygen with polycrystalline tungsten may be governed principally by the structure of the metal surface. Therefore, the interaction of oxygen with the surfaces of a tungsten single crystal, oriented in different ways with respect to the crystallographic axes was studied. It was established that the surface layers of the target atoms formed sections of the tungsten lattice parallel to the crystallographic planes determined by the x-ray diffraction method. The dependence of the work function of the [100] and [110] faces of a tungsten single crystal on the duration of adsorption of a molecular beam of oxygen of constant intensity, and the changes in the work function of the [100] and [110] faces due to adsorption and desorption of oxygen are given. (J.F.P.)

15987 ON THE COLLECTIVE THEORY OF BOHM AND PINES. **Sips, V. (Institut Rudjer Boskovic, Zagreb). Z. Phys., 190: 205-8(1966). (In German).**
Starting from the longitudinal electron-phonon hamiltonian and performing two suitable canonical transformations, the hamiltonian of separated plasmons and electrons is derived. The result obtained is in good agreement with the result found by the method of the extended hamiltonian and the corresponding subsidiary conditions. The proposed approach may be applied to those problems in which longitudinal phonons are of no interest. (auth)

15988 QUASI-PARTICLE SPECTRUM AND ELECTRIC CONDUCTIVITY OF THE SMALL POLARON. **Schnakenberg, J. (Univ., Cologne). Z. Phys., 190: 209-25(1966). (In German).**
The quasi-particle spectrum of the small polaron is calculated in a slightly generalized Holstein model by means of a second order perturbation expansion of the self energy in the Green's function formalism. The results are applied to the calculation of the electrical conductivity of the model from Kubo's formula. (auth)

15989 DECAY TIME OF SCINTILLATION OF ANTHRACENE AND p-TERPHENYL SINGLE CRYSTALS AS A FUNCTION OF DIRECTIONAL INTENSITY IN BOMBARDMENT WITH α-PARTICLES. **Brinkmeier, Fritz (Univ., Goettingen, Ger.). Z. Phys., 190: 316-26(1966). (In German).**
Single crystals of anthracene and p-terphenyl were bombarded with α-particles. The angle of incidence with respect to the crystal axes was varied. The directional intensity of the scintillation light was investigated as function of the decay time of the scintillator. During the first 100 nsec after the excitation of the crystal the anisotropy of the scintillation light yield decreases starting with a value larger than that measured with pulses of 1000 nsec length. For the next 900 nsec the anisotropy remains nearly constant being still higher than 1. Therefore the anisotropy of the fast component of the scintillation light is larger than the anisotropy of the slow component. The results are discussed with reference to Birk's formula. (auth)

15990 NON-ISOTROPIC EXCHANGE INTERACTIONS IN THE RARE EARTH METALS [Thesis]. **Specht, Frederick. Houston, Tex., Rice Univ., 1965. 120p.**
The non-isotropic contribution to the indirect exchange interaction in the rare earth metals is calculated in lowest order, taking into account the non-sphericity of the 4f shell. With a free electron gas model for the conduction band, non-isotropic corrections to the zeroth order isotropic term are found to be several tens of a per cent, ranging from 20% in the case of holmium to 70% in the case of thulium. In addition to the non-isotropic exchange interaction an anisotropic crystal field term is obtained. It is shown that the anisotropic contributions considerably alter the nature of the interaction from that based on a simple isotropic theory. The expression for the effective exchange hamiltonian is obtained by using the S-matrix expansion in conjunction with second quantization. In order to deal with the N particle functions of the 4f shell a generalization of second quantization is developed, which can handle eigenfunctions with an arbitrary number of arguments. In expressing the interaction in terms of the total angular momentum operator of the 4f shell the reduced matrix element $\beta_k(j_1,j_2)$ is required where β_k is defined by the relation $Y_{kq}(j_1) \rightarrow \beta_k(j_1,j_2,j)\ Y_{kq}(j)$ of the Wigner-Eckart theorem. A general expression for β_k is derived for the two cases $j = j_1 + j_2$ and $j = j_1 - j_2$. (Dissertation Abstr.)

15991 MAGNETIC INTERACTIONS IN THE RARE EARTH ETHYL SULFATES [Thesis]. **Dweck, Joel Allen. Providence, Brown Univ., 1965. 110p.**
The interactions between magnetic rare earth ions in the isomorphic ethyl sulfate salts were investigated under the experimental condition $h\nu > kT$, and consequently the spins are aligned by the external magnetic field. Paramagnetic resonance under these conditions is found to show behavior

qualitatively similar to ferromagnetic resonance. The spin-spin interactions may be determined from the line shifts at low temperatures, and from the observation of resolved structure that results from the resonance absorption of ions having a near neighbor ion whose spin is antiparallel to the magnetic field. A superheterodyne cavity spectrometer operating at 35kMc/sec and a waveguide spectrometer operating at 35 and 70kMc/sec were constructed. An all-glass ^3He cryostat was employed to reach temperatures down to 0.3°K. The resonance spectrum of the S-state ion Gd^{3+} in the paramagnetic dysprosium ethyl sulfate, was investigated. The shift of the central gadolinium fine structure line at low temperatures was found to agree with that calculated from a lattice summation of the dipolar interactions with the dysprosium ions. Resolved structure, due to the interaction of a gadolinium ion with particular near neighbor dysprosium ions that are aligned antiparallel to the external field, is observed. The interaction between the gadolinium and dysprosium ions is found to be predominantly dipolar. The effects of the dipolar fields on the angular variation of the gadolinium fine structure splitting are also demonstrated. Structure on the gadolinium lines, more readily observed in the diamagnetic yttrium and lanthanum ethyl sulfates, is discussed, and the possibility that the structure results from interactions with the protons in the waters of hydration is explored. Although crystal field theory predicts that no resonance should be observable for Dy^{3+} in the C_{3h} symmetry of the ethyl sulfates, this spectrum was observed. The spectrum of dysprosium (0.5%) in yttrium ethyl sulfate is found to consist of a single main line and many smaller hyperfine lines, when the magnetic field is parallel to the c-axis. As the field is rotated away from this axis, the lines first broaden and then split into several resolvable components that continue to spread apart. This unusual behavior was explained in terms of a defect model. The anomalous behavior of cerium ethyl sulfate at low temperatures was investigated. At temperatures where all spins are aligned, the total nondipolar interaction of a cerium ion with all of its neighboring cerium ions is found to be antiferromagnetic, and to have the magnitude $(.113 \pm .003)\ cm^{-1}$. The effects of an ionic electric quadrupole-quadrupole (QQ) coupling between cerium ions on the resonance spectrum were calculated to second order. Several unusual qualitative features of the resonance spectrum may be explained on the basis of a QQ coupling between cerium ions. (Dissertation Abstr.)

15992 MAGNETIC HYPERFINE INTERACTIONS IN ^{149}Sm IN FERROMAGNETIC $SmAl_2$ [Thesis]. Lesikar, Arnold Vincent. Pasadena, Calif., California Inst. of Tech., 1965. 68p.

The internal field acting at the samarium nucleus in $SmAl_2$ is investigated theoretically and experimentally. The internal field is computed in the molecular field approximation assuming a crystalline electric field to act on the trivalent samarium ion. Admixtures of the first excited multiplet of the ion by the exchange and crystalline electric field are included in the calculation and lead to an increase of no more than 10% in the theoretically predicted internal field from the values predicted when the admixture is neglected if a crystal field interaction of reasonable size is assumed. The internal field resulting from theory is compared with the values resulting from Mössbauer studies of the hyperfine structure of the 22-kev gamma transition in ^{149}Sm. The best fit made to the experimentally observed Mössbauer absorption patterns leads to an internal field much smaller than that predicted by theory. Possible sources of this disagreement between theory and experiment are discussed. (Dissertation Abstr.)

15993 CALCULATION OF ELECTRICAL AND RADIATION STORAGE TIME IN TRANSISTORS. Gage, Donald S. (Boeing Co., Seattle). 37p. (CONF-650707-10). ORINS, Gmelin, AED-CONF-65-152-17.

From IEEE Annual Conference on Nuclear and Space Radiation Effects, Ann Arbor, Mich.

The conventional viewpoint of saturation in junction transistors, from a device point of view, considers the excess minority carriers in the base region. A different viewpoint considers the majority carriers in the base. The important elements then are the number of these carriers stored in the transistor and whether they are stored in the active base region, the extrinsic base region, the collector body, or the epitaxial layer. The storage of carriers in the active base region plays a relatively minor role in the storage effect for most modern transistors because of the relatively small volume of semiconductor material involved. In alloy, diffused, and epitaxial transistors the storage of carriers (electrons in a p-n-p transistor) is shown to be in the last three regions named above, respectively; in none of these transistor types is the storage region identifiable as the active base region. Detailed calculations of the primary photocurrent were made for three practical transistor construction types that relate this current to basic device parameters and to the electrical storage time. In addition, the radiation storage time was calculated in terms of the electrical storage time for epitaxial transistors. Examples of these calculations are given and the results presented. Experimental measurement of the electrical storage time of several epitaxial transistors, including three different types for which accurate basic parameter information is available, is shown to be in excellent agreement with the calculated value for each transistor type. (auth)

REACTOR TECHNOLOGY

General

Refer also to abstract 14504.

15994 (ANL–7152) REACTOR DEVELOPMENT PROGRAM PROGRESS REPORT, JANUARY 1966. (Argonne National Lab., Ill.). Feb. 24, 1966. Contract W-31-109-eng-38. 105p. Dep. mn. CFSTI $4.00 cy, $0.75 mn.

Separate abstracts were prepared for the 4 included sections. (M.O.W.)

15995 (BNL–966) DESCRIPTION OF THE ENDF SERVICE ROUTINES. Honeck, Henry C.; Felberbaum, Joan (Brookhaven National Lab., Upton, N. Y.). Dec. 1965. Contract AT-30-2-GEN-16. 124p. Dep. mn. CFSTI $4.00 cy, $0.75 mn.

A series of computer programs associated with the Evaluated Nuclear Data File (ENDF) at BNL are described. These routines are designated as service routines and perform simple transfers and checking of data between cards and tapes. The routines, written in Fortran II, are intended primarily for use at the ENDF Center at BNL. (auth)

15996 MEANS OF APPROACHING NATURAL CONVECTION EFFECTS IN A HOMOGENEOUS REACTOR. Warschauer, K. A.; Huffenus, J. P. (K.E.M.A., Arnhem, Netherlands). Houille Blanche, No. 1, 61-5(1965). (In French).

Measurements of velocities and mixing were made on a simulated model of a homogeneous reactor in order to determine residence time in the core. Concentrations were measured using conductivity probes, and residence time was related to these concentrations. Experiments were carried out for flow rates from 2 to 11.8 l/sec and Reynolds numbers from 51,000 to 300,000. Maximum relative age found near the center was 1.32 ± 3%. No effects on residence time due to differences in flow rate or density were found. (M.J.T.)

Auxiliaries and Components

Refer also to abstracts 14847 and 14848.

15997 (CEA-R–2856) ETUDE AERODYNAMIQUE DE L'ECOULEMENT FLUIDE DANS UN CANAL DE REACTEUR CHARGE EN ELEMENTS COMBUSTIBLES ANNULAIRES REFROIDIS INTERIEUREMENT ET EXTERIEUREMENT. (Aerodynamic Study of the Fluid Flow in the Channel of a Reactor Filled with Internally and Externally Cooled Fuel Elements). Rousseau, Jean-Claude (Commissariat a l'Energie Atomique, Saclay (France). Centre d'Etudes Nucleaires). Nov. 1965. 62p. Dep. mn.

A study is made of the problem of the flow-rate and pressure distributions along the length of two volumes, internal and external, bounded by a series of non-contiguous annular elements placed along the channel axis. It is observed that the phenomenon can easily be represented by equations. The theoretical expressions observed are particularly simple when the distances between the elements are above a certain minimum value. The experimental work has made it possible to show that the theoretical formulation derived is valid with a very great accuracy. The experimental study was carried out in the case of a very small spacing between the elements. It was shown that the hypothesis made for deriving the theoretical expressions was perfectly justified. The problem of evaluating the pressure-drops between the ends of a series of annular elements was considered. (auth)

15998 (EUR-2117.n) SLIJTAGEONDERZOEK AAN REACTORONDERDELEN. (Wear Research on Reactor Parts). Weltevreden, P. S. (Nederlandse Organisatie voor Toegenpast Natuurwetenschappelijk Onderzoek, The Hague. Metaalinstituut). Mar. 1965. Contract 040-61-9 ORGN. 17p. (CONF-640408-1). Dep.mn.

From Wear Congress "Assocn. for Knowledge of Materials," Utrecht.

Wear research on SAP is described as part of a design study for the ORGEL reactor. Before describing the wear research itself a concise description is given of the reactor concept. From this description follows the background and the necessity of the wear study. After specification of the experimental conditions, a description is given of the wear machine constructed for this study. In this machine the operating conditions of a pressure tube are represented as closely as possible. Frequency, amplitude, and contact force are continuously checked. To obtain reference values, the combinations SAP/SAP, steel/steel and SAP/steel are studied first. Given low wear resistance of SAP, a general screening follows in order to find a material showing little wear against SAP, meanwhile giving no damage at all to the SAP. This screening results in the selection of a few materials showing the requested properties. (auth)

15999 (NAA-SR–11739) MODULAR STEAM GENERATOR FABRICATION. Bogaert, L. T. (Atomics International, Canoga Park, Calif.). [nd]. Contract AT(11-1)-Gen-8. 47p. Dep. mn. CFSTI $2.00 cy, $0.50 mn.

The fabrication is described and recommended changes in the design and fabrication procedures of future modular steam generators are presented. (W.L.G.)

16000 (NYO–2655-1) AN INVESTIGATION OF THE EFFECT OF MECHANICALLY INDUCED VIBRATIONS ON HEAT TRANSFER RATES IN A PRESSURIZED WATER SYSTEM. Jordan, E. D.; Steffens, J. (Catholic Univ. of America, Washington, D. C. Div. of Nuclear Science and Engineering). July 1965. Contract AT(30-1)-2655. 105p. Dep. mn. CFSTI $4.00 cy, $0.75 mn.

The vibration of solids at high temperature in a high pressure water media was investigated. A high pressure vibrational test section was designed, built and tested as an addition to an existing pressurized water heat transfer loop. An electrodynamic vibration system mechanically vibrated an electrically heated rod which is transferring heat to pressurized water flowing past the rod. A constant experimental geometry was investigated with convective heat transfer rates investigated in the region of heat fluxes from 50,000 to 80,000 Btu/hr/ft^2, flow Reynolds number from 7000 to 8500, and ΔT (difference between average heater temperature and average water temperature) from 90°F to 210°F. Results of the analyses are presented. (M.O.W.)

16001 REVIEW OF CONTAINMENT PHILOSOPHY AND DESIGN PRACTICE. Gall, W. R. Nucl. Safety, 7: 81-6; 88 (Fall 1965).

Engineered safeguards such as containment, pressure- and temperature-reducing systems, air-cleaning systems, and core-spray and injection systems provide protection for the public so that reactors may be located at sites nearer populated areas than is considered safe without these safeguards under current ground rules. A review of recent design practice indicates that the effect of engineered safeguards is to reduce the radii of the required exclusion and low-population zones. (auth)

16002 STUDY OF CABLE-WRAPPED PRESSURE VESSEL FOR NUCLEAR REACTORS. Braun, Howard E.; Wesner, John W. Jr. (Westinghouse Electric Corp., Pittsburgh). New York, American Society of Mechanical Engineers, 1965, Preprint No. 65-WA/NE-4, 12p., $1.50. (CONF-651110–19). ORINS.

From American Society of Mechanical Engineers, Annual Winter Meeting, Chicago.

This is a preliminary feasibility and incentive study of wire or cable reinforced steel vessels for large high pressure nuclear reactors. The straight cylindrical section is made of several welded thin courses reinforced on the outside with axial and hoop cables to assist the shell in carrying biaxial loading. The goals of the study were improved cost effectiveness of materials, lead time, and shipping considerations. Some of the parameters considered are: Vessel wall material, axial and hoop stress distribution between the solid wall and reinforcing cable, cable size, wire stress level as percent of ultimate, and the number of hoop layers of reinforcing. Computer solutions of many possible configurations are given. (auth)

16003 IMPROVEMENTS RELATING TO NUCLEAR REACTOR FUELLING ARRANGEMENTS. Howard, John Alban; Wall, Philip Martin (to English Electric Co., Ltd.). British Patent 1,017,237. Jan. 19, 1966. Filed Nov. 7, 1961.

In a fueling arrangement for a reactor, the fuel elements are arranged in a line with each element being supported by the element next below it so as to form a string of elements for insertion into a vertical channel. Two or more wires are secured at their lower ends to the lower ends of the string of fuel element. The upper ends of the wires are suspended from wire-supporting means arranged for connection to lowering means for lowering the string of elements into the fuel channel. Wire-releasing means are provided at the lower end of the string of elements and are arranged to automatically release the wires when the fuel elements reach their operative position. (B.L.M.)

16004 FLOW REGULATOR VALVE. Webb, John (to United Kingdom Atomic Energy Authority). British Patent 1,017,350. Jan. 19, 1966. Filed Nov. 23, 1964.

A flow regulator valve for insertion in a number of flow paths to enable the flows to be adjusted relatively comprises two or more impedance means, which in the absence of all others have a substantially invariable individual flow impedance. The impedance means are in the form of orifice plates disposed transverse of the duct in a line so that the plates can be brought together by a screw type mechanism to become effectively one plate. When the valve is to introduce its maximum impedance to flow, the plates are spaced apart along the flow path and have a collective flow impedance no more than the sum of their individual impedances. Bringing the plates together to reduce their separation reduces the collective impedance of the plates and hence of the valve. (B.L.M.)

16005 LOCATING DEVICE. Wallis, John Dawtrey (to English Electric Co., Ltd.). British Patent 1,017,401. Jan. 19, 1966. Filed June 9, 1961.

A device is described for locating two nuclear fuel elements one above the other in predetermined relative angular orientation about a common axis. The device comprises at least one first guide surface and at least one first thrust surface at one end of one fuel element and at least one second guide surface and at least one second thrust surface fixed at the co-operating end of the other fuel element. The first guide surface(s) is arranged for co-operation with the second guide surface(s), and the guide surfaces are inclined with respect to a common axis so as to guide the fuel elements towards orientation when and as one element comes into contact with the other axially. The first and second thrust surface(s) are arranged for co-operation to maintain the orientation when the upper fuel element is supported on the lower. (B.L.M.)

16006 IMPROVEMENTS RELATING TO ELECTRIC SAFETY SYSTEMS FOR NUCLEAR REACTORS. Moores, Harry (to English Electric Co., Ltd.). British Patent 1,017,992. Jan. 26, 1966. Filed May 5, 1961.

An electric safety system for a nuclear reactor includes a direct current safety circuit that is arranged to operate nuclear reactor shutdown equipment. In the circuit at least one group of three parallel pairs of relay contact pairs are connected in series. The contact pairs in the group are operable by a group of three relay coils in response to changes in some parameter in the reactor and are so arranged that the safety circuit is opened only if more than one relay coil in each group of three operates to open its corresponding contact pairs. Means are provided to indicate whether a contact pair is open or closed. Provision is also made for applying an a-c current to the safety circuit. (B.L.M.)

16007 IMPROVEMENTS RELATING TO NUCLEAR REACTORS. Clayton, Kenneth Frank; Long, Everett (to English Electric Co., Ltd.). British Patent 1,018,618. Jan. 26, 1966. Filed Feb. 14, 1962.

Storage equipment for use in a nuclear reactor for storing and cooling fuel elements after removal from the core includes tube-like elements containing means designed to hold the elements and to contain a protective fluid. Cooling means are provided for allowing a coolant gas at atmospheric pressure and at a temperature substantially below that of the elements to circulate by convection around the outside of the element storage compartment or building. This circulation of the coolant gas causes the fuel elements to be cooled by only indirect heat exchange with the coolant gas. The element-containing compartment and the irradiated fuel elements contained within the compartment are sealed from the parts of the equipment containing the coolant gas to prevent contamination. (B.L.M.)

16008 FUEL ELEMENT HANDLING APPARATUS FOR NUCLEAR REACTORS. Clayton, Kenneth Frank (to English Electric Co., Ltd.). British Patent 1,018,662. Jan. 26, 1966. Filed Mar. 22, 1962.

Fuel element handling apparatus for a nuclear reactor is described that provides vertical access to a number of parallel channels or tubes for containing fuel elements. The channels are arranged on a number of pitch circles concentric with a central axis of the apparatus with more than one channel on at least one of the pitch circles. The apparatus includes a vertical inlet duct, guide tubes arranged with the lower end of one guide tube on each of the pitch circles, and tube-selecting means for bringing the inlet duct into communication with the upper end of each guide tube in turn. The guide tubes are rotatable together about the central axis so that each guide tube communicates successively with each channel on the corresponding pitch circle. (B.L.M.)

16009 PRESSURE VESSELS. Young, Alexander Gillies (to English Electric Co. Ltd.). British Patent 1,019,282. Feb. 2, 1966. Filed Jan. 5, 1962.

A liner comprises a fluid-tight skin portion covering the internal surface of a concrete pressure vessel, part of which is in spherical form. A frame including a number of members arranged to define the surface of the spherical portion is arranged in rigid relation with and on one side of the liner and embedded in the concrete. The frame members define geodetic lines arranged so as to form a number of substantially congruent spherical triangles or approximately triangular figures. Other frame members divide the triangles or triangular figures according to a triangular grid into a number of minor figures. Preferably, the skin portion of the liner is formed by a number of separate plate members joined together at their sides. (B.L.M.)

16010 NUCLEAR REACTOR. (to United Kingdom Atomic Energy Authority). French Patent 1,345,862. Nov. 4, 1963. Priority date Dec. 20, 1961, Great Britain.

A method is provided for the removal of fission product metals from the coolant gas stream of a nuclear reactor. The gas stream passes through a filter bed in the form of a packing of discrete solid bodies such as rings, rods, tubes, beads and thin filaments or threads of the solid. These bodies are formed of a "glass-like" solid which has sufficient stability to withstand a temperature of at least 700°C without the bodies fusing together and possessing a sufficiently high diffusion coefficient to allow the absorbed fission products to diffuse into the whole mass of the material. (IIB)

16011 GAS-LIQUID MIXING DEVICE FOR STEAM COOLED REACTOR. (to EURATOM). French Patent

1,359,123. Mar. 16, 1964. Priority date Dec. 11, 1961, United States.

An arrangement is provided for mixing steam and water in a fog-cooled reactor. A plurality of coolant tubes vertically extending within a pressure vessel are disposed between a pair of upper and lower flat horizontal plates. The tubes are surrounded by a wall forming an annular space with the pressure vessel. Liquid water is admitted into the annular space adjacent to the bottom of the vessel and passes into the spaces between the coolant tubes. Dry steam enters the vessel through an inlet disposed in the bottom of it and penetrates into the base openings of the coolant tubes. The steam-water mixing device is formed in each of the coolant tubes, consisting of a diverging section extending upwardly from the lower plate, which section has a plurality of small openings to permit liquid water to enter in the form of fine droplets to mix with the steam therein. The water-steam mixture then travels upwards through and out of the top of said tubes, withdrawing the fission heat of the reactor. (IIB)

16012 NUCLEAR REACTOR CONTROL MECHANISM. (to United Kingdom Atomic Energy Authority). French Patent 1,367,389. June 8, 1964. Priority date Aug. 30, 1962, Great Britain.

A reactivity control element is driven by a fluid-operated piston and cylinder. The cylinder is movable while the piston is fixed. This control mechanism is compact and suitable for incorporation as a unit into a reactor vessel with a consequent reduction in the required penetrations through the vessel. The control mechanism is incorporated in a nuclear reactor having a core cooled by circulated coolant and may be so connected to the reactor coolant circuit that the pressure difference between the interior and the exterior of the control element is equal to the coolant pressure differential across the core. (IIB)

16013 THIN-WALLED NUCLEAR REACTOR. (to Aktiebolaget Atomenergi). French Patent 1,368,813. June 29, 1964. Priority date June 6, 1962, Sweden.

A pressure vessel of pre-stressed concrete is provided with an opening at the top and contains a comparatively thin-walled reactor tank of stainless steel. This tank is also provided with an opening at the top through which the reactor vessel is in open communication with the space between the reactor vessel and the pressure vessel. This space is filled with a gas which does not condense at normal temperatures and which has the same pressure as the steam pressure in the reactor vessel. (IIB)

16014 REACTOR CONTROL SYSTEM. Parkinson, Thomas Franklin; Dalton, George Ronald; Blair, Donald James; Driscoll, Michael John. U. S. Patent 3,228,847. Jan. 11, 1966. Filed Jan. 29, 1963.

A control system for a reactor adapted to maintain a self-sustained reaction comprises a control tube extending into the active portion of the reactor and fluid-movable neutronic reacting particles arranged in the tube. The tube may be of cylindrical or cruciform configuration and has an enlarged cross section in the midportion extending into the active region to minimize peak-to-average power ratio. The mean diameter of the particles is of the order of less than $1/10$ of the mean diameter of the tube, and the flow of the particles through the tube is maintained at such a rate that the particles flow through the tube in a substantially non-contacting fashion so that an almost continuous variation in density of the particles is produced along the length of the tube. (B.L.M.)

16015 NUCLEAR REACTOR CORE HAVING MEANS FOR VARYING INCLINATION OF FUEL ASSEMBLIES. Astley, E. R.; Finch, L. M. (to U. S. Atomic Energy Commission). U. S. Patent 3,230,146. Jan. 18, 1966.

A nuclear reactor comprising a plurality of spaced elongated fuel assemblies disposed around a central axial fuel assembly and means for rotating the upper portions of said spaced fuel assemblies around the central fuel assembly while holding the lower portions thereof in a fixed position to control the reactor is described. (AEC)

16016 METHOD AND APPARATUS FOR CONTROLLING REACTIVITY. Hitchcock, J. M. (to U. S. Atomic Energy Commission). U. S. Patent 3,230,147. Jan. 18, 1966.

A method for controlling the reactivity of a nuclear reactor is given. The method comprises the steps of introducing a series of bodies of non-fissile neutron absorbing material into the core structure of the reactor, said bodies of neutron absorbing material being introduced into the reactor core structure in sequence along a line passing through the nuclear reactor core structure and the series of bodies increasing in neutron absorbing capacity from one body to the next in the series; and moving the series of bodies as a whole into and out of reactor core structure so that the number of the series of bodies contained wholly or partially by the reactor core structure is varied. The series of bodies of non-fissile neutron absorbing material begins with a minimum capacity at the body which is first inserted into the nuclear reactor core structure and ends with a maximum capacity at the body which is last introduced into the reactor core. (AEC)

16017 MEANS FOR MOUNTING PRESSURE POWER TUBES IN A NUCLEAR REACTOR. Boiron, Pierre Georges (to EURATOM). U. S. Patent 3,230,149. Jan. 18, 1966. Filed July 29, 1963.

A mounting combination for the pressure tube in a nuclear power reactor having a pile body defining a reaction tank with a top and bottom wall and at least one pressure tube projecting through the walls comprises an upper and lower connector located on either side of the heart of the reactor. The upper connector is formed by an upper sleeve secured to the top wall of the tank and surrounding the upper end of the pressure tube in spaced relation. The upper end of the pressure tube is secured to the sleeve in a fluid-tight engagement, and an upward extension on the sleeve beyond the upper end of the pressure tube has an orifice shaped to receive a fuel assembly, which is secured on the extension and suspended from it for loading into the pressure tube. Coolant fluid is circulated between the sleeve and pressure tube and between the fuel element and the pressure tube. The lower connector is formed of a lower sleeve surrounding the lower end of the pressure tube and sealing means between the lower end of the pressure tube and the sleeve that permits relative axial movement between these two parts. (B.L.M.)

16018 NUCLEAR REACTOR CONTROL SYSTEM. Hennig, Robert J. (to Atomic Power Development Associates, Inc.). U. S. Patent 3,231,473. Jan. 25, 1966. Filed Mar. 31, 1960.

In a nuclear reactor having an active core, a control system includes means for defining a closed path of circulation through the active core. A portion of the closed path comprises a number of upstanding passages extending upwardly through and above the active core portion and disposed across the core. Rod-shaped poison members are disposed in each passage, and each rod has a diameter less than that of the passage to provide clearance for the flow of a liquid through the passages. A liquid, such as molten Na, is circulated through the passages at such a velocity as to regulate the elevation of the poison members in the passages. Under emergency conditions, the direction of flow of the liquid can be reversed so as to drive the rods into the reactor core at a very high velocity to immediately terminate the chain reaction. (B.L.M.)

Criticality Studies

Refer also to abstracts 14860 and 14996.

16019 (BMI-X-10154) AN EVALUATION OF THE APPLICABILITY OF EXISTING DATA TO THE ANALYTICAL DESCRIPTION OF A NUCLEAR-REACTOR ACCIDENT. Quarterly Progress Report, October–December 1965. Sunderman, Duane N.; Morrison, David L.; Gieseke, James A.; Ritzman, Robert L.; Walters, Craig T.; Genco, Joseph M. (Battelle Memorial Inst., Columbus, Ohio).

Jan. 1, 1966. Contract W-7405-eng-92. 51p. (EURAEC-1571). Dep. mn. CFSTI $3.00 cy, $0.50 mn.

Work Performed under United States–Euratom Joint Research and Development Program.

Coolant-loss or blowdown accidents are studied for two high-power reactor concepts. One is a pressurized-water reactor and the other is a boiling-water reactor, and both are fueled with urania rods, clad in stainless steel or zirconium. Experimental studies are carried out of these accidents in the LOFT facility. Analytical studies of the relevant heat-transfer and thermodynamic parameters, fission-product chemistry variables, and aerosol, particle, and gas dynamics are carried out. Clad-water reactions are investigated systematically. The use of the NURLOC computer code for these studies is discussed. 51 references. (T.F.H.)

16020 (CEA-R-2836) REPONSE IMPULSIONNELLE SPATIO-TEMPORELLE D'UN REACTEUR CYLINDRIQUE EN REGIME SOUS-CRITIQUE. (Space-Time Dependent Impulse Response of a Subcritical Cylindrical Reactor). Cazemajou, Jean (Commissariat a l'Energie Atomique, Saclay (France). Centre d'Etudes Nucleaires). Nov. 1965. 34p. Dep. mn.

A new formulation of the spatial dependent impulse response of a subcritical reactor in a cylindrical geometry is proposed. An expression of the transfer function between a point source at the center of coordinates and the flux at a given point (r,z) is obtained by solving, by means of Laplace transform, the one group diffusion equation. In this transfer function, variables r and p (p being the Laplace variable) remain linked within a modified Bessel function. Taking the inverse Laplace transform is done by two different ways: using the Mellin-Fourier method which separates variables r and t. This method makes it possible to establish that there is identity between the classical formulation and the new one and using an inverse Laplace transform which keeps variables r and t linked. This method requires to approximate the inverse Laplace transform of the end factor. It is then possible to replace the radial harmonics modes series of the classical expression by a single function. (auth)

16021 (CEA-R-2890) LA COLLISION ANISOTROPE DANS LES PROBLEMES DE CELLULE. (The Anisotropic Collision in Cell Problems). Benoist, Pierre (Commissariat a l'Energie Atomique, Saclay (France). Centre d'Etudes Nucleaires). Nov. 1965. 19p. Dep. mn.

A general expression allowing the calculation of the influence on cell factors of an anisotropic component of the scattering law in a given medium is established, in the framework of the integral transport theory. This expression is applied to the problems of the thermal utilization factor, fast fission factor and diffusion coefficients. In the case of the thermal utilization factor, it is shown that the introduction of the transport cross section is justified rigorously in the moderator. In the fuel, it is not very much theoretically justified although it leads to good results for rather big rods; a very simple formula is then established from the general expression, allowing the calculation of the correction to effect on f, without using the transport cross section; this formula leads, for all the rod diameters considered, to results in very good agreement with reference values obtained by the S_8 method. An analogous formula for the fast fission factor is established. (auth)

16022 (EUR-2627.e) NEUTRON TRANSPORT IN A SPHERICAL REACTOR, A STUDY IN THE APPLICATION OF THE j_N APPROXIMATION OF THE MULTIPLE COLLISION METHOD. Asaoka, T. (European Atomic Energy Community, Ispra (Italy). Joint Nuclear Research Center). Nov. 5, 1965. 32p. Dep. mn.

The j_N approximation to the solution of neutron transport problems emerges in the course of developing the multiple collision method, which is based on the random walk approach. By means of the j_N method, transport problems for a multiregion spherical reactor, where the total neutron cross sections are independent of the spatial region (position), are treated in the context of a multigroup model under the assumption that the scattering of neutrons is spherically symmetric in the laboratory system. The critical radii for bare spheres, calculated by using the j_N approximation in combination with a one-group model, are compared with those obtained from the S_N method and the exact values. In addition, by fixing the radius, the values of k_{eff} and the asymptotic time-constant (or the so-called Rossi-α) are calculated and the flux distributions corresponding to these two calculations are compared with each other. For a subcritical system, the flux obtained from the time-constant calculation decreases more slowly as the radial coordinate increases than that obtained from the k_{eff} calculation. In order to give a numerical illustration of the multigroup model, calculations are performed on two fast neutron critical assemblies, Godiva and Jezebel, and the results are compared with those of the S_4 approximation and experiment. It can be seen from these results that the j_3 approximation gives a result comparably accurate to the S_4 calculation for all bare systems of interest. (auth)

16023 (IITRI-578P21-16) STUDIES OF REACTOR CONTAINMENT. Progress Report, October–November 1965. Eichler, J. B.; Gallagher, E. V.; Lieberman, P.; Singer, T. (comps.) (IIT Research Inst., Chicago, Ill.). Contract AT(11-1)-578. 54p. (IITRI-T6042-16). Dep. mn. CFSTI $3.00 cy, $0.50 mn.

Experiments are carried out and analyzed on: the dynamic and kinetic characteristics of shock-wave impingement on Foamglass, a crushable solid; and water decompression into air-filled cavities, with concomitant shock wave generation, under one-dimensional conditions and with the water initially in a state characteristic of pressurized-water or boiling reactors. (T.F.H.)

16024 (RFR-231) FLUX-SHAPE EIGENFUNCTION TABLES FOR TWO-ZONE SLABS. Norinder, Olov (Aktiebolaget Atomenergi, Stockholm (Sweden)). Mar. 13, 1963. 32p. Dep. mn.

The spatial stability of neutron flux distributions can be investigated by considering the flux-shape eigenfunctions as described by Randall and St. John. The eigenfunction properties entering into such calculations are tabulated for the zero (fundamental), first, and second flux eigenfunctions of a two-zone symmetric slab. The tables are particularly intended for xenon stability calculations and, there, also present some properties of xenon distributions. Formulas for calculating xenon spatial stability are included. (auth)

16025 (RFR-232) FLUX-SHAPE EIGENFUNCTION TABLES FOR TWO-ZONE CYLINDERS. Norinder, Olov (Aktiebolaget Atomenergi, Stockholm (Sweden)). Apr. 17, 1963. 18p. Dep. mn.

The spatial stability of neutron flux distributions can be investigated by considering the flux-shape eigenfunctions as described by Randall and St. John. The eigenfunction properties entering into such calculations are tabulated for the fundamental mode and for the first, second and third azimuthal modes of a two-zone cylinder. The tables are particularly intended for xenon stability calculations and therefore also present some properties of xenon distributions. (auth)

16026 (UJV-1459/65) VYPOCET HAVARIJNI DYNAMIKY JADERNYCH REAKTORU. (Dynamics of Accidents in Nuclear Reactors). Pfann, J. (Ustav Jaderneho Vyzkumu, Ceskoslovenska Akademie Ved, Rez). 1965. 36p. Dep. mn.

The transient state equations of reactors are presented. The method of numerical solution of the equations and an ALGOL program "DYNAMIKA REAKTORU" for solving transient and accidental processes in heavy water moderated, gas cooled reactors with fuel element rods are described. (M.O.W.)

16027 REACTIVITY MEASUREMENTS BY REACTOR NOISE ANALYSIS USING TWO-DETECTOR CORRELATION METHOD. Nomura, Tsutomu (Nippon Atomic Industry Group Co., Kawasaki-shi, Japan). J. Nucl. Sci. Technol. (Tokyo), 3: 14-19(Jan. 1966).

For a subcritical reactor, power spectral density measurement of neutron fluctuations can be used to evaluate the quantity $\alpha = (1 - \rho/\beta)\beta/l$, where ρ/β, the reactivity, can be determined using the quantity β/l measured at critical state. In an actual experiment, however, chamber noise is a hindrance, particularly at the highly subcritical state. The correlation technique was used to eliminate the chamber noise component, thereby considerably extending the possible range of reactivity determination by reactor noise analysis. (auth)

16028 MEASUREMENTS OF SPATIAL DISTRIBUTION OF CADMIUM RATIO IN HETEROGENEOUS LATTICES. Kadotani, Hiroyuki (Tokyo Inst. of Tech.). J. Nucl. Sci. Technol. (Tokyo), 3: 27-31(Jan. 1966).

Spatial distributions of the Cd-ratio of Au foils were measured for various lattice pitches in a natural uranium-light water system. Comparison of the experimental results with theoretical calculations using the THERMOS-code showed some divergence of the theoretical Cd-ratio toward larger than experimental values in the fuel rod. (auth)

16029 NUCLEAR-POWER-EXCURSION SIMULATION IN FRANCE. Pascouet, A. Nucl. Safety, 7: 20-5; 42 (Fall 1965).

The possible mechanical effects of nuclear power excursions in water-cooled and -moderated reactors are of concern to reactor designers and operators. An investigation of means for simulating nuclear power excursions led to the development of explosive simulation charges with time-dependent power releases. Release comparable with the maximum BORAX-I power release is obtained within a given volume. The data are in good agreement with those deduced from experiments performed on various reactors and were used to establish likely orders of magnitude for the mechanical structural response. The simulation provides for the experimental investigation of boiling phenomena near fuel plates and cladding behavior during reactor transients. (auth)

16030 KRITICHESKIE PARAMETRY GOMOGENNIKH RAZMNOZHAYUSHCHIKH SISTEM. (Critical Parameters of Homogeneous Multiplying Systems). Marchuk, G. I.; Kocherin, V. I.; Nevinitsa, A. I.; Uanadze, O. P. Moscow, Atomizdat, 1965. 144p.

Information on the critical parameters of reactors with various spectra is presented, obtained from neutron-physics and computer calculations of homogeneous systems. The basic theoretical methods for reactor calculations are described, including methods for calculating the spatial-angular moments of the neutron distribution function, the neutron diffusion length, kinetic effects, reactor critical masses, and multigroup constants. Homogeneous reactors with graphite, beryllium, and boron moderators are discussed. Results of calculations are correlated with experimental data. Tables of the critical masses and other physical parameters of homogeneous multiplying systems are presented. (M.J.T.)

16031 CRITICALITY DATA AND ITS APPLICATION TO PLANT CLEARANCE. Chalmers, J. H. (United Kingdom Atomic Energy Authority, Risley, Eng.). Vienna, International Atomic Energy Agency, 1965, Preprint No. SM-70/8, 17p. (CONF-651103-18). ORINS.

From IAEA Symposium on Criticality Control of Fissile Materials, Stockholm.

The results of a theoretical parametric survey of critical data for single homogeneous units of a number of compounds of uranium and plutonium are presented. Included are parameters for uranium metal-water systems between 93 and 5% enrichment; uranium oxide-water systems at 93% and from 10 to 2% enrichment; plutonium metal, nitrate, oxalate and oxide-water systems. The last mentioned include the effect on mass and volume of 5 and 15% ^{240}Pu. The effects of the addition of nitric acid to both uranium and plutonium metal-water mixtures are considered within N/fissile ratios of 2–70 and 4–70 respectively. Also included are parameters for lattice arrangements of unclad uranium oxide rods of various diameters for enrichments between 1.3 and 5%. The method of calculation used for the majority of this work was diffusion theory using four energy groups. In some instances Monte Carlo calculations were made as a check on diffusion theory, in others Monte Carlo was used throughout. Some comparison is made with the results of other workers and with experiments in those instances where meaningful data checks are available. The application of single unit data to multi-body systems for plant clearance purposes is briefly discussed, and reference is made to other methods of calculation capable of dealing with arrays of non-standard geometries and units of complex shapes. (auth)

16032 CRITICALITY PARAMETERS FOR MIXTURES OF PLUTONIUM OXIDE, URANIUM OXIDE AND WATER. Chalmers, J. H. (United Kingdom Atomic Energy Authority, Risley, Eng.). Vienna, International Atomic Energy Agency, 1965, Preprint No. SM-70/9, 12p. (CONF-651103-19). ORINS.

From IAEA Symposium on Criticality Control of Fissile Materials, Stockholm.

Homogeneous mixtures of plutonium and uranium oxides with water in various proportions are considered and estimates of the critical parameters of these mixtures based upon diffusion theory calculations using four energy groups are presented. No experimental results are available to directly check the accuracy of these calculations. Using the same method of calculation, however, the experimental results quoted for 0.372 in. dia. rods in hexagonal lattice arrangement in water were reproduced to within ±1.1% in k_{eff}. These rods contained 1.5% PuO_2 in UO_2 depleted to 0.22% ^{235}U. The results of some Monte Carlo check calculations on homogeneous mixtures are quoted; these predict lower critical masses. Comparison is also made with Marchuk's results. The mixtures considered are assumed to be mechanical mixtures of water with PuO_2/UO_2 having a crystal density of 11.2 gm/cc. Marchuk's calculations are based on a PuO_2/UO_2 density of 6.0 gm/cc. The comparisons with his results assume the same density. (auth)

16033 A VARIATIONAL APPROACH TO THE EFFECT OF BOUNDARY PERTURBATIONS WHEN THE MULTI-GROUP DIFFUSION EQUATIONS APPLY. Spinks, N. (Australian Atomic Energy Commission, Lucas Heights, New South Wales). 14p. (CONF-650602-71). ORINS. Gmelin, AED-CONF-65-125-107.

From American Nuclear Society 11th Annual Meeting, Gatlinburg, Tenn.

Variational principles are given which allow perturbations of the surface defining the boundary of a region in which the multi-group diffusion equations apply. The perturbation may take the form of a change in boundary conditions or a change in the boundary shape. The principles are useful for determining the reactivity worth of control rods when the shape of the rod makes a direct calculation difficult. In addition, from a single flux and adjoint flux calculation, the worths of a host of control rods of slightly different compositions (boundary conditions) and slightly different shapes and sizes can be determined. The application of the principle to the output from finite difference computer codes is discussed. (auth)

16034 THE CRITICALITY OF INTERACTING ARRAYS. Abbey, F. (United Kingdom Atomic Energy Authority, Risley, Eng.). Vienna, International Atomic Energy Agency, 1965, Preprint No. SM-70/6, 39p. (CONF-651103-16). ORINS.

From IAEA Symposium on Criticality Control of Fissile Materials, Stockholm.

Central to an understanding of the criticality of interacting arrays is a knowledge of the quantitative relation between the reactivity and separation of units. An examination of this relation for regular arrays of spheres is made in terms of a simple theoretical model which focuses attention on the interaction probabilities between pairs of units, i.e., the proportion of the neutrons emitted by one unit which reach another. Formulation of balance equations connecting the fluxes entering and leaving each unit then allows assessment of the criticality of the array.

The interaction probabilities are taken as mean fractional solid angles. Attention is drawn to the possibility of using Monte Carlo methods for the evaluation of interaction probabilities for systems of complex geometry and the GEM Monte Carlo code for the IBM 7090 is used to evaluate cases where other spheres in an array partially intervene between source and target spheres. The values obtained are separately tabulated as being of interest outside the particular arrays considered. A new code incorporating a specially simplified variant of GEM and provision for solution of the neutron balance equations is described as a ready means for estimation of the criticality of arrays for which the unit reactivities are known. A related discussion of factors affecting the criticality of arrays is presented. Factors considered include the size, shape, composition and density of units, proximity to reflectors and the mixing of units of differing types. Comparison is made between the theoretical model and published critical data for both unreflected and reflected arrays. Recently reported data for systems of this kind from both experimental and calculational sources allow a reasonably comprehensive comparison. New results are also given on the effect of moving units out of the plane of a two dimensional array and on the interaction of small numbers of slab tanks. The latter is seen as a special case and is investigated in some detail; a simple empirical correlation is given for air spacing and it is shown that there is little to be gained by attempting decoupling with shielding materials. (auth)

Design and Feasibility

16035 GRAPHITE–GAS REACTORS. Crespi, M. Alicia (Junta de Energia Nuclear, Madrid). Energia Nucl. (Madrid), 9: 345-56(Sept.-Oct. 1965). (In Spanish).

After a brief review of the characteristics of light water and heavy water gas-cooled graphite reactors and a comparative economic study of the various types, a survey was made of the present developments and of the evolution hoped for reactors moderated by graphite and cooled by gas. The developments in England, France, and United States are emphasized. (J.S.R.)

16036 THE CONCEPT OF A FAST BREEDER REACTOR WITH FUSED SALT FUEL AND BOILING MERCURY "WARS". Taube, Mieczyslaw; Wierusz, Andrzej; Kowalew, Andrzej; Mielcarski, Mieczyslaw; Poturaj-Gutniak, Stefan (Inst. of Nuclear Research, Warsaw). Nukleonika, 10: 637(1965).

The fast breeder concept using a fused fuel of $^{239}PuCl_3$, $^{238}UCl_3$, NaCl, and KCl in boiling Hg coolant is described. (M.C.G.)

16037 THE CONCEPT OF SALT-BOILING FAST BREEDER REACTOR "SAWA". Taube, Miecyslaw; Mielcarski, Mieczyslaw; Kowalew, Andrezej; Poturaj-Gutniak, Stefan (Inst. of Nuclear Research, Warsaw). Nukleonika, 10: 639-40(1965).

A fast breeder reactor concept is proposed in which the core consists of the following fused chlorides: $^{239}PuCl_3$ as the fissionable material, $^{238}UCl_3$ as the fertile material, NaCl as the inactive diluent, and $AlCl_3$ as the coolant. (M.C.G.)

16038 NUCLEAR REACTOR. (to United Kingdom Atomic Energy Authority). French Patent 1,304,929. Aug. 20, 1962. Priority date Nov. 4, 1960, Great Britain.

A fuel element in the core of a nuclear reactor has a multiplying region containing fissile material and a non-multiplying region. The fuel element is mounted for rotation to afford control of the reactor by interchange of the positions of the multiplying region and non-multiplying region. A reactor core may comprise a plurality of rotary fuel elements. (IIB)

16039 NUCLEAR REACTOR. (to Nuclear Materials and Equipment Corp.). French Patent 1,327,306. Apr. 8, 1963. Priority date Sept. 5, 1961, United States.

Pu-240 has a strong neutron resonance-capture peak at 1.055 ev. The effective cross section of Pu-240 to neutrons is strongly affected by the neutron energy and may be set to decrease as the energy of the neutrons averaged over the whole spectrum decreases. These properties of Pu-240 can be used in a nuclear reactor to minimize inherently the reactivity variation during irradiation. This may be accomplished by causing excess neutrons to be absorbed preferentially in the Pu-240 thereby yielding the fissile isotope Pu-241 rather than by having them absorbed in a strictly parasitic control material. When a reactor is fueled with plutonium alone or together with other fissile or fertile materials, said plutonium including the isotope Pu-240, this reactor may be characterized by the amount of the isotope or by the moderation in such a way that the effective neutron-absorption cross section of Pu-240 decreases substantially as the time of operation of said reactor increases. By virtue of the decreasing cross section of Pu-240 as the average neutron energy decreases during fuel consumption, the plutonium becomes a self-stabilizing or self-compensating fuel. The quantity of the plutonium, its isotopic composition and the moderation of the reactor should thus be such as to compensate for the loss of reactivity of the fuel as the reactor operates. (IIB)

16040 NUCLEAR REACTOR WITH CORE SUBMERGED IN A LIQUID METAL. (to United Kingdom Atomic Energy Authority). French Patent 1,353,703. Jan. 20, 1964. Priority date Feb. 14, 1962, Great Britain.

A reactor tank contains liquid metal as a primary coolant Submerged in this primary coolant are the reactor core together with a primary pump and a primary heat exchanger. In a primary coolant circuit the coolant is circulated from the tank through the pump, core and primary heat exchanger back to the tank. An auxiliary cooling coil with an auxiliary coolant is arranged to promote circulation in the primary cooling circuit by natural convection of the primary coolant. An auxiliary heat exchanger is located outside the reactor tank and is connected to the auxiliary cooling coil to abstract heat from the primary coolant by natural convection circulation of the auxiliary coolant. (IIB)

16041 NUCLEAR REACTOR. (to United Kingdom Atomic Energy Authority). French Patent 1,355,945. Feb. 10, 1964. Priority date Apr. 13, 1962, Great Britain.

In a nuclear reactor the neutron moderation is achieved by an equilibrium mixture of, on the one hand, a solid acceptor material containing a neutron moderator and, on the other hand, the same moderator in a fluid phase. The reactivity of the reactor is controlled by variation of the equilibrium conditions, so as to vary the moderator content of the acceptor material. (IIB)

16042 NUCLEAR REACTOR. (to United Kingdom Atomic Energy Authority). French Patent 1,360,063. Mar. 23, 1964. Priority date June 4, 1962, Great Britain.

The core of a nuclear reactor is formed by hexagonal fuel elements clustered so as to be in contact with one another except at interspaces for permitting coolant flow. The full-group fuel assembly of the core comprises six similar subgroup fuel assemblies arranged symmetrically to define a void. Each subgroup fuel assembly comprises twenty-one fuel elements arranged in a hexagonal group of nineteen. The central void defines a control rod channel. (IIB)

16043 PEBBLE BED NUCLEAR REACTOR. (to United Kingdom Atomic Energy Authority). French Patent 1,365,532. May 25, 1964. Priority date June 1, 1962, Great Britain.

A pebble bed nuclear reactor has a graphite core structure which defines seven reactor vessels to receive beds of fuel elements in the form of spherical balls. The vessels are arranged so that six vessels are grouped with equal spacing in a circle around a central vessel. The core structure is built of graphite bricks so that it is wholly of refractory material. It is constituted by a circular outer wall strengthened by restraining hoops, core bottoms each constituted as an inverted arch with graphite bricks of keystone shape and defining conical bases for the reactor

vessels, core partitions also of graphite which separate the reactor vessels and core lids which close the reactor vessels. Each reactor vessel has a fuel inlet and a fuel outlet. (IIB)

16044 NUCLEAR REACTOR. (to United Kingdom Atomic Energy Authority). French Patent 1,367,390. June 8, 1964. Priority date Aug. 30, 1962, Great Britain.

A liquid-moderated nuclear reactor has a hollow neutron-absorbing control element which displaces liquid moderator, e.g., water, when it moves. A filler element is placed within the liquid moderator in such a way that it is surrounded by the control element when the control element is located within the core. The filler element is without fissile content and is substantially made of moderator material having a neutron slowing-down power less than that of the liquid moderator displaced by the filler element. When the control element is withdrawn from the reactor core, the thermal neutron flux in the region vacated by it does not show the flux peaking, which would occur in this region were it occupied solely by the displaced neutron moderating liquid. (IIB)

16045 NUCLEAR REACTOR. (to United Kingdom Atomic Energy Authority). French Patent 1,370,966. July 20, 1964. Priority date Sept. 19, 1962, Great Britain.

The core of the reactor together with a heat transfer fluid are separated from a reactor coolant passing through the core. The circuit for the heat transfer fluid has a riser section containing fuel elements and a downcomer section to return the fluid from the top to the bottom of the riser section. The downcomer section is arranged to be cooler over its whole length than the riser section by unequal distribution of fuel elements between the two sections, so as to promote natural convection circulation of the heat transfer fluid. (IIB)

Fuels

Refer also to abstracts 14435 and 14438.

16046 BURNUP DETERMINATIONS OF NUCLEAR FUEL ELEMENTS USING MASS SPECTROMETRIC METHODS. Viehboeck, F. P. (Oesterreichische Studiengesellschaft fuer Atomenergie, Siebersdorf, Austria). Acta Phys. Austr., 20: 314-24(1965). (In German).

The mass spectrometric method for burnup determination is described. The theory of the determination, using uranium isotope ratios, is given. A thermal three-filament surface ionization source and an ion source for high-temperature fuels are described. (J.S.R.)

16047 FUELS FOR FAST NEUTRON REACTORS. Sebilleau, F. (CEA, Paris). Energie Nucl., 7: 418-27 (Nov. 1965). (In French).

Two parameters that are characteristic of fast neutron piles are high specific power per unit volume of the core and high burn-up. These two conditions that determine the main characteristics of the fuel elements are discussed. Fuel canning materials are described. (auth)

16048 IMPROVEMENTS IN FUEL ELEMENTS FOR NUCLEAR REACTORS. Wallis, John Dawtrey (to English Electric Co., Ltd.). British Patent 1,017,201. Jan. 19, 1966. Filed May 11, 1961.

A fuel element for a reactor includes a generally cylindrical can and a fuel rod fitting within the can. The rod has at least one groove on its surface with the ends of the, or each, groove being axially displaced, and corresponding portion(s) of the can are deformed during manufacture of the fuel element so as to fit closely within the grooves to prevent relative rotation of the can and fuel rod at all times when the fuel element is within the reactor. (B.L.M.)

16049 IMPROVEMENTS IN NUCLEAR REACTORS. Beurtheret, Charles (to Compagnie Francaise Thomson-Houston). British Patent 1,018,432. Jan. 26, 1966. Filed Jan. 28, 1963.

A sheathing arrangement is described for parallel fuel rods of fissile material immersed in a liquid that acts as a coolant and that may also act as a moderator. The sheath enclosing each rod has radial appendages, the tips of which are cooled by an auxiliary circulation of liquid independent of the principal circulation over the rest of the surface of the sheath. The radial appendages may take the form of protuberances arranged in rows parallel to the axes of the rods or longitudinal fins. Arrangements of the sheathed rods in certain manners define conduits for both the main and auxiliary coolants. (B.L.M.)

16050 FUEL ASSEMBLIES IN A NUCLEAR REACTOR. (to Societe Belge pour l'Industrie Nucleaire). French Patent 1,329,610. May 6, 1963. Priority date Mar. 9, 1961, Belgium.

A structure comprising fuel elements, a support for those elements, a member for reactivity control and an actuating mechanism for this member is adapted to be removed as a unit from the reactor vessel and to be re-introduced as a unit into the reactor vessel. (IIB)

16051 ASSEMBLY OF FUEL ELEMENTS FOR A NUCLEAR REACTOR. (to Societe Belge pour l'Industrie Nucleaire). French Patent 1,329,611. May 6, 1963. Priority date Mar. 9, 1961, Belgium.

The fuel elements in a nuclear reactor are fixed to a hollow cylindrical support. The fuel elements are arranged around this hollow support in a plurality of rows enclosing it only partially. The advantage of this assembly is that all the fuel elements are supported by a central tube, which has a high mechanical strength and that the space within the central tube can be used for inserting reactor members, for example, absorbing rods or a liquid moderator. (IIB)

16052 MEANS FOR FLATTENING NEUTRON FLUX DISTRIBUTION IN THE AXIAL DIRECTION OF A NUCLEAR REACTOR. (to EURATOM). French Patent 1,361,744. Apr. 13, 1964. Priority date Aug. 31, 1962, Belgium.

Some fuel elements comprise a rigid longitudinal metal frame formed with longitudinal grooves in which nuclear fuel plates are secured. In order to obtain a flux flattening in the reactor, some, but not all, of the fuel-containing channels are devoid of fissile fuel on each side of a plane intermediate and perpendicular to the length of the channels. (IIB)

16053 METHOD AND CONTACT MATERIAL FOR CHEMICAL CONVERSION IN PRESENCE OF NUCLEAR FISSION FRAGMENTS. Fellows, Albert T. (to Socony Mobil Oil Co., Inc.). U. S. Patent 3,228,848. Jan. 11, 1966. Filed Apr. 22, 1960.

Modification of the particles of contact material described in the U. S. Pat. 3,228,848 for the use in processes utilizing the energy of nuclear fission for the conduct of chemical conversions of fluid reactants to fluid products of different composition is described. The microporous solid particles have nominal diameters within the range of about 100 μ to about 1 in., and each particle consists of a microporous inner portion comprising a mixture of carrier material and fissionable material surrounded by a microporous outer portion. The center portion serves as a fission products-forming area in which high energy, normally solid, fission products are formed and from which the energy is transferred to the reactants since the pores admit the chemical fluid reactants. The outer porous material layer serves to retain the fission particles within the particle and is 10 to 100 μ in thickness. (B.L.M.)

16054 UTILIZATION OF NUCLEAR FISSION FOR CHEMICAL REACTIONS. Fellows, Albert T. (to Socony Mobil Oil Co., Inc.). U. S. Patent 3,228,849. Jan. 11, 1966. Filed Apr. 22, 1960.

A method similar to that described in U. S. Pat. 3,228,848 is patented for utilizing the energy of nuclear fission for chemical conversions of fluid reactants to fluid products of different composition by conversions that require a substantial amount of energy. The porous material for carrying out

the reactions comprises particles of a solid inorganic carrier having a large surface area and a pore volume of 5 to 70% of the total particle volume. The pores have a radius in the range of about 4 Å to 100 μ, and the fissionable material having a grain size of less than 6 μ is dispersed in the porous material in a concentration sufficient to render the contact material capable of effecting a neutron-multiplying fission reaction in the presence of a suitable neutron flux. Active contact sites are formed on the contact material by virtue of the transfer of energy to the contact material from the high energy, normally solid, fission fragments formed during the fission reaction and retained in the contact material. The contact sites in turn transfer the energy to the fluid chemical reactants. (B.L.M.)

16055 CHEMICAL CONVERSION IN PRESENCE OF NUCLEAR FISSION FRAGMENTS. Fellows, Albert T. (to Socony Mobil Oil Co., Inc.). U. S. Patent 3,228,850. Jan. 11, 1966. Filed Apr. 22, 1960.

A new and improved particulate contact material is described for use in processes utilizing the energy of nuclear fission for chemical conversion. The particle is composed of a core portion that is substantially free of fissionable material and has a nominal diameter in excess of about 50 μ and a fissionable material-containing portion surrounding the core and having a thickness within the range of 30 to 25,000 μ. Preferably, the core portion is composed of a material having good moderating properties or neutron-thermalizing properties. The fissionable material is dispersed within a microporous carrier material. The particle is adapted to prevent substantial initial escape of normally solid fission fragments by proper shaping and sizing or by encasing the fissionable material-containing portion of the particle in a shell of porous, solid material having a thickness of about 10 to 100 μ. A method for utilizing a mass of these particles in a reactor as a critical mass and as a contact mass for the conduct of chemonuclear conversions is described in detail. (B.L.M.)

16056 METAL-CLAD FUEL ELEMENT WITH COPPER FOIL INTERLAYER. Martin, W. R.; Weir, J. R. (to U. S. Atomic Energy Commission). U. S. Patent 3,230,150. Jan. 18, 1966.

Metal-clad reactor fuel elements which have a copper foil disposed between the cladding and the fuel core, such as stacked UO_2 pellets, to prevent permanent axial elongation of the fuel element are described. (AEC)

16057 FUEL ELEMENT FOR A NUCLEAR REACTOR. Mills, L. E.; Hauth, J. J.; Bloomster, C. H.; Carroll, D. F. (to U. S. Atomic Energy Commission). U. S. Patent 3,230,151. Jan. 18, 1966.

A fuel element for a nuclear reactor including a ceramic fuel containing a relatively low amount of fissionable material having an axial void therein and a slender wire of metallic fuel containing a relatively high amount of fissionable material disposed in the axial void, the axial void being substantially larger than the wire, is described. (AEC)

16058 COMPARTMENTED NUCLEAR REACTOR FUEL ROD AND METHOD OF MAKING. Kerze, F. Jr. (to U. S. Atomic Energy Commission). U. S. Patent 3,230,152. Jan. 18, 1966.

Compartmented nuclear reactor fuel rods are described in which the fuel is in pellet form. The fuel rod consists of an elongated tubular cladding having dished spacing disks whose peripheries are in wedged contact with the interior wall of the cladding thus forming longitudinal compartments for the fuel pellets. The purpose of compartmenting the fuel is to prevent ratchetting or movement of the fuel pellets which can lead to fuel rod distortion during thermal cycling. (AEC)

Power and Power-Breeder Reactors

Refer also to abstracts 14946 and 15717.

16059 (ACNP–65600) PATHFINDER ATOMIC POWER PLANT. FLOODING COEFFICIENT, CORE PRESSURIZATION, AND TEMPERATURE COEFFICIENT TESTS. Smith, J. A.; Fisher, J. R.; Lacy, P. S. (Allis-Chalmers Mfg. Co., Bethesda, Md. Atomic Energy Div.). Nov. 30, 1965. Contract AT(11-1)589. 30p. Dep. mn. CFSTI $2.00 cy, $0.50 mn.

For Northern States Power Co., Minneapolis, Minn. and Central Utilities Atomic Power Associates.

Testing activities on the flooding coefficient, core pressurization, and temperature coefficient of the Sioux Falls reactor with a hot or cold core are reported, for pressures and temperatures from ambient to 550 psi and 480°F. (T.F.H.)

16060 (ANL–7152, pp 1-49) LIQUID-METAL-COOLED REACTORS. (Argonne National Lab., Ill.).

Improvements in various components of the EBR-II are discussed. Power distributions and reactivity worth calculations were made in the ZPR-III, ZPR-VI, and ZPPR critical assemblies. Research on fast reactor fuel development and processing is presented. A brief discussion of progress in the sodium technology program is included. (M.O.W.)

16061 (BAW–296) RADIOCHEMISTRY OF NUCLEAR FUELS. Quarterly Progress Report No. 3, February 1, 1965–April 30, 1965. Bishop, W. N.; Dewell, E. H. (Babcock and Wilcox Co., Lynchburg, Va.). Contract AT(30-1)-3376. 43p. Dep. mn. CFSTI $2.00 cy, $0.50 mn.

Problems involved in calculating reactor fuel burnup were studied, and equations that relate the experimental measurements to burnup were derived. The conditions that are required for using simplified expressions for burnup are given. The neutron flux and exposure time conditions under which several possible burnup monitors are useful were determined. The parameters whose errors significantly affect the error in burnup were found for various exposure conditions and for several monitors. (auth)

16062 (CVNA–175) CVTR CONTROL ROD PERFORMANCE TEST. Kortheuer, John (Carolinas Virginia Nuclear Power Associates, Inc., Parr, S. C.). Apr. 8, 1963. 42p.

The data that were taken during the precritical control rod performance test at the CVTR are presented. (D.C.W.)

16063 (CVNA–241) CVTR ORGANIC LOOP FEASIBILITY XTUDY. Carolinas Virginia Tube Reactor Post-Construction Research and Development Program, Task CVPC-32. Smith, J. Ed.; Alligood, Fred M. (Carolinas Virginia Nuclear Power Associates, Inc., Parr, S. C.). [nd]. Contract AT(30-1)-2289. 19p. Dep. mn. CFSTI $1.00 cy, $0.50 mn.

The results of a preliminary study on the feasibility of installing an organic cooled loop in the CVTR are presented. A feasible loop with areas designated for equipment location and an approximate time and cost analysis for its installation are described. (M.O.W.)

16064 (EUR–2420.d,f,i,n,e) INSTRUMENTATION AND CONTROL IN THE GARIGLIANO AND LATINA NUCLEAR POWER PLANTS. (European Atomic Energy Community). Oct. 1965. 248p. (In German, French, Italian, Dutch, and English). Dep. mn.

Separate abstracts were prepared for the 10 included papers. (M.O.W.)

For abstracts of individual papers see: 16065–16074.

16065 (EUR-2420.d,f,i,n,e, pp 17-49) LA STRUMENTAZIONE "IN-CORE" DEL REATTORE DELLA CENTRALE SENN DEL GARIGLIANO. (In-Core Instrumentation for the Reactor of the SENN Power Plant at Garigliano). Di Grazia, Giovanni (FIAT, Turin (Italy). Sezione Energia Nucleare).

The in-core instrumentation fitted in the 150 Mw(e) SENN reactor and consisting of 80 fission microchambers is described. A description of the devices for manipulating

and counting the Ti-Cu wires used to determine the axial power pattern in the microchamber position necessary for calibration operations, and also the procedure adopted for carrying out the calibration itself is included. In addition, there is a description of the method used to introduce this instrumentation into the safety device and the method followed in calculating the burnout ratio, using this instrumentation. (auth)

16066 (EUR-2420.d,f,i,n,e, pp 51-115) L'AUTOCONTROLLO DELLA CENTRALE DI LATINA. (Controls for the Latina Power Plant). Dondi, Giovanni (European Atomic Energy Community, Ispra (Italy). Joint Nuclear Research Center).

A detailed description is given of the three control circuits of the Latina power plant and of their behavior in various operational conditions. An analysis of the safety problems bound up with the functioning of the autocontrol is presented. A compilation of certain characteristics of autocontrol parameters and a review of the test program scheduled for its coming into service are included. (auth)

16067 (EUR-2420.d,f,i,n,e, pp 117-31) AUTOMATISMES-SECURITIES-SALLE DE COMMANDE DE LA CENTRALE DE LATINA. (Automatic Devices-Safety Equipment-Control Room of the Latina Power Plant). Grauvogel, Antoine (Electricite de France, Chinon).

Operation of the Latina Power Plant was investigated from the following three aspects; control, neutron measurements, and safety devices. Control is exercised from a central control room as regards supervision and general handling operations and from local panels as regards specific handling operations for each item of equipment. The neutron measurements involve a large number of chains the ranges and overlaps of which afford excellent knowledge of the reactor. The safety chains are set up from diagrams which are of a complex nature but make it possible to avoid unscheduled releases; various matching-up systems are used and by means of three identical chains a two-out-of-three coincidence in the rod-drop order is achieved. (auth)

16068 (EUR-2420.d,f,i,n,e, pp 133-45) CONTROLE NEUTRONIQUE DU REACTEUR DU GARIGLIANO. (Neutronic Control of Garigliano Reactor). Lafaurie, Denis (Compagnie Francaise Thomson-Houston, Paris).

The reactor's nuclear control gear and the principles on which it operates are described. In particular, discussions are presented on: (1) the out-of-core neutron power measurement systems, which are used for piloting the reactor during startup and power run-up, certain of them also serving as safety devices during operation at rated power, (2) the in-core flux measuring instruments, which constitute an innovation in neutronics control, and make for rationalized use of fuel, and (3) environmental radioactivity measurements for surveillance and health and safety purposes. Flow schemes and layout diagrams are included. (auth)

16069 (EUR-2420.d,f,i,n,e, pp 147-80) SISTEMA BARRE DI CONTROLLO DEL REATTORE SENN. (Control Rod System for the SENN Reactor). Leonelli, Franco (European Atomic Energy Community, Ispra (Italy). Joint Nuclear Research Center); Nicoloso, Ennio (Ente Nazionale per l'Energia Elettrica, Latina (Italy)).

The main facts concerning the control rod system at the SENN Garigliano power plant are presented. The subject is treated in three sections—a description of the system and its various component parts, a description of its operation, both electrical and hydraulic, and an analysis of possible breakdown in the system. The action to take in the event of various possible failures is discussed. (auth)

16070 (EUR-2420.d,f,i,n,e, pp 181-9) DETECTION DE RUPTURES DE GAINES DANS LA CENTRALE DE LATINA. (Detection of Can Ruptures in the Latina Power Plant). Menetrey, Maurice (Electricite de France, Chinon).

The burst-slug detection system comprises altogether nine detection instruments (6 normal detectors, 1 "DRGG" [general burst slug detection] detector and 2 repeaters). Detection is effected by the collection of radioactive ions on an electrically charged wire. The gas drawn off in each channel by a double annular sampler is switched to a detector by means of two pneumatic selectors. The primary selector is located in the charging plug itself, so that the number of tubes issuing from the reactor is very small. All counts performed by the detectors are relayed to recorders installed in the control room. When a detector gives an alarm the defective cluster is switched manually to repeater from the secondary selector station; identification of the defective channel takes place on two cycles. (auth)

16071 (EUR-2420.d,f,i,n,e, pp 191-202) BESCHREIBUNG EER TURBINENREGELUNG UND ERFAHRUNGEN IM SENN-KRAFTWERK BEI DER INBETRIEBNAHME DER TURBINE. (Description of the Turbine Regulation and Experience at SENN Power Station on Turbine Startup). Staebler, Karl (Bayernwerk, A. G., Munich (West Germany)).

The three-casing, single-shaft turbine in the SENN atomic power plant is supplied with primary steam at 70 atm. over from a boiling water reactor and also with secondary steam via a condensate circuit and steam generator. One feature of twin-cycle boiling water reactors is that the generation of heat can be regulated above a certain power (about 70% full-load) by changing the quantity of secondary steam, without necessitating regulation of the neutron flux in the core by means of the control rods. The reactor pressure is maintained constant by adjusting the primary steam valves and, if necessary, opening a bypass valve to the condenser. The regulating equipment also includes devices for aperture control and revolution adjustment (synchronizer) and a centrifugal governor. The turbine, condenser and generator are protected by control devices in the turbine valves, the reactor and the generator output switch. (auth)

16072 (EUR-2420.d,f,i,n,e, pp 203-14) CONSIDERAZIONI SULL'ESERCIZIO DELLA CENTRALE DI LATINA IN FUNZIONE DELLE SUE CARATTERISTICHE DI REGOLAZIONE. (Considerations of Regulating Characteristics During the Operation of the Latina Power Plant). Valant, Paolo (Comitato Nazionale per l'Energia Nucleare, Rome (Italy)).

A description is given of the regulating system at the Latina power plant, together with some observations on the requirements called for by the characteristics of the electric grids and by operation of the power plant. The capacity of this type of plant to bear abrupt load changes and to provide the initial load increases and modulations over long and short periods is discussed. In addition, it is shown that for present requirements the Latina plant, and indeed virtually all existing nuclear power plants, will be called upon to provide a basic service for demands of a strictly economic nature. There are, however, good prospects that power reactors of this type will take part in the frequency regulation of the entire grid, especially when, in the not far distant future, a considerable number of power plants will be capable of performing this task, so that the burden will be less heavy than it is today. (auth)

16073 (EUR-2420.d,f,i,n,e, pp 215-25) REGOLAZIONE DELLA POTENZA PER CENTRALI ELETTRONUCLEARI DEL TIPO BWR-CICLO DUALE-CENTRALE DEL GARIGLIANO. (Regulation of the Output of a Electronuclear Power Plant of the BWR-Type Dual-Cycle Garigliano Power Plant). Valant, Paolo (Comitato Nazionale per l'Energia Nucleare, Rome (Italy)).

The possibilities of regulating the output of BWR dual-cycle power plants are discussed. An automatic control system is described. In particular, an out-line is given of the characteristics of the regulation and control system in the SENN plant with special attention being devoted to the turbine regulation system, whose various preventive devices and safeguards are analyzed. Finally, mention is made of several operations of a more critical nature, such as the controlled startup and shutdown of the reactor and the method of operating the system in exceptional cases such as an unscheduled pressure drop, scram insertion, or low vacuum in the condenser. (auth)

16074 (EUR-2420.d,f,i,n,e, pp 227-48) THE CONTROL ROD DRIVE SYSTEM OF THE GARIGLIANO NUCLEAR POWER PLANT, SENN, ITALY. Staebler, Karl (Bayernwerk, A. G., Munich (West Germany)); Woldringh, Sebo H. (Samenwerkende Electriciteits-Productiebedrijven, N. V., Arnhem (Nederlands)).

A description is given of the control rod drive mechanism and the actuating hydraulic system as used in the Garigliano Nuclear Power Plant. The changes in this design with respect to the early offer as well as to the Dresden design are discussed. Before the preoperational test of the control rod drive mechanism, tests were performed on the actuating hydraulic system, using a dummy for the drive mechanism. These tests and the preoperational tests proper are described and the results, which were very successful, are given. Some evaluation of the safety of the mechanical and hydraulic systems will be presented; the influence of the malbehavior of these systems on the reactor plant are not analyzed, only some data on reactivities are given. In general it is thought that the control rod drive system is of reliable design and of good workmanship. (auth)

16075 (GAMD-6519) RAD 2: A COMPUTER PROGRAM FOR CALCULATING FISSION PRODUCT RADIOACTIVITIES. Vanslager, F. E. (General Atomic, San Diego, Calif. John Jay Hopkins Lab. for Pure and Applied Science). July 23, 1965. Contract AT(04-3)-167. 33p. Dep. mn. CFSTI $2.00 cy, $0.50 mn.

The computer program RAD 2, a FORTRAN IV program that is designed to calculate fission-product activity distributions in a high-temperature gas-cooled reactor system, is described. The equations used by the program are given, and a program listing is included. (D.C.W.)

16076 (JAERI-1088) FEASIBILITY CALCULATION FOR THE JPDR-II CORE DESIGN; ONE-DIMENSIONAL NUCLEAR THERMAL AND HYDRAULIC CALCULATION. Mochizuki, Kelichi; Ishikawa, Michio; Kuge, Yasushi; Kobori, Tetsuo; Naitoh, Yoshitaka (Japan Atomic Energy Research Inst., Tokyo). July 1965. 43p. (In Japanese). Dep. mn.

In connection with the project of doubling-up the power density of the JPDR core by changing from the natural circulation to the forced circulation, a feasibility study was carried out on the core nuclear thermal and hydraulic characteristics. "KYNAK" was employed for this survey calculation, which is the IBM 7044 computer code—one dimensional, nuclear thermal and hydraulic calculation of the forced—circulation BWR core. By changing the values of such parameters as thermal power, fuel rod diameter, coolant flow, and inlet subcooling, the optimum values of the parameters were obtained, which would satisfy the minimum burnout ratio, maximum fuel temperature, maximum heat flux, flow pressure drop through the core and k_{eff} in the specified design criteria. It was found from the calculations that the high power density desired was obtainable within the limitations specified by the design criteria, when using the fuel assembly of 7×7 or 8×8 small-diameter rods lattice, the coolant flow of $1.8 \sim 2.0$ m/sec and the core inlet enthalpy of $280 \sim 285$ kcal/kg. Calculations were also made of the optimum coolant flow distribution in the core and the pumping power required by the forced circulation when the power was 90 Mw thermal. (auth)

16077 (NAA-SR-11628) PIQUA NUCLEAR POWER FACILITY REACTOR OPERATIONS ANALYSIS PROGRAM. Semiannual Progress Report No. 6, January 1–June 30, 1965. Cataldo, H.; DeBear, W. S.; Fukushima, T. Y.; Jenkins, O. G.; Lew, D. E.; Mills, R. M.; Perret, J. D.; Rubinstein, H. J.; Shepard, R. C. (Atomics International, Canoga Park, Calif.). Dec. 15, 1965. Contract AT-11-1-GEN-8. 134p. Dep. mn; CFSTI $4.00 cy, $1.00 mn.

Seven sections are included; separate abstracts have been prepared for all. (T.F.H.)

For abstracts of individual sections see: 16078–16084.

16078 (NAA-SR-11628, pp 9-16) REVIEW OF OPERATIONS. (Atomics International, Canoga Park, Calif.).

A resume is presented in tabular and graphic form of the operation of PNPF. (T.F.H.)

16079 (NAA-SR-11628, pp 17-50) NUCLEAR ANALYSIS. (Atomics International, Canoga Park, Calif.).

The Piqua reactor reactivity history, the differences between experimental and theoretical determinations of the parameters of its core, core changes and manipulations, power variations, coolant impurity levels, fuel-element temperatures, and scram experiences are tabulated and discussed. (T.F.H.)

16080 (NAA-SR-11628, pp 51-78) SYSTEMS AND COMPONENTS ANALYSIS. (Atomics International, Canoga Park, Calif.).

Analyses are reported of the PNPF main heat-transfer system; the performance of the in-vessel and degasifier filters; the operations of the coolant distillation system, the waste-fired boiler, the aqueous-waste and waste-gas systems, and failed-element location systems; and the radiation levels around the plant. (T.F.H.)

16081 (NAA-SR-11628, pp 79-104) COOLANT CHEMISTRY AND ANALYSIS. (Atomics International, Canoga Park, Calif.).

PNPF coolant chemistry parameters are reviewed and tabulated from startup through May 1965. (T.F.H.)

16082 (NAA-SR-11628, pp 105-7) EFFECT OF OXYGEN ON IRRADIATED COOLANT. (Atomics International, Canoga Park, Calif.).

A sample of irradiated Piqua reactor coolant is oxidized for 24 hr at 160°C; the oxidation is then continued at various temperatures for varying durations. The effects of this oxidation on carbonyl-bound oxygen contents, total oxygen contents, and colloidal-particle contents are measured. (T.F.H.)

16083 (NAA-SR-11628, pp 108-23) POST-IRRADIATION EXAMINATION OF FUEL ELEMENT P-1091 (F-13). (Atomics International, Canoga Park, Calif.).

The fuel element in question is one removed from PNPF following a history of steadily increasing outlet temperature and relative power. The inspections and measurements carried out include gross observations, dimensional variations, density variations, metallographic characteristics, and gamma-scan activities. (T.F.H.)

16084 (NAA-SR-11628, pp 124-34) EXAMINATION OF SECOND SET OF IN-VESSEL FILTERS. (Atomics International, Canoga Park, Calif.).

The PNPF organic coolant is filtered upstream of the core by means of 67 glass-fiber cartridge filters. The second complete loading of filters operated for 2559 Mwdt before the filter pressure-drop reached the excessive value of 10 psi, whereupon 15 filters were replaced and inspected. Examination results on these filters are given. (T.F.H.)

16085 (SWRI-1228-4-15) EVALUATION OF THE SERVICEABILITY OF THE ELK RIVER REACTOR PRESSURE VESSEL. Quarterly Report, October 1, 1965–December 31, 1965. Lautzenheiser, C. E. (Southwest Research Inst., San Antonio, Tex.). Jan. 20, 1966. Contract AT(11-1)-1228. 18p. Dep. mn. CFSTI $1.00 cy, $0.50 mn.

A study of the effect of neutron irradiation on the tensile properties, nil-ductility transition temperature, and low-cycle fatigue strength of the vessel steels and dissimilar welds is outlined, and the status of ultrasonic equipment for the inspection of nozzle areas is summarized. (D.C.W.)

16086 (TID-22651) ADDITIONAL CRITICAL HEAT FLUX DATA FOR LARGE DIAMETER, INTERNALLY HEATED, ECCENTRIC ANNULI AT 1000 PSIA. Topical Report No. 8. Matzner, Bruce; Casterline, J. E. (Columbia Univ., New York. Dept. of Chemical Enginering). Jan. 21, 1966. Contract AT(30-3)-187. 16p. Dep. mn. CFSTI $1.00 cy, $0.50 mn.

The critical heat flux of the following two test sections was investigated; (1) eccentricity of 42% (0.060" minimum gap) of the 3.8" heater in the 4.0" housing tube, and (2) eccentricity of 42% of the 3.8" heater in the 4.0" housing tube with a roughened housing tube wall in the form of 0.035" high stripping rings placed 3.5" apart. The results are presented. (M.O.W.)

16087 (TRG-Report-1115) ECONOMICS OF ALTERNATIVE NUCLEAR POWER PROGRAMMES BASED ON GAS-COOLED GRAPHITE AND FAST REACTORS. Iliffe, C. E. (Reactor Group, United Kingdom Atomic Energy Authority, Risley (England)). 1965. 53p. Dep. BIS $1.60. HMSO 8s.

The DISCOUNT computer program was used to evaluate discounted unit costs and minimum plutonium selling prices for various alternative nuclear power programs. The buildup of plutonium stocks and the installed capacity of different reactor types, with their load factors, is also given. The reactor types involved are Magnox, Large Magnox, A.G.R. and the Fast Reactor. The lowest discounted unit cost is obtained when the 5000 Mw(e) Magnox program is followed by A.G.R.s and carbide-fueled fast reactors. If nuclear power expands only to take up the base load, this lowest cost is 0.465 d/u.s.o. If all conventional stations are ultimately replaced by nuclear ones, the cost is 0.509 d/u.s.o. These costs increase by 0.021 and 0.015 d/u.s.o. respectively when the carbide fuel at 5% burnup is replaced by a 60% stainless steel/oxide cermet at 10% burnup. Also, the cermet-fueled fast reactors require at least as many A.G.R.s to support them while the carbide-fueled fast reactors can ultimately dispense with thermal reactor support altogether. A further replacement of the cermet-fuled fast reactors by plutonium-burning A.G.R.s leads to further increases in discounted unit cost of over 0.03 d/u.s.o. An estimate is given of the reductions in discounted unit cost on reducing the stainless steel (S.S.) content of the cermet fuel or doubling the burnup of the carbide fuel. The effect of interest rate and order of load factor is also considered. A comparison is made between fast reactor unit cost based on a fixed value of plutonium and discounted unit cost. Both are found to vary in a similar manner with changes in fast reactor specification. The proportion of electricity generation from fast reactors is plotted against inverse doubling time and plutonium inventory and enables rapid estimates to be made of discounted unit cost. Minimum selling prices for plutonium are determined for each nuclear power program for various quantities of plutonium sold. The effects on these prices of reactor capital costs, order of load factor and interest rate are also considered. (auth)

16088 (WAPD-299) DECONTAMINATION OF THE SHIPPINGPORT ATOMIC POWER STATION. Abrams, C. S.; Salterelli, E. A. (eds.) (Bettis Atomic Power Lab., Pittsburgh, Pa.). Jan. 1966. Contract AT-11-1-GEN-14. 81p. Dep. mn. CFSTI $3.00 cy, $0.75 mn.

A description of the decontamination system is presented. The various operations of the system are described. Data taken prior, during, and after decontamination point out the effectiveness of the decontamination process. (M.O.W.)

16089 (WAPD-MRP-114) PRESSURIZED WATER REACTOR (PWR) PROJECT. Technical Progress Report, July 24–October 21, 1965. (Bettis Atomic Power Lab., Pittsburgh, Pa.). Contract AT(11-1)-Gen-14. 104p. Dep. mn; CFSTI $2.50 cy, $0.75 mn.

Trends in PWR core flow and pressure drop, ascribed to the deposition of corrosion products in coolant channels, are measured and evaluated. PWR Core 2 is taken to full power, 150 Mw(e) equivalent, with agreement between predictions and measurements made by core instrumentation. The core power capability is evaluated to assure satisfactory operation at full power. It is established that FEDAL system flow rate affects core thermocouple accuracy. A study is completed, which shows little gain achievable by resetting blanket orifices. An attenuation factor to apply to pressure waves resulting from check valve closure is evaluated for application to stress analysis of the fuel clusters. Six PWR Core 2 Seed 1 plate elements are irradiated through 405 power cycles with no loop activity bursts. Preliminary visual inspection indicates no cladding rupture or excessive clad bulging. Analysis of the beginning-of-life cold, clean criticality physics tests using both the conventional and the TNT02 synthesis techniques is completed. The opposite variation in calculated eigenvalue as a function of controlling rod bank height exhibited by the two methods is seen to result from the relative difference in differential reactivity worths. Power operation with Core 2 continued until October 13, 1965, when the reactor was shut down and a series of periodic physics tests initiated. PWR-2 Seed 2 plate elements continue to behave as predicted in the VH-3 irradiation loop. Metallographic examination of PWR-2 Seed 2 poison plates, designed with interlocking hooks to provide internal void spacing, shows a single brittle crack at the base of the hooks. This has no detrimental effect on plate operation. (auth)

16090 (WAPD-T-1841) PRESCRIPTION FOR DIFFUSION THEORY REPRESENTATION OF FUEL CLUSTERS CONTAINING CONTROL RODS BASED ON MONTE CARLO CORRELATION OF CAPTURE PROBABILITIES. Flanagan, Charles A. (Bettis Atomic Power Lab., West Mifflin, Pa.). Nov. 1965. Contract AT-11-1-GEN-14. 18p. (CONF-651101–69). Dep. mn. CFSTI $1.00 cy, $0.50 mn.

From 13th Conference on Remote Systems Technology, Washington, D. C.

A method is described for force fitting P-1 approximation calculations which contain explicitly represented control rods by correlating capture probabilities determined by Monte Carlo calculations. The method is empirically based. The method, where tested, appears to improve calculational results in two- and three-dimensions relative to experiment. (auth)

16091 (WCAP–6078) YANKEE CORE EVALUATION PROGRAM. Semi-Annual Progress Report for the Period Ending September 30, 1965. O'Boyle, M. J. (comp. and ed.) (Westinghouse Electric Corp., Pittsburgh, Pa. Atomic Power Div.). Oct. 1965. Contract AT(30-1)-3017. 65p. Dep. mn; CFSTI $3.00 cy, $0.75 mn.

The irradiation and testing of fuel elements to high burnups in Yankee Power Reactor is summarized. The objectives of the studies reported are to analyze the Yankee Core I performance, and to reconcile the theoretical and experimental determinations of this performance. (T.F.H.)

16092 THE WINDSCALE ADVANCED GAS-COOLED REACTOR. Andrews, J. S. V. Energie Nucl., 7: 410-17(Nov. 1965).

The design of the Windscale A.G.R. and its auxiliary equipment are discussed, and an account is given of the commissioning of the reactor and of its operation over two-and-a-half years to the autumn of 1965. The experimental work carried out is outlined, with special reference to the satisfactory behavior of the fuel. Finally an indica- is given of possible future developments in gas-cooled reactor technology arising from this work. (auth)

16093 DEPENDENCE OF BREEDING UPON SOME DESIGN PARAMETERS OF LARGE FAST REACTORS. Moorhead, T. P.; Belcher, A. S. B. (Atomic Energy Research Establishment, Winfrith, Eng.). EuroNuclear, 2: 599-603(Dec. 1965).

The dependence of breeding upon some of the more important reactor parameters is examined, an important general design requirement for good breeding is deduced, and breeding in oxide and carbide fuels is compared. The results were obtained from a number of closely related computer cases, in which chosen parameters were altered one at a time, and the fuel enrichment, Pu in (U + Pu), adjusted to maintain criticality. It is generally concluded that for the type of system studied any effect which tends to increase enrichment or to soften the spectrum also worsen breeding, and vice versa. (J.F.P.)

16094 DODEWAARD NUCLEAR POWER STATION. Mostert, P. EuroNuclear, 3: 37-40(Jan. 1966).

The design and construction of the 50-Mw(e) boiling-water Dodewaard Nuclear Power Station is discussed. The reactor has a single direct primary circuit in which steam from the reactor goes directly to the turbine. The Zircaloy-2-clad UO_2 fuel elements are cooled by natural convection, which is increased by a "chimney" on top of each group of four elements. The core consists of 156 fuel elements and 37 control rods. For reactor containment the pressure suppression system is used. (M.C.G.)

16095 SECONDARY SHUTDOWN SYSTEMS OF NUCLEAR POWER REACTORS. Walker, C. S. Nucl. Safety, 7: 45-52; 62-4(Fall 1965).

Current practices regarding secondary shutdown systems in a large sample of reactors in the United States, the United Kingdom, France, and Canada are summarized. Most of the reactor facilities examined are equipped with alternate shutdown devices, designated as secondary shutdown systems; however, there is a rather large variation in the independence and performance of the actual systems employed. Also, basically similar systems, such as those for injecting boron solutions into water-moderated reactors, vary greatly with respect to procedures and time intervals required to complete operation. Not all the reactors examined have secondary shutdown systems, and there is no simple manner of determining whether a particular reactor needs a secondary shutdown system. (auth)

16096 TESTING OF CONTROL-ROD DRIVES. Bates, A. E. G. Nucl. Safety, 7: 57-62; 65-6(Fall 1965).

Control-rod-drive development and testing programs for a number of representative power reactors indicated that satisfactory rod drive may require an expensive and lengthy program. The predominant difficulties encountered were associated with "old art" rather than with the effects of nuclear radiation. Development programs will probably be required for each new type of power reactor. A versatile test stand is essential, but satisfactory completion of required tests does not guarantee trouble-free operation. (auth)

16097 NPD REACTOR OPERATING EXPERIENCE. Hake, G. (Atomic Energy of Canada Ltd., Chalk River). Nucl. Safety, 7: 106-13; 134(Fall 1965).

The performance of the NPD reactor up to the end of 1964 is reviewed. The reactor was built to demonstrate the concept of a pressure-tube reactor cooled and moderated with heavy water and fueled with natural uranium. The operation demonstrated a high station-capacity factor and the satisfactory conservation of heavy water. The design is shown to be sound and the reactor safe. Safety features characteristic of Canadian reactors are identified, and component performance and failures are discussed. Improvements made to the station are described. The adoption of the "dry-room" principle is considered one of the most important in that both heavy-water losses and the tritium hazard were reduced. (auth)

16098 BONUS SUPERHEATER FAILURE. King, E. M.; Long, E. L. Nucl. Safety, 7: 113-18; 134-5(Fall 1965).

On Nov. 11, 1964, while operating at about 5 Mw, BONUS recorded a power transient when the steam flow was reduced for about 2½ min as a result of operator error. Subsequently, fission-product-activity levels increased in several locations. There was no significant exposure to BONUS plant personnel nor to off-site personnel; there was no significant release of radioisotopes to the surrounding area. A failed superheater assembly was located by a series of radiation surveys within the reactor vessel, and the assembly was shipped to ORNL for examination. Hot-cell examination revealed that two fuel rods in the assembly had swollen on the diameter the entire length of the cladding and that one of these had an 11.5-in. rupture near the bottom end. In addition, an assembly that had never been placed in reactor service was examined. The most significant observations that could be related to failure of the rods involved the weldments. Metallographic examination revealed hot cracks (i.e., cracks that formed during welding) in the vent-plug welds. Since the defects in the welds afforded continuous paths from the interior to the exterior of the fuel rods, it was possible to conclude that the failures experienced were of a waterlogging type that occurred during the transient. (auth)

16099 NUCLEAR FUELS. Prakash, Brahm (Atomic Energy Establishment, Trombay, Bombay). Trans. Indian Inst. Metals, 17: 1-4(Mar. 1964).

Experience in the development of nuclear power reactors in India is considered from the point of view of fuel element problems. The choice of fuel for a particular nuclear reactor is discussed. Ideally, cost of first fabrication should be low; the fuel should be capable of releasing heat at high temperatures and undergo no perceptible change in its dimensions in the reactor; it should give a high burnup; and the discharged fuel should be capable of reprocessing at low costs to recover the residual fissile material in it. Relative advantages and problems with ^{233}U, ^{235}U, and ^{239}Pu are discussed. The nuclear power generation program in India is envisaged to develop in three stages: first-generation reactors based on natural U, which will provide Pu as a by-product; second generation reactors to be converters (Pu-Th), which will produce power and yield fissile ^{233}U as a by-product; and third generation reactors to be breeders (^{233}U, Th), which will generate power and produce more ^{233}U than they will consume. For application in low-temperature Pu-producing reactors, with or without power generation, and for research reactors such as the CIR (Canada-India Reactor), unalloyed β-quenched U possesses excellent nuclear properties and reasonably good mechanical and physical properties. Fuel elements for the CIR are in regular production. The processes in their fabrication are outlined. It was decided to set up a Candu type (200 Mw(e)) nuclear power plant at Rana Pratap Sagar, Rajasthan, in collaboration with Canada. This reactor will be fueled with natural UO_2 and will use heavy water as a moderator and as coolant. The UO_2 in the fuel elements will be in the form of sintered pellets canned in Zircaloy tubes. Procedures for fabricating the pellets are described. In reactors operating on enriched UO_2, much higher burnups can be obtained. Thus a minimum fuel burnup of 16,500 Mwd/Te is specified for the 380 Mw(e) Tarapur Power Station, which will use an enrichment of about 2.23%, and will be moderated and cooled with ordinary water. The Candu type reactor in Rajasthan and Tarapur Reactor will yield high-burnup plutonium, so that remote fabrication methods are being adopted for its safe handling. Because of India's thorium deposits, the Th-^{233}U cycle is being considered. (BBB)

16100 FABRICATION PROCEDURES FOR ENRICO FERMI FAST BREEDER REACTOR FUEL ELEMENTS. Donnelly, R. G.; Thurber, W. C.; Slaughter, G. M. (Oak Ridge National Lab., Tenn.). Weld. J. (N. Y.), 44: 1027-34(Dec. 1965). (ORNL-P-931).

A program was carried out to develop procedures for fabricating the proposed Core B fuel element of the Enrico Fermi Fast Breeder Reactor. The element consists of fourteen 0.112-in.-thick fuel plates spaced 0.054-in. apart to form a rigid bundle 2.270 in. high × 2.386 in. wide × 20.094 in. long fabricated to extremely close tolerances. The attachment of a multiplicity of additional components, such as spacers, bushings, wear balls, and seal strips, was also required. Over 100 individual parts were joined for each fuel element in a single brazing operation. A total of six dummy solid stainless steel and seven prototype elements containing depleted UO_2 was successfully fabricated by furnace brazing. A nickel-chromium-silicon brazing alloy chosen for this application met all brazing, corrosion, strength, and nuclear requirements. Special techniques were developed to obtain the close tolerances desired, and special procedures were conceived for inspecting the various critical dimensions of the element. (auth)

16101 TRANSIENT DNB TEST ON CVTR FUEL ASSEMBLY. Tong, L. S. (Westinghouse Electric Corp., Pittsburgh); Bishop, A. A.; Casterline, J. E.; Matzner, B. New York, American Society of Mechanical Engineers, 1965, Preprint No. 65-WA/NE-3, 6p., $1.50. (CONF-651110-18). ORINS.

From American Society of Mechanical Engineers, Annual Winter Meeting, Chicago.

Transient DNB was tested on an electric heater mockup of a CVTR fuel assembly under two types of transient conditions. The power transient of a reactivity accident was simulated by a ramp increase of electric power to the heaters. The flow transient of a loss of flow accident was sim-

ulated by a controlled flow coast down in a testing loop. The data of the steady state DNB tests are all greater than the predicted value based on the W-2 modified correlation. The power transient test results indicate that the CVTR reactor, operating at 65 MWt with 80 percent flow, can stand a power excursion of 40 percent without reaching DNB. The flow transient test results indicate that the CVTR reactor, operating at 65 MWt continuously without power decay, can stand a flow coast down up to 10 sec without reaching DNB. The results with power decay (reactor scram) are even more encouraging. The test section can operate at 67 percent overpower and then experience a flow coast down without reaching DNB. (auth)

16102 OPERATING METHOD FOR A FAST BREEDER REACTOR AS A POWER REACTOR. (to Walther and Cie. AG). French Patent 1,190,253. Oct. 12, 1959. Priority date Jan. 18, 1957, Germany.

The fast breeder reactor vessel is filled with a liquid fissile material in the form of a molten metal, metal alloy, suspension or molten salt. Through the vessel the coolant is passed in pipes for the purpose of withdrawing the heat generated by the nuclear reaction. The major part of the fissile material is retained in the reactor vessel and a minor part is withdrawn therefrom for purification and regeneration, to be returned to the vessel after this operation. The amount withdrawn and returned is sufficient to ensure that the concentration of the fissile material remains approximately at its original level and that the concentration of the fission products is maintained at a constant low level. The reactor vessel is blanketed by a breeder vessel containing the fertile material in liquid form and is also fitted with cooling pipes. (IIB)

16103 METHOD OF OBTAINING A UNIFORM OUTPUT DENSITY IN GAS-COOLED HIGH TEMPERATURE NUCLEAR REACTORS. (to Brown, Boveri and Cie, AG). French Patent 1,305,299. Aug. 20, 1962. Priority date Mar. 4, 1961, Germany.

In nuclear reactors in which shaped bodies containing fissile material are used, this fissile material forms a mound or heap. The neutron density at the center of the mound is, for geometrical reasons, greater than that in the peripheral zones, since the product of neutron density and microscopic local fission cross section is proportional to the local output density. In order to obtain a maximum total output, the angle of slope of the mound should be reduced. This is achieved by discharging the shaped bodies downwardly through a discharge duct which is disposed in the axis of the cylindrical core. As long as no fresh shaped bodies are added from above during the discharge, the upper sloping cone of the mound collapses first, and a substantially plane shape of the surface is obtained. (IIB)

16104 NUCLEAR REACTOR WITH ASYMMETRICAL POWER RATING DISTRIBUTION. (to General Electric Co. Ltd.). French Patent 1,351,029. Dec. 23, 1963. Priority date Mar. 13, 1962, Great Britain.

It has been the practice in gas-cooled nuclear reactors to maintain a symmetrical power rating distribution in the direction of coolant flow approximating a cosine law. This power distribution is quite impossible to obtain in practice. According to the invention neutron absorbing rods are disposed in passages formed in the core in order to control the neutron flux within the core so as to maintain a desired power rating distribution. These rods are suspended by wires from hoists whereby their axial position can be adjusted. Without the rods the neutron flux, and hence the power rating, would tend to be symmetrical in the axial direction. It is found that if the rods are 0.65 L in length, where L is the length of the core passages, and are placed so that their centers are at a distance of 0.65 L from the lower face of the core then the power rating is suitably asymmetrically distributed; in this way the total power output can be increased by about 7% for a constant coolant mass flow. (IIB)

16105 BOILING WATER NUCLEAR REACTOR WITH BREEDER BLANKET SUPERHEATER. Bryan, Roland T. (to Babcock and Wilcox Co.). U. S. Patent 3,228,846. Jan. 11, 1966. Filed Mar. 6, 1961.

A boiling water reactor includes a pressure vessel having an upper steam space and a lower water space with an upright core structure occupying a substantial volume within the water space. A number of removable solid fissile fuel elements are operably arranged in the core chamber to release heat during the chain reaction. A number of steam and water separating devices are superjacent to the core chamber. A closed fertile material blanket chamber longitudinally embraces the core chamber. A number of fuel elements are arranged to operate in the blanket chamber to emit heat in the presence of a high neutron flux. Steam conduit means pass steam from the steam and water separating devices through the blanket chamber where the heat from the fuel elements superheats the steam and cools the fertile material. (B.L.M.)

16106 NUCLEAR REACTOR PLANT. Kaegi, Jakob (to Sulzer Freres, S.A.). U. S. Patent 3,231,475. Jan. 25, 1966. Priority date May 17, 1960, Switzerland.

A nuclear plant includes a heterogeneous reactor in which the fuel elements are cooled by a vapor that is vaporized outside the reactor and that leaves the reactor at a temperature considerably higher than that for conventional plants of this type. At least two groups of cooling conduits are provided in the reactor. Vapor is supplied from the evaporating means to the first group of cooling conduits. After superheating in the first group, the superheated vapor is conducted by means of a pipe to the second group of cooling conduits for further superheating prior to discharge to a heat consumer. Additional conduit means are provided for conducting some of the vapor superheated in the first group of cooling conduits to the evaporating means for evaporating the liquid operating medium. (B.L.M.)

Process Heat Reactors

16107 (JPRS-33406) THE USE OF REACTORS OF THE BELOYARSK ATOMIC POWER PLANT TYPE FOR DUAL-PURPOSE DESALINIZATION SYSTEMS. Koryakin, Yu. I.; Loginov, A. A.; Mikhan, V. I.; Monchinskii, A. G. Translation of paper No. SWD/57 presented at the First International Symposium on Desalination of Water, Washington, D. C., October 3–9, 1965. 15p. (TT–65–33980). CFSTI $1.00 cy, $0.50 mn.

An evaluation of the power potentialities and economic indices of reactors of the Beloyarsk type gives grounds to consider these reactors to be very promising for a combined production of electric power and desalted water, especially under the conditions when these two types of the product are equally important and necessary. (auth)

16108 (JPRS-33459) THE APPLICATION OF NUCLEAR POWER INSTALLATION FOR WATER DESALINATION WITH SIMULTANEOUS PRODUCTION OF ELECTRIC POWER. Dmitriev, I. D. Translation of paper No. SWD/72 presented at the First International Symposium on Desalination of Water, Washington, D. C., October 3–9, 1965. 12p. (TT–65–34033). CFSTI $1.00 cy, $0.50 mn.

Among the versions under investigation utilizing turbines with controllable steam diversion, the most convenient seems to be the atomic energy station with fast neutron reactors producing desalinated water at a cost of 4.5 kop/m^3. The calculations do not pretend to shed complete light on the question under investigation, and consequently cannot be extended to all specific cases of fresh water production by means of nuclear reactor heat. (auth)

16109 THE U. S. HEAVY WATER-ORGANIC COOLED REACTOR PROGRAMME AND CANADIAN-U.S. CO-OPERATION. Ramey, James T. Nucl. Energy, 348-53 (Nov.-Dec. 1965).

The evolution, developmental status, and potential as an economic energy source of the heavy water-moderated, organic-cooled reactor concept are considered. Reference

designs are being prepared for a 1000 Mw(e) power-only plant and an 8300 Mw(t) combination power-desalting plant. Studies are being made of SAP and zirconium alloys as fuel element cladding and pressure tube materials and of UO_2 and UC as fuel materials. It was concluded that the heavy water-moderated, organic-cooled reactor has the necessary potential for extrapolation to very large sizes. that it has good fuel utilization characteristics, that in sizes above 1000 Mw(t) the energy cost is low, and that it can be developed for economic commercial application by the mid-1970's. (M.C.G.)

Propulsion and Space

See also ENGINEERING — Space Propulsion

Refer also to abstracts 14727, 14785, and 15932.

16110 (AD–620650) OUT-OF-PILE THERMIONIC SPACE POWER SYSTEMS USING A GASEOUS HEAT-TRANSFER FLUID. Leonard, Anthony (RAND Corp., Santa Monica, Calif.). Sept. 1965. Contract AF49(638)-700. 50p. (RM–4469-PR). CFSTI $2.00 cy, $0.50 mn.

A study is made of the potential of space power systems composed of a high-temperature gas-cooled reactor and out-of-pile thermionic converters. Emphasis is placed on the creep-rupture problem and the optimization of the radiator-converter configuration. Expressions for thermionic-converter efficiency and power density as a function of emitter temperature and collector temperature are developed. For a system using 750-psi He at a maximum gas temperature of 3600°F, a specific mass of about 13 lb/kw is estimated, excluding power conditioner and shield masses. A 1000-psi system using Ne would have a specific mass of about 17 lb/kw. (TAB)

16111 (N65–16315) STUDY OF RANKINE-CYCLE SPACE NUCLEAR POWER SYSTEMS. Cox, A. Lucile; Blanton, Roy W. Jr. (Brown Engineering Co., Inc., Huntsville, Ala. Research Labs.). Aug. 1964. Contract NAS8-5289. 230p. (NASA-CR-60553; R–113). CFSTI $6.00 cy, $1.25 mn.

The effects of various parameters on the specific weight are presented for a number of configurations and operating fluids. It is shown that when shielding for manned vehicles is required, the minimum specific weights occur at temperature ratios across the turbine much lower than the 0.75 generally found for unmanned systems. Suggestions for improved power systems are included. (STAR)

16112 (SC-RR–65-551) ROVER POSTOPERATIONAL DESTRUCT INSTRUMENTATION DEVELOPMENT. Berry, R. E.; Martin, J. P. (Sandia Corp., Albuquerque, N. Mex.). Dec. 1965. Contract AT(29-1)-789. 119p. Dep. mn. CFSTI $4.00 cy, $1.00 mn.

Development tests in preparation for a full-scale destruct test of the ROVER/NERVA space propulsion engine are reported. The development tests furnish the following information: the debris pattern from a four-explosive-charge scale model is a four-jet pattern with the jets originating at 45 degrees between the explosive charges; the debris size and distribution is repeatable and the size ranges from 0.5 to 4760 microns; the velocity of the debris particles is about 350 to 450 feet per second; scale models simulating the real item must be used to be assured of proper debris distribution pattern; rotating polystyrene foam particle catchers and velocity measuring devices are satisfactory and will yield the desired data; air sampling is necessary to obtain information on the particle sizes below 20 microns; 2-pound per cubic foot foam is superior for particle collection; and the pressure generated is about 50 percent of the pressure created by an uncased charge of the same weight. The development tests provide techniques, instrumentation, and physical layout information needed for performing a full-scale destruct test on a mockup ROVER/NERVA space propulsion engine. (auth)

16113 (SC-RR–66-22) A COMPARISON OF THE RESULTS OF THE SANDIA CORPORATION TTA TRAJECTORY PROGRAM AND THE ATOMICS INTERNATIONAL RESTORE TRAJECTORY PROGRAM. Spahr, H. R. (Sandia Corp., Albuquerque, N. Mex.). Feb. 1966. Contract AT(29-1)-789. 60p. Dep. mn. CFSTI $3.00 cy, $0.75 mn.

The results of the Sandia Corporation TTA and the Atomics International RESTORE trajectory programs are compared. Initial conditions used for both trajectories correspond to an orbital decay trajectory which is very sensitive to any variation in initial conditions or input data. The comparison of the results, which indicated relatively small differences between the two trajectories, verified the accuracy of the trajectory programs. (auth)

16114 MONTE CARLO CALCULATION OF THE TRANSMISSION OF GAMMA RAYS FROM A LINE ISOTROPIC SOURCE THROUGH STEEL PIPES. Umeda, Iwao. Nippon Kokan Tech. Rep.-Overseas, No. 4, 97-104(Feb. 1965).

On a nuclear powered ship, radiation protection for passengers and crews is of paramount importance. From an economic point, radiation shielding, while designed to efficiently absorb radiation emitting from the reactor should be as small and light as possible. The steel piping of a ship utilizing nuclear energy constitutes an assembly of many line radioactive sources. The steel pipes act as an effective shield against these line sources. In order to quantitatively determine such shielding properties, the transmission of gamma rays from the line sources through steel pipes by the Monte Carlo method was calculated. Calculation procedure described and examples of calculation of the buildup factors, the energy spectra and the collision numbers of transmitted gamma rays through the pipe, for the cases where ^{60}Co and ^{137}Cs line sources are shielded with steel pipes having a wall thickness of 10.0 to 51.5 mm are cited. The case histories of 5000 photons for ^{60}Co and 10,000 photons for ^{137}Cs were followed on the IBM 7090 digital computer. (Rev. Metal Lit.)

16115 SPACE AND NUCLEAR ENERGY. Tape, Gerald F. Nucl. Energy, 343-7(Nov.-Dec. 1965).

The utilization of nuclear energy in space missions is discussed. On-board electric power requirements are reviewed. The advantages of isotopic space power systems over solar-powered units are discussed. The development of SNAP-9A, SNAP-19, SNAP-25, SNAP-11, and SNAP-27 generators is described. The SNAP reactors being developed are also considered: SNAP-10A, SNAP-8, and SNAP-50. Progress in nuclear rocket propulsion is also reviewed. The major portion of the work was on graphite reactor systems. (M.C.G.)

16116 SUDOVYE ATOMNYE ENERGETICHESKIE USTANOVKI. PUTI I PERSPEKTIVY RAZVITIYA. (Naval Nuclear Power Installations. The Means and Perspectives of their Development). Pozdeev, A. V. Leningrad, Izdatel'stvo Sudostroenie, 1964. 820p.

The use of nuclear power plants on ships of the marine transport fleet is examined. Basic principles and technology of nuclear energy production and reactors are reviewed. The development and operating conditions of nuclear ships in other countries are surveyed. The construction, economics, and safety considerations of nuclear ships, using steam turbines and gas turbines, are considered, and future prospectives are discussed. (M.J.T.)

16117 IMPROVEMENTS RELATING TO NUCLEAR REACTORS. (to Allis-Chalmers Mfg. Co.). French Patent 1,314,117. Nov. 26, 1962. Priority date Jan. 5, 1961, United States.

A horizontally disposed nuclear reactor is adapted for use in mobile units and particularly in submarine vessels as a source of propelling power. The pressure vessel and the reactor auxiliary equipment are disposed in the lower portion and along the longitudinal axis of a submarine hull. A hatchway aligned with the fueling port of the pressure vessel is arranged in the upper portion of the hull and is suitably sealed by a removable hatch. (IIB)

Research and Test Reactors

16118 (AE-212) CENTRAL REACTIVITY MEASUREMENTS ON ASSEMBLIES 1 AND 3 OF THE FAST REACTOR FR0. Londen, S-O. (Aktiebolaget Atomenergi, Stockholm (Sweden)). Jan. 1966. 47p. Dep. mn.

The reactivity effects of small samples of various materials were measured by the period method at the core center of Assemblies 1 and 3 of the fast zero power FR0. For some materials the reactivity change as a function of sample size was determined experimentally. The core of Assembly 1 consisted only of uranium enriched to 20% whereas the core of Assembly 3 was diluted with 30% graphite. The results were compared with calculated values obtained with a second-order transport-theoretical perturbation model and using differently shielded cross sections depending upon sample size. Qualitative agreement was generally found, although discrepancies still exist. The spectrum perturbation caused by the experimental arrangement was analyzed and found to be rather important. (auth)

16119 (ANL-7152, pp 73-86) ADVANCED SYSTEMS RESEARCH AND DEVELOPMENT. (Argonne National Lab., Ill.).

Reactivity worth calculations were made for the AARR control elements Hf and $Eu_2O_3-TiO_2-SS$. Neutron fission spectra were calculated for various fuel loadings. Separate brief discussions on the AARR are presented on heat transfer, fuel and materials development, reactor vessel, control rod drive mechanism, and experimental facilities. (M.O.W.)

16120 (BNWL-176) DETERMINATION OF MAXIMUM NUCLEAR TUBE POWERS BASED ON BOILING BURNOUT. Hesson, G. M. (Battelle-Northwest, Richland, Wash. Pacific Northwest Lab.). Dec. 1965. Contract AT(45-1)-1830. 17p. Dep. mn. CFSTI $1.00 cy, $0.50 mn.

A method is described to define the maximum tube power of a pressure tube reactor as limited by boiling burnout. The method divides all those factors involved in a boiling burnout analysis into two groups and a factor called a consequence factor. The two groups consist of: those whose value and effect can be defined with reasonable accuracy, and those whose value or effect is uncertain but which must be estimated. The consequence factor is determined from an assessment of the consequences of boiling burnout. These factors and the relation they impose between the boiling burnout heat flux and the average heat flux derived from the measured tube power are presented. (M.O.W.)

16121 (BNWL-197) NEUTRONIC CONSIDERATIONS IN THE SELECTION OF A DRIVER FUEL FOR THE FAST TEST REACTOR (FTR). Little, W. W. Jr.; Hardie, R. W. (Battelle-Northwest, Richland, Wash. Pacific Northwest Lab.). Dec. 1965. Contract AT(45-1)-1830. 37p. Dep. mn. CFSTI $3.00 cy, $0.50 mn.

The neutronic characteristics of four possible driver fuels for the Fast Test Reactor (FTR) were studied using the Russian 26-group data compilation. The fuels investigated were PuO_2-SS, UO_2-SS, $PuO_2-^{238}UO_2$, and $UO_2-^{238}UO_2$. Since a high flux is of paramount importance in a test reactor, low inventory plutonium fueled cores were found to be more suitable than uranium cores for use in the FTR. For core volumes of approximately 600 liters, it was found that cermet fuels appear preferable to ceramic fuels due to the small Doppler and perhaps unreliable thermal expansion coefficient of the ceramic fuel. If compromises in flux are acceptable, the Doppler coefficient in the ceramic fuel could be enhanced by using a BeO moderator. (auth)

16122 (JAERI-6016) A USER'S MANUAL FOR JRR-4 EXPERIMENTAL FACILITIES. Miyasaka, S. (Japan Atomic Energy Research Inst., Tokyo). Aug. 1965. 95p. (In Japanese). Dep. mn.

JRR-4 is the swimming pool type reactor which is constructed for shielding research. The design of the experimental facilities of the JRR-4 is included. The techniques for operation are discussed. (auth)

16123 (KFK-350) UNTERKRITISCHE ANORDNUNGEN, KRITISCHE ANORDNUNGEN UND PULSREAKTOREN ZUM STUDIUM SCHNELLER REAKTOREN. (Subcritical, Critical, and Burst Facilities in Fast Reactor Physics Research). Homma, H.; Patzelt, H.; Stahl, S. (Kernforschungsanlage, Karlsruhe (West Germany)). Sept. 1965. 198p. Dep. mn.

A survey is presented of the fast subcritical, critical, intermediary critical, couples fast-thermal critical, and fast pulse reactor assemblies now in operation. The site of the installation, their out-put, technical data, and literature references are tabulated. (J.S.R.)

16124 (ORNL-TM-1388) HFIR CLADDING-FAILURE DETECTOR. DeLorenzo, J. T. (Oak Ridge National Lab., Tenn.). Dec. 8, 1965. Contract W-7405-eng-26. 7p. Dep. mn. CFSTI $1.00 cy, $0.50 mn.

The HFIR Cladding-Failure Detector monitors a sample stream of primary coolant water from the exit of the reactor to detect the release of fission product activity from small defects, such as blisters, in the full cladding. The operation of the system is briefly described and a procedure for determining the settings for the pulse amplifier, pulse-height discriminator, and high-voltage supply is given. (auth)

16125 (ORNL-TM-1393) DESCRIPTION OF FACILITY RADIATION AND CONTAMINATION ALARM SYSTEMS INSTALLED IN THE HIGH-FLUX ISOTOPE REACTOR FACILITY, BUILDING 7900. Russell, J. A. Jr.; Knowles, D. J. (Oak Ridge National Lab., Tenn.). Dec. 8, 1965. Contract W-7405-eng-26. 18p. Dep. mn. CFSTI $1.00 cy, $0.50 mn.

Facility radiation and contamination systems were installed in the High Flux Isotope Reactor Facility, to continuously and automatically monitor the gamma radiation level and air contamination level in the entire facility. The monitoring instruments in the network are used to provide health physics monitoring information, local alarms when abnormal conditions occur, and remote alarms on a central monitoring panel located on the reactor control panel. Nine monitrons continuously monitor for gamma radioactivity. Five of these monitrons are used in the facility radiation alarm system. Nine constant air monitors continuously sample the air in the building for radioactive (beta-gamma) particulate material. Six of these constant air monitors are used in the facility contamination alarm system. A description of the facilities is presented. (M.O.W.)

16126 THE ISPRA-2 REACTOR CONTROL SYSTEM. Conti, M. (CNEN, CSN, Casaccia, Italy); Fioroni, F.; Galli de Paratesi, S. Comit. Naz. Energia Nucl. Notiz., 11: 34-50(Nov. 1965). (In Italian).

A description is given of the control system for the Ispra-2 swimming pool reactor, at present in operation at C.N.E.N.'s Casaccia Nuclear Research Center. This is the first system of 100% Italian design in this field. (auth)

16127 RESEARCH CENTERS IN EUROPE. NO. 12. SEIBERSDORF. EuroNuclear, 2: 607-14(Dec. 1965).

A description of the organization and work at the Seibersdorf center is given. Most of the work is of a fundamental nature. But work was also done on coated fuel particles for the DRAGON project of the ENEA. The work of the IAEA laboratory consists for the most part in providing highly specialized services for member countries in the fields of radioactive analysis and standardization, as well as studies, and co-ordination work on agricultural and medical applications of nuclear radiations. Future projects at Seibersdorf are also mentioned. (J.F.P.)

16128 OPERATING EXPERIENCE WITH A HEAVY WATER REFLECTOR TANK. Martin, Robert D. (Univ. of Michigan, Ann Arbor). 45p. (CONF-650710-14). ORINS. Gmelin, AED-CONF-65-192-11.

From American Nuclear Society Meeting on Reactor Operating Experience, Jackson Lake Lodge, Wyo.

A reflector modification at the University of Michigan pool reactor converted two radial beam ports into tangential ports. Initial test results showed a thermal flux increase of

1.8 for the two beam ports involved. The modification was made by installing a rectangular, vented, aluminum tank containing 45 gallons of D_2O immediately adjacent to one full face of the reactor core. The tank was provided with internal void chambers which act as the port source planes. The void chambers have the same cross-sectional dimensions as the beam port collimators and are aligned with the collimator centerlines. While the design calculations for the tank predicted a reactivity worth of +.04 $\Delta k/k$ compared to light water, tests have shown the tank worth to be approximately +.02 $\Delta k/k$. This lower positive reactivity worth required that the operating core mass be increased by 12% to provide the excess reactivity required for routine 2 MW operation. Remotely inflatable metal bellows assemblies were used to replace the water gap between the beam ports and the tank void chambers. Bellows pressures above 10 psig afford no beam intensity increase while a reduction to 9 psig reduces beam port neutron intensity more than 32% at the tangential ports. The analysis of reactor operating hazards considered increased core power density and reactivity changes from tank movements. All these were found to be of no greater consequence than hazards already evaluated for the Ford Nuclear Reactor. Calculation of the hazard of D_2O passing through the core following a tank rupture, showed that the reactivity effect of all H_2O-D_2O volume fractions would be negative compared to light water for the FNR core. The Maximum Credible Accident was postulated to be the release into the reactor pool of the tritium produced in the tank. To avoid exceeding the limits specified in 10 CFR 20 in either the building or outside air following such a release, the tank tritium inventory will be kept below 50 curies. The tritium level is assayed every 800 MWH. (auth)

16129 EXPERIMENTAL FACILITIES IN A HIGH FLUX POOL-TYPE TEST REACTOR. **Robertshaw, Richard D. (General Electric Co., Pleasanton, Calif.). New York, American Society of Mechanical Engineers, 1965, Preprint No. 65-WA/NE-1, 5p., $1.50. (CONF-651110-17). ORINS.**

From American Society of Mechanical Engineers, Annual Winter Meeting, Chicago.

The unique General Electric high flux test reactor is described, including the location of the various experimental facilities in the reactor. The experimental facilities located inside the reactor pressure vessel are described in detail. The various types of experimental facilities located in the pool adjacent to the reactor are described in detail with illustrations. These pool facilities include not only stationary-tubes, but also movable facilities used to control the radiation exposure rate. (auth)

16130 THERMAL COLUMN PNEUMATIC FACILITY. **de Saint Maurice, Arthur B.; Canfield, Richard T. (Columbia Univ., New York). 20p. (CONF-650710-15). ORINS. Gmelin, AED-CONF-65-192-12.**

From American Nuclear Society Meeting on Reactor Operating Experience, Jackson Lake Lodge, Wyo.

A pneumatic rabbit facility was installed in the thermal column for the Industrial Reactor Laboratories' 5 Mw pool research reactor. This pneumatic system has greatly increased the flexibility of the graphite thermal column by providing accessibility during reactor full power operation. Previously, sample insertions and removals were possible only during reactor shutdown periods. The unique feature of the pneumatic facility is that the rabbit track and vent line were machined in two standard graphite stringers which when connected end-to-end provide full penetration of the thermal column. An "S" shape contoured track precludes radiation streaming and the graphite surface is ideal for rabbit travel eliminating the necessity of a liner which could conceivably have presented flux perturbation and column contamination problems. (auth)

16131 MATERIAL TEST NUCLEAR REACTOR. **(to Hitachi, Ltd.). French Patent 1,369,644. July 6, 1964. Priority date Sept. 12, 1962, Japan.**

The problem which arises from a light water moderated material test reactor is the fact that it has a rather large heating caused by the gamma radiation and is therefore greatly restricted in its design with respect to the formation of in-pile loops. A heavy water reactor has a gamma heating which is smaller but on the other hand, when a test piece is inserted, the heavy water reactor results in a large reactivity change and a large neutron flux change. In order to do away with these inconveniences a new material test reactor employs a mixture of light water and heavy water as the moderator. (IIB)

WASTE DISPOSAL AND PROCESSING

See also BIOLOGY AND MEDICINE — Ecology
CHEMISTRY — Radiochemistry
CHEMISTRY — Separation Processes and Procedures
HEALTH AND SAFETY

Refer also to abstracts 14466 and 14753.

16132 (BNL–8558) NEUTRON BURNING OF LONG-LIVED FISSION PRODUCTS FOR WASTE DISPOSAL. Steinberg, Meyer; Wotzak, Gregory; Manowitz, Bernard (Brookhaven National Lab., Upton, N. Y.). Sept. 1964. Contract AT-30-2-GEN-16. 27p. Dep. mn; CFSTI $2.00 cy, $0.50 mn.

A discussion is presented of the economics of ^{85}Kr, ^{90}Sr, and ^{137}Cs waste processing by in-pile nuclear "burning" to yield stable or short-lived products. In the process, the Cs and Kr effluents from a reactor are fed into gaseous diffusion plants to increase the ^{137}Cs and ^{85}Kr contents, respectively, to 90%. ^{90}Sr is fed into the "burner" reactor directly, with no isotopic separation, along with the 90%-pure Cs and Kr radioisotopes. After suitable burning times, the irradiated radioisotopes are recycled through the separation processes and back into the "burner." (T.F.H.)

16133 (IDO–14672) LEACHABILITY OF GLASS PREPARED FROM HIGHLY RADIOACTIVE CALCINED ALUMINA WASTE. Paige, B. E. (Phillips Petroleum Co., Idaho Falls, Idaho. Atomic Energy Div.). Feb. 1966. Contract AT(10-1)-205. 32p. Dep. mn. CFSTI $2.00 cy, $0.50 mn.

Alumina-phosphate glass was prepared from full-level radioactive calcine produced in the Waste Calcining Facility at the Idaho Chemical Processing Plant. The glass was prepared from 25 weight percent alumina calcine, 40.5 percent P_2O_5 and 18.6 percent Na_2O added as $NaH_2PO_4 \cdot H_2O$, and 15.9 percent PbO. The details of preparation and the effect of radiation and heat treatment on the glass are reported. Leaching data obtained for fission products and the glass components are compared for the glass in distilled water at 25 and 94°C. A specially designed apparatus which circulated the water continuously was used. The high level of activity made it feasible to use a single molded piece permitting the surface area and other experimental conditions to be defined to a far greater degree than is feasible with the crushed glass techniques required for low levels of activity. Devitrification by heating for 30 days at 450°C was found to have no effect on the leaching rate. (auth)

16134 (IEA–102) WASTE DISPOSAL PROBLEMS AT THE INSTITUTO DE ENERGIA ATOMICA. Costa Rodrigues, Jose Maria (Instituto de Energia Atomica, Sao Paulo (Brazil)). Aug. 1965. 28p. (CONF-631104–9). Dep. mn.

From the Meeting on the Utilization of Research Reactors, Sao Paulo, Brazil.

A preliminary evaluation of the radioactive liquid waste problem at the Instituto de Energia Atômica is presented. Several types of wastes produced at present, or expected in the near future, are described or tentatively evaluated. The natural drainage system of this area is also briefly described and the annual flowrates indicated. Dispersion of radioactive liquid wastes into the available near-by streams was examined and the construction of a treatment plant is suggested. (auth)

16135 (RL–SA–62) STORAGE FACILITIES FOR HANFORD HIGH-LEVEL FISSION WASTE CONTAINERS. Barnes, J. W. (Isochem Inc., Richland, Wash.). [1966]. Contract AT(45-1)-1851. 22p. (CONF-660208–2). Dep. mn. CFSTI $1.00 cy, $0.50 mn.

From Symposium on Solidification and Long-Term Storage of Highly Radioactive Wastes, Richland, Wash.

A facility designed for the surveillance and long term storage of high level waste containers produced under the Hanford Waste Management Program is described. This facility is located in an existing canyon type structure to assure maximum containment. A closed loop high purity water system with dual heat exchangers and circulating pumps is provided. Equipment and container handling are designed for remote operation and maintenance. Instrumentation is provided for monitoring and surveillance of fission waste containers. Flexibility exists for safely handling containers and waste streams in the event of a container failure. Alternative storage vaults and cooling systems are also considered. (auth)

16136 RADIOACTIVE WASTE: GENERAL CHARACTERISTICS. Iranzo, Emilio (Junta de Energia Nuclear, Madrid). Energia Nucl. (Madrid), 9: 365-76(Sept.-Oct. 1965). (In Spanish).

The origin of radioactive wastes is summarized briefly. The nature of the waste from reactors, fuel processing plants, uranium ores and fabricating plants, radioisotope production, and nuclear accidents is discussed. (J.S.R.)

16137 LIQUID- AND GASEOUS-WASTE-EFFLUENT SAMPLING AND MONITORING. Knowles, D. J. Nucl. Safety, 7: 52-6; 64-5(Fall 1965).

Literature published since 1960 in the field of waste treatment and disposal covering developments in instrumentation and techniques of sampling and monitoring gaseous and liquid waste is reviewed. The references include foreign papers as well as those of U. S. origin. General comments on waste-effluent-monitoring apparatus are made. (auth)

16138 AN INVESTIGATION OF THE USABILITY OF SOME FLOCCULANTS FOR TREATMENT OF RADIOACTIVE WASTE WATER BY MINERAL SORBENTS. Oglaza, Jan; Siemaszko, Aleksander. Nukleonika, 10: 519-22(1965). (In Polish).

Investigations were carried out with the water of the Vistula River, having a hardness of 13° north. The sorbents used were raw bentonite of the "Jawar" diggings, bentonite loam from the Chmielnik region, and silicious earth from the Lechowek pit, and as flocculants, Separan 2610 (polyacrylamide), and swelling-type shavings NTL. The water was contaminated with ^{137}Cs and ^{144}Ce with carriers of CsCl and $Ce(NO_3)_3 \cdot 6H_2O$ in quantities of 0.5 mg/liter and an activity of 10 to 20 μC/liter. In the first stage of the investigation, the rate of growth of the clear column was measured, as observed visually, for the 3 sorbents with and without flocculants. Also, the activity was measured with a collimated radiation detector viewing only the center of the column. This stage showed that the shavings gave a large increase in settling out of the radioactivity, and the Separan gave a considerably larger increase. In the second stage, the amount of radioactivity found in the sediment was first measured as a function of the mass of sorbent added, with 2 mg/liter of Separan. Next, without flocculants, the rate of decontamination of the water was measured as a function of time after the mixing ceased. The addition of flocculants increased the rate of sedimentation and the rate of decontamination, and resulted in a great improvement in producing a very distinct boundary of the clear column of the fluid, making decanting much more feasible. (TTT)

16139 WASTE FRACTIONIZATION PLANT /WAFRAX/ (Engineering Materials). (General Electric Co., Richland, Wash. Hanford Atomic Products Operation). (CAPE–1269).

104 drawings.

Engineering drawings of the WAFRAX Plant and associated equipment used for the fractionization of waste are included. The facility has a "hot side" that consists of 40 cells and canyon equipment and a "cold side" that contains the storage facilities and aqueous make-up equipment. Facilities to remove ^{90}Sr and ^{137}Cs from current and stored wastes are located in 35 of the 40 cells. Cesium recovery equipment, including ion exchangers, is located in cells 17 thru 21. Strontium or mixed Cs and Sr packaging facilities are located in cells 14 and 15. Facilities are provided in cells 9, 10, 16, and 22 thru 25 for the collection and disposal of liquid process waste, cell drainage, steam condensate from process vessels, off-gases, and organic waste. Pressure vessels and tanks are located on the "cold side" to store nitric, formic, and acetic acids; carbon dioxide; anhydrous ammonia; ammonia; carbonate; sodium hydroxide; ethylenediamine tetraacetic acid; and organic solvents. Operations and maintenance are remotely controlled. (For details, see TID-4100). (M.C.G.)

16140 DETERMINATION OF THE URANIUM CONTENT IN SCRAPS. Nakajima, K.; Saito, N. (Atomic Fuel Corp., Tokyo). Vienna, International Atomic Energy Agency, 1965, Preprint No. SM-67/5, 17p. (CONF-650803-36). ORINS.

From IAEA Symposium on Nuclear Materials Management, Vienna.

Uranium accountability problems related to recovered precipitate cakes and metal scraps are described. Waste solution from the uranium refining pilot plant utilizing the Excer process is neutralized and sent to aging tanks. Condensed slurry-type precipitates are filtered with a filter press. To determine the uranium content of the cakes, sampling experiments were continued over a two-year period in practical operation, and the following values were obtained for 171 lots: average uranium content $\overline{X}$, 10.29%; variation between lots σ_L^2, 4.36%; variation between filter plates σ_b^2, 0.014%; variation within filter plates σ_W^2, 2.02%; and accuracy of reduction and analysis $\sigma_R^2 + \sigma_M^2$, 0.349%. Based on these results, a proper sampling plan was established. In this plan variance of the mean value $V(\overline{X})$ was 4.65%, variation without σ_L^2 was 0.29%, and the coefficient of variation was about 5%. In the case of precipitate cakes as feed materials for a recovery process, derived values from this sampling method agreed satisfactorily with the analysis of the resulting product. Since the uranium metal scrap in the form of turnings or sawdust catches fire easily in the air it is difficult to use the direct weighing method. Therefore, the weight-volume-density method was adopted. It was found that a lower density liquid and a higher density scrap sample resulted in a higher degree of precision and also that measurement errors of liquid density and total volume seriously affected derived scrap weight. Uranium metal scraps were oxidized even under machine oil, and oxidized fine particles caused a measurement error. (auth)

16141 A NEW GLASS CONTAINING RADIOACTIVE WASTE OXIDES. Grover, John Roger; Jones, Alan David (to United Kingdom Atomic Energy Authority). British Patent 1,019,373. Feb. 2, 1966. Filed Aug. 10, 1962.

A glass having a melting point in the range of 850 to 1100°C consists essentially of glass forming oxides and from 20 to 50% by weight of waste oxides resulting from the treatment to remove the U and Pu from irradiated metallic U nuclear fuel having a burnup in excess of 3000 Mwday/ton. The glass forming oxides are selected from the oxides of Ca, B, Na, P, Si, Pb, Mo, Zn, Al, and Fe. The glass is formed by melting the oxides in a steel containing vessel. After the glass is formed, the vessel may be sealed and the entire body disposed of as a means of waste disposal. The sealed glass containing vessel may be used also as a radiation source providing a mixed spectrum of gamma rays substantially free of beta rays or alpha particles. (B.L.M.)

16142 METHOD FOR THE SOLIDIFICATION OF AQUEOUS ATOMIC WASTE. Alberti, Rudolf. German Patent 1,199,414. Aug. 26, 1965. Filed Mar. 18, 1961.

The method consists of introducing radioactive liquid from below into a container filled with hydraulic binding agent, of impregnating the block of radioactive liquid and binding agent with melts, solutions, or emulsions of paraffins, lacquers, or silicones, or aqueous solutions of inorganic, solidifying substances like water glass. (Gmelin Inst.)

GENERAL AND MISCELLANEOUS

16143 (AD–620276) BETA PARTICLE STANDARDS FOR ^{14}C AND OTHER ELEMENTS IN THE FORM OF RADIOACTIVE MONOLAYERS. Beischer, Dietrich E. (Naval School of Aviation Medicine, Pensacola, Fla.). May 23, 1950. 15p. (NM–001-059.16-03). CFSTI $1.00 cy, $0.50 mn.

The properties of radioactive monolayers for use as beta sources are discussed. The use of radioactive monolayers as standards in assay work, radioautography, and dosage determinations by means of G-M counters is recommended. (D.C.W.)

16144 (AED-C–32-1(Vol.1 and Vol.2)) DIRECTORY OF THE NUCLEAR INDUSTRY, USA. Financial Data; Review of Products and Services; Industrial Literature. (Zentralstelle fuer Atomkernenergie-Dokumentation, Gmelin-Institut fuer Anorganische Chemie und Grezgebiete, Frankfurt am Main (West Germany)). 1965. 764p. Gmelin, Frankfurt, W. Ger. or Larchmont, N. Y. $5.00.

Basic data on some 300 American companies in the nuclear field are included. The handbook consists of 2 parts: a Company Directory and an Index. The Company Directory includes the following data: registered firm name, address, and code number; subsidiary companies or divisions active in the nuclear field; classification of manufacturing programs or services through descriptors; basic financial data; and listing of industrial literature issued by the company which is on file at the ZAED. The Index is made up of products with descriptors, characterizing the activity of each firm. A code number is given for each firm. (P.C.H.)

16145 (BNWL–113-7) PLUTONIUM ABSTRACTS. Volume 5, Number 7. (Battelle-Northwest, Richland, Wash. Pacific Northwest Lab.). Aug. 30, 1965. Contract AT(45-1)-1830. 19p. Dep. mn. CFSTI $1.00 cy, $0.50 mn.

Forty-one references are given to reports and journals published during 1961 and 1965 through July. The subject fields covered include: biology and medicine; chemistry; health and safety; metallurgy; physics; and reactor technology. (P.C.H.)

16146 (COO–888-39) PENETRATION OF ORGANIC COMPOUNDS THROUGH ISOLATED CUTICULAR MEMBRANES WITH SPECIAL REFERENCE TO ^{14}C UREA. Yamada, Y.; Wittwer, S. H.; Bukovac, M. J. (Michigan State Univ., East Lansing. Dept. of Horticulture). July 20, 1964. Contract AT(11-1)-888. 23p. Dep. mn. CFSTI $1.00 cy, $0.50 mn.

Rates of penetration of ^{14}C-labeled urea, and in some instances maleic hydrazide and N,N-dimethylaminosuccinamic acid (in NSA index as N,N-dimethylsuccinamic acid), through enzymically isolated astomatous tomato fruit and stomatous onion leaf cuticular membranes were determined. Results were related to previous permeability studies with inorganic ions and with binding on cuticular surfaces and dialyzing membranes. Retention of urea was essentially the same on the outer and inner surfaces of both types of cuticles, and 10 to 20 times greater than on the surface of a dialyzing membrane. Penetration of all three organic compounds through tomato fruit cuticles was greater from the outer to the inner surface than in the opposite direction. With the onion leaf cuticle, however, influx and efflux of urea was approximately equal. Permeability of urea through tomato fruit cuticles was twice that of N,N-dimethylaminosuccinamic acid and 6 times that for maleic hydrazide. The amounts of urea which penetrated the tomato fruit cuticle exceeded by 10 to 20 times the inorganic ions (Rb^+, Ca^{2+}, Cl^-, SO_4^{2-}), and increased, but not proportionally, with the concentration of urea in the test solution. (auth)

16147 (COO–888-45) PERMEABILITY OF IRON AND IRON CHELATES THROUGH CUTICULAR MEMBRANES. Kannan, S.; Wittwer, S. H.; Yamada, Y. (Michigan State Univ., East Lansing. Dept. of Horticulture). [1965]. Contract AT(11-1)-888. 10p. Dep. mn. CFSTI $1.00 cy, $0.50 mn.

Permeability studies of isotopically labeled iron chelates and chelate components were conducted with enzymically isolated cuticular membranes derived from ripe tomato fruit. The cuticle was almost an impermeable barrier to $^{59}FeSO_4$, but permeability of ^{59}Fe chelated with EDTA–^{14}C or EDDHA–^{14}C was increased to 50 to 100-fold, and to rates comparable for those of other cations. Penetration for both the metal and ligands was greater at pH 3 than 6, and was much less for cuticular than for a dialyzing membrane. The results are related to failures of iron sprays to alleviate iron deficiency disorders on the leaves of many species, and are suggestive of new approaches in the foliar nutrition of some crop plants. (auth)

16148 (NYO–2779-9) ALPHARADIOGRAPHIC AND HISTOLOGICAL OBSERVATIONS ON THE SKELETAL EFFECTS OF HYPO AND HYPERVITAMINOSES A AND D IN THE RAT. Belanger, Leonard F.; Clark, Irwin (British Columbia Univ., Vancouver. Faculty of Medicine. Columbia Univ., New York. Coll. of Physicians and Surgeons). [1964]. Contract AT(30-1)-2779. 25p. Dep. mn. CFSTI $1.00 cy, $0.50 mn.

Male rats were fed a diet deficient in either vitamin A or vitamin D or A and D. Some were then given large doses of vitamin A, D or A and D by stomach tube. Sections of the tibia demineralized in EDTA after the administration of a tracer dose of ^{210}Po produced histological and radiographic evidence of slight retardation of growth, maturation, and resorption in D deficiency. In A deficiency and in combined A and D deficiency, there is defective matrix synthesis, formation of persistent globular masses and decrease in osteocytic resorption (osteolysis). In hypervitaminosis D, slightly increased periosteal growth and greatly increased osteolysis were observed, while in hypervitaminosis A, large growth of cancellous bone at periosteum and stimulation of osteolysis in new and old bone were observed. In combined A and D hypervitaminosis, as above with greater immaturity of new growth, increased fragility and spontaneous fractures were observed. (43 references.) (auth)

16149 (NYO–2779-10) DEMINERALIZATION WITH E.D.T.A. BY CONSTANT REPLACEMENT. Belanger, Leonard F.; Copp, D. Harold; Morton, Margaret A. (British Columbia Univ., Vancouver. Faculty of Medicine). [1963]. Contract AT(30-1)-2779. 17p. Dep. mn. CFSTI $1.00 cy, $0.50 mn.

An apparatus for demineralization of hard tissues by constant replacement of a saturated solution of EDTA is described. The method allows for more rapid demineralization through better Ca chelation. EDTA demineralization preserves cells and matrix constituents particularly the mucopolysaccharides as demonstrated by staining, alpharadiography, phase contrast microscopy, and microincineration. Cold acetone fixation followed by cold EDTA demineralization retains several enzymic activities. (auth)

16150 (ORNL–3909) THE MINIMUM SIGNIFICANT NUMBER OF SUCCESSES IN A BINOMIAL SAMPLE. Kastenbaum, Marvin A. (Oak Ridge National Lab., Tenn.); Bowman, K. O. (Oak Ridge Gaseous Diffusion Plant, Tenn.). Feb. 1966. Contract W-7405-eng-26. 68p. Dep. mn. CFSTI $3.00 cy, $0.75 mn.

In the field of sampling inspection one often wishes to know the smallest number of successes (or failures), c, in n independent Bernouilli trials such that $\sum_{r=c}^{n} \binom{n}{r} p^r(1-p)^{n-r} \leq \alpha$, where p is the probability of successes in a single trial, and $0 \leq \alpha \leq 1$ is a specified level of significance. Numerical tables were calculated to provide minimum values of c, for a given n, p, and α. Values of

c are given for all combinations of n = 1(1)200, p = 0.01 (0.01) 0.99, and α = 0.01, 0.05, 0.10. (M.O.W.)

16151 (RFP-647) VAPOR DEPOSITED FILM DISTRIBUTION ON CURVED SUBSTRATE SURFACES. Beno, R. L. (Rocky Flats Div., Dow Chemical Co., Golden, Colo.). Mar. 1, 1966. Contract AT(29-1)-1106. 8p. Dep. mn. CFSTI $1.00 cy, $0.50 mn.

A comparison between calculated and experimental film thickness distribution on curved substrate surfaces is described. Using copper as evaporant, the emission characteristics of a tantalum crucible and a surface emitting pan source are compared. Two simultaneously emitting tantalum crucibles, situated beneath the exterior of a hemispheric substrate surface, did not upset distributions as determined by Knudsen's cosine law. (auth)

16152 (TID-3732) BIBLIOGRAPHIES OF ATOMIC ENERGY LITERATURE. Issued or in Progress During the Period, October-November 1965. (Division of Technical Information Extension (AEC), Oak Ridge, Tenn.). 18p. DTI Extension Free.

References (105) are given to bibliographies of interest to the atomic energy program issued or in preparation during the period Oct. to Nov. 1965. The references are listed according to corporate author. Report number and author and subject indexes are included. (P.C.H.)

16153 (UCRL-16472) MEASUREMENT OF HEAT RELEASED ON SOLID SURFACES. Muller, Rolf H.; Nobbe, Louis B. (Lawrence Radiation Lab., Univ. of California, Berkeley). Dec. 1965. Contract W-7405-eng-48. 39p. Dep. mn. CFSTI $2.00 cy, $0.50 mn.

The measurement of reaction enthalpies on solid surfaces of simple, well-defined geometry requires a quantitative knowledge of heat dissipation and the measurement of exceedingly small temperature differences. Both of these problems are analyzed theoretically with particular reference to the determination of heats of adsorption and immersion using presently available instrumentation. (auth)

16154 (Y-1420(Rev.1)) AN EXTENSION OF APT TO OBTAIN CENTROID AND INERTIA INFORMATION. Fowler, A. H.; Wilson, C. W. (Union Carbide Corp., Oak Ridge, Tenn. Y-12 Plant). Feb. 16, 1966. Contract W-7405-eng-26. 27p. Dep. mn. CFSTI $2.00 cy, $0.50 mn.

Computer routines are described which can be used with the APT system to obtain centroids and inertias of plane surfaces and solids of revolution. (auth)

16155 EUROPEAN TARIFFS AND NUCLEAR ENERGY. Conde, M. Rodriguez (Junta de Energia Nuclear, Madrid). Energia Nucl. (Madrid), 9: 359-63(Sept.-Oct. 1965). (In Spanish).

The tariffs imposed on nuclear materials and instrumentation in the European Community are briefly summarized and tabulated. (J.S.R.)

16156 RESEARCH CENTRES IN EUROPE—NO. 13. JUELICH. EuroNuclear, 3: 45-52(Jan. 1966).

The organization and facilities at the Juelich Nuclear Research Center are discussed. The FRJ-1 (Merlin) and FRJ-2 (DIDO) research reactors and their irradiation facilities are described. Beam and loop experiments in these reactors are outlined. Work in reactor technology is being carried out by component testing, materials testing, and design development. Research progress in plasma physics, medicine, zoology, botany and microbiology, agriculture, and chemistry are reviewed. Development of the AVR Pebble Bed reactor is discussed. (M.C.G.)

16157 FRESH WATER FROM THE SEA. Proceedings of the International Symposium held in Milan, April 20-21, 1964. Girelli, Alberto (ed.). New York, Pergamon Press, 1965. 200p. $9.00. (CONF-640415).

Eight papers presented at the symposium are given. Topics covered include: Application of ion exchange for conversion of saline water into fresh water, sea and brackish water desalting in Japan, developments in obtaining fresh water from sea water in Germany, British activities in desalination development and research, desalination research in Italy, the state of desalination research in Israel, evolution of the distillation process for sea water conversion, and the role of the United Nations Department of Economic and Social Affairs in the field of water desalination. (M.C.G.)

CORPORATE AUTHOR INDEX

This index contains entries for this period for all report literature and, in addition, for certain published literature items for which it is felt that a corporate approach is especially desirable, e.g., symposia, conference proceedings, and meetings.

Each entry under a corporate author is a shortened version of the title of the publication, followed by the *NSA* volume and abstract number. Report numbers are given in parentheses.

The phrase "Progress report" is abbreviated as "Prog. rpt.," permitting a more rapid and complete alphabetical arrangement of the titles without changing the location of the progress report titles in relation to the other titles.

A

AEROJET-GENERAL NUCLEONICS, SAN RAMON, CALIF.
Prog. rpt. on alkali metals evaluation, 7–9/65, 20: 15028 (AGN-8166)

AERONAUTICAL RESEARCH LABS., WRIGHT-PATTERSON AFB, OHIO.
On K-level widths, 20: 15239 (CONF-233(Vol.3), pp 419-39)

AEROPROJECTS, INC., WEST CHESTER, PA.
Prog. rpt. on ultrasonic instrumentation for nuclear applications, 12/65–1/66, 20: 14700 (NYO-3622-1)

AEROSPACE RESEARCH LABS., WRIGHT-PATTERSON AFB, OHIO.
$L_1L_{2,3}M_{4,5}$ Coster-Kronig transition rates, 20: 15238 (CONF-233(Vol.3), pp 398-418)

AIR FORCE CAMBRIDGE RESEARCH LABS., L. G. HANSCOM FIELD, MASS.
Radiochemical procedures for selected radionuclides in environmental samples, 20: 14430 (AD-620219)

AKADEMIYA NAUK SSSR, NOVOSIBIRSK. INSTITUT YADERNOI FIZIKI.
Experimental investigation of charge-transfer proton injection into cyclic accelerators and storage rings, 20: 15162 (NP-15785)

AKTIEBOLAGET ATOMENERGI, STOCKHOLM (SWEDEN).
Bibliography on radiation effects on solid, U based nuclear fuel materials, Vol. 5, No. 4, 20: 15137 (VDIT-16(5.4))
Central reactivity measurements on assemblies 1 and 3 of reactor FR0, 20: 16118 (AE-212)
Flux-shape eigenfunction tables for two-zone slabs, 20: 16024 (RFR-231)
Flux-shape eigenfunction tables for two-zone cylinders, 20: 16025 (RFR-232)
Prog. rpt. on personnel dosimetry, annual, 1964, 20: 14782 (AE-211)

ALLIS-CHALMERS MFG. CO., BETHESDA, MD. ATOMIC ENERGY DIV.
Pathfinder flooding coefficient, core pressurization, and temperature coefficient tests, 20: 16059 (ACNP-65600)

AMERICAN SCIENCE AND ENGINEERING, INC., CAMBRIDGE, MASS.
Prog. rpt. on measurements of low energy electron precipitations associated with auroral disturbances and trapped radiation belts, final, 3/63–9/65, 20: 15589 (ASE-1125)

ANCKER HOSPITAL, ST. PAUL, MINN.
Blood supply to hepatic V2 carcinoma implants as measured by radioactive microspheres, 20: 14405 (COO-1305-2)

ARGONNE NATIONAL LAB., ILL.
Advanced systems research and development, 20: 16119 (ANL-7152, pp 73-86)
Automatic handling of data from large-scale dog radiation experiment using general purpose computer, 20: 14238 (CONF-650560-13)
Checker-playing program for IPL-VC computer, 20: 14949 (ANL-7109)
Corrections for x-ray intensity data obtained from electron microprobes, 20: 14431 (ANL-7078)
General reactor technology, 20: 15032 (ANL-7152, pp 50-72)
Glovebox amalgamation for determination of oxygen in alkali metals, 20: 14432 (ANL-7123)
Growth and annealing of evaporated aluminum–silicon films, 20: 15030 (ANL-7102)
High-temperature thermal diffusivity of UO_2 under transient conditions, 20: 15031 (ANL-7116)
Liquid-metal-cooled reactors, 20: 16060 (ANL-7152, pp 1-49)
Mass transfer of U spheres to flowing molten Cd in laminar and turbulent flow, 20: 14975 (ANL-7091)
Mechanical properties of uranium compounds, 20: 15029 (ANL-7070)
Nuclear safety, 20: 15033 (ANL-7152, pp 87-96)
Prog. rpt. on reactor development, 1/66, 20: 15994 (ANL-7152)
Self-sustained hydrodynamic oscillations in natural-circulation two-phase-flow boiling loop, 20: 14684 (ANL-7073)
Theory of migration and coalescence of bubbles in solids, 20: 15132 (ANL-7079)

ARKANSAS UNIV., FAYETTEVILLE. DEPT. OF CHEMISTRY.
Measurement of the M/L-capture ratio in 30-million-year ^{205}Pb decay, 20: 15714 (CONF-233(Vol.2), pp 369-70)

ARMY GENERAL EQUIPMENT TEST ACTIVITY, FORT LEE, VA.
Research test of irradiated beef, ham, and shrimp, 20: 14931 (NP-15677)

ARMY QUARTERMASTER RESEARCH AND ENGINEERING FIELD EVALUATION AGENCY, FORT LEE, VA.
Research test of irradiated beef, pork sausage, and shrimp, 20: 14930 (NP-15676)

ASTRA, INC., RALEIGH, N. C.
Check on weight of space radiators for steam systems, 20: 14688 (N65-20692)

ATOMIC ENERGY CENTRE, DACCA (PAKISTAN). HEALTH PHYSICS DIV.
Radiation safety regulations for atomic energy centre, Dacca, 20: 14783 (AECD/HP/2)

ATOMIC ENERGY OF CANADA LTD., CHALK RIVER (ONTARIO).
Automatic sample changing systems utilizing AECL-2041 digital read-out system, 20: 14846 (AECL-2517)

ATOMIC ENERGY OF CANADA LTD., CHALK RIVER (ONTARIO). CHALK RIVER NUCLEAR LABS.
Angular correlation and internal conversion studies in ^{125}I and ^{127}I, 20: 15701 (CONF-233(Vol.2), pp 128-41)
Anomalous L-subshell conversion of some hindered E1 transitions in the rare earth region, 20: 15703 (CONF-233(Vol.2), pp 148-57)
Atomic M-level widths in ^{151}Sm, 20: 15241 (CONF-233(Vol.3), pp 454-64)
K-shell fluorescence yields of V, Cr, and Cu, 20: 15242 (CONF-233(Vol.3), pp 465-79)

ATOMIC ENERGY RESEARCH ESTABLISHMENT, HARWELL (ENGLAND).
Prog. rpt. on direct biological monitoring, 1963–64, 20: 14784 (AERE-R-5015)

ATOMIC WEAPONS RESEARCH ESTABLISHMENT, ALDERMASTON (ENGLAND).
Calculation of group averaged neutron cross sections (FORTRAN for IBM-7030), 20: 15665 (AWRE-O-103/65)
Permeation and diffusion of hydrogen in molybdenum, 20: 14976 (AWRE-O-16/66)
Versatile and cheap vacuum leak, 20: 14730 (AWRE-O-10/66)

ATOMICS INTERNATIONAL, CANOGA PARK, CALIF.
Coolant chemistry and analysis, 20: 16081 (NAA-SR-11628, pp 79-104)
Effect of oxygen on irradiated coolant, 20: 16082 (NAA-SR-11628, pp 105-7)
Examination of second set of in-vessel filters, 20: 16084 (NAA-SR-11628, pp 124-34)
Modular steam generator fabrication, 20: 15999 (NAA-SR-11739)
Nuclear analysis, 20: 16079 (NAA-SR-11628, pp 17-50)
Post-irradiation examination of Piqua fuel element, 20: 16083 (NAA-SR-11628, pp 108-23)

Prog. rpt. on Piqua power facility operations analysis, semiannual, 1–6/65, 20: 16077 (NAA-SR-11628)
Review of operations, 20: 16078 (NAA-SR-11628, pp 9-16)
Systems and components analysis, 20: 16080 (NAA-SR-11628, pp 51-78)

B

BABCOCK AND WILCOX CO., LYNCHBURG, VA.
Prog. rpt. on radiochemistry of nuclear fuels, 5–7/65, 20: 14433 (BAW-298)
Prog. rpt. on radiochemistry of nuclear fuels, 2–4/65, 20: 16061 (BAW-296)
BATTELLE INSTITUT E. V., FRANKFURT AM MAIN (WEST GERMANY).
Application of tracer systems to localize failed fuel elements, 20: 14848 (BMwF-FBK-65-02)
Study to find detector situated within radiation field of reactor core which will indicate fission products in coolant under operating conditions, 20: 14847 (BMwF-FBK-65-01)
BATTELLE MEMORIAL INST., COLUMBUS, OHIO.
Prog. rpt. on applicability of existing data to analytical description of a nuclear-reactor accident, 10–12/65, 20: 16019 (BMI-X-10154)
Prog. rpt. on civilian applications, 12/65, 20: 14957 (BMI-1754)
Prog. rpt. on refractory metals, 9–11/64, 20: 15049 (N65-16256)
BATTELLE-NORTHWEST, RICHLAND, WASH. PACIFIC NORTHWEST LAB.
Adsorption of trace ions from intermediate-level radioactive wastes by ion exchange, 20: 14434 (BNWL-180)
Chemical analysis of spent power reactor fuels, 20: 14435 (BNWL-SA-503)
Comparison of double diffracting x-ray unit with standard x-ray diffraction unit, 20: 14823 (RL-REA-2595, pp 73-9)
Environmental monitoring, 20: 14786 (BNWL-SA-465)
Fission product recovery research at Battelle-Northwest, 20: 14436 (BNWL-SA-504)
Geophysical seismic evaluation study at Hanford, 20: 14753 (BNWL-47)
Line broadening in irradiated molybdenum, 20: 15136 (RL-REA-2595, pp 51-62)
Low-temperature allotropic transformations in plutonium, 20: 15034 (BNWL-49)
Maximum nuclear tube powers based on boiling burnout, 20: 16120 (BNWL-176)
Neutronic considerations in selection of driver fuel for FTR, 20: 16121 (BNWL-197)
Plutonium Abstracts, Vol. 5, No. 7, 20: 16145 (BNWL-113-7)
Prog. rpt. on W–Tc alloys, 10/65–1/66, 20: 15035 (BNWL-196)
Pu release studies. I., 20: 15036 (BNWL-205)
SNPO and SNAP biological studies, 20: 14785 (BNWL-182)
Storage of long-lived fission products on alumino-silicate zeolites, 20: 14466 (RL-SA-58)
Texture studies in monoclinic plutonium, 20: 15944 (RL-REA-2595, pp 12-14)
BAYERNWERK, A. G., MUNICH (WEST GERMANY).
Control rod drive system of Garigliano nuclear power plant, SENN, 20: 16074 (EUR-2420.d,f,i,n,e, pp 227-48)
Description of the turbine regulation and experience at SENN-power station on turbine startup, 20: 16071 (EUR-2420.d,f,i,n,e, pp 191-202)
BERNE UNIV. (SWITZERLAND). PHYSIKALISCHES INSTITUT.
Rare gas measurements in 30 stone meteorites, 20: 15193 (NP-15654)
BETTIS ATOMIC POWER LAB., PITTSBURGH, PA.
Decontamination of Shippingport atomic power station, 20: 16088 (WAPD-299)
Evaluation of low-density single-phase cubic $ZrO_2 + UO_2$ fuels stabilized with CaO, 20: 15138 (WAPD-292)
Prog. rpt. on PWR project, 7/24–10/21/65, 20: 16089 (WAPD-MRP-114)
SHREW—FORTRAN code for computing angular distributions, polarizations and transport cross sections of neutrons scattered by spinless targets, 20: 15670 (WAPD-TM-524)
BETTIS ATOMIC POWER LAB., WEST MIFFLIN, PA.
Diffusion theory representation of fuel clusters containing control, 20: 16090 (WAPD-T-1841)
BOSTON UNIV., MASS.
Prog. rpt. on radiation chemistry of organic compounds, 2/65–1/66, 20: 14579 (NYO-2383-15)
BRANDEIS UNIV., WALTHAM, MASS. DEPT. OF CHEMISTRY.
Analytic continuation of an S_{11} pion-nucleon amplitude to the P_{11} amplitude, 20: 15312 (MIT-2098-86)
BRITISH COLUMBIA UNIV., VANCOUVER. FACULTY OF MEDICINE.
Alpha-radiographic and histological observations on skeletal effects of hypo and hypervitaminoses A and D in the rat, 20: 16148 (NYO-2779-9)
Demineralization with EDTA by constant replacement, 20: 16149 (NYO-2779-10)
BROOKHAVEN NATIONAL LAB., UPTON, N. Y.
Accelerators of the future, 20: 15156 (BNL-741(Rev.))
Changes in leaves of *Quercus Alba* exposed to chronic gamma radiation, 20: 14289 (BNL-9509)
Conference on genetic control of differentiation, Brookhaven National Lab., 6/65, 20: 14231 (BNL-931)
Description of evaluated nuclear data file service routines, 20: 15995 (BNL-966)
Growth of tracks from segments, 20: 14849 (BNL-9720)
High-temperature liquid-metal technology review, Vol. 3, No. 6, 12/65, 20: 14958 (BNL-972)
Neutron burning of long-lived fission products for waste disposal, 20: 16132 (BNL-8558)
Parametric radiation detector preamplifier, 20: 14851 (BNL-9980)
Structure of Brookhaven FSD system for analysis of bubble chamber film, 20: 14850 (BNL-9763)
Transverse coherent instability of bunched beams, 20: 15170 (SLAC-49, pp 36-48)
BROWN, BOVERI UND CIE A. G., MANNHEIM (WEST GERMANY).
Influence of CsF on emitter work function and the performance of Cs diodes, 20: 15297 (CONF-640921, pp 101-9)
BROWN ENGINEERING CO., INC., HUNTSVILLE, ALA. RESEARCH LABS.
Study of Rankine-cycle space nuclear power systems, 20: 16111 (N65-16315)
BROWN UNIV., PROVIDENCE, R. I. DIV. OF ENGINEERING.
Prog. rpt. on mechanical properties of metals, 2/65–1/66, 20: 15055 (NYO-2394-19)
BRUSSELS UNIV. (BELGIUM).
Double ionization accompanying ^{6}He decay, 20: 15715 (CONF-233 (Vol.3), pp 505-9)
BUREAU OF MINES, ALBANY, OREG. ALBANY METALLURGY RESEARCH CENTER.
Electric-arc furnace reduction of tin slag for production of columbium–tantalum-bearing alloy, 20: 14956 (BM-RI-6734)
Prog. rpt. on metallurgy, 10–12/65, 20: 14968 (USBM-RC-1220)
BUREAU OF MINES, MORGANTOWN, W. VA. MORGANTOWN COAL RESEARCH CENTER.
Prog. rpt. on high-temperature energy system, 8–10/65, 20: 14671 (TID-22394)

C

CAIRO UNIV. (EGYPT). FACULTY OF ENGINEERING.
L auger spectra in j-j coupling, 20: 15237 (CONF-233(Vol.3), pp 371-97)
CAMBRIDGE ELECTRON ACCELERATOR, MASS.
Summary of research operations at Cambridge electron accelerator, 1/66, 20: 15306 (CEAL-1026)
Wake fields of charged particle traveling in vacuum chamber with resistive walls, 20: 15169 (SLAC-49, pp 32-5)
CAROLINAS VIRGINIA NUCLEAR POWER ASSOCIATES, INC., PARR, S. C.
CVTR control rod performance test, 20: 16062 (CVNA-175)
CVTR organic loop feasibility study, 20: 16063 (CVNA-241)
Meteorological program at Parr, South Carolina, 20: 14732 (CVNA-172)
CATHOLIC UNIV. OF AMERICA, WASHINGTON, D. C. DEPT. OF SPACE SCIENCE AND APPLIED PHYSICS.
MHD boundary layer between parallel streams of different magnetic fields and temperatures, 20: 15570 (N65-21084)
CATHOLIC UNIV. OF AMERICA, WASHINGTON, D. C. DIV. OF NUCLEAR SCIENCE AND ENGINEERING.
Effect of mechanically induced vibrations on heat transfer rates in pressurized water system, 20: 16000 (NYO-2655-1)
Feasibility of short-lived radioisotope tracer system for detection of hidden materials, 20: 14451 (NYO-2586-2)
CENTRAL UTILITIES ATOMIC POWER ASSOCIATES.
Pathfinder flooding coefficient, core pressurization, and temperature coefficient tests, 20: 16059 (ACNP-65600)
CENTRE NATIONAL DE LA RECHERCHE SCIENTIFIQUE, ORSAY (FRANCE). CENTRE DE SPECTROMETRIE NUCLEAIRE ET DE SPECTROMETRIE DE MASSE.
The L,M,N Auger spectra and the Coster-Kroenig transitions of heavy elements, 20: 15240 (CONF-233(Vol.3), pp 440-53)
CENTRE NATIONAL DE RECHERCHES METALLURGIQUES, LIEGE (BELGIUM).
Prog. rpt. on embrittlement of reactor vessel steels, 7–9/65, 20: 15039 (EURAEC-1475)
CHEMICAL RESEARCH AND DEVELOPMENT LABS., EDGEWOOD ARSENAL, MD. EXPERIMENTAL ENGINEERING DIV.
Seventeenth materials review, 20: 14506 (CRDL-SP-5-7)
CHICAGO UNIV., ILL. INST. FOR COMPUTER RESEARCH.
Prog. rpt. on computer research, 11/65, 20: 14950 (COO-614-41)
COLORADO UNIV., BOULDER.
Representative models of observed solar wind, 20: 15190 (AD-620407)

COLUMBIA UNIV., NEW YORK. COLL. OF PHYSICIANS AND SURGEONS.
Alpha-radiographic and histological observations on skeletal effects of hypo and hypervitaminoses A and D in the rat, 20: 16148 (NYO-2779-9)
COLUMBIA UNIV., NEW YORK. ENGINEERING RESEARCH LABS.
Additional critical heat flux data for large-diameter, internally heated, eccentric annuli at 1000 psia, 20: 16086 (TID-22651)
COMBUSTION ENGINEERING, INC., WINDSOR, CONN. NUCLEAR DIV.
Analytical and experimental methods of determining heavy-isotope content of operating fuel elements, 20: 14438 (CEND-540)
COMISION NACIONAL DE ENERGIA ATOMICA, BUENOS AIRES (ARGENTINA).
Detector for reprocessing cells, 20: 14853 (CNEA-159)
COMISION NACIONAL DE ENERGIA NUCLEAR, MEXICO CITY.
Bibliography on conversion of salt and brackish waters into fresh water (1954–1964), 20: 14510 (NP-15834)
COMITATO NAZIONALE PER L'ENERGIA NUCLEARE, CASACCIA (ITALY). CENTRO DI STUDI NUCLEARI.
Bibliography on underground nuclear explosions, 20: 14661 (NP-15867)
COMITATO NAZIONALE PER L'ENERGIA NUCLEARE, ROME (ITALY).
Method for determination of intermediate neutron spectrum in reactor, 20: 14860 (RT/FI(65)-33)
Regulating characteristics during the operation of Latina power plant, 20: 16072 (EUR-2420.d,f,i,n,e, pp 203-14)
Regulation of output of electronuclear power plant of the BWR-type dual-cycle Garigliano power plant, 20: 16073 (EUR-2420.d,f,i,n,e, pp 215-25)
Small-angle elastic scattering of polarized protons in photographic emulsions, 20: 15314 (RT/FI(65)35)
COMITATO NAZIONALE ENERGIA NUCLEARE, ROME (ITALY). DIVISIONE DI BIOLOGIA E PROTEZIONE SANITARIA.
Control of polyphenyls in work environments, 20: 14467 (RT/PROT(64)-20)
COMMISSARIAT A L'ENERGIE ATOMIQUE, FONTENAY-AUX-ROSES (FRANCE). CENTRE D'ETUDES NUCLEAIRES.
Voltammetry of uranyl chloride in LiCl–KCl eutectic, 20: 14437 (CEA-R-2879)
COMMISSARIAT A L'ENERGIE ATOMIQUE, SACLAY (FRANCE). CENTRE D'ETUDES NUCLEAIRES.
Absolute measurement of activity of electron-capture nuclides, 20: 15690 (CEA-R-2813)
Aerodynamic study of the fluid flow in channel of reactor filled with internally and externally cooled fuel elements, 20: 15997 (CEA-R-2856)
Contribution to the study of the α-α interaction, 20: 15689 (CEA-R-2786)
Detection of fission fragments by secondary emission, 20: 14852 (CEA-R-2862)
Diffusion of iron, of silver and of carbon in beryllium, 20: 15037 (CEA-R-2621)
Electronic radiation of a plasma in a magnetic field, 20: 15870 (CEA-R-2881)
Heat transfer and pressure drops along surfaces fitted with herring bone fins, 20: 14685 (CEA-R-2471)
Measurement of resonance absorption integrals (Mn, Fe, Co, Ni, Cu, Zr, Mo), 20: 15691 (CEA-R-2840)
Release, properties, and trapping of radioactive iodines in waste gases, 20: 14787 (CEA-Bib-64)
Space-time dependent impulse response of a subcritical cylindrical reactor, 20: 16020 (CEA-R-2836)
The anisotropic collision in cell problems, 20: 16021 (CEA-R-2890)
COMPAGNIE FRANCAISE THOMSON–HOUSTON, PARIS.
Neutronic control of Garigliano reactor, 20: 16068 (EUR-2420.d,f,i,n,e, pp 133-45)
CONNECTICUT UNIV., STORRS. DEPT. OF PHYSICS.
Coincidence study of O^+ on Kr collisions, 20: 15249 (TID-22643)
CORNELL UNIV., ITHACA, N. Y. MATERIALS SCIENCE CENTER.
Electron spin resonance identification of N_2^- in irradiated sodium azide, 20: 15942 (NYO-2150-11)
COSMIC, INC., WASHINGTON, D. C.
Development of charged colloid source for electrostatic propulsion, 20: 14725 (N65-15876)

D

DEPARTMENT OF MINES AND TECHNICAL SURVEYS (CANADA). MINES BRANCH.
Corrosion behavior of U-bearing resulfurized Cr stainless steel, 20: 14983 (NP-15875)
DEPARTMENT OF NATIONAL HEALTH AND WELFARE, OTTAWA (ONTARIO). RADIATION PROTECTION DIV.
Canadian fallout data for October 1965, 20: 14737 (NP-15853, pp 8-20)
Data from radiation protection programs, 20: 14735 (NP-15853)
Reactor environment monitoring for October 1965, 20: 14738 (NP-15853, pp 21-33)
^{90}Sr in 1964 Canadian hard red spring wheat, 20: 14736 (NP-15853, pp 3-7)
DIVISION OF ISOTOPES DEVELOPMENT (AEC), WASHINGTON, D. C.
New developments and trends in isotope industry, 20: 14929 (CONF-651132-1)
DIVISION OF RAW MATERIALS (AEC), WASHINGTON, D. C.
Uranium exploration in Chile, 20: 14779 (RME-4569(Rev.))
DIVISION OF TECHNICAL INFORMATION EXTENSION, (AEC), OAK RIDGE, TENN.
Bibliographies of atomic energy literature, 20: 16152 (TID-3732)
DU PONT DE NEMOURS (E. I.) & CO., AIKEN, S. C. SAVANNAH RIVER LAB.
Chemical processing of Cm, 20: 14636 (CONF-660305-7)
Evaluation of commercial n-paraffin mixtures for purex diluent, 20: 14637 (DP-1034)
Large-scale ^{60}Co heat sources, 20: 14945 (CONF-660305-14)
Radioisotope production capabilities of U. S. power reactors, 20: 14946 (DP-1015)
Recovery and purification of ^{147}Pm, 20: 14635 (CONF-660305-5)
^{244}Cm for radioisotopic heat sources work at Savannah River Laboratory, 20: 15038 (CONF-660305-12)

E

EIDGENOESSISCHE TECHNISCHE HOCHSCHULE, ZURICH (SWITZERLAND).
Exact and approximate solutions of many-group transport equations in even geometry, 20: 15667 (EIR-72)
ELECTRICITE DE FRANCE, CHINON.
Automatic devices—safety equipment—control room of the Latina power plant, 20: 16067 (EUR-2420.d,f,i,n,e, pp 117-31)
Detection of can ruptures in the Latina power plant, 20: 16070 (EUR-2420.d,f,i,n,e, pp 181-9)
ENTE NAZIONALE PER L'ENERGIA ELETTRICA, LATINA (ITALY).
Control rod system for the SENN reactor, 20: 16069 (EUR-2420.d,f,i,n,e, pp 147-80)
EUROPEAN ATOMIC ENERGY COMMUNITY.
Automatic devices—safety equipment—control room of the Latina power plant, 20: 16067 (EUR-2420.d,f,i,n,e, pp 117-31)
Control rod drive system of Garigliano nuclear power plant, SENN, 20: 16074 (EUR-2420.d,f,i,n,e, pp 227-48)
Control rod system for the SENN reactor, 20: 16069 (EUR-2420.d,f,i,n,e, pp 147-80)
Controls for the Latina power plant, 20: 16066 (EUR-2420.d,f,i,n,e, pp 51-115)
Description of the turbine regulation and experience at SENN-power station on turbine startup, 20: 16071 (EUR-2420.d,f,i,n,e, pp 191-202)
Detection of can ruptures in the Latina power plant, 20: 16070 (EUR-2420.d,f,i,n,e, pp 181-9)
In-core instrumentation for the reactor of the SENN power plant at Garigliano, 20: 16065 (EUR-2420.d,f,i,n,e, pp 17-49)
Influence of molecular structure on composition of steroids in solution by autoirradiation, 20: 14578 (EUR-2435.f)
Instrumentation and control in Garigliano and Latina nuclear power plants, 20: 16064 (EUR-2420.d,f,i,n,e)
Neutronic control of Garigliano reactor, 20: 16068 (EUR-2420.d,f,i,n,e, pp 133-45)
Regulating characteristics during the operation of Latina power plant, 20: 16072 (EUR-2420.d,f,i,n,e, pp 203-14)
Regulation of output of electronuclear power plant of the BWR-type dual-cycle Garigliano power plant, 20: 16073 (EUR-2420.d,f,i,n,e, pp 215-25)
Wear research on reactor parts, 20: 15998 (EUR-2117.n)
EUROPEAN ATOMIC ENERGY COMMUNITY, ISPRA (ITALY). JOINT NUCLEAR RESEARCH CENTER.
Control rod system for the SENN reactor, 20: 16069 (EUR-2420.d,f,i,n,e, pp 147-80)
Controls for the Latina power plant, 20: 16066 (EUR-2420.d,f,i,n,e, pp 51-115)
Neutron transport in a spherical reactor, 20: 16022 (EUR-2627.e)
One-group collision probability code for cylinders and slabs, 20: 15668 (EUR-2624.e)
EUROPEAN COMPANY FOR THE CHEMICAL PROCESSING OF IRRADIATED FUELS, MOL (BELGIUM).
Aqueous processing of graphite-carbide fuel elements, 20: 14638 (NP-15753)
EUROPEAN ORGANIZATION FOR NUCLEAR RESEARCH, GENEVA (SWITZERLAND).
Choice of substances for polarized proton targets, 20: 15692 (CERN-66-3)
Excitation of delay-type magnets by short pulses, 20: 15157 (CERN-66-1)
Incoherent beams blow-up in colliding beams, 20: 15174 (SLAC-49,

pp 71-3)
Report on design study of intersecting storage rings (ISR) for CERN proton synchrotron, 20: 15158 (CERN-542)

F

FENIX AND SCISSON, INC., TULSA, OKLA.
Mining on Nevada Test Site, 20: 14754 (NVO-38-1)
FIAT, TURIN (ITALY). SEZIONE ENERGIA NUCLEARE.
In-core instrumentation for the reactor of the SENN power plant at Garigliano, 20: 16065 (EUR-2420.d,f,i,n,e, pp 17-49)
FREIE UNIVERSITAET, BERLIN (WEST GERMANY). I. PHYSIKALISCHES INSTITUT.
Development of 100-Mev FFAG electron synchrotron: broad-band adaptation of accelerator electrodes, 20: 15161 (NP-15273)

G

GENERAL ATOMIC, SAN DIEGO, CALIF.
Thermionic reactor reliability, 20: 15292 (AD-620511)
GENERAL ATOMIC, SAN DIEGO, CALIF. JOHN JAY HOPKINS LAB. FOR PURE AND APPLIED SCIENCE.
Evaluation of vapor-deposited tungsten tubing, 20: 15048 (N65-16231)
Prog. rpt. on application of neutron activation analysis in scientific crime detection, 5/62–10/63, 20: 14439 (GA-5556)
Prog. rpt. on cathodes for thermionic reactors, 4/63, 20: 15046 (N65-15820)
Prog. rpt. on mechanical properties of reactor materials, annual, 11/64–10/65, 20: 15040 (GA-6721)
Prog. rpt. on thermionic materials for space power applications, 10/63, 20: 14959 (N65-20797)
Prog. rpt. on thermionic materials for space power applications, 9/63, 20: 14960 (N65-20798)
Prog. rpt. on thermionic materials for space power application, 12/63, 20: 14961 (N65-20801)
Prog. rpt. on thermionic materials for space power applications, 1/64, 20: 14962 (N65-20803)
RAD 2: computer program for calculating fission product radioactivities, 20: 16075 (GAMD-6519)
GENERAL ELECTRIC CO., CINCINNATI, OHIO. NUCLEAR MATERIALS AND PROPULSION OPERATION.
Properties of some refractory metals. V., 20: 15041 (GEMP-397)
GENERAL ELECTRIC CO., PHILADELPHIA, PA. MISSILE AND SPACE DIV.
Investigation of plasma accelerator (cyclotron resonance propulsion system), 20: 14726 (NASA-CR-54746)
Navigator study of electric propulsion for unmanned scientific missions, 20: 14724 (65SD5322-A)
Prog. rpt. on surface contouring as applied to semiconductor radiation detectors, semiannual, 1–6/65, 20: 14858 (NYO-3246-5)
GENERAL ELECTRIC CO., PLEASANTON, CALIF. VALLECITOS ATOMIC LAB.
A fresh look at the Child-Langmuir problem, 20: 15295 (CONF-640921, pp 47-77)
GENERAL ELECTRIC CO., RICHLAND, WASH. HANFORD ATOMIC PRODUCTS OPERATION.
Administering criticality control in Hanford Atomic Products Operation non-reactor environment, 20: 14790 (RL-SA-43A)
Comparison of double diffracting x-ray unit with standard x-ray diffraction unit, 20: 14823 (RL-REA-2595, pp 73-9)
Conference on applications of x-ray diffraction in the atomic energy field, Richland, Wash., 2/65, 20: 15943 (RL-REA-2595)
Determination of residual stress in uranium with an x-ray diffractometer, 20: 15945 (RL-REA-2595, pp 43-50)
Large scale processing and source preparation of separated fission products, 20: 14641 (RL-SA-59)
Line broadening in irradiated molybdenum, 20: 15136 (RL-REA-2595, pp 51-62)
Prog. rpt. on batch electrorefining of Pu metal, 5/65, 20: 14967 (RL-SEP-503-1)
Stirred-bed gas-solids reactor for preparing plutonium trichloride, 20: 14669 (RL-SEP-414)
Storage of long-lived fission products on alumino-silicate zeolites, 20: 14466 (RL-SA-58)
Texture studies in monoclinic plutonium, 20: 15944 (RL-REA-2595, pp 12-14)
Zirconium fire experience, 20: 15001 (HW-66930)
GENERAL ELECTRIC CO., SAN JOSE, CALIF. ADVANCED PRODUCTS OPERATION.
Sodium mass transfer. XIX., 20: 14979 (GEAP-4835)
GENERAL ELECTRIC CO., SAN JOSE, CALIF. ATOMIC POWER EQUIPMENT DEPT.
Dependence of transition boiling heat transfer on loop flow disturbances, 20: 14687 (GEAP-4785)
Prog. rpt. on accurate nuclear fuel burnup analyses, 2–5/65, 20: 15133 (GEAP-4893)
Prog. rpt. on accurate nuclear fuel burnup analyses, 6–8/65, 20: 15717 (GEAP-4950)
Prog. rpt. on specific Zr alloy design program, 1/66, 20: 14980 (GEAP-5065)
GENERAL MOTORS CORP., SANTA BARBARA, CALIF. DEFENSE RESEARCH LABS.
Bathyphotometric studies of light regime of organisms of deep scattering layers, 20: 14235 (SAN-584-1)
Dissociation and evaporation of TaC, HfC, and ZrC at elevated temperatures, 20: 15052 (NP-15880)
GENEVA UNIV. (SWITZERLAND). BIOPHYSICAL LAB.
X-ray inactivation of lambda phages. I, II, 20: 14260 (NP-15856)
GEORGIA INST. OF TECH., ATLANTA.
Bibliography on atomic and molecular processes, 1964, 20: 15248 (ORNL-AMPIC-3)
GEORGIA INST. OF TECH., ATLANTA. ENGINEERING EXPERIMENT STATION.
Prog. rpt. on mechanical properties of slip-cast fused silica, final, 7/64–6/65, 20: 15058 (SC-DC-66-1130)
GEORGIA UNIV., ATHENS.
Infrared spectra of neoprene before and after gamma irradiation, 20: 14585 (TID-22652)
GLASGOW UNIV. (SCOTLAND). DEPT. OF NATURAL PHILOSOPHY.
Ratio of K-capture to positron emission in decay of ^{13}N, 20: 15712 (CONF-233(Vol.2), pp 359-64)
GOSUDARSTVENNYI KOMITET PO ISPOL'ZOVANIYU ATOMNOI ENERGII SSSR, MOSCOW. SOYUZNYI NAUCHNO-ISSLEDOVATEL'SKII INSTITUT PRIBOROSTROENIYA.
Type 9014-01 alpha-radiation ionization spectrometer and its uses for measuring small concentrations of aerosols of alpha-active isotopes, 20: 14857 (NP-15448)
Impurities in Cs in thermionic converters, 20: 15298 (FEI-22)
GRENOBLE UNIV. (FRANCE). LABORATOIRE DE PHYSIQUE NUCLEAIRE.
Orbital electron capture by the nucleus, 20: 15695 (CONF-233(Vol.1), pp 30-59)

H

HARVARD UNIV., CAMBRIDGE, MASS.
Summary of research operations at Cambridge electron accelerator, 1/66, 20: 15306 (CEAL-1026)
HIGH ALTITUDE OBSERVATORY, BOULDER, COLO.
Bibliography on effects of short-wave and particle radiation on glasses, 20: 15134 (N65-15819)
HOPITAL ST. PIERRE, LOUVAIN (BELGIUM). LABORATOIRE DE RECHERCHES DE LA CLINIQUE MEDICALE.
Influence of molecular structure on composition of steroids in solution by autoirradiation, 20: 14578 (EUR-2435.f)
HUGHES AIRCRAFT CO., FULLERTON, CALIF.
Prog. rpt. on radiation effects on microelectronic circuits, 5–7/65, 20: 14918 (ECOM-01313-1)

I

IIT RESEARCH INST., CHICAGO, ILL.
Prog. rpt. on reactor containment, 10–11/65, 20: 16023 (IITRI-578P21-16)
Prog. rpt. on yield phenomena and fracture of hydrided Zr, 10–12/65, 20: 15042 (IITRI-578-P27-14)
ILLINOIS INST. OF TECH., CHICAGO.
Vacuum polarization in μ-mesic atoms, 20: 15246 (CONF-233(Vol.3), pp 520-8)
ILLINOIS UNIV., URBANA. COORDINATED SCIENCE LAB.
Thermodynamic properties of an electron plasma, 20: 15869 (AD-628317)
ILLINOIS UNIV., URBANA. ENGINEERING EXPERIMENT STATION.
Admittance and resonance probe characteristics of a spherical plasma probe, 20: 15868 (AD-628186)
ILLINOIS UNIV., URBANA. GASEOUS ELECTRONICS LAB.
Collision frequency measurements in oxygen and helium magneto-plasma afterglows, 20: 15867 (AD-620664)
INSTITUT DE SOUDURE, PARIS (FRANCE).
Welding tests on section taken from heavy-gage plates of rolled steel, 20: 15000 (EURAEC-1517)
INSTITUT FUER PLASMAPHYSIK, G.M.B.H. GARCHING (WEST GERMANY).
Calculation of two-dimensional magnetic field of even number of Ioffe bars by complex analysis, 20: 15878 (IPP-6/42)
Development of a laser amplifier and application in plasma diagnostics, 20: 15873 (IPP-1/42)
Influence of rotation and magnetic fields on thermal instability of fluid

sphere, 20: 15876 (IPP-6/33)
Measurements of electron temperature in an argon–potassium plasma, 20: 15874 (IPP-3/31)
Plane magnetohydrostatic equilibria with interior field, 20: 15877 (IPP-6/41)
Population densities of discrete energy levels in a stationary nonthermal hydrogen arc, 20: 15875 (IPP-3/32)
Prog. rpt. on plasma physics, annual, 1964, 20: 15882 (NP-15868)
Radial and axial distribution of the electron density of theta pinch as function of time, 20: 15871 (IPP-1/38)
Three-dimensional normal modes of Vlasov plasma with and without magnetic field, 20: 15879 (IPP-6/43)
Time-resolved profile measurements of impurity lines in theta pinch discharge, 20: 15872 (IPP-1/41)

INSTITUT NATIONAL DES SCIENCES ET TECHNIQUES NUCLEAIRES, PARIS (FRANCE).
A fresh look at the Child-Langmuir problem, 20: 15295 (CONF-640921, pp 47-77)
Conference on thermionic conversion, Saclay, 9/64, 20: 15293 (CONF-640921)
Influence of CsF on emitter work function and the performance of Cs diodes, 20: 15297 (CONF-640921, pp 101-9)
Recent progress in fundamental and applied thermionic converter technology, 20: 15294 (CONF-640921, pp 9-45)
Utilization of impregnation compounds in graphite in thermionic conversion, 20: 15296 (CONF-640921, pp 81-99)

INSTITUTE OF NUCLEAR PHYSICS, KRAKOW (POLAND).
Octupole coulomb excitation of ^{208}Pb, 20: 15719 (INP-431/PL)

INSTITUTE OF NUCLEAR RESEARCH, WARSAW (POLAND).
Application of noise technique to diagnostics of magnetohydrodynamics, 20: 15569 (INR-626/IX/R)

INSTITUTO DE ENERGIA ATOMICA, SAO PAULO (BRAZIL).
Waste disposal problems, 20: 16134 (IEA-102)

INSTITUTO DE INVESTIGACIONES GEOLOGICAS, SANTIAGO (CHILE).
Uranium exploration in Chile, 20: 14779 (RME-4569(Rev.))

INSTITUTT FOR ATOMENERGI, KJELLER (NORWAY).
Radiochemical and nuclear studies of short-lived fission products ^{146}Ce, ^{146}Ce, and ^{147}Ce, 20: 15722 (KR-76)

INSTITUUT VOOR KERNPHYSISCH ONDERZOEK, AMSTERDAM (NETHERLANDS).
E2 conversion coefficients in ^{152}Sm, ^{154}Gd, and ^{160}Dy, 20: 15705 (CONF-233(Vol.2), pp 177-90)
Some allowed K-capture to positron ratios, 20: 15711 (CONF-233(Vol.2), pp 345-58)

INTERNATIONAL ATOMIC ENERGY AGENCY, VIENNA (AUSTRIA).
Angular correlation and internal conversion studies in ^{125}I and ^{127}I, 20: 15701 (CONF-233(Vol.2), pp 128-41)
Anomalous L-subshell conversion of some hindered E1 transitions in the rare earth region, 20: 15703 (CONF-233(Vol.2), pp 148-57)
Application to lens-type spectrometer of internal-external conversion IEC method for determination of internal conversion coefficients, 20: 15710 (CONF-233(Vol.2), pp 252-5)
Atomic M-level widths in ^{151}Sm, 20: 15241 (CONF-233(Vol.3), pp 454-64)
Atomic readjustment following formation of inner shell vacancies, 20: 15245 (CONF-233(Vol.3), pp 494-504)
Comparison of recent precision results of orbital electron capture ratios with theory, 20: 15713 (CONF-233(Vol.2), pp 365-8)
Conference on role of atomic electrons in nuclear transformations, Warsaw, 9/63, 20: 15236 (CONF-233(Vol.3))
Conference on role of atomic electrons in nuclear transformations, Warsaw, Poland, 9/63, 20: 15693 (CONF-233(Vol.1))
Conference on role of atomic electrons in nuclear transformations, Warsaw, 9/63, 20: 15697 (CONF-233(Vol.2))
Double ionization accompanying ^{6}He decay, 20: 15715 (CONF-233 (Vol.3), pp 505-9)
Experimental and theoretical studies of L-conversion electron directional correlations, 20: 15699 (CONF-233(Vol.2), pp 117-19)
E2 conversion coefficients in ^{110}Cd and ^{132}Xe, 20: 15704 (CONF-233 (Vol.2), pp 164-76)
E2 conversion coefficients in ^{152}Sm, ^{154}Gd, and ^{160}Dy, 20: 15705 (CONF-233(Vol.2), pp 177-90)
Influence of nuclear charge distribution on β decay, 20: 15716 (CONF-233(Vol.3), pp 529-37)
Internal conversion, 20: 15694 (CONF-233(Vol.1), pp 1-29)
Internal pair formation and electroexcitation of nuclei, 20: 15696 (CONF-233(Vol.1), pp 60-86)
K-conversion coefficient of the 412-kev E2 transition in ^{198}Hg, 20: 15707 (CONF-233(Vol.2), pp 198-212)
K-conversion process of the 412-kev E2 transition in ^{198}Hg, 20: 15708 (CONF-233(Vol.2), pp 213-19)
K-shell conversion coefficients for pure E2 transitions in deformed nuclei, 20: 15706 (CONF-233(Vol.2), pp 191-7)
K-shell fluorescence yields of V, Cr, and Cu, 20: 15242 (CONF-233(Vol.3), pp 465-79)
KLL-Auger spectrum of manganese, 20: 15243 (CONF-233(Vol.3), pp 480-6)
L auger spectra in j-j coupling, 20: 15237 (CONF-233(Vol.3), pp 371-97)
$L_1L_{2,3}M_{4,5}$ Coster-Kronig transition rates, 20: 15238 (CONF-233(Vol.3), pp 398-418)
Measurement of the M/L-capture ratio in 30-million-year ^{205}Pb decay, 20: 15714 (CONF-233(Vol.2), pp 369-70)
On K-level widths, 20: 15239 (CONF-233(Vol.3), pp 419-39)
Orbital electron capture by the nucleus, 20: 15695 (CONF-233(Vol.1), pp 30-59)
Particle parameter of the $2^+ \rightarrow 0^+$ E2 transition in ^{152}Sm, 20: 15698 (CONF-233(Vol.2), pp 109-16)
Particle parameter of the $2^+ \rightarrow 0^+$ E2 transition in ^{170}Yb, 20: 15700 (CONF-233(Vol.2), pp 120-7)
Photoelectron scattering and consequences for determination of internal conversion coefficients by the IEC method, 20: 15709 (CONF-233 (Vol.2), pp 247-51)
Ratio of K-capture to positron emission in decay of ^{13}N, 20: 15712 (CONF-233(Vol.2), pp 359-64)
Seminar on high-energy physics and elementary particles, Trieste, 5–6/65, 20: 15315 (STI/PUB/117)
Some allowed K-capture to positron ratios, 20: 15711 (CONF-233(Vol.2), pp 345-58)
Studies of Auger effect in light elements, 20: 15244 (CONF-233(Vol.3), pp 487-93)
Symposium on non-destructive testing in nuclear technology. Vol. I., Bucharest, 5/65, 20: 14701 (STI/PUB/105(Vol.1))
The L,M,N Auger spectra and the Coster-Kroenig transitions of heavy elements, 20: 15240 (CONF-233(Vol.3), pp 440-53)
Vacuum polarization in μ-mesic atoms, 20: 15246 (CONF-233(Vol.3), pp 520-8)

INTERNATIONAL CENTRE FOR THEORETICAL PHYSICS, TRIESTE (ITALY).
Evaluation of $N^{\frac{3}{2}}_{3}N$ weak coupling constants, 20: 15308 (IC/66/13)
Impossibility of having exact U(6) group based upon algebra of currents, 20: 15444 (IC/66/14)

INTERNATIONAL UNION OF PURE AND APPLIED PHYSICS.
Angular correlation and internal conversion studies in ^{125}I and ^{127}I, 20: 15701 (CONF-233(Vol.2), pp 128-41)
Anomalous L-subshell conversion of some hindered E1 transitions in the rare earth region, 20: 15703 (CONF-233(Vol.2) , pp 148-57)
Application to lens-type spectrometer of internal-external conversion method for determination of internal conversion coefficients, 20: 15710 (CONF-233(Vol.2), pp 252-5)
Atomic M-level widths in ^{151}Sm, 20: 15241 (CONF-233(Vol.3), pp 454-64)
Atomic readjustment following formation of inner shell vacancies, 20: 15245 (CONF-233(Vol.3), pp 494-504)
Comparison of recent precision results of orbital electron capture ratios with theory, 20: 15713 (CONF-233(Vol.2), pp 365-8)
Conference on role of atomic electrons in nuclear transformations, Warsaw, Vol. 3, 9/63, 20: 15236 (CONF-233(Vol.3))
Conference on role of atomic electrons in nuclear transformations, Warsaw, Poland, 9/63, 20: 15693 (CONF-233(Vol.1))
Conference on role of atomic electrons in nuclear transformations, Warsaw, 9/63, 20: 15697 (CONF-233(Vol.2))
Double ionization accompanying ^{6}He decay, 20: 15715 (CONF-233 (Vol.3), pp 505-9)
Experimental and theoretical studies of L-conversion electron directional correlations, 20: 15699 (CONF-233(Vol.2), pp 117-19)
E2 conversion coefficients in ^{110}Cd and ^{132}Xe, 20: 15704 (CONF-233 (Vol.2), pp 164-76)
E2 conversion coefficients in ^{152}Sm, ^{154}Gd, and ^{160}Dy, 20: 15705 (CONF-233(Vol.2), pp 177-90)
Influence of nuclear charge distribution on β decay, 20: 15716 (CONF-233(Vol.3), pp 529-37)
Internal conversion, 20: 15694 (CONF-233(Vol.1), pp 1-29)
Internal pair formation and electroexcitation of nuclei, 20: 15696 (CONF-233(Vol.1), pp 60-86)
K-conversion coefficient of the 412-kev E2 transition in ^{198}Hg, 20: 15707 (CONF-233(Vol.2), pp 198-212)
K-conversion process of the 412-kev E2 transition in ^{198}Hg, 20: 15708 (CONF-233(Vol.2), pp 213-19)
K-shell conversion coefficients for pure E2 transitions in deformed nuclei, 20: 15706 (CONF-233(Vol.2), pp 191-7)
K-shell fluorescence yields of V, Cr, and Cu, 20: 15242 (CONF-233(Vol.3), pp 465-79)
KLL-Auger spectrum of manganese, 20: 15243 (CONF-233(Vol.3), pp 480-6)
L auger spectra in j-j coupling, 20: 15237 (CONF-233(Vol.3), pp 371-97)
$L_1L_{2,3}M_{4,5}$ Coster-Kronig transition rates, 20: 15238 (CONF-233(Vol.3), pp 398-418)
Measurement of the M/L-capture ratio in 30-million-year ^{205}Pb decay,

20: 15714 (CONF-233(Vol.2), pp 369-70)
On K-level widths, 20: 15239 (CONF-233(Vol.3), pp 419-39)
Orbital electron capture by the nucleus, 20: 15695 (CONF-233(Vol.1), pp 30-59)
Particle parameter of the $2^+ \rightarrow 0^+$ E2 transition in ^{152}Sm, 20: 15698 (CONF-233(Vol.2), pp 109-16)
Particle parameter of the $2^+ \rightarrow 0^+$ E2 transition in ^{170}Yb, 20: 15700 (CONF-233(Vol.2), pp 120-7)
Photoelectron scattering and consequences for determination of internal conversion coefficients by the IEC method, 20: 15709 (CONF-233 (Vol.2), pp 247-51)
Ratio of K-capture to positron emission in decay of ^{13}N, 20: 15712 (CONF-233(Vol.2), pp 359-64)
Some allowed K-capture to positron ratios, 20: 15711 (CONF-233(Vol.2), pp 345-58)
Studies of Auger effect in light elements, 20: 15244 (CONF-233(Vol.3), pp 487-93)
The L,M,N Auger spectra and the Coster-Kroenig transitions of heavy elements, 20: 15240 (CONF-233(Vol.3), pp 440-53)
Vacuum polarization in μ-mesic atoms, 20: 15246 (CONF-233(Vol.3), pp 520-8)
30.7-Kev anomalous electric dipole transition, 20: 15702 (CONF-233 (Vol.2), pp 142-7)

ISOCHEM INC., RICHLAND, WASH.
Large-scale processing and source preparation of separated fission products, 20: 14641 (RL-SA-59)
Storage facilities for Hanford high-level fission waste containers, 20: 16135 (RL-SA-62)

J

JAPAN ATOMIC ENERGY RESEARCH INST., TOKYO.
Centralized field radiological monitoring system at nuclear installation, 20: 14855 (JAERI-1090)
Feasibility calculation for JPDR-II core design; one-dimensional nuclear thermal and hydraulic calculation, 20: 16076 (JAERI-1088)
Radiation leak test of shielded cells at reprocessing analytical facility, 20: 14788 (JAERI-1089)
User's manual for JRR-4 experimental facilities, 20: 16122 (JAERI-6016)

JOHNS HOPKINS UNIV., BALTIMORE, MD. DEPT. OF MECHANICS.
Hall effect in two-dimensional flow along an insulating plane, 20: 15568 (AD-620324)

JOINT INST. FOR NUCLEAR RESEARCH, DUBNA (USSR). LAB OF NUCLEAR PROBLEMS.
Angular distribution of high energy neutrons emitted in absorbing polarized μ^- mesons in calcium, 20: 15721 (JINR-E-2517)
Asymmetry in angular distribution of high-energy neutrons from μ^- capture in sulfur, 20: 15720 (JINR-E-2516)
Production cross section of charged pions in (n,p) collisions at 585 Mev, 20: 15310 (JINR-P-2508)

JOINT INST. FOR NUCLEAR RESEARCH, DUBNA (USSR). LAB OF NUCLEAR REACTIONS.
Octupole coulomb excitation of ^{208}Pb, 20: 15719 (INP-431/PL)

JOINT INST. FOR NUCLEAR RESEARCH, DUBNA (USSR). LAB OF THEORETICAL PHYSICS.
Possible mechanism of CP violation, 20: 15309 (JINR-E-2563)

K

KANSAS ENGINEERING EXPERIMENT STATION, MANHATTAN.
Effect of neutron irradiated on transistor current gain, 20: 14920 (TID-22664)

KANSAS STATE UNIV., MANHATTAN. DEPT. OF CHEMISTRY.
Prog. rpt. on low energy investigations of radiation chemistry, final, 2/64–5/65, 20: 14584 (TID-22444)

KERNFORSCHUNGSANLAGE, JUELICH (WEST GERMANY). INSTITUT FUER REAKTORWERKSTOFFE.
Dispersion curves for rotation oscillations of tetrahedral molecules in face-centered lattice with tetragonal molecular orientation, 20: 15940 (JUL-292-RW)

KERNFORSCHUNGSANLAGE, JUELICH (WEST GERMANY). ZENTRALABTEILUNG STRAHLENSCHUTZ.
Detection of incorporated plutonium, 20: 14239 (JUL-312-ST)

KERNFORSCHUNGSZENTRUM, KARLSRUHE (WEST GERMANY).
Subcritical, critical, and burst facilities in fast reactor physics research, 20: 16123 (KFK-350)

KERNFORSCHUNGSZENTRUM, KARLSRUHE (WEST GERMANY). INSTITUT FUER EXPERIMENTELLE KERNPHYSIK.
Construction and properties of analyzer for measurement of neutron polarization, 20: 14856 (KFK-345)

KNOLLS ATOMIC POWER LAB., SCHENECTADY, N. Y.
Doppler coefficient of thorium oxide, 20: 15732 (TID-21654)
Neutron measurement by track imaging in insulating materials, 20: 14854 (CONF-660304-3)
Variational methods in the calculation of spatially dependent spectra, 20: 15666 (CONF-660204-4)

L

LABORATORI NAZIONALI DI FRASCATI, COMITATO NAZIONALE PER L'ENERGIA NUCLEARE (ITALY).
External beam of Frascati electron synchrotron, 20: 15159 (LNF-65/36)
Instrument for measuring magnetic fields in range 0.01 to 20 gauss with peaking-strips, 20: 15160 (LNF-65/44)
Theory of coherent bunch motion in electron-positron storage rings, 20: 15173 (SLAC-49, pp 61-8)
Vector boson hunting with Adone, 20: 15311 (LNF-65/47)

LAWRENCE RADIATION LAB., UNIV. OF CALIFORNIA, BERKELEY.
Apparatus for heat capacity measurements in range 0.24 to 20°K, 20: 15061 (UCRL-11580)
Asymptotic perturbation fields of longitudinally bunched beam within rectangular pipe with resistive walls, 20: 15168 (SLAC-49, pp 23-31)
Behavior of droplets evaporating in high temperature convective environments, 20: 14692 (UCRL-16656)
Dislocation mechanisms of Mo single crystals, 20: 15946 (UCRL-16643)
Dislocation mechanisms in deformation of high-purity tantalum at low temperatures, 20: 15947 (UCRL-16645)
Effect of LiF on densification of MgO, 20: 15010 (UCRL-16534)
Influence of dielectric media on electromagnetic fields of coasting beam in straight rectangular pipe, 20: 15172 (SLAC-49, pp 52-8)
Longitudinal dispersion in single-phase liquid flow through ordered and random packings, 20: 14691 (UCRL-10696(Rev.)(Pt.2))
Longitudinal wake fields of pulse of charge moving down straight pipe of circular cross section with finite conductivity, 20: 15167 (SLAC-49, pp 18-22)
Measurement of heat released on solid surfaces, 20: 16153 (UCRL-16472)
Photobiochemistry—dehydration condensation in aqueous solution, 20: 14233 (UCRL-16566)
Production properties and decay modes of the ϕ meson, 20: 15316 (UCRL-16526)
Spiral reader control and data acquisition with PDP-4, 20: 14861 (UCRL-16555)
Strain aging of iron alloys, 20: 15063 (UCRL-16585)
Theory of coherent bunch motion in electron-positron storage rings, 20: 15173 (SLAC-49, pp 61-8)
Thermodynamic properties of metals and alloys, 20: 14514 (UCRL-11821)
Threshold detector applications to neutron spectroscopy at Berkeley accelerators, 20: 15175 (UCRL-16312)
Transverse coherent instability of bunched beams, 20: 15170 (SLAC-49, pp 36-48)
Vapor pressure of Pb and activity measurements on liquid Pb–Sn alloys, 20: 15062 (UCRL-16514)
Vaporization studies of lanthanum fluoride, 20: 14515 (UCRL-16649)

LAWRENCE RADIATION LAB., UNIV. OF CALIFORNIA, LIVERMORE.
Apparent CP noninvariance and the neutrino sea, 20: 15446 (UCRL-12380-T)
Charge transfer cross sections for H^+, H_2^+, or H_3^+ on H_2 from 2 to 55 kev, 20: 15250 (UCRL-6987(Rev.1))
Dispersion relation for relativistic streams of finite radius, 20: 15885 (UCRL-12207(Rev.1))
Free field motion near nuclear explosion in salt: project salmon, 20: 14663 (UCRL-14463(Rev.1))
Mechanical properties of some uranium alloys, 20: 15060 (UCRL-7771)
Neutron-neutron interaction in triton-triton reaction, 20: 15733 (UCRL-7769)
Numerical simulation of seismic disturbances, 20: 14755 (UCRL-7929)
Prog. rpt. on controlled thermonuclear research, semiannual, 1–6/65, 20: 15886 (UCRL-14285)
Radial wave equations for a vector meson in a spherically symmetric potential, 20: 15447 (UCRL-14698-T)
Salmon seismic experiment, 20: 14664 (UCRL-14487(Rev.1))
Some analytical methods for explosives and explosive simulants, 20: 14470 (UCRL-7873)
Use of one- and two-dimensional hydrodynamic machine calculations in high explosive research, 20: 15571 (UCRL-14531)

LITTON SYSTEMS, INC., ST. PAUL, MINN. APPLIED SCIENCE DIV.
Large volume impactor collector, 20: 14815 (COO-401-139)

LOCKHEED–GEORGIA CO., MARIETTA.
Meteorological program at Parr, South Carolina, 20: 14732 (CVNA-172)

LOCKHEED NUCLEAR PRODUCTS, MARIETTA, GA.
Data compilation and evaluation of space shielding problems, 20: 15930 (NP-15697(Vol.2))

LOS ALAMOS SCIENTIFIC LAB., UNIV. OF CALIFORNIA, N. MEX.
Coated particle fuel elements for UHTREX, 20: 15002 (LA-3378)

Computer analysis of cell volume distributions, 20: 14232 (LA-3440)
Determination of nitride nitrogen in plutonium metal, alloys, and compounds, 20: 14440 (LA-3452)
High yield ^{233}U casting operations, 20: 15003 (LA-DC-7510)
Solubilities of selected elements in liquid Pu. VII., 20: 15043 (LA-3436)
Thermodynamic properties of Pu compounds from EMF measurements. I., 20: 14507 (LA-3399)

M

MALLINCKRODT CHEMICAL WORKS, WELDON SPRING, MO. URANIUM DIV.
Energy dispersion system for light element analysis with electron microprobe, 20: 14442 (MCW-1493, pp 5-13)
Prog. rpt. on feed materials, 11/65, 20: 14441 (MCW-1493)
Spectrochemical method for simultaneous determination of calcium, lithium, and potassium in high-purity thorium compounds, 20: 14443 (MCW-1493, pp 27-30)
X-ray determination of crystallite size of thoria, 20: 15044 (MCW-1493, pp 15-25)
MARQUETTE UNIV., MILWAUKEE, WIS.
Comparison of recent precision results of orbital electron capture ratios with theory, 20: 15713 (CONF-233(Vol.2), pp 365-8)
MARYLAND UNIV., COLLEGE PARK. DEPT. OF PHYSICS AND ASTRONOMY.
Anomalous propagation in a quantum plasma and magnon-helicon coupling, 20: 15941 (NP-15698)
Electron-phonon renormalization effects in high magnetic fields, 20: 15939 (AD-620189)
MASCHINENFABRIK AUGSBURG-NUERNBERG A. G., NUREMBERG (WEST GERMANY).
Prog. rpt. on critical heat flux in boiling water, 4–6/65, 20: 14686 (EURAEC-1448)
MASONIC MEDICAL RESEARCH LAB., UTICA, N. Y.
Prog. rpt. on effects of age and radiation on nucleic acid metabolism and protein synthesis in nervous system tissues, 3/15/65–1/1/66, 20: 14242 (TID-22591)
MASSACHUSETTS INST. OF TECH., CAMBRIDGE.
Analytic continuation of an S_{11} pion-nucleon amplitude to the P_{11} amplitude, 20: 15312 (MIT-2098-86)
The angular distributions and energy spectra of photoneutrons from heavy elements, 20: 15724 (MIT-2098-224)
Theoretical background for thermionic conversion including space-charge theory, 20: 15299 (NASA-TN-D-3324)
MASSACHUSETTS INST. OF TECH., CAMBRIDGE. LAB. FOR INSULATION RESEARCH.
Prog. rpt. on electron-ionization cross sections, semiannual, 12/16/64–6/15/65, 20: 15235 (AD-620289)
MASSACHUSETTS INST. OF TECH., CAMBRIDGE. LAB. FOR NUCLEAR SCIENCE.
The energy and angular distribution of photoneutrons from heavy elements, 20: 15723 (MIT-2098-162)
MASSACHUSETTS UNIV., AMHERST.
Changes in leaves of *Quercus Alba* exposed to chronic gamma radiation, 20: 14289 (BNL-9509)
MAX-PLANCK-INSTITUT FUER PHYSIK UND ASTROPHYSIK, MUNICH (WEST GERMANY).
Determination of electron density from line merging, 20: 15881 (MPI-PAE/PL-7/65)
Prog. rpt. on plasma physics, annual, 1964, 20: 15882 (NP-15868)
Variation of the adiabatic invariant of the harmonic oscillator, 20: 15623 (MPI-PAE/P1.15/65)
MIAMI UNIV., CORAL GABLES, FLA. DEPT. OF PHYSICS.
30.7-Kev anomalous electric dipole transition, 20: 15702 (CONF-233 (Vol.2), pp 142-7)
MICHIGAN STATE UNIV., EAST LANSING. DEPT. OF HORTICULTURE.
Penetration of organic compounds through isolated cuticular membranes with special reference to ^{14}C urea, 20: 16146 (COO-888-39)
Permeability of iron and iron chelates through cuticular membranes, 20: 16147 (COO-888-45)
MICHIGAN UNIV., ANN ARBOR.
Choral hydrate 800 rad dosimeter, 20: 14583 (TID-21634)
MINNESOTA UNIV., MINNEAPOLIS. MEDICAL SCHOOL.
Blood supply to hepatic V2 carcinoma implants as measured by radioactive microspheres, 20: 14405 (COO-1305-2)
MISSISSIPPI UNIV., JACKSON. DEPT. OF PHYSIOLOGY AND BIOPHYSICS.
Prog. rpt. on cardiac damage, final, 1965, 20: 14292 (TID-22563)
MISSOURI UNIV., COLUMBIA.
Heat-generated pressure oscillations in closed end pipe, 20: 14690 (SC-DC-66-1293)
MOSCOW STATE UNIV. (USSR). SCIENTIFIC RESEARCH INST. OF NUCLEAR PHYSICS.
Investigation of the transition effect, 20: 15317 (ORNL-tr-677)
MOUND LAB., MIAMISBURG, OHIO.
Prog. rpt., 6/65, 20: 14444 (MLM-1268)
MSA RESEARCH CORP., CALLERY, PA.
Prog. rpt. on measurement of impurities in Na, 10–12/65, 20: 14445 (MSAR-66-10)
MSA RESEARCH CORP., EVANS CITY, PA.
Prog. rpt. on effect of high-temperature Na on steels, 10–12/65, 20: 14981 (MSAR-66-09)
MUNICH UNIV. (WEST GERMANY).
Preparation and roentgenographic study of highly radioactive material, 20: 14509 (NP-15826)

N

NATIONAL AERONAUTICS AND SPACE ADMINISTRATION, CLEVELAND, OHIO. LEWIS RESEARCH CENTER.
Current distribution in an array of superconducting thin films, 20: 15643 (NASA-TN-D-3293)
Distortion of atomic-beam velocity distributions due to classical hard-sphere gas scattering, 20: 15247 (N65-15530)
Experimental study of effect of simulated reactor core position on nozzle heat transfer, 20: 14727 (NASA-TM-X-1208)
Magnetic susceptibilities of compositions in tantalum–tantalum carbide system, 20: 15045 (N65-15534)
Rates of hydrogen–graphite reaction between 1550° and 2260°C, 20: 14508 (N65-20481)
Simulated nuclear heating of liquid hydrogen in propellant tank, 20: 14728 (NASA-TN-D-3328)
Theoretical background for thermionic conversion including space-charge theory, 20: 15299 (NASA-TN-D-3324)
Thermal neutron flux perturbation by Dy–Al foils in H_2O and UO_2F_2–H_2O solutions, 20: 15669 (NASA-TN-D-3237)
NATIONAL AERONAUTICS AND SPACE ADMINISTRATION, GREENBELT, MD. GODDARD SPACE FLIGHT CENTER.
Liouville's equation and n-body problem, 20: 15148 (N65-20165)
Solar cycle effects on inner-zone protons, 20: 15590 (NASA-TN-D-3086)
NATIONAL AERONAUTICS AND SPACE ADMINISTRATION, HOUSTON, TEX. MANNED SPACECRAFT CENTER.
Model solar proton environments for manned spacecraft design, 20: 15191 (N65-20996)
NATIONAL AERONAUTICS AND SPACE ADMINISTRATION, HUNTSVILLE, ALA. GEORGE C. MARSHALL SPACE FLIGHT CENTER.
Solar flare environment, 20: 15192 (N65-21000)
NATIONAL AERONAUTICS AND SPACE ADMINISTRATION, WASHINGTON, D. C.
Bibliography on welding methods, 20: 15005 (NASA-SP-5024)
NATIONAL INST. FOR RESEARCH IN NUCLEAR SCIENCE, CHILTON (ENGLAND). RUTHERFORD HIGH ENERGY LAB.
Accelerator physics measurements, 20: 15165 (RHEL/R-112, pp 12-22)
Experimental techniques and apparatus, 20: 14822 (RHEL/R-112, pp 99-128)
Introduction to the higher symmetries, 20: 15445 (RHEL/R-102)
Prog. rpt., annual, PLA division, 1965, 20: 15164 (RHEL/R-112)
Proton-induced reactions, 20: 15729 (RHEL/R-112, pp 37-66)
Proton scattering, 20: 15728 (RHEL/R-112, pp 23-36)
Theoretical studies, 20: 15730 (RHEL/R-112, pp 67-98)
NATIONAL LEAD CO. OF OHIO, CINCINNATI.
Comparison of electrolytic and ferrosilicon-process magnesiums for uranium production, 20: 15050 (NLCO-970, pp 3.1-4)
Controlling furnace cycle with infrared pyrometers in casting of large uranium ingots, 20: 15006 (NLCO-970, pp 4.1-5)
Determination of ^{235}U by gamma-ray spectroscopy, 20: 14449 (NLCO-970, pp 7.1-5)
Determination of beta activities in plant effluents, 20: 14450 (NLCO-970, pp 8.1-4)
Development of thorium purification system, 20: 14448 (NLCO-970, pp 1.1-22)
Effect of furnace heating element arrangement on uranium metal quality, 20: 14964 (NLCO-970, pp 2.1-7)
Inhibition of corrosion of type-304L stainless steel from fluorides in nitric acid solutions, 20: 14982 (NLCO-970, pp 6.1-4)
Prog. rpt., 10–12/65, 20: 14963 (NLCO-970)
Thermoelectric cooling of cutting tools, 20: 14689 (NLCO-970, pp 5.1-7)
NATIONAL MARINE CONSULTANTS, ANAHEIM, CALIF.
Mono lake wave experiment: feasibility study, 20: 14660 (AD-620468)
NATIONAL RADIATION LAB., CHRISTCHURCH (NEW ZEALAND).
Prog. rpt. on fallout in New Zealand, 7–9/65, 20: 14734 (NP-15844)
NATIONAL TAIWAN UNIV., TAIPEI (CHINA). DEPT. OF AGRONOMY.
^{14}C-labeled urea and ^{32}P-labeled phosphate to investigate foliar-applied fertilizer for rice growing in reclaimed tidal lands, 20: 14240 (NP-15670)

NAVAL CIVIL ENGINEERING LAB., PORT HUENEME, CALIF.
Monte Carlo calculations of gamma-ray streaming through coplanar and noncoplanar ducts, 20: 15929 (AD-627890)
NAVAL ORDNANCE LAB., WHITE OAK, MD.
Anomalous propagation in a quantum plasma and magnon-helicon coupling, 20: 15941 (NP-15698)
NAVAL POSTGRADUATE SCHOOL, MONTEREY, CALIF.
Half-life measurements of some neutron induced isomers, 20: 15688 (AD-620384)
NAVAL RADIOLOGICAL DEFENSE LAB., SAN FRANCISCO, CALIF.
Gamma-ray energy pseudospectra for ^{235}U fission products and for various times after fission, 20: 14733 (AD-628982)
Isolation of streptococcus equi from burros, 20: 14288 (AD-627986)
Recovery of rat kidney from x irradiation, 20: 14258 (AD-627569)
Time history of biological response to ionizing radiation, 20: 14287 (AD-626996)
NAVAL SCHOOL OF AVIATION MEDICINE, PENSACOLA, FLA.
Beta particle standards for ^{14}C and other elements in form of radioactive monolayers, 20: 16143 (AD-620276)
NEDERLANDSE ORGANISATIE VOOR TOEGEPAST NATUURWETENSCHAPPELIJK ONDERZOEK, DELFT. CENTRAAL LABORATORIUM.
Measurements of wall-thickness variations in long straight tubes, 20: 14816 (EUR-2512.n)
NEDERLANDSE ORGANISATIE VOOR TOEGEPAST NATUURWETENSCHAPPELIJK ONDERZOEK, THE HAGUE. METAALINSTITUUT.
Wear research on reactor parts, 20: 15998 (EUR-2117.n)
NEW BRUNSWICK LAB. (AEC), N. J.
Evaluation of methods in TID-7029, "selected measurement methods for plutonium and uranium in nuclear fuel cycle", 20: 14447 (NBL-231)
NEW MEXICO UNIV., ALBUQUERQUE. BUREAU OF ENGINEERING RESEARCH.
Heat-generated pressure oscillations in closed end pipe, 20: 14690 (SC-DC-66-1293)
NEW YORK STATE VETERINARY COLL., ITHACA, N. Y. DEPT. OF PHYSICAL BIOLOGY.
Prog. rpt. on fission product metabolism and response in animals, 1/64–12/65, 20: 14243 (TID-22626)
NEW YORK UNIV., N. Y. DEPT. OF METALLURGY AND MATERIALS SCIENCES.
Prog. rpt. on thermodynamic properties of intermetallic compounds, 10/65, 20: 15056 (NYO-2916-10)
NOBEL INST. OF PHYSICS, STOCKHOLM (SWEDEN).
Application to lens-type spectrometer of internal-external conversion method for determination of internal conversion coefficients, 20: 15710 (CONF-233(Vol.2), pp 252-5)
Photoelectron scattering and consequences for determination of internal conversion coefficients by the IEC method, 20: 15709 (CONF-233 (Vol.2), pp 247-51)
Studies of Auger effect in light elements, 20: 15244 (CONF-233(Vol.3), pp 487-93)
NORSK HYDRO'S INST. FOR CANCER RESEARCH, OSLO.
^{137}Cs in people and food in Norway, 1963–1965, 20: 14739 (TID-22655)
NORSK RADIUMHOSPITAL, OSLO.
^{137}Cs in people and food in Norway, 1963–1965, 20: 14739 (TID-22655)
NORTHERN STATES POWER CO., MINNEAPOLIS, MINN.
Pathfinder flooding coefficient, core pressurization, and temperature coefficient tests, 20: 16059 (ACNP-65600)
NUCLEAR ENERGY INFORMATION CENTER, WARSAW (POLAND).
Angular correlation and internal conversion studies in ^{125}I and ^{127}I, 20: 15701 (CONF-233(Vol.2), pp 128-41)
Anomalous L-subshell conversion of some hindered E1 transitions in the rare earth region, 20: 15703 (CONF-233(Vol.2), pp 148-57)
Application to lens-type spectrometer of internal-external conversion IEC method for determination of internal conversion coefficients, 20: 15710 (CONF-233(Vol.2), pp 252-5)
Atomic M-level widths in ^{151}Sm, 20: 15241 (CONF-233(Vol.3), pp 454-64)
Atomic readjustment following formation of inner shell vacancies, 20: 15245 (CONF-233(Vol.3), pp 494-504)
Comparison of recent precision results of orbital electron capture ratios with theory, 20: 15713 (CONF-233(Vol.2), pp 365-8)
Conference on role of atomic electrons in nuclear transformations, Warsaw, 9/63, 20: 15236 (CONF-233(Vol.3))
Conference on role of atomic electrons in nuclear transformations, Warsaw, Poland, 9/63, 20: 15693 (CONF-233(Vol.1))
Conference on role of atomic electrons in nuclear transformations, Warsaw, 9/63, 20: 15697 (CONF-233(Vol.2))
Double ionization accompanying ^{6}He decay, 20: 15715 (CONF-233 (Vol.3), pp 505-9)
Experimental and theoretical studies of L-conversion electron directional correlations, 20: 15699 (CONF-233(Vol.2), pp 117-19)
E2 conversion coefficients in ^{110}Cd and ^{132}Xe, 20: 15704 (CONF-233 (Vol.2), pp 164-76)
E2 conversion coefficients in ^{152}Sm, ^{154}Gd, and ^{160}Dy, 20: 15705 (CONF-233(Vol.2), pp 177-90)
Influence of nuclear charge distribution on β decay, 20: 15716 (CONF-233(Vol.3), pp 529-37)
Internal conversion, 20: 15694 (CONF-233(Vol.1), pp 1-29)
Internal pair formation and electroexcitation of nuclei, 20: 15696 (CONF-233(Vol.1), pp 60-86)
K-conversion coefficient of the 412-kev E2 transition in ^{198}Hg, 20: 15707 (CONF-233(Vol.2), pp 198-212)
K-conversion process of the 412-kev E2 transition in ^{198}Hg, 20: 15708 (CONF-233(Vol.2), pp 213-19)
K-shell conversion coefficients for pure E2 transitions in deformed nuclei, 20: 15706 (CONF-233(Vol.2), pp 191-7)
K-shell fluorescence yields of V, Cr, and Cu, 20: 15242 (CONF-233(Vol.3), pp 465-79)
KLL-Auger spectrum of manganese, 20: 15243 (CONF-233(Vol.3), pp 480-6)
L auger spectra in j-j coupling, 20: 15237 (CONF-233(Vol.3), pp 371-97)
$L_1L_{2,3}M_{4,5}$ Coster-Kronig transition rates, 20: 15238 (CONF-233(Vol.3), pp 398-418)
Measurement of the M/L-capture ratio in 30-million-year ^{205}Pb decay, 20: 15714 (CONF-233(Vol.2), pp 369-70)
On K-level widths, 20: 15239 (CONF-233(Vol.3), pp 419-39)
Orbital electron capture by the nucleus, 20: 15695 (CONF-233(Vol.1), pp 30-59)
Particle parameter of the $2^+ \rightarrow 0^+$ E2 transition in ^{152}Sm, 20: 15698 (CONF-233(Vol.2), pp 109-16)
Particle parameter of the $2^+ \rightarrow 0^+$ E2 transition in ^{170}Yb, 20: 15700 (CONF-233(Vol.2), pp 120-7)
Photoelectron scattering and consequences for determination of internal conversion coefficients by the IEC method, 20: 15709 (CONF-233 (Vol.2), pp 247-51)
Ratio of K-capture to positron emission in decay of ^{13}N, 20: 15712 (CONF-233(Vol.2), pp 359-64)
Some allowed K-capture to positron ratios, 20: 15711 (CONF-233(Vol.2), pp 345-58)
Studies of Auger effect in light elements, 20: 15244 (CONF-233(Vol.3), pp 487-93)
The L,M,N Auger spectra and the Coster-Kroenig transitions of heavy elements, 20: 15240 (CONF-233(Vol.3), pp 440-53)
Vacuum polarization in μ-mesic atoms, 20: 15246 (CONF-233(Vol.3), pp 520-8)
30.7-Kev anomalous electric dipole transition, 20: 15702 (CONF-233 (Vol.2), pp 142-7)
NUCLEAR MATERIALS AND EQUIPMENT CORP., APOLLO, PA.
Prog. rpt. on development and testing of UO_2–PuO_2 fast reactor fuels, 10–12/65, 20: 14965 (NUMEC-3524-12)
Prog. rpt. on growth of single crystals of Pu, 10–12/65, 20: 15053 (NUMEC-3428-17)
Prog. rpt. on irradiation testing of UO_2–PuO_2 fuels, 10–12/65, 20: 15135 (NUMEC-3432-18)
Prog. rpt. on UO_2–PuO_2–ZrO_2 fuel development, 10–12/65, 20: 15054 (NUMEC-3505-11)
NUKLEAR-CHEMIE UND -METALLURGIE G.M.B.H., WOLFGANG AM MAIN (WEST GERMANY).
Prog. rpt. on fabrication of UO_2 powders and processing into fuel elements, 4–6/65, 20: 14999 (EURAEC-1466)

O

OAK RIDGE GASEOUS DIFFUSION PLANT, TENN.
Minimum significant number of successes in a binomial sample, 20: 16150 (ORNL-3909)
OAK RIDGE NATIONAL LAB., TENN.
Analytical biochemistry, 20: 14456 (ORNL-3889, pp 32-5)
Analytical chemistry for reactor projects, 20: 14454 (ORNL-3889, pp 17-24)
Analytical instrumentation, 20: 14452 (ORNL-3889, pp 1-12)
Analytical studies of molten-salt systems, 20: 14453 (ORNL-3889, pp 12-14)
Atomic readjustment following formation of inner shell vacancies, 20: 15245 (CONF-233(Vol.3), pp 494-504)
Attempted determination of nitrate in fired thoria using infrared techniques, 20: 14468 (TID-22505)
Bibliography on atomic and molecular processes, 1964, 20: 15248 (ORNL-AMPIC-3)
Charge-sensitive preamplifier, ORNL model RC11-4-2X, 20: 14859 (ORNL-TM-1390)
Curium processing experience, 20: 14639 (ORNL-P-1963)
Densification and sintering of thoria and thoria gels, 20: 15009 (TID-22491)
Description of facility radiation and contamination alarm systems installed in HFIR facility, 20: 16125 (ORNL-TM-1393)
Effects of radiation on analytical methods, 20: 14581 (ORNL-3889,

pp 14-16)
Flooding in perforated-plate pulsed extraction columns, 20: 14462 (ORNL-3890)
HFIR cladding-failure detector, 20: 16124 (ORNL-TM-1388)
Hot presses for glove box and manipulator cell, 20: 14666 (ORNL-P-1946)
Inelastic scattering and the distorted wave method, 20: 15726 (ORNL-P-1957)
Infrared and nuclear magnetic resonance spectrometry, 20: 14459 (ORNL-3889, pp 44-6)
Inorganic preparations, 20: 14511 (ORNL-3889, pp 71-3)
Machine to transfer powdered radioactive fuel remotely, 20: 14668 (ORNL-TM-1397)
Mass spectrometry, 20: 14458 (ORNL-3889, pp 39-43)
Minimum significant number of successes in a binomial sample, 20: 16150 (ORNL-3909)
Nuclear and radiochemical analyses, 20: 14461 (ORNL-3889, pp 48-70)
Optical and electron microscopy, 20: 14460 (ORNL-3889, pp 46-8)
Organic preparations, 20: 14576 (ORNL-3889, pp 73-7)
±32 volt power supply, ORNL model RC11-4-2E, 20: 14818 (ORNL-TM-1391)
Preparation of megacurie quantities of ^{137}Cs salts and source compounds, 20: 14626 (ORNL-P-1944)
Preparation of UO_2 microspheres by a sol-gel technique, 20: 15008 (ORNL-3874)
Prog. rpt. on analytical chemistry, annual, 1965, 20: 14428 (ORNL-3889)
Prog. rpt. on chemical applications of nuclear explosions (CANE), 10-12/65, 20: 14662 (ORNL-TM-1394)
Radiation densities and TBP radiolysis during thorex short decay runs, 20: 14580 (ORNL-2764)
Radioisotope sources and source testing, 20: 14789 (ORNL-P-1910)
Special research and development problems, 20: 14455 (ORNL-3889, pp 25-32)
Structural analysis of shipping casks. Vol. I., 20: 14667 (ORNL-TM-1312(Vol. I))
Survey of head-end processes for recovery of uranium and thorium from graphite-base reactor fuels, 20: 14640 (ORNL-TM-1411)
Vapor pressures of gaseous products from chemical reactions of sol-gel fuels, 20: 14512 (ORNL-TM-1418)
X-ray and spectrochemical analyses, 20: 14457 (ORNL-3889, pp 36-9)

OESTERREICHISCHE STUDIENGESELLSCHAFT FUER ATOMENERGIE G.M.B.H., SEIBERSDORF. INSTITUT FUER CHEMIE.
Radiation chemical carboxylation of polychloride compounds for trichloroacetic acid, 20: 14582 (SGAE-CH-25/1965)

OFFICE NATIONAL D'ETUDES ET DE RECHERCHES AEROSPATIALES, CHATILLON-SOUS-BAGNEUX (FRANCE).
Spectrographic analysis of Nb-Zr alloys, 20: 14446 (N64-25607)

OHIO STATE UNIV., COLUMBUS.
Construction of lithium drifted germanium solid state detector system with special attention to ^{105}Ag and ^{192}Ir, 20: 14845 (AD-620434)

OHIO STATE UNIV. RESEARCH FOUNDATION, COLUMBUS.
Prog. rpt. on K-meson experiments at ZGS, final, 2/63-9/65, 20: 15307 (COO-1261-22)

P

PARAMETRICS, INC., WALTHAM, MASS.
Low-level radiation altimeter system study, 20: 14817 (N65-20421)
Rocket-borne air density measurement system utilizing electron-bremsstrahlung, 20: 15588 (AD-620682)

PARIS UNIV. (FRANCE).
Contribution to the study of the α-α interaction, 20: 15689 (CEA-R-2786)

PARIS UNIV. (FRANCE). FACULTE DES SCIENCES.
Measurement of recoil protons in the elastic electron-proton scattering, 20: 15313 (NP-15822)

PARIS UNIV. (FRANCE). LABORATOIRE DE PHYSIQUE.
Diffusion of iron, of silver and of carbon in beryllium, 20: 15037 (CEA-R-2621)

PARIS UNIV., ORSAY (FRANCE). INSTITUT DU RADIUM.
30.7-Kev anomalous electric dipole transition, 20: 15702 (CONF-233 (Vol.2), pp 142-7)

PETROLEUM CONSULTANTS, HOUSTON, TEX.
Mining on Nevada Test Site, 20: 14754 (NVO-38-1)

PHILIPPINE ATOMIC ENERGY COMMISSION, MANILA.
Production of colloidal ^{198}Au, 20: 14627 (PAEC(D)IS-651)
Studies on coconut oil. II., 20: 14463 (PAEC(D)CH-652)

PHILLIPS PETROLEUM CO. IDAHO FALLS, IDAHO., ATOMIC ENERGY DIV.
Leachability of glass prepared from highly radioactive calcined alumina waste, 20: 16133 (IDO-14672)
Measurement of absolute value of η for ^{233}U, ^{235}U, and ^{239}Pu using monochromatic neutrons, 20: 15718 (IDO-17083)

PITMAN-DUNN RESEARCH INST., FRANKFORD ARSENAL, PHILADELPHIA, PA.
Shaped Mg-Li castings, 20: 15007 (NP-15881)

POLISH ACADEMY OF SCIENCES, WARSAW.
Angular correlation and internal conversion studies in ^{125}I and ^{127}I, 20: 15701 (CONF-233(Vol.2), pp 128-41)
Anomalous L-subshell conversion of some hindered E1 transitions in the rare earth region, 20: 15703 (CONF-233(Vol.2), pp 148-57)
Application to lens-type spectrometer of internal-external conversion IEC method for determination of internal conversion coefficients, 20: 15710 (CONF-233(Vol.2), pp 252-5)
Atomic M-level widths in ^{151}Sm, 20: 15241 (CONF-233(Vol.3), pp 454-64)
Atomic readjustment following formation of inner shell vacancies, 20: 15245 (CONF-233(Vol.3), pp 494-504)
Comparison of recent precision results of orbital electron capture ratios with theory, 20: 15713 (CONF-233(Vol.2), pp 365-8)
Conference on role of atomic electrons in nuclear transformations, Warsaw, Vol. 3, 9/63, 20: 15236 (CONF-233(Vol.3))
Conference on role of atomic electrons in nuclear transformations, Warsaw, Poland, 9/63, 20: 15693 (CONF-233(Vol.1))
Conference on role of atomic electrons in nuclear transformations, Warsaw, 9/63, 20: 15697 (CONF-233(Vol.2))
Double ionization accompanying ^{6}He decay, 20: 15715 (CONF-233 (Vol.3), pp 505-9)
Experimental and theoretical studies of L-conversion electron directional correlations, 20: 15699 (CONF-233(Vol.2), pp 117-19)
E2 conversion coefficients in ^{110}Cd and ^{132}Xe, 20: 15704 (CONF-233 (Vol.2), pp 164-76)
E2 conversion coefficients in ^{152}Sm, ^{154}Gd, and ^{160}Dy, 20: 15705 (CONF-233(Vol.2), pp 177-90)
Influence of nuclear charge distribution on β decay, 20: 15716 (CONF-233(Vol.3), pp 529-37)
Internal conversion, 20: 15694 (CONF-233(Vol.1), pp 1-29)
Internal pair formation and electroexcitation of nuclei, 20: 15696 (CONF-233(Vol.1), pp 60-86)
K-conversion coefficient of the 412-kev E2 transition in ^{198}Hg, 20: 15707 (CONF-233(Vol.2), pp 198-212)
K-conversion process of the 412-kev E2 transition in ^{198}Hg, 20: 15708 (CONF-233(Vol.2), pp 213-19)
K-level widths, 20: 15239 (CONF-233(Vol.3), pp 419-39)
K-shell conversion coefficients for pure E2 transitions in deformed nuclei, 20: 15706 (CONF-233(Vol.2), pp 191-7)
K-shell fluorescence yields of V, Cr, and Cu, 20: 15242 (CONF-233(Vol.3), pp 465-79)
KLL-Auger spectrum of manganese, 20: 15243 (CONF-233(Vol.3), pp 480-6)
L auger spectra in j-j coupling, 20: 15237 (CONF-233(Vol.3), pp 371-97)
$L_1L_{2,3}M_{4,5}$ Coster-Kronig transition rates, 20: 15238 (CONF-233(Vol.3), pp 398-418)
L,M,N Auger spectra and the Coster-Kroenig transitions of heavy elements, 20: 15240 (CONF-233(Vol.3), pp 440-53)
Measurement of the M/L-capture ratio in 30-million-year ^{205}Pb decay, 20: 15714 (CONF-233(Vol.2), pp 369-70)
Orbital electron capture by the nucleus, 20: 15695 (CONF-233(Vol.1), pp 30-59)
Particle parameter of the $2^+ \rightarrow 0^+$ E2 transition in ^{152}Sm, 20: 15698 (CONF-233(Vol.2), pp 109-16)
Particle parameter of the $2^+ \rightarrow 0^+$ E2 transition in ^{170}Yb, 20: 15700 (CONF-233(Vol.2), pp 120-7)
Photoelectron scattering and consequences for determination of internal conversion coefficients by the IEC method, 20: 15709 (CONF-233 (Vol.2), pp 247-51)
Ratio of K-capture to positron emission in decay of ^{13}N, 20: 15712 (CONF-233(Vol.2), pp 359-64)
Some allowed K-capture to positron ratios, 20: 15711 (CONF-233(Vol.2), pp 345-58)
Studies of Auger effect in light elements, 20: 15244 (CONF-233(Vol.3), pp 487-93)
Vacuum polarization in μ-mesic atoms, 20: 15246 (CONF-233(Vol.3), pp 520-8)
30.7-Kev anomalous electric dipole transition, 20: 15702 (CONF-233 (Vol.2), pp 142-7)

PRATT AND WHITNEY AIRCRAFT, EAST HARTFORD, CONN.
Prog. rpt. on determination of emisavity of materials, semiannual, 5/15-11/14/65, 20: 15057 (PWA-2750)

PRINCETON-PENNSYLVANIA ACCELERATOR, PRINCETON, N. J.
Experimental investigation of some neutron-deficient nuclei, 20: 15727 (PPAD-572F)
Princeton-Pennsylvania 3-Bev proton synchrotron parameters, 20: 15163 (PPAD-279D(Rev.))

R

RAND CORP., SANTA MONICA, CALIF.

Equatorial transmission of geomagnetic micropulsations through the ionosphere and lower exosphere, 20: 15591 (RM-4858)
Out-of-pile thermionic space power systems using a gaseous heat-transfer fluid, 20: 16110 (AD-620650)

REACTOR GROUP, UNITED KINGDOM ATOMIC ENERGY AUTHORITY, RISLEY (ENGLAND).
Economics of alternative nuclear power programs based on gas-cooled graphite and fast reactors, 20: 16087 (TRG-Report-1115)

RENSSELAER POLYTECHNIC INST., TROY, N. Y. DEPT. OF NUCLEAR ENGINEERING AND SCIENCE.
Prog. rpt. on linear accelerator project, 10–12/65, 20: 15731 (RPI-328-49)

ROCKY FLATS DIV., DOW CHEMICAL CO., GOLDEN, COLO.
Automatic recording, low-temperature dilatometer, 20: 14821 (RFP-668)
Critical temperature of plutonium-chlorinated solvent reactions, 20: 14513 (RFP-688)
Effect of composition on corrosion of plutonium metal, 20: 14984 (RFP-511)
Improved electrodeless toroidal conductivity analyzer, 20: 14465 (RFP-657)
Impurity analysis of plutonium peroxide and plutonium fluoride, 20: 14464 (RFP-599)
Optical determination of depth of defects by replication techniques, 20: 14966 (RFP-673)
Precision back-reflection laue camera, 20: 14820 (RFP-636)
Thin film evaporation rate monitor, 20: 14819 (RFP-602)
Vapor-deposited film distribution on curved substrate surfaces, 20: 16151 (RFP-647)

ROSCOE B. JACKSON MEMORIAL LAB., BAR HARBOR, MAINE.
Prog. rpt. on attempts to delineate inborn anemias in mice, 2/65–1/66, 20: 14290 (NYO-1800-12)

S

SAMENWERKENDE ELECTRICITEITS-PRODUCTIEBEDRIJVEN, N. V., ARNHEM (NETHERLANDS).
Control rod drive system of Garigliano nuclear power plant, SENN, 20: 16074 (EUR-2420.d,f,i,n,e, pp 227-48)

SANDIA CORP., ALBUQUERQUE, N. MEX.
Coincidence study of O^+ on Kr collisions, 20: 15249 (TID-22643)
Comparison of results of Sandia TTA trajectory program and Atomics International RESTORE trajectory program, 20: 16113 (SC-RR-66-22)
Computer program for performing reliability analyses, 20: 14824 (SC-TM-65-523)
Design considerations for ion plating, 20: 14670 (SC-R-65-997)
Prog. rpt. on mechanical properties of slip-cast fused silica, final, 7/64–6/65, 20: 15058 (SC-DC-66-1130)
Rover postoperational destruct instrumentation development, 20: 16112 (SC-RR-65-551)

SHEFFIELD UNIV. (ENGLAND). DEPT. OF APPLIED MATHEMATICS.
Explanation of the Appleton anomaly of the F2 layer. II., 20: 15586 (AD-620243)
Magnetohydrostatic cavity formed around a system of line currents in an infinitely conducting atmosphere, 20: 15587 (AD-620244)

SOCIETE D'ETUDES, DE RECHERCHES ET D'APPLICATIONS POUR L'INDUSTRIE, BRUSSELS (BELGIUM).
Dynamic corrosion tests on carbon and stainless steels in pressurized water, 20: 14978 (EURAEC-1546)
Prog. rpt. on steel corrosion, 7–10/65, 20: 14977 (EURAEC-1500)

SOUTHWEST RESEARCH INST., SAN ANTONIO, TEX.
Prog. rpt. on Elk River reactor pressure vessel, 10–12/65, 20: 16085 (SWRI-1228-4-15)
Prog. rpt. on fatigue strength of pressure vessels, 1/66, 20: 15059 (SWRI-1228-1-20)

SPACE TECHNOLOGY LABS., INC., REDONDO BEACH, CALIF. SOLID STATE PHYSICS LAB.
Prog. rpt. on effects of proton irradiation on solar cells, 1/65, 20: 14919 (N65-20653)

STANFORD LINEAR ACCELERATOR CENTER, STANFORD UNIV., CALIF.
Asymptotic perturbation fields of longitudinally bunched beam within rectangular pipe with resistive walls, 20: 15168 (SLAC-49, pp 23-31)
Incoherent beams blow-up in colliding beams, 20: 15174 (SLAC-49, pp 71-3)
Influence of dielectric media on electromagnetic fields of coasting beam in straight rectangular pipe, 20: 15172 (SLAC-49, pp 52-8)
Longitudinal wake fields of pulse of charge moving down straight pipe of circular cross section with finite conductivity, 20: 15167 (SLAC-49, pp 18-22)
Storage ring summer study, 1965, on instabilities in stored particle beams, 20: 15166 (SLAC-49)
Theory of coherent bunch motion in electron-positron storage rings, 20: 15173 (SLAC-49, pp 61-8)
Transverse coherent instability of bunched beams, 20: 15170 (SLAC-49, pp 36-48)
Transverse stability of ultra-relativistic multiple-bunched beams, 20: 15171 (SLAC-49, pp 49-51)
Wake fields of charged particle traveling in vacuum chamber with resistive walls, 20: 15169 (SLAC-49, pp 32-5)

STANFORD RESEARCH INST., MENLO PARK, CALIF.
Disintegration rate multipliers in beta-emitter dose calculations, 20: 14403 (NP-15714)
Prog. rpt. on growth of carbide crystals, 9–12/64, 20: 15047 (N65-15919)

STANFORD UNIV., CALIF. INST. FOR PLASMA RESEARCH.
Electron beam probing of cathode sheath and beam-plasma interaction, 20: 15884 (SU-IPR-33)
Instability of steady state of plasma in uniform electric field, 20: 15883 (SU-IPR-31)

STANFORD UNIV., CALIF. MICROWAVE LAB.
Instability and amplification in finite beam-plasma systems. I., 20: 15880 (ML-1292)

STATE UNIV. OF NEW YORK, BROOKLYN. DEPT. OF ANATOMY.
Prog. rpt. on effects of radiation on cartilage and bone, annual, 12/63–12/64, 20: 14291 (TID-22494)

STATENS RADIOLOGISK-FYSISKE LABORATORIUM, OSLO (NORWAY).
^{137}Cs in people and food in Norway, 1963–1965, 20: 14739 (TID-22655)

STOCKHOLM UNIV. (SWEDEN).
K-conversion process of the 412-kev E2 transition in ^{198}Hg, 20: 15708 (CONF-233(Vol.2), pp 213-19)

STOCKHOLM UNIV. (SWEDEN). INST. OF PHYSICS.
Internal conversion, 20: 15694 (CONF-233(Vol.1), pp 1-29)

SWEDISH STATE POWER BOARD, STOCKHOLM.
Heat resistance of concrete, 20: 15051 (NP-15876)

T

TATA INST. OF FUNDAMENTAL RESEARCH, BOMBAY (INDIA).
K-shell conversion coefficients for pure E2 transitions in deformed nuclei, 20: 15706 (CONF-233(Vol.2), pp 191-7)

TECHNICAL OPERATIONS RESEARCH, BURLINGTON, MASS.
Structure shielding from simulated fallout gamma radiation, 20: 15931 (TO-B-65-27)

TECHNION–ISRAEL INST. OF TECH., HAIFA.
Prog. rpt. on physico-chemical-biological processes affecting dispersion of radionuclides, final, 12/61–12/64, 20: 14731 (NP-159861)

TECHNISCHE HOGESCHOOL, DELFT (NETHERLANDS).
K-conversion coefficient of the 412-kev E2 transition in ^{198}Hg, 20: 15707 (CONF-233(Vol.2), pp 198-212)

TENNESSEE UNIV., MEMPHIS. DEPT. OF PHYSIOLOGY AND BIOPHYSICS.
Metabolism of methyl palmitate, 20: 14241 (TID-21437)

TEXAS AGRICULTURAL AND MECHANICAL UNIV., COLLEGE STATION.
Pulse shape discrimination considerations in dual crystal gamma-ray scintillation detector, 20: 14844 (AD-620395)

THERMO ELECTRON ENGINEERING CORP., WALTHAM, MASS.
Recent progress in fundamental and applied thermionic converter technology, 20: 15294 (CONF-640921, pp 9-45)

U

UNION CARBIDE CORP., OAK RIDGE, TENN. Y-12 PLANT.
Automated air sampling by use of aperture cards, 20: 14791 (Y-1501)
Extension of APT to obtain centroid and inertia information, 20: 16154 (Y-1420(Rev.1))
Penetration tests, 20: 14702 (Y-1490)

UNION CARBIDE CORP., PARMA, OHIO. CARBON PRODUCTS DIV.
Prog. rpt. on protective coatings for refractory metals, 10/23/64–1/23/65, 20: 15004 (N65-20790)

UNITED STATES–EURATOM JOINT RESEARCH AND DEVELOPMENT PROGRAM.
Dependence of transition boiling heat transfer on loop flow disturbances, 20: 14687 (GEAP-4785)
Dynamic corrosion tests on carbon and stainless steels in pressurized water, 20: 14978 (EURAEC-1546)
Prog. rpt. on applicability of existing data to analytical description of a nuclear-reactor accident, 10–12/65, 20: 16019 (BMI-X-10154)
Prog. rpt. on critical heat flux in boiling water, 4–6/65, 20: 14686 (EURAEC-1448)
Prog. rpt. on embrittlement of reactor vessel steels, 7–9/65, 20: 15039 (EURAEC-1475)
Prog. rpt. on fabrication of UO_2 powders and processing into fuel elements, 4–6/65, 20: 14999 (EURAEC-1466)
Prog. rpt. on specific Zr alloy design program, 1/66, 20: 14980 (GEAP-5065)
Prog. rpt. on steel corrosion, 7–10/65, 20: 14977 (EURAEC-1500)
Prog. rpt. on yield phenomena and fracture of hydrided Zr, 10–12/65,

20: 15042 (IITRI-578-P27-14)
Welding tests on section taken from heavy-gage plates of rolled steel, 20: 15000 (EURAEC-1517)

UPPSALA UNIV., (SWEDEN). INST. OF PHYSICS.
Experimental and theoretical studies of L-conversion electron directional correlations, 20: 15699 (CONF-233(Vol.2), pp 117-19)

USTAV JADERNEHO VYZKUMU, CESKOSLOVENSKA AKADEMIE VED, REZ.
Dynamics of accidents in nuclear reactors, 20: 16026 (UJV-1459/65)
Gamma transitions in ^{153}Eu, 20: 15734 (ZfK-PhA-18)
Influence of nuclear charge distribution on β decay, 20: 15716 (CONF-233(Vol.3), pp 529-37)

UTAH UNIV., SALT LAKE CITY. INST. OF METALS AND EXPLOSIVES RESEARCH.
Attempted determination of nitrate in fired thoria using infrared techniques, 20: 14468 (TID-22505)
Densification and sintering of thoria and thoria gels, 20: 15009 (TID-22491)

V

VANDERBILT UNIV., NASHVILLE, TENN.
Application to lens-type spectrometer of internal-external conversion IEC method for determination of internal conversion coefficients, 20: 15710 (CONF-233(Vol.2), pp 252-5)
E2 conversion coefficients in ^{110}Cd and ^{132}Xe, 20: 15704 (CONF-233 (Vol.2), pp 164-76)
E2 conversion coefficients in ^{152}Sm, ^{154}Gd, and ^{160}Dy, 20: 15705 (CONF-233(Vol.2), pp 177-90)
KLL-Auger spectrum of manganese, 20: 15243 (CONF-233(Vol.3), pp 480-6)
Particle parameter of the $2^+ \rightarrow 0^+$ E2 transition in ^{152}Sm, 20: 15698 (CONF-233(Vol.2), pp 109-16)
Particle parameter of the $2^+ \rightarrow 0^+$ E2 transition in ^{170}Yb, 20: 15700 (CONF-233(Vol.2), pp 120-7)

VEB ENTWICKLUNG UND PROJEKTIERUNG KERNTECHNISCHER ANLAGEN, BERLIN (EAST GERMANY).
Nuclear data on production of γ rays through interaction with fast neutrons, 20: 15725 (NP-14855)

VIENNA UNIV. (AUSTRIA). ANALYTISCHES INSTITUT.
Prog. rpt. on ion exchange separation of U and Th in mixed and non-aqueous solvents, final, 1965, 20: 14469 (TID-22650)

VIRGINIA UNIV., CHARLOTTESVILLE.
Internal pair formation and electroexcitation of nuclei, 20: 15696 (CONF-233(Vol.1), pp 60-86)

W

WALTER REED ARMY INST. OF RESEARCH, WASHINGTON, D. C. BEHAVIORAL RADIOLOGY LAB.
Effects of exposure to mixed fission spectrum delivered in single "pulse" and x-rays delivered at slower rate upon conditioned avoidance behavior of primates, 20: 14286 (AD-625837)

WESTINGHOUSE ELECTRIC CORP., PITTSBURGH, PA. ATOMIC POWER DIV.
Prog. rpt. on Yankee core evaluation, semi-annual, 9/65, 20: 16091 (WCAP-6078)

Y

YUGOSLAV ACADEMY OF SCIENCES AND ARTS, ZAGREB. INST. FOR MEDICAL RESEARCH.
Prog. rpt. on mechanism of initial radiation effects, final, 11/63–10/65, 20: 14259 (NP-15855)

Z

ZENTRALINSTITUT FUER KERNFORSCHUNG, ROSSENDORF BEI DRESDEN (EAST GERMANY).
Gamma transitions in ^{153}Eu, 20: 15734 (ZfK-PhA-18)

ZENTRALSTELLE FUER ATOMKERNENERGIE-DOKUMENTATION, GMELIN-INSTITUT FUER ANORGANISCHE CHEMIE UND GRENZGEBIETE, FRANKFURT AM MAIN (WEST GERMANY).
Directory of the nuclear industry, USA, 20: 16144 (AED-C-32-1 (Vol.1 and Vol.2))

PERSONAL AUTHOR INDEX

Each entry after an author's name is a shortened version of the title of the report or article, followed by the *NSA* volume and abstract number. Report numbers are given in parentheses.

The phrase "Progress report" is abbreviated as "Prog. rpt.," permitting a more rapid and complete alphabetical arrangement of the titles without changing the location of the progress report titles in relation to the other titles.

Because of problems involving the mechanical preparation of this index, all accent marks are omitted. The following changes in spelling have been introduced to reduce some of the confusion which might result from omitting the accents:

ä	becomes	ae
ö		oe
ø		oe
ü		ue (except in transliterated Chinese names)

A

ABASHIAN, A., Decay spectrum of $K^0_{\mu 3}$, 20: 15331

ABBEY, F., Criticality of interacting arrays, 20: 16034

ABBOTT, A. E., Controlling furnace cycle with infrared pyrometers in casting of large uranium ingots, 20: 15006 (NLCO-970, pp 4.1-5)

ABE, Haruhiko, Microwave radiation from a bounded plasma, 20: 15893

ABE, Mitsuo, Ion adsorptive properties of insoluble tetra-, penta-, hexavalent metal hydrous oxides, 20: 14651

ABKIN, A. D., Radiation polymerization of vinyl chloride in solid solutions at low temperatures, 20: 14594

ABOLINS, M. A., Reaction $\pi^- d \to \pi^- d \pi^+ \pi^-$ at 3.7 Bev/c, 20: 15409

ABOLINS, M. A., Study of the A and B mesons, 20: 15408

ABRAHAM, S., Improved methods for liquid scintillation assay of (A) ^{14}C-compounds on paper chromatograms and (B) ^{14}C-protein, 20: 14479

ABRAMS, C. S., Decontamination of Shippingport atomic power station, 20: 16088 (WAPD-299)

ABRAMS, R. J., Decay spectrum of $K^0_{\mu 3}$, 20: 15331

ABROYAN, I. A., Conductivity induced in Ge by bombardment with K ions, 20: 15978

ACHARYA, R., Bhabha's irreducible spin (½,½) equation as basis of strong-interaction symmetries, 20: 15471

ACHENER, P. Y., Prog. rpt. on alkali metals evaluation, 7–9/65, 20: 15028 (AGN-8166)

ACTON, Loren W., Observations of cosmic x-rays, 20: 15220

ADAIR, Robert K., Probable momentum spectra in atmosphere of long-lived heavy triplets produced by primary cosmic rays, 20: 15287

ADAMS, G. E., Transient species produced in irradiated water and aqueous solutions containing oxygen, 20: 14614

ADAMS, R. M., Administration of nuclear safety at ANL, 20: 14800

ADELMAN, Stuart Lee, Angular distributions of the K*(888) and N*(1425) from $K^- p$ collisions at 1.5 Bev/c, 20: 15429

AFGAN, N., New method of burnout detection, 20: 14694

AGUILERA NAVARRO, V. C., Applications of Gel'fand-Moshinsky bases in unitary symmetry and its breaking, 20: 15455

AHMAVAARA, Yrjoe, Structure of space and formalism of relativistic quantum theory. III., 20: 15629

AHMAVAARA, Yrjoe, Structure of space and formalism of relativistic quantum theory. IV., 20: 15630

AHMED, K., W spin and the rotation group in four dimensions, 20: 15467

AHRENS, T., Existence of weakly interacting charge-retention currents, 20: 15327

AIELLO, W. P., Vela satellite system detector electronics, 20: 15596

AINSWORTH, Alan, Remote-control manipulators, 20: 14681

AITCHISON, I. J. R., Final-state interactions among three particles. II., 20: 15476

AKIMOTO, Yumi, Production of spherical uranium nuclear fuel substances, 20: 14575

AKININA, Z. S., Chemical and thermal stability of scandium borides, 20: 14531

ALBERTI, Rudolf, Method for the solidification of aqueous atomic waste, 20: 16142

ALBRIDGE, R. G., KLL-Auger spectrum of manganese, 20: 15243 (CONF-233(Vol.3), pp 480-6)

ALEKPEROV, R. A., Uranium extraction from aqueous solutions with naphthenic acid, 20: 14642

ALEKSEEV, F. A., Present status of nuclear geophysics and prospects for future development, 20: 14770

ALEKSEEV, V. L., Investigation of excited states $^{104,104*}Rh$ by observation of γ rays from (n,γ) reaction, 20: 15754

ALESSANDRINI, Victor A., Faddeev-type equations for the four-body problem, 20: 15456

ALFIMENKOV, V. P., Determination of neutron resonance spins in ^{165}Ho nuclei, 20: 15681

ALGER, Donald L., Thermal neutron flux perturbation by Dy–Al foils in H_2O and UO_2F_2–H_2O solutions, 20: 15669 (NASA-TN-D-3237)

ALIEV, N. G., Thermal conductivity of holmium and erbium from 2 to 100°K, 20: 15117

ALKHAZOV, D. G., Polarized γ radiation emitted during Coulomb excitation, 20: 15759

ALLABY, J. V., π-pair photoproduction below 1 Bev, 20: 15332

ALLAIN, C., Control methods used in department of metallurgy for structural and fuel elements, 20: 14711

ALLEAU, T., Utilization of impregnation compounds in graphite in thermionic conversion, 20: 15296 (CONF-640921, pp 81-99)

ALLEN, J. R., Pathologic alterations produced by total body x-irradiation in monkeys, 20: 14302

ALLEN, L. S., Theoretical and experimental model results in neutron lifetime logging, 20: 14775

ALLEN, Leland C., Fluorides and oxides of helium and neon, 20: 14541

ALLEN, M., Transverse stability of ultra-relativistic multiple-bunched beams, 20: 15171 (SLAC-49, pp 49-51)

ALLEN, R. G., Meteorological program at Parr, South Carolina, 20: 14732 (CVNA-172)

ALLIGOOD, Fred M., CVTR organic loop feasibility study, 20: 16063 (CVNA-241)

ALMOND, P. R., Energy dependence of lithium fluoride dosimeters at high energies, 20: 14888

ALMOND, Peter Richard, Reaction $^{11}B(d,n)^{12}C$ and calorimetric dosage calibration and determination of absorbed dose for proton irradiation, 20: 15858

ALTENBRUNN, H. J., DPN degradation and synthesis of lymphosarcoma ascites cells after x irradiation, 20: 14370

ALVAREZ, R. A., Photoproduction of π^+ from H at energies near the first resonance, 20: 15340

ALYEA, E. D. Jr., $\pi^+ p$ Interactions at 781 Mev, 20: 15341

AMALRIC, R., High-energy radiations in France. (Present equipment and future prospects), 20: 14425

AMBACH, W., Investigation of radioactivity of snow layers of Alpine glacier for establishment of dating boundaries, 20: 14740

AMBLARD, B., Reactions $\pi^- + p \to \pi^0 + n$ and $\pi^- + p \to \eta + n$ at high energies, 20: 15380

AMMAR, R., V-2-prong K-p interactions at 5.5 Bev/c, 20: 15416

AMMENTORP-SCHMIDT, Frits, X-ray fluorescence analysis of technetium and molybdenum in solutions, 20: 14497

AMOSOV, V. M., Synthesis and properties of intermediate lanthanum,

cerium, praseodymium, and neodymium tungstates, 20: 14534
ANASTASIJEVIC, P., New method of burnout detection, 20: 14694
ANDERSEN, Anne Marie, Relationship between hematocrit and solubility of ^{133}Xe in blood, 20: 14415
ANDERSON, Charles Keller, Representative models of observed solar wind, 20: 15190 (AD-620407)
ANDERSON, Kenneth N., Operation Red Dog, 20: 14808
ANDERSON, Philip Douglass, Thermodynamic properties of metals and alloys, 20: 14514 (UCRL-11821)
ANDERSSON, Bengt, Ion waves on bounded plasmas, 20: 15901
ANDREESCU, M., Statistics of scaled pulses, 20: 14890
ANDREW, J. F., Compressibility of oriented alpha plutonium, 20: 15095
ANDREWS, J. S. V., Windscale advanced gas-cooled reactor, 20: 16092
ANDREWS, R. C., Prog. rpt. on measurement of impurities in Na, 10-12/65, 20: 14445 (MSAR-66-10)
ANGELOVIC, Joseph W., Some effects of accumulated radium on productivity of algae, 20: 14381
ANGERMAN, C. L., Influence of stress on hydride habit plane in Zircaloy-2, 20: 15120
ANGERMAN, C. L., Large-scale ^{60}Co heat sources, 20: 14945 (CONF-660305-14)
ANTON, H. F., Development of charged colloid source for electrostatic propulsion, 20: 14725 (N65-15876)
ANTONOV, A. V., Use of pulsed neutron generator to determine neutron diffusion parameters of rocks and fluids, 20: 14772
ANTONOVA, L. I., Roentgenographic studies of lanthanum tellurides, 20: 14530
APPEL, J. C., Prog. rpt. on mechanical properties of reactor materials, annual, 11/64–10/65, 20: 15040 (GA-6721)
APPLETON, J. P., Electrical precursors of ionizing shock waves, 20: 15577
ARAJS, S., Search for low-temperature anomalies in electrical resistivity of dilute gold–erbium alloys, 20: 15083
ARAJS, S., Thermal conductivity, electrical resistivity, and Lorenz function of polycrystalline erbium between 5 and 300°K, 20: 15107
ARAKI, Gentaro, Shell model with $\sigma \cdot \chi$ potential, 20: 15791
ARAKI, H., Equivalence of locality and paralocality in free parafield theory, 20: 15468
ARAKI, K., ESR study of free radicals formed by γ-irradiation of poly (ethylene terephthalate), 20: 14606
ARANGUREN, V., Response to radiotherapy of aortic-femoral prosthesis, 20: 14345
ARANGUREN, Visitacion, Effects of radiotherapy on artificial grafts of thoracic aorta, 20: 14344
ARBUZOV, B. A., Possible mechanism of CP violation, 20: 15309 (JINR-E-2563)
ARBUZOV, M. P., X-ray studies of oxidation of Ni_3Al–Ni_3Nb alloys, 20: 14990
ARCHAMBEAU, C. B., Data processing techniques for detection and interpretation of teleseismic signals, 20: 14762
ARD, W. B., Use of silicon solar cells as detectors of energetic electrons from plasmas, 20: 15916
ARIENT, M., Hematological changes in radiation sickness. V., 20: 14314
ARMENSKII, E. V., Measurements of mean energy of electron beams in low-energy linear accelerators, 20: 15179
ARMSTRONG, W. M., Creep of single-crystal UO_2, 20: 15086
ARNELL, S. E., Anticoincidence spectrometers for nuclear reaction studies, 20: 14865
ARNETT, R. A., Ocean-bottom seismograph, 20: 14765
ARNOLD, Dan McCoy, (n,2n) Excitation functions of several low-neutron excess nuclei, 20: 15863
ARNOLD, G. P., Thermal expansion of uranium dicarbide and uranium sesquicarbide, 20: 15093
ARNOL'DOV, M. N., Impurities in Cs in thermionic converters, 20: 15298 (FEI-22)
ARNOULT, Claire, Hyperfine structure of low-lying levels of Tb $4f^9 5d6s^2$ configuration, 20: 15254
ARONSON, Raphael, Transfer-matrix method for γ and neutron penetration, 20: 15934
ARSENIN, V. Ya., Analyzing spectra of γ quanta and fast neutrons measured by means of single-crystal scintillation spectrometers, 20: 14869
ARTANDI, C., Aims and standards of sterilization treatments, 20: 14234
ASAAD, W. N., L auger spectra in j-j coupling, 20: 15237 (CONF-233(Vol.3), pp 371-97)
ASAOKA, T., Neutron transport in a spherical reactor, 20: 16022 (EUR-2627.e)
ASARO, F., Charge and energy distributions of recoils from ^{226}Th alpha decay, 20: 15822
ASHLINE, Ronald Olive, Aqueous phase oxidation of cyclohexane using gamma radiation, 20: 14625
ASHWOOD-SMITH, M. J., Chemical protection against x-irradiation and protection of cells from freezing damage, 20: 14394
ASLUND, Nils, Rotational analysis of perturbed C and D states of BaH and BaD, 20: 14517
ASLUND, Nils, Spectra of SnH and SnD, 20: 15251
ASTLEY, E. R., Nuclear reactor core having means for varying inclination of fuel assemblies, 20: 16015
ATKINS, M., Total absorption x-ray calorimeter, 20: 14908
ATKINSON, H. H., Differential cross sections and polarization effects in pion-proton elastic scattering at 875 to 1579 Mev/c, 20: 15372
ATKINSON III, Reilly, B exchange in π-ω scattering and spin of the B meson, 20: 15357
AUDIAS, Arlette, Detection of fission fragments by secondary emission, 20: 14852 (CEA-R-2862)
AUSLOOS, P., Gas-phase radiolysis of cyclopentane, 20: 14599
AVERY, Lorne, Bibliography on effects of short-wave and particle radiation on glasses, 20: 15134 (N65-15819)
AZIMOV, S. A., Azimuthal angular distribution of shower particles and gray tracks made by cosmic-ray particles in photoemulsion, 20: 15290

B

BAACKE, J., Pion-nucleon scattering at high energies, 20: 15376
BABICHEVA, E. V., ^{90}Sr, stable strontium and calcium in soil and vegetable food products, 20: 14236
BABUSHKINA, N. A., Galvanomagnetic properties of holmium, 20: 15983
BACHURINA, T. I., Activity of cardiovascular system during radiation injuries, 20: 14371
BACON, T. C., Observations of $Y_1^*(1405)$ and $Y_1^*(1358)$ resonances in π-N collisions at 1.68 Bev/c, 20: 15404
BACON, T. C., Production and decay of ρ^0 and ω mesons in π^+n and π^-p interactions at 1.7 Bev/c, 20: 15403
BAECHMANN, K., Influence of complex stabilities on electron transfer reactions, 20: 14574
BAER, Rudolf L., Photobiology of Lupus erythematosus, 20: 14309
BAGINSKI, W. A., Properties of an yttrium-containing columbium alloy, 20: 15119
BAGSHAW, Malcolm A., Serum concentration: effects on cycle and x-ray sensitivity of mammalian cells, 20: 14400
BAHCALL, John N., Non-resonant nuclear reactions at stellar temperatures, 20: 15221
BAHCALL, John N., Observational test of theories of neutron-star cooling, 20: 15201
BAIER, V. N., Radiative polarization of electrons in a magnetic field, 20: 15638
BAILY, N. A., Response of p-i-n junctions to beta rays. II., 20: 14886
BAKER, L. Jr., Metal–water reactions, 20: 14996
BALDWIN, Richard, Engineering aspects of multichannel processing based on measured noise correlations, 20: 14763
BALIS, M. Earl, Effect of amino acids on thymine dimerization, 20: 14272
BALL, J. S., One-boson-exchange model of NN and NN-interaction, 20: 15345
BALL, Otis G., Advanced cancer of bladder: management with irradiation, 20: 14414
BALLINGER, Edward R., Radiation dosimeter system using cadmium-backed copper foil, 20: 14915
BALOCK, J. W., Differential effect of gamma radiation on fruit flies and fruit fly parasites, 20: 14935
BALTAY, C., p-p Annihilations into K and π mesons at 3.7 Bev/c, 20: 15338
BAMFORD, Sophia, Evaluation for genetic damage in offspring of women with high-level gonadal irradiation, 20: 14348
BANSAL, Ram Krishan, Core polarization in transfer reactions via shell model and sum-rule techniques, 20: 15852
BARANOV, V. I., ^{90}Sr, stable strontium and calcium in soil and vegetable food products, 20: 14236
BARCH, W. E., Structure shielding from simulated fallout gamma radiation, 20: 15931 (TO-B-65-27)
BARD, R. J., Coated particle fuel elements for UHTREX, 20: 15002 (LA-3378)
BARDENSHTEIN, S. B., Structure of radiation chlorinated and sulfochlorinated polyethylene, 20: 14621
BAREYRE, P., Recoil proton polarization measurements in pion-nucleon scattering, 20: 15373
BARFIELD, Michael, Electron correlation and nuclear spin-spin coupling constant. I., 20: 14543
BARKER, Bruce M., Meson resonances and nuclear forces, 20: 15817
BARMAWI, M., Regge-pole contribution to vector-meson production, 20: 15354
BARNES, J. W., Storage facilities for Hanford high-level fission waste containers, 20: 16135 (RL-SA-62)
BARNES, R. G., Paramagnetic resonance of cobalt in intermetallic compounds, 20: 15963
BARNETT, C. F., Bibliography on atomic and molecular processes, 1964, 20: 15248 (ORNL-AMPIC-3)
BARRICELLI, Nils Aall, Stimulation of recombination in multiplicity-

reactivated bicomplexes and genetic map length of phage T4, 20: 14328
BARSUKOV, V. S., Oxygen effect on post-irradiation restoration of yeast cells, 20: 14399
BARTHOLOMEW, George L., Neutron shielding using composition comprising graphite, boron carbide and carbonized residue, 20: 15027
BARTL, A., Radiation correctors of e-p scattering, 20: 15319
BARTLEY, J. C., Improved methods for liquid scintillation assay of (A) ^{14}C-compounds on paper chromatograms and (B) ^{14}C-protein, 20: 14479
BARTON, Gabriel, Introduction to dispersion techniques in field theory, 20: 15565
BARTUSEK, M., Complexes of uranyl with phenolic ligands. II., 20: 14522
BARUT, A. O., Invariant amplitudes and interpretation of SU(3)- and SU(6)-type symmetries, 20: 15547
BASILADZE, S. G., Production cross section of charged pions in (n,p) collisions, 20: 15310 (JINR-P-2508)
BASSICHIS, W. H., Analytical expressions for inelastic scattering cross sections, 20: 15743
BATES, A. E. G., Testing of control-rod drives, 20: 16096
BATES, David V., Deposition and retention models for internal dosimetry of human respiratory tract, 20: 14796
BATLLE DE PABON, Hilda, Radiation-induced bromination of 2,3-dimethylbutane, 20: 14591
BATT, Russell Howard, Apparatus for heat capacity measurements in range 0.24 to 20°K, 20: 15061 (UCRL-11580)
BAUER, Robert, Experimental investigations on HeLa cells after separated and combined use of decortilen and x radiation, 20: 14375
BAUMANN, G., Double emission of hammer tracks from heavy emulsion nuclei in high-energy interactions, 20: 15792
BAYBARZ, R. D., Curium processing experience, 20: 14639 (ORNL-P-1968)
BAYET, Michel, Kinetic theory of weakly ionized homogeneous plasma. III., 20: 15888 (SC-T-65-775)
BAYET, Michel, Kinetic theory of weakly ionized homogeneous plasma. IV., 20: 15889 (SC-T-65-776)
BEARD, S. J., Large-scale processing and source preparation of separated fission products, 20: 14641 (RL-SA-59)
BEAVER, Wallace W., Sintered intermetallic bodies composed of aluminum and niobium or tantalum, 20: 15026
BEBB, H. Barry, Multiphoton ionization of rare gas and hydrogen atoms, 20: 15276
BECHDOLFF, A., Double emission of hammer tracks from heavy emulsion nuclei in high-energy interactions, 20: 15792
BECK, J., Relativistic effects in many-electron hyperfine structure. I. Theory, 20: 15264
BECK, Juergen, Radiation transmitter, 20: 14864
BECKER, F., Theory of double-charge-exchange nuclear reactions with π mesons, 20: 15813
BECKER, K., Photographic, glass or thermoluminescence dosimetry, 20: 14907
BEEKHUIS, H., Beta decay of ^{147}Nd, 20: 15810
BEENAKKER, J. J. M., Polarizability of hydrogen-isotopes and of ortho and para hydrogen, 20: 15262
BEHNE, D., Attempts at material separation in an electrolytic counter-current exchange process. VI., 20: 14947
BEHRENDS, R. E., Bosons, A parity, and G_2, 20: 15473
BEHRENDS, R. E., Electromagnetic interactions and G_2, 20: 15475
BEHRENDS, R. E., Weak interactions and G_2, 20: 15474
BEISCHER, Dietrich E., Beta particle standards for ^{14}C and other elements in form of radioactive monolayers, 20: 16143 (AD-620276)
BELANGER, Leonard F., Alpha-radiographic and histological observations on skeletal effects of hypo and hypervitaminoses A and D in the rat, 20: 16148 (NYO-2779-9)
BELANGER, Leonard F., Demineralization with EDTA by constant replacement, 20: 16149 (NYO-2779-10)
BELCHER, A. S. B., Dependence of breeding upon design parameters of large fast reactors, 20: 16093
BELINFANTE, J. G., Symmetry properties of bootstrap models, 20: 15556
BELL, J., Effect of minor impurities on positron annihilation lifetime spectrum in argon, 20: 15436
BELLAMY, E. H., Elastic scattering of negative pions on protons near 2 Bev/c, 20: 15377
BELLAMY, Roy Graham, Improvements in or relating to nuclear fuel materials, 20: 15022
BELLAMY, Roy Graham, Improvements in or relating to nuclear fuel materials, 20: 15023
BELLAMY, Roy Graham, Improvements in or relating to nuclear fuel materials, 20: 15024
BELTRAMETTI, E., Small-angle elastic scattering of polarized protons in photographic emulsions, 20: 15314 (RT/FI(65)35)
BELYAEV, B. N., Pair-producing conversion transitions in ^{72}Ge, 20: 15834
BELYAKOV, A. N., Uniform irradiation of surfaces by pulsed electron beams, 20: 15178
BENECKE, Mark William, Effect of LiF on densification of MgO, 20: 15010 (UCRL-16534)
BENES, Jiri, Oxidation products of unsaturated fatty acids in irradiated organism, 20: 14379
BENESOVSKY, F., Some new η carbides, 20: 15103
BENESOVSKY, F., Systems niobium–chromium–carbon and tantalum–chromium–carbon, 20: 15108
BENISZ, Jerzy, Estimation of maximal concentration of thorium and uranium which can be introduced into nuclear emulsion, 20: 14877
BENJAMIN, John S., Intermediate phases in ternary system Nb(Cb)–Ni–Al at 1140°C, 20: 15121
BENNEMANN, K. H., Superconductivity in ferromagnetic alloys, 20: 15648
BENNETT, Willard H., Means for producing focused high density electron streams, 20: 14843
BENO, R. L., Thin film evaporation rate monitor, 20: 14819 (RFP-602)
BENO, R. L., Vapor-deposited film distribution curved substrate surfaces, 20: 16151 (RFP-647)
BENOIST, Pierre, The anisotropic collision in cell problems, 20: 16021 (CEA-R-2890)
BENSON, Joy Lynn, Mass spectrometric determination of the mass of ^{1}H, 20: 15853
BERG, J. M., Correlated electrical and x-ray measurements in flash x-ray discharges, 20: 15573
BERGER, J.-P., Irradiation with ^{90}Sr of superior sympathetic cervical ganglion of rat in vitro, 20: 14332
BERGWALL, S., Anomaly in band structure of terbium metal, 20: 15106
BERKAS, Ernest M., Comparison of wound healing between irradiated and nonirradiated patients after radical neck dissection, 20: 14303
BERLEY, D., Search for decay $\eta \to \pi^0 + e^+ + e^-$, 20: 15333
BERLOVICH, E. E., Applicability of the Ikegami-Udagava method for considering pairing correlations, 20: 15766
BERLOVICH, E. E., Peculiarities of electric dipole transitions in deformed odd nuclei, 20: 15765
BERMAN, R., Effect of isotopes on lattice heat conduction. II. Solid helium, 20: 15652
BERMAN, R., Effect of isotopes on lattice heat conduction. I., 20: 15970
BERMAN, S. M., Spin and parity determination of resonances, 20: 15431
BERNARD, Davy Lee, Equilibrium charge states of ^{16}O ions. I and II., 20: 15854
BERNARDINI, C., Vector boson hunting with Adone, 20: 15311 (LNF-65/47)
BERNSTEIN, M. J., Time-resolved profile measurements of impurity lines in theta pinch discharge, 20: 15872 (IPP-1/41)
BERNSTEIN, Seldon E., Prog. rpt. on attempts to delineate inborn anemias in mice, 2/65–1/66, 20: 14290 (NYO-1800-12)
BERRY, R. E., Rover postoperational destruct instrumentation development, 20: 16112 (SC-RR-65-551)
BERSENEVA, G. T., Precipitation of scandium from hydrochloric acid solutions by sodium silicofluoride, 20: 14566
BERTHO, E., Response to radiotherapy of aortic-femoral prosthesis, 20: 14345
BERTHO, Emile, Effects of radiotherapy on artificial grafts of thoracic aorta, 20: 14344
BERTIN, A., Radiation-induced noise in semiconductor counters, 20: 14923
BERTOTTI, B., Ion waves in bounded plasma, 20: 15900
BERTOZZI, W., The energy and angular distribution of photoneutrons from heavy elements, 20: 15723 (MIT-2098-162)
BERTSCH, George F., Deformations in perturbation theory, 20: 15809
BESANT, C. B., Diffusion length of thermal neutrons in water between 18 and 255°C, 20: 15679
BETHKE, George W., Investigation of plasma accelerator (cyclotron resonance propulsion system), 20: 14726 (NASA-CR-54746)
BETTS, D. S., Viscosity and acoustic impedance of liquid ^{3}He, 20: 15583
BEURTHERET, Charles, Improvements in nuclear reactors, 20: 16049
BEVINGTON, P. R., Elastic and inelastic neutron scattering by silicon and sulfur, 20: 15811
BHATNAGAR, Prem Lata, Adult emergence of house fly, musca domestica, from x-irradiated pupae, 20: 14306
BIALYNICKI-BIRULA, I., Simplified renormalization theory in mesodynamics, 20: 15453
BIDE, R. W., Biochemical effects of x-irradiation on erythrocytes, 20: 14275
BIEBL, Richard, Variations of resistance against α radiations with time of day, 20: 14361
BIEDENHARN, L. C., Coulomb excitation, 20: 15848
BIEFER, G. J., Corrosion behavior of U-bearing resulfurized Cr stainless steel, 20: 14983 (NP-15875)
BIELACZYC, Czeslaw, Thermalization process of neutrons from Po–Be neutron sources in a paraffin moderator, 20: 15683
BIERMAN, A., Calibration of ^{60}Co source by comparison with a weak radium standard, 20: 14927
BIERMAN, D. J., Structure in electron energy spectrum from multi-kev Ar^+–Au and Ar^+–Cu collisions, 20: 15261
BIESENBERGER, Kurt, Determination of very small hafnium contents in

zirconium dioxide preparations by means of x-ray spectral analysis after enrichment by means of partition process, 20: 14496
BIETTI, A., Sum rules for magnetic quadrupole and electric dipole moments, 20: 15365
BILDSTEIN, H., Radiation chemical carboxylation of polychloride compounds for trichloroacetic acid, 20: 14582 (SGAE-CH-25/1965)
BINFORD, Robert T. Jr., Radiation and infants' teeth, 20: 14322
BIRD, L. L., Low-level radiation altimeter system study, 20: 14817 (N65-20421)
BIRGE, Robert W., Spin and parity of Y^{0}(1815) and the Y*(1765), 20: 15414
BISHOP, A. A., Transient DNB test on CVTR fuel assembly, 20: 16101
BISHOP, J. M., K^+p interactions at 3.6 Bev/c, 20: 15415
BISHOP, J. M., Results on π^--p and K^+-p interactions at high energy. B., 20: 15407
BISHOP, W. N., Prog. rpt. on radiochemistry of nuclear fuels, 5–7/65, 20: 14433 (BAW-298)
BISHOP, W. N., Prog. rpt. on radiochemistry of nuclear fuels, 2–4/65, 20: 16061 (BAW-296)
BISWAS, S. N., Current algebras and nonleptonic K-meson decays, 20: 15366
BISWAS, S. N., Deviations from charge independence in n-p and n-n scattering lengths by S-matrix methods, 20: 15356
BITZER, E. B., Prog. rpt. on protective coatings for refractory metals, 10/23/64–1/23/65, 20: 15004 (N65-20790)
BIZZARRI, U., External beam of Frascati electron synchrotron, 20: 15159 (LNF-65/36)
BLACK, J. L., Energy levels of ^{90}Y, 20: 15799
BLACKALL, P., Search for hyperon resonances with spark chambers, 20: 15417
BLAIR, Donald James, Reactor control system, 20: 16014
BLAKE, C. A. Jr., Prog. rpt. on chemical applications of nuclear explosions (CANE), 10–12/65, 20: 14662 (ORNL-TM-1394)
BLANCHARD, R. C., Solar cycle effects on inner-zone protons, 20: 15590 (NASA-TN-D-3086)
BLANCHARD, Robert J. W., Blood supply to hepatic V2 carcinoma implants as measured by radioactive microspheres, 20: 14405 (COO-1305-2)
BLANKENBECLER, R., Linear integral equations for relativistic multichannel scattering, 20: 15351
BLANPIED, W. A., Evidence for hyperon states with masses greater than 1900 Mev, 20: 15424
BLANTON, Roy W. Jr., Study of Rankine-cycle space nuclear power systems, 20: 16111 (N65-16315)
BLATT, Charles J., Comparison of wound healing between irradiated and nonirradiated patients after radical neck dissection, 20: 14303
BLATZ, Hanson, Effective control of x-ray exposure in dentistry, 20: 14419
BLAU, Lawrence Martin, Quantitative spectroscopic studies using the $(^3He,\alpha)$ reaction, 20: 15855
BLEHM, S., Effect of x-irradiation on cell size distribution of thymus lymphocytes, 20: 14318
BLETCHLY, J. D., Effect of γ-radiation on some wood-boring insects, 20: 14305
BLEWETT, John P., Accelerators of the future, 20: 15156 (BNL-741 (Rev.))
BLICHERT-TOFT, P. H., Decay of ^{153}Sm(47h) to ^{153}Eu, 20: 15795
BLICKENS, D. A., Metabolism of methyl palmitate, a phagocytic and immunologic depressant, and its influence on tissue lipids, 20: 14241 (TID-21437)
BLOOD, R. E., Prog. rpt. on specific Zr alloy design program, 1/66, 20: 14980 (GEAP-5065)
BLOOMBERG, Howard Warren, Relation between moment equations and kinetic equation in a collisionless plasma, 20: 15917
BLOOMSTER, C. H., Fuel element for a nuclear reactor, 20: 16057
BLUE, E., A fresh look at the Child-Langmuir problem, 20: 15295 (CONF-640921, pp 47-77)
BLUM, N. A., Isomer-shift measurement in ^{182}W, 20: 15820
BOAG, J., Problems involved in delivering adequate radiation dose to complex samples, 20: 14814
BOAG, J. W., Transient species produced in irradiated water and aqueous solutions containing oxygen, 20: 14614
BOBLETER, O., Device for measuring continuously alpha activity of flowing solutions, 20: 14871
BOBLETER, O., Kinetic investigations on ion exchange processes with regard to uranium fission-product separation, 20: 14643
BOBYKIN, B. V., Deflecting properties and dispersion of electrostatic prism spectrometer, 20: 14868
BOCA, I., Polarization of protons from elastic and inelastic scattering on ^{24}Mg, 20: 15806
BOCCHI, R., Costal fractures as consequence of radiation treatment of breast cancer, 20: 14369
BOCHKAREV, V. V., Imitators of short-living isotopes of iodine, 20: 14928
BODENHEIMER, Peter, Studies in stellar evolution. III., 20: 15196
BOEBEL, G., Small-angle elastic scattering of polarized protons in photographic emulsions, 20: 15314 (RT/FI(65)35)
BOEHM, H., Study on the high-temperature embrittlement of austenitic chromium–nickel steel and nickel alloys by neutron irradiation, 20: 15141
BOEHME, D. K., Mass spectrometric sampling probe for discharge plasmas, 20: 15915
BOEHMER, Winfried, Determination of very small hafnium contents in zirconium dioxide preparations by means of x-ray spectral analysis after enrichment by means of partition process, 20: 14496
BOFFI, S., Coherence properties of fermion beams, 20: 15328
BOFFI, V. C., Neutron diffusion parameters in benzene, 20: 15676
BOGAERT, L. T., Modular steam generator fabrication, 20: 15999 (NAA-SR-11739)
BOGART, Donald, Thermal neutron flux perturbation by Dy–Al foils in H_2O and UO_2F_2–H_2O solutions, 20: 15669 (NASA-TN-D-3237)
BOGDANOVICH, E., Investigation of 9 Bev/c π^- meson interactions with xenon nuclei accompanied by Λ and K^0 particle production, 20: 15841
BOIRON, Pierre Georges, Means for mounting pressure power tubes in a nuclear reactor, 20: 16017
BOKSHTEIN, S. Z., Structure of grain boundaries in molybdenum and its alloys with zirconium and rhenium, 20: 15128
BOKSHTEIN, S. Z., Volume and boundary diffusion of tungsten molybdenum, 20: 15126
BOLDMAN, Donald R., Experimental study of effect of simulated reactor core position on nozzle heat transfer, 20: 14727 (NASA-TM-X-1208)
BOLEY, B. A., Symposium on high temperature structures and materials, N.Y., N.Y., 1/63, 20: 15129
BOLOTIN, V. F., Type 9014-01 alpha-radiation ionization spectrometer and its uses for measuring small concentrations of aerosols of alpha-active isotopes, 20: 14857 (NP-15448)
BOMSE, F., Single-particle exchange in 3-particle final states of the reaction K^+p at 2.26 Bev/c, 20: 15422
BONDAR, I. A., Polymorphism of rare earth pyrosilicates, 20: 14537
BONFER, D. C., Comparison of electrolytic and ferrosilicon-process magnesiums for uranium production, 20: 15050 (NLCO-970, pp 3.1-4)
BONFER, D. C., Effect of furnace heating element arrangement on uranium metal quality, 20: 14964 (NLCO-970, pp 2.1-7)
BONILLA, Charles F., Shipping container for spent nuclear reactor fuel elements, 20: 14678
BONNET, P., Low-voltage radiography in detecting flaws in thin-walled sintered aluminum powder (SAP) tubes, 20: 14706
BONNOR, W. B., Exact solution of Einstein-Maxwell equations referring to magnetic dipole, 20: 15155
BONNOR, W. B., Gravitational waves from isolated sources, 20: 15637
BONTSCHEV, Zv., Moessbauer effect in tin, 20: 14567
BORCHERS, H. J., Local ring and quantum field theory, 20: 15517
BORDARIER, Y., Hyperfine structure of Eu I, 20: 15263
BORGEAUD, P., Reactions $\pi^- + p \to \pi^0 + n$ and $\pi^- + p \to \eta + n$ at high energies, 20: 15380
BORGHINI, M., Choice of substances for polarized proton targets, 20: 15692 (CERN-66-3)
BORGHINI, M., Dynamic polarization of nuclei by electron-nucleus dipolar coupling ("effet solide"), 20: 15819
BORISOGLEBSKII, L. A., Absolute (reduced) and relative probabilities for E0 conversion, 20: 15771
BORNSTEIN, N. S., Diffusivity data on formation of niobium carbide surface films, 20: 14992
BORODULIN, A. I., Measurements of mean energy of electron beams in low-energy linear accelerators, 20: 15179
BOROOKHIM, Manouchehr, Effect of neutron irradiated on transistor current gain, 20: 14920 (TID-22664)
BOROWCZIK, M., Probe for complex study of physical properties of soils, 20: 14773
BORSARU, M., Polarization of protons from elastic and inelastic scattering on ^{24}Mg, 20: 15806
BORUSEVICH, L. K., X-ray structure and metallographic studies of Nb–Co–C systems, 20: 15077
BOSE, S. K., Current algebras and nonleptonic K-meson decays, 20: 15366
BOSI, G., Analysis of beta spectra by measurements in crossed electric and magnetic fields, 20: 14882
BOSKMA, P., Beta decay of ^{147}Nd, 20: 15810
BOSWELL, A. L., Egg mortality after gamma irradiation of adults of omnivorous leaf roller, 20: 14340
BOUCHEZ, R., Orbital electron capture by the nucleus, 20: 15695 (CONF-233(Vol.1), pp 30-59)
BOUGNOT, G., Lifetimes of first excited states of ^{19}F and ^{25}Mg, 20: 15780
BOUNDS, C. L., Effect of isotopes on lattice heat conduction. II. Solid helium, 20: 15652
BOURAT, Guy, Method for liquid-liquid extraction of beryllium, 20: 14658
BOURNE, Leonard, Improvements in or relating to nuclear fuel materials, 20: 15022
BOURNE, Leonard, Improvements in or relating to nuclear fuel materials,

20: 15023
BOURNE, Leonard, Improvements in or relating to nuclear fuel materials, 20: 15024
BOWERSOX, D. F., Solubilities of selected elements in liquid Pu. VII., 20: 15043 (LA-3436)
BOWES, William A., Uranium exploration in Chile, 20: 14779 (RME-4569 (Rev.))
BOWMAN, A. L., Thermal expansion of uranium dicarbide and uranium sesquicarbide, 20: 15093
BOWMAN, F. E., Texture studies in monoclinic plutonium, 20: 15944 (RL-REA-2595, pp 12-14)
BOWMAN, K. O., Minimum significant number of successes in a binomial sample, 20: 16150 (ORNL-3909)
BOYARKINA, A. N., Coherent effects in association replacement reactions, 20: 15838
BOYD, H. W., E2 conversion coefficients in ^{110}Cd and ^{132}Xe, 20: 15704 (CONF-233(Vol.2), pp 164-76)
BOYD, W., Choral hydrate 800 rad dosimeter, 20: 14583 (TID-21634)
BRADFORD, J. C., Data processing techniques for detection and interpretation of teleseismic signals, 20: 14762
BRADLEY, W. F., Structure refinement of La_2Te_3, Th_3P_4 type structure, 20: 14524
BRADNER, H., Coherence measurements with time sampling ocean-bottom seismometers, 20: 14766
BRANDT, John C., Chemical composition of photosphere and corona as influenced by solar wind, 20: 15222
BRANSDEN, B. H., Analysis of pion-nucleon scattering and lower nucleon isobars, 20: 15381
BRAUN, H., Double emission of hammer tracks from heavy emulsion nuclei in high-energy interactions, 20: 15792
BRAUN, Howard E., Study of cable-wrapped pressure vessel for nuclear reactors, 20: 16002
BRAY, P. J., A nuclear magnetic resonance study of decomposition in neutron-irradiated LiF, 20: 14602
BRAY, P. J., Thermal history of LiF single crystals during neutron irradiation, 20: 14603
BREELING, Jim, Nuclear medicine's two explosive decades, 20: 14427
BREIPOHL, A. M., Computer program for performing reliability analyses, 20: 14824 (SC-TM-65-523)
BREITWIESER, Roland, Theoretical background for thermionic conversion including space-charge theory, 20: 15299 (NASA-TN-D-3324)
BREWER, A. W., Precision back-reflection Laue camera, 20: 14820 (RFP-636)
BRILL, Dieter R., Cartan frames and general relativistic Dirac equation, 20: 15457
BRINKLEY, Diana, Choroido-retinal damage as complication of radiotherapy, 20: 14297
BRINKMEIER, Fritz, Decay time of scintillation of anthracene and p-terphenyl single crystals, 20: 15989
BRISCOE, H. W., Data recording and processing for experimental large aperture seismic array, 20: 14761
BROCK, J. C. F., Effect of isotopes on lattice heat conduction. I., 20: 15970
BRODI, G., Controlling furnace cycle with infrared pyrometers in casting of large uranium ingots, 20: 15006 (NLCO-970, pp 4.1-5)
BRODSKY, Allen, Balancing benefit versus risk in control of consumer items containing radioactive material, 20: 14792
BRODY, Kenneth R., Production of ^{75}Se-selenocystine by neutron activation, 20: 14630
BRONFIN, M. B., Diffusion of rhenium in molybdenum, 20: 15127
BRONFIN, M. B., Structure of grain boundaries in molybdenum and its alloys with zirconium and rhenium, 20: 15128
BRONFIN, M. B., Volume and boundary diffusion of tungsten in molybdenum, 20: 15126
BROOKS, W. L., Prog. rpt. on direct biological monitoring, 1963–64, 20: 14784 (AERE-R-5015)
BROOME, P. W., Data processing techniques for detection and interpretation of teleseismic signals, 20: 14762
BROS, J., Axiomatic field theory, 20: 15514
BROVERMAN, I., Prog. rpt. on yield phenomena and fracture of hydrided Zr, 10–12/65, 20: 15042 (IITRI-578-P27-14)
BROWER, Moonyeen S., Changes in leaves of Quercus alba exposed to chronic gamma radiation, 20: 14289 (BNL-9509)
BROWN, F., Angular correlation and internal conversion studies in ^{125}I and ^{127}I, 20: 15701 (CONF-233(Vol.2), pp 128-41)
BROWN, Harold, Navigator study of electric propulsion for unmanned scientific missions, 20: 14724 (65SD5322-A)
BROWN, K. B., Prog. rpt. on chemical applications of nuclear explosions (CANE), 10–12/65, 20: 14662 (ORNL-TM-1394)
BROWN, Karl P. Jr., Shipping container for spent nuclear reactor fuel elements, 20: 14678
BROWN, R. E., Geophysical seismic evaluation study at Hanford, 20: 14753 (BNWL-47)
BROWN, R. I., Polarization of photons scattered by ^{14}N, 20: 15783
BROWN, Stephen L., Disintegration rate multipliers in beta-emitter dose calculations, 20: 14403 (NP-15714)
BROWN, Steven H., Shipping container for spent nuclear reactor fuel elements, 20: 14678
BROWN, W. G., Cis-trans isomerization in solid matrices by γ irradiation, 20: 14596
BROWNELL, L. E., Choral hydrate 800 rad dosimeter, 20: 14583 (TID-21634)
BROWNING, Thomas H., Morphologic response of mucosa of human small intestine to x-ray exposure, 20: 14339
BRUBAKER, C. H. Jr., Exchange of ^{18}O between water and orthotungstate and between water and 12-tungstocobaltate(III), 20: 14525
BRUCKER, W., Influence of x rays on phosphate metabolism of phycomyces, 20: 14264
BRUNEAU, J., Response to radiotherapy of aortic-femoral prosthesis, 20: 14345
BRUNEAU, R., Isotope tests of kidney function in pelvic and abdominal irradiation, 20: 14296
BRUNETON, C., Reactions $\pi^- + p \rightarrow \pi^0 + n$ and $\pi^- + p \rightarrow \eta + n$ at high energies, 20: 15380
BRUSSAARD, P. J., Coulomb excitation, 20: 15848
BRUSTAD, T., Inactivation and induction of free radicals in dried trypsin, 20: 14273
BRYAN, D. E., Prog. rpt. on application of neutron activation of analysis in scientific crime detection, 5/62–10/63, 20: 14439 (GA-5556)
BRYAN, Roland T., Boiling water nuclear reactor with breeder blanket superheater, 20: 16105
BRYNJOLFSSON, A., Effect of ionizing radiation in producing sterility in pharmaceutical products: cells, 20: 14388
BRYNJOLFSSON, Ari, Method of irradiating objects with high energy electrons, 20: 15188
BUCCINO, S. G., Elastic and inelastic neutron scattering by silicon and sulfur, 20: 15811
BUCHANAN, C. D., Recent high-energy electron investigations at Stanford Univ., 20: 15439
BUCKLEY, Arthur Hever, Radioactive composition, 20: 14721
BUCKLEY, T. F., Elastic scattering of negative pions on protons near 2 Bev/c, 20: 15377
BUDBERG, P. B., Constitution diagram of Ti–Nb–Cr system, 20: 15078
BUDKER, G. I., Experiments with charge exchange injection in storage ring, 20: 15177
BUDKER, G. I., Experimental investigation of charge-transfer injection of proton into cyclic accelerators and storage rings, 20: 15163 (NP-15785)
BUDKER, G. I., High-current positron source, 20: 15176
BUECHLI, K., Elimination of salmonellae from proteinaceous foods with irradiation, 20: 14933
BUEHLER, E., Rapid quenching of reactive and refractory alloys from liquid state, 20: 15020
BUERKER, U., Transition radiation from thin silver foils, 20: 15968
BUKHANEVICH, V. F., Study of niobium and tantalum sulfides, 20: 14554
BUKOVAC, M. J., Penetration of organic compounds through isolated cuticular membranes with special reference to ^{14}C ures, 20: 16146 (COO-888-39)
BUON, Jean, Measurement of recoil protons in the elastic electron-proton scattering, 20: 15313 (NP-15822)
BURBIDGE, E. Margaret, Optical evidence suggesting occurrence of violent outburst in NGC 1275, 20: 15205
BURBIDGE, G. R., Optical evidence suggesting occurrence of violent outburst in NGC 1275, 20: 15205
BURCH, P. R. J., Coincident gamma-ray spectrometer and its application to measurements of low-level radioactivity, 20: 14885
BURDIN, K. S., Studies of potassium release from γ-irradiated cells, 20: 14282
BURGETT, R., Prog. rpt. on NLCO activities, 10–12/65, 20: 14963 (NLCO-970)
BURIN, Kl., Moessbauer effect in tin, 20: 14567
BURNETT, George W., Radiation and infants' teeth, 20: 14322
BURNEY, G. A., Chemical processing of Cm, 20: 14636 (CONF-660305-7)
BURYKINA, A. L., Behavior of new materials working in contact with solid metals, compounds, and melts, 20: 14989
BUSCH, Raymond Andrew, Strain aging of iron alloys, 20: 15063 (UCRL-16585)
BUSCHERT, R. C., Atomic structure and correlation in liquid binaries by x-ray and neutron diffraction with application to NaK, 20: 15080
BUSCHERT, R. C., Measurement of length changes to 0.1 A in irradiated germanium at low temperature, 20: 15147
BUSSIERE, Paul, Thermal decomposition of β lead dioxides of different texture, 20: 14548
BUSZA, W., Elastic scattering of negative pions on protons near 2 Bev/c, 20: 15377
BUTTON, Edward J., Half-life measurements of some neutron induced isomers, 20: 15688 (AD-620384)

BUTTON-SHAFER, Janice, Spin and parity of the Ξ^* (1530 Mev), 20: 15464
BYERS, N., CP violation in K decay, 20: 15434
BYERS, N., πp Charge-exchange scattering and coherent droplet model of high-energy exchange processes, 20: 15342

C

CABASSA, N., Effects of experimental dysprotidemia on Hamolsky's test responses, 20: 14276
CABELL, M. J., Mass spectrometric measurements of ratio of thermal neutron capture to fission for ^{241}Pu, 20: 15774
CAGLIOTI, G., Coherence properties of fermion beams, 20: 15328
CAHN, J. H., Collision frequency measurements in oxygen and helium magnetoplasma afterglows, 20: 15867 (AD-620664)
CALDWELL, R. L., Theoretical and experimental model results in neutron lifetime logging, 20: 14775
CALLAN, Edwin J., $L_1L_{2,3}M_{4,5}$ Coster-Kronig transition rates, 20: 15238 (CONF-233(Vol.3), pp 398-418)
CALLAN, Edwin J., On K-level widths, 20: 15239
CALLEN, Earl, Anomalous propagation in a quantum plasma and magnon-helicon coupling, 20: 15941 (NP-15698)
CALVERT, Wynne, Observations of ionospheric irregularities and plasma resonances, 20: 15622
CAMBELL, Ali Bulent, Cylindrically symmetric plasma source, 20: 15914
CAMERON, A. E., Mass spectrometry, 20: 14458 (ORNL-3889, pp 39–43)
CAMERON, A. E., Reliable sample changer for mass spectrometer, 20: 14829
CAMERON, J. F., Apparatus for concentration and measurement of low tritium activities, 20: 14503
CAMERON, J. F., Review of design and application of radioisotope instruments in industry, 20: 14835
CAMP, Eldridge K., Application and electroplating of Re, 20: 15016
CAMPBELL, D., ESR study of free radicals formed by γ-irradiation of poly(ethylene terephthalate), 20: 14606
CAMPBELL, G. M., Thermodynamic properties of Pu compounds from EMF measurements. I., 20: 14507 (LA-3399)
CAMPONOVO, F., Vesico-ureteral reflux after irradiation of urinary bladder, 20: 14411
CANFIELD, Richard T., Thermal column pneumatic facility, 20: 16130
CANNARA, A., Electron beam probing of cathode sheath and beam-plasma interaction, 20: 15884 (SU-IPR-33)
CANOBBIO, Ernesto, Electronic radiation of a plasma in a magnetic field, 20: 15870 (CEA-R-2881)
CAPLAN, Charles, Stimulation of recombination in multiplicity-reactivated bicomplexes and genetic map length of phage T4, 20: 14328
CAPPELAERE, P., Systematic microscopic study of effect of ionizing radiation on animal cells in culture. II., 20: 14321
CARA, J., Absolute cross sections and excitation functions for deuteron-induced reactions on chromium between 2 and 12 Mev, 20: 15808
CARACOCHE, M. C., Isomeric cross-section ratios for ^{134m}Cs, ^{134}Cs, and ^{133m}Ba, ^{133}Ba formed in (d,p) and (d,2n) reactions, 20: 15778
CARDOSO-MARTINHO, Eduardo, Measurement of resonance absorption integrals (Mn, Fe, Co, Ni, Cu, Zr, Mo), 20: 15691 (CEA-R-2840)
CAREY, W. T., Penetration tests, 20: 14702 (Y-1490)
CARHART, R., Nonleptonic decays of the intermediate vector meson, 20: 15362
CARLSON, Thomas A., Atomic readjustment following formation of inner shell vacancies, 20: 15245 (CONF-233(Vol.3), pp 494-504)
CARMONY, D. D., K$^-$p interactions at 3.8 Bev/c, 20: 15418
CARMONY, D. D., Reaction $\pi^-d \to \pi^-d\pi^+\pi^-$ at 3.7 Bev/c, 20: 15409
CARMONY, D. D., Study of the A and B mesons, 20: 15408
CAROVILLANO, Robert L., Axisymmetric plasmasphere resonances, toroidal mode, 20: 15592
CARPENTER, E. W., Historical review of seismometer array development, 20: 14757
CARPENTER, F. D., Prog. rpt. on thermionic materials for space power applications, 10/63, 20: 14959 (N65-20797)
CARPENTER, F. D., Prog. rpt. on thermionic materials for space power applications, 9/63, 20: 14960 (N65-20798)
CARPENTER, F. D., Prog. rpt. on cathodes for thermionic reactors, 4/63, 20: 15046 (N65-15820)
CARR, Leo J., Radiation dosimeter system using cadmium-backed copper foil, 20: 14915
CARROLL, A. S., Pion-proton charge-exchange scattering near 2.0 Bev/c, 20: 15378
CARROLL, D. F., Fuel element for a nuclear reactor, 20: 16057
CARROLL, R. M., Fission-product release from fuels, 20: 15144
CARTER, J. R. Jr., Effect of electron energy on defect introduction in silicon, 20: 14925
CARTER, R. D., Administering criticality control in Hanford Atomic Products Operation non-reactor environment, 20: 14790 (RL-SA-43A)
CASARETT, George W., Experimental radiation carcinogenesis, 20: 14360
CASEY, Kendall Francis Jr., Cherenkov and transition radiation in a periodic medium, 20: 15558
CASTERLINE, J. E., Additional critical heat flux data for large-diameter, internally heated, eccentric annuli at 1000 psia, 20: 16086 (TID-22651)
CASTERLINE, J. E., Critical heat flux in long tubes at 1000 psi with and without swirl promoters, 20: 14695
CASTERLINE, J. E., Transient DNB test on CVTR fuel assembly, 20: 16101
CASTIGLIONI, M., Acceleration of negative ions in Milan AVF cyclotron, 20: 15180
CASTILHO ALCARAS, J. A., Applications of Gel'fand-Moshinsky bases in unitary symmetry and its breaking, 20: 15455
CATALDO, H., Prog. rpt. on Piqua power facility operations analysis, semiannual, 1–6/65, 20: 16077 (NAA-SR-11628)
CATHCART, J. V., Polarized light microscopy of pyrolytic carbon deposits, 20: 15089
CAUSEY, A. R., Creep of single-crystal UO_2, 20: 15086
CAVALIERE, A., Ion waves in bounded plasma, 20: 15900
CAZEMAJOU, Jean, Space-time dependent impulse response of a sub-critical cylindrical reactor, 20: 16020 (CEA-R-2836)
CENJA, M., Polarization of protons from elastic and inelastic scattering on ^{24}Mg, 20: 15806
CERCIGNANI, Carlo, Linearized Rayleigh's problem in magnetogas-dynamics, 20: 15578
CHAI, Kai-yung, Nonisochronous phenomenon in an isochronous cyclotron, 20: 15186
CHALMERS, J. H., Criticality data and its application to plant clearance, 20: 16031
CHALMERS, J. H., Criticality parameters for mixtures of plutonium oxide, uranium oxide and water, 20: 16032
CHALOV, P. I., Relative levels of fission fragment fallout from stratosphere, 20: 14742
CHAMBERS, E. S., Charge transfer cross sections for H^+, H_2^+, or H_3^+ on H_2 from 2 to 55 kev, 20: 15250 (UCRL-6987(Rev.1))
CHAMBERS, R. H., Prog. rpt. on mechanical properties of reactor materials, annual, 11/64–10/65, 20: 15040 (GA-6721)
CHAND, Ramesh, Tests of isospin purity of Σ^0 and Λ^0 hyperons, 20: 15401
CHANDLER, H. K., Effect of irradiation temperature on radiosensitizing activity of vitamin K_5, 20: 14395
CHANDRASEKHAR, S., Post-Newtonian equations of hydrodynamics in general relativity, 20: 15626
CHANDRASEKHAR, S., Post-Newtonian effects of general relativity on the equilibrium of uniformly rotating bodies. I., 20: 15627
CHANDRASEKHAR, S., Stability of gaseous masses for radial and non-radial oscillations in post-Newtonian approximation of general relativity, 20: 15210
CHANG, C. C., MHD boundary layer between parallel streams of different magnetic fields and temperatures, 20: 15570 (N65-21084)
CHANG, Chia-Hwa, Mass formulas for the 189 multiplet of SU(6), 20: 15478
CHANG, Han, Protective effects of streptomycin against radiation damage of chromosomes of germinal cells of mammals, 20: 14404
CHANG, N. P., Generalized definition of P and C, 20: 15486
CHANG, Run-hwa, Angular distribution of high-energy neutrons emitted in absorbing polarized μ^- mesons in calcium, 20: 15721 (JINR-E-2517)
CHARLESBY, A., Potential modifying factors in sterilization and inactivation, 20: 14390
CHARLOT, Gaston, Ion exchange methods of separating zirconium and hafnium, 20: 14657
CHASE, H. B., Radiobiological aspects of supersonic transport, 20: 14797
CHASE, R. L., Parametric radiation detector preamplifier, 20: 14851 (BNL-9980)
CHEN, Michael Ming, Validity conditions of transport property measurements using arc columns, 20: 15926
CHEN, Shek C., Comparison of wound healing between irradiated and nonirradiated patients after radical neck dissection, 20: 14303
CHERKASHIN, E. E., New ternary compounds with $W_2Cr_{21}C_6$ type structure, 20: 14532
CHERNICK, C. L., Refractive index and molar refraction of xenon oxide tetrafluoride, 20: 14528
CHERNOGOROVA, V. A., Angular distribution of high-energy neutrons emitted in absorbing polarized μ^- mesons in calcium, 20: 15721 (JINR-E-2517)
CHERNOGOROVA, V. A., Asymmetry in angular distribution of high-energy neutrons from μ^- capture in sulfur, 20: 15720 (JINR-E-2516)
CHERRY, J. T., Numerical simulation of seismic disturbances, 20: 14755 (UCRL-7929)
CHEUNG, K. Y., Thermal-neutron pulse propagation, 20: 15678
CHEVALIER, Gerard, Release, properties, and trapping of radioactive iodines in waste gases, 20: 14787 (CEA-Bib-64)
CHI, J. W. H., Slug flow and film boiling of hydrogen, 20: 14697
CHIKHLADZE, V. L., Decay scheme of ^{109}Sn, 20: 15752
CHIKHLADZE, V. L., Isomeric transitions of $^{114*}In$ and $^{118*}Te$, 20: 15753

CHILTON, A. B., New variant to exponential transformation technique in Monte Carlo shielding calculations, 20: 15937
CHILTON, C. J., Comparison between solar x-ray emission and vlf sudden phase anomalies, 20: 15603
CHIN, Choo-wen, Opacity due to Compton scattering at relativistic temperatures in semide-generate electron gas, 20: 15209
CHINOWSKY, William, Single-pion production by 1.96-Bev/c K+ mesons, 20: 15335
CHIOFI, K., Coherent effects in association replacement reactions, 20: 15838
CHIOTTI, P., Reactions of uranium carbide in KCl–LiCl/zinc system, 20: 14991
CHORNII, Z. P., Spectral composition of radioluminescence, 20: 14611
CHOW, Y. W., Isomer-shift measurement in ^{182}W, 20: 15820
CHOY, Thomas K., Determination of gold in cosmic dust collection by nuclear activation analysis, 20: 14475
CHRIST, R., Prog. rpt. on fabrication of UO_2 powders and processing into fuel elements, 4–6/65, 20: 14999 (EURAEC-1466)
CHRISTIE, W. H., Reliable sample changer for mass spectrometer, 20: 14829
CHRISTOV, D., Moessbauer effect in tin, 20: 14567
CHU, Chun, ^{14}C-labeled urea and ^{32}P-labeled phosphate to investigate foliar-applied fertilizer for rice growing in reclaimed tidal lands, 20: 14240 (NP-15670)
CHUBURKOV, Yu. T., Extraction of curium and fermium with thenoyltrifluoroacetone, 20: 14654
CHUBURKOV, Yu. T., Preparation of ^{242}Pu and ^{242}Cm from neutron-irradiated ^{241}Am, 20: 14631
CHUDAKOV, V. M., Azimuthal angular distribution of shower particles and gray tracks made by cosmic-ray particles in photoemulsion, 20: 15290
CHUPRINA, V. G., X-ray studies of oxidation of Ni_3Al–Ni_3Nb alloys, 20: 14990
CHURAEV, N. V., Measurement of moisture in organic soils by neutron method, 20: 14756
CHUTKIN, O. A., Type 9014-01 alpha-radiation ionization spectrometer and its uses for measuring small concentrations of aerosols of alpha-active isotopes, 20: 14857 (NP-15448)
CIECHANOWICZ, W., Application of noise technique to diagnostics of magnetohydrodynamics, 20: 15569 (INR-626/IX/R)
CINDRO, N., Isomeric cross-section ratios for 14.6-Mev neutron-induced reactions, 20: 15773
CIOHODARU, Lucia, Determination of thorium in different monazite ore samples, 20: 14491
CLARK, Irwin, Alpha-radiographic and histological observations on skeletal effects of hypo and hypervitaminoses A and D in the rat, 20: 16148 (NYO-2779-9)
CLARK, W. H., Malignant mixed muellerian neoplasms (mixed mesodermal tumors), 20: 14300
CLARK, W. I., Comparison of double diffracting x-ray unit with standard x-ray diffraction unit, 20: 14832 (RL-REA-2595, pp 73-9)
CLARK, W. I., Conference on applications of x-ray diffraction in the atomic energy field, Richland, Wash., 2/65, 20: 15943 (RL-REA-2595)
CLARKE, C. H., Recombination among uv-induced adenine-1 mutants of Schizosaccharomyces pombe, 20: 14327
CLARKE, J. T., Surface area measurements, 20: 14973
CLARKE, William D., Bathyphotometric studies of light regime of organisms of deep scattering layers, 20: 14235 (SAN-584-1)
CLAUSS, M. A., Embrittlement of tantalum by hydrogen, at room temperature, 20: 15130
CLAYTON, C. G., Review of design and application of radioisotope instruments in industry, 20: 14835
CLAYTON, George D., Threshold-limit values in industrial hygiene, 20: 14805
CLAYTON, Kenneth Frank, Fuel element handling apparatus for nuclear reactors, 20: 16008
CLAYTON, Kenneth Frank, Improvements relating to nuclear reactors, 20: 16007
CLEGG, A. B., Pion-proton charge-exchange scattering near 2.0 Bev/c, 20: 15378
CLENDINNING, W., Total absorption x-ray calorimeter, 20: 14908
COATS, James W., Experimental study of effect of simulated reactor core position on nozzle heat transfer, 20: 14727 (NASA-TM-X-1208)
COBURN, Jack W., Renal concentrating defect in canine radiation nephritis, 20: 14342
COCHAVI, S., Excitation of isobaric analog states by (p,n) reactions, 20: 15804
COCHRAN, J. S., Large-scale processing and source preparation of separated fission products, 20: 14641 (RL-SA-59)
COCKS, F. H., Segregation of Ta at very low concentrations in Nb, 20: 14969
COGNEAU, M., Absolute cross sections and excitation functions for deuteron-induced reactions on chromium between 2 and 12 Mev, 20: 15808
COHEN, Jeffrey M., Cartan frames and general relativistic Dirac equation, 20: 15457
COHEN, R. L., Ultrastable triangle and square wave generator, 20: 14827
COHEN, S. G., Isomer-shift measurement in ^{182}W, 20: 15820
COHN, Stanton H., Decrement in radiostrontium retention following stable strontium prefeeding in growing rat, 20: 14251
COJOCARU, V., Determination of thorium in different monazite ore samples, 20: 14491
COLE, J., Single-particle exchange in 3-particle final states of the reaction K+p at 2.26 Bev/c, 20: 15422
COLE, L. J., Recovery of rat kidney from x irradiation, 20: 14258 (AD-627569)
COLE, Leonard J., Radiation carcinogenesis: sequence of events, 20: 14373
COLEMAN, C. E., Hydrogen embrittlement of zirconium in slow-bend tests, 20: 14993
COLEMAN, S., Fun with SU(3), 20: 15531
COLLARD, H., Recent high-energy electron investigations at Stanford Univ., 20: 15439
COLLINS, P. D. B., Inadequacies of new form of strip approximation for the π-π scattering amplitude, 20: 15359
COLLINS, P. D. B., S-wave π-π scattering amplitudes in new form of the strip approximation, 20: 15358
COLOMBIE, Michel, Influence of carbon concentration on morphology of uranium–molybdenum, 20: 15070
COMAR, C. L., Prog. rpt. on fission product metabolism and response in animals, 1/64–12/65, 20: 14243 (TID-22626)
CONDE, M. Rodriguez, European tariffs and nuclear energy, 20: 16155
CONNER, J. P., Comparison between solar x-ray emission and vlf sudden phase anomalies, 20: 15603
CONSOLI, Terenzio, Electronic radiation of a plasma in a magnetic field, 20: 15870 (CEA-R-2881)
CONSTANTINESCU, M., Paramagnetic centers formed by irradiation in oxygenated compounds of Se. I., 20: 15972
CONSTANTINESCU, O., Paramagnetic centers formed by irradiation in oxygenated compounds of Se. I., 20: 15972
CONTE, M., External beam of Frascati electron synchrotron, 20: 15159 (LNF-65/36)
CONTI, M., ISPRA-2 reactor control system, 20: 16126
CONWAY, J. B., Properties of some refractory metals. V., 20: 15041 (GEMP-397)
COOMBES, Charles A., Scalar pion-nucleon interaction, 20: 15325
COPP, D. Harold, Demineralization with EDTA by constant replacement, 20: 16149 (NYO-2779-10)
COPPI, B., New model of solar flares, 20: 15214
CORBETT, I. F., Pion-proton charge-exchange scattering near 2.0 Bev/c, 20: 15378
CORBETT, W. J., Prog. rpt. on mechanical properties of slip-cast fused silica, final, 7/64–6/65, 20: 15058 (SC-DC-66-1130)
CORBIN, L. T., Analytical chemistry for reactor projects, 20: 14454 (ORNL-3889, pp 17-24)
CORNELL, D. A., Paramagnetic resonance of cobalt in intermetallic compounds, 20: 15963
CORREA, Pelayo, Radium isotope accumulation in animal thyroids, 20: 14254
COSTACHEL, O., Formation of lipid peroxides in tissues of irradiated and radioprotected rats, 20: 14293
COSTA RODRIGUES, Jose Maria, Waste disposal problems, 20: 16134 (IEA-102)
COSTIGLIOLO, Furio, Detector for reprocessing cells, 20: 14853 (CNEA-159)
COTTIER, H., Response to antigen stimulus by lymphoreticular system, 20: 14354
COUBLE, Edward, Radiochemical procedures for selected radionuclides in environmental samples, 20: 14430 (AD-620219)
COURANT, E. D., Transverse coherent instability of bunched beams, 20: 15170 (SLAC-49, pp 36-48)
COURTNEY, F. E., Meteorological program at Parr, South Carolina, 20: 14732 (CVNA-172)
COWELL, W. R., Checker-playing program for IPL-VC computer, 20: 14949 (ANL-7109)
COX, A. Lucile, Study of Rankine-cycle space nuclear power systems, 20: 16111 (N65-16315)
COX, C. R., Differential cross sections and polarization effects in pion-proton elastic scattering at 875 to 1579 Mev/c, 20: 15372
COX, W. L., Structure refinement of La_2Te_3, Th_3P_4 type structure, 20: 14524
COZ, Marcel, Channels projection operators and the Pauli principle, 20: 15744
CRAIG, R. M., Elastic and inelastic scattering of 20- to 28-Mev polarized protons by carbon, 20: 15805
CRANNELL, C., Recent high-energy electron investigations at Stanford Univ., 20: 15439
CRAWFORD, C. K., Prog. rpt. on electron-ionization cross sections,

semiannual, 12/16/64–6/15/65, 20: 15235 (AD-620289)
CRAWFORD, Frank S. Jr., Study of the decay $\eta^0 \rightarrow \pi^+ + \pi^- + \gamma$, 20: 15367
CRAWFORD, J. H. Jr., Radiation damage in solids: survey, 20: 15139
CRAWFORD, W. M., Corrosion behavior of U-bearing resulfurized Cr stainless steel, 20: 14983 (NP-15875)
CREAMER, B., Recovery of intestinal mucosa in rat after x-irradiation of exteriorized intestine, 20: 14364
CRESPI, M. Alicia, Graphite-gas reactors, 20: 16035
CRIMI, Gilles F., Investigation of plasma accelerator (cyclotron resonance propulsion system), 20: 14726 (NASA-CR-54746)
CRISTALLINI, C., Raman polarization studies of several nitrato complexes, 20: 14529
CRISTOFORI, F., Statistics of eigenvalues of random matrices, 20: 15784
CRISTU, M. I., Gamma radiation from interaction of neutrons with iodine nuclei, 20: 15831
CROFT, W. L., Particle parameter of the $2^+ \rightarrow 0^+$ E2 transition in ^{170}Yb, 20: 15700 (CONF-233(Vol.2), pp 120-7)
CROMBIE, D. D., Use of vlf measurements for obtaining information on the lower ionosphere (especially during solar flares), 20: 15604
CROSBY, E. H., Energy dependence of lithium fluoride dosimeters at high energies, 20: 14888
CROUCH, H. R. Jr., High-energy photoproduction of nucleon and pionic resonances, 20: 15425
CROUSE, D. J., Prog. rpt. on chemical applications of nuclear explosions (CANE), 10–12/65, 20: 14662 (ORNL-TM-1394)
CROWE, Kenneth M., π-π interaction in reaction $\pi^- + p \rightarrow \pi^0 + \pi^0 + n$ at 378 Mev, 20: 15368
CSONKA, P. L., Apparent CP noninvariance and the Neutrino Sea, 20: 15446 (UCRL-12380-T)
CUEER, P., Double emission of hammer tracks from heavy emulsion nuclei in high-energy interactions, 20: 15792
CUNANAN, S. A., Studies on coconut oil, 20: 14463 (PAEC(D)CH–652)
CUNNINGHAM, S. P., Ground-based optical detection of deep space nuclear detonations, 20: 15608
CURRIE, D. G., Poincare-invariant equations of motion for classical particles, 20: 15153
CURRIE, Douglas G., New class of invariance transformations in classical hamiltonian particle dynamics, 20: 15150
CURTISS, C. F., Low-energy atomic collisions. I., 20: 14545
CUSSON, Ronald Yvon, Scattering of alpha particles in ^{7}Li, 20: 15859
CUTKOSKY, R. E., Self-consistent broken symmetries, 20: 15557
CUTKOSKY, R. E., Simple bootstrap rules, 20: 15555
CUTKOSKY, R. E., Symmetry properties of bootstrap models, 20: 15556
CZAJKOWSKI, M., Sensitized fluorescence in vapors of alkali metals. V., 20: 15253
CZARNECKI, E., Measurement methods to impart linearity of scale to radioisotope instruments, 20: 14836
CZERWONKO, J., Superconductivity with pairs in triplet of spins, 20: 15644
CZYZ, W., Electric dipole sum rules and inelastic electron scattering form factors of 1^-, $T = 1$ states in light nuclei, 20: 15746

D

DABEK, Tadeusz, Detecting probes operating in single-cable system of pulse transmission and power supply, 20: 14876
D'ACUNZO, L., Effects of polymerized heterologous RNA on ascite tumors, 20: 14397
D'ACUNZO, L., Radioprotective effects of ribonucleic acid on normal and tumor tissues, 20: 14401
DAHL, Orin I., Enhancements in interactions of 3.2 Bev/c π^- with deuterium, 20: 15405
DAIRIKI, Ned T., π-π interaction in reaction $\pi^- + p \rightarrow \pi^0 + \pi^0 + n$ at 378 Mev, 20: 15368
DALITZ, R. H., Remarks on study of pion-nucleon interaction, 20: 15371
DALTON, George Ronald, Reactor control system, 20: 16014
DAMERELL, C. S. J., Pion-proton charge-exchange scattering near 2.0 Bev/c, 20: 15378
DANDL, R. A., Device having high-gradient cusp geometry, 20: 15928
DANDL, R. A., Use of silicon solar cells as detectors of energetic electrons from plasmas, 20: 15916
DANFORTH, John P., Variable specific gravity radioactive source holder, 20: 14683
D'ANGELO, N., Kelvin-Helmholtz instability in a cesium plasma, 20: 15906
DANIELS, A. U., Densification and sintering of thoria and thoria gels. XXVII., 20: 15009 (TID-22491)
DANOS, M., Nuclear giant quadrupole resonance, 20: 15823
DANYSZ, A., Radioprotective action of methandrostenolone, 20: 14392
DANYSZ, Andrzej, Effective mechanism of radioprotective substance methandrostenolone. II., 20: 14402
DAR, A., Analytical expressions for inelastic scattering cross sections, 20: 15743
DARCEY, W., Energy levels of ^{90}Y, 20: 15799
DARRIULAT, Pierre, Contribution to the study of the α-α interaction, 20: 15689 (CEA-R-2786)
DAUER, M., Adult emergence of house fly, musca domestica, from x-irradiated pupae, 20: 14306
DAVEY, C. N., Automation of tube-thickness measurements using ultrasonics, 20: 14718
DAVIES, H., High-energy γ rays from pion capture, 20: 15794
DAVIES, H., Reaction $(\pi^-, 2n)$ in ^{6}Li and ^{7}Li, 20: 15793
DAVIES, W. E. R., Cooperative effects in scattering of laser beam from a plasma, 20: 15911
DAVILA, A. T., Production of colloidal ^{198}Au, 20: 14627 (PAEC(D)IS-651)
DAVIS, F. C., Machine to transfer powdered radioactive fuel remotely, 20: 14668 (ORNL-TM-1397)
DAVIS, R., V-2-prong K$^-$p interactions at 5.5 Bev/c, 20: 15416
DAVIS, Wallace Jr., Radiation densities and TBP radiolysis during thorex short decay runs, 20: 14580 (ORNL-2764)
DAWSON, John M., Kinetic structure of a plasma, 20: 15899
DAYTON, Russell W., Prog. rpt. on civilian applications, 12/65, 20: 14957 (BMI-1754)
DE ALFARO, V., Differential properties of Feynman amplitudes, 20: 15525
DE ALFARO, V., Potential scattering, 20: 15566
DEAN, Phillip N., Computer analysis of cell volume distributions, 20: 14232 (LA-3440)
DEAN, W. C., Data processing techniques for detection and interpretation of teleseismic signals, 20: 14762
DEARMAN, Henry H., EPR studies of defect sites in thulium ethylsulfate crystals, 20: 14547
DE BEAR, W. S., Prog. rpt. on Piqua power facility operations analysis, semiannual, 1–6/65, 20: 16077 (NAA-SR-11628)
DECOURS, Jacques, Influence of carbon concentration on morphology of uranium–molybdenum, 20: 15070
DE DORLODOT, P., Dynamic corrosion tests on carbon and stainless steels in pressurized water, 20: 14978 (EURAEC-1546)
DEDOV, V. B., Preparation of ^{242}Pu and ^{242}Cm from neutron-irradiated ^{241}Am, 20: 14631
DE GENNES, P. G., Excitation spectrum of superimposed normal and superconducting films, 20: 15653
DE GROOT, J. J., Polarizability of hydrogen-isotopes and of ortho and para hydrogen, 20: 15262
DEHMELT, H. G., Ultrahigh resolution $\Delta F = 0, \pm 1$ (^{3}He)$^+$ HFS spectra by ion-storage collision technique, 20: 15260
DEINZER, W., Models for carbon-burning stars, 20: 15194
DEIRMENDJIANA, Astrik, Magnetohydrostatic cavity formed around a system of line currents in an infinitely conducting atmosphere, 20: 15587 (AD-620244)
DE JAGER, C., Symposium on solar spectrum, Utrecht, 8/63, 20: 15234
DELAFIELD, H. J., Gamma-ray exposure measurements in man phantom related to personnel film dosimetry, 20: 14806
DELBOURGO, R., Relativistic extension of non-compact symmetry groups, 20: 15370
DELBOURGO, R., $\bar{U}(12)$ symmetry, 20: 15537
DELCROIX, Jean-Loup, Kinetic theory of weakly ionized homogeneous plasma. III., 20: 15888 (SC-T-65-775)
DELCROIX, Jean-Loup, Kinetic theory of weakly ionized homogeneous plasma. IV., 20: 15889 (SC-T-65-776)
DEL FAVERO, A., Variations of hepatic lipid components in mouse after whole-body irradiation with lethal dose, 20: 14268
DELLER, D. J., Measurement of ^{47}Ca absorption by whole-body gamma spectrometry, 20: 14247
DE LORENZO, J. T., Charge-sensitive preamplifier, ORNL model RC11-4-2X, 20: 14859 (ORNL-TM-1390)
DE LORENZO, J. T., HFIR cladding-failure detector, 20: 16124 (ORNL-TM-1388)
DE LORENZO, J. T., ±32 Volt power supply, ORNL model RC11-4-2E, 20: 14818 (ORNL-TM-1391)
DE MEESTER, P., Microradiographic fuel investigation in thin layers, 20: 14704
DEMEUR, M., Double ionization accompanying ^{6}He decay, 20: 15715 (CONF-233(Vol.3), pp 505-9)
DEMIDOV, A. M., Gamma spectrum produced by thermal neutron capture in palladium, 20: 15755
DEMIDOV, A. M., Gamma spectrum produced by thermal neutron capture in gold, 20: 15756
DEMIDOV, A. M., Nuclear levels of ^{168}Er excited by the (n,γ) reaction, 20: 15757
DEMIRKHANOV, R. A., Atomic masses of stable neodymium, praseodymium, cerium, and lanthanum isotopes, 20: 15769
DEMUS, S., Measurement methods to impart linearity of scale to radioisotope instruments, 20: 14836
DENIG, Richard, Rapid extraction by quasi-solid extraction agent, 20: 14656

DENISKIN, V. P., Eddy-current method for multi-parameter testing of structural components, 20: 14708
DENISSE, Jean-Francois, Kinetic theory of weakly ionized homogeneous plasma. III., 20: 15888 (SC-T-65-775)
DENISSE, Jean-Francois, Kinetic theory of weakly ionized homogeneous plasma. IV., 20: 15889 (SC-T-65-776)
DENNEY, J. M., Prog. rpt. on effects of proton irradiation on solar cells, 1/65, 20: 14919 (N65-20653)
DENNIS, J. A., Neutron flux and energy measurements, 20: 14883
DE PINHO, A. G., Rotational levels of odd-odd light deformed nuclei, 20: 15814
DEPONNIER, P., Orbital electron capture by the nucleus, 20: 15695 (CONF-233(Vol.1), pp 30-59)
DE RAAD, J. A., Quality selection of Zircaloy-2 canning tubes by ultrasonic testing on small defects, 20: 14714
DERADO, I., Single-pion production in π^-p interactions between 600 and 900 Mev, 20: 15411
DERRICK, M., V-2-prong K$^-$p interactions at 5.5 Bev/c, 20: 15416
DESAI, Bipin R., πN charge-exchange scattering and the ρ trajectory, 20: 15364
DESAI, Rashmi C., Atomic motions in rigid sphere gas as a problem in neutron transport, 20: 15675
DE SAINT MAURICE, Arthur B., Thermal column pneumatic facility, 20: 16130
DESSERT, Robert Allen, Construction of lithium drifted germanium solid state detector system with special attention to ^{105}Ag and ^{192}Ir, 20: 14845 (AD-620434)
DESTRIBATS, Marie-Therese, Automatic inspection of Co-laminated elements, 20: 14715
DESTRIBATS, Marie-Therese, Control methods used in department of metallurgy for structural and fuel elements, 20: 14711
DETILLEUX, E., Aqueous processing of graphite–carbide fuel elements, 20: 14638 (NP-15753)
DEVIN, B., Utilization of impregnation compounds in graphite in thermionic conversion, 20: 15296 (CONF-640921, pp 81-99)
DE VRIES, R. F., Spectroscopic determination of electron temperature in a helium plasma, 20: 15908
DE WAARD, H., Beta decay of ^{147}Nd, 20: 15810
DE WAART, J., Elimination of salmonellae from proteinaceous foods with irradiation, 20: 14933
DEWELL, E. H., Prog. rpt. on radiochemistry of nuclear fuels, 2–4/65, 20: 16061 (BAW-296)
DE WIT, S. A., Some allowed K-capture to positron ratios, 20: 15711 (CONF-233(Vol.2), pp 345-58)
DEYEV, V. I., Mechanism of boiling of liquid sodium on heating surface at free convection, 20: 14693 (AD-625791)
DICKIE, Alan Bain, Improvements in fluid flow control valves, 20: 14676
DICKINSON, H., Systems for detection and identification of nuclear explosions in the atmosphere and in space, 20: 15594
DICKSON, J. M., Prog. rpt., annual, PLA division, 1965, 20: 15164 (RHEL/R-112)
DIENST, W., Study of the high-temperature embrittlement of austenitic chromium–nickel steel and nickel alloys by neutron irradiation, 20: 15141
DIENSTBIER, Z., Hematological changes in radiation sickness. V., 20: 14314
DIENSTBIER, Z., Influence of x-radiation, on urinary excretion of inorganic phosphates and ammonia, 20: 14270
DIENSTBIER, Zdenek, Activity of pyridine nucleotidase in whole-body x-irradiated rats, 20: 14362
DIETRICH, K., Self-consistent calculation of nuclear equilibrium deformations, 20: 15843
DI GRAZIA, Giovanni, In-core instrumentation for the reactor of the SENN power plant at Garigliano, 20: 16065 (EUR-2420.d,f,i,n,e, pp 17-49)
DILLAMORE, I. L., Preferred orientation in wrought and annealed metals, 20: 15099
DI LUZIO, N. R., Metabolism of methyl palmitate, a phagocytic and immunologic depressant, and its influence on tissue lipids, 20: 14241 (TID-21437)
DIMCZEW, Todor, Low-background beta scintillation counting without shielding, 20: 14873
DIMCZEW, Todor, Some spectrometer properties of counter with thin plastic phosphor used for measuring β-particles of ^{90}Sr + ^{90}Y, 20: 14874
DIMOND, Noreen A., Radiochemical procedures for selected radionuclides in environmental samples, 20: 14430 (AD-620219)
DIMOV, G. I., Experimental investigation of charge-transfer injection of proton into cyclic accelerators and storage rings, 20: 15162 (NP-15785)
DIMOV, G. I., Experiments with charge exchange injection in storage ring, 20: 15177
DIONISIO, J. Sant'Ana, The L,M,N Auger spectra and the Coster-Kroenig transitions of heavy elements, 20: 15240 (CONF-233(Vol.3), pp 440-53)
DIPERT, Merlin H., Automatic handling of data from large-scale dog radiation experiment using general purpose computer, 20: 14238 (CONF-650560-13)
DIVINE, Neil, Numerical evaluation of degenerate equation of state, 20: 15213
DIVINE, Neil, Structure and evolution of model helium stars, 20: 15195
DJORDJEVIC, O., Metabolism of nucleic acids in uv-irradiated L-strain cells treated with native deoxyribonucleic acid, 20: 14355
DMITRIEV, I. D., Application of nuclear power installation for water desalination with simultaneous production of electric power, 20: 16108 (JPRS-33459)
DMITRIEV, V. N., Radioactivity of air over Atlantic Ocean in May to July, 1964, 20: 14743
DOBROVOLSKII, T., Investigation of 9 Bev/c π^- meson interactions with xenon nuclei accompanied by Λ and K^0 particle production, 20: 15841
DOCKERY, John Thomas, Y*(1660)—spin and parity determination, 20: 15397
DODD, P. H., Logging system and computer program to determine rock density of uranium deposits, 20: 14778
DODDS, J., Coherence measurements with time sampling ocean-bottom seismometers, 20: 14766
DODGE, F. T., Magnetohydrodynamic squeeze film energy converters, 20: 15304
DODSON, Helen W., Unexpected time distributions of terrestrial detection of solar cosmic-ray events, 20: 15233
DOEPKER, R. D., Gas-phase radiolysis of cyclopentane, 20: 14599
DOHERTY, R. H., Techniques for detection of high-altitude nuclear explosions, 20: 15612
DOLL, W. R. S., Evaluation of risk from radiation, 20: 14331
DOLPHIN, G. W., Dosimetry of gastrointestinal tract, 20: 14795
DONAHUE, T. M., Detection of high-altitude explosions by observation of air fluorescence, 20: 15610
DONDES, S., Spectroscopic study of alpha-ray-induced luminescence in gases. I., 20: 14617
DONDI, Giovanni, Controls for the Latina power plant, 20: 16066 (EUR-2420.d,f,i,n,e, pp 51-115)
DONNELLY, R. G., Fabrication procedures for Enrico Fermi fast breeder reactor fuel elements, 20: 16100
DOOHER, J., Effect of intermediate vector mesons on neutrino production of lepton pairs, 20: 15347
DOOHER, J., Nonleptonic decays of the intermediate vector meson, 20: 15362
DOOLEN, Gary D., Nucleon as a composite particle state, 20: 15352
DOOLEN, Gary D., Self-consistent determination of position and width of the 33 π in resonance, 20: 15353
DORE, J.-C., Elastic and inelastic scattering of 20- to 28-Mev polarized protons by carbon, 20: 15805
DORNBRACK, G., Injuries in the mouth-jaw region following irradiation, 20: 14324
DORN, D. W., Neutron-neutron interaction in triton-triton reaction, 20: 15733 (UCRL-7769)
DOROKHOV, V. V., Atomic masses of stable neodymium, praseodymium, cerium, and lanthanum isotopes, 20: 15769
DOROSHENKO, G. G., Analyzing spectra of γ quanta and fast neutrons measured by means of single-crystal scintillation spectrometers, 20: 14869
DORY, J., Automatic inspection of Co-laminated elements, 20: 14715
DOTHAN, Yossef, Band spectra generated by non-compact algebra, 20: 15506
DOUGLASS, D. H. Jr., Subharmonic structure in Pb–Pb superconductive tunneling junctions, 20: 15651
DOWELL, J. D., Search for hyperon resonances with spark chambers, 20: 15417
DOWNS, Angela M., Magnetohydrostatic cavity formed around a system of line currents in an infinitely conducting atmosphere, 20: 15587 (AD-620244)
DRAGON, V., Formation of lipid peroxides in tissues of irradiated and radioprotected rats, 20: 14293
DRAHOVSKY, D., Urinary excretion of pseudouridine in course of x-ray therapy, 20: 14269
DRAPER, J. E., Thermal and resonance neutron capture in Cl, Sc, V, Co, and Ir, 20: 15787
DRELL, S. D., Special models and predictions for photoproduction above 1 Bev, 20: 15442
DREVER, R. W. P., Ratio of K-capture to positron emission in decay of ^{13}N, 20: 15712 (CONF-233(Vol.2), pp 359-64)
DREVINSKY, Peter J., Radiochemical procedures for selected radionuclides in environmental samples, 20: 14430 (AD-620219)
DRIESSENS, J., Systematic microscopic study of effect of ionizing radiation on animal cells in culture. II., 20: 14321
DRISCOLL, Michael John, Reactor control system, 20: 16014
DRORY, Ch., Excitation of isobaric analog states by (p,n) reactions, 20: 15804
DROSG, Manfred, Moessbauer effect of 46.5-kev line of ^{183}W, 20: 15737
DROULLARD, R. F., Logging system and computer program to determine rock density of uranium deposits, 20: 14778

DRUCKER, D. C., Prog. rpt. on mechanical properties of metals, 2/65–1/66, 20: 15055 (NYO-2394-19)
DUBOVIK, V. M., Ionization losses of spin-½ particles, 20: 15269
DUDA, Renate, Determination of trace impurities in UO_2 fuel materials, 20: 14494
DUERRSCHNABEL, W., Prog. rpt. on fabrication of UO_2 powders and processing into fuel elements, 4–6/65, 20: 14999 (EURAEC-1466)
DUFFEY, Dick, Derivative neutron activation analysis, 20: 14502
DUKE, P. J., Differential cross sections and polarization effects in pion-proton elastic scattering at 875 to 1579 Mev/c, 20: 15372
DUMITRESCU, O., Reduced widths for nucleon emission in shell-model intermediate coupling, 20: 15830
DUMONT, Allan E., Studies in I metabolism. III., 20: 14249
DUMOVA, A. A., Analyzing spectra of γ quanta and fast neutrons measured by means of single-crystal scintillation spectrometers, 20: 14869
DUNMYRE, G. R., Search for low-temperature anomalies in electrical resistivity of dilute gold–erbium alloys, 20: 15083
DUNMYRE, G. R., Thermal conductivity, electrical resistivity, and Lorenz function of polycrystalline erbium between 5 and 300°K, 20: 15107
DUNNE, S. A., W spin and the rotation group in four dimensions, 20: 15467
DUNSTER, H. J., Evaluation of risk from radiation, 20: 14331
DUPLAN, J. F., Protection of mouse against lethal effects of x rays by sodium hyposulfite, 20: 14393
DURKEE, Robin K., Thermoluminescent dosimeter shield, 20: 14914
DUTREIX, J., High-energy radiations in France. (Present equipment and future prospects), 20: 14425
DUTT, G. C., Reaction mechanism for $^{11}B(\alpha,n)^{14}N$ reaction, 20: 15790
DUTTO, G., Acceleration of negative ions in Milan AVF cyclotron, 20: 15180
DWECK, Joel Allen, Magnetic interactions in rare earth ethyl sulfates, 20: 15991
DYATLOV, V. K., Isomeric transitions of $^{114*}In$ and $^{115*}Te$, 20: 15753
DYRSET, J., Inactivation and induction of free radicals in dried trypsin, 20: 14273
DZHAFAROV, I. G., Neutrino-nucleon interactions with lepton production, 20: 15387
DZNAGATSPANYAN, R. V., Structure of radiation chlorinated and sulfochlorinated polyethylene, 20: 14621
DZNELEPOV, B. S., Gamma radiation of ^{152}Eu in energy range 1380 to 1900 kev, 20: 15832
DZHELEPOV, B. S., New data on decay of $^{184*}Re$, 20: 15750
DZIUNIKOWSKI, Bohdan, Debalancing of differential x-ray filters, 20: 14487
DZKUYA, M. I., Atomic masses of stable neodymium, praseodymium, cerium, and lanthanum isotopes, 20: 15769

E

EARL, John Alfred, Insulating vitreous material, 20: 15131
EASTWOOD, T. A., Neutron flux measurements with cobalt, 20: 14867
EBERHAGEN, A., Time-resolved profile measurements of impurity lines in theta pinch discharge, 20: 15872 (IPP-1/41)
EBERHARDT, P., Rare gas measurements in 30 stone meteorites, 20: 15193 (NP-15654)
EBERLINE, Howard C., Fast and slow neutron counter, 20: 14913
EBERLINE, Howard C., High level remote radiation monitor, 20: 14911
EDELMAN, Ralph E., Shaped Mg–Li castings, 20: 15007 (NP-15881)
EDER, Gernot, Terrestrial neutrinos, 20: 14750
EDING, H. J., Prog. rpt. on growth of carbide crystals, 9–12/64, 20: 15047 (N65-15919)
EDINGTON, J. W., Prog. rpt. on refractory metals, 9–11/64, 20: 15049 (N65-16256)
EDSMYR, Folke, Vesico-ureteric reflux in connection with supervoltage therapy for bladder carcinoma, 20: 14298
EDVARDSSON, K. A., Prog. rpt. on personnel dosimetry, annual, 1964, 20: 14782 (AE-211)
EDVINSSON, Gunnar, Rotational analysis of perturbed C and D states of BaH and BaD, 20: 14517
EDWARDS, David L., Mixed heterologous mesenchymal sarcomas (mixed mesodermal sarcomas) of uterus, 20: 14301
EFENDIEVA, N. G., Uranium extraction from aqueous solutions with naphthenic acid, 20: 14642
EFIMOV, Yu. V., Reactions of vanadium with liquid elements of periodic table, 20: 14538
EGAMI, Nobuo, Inhibitory effect of x-irradiation on development of ovaries of fish, Oryzias latipes, in sexually inactive seasons, 20: 14307
EGOROV, Yu. S., Decay of ^{90}Mo, 20: 15751
EHLERS, Robert C., Experimental study of effect of simulated reactor core position on nozzle heat transfer, 20: 14727 (NASA-TM-X-1208)
EHLOTZKY, F., Double bremsstrahlung, 20: 15318
EHRENSTEIN, Gerald Marvin, Hyperfine structure in ^{17}OH, 20: 15272
EHRHARDT, E., DPN degradation and synthesis of lymphosarcoma ascites cells after x irradiation, 20: 14370
EICHELBERGER, J. F., Prog. rpt., 6/65, 20: 14444 (MLM-1268)
EICHLER, J. B., Prog. rpt. on reactor containment, 10–11/65, 20: 16023 (IITRI-578P21-16)
EILENBERGER, Gert, General approximation method for the free energy functional of superconducting alloys, 20: 15654
EINHORN, Jerzy, Hypothyroidism following ^{131}I treatment for hyperthyroidism, 20: 14338
EISMONT, V. P., Deuteron fission of ^{232}Th and dependence of fragment kinetic energy on excitation energy of the fissile nucleus, 20: 15840
EISNER, H., Investigation of radioactivity of snow layers of Alpine glacier for establishment of dating boundaries, 20: 14740
ELISEEV, A. A., Roentgenographic studies of lanthanum tellurides, 20: 14530
ELLIOTT, R. J., Localized vibrations of H^- and D^- ions in alkaline earth fluorides, 20: 15969
ELY, Robert P., Spin and parity of $Y_1^*(1815)$ and the $Y^*(1765)$, 20: 15414
ELZE, J., Growth conditions and properties of thick anodic produced oxide layers on zirconium, 20: 14995
EMURA, Satoru, Radiation leak test of shielded cells at reprocessing analytical facility, 20: 14788 (JAERI-1089)
ENGEL, R. D., Detection of daytime nuclear bursts below 150 km by prompt vlf phase anomalies, 20: 15602
ENGLER, A., Observations of $Y_1^*(1405)$ and $Y_1^*(1358)$ resonances in π-N collisions at 1.68 Bev/c, 20: 15404
ENOCH, Jacob, Steady-state structure and low-frequency oscillations of an infinitely long E layer, 20: 15905
ENTICKNAP, R. G., Large aperture seismic array signal handling system, 20: 14760
ERBER, T., Vacuum polarization in μ-mesic atoms, 20: 15246 (CONF-233(Vol.3), pp 520-8)
ERDAHL, Robert M., Fluorides and oxides of helium and neon, 20: 14541
ERMAKOV, V. A., Preparation of ^{242}Pu and ^{242}Cm from neutron-irradiated ^{241}Am, 20: 14631
ERMAN, Peter, Anomalies of E2 conversion coefficients in the deformed-nucleus region, 20: 15745
ERMAN, Peter, Photoelectron scattering and consequences for determination of internal conversion coefficients by the IEC method, 20: 15709 (CONF-233(Vol.2), pp 247-51)
ERMAN, Peter, Studies of Auger effect in light elements, 20: 15244 (CONF-233(Vol.3), pp 487-93)
ERMOLOV, P. F., Production cross section of charged pions in (n,p) collisions, 20: 15310 (JINR-P-2508)
ERNST, Frederick J., Masses and couplings of $P_{\frac{1}{2}}$ octet and $P_{\frac{3}{2}}$ decuplet, 20: 15509
ERVIN, G. Jr., Oriented growth of oxidation products on single crystals of uranium monocarbide, 20: 14985
ERWIN, A. R., K^+p interactions at 3.6 Bev/c, 20: 15415
ERWIN, A. R., Results on π^--p and K^+-p interactions at high energy. A., 20: 15406
ERWIN, A. R., Results on π^--p and K^+-p interactions at high energy. B., 20: 15407
ESPI, G., Lifetimes of first excited states of ^{19}F and ^{25}Mg, 20: 15780
ETTERS, Richard David, Theory of many-boson systems, 20: 15560
EUBANKS, I. D., Chemical processing of Cm, 20: 14636 (CONF-660305-7)
EUGSTER, O., Rare gas measurements in 30 stone meteorites, 20: 15193 (NP-15654)
EVANS, D. Fennell, Conductance of ions in light and heavy water at 25°, 20: 14540
EVANS, J. A., Permeation and diffusion of hydrogen in molybdenum, 20: 14976 (AWRE-O-16/66)
EVANS, J. A., Versatile and cheap vacuum leak, 20: 14730 (AWRE-O-10/66)
EVANS, J. S., Experimental investigation of some neutron-deficient nuclei, 20: 15727 (PPAD-572F)
EVANS, L., Relativistic effects in many-electron hyperfine structure. II., 20: 15265
EVANS, L., Relativistic effects in many-electron hyperfine structure. III., 20: 15266
EVE, I. S., Dosimetry of gastrointestinal tract, 20: 14795
EVE, I. S., Physiology of gastrointestinal tract in relation to radiation doses, 20: 14794
EVERETT, Mark Allen, Ultraviolet erythema, 20: 14310
EVERHART, Edgar, Coincidence study of O^+ on Kr collisions, 20: 15249 (TID-22648)
EVSEEV, V. S., Angular distribution of high-energy neutrons emitted in absorbing polarized μ^- mesons in calcium, 20: 15721 (JINR-E-2517)
EVSEEV, V. S., Asymmetry in angular distribution of high-energy neutrons from μ^- capture in sulfur, 20: 15720 (JINR-E-2516)
EWAN, G. T., Anomalous L-subshell conversion of some hindered E1 transitions in the rare earth region, 20: 15703 (CONF-233(Vol.2), pp 148-57)
EXNER, H. E., Observations on milling of hard metal powders, 20: 15015

F

FADEEVA, V. I., Diffuse scattering of x rays by HfC–ZrC solid solutions, 20: 15074

FAIRCHILD, R. G., Development and dosimetry of "epithermal" neutron beam for possible use in neutron capture therapy. II., 20: 14421

FALK, F., Experimental and theoretical studies of L-conversion electron directional correlations, 20: 15699 (CONF-233(Vol.2), pp 117-19)

FANG, Shou-sien, Nonisochronous phenomenon in an isochronous cyclotron, 20: 15186

FARKAS, J., Observations on biochemical changes in irradiated spores of Bacillus cereus, 20: 14263

FARMER, Herbert Edward, Radioactive composition, 20: 14721

FARRELL, Sherman R., Rotatable charged particle beam deflector, 20: 15189

FARVAR, M. A., Choral hydrate 800 rad dosimeter, 20: 14583 (TID-21634)

FEDOROV, G. V., Hall effect in terbium and thulium, 20: 15071

FEDOROV, T. F., Phase equilibria in system molybdenum–chromium–carbon, 20: 15111

FEDOROV, T. F., X-ray structure and metallographic studies of Nb–Co–C systems, 20: 15077

FEDOROV, V. S., Kinetics of re-extraction of uranyl nitrate from alkyl-phosphate solutions in water. I., 20: 14655

FEDOTOV, D. N., Uranium in paleozoic deposits of Northern Tien Shan, 20: 14780 (AEC-tr-6579)

FEIGE, Y., Calibration of ^{60}Co source by comparison with a weak radium standard, 20: 14927

FEITELBERG, Sergei, Studies in I metabolism. IV., 20: 14250

FELBERBAUM, Joan, Description of evaluated nuclear data file service routines, 20: 15995 (BNL-966)

FELDMAN, Karl Thomas Jr., Heat-generated pressure oscillations in closed end pipe, 20: 14690 (SC-DC-66-1293)

FELLOWS, Albert T., Chemical conversion in presence of nuclear fission fragments, 20: 16053

FELLOWS, Albert T., Chemical conversion in presence of nuclear fission fragments, 20: 16055

FELLOWS, Albert T., Utilization of nuclear fission for chemical reactions, 20: 16054

FENISH, R. G., Prog. rpt. on protective coatings for refractory metals, 10/23/64–1/23/65, 20: 15004 (N65-20790)

FENRICK, Harold W., Electron spin resonance spectra of γ-irradiated polycrystalline alkyl iodides, 20: 14597

FERGASON, L. A., Energy dispersion system for light element analysis with electron microprobe, 20: 14442 (MCW-1493, pp 5–13)

FERRARI, H. M., Migration of pores in uranium dioxide, 20: 15094

FERRARI, Lawrence August, Behavior of runaway electrons in a plasma betatron, 20: 15919

FERRARO, J. R., Raman polarization studies of several nitrato complexes, 20: 14529

FERREIRA, P. Leal, Applications of Gel'fand-Moshinsky bases in unitary symmetry and its breaking, 20: 15455

FERWERDA, Hedzer A., Fronsdal's model for leptonic interactions, 20: 15360

FIBICH, Moshe, Phonon effects in superconductors, 20: 15664

FICKINGER, W. J., Production and decay of ρ^0 and ω mesons in π^+n and π^-p interactions at 1.7 Bev/c, 20: 15403

FIELD, E. C., Detection of daytime nuclear bursts below 150 km by prompt vlf phase anomalies, 20: 15602

FIELD, E. C., Equatorial transmission of geomagnetic micropulsations through the ionosphere and lower exosphere, 20: 15591 (RM-4858)

FIELD, Michael, Machining difficult materials—molybdenum alloys, 20: 15014

FIELDS, T., V-2-prong K$^-$p interactions at 5.5 Bev/c, 20: 15416

FILATOV, E. S., Mechanism of elementary hot reactions, 20: 14620

FILIPKOVSKII, A., Investigation of 9 Bev/c π^- meson interactions with xenon nuclei accompanied by Λ and K^0 particle production, 20: 15841

FILIPP, Radislav, Problems of controlling defects in materials used for first Czechoslovak nuclear-power station, 20: 14709

FILIPPOV, A. T., Calculation of radiative corrections in non-renormalizable field theory, 20: 15528

FILIPPOV, A. T., Possible mechanism of CP violation, 20: 15309 (JINR-E-2563)

FINCH, L. M., Nuclear reactor core having means for varying inclination of fuel assemblies, 20: 16015

FINGERHUT, Aaron, G., Electron beam produced lichtenberg figures, 20: 14607

FINK, R. W., Comparison of recent precision results of orbital electron capture ratios with theory, 20: 15713 (CONF-233(Vol.2), pp 365-8)

FINK, R. W., Measurement of the M/L-capture ratio in 30-million-year ^{205}Pb decay, 20: 15714 (CONF-233(Vol.2), pp 369-70)

FINKEL, V. A., Crystal structure of gadolinium at 120 to 370°K, 20: 15124

FIORONI, F., ISPRA-2 reactor control system, 20: 16126

FIORY, A. T., Observation of a "Peltier" effect in a type-II superconductor, 20: 15649

FISCHER, H., Excitation of delay-type magnets by short pulses, 20: 15157 (CERN-66-1)

FISCHER, Werner, Determination of very small hafnium contents in zirconium dioxide preparations by means of x-ray spectral analysis after enrichment by means of partition process, 20: 14496

FISCHMEISTER, H. F., Observations on milling of hard metal powders, 20: 15015

FISH, Birney R., Deposition and retention models for internal dosimetry of human respiratory tract, 20: 14796

FISHER, D. J., Analytical instrumentation, 20: 14452 (ORNL-3889, pp 1–12)

FISHER, G. P., Decay spectrum of $K^0_{\mu 3}$, 20: 15331

FISHER, J. R., Pathfinder flooding coefficient, core pressurization, and temperature coefficient tests, 20: 16059 (ACNP-65600)

FISHER, Michael E., Stability of many-particle systems, 20: 15151

FISHER, Philip C., Observations of cosmic x-rays, 20: 15220

FISK, H. E., Observations of Y^*_1(1405) and Y^*_1(1358) resonances in π-N collisions at 1.68 Bev/c, 20: 15404

FIVEL, Daniel I., Solution of scattering and bound-state problems by construction of approximate dynamical symmetries, 20: 15483

FLAMMERSFELD, A., Excited levels of ^{79}Br, 20: 15802

FLAMMERSFELD, A., Measurement of excitation cross sections for K ionization by impact of low-energy negaton and positons, 20: 15257

FLANAGAN, Charles A., Diffusion theory representation of fuel clusters containing control rods, 20: 16090 (WAPD-T-1841)

FLATAU, Bogumila, Thermalization process of neutrons from Po–Be neutron sources in a paraffin moderator, 20: 15683

FLECK, P. L., Data recording and processing for experimental large aperture seismic array, 20: 14761

FLINN, E. A., Data processing techniques for detection and interpretation of teleseismic signals, 20: 14762

FLORKOWSKI, T., Excitation of characteristic radiation in elements of $14 \leq Z \leq 50$, 20: 15258

FLUHARTY, R. G., Measurement of absolute value of eta for ^{233}U, ^{235}U and ^{239}Pu using monochromatic neutrons, 20: 15718 (IDO-17083)

FOERSTER, F., Automatic inspection of nuclear-reactor tubes during production and processing, using eddy-current methods, 20: 14720

FOERSTER, F., Measurement of physical properties of reactor components and irradiated materials, 20: 14719

FOGEL', Ya. M., Interaction of oxygen with a Nb surface, 20: 15976

FOIS, M., Acceleration of negative ions in Milan AVF cyclotron, 20: 15180

FONDANAICHE, Jean-Claude, Voltammetry of uranyl chloride in LiCl–KCl eutectic, 20: 14437 (CEA-R-2879)

FORBES, C. B., LASA sensing system design, installation, and operation, 20: 14759

FORSHUFVUD, Sten, Napoleon's illness 1816–1821 in light of activation analyses of hairs from various dates, 20: 14478

FORTSON, E. N., Ultrahigh resolution $\Delta F = 0, \pm 1$ (^{3}He)$^+$ HFS spectra by ion-storage collision technique, 20: 15260

FOSTER, M., Experimental evidence on C violation in η decay, 20: 15430

FOSTER, M., Search for the decay $\eta^0 \rightarrow \pi^0 e^+ e^-$, 20: 15427

FOU, Cheng-Ming, Reaction ^{58}Ni(^{3}He,α)^{57}Ni, 20: 15860

FOUILLOUX, Pierre, Thermal decomposition of β lead dioxides of different texture, 20: 14548

FOULKS, R., Coherence measurements with time sampling ocean-bottom seismometers, 20: 14766

FOULQUIER, H., Remote-controlled automatic welding in construction of nuclear reactor, 20: 15019

FOULQUIER, H. E., Industrial ultrasonic inspection of stainless-steel claddings for EL4 reactor, 20: 14717

FOUQUE, Daniel, Thermal decomposition of β lead dioxides of different texture, 20: 14548

FOWLER, A. H., Extension of APT to obtain centroid and inertia information, 20: 16154 (Y-1420(Rev.1))

FOWLER, E. E., New developments and trends in isotope industry, 20: 14929 (CONF-651132-1)

FOWLER, M., Electron-phonon renormalization effects in high magnetic fields, 20: 15939 (AD-620189)

FRAHM, C. P., Existence of weakly interacting charge-retention currents, 20: 15327

FRANA, J., Gamma transitions in ^{153}Eu, 20: 15734 (ZfK-PhA-18)

FRANCIS, N. C., Variational methods in the calculation of spatially dependent spectra, 20: 15666 (CONF-660204-4)

FRANCO, V., High-energy deuteron cross sections, 20: 15361

FRANKE, H., Effect of radiation in liver cells of pregnant rats and their fetuses, 20: 14294

FRANKE, H., Reaction of fine structures in fetal rat liver cell to whole-body irradiation of 400 R, 20: 14262

FRANKE, Renate, Determination of trace impurities in UO_2 fuel materials, 20: 14494

FRANKEL, R. B., Isomer-shift measurement in ^{182}W, 20: 15820

FRANKEVICH, D. P., Compounds with structures of Th_6Mn_{23} type in alloys of rare earth metals with manganese and iron, 20: 15110
FRECK, David Vernon, Improvements relating to radiation detectors, 20: 14909
FRECK, David Vernon, Improvements relating to radiation detectors, 20: 14910
FREUDENTHAL, A. M., Symposium on high temperature structures and materials, N.Y., N.Y., 1/63, 20: 15129
FREVERT, E., Effective cross section for (n,^{3}He) process on ^{55}Mn, ^{59}Co, ^{75}As, and ^{103}Rh at 14.8 Mev, 20: 15739
FREVERT, L., Excited levels of ^{79}Br, 20: 15802
FREYER, H. D., Attempts at material separation in an electrolytic countercurrent exchange process. VI., 20: 14947
FRICK II, Henry Clay, Pelvic lymph node dissection following radiotherapy for cancer of cervix: re-evaluation, 20: 14409
FRIDRICH, Raimund, Function of reticuloendothelial system after local radiation burden to liver, 20: 14374
FRIED, Burton D., Low-frequency spatial response of a collisional electron plasma, 20: 15904
FRIEDBERG, F., Radiation degradation of polyamino acids in solid state, 20: 14588
FRIEDLAENDER, E. M., Multiplicity of neutral pions produced in 9 Bev/c two-prong π^--p interactions, 20: 15384
FRIEDRICH, L. A., Diffusivity data on formation of niobium carbide surface films, 20: 14992
FRISHMAN, Yitzhak, Corollaries of the Goldstone theorem, 20: 15487
FRITZ, K. M., Determination of ^{235}U by gamma-ray spectroscopy, 20: 14449 (NLCO-970, pp 7.1–5)
FRITZ, Karl, Radial wave equations for a vector meson in a spherically symmetric potential, 20: 15447 (UCRL-14698-T)
FRONSDAL, C., Theory of representations of non-compact Lie algebras, 20: 15541
FROSCH, R. A., Principles of experimental large aperture seismic array (LASA), 20: 14758
FUBINI, S., Use of dispersion methods in study of symmetries, 20: 15549
FUERST-RAUCH, M., Reaction ^{16}O(n,α)^{13}C around 14 Mev, 20: 15738
FUJIMOTO, Takashi, Spectroscopic studies on helium plasma heated by reflected shock in T tube, 20: 15896
FUJINAGA, Taitiro, Gaschromatographic determination of scandium as acetylacetonate and trifluoroacetylacetonate, 20: 14486
FUKUDA, Kuniya, Spectroscopic studies on helium plasma heated by reflected shock in T tube, 20: 15896
FUKUSHIMA, T. Y., Prog. rpt. on Piqua power facility operations analysis, semiannual, 1–6/65, 20: 16077 (NAA-SR-11628)
FUNK, E. G., Decay of ^{153}Sm(47h) to ^{153}Eu, 20: 15795
FUNKE, L., Gamma transitions in ^{153}Eu, 20: 15734 (ZfK-PhA-18)
FURLAN, G., Evaluation of $N^{\frac{1}{2}}N$ weak coupling constants, 20: 15308
FURLAN, G., Use of dispersion methods in study of symmetries, 20: 15549
FURNICA, G., Biochemical study on radioprotection processes, 20: 14391
FURNICA, M., Biochemical study on radioprotection processes, 20: 14391
FURNICA, M., Formation of lipid peroxides in tissues of irradiated and radioprotected rats, 20: 14293
FURNICA, M., Rate of peroxidation of homogenized tissues during their irradiation in vitro, 20: 14261
FURSMAN, Oliver C., Electric-arc furnace reduction of tin slag for production of columbium–tantalum-bearing alloy, 20: 14956 (BM-RI-6734)
FURTH, H. P., Apparatus for magnetically confining a plasma, 20: 15927
FURUKAWA, Kiyoshi, Estimation of gamma-ray energy absorbed in gaseous media, 20: 14870
FUSCHINI, E., Internal Compton effect at small angles, 20: 15815

G

GADETSKII, O. G., Influence of pairing correlations on E1 transitions in deformed nuclei, 20: 15764
GADIYAR, H. S., Kinetics of uranium-dioxide sintering between 950°C and 1500°C in dry hydrogen atmosphere, 20: 15082
GAGE, Donald S., Calculation of electrical and radiation storage time in transistors, 20: 15993
GAILLARD, R., Welding tests on section taken from heavy-gage plates of rolled steel, 20: 15000 (EURAEC-1517)
GALBRAITH, W., Experimental verification of the Johnson-Treiman relationship, 20: 15428
GALBRAITH, W., Pion-nucleon resonances and their effect upon $\pi^{\pm}$p total cross sections, 20: 15379
GALL, W. R., Review of containment philosophy and design practice, 20: 16001
GALLAGHER, E. V., Prog. rpt. on reactor containment, 10–11/65, 20: 16023 (IITRI-S78P21-16)
GALLI DE PARATESI, S., ISPRA-2 reactor control system, 20: 16126
GAL'PERIN, L. N., Polarized γ radiation emitted during Coulomb excitation, 20: 15759
GAMBA, A., Jordan algebra M_3^1, 20: 15543
GAMBLIN, Rodger Lotis, Polarization and relaxation processes in ^{3}He gas, 20: 15274
GAMMEL, J. L., Application of Pade approximant to scattering theory, 20: 15363
GANGRSKII, Yu. P., Interference effects in Coulomb excitation of 2^+ levels in even-even nuclei, 20: 15768
GARDNER, Leonard B., Monte Carlo calculations of gamma-ray streaming through coplanar and noncoplanar ducts, 20: 15929 (AD-627890)
GARFINKEL, A., Results on π^--p and K^+-p interactions at high energy. A., 20: 15406
GARG, Virendra Nath, Conductometric determination of lanthanum as normal selenite, 20: 14484
GARLOCK, Edward A. Jr., Protective shelter, 20: 14723
GATELY, P., Calculation of group averaged neutron cross sections (FORTRAN for IBM-7030), 20: 15665 (AWRE-O-103/65)
GATTO, R., Kinetic supermultiplets of $\bar{U}(12)$. II., 20: 15479
GATTO, R., Relation between D/F and G_A/G_V from current algebra, 20: 15488
GATTO, R., Theoretical aspects of colliding-beam experiments, 20: 15443
GATZ, Carole R., Temperature-independent factor in isotopic rate-constant ratios, 20: 14544
GAUDIOSI, G., Dependence of transition boiling heat transfer on loop flow disturbances, 20: 14687 (GEAP-4785)
GAUNTNER, James W., Simulated nuclear heating of liquid hydrogen in propellant tank, 20: 14728 (NASA-TN-D-3328)
GAVRILYUK, V. M., Proof of existence of positive charge in adsorbed Th atoms, 20: 15985
GAY, William I., Ionizing radiation for measuring biological phenomena, 20: 14386
GAZELLE, Roland J., Radiation barrier panels, 20: 14682
GEBALLE, R., Structure in electron energy spectrum from multi-kev Ar^+–Au and Ar^+–Cu collisions, 20: 15261
GEDEONOV, L. I., Radioactivity of air over Atlantic Ocean in May to July, 1964, 20: 14743
GEIER, Gerhard, Exchange of ^{18}O between water and orthotungstate and between water and 12-tungstocobaltate(III), 20: 14525
GEIGER, J. S., Angular correlation and internal conversion studies in ^{125}I and ^{127}I, 20: 15701 (CONF-233(Vol.2), pp 128-41)
GEIGER, J. S., Atomic M-level widths in ^{151}Sm, 20: 15241 (CONF-233 (Vol.3), pp 454-64)
GEISS, J., Rare gas measurements in 30 stone meteorites, 20: 15193 (NP-15654)
GELERINTER, Edward, Electron spin resonance identification of N_3^- in irradiated sodium azide, 20: 15942 (NYO-2150-11)
GEMMELL, Gordon D., Method of treating columbium-base alloy, 20: 14972
GENCO, Joseph M., Prog. rpt. on applicability of existing data to analytical description of a nuclear-reactor accident, 10–12/65, 20: 16019 (BMI-X-10154)
GENEST, L., Response to radiotherapy of aortic-femoral prosthesis, 20: 14345
GENEST, Leopold, Effects of radiotherapy on artificial grafts of thoracic aorta, 20: 14344
GENS, T. A., Vapor pressures of gaseous products from chemical reactions of sol-gel fuels, 20: 14512 (ORNL-TM-1418)
GEORGE, T. M., Particle parameter of the $2^+ \rightarrow 0^+$ E2 transition in ^{152}Sm, 20: 15698 (CONF-233(Vol.2), pp 109-16)
GEORGESCU, Iulia I., Determination of thorium in different monazite ore samples, 20: 14491
GEORGIEVA, I. Ya., Corrosion resistance of binary niobium alloys, 20: 14997
GEORGIEVA, I. Ya., Regular changes in hardness of binary niobium alloys, 20: 15073
GERASIMOV, A. B., Low-temperature annealing of germanium, irradiated with fast electrons, 20: 15984
GERASIMOV, G. N., Radiation polymerization of vinyl chloride in solid solutions at low temperatures, 20: 14594
GERASIMOV, V. G., Eddy-current method for multi-parameter testing of structural components, 20: 14708
GERBER, J. P., Double emission of hammer tracks from heavy emulsion nuclei in high-energy interactions, 20: 15792
GERHOLM, T. R., Internal conversion, 20: 15694 (CONF-233(Vol.1), pp 1-29)
GEROCH, R. P., Electromagnetism as an aspect of geometry, 20: 15624
GERSTEIN, I. S., Vertex poles and bound states in Lee model, 20: 15469
GERSTENBERG, E., Treatment of hemangioma of skin, 20: 14418
GERSTENKORN, Simon, Hyperfine structure of low-lying levels of Tb $4f^95d6s^2$ configuration, 20: 15254
GIACCONI, R., Solar x-ray images obtained using grazing incidence optics, 20: 15203
GIAUX, G., Systematic microscopic study of effect of ionizing radiation on animal cells in culture. II., 20: 14321
GIBBERD, M. C., Atrial fibrillation in thyrotoxicosis treated with radioiodine, 20: 14424

GIBBONS, J. H., Lack of structure in ^{235}U fission cross section, 20: 15818
GIBSON, R., Permeation and diffusion of hydrogen in molybdenum, 20: 14976 (AWRE-O-16/66)
GIBSON, R., Versatile and cheap vacuum leak, 20: 14730 (AWRE-O-10/66)
GIESECKE, J., Pion-nucleon scattering at high energies, 20: 15376
GIESEKE, James A., Prog. rpt. on applicability of existing data to analytical description of a nuclear-reactor accident, 10–12/65, 20: 16019 (BMI-X-10154)
GIESSEN, Bill C., Intermediate phases in ternary system Nb(Cb)–Ni–Al at 1140°C, 20: 15121
GIGLI, A., Small-angle elastic scattering of polarized protons in photographic emulsions, 20: 15314 (RT/FI(65)35)
GIGNOUX, D., Development of charged colloid source for electrostatic propulsion, 20: 14725 (N65-15876)
GILLESPIE, John F., Comparative studies of effect of methods of sterilization on absorption of chromic catgut, 20: 14932
GILLY, L., Absolute cross sections and excitation functions for deuteron-induced reactions on chromium between 2 and 12 Mev, 20: 15808
GILMORE, R. R., High yield ^{233}U casting operations, 20: 15003 (LA-DC-7510)
GILMORE, Shirley Ann, Influence of total dose and of age on effects of proton irradiation of spinal cords of young rats, 20: 14299
GINSBERG, Edward S., Radiative corrections to K^+_{l3} decays, 20: 15349
GINSBURG, I. F., Summation of ladder graphs at high energies, 20: 15501
GINTZBURG, M. A., Origin of radiation belts, 20: 15593
GIRELLI, Alberto, Symposium on fresh water from the sea, Milan, 4/64, 20: 16157
GIROLAMI, Antonio, Studies in I metabolism. III., 20: 14249
GIUDICI, G., Effects of polymerized heterologous RNA on ascite tumors, 20: 14397
GIUDICI, G., Radioprotective effects of ribonucleic acid on normal and tumor tissues, 20: 14401
GIUPPONI, P., Ion waves in bounded plasma, 20: 15900
GLAD, Blaine W., Quantum yield studies of dye-sensitized photoinactivation of trypsin, 20: 14274
GLASER, H., Radial and axial distribution of the electron density of theta pinch as function of time, 20: 15871 (IPP-1/38)
GLASHOW, S. L., Electrodynamic mass formula in SU(3) and SU(6), 20: 15535
GLAUBER, R. J., High-energy deuteron cross sections, 20: 15361
GLAZOV, V. M., Application of several radioactive isotopes in radiochemical analysis, 20: 14488
GLICK, Arnold J., Anomalous propagation in a quantum plasma and magnon-helicon coupling, 20: 15941 (NP-15698)
GLOECKLE, Walter, Analytical properties of S matrix in many-channel scattering, 20: 15505
GLORE, J. P., Vela satellite system detector electronics, 20: 15596
GLUSHKOVA, V. B., Infrared spectra of products of Nd_2O_3 reaction with water, 20: 14568
GNATOVICH, V., Collective levels in odd-A deformed nuclei in the rare earth region, 20: 15833
GOBLE, D. F., Liquid helium and the properties of finite Bose-Einstein assemblies, 20: 15645
GODBOLD, B. C., Current practice in survey of working environments, 20: 14812
GODBOLD, B. C., Recent advances in monitoring for airborne radioactivity, 20: 14811
GODBOLD, B. C., Symposium on radiological monitoring of environment, Berkeley, Gloucestershire, 10/63, 20: 14810
GODINA, N. A., Formation of lanthanum, praseodymium and neodymium aluminates, 20: 14539
GOELER, S. V., Kelvin-Helmholtz instability in a cesium plasma, 20: 15906
GOETZE, E., Effect of radiation in liver cells of pregnant rats and their fetuses, 20: 14294
GOETZE, E., Reaction of fine structures in fetal rat liver cell to whole-body irradiation of 400 R, 20: 14262
GOLD, Albert, Multiphoton ionization of rare gas and hydrogen atoms, 20: 15276
GOLDBERG, H., Analytic continuation of an S_{11} pion-nucleon amplitude to the P_{11} amplitude, 20: 15312 (NIT-2098-86)
GOLDBLITH, S. A., Effect of irradiation temperature on radiosensitizing activity of vitamin K_5, 20: 14395
GOLDBLITH, S. A., Radiation preservation of food, 20: 14938
GOLDHABER, Gerson, Single-pion production by 1.96-Bev/c K+ mesons, 20: 15335
GOLDHABER, Sulamith, Single-pion production by 1.96-Bev/c K+ mesons, 20: 15335
GOLDRICK, W. B., Modular system of logic for the Vela satellite program, 20: 15597
GOLDSMITH, M., SHREW—FORTRAN code for computing angular distributions, polarizations and transport cross sections of neutrons scattered by spinless targets, 20: 15670 (WAPD-TM-524)
GOLINSKI, M., Solvent extraction of molybdenum and uranium from sulfate solutions with tri-n-octylamine, 20: 14653
GOLUB, A. M., Reactions of lanthanum nitrate with ammonium carbonate in solution, 20: 14535
GOLUBKOV, A. V., Transport mechanism in samarium sulfide, 20: 15981
GOMBERG, H. J., Total absorption x-ray calorimeter, 20: 14908
GOMIDE, F. M., Static cosmological model and redshift for radio galaxies, 20: 15224
GON, Eliezer, Pulsed-source measurement of neutron diffusion parameters in water, 20: 15686
GONCHAROVA, E. V., Transport mechanism in samarium sulfide, 20: 15981
GONDA, K., Acceleration of uranium(IV)–(VI) electron exchange reaction by hydrochloric acid, 20: 14570
GONDI, P., Radiation-induced noise in semiconductor counters, 20: 14923
GOOD, M., Experimental evidence on C violation in η decay, 20: 15430
GOOD, M., Search for the decay $\eta^0 \to \pi^0 e^+ e^-$, 20: 15427
GOODINGS, J. M., Mass spectrometric sampling probe for discharge plasmas, 20: 15915
GOODMAN, L. J., Development and dosimetry of "epithermal" neutron beam for possible use in neutron capture therapy. II., 20: 14421
GOODMAN, R. H., Use of on-line computer for Moessbauer experiments, 20: 15973
GORDUS, A., Total absorption x-ray calorimeter, 20: 14908
GORENFLO, Rudolf, Calculation of two-dimensional magnetic field of even number of Ioffe bars by complex analysis, 20: 15878 (IPP-6/42)
GORENFLO, Rudolf, Plane magnetohydrostatic equilibria with interior field, 20: 15877 (IPP-6/41)
GORIN, E., Process for producing tritiated organic compounds, 20: 14633
GORSKII, V. V., Flaw detection in thin-walled tubes, 20: 14713
GOSHAW, A., K+p interactions at 3.6 Bev/c, 20: 15415
GOTO, Tetsuo, Elastic sphere model of elementary particles and relation to quadri-local field model, 20: 15493
GOULD, Robert J., Opacity of universe to high-energy photons, 20: 15226
GOWEN, John W., Effects of x-irradiation upon post-natal growth in mouse, 20: 14315
GRABER, H., Gamma transitions in ^{153}Eu, 20: 15734 (ZfK-PhA-18)
GRACE, M. A., ^{54}Fe: spins and decay modes of low-lying excited states, 20: 15786
GRAD, Harold, Variational principle for a guiding-center plasma, 20: 15898
GRADZKI, F., Excitation function of $^{29}Si(n,\alpha_0)^{26}Mg$ reaction for neutron energies around 14 Mev, 20: 15800
GRAHAM, R. L., Atomic M-level widths in ^{151}Sm, 20: 15241 (CONF-233(Vol.3), pp 454-64)
GRANATKIN, B. V., Use of pulsed neutron generator to determine neutron diffusion parameters of rocks and fluids, 20: 14772
GRANJON, H., Welding tests on section taken from heavy-gage plates of rolled steel, 20: 15000 (EURAEC-1517)
GRANT, Nicholas J., Intermediate phases in ternary system Nb(Cb)–Ni–Al at 1140°C, 20: 15121
GRANT, P. J., Diffusion length of thermal neutrons in water between 18 and 255°C, 20: 15679
GRASS, F., Device for measuring continuously alpha activity of flowing solutions, 20: 14871
GRAUVOGEL, Antoine, Automatic devices—safety equipment—control room of the Latina power plant, 20: 16067 (EUR-2420.d,f,i,n,e, pp 117-31)
GRAY, Mary Jane, Pelvic lymph node dissection following radiotherapy for cancer of cervix: re-evaluation, 20: 14409
GRAY, R. J., Polarized light microscopy of pyrolytic carbon deposits, 20: 15089
GRECHUSHNIKOV, B. N., Electron paramagnetic resonance of atomic hydrogen in beryllium, 20: 15982
GREEN, J. P., Isotope tests of kidney function in pelvic and abdominal irradiation, 20: 14296
GREEN, P. E. Jr., Principles of experimental large aperture seismic array (LASA), 20: 14758
GREENBERG, J. S., Evidence for hyperon states with masses greater than 1900 Mev, 20: 15424
GREENBERG, O. W., Equivalence of locality and paralocality in free parafield theory, 20: 15468
GREENE, A. C., Thermal history of LiF single crystals during neutron irradiation, 20: 14603
GREENING, J. R., Current practice in survey of working environments, 20: 14812
GREENLEES, G. W., Elastic and inelastic scattering of 20- to 28-Mev polarized protons by carbon, 20: 15805
GREGORIO, E. G., Production of colloidal ^{198}Au, 20: 14627 (PAEC(D)IS-651)
GREGORIO, Reynaldo G., Radioisotopes in internal radiation therapy, 20: 14406

GREIFINGER, C., Equatorial transmission of geomagnetic micropulsations through the ionosphere and lower exosphere, 20: 15591 (RM-4858)
GREINER, W., Nuclear giant quadrupole resonance, 20: 15823
GRIBANOV, Yu. I., Device for x-ray structural analysis of radioactive materials, 20: 15064 (AD-625748)
GRIFFIN, D. A., Bibliography on atomic and molecular processes, 1964, 20: 15248 (ORNL-AMPIC-3)
GRIGOR'EV, E. P., Decay of ^{90}Mo, 20: 15751
GRIGOR'EV, K. A., Uranium in paleozoic deposits of Northern Tien Shan, 20: 14780 (AEC-tr-6579)
GRIGOREV, V. N., Pair-producing conversion transitions in ^{72}Ge, 20: 15834
GRIGORY, S. C., Prog. rpt. on fatigue strength of pressure vessels, 1/66, 20: 15059 (SWRI-1228-1-20)
GRODZINS, L., Isomer-shift measurement in ^{182}W, 20: 15820
GROENIER, W. S., Flooding in perforated-plate pulsed extraction columns, 20: 14462 (ORNL-3890)
GROMOV, K., Collective levels in odd-A deformed nuclei in the rare earth region, 20: 15833
GROSHEV, L. V., Gamma spectrum produced by thermal neutron capture in palladium, 20: 15755
GROSHEV, L. V., Gamma spectrum produced by thermal neutron capture in gold, 20: 15756
GROSHEV, L. V., Nuclear levels of ^{168}Er excited by the (n,γ) reaction, 20: 15757
GROSHEV, L. V., Nuclear levels of ^{166}Ho from (n,γ) reaction, 20: 15758
GROSS, Franz, Relativistic corrections to impulse approximation in elastic e-d scattering, 20: 15348
GROSSE, G., Purity and sorption tests of solutions of radionuclides, 20: 15747
GROSSO, P., Determination of trace elements in iron by neutron-activation techniques, 20: 14471
GROTENHUIS, Ivan, Blood supply to hepatic V2 carcinoma implants as measured by radioactive microspheres, 20: 14405 (COO-1305-2)
GROTZKY, V. K., Optical determination of depth of defects by replication techniques, 20: 14966 (RFP-673)
GROVE, G. R., Prog. rpt., 6/65, 20: 14444 (MLM-1268)
GROVER, George M., Evaporation-condensation heat transfer device, 20: 14699
GROVER, John Roger, New glass containing radioactive waste oxides, 20: 16141
GROVER, R., Propagation of shocks in exponentially decreasing atmospheres, 20: 15217
GRUBB, William B. Jr., Role of radiation therapy in treatment of chenodectomas of Glomus jugulare, 20: 14417
GRUBER, E. E., Theory of migration and coalescence of bubbles in solids, 20: 15132 (ANL-7079)
GRUENWALD S., Rodolfo, Uranium exploration in Chile, 20: 14779 (RME-4569(Rev.))
GRYNBERG, M., n-Pion configurational wave functions with definite symmetry, 20: 15450
GUBERMAN, Sh. A., Application of similitude theory to study of radiation transfer processes, 20: 14776
GUBERMAN, Sh. A., Nuclear geophysical methods applied to geophysical research data, 20: 14777
GUENIN, Marcel, Axiomatic foundations of quantum theories, 20: 15631
GUERRIERO, L., Charge exchange scattering near N*(1510) and N*(1690) resonances, 20: 15374
GUERSEY, F., Remarks on relativistic formulations of SU(6), 20: 15546
GUETLBAUER, F., Radiation chemical carboxylation of polychloride compounds for trichloroacetic acid, 20: 14582 (SGAE-CH-25/1965)
GUINN, V. P., Prog. rpt. on application of neutron activation of analysis in scientific crime detection, 5/62–10/63, 20: 14439 (GA-5556)
GULYAEV, A. P., Corrosion resistance of binary niobium alloys, 20: 14997
GULYAEV, A. P., Regular changes in hardness of binary niobium alloys, 20: 15073
GUNTER, K., Charge and energy distributions of recoils from ^{226}Th alpha decay, 20: 15822
GUNTHER, Wolfgang H. H., Production of ^{75}Se-selenocystine by neutron activation, 20: 14630
GUPTA, Suraj N., Meson resonances and nuclear forces, 20: 15817
GURLAND, J., Prog. rpt. on mechanical properties of metals, 2/65–1/66, 20: 15055 (NYO-2394-19)
GURZA, Tomas, Bibliography on conversion of salt and brackish waters into fresh water (1954–1964), 20: 14510 (NP-15834)
GUSEV, V. M., Silicon solar cells produced by ion bombardment, 20: 15302
GUSEVA, M. I., Silicon solar cells produced by ion bombardment, 20: 15302
GUSINSKII, G. M., Polarized γ radiation emitted during Coulomb excitation, 20: 15759
GUSMANO, Ernest A., Decrement in radiostrontium retention following stable strontium prefeeding in growing rat, 20: 14251
GUYTON, Arthur C., Prog. rpt. on cardiac damage, final, 1965, 20: 14292 (TID-22563)
GVOZDEV, B. A., Extraction of curium and fermium with thenoyltrifluoroacetone, 20: 14654
GVOZDEV, B. A., Preparation of ^{242}Pu and ^{242}Cm from neutron-irradiated ^{241}Am, 20: 14631
GVOZDEV, V. S., Pair-producing conversion transitions in ^{72}Ge, 20: 15834
GYGAX, Susa, Critical field of superconducting indium–lead alloys, 20: 15105

H

HAENDEL, S. K., Correlated electrical and x-ray measurements in flash x-ray discharges, 20: 15573
HAENSGEN, H., Neutron polarization in reaction D(d,n)^{3}He at low deuteron energies, 20: 15735 (ANL-Trans-265)
HAGEN, Ulrich, Radiosensitivity of DNA. III., 20: 14283
HAHN, George M., Serum concentration: effects on cycle and x-ray sensitivity of mammalian cells, 20: 14400
HAISSINSKY, Moise, Gamma radiolysis of alkaline and neutral solutions. I., 20: 14600
HAISSINSKY, Moise, Gamma radiolysis of alkaline and neutral solutions. II., 20: 14601
HAKE, G., NPD reactor operating experience, 20: 16097
HAKKILA, E. A., Determination of nitride nitrogen in plutonium metal, alloys, and compounds, 20: 14440 (LA-3452)
HALDEN, F. A., Prog. rpt. on growth of carbide crystals, 9–12/64, 20: 15047 (N65-15919)
HALLOWES, K. H., Alpha particle hygrometer, 20: 14840
HALPRIN, Arthur, Production processes in nuclear Coulomb field, 20: 15562
HAMILTON, J. H., Application to lens-type spectrometer of internal-external conversion IEC method for determination of internal conversion coefficients, 20: 15710 (CONF-233(Vol.2), pp 252-5)
HAMILTON, J. H., E2 conversion coefficients in ^{110}Cd and ^{132}Xe, 20: 15704 (CONF-233(Vol.2), pp 164-76)
HAMILTON, J. H., E2 conversion coefficients in ^{152}Sm, ^{154}Gd and ^{160}Dy, 20: 15705 (CONF-233(Vol.2), pp 177-90)
HAMILTON, J. H., Particle parameter of the $2^+ \rightarrow 0^+$ E2 transition in ^{152}Sm, 20: 15698 (CONF-233(Vol.2), pp 109-16)
HAMILTON, J. H., Particle parameter of the $2^+ \rightarrow 0^+$ E2 transition in ^{170}Yb, 20: 15700 (CONF-233(Vol.2), pp 120-7)
HAMMER, D. C., Viscosity coefficients and the phonon density temperature dependence in liquid ^{4}He, 20: 15646
HANKE, G., Angular distribution of protons of reaction ^{11}B(d,p$_{0,1}$)^{12}B at 0.7 to 1.7 Mev, 20: 15847
HANLON, J. E., Dislocation-relaxation internal-friction peak in columbium and Cb–5% Zr, 20: 15122
HANNA, R. C., Prog. rpt., annual, PLA division, 1965, 20: 15164 (RHEL/R-112)
HANRAHAN, Leo R., Reversible interreferenced power supply for double focusing mass spectrometers, 20: 14830
HANSEN, H., Measurement of excitation cross sections for K ionization by impact of low-energy negaton and positons, 20: 15257
HANSON, L. A., Reaction of uranium carbide with nitrogen, 20: 14994
HARA, Y., Nonleptonic decays of hyperons, 20: 15369
HARACZ, Richard D., Meson resonances and nuclear forces, 20: 15817
HARARI, H., Reduction of direct products of irreducible representations of SU(n), 20: 15458
HARARI, H., Review of experimental tests of SU(3) in scattering reactions, 20: 15532
HARBER, Leonard C., Photobiology of Lupus erythematosus, 20: 14309
HARBUR, D. R., High yield ^{233}U casting operations, 20: 15003 (LA-DC-7510)
HARCHOL, M., Excitation of isobaric analog states by (p,n) reactions, 20: 15804
HARDIE, D., Hydrogen embrittlement of zirconium in slow-bend tests, 20: 14993
HARDIE, R. W., Neutronic considerations in selection of driver fuel for FTR, 20: 16121 (BNWL-197)
HARDISON, H. V., Portable beta-gamma hand and shoe monitor, 20: 14866
HARDY, Alva C., Model solar proton environments for manned spacecraft design, 20: 15191 (N65-20996)
HARDY, Gy., Investigations in field of radiation-induced solid state polymerization, 20: 14586
HARDY, J. W., Propagation of shocks in exponentially decreasing atmospheres, 20: 15217
HARDY, Walter N., Nuclear spin relaxation in gaseous H_2 at low densities, 20: 15574
HARGRACES, R., High-energy photoproduction of nucleon and pionic resonances, 20: 15425
HARM, Walter, Host-cell reactivation of non-lethal ultraviolet effects, 20: 14357

HARM, Walter, Suppression of phage T4 by coinfection with uv-inactivated homologous phage, 20: 14271
HARMISON, Lowell T., Derivative neutron activation analysis, 20: 14502
HARMON, T. G., Optical and electron microscopy, 20: 14460 (ORNL-3889, pp 46–8)
HARMSEN, D. M., Double emission of hammer tracks from heavy emulsion nuclei in high-energy interactions, 20: 15792
HARRIS, Everett L. Jr., Three-phase, 1.5-Mw, electronic line regulator for Berkeley 88-inch cyclotron, 20: 15183
HARRIS, Payne S., Radiation dosimeter system using cadmium-backed copper foil, 20: 14915
HARRISON, E. R., Equation of state of matter at supernuclear density, 20: 15212
HART, E. L., Search for decay $\eta \rightarrow \pi^0 + e^+ + e^-$, 20: 15333
HART, G. E., Improved electrodeless toroidal conductivity analyzer, 20: 14465 (RFP–657)
HART, G. E., Thin film evaporation rate monitor, 20: 14819 (RFP-602)
HART, R. K., Growth and annealing of evaporated aluminum–silicon films, 20: 15030 (ANL-7102)
HART, Raymond K., Corrections for x-ray intensity data obtained from electron microprobes, 20: 14431 (ANL-7078)
HARTECK, P., Spectroscopic study of alpha-ray-induced luminescence in gases. I., 20: 14617
HASHIZUME, Tadashi, Estimation of genetically significant dose due to therapeutic radiation in Japan, 20: 14799
HASIMOTO, H., Hall effect in two-dimensional flow along an insulating plane, 20: 15568 (AD-620324)
HASSAN, M. Y. M., Equilibrium deformations of the odd-mass nuclei in rare-earth region, 20: 15788
HASSELBERG, G., Observations on vacuum polarization in external fields, 20: 15639
HASSELGREN, A., Anticoincidence spectrometers for nuclear reaction studies, 20: 14865
HATANO, Akira, Electron interaction and positron annihilation in electron gases, 20: 15383
HATCH, L. P., Fluidized bed reprocessing of graphite matrix nuclear fuel, 20: 14647
HATCH, Theodore F., Deposition and retention models for internal dosimetry of human respiratory tract, 20: 14796
HATEGAN, C., Polarization of protons from elastic and inelastic scattering on ^{24}Mg, 20: 15806
HATTA, Yoshisuke, External excitation of standing waves in r-f discharge, 20: 15912
HAUCK, H.-J., Study on the high-temperature embrittlement of austenitic chromium–nickel steel and nickel alloys by neutron irradiation, 20: 15141
HAUG, A., Influence of pH and oxygen on 315 μ inactivation and thymine dimerization in mutants of bacteriophage T4, 20: 14356
HAUSNER, Henry H., Beryllium, its metallurgy and properties, 20: 15125
HAUTH, J. J., Fuel element for a nuclear reactor, 20: 16057
HAWKINS, Donald Thomson, Vapor pressure of Pb and activity measurements on liquid Pb–Sn alloys, 20: 15062 (UCRL-16514)
HAYASHI, Chushiro, Advanced phases of evolution of population II stars, 20: 15227
HAYBRON, R. M., Inelastic scattering of high-energy protons in collective theory of excitations, 20: 15797
HAYDEN, G. A., Radiation degradation of polyamino acids in solid state, 20: 14588
HAYES, W., Localized vibrations of H^- and D^- ions in alkaline earth fluorides, 20: 15969
HEARD, K. S., Differential cross sections and polarization effects in pion-proton elastic scattering at 875 to 1579 Mev/c, 20: 15372
HEATON, Leroy, Atomic structure and correlation in liquid binaries by x-ray and neutron diffraction with application to NaK, 20: 15080
HEGEDUES, E., Uniformization of the scaler self-energy diagram, 20: 15495
HEICHE, Gerhard, Anomalous propagation in a quantum plasma and magnon-helicon coupling, 20: 15941 (NP-15698)
HEINEMANN, K., Angular distribution of 440-kev γ rays from reaction $^{23}Na(p,p'\gamma)^{23}Na$, 20: 15846
HEKHUIS, G. L., Radiobiological aspects of supersonic transport, 20: 14797
HELLWEGE, K. H., Absorption spectrum of Ce^{3+}-ions and crystal field in La(Ce)Cl, 20: 14553
HELMHOLZ, A. C., Charge and energy distributions of recoils from ^{226}Th alpha decay, 20: 15822
HENDRICKS, T. J., K-p interactions at 3.8 Bev/c, 20: 15418
HENDRY, Archibald W., Introduction to the higher symmetries, 20: 15445 (RHEL/R-102)
HENKE, H., Influence of 5-hydroxytryptamine (serotonin) on radioinduced mutation rate in Drosophila melanogaster, 20: 14398
HENKEL, D., Prog. rpt. on critical heat flux in boiling water, 4–6/65, 20: 14686 (EURAEC-1448)
HENNELLY, Edward J., Radioisotope production capabilities of U. S. power reactors, 20: 14946 (DP-1015)
HENNICO, Alphonse, Longitudinal dispersion in single-phase liquid flow through ordered and random packings, 20: 14691 (UCRL-10696(Rev.) (Pt.2))
HENNIG, Robert J., Nuclear reactor control system, 20: 16018
HENNINGER, E. H., Atomic structure and correlation in liquid binaries by x-ray and neutron diffraction with application to NaK, 20: 15080
HENRY, L. L., Classical treatment of dispersion forces, 20: 15152
HENYEY, Louis, Studies in stellar evolution. III., 20: 15196
HENZEL, H., Application of tracer systems to localize failed fuel elements, 20: 14848 (BMwF-FBK-65-02)
HERBERT, R., Use of ^{99m}Tc as clinical tracer element, 20: 14423
HERBIN, Y., Systematic microscopic study of effect of ionizing radiation on animal cells in culture. II., 20: 14321
HERENGUEL, J., Gaines fabrication plant for nuclear fuel at Trefimetaux, 20: 15018
HERMANN, R., Properties of representations of non-compact groups, 20: 15542
HERMANN, Robert, Lie groups for physicists, 20: 14955
HERMANS, L. J. F., Polarizability of hydrogen-isotopes and of ortho and para hydrogen, 20: 15262
HERMANSDORFER, H., Time resolved profile measurements of impurity lines in theta pinch discharge, 20: 15872 (IPP-1/41)
HERNQUIST, R. A., Computer program for performing reliability analyses, 20: 14824 (SC-TM-65-523)
HERRLANDER, C. J., Anomalous L-subshell conversion of some hindered E1 transitions in the rare earth region, 20: 15703 (CONF-233(Vol.2), pp 148-57)
HERRMANN, Guenter, Rapid extraction by quasi-solid extraction agent, 20: 14656
HESKETH, R. V., Vacancy clusters and loops in ion-bombarded copper, 20: 15146
HESS, W. N., Solar cycle effects on inner-zone protons, 20: 15590 (NASA-TN-D-3086)
HESSON, G. M., Maximum nuclear tube powers based on boiling burnout, 20: 16120 (BNWL-176)
HEUER, P. M., Stored energy in neutron-irradiated beryllium oxide, 20: 15142
HEWITT, David, Childhood cancer in twins, 20: 14319
HEWSON-BROWNE, R. C., Magnetohydrostatic cavity formed around a system of line currents in an infinitely conducting atmosphere, 20: 15587 (AD-620244)
HICKMAN, Bernard T., Advanced cancer of bladder: management with irradiation, 20: 14414
HIEBERT, Richard D., Radiation dosimeter system using cadmium-backed copper foil, 20: 14915
HIGASHI, Shigeru, Cosmic ray intensities under sea-water at depths down to 1,500 meters, 20: 15289
HILBERT, J. W., Response of p-i-n junctions to beta rays. II., 20: 14886
HILGERTOVA, Jirina, Activity of pyridine nucleotidase in whole-body x-irradiated rats, 20: 14362
HILL, C. W., Data compilation and evaluation of space shielding problems, 20: 15930 (NP-15697(Vol.2))
HILL, D. G., Observations of $Y_1^*(1405)$ and $Y_1^*(1358)$ resonances in π-N collisions at 1.68 Bev/c, 20: 15404
HILL, D. G., Production and decay of ρ^0 and ω mesons in π^+n and π^-p interactions at 1.7 Bev/c, 20: 15403
HILTON, P. J., Atrial fibrillation in thyrotoxicosis treated with radio-iodine, 20: 14424
HIRAKIS, E. C., Diffusivity data on formation of niobium carbide surface films, 20: 14992
HIRO, Sanju, 30-Mev flux-forced field-biased betatron, 20: 15181
HIROWATARI, Tomoyuki, γ shielding property, strength and workmanship of built-up type lead slab structure, 20: 15932 (ORNL-tr-843)
HIRSCHMAN, Albert, Prog. rpt. on effects of radiation on cartilage and bone, annual, 12/63–12/64, 20: 14291 (TID-22494)
HISANO, Kumao, Far-infrared vibration mode in $SrCl_2$, 20: 15958
HITCHCOCK, J. M., Method and apparatus for controlling reactivity, 20: 16016
HJAERNE, L., Method for predicting penetration and slowing down of neutrons in reactor shields, 20: 15935
HODGSON, A. E. M., Alpha particle hygrometer, 20: 14840
HOEHLER, G., Experimental techniques, 20: 14841
HOEHLER, G., Pion-nucleon scattering at high energies, 20: 15376
HOEHLER, G., Recent high-energy electron investigations at Stanford Univ., 20: 15439
HOEHLER, G., Review of nucleon form factors, 20: 15440
HOEHLER, G., Special models and predictions for pion photoproduction (low energies), 20: 15441
HOEHLER, G., Special models and predictions for photoproduction above 1 Bev, 20: 15442
HOEHLER, G., Strong interactions of elementary particles in Bev region, 20: 15438

HOEHLER, G., Symposium on electron and photon interactions at high energies, Hamburg, 6/65. I., 20: 15437
HOEHLER, G., Theoretical aspects of colliding-beam experiments, 20: 15443
HOEHLER, G., Use of bubble chambers and spark chambers at electron accelerators, 20: 15187
HOENIG, Arnost, Computation of thickness of steel shielding walls against γ radiation, 20: 15933 (ORNL-tr-1060)
HOERL, Erwin M., Possibility of application of scattering of γ quanta to determination of phonon properties, 20: 15948
HOERLIN, H., Los Alamos air fluorescence detection system, 20: 15609
HOFER, Kurt, Variations of resistance against α radiations with time of day, 20: 14361
HOFFMAN, D. C., Radiochemical and nuclear studies of short-lived fission products ^{145}Ce, ^{146}Ce, and ^{147}Ce, 20: 15722 (KR-76)
HOFFMANN, Marga, Recrystallization of Cb_3Sn, 20: 15113
HOFMAN, Walter, Neutron diffuser, 20: 15687
HOFSTADTER, R., Proton form factors from elastic electron-proton scattering, 20: 15337
HOGAN, M. A., Gamma-ray energy pseudospectra for ^{235}U fission products and for various times after fission, 20: 14733 (AD-628982)
HOH, F. C., Stability of sheet pinch, 20: 15903
HOKI, Shiro, Diffusion length of thermal neutrons in terphenyl (Santowax-R) at temperatures up to 400°C, 20: 15680
HOLLADAY, W. G., Poles and resonances in process $\pi^+ + p \rightarrow \Sigma^+ + K^+$, 20: 15400
HOLLAND, J. W., Thermionic reactor reliability, 20: 15292 (AD-620511)
HOLLAND, W., Prog. rpt. on thermionic materials for space power applications, 10/63, 20: 14959 (N65-20797)
HOLLANDSWORTH, C. E., Elastic and inelastic neutron scattering by silicon and sulfur, 20: 15811
HOLMBERG, L., K-conversion process of the 412-kev E2 transition in ^{198}Hg, 20: 15708 (CONF-233(Vol.2), pp 213-19)
HOLSOPPLE, H. L., Organic preparations, 20: 14576 (ORNL-3889, pp 73-7)
HOLSTEN, Richard David, Organization and metabolism in cultured plant cells, 20: 14383
HOLT, Ben D., Glovebox amalgamation for determination of oxygen in alkali metals, 20: 14432 (ANL-7123)
HOLT, J. Garrett, Energy dependence of lithium fluoride dosimeters and high electron energies, 20: 14887
HOMES, A., Prog. rpt. on direct biological monitoring, 1963–1964, 20: 14784 (AERE-R-5015)
HOMMA, H., Subcritical, critical, and burst facilities in fast reactor physics research, 20: 16123 (KFK-350)
HONECK, Henry C., Description of evaluated nuclear data file service routines, 20: 15995 (BNL-966)
HONSTEAD, J. F., Environmental monitoring, 20: 14786 (BNWL-SA-465)
HOOD, Ramon, Radioisotope production capabilities of U. S. power reactors, 20: 14946 (DP-1015)
HOOPER, H. O., A nuclear magnetic resonance study of decomposition in neutron-irradiated LiF, 20: 14602
HOOPER, H. O., Thermal history of LiF single crystals during neutron irradiation, 20: 14603
HOOPER, J. W., Bibliography on atomic and molecular processes, 1964, 20: 15248 (ORNL-AMPIC-3)
HOPE, C. S., Metabolic theory of cell survival curves, 20: 14359
HOPKINS, H. W. K., Observations of Y$_1^*$(1405) and Y$_1^*$(1358) resonances in π-N collisions at 1.68 Bev/c, 20: 15404
HOPKINS, H. W. K., Production and decay of ρ^0 and ω mesons in π^+n and π^-p interactions at 1.7 Bev/c, 20: 15403
HORNBACK, C. E., Techniques for detection of high-altitude nuclear explosions, 20: 15612
HORNER, M. H., Prog. rpt. on thermionic materials for space power applications, 10/63, 20: 14959 (N65-20797)
HORNER, M. H., Prog. rpt. on thermionic materials for space power applications, 9/63, 20: 14960 (N65-20798)
HORNER, M. H., Prog. rpt. on cathodes for thermionic reactors, 4/63, 20: 15046 (N65-15820)
HORNER, P., Size effect of radiation-induced dimensional changes of graphite, 20: 15143
HORVAT, D., Limitations of ^{192}Ir as radiographic source for control of reactor pressure-vessels, 20: 14705
HOSHI, Reiun, Advanced phases of evolution of population II stars, 20: 15227
HOUGH, Paul V. C., Structure of Brookhaven FSD system for analysis of bubble chamber film, 20: 14850 (BNL-9763)
HOWARD, John Albon, Improvements relating to nuclear reactor fuelling arrangements, 20: 16003
HOWELL, W. D., Automatic sample changing systems utilizing AECL-2041 digital read-out system, 20: 14846 (AECL-2517)
HOWL, D. A., Thermal conductivity of springfields adjusted uranium in temperature range 160–620°C, 20: 15084
HRADECONA, Zdenka, X-ray inactivation of lambda phages. I, II, 20: 14260 (NP-15856)
HROVAT, M., Diffusion of uranium in graphite, 20: 15087
HRYNKIEWICZ, A. Z., Octupole Coulomb excitation of ^{208}Pb, 20: 15719 (INP-431/PL)
HRYNKIEWICZ, A. Z., Quadrupole splitting of 14.4-kev γ line of ^{57}Fe in Fe sulfates, 20: 15775
HSU, Loke Soo, Microscopic models for vibrational states in nuclei, 20: 15851
HU, Ning, Dispersion-relation treatment of low-energy pion-nucleon scattering, 20: 15385
HUDSON, R. G., Prog. rpt. on thermionic materials for space power applications, 10/63, 20: 14959 (N65-20797)
HUDSON, R. G., Prog. rpt. on thermionic materials for space power applications, 9/63, 20: 14960 (N65-20798)
HUDSON, R. G., Prog. rpt. on cathodes for thermionic reactors, 4/63, 20: 15046 (N65-15820)
HUFFENUS, J. P., Means of approaching natural convection effects in a homogeneous reactor, 20: 15996
HUFNAGEL, Charles A., Comparative studies of effect of methods of sterilization on absorption of chromic catgut, 20: 14932
HUGHES, E. B., Proton form factors from elastic electron-proton scattering, 20: 15337
HUGHES, V. W., Evidence for hyperon states with masses greater than 1900 Mev, 20: 15424
HULTBERG, S., Application to lens-type spectrometer of internal-external conversion IEC method for determination of internal conversion coefficients, 20: 15710 (CONF-233(Vol.2), pp 252-5)
HULTBERG, Soelve, Anomalies of E2 conversion coefficients in the deformed-nucleus region, 20: 15745
HULTBERG, Soelve, Photoelectron scattering and consequences for determination of internal conversion coefficients by the IEC method, 20: 15709 (CONF-233(Vol.2), pp 247-51)
HULTZSCH, H., Gamma spectrum of ^{214}Po(RaC'), 20: 15844
HUMPHREY, H. W., Determination of ^{235}U by gamma-ray spectroscopy, 20: 14449 (NLCO-970, pp 7.1-5)
HUMPHREY, H. W., Determination of beta activities in plant effluents, 20: 14450 (NLCO-970, pp 8.1–4)
HUNGATE, F. P., Symposium on radiation and terrestrial ecosystems, 20: 14237
HUNT, Vilma R., Distribution of ^{210}Po in pulmonary tissues of cigarette smokers, 20: 14798
HUNTER, Willard L., Electric-arc furnace reduction of tin slag for production of columbium–tantalum-bearing alloy, 20: 14956 (BM-RI-6734)
HUNTLEY, Sidney C., Simulated nuclear heating of liquid hydrogen in propellant tank, 20: 14728 (NASA-TN-D-3328)
HUNZIKER, W., Space-time behavior of Schroedinger wave functions, 20: 15632
HURDLOW, W. R., Numerical simulation of seismic disturbances, 20: 14755 (UCRL-7929)
HURE, Jacques, Ion exchange methods of separating zirconium and hafnium, 20: 14657
HUSSAIN, F., pp-Annihilations into two mesons within broken inhomogeneous Ū(12) symmetry scheme, 20: 15346
HYMAN, L., V-2-prong K⁻p interactions at 5.5 Bev/c, 20: 15416
HYNST, A., Determination of hydrogen in hydrocarbons by neutron activation, 20: 14480
HYODO, Yasuko, Inhibitory effect of x-irradiation on development of ovaries of fish, Oryzias latipes, in sexually inactive seasons, 20: 14307

I

IBEN, Icko Jr., Stellar evolution. II., 20: 15207
ICHIKAWA, Y. H., Thermodynamic properties of an electron plasma, 20: 15869 (AD-628317)
ICHTCHENKO, Georges, Electronic radiation of a plasma in a magnetic field, 20: 15870 (CEA-R-2881)
IDA, Masakuni, Properties of noncomposite particles, 20: 15491
IDEHARA, Toshitaka, Microwave radiation from a bounded plasma, 20: 15893
IJAZ, M. A., Exchange mechanism in p-p interactions at 2.80 Bev/c, 20: 15423
IKEDA, Hiroshi, 30-Mev flux-forced field-biased betatron, 20: 15181
IKEGAMI, Akira, Tritium-hydrogen exchange of poly-l-glutamic acid in aqueous solutions, 20: 14628
ILIESCU, E., Polarization of protons from elastic and inelastic scattering on ^{24}Mg, 20: 15806
ILIFFE, C. E., Economics of alternative nuclear power programs based on gas-cooled graphite and fast reactors, 20: 16087 (TRG-Report-1115)
INGALL, David, Evaluation for genetic damage in offspring of women with high-level gonadal irradiation, 20: 14348
INGLEY, J., Neutron-neutron interaction in triton-triton reaction, 20: 15733 (UCRL-7769)
INGOLD, J. H., A fresh look at the Child-Langmuir problem, 20: 15295

(CONF-640921, pp 47-77)
INNIGER, H., Non-destructive testing of plutonium-enriched fuel rods, 20: 14707
INOMATA, Akira, Geometrical and gauge theoretical investigations on elementary particle interactions, 20: 15561
INUISHI, Yoshio, Radiation damage of carrier life time in p type Si, 20: 14922
IOSIFESCU, M., Reduced widths for nucleon emission in shell-model intermediate coupling, 20: 15830
IRANZO, Emilio, Radioactive waste: general characteristics, 20: 16136
ISAACSON, R. E., Administering criticality control in Hanford Atomic Products Operation non-reactor environment, 20: 14790 (RL-SA-43A)
ISAKOV, V. I., Influence of second-order effects on the angular correlations of Coulomb-excited nuclei, 20: 15767
ISAKOV, V. I., Interference effects in Coulomb excitation of 2^+ levels in even-even nuclei, 20: 15768
ISHCHUK, V. A., Characteristics of interaction of oxygen with surface of a tungsten single crystal, 20: 15986
ISHIDA, Ryoei, Spectrophotometric determination of thorium(IV) with chromazurols, 20: 14485
ISHIDA, Ryohei, Plasma jet applied spectroscopic source for alkali earth analysis, 20: 14492
ISHIDA, Shin, Magnetic moments of baryons and fundamental triplet, 20: 15492
ISHIGURE, Kenkichi, Radiation-induced copolymerization of tetrafluoroethylene with isobutylene. I., 20: 14608
ISHIHARA, Toyohide, Centralized field radiological monitoring system at nuclear installation, 20: 14855 (JAERI-1090)
ISHII, Keishi, Spectroscopic studies on helium plasma heated by reflected shock in T tube, 20: 15896
ISHIKAWA, Michio, Feasibility calculation for JPDR-II core design; one-dimensional nuclear thermal and hydraulic calculation, 20: 16076 (JAERI-1088)
ISLAM, M. M., Energy levels of ^{90}Y, 20: 15799
ITO, Takuji, Ion adsorptive properties of insoluble tetra-, penta-, hexavalent metal hydrous oxides, 20: 14651
ITOH, N., Photochemistry of V centers in alkali halides x-rayed near 200°K, 20: 14604
IVANCHENKO, I. M., Phase-shift analysis of elastic πN scattering at 240 Mev, 20: 15388
IVANOV, V. A., Nuclear levels of ^{168}Er excited by the (n,γ) reaction, 20: 15757
IVANOV, V. D., Content of submicroscopic aerosols of short-lived daughter products of radon in mine air, 20: 14747
IVANOVSKAYA, I. A., Investigation of 9 Bev/c π^- meson interactions with xenon nuclei accompanied by Λ and K^0 particle production, 20: 15841
IVANOVSKII, M. N., Impurities in Cs in thermionic converters, 20: 15298 (FEI-22)
IWASHITA, Takeki, Decay of ^{159}Eu, 20: 15782
IZVEKOVA, M. L., Nuclear geophysical methods applied to geophysical research data, 20: 14777

J

JACKLIN, S. W., Egg mortality after gamma irradiation of adults of omnivorous leaf roller, 20: 14340
JACKSON, J. D., Summary of session of production mechanisms, 20: 15510
JACOBS, H., Detection of incorporated plutonium, 20: 14239 (JUL-312-ST)
JACQUES, Gabriel L., Longitudinal dispersion in single-phase liquid flow through ordered and random packings, 20: 14691 (UCRL-10696(Rev.) (Pt.2))
JAECH, J. L., Prog. rpt. on accurate nuclear fuel burnup analyses, 6–8/65, 20: 15717 (GEAP-4950)
JAECH, J. L., Prog. rpt. on specific Zr alloy design program, 1/66, 20: 14980 (GEAP-5065)
JAFFE, A. A., Excitation of isobaric analog states by (p,n) reactions, 20: 15804
JAIMES, Salvador, Host response to eggs of schistosoma mansoni. IV., 20: 14304
JAIN, Ashok, Energy levels in Thomas-Fermi dirac atom, 20: 15267
JAIN, Kamal C., Self-sustained hydrodynamic oscillations in natural-circulation two-phase-flow boiling loop, 20: 14684 (ANL-7073)
JAKSIC, B., Differential properties of Feynman amplitudes, 20: 15525
JAMES, Frederick E., Interactions of π^+ mesons with protons at 2.08 Bev/c, 20: 15334
JAMESON, Robert T., Machining difficult materials—molybdenum alloys, 20: 15014
JANA, Manas K., X-ray induced female sterility in Phaseolus mungo, 20: 14347
JANKOWSKA, Helena, Studies of adsorption of I on activated C. II., 20: 15065 (ORNL-tr-1018)
JANKOWSKI, F. J., Effect of low-intensity radiation on man, 20: 14352
JANKOWSKI, S., Cis-trans isomerization in solid matrices by γ irradiation, 20: 14596
JANNEY, Gareth Maynard, Visible spectra of two stable isotopic species of yttrium monochloride, 20: 14569
JANNUSSIS, A., Relativistic motion of an electron in external homogeneous magnetic fields, 20: 15640
JANOWITZ, G. S., Hall effect in two-dimensional flow along an insulating plane, 20: 15568 (AD-620324)
JANSEN, J., Low-voltage radiography in detecting flaws in thin-walled sintered aluminum powder (SAP) tubes, 20: 14706
JANSEN, J. F. W., E2 conversion coefficients in ^{152}Sm, ^{154}Gd and ^{160}Dy, 20: 15705 (CONF-233(Vol.2), pp 177-90)
JANSSENS, T., Proton form factors from elastic electron-proton scattering, 20: 15337
JASKOLA, M., Excitation function of $^{29}Si(n,\alpha_0)^{26}Mg$ reaction for neutron energies around 14 Mev, 20: 15800
JAWOROWSKI, Zbigniew, Radiation dose from radium D to human bones, 20: 14353
JAWOROWSKI, Zbigniew, Scintillation cell for determination of ^{222}Rn, 20: 14881
JEAN, A. G., Techniques for detection of high-altitude nuclear explosions, 20: 15612
JEFFERSON, S., Commissioning gamma radiation processing plant, 20: 14944
JEFFRIES, C. D., Sizable proton polarization using a spin refrigerator, 20: 15964
JENA, P. K., Kinetics of uranium-dioxide sintering between 950°C and 1500°C in dry hydrogen atmosphere, 20: 15082
JENGO, R., Evaluation of $N_{\frac{1}{2},N}$ weak coupling constants, 20: 15308
JENKINS, E. W., Experimental verification of the Johnson-Treiman relationship, 20: 15428
JENKINS, O. G., Prog. rpt. on Piqua power facility operations analysis, semiannual, 1–6/65, 20: 16077 (NAA-SR-11628)
JESTER, A., Influence of CsF on emitter work function and the performance of Cs diodes, 20: 15297 (CONF-640921, pp 101-9)
JIRACEK, V., Influence of x-radiation, on urinary excretion of inorganic phosphates and ammonia, 20: 14270
JOHLER, J. R., Propagation of ground wave electromagnetic signal, with particular reference to pulse of nuclear origin, 20: 15606
JOHNSON, A. J., Impurity analysis of plutonium peroxide and plutonium fluoride, 20: 14464 (RFP–599)
JOHNSON, C. M., Improved electrodeless toroidal conductivity analyzer, 20: 14465 (RFP–657)
JOHNSON, Hugh M., Observations of cosmic x-rays, 20: 15220
JOHNSON, P. B., Angular correlation study of reaction $\pi^- p \to \pi^- \pi^+ p \pi^-$ at 2.7 Bev/c, 20: 15410
JOHNSON, Richard, Fluidized bed reprocessing of graphite matrix nuclear fuel, 20: 14647
JOHNSON, Robert Lewis, Transport effects in the neutron wave experiment, 20: 15685
JOLLEY, W. G., Conference on applications of x-ray diffraction in the atomic energy field, Richland, Wash., 2/65, 20: 15943 (RL-REA-2595)
JOLLEY, W. G., Determination of residual stress in uranium with an x-ray diffractometer, 20: 15945 (RL-REA-2595, pp 43-60)
JOLLY, Rajinder Kumar, Elastic and inelastic scattering of 15-Mev deuterons from nuclei, 20: 15850
JONES, Alan David, New glass containing radioactive waste oxides, 20: 16141
JONES, D. C., Persistent metabolic effect of x-rays or neutrons, 20: 14368
JONES, D. P., Differential cross sections and polarization effects in pion-proton elastic scattering at 875 to 1579 Mev/c, 20: 15372
JONES, G. D., Localized vibrations of H^- and D^- ions in alkaline earth fluorides, 20: 15969
JONES, J. K., Current practice in survey of working environments, 20: 14812
JONES, J. K., Recent advances in monitoring for airborne radioactivity, 20: 14811
JONES, J. K., Symposium on radiological monitoring of environment, Berkeley, Gloucestershire, 10/63, 20: 14810
JONES, J. L., Structure shielding from simulated fallout gamma radiation, 20: 15931 (TO-B-65-27)
JONES, L. V., Prog. rpt., 6/65, 20: 14444 (MLM-1268)
JONES, L. V., Radioactive radiation emitting sources, 20: 14634
JONES, P. M. S., Permeation and diffusion of hydrogen in molybdenum, 20: 14976 (AWRE-O-16/66)
JONES, P. M. S., Versatile and cheap vacuum leak, 20: 14730 (AWRE-O-10/66)
JONES, Sam T., Radiation-induced mutations in southern peas, 20: 14341
JORDAN, E. D., Effect of mechanically induced vibrations on heat transfer rates in pressurized water system, 20: 16000 (NYO-2655-1)
JORDAN, E. D., Feasibility of short-lived radioisotope tracer system for detection of hidden materials, 20: 14451 (NYO-2586–2)
JORDAN, Willard C., Observations of cosmic x-rays, 20: 15220
JOSEPH, D. W., Possible alternative to SU(6), 20: 15508

JOSET, F., Modification of conjugation in Escherichia coli K-12 by ultraviolet irradiation, 20: 14329
JOSHI, M. C., K-shell conversion coefficients for pure E2 transitions in deformed nuclei, 20: 15706 (CONF-233(Vol.2), pp 191-7)
JOUSSET, J. C., Annealing of uranium quenched from 100 to 4.2°K, 20: 15066
JOYEUX, J., Preparation by levitation melting in argon of homogeneous aluminum alloys for neutron measurements, 20: 15013
JUDD, B. R., Hyperfine structure of Eu I, 20: 15263
JUNGK, G., Photoconductivity and p-n photoeffect in SiC during excitation with x radiation, 20: 15967

K

KABISHCHER, E. I., Influence of atmospheric precipitation on fallout of radioactive substances from atmosphere, 20: 14746
KACHIKIN, V. I., Content of submicroscopic aerosols of short-lived daughter products of radon in mine air, 20: 14747
KACSER, C., Final-state interactions among three particles. II., 20: 15476
KACZOR, Krystyna, Absolute activity measurement of weakly radioactive preparations, 20: 14896
KADNER, M., Application of tracer systems to localize failed fuel elements, 20: 14848 (BMwF-FBK-65-02)
KADOTANI, Hiroyuki, Measurements of spatial distribution of cadmium ratio in heterogeneous lattices, 20: 16028
KADYSHEVSKII, V. G., Symmetry group ISL(6): representations and invariants, 20: 15498
KAEGI, Jakob, Nuclear reactor plant, 20: 16106
KAHN, F. D., Radiation from cosmic-ray air showers, 20: 15288
KAINUMA, Yoshiro, An elementary theory of inelastic scattering of fast electrons by thin crystals, 20: 15956
KAKIHANA, H., Acceleration of uranium(IV)–(VI) electron exchange reaction by hydrochloric acid, 20: 14570
KALECINSKI, J., Yield of molecular hydrogen in γ-irradiated alkaline solutions of chromite(III) and chromate(VI), 20: 14589
KALINICHEV, Yu. V., Gamma radiation of ^{152}Eu in energy range 1380 to 1900 kev, 20: 15832
KALISZ, Jozef, Fast multiple coincidence circuit using avalanche transistors, 20: 14880
KALIX, E., Application of tracer systems to localize failed fuel elements, 20: 14848 (BMwF-FBK-65-02)
KALKSTEIN, Marvin I., Radiochemical procedures for selected radionuclides in environmental samples, 20: 14430 (AD-620219)
KALMUS, George E., Spin and parity of Y$_1^0$(1815) and the Y*(1765), 20: 15414
KAMALYAN, L. A., X-radiation influence on smallpox vaccine virus in chicken embryo, 20: 14281
KAMINISI, Keisuke, Electron degeneracy at extremely high temperatures, 20: 15229
KAMINKER, D. M., Investigation of excited states ^{104,104*}Rh by observation of γ rays from (n,γ) reaction, 20: 15754
KAMINSKA, Urszula, Absolute activity measurement of weakly radioactive preparations, 20: 14896
KAMIYAMA, Hiroshi, Spiral distribution of the polar Es ionization, 20: 15614
KAMKE, D., Angular distribution of protons of reaction $^{11}B(d,p_{0,1})^{12}B$ at 0.7 to 1.7 Mev, 20: 15847
KANAZAWA, Hideo, Electron interaction and positron annihilation in electron gases, 20: 15383
KANAZIR, D., Metabolism of nucleic acids in uv-irradiated L-strain cells treated with native deoxyribonucleic acid, 20: 14355
KANCHELI, O. V., Threshold behavior of partial amplitudes of inelastic processes, 20: 15500
KANE, G., Single-particle exchange in 3-particle final states of the reaction K+p at 2.26 Bev/c, 20: 15422
KANEYASU, Yoshiko, Skin contamination by radioactive substances, 20: 14253
KANKI, Takeshi, Nucleon as a composite particle state, 20: 15352
KANKI, Takeshi, Self-consistent determination of position and width of the 33 π in resonance, 20: 15353
KANNAN, S., Permeability of iron and iron chelates through cuticular membranes, 20: 16147 (COO-888-45)
KAPLAN, A. L., Structure shielding from simulated fallout gamma radiation, 20: 15931 (TO-B-65-27)
KAPLAN, I. G., Distribution of energy of ionizing radiation in molecular mixtures, 20: 14595
KAPLAN, Louis L., Nuclear blast effects on components and equipment, 20: 14921
KAPPELMANN, F. A., Method for separating americium and curium from lanthanide rare earths and yttrium, 20: 14659
KARDASH, N. S., Redistribution of initially absorbed energy in radiolysis and photolysis of acyl peroxide solutions, 20: 14619
KARLSSON, R. H., Total hemispherical emittance of plutonium at 89°C, 20: 15088
KARMILOV, A. G., Device for x-ray structural analysis of radioactive materials, 20: 15064 (AD-625748)
KARTMAZOV, G. N., Interaction of oxygen with a Nb surface, 20: 15976
KARZHAVINA, E. N., Neutron resonances of Yb isotopes, 20: 15839
KASHIWAGI, Michio, Radical pairs trapped in x-irradiated single crystals of dimethylglyoxime-O, O-d_2, glyoxime, and methylglyoxime, 20: 14598
KASHUBA, I. E., Elastic scattering of medium-energy neutrons and the optical nuclear model, 20: 15770
KASTENBAUM, Marvin A., Minimum significant number of successes in a binomial sample, 20: 16150 (ORNL-3909)
KASTRUP, H. A., Conformal group in space-time, 20: 15470
KATKOV, V. M., Radiative polarization of electrons in a magnetic field, 20: 15638
KATO, Kiyoe, Electrical conductivity of a turbulent plasma, 20: 15895
KATO, T. R., Inhibition of corrosion of type-304L stainless steel from fluorides in nitric acid solutions, 20: 14982 (NLCO-970, pp 6.1-4)
KATO, Toyooki, Amine extraction of radioruthenium as chlorocomplex, 20: 14650
KATO, Yoshio, Effect on geomagnetic micropulsation of solar eclipse of 20 July 1963, 20: 15617
KATO, Yoshio, Effect on the geomagnetic field of total solar eclipse of February 5, 1962, 20: 15618
KATO, Yoshio, Effect of the anisotropic ionosphere on hydromagnetic oscillations, 20: 15619
KATO, Yoshio, Polarization of the long period geomagnetic pulsation, pc5, 20: 15615
KATO, Yoshio, Possible mechanism for rules of polarization of pc5 geomagnetic pulsations, 20: 15616
KATZ, Amnon, Corollaries of the Goldstone theorem, 20: 15487
KATZSCHMANN, R., Influence of La_2O_3 and ThO_2 on crystallization behavior of optical glasses, 20: 15075
KAUFMAN, Allan N., Low-frequency spatial response of a collisional electron plasma, 20: 15904
KAUN, K.-H., Gamma transitions in ^{153}Eu, 20: 15734 (ZfK-PhA-18)
KAWARABAYASHI, Ken, Partially conserved axial-vector current and decays of vector mesons, 20: 15485
KAWASAKI, S., Diffusion of xenon in metals, 20: 15090
KEANE, A. T., Radium isotope accumulation in animal thyroids, 20: 14254
KEEN, B. E., Viscosity and acoustic impedance of liquid ^{3}He, 20: 15583
KEIL, E., Incoherent beams blow-up in colliding beams, 20: 15174 (SLAC-49, pp 71-3)
KEILHOLTZ, G. W., Release and transport of fission-product iodine and its removal from reactor containment systems, 20: 14804
KEIPER, A., Photoconductivity and p-n photoeffect in SiC during excitation with x radiation, 20: 15967
KELER, E. K., Formation of lanthanum, praseodymium and neodymium aluminates, 20: 14539
KELLER, Barbara K., Effects of exposure to mixed fission spectrum delivered in single "pulse" and x-rays delivered at slower rate upon conditioned avoidance behavior of primates, 20: 14286 (AD-625837)
KELLER, C., Synthesis of transcurium elements by nuclear reactions with heavy ions, 20: 15740
KELLER, Richard H., Mixed heterologous mesenchymal sarcomas (mixed mesodermal sarcomas) of uterus, 20: 14301
KELLEY, M. T., Analytical instrumentation, 20: 14452 (ORNL-3889, pp 1–12)
KELLEY, M. T., Analytical chemistry for reactor projects, 20: 14454 (ORNL-3889, pp 17–24)
KELLEY, M. T., Inorganic preparations, 20: 14511 (ORNL-3889, pp 71–3)
KELLEY, M. T., Optical and electron microscopy, 20: 14460 (ORNL-3889, pp 46–8)
KEL'MAN, V. M., Deflecting properties and dispersion of electrostatic prism spectrometer, 20: 14868
KELSEY, J. C., Value of radiation sterilization in hospital practice, 20: 14943
KEMP, M. A. R., Differential cross sections and polarization effects in pion-proton elastic scattering at 875 to 1579 Mev/c, 20: 15372
KENDALL, G., High-energy photoproduction of nucleon and pionic resonances, 20: 15425
KENDALL, P. C., Explanation of the Appleton anomaly of the F2 layer. II., 20: 15586 (AD-620243)
KENNEY, V. P., Single-pion production in π−p interactions between 600 and 900 Mev, 20: 15411
KERIMOV, B. K., Neutrino-nucleon interactions with lepton production, 20: 15387
KERNAN, Anne, Spin and parity of Y$_1^0$(1815) and the Y*(1765), 20: 15414
KERR, R. J., Device having high-gradient cusp geometry, 20: 15928
KERWICK, Walter, Variable specific gravity radioactive source holder, 20: 14683
KERZE, F. Jr., Compartmented nuclear reactor fuel rod and method of making, 20: 16058

KESSEL, Quentin C., Coincidence study of O^+ on Kr collisions, 20: 15249 (TID-22648)
KHANSEVAROV, R. Yu., Defects formed in indium antimonide by γ irradiation, 20: 15979
KHARLAMOV, V., Methods for analysis of radioactive preparations, 20: 14501
KHAZEMOV, F. F., Lanthanum trichloride reaction with fused eutectic mix of Li and K chlorides, 20: 14565
KHMEL'NITSKII, Yu. L., Oxidation of technical paraffin wax with oxygen under action of γ-irradiation, 20: 14612
KHODULEV, B. S., Flaw detection in thin-walled tubes, 20: 14713
KHOMIKOVSKII, P. M., Radiation polymerization of vinyl chloride in solid solutions at low temperatures, 20: 14594
KHORUZHII, S. S., Reduction formulas in Wightman axiomatics, 20: 15502
KHROMOV, V. V., Separation of spatial and angular variables in solving neutron transport equation, 20: 15673
KHUDAKOV, S. V., Nuclear moments of inertia, 20: 15835
KHULELIDZE, D. E., Decay scheme of ^{109}Sn, 20: 15752
KHULELIDZE, D. E., Isomeric transitions of ^{114*}In and ^{118*}Te, 20: 15753
KHURI, N. N., Univalent functions and scattering amplitudes at high energies, 20: 15519
KIBBLE, T. W. B., Quantum theory of gravitation, 20: 15642
KIEL, G. R., Administering criticality control in Hanford Atomic Products Operation non-reactor environment, 20: 14790 (RL-SA-43A)
KIERSTEAD, Henry A., Evidence against an intermediate state between He I and He II, 20: 15582
KIHLBERG, Arne, Unitary representations of class of pseudo-orthogonal groups, 20: 14951
KILBINGER, F., Asymmetry in angular distribution of high-energy neutrons from μ^- capture in sulfur, 20: 15720 (JINR-E-2516)
KILCHER, Pierrette, Transitions in ^{188}Pt, 20: 15781
KIM, Y. S., Perturbed bound-state poles in potential scattering. I., 20: 15480
KIMELDORF, D. J., Persistent metabolic effect of x-rays or neutrons, 20: 14368
KING, E. M., Bonus superheater failure, 20: 16098
KING, F. D. R., Large-scale ^{60}Co heat sources, 20: 14945 (CONF-660305-14)
KING, T. A., Time dependence of scintillation intensity in aromatic materials, 20: 14615
KINOSHITA, Kisei, Many-pole amplitudes and elementarity. II., 20: 15490
KIRCHGESSNER, J., Princeton-Pennsylvania 3-Bev proton synchrotron parameters, 20: 15163 (PPAD-279D(Rev.))
KIRICHENKO, V. N., Content of submicroscopic aerosols of short-lived daughter products of radon in mine air, 20: 14747
KIRKBRIGHT, G. F., Spectrofluorimetric determination of microgram amounts of Sc. II., 20: 14476
KIRSH, A. A., Content of submicroscopic aerosols of short-lived daughter products of radon in mine air, 20: 14747
KISER, Robert W., Prog. rpt. on low energy investigations of radiation chemistry, final, 2/64–5/65, 20: 14584 (TID-22444)
KISHKIN, S. T., Structure of grain boundaries in molybdenum and its alloys with zirconium and rhenium, 20: 15128
KISHKIN, S. T., Volume and boundary diffusion of tungsten in molybdenum, 20: 15126
KISPERT, R. C., Development of thorium purification system, 20: 14448 (NLCO-970, pp 1.1–22)
KISS, I., Observations on biochemical changes in irradiated spores of Bacillus cereus, 20: 14263
KISS, Istvan, Production of heavy isotopes of hydrogen and of their compounds, 20: 14948
KISSINGER, H. E., Line broadening in irradiated molybdenum, 20: 15136 (RL-REA-2595, pp 51-62)
KITAGAKI, T., Princeton-Pennsylvania 3-Bev proton synchrotron parameters, 20: 15163 (PPAD-279D(Rev.))
KITAMURA, Takashi, Cosmic ray intensities under sea-water at depths down to 1,500 meters, 20: 15289
KITCHING, P., Evidence for hyperon states with masses greater than 1900 Mev, 20: 15424
KITCHINGMAN, W. J., $\beta \rightarrow \alpha$ phase change in pure uranium, 20: 15092
KIYAMA, Satoru, Electrical conductivity of a turbulent plasma, 20: 15895
KLAPISCH, M., Hyperfine structure of Eu I, 20: 15263
KLEEMAN, Charles R., Renal concentrating defect in canine radiation nephritis, 20: 14342
KLEIN, Deane T., Photoprotection against genetic damage in neurospora caused by x-rays, 20: 14358
KLEIN, H., Electron capture (P_L/P_K) ratio in decay of ^{204}Tl, 20: 15796
KLEIN, P. R., Angular correlation study of reaction $\pi^- p \rightarrow \pi^- \pi^+ p \pi^-$ at 2.7 Bev/c, 20: 15410
KLEIN, Richard M., Photoprotection against genetic damage in neurospora caused by x-rays, 20: 14358
KLEINE, T. O., Autoradiographic studies of uptake of ^{131}I and $^{35}SCN^-$ in thyroid, salivary glands, trachea, and other organs of guinea pig, 20: 14245
KLEPFER, H. H., Prog. rpt. on specific Zr alloy design program, 1/66, 20: 14980 (GEAP-5065)
KLYNNING, Lennart, Spectra of SnH and SnD, 20: 15251
KLYUKVINA, V. P., Accumulation of F centers in KCl crystals, 20: 15980
KNAAP, H. F. P., Polarizability of hydrogen-isotopes and of ortho and para hydrogen, 20: 15262
KNIGHT, Kenneth Douglas, Photoproduction at medium energies, 20: 15394
KNOPP, C. F., Cylindrically symmetric plasma source, 20: 15914
KNORR, G., Variation of the adiabatic invariant of the harmonic oscillator, 20: 15623 (MPI-PAE/P1.15/65)
KNOWLES, D. J., Description of facility radiation and contamination alarm systems installed in HFIR facility, 20: 16125 (ORNL-TM-1393)
KNOWLES, D. J., Liquid- and gaseous-waste-effluent sampling and monitoring, 20: 16137
KNOWLES, Paul H., Uranium exploration in Chile, 20: 14779 (RME-4569 (Rev.))
KNUDSEN, P., Non-destructive testing methods applied to multi-finned sap tubing for nuclear-fuel elements, 20: 14712
KNUDSON, Alvin R., Nuclear radiation detection system using plurality of detectors, 20: 14916
KNUTSON, C. D., A nuclear magnetic resonance study of decomposition in neutron-irradiated LiF, 20: 14602
KOBORI, Tetsuo, Feasibility calculation for JPDR-II core design; one-dimensional nuclear thermal and hydraulic calculation, 20: 16076 (JAERI-1088)
KOCH, J. C., Controlling furnace cycle with infrared pyrometers in casting of large uranium ingots, 20: 15006 (NLCO-970, pp 4.1-5)
KOCH, Siegfried, Measurement of ash content of lignite by γ irradiation technique with radionuclide ^{170}Tm, 20: 14493
KOCHAROV, G. E., Effects of neutrino background on shape of β spectra, 20: 15326
KOCHEGURA, N., Alteration of anti-friction and strength characteristics of engineering materials, subjected to neutron irradiation, 20: 15140
KOCHERIN, V. I., Critical parameters of homogeneous breeding systems, 20: 16030
KOFRANEK, Vl., Hematological changes in radiation sickness. V., 20: 14314
KOHMURA, Toshitake, Nuclear reactions by a low-energy pion, 20: 15827
KOHMURA, Toshitake, Wave functions in hypernuclei and nuclear compressibility, 20: 15826
KOLANKOWSKI, Stanislaw, Absolute activity measurement of weakly radioactive preparations, 20: 14896
KOLAR, Z., Isomeric cross-section ratios for 14.6-Mev neutron-induced reactions, 20: 15773
KOLBASOV, V. I., Structure of radiation chlorinated and sulfochlorinated polyethylene, 20: 14621
KOLHN H., Erik, Uranium exploration in Chile, 20: 14779 (RME-4569 (Rev.))
KOLOUSEK, J., Influence of x-radiation, on urinary excretion of inorganic phosphates and ammonia, 20: 14270
KOLTUNOV, Yu. B., Studies of potassium release from γ-irradiated cells, 20: 14282
KOMISSAROVA, L. N., Binary oxides in ZrO_2–Nb_2O_5 systems, 20: 15079
KONIJN, J., Some allowed K-capture to positron ratios, 20: 15711 (CONF-233(Vol.2), pp 345-58)
KONOVALENKO, B. M., Low-temperature annealing of germanium, irradiated with fast electrons, 20: 15984
KOPANETS, E. G., Measurement of linear polarization of 1.97-Mev γ rays in reaction $^{36}Ar(p,p'\gamma)^{36}Ar$, 20: 15760
KOPANETS, E. G., Nuclear levels of ^{27}Al at excitation energies of 10.495 and 3.95 Mev, 20: 15761
KOPELMAN, Jay B., Moderation and cascade times of negative pions and negative kaons in liquid helium, 20: 15273
KOPOLDOVA, J., Radiation chemical reactions in aqueous oxygenated and oxygen-free solutions of aliphatic dipeptides and tripeptides, 20: 14616
KOPP, Ingvar, Rotational analysis of perturbed C and D states of BaH and BaD, 20: 14517
KOPTA, S., Octupole Coulomb excitation of ^{208}Pb, 20: 15719 (INP-431/PL)
KOPYTIN, I. V., Influence of strong interactions between nucleons in nuclei on forbidden β decay, 20: 15836
KORBEL, Kazimierz, Detecting probes operating in single-cable system of pulse transmission and power supply, 20: 14876
KORDUS, Aleksander, Conductivity measurements concerning low-temperature plasmas used in MGD generators, 20: 15897
KOREN, Kristian, ^{137}Cs in people and food in Norway, 1963–1965, 20: 14739 (TID-22655)
KORKISCH, J., Prog. rpt. on ion exchange separation of U and Th in mixed and nonadequate solvents, final, 1965, 20: 14469 (TID-22650)
KORNILOV, I. I., Constitution diagram of Ti–Nb–Cr system, 20: 15078

KOROBEINIKOVA, V. G., Phase diagram of columbium–nickel system, 20: 15115
KOROLEV, B. M., Structure of radiation chlorinated and sulfochlorinated polyethylene, 20: 14621
KORPAK, W., Solvent extraction of molybdenum and uranium from sulfate solutions with tri-n-octylamine, 20: 14653
KORPUSOV, G. V., Density and viscosity of solutions of system: organic solvent–rare earth nitrate solutions, 20: 14648
KORTHEUER, John, CVTR control rod performance test, 20: 16062 (CVNA-175)
KORYAGIN, V. F., Electron paramagnetic resonance of atomic hydrogen in beryllium, 20: 15982
KORYAKIN, Yu. I., Use of reactors of Beloyarsk atomic power plant type for dual-purpose desalinization systems, 20: 16107 (JPRS-33406)
KORZH, I. A., Elastic scattering of medium-energy neutrons and the optical nuclear model, 20: 15770
KOSIARA, A., Excitation of characteristic radiation in elements of $14 \leq Z \leq 50$, 20: 15258
KOSTELNICEK, R. J., Admittance and resonance probe characteristics of a spherical plasma probe, 20: 15868 (AD-628186)
KOSTIC, Lj., Metabolism of nucleic acids in uv-irradiated L-strain cells treated with native deoxyribonucleic acid, 20: 14355
KOSTYRKO, Andrzej, Scintillation cell for determination of ^{222}Rn, 20: 14881
KOTEL'NIKOV, G. N., Singularities in uranium–radium series equilibrium shift in uranium deposits with solid bitumens, 20: 14781
KOTEL'NIKOV, V. N., New data on atmospheric radioactivity and fallout density near Black Sea, 20: 14741
KOUNOSU, Shigeru, Neutral decay modes of the η meson, 20: 15395
KOURI, Donald J., Low-energy atomic collisions. I., 20: 14545
KOVACS, Valeria, Isotopic exchange between iodo amino acids and ^{131}I on chromatographic paper, 20: 14632
KOVAR, M., Determination of hydrogen in hydrocarbons by neutron activation, 20: 14480
KOVBA, L. M., Binary oxides in ZrO_2–Nb_2O_5 systems, 20: 15079
KOVETZ, Attay, Influence of rotation and magnetic fields on thermal instability of fluid sphere, 20: 15876 (IPP-6/33)
KOWALEW, Andrzej, Concept of fast breeder reactor with fused salt fuel and boiling mercury "wars", 20: 16036
KOWALEW, Andrzej, Concept of salt-boiling fast breeder reactor, 20: 16037
KOWALIK, S., Measurement methods to impart linearity of scale to radioisotope instruments, 20: 14836
KOWALSKI, S., The energy and angular distribution of photoneutrons from heavy elements, 20: 15723 (MIT-2098-162)
KOWNACKI, Jan, Proportional counter as spectrometer for low-energy γ and β rays, 20: 14879
KOYANAGI, Takemi, Confidence test of radiation counter, 20: 14889
KOZA, F., Determination of hydrogen in hydrocarbons by neutron activation, 20: 14480
KOZHEVNIKOV, D. A., Application of similitude theory to study of radiation transfer processes, 20: 14776
KOZHEVNIKOV, D. A., Over-all pattern and characteristics of stationary distribution of neutrons, 20: 14774
KOZYREV, V. I., Uranium in paleozoic deposits of Northern Tien Shan, 20: 14780 (AEC-tr-6579)
KRAEMER, R., Single-particle exchange in 3-particle final states of the reaction K+p at 2.26 Bev/c, 20: 15422
KRAEMER, R. W., Observations of $Y_1^*(1405)$ and $Y_1^*(1358)$ resonances in π-N collisions at 1.68 Bev/c, 20: 15404
KRAMER, G., Symposium on electron and photon interactions at high energies, Hamburg, 6/65. I., 20: 15437
KRASNOSHCHEKOV, M., Alteration of anti-friction and strength characteristics of engineering materials, subjected to neutron irradiation, 20: 15140
KRASNOV, Yu. N., Lanthanum trichloride reaction with fused eutectic mix of Li and K chlorides, 20: 14565
KRAUSE, Albert, Production of rare earths from kola-apatite, 20: 14520
KRAUSE, L., Sensitized fluorescence in vapors of alkali metals. V., 20: 15253
KRAUSE, M. O., Bibliography on atomic and molecular processes, 1964, 20: 15248 (ORNL-AMPIC-3)
KRAUSE, Manfred O., Atomic readjustment following formation of inner shell vacancies, 20: 15245 (CONF-233(Vol.3), pp 494-504)
KRAYBILL, Henry L., Interactions of π^+ mesons with protons at 2.08 Bev/c, 20: 15334
KRIPYAKEVICH, P. I., Compounds with structures of Th_6Mn_{23} type in alloys of rare earth metals with manganese and iron, 20: 15110
KROEGER, Henry R., Check on weight of space radiators for steam systems, 20: 14688 (N65-20692)
KRONGAUZ, V. A., Distribution of initially absorbed energy in radiolysis and photolysis of acyl peroxide solutions, 20: 14619
KRSMANOVIC-SIMIC, Drago, Radioresistance of nucleohistone, 20: 14592
KRUEGER, F. Wolfgang, Nuclear data on production of γ rays through interaction with fast neutrons, 20: 15725 (NP-14855)
KRUGER, O. L., Phase relations and structures in uranium–platonium–fissium alloys, 20: 15085
KRULIKOWSKI, C., Probe for complex study of physical properties of soils, 20: 14773
KRUPP, P., Early action of gamma radiations on electrical brain activity and behavior in rabbit, 20: 14326
KRUPP, P. J., Malignant mixed muellerian neoplasms (mixed mesodermal tumors), 20: 14300
KRUSHINSKII, A. N., Preparation of complex carbide alloys containing scandium carbide, 20: 15017
KRUSZEWSKA, Jadwiga, Effective mechanism of radioprotective substance methandrostenolone. II., 20: 14402
KRUTILINA, T. A., Characteristics of interaction of oxygen with surface of a tungsten single crystal, 20: 15986
KSANDA, C. F., Gamma-ray energy pseudospectra for ^{235}U fission products and for various times after fission, 20: 14733 (AD-628982)
KSHIRSAGAR, Sharad, Occurrence of squamous carcinoma and osteosarcoma in young rabbits injected with ^{90}Sr(50-100 μC/kg), 20: 14316
KU, Yuen-liang, ^{14}C-labeled urea and ^{32}P-labeled phosphate to investigate foliar-applied fertilizer for rice growing in reclaimed tidal lands, 20: 14240 (NP-15670)
KUBAREV, Yu. V., Source of gas-discharge plasma, 20: 15887 (AD-625789)
KUBISZ, J., Quadrupole splitting of 14.4-kev γ line of ^{57}Fe in Fe sulfates, 20: 15775
KUBO, Hiroshi, Microwave radiation from a bounded plasma, 20: 15893
KUCAN, Zeljko, Inactivation of isolated Escherichia coli ribosomes by gamma irradiation, 20: 14363
KUCERA, Karel, Influence of cortisone and ACTH treatment on serum glycoprotein levels in x-irradiated rats, 20: 14378
KUCHITSU, Kozo, Third-order potential constants of bent XY_2 molecules, 20: 14559
KUCHOWICZ, Bronislaw, Origin of chemical elements in stars. VIII., 20: 15231
KUDO, Yoshiteru, Effect of final-state interactions in $(\alpha,2\alpha)$ reactions, 20: 15825
KUEHN, W., Radiometric method for continuous cross-section measurement of hot rolled wires, 20: 14838
KUEHNELT, H., Higher symmetry of leptons, 20: 15448
KUENKEL, H. A., Influence of 5-hydroxytryptamine (serotonin) on radio-induced mutation rate in Drosophila melanogaster, 20: 14398
KUGE, Yasushi, Feasibility calculation for JPDR-II core design; one-dimensional nuclear thermal and hydraulic calculation, 20: 16076 (JAERI-1088)
KUICH, G., Coherent extinction and second order neutron scattering on single crystals, 20: 15671
KULGAWCZUK, D. S., Quadrupole splitting of 14.4-kev γ line of ^{57}Fe in Fe sulfates, 20: 15775
KULKE, W., Use of ^{99m}Tc as clinical tracer element, 20: 14423
KUMAMOTO, Tooru, Gaschromatographic determination of scandium as acetylacetonate and trifluoroacetylacetonate, 20: 14486
KUMAR, Aditya, Deviations from charge independence in n-p and n-n scattering lengths by S-matrix methods, 20: 15356
KUMAR, Sudhir, Physiological and biochemical studies of incompatibility in Oenothera organensis, 20: 14382
KUNICKI, Adam, Universal laboratory monitor model MSP-2, 20: 14872
KUNZ, C., Spectroscopic study of alpha-ray-induced luminescence in gases. I., 20: 14617
KUNZ, J., Autoradiographic and fluorescence microscopic studies of aortic mucopolysaccharide after local exposure to ^{90}Sr–^{90}Y radiation, 20: 14295
KUNZ, W., Superconductivity of fusion samples of systems Nb–Sn, Nb–Al, Nb–Ga, V–Si, and V–Ga, 20: 15123
KURILOVA, L., Complexes of uranyl with phenolic ligands. III., 20: 14481
KURILOVA, L., Uranyl complexes with phenolic ligands. IV., 20: 14482
KURINNYI, V. I., Silicon solar cells produced by ion bombardment, 20: 15302
KURITA, Yukio, Radical pairs trapped in x-irradiated single crystals of dimethylglyoxime-O, O-d_2, glyoxime, and methylglyoxime, 20: 14598
KUSHAKEVICH, Yu. P., Isomeric transitions of $^{114*}In$ and $^{115*}Te$, 20: 15753
KUSMA, J. B., Crystal structures of YAg_2, YAu_2, and YZn_{12}, 20: 15102
KUZMA, Y. B., Phase equilibria in system molybdenum–chromium–carbon, 20: 15111
KUZ'MA, Yu. B., New ternary compounds with $W_2Cr_{21}C_6$ type structure, 20: 14532
KUZ'MA, Yu. B., Zirconium–cobalt–boron system, 20: 14533
KUZNETSOV, L. I., Roentgenographic studies of lanthanum tellurides, 20: 14530
KUZNIECOV, I., Octupole Coulomb excitation of ^{208}Pb, 20: 15719 (INP-431/PL)
KVIN, V. E., Study of homogeneous sintered tungsten–hafnium alloy,

20: 15021
KYCIA, T. F., Experimental verification of the Johnson-Treiman relationship, 20: 15428

L

LACH, J., p-p Annihilations into K and π mesons at 3.7 Bev/c, 20: 15338
LACINA, B., Neutron-neutron interaction in triton-triton reaction, 20: 15733 (UCRL-7769)
LACY, P. S., Pathfinder flooding coefficient, core pressurization, and temperature coefficient tests, 20: 16059 (ACNP-65600)
LADEFOGED, Jorgen, Relationship between hematocrit and solubility of ^{133}Xe in blood, 20: 14415
LAFAURIE, Denis, Neutronic control of Garigliano Reactor, 20: 16068 (EUR-2420.d,f,i,n,e, pp 133-45)
LA FAVE, James W., Blood supply to hepatic V2 carcinoma implants as measured by radioactive microspheres, 20: 14405 (COO-1305-2)
LAHIRI, S. K., Method for studying maturation time of average bone marrow cell in rat using ^{32}P as tracer, 20: 14248
LAKH, V. I., Zirconium–cobalt–boron system, 20: 14533
LAKSHMANAN, S., Derivative neutron activation analysis, 20: 14502
LALANNE, C. M., High-energy radiations in France. (Present equipment and future prospects), 20: 14425
LAM, Carroll F., Pulse shape discrimination considerations in dual crystal gamma-ray scintillation detector, 20: 14844 (AD-620395)
LAMBERTS, H. B., Deposition of radioactive Ba and Sr in aortic wall, 20: 14252
LAMBORIZIO, C., Small-angle elastic scattering of polarized protons in photographic emulsions, 20: 15314 (RT/FI(65)35)
LAMPE, Isadore, Role of radiation therapy in treatment of chemodectomas of Glomus jugulare, 20: 14417
LAMSA, J. W., Single-pion production in π^-p interactions between 600 and 900 Mev, 20: 15411
LANCZOS, C., Metrical lattice and problem of electricity, 20: 15633
LANDAU, Ronald W., Dispersion relation for relativistic streams of finite radius, 20: 15885 (UCRL-12207(Rev.1))
LANDER, R. L., K-p interactions at 3.8 Bev/c, 20: 15418
LANDER, R. L., Reaction $\pi^-d \rightarrow \pi^-d\,\pi^+\pi^-$ at 3.7 Bev/c, 20: 15409
LANDER, R. L., Study of the A and B mesons, 20: 15408
LANDOVITZ, L. F., Bosons, A parity, and G_2, 20: 15473
LANDSTEINER, Ernest K., Urinary complications following combined interstitial radiation and node dissection therapy for cervical cancer, 20: 14377
LANGEBARTEL, R. G., Liouville's equation and n-body problem, 20: 15148 (N65-20165)
LANGHOFF, H., Excited levels of ^{79}Br, 20: 15802
LANGPAPE, R., Influence of CsF on emitter work function and the performance of Cs diodes, 20: 15297 (CONF-640921, pp 101-9)
LA PAGLIA, S. R., Theoretical transition probabilities, 20: 15275
LAPIERE, C. M., Effect of x rays on reversibility of collagen gel, 20: 14593
LAPSHOV, Y. K., High-temperature heaters made with niobium and zirconium carbides, 20: 15112
LARIONOV, V. V., Natural radioactivity of carbonate rocks, 20: 14752
LARKINS, John H., Radiation dosimeter system using cadmium-backed copper foil, 20: 14915
LA SALLE, Richard Alan, Alpha-alpha angular correlation studies of reaction $^{12}C(\alpha,\alpha')^{12*}C(\alpha_0)^8Be$, 20: 15862
LASHOF, Joyce C., Childhood cancer in twins, 20: 14319
LASHOF, Joyce C., Oxford survey of childhood cancers progress report III, 20: 14346
LASLETT, L. Jackson, Asymptotic perturbation fields of longitudinally bunched beam within rectangular pipe with resistive walls, 20: 15168 (SLAC-49, pp 23-31)
LASLETT, L. Jackson, Influence of dielectric media on electromagnetic fields of coasting beam in straight rectangular pipe, 20: 15172 (SLAC-49, pp 52-8)
LATAL, H., Remarks on regularization, 20: 15320
LAU, Silvanus Siu-wai, Dislocation mechanisms of Mo single crystals, 20: 15946 (UCRL-16643)
LAUBE, E., Crystal structures of YAg_2, YAu_2, and YZn_{12}, 20: 15102
LAUGHLIN, John S., Energy dependence of lithium fluoride dosimeters and high electron energies, 20: 14887
LAUMETS, E., Gamma-ray energy pseudospectra for ^{235}U fission products and for various times after fission, 20: 14733 (AD-628982)
LAUMETS, E., Time history of biological response to ionizing radiation, 20: 14287 (AD-626996)
LAUTZENHEISER, C. E., Prog. rpt. on Elk River reactor pressure vessel, 10–12/65, 20: 16085 (SWRI-1228-4-15)
LA VALLE, D. E., Inorganic preparations, 20: 14511 (ORNL-3889, pp 71–3)
LAWLEY, A., Friction stress and micro-yielding of beryllium, 20: 15067
LAYTON, Richard Gary, Excitation of oxygen by 18- to 102-Kev protons, 20: 15271
LAZAREV, A. N., Polymorphism of rare earth pyrosilicates, 20: 14537
LEARY, J. A., Solubilities of selected elements in liquid Pu. VII., 20: 15043 (LA-3436)
LEARY, J. A., Thermodynamic properties of Pu compounds from EMF measurements. I., 20: 14507 (LA-3399)
LEBEDEV, I. A., Preparation of ^{242}Pu and ^{242}Cm from neutron-irradiated ^{241}Am, 20: 14631
LEBLANC, J. M., Non-destructive testing of plutonium-enriched fuel rods, 20: 14707
LEDINGHAM, K. W. D., Ratio of K-capture to positron emission in decay of ^{13}N, 20: 15712 (CONF-233(Vol.2), pp 359-64)
LEDNEY, I. A., Device for x-ray structural analysis of radioactive materials, 20: 15064 (AD-625748)
LEE, B. W., Selected topics in unitary symmetry and weak interactions, 20: 15533
LEE, Hyung Joon, Absorption of sound in superconductors of the second kind, 20: 15663
LEE, M., Transverse stability of ultra-relativistic multiple-bunched beams, 20: 15171 (SLAC-49, pp 49-51)
LEGRAND, Jean, Absolute measurement of activity of electron-capture nuclides, 20: 15690 (CEA-R-2813)
LEIMDOERFER, M., Method for predicting penetration and slowing down of neutrons in reactor shields, 20: 15935
LEIST, N. R., Development of thorium purification system, 20: 14448 (NLCO-970, pp 1.1–22)
LEITER, Edgar, Radiation transmitter, 20: 14864
LEMBERG, I. Kh., Interference effects in Coulomb excitation of 2^+ levels in even-even nuclei, 20: 15768
LEMBERG, I. Kh., Polarized γ radiation emitted during Coulomb excitation, 20: 15759
LENGEMANN, F. W., Prog. rpt. on fission product metabolism and response in animals, 1/64–12/65, 20: 14243 (TID-22626)
LEONARD, Anthony, Out-of-pile thermionic space power systems using a gaseous heat-transfer fluid, 20: 16110 (AD-620650)
LEONELLI, Franco, Control rod system for the SENN reactor, 20: 16069 (EUR-2420.d,f,i,n,e, pp 147-80)
LEONTIC, B., Search for hyperon resonances with spark chambers, 20: 15417
LEONTIC, B. A., Experimental verification of the Johnson-Treiman relationship, 20: 15428
LEPINSKIKH, B. M., Surface ductility and density of oxide melts containing vanadium or niobium pentoxides, 20: 15076
LERCH, P., Irradiation with ^{90}Sr of superior sympathetic cervical ganglion of rat in vitro, 20: 14332
LERCHE, I., Radiation from cosmic-ray air showers, 20: 15288
LERNER, M. W., Evaluation of methods in TID-7029, "selected measurement methods for plutonium and uranium in nuclear fuel cycle", 20: 14447 (NBL-231)
LESIKAR, Arnold Vincent, Magnetic hyperfine interactions in ^{149}Sm in ferromagnetic $SmAl_2$, 20: 15992
LESK, Arthur M., Fluorides and oxides of helium and neon, 20: 14541
LESKOV, S. A., Uranium in paleozoic deposits of Northern Tien Shan, 20: 14780 (AEC-tr-6579)
LESUEUR, R., Utilization of impregnation compounds in graphite in thermionic conversion, 20: 15296 (CONF-640921, pp 81-99)
LEUTZ, H., Electron capture (P_L/P_K) ratio in decay of ^{204}Tl, 20: 15796
LEVENSON, M., Administration of nuclear safety at ANL, 20: 14800
LEVEQUE, Paul, Results of tritium activity measurement of some waters of southwest, 20: 14744
LEVINA, M. E., Study of $NaBeF_3$–$NaPO_3$ system by emanation method, 20: 14557
LEVINA, M. E., Study of $KBeF_3$–KPO_3 system by emanation method, 20: 14558
LEVINSKAYA, M. Kh., Interaction of diborides of vanadium, niobium and tantalum with carbon, 20: 14555
LEVINSKAYA, M. Kh., Studies of carbidization of titanium and zirconium nitrates, 20: 15072
LEVINSKII, Y. V., Interaction of diborides of vanadium, niobium and tantalum with carbon, 20: 14555
LEVINSKII, Yu. V., Studies of carbidization of titanium and zirconium nitrates, 20: 15072
LEVINSON, L. S., Heat content of crystal-bar thorium, 20: 14550
LEW, D. E., Prog. rpt. on Piqua power facility operations analysis, semi-annual, 1–6/65, 20: 16077 (NAA-SR-11628)
LEWA, Czeslaw, Thermalization process of neutrons from Po–Be neutron sources in a paraffin moderator, 20: 15683
LEWIN, W. H. G., K-conversion coefficient of the 412-kev E2 transition in ^{198}Hg, 20: 15707 (CONF-233(Vol.2), pp 198-212)
LEWIS, G. M., Search for hyperon resonances with spark chambers, 20: 15417
LEWIS, R. E., Preparation of megacurie quantities of ^{137}Cs salts and source compounds, 20: 14626 (ORNL-P-1944)

LEY, F. J., Effects of ionizing radiations in producing sterility in spores, 20: 14389
LIBOTTE, P., Non-destructive testing of plutonium-enriched fuel rods, 20: 14707
LICCIARDELLO, J. J., Effect of irradiation temperature on radiosensitizing activity of vitamin K_5, 20: 14395
LICHTENBERG, D. B., Peripheral model of meson-nucleon collisions, 20: 15419
LICHTENBERG, Franz V., Host response to eggs of schistosoma mansoni. IV., 20: 14304
LICHTIN, Norman N., Prog. rpt. on radiation chemistry of organic compounds, 2/65–1/66, 20: 14579 (NYO-2383-15)
LIDIARD, A. B., Self-diffusion of uranium in UO_2, 20: 15091
LIE, T. J., Thermodynamic properties of an electron plasma, 20: 15869 (AD-628317)
LIEBERMAN, P., Prog. rpt. on reactor containment, 10–11/65, 20: 16023 (IITRI-578P21-16)
LIEBMANN, B., Prog. rpt. on fabrication of UO_2 powders and processing into fuel elements, 4–6/65, 20: 14999 (EURAEC-1466)
LIEBOWITZ, H., Symposium on high temperature structures and materials, N.Y., N.Y., 1/63, 20: 15129
LIEBSCHUTZ, A. M., Prog. rpt. on radiation effects on microelectronic circuits, 5–7/65, 20: 14918 (ECOM-01313-1)
LIEBSTER, J., Radiation chemical reactions in aqueous oxygenated and oxygen-free solutions of aliphatic dipeptides and tripeptides, 20: 14616
LIESER, K. H., Influence of complex stabilities on electron transfer reactions, 20: 14574
LIESER, K. H., Kinetics and mechanism of heterogeneous exchange reactions on surface of ionic crystals, 20: 14572
LIGENSA, R., Nuclear giant quadrupole resonance, 20: 15823
LIN, C. C., Gravitational collapse of uniform spheroid, 20: 15206
LIN, C.-S., Large aperture seismic array signal handling system, 20: 14760
LINDACKERS, Karl-Heinz, Different methods for determination of radioactivity in air, 20: 14745
LINDGREN, Bo, Rotational analysis of perturbed C and D states of BaH and BaD, 20: 14517
LINDGREN, Bo, Spectra of SnH and SnD, 20: 15251
LINDGREN, J. R., Evaluation of vapor-deposited tungsten tubing, 20: 15048 (N65-16231)
LINDGREN, J. R., Prog. rpt. on thermionic materials for space power applications, 9/63, 20: 14960 (N65-20798)
LINDGREN, Martin, Record form for external beam therapy designed specially for ^{60}Co treatment with stationary fields, 20: 14408
LINDSAY, J. C., Solar x-ray images obtained using grazing incidence optics, 20: 15203
LINDSEY, James S., Final-state interaction involving hyperons, 20: 15412
LINDSEY, James S., Spin and parity of the Ξ^* (1530 Mev), 20: 15464
LINDSEY, James Seward, Production properties and decay modes of the θ meson, 20: 15316 (UCRL-16526)
LINEKIN, David Maynard, Onsager-Feynman quantized vortex line theory of rotating liquid helium II, 20: 15661
LINGANE, James J., Analytical chemistry of selected metallic elements, 20: 14500
LINKLETTER, D., Effect of x-irradiation on cell size distribution of thymus lymphocytes, 20: 14318
LIPKIN, H. J., Introduction to SU(3), 20: 15529
LIPKIN, H. J., Now we are SU(6), 20: 15534
LIPKIN, H. J., Properties of mesons in SU(3), 20: 15530
LIPKIN, H. J., W spin and SU(12) subgroups, 20: 15539
LISITSYN, V. M., Generation of vacancies in KBr–Sr irradiated by a proton beam, 20: 15977
LISTER, B. A. J., Recent advances in monitoring for airborne radioactivity, 20: 14811
LITTLE, John B., Distribution of ^{210}Po in pulmonary tissues of cigarette smokers, 20: 14798
LITTLE, W. W. Jr., Neutronic considerations in selection of driver fuel for FTR, 20: 16121 (BNWL-197)
LIU, Lien-sou, Assignments of higher resonances in SU(12), 20: 15496
LIVINGSTON, J. T., ^{244}Cm for radioisotopic heat sources work at Savannah River laboratory, 20: 15038 (CONF-660305-12)
LIVINGSTON, M. Stanley, Summary of research operations at Cambridge electron accelerator, 1/66, 20: 15306 (CEAL-1026)
LLOYD, M. H., Method of preparing compactible thorium oxide–plutonium oxide particles, 20: 15025
LOCHSTET, William Albert, Photonuclear activation of carbon over the giant resonance, 20: 15861
LOCKHART, R. W., Sodium mass transfer. XIX., 20: 14979 (GEAP-4835)
LOCKWOOD, John A., Cosmic ray neutron intensity monitor. Part B., 20: 15278
LOCKWOOD, John A., Cosmic ray neutron intensity monitor. Part B., 20: 15280
LOCKWOOD, John A., Cosmic ray neutron intensity monitor. Part B., 20: 15282
LOCKWOOD, John A., Cosmic ray neutron intensity monitor. Part B., 20: 15284
LOCKWOOD, John A., Cosmic ray neutron intensity monitor. Part B., 20: 15286
LODHI, M. A. K., Elastic electron scattering by ^6Li, 20: 15866
LOGINOV, A. A., Use of reactors of Beloyarsk atomic power plant type for dual-purpose desalinization systems, 20: 16107 (JPRS-33406)
LOIACONO, Raffaele, Tests on components for Eurex 2AW plant, 20: 14644
LOKEN, J., V-2-prong K⁻p interactions at 5.5 Bev/c, 20: 15416
LOLEY, F., Microchemical analysis of dust samples for long-lived uranium fission products, 20: 14472
LOMON, E. L., Analytic continuation of an S_{11} pion-nucleon amplitude to the P_{11} amplitude, 20: 15312 (MIT-2098-86)
LOMOVA, M. A., Lipase activity in fatty tissues and liver following γ irradiation, 20: 14279
LONDEN, S.-O., Central reactivity measurements on assemblies 1 and 3 of reactor FR0, 20: 16118 (AE-212)
LONG, E. L., Bonus superheater failure, 20: 16098
LONG, Everett, Improvements relating to nuclear reactors, 20: 16007
LOPEZ-MENCHERO, E., Aqueous processing of graphite-carbide fuel elements, 20: 14638 (NP-15753)
LOPUSZANSKI, Jan, Problems in quantum theory of fields, 20: 15489
LOTHROP, Fred H. G., Bevatron beam spill by amplitude modulation, 20: 15185
LOUIE, James, Spin and parity of Y$_1^*$(1815) and the Y*(1765), 20: 15414
LOUTHAN, M. R. Jr., Influence of stress on hydride habit plane in Zircaloy-2, 20: 15120
LOVELACE, C., Pion-nucleon phase shifts and their implications, 20: 15382
LOWE, J., Elastic and inelastic scattering of 20- to 28-Mev polarized protons by carbon, 20: 15805
LOWE, J. T., Recovery and purification of ^{147}Pm, 20: 14635 (CONF-660305-5)
LU, D. C., Evidence for hyperon states with masses greater than 1900 Mev, 20: 15424
LUCAS, Arthur C., Thermoluminescent dosimeter shield, 20: 14914
LUEHRS, G., Gamma spectrum of $^{214}Po(RaC')$, 20: 15844
LUI, Yau-Yin, KLL-Auger spectrum of manganese, 20: 15243 (CONF-233(Vol.3), pp 480-6)
LUKASIK, S. J., Computer simulation of satellite systems, 20: 15599
LUK'YANOV, V. K., Inelastic scattering of heavy particles with excitation of collective nuclear states, 20: 15763
LUMBA, L. G., Production of colloidal ^{198}Au, 20: 14627 (PAEC(D)IS-651)
LUND, S. A., Non-destructive testing methods applied to multi-finned sap tubing for nuclear-fuel elements, 20: 14712
LUNDBY, A., Search for hyperon resonances with spark chambers, 20: 15417
LUNGU, S., Radiation-induced stress relaxation and flow in vitreous silica, 20: 15971
LUOMA, W., Prog. rpt. on determination of emissivity of materials, semiannual, 5/15–11/14/65, 20: 15057 (PWA-2750)
LUSHCHIKOV, V. I., Determination of neutron resonance spins in ^{165}Ho nuclei, 20: 15681
LUTSENKO, V. N., Nuclear levels of ^{168}Er excited by the (n,γ) reaction, 20: 15757
LUX, Franz, X-ray fluorescence analysis of technetium and molybdenum in solutions, 20: 14497
LVOVA, M. A., Imitators of short-living isotopes of iodine, 20: 14928
LYEM, Arthur, Seventeenth materials review, 20: 14506 (CRDL-SP-5-7)
LYNCH, H. L., π-pair photoproduction below 1 Bev, 20: 15332
LYNN, Y. M., Magnetohydrodynamic shocks in nonaligned flow, 20: 15576
LYON, W. S., Nuclear and radiochemical analyses, 20: 14461 (ORNL-3889, pp 48–70)
LYON, W. S., Radioactivation analysis as analytical tool, 20: 14477
LYSKOVICH, A. B., Spectral composition of radioluminescence, 20: 14611
LYUTAYA, M. D., Chemical and thermal stability of scandium borides, 20: 14531

M

MA, Chung-chi, Assignments of higher resonances in SU(12), 20: 15496
MAC DONALD, H. F., Localized vibrations of H⁻ and D⁻ ions in alkaline earth fluorides, 20: 15969
MAC DOWELL, S. W., CP violation in K decay, 20: 15434
MACHIDA, T., Errors of gamma-scattering density meter and its design for low density measurement, 20: 14837
MACKLIN, R. L., Lack of structure in ^{235}U fission cross section, 20: 15818
MAC NEIL, R. L., Structure shielding from simulated fallout gamma radiation, 20: 15931 (TO-B-65-27)
MADSHUS, Kjell, ^{137}Cs in people and food in Norway, 1963–1965,

20: 14739 (TID-22655)
MAIANI, L., Kinetic supermultiplets of U(12). II., 20: 15479
MAIANI, L., Relation between D/F and G_A/G_V from current algebra, 20: 15488
MAIDUKOVA, T. P., Reactions of lanthanum nitrate with ammonium carbonate in solution, 20: 14535
MAIER, Richard Georg, Recrystallization of Cb_3Sn, 20: 15113
MAIER, Yo, New complexes. III., 20: 14521
MAJERCZYK, J., Influence of composition and density of soils on readings of neutron moisture meters, 20: 14771
MAJEWSKI, W., Bootstrap mechanism and charge independence of strong interactions, 20: 15454
MAJOR, F. G., Ultrahigh resolution $\Delta F = 0, \pm 1$ (^3He)+ HFS spectra by ion-storage collision technique, 20: 15260
MAKIN, M. J., Effect of solute concentration on formation of loops in aluminum–magnesium alloys during fission fragment irradiation, 20: 15145
MALAMAND, Frima, Spectrographic analysis of Nb–Zr alloys, 20: 14446 (N64-25607)
MALDAGUE, P., Protection of mouse against lethal effects of x rays by sodium hyposulfite, 20: 14393
MALHERBE, Jean, Heat transfer and pressure drops along surfaces fitted with herring bone fins, 20: 14685 (CEA-R-2471)
MALIK, F. B., Variational derivation of the pairing equation in a finite nucleus, 20: 15742
MALINOVSKII, O. V., Oxygen effect on post-irradiation restoration of yeast cells, 20: 14399
MALISSA, H., Microchemical analysis of dust samples for long-lived uranium fission products, 20: 14472
MALOYAN, A. G., Gamma radiation of ^{152}Eu in energy range 1380 to 1900 kev, 20: 15832
MALTSEV, V. M., Investigation of 9 Bev/c π^- meson interactions with xenon nuclei accompanied by Λ and K^0 particle production, 20: 15841
MALTSEVA, L. F., High-temperature heaters made with niobium and zirconium carbides, 20: 15112
MALVANO, R., Determination of trace elements in iron by neutron-activation techniques, 20: 14471
MALVEN, R., Field control of telecobalt therapy by gamma-ray television, 20: 14407
MANAKOV, A. I., Surface ductility and density of oxide melts containing vanadium or niobium pentoxides, 20: 15076
MANDELSTAM, S., Kronecker-delta singularities in j-plane, 20: 15521
MANDZUKOV, Iv., Moessbauer effect in tin, 20: 14567
MANG, H. J., Self-consistent calculation of nuclear equilibrium deformations, 20: 15843
MANI, G. S., Reaction mechanism for $^{11}B(\alpha,n)^{14}N$ reaction, 20: 15790
MANI, H. S., SU(n) crossing matrices for baryon-meson scattering, 20: 15322
MANISTA, Eugene J., Distortion of atomic-beam velocity distributions due to classical hard-sphere gas scattering, 20: 15247 (N65-15530)
MANOILOVA, I. G., Transport mechanism in samarium sulfide, 20: 15981
MANOWITZ, Bernard, Neutron burning of long-lived fission products for waste disposal, 20: 16132 (BNL-8558)
MANTEIFEL', V. M., Role of the mitochondrial apparatus of lymphocytes in their response to ionizing radiation, 20: 14335
MAR, B. W., Electron shielding analysis for space vehicles, 20: 15936
MAR, Raymond W., Vaporization studies of lanthanum fluoride, 20: 14515 (UCRL-16649)
MARCHUK, G. I., Critical parameters of homogeneous breeding systems, 20: 16030
MARCINKOWSKI, Andrzej, Proportional counter as spectrometer for low-energy γ and β rays, 20: 14879
MARIC, Z., Theory of double-charge-exchange nuclear reactions with π mesons, 20: 15813
MARINOV, M. S., Strong interactions and relativized SU(6) symmetry U(12). Meson-baryon scattering, 20: 15390
MARISCHEV, V. A., Structure of grain boundaries in molybdenum and its alloys with zirconium and rhenium, 20: 15128
MARK, Hans, New applications for nuclear energy, 20: 14665
MARKELOV, V. N., New data on atmospheric radioactivity and fallout density near Black Sea, 20: 14741
MARKL-MUSYL, I., Device for measuring continuously alpha activity of flowing solutions, 20: 14871
MARKOVSKII, E., Alteration of anti-friction and strength characteristics of engineering materials, subjected to neutron irradiation, 20: 15140
MARMER, E. N., High-temperature heaters made with niobium and zirconium carbides, 20: 15112
MAROLI, C., Kinetic theory of high-frequency resonance gas discharge breakdown, 20: 15575
MARONI, C., Internal Compton effect at small angles, 20: 15815
MARSHALL III, J. Howard, $K^+\Lambda$ photoproduction from hydrogen, 20: 15393
MARSHALL, R. W., Prog. rpt. on radiation effects on microelectronic circuits, 5–7/65, 20: 14918 (ECOM-01313-1)
MARSHALL, S. W., Effect of crystal size on Moessbauer recoil-free fraction in ^{197}Au, 20: 15962
MARSHALL, T. W., Classical treatment of dispersion forces, 20: 15152
MARSICO, B., Neutron diffusion parameters in benzene, 20: 15676
MARTALOGU, N., Polarization of protons from elastic and inelastic scattering on ^{24}Mg, 20: 15806
MARTI, K., Rare gas measurements in 30 stone meteorites, 20: 15193 (NP-15654)
MARTIN, A., Qualitative and quantitative consequences of analyticity and unitarity, 20: 15518
MARTIN, D. W., Bibliography on atomic and molecular processes, 1964, 20: 15248 (ORNL-AMPIC-3)
MARTIN, H. J. Jr., π^+p Interactions at 781 Mev, 20: 15341
MARTIN, Heather, Measurement of ^{47}Ca absorption by whole-body gamma spectrometry, 20: 14247
MARTIN, J. P., Rover postoperational destruct instrumentation development, 20: 16112 (SC-RR-65-551)
MARTIN, Joan C., Spatial avoidance in paradigm in which ionizing irradiation precedes spatial confinement, 20: 14366
MARTIN, Robert D., Operating experience with a heavy water reflector tank, 20: 16128
MARTIN, W. R., Metal-clad fuel element with copper foil interlayer, 20: 16056
MARTINEZ, J. L., Thin film evaporation rate monitor, 20: 14819 (RFP-602)
MARTINIS, M., W spin and the rotation group in four dimensions, 20: 15467
MARTINSON, R. M., Large aperture seismic array signal handling system, 20: 14760
MARTNA, J., Heat resistance of concrete, 20: 15051 (NP-15876)
MARUYAMA, Shizuo, Estimation of genetically significant dose due to therapeutic radiation in Japan, 20: 14799
MARUYAMA, Y., X-ray and fast neutron survival response of 5-bromodeoxycytidine-treated bone marrow cells, 20: 14333
MASHOVETS, T. V., Defects formed in indium antimonide by γ irradiation, 20: 15979
MASI, G., Control of polyphenyls in work environments, 20: 14467 (RT/PROT(64)–20)
MATHEWS, P. M., Relativistic Schroedinger equations for particles of arbitrary spin, 20: 15567
MATHEWS, William G., Time evolution of H II region, 20: 15199
MATINYAN, S. G., Threshold behavior of partial amplitudes of inelastic processes, 20: 15500
MATOUSEK, J., Systematic observation of long lived radioactivity in Pilsen region, 20: 14813
MATSUBARA, Takeo, Diffusion length of thermal neutrons in terphenyl (Santowax-R) at temperatures up to 400°C, 20: 15680
MATTOX, D. M., Design considerations for ion plating, 20: 14670 (SC-R-65-997)
MATUMURA, On, Far-infrared vibration mode in $SrCl_2$, 20: 15958
MATZNER, B., Critical heat flux in long tubes at 1000 psi with and without swirl promoters, 20: 14695
MATZNER, B., Transient DNB test on CVTR fuel assembly, 20: 16101
MATZNER, Bruce, Additional critical heat flux data for large-diameter, internally heated, eccentric annuli at 1000 psia, 20: 16086 (TID-22651)
MAUNG, Tin, π-π Interaction in reaction $\pi^- + p \rightarrow \pi^0 + \pi^0 + n$ at 378 Mev, 20: 15368
MAURO, S., Excitation spectrum of superimposed normal and superconducting films, 20: 15653
MAUTNER, Henry G., Production of ^{75}Se-selenocystine by neutron activation, 20: 14630
MAUTZ, E. W., Comparison of electrolytic and ferrosilicon-process magnesiums for uranium production, 20: 15050 (NLCO-970, pp 3.1-4)
MAUTZ, E. W., Effect of furnace heating element arrangement on uranium metal quality, 20: 14964 (NLCO-970, pp 2.1-7)
MAVRODIN, Marie, New ytterbium compounds with organic acids, 20: 14490
MAXEY, T. J., Redundancy design for Vela spacecraft, 20: 15598
MAY, F., Counting of neutrons at small counting rates: elimination of γ background and electronic disturbances, 20: 14863
MAYINGER, F., Prog. rpt. on critical heat flux in boiling water, 4–8/65, 20: 14686 (EURAEC-1448)
MAYMAN, S., Nondestructive measurement of burnup by γ-ray spectroscopy, 20: 14504
MC ALLISTER, R. A., Flooding in perforated-plate pulsed extraction columns, 20: 14462 (ORNL-3890)
MC BRIDE, J. P., Preparation of UO_2 microspheres by sol-gel technique, 20: 15008 (ORNL-3874)
MC CALLUM, K. J., Radiolysis of trifluoroethanol, 20: 14590
MC CARTHY, Arthur Lancelot, Survey of isomers with half lives in the range 5 to 1000 microseconds, 20: 15856
MC CLANAHAN, R. J., Sterilization of carrot rust fly by irradiation with ^{137}Cs, 20: 14317
MC COLL, J. R., Sizable proton polarization using a spin refrigerator,

20: 15964
MC COMBS, H. Lewis, Distribution of ^{210}Po in pulmonary tissues of cigarette smokers, 20: 14798
MC CORMICK, Norman Joseph, One-speed neutron transport problems in plane geometry, 20: 15684
MC CRIGHT, R. D., Thermoelectric cooling of cutting tools, 20: 14689 (NLCO-970, pp 5.1-7)
MC CUNE, J. E., Three-dimensional normal modes of Vlasov plasma with and without magnetic field, 20: 15879 (IPP-6/43)
MC DANIEL, E. W., Bibliography on atomic and molecular processes, 1964, 20: 15248 (ORNL-AMPIC-3)
MC DONALD, F. A., Application of Pade approximant to scattering theory, 20: 15363
MC DONALD, R. R., Automatic recording, low-temperature dilatometer, 20: 14821 (RFP-668)
MC DONALD, R. R., Precision back-reflection Laue camera, 20: 14820 (RFP-636)
MC DONALD, W. G., Ocean-bottom seismic observatories, 20: 14767
MC DONELL, W. R., ^{244}Cm for radioisotopic heat sources work at Savannah River laboratory, 20: 15038 (CONF-660305-12)
MC DUFF, Henry C. Jr., Urinary complications following combined interstitial radiation and node dissection therapy for cervical cancer, 20: 14377
MC FEE, A. F., Skeletal defects in prenatally irradiated sheep, cattle and swine, 20: 14337
MC GILLIS, D. A., Sensitized fluorescence in vapors of alkali metals. V., 20: 15253
MC GONNAGLE, W. J., Non-destructive testing in reactor pressure-vessel fabrication, 20: 14710
MC GRATH, R. A., Breakdown of DNA in x-irradiated Escherichia coli, 20: 14265
MC GUIRE, Eugene Joseph, Model for atomic excited states, 20: 15270
MC HENRY, R. E., Hot presses for glove box and manipulator cell, 20: 14666 (ORNL-P-1946)
MC KEE, D. W., Catalytic activity of noble metal alloys, 20: 14542
MC KINLEY, John M., Simultaneous determination of parameters of the core-particle model in ^{197}Au, 20: 15803
MC NUTT, James E., Method of treating columbium-base alloy, 20: 14972
MEAKIN, J. D., Friction stress and micro-yielding of beryllium, 20: 15067
MEDNIKOVA, L. S., Deflecting properties and dispersion of electrostatic prism spectrometer, 20: 14868
MEDVEDEV, B. I., Nuclear moments of inertia, 20: 15835
MEECHAM, W. C., Simplified normal mode treatment of long-period acoustic-gravity waves in the atmosphere, 20: 15611
MEER, M., Experimental evidence on C violation in η decay, 20: 15430
MEER, M., Search for the decay $\eta^0 \rightarrow \pi^0 e^+ e^-$, 20: 15427
MEERT, M., Double ionization accompanying ^6He decay, 20: 15715 (CONF-233(Vol.3), pp 505-9)
MEFOD'EVA, M. P., Formation of pentavalent neptunium complexes in lactate and glycolate solutions, 20: 14556
MEIJER, A. C., Measurements of wall-thickness variations in long straight tubes, 20: 14816 (EUR-2512.n)
MEILING, V., Applicability of the Ikegami-Udagava method for considering pairing correlations, 20: 15766
MEISEL, Lawrence V., Electron drift velocity in gas filled, cylindrical, thermionic diodes, 20: 15303
MEISEL', M. N., Role of the mitochondrial apparatus of lymphocytes in their response to ionizing radiation, 20: 14335
MELAIKA, E. A., Prog. rpt. on alkali metals evaluation, 7-9/65, 20: 15028 (AGN-8166)
MELEKHONOVA, I. I., Oxidation of technical paraffin wax with oxygen under action of γ-irradiation, 20: 14612
MELIK-GAIKAZYAN, I. Ya., Generation of vacancies in KBr–Sr irradiated by a proton beam, 20: 15977
MELISSINOS, A. C., π-meson production in p-p collisions, 20: 15336
MELISSINOS, A. C., Production processes in low-energy p-p collision, 20: 15426
MELTZER, C. M., Observations of $Y_1^*(1405)$ and $Y_1^*(1358)$ resonances in π-N collisions at 1.68 Bev/c, 20: 15404
MELVIN, M. A., Orbits in a magnetic universe, 20: 15634
MENDELSON, M. R., First-order solutions of one-speed transport equations in plane multiregion geometries, 20: 15674
MENETREY, Maurice, Detection of can ruptures in the Latina power plant, 20: 16070 (EUR-2420.d,f,i,n,e, pp 181-9)
MERCER, B. W., Adsorption of trace ions from intermediate-level radioactive wastes by ion exchange, 20: 14434 (BNWL-180)
MERCER, B. W., Storage of long-lived fission products on alumino-silicate zeolites, 20: 14466 (RL-SA-58)
MERCER, Thomas T., Deposition and retention models for internal dosimetry of human respiratory tract, 20: 14796
MERKULEV, Yu. A., Use of pulsed neutron generator to determine neutron diffusion parameters of rocks and fluids, 20: 14772
MERKULOV, A. G., Precipitation of scandium from hydrochloric acid solutions by sodium silicofluoride, 20: 14566
MERLO, J. P., Reaction $\pi N \rightarrow \pi N^*(1238)$ near the N*(1510) and the N*(1690) resonances, 20: 15375
MERRITT, Janet S., Atomic M-level widths in ^{151}Sm, 20: 15241 (CONF-233(Vol.3), pp 454-64)
MERRITT, Janet S., K-shell fluorescence yields of V, Cr, and Cu, 20: 15242 (CONF-233(Vol.3), pp 465-79)
MERTA, Andrzej, Application of motor-car engine for control of air pollution with radioactive aerosols, 20: 14672
MERTL, F., Systematic observation of long lived radioactivity in Pilsen region, 20: 14813
MESHCHERYAKOV, V. A., Interactions $\gamma 3\pi$ and $\rho\pi\gamma$, 20: 15389
MESTEL, L., Gravitational collapse of uniform spheroid, 20: 15206
METTLER, Alan J., Monte Carlo calculations of gamma-ray streaming through coplanar and noncoplanar ducts, 20: 15929 (AD-627890)
MEWE, R., Spectroscopic determination of electron temperature in a helium plasma, 20: 15908
MEYER-BERKHOUT, U., Search for hyperon resonances with spark chambers, 20: 15417
MEYER-BERKHOUT, U., Symposium on electron and photon interactions at high energies, Hamburg, 6/65. I., 20: 15437
MEYEROTT, Arthur J., Observations of cosmic x-rays, 20: 15220
MICHA, David A., Angular distribution of products of hydrogen atom-hydrogen molecule reactions, 20: 15252
MICHA, David A., Exchange reaction of H and H_2, 20: 14518
MICHAEL, B. D., Transient species produced in irradiated water and aqueous solutions containing oxygen, 20: 14614
MICHALYAK, S., Experimental investigation of transient radiation, 20: 15268
MICHELSEN, O. B., Radiochemical and nuclear studies of short-lived fission products ^{145}Ce, ^{146}Ce, and ^{147}Ce, 20: 15722 (KR-76)
MICHIYOSHI, Itaru, Current-voltage characteristics of Cs thermionic converters operated at relatively low temperature, 20: 15301
MIDDLEMAS, N., Pion-proton charge-exchange scattering near 2.0 Bev/c, 20: 15378
MIELCARSKI, Mieczyslaw, Concept of fast breeder reactor with fused salt fuel and boiling mercury "wars", 20: 16036
MIELCARSKI, Mieczyslaw, Concept of salt-boiling fast breeder reactor, 20: 16037
MIHELICH, J. W., Decay of ^{153}Sm(47h) to ^{153}Eu, 20: 15795
MIKHALYAK, S., Investigation of the transition effect, 20: 15317 (ORNL-tr-677)
MIKHAN, V. I., Use of reactors of Beloyarsk atomic power plant type for dual-purpose desalinization systems, 20: 16107 (JPRS-33406)
MILEY, D. V., Optical determination of depth of defects by replication techniques, 20: 14966 (RFP-673)
MILEY, G. H., Thermal-neutron pulse propagation, 20: 15678
MILLER, David B., Investigation of plasma accelerator (cyclotron resonance propulsion system), 20: 14726 (NASA-CR-54746)
MILLER, Donald H., Enhancements in interactions of 3.2 Bev/c π^- with deuterium, 20: 15405
MILLER, I., Single-particle exchange in 3-particle final states of the reaction K+p at 2.26 Bev/c, 20: 15422
MILLER, J. N., Attenuation of virulent Treponema pallidum by means of gamma irradiation, 20: 14308
MILLER, K. T., Oriented growth of oxidation products on single crystals of uranium monocarbide, 20: 14985
MILLER, Richard H., Prog. rpt. on computer research, 11/65, 20: 14950 (COO-614-41)
MILLER, V. V., Use of pulsed neutron generator to determine neutron diffusion parameters of rocks and fluids, 20: 14772
MILLS, L. E., Fuel element for a nuclear reactor, 20: 16057
MILLS, Norman David, Low-temperature thermal expansion of Ho and Er sesquioxides, 20: 15660
MILLS, R. G., Evaluation of vapor-deposited tungsten tubing, 20: 15048 (N65-16231)
MILLS, R. M., Prog. rpt. on Piqua power facility operations analysis, semiannual, 1-6/65, 20: 16077 (NAA-SR-11628)
MILLS, W. R. Jr., Theoretical and experimental model results in neutron lifetime logging, 20: 14775
MINEHART, R. C., Evidence for hyperon states with masses greater than 1900 Mev, 20: 15424
MINOR, A., Influence of CsF on emitter work function and the performance of Cs diodes, 20: 15297 (CONF-640921, pp 101-9)
MISHIMA, J., Pu release studies. I., 20: 15036 (BNWL-205)
MISHIMA, Yasushi, Cosmic ray intensities under sea-water at depths down to 1,500 meters, 20: 15289
MISHIMA, Yoshitsugu, Some preliminary tests on beryllium ingot, produced by arc-melting, 20: 15118
MITCHELL, E. P., Prog. rpt. on radiation effects on microelectronic circuits, 5-7/65, 20: 14918 (ECOM-01313-1)
MITCHELL, Thomas P., Evolution of solar magnetic field, 20: 15223
MITRA, A. N., $\eta\pi\pi$ Model of χ^0 and a possible η-π resonance, 20: 15355

MITRA, A. N., Nonrelativistic quark model for baryons, 20: 15477
MITSUTANI, Akio, Effect of preirradiation on activated charcoal, 20: 14609
MITTELMANN, Alice, Studies in I metabolism. IV., 20: 14250
MITYUSHOVA, N. M., Oxygen effect on post-irradiation restoration of yeast cells, 20: 14399
MIWA, H., Beta-ray back-scattered type thickness gage for galvanizing process, 20: 14839
MIYAKOSHI, Junichi, γ Shielding property, strength and workmanship of built-up type lead slab structure, 20: 15932 (ORNL-tr-843)
MIYAMOTO, Shigeneri, Cosmic ray intensities under sea-water at depths down to 1,500 meters, 20: 15289
MIYASAKA, S., User's manual for JRR-4 experimental facilities, 20: 16122 (JAERI-6016)
MIZUKOSHI, T., Beta-ray back-scattered type thickness gage for galvanizing process, 20: 14839
MIZUNO, Yukio, Electron interaction and positron annihilation in electron gases, 20: 15383
MOCCIA, Achille, Tests on components for Eurex 2AW plant, 20: 14644
MOCHIZUKI, Keiichi, Feasibility calculation for JPDR-II core design; one-dimensional nuclear thermal and hydraulic calculation, 20: 16076 (JAERI-1088)
MOCOROA, A., Isomeric cross-section ratios for ^{134m}Cs, ^{134}Cs, and ^{133m}Ba, ^{133}Ba formed in (d,p) and (d,2n) reactions, 20: 15778
MODESITT, G. E., Statistical analysis of spacecraft replenishment, 20: 15600
MODISETTE, Jerry L., Model solar proton environments for manned spacecraft design, 20: 15191 (N65-20996)
MOECK, E. O., Critical heat flux in long tubes at 1000 psi with and without swirl promoters, 20: 14695
MOEHL, D., Development of 100-Mev FFAG electron synchroton: broad-band adaptation of accelerator electrodes, 20: 15161 (NP-15273)
MOHAN, Gyan, SU(n) crossing matrices for baryon-meson scattering, 20: 15322
MOHAN RAO, Pendurty Krishna, Biological effects of multiple treatments with radiation and diethyl sulfate on barley, 20: 14384
MOHINDRA, V. K., Canadian fallout data for October 1965, 20: 14737 (NP-15853, pp 8-20)
MOHINDRA, V. K., Reactor environment monitoring for October 1965, 20: 14738 (NP-15853, pp 21-33)
MOLE, R. H., Radiobiological aspects of supersonic transport, 20: 14797
MOLER, R. B., Measurement of the M/L-capture ratio in 30-million-year ^{205}Pb decay, 20: 15714 (CONF-233(Vol.2), pp 369-70)
MOLINARI, V. G., Neutron diffusion parameters in benzene, 20: 15676
MONCHINSKII, A. G., Use of reactors of Beloyarsk atomic power plant type for dual-purpose desalinization systems, 20: 16107 (JPRS-33406)
MONGA, S. K., Hypertriton binding energy with nonlocal separable potentials, 20: 15812
MONIER, L. F., Detection of pulse pile-ups with pulse overlap to pulse height converter, 20: 14828
MONNIER, Marcel, Early action of gamma radiations on electrical brain activity and behavior in rabbit, 20: 14326
MONTGOMERY, Donald W., Device for storage of heat evolving material, 20: 14679
MONTGOMERY, Leslie D., High-temperature thermal diffusivity of UO_2 under transient conditions, 20: 15031 (ANL-7116)
MONTVAY, Istvan, Dirac's δ function and the distribution theory, 20: 15628
MOON, Joon Sang, Longitudinal dispersion in single-phase liquid flow through ordered and random packings, 20: 14691 (UCRL-10696(Rev.) (Pt.2))
MOORE, Barry Hilton, Infrared spectra of neoprene before and after gamma irradiation, 20: 14585 (TID-22652)
MOORE, R. L., Fission product recovery research at Battelle-Northwest, 20: 14436 (BNWL-SA-504)
MOORE, R. T., Techniques for détection of high-altitude nuclear explosions, 20: 15612
MOORES, Harry, Improvements relating to electric safety systems for nuclear reactors, 20: 16006
MOORHEAD, T. P., Dependence of breeding upon design parameters of large fast reactors, 20: 16093
MOORHOUSE, R. G., Analysis of pion-nucleon scattering and lower nucleon isobars, 20: 15381
MORAGA B., Aldo, Uranium exploration in Chile, 20: 14779 (RME-4569 (Rev.))
MORGAN, A., Prog. rpt. on direct biological monitoring, 1963–64, 20: 14784 (AERE-R-5015)
MORGAN, J. R., Compressibility of oriented alpha plutonium, 20: 15095
MORGENSTERN, J. C., Propagation of ground wave electromagnetic signal, with particular reference to pulse of nuclear origin, 20: 15606
MORI, Kenji, Stress corrosion cracking of Ti and Zr in HCl–methanol solutions, 20: 14988
MORINO, Yonezo, Third-order potential constants of bent XY_2 molecules, 20: 14559
MORITA, Kazuo, Radiation treatment of cancer of lung, 20: 14420
MORIYAMA, Hideo, Studies on x-agent. XLIV., 20: 14622
MORRISON, David L., Prog. rpt. on applicability of existing data to analytical description of a nuclear-reactor accident, 10–12/65, 20: 16019 (BMI-X-10154)
MORROW, Paul E., Deposition and retention models for internal dosimetry of human respiratory tract, 20: 14796
MORTADA, Aly, Supervoltage x-irradiation of epithelial tumours of lacrimal gland, 20: 14410
MORTON, Margaret A., Demineralization with EDTA by constant replacement, 20: 16149 (NYO-2779-10)
MORTON, P. L., Longitudinal wake fields of pulse of charge moving down straight pipe of circular cross section with finite conductivity, 20: 15167 (SLAC-49, pp 18-22)
MOSER, Manny H., Transfers of water and electrolytes across granulation tissue in patients following burns, 20: 14255
MOSKVIN, A. I., Formation of pentavalent neptunium complexes in lactate and glycolate solutions, 20: 14556
MOSLEY, W. C. Jr., ^{244}Cm for radioisotopic heat sources work at Savannah River laboratory, 20: 15038 (CONF-660305-12)
MOSSEL, D. A. A., Elimination of salmonellae from proteinaceous foods with irradiation, 20: 14933
MOSTERT, P., Dodewaard nuclear power station, 20: 16094
MOTT, J., V-2-prong K$^-$p interactions at 5.5 Bev/c, 20: 15416
MOTZ, Robin O., Alfven wave generation in a spherical system, 20: 15581
MOWER, Lyman, Decay theory of closely coupled unstable states, 20: 15816
MUELLER, J. H., Development of thorium purification system, 20: 14448 (NLCO-970, pp 1.1–22)
MUELLER, N., Prog. rpt. on fabrication of UO_2 powders and processing into fuel elements, 4–6/65, 20: 14999 (EURAEC-1466)
MUELLER, P., Automatic inspection of nuclear-reactor tubes during production and processing, using eddy-current methods, 20: 14720
MUELLER, P., Measurement of physical properties of reactor components and irradiated materials, 20: 14719
MUELLER, Robert A., Thermal neutron flux perturbation by Dy–Al foils in H_2O and UO_2F_2–H_2O solutions, 20: 15669 (NASA-TN-D-3237)
MUENZER, H., Reaction $^{18}O(n,\alpha)^{15}C$ around 14 Mev, 20: 15738
MUIRHEAD, H., High-energy γ rays from pion capture, 20: 15794
MUIRHEAD, H., Reaction (π^-,2n) in ^{6}Li and ^{7}Li, 20: 15793
MUKAIYAMA, Takeshi, Diffusion length of thermal neutrons in terphenyl (Santowax-R) at temperatures up to 400°C, 20: 15680
MULLER, Rolf H., Measurement of heat released on solid surfaces, 20: 16153 (UCRL-16472)
MUNEY, W. S., Solar x-ray images obtained using grazing incidence optics, 20: 15203
MUNIR, B. A., Conference on resonant particles, Ohio University, 6/65, 20: 15398
MUNIR, B. A., Exchange mechanism in p-p interactions at 2.80 Bev/c, 20: 15423
MURPHREE, R. L., Skeletal defects in prenatally irradiated sheep, cattle and swine, 20: 14337
MURPHREE, R. L., Sperm production by chronically irradiated bulls, 20: 14336
MURPHY, P. G., Differential cross sections and polarization effects in pion-proton elastic scattering at 875 to 1579 Mev/c, 20: 15372
MURRAY, B. C., Ground-based optical detection of deep space nuclear detonations, 20: 15608
MURRAY, Joseph J., Spin and parity of the Ξ^* (1530 Mev), 20: 15464
MUSAL, Henry M. Jr., Parameters and governing equations for compressible anisotropic plasma, 20: 15913
MUTA, Nobuyoshi, Radiation treatment of cancer of lung, 20: 14420
MUTCHLER, G. S., The energy and angular distribution of photoneutrons from heavy elements, 20: 15723 (MIT-2098-162)
MUTCHLER, Gordon Sinclair, The angular distributions and energy spectra of photoneutrons from heavy elements, 20: 15724 (MIT-2098-224)
MYDOSH, John A., Critical currents in superconducting films, 20: 15662
MYERS, D. K., Biochemical effects of x-irradiation on erythrocytes, 20: 14275
MYERS, O. E., Kinetics of trihalide exchange, 20: 14573
MYRE, W. C., Modular system of logic for the Vela satellite program, 20: 15597

N

NABICHVRISHVILI, V. A., Polarized γ radiation emitted during Coulomb excitation, 20: 15759
NADYKTO, B. T., Interaction of oxygen with a Nb surface, 20: 15976
NAG, B. D., Method for studying maturation time of average bone marrow cell in rat using ^{32}P as tracer, 20: 14248
NAGAHATA, Yasuo, γ Shielding property, strength and workmanship of built-up type lead slab structure, 20: 15932 (ORNL-tr-843)
NAGASAKI, R., Diffusion of xenon in metals, 20: 15090
NAGAYA, Yutaka, Radioactive contamination of Indo-Antarctic Ocean water

in early parts of 1961 and 1962, 20: 14749
NAGY, L., Investigations in field of radiation-induced solid state polymerization, 20: 14586
NAIK, Mool Chandra, Diffusion of iron, of silver and of carbon in beryllium, 20: 15037 (CEA-R-2621)
NAITOH, Yoshitake, Feasibility calculation for JPDR-II core design; one-dimensional nuclear thermal and hydraulic calculation, 20: 16076 (JAERI-1088)
NAKAGAWA, Yasuaki, Neutron-diffraction study of Cr_2As, 20: 15954
NAKAHARA, Yoshinori, Radiation leak test of shielded cells at reprocessing analytical facility, 20: 14788 (JAERI-1089)
NAKAJIMA, K., Determination of uranium content in scraps, 20: 16140
NAKAJIMA, S., Superconductivity in ferromagnetic alloys, 20: 15648
NAKAMURA, Hiroki, Collisional excitation transfer between atoms in near-resonant processes, 20: 15255
NAKANO, Takeo, Radiation damage of carrier life time in p type Si, 20: 14922
NAKASIMA, Kenshiro, Radiation damage of carrier life time in p type Si, 20: 14922
NAKAYAMA, Toshio, Kinetic structure of a plasma, 20: 15899
NAMBOODIRI, M. N., Isomeric cross-section ratios in (n,γ) reactions on ^{130}Te and ^{110}Pd, 20: 15777
NAMBU, Y., Nonleptonic decays of hyperons, 20: 15369
NAQVI, J. H., Deuteron photodisintegration with a separable two-nucleon potential, 20: 15789
NARAYANASWAMY, P., Bhabha's irreducible spin (½,½) equation as basis of strong-interaction symmetries, 20: 15471
NARIAI, Hidekazu, A simple and well-adjusted exterior metric for collapsing or anti-collapsing star, 20: 15228
NASH, Donald J., Effects of x-irradiation upon post-natal growth in mouse, 20: 14315
NASSIFF, S. J., Isomeric cross-section ratios for ^{134m}Cs, ^{134}Cs, and ^{133m}Ba, ^{133}Ba formed in (d,p) and (d,2n) reactions, 20: 15778
NAUMOVA, I. I., Quantitative determination of nickel and iron in ferromagnetic films by neutron activation, 20: 14489
NEEB, Karl Heinz, Determination of trace impurities in UO_2 fuel materials, 20: 14494
NEEL, R. B., Chemical processing of Cm, 20: 14636 (CONF-660305-7)
NE'EMAN, Yuval, Band spectra generated by non-compact algebra, 20: 15506
NEFKENS, B. M. K., Decay spectrum of $K^o_{\mu 3}$, 20: 15331
NEIDER, R., Microradiographic fuel investigation in thin layers, 20: 14704
NELEPO, B. A., New data on atmospheric radioactivity and fallout density near Black Sea, 20: 14741
NELEPO, B. A., Radioactivity of air over Atlantic Ocean in May to July, 1964, 20: 14743
NELKIN, Mark, Atomic motions in rigid sphere gas as a problem in neutron transport, 20: 15675
NELKIN, Mark, Brillouin scattering by gases as test of Boltzmann equation, 20: 15580
NELMS, J. R., Spectrochemical method for simultaneous determination of calcium, lithium, and potassium in high-purity thorium compounds, 20: 14443 (MCW-1493, pp 27-30)
NELSON, Arne, Placental transfer of ^{85}Sr in mice, 20: 14244
NELSON, Neal S., Ionizing radiation for measuring biological phenomena, 20: 14386
NELSON, R. D., Low-temperature allotropic transformations in plutonium, 20: 15034 (BNWL-49)
NESS, Norman F., Extension of photospheric magnetic field into interplanetary space, 20: 15215
NESTEROVSKII, V. V., Oxidation of technical paraffin wax with oxygen under action of γ-irradiation, 20: 14612
NEUFELD, Jacob, Calculation of radiation dose from protons and neutrons to 400 Mev, 20: 14330
NEUMANN, Leo, Survey of chemical technology in nuclear industry, 20: 14429
NEUMANN, N. F., Energy dispersion system for light element analysis with electron microprobe, 20: 14442 (MCW-1493, pp 5-13)
NEVINITSA, A. I., Critical parameters of homogeneous breeding systems, 20: 16030
NEWBOLT, W. B., E2 conversion coefficients in ^{110}Cd and ^{132}Xe, 20: 15704 (CONF-233(Vol.2), pp 164-76)
NEWCOMBE, H. B., Radiobiological aspects of supersonic transport, 20: 14797
NEWHOUSE, T. W., Ocean-bottom seismograph, 20: 14765
NEWTON, D., Pion-proton charge-exchange scattering near 2.0 Bev/c, 20: 15378
NEZRICK, F. A., Fission-antineutrino interaction with protons, 20: 15330
NICHOLAS, M., Wetting of UC by copper and gold, 20: 14551
NICHOLS, J. P., Storage of irradiated fuel elements at reactor plants, 20: 14803
NICROSINI, F., Variations of hepatic lipid components in mouse after whole-body irradiation with lethal dose, 20: 14268
NIEMEYER, R. G., Radioisotope sources and source testing, 20: 14789 (ORNL-P-1910)
NIEWODNICZANSKI, Jerzy, Debalancing of differential x-ray filters, 20: 14487
NIKITIN, F. V., Evaluation of gamma-emitter activity in x-ray absorption analysis, 20: 14498
NIKITIN, G. A., Flaw detection in thin-walled tubes, 20: 14713
NIKLAUS, J. P., Measurement of free and incoherent neutron cross sections of silicon and lead, 20: 15682
NIKOLENKO, V. G., Determination of neutron resonance spins in ^{165}Ho nuclei, 20: 15681
NILSON, Arne E., Vesico-ureteric reflux in connection with supervoltage therapy for bladder carcinoma, 20: 14298
NILSSON, Jan S., Consistent theory of weak interactions, 20: 15481
NINAN, C. A., Naturally occurring haploid embryo in coconut palm (Cocos nucifera L.), 20: 14320
NISHIJIMA, K., Arbitrariness in choice of field operators, 20: 15516
NISHIMAKI, Ko, γ Shielding property, strength and workmanship of built-up type lead slab structure, 20: 15932 (ORNL-tr-843)
NISTOR, C., Statistics of scaled pulses, 20: 14890
NITU, R., Multiplicity of neutral pions produced in 9 Bev/c two-prong π^-p interactions, 20: 15384
NOBBE, Louis B., Measurement of heat released on solid surfaces, 20: 16153 (UCRL-16472)
NOLAN, James F., Mixed heterologous mesenchymal sarcomas (mixed mesodermal sarcomas) of uterus, 20: 14301
NOMURA, Tsutomu, Reactivity measurements by reactor noise analysis using two-detector correlation method, 20: 16027
NONEMAN, E. M., Redundancy design for Vela spacecraft, 20: 15598
NORDBERG, Ulla-Brita, Record form for external beam therapy designed specially for ^{60}Co treatment with stationary fields, 20: 14408
NORINDER, Olov, Flux-shape eigenfunction tables for two-zone slabs, 20: 16024 (RFR-231)
NORINDER, Olov, Flux-shape eigenfunction tables for two-zone cylinders, 20: 16025 (RFR-232)
NORRIS, W. P., Automatic handling of data from large-scale dog radiation experiment using general purpose computer, 20: 14238 (CONF-650560-13)
NORTH, J. C., Measurement of length changes to 0.1 A in irradiated germanium at low temperature, 20: 15147
NORTON, F. J., Catalytic activity of noble metal alloys, 20: 14542
NORTON, R. E., Interpretation for singularities in the physical region, 20: 15524
NOTTELMANN, Werner, Radiation transmitter, 20: 14864
NOTTINGHAM, Wayne B., Theoretical background for thermionic conversion including space-charge theory, 20: 15299 (NASA-TN-D-3324)
NOVAK, V., New complexes. III., 20: 14521
NOVAKOVIC, M., New method of burnout detection, 20: 14694
NOWELL, Peter C., Radiation carcinogenesis: sequence of events, 20: 14373
NOWOTNY, H., Some new η carbides, 20: 15103
NOWOTNY, H., Systems niobium–chromium–carbon and tantalum–chromium–carbon, 20: 15108
NUVOLONE, U., Polyvinylpyrrolidone in treatment of radiation sickness. Radiotoxins, 20: 14396
NYSTROEM, U., Ultrasonic detection of longitudinal defects in thin-wall cladding tubes, 20: 14716

O

OBENCHAIN, R., LASA sensing system design, installation, and operation, 20: 14759
OBOLONCHIK, V. A., Study of niobium and tantalum sulfides, 20: 14554
O'BOYLE, M. J., Prog. rpt. on Yankee core evaluation, semiannual, 9/65, 20: 16091 (WCAP-6078)
O'DONNELL, P. J., Analysis of pion-nucleon scattering and lower nucleon isobars, 20: 15381
OEHME, R., Lorentz covariant supermultiplet scheme, 20: 15538
OGANESYAN, K. O., Production cross section of charged pions in (n,p) collisions, 20: 15310 (JINR-P-2508)
OGAWA, Shinji, Ferromagnetic resonance in $ZrZn_2$, 20: 15960
OGIMOTO, Takesi, Small wave-function renormalization constants implied by a partially conserved axial-vector current, 20: 15402
OGLAZA, Jan, Flocculants for treatment of radioactive waste water by mineral sorbents, 20: 16138
OGORODNIKOV, B. I., Content of submicroscopic aerosols of short-lived daughter products of radon in mine air, 20: 14747
O'HALLORAN, Thomas, Single-pion production by 1.96-Bev/c K+ mesons, 20: 15335
OHAMA, Nobuhiko, Far-infrared vibration mode in $SrCl_2$, 20: 15958
OHTSUKI, Yoshihiko H., Relativistic dynamical theory of electron diffraction containing inelastic scatterings, 20: 15959
OKA, Yoshinosa, Amine extraction of radioruthenium as chlorocomplex, 20: 14650

OKABAYASHI, Takao, Extension of inversion with a non-Abelian group of parity tripod, 20: 15494
OKABE, Shigeru, Energy monitor for electron beams, 20: 15184
OKADA, Shigefumi, Study of mechanisms of radiation-induced reproductive death of mammalian cells in culture, 20: 14367
OKADA, Tokuji, Radiation chemistry of cyclic dienes. I., 20: 14610
OKASAKA, Rei, Spectroscopic studies on helium plasma heated by reflected shock in T tube, 20: 15896
OKUBO, Susumu, Impossibility of having exact U(6) group based upon algebra of currents, 20: 15444 (IC/66/14)
OKUN, L., Neutral α particles, 20: 15504
OKUN, L. B., Possible properties of CP-violating non-leptonic interactions, 20: 15433
OKUN, L. B., Quarks: astrophysical and physico-chemical aspects, 20: 15435
OLAH, George A., Kinetic isotope effects and their role in study of mechanism of electrophilic aromatic substitutions, 20: 14577
OLES, A., Study of UAs_2 by neutron diffraction, 20: 15949
OLIVER, R., Whole-body counter for clinical measurements utilizing "shadow shield" technique, 20: 14422
OLSEN, C. S., Attempted determination of nitrate in fired thoria using infrared techniques, 20: 14468 (TID-22505)
OLSEN, Robert L., Ultraviolet erythema, 20: 14310
OLSON, F. A., Attempted determination of nitrate in fired thoria using infrared techniques, 20: 14468 (TID-22505)
OLSSON, P. O. M., Hypergeometric function of two variables of importance in perturbation theory. I., 20: 14952
ONO, H., Errors of gamma-scattering density meter and its design for low density measurement, 20: 14837
ONO, Yoshimi, Effects of ionizing radiation to central nervous system, 20: 14350
ONO, Yusuke, Gaschromatographic determination of scandium as acetylacetonate and trifluoroacetylacetonate, 20: 14486
ONUFRIEV, V. G., Decay scheme of ^{109}Sn, 20: 15752
ONUFRIEV, V. G., Isomeric transitions of $^{114*}In$ and $^{115*}Te$, 20: 15753
ONUKI, Mamoru, Radiation leak test of shielded cells at reprocessing analytical facility, 20: 14788 (JAERI-1089)
OOSAWA, Fumio, Tritium-hydrogen exchange of poly-l-glutamic acid in aqueous solutions, 20: 14628
OPAVSKY, Werner, X-ray fluorescence analysis of technetium and molybdenum in solutions, 20: 14497
O'RAIFEARTAIGH, L., Interpretation of $\bar{U}$ symmetries, 20: 15507
ORAM, Derek William, Improvements relating to co-operating contact assemblies, 20: 14842
ORBELI, A. L., Paramagnetic resonance of free silver atoms formed in frozen solutions of silver salts irradiated at 77°K, 20: 15975
OREN, O. H., Prog. rpt. on physico-chemical-biological processes affecting dispersion of radionuclides, final, 12/61–12/64, 20: 14731 (NP-159861)
ORKISZ, Zuzanna, Estimation of maximal concentration of thorium and uranium which can be introduced into nuclear emulsion, 20: 14877
ORLICH, E., Absorption spectrum of Ce^{3+}-ions and crystal field in La(Ce) Cl, 20: 14553
ORR, J. S., Metabolic theory of cell survival curves, 20: 14359
OSBORN, G. K., Persistent metabolic effect of x-rays or neutrons, 20: 14368
OSHIMA, Keichi, Radiation-induced copolymerization of tetrafluoroethylene with isobutylene. I., 20: 14608
OSINSKI, P., Influence of molecular structure on decomposition of steroids in solution by autoirradiation, 20: 14578 (EUR-2435.f)
OSSWALD, M., Electron microscopic studies of teeth irradiated with ultrahard radiation, 20: 14323
OSSWALD, M., Injuries in the mouth-jaw region following irradiation, 20: 14324
OSTERLAND, G., Treatment of hemangioma of skin, 20: 14418
OSTERLE, J. F., Magnetohydrodynamic squeeze film energy converters, 20: 15304
OTERO, Alberto Rodrigo, Cleaning of filters in fluidized beds. II., 20: 14645
OTOKOZAWA, Jun, Magnetic moments of baryons and fundamental triplet, 20: 15492
OTTER, A. J., Eddy-current testing of finned fuel cladding, 20: 14703
OTTINGER, C. L., Preparation of megacurie quantities of ^{137}Cs salts and source compounds, 20: 14626 (ORNL-P-1944)
OVERTON, T. R., Coincident gamma-ray spectrometer and its application to measurements of low-level radioactivity, 20: 14885

P

PACHOLCZYK, A. G., Evolution of extended radio sources, 20: 15200
PAGE, N. P., Isolation of Streptococcus equi from burros, 20: 14288 (AD-627986)
PAGE, William E., Classical limit of radiative and damping corrections to meson scattering, 20: 15563
PAGELS, Joanne A., Automatic handling of data from large-scale dog radiation experiment using general purpose computer, 20: 14238 (CONF-650560-13)
PAGNAMENTA, Antonio, V 6-bound state and uniqueness in three-particle sector of Lee model, 20: 15459
PAIGE, B. E., Leachability of glass prepared from highly radioactive calcined alumina waste, 20: 16133 (IDO-14672)
PAINE, Robert M., Sintered intermetallic bodies composed of aluminum and niobium or tantalum, 20: 15026
PALATHINGAL, Jose Chekkov, Beta-neutrino angular correlation and nuclear matrix elements in first-forbidden nonunique β decay, 20: 15857
PAL'GUEV, S. F., Structure, electric conductivity, and conductivity characteristics in ternary system (0.75 CeO_2–0.25 ZrO_2)–CaO, 20: 14536
PAN, Mao-lyan, Electron-beam welding of molybdenum, 20: 15012
PAN, Tsziluan, Electron-beam welding of molybdenum, 20: 15012
PAN, V. M., Phase diagram of columbium–nickel system, 20: 15115
PANDE, Lalit K., SU(n) crossing matrices for baryon-meson scattering, 20: 15322
PANEK, R., Radioprotective action of methandrostenolone, 20: 14392
PANEK, Ryszard, Effective mechanism of radioprotective substance methandrostenolone. II., 20: 14402
PANOFSKY, W. K. H., Experimental techniques, 20: 14841
PAO, H. P., MHD boundary layer between parallel streams of different magnetic fields and temperatures, 20: 15570 (N65-21084)
PAPROCKI, Stan J., Prog. rpt. on civilian applications, 12/65, 20: 14957 (BMI-1754)
PARASKEVOUDAKIS, P., Total absorption x-ray calorimeter, 20: 14908
PARFENOV, G. P., Development of dominant lethality in fruit flies exposed to vibration, acceleration, and gamma radiation, 20: 14343
PARK, A. B., Nuclear accidents and our food supply, 20: 14748
PARKER, E. N., Dynamical properties of stellar coronas and stellar winds. V., 20: 15216
PARKER, E. N., Suprathermal hydromagnetic waves, 20: 15198
PARKER, K., Calculation of group averaged neutron cross sections (FORTRAN for IBM-7030), 20: 15665 (AWRE-O-103/65)
PARKER, Lee W., Longitudinal plasma waves in the low-frequency limit, 20: 15902
PARKHOMENKO, I. M., Studies of potassium release γ-irradiated cells, 20: 14282
PARKINSON, Thomas Franklin, Reactor control system, 20: 16014
PARLANGE, Francois, Electronic radiation of a plasma in a magnetic field, 20: 15870 (CEA-R-2881)
PARR, E. E., Prog. rpt. on alkali metals evaluation, 7–9/65, 20: 15028 (AGN-8166)
PASCARU, I., Paramagnetic centers formed by irradiation in oxygenated compounds of Se. I., 20: 15972
PASCHALL, Hunter H., Research test of irradiated beef, pork sausage, and shrimp, 20: 14930 (NP-15676)
PASCHALL, Hunter H., Research test of irradiated beef, ham, and shrimp, 20: 14931 (NP-15677)
PASCOUET, A., Nuclear-power-excursion simulation in France, 20: 16029
PASCUAL, O. S., Studies on coconut oil, 20: 14463 (PAEC(D)CH–652)
PASOTTI, C., Variations of hepatic lipid components in mouse after whole-body irradiation with lethal dose, 20: 14268
PASZYC, S., Photolysis and radiolysis of nitromethane and nitroethane, 20: 14613
PATE, W. A., Machine to transfer powdered radioactive fuel remotely, 20: 14668 (ORNL-TM-1397)
PATIL, Sharashchandra H., Reciprocity, normality of K^0-$\bar{K}^0$ mass matrix, and CP violation in weak interactions, 20: 15350
PATOCKA, S., Systematic observation of long lived radioactivity in Pilsen region, 20: 14813
PATZELT, H., Subcritical, critical, and burst facilities in fast reactor physics research, 20: 16123 (KFK-350)
PAUN, I., Paramagnetic centers formed by irradiation in oxygenated compounds of Se. I., 20: 15972
PAVLICSEK, I., Activation of ^{113m}In by gamma rays of ^{60}Co, 20: 15748
PAVLOTSKAYA, F. I., ^{90}Sr, stable strontium and calcium in soil and vegetable food products, 20: 14236
PAYNE, B. R., Apparatus for concentration and measurement of low tritium activities, 20: 14503
PAYNE, J. A., Ratio of K-capture to positron emission in decay of ^{13}N, 20: 15712 (CONF-233(Vol.2), pp 359-64)
PEARCE, W. A., Deduction of potentials from scattering phase shifts. I., 20: 15463
PECCI, Joseph, Radiochemical procedures for selected radionuclides in environmental samples, 20: 14430 (AD-620219)
PEEBLES, P. J. E., Black-body radiation content of universe and formation of galaxies, 20: 15204
PEEKNA, A., Results on π^--p and K^+-p interactions at high energy. A., 20: 15406
PEIMBERT, Manuel, Search for deuterium in stellar spectra. II., 20: 15197

PEKER, L. K., Five-particle isomer state in ^{125}Xe, 20: 15837
PELCE, Jacques, Heat transfer and pressure drops along surfaces fitted with herring bone fins, 20: 14685 (CEA-R-2471)
PELEKHOV, V. I., Nuclear levels of ^{168}Er excited by the (n,γ) reaction, 20: 15757
PELLEGRINI, C., Theory of coherent bunch motion in electron-positron storage rings, 20: 15173 (SLAC-49, pp 61-8)
PENCHEV, G. I., Investigation of 9 Bev/c π^- meson interactions with xenon nuclei accompanied by Λ and K^0 particle production, 20: 15841
PEPPER, Stephen V., Strong pair interactions of the weak intermediate boson with hadrons, 20: 15396
PERACCHIA, G., Costal fractures as consequence of radiation treatment of breast cancer, 20: 14369
PEREC, M., Production of UO_2 electrochemical reduction of U(VI) in NaC solutions. II., 20: 14552
PEREY, F. G., Inelastic scattering and the distorted wave method, 20: 15726 (ORNL-P-1957)
PEREZ, A. Perez y, Response to radiotherapy of aortic-femoral prosthesis, 20: 14345
PEREZ, Alberto Perez y, Effects of radiotherapy on artificial grafts of thoracic aorta, 20: 14344
PERKINS, C. W., Prog. rpt. on radiation effects on microelectronic circuits, 5–7/65, 20: 14918 (ECOM-01313-1)
PERKINS, R. W., Radium isotope accumulation in animal thyroids, 20: 14254
PERNICK, Benjamin J., Plasma production by kinetic impact, 20: 15920
PERRERS-Taylor, Marjorie, Choroido-retinal damage as complication of radiotherapy, 20: 14297
PERRETT, J. D., Prog. rpt. on Piqua power facility operations analysis, semiannual, 1–6/65, 20: 16077 (NAA-SR-11628)
PERRY, John F. Jr., Blood supply to hepatic V2 carcinoma implants as measured by radioactive microspheres, 20: 14405 (COO-1305-2)
PETERS, Karl, Experimental investigations on HeLa cells after separated and combined use of decortilen and x radiation, 20: 14375
PETERSON, C. A. W., Mechanical properties of some uranium alloys, 20: 15060 (UCRL-7771)
PETERSON, J. P. Jr., Half life of ^{149}Nd, 20: 15779
PETERSON, J. P. Jr., Prog. rpt. on accurate nuclear fuel burnup analyses, 6–8/65, 20: 15717 (GEAP-4950)
PETERSON, J. P. Jr., Prog. rpt. on accurate nuclear fuel burnup analyses, 2–5/65, 20: 15133 (GEAP-4893)
PETERSON, Lawrence F., Upper limits of cosmic gamma-ray flux from OSO-1, 20: 15291
PETITT, G. A., Elastic and inelastic neutron scattering by silicon and sulfur, 20: 15811
PETKOV, I. Zh., Inelastic scattering of heavy particles with excitation of collective nuclear states, 20: 15763
PETRUKHIN, N. V., Determination of radiocesium in environment, 20: 14483
PETTERSSON, B. G., Internal conversion, 20: 15694 (CONF-233(Vol.1), pp 1-29)
PETTERSSON, B. G., K-conversion process of the 412-kev E2 transition in ^{198}Hg, 20: 15708 (CONF-233(Vol.2), pp 213-19)
PETTERSSON, B. G., Particle parameter of the $2^+ \rightarrow 0^+$ E2 transition in ^{170}Yb, 20: 15700 (CONF-233(Vol.2), pp 120-7)
PEVSNER, A., Single-particle exchange in 3-particle final states of the reaction K^+p at 2.26 Bev/c, 20: 15422
PEYROT, J. P., Industrial ultrasonic inspection of stainless-steel claddings for EL4 reactor, 20: 14717
PFALZNER, Paul M., Attenuation coefficient: finite or infinitesimal, 20: 15329
PFANN, J., Dynamics of accidents in nuclear reactors, 20: 16026 (UJV-1459/65)
PFIRSCH, D., Distribution functions of particle trajectories in plain magnetic fields, 20: 15620
PFIRSCH, D., Variation of the adiabatic invariant of the harmonic oscillator, 20: 15623 (MPI-PAE/P1.15/65)
PHELPS, B. A., Size effect of radiation-induced dimensional changes of graphite, 20: 15143
PHILIPS, S. A., Fabrication of electric discharge tube in gas containing tritium, 20: 14825 (CEA-tr-X-356)
PHILLIPS, A. C., Application of Faddeev equations to the three-nucleon problem, 20: 15343
PHILLIPS, R. H., Experimental verification of the Johnson-Treiman relationship, 20: 15428
PHILLIPS, T. L., Recovery of rat kidney from x irradiation, 20: 14258 (AD-627569)
PICARD, Horacio, Detector for reprocessing cells, 20: 14853 (CNEA-159)
PICARD, J., Rotational levels of odd-odd light deformed nuclei, 20: 15814
PICASSO, E., Small-angle elastic scattering of polarized protons in photographic emulsions, 20: 15314 (RT/FI(65)35)
PICKETT, A. G., Prog. rpt. on fatigue strength of pressure vessels, 1/66, 20: 15059 (SWRI-1228-1-20)
PICKWICK, K. M., $\beta \rightarrow \alpha$ phase change in pure uranium, 20: 15092
PIERCE, E. E., Hot presses for glove box and manipulator cell, 20: 14666 (ORNL-P-1946)
PIERCE, E. T., Nuclear explosion phenomena and their bearing on radio detection of the explosions, 20: 15601
PIERRE, Bernard, Heat transfer and pressure drops along surfaces fitted with herring bone fins, 20: 14685 (CEA-R-2471)
PIETSCHMANN, Herbert V. R., Consistent theory of weak interactions, 20: 15481
PIKELNER, S. B., Quarks: astrophysical and physico-chemical aspects, 20: 15435
PILNEY, D. G., Growth and annealing of evaporated aluminum–silicon films, 20: 15030 (ANL-7102)
PINI, M., Effects of polymerized heterologous RNA on ascite tumors, 20: 14397
PINI, Mario, Radioprotective effects of ribonucleic acid on normal and tumor tissues, 20: 14401
PINKAU, Klaus, Design calculations for ionization spectrometers: cascade development, 20: 14892
PINKERTON, Arthur P., Energy dependence of lithium fluoride dosimeters and high electron energies, 20: 14887
PINKNEY, R. J., Automatic recording, low-temperature dilatometer, 20: 14821 (RFP-668)
PITTS, S. H. Jr., Critical temperature of plutonium-chlorinated solvent reactions, 20: 14513 (RFP-688)
PLACIDI, M., Instrument for measuring magnetic fields in range 0.01 to 20 gauss with peaking strips, 20: 15160 (LNF-65/44)
PLAKSIN, I. N., Evaluation of gamma-emitter activity in x-ray absorption analysis, 20: 14498
PLATZEK, P., Measurements of wall-thickness variations in long straight tubes, 20: 14816 (EUR-2512.n)
PLEITZ, Wolfgang, Light yield of plastic scintillator NE 102A for electrons of 3 to 11 kev, 20: 14895
PLUMLEE, D. E., Sodium mass transfer. XIX., 20: 14979 (GEAP-4835)
PLYUSHCHEV, V. E., Synthesis and properties of intermediate lanthanum, cerium, praseodymium, and neodymium tungstates, 20: 14534
PNEUMAN, G. W., Evolution of solar magnetic field, 20: 15223
PODOBNIK, B., Direct spectrographic determination of impurities in uranium tetrafluoride, 20: 14473
POHL, L. E., Sodium mass transfer. XIX., 20: 14979 (GEAP-4835)
POIRIER, C. P., π^+p Interactions at 781 Mev, 20: 15341
POIRIER, J. A., Single-pion production in π^-p interactions between 600 and 900 Mev, 20: 15411
POIZAT, J. C., Lifetimes of first excited states of ^{19}F and ^{25}Mg, 20: 15780
POKROVSKY, S. I., Determination of radiocesium in environment, 20: 14483
POLETTI, A. R., ^{54}Fe: spins and decay modes of low-lying excited states, 20: 15786
POLIVANOV, M. C., Causal S matrix in the axiomatic approach, 20: 15515
POLKINGHORNE, J. C., Analytic properties of Feynman integrals, 20: 15523
POLLARD, E. C., Effect of ionizing radiation in producing sterility in pharmaceutical products: viruses, 20: 14387
POLLOCK, F., Continuous γ radiation accompanying β decay, 20: 15801
POLLOCK, F., Quantum theory of vortex ring formation in superfluid helium, 20: 15647
POOLE, D. M., Wetting of UC by copper and gold, 20: 14551
POPA, M. S., Gamma radiation from interaction of neutrons with iodine nuclei, 20: 15831
POPESCU, Fl. G., Diffusion of fission product activity through fuel coatings, 20: 15114
POPOV, A. B., Neutron resonances of Yb isotopes, 20: 15839
POPOV, A. G., Experimental investigation of charge-transfer injection of proton into cyclic accelerators and storage rings, 20: 15162 (NP-15785)
POPOV, A. G., Experiments with charge exchange injection in storage ring, 20: 15177
POPOV, V. K., Flaw detection in thin-walled tubes, 20: 14713
POPOVA, A. M., Solution of three-nucleon interaction problem, 20: 15386
POPOVA, N. M., X-ray structure and metallographic studies of Nb–Co–C systems, 20: 15077
PORTER, John Robert, Multipole formalism for test particles in general relativity, 20: 15641
POSE, H., Neutron polarization in reaction $D(d,n)^3He$ at low deuteron energies, 20: 15735 (ANL-Trans-265)
POSPISIL, J., Hematological changes in radiation sickness. V., 20: 14314
POSPISIL, Jan, Activity of pyridine nucleotidase in whole-body x-irradiated rats, 20: 14362
POSPISIL, M., Individual differences in radiation mortality of mice as predicted from pre-irradiation stress responses, 20: 14266
POSTON, J. R., W spin and the rotation group in four dimensions, 20: 15467

POTTS, B. C., Utilization of riometers for detection of nuclear explosions in space, 20: 15607
POTURAJ-GUTNIAK, Stefan, Concept of fast breeder reactor with fused salt fuel and boiling mercury "wars", 20: 16036
POTURAJ-GUTNIAK, Stefan, Concept of salt-boiling fast breeder reactor, 20: 16037
POWELL, D. B., Packaging requirements for radiation-sterilized items, 20: 14942
POZDEEV, A. V., Naval nuclear power installations. Means and perspectives of their development, 20: 16116
POZZO, S., Method for determination of intermediate neutron spectrum in reactor, 20: 14860 (RT/FI(65)-33)
PRADAL, J., Self-consistent calculation of nuclear equilibrium deformations, 20: 15843
PRAKASH, Brahm, Nuclear fuels, 20: 16099
PRANGE, R. E., Electron-phonon renormalization effects in high magnetic fields, 20: 15939 (AD-620189)
PRASAD, K. G., K-shell conversion coefficients for pure E2 transitions in deformed nuclei, 20: 15706 (CONF-233(Vol.2), pp 191-7)
PRASAD, Sarju, Conductometric determination of lanthanum as normal selenite, 20: 14484
PREDAZZI, E., Integral representations for scattering amplitudes. I., 20: 15451
PREDAZZI, E., Integral representations for scattering amplitudes. II., 20: 15321
PRELESNIK, B. V., Neutron coherent scattering amplitude of cesium, 20: 15736
PRENTICE, J. D., Differential cross sections and polarization effects in pion-proton elastic scattering at 875 to 1579 Mev/c, 20: 15372
PRENTISS, D. D., Ocean-bottom seismic observatories, 20: 14767
PREPARATA, G., Kinetic supermultiplets of $\bar{U}(12)$. II., 20: 15479
PREPARATA, G., Relation between D/F and G_A/G_V from current algebra, 20: 15488
PRETTRE, Marcel, Thermal decomposition of β lead dioxides of different texture, 20: 14548
PRICE, Clair E., Refractory composition, 20: 14974
PRICE, LeRoy R., Study of the decay $\eta^0 \to \pi^+ + \pi^- + \gamma$, 20: 15367
PRICE, Nancy J., Probable momentum spectra in atmosphere of long-lived heavy triplets produced by primary cosmic rays, 20: 15287
PRINS, G., Preparation and properties of uranium carbides, 20: 15011
PRIVE, Lucien, Effects of radiotherapy on artificial grafts of thoracic aorta, 20: 14344
PRONIEWSKI, Henryk, Effective mechanism of radioprotective substance methandrostenolone. II., 20: 14402
PRONYAKIN, V. T., Flaw detection in thin-walled tubes, 20: 14713
PROT, A., Control methods used in department of metallurgy for structural and fuel elements, 20: 14711
PROT, A. C., Industrial ultrasonic inspection of stainless-steel claddings for EL4 reactor, 20: 14717
PUCK, T. T., Cellular aspects of mammalian radiation syndrome. II., 20: 14365
PUGH, Robert E., S-operator theory. II., 20: 15635
PUSHLENKOV, M. F., Kinetics of re-extraction of uranyl nitrate from alkylphosphate solutions in water. I., 20: 14655
PUSTYL'NIK, A. I., Density and viscosity of solutions of system: organic solvent–rare earth nitrate solutions, 20: 14648
PYATOV, N. I., Influence of pairing correlations on E1 transitions in deformed nuclei, 20: 15764

Q

QUANG, B. D., Existence of weakly interacting charge-retention currents, 20: 15327
QUERCIA, I. F., External beam of Frascati electron synchrotron, 20: 15159 (LNF-65/36)
QUINBY, T. C., Hot presses for glove box and manipulator cell, 20: 14666 (ORNL-P-1946)
QUINCY, R. B., Inorganic preparations, 20: 14511 (ORNL-3889, pp 71-3)
QUIQUEMELLE, B., One-group collision probability code for cylinders and slabs, 20: 15668 (EUR-2624.e)
QUIRK, T. W., Pion-proton charge-exchange scattering near 2.0 Bev/c, 20: 15378
QUISENBERRY, K. S., Doppler coefficient of thorium oxide, 20: 15732 (TID-21654)

R

RAAEN, Helen P., Prog. rpt. on analytical chemistry, annual, 1965, 20: 14428 (ORNL-3889)
RADEKA, V., Parametric radiation detector preamplifier, 20: 14851 (BNL-9980)
RADFORD, Edward P. Jr., Distribution of ^{210}Po in pulmonary tissues of cigarette smokers, 20: 14798
RADOSKI, Henry R., Axisymmetric plasmasphere resonances: toroidal mode, 20: 15592
RAFFETY, J. C., Plant for removal of radon by aeration, 20: 14649
RAHM, D. C., Search for decay $\eta \to \pi^0 + e^+ + e^-$, 20: 15333
RAINWATER, James, Increasing synchrocyclotron currents and space charge limit, 20: 15182
RAJAGOPALAN, M., Isomeric cross-section ratios in (n,γ) reactions on ^{130}Te and ^{110}Pd, 20: 15777
RAKOW, Adalbert, Measurement of standard ion doses in solid and fluid media. I., 20: 14894
RAM, Paras, Kinetics of uranium-dioxide sintering between 950°C and 1500°C in dry hydrogen atmosphere, 20: 15082
RAMANIAH, M. V., Isomeric cross-section ratios in (n,γ) reactions on ^{130}Te and ^{110}Pd, 20: 15777
RAMASASTRY, C., Paramagnetism of color centers in sodium chlorate crystals, 20: 15961
RAMER, S., Population densities of discrete energy levels in a stationary nonthermal hydrogen arc, 20: 15875 (IPP-3/32)
RAMEY, James T., U. S. heavy water organic-cooled reactor program and Canadian–U. S. cooperation, 20: 16109
RAMSDEN, S. A., Cooperative effects in scattering of laser beam from a plasma, 20: 15911
RANDOLPH, Philip, Salmon seismic experiment, 20: 14664 (UCRL-14487 (Rev.1))
RANGANATHAN, S., Time-dependent correlations in Maxwell gas, 20: 15579
RANJI, Sampath, Dislocation mechanisms in deformation of high-purity tantalum at low temperatures, 20: 15947 (UCRL-16645)
RAO, M. N., Ruthenium and rhodium isotopes in spontaneous fission of ^{238}U, 20: 15776
RAPOPORT, L. P., Influence of strong interactions between nucleons in nuclei on forbidden β decay, 20: 15836
RASHID, M. A., $\bar{U}(12)$ symmetry, 20: 15537
RASMUSSEN, N. C., Nondestructive measurement of burnup by γ-ray spectroscopy, 20: 14504
RASOR, N. S., Recent progress in fundamental and applied thermionic converter technology, 20: 15294
RASPOTNIK, S. L., SHREW—FORTRAN code for computing angular distributions, polarizations and transport cross sections of neutrons scattered by spinless targets, 20: 15670 (WAPD-TM-524)
RASSAERTS, H., Systems niobium–chromium–carbon and tantalum–chromium–carbon, 20: 15108
RASULKULOV, M. S., Azimuthal angular distribution of shower particles and gray tracks made by cosmic-ray particles in photoemulsion, 20: 15290
RAUCH, H., Coherent extinction and second order neutron scattering on single crystals, 20: 15671
RAVEENDRANATH, T. G., Naturally occurring haploid embryo in coconut palm (Cocos nucifera L.), 20: 14320
RAVINDRAN, N., Isomeric cross-section ratios in (n,γ) reactions on ^{130}Te and ^{110}Pd, 20: 15777
RAY, J. A., Bibliography of atomic and molecular processes for 1964, 20: 15248 (ORNL-AMPIC-3)
RAYMOND, J. R., Geophysical seismic evaluation study at Hanford, 20: 14753 (BNWL-47)
RAZBITNOI, V. M., Preparation of ^{242}Pu and ^{242}Cm from neutron-irradiated ^{241}Am, 20: 14631
READ, A. L., Experimental verification of the Johnson-Treiman relationship, 20: 15428
REAY, N. W., π-meson production in p-p collisions, 20: 15336
RECTOR, J. W., Development of thorium purification system, 20: 14448 (NLCO-970, pp 1.1–22)
REECE, William Omar, Effects of exercise and inhaled yttrium oxide on blood lactic acid, 20: 14257
REED, J. T., π-meson production in p-p collisions, 20: 15336
REED, M. C., Checker-playing program for IPL-VC computer, 20: 14949 (ANL-7109)
REEDER, S. D., Measurement of absolute value of eta for ^{233}U, ^{235}U and ^{239}Pu using monochromatic neutrons, 20: 15718 (IDO-17083)
REES, J., Transverse stability of ultra-relativistic multiple-bunched beams, 20: 15171 (SLAC-49, pp 49-51)
REGGE, T., Differential properties of Feynman amplitudes, 20: 15525
REGGE, T., Potential scattering, 20: 15566
REIBEL, Kurt, Prog. rpt. on K-meson experiments at ZGS, final, 2/63–9/65, 20: 15307 (COO-1261-22)
REIDY, J. J., Decay of ^{187}W using 2-m curved-crystal spectrometer, 20: 15807
REIDY, W. P., Solar x-ray images obtained using grazing incidence optics, 20: 15203
REIDY, William P., Prog. rpt. on measurements of low energy electron precipitations associated with auroral disturbances and trapped radiation belts, final, 3/63–9/65, 20: 15589 (ASE-1125)
REIFFENSTEIN, E., Some new η carbides, 20: 15103
REILLY, J. J., Fluidized bed reprocessing of graphite matrix nuclear fuel,

20: 14647
REMES, F., Fission-antineutrino interaction with protons, 20: 15330
REINHARDT, Kelus, Determination of very small hafnium contents in zirconium dioxide preparations by means of x-ray spectral analysis after enrichment by means of partition process, 20: 14496
REITER, G. F., Instability of steady state of plasma in uniform electric field, 20: 15883 (SU-IPR-31)
REITER, H., Repair of damage induced by monofunctional alkylating agent in transformable, ultraviolet-sensitive strain of Bacillus subtilis, 20: 14267
REMIDDI, E., Evaluation of $N^{\frac{1}{2}}_{\frac{1}{2}}N$ weak coupling constants, 20: 15308
RENGAN, K., Isomeric cross-section ratios in (n,γ) reactions on ^{130}Te and ^{110}Pd, 20: 15777
RENNINGER, G. H., Symmetry properties of bootstrap models, 20: 15556
RENZLER, G., Instrument for measuring magnetic fields in range 0.01 to 20 gauss with peaking strips, 20: 15160 (LNF-65/44)
RESMINI, F., Acceleration of negative ions in Milan AVF cyclotron, 20: 15180
RESNICK, R., Dissociation and evaporation of TaC, HfC, and ZrC at elevated temperatures, 20: 15052 (NP-15880)
RESTER, Robert R., Radiation control in Mississippi, 20: 14807
REXER, J., Prog. rpt. on protective coatings for refractory metals, 10/23/64–1/23/65, 20: 15004 (N65-20790)
REYNOLDS, R. L., Skeletal defects in prenatally irradiated sheep, cattle and swine, 20: 14337
REYNOLDS, R. Stanton, Unattended seismological observatory, 20: 14764
REYNOLDS, Togwedd, Choroido-retinal damage as complication of radiotherapy, 20: 14297
REYNOLDS, W. L., Chloride ion catalyzed iron(II) + iron(III) isotope exchange in dimethylsulfoxide, 20: 14571
REZANKA, I., Gamma transitions in ^{153}Eu, 20: 15734 (ZfK-PhA-18)
RHODES, John Rathbone, Improvements in or relating to radiometric analysis techniques, 20: 14505
RICHARDSON, J. E., Use of on-line computer for Moessbauer experiments, 20: 15973
RICHIR, Marc, Radioresistance of nucleohistone, 20: 14592
RICHTER, Burton, Storage ring summer study, 1965, on instabilities in stored particle beams, 20: 15166 (SLAC-49)
RICHTER, F. W., Angular distribution of 440-kev γ rays from reaction ^{23}Na(p,p'γ)^{23}Na, 20: 15846
RICHTER, Herfried, Production of rare earths from kola-apatite, 20: 14520
RICKARDS, G. K., Vacancy clusters and loops in ion-bombarded copper, 20: 15146
RIDER, B. F., Half life of ^{149}Nd, 20: 15779
RIDER, B. F., Prog. rpt. on accurate nuclear fuel burnup analyses, 6–8/65, 20: 15717 (GEAP-4950)
RIDER, B. F., Prog. rpt. on accurate nuclear fuel burnup analyses, 2–5/65, 20: 15133 (GEAP-4893)
RIDGWAY, K. R., Administering criticality control in Hanford Atomic Products Operation non-reactor environment, 20: 14790 (RL-SA-43A)
RIEDEL, J. T., Separation of isotope ^{10}B by exchange distillation, 20: 14629
RIEDMUELLER, W., Measurements of electron temperature in an argon–potassium plasma, 20: 15874 (IPP-3/31)
RINARD, Phillip M., Simultaneous determination of parameters of the core-particle model in ^{197}Au, 20: 15803
RITCHIE, W. B., Data compilation and evaluation of space shielding problems, 20: 15930 (NP-15697(Vol.2))
RITSON, D. M., π-pair photoproduction below 1 Bev, 20: 15332
RITZERFELD, W., Morphologic and physiologic changes in staphylococci from streptomycin and ^{60}Co treatment, 20: 14313
RITZMAN, Robert L., Prog. rpt. on applicability of existing data to analytical description of a nuclear-reactor accident, 10–12/65, 20: 16019 (BMI-X-10154)
RIVERS, R. J., Gauge approximations in mesodynamics, 20: 15460
ROBERTS, F. P., Chemical analysis of spent power reactor fuels, 20: 14435 (BNWL-SA-503)
ROBERTS, W. T., Preferred orientation in wrought and annealed metals, 20: 15099
ROBERTS, W. T., Solar flare environment, 20: 15192 (N65-21000)
ROBERTSHAW, Richard D., Experimental facilities in high-flux pool-type test reactor, 20: 16129
ROBERTSON, J. S., Radiobiological aspects of supersonic transport, 20: 14797
ROBIN, Gerard, Industrial applications of radioactive tracers, 20: 14934
ROBINSON, C. G., Prog. rpt. on fatigue strength of pressure vessels, 1/66, 20: 15059 (SWRI-1228-1-20)
ROBINSON, D. K., Observations of $Y^{\frac{1}{2}}_{\frac{1}{2}}$(1405) and $Y^{\frac{1}{2}}_{\frac{1}{2}}$(1358) resonances in π-N collisions at 1.68 Bev/c, 20: 15404
ROBINSON, D. K., Production and decay of ρ^0 and ω mesons in π^+n and π^-p interactions at 1.7 Bev/c, 20: 15403
ROBINSON, David W., Transfers of water and electrolytes across granulation tissue in patients following burns, 20: 14255
ROBINSON, K. W., Wake fields of charged particle traveling in vacuum chamber with resistive walls, 20: 15169 (SLAC-49, pp 32-5)
ROBINSON, W. C., Reactions of uranium carbide in KCl–LiCl/zinc system, 20: 14991
ROCHLIN, G. I., Subharmonic structure in Pb–Pb superconductive tunneling junctions, 20: 15651
ROCKSTEIN, M., Adult emergence of house fly, musca domestica, from x-irradiated pupae, 20: 14306
RODDY, F. M., Prog. rpt. on electron-ionization cross sections, semiannual, 12/16/64–6/15/65, 20: 15235 (AD-620289)
RODE, L. G., Measurement of moisture in organic soils by neutron method, 20: 14756
RODGERS, S. J., Prog. rpt. on measurement of impurities in Na, 10–12/65, 20: 14445 (MSAR-66-10)
RODZIKOVSKAYA, S. V., Study of niobium and tantalum sulfides, 20: 14554
ROENNBAECK, Curt, Placental transfer of ^{85}Sr in mice, 20: 14244
ROESSNER, W., Deoxyribonuclease II and deoxyribonucleic acid in rat thymus after action of radiomimetic drugs and x irradiation, 20: 14311
ROESSNER, W., Effect of radiomimetic drugs and x irradiations on permeability of blood-brain barrier to Evans blue, 20: 14312
ROF, Juan Sancho, Cleaning of filters in fluidized beds. II., 20: 14645
ROGANOV, V. S., Angular distribution of high-energy neutrons emitted in absorbing polarized μ^- mesons in calcium, 20: 15721 (JINR-E-2517)
ROGANOV, V. S., Asymmetry in angular distribution of high-energy neutrons from μ^- capture in sulfur, 20: 15720 (JINR-E-2516)
ROGERS, Leo A., Free field motion near nuclear explosion in salt: Project Salmon, 20: 14663 (UCRL-14463(Rev.1))
ROGERS, S. C., Radiation degradation of polyamino acids in solid state, 20: 14588
ROGERS, S. J., Effect of isotopes on lattice heat conduction. II. Solid helium, 20: 15652
ROHRER, W. M. Jr., Burnout in steam–water flows with axially nonuniform heat flux, 20: 14696
ROL, P. K., Structure in electron energy spectrum from multi-kev Ar^+–Au and Ar^+–Cu collisions, 20: 15261
ROMANOWSKI, T. A., Prog. rpt. on K-meson experiments at ZGS, final, 2/63–9/65, 20: 15307 (COO-1261-22)
ROMANSKII, I. A., Structure of radiation chlorinated and sulfochlorinated polyethylene, 20: 14621
ROMNEY, C. F., Principles of experimental large aperture seismic array (LASA), 20: 14758
ROOYMANS, C. J. M., High-pressure phase transition of europium telluride, 20: 15974
ROSE, M. E., Internal pair formation and electroexcitation of nuclei, 20: 15696 (CONF-233(Vol.1), pp 60-86)
ROSE, R. G., Migration of pores in uranium dioxide, 20: 15094
ROSE, R. M., Segregation of Ta at very low concentrations in Nb, 20: 14969
ROSENBLUTH, M. N., Apparatus for magnetically confining a plasma, 20: 15927
ROSENGREN, B., Field control of telecobalt therapy by gamma-ray television, 20: 14407
ROSHCHINA, L. I., Accumulation of F centers in KCl crystals, 20: 15980
ROSKIES, Ralph, Internal symmetry and mass splitting, 20: 15461
ROSOFF, Betty, Effects of chelating agents in man, 20: 14256
ROSSETTI, C., Use of dispersion methods in study of symmetries, 20: 15549
ROSZTOCZY, Zoltan R., Analytical and experimental methods of determining heavy-isotope content of operating fuel elements, 20: 14438 (CEND-540)
ROTELLI, P., pp-Annihilations into two mesons wihin broken inhomogeneous U(12) symmetry scheme, 20: 15346
ROTENBERG, M. A., Gravitational waves from isolated sources, 20: 15637
ROTTER, Ingrid, Genealogical coefficients for α particles, 20: 15741
ROUANET, Pierre, Influence of carbon concentration on morphology of uranium–molybdenum, 20: 15070
ROUBAL, W. T., Damage to proteins, enzymes, and amino acids by peroxidizing lipids, 20: 14587
ROULEAU, W. T., Magnetohydrodynamic squeeze film energy converters, 20: 15304
ROUSE, Gerald Russell, Elastic electron-proton scattering at forward angles, 20: 15391
ROUSSEAU, Jean-Claude, Aerodynamic study of fluid flow in channel of reactor filled with internally and externally cooled fuel elements, 20: 15997 (CEA-R-2856)
ROWLAND, M. C., Sodium mass transfer. XIX., 20: 14979 (GEAP-4835)
ROXBURGH, Ian W., Fission theory of origin of binary stars, 20: 15219
ROY, Maurice, Conference on aeronautical sciences, Stockholm, 8/62, 20: 14729
RUBIN, P., Isotope tests of kidney function in pelvic and abdominal irradiation, 20: 14296
RUBINI, Milton E., Renal concentrating defect in canine radiation nephritis, 20: 14342

RUBINSTEIN, H. J., Prog. rpt. on Piqua power facility operations analysis, semiannual, 1–6/65, 20: 16077 (NAA-SR-11628)
RUBINSTEIN, R., Experimental verification of the Johnson-Treiman relationship, 20: 15428
RUBY, Peter R., Prog. rpt. on measurements of low energy electron precipitations associated with auroral disturbances and trapped radiation belts, final, 3/63–9/65, 20: 15589 (ASE-1125)
RUEHL, W., SL(6.C) model as relativistically invariant formulation of SU(6) symmetry, 20: 15536
RUELLE, David, Stability of many-particle systems, 20: 15151
RUF, H., Activation analytical determination of very small iridium contents in uranium oxide, 20: 14495
RUIZ, C. P., Half life of ^{149}Nd, 20: 15779
RUIZ, C. P., Prog. rpt. on accurate nuclear fuel burnup analyses, 6–8/65, 20: 15717 (GEAP-4950)
RUIZ, C. P., Prog. rpt. on accurate nuclear fuel burnup analyses, 2–5/65, 20: 15133 (GEAP-4893)
RUSH, John Edwin Jr., Two-resonance model for Λ–K^0 production, 20: 15392
RUSSELL, Elizabeth S., Prog. rpt. on attempts to delineate inborn anemias in mice, 2/65–1/66, 20: 14290 (NYO-1800-12)
RUSSELL, J. A. Jr., Description of facility radiation and contamination alarm systems installed in HFIR facility, 20: 16125 (ORNL-TM-1393)
RUSSELL, J. C., Radiolysis of trifluoroethanol, 20: 14590
RUSSELL, R. Scott, Evaluation of risk from radiation, 20: 14331
RUST, John H., Ionizing radiation for measuring biological phenomena, 20: 14386
RUSU, M., Statistics of scaled pulses, 20: 14890
RYABUKHIN, Yu. S., Uniform irradiation of surfaces by pulsed electron beams, 20: 15178
RYABYKH, O. I., Nuclear geophysical methods applied to geophysical research data, 20: 14777
RYADOV, V. G., Determination of radiocesium in environment, 20: 14483
RYBAKOV, V. P., Decay scheme of ^{119*}Te, 20: 15762
RYBIN, V. M., Measurements of mean energy of electron beams in low-energy linear accelerators, 20: 15179
RYON, A. D., Flooding in perforated-plate pulsed extraction columns, 20: 14462 (ORNL-3890)
RYPAR, Vratislav, Survey of chemical technology in nuclear industry, 20: 14429

S

SABIROVA, T. M., Radiation polymerization of vinyl chloride in solid solutions at low temperatures, 20: 14594
SACHS, David L., Low-frequency spatial response of a collisional electron plasma, 20: 15904
SACHS, R. G., Phenomenological theory of CP-violating K^0 decays, 20: 15432
SAELENS, Richard G., Nuclear blast effects on components and equipment, 20: 14921
SAHNI, R. J., Angular correlation study of reaction $\pi^- p \to \pi^- \pi^+ p\ \pi^-$ at 2.7 Bev/c, 20: 15410
SAHOURIA, Jack S., Spin and parity of Y$^*_1$(1815) and the Y*(1765), 20: 15414
SAIA, Anthony, Shaped Mg–Li castings, 20: 15007 (NP-15881)
SAINT-JAMES, Rose, Ion exchange methods of separating zirconium and hafnium, 20: 14657
ST. ROMAIN, M. J., Malignant mixed muellerian neoplasms (mixed mesodermal tumors), 20: 14300
SAITO, N., Determination of uranium content in scraps, 20: 16140
SAITO, Takeo, Statistical studies on three types of geomagnetic continuous pulsations. I., 20: 15613
SAKAI, Toshio, γ Shielding property, strength and workmanship of built-up type lead slab structure, 20: 15932 (ORNL-tr-843)
SAKANO, Kosuke, Current-voltage characteristics of Cs thermionic converters operated at relatively low temperature, 20: 15301
SAKURAI, Hiroshi, Radiation chemistry of cyclic dienes. I., 20: 14610
SALAM, A., Relativistic extension of non-compact symmetry groups, 20: 15370
SALAM, Abdus, Ü(12) symmetry, 20: 15537
SALANT, E. O., Observations of Y$^*_1$(1405) and Y$^*_1$(1358) resonances in π-N collisions at 1.68 Bev/c, 20: 15404
SALANT, E. O., Production and decay of ρ^0 and ω mesons in π^+n and π^-p interactions at 1.7 Bev/c, 20: 15403
SALATHE, Eric Poul, Two-dimensional magnetohydrodynamics, 20: 15585
SALBYJ, Bohdan M., Post-irradiation survival of Staphylococcus aureus in sea foods, 20: 14936
SALES, A. T., Prog. rpt. on mechanical properties of slip-cast fused silica, final, 7/64–6/65, 20: 15058 (SC-DC-66-1130)
SALIBEKOV, S. E., Interaction of diborides of vanadium, niobium and tantalum with carbon, 20: 14555
SALIBEKOV, S. E., Studies of carbidization of titanium and zirconium nitrates, 20: 15072
SALPETER, E. E., Models for carbon-burning stars, 20: 15194
SALTER, Robert Mundhenk Jr., Neutron-neutron s-wave scattering length from the reaction $\pi^- + d \to 2n + \gamma$, 20: 15511
SALTERELLI, E. A., Decontamination of Shippingport atomic power station, 20: 16088 (WAPD-299)
SAMODELOV, A. P., Precipitation of scandium from hydrochloric acid solutions by sodium silicofluoride, 20: 14566
SAMSONOV, G. V., High-temperature heaters made with niobium and zirconium carbides, 20: 15112
SAMUELI, J. J., Lifetimes of first excited states of ^{19}F and ^{25}Mg, 20: 15780
SAMUELS, E. R., Canadian fallout data for October 1965, 20: 14737 (NP-15853, pp 8-20)
SAMUELS, E. R., Reactor environment monitoring for October 1965, 20: 14738 (NP-15853, pp 21-33)
SAMUELS, E. R., ^{90}Sr in 1964 Canadian hard red spring wheat, 20: 14736
SANDARS, P. G. H., Relativistic effects in many-electron hyperfine structure. I. Theory, 20: 15264
SANDARS, P. G. H., Relativistic effects in many-electron hyperfine structure. II., 20: 15265
SANDARS, P. G. H., Relativistic effects in many-electron hyperfine structure. III., 20: 15266
SANDENAW, T. A., Heat capacities of $NbC_{0.702}$, $NbC_{0.825}$, $NbC_{0.980}$, and Nb_2C below 320°K, 20: 15097
SANDERS, Merwyn, Automated air sampling by use of aperture cards, 20: 14791 (Y-1501)
SANDERS, William A., Rates of hydrogen–graphite reaction between 1550° and 2260°C, 20: 14508 (N65–20481)
SANDS, Matthew, Storage ring summer study, 1965, on instabilities in stored particle beams, 20: 15166 (SLAC-49)
SANDULESCU, A., Reduced widths for nucleon emission in shell-model intermediate coupling, 20: 15830
SANDWEISS, J., p-p Annihilations into K and π mesons at 3.7 Bev/c, 20: 15338
SANTORO, Gilbert J., Magnetic susceptibilities of compositions in tantalum–tantalum carbide system, 20: 15045 (N65-15534)
SARASWATI, V., Quadrupole coupling constants of deuteron in polycrystalline glycine compounds, 20: 15957
SARAZIN, A., Lifetimes of first excited states of ^{19}F and ^{25}Mg, 20: 15780
SARGENT, C. P., The energy and angular distribution of photoneutrons from heavy elements, 20: 15723 (MIT-2098-162)
SASLAW, W. C., Overshooting from stellar convective cores, 20: 15208
SASS, A. R., Current distribution in an array of superconducting thin films, 20: 15643 (NASA-TN-D-3293)
SASTRY, S. B. S., Paramagnetism of color centers in sodium chlorate crystals, 20: 15961
SATO, Noriyoshi, External excitation of standing waves in r-f discharge, 20: 15912
SATO, Tadashi, Effects of radiation on seeds of Phleum pratense L., 20: 14349
SATO, Yoshiaki, Effect of the anisotropic ionosphere on hydromagnetic oscillations, 20: 15619
SAUERBIER, W., Influence of pH and oxygen on 315 μ inactivation and thymine dimerization in mutants of bacteriophage T4, 20: 14356
SAUR, E., Superconductivity of fusion samples of systems Nb–Sn, Nb–Al, Nb–Ga, V–Si, and V–Ga, 20: 15123
SAWYER, R. F., Dynamical question bearing on calculations of mass shifts in S-matrix theory, 20: 15466
SAX, R. L., Data processing techniques for detection and interpretation of teleseismic signals, 20: 14762
SAXENA, R. P., Deviations from charge independence in n-p and n-n scattering lengths by S-matrix methods, 20: 15356
SAYER, Robert M., Ultraviolet erythema, 20: 14310
SCANDOLA, G., Radiation-induced noise in semiconductor counters, 20: 14923
SCANDRETT, J. H., π^+p Interactions at 781 Mev, 20: 15341
SCHAACK, G., Absorption spectrum of Ce^{3+}-ions and crystal field in La(Ce)Cl, 20: 14553
SCHAD, O., Prog. rpt. on critical heat flux in boiling water, 4–6/65, 20: 14686 (EURAEC-1448)
SCHAEFER, D. W., Electronic spectra of solutions of europium and ytterbium in liquid ammonia, 20: 14526
SCHAEFER, H. J., Radiobiological aspects of supersonic transport, 20: 14797
SCHARF, Waldemar, Universal laboratory monitor model MSP-2, 20: 14872
SCHECHTER, J., Nonleptonic decays of hyperons, 20: 15369
SCHEIDECKER, M., Gaines fabrication plant for nuclear fuel at Trefimetaux, 20: 15018
SCHENKEL, R., Effect of pyridoxal on strontium content of skeleton, 20: 14246
SCHIKARSKI, L., Prog. rpt. on fabrication of UO_2 powders and processing into fuel elements, 4–6/65, 20: 14999 (EURAEC-1466)

SCHILDKNECHT, H., Structural information and identification of organic substances by means of "electron pyrolysis". I., 20: 14623
SCHILLER, D. H., Uniformization of the scalar self-energy diagram, 20: 15495
SCHINDEWOLF, U., Enrichment of deuterium, 20: 14519
SCHINDLER, H., Multistage plasma acceleration and heating, 20: 15892
SCHINDLER, R., Animal cell in cell cultures, 20: 14385
SCHIPPISI, G. Gagnoni, Costal fractures as consequence of radiation treatment of breast cancer, 20: 14369
SCHIRMER, G., Neutron polarization in reaction D(d,n)^{3}He at low deuteron energies, 20: 15735 (ANL-Trans-265)
SCHLEICHORS, H., DPN degradation and synthesis of lymphosarcoma ascites cells after x irradiation, 20: 14370
SCHLOERB, Paul R., Transfers of water and electrolytes across granulation tissue in patients following burns, 20: 14255
SCHLOESSER, J., Correlation among pore-size distribution, permeability, and diffusion in graphite, 20: 15104
SCHLUETER, Arnulf, Plane magnetohydrostatic equilibria with interior field, 20: 15877 (IPP-6/41)
SCHMAGLOWSKI, S., DPN degradation and synthesis of lymphosarcoma ascites cells after x irradiation, 20: 14370
SCHMATZ, W., Measurement of free and incoherent neutron cross sections of silicon and lead, 20: 15682
SCHMID, A., Effect of pyridoxal on strontium content of skeleton, 20: 14246
SCHMIDLIN, P., Measurement of two β-γ directional correlations in decay of ^{126}I, 20: 15845
SCHMIDT, James F., Experimental study of effect of simulated reactor core position on nozzle heat transfer, 20: 14727 (NASA-TM-X-1208)
SCHMIDT, W. C., Storage of long-lived fission products on alumino-silicate zeolites, 20: 14466 (RL-SA-58)
SCHNAKENBERG, J., Quasi-particle spectrum and electric conductivity of the small polaron, 20: 15988
SCHOEBEL, J.-D., Cobalt corner in the tri-component system cobalt–niobium–boron, 20: 15100
SCHOETT, W., Excited levels of ^{79}Br, 20: 15802
SCHOLZ, L. C., Computer simulation of satellite systems, 20: 15599
SCHONDORF, K.-W., Treatment of hemangioma of skin, 20: 14418
SCHREDER, Gerald, Opacity of universe to high-energy photons, 20: 15226
SCHRODER, C. M., Isolation of Streptococcus equi from burros, 20: 14288 (AD-627986)
SCHROER, B., Some remarks on non-renormalizable quantum field theories, 20: 15527
SCHULTZ, Warner W., Neutron measurement by track imaging in insulating materials, 20: 14854 (CONF-660304-3)
SCHULZ, M. D., Tonsil and palatine arch cancer-treatment by radiotherapy, 20: 14416
SCHWARZSCHILD, M., Overshooting from stellar convective cores, 20: 15208
SCHWEINGRUBER, F., V-2-prong K$^-$p interactions at 5.5 Bev/c, 20: 15416
SCIASCIA, R., Effects of experimental dysprotidemia on Hamolsky's test responses, 20: 14276
SCOTTI, A., One-boson-exchange model of NN and NN-interaction, 20: 15345
SCOZZAFAVA, R., Neutron diffusion parameters in benzene, 20: 15676
SEBILLEAU, F., Fuels for fast neutron reactors, 20: 16047
SEELIGER, D., Neutron polarization in reaction D(d,n)^{3}He at low deuteron energies, 20: 15735 (ANL-Trans-265)
SEGAL, Robert Lloyd, Studies in I metabolism. III., 20: 14249
SEGAL, Robert Lloyd, Studies in I metabolism. IV., 20: 14250
SEHGAL, Bal Raj, Neutron thermalization and diffusion in nonisothermal media, 20: 15677
SEIDEL, Thomas Edward, Position-dependent superconductivity by thermal and electrical conductivity in superconducting films, 20: 15656
SEIDLITZ, Leo, Enhancements in interactions of 3.2 Bev/c π^- with deuterium, 20: 15405
SEIGLE, L., Dissociation and evaporation of TaC, HfC, and ZrC at elevated temperatures, 20: 15052 (NP-15880)
SEIP, Hans M., Studies on failure of first Born approximation in electron diffraction. I., 20: 14516
SELF, S. A., Instability and amplification in finite beam-plasma systems. I., 20: 15880 (ML-1292)
SELIG, H., Refractive index and molar refraction of xenon oxide tetrafluoride, 20: 14528
SELIG, Henry, Complexes of xenon oxide tetrafluoride, 20: 14523
SELIG, Walter, Some analytical methods for explosives and explosive simulants, 20: 14470 (UCRL-7873)
SELITSKII, Yu. A., Deuteron fission of ^{232}Th and dependence of fragment kinetic energy on excitation energy of the fissile nucleus, 20: 15840
SELLERS, Bach, Rocket-borne air density measurement system utilizing electron-bremsstrahlung, 20: 15588 (AD-620682)
SEMTURS, F., Counting of neutrons at small counting rates: elimination of γ background and electronic disturbances, 20: 14863
SENNETT, C. T., Localized vibrations of H$^-$ and D$^-$ ions in alkaline earth fluorides, 20: 15969
SEPEL, T., Complexes of uranyl with phenolic ligands. III., 20: 14481
SEPEL, T., Uranyl complexes with phenolic ligands. IV., 20: 14482
SERANO C., Mario, Uranium exploration in Chile, 20: 14779 (RME-4569 (Rev.))
SEREBRYAKOV, V. V., Summation of ladder graphs at high energies, 20: 15501
SERGEEV, A. G., Gamma radiation of ^{152}Eu in energy range 1380 to 1900 kev, 20: 15832
SERGEEV, V. O., Decay of ^{90}Mo, 20: 15751
SERIN, B., Observation of a "Peltier" effect in a type-II superconductor, 20: 15649
SESHADRI, S. R., Radiation from a current strip in uniaxially anisotropic plasma medium, 20: 15891
SESSLER, A. M., Longitudinal wake fields of pulse of charge moving down straight pipe of circular cross section with finite conductivity, 20: 15167 (SLAC-49, pp 18-22)
SESSLER, A. M., Storage ring summer study, 1965, on instabilities in stored particle beams, 20: 15166 (SLAC-49)
SESSLER, A. M., Theory of coherent bunch motion in electron-positron storage rings, 20: 15173 (SLAC-49, pp 61-8)
SESSLER, A. M., Transverse coherent instability of bunched beams, 20: 15170 (SLAC-49, pp 36-48)
SESSLER, Andrew M., Asymptotic perturbation fields of longitudinally bunched beam within rectangular pipe with resistive walls, 20: 15168 (SLAC-49, pp 23-31)
SETO, Yoshio, Radioactive contamination of Indo-Antarctic Ocean water in early parts of 1961 and 1962, 20: 14749
SEYFARTH, Rudolf, Determination of trace impurities in UO_2 fuel materials, 20: 14494
SHABUROV, V. A., Investigation of excited states ^{104,104*}Rh by observation of γ rays from (n,γ) reaction, 20: 15754
SHADIEV, N., Gamma spectrum produced by thermal neutron capture in palladium, 20: 15755
SHADIEV, N., Gamma spectrum produced by thermal neutron capture in gold, 20: 15756
SHADIEV, N., Nuclear levels of ^{168}Er excited by the (n,γ) reaction, 20: 15757
SHADIEV, N., Nuclear levels of ^{166}Ho from (n,γ) reaction, 20: 15758
SHAFFER, R. A., Mass of the muon and charged-meson decay rates, 20: 15344
SHAHANI, C. J., Ruthenium and rhodium isotopes in spontaneous fission of ^{238}U, 20: 15776
SHAHN, Ezra, Fate of DNA injected into host cell from uv irradiated T4 bacteriophages, 20: 14285
SHAKHOVA, K. I., Constitution diagram of Ti–Nb–Cr system, 20: 15078
SHALEK, R. J., Energy dependence of lithium fluoride dosimeters at high energies, 20: 14888
SHANGIN-BEREZOVSKII, G. N., Frequency and spectrum of chlorophyll mutations following ethylenimine treatment of second generation seeds of γ-irradiated barley, 20: 14334
SHAO, Wei, Protective effects of streptomycin against radiation damage of chromosomes of germinal cells of mammals, 20: 14404
SHAPIRO, F. L., Determination of neutron resonance spins in ^{165}Ho nuclei, 20: 15681
SHAPIRO, I. S., Direct reactions with two-nucleon transfer, 20: 15798
SHARMA, R. P., K-shell conversion coefficients for pure E2 transitions in deformed nuclei, 20: 15706 (CONF-233(Vol.2), pp 191-7)
SHARNEY, Lena, Studies in I metabolism. III., 20: 14249
SHARNEY, Lena, Studies in I metabolism. IV., 20: 14250
SHARP, D. H., S-matrix perturbation theory, 20: 15526
SHARP, Joseph C., Effects of exposure to mixed fission spectrum delivered in single "pulse" and x-rays delivered at slower rate upon conditioned avoidance behavior of primates, 20: 14286 (AD-625837)
SHARPE, C., Automation of tube-thickness measurements using ultrasonics, 20: 14718
SHCHEGELSKII, V. A., Phase-shift analysis of elastic πN scattering at 240 Mev, 20: 15388
SHEA, J. J., Development of charged colloid source for electrostatic propulsion, 20: 14725 (N65-15876)
SHEARD, Harold, Irradiation of food, 20: 14937
SHELINE, R. K., Centrifugal stretching and Coriolis-force antipairing effects in ^{182}W, 20: 15821
SHEPARD, R. C., Prog. rpt. on Piqua power facility operations analysis, semiannual, 1–6/65, 20: 16077 (NAA-SR-11628)
SHEPHARD, W. D., Single-pion production in π^-p interactions between 600 and 900 Mev, 20: 15411
SHEPHERD, R. T. H., Use of ^{99m}Tc as clinical tracer element, 20: 14423
SHERMAN, Alfred I., Chemotherapeutic agents and radioisotopes in nonoperative treatment of gynecologic cancers, 20: 14413
SHERSHEV, B. S., Study of $NaBeF_3$–$NaPO_3$ system by emanation method,

20: 14557
SHERSHEV, B. S., Study of $KBeF_3$–KPO_3 system by emanation method, 20: 14558
SHIDA, Shoji, Estimation of gamma-ray energy absorbed in gaseous media, 20: 14870
SHIH, Ching-yuan, ^{14}C-labeled urea and ^{32}P-labeled phosphate to investigate foliar-applied fertilizer for rice growing in reclaimed tidal lands, 20: 14240 (NP-15670)
SHIH, H. C., Vacuum polarization in μ-mesic atoms, 20: 15246 (CONF-233(Vol.3), pp 520-8)
SHIMA, Yuokov, Photon splitting in a nuclear electric field, 20: 15339
SHIMAHARA, Hiroko, Electrical conductivity of a turbulent plasma, 20: 15895
SHIMCHAK, M., Angular distribution of high-energy neutrons emitted in absorbing polarized μ^- mesons in calcium, 20: 15721 (JINR-E-2517)
SHIMCHAK, M., Asymmetry in angular distribution of high-energy neutrons from μ^- capture in sulfur, 20: 15720 (JINR-E-2516)
SHIMELEVICH, Yu. S., Use of pulsed neutron generator to determine neutron diffusion parameters of rocks and fluids, 20: 14772
SHIMIZU, M., Beta-ray back-scattered type thickness gage for galvanizing process, 20: 14839
SHIMODAIRA, Hajime, Magnetic moments of baryons and fundamental triplet, 20: 15492
SHIMOSE, Takeaki, Stress corrosion cracking of Ti and Zr in HCl–methanol solutions, 20: 14988
SHINDO, Mitsuo, γ Shielding property, strength and workmanship of built-up type lead slab structure, 20: 15932 (ORNL-tr-843)
SHINOHARA, Kenichi, Graft copolymerization of polymer, initiated by electron irradiation, in the presence of monomer vapor. IV., 20: 14618
SHIOBARA, Shinji, Application of microwave scattering theory to measurement of underdense cylindrical plasmas, 20: 15894
SHIOZAKI, Masaru, Radioactive contamination of Indo-Antarctic Ocean water in early parts of 1961 and 1962, 20: 14749
SHIRKOV, D. V., Dispersion description of low-energy scattering, 20: 15522
SHISHELOV, I. A., New data on decay of $^{184*}Re$, 20: 15750
SHKARLET, Yu. M., Eddy-current method for multi-parameter testing of structural components, 20: 14708
SHOBE, L. R., Structural analysis of shipping casks. Vol. I, 20: 14667 (ORNL-TM-1312(Vol.1))
SHOEMAKER, F. C., Princeton-Pennsylvania 3-Bev proton synchrotron parameters, 20: 15163 (PPAD-279D(Rev.))
SHONO, Yoshiyuki, Unified derivation of the cranking model and Peierls-Yoccoz method. I., 20: 15828
SHOOK, Donald F., Thermal neutron flux perturbation by Dy–Al foils in H_2O and UO_2F_2–H_2O solutions, 20: 15669 (NASA-TN-D-3237)
SHOREY, W. R. J., Automatic sample changing systems utilizing AECL-2041 digital read-out system, 20: 14846 (AECL-2517)
SHORTER, R. G., Recovery of intestinal mucosa in rat after x-irradiation of exteriorized intestine, 20: 14364
SHTAL', M. Z., Decay scheme of $^{119*}Te$, 20: 15762
SHU, F. H., Gravitational collapse of uniform spheroid, 20: 15206
SHURANI, P., Mass formula problem in the ISL(6) group, 20: 15499
SHVACHKO, V. I., Interaction of oxygen with a Nb surface, 20: 15976
SHVARTSMAN, M. D., Natural radioactivity of carbonate rocks, 20: 14752
SIDDIQI, Aziz Ahmad, Radiation safety regulations for atomic energy centre, Dacca, 20: 14783 (AECD/HP/2)
SIEMASZKO, Aleksander, Flocculants for treatment of radioactive waste water by mineral sorbents, 20: 16138
SIEMON, R., Total absorption x-ray calorimeter, 20: 14908
SIEWERT, C. E., Exact solution of equations of radiative transfer for local thermodynamic equilibrium in the nongray case, 20: 15572
SIGMAR, D. J., Cluster expansion of thermal averages in slow neutron scattering in real gases, 20: 15672
SIKULOVA, J., Individual differences in radiation mortality of mice as predicted from pre-irradiation stress responses, 20: 14266
SILINI, G., X-ray and fast neutron survival response of 5-bromodeoxycytidine-treated bone marrow cells, 20: 14333
SILVER, Solomon, Studies in I metabolism. III., 20: 14249
SILVERT, William Lawrence, Theory of nonhomogeneous superconductors, 20: 15655
SIMMONS, J. H., Current distribution in an array of superconducting thin films, 20: 15643 (NASA-TN-D-3293)
SIMONOV, V. V., Phospholipids in liver cells and intestinal mucous in rabbits exposed to whole-body γ irradiation, 20: 14278
SIMPSON, John A., Cosmic ray neutron intensity monitor. Part A., 20: 15277
SIMPSON, John A., Cosmic ray neutron intensity monitor. Part A., 20: 15279
SIMPSON, John A., Cosmic ray neutron intensity monitor. Part A., 20: 15281
SIMPSON, John A., Cosmic ray neutron intensity monitor. Part A., 20: 15283
SIMPSON, John A., Cosmic ray neutron intensity monitor. Part A., 20: 15285
SIMPSON, K. M., Data compilation and evaluation of space shielding problems, 20: 15930 (NP-15697(Vol.2))
SIMSON, R., Measurement of free and incoherent neutron cross sections of silicon and lead, 20: 15682
SINANOGLU, Oktay, Theoretical transition probabilities, 20: 15275
SINCLAIR, Kenneth F., Scintillation selector for low energy charged particles, 20: 14912
SINGER, Sidney, Vela satellite program for detection of high-altitude nuclear detonations, 20: 15595
SINGER, T., Prog. rpt. on reactor containment, 10–11/65, 20: 16023 (IITRI-578P21-16)
SINGH, R., Single-particle exchange in 3-particle final states of the reaction K^+p at 2.26 Bev/c, 20: 15422
SINGH, Virendra, SU(n) crossing matrices for baryon-meson scattering, 20: 15322
SINGH, Zorawar Khangura, Compound elastic scattering of 3.15-Mev neutrons by ^{40}Ca, 20: 15865
SINHA, S. P., Spectroscopic investigations of some neodymium complexes, 20: 14560
SINNAMON, Gerald F., Prog. rpt. on measurements of low energy electron precipitations associated with auroral disturbances and trapped radiation belts, final, 3/63–9/65, 20: 15589 (ASE-1125)
SIPS, V., Collective theory of Bohm and Pines, 20: 15987
SIRLIN, A., Weak interactions and G_2, 20: 15474
SISTLER, J., Application to lens-type spectrometer of internal-external conversion IEC method for determination of internal conversion coefficients, 20: 15710 (CONF-233(Vol.2), pp 252-5)
SJOEDEN, Ann-Marie, Placental transfer of ^{85}Sr in mice, 20: 14244
SKLADANOWSKI, Z., Equilibrium deformations of the odd-mass nuclei in rare-earth region, 20: 15788
SKODA, J., Urinary excretion of pseudouridine in course of x-ray therapy, 20: 14269
SKREB, Yvette, Prog. rpt. on mechanism of initial radiation effects, final, 11/63–10/65, 20: 14259 (NP-15855)
SKREBTSOV, A. N., Radioisotope study of open-hearth process, 20: 14939
SKURNICK, I. D., Current distribution in an array of superconducting thin films, 20: 15643 (NASA-TN-D-3293)
SLAUGHTER, G. M., Fabrication procedures for Enrico Fermi fast breeder reactor fuel elements, 20: 16100
SLESAREV, I. S., Separation of spatial and angular variables in solving neutron transport equation, 20: 15673
SMART, Wesley M., Spin and parity of $Y_1^*(1815)$ and the $Y^*(1765)$, 20: 15414
SMEDAL, Magnus I., Evaluation for genetic damage in offspring of women with high-level gonadal irradiation, 20: 14348
SMIRNOV, A. I., Investigation of excited states $^{104,104*}Rh$ by observation of γ rays from (n,γ) reaction, 20: 15754
SMIRNOV, M. V., Electrolysis of Ce in chloride-fluoride systems, 20: 14564
SMIRNOV, M. V., Lanthanum trichloride reaction with fused eutectic mix of Li and K chlorides, 20: 14565
SMIRNOV, M. V., Polarization of Mo cathode in LiCl–KCl and NaCl–KCl, 20: 14562
SMIRNOV, M. V., Reaction of trivalent Ce ions with fluoride anions, 20: 14563
SMIRNOV, N. V., Anodic dissolution of Ce metal, 20: 14561
SMIRNOV, V. N., Measurements of mean energy of electron beams in low-energy linear accelerators, 20: 15179
SMIRNOV, Yu. N., Crystal structure of gadolinium at 120 to 370°K, 20: 15124
SMITH, Alan R., Threshold detector applications to neutron spectroscopy at Berkeley accelerators, 20: 15175 (UCRL-16312)
SMITH, Arvin H., Progress in photovoltaic energy conversion, 20: 15305
SMITH, Bob H., Three-phase, 1.5-Mw, electronic line regulator for Berkeley 88-inch cyclotron, 20: 15183
SMITH, Dean Leroy Jr., Mass and energy transfer between confined plasma jet and gaseous coolant, 20: 15584
SMITH, F. F., Egg mortality after gamma irradiation of adults of omnivorous leaf roller, 20: 14340
SMITH, F. R., Prog. rpt. on accurate nuclear fuel burnup analyses, 6–8/65, 20: 15717 (GEAP-4950)
SMITH, F. R., Prog. rpt. on accurate nuclear fuel burnup analyses, 2–5/65, 20: 15133 (GEAP-4893)
SMITH, Gerald A., Final-state interaction involving hyperons, 20: 15412
SMITH, Gerald A., Spin and parity of the Ξ^* (1530 Mev), 20: 15464
SMITH, Hamilton, Napoleon's illness 1816–1821 in light of activation analyses of hairs from various dates, 20: 14478
SMITH, J. A., Pathfinder flooding coefficient, core pressurization, and temperature coefficient tests, 20: 16059 (ACNP-65600)
SMITH, J. Ed., CVTR organic loop feasibility study, 20: 16063 (CVNA-241)
SMITH, J. H., Decay spectrum of $K^0_{2\mu}$, 20: 15331

SMITH, J. Lloyd, Legal aspects of radiation-safety program, 20: 14801
SMITH, J. R., Measurement of absolute value of eta for ^{233}U, ^{235}U and ^{239}Pu using monochromatic neutrons, 20: 15718 (IDO-17083)
SMITH, L. T., Exchange mechanisms in K–p reactions at 1.8 and 1.95 Bev/c, 20: 15420
SMITH, O. Glenn, Burnout in steam–water flows with axially nonuniform heat flux, 20: 14696
SMITH, P. K., ^{244}Cm for radioisotopic heat sources work at Savannah River laboratory, 20: 15038 (CONF-660305-12)
SMITH, P. W., Large-scale processing and source preparation of separated fission products, 20: 14641 (RL-SA-59)
SMITH, R. C., Malignant mixed muellerian neoplasms (mixed mesodermal tumors), 20: 14300
SMITH, Thomas M., Half-life measurements of some neutron induced isomers, 20: 15688 (AD-620384)
SMOLIN, M. D., Electric transport of components in Mo–W system, 20: 15116
SMRZ, Pavel, Absorptive corrections to the nucleon exchange term in elastic πN scattering, 20: 15324
SNELLMAN, H., Experimental and theoretical studies of L-conversion electron directional correlations, 20: 15699 (CONF-233(Vol.2), pp 117-19)
SNOEK, C., Structure in electron energy spectrum from multi-kev Ar^+–Au and Ar^+–Cu collisions, 20: 15261
SNOW, G. A., Low-energy hyperon-proton reactions, 20: 15413
SNYDER, Bernard Joseph, Gamma ray scintillation detector efficiencies, 20: 14897
SNYDER, W. S., Calculation of radiation dose from protons and neutrons to 400 Mev, 20: 14330
SNYDER, W. S., Radiobiological aspects of supersonic transport, 20: 14797
SOBCZYNSKI, Zbigniew, Absolute activity measurement of weakly radioactive preparations, 20: 14896
SOBCZYNSKI, Zbigniew, Thermalization process of neutrons from Po–Be neutron sources in a paraffin moderator, 20: 15683
SOBUE, Hiroshi, Radiation-induced copolymerization of tetrafluoroethylene with isobutylene. I., 20: 14608
SOCOLOW, R., Electrodynamic mass formula in SU(3) and SU(6), 20: 15535
SODAN, H., Gamma transitions in ^{153}Eu, 20: 15734 (ZfK-PhA-18)
SODEK, Bernard A. Jr., Viscous effects in a hydromagnetic waveguide, 20: 15925
SOFFER, A., Effects of chelating agents in man, 20: 14256
SOINE, T. S., Prog. rpt. on batch electrorefining of Pu metal, 5/65, 20: 14967 (RL-SEP-503-1)
SOINE, T. S., Stirred-bed gas-solids reactor for preparing plutonium trichloride, 20: 14669 (RL-SEP-414)
SOKOLOV, A. A., Neutrino-nucleon interactions with lepton production, 20: 15387
SOKOLOVSKII, Yu. S., Anodic dissolution of Ce metal, 20: 14561
SOKOLOVSKII, Yu. S., Electrolysis of Ce in chloride-fluoride systems, 20: 14564
SOKOLOVSKII, Yu. S., Polarization of Mo cathode in LiCl–KCl and NaCl–KCl, 20: 14562
SOKOLOVSKII, Yu. S., Reaction of trivalent Ce ions with fluoride anions, 20: 14563
SOLDAT, J. K., Environmental monitoring, 20: 14786 (BNWL-SA-465)
SOLLFREY, William, Effects of propagation on high-frequency electromagnetic radiation from low-altitude nuclear explosions, 20: 15605
SOLOV'EV, A. N., Mechanism of boiling of liquid sodium on heating surface at free convection, 20: 14693 (AD-625791)
SOLOVEV, L. D., Interactions $y3\pi$ and $p\pi\gamma$, 20: 15389
SOLOVEV, S. M., Deuteron fission of ^{232}Th and dependence of fragment kinetic energy on excitation energy of the fissile nucleus, 20: 15840
SOMMER, L., Complexes of uranyl with phenolic ligands. III., 20: 14481
SOMMER, L., Uranyl complexes with phenolic ligands. IV., 20: 14482
SONA, P. G., Statistics of eigenvalues of random matrices, 20: 15784
SONDHAUS, C., Radiobiological aspects of supersonic transport, 20: 14797
SONG, Xing-chang, Intermediate boson theory in SU(6) symmetry, 20: 15497
SONKA, Jiri, Activity of pyridine nucleotidase in whole-body x-irradiated rats, 20: 14362
SONNABEND, E., Radiation tolerance of patient in extra-oral radiography, 20: 14412
SOOP, Mattias, JWKB approximation for barrier transmission, 20: 15625
SOROKIN, A. A., Decay scheme of $^{119}*Te$, 20: 15762
SOVKA, J. A., Nondestructive measurement of burnup by γ-ray spectroscopy, 20: 14504
SOVTSOV, M. I., Decay of ^{99}Mo, 20: 15751
SPACU, P., New ytterbium compounds with organic acids, 20: 14490
SPAHR, H. R., Comparison of results of Sandia TTA trajectory program and Atomics International RESTORE trajectory program, 20: 16113 (SC-RR-66-22)
SPALLER, A. E., Structural analysis of shipping casks. Vol. I., 20: 14667 (ORNL-TM-1312(Vol.1))
SPARGO, Edward, Quasi-classical solution to the Dirac equation, 20: 15559
SPECHT, Frederick, Nonisotropic exchange interactions in rare earth metals, 20: 15990
SPENCER, Herta, Effects of chelating agents in man, 20: 14256
SPENCER, Richard P., Production of ^{75}Se-selenocystine by neutron activation, 20: 14630
SPENER, G., Diffusion of uranium in graphite, 20: 15087
SPENKO, M., Direct spectrographic determination of impurities in uranium tetrafluoride, 20: 14473
SPIKES, John D., Quantum yield studies of dye-sensitized photoinactivation of trypsin, 20: 14274
SPINKS, N., Variational approach to effect of boundary perturbations when the multigroup diffusion equations apply, 20: 16033
SPIRIDON, M., Rate of peroxidation of homogenized tissues during their irradiation in vitro, 20: 14261
SPRACKLEN, Howard P., Nuclear radiation detector with control grid, 20: 14917
SPRINKLE, Ellen A., Saturation curve in cylindrical and spherical ionization chambers, 20: 14884
SRIVASTAVA, Y. N., Kronecker delta-type singularities and Reggeization, 20: 15465
SROUBEK, Z., Electron spin resonance of NO_3 in irradiated $NaNO_3$, 20: 15965
STADELMAIER, H. H., Cobalt corner in the tri-component system cobalt–niobium–boron, 20: 15100
STADNYKH, B. I., Zirconium–cobalt–boron system, 20: 14533
STAEBLER, Karl, Control rod drive system of Garigliano nuclear power plant, 20: 16074 (EUR-2420.d,f,i,n,e, pp 227-48)
STAEBLER, Karl, Description of the turbine regulation and experience at SENN power station on turbine startup, 20: 16071 (EUR-2420.d,f,i,n,e, pp 191-202)
STAFFURTH, J. S., Atrial fibrillation in thyrotoxicosis treated with radioiodine, 20: 14424
STAHL, S., Subcritical, critical, and burst facilities in fast reactor physics research, 20: 16123 (KFK-350)
STANKOVA, O., Complexes of uranyl with phenolic ligands. II., 20: 14522
STANLEY, Alan G., Effect of electron irradiation on N-channel MOS transistors, 20: 14924
STANLEY, P., Calculation of group averaged neutron cross sections (FORTRAN for IBM-7030), 20: 15665 (AWRE-O-103/65)
STAPP, H. P., Analytic S-matrix theory, 20: 15512
STARBUCK, J. W., X-ray determination of crystallite size of thoria, 20: 15044 (MCW-1493, pp 15-25)
STARK, K. M., Metabolic theory of cell survival curves, 20: 14359
STASHKOV, A. M., Early reaction of adrenal cortex in dogs exposed to radiation, 20: 14280
STASOVSKAYA, V. V., Measurement of abrasive capacity of powders of carbides and borides of refractory metals, 20: 15109
STAUDENMAIER, H.-M., Construction and properties of analyzer for measurement of neutron polarization, 20: 14856 (KFK-345)
STAUTBERG, J. L., Single-pion production in π^-p interactions between 600 and 900 Mev, 20: 15411
STEDMAN, Jon D., Spiral reader control and data acquisition with PDP-4, 20: 14861 (UCRL-16555)
STEELE, F. K., Comparison between solar x-ray emission and vlf sudden phase anomalies, 20: 15603
STEEN, H. B., Inactivation and induction of free radicals in dried trypsin, 20: 14273
STEENBECK, L., DPN degradation and synthesis of lymphosarcoma ascites cells after x irradiation, 20: 14370
STEFFENS, J., Effect of mechanically induced vibrations on heat transfer rates in pressurized water system, 20: 16000 (NYO-2655-1)
STEIGERWALD, E. A., Permeability to hydrogen of metals with metallic coatings, 20: 14987
STEIN, E. M., Survey of representations of non-compact groups, 20: 15540
STEINBERG, Meyer, Neutron burning of long-lived fission products for waste disposal, 20: 16132 (BNL-8558)
STEINBERG, Neil Ira, Gamma radiation induced graft copolymerization of styrene and polyethylene, 20: 14624
STEINFINK, H., Structure refinement of La_2Te_3, Th_3P_4 type structure, 20: 14524
STEINITZ, R., Dissociation and evaporation of TaC, HfC, and ZrC at elevated temperatures, 20: 15052 (NP-15880)
STEINMAN, Gary David, Photobiochemistry–dehydration condensation in aqueous solution, 20: 14233 (UCRL-16566)
STEINMANN, O., Renormalizability in LSZ perturbation theory, 20: 15452
STEINMANN, W., Transition radiation from thin silver foils, 20: 15968
STEPANOV, A. V., Radioactivity of air over Atlantic Ocean in May to July, 1964, 20: 14743
STEPIEN, K., Hydromagnetic oscillations of nonuniform plasma. I.,

20: 15890
STERLING, Lehman N., Mixed heterologous mesenchymal sarcomas (mixed mesodermal sarcomas) of uterus, 20: 14301
STERLINSKI, Slawomir, Method for simultaneous counting of source and background for short-lived radioisotopes near determination limit, 20: 14878
STERNBERG, Joseph, Placental transfer of fission products and effects on fetal development, 20: 14372
STERNBERG, W. H., Malignant mixed muellerian neoplasms (mixed mesodermal tumors), 20: 14300
STERNER, J. H., Atomic energy for society and balance between hazard and gain, 20: 14802
STERNGLASS, E. J., Molecular structure of meson and baryon resonance states, 20: 15399
STETSON, R. F., Use of silicon solar cells as detectors of energetic electrons from plasmas, 20: 15916
STEWART, Alice, Oxford survey of childhood cancers progress report III, 20: 14346
STEWART, Alice M., Childhood cancer in twins, 20: 14319
STEWART, G. H., Conference on ceramics, Noordwijk aan Zee, Vol. 2, 5/63, 20: 14970
STOCKMEYER, R., Dispersion curves for rotation oscillations of tetrahedral molecules in face-centered lattice with tetragonal molecular orientation, 20: 15940 (JUL-292-RW)
STOECKER, W. C., X-ray determination of crystallite size of thoria, 20: 15044 (MCW-1493, pp 15-25)
STOECKERT, Heinz, Determination of trace impurities in UO_2 fuel materials, 20: 14494
STOELAN, Birger, Study of many-fermion systems, 20: 15564
STOLARSKI, G. Z. A., Stored energy in neutron-irradiated beryllium oxide, 20: 15142
STONEHILL, D. L., Growth of tracks from segments, 20: 14849 (BNL-9720)
STONEHILL, D. L., p-p Annihilations into K and π mesons at 3.7 Bev/c, 20: 15338
STONEHILL, D. L., Search for decay $\eta \rightarrow \pi^0 + e^+ + e^-$, 20: 15333
STONEHOUSE, Albert James, Sintered intermetallic bodies composed of aluminum and niobium or tantalum, 20: 15026
STORK, D. H., Exchange mechanisms in K⁻p reactions at 1.8 and 1.95 Bev/c, 20: 15420
STORMS, E. K., Heat capacities of $NbC_{0.702}$, $NbC_{0.825}$, $NbC_{0.980}$, and Nb_2C below 320°K, 20: 15097
STOTHERS, Richard, Evolution of O stars. III., 20: 15218
STOYANTSOVA, Z. P., Roentgenographic studies of lanthanum tellurides, 20: 14530
STRASHINSKAYA, L. V., Behavior of new materials working in contact with solid metals, compounds, and melts, 20: 14989
STRATHDEE, J., Relativistic extension of non-compact symmetry groups, 20: 15370
STRATHDEE, J., $\bar{U}(12)$ symmetry, 20: 15537
STRAUCH, Karl, Use of bubble chambers and spark chambers at electron accelerators, 20: 15187
STRAUSS, B., Repair of damage induced by monofunctional alkylating agent in transformable, ultraviolet-sensitive strain of Bacillus subtilis, 20: 14267
STREATER, R. F., Broken symmetries and the Goldstone theorem, 20: 15552
STREKALOVSKII, V. N., Structure, electric conductivity, and conductivity characteristics in ternary system (0.75 CeO_2–0.25 ZrO_2)–CaO, 20: 14536
STREMNITZER, H., Results of isospin exchange relations for pion production amplitudes, 20: 15449
STRENG, A. G., Photochemical formation of krypton difluoride from krypton and fluorine or oxygen difluoride, 20: 14527
STRENG, L. V., Photochemical formation of krypton difluoride from krypton and fluorine or oxygen difluoride, 20: 14527
STRINDEHAG, Ove M., Optical reflectors for use in internal sample aqueous Cherenkov counters, 20: 14893
STRINI, G., Acceleration of negative ions in Milan AVF cyclotron, 20: 15180
STROEM, Staffan, Construction of representations of inhomogeneous Lorentz group by means of contraction of representations of (1 + 4) de Sitter group, 20: 14954
STROEM, Staffan, Contraction of representations of Lorentz group to representations of Euclidean group, 20: 14953
STROEMME, Aksel, ^{137}Cs in people and food in Norway, 1963–1965, 20: 14739 (TID-22655)
STROGONOV, Yu. D., Studies of carbidization of titanium and zirconium nitrates, 20: 15072
STROHAL, P., Isomeric cross-section ratios for 14.6-Mev neutron-induced reactions, 20: 15773
STRUZYNSKI, R. E., Continuous γ radiation accompanying β decay, 20: 15801
STUMP, R., p-p Annihilations into K and π mesons at 3.7 Bev/c, 20: 15338
STURCKEN, E. F., ^{244}Cm for radioisotopic heat sources work at Savannah River laboratory, 20: 15038 (CONF-660305-12)
STURGES, Donald G., Neutron shielding using composition comprising graphite, boron carbide and carbonized residue, 20: 15027
STURROCK, P. A., New model of solar flares, 20: 15214
STURROCK, W. R., Creep of single-crystal UO_2, 20: 15086
SUBBOTIN, V. I., Impurities in Cs in thermionic converters, 20: 15298 (FEI-22)
SUBOTOWICZ, Mieczyslaw, Measurement of matrix elements for first forbidden β transitions. II., 20: 15824
SUBRAHMANYAM, Vishnubhotla, Alpha-decay studies of protactinium isotopes, 20: 15864
SUCCI, C., Acceleration of negative ions in Milan AVF cyclotron, 20: 15180
SUDARSHAN, E. C. G., Theory of approximate symmetries, 20: 15548
SUEHIRO, Yoshiyuki, Production of spherical uranium nuclear fuel substances, 20: 14575
SUEOKA, Osamu, Plasma oscillation of electrons in Be, Mg, Al, Si, Ge, Sn, Sb, and Bi, 20: 15951
SUEOKA, Osamu, Plasma oscillation of electrons in Al–Be, Al–Ge, and Al–Sn eutectoids, 20: 15952
SUEOKA, Osamu, Plasma oscillation of valence electrons and exciton in alkali halides, 20: 15953
SUEOKA, Osamu, Plasma oscillation of conduction electron in Na, 20: 15955
SUEPTITZ, P., Diffusion and isotopic effects of ^{22}Na and ^{24}Na on silver chloride, 20: 15966
SUESSMANN, G., Dipole approximation in nonlocal potential, 20: 15842
SUGAHARA, Tsutomu, Radiosensitivity and nonprotein SH compounds in mammalian tissues, 20: 14351
SUGAR, R., Linear integral equations for relativistic multi-channel scattering, 20: 15351
SUGAWARA, Tadashi, Low temperature resistivity of yttrium-based alloys containing small amounts of rare earth metals, 20: 15098
SUGIMOTO, Daiichiro, Advanced phases of evolution of population II stars, 20: 15227
SUGLUBOV, D. N., Infrared spectra of products of Nd_2O_3 reaction with water, 20: 14568
SUKHINA, B. N., Experimental investigation of charge-transfer injection of proton into cyclic accelerators and storage rings, 20: 15162 (NP-15785)
SUKHINA, B. N., Experiments with charge exchange injection in storage ring, 20: 15177
SUMBAEV, O. I., Investigation of excited states $^{104,104*}Rh$ by observation of γ rays from (n,γ) reaction, 20: 15754
SUN, C., V-2-prong K⁻p interactions at 5.5 Bev/c, 20: 15416
SUNDARESAN, M. K., $\eta\pi\pi$ Model of χ^0 and a possible η-π resonance, 20: 15355
SUNDERMAN, Duane N., Prog. rpt. on applicability of existing data to analytical description of a nuclear-reactor accident, 10–12/65, 20: 16019 (BMI-X-10154)
SUTTON, G. H., Ocean-bottom seismic observatories, 20: 14767
SUYAMA, Naohiro, Radiation leak test of shielded cells at reprocessing analytical facility, 20: 14788 (JAERI-1089)
SUZUKI, Mahiko, Partially conserved axial-vector current and decays of vector mesons, 20: 15485
SVECHNIKOV, V. N., Phase diagram of columbium–nickel system, 20: 15115
SVICHEKOVA, M., New complexes. III., 20: 14521
SVIRIDOV, Yu. K., Experimental investigation of charge-transfer injection of proton into cyclic accelerators and storage rings, 20: 15162 (NP-15785)
SVIRIDOV, Yu. K., Experiments with charge exchange injection in storage ring, 20: 15177
SWAIN, C. Gardner, Conductance of ions in light and heavy water at 25°, 20: 14540
SWAIN, R. J., LASA sensing system design, installation, and operation, 20: 14759
SWAN, P., Deduction of potentials from scattering phase shifts. I., 20: 15463
SWARTZENDRUBER, D. C., Breakdown of DNA in x-irradiated Escherichia coli, 20: 14265
SWENSON, C. A., Lithium metal: experimental equation of state, 20: 15096
SYKES, E. C., Some mechanical properties of uranium at intermediate strain rates and temperatures, 20: 15081
SZANTAI, Ionos, Isotopic exchange between iodo amino acids and ^{131}I on chromatographic paper, 20: 14632
SZAWLOWSKI, Marek, Semiconductor p-n junction detector for nuclear radiation as electric signal source, 20: 14875
SZYMANSKI, Z., Equilibrium deformations of the odd-mass nuclei in rare-earth region, 20: 15788
SZYMCZYK, S., Octupole Coulomb excitation of ^{208}Pb, 20: 15719 (INP-431/PL)

T

TABATA, Tatsuo, Energy monitor for electron beams, 20: 15184

TABATA, Yoneho, Radiation-induced copolymerization of tetrafluoroethylene with isobutylene. I., 20: 14608

TACKETT, James Edwin, Properties and infrared spectra of several metal chelates, 20: 14499

TADA, Hiromitsu, Diffusion length of thermal neutrons in terphenyl (Santowax-R) at temperatures up to 400°C, 20: 15680

TAFT, H. D., p-p Annihilations into K and π mesons at 3.7 Bev/c, 20: 15338

TAGLIAFERRI, G., Acceleration of negative ions in Milan AVF cyclotron, 20: 15180

TAKAHASI, Tomotsu, Cosmic ray intensities under sea-water at depths down to 1,500 meters, 20: 15289

TAKAMATSU, Toshiaki, Graft copolymerization of polymer, initiated by electron irradiation, in the presence of monomer vapor. IV., 20: 14618

TAKAMUKU, Setsuo, Radiation chemistry of cyclic dienes. I., 20: 14610

TAKAMURA, Akira, Stress corrosion cracking of Ti and Zr in HCl–methanol solutions, 20: 14988

TAKAYANAGI, Kazuo, Excitation of molecular vibration by slow electrons, 20: 15256

TAKEUCHI, Masa, Vertical distributions of fallout gamma-ray sources in ground soil in eastern Japan, 20: 14751

TAKVALE, R., Neutrino-nucleon interactions with lepton production, 20: 15387

TAMAO, Tsutomu, Possible mechanism for rules of polarization of pc5 geomagnetic pulsations, 20: 15616

TAMARKIN, P., Systems for detection and identification of nuclear explosions in the atmosphere and in space, 20: 15594

TAMURA, Masami, Electron-photon shower study by the Monte Carlo method, 20: 15938

TAMURA, Tsuneo, Selective sorption reactions of strontium with soil minerals, 20: 14652

TANAKA, K., Radiative decay of vector mesons in SU(6), 20: 15472

TANAKA, Momoru, γ Shielding property, strength and workmanship of built-up type lead slab structure, 20: 15932 (ORNL-tr-843)

TANAKA, Osamu, 30-Mev flux-forced field-biased betatron, 20: 15181

TANG, Ting-wei, Generation of the third-harmonic current density in a plasma, 20: 15909

TANNER, Raymond L., Electron beam produced lichtenberg figures, 20: 14607

TAO, S. J., Effect of minor impurities on positron annihilation lifetime spectrum in argon, 20: 15436

TAPE, Gerald F., Space and nuclear energy, 20: 16115

TAPPEL, A. L., Damage to proteins, enzymes, and amino acids by peroxidizing lipids, 20: 14587

TARAN, Yu. V., Determination of neutron resonance spins in ^{165}Ho nuclei, 20: 15681

TARASOV, V. K., Applicability of the Ikegami-Udagava method for considering pairing correlations, 20: 15766

TARIMER, N., Dynamical quantum numbers implied by representation types of Poincare group, 20: 15544

TATE, P. A., Saturation curve in cylindrical and spherical ionization chambers, 20: 14884

TATTERSALL, K., Problems of microbial contamination in prepacked preparations, 20: 14941

TAUB, J. M., Coated particle fuel elements for UHTREX, 20: 15002 (LA-3378)

TAUBE, Miecyslaw, Concept of salt-boiling fast breeder reactor, 20: 16037

TAUBE, Mieczyslaw, Concept of fast breeder reactor with fused salt fuel and boiling mercury "wars", 20: 16036

TAUSNER, M., Effect of intermediate vector mesons on neutrino production, 20: 15347

TAUTFEST, G. W., Angular correlation study of reaction $\pi^- p \to \pi^- \pi^+ p \pi^-$ at 2.7 Bev/c, 20: 15410

TAVKHELIDZE, A., Electromagnetic form factors in composite models of elementary particles (relativistic models), 20: 15551

TAVKHELIDZE, A., Higher symmetries and composite models of elementary particles, 20: 15550

TAYLOR, J. G. V., K-shell fluorescence yields of V, Cr, and Cu, 20: 15242 (CONF-233(Vol.3), pp 465-79)

TAYLOR, J. R., Navigator study of electric propulsion for unmanned scientific missions, 20: 14724 (65SD5322-A)

TAYLOR, John R., Cluster decomposition of S-matrix elements, 20: 15484

TAZZARI, S., Instrument for measuring magnetic fields in range 0.01 to 20 gauss with peaking strips, 20: 15160 (LNF-65/44)

TEICHMANN, J., On the propagation of electromagnetic waves in a plasma with heavy positive and negative ions, 20: 15910

TEMPEL, K., Deoxyribonuclease II and deoxyribonucleic acid in rat thymus after action of radiomimetic drugs and x irradiation, 20: 14311

TEMPEL, K., Effect of radiomimetic drugs and x irradiations on permeability of blood-brain barrier to Evans blue, 20: 14312

TENISHEVA, T. F., Polymorphism of rare earth pyrosilicates, 20: 14537

TEREE, Thomas M., Decrement in radiostrontium retention following stable strontium prefeeding in growing rat, 20: 14251

TERFLOTH, H. P., Study to find detector situated within radiation field of reactor core which will indicate fission products in coolant under operating conditions, 20: 14847 (BMwF-FBK-65-01)

TER-POGOSYAN, R. A., X-radiation influence on smallpox vaccine virus in chicken embryo, 20: 14281

TESTA, C., Control of polyphenyls in work environments, 20: 14467 (RT/PROT(64)–20)

TESTAGUZZA, Gino, Laminated radiation resistant panels, 20: 14680

THAL, Marie-Florence, Release, properties, and trapping of radioactive iodines in waste gases, 20: 14787 (CEA-Bib-64)

THANOS, S. N., Ocean-bottom seismic observatories, 20: 14767

THEVENET, B., Search for decay $\eta \to \pi^0 + e^+ + e^-$, 20: 15333

THIESSEN, K., Photoconductivity and p-n photoeffect in SiC during excitation with x radiation, 20: 15967

THOMAS, E. W., Bibliography on atomic and molecular processes, 1964, 20: 15248 (ORNL-AMPIC-3)

THOMAS, M. F., ^{54}Fe: spins and decay modes of low-lying excited states, 20: 15786

THOMAS, Robert Leighton, Ultrasonic longitudinal wave attenuation in superconducting tin, 20: 15659

THOMASON, P. F., Infrared and nuclear magnetic resonance spectrometry, 20: 14459 (ORNL-3889, pp 44–6)

THOMASON, P. F., Organic preparations, 20: 14576 (ORNL-3889, pp 73-7)

THOME, P., Control methods used in department of metallurgy for structural and fuel elements, 20: 14711

THOME, P., Remote-controlled automatic welding in construction of nuclear reactor, 20: 15019

THOMPSON, D. S., Electronic spectra of solutions of europium and ytterbium in liquid ammonia, 20: 14526

THOMPSON, F. E., Modular system of logic for the Vela satellite program, 20: 15597

THOMPSON, J. C. Jr., Prog. rpt. on fission product metabolism and response in animals, 1/64–12/65, 20: 14243 (TID-22626)

THOMPSON, M. A., Effect of composition on corrosion of plutonium metal, 20: 14984 (RFP-511)

THOMPSON, M. A., Results on π^--p and K^+-p interactions at high energy. A., 20: 15406

THOMPSON, M. C., Chemical processing of Cm, 20: 14636 (CONF-660305-7)

THOMPSON, M. C., ^{244}Cm for radioisotopic heat sources work at Savannah River laboratory, 20: 15038 (CONF-660305-12)

THOMPSON, R. C., SNPO and SNAP biological studies, 20: 14785 (BNWL-182)

THOMPSON, William Alexander Jr., Crystalline anisotropy of superconducting energy gap in aluminum, 20: 15658

THOMSON, Karl V., Design calculations for ionization spectrometers: cascade development, 20: 14892

THOR, Anders J., Binding energy and the quadrupole moment of the deuteron, 20: 15323

THORNE, Kip S., Gravitational collapse and death of a star, 20: 15230

THOSAR, B. V., K-shell conversion coefficients for pure E2 transitions in deformed nuclei, 20: 15706 (CONF-233(Vol.2), pp 191-7)

THRESHER, J. J., Differential cross sections and polarization effects in pion-proton elastic scattering at 875 to 1579 Mev/c, 20: 15372

THUN, J. E., Experimental and theoretical studies of L-conversion electron directional correlations, 20: 15699 (CONF-233(Vol.2), pp 117-19)

THURBER, W. C., Fabrication procedures for Enrico Fermi fast breeder reactor fuel elements, 20: 16100

THYAGARAJAN, R., F-bands in NaBr–NaCl mixed crystals, 20: 14605

TICHO, H. K., Exchange mechanisms in K-p reactions at 1.8 and 1.95 Bev/c, 20: 15420

TIKHOMIROV, V. R., Determination of radiocesium in environment, 20: 14483

TIKHONOV, A. N., Analyzing spectra of γ quanta and fast neutrons measured by means of single-crystal scintillation spectrometers, 20: 14869

TILGER, C. A., π^+p interactions at 781 Mev, 20: 15341

TIMASHEV, S. F., Direct reactions with two-nucleon transfer, 20: 15798

TIMOSHIN, I. Yu., Experimental investigation of charge-transfer injection of proton into cyclic accelerators and storage rings, 20: 15162 (NP-15785)

TIMOSHIN, I. Yu., Experiments with charge exchange injection in storage ring, 20: 15177

TIMOV, V. V., Silicon solar cells produced by ion bombardment, 20: 15302

TIRONI, Gino, Linearized Rayleigh's problem in magnetogasdynamics, 20: 15578

TISHKIN, P. A., New data on decay of ^{184*}Re, 20: 15750

TISLJAR-LENTULIS, G. M., Method for measurement of ionization curves by

means of scintillation counters, 20: 14891
TITOV, A. I., Conductivity induced in Ge by bombardment with K ions, 20: 15978
TITTMANN, Bernard Rainer Michel, Amplitude-dependent ultrasonic attenuation in superconducting lead, 20: 15657
TKEBUCHAVA, F. G., Interactions $y3\pi$ and $p\pi\gamma$, 20: 15389
TODOROV, I. T., Symmetry group ISL(6): representations and invariants, 20: 15498
TOERNKVIST, S., Experimental and theoretical studies of L-conversion electron directional correlations, 20: 15699 (CONF-233(Vol.2), pp 117-19)
TOKUOKA, Zensuke, Generating relations of sub-algebras in Duffin-Kemmer algebra, 20: 15462
TOLL, J. S., Equivalence of locality and paralocality in free parafield theory, 20: 15468
TOLL, J. S., Two, three, and four point functions in quantum field theory, 20: 15513
TOLOS, W. P., Development of thorium purification system, 20: 14448 (NLCO-970, pp 1.1–22)
TOMASCH, W. J., Energy spacing of geometrical resonance structure in thick films of superconducting In, 20: 15650
TOMASINI, G., Small-angle elastic scattering of polarized protons in photographic emulsions, 20: 15314 (RT/FI(65)35)
TOMISHIMA, Yasuo, Energy levels in Thomas-Fermi dirac atom, 20: 15267
TOMITA, Kenji, A simple and well-adjusted exterior metric for collapsing or anti-collapsing star, 20: 15228
TOMIYASU, H., Acceleration of uranium(IV)–(VI) electron exchange reaction by hydrochloric acid, 20: 14570
TOMOZAWA, Yukio, Reciprocity, normality of K^0-$\bar{K}^0$ mass matrix, and CP violation in weak interactions, 20: 15350
TONG, L. S., Burnout in steam–water flows with axially nonuniform heat flux, 20: 14696
TONG, L. S., Transient DNB test on CVTR fuel assembly, 20: 16101
TONOLINI, F., Statistics of eigenvalues of random matrices, 20: 15784
TOOPER, Robert F., Adiabatic fluid spheres in general relativity, 20: 15211
TORGERSON, R. T., Properties of an yttrium-containing columbium alloy, 20: 15119
TORGESON, D. R., Paramagnetic resonance of cobalt in intermetallic compounds, 20: 15963
TOTSKII, I. A., Elastic scattering of medium-energy neutrons and the optical nuclear model, 20: 15770
TOTTLE, C. R., Mechanical properties of uranium compounds, 20: 15029 (ANL-7070)
TOVSTOLES, K. V., Kidney function in cases of subcutaneous trauma combined with radiation sickness, 20: 14325
TRAINOR, L. E. H., Liquid helium and the properties of finite Bose-Einstein assemblies, 20: 15645
TRAKHTENBERT, L. I., Eddy-current method for multi-parameter testing of structural components, 20: 14708
TRAMS, A., Influence of 5-hydroxytryptamine (serotonin) on radioinduced mutation rate in Drosophila melanogaster, 20: 14398
TRAUTMANN, Norbert, Rapid extraction by quasi-solid extraction agent, 20: 14656
TRAYLOR, E. Dean, Mass transfer of U spheres to flowing molten Cd in laminar and turbulent flow, 20: 14975 (ANL-7091)
TREMILLON, Bernard, Ion exchange methods of separating zirconium and hafnium, 20: 14657
TRIER, Jerry S., Morphologic response of mucosa of human small intestine to x-ray exposure, 20: 14339
TRIFTSHAEUSER, W., Measurement of free and incoherent neutron cross sections of silicon and lead, 20: 15682
TRIPARD, G. E., Detection of pulse pile-ups with pulse overlap to pulse height converter, 20: 14828
TROSTEL, Louis J. Jr., Stability of alumina and zirconia in hydrogen, 20: 14986
TROZERA, T. A., Prog. rpt. on mechanical properties of reactor materials, annual, 11/64–10/65, 20: 15040 (GA-6721)
TRUKHLYAEV, P. S., Preparation of ^{242}Pu and ^{242}Cm from neutron-irradiated ^{241}Am, 20: 14631
TRUNOV, V. K., Binary oxides in ZrO_2–Nb_2O_5 systems, 20: 15079
TSCHERNER, Manfred, Different methods for determination of radioactivity in air, 20: 14745
TSCHIRF, E., Experiments in development of neutron dosimeter, 20: 14862
TSEVELEV, M. A., Relative levels of fission fragment fallout from stratosphere, 20: 14742
TSUJI, Yoshio, Diffusion length of thermal neutrons in terphenyl (Santowax - R) at temperatures up to 400°C, 20: 15680
TSUKERMAN, S. A., Study of homogeneous sintered tungsten–hafnium alloy, 20: 15021
TSUMORI, Kunihiko, Energy monitor for electron beams, 20: 15184
TSYLOV, Yu. A., Density and viscosity of solutions of system: organic solvent-rare earth nitrate solutions, 20: 14648
TSYTKO, S. P., Measurement of linear polarization of 1.97-Mev γ rays in reaction $^{36}Ar(p,p'\gamma)^{36}Ar$, 20: 15760
TSYTKO, S. P., Nuclear levels of ^{27}Al at excitation energies of 10.495 and 3.95 Mev, 20: 15761
TUBIS, Arnold, Nucleon as a composite particle state, 20: 15352
TUBIS, Arnold, Self-consistent determination of position and width of the 33 π in resonance, 20: 15353
TUCKER, P. A., Radioactive radiation emitting sources, 20: 14634
TUNKELANG, B., Bosons, A parity, and G_2, 20: 15473
TURCHINETZ, W., The energy and angular distribution of photoneutrons from heavy elements, 20: 15723 (MIT-2098-162)
TURKIEWICZ, I. M., Excitation function of $^{29}Si(n,\alpha_0)^{26}Mg$ reaction for neutron energies around 14 Mev, 20: 15800
TURKIEWICZ, J., Excitation function of $^{29}Si(n,\alpha_0)^{26}Mg$ reaction for neutron energies around 14 Mev, 20: 15800
TURNER, D. T., ESR study of free radicals formed by γ-irradiation of poly(ethylene terephthalate), 20: 14606
TURNER, J. E., Calculation of radiation dose from protons and neutrons to 400 Mev, 20: 14330
TURRIN, A., External beam of Frascati electron synchrotron, 20: 15159 (LNF-65/36)
TWITTY, B. L., Determination of ^{235}U by gamma-ray spectroscopy, 20: 14449 (NLCO-970, pp 7.1–5)
TWITTY, B. L., Determination of beta activities in plant effluents, 20: 14450 (NLCO-970, pp 8.1–4)
TYURYUKANOVA, E. B., ^{90}Sr, stable strontium and calcium in soil and vegetable food products, 20: 14236

U

UDAGAWA, T., Centrifugal stretching and Coriolis-force antipairing effects in ^{182}W, 20: 15821
UDGAONKAR, B. M., Bootstraps, 20: 15553
UDUPA, K. B., Method for studying maturation time of average bone marrow cell in rat using ^{32}P as tracer, 20: 14248
UENO, Yori, Radiosensitivity and nonprotein SH compounds in mammalian tissues, 20: 14351
UGLOW, A. G., Size effect of radiation-induced dimensional changes of graphite, 20: 15143
UHLMANN, W., Bibliography on radiation effects on solid, U based nuclear fuel materials, Vol. 5, No. 4, 20: 15137 (VDIT-16(5.4))
UHRICH, David L., Measurement of lattice constant in dihydrides of gadolinium–yttrium alloys, 20: 14546
UJLAKI, Endre, Moessbauer effect of 46.5-kev line of ^{183}W, 20: 15737
ULLAH, Nazakat, Asymptotic solution for Brownian motion of eigenvalues of a random matrix, 20: 15785
ULLMAIER, H. A., Measurement of ionization in liquid argon due to x-rays, 20: 15259
UMANSKII, Ya. S., Diffuse scattering of x rays by HfC–ZrC solid solutions, 20: 15074
UMEDA, Iwao, Transmission of γ rays from line isotropic source through steel pipes, 20: 16114
UPTON, A. C., Radiobiological aspects of supersonic transport, 20: 14797
URAY, Zoltan, Isotopic exchange between iodo amino acids and ^{131}I on chromatographic paper, 20: 14632
URBAN, P., Higher symmetry of leptons, 20: 15448
USAKOVSKAYA, T. S., Effects of ionizing radiation on DNA in nucleoprotein complex, 20: 14277
UTSUMI, Takeshi, Polarization of the long period geomagnetic pulsation, pc5, 20: 15615
UZNADZE, O. P., Critical parameters of homogeneous breeding systems, 20: 16030

V

VALANT, Paolo, Regulating characteristics during the operation of Latina power plant, 20: 16072 (EUR-2420.d,f,i,n,e, pp 203-14)
VALANT, Paolo, Regulation of output of electronuclear power plant of the BWR-type dual-cycle Garigliano power plant, 20: 16073 (EUR-2420.d,f,i,n,e, pp 215-25)
VALENTIN, Jacques, 30.7-Kev anomalous electric dipole transition, 20: 15702 (CONF-233(Vol.2), pp 142-7)
VALERINO, Michael F., Analytical and experimental methods of determining heavy-isotope content of operating fuel elements, 20: 14438 (CEND-540)
VALLADAS, G., Reaction $\pi N \rightarrow \pi N^*(1238)$ near the $N^*(1510)$ and the $N^*(1690)$ resonances, 20: 15375
VAL'TER, A. K., Measurement of linear polarization of 1.97-Mev γ rays in reaction ^{36}Ar $(p,p'\gamma)^{36}Ar$, 20: 15760
VAL'TER, A. K., Nuclear levels of ^{27}Al at excitation energies of 10.495 and 3.95 Mev, 20: 15761
VAN ANDEL, J. G., Deposition of radioactive Ba and Sr in aortic wall, 20: 14252

VAN AUDENHOVE, J., Preparation by levitation melting in argon of homogeneous aluminum alloys for neutron measurements, 20: 15013
VAN CANEGHEM, P., Effect of x rays on reversibility of collagen gel, 20: 14593
VAN DAM, H., Instantaneous and asymptotic conservation laws for classical relativistic mechanics of interacting point particles, 20: 15154
VANDEN BERG, Henry J. Jr., Comparison of wound healing between irradiated and nonirradiated patients after radical neck dissection, 20: 14303
VAN DER LAARSE, J. D., Rapid method for simultaneous determination of total carbon and ^{14}C in small samples, 20: 14474
VAN DER LINDE, A., Quality selection of Zircaloy-2 canning tubes by ultrasonic testing on small defects, 20: 14714
VANDERVELL, H. D., Prog. rpt. on direct biological monitoring, 1963–64, 20: 14784 (AERE-R-5015)
VANDERVOORT, R. R., Mechanical properties of some uranium alloys, 20: 15060 (UCRL-7771)
VAN DER WEG, W. F., Structure in electron energy spectrum from multi-kev Ar^+–Au and Ar^+–Cu collisions, 20: 15261
VAN DE VORST, Albert, Radioresistance of nucleohistone, 20: 14592
VAN EIJK, C. W. E., K-conversion coefficient of the 412-kev E2 transition in ^{198}Hg, 20: 15707 (CONF-233(Vol.2), pp 198-212)
VAN HOVE, L., Consequences of analyticity in energy for high-energy scattering, 20: 15520
VAN HOVE, L., Strong interactions of elementary particles in Bev region, 20: 15438
VANINBROUKX, R., Purity and sorption tests of solutions of radionuclides, 20: 15747
VAN KLINKEN, J., Beta decay of ^{147}Nd, 20: 15810
VAN LANCKER, J. L., Pathologic alterations produced by total body x-irradiation in monkeys, 20: 14302
VAN LEUVEN, H. C. E., Rapid method for simultaneous determination of total carbon and ^{14}C in small samples, 20: 14474
VAN MIDDLESWORTH, L., Radium isotope accumulation in animal thyroids, 20: 14254
VAN NOOIJEN, B., K-conversion coefficient of the 412-kev E2 transition in ^{198}Hg, 20: 15707 (CONF-233(Vol.2), pp 198-212)
VANSLAGER, F. E., RAD 2: computer program for calculating fission product radioactivities, 20: 16075 (GAMD-6519)
VAN TUYL, H. H., Chemical analysis of spent power reactor fuels, 20: 14435 (BNWL-SA-503)
VAN VOROUS, T., Thin film evaporation rate monitor, 20: 14819 (RFP-602)
VAN WAGONER, Mark B., Laminated radiation resistant panels, 20: 14680
VARDYA, M. S., Studies in stellar evolution. III., 20: 15196
VARTEVANYAN, Zh. Ts., X-radiation influence on smallpox vaccine virus in chicken embryo, 20: 14281
VASILENKO, S. S., Pair-producing conversion transitions in ^{72}Ge, 20: 15834
VASIL'EV, A. G., Uniform irradiation of surfaces by pulsed electron beams, 20: 15178
VASYUTINSKII, B. M., Interaction of oxygen with a Nb surface, 20: 15976
VAUGHAN, Janet, Occurrence of squamous carcinoma and osteosarcoma in young rabbits injected with ^{90}Sr(50-100 μC/kg), 20: 14316
VAUGHEN, V. C. A., Curium processing experience, 20: 14639 (ORNL-P-1968)
VEATCH, G. E., Collision frequency measurements in oxygen and helium magnetoplasma afterglows, 20: 15867 (AD-620664)
VEDULA, Yu. S., Proof of existence of positive charge in adsorbed Th atoms, 20: 15985
VEJVODA, E., Impurity analysis of plutonium peroxide and plutonium fluoride, 20: 14464 (RFP–599)
VERDEYEN, J. T., Collision frequency measurements in oxygen and helium magnetoplasma afterglows, 20: 15867 (AD-620664)
VERES, A., Activation of ^{113m}In by gamma rays of ^{60}Co, 20: 15748
VERMEULEN, G., Aqueous processing of graphite–carbide fuel elements, 20: 14638 (NP-15753)
VERMEULEN, Theodore, Longitudinal dispersion in single-phase liquid flow through ordered and random packings, 20: 14691 (UCRL-10696 (Rev.)(Pt.2))
VERONESI, P., Internal Compton effect at small angles, 20: 15815
VETTE, James I., Protons and electrons in the inner radiation zone, 20: 15621
VETTE, James I., Space radiation environment, 20: 15232
VIDAL, C.-R., Determination of electron density from line merging, 20: 15881 (MPI-PAE/PL-7/65)
VIDAL, Rene, Measurement of resonance absorption integrals (Mn, Fe, Co, Ni, Cu, Zr, Mo), 20: 15691 (CEA-R-2840)
VIEHBOECK, F. P., Burnup determinations of nuclear fuel elements using mass spectrometric methods, 20: 16046
VIGEHOLM, B., Effect of solute concentration on formation of loops in aluminum–magnesium alloys during fission fragment irradiation, 20: 15145
VIGNAU, H., Isomeric cross-section ratios for ^{134m}Cs, ^{134}Cs, and ^{133m}Ba, ^{133}Ba formed in (d,p) and (d,2n) reactions, 20: 15778
VIGNEAUX, Michel, Results of tritium activity measurement of some waters of southwest, 20: 14744
VIJAYARAGHAVAN, R., Quadrupole coupling constants of deuteron in polycrystalline glycine compounds, 20: 15957
VILLAR, G. E., Suggested modification to periodic chart, 20: 14549
VINDUSKA, M., Influence of nuclear charge distribution on β decay, 20: 15716 (CONF-233(Vol.3), pp 529-37)
VINSON, Terence M., Model solar proton environments for manned spacecraft design, 20: 15191 (N65-20996)
VITEK, F., Hematological changes in radiation sickness. V., 20: 14314
VITTITOE, C. N., Single-pion production in π^-p interactions between 600 and 900 Mev, 20: 15411
VITTORIO, P. V., Effect of x-irradiation on cell size distribution of thymus lymphocytes, 20: 14318
VLADIMIROV, L. A., Analyzing spectra of γ quanta and fast neutrons measured by means of single-crystal scintillation spectrometers, 20: 14869
VLADIMIROVA, Z. A., Binary oxides in ZrO_2–Nb_2O_5 systems, 20: 15079
VOGEL, R. S., Spectrochemical method for simultaneous determination of calcium, lithium, and potassium in high-purity thorium compounds, 20: 14443 (MCW-1493, pp 27-30)
VOINOVA, N. A., Gamma radiation of ^{152}Eu in energy range 1380 to 1900 kev, 20: 15832
VOLCHENKOVA, Z. S., Structure, electric conductivity, and conductivity characteristics in ternary system (0.75 CeO_2–0.25 ZrO_2)–CaO, 20: 14536
VOLKENSHTEIN, N. V., Hall effect in terbium and thulium, 20: 15071
VOLKENSHTEIN, N. V., Thermal conductivity of holmium and erbium from 2 to 100°K, 20: 15117
VOLKERT, O., Structural information and identification of organic substances by means of "electron pyrolysis". I., 20: 14623
VOLKOV, V. V., Preparation of ^{242}Pu and ^{242}Cm from neutron-irradiated ^{241}Am, 20: 14631
VOLTZ, R., Time dependence of scintillation intensity in aromatic materials, 20: 14615
VON BAECKMANN, A., Activation analytical determination of very small iridium contents in uranium oxide, 20: 14495
VON BAEYER, Hans C., Absorptive corrections to the nucleon exchange term in elastic πN scattering, 20: 15324
VON KARMAN, Theodore, Conference on aeronautical sciences, Stockholm, 8/62, 20: 14729
VOROB'EV, L. D., Dispersion sum rules and SU(6) symmetry, 20: 15503
VOROB'EV, V. V., Crystal structure of gadolinium at 120 to 370°K, 20: 15124
VOROSHILOV, Y. V., Compounds with structures of Th_6Mn_{23} type in alloys of rare earth metals with manganese and iron, 20: 15110
VOROSHILOV, Yu. V., New ternary compounds with $W_2Cr_{21}C_6$ type structure, 20: 14532
VOROSHILOV, Yu. V., Zirconium–cobalt–boron system, 20: 14533
VYAKHOREV, V. G., Eddy-current method for multi-parameter testing of structural components, 20: 14708

W

WACHTEL, L. W., Recovery of rat kidney from x irradiation, 20: 14258 (AD-627569)
WACHTEL, S. J., Fluidized bed reprocessing of graphite matrix nuclear fuel, 20: 14647
WADA, G., Chloride ion catalyzed iron(II) + iron(III) isotope exchange in dimethylsulfoxide, 20: 14571
WADSWORTH, M. E., Attempted determination of nitrate in fired thoria using infrared techniques, 20: 14468 (TID-22505)
WADSWORTH, M. E., Densification and sintering of thoria and thoria gels. XXVIII., 20: 15009 (TID-22491)
WAGENER, K., Attempts at material separation in an electrolytic countercurrent exchange process. VI., 20: 14947
WAGONER, Robert V., Possible mechanism for producing strong radio sources, 20: 15225
WAKERLEY, Sheila E., Metabolic theory of cell survival curves, 20: 14359
WALCZAK, T., Octupole Coulomb excitation of ^{208}Pb, 20: 15719 (INP-431/PL)
WALDMAN, J., Structure shielding from simulated fallout gamma radiation, 20: 15931 (TO-B-65-27)
WALDSCHMIDT, Marianne, Behavior of succinic acid dehydrogenase and NADH-cytochrome-c reductase in liver, spleen, and thymus mitochondria of rats after irradiation in vivo, 20: 14376
WALI, K. C., Masses and couplings of $P_{\frac{1}{2}}$ octet and $P_{\frac{3}{2}}$ decuplet, 20: 15509
WALKER, A., Raman polarization studies of several nitrato complexes, 20: 14529
WALKER, C. S., Secondary shutdown systems of nuclear power reactors,

20: 16095
WALKER, W. D., K+p interactions at 3.6 Bev/c, 20: 15415
WALKER, W. D., Results on π−-p and K+-p interactions at high energy. A., 20: 15406
WALKER, W. D., Results on π−-p and K+-p interactions at high energy. B., 20: 15407
WALL, Philip Martin, Improvements relating to nuclear reactor fuelling arrangements, 20: 16003
WALLACE, R., Radiobiological aspects of supersonic transport, 20: 14797
WALLACE, T. C., Thermal expansion of uranium dicarbide and uranium sesquicarbide, 20: 15093
WALLERSTEIN, George, Internal evolution of helium stars, 20: 15202
WALLERSTEIN, George, Search for deuterium in stellar spectra. II., 20: 15197
WALLINGFORD, J. S., Orbits in a magnetic universe, 20: 15634
WALLIS, John Dewtrey, Improvements in fuel elements for nuclear reactors, 20: 16048
WALLIS, John Dewtrey, Locating device, 20: 16005
WALLMAN, H., Field control of telecobalt therapy by gamma-ray television, 20: 14407
WALTER, S., Enrichment of deuterium, 20: 14519
WALTERS, Craig T., Prog. rpt. on applicability of existing data to analytical description of a nuclear-reactor accident, 10–12/65, 20: 16019 (BMI-X-10154)
WALTMAN, F. D., Mining on Nevada Test Site, 20: 14754 (NVO-38-1)
WALTON, J. D. Jr., Prog. rpt. on mechanical properties of slip-cast fused silica, final, 7/64–6/65, 20: 15058 (SC-DC-66-1130)
WALWORTH, Claire B., Refractory composition, 20: 14974
WANG, Chzhi-lunn, Electron-beam welding of molybdenum, 20: 15012
WANG, Ling-Lie Chau, Constructing helicity amplitudes free from kinematic singularities and zeros, 20: 15482
WANG, Nai-yen, Neutron resonances of Yb isotopes, 20: 15839
WANG, Tu-kung, Protective effects of streptomycin against radiation damage of chromosomes of germinal cells of mammals, 20: 14404
WAPSTRA, A. H., K-conversion coefficient of the 412-kev E2 transition in ^{199}Hg, 20: 15707 (CONF-233(Vol.2), pp 198-212)
WAPSTRA, A. H., Some allowed K-capture to positron ratios, 20: 15711 (CONF-233(Vol.2), pp 345-58)
WARNER, G. T., Whole-body counter for clinical measurements utilizing "shadow shield" technique, 20: 14422
WARNER, H. R., Evaluation of low-density single-phase cubic ZrO_2 + UO_2 fuels stabilized with CaO, 20: 15138 (WAPD-292)
WARNOCK, Robert, Masses and couplings of $P_{\frac{1}{2}}$ octet and $P_{\frac{3}{2}}$ decuplet, 20: 15509
WARNOCK, Robert L., Vector exchange in K-N scattering as test of broken M(12) symmetry, 20: 15421
WARSCHAUER, K. A., Means of approaching natural convection effects in a homogeneous reactor, 20: 15996
WARZEE, M., Dynamic corrosion tests on carbon and stainless steels in pressurized water, 20: 14978 (EURAEC-1546)
WASILEWSKA, M., Excitation of characteristic radiation in elements of $14 \leq Z \leq 50$, 20: 15258
WASSEN, Anders, Napoleon's illness 1816–1821 in light of activation analyses of hairs from various dates, 20: 14478
WASSERMAN, R. H., Prog. rpt. on fission product metabolism and response in animals, 1/64–12/65, 20: 14243 (TID-22626)
WASSON, O. A., Thermal and resonance neutron capture in Cl, Sc, V, Co, and Ir, 20: 15787
WATANABE, Hiroshi, Neutron-diffraction study of Cr_2As, 20: 15954
WATANABE, Ikuo, Study of mechanisms of radiation-induced reproductive death of mammalian cells in culture, 20: 14367
WATASE, Yuzuru, Cosmic ray intensities under sea-water at depths down to 1,500 meters, 20: 15289
WATERBURY, G. R., Determination of nitride nitrogen in plutonium metal, alloys, and compounds, 20: 14440 (LA-3452)
WATSON, D. L., Elastic and inelastic scattering of 20- to 28-Mev polarized protons by carbon, 20: 15805
WATY, J., Dynamic corrosion tests on carbon and stainless steels in pressurized water, 20: 14978 (EURAEC-1546)
WAUGH, J. S., Electronic spectra of solutions of europium and ytterbium in liquid ammonia, 20: 14526
WEAVER, B. S., Method for separating americium and curium from lanthanide rare earths and yttrium, 20: 14659
WEBB, John, Flow regulator valve, 20: 16004
WEBELER, R. W. H., Viscosity coefficients and the phonon density temperature dependence in liquid ^{4}He, 20: 15646
WEGST, M., Total absorption x-ray calorimeter, 20: 14908
WEIGEL, Dominique, Thermal decomposition of β lead dioxides of different texture, 20: 14548
WEIGEL, Fritz, Preparation and roentgenographic study of highly radioactive material, 20: 14509 (NP-15826)
WEIGEL, M., Dipole approximation in nonlocal potential, 20: 15842
WEINBERG, A., K+p interactions at 3.6 Bev/c, 20: 15415
WEINBERG, A., Results on π−-p and K+-p interactions at high energy. A., 20: 15406
WEINBERG, A. F., Evaluation of vapor-deposited tungsten tubing, 20: 15048 (N65-16231)
WEINBERG, A. F., Prog. rpt. on cathodes for thermionic reactors, 4/63, 20: 15046 (N65-15820)
WEINREICH, Marcel I., Kinetic theory of weakly ionized homogeneous plasma. III., 20: 15888 (SC-T-65-775)
WEINREICH, Marcel I., Kinetic theory of weakly ionized homogeneous plasma. IV., 20: 15889 (SC-T-65-776)
WEINSTEIN, D., Prog. rpt. on yield phenomena and fracture of hydrided Zr, 10–12/65, 20: 15042 (IITRI-S78-P27-14)
WEIR, J. R., Metal-clad fuel element with copper foil interlayer, 20: 16056
WEISS, E., Prog. rpt. on critical heat flux in boiling water, 4–6/65, 20: 14686 (EURAEC-1448)
WEISSGLAS, Peter, Ion waves on bounded plasmas, 20: 15901
WELCH, P. R., Sperm production by chronically irradiated bulls, 20: 14336
WELKER, Klaus, Moving-field irradiation with wedge filters in ^{60}Co teletherapy, 20: 14426
WELLS, F. H., Automation of tube-thickness measurements using ultrasonics, 20: 14718
WELLSTEIN, Hans, Radiosensitivity of DNA. III., 20: 14283
WELTER, Helmut, Calculation of two-dimensional magnetic field of even number of Ioffe bars by complex analysis, 20: 15878 (IPP-6/42)
WELTEVREDEN, P. S., Wear research on reactor parts, 20: 15998 (EUR-2117.n)
WELTI, H.-J., Irradiation with ^{90}Sr of superior sympathetic cervical ganglion of rat in vitro, 20: 14332
WELTY, William H., Air intake stack and filter cartridge for fallout shelters, 20: 14722
WERTH, Glenn, Salmon seismic experiment, 20: 14664 (UCRL-14487 (Rev.1))
WESNER, John W. Jr., Study of cable-wrapped pressure vessel for nuclear reactors, 20: 16002
WESS, K., Radiation chemical carboxylation of polychloride compounds for trichloroacetic acid, 20: 14582 (SGAE-CH-25/1965)
WEST, T. S., Spectrofluorimetric determination of microgram amounts of Sc. II., 20: 14476
WESTERVELT, D. R., Los Alamos air fluorescence detection system, 20: 15609
WESTGARD, J. B., Observations of Y*(1405) and Y*(1358) resonances in π-N collisions at 1.68 Bev/c, 20: 15404
WHEELER, Owen H., Radiation-induced bromination of 2,3-dimethylbutane, 20: 14591
WHELTON, James A., Evaluation for genetic damage in offspring of women with high-level gonadal irradiation, 20: 14348
WHITE, J. C., Analytical studies of molten-salt systems, 20: 14453 (ORNL-3889, pp 12-14)
WHITE, J. C., Analytical chemistry for reactor projects, 20: 14454 (ORNL-3889, pp 17-24)
WHITE, J. C., Analytical biochemistry, 20: 14456 (ORNL-3889, pp 32-5)
WHITE, J. C., Effects of radiation on analytical methods, 20: 14581 (ORNL-3889, pp 14-16)
WHITE, J. C., Infrared and nuclear magnetic resonance spectrometry, 20: 14459 (ORNL-3889, pp 44-6)
WHITE, J. C., Nuclear and radiochemical analyses, 20: 14461 (ORNL-3889, pp 48–70)
WHITE, J. C., Organic preparations, 20: 14576 (ORNL-3889, pp 73-7)
WHITE, J. C., Special research and development problems, 20: 14455 (ORNL-3889, pp 25–32)
WICHTL, O., X irradiation in pregnancy, 20: 14380
WICKLUND, Harriet, Hypothyroidism following ^{131}I treatment for hyperthyroidism, 20: 14338
WIEDENBECK, M. L., Decay of ^{187}W using 2-m curved-crystal spectrometer, 20: 15807
WIERNIK, G., Recovery of intestinal mucosa in rat after x-irradiation of exteriorized intestine, 20: 14364
WIERUSZ, Andrzej, Concept of fast breeder reactor with fused salt fuel and boiling mercury "wars", 20: 16036
WIESNER, L., Radiometric method for continuous cross-section measurement of hot rolled wires, 20: 14838
WIGNER, E. P., Instantaneous and asymptotic conservation laws for classical relativistic mechanics of interacting point particles, 20: 15154
WIJFFELS, Joannes Baptista, Behavior of droplets evaporating in high temperature convective environments, 20: 14692 (UCRL-16656)
WIKHAMMER, G. A., Critical heat flux in long tubes at 1000 psi with and without swirl promoters, 20: 14695
WILCOX, John M., Extension of photospheric magnetic field into interplanetary space, 20: 15215
WILENZICK, R. M., Effect of crystal size on Moessbauer recoil-free fraction in ^{197}Au, 20: 15962

WILHITE, Richard N., Evaluation of commercial n-paraffin mixtures for purex diluent, 20: 14637 (DP-1034)
WILIP, Elmar K., Neutron polarization in reaction D(d,n)^{3}He at low deuteron energies, 20: 15735 (ANL-Trans-265)
WILKEY, D. Dennis, Isomer of ^{130}I, 20: 15772
WILKINS, M., Mass spectrometric measurements of ratio of thermal neutron capture to fission for ^{241}Pu, 20: 15774
WILKINS, Mark L., Use of one- and two-dimensional hydrodynamic machine calculations in high explosive research, 20: 15571 (UCRL-14531)
WILKS, J., Viscosity and acoustic impedance of liquid ^{3}He, 20: 15583
WILL, Wolfram, Measurement of standard ion doses in solid and fluid media. I., 20: 14894
WILLARD, John E., Electron spin resonance spectra of γ-irradiated polycrystalline alkyl iodides, 20: 14597
WILLARD, John E., Isomer of ^{130}I, 20: 15772
WILLENS, R. H., Rapid quenching of reactive and refractory alloys from liquid state, 20: 15020
WILLIAMS, C. W., Refractive index and molar refraction of xenon oxide tetrafluoride, 20: 14528
WILLIAMS, D. V. J., Calculation of group averaged neutron cross sections (FORTRAN for IBM-7030), 20: 15665 (AWRE-O-103/65)
WILLIAMS, R. W., Breakdown of DNA in x-irradiated Escherichia coli, 20: 14265
WILLIAMS, W. S. C., Pion-proton charge-exchange scattering near 2.0 Bev/c, 20: 15378
WILLIAMSON, Margaret, Occurrence of squamous carcinoma and osteosarcoma in young rabbits injected with ^{90}Sr(50-100 μC/kg), 20: 14316
WILLIS, W. J., Search for decay $\eta \rightarrow \pi^0 + e^+ + e^-$, 20: 15333
WILLMARTH, T. E., Optical and electron microscopy, 20: 14460 (ORNL-3889, pp 46–8)
WILSON, C. W., Extension of APT to obtain centroid and inertia information, 20: 16154 (Y-1420(Rev.1))
WILSON, Richard, Review of nucleon form factors, 20: 15440
WINDELBAND, Rolf, Measurement of ash content of lignite by γ irradiation technique with radionuclide ^{170}Tm, 20: 14493
WINDLE, D. W., Explanation of the Appleton anomaly of the F2 layer. II., 20: 15586 (AD-620243)
WINKELMAN, J. R., Techniques for detection of high-altitude nuclear explosions, 20: 15612
WINKLER, A., Urinary excretion of pseudouridine in course of x-ray therapy, 20: 14269
WINTERHOFF, D. H., Morphologic and physiologic changes in staphylococci from streptomycin and ^{60}Co treatment, 20: 14313
WIRSING, Edward Jr., Fluidized bed reprocessing of graphite matrix nuclear fuel, 20: 14647
WIRTH, W., Vesico-ureteral reflux after irradiation of urinary bladder, 20: 14411
WISECUP, W. G., Isolation of Streptococcus equi from burros, 20: 14288 (AD-627986)
WITTE, H. O., Survey of head-end processes for recovery of uranium and thorium from graphite-base reactor fuels, 20: 14640 (ORNL-TM-1411)
WITTEMAN, W. G., Thermal expansion of uranium dicarbide and uranium sesquicarbide, 20: 15093
WITTENBERG, L. J., Radioactive radiation emitting sources, 20: 14634
WITTWER, S. H., Penetration of organic compounds through isolated cuticular membranes with special reference to ^{14}C urea, 20: 16146 (COO-888-39)
WITTWER, S. H., Permeability of iron and iron chelates through cuticular membranes, 20: 16147 (COO-888-45)
WOLDRINGH, Sebo H., Control rod drive system of Garigliano nuclear power plant, 20: 16074 (EUR-2420.d,f,i,n,e, pp 227-48)
WOLF, J. D., Dislocation-relaxation internal-friction peak in columbium and Cb–5% Zr, 20: 15122
WOLF, R. C., Pathologic alterations produced by total body x-irradiation in monkeys, 20: 14302
WOLF, Richard A., Observational test of theories of neutron-star cooling, 20: 15201
WOLFRAM, T., Energy spacing of geometrical resonance structure in thick films of superconducting In, 20: 15650
WOLICKI, Eligius A., Nuclear radiation detection system using plurality of detectors, 20: 14916
WONG, D. Y., One-boson-exchange model of NN and NN-interaction, 20: 15345
WOOD, R. V. Jr., Large aperture seismic array signal handling system, 20: 14760
WOOD, T. H., Modification of conjugation in Escherichia coli K-12 by ultraviolet irradiation, 20: 14329
WOODGATE, G. K., Relativistic effects in many-electron hyperfine structure. II., 20: 15265
WOODGATE, G. K., Relativistic effects in many-electron hyperfine structure. III., 20: 15266
WOODWARD, C., Spectrofluorimetric determination of microgram amounts of Sc. II., 20: 14476
WOOLLETT, Edwin Lee, Kinetic equation for a warm plasma, 20: 15918
WORTHLEY, B. W., Measurement of ^{47}Ca absorption by whole-body gamma spectrometry, 20: 14247
WOTZAK, Gregory, Neutron burning of long-lived fission products for waste disposal, 20: 16132 (BNL-8558)
WOULDS, J. N., High-energy γ rays from pion capture, 20: 15794
WOULDS, J. N., Reaction (π^-,2n) in ^{6}Li and ^{7}Li, 20: 15793
WRIGHT, H. W., Optical and electron microscopy, 20: 14460 (ORNL-3889, pp 46–8)
WRIGHT, Harvel, Calculation of radiation dose from protons and neutrons to 400 Mev, 20: 14330
WRIGHT, Kenneth, Evaluation for genetic damage in offspring of women with high-level gonadal irradiation, 20: 14348
WULFF, J., Segregation of Ta at very low concentrations in Nb, 20: 14969
WULFF, Verner J., Prog. rpt. on effects of age and radiation on nucleic acid metabolism and protein synthesis in nervous system tissues, 3/15/65–1/1/66, 20: 14242 (TID-22591)

X

XUONG, Nguyen-huu, K$^-$p interactions at 3.8 Bev/c, 20: 15418
XUONG, Nguyen-Huu, Mass formulas for the 189 multiplet of SU(6), 20: 15478
XUONG, Nguyen-huu, Reaction $\pi^-d \rightarrow \pi^-d\,\pi^+\pi^-$ at 3.7 Bev/c, 20: 15409
XUONG, Nguyen-huu, Study of the A and B mesons, 20: 15408

Y

YABUKI, Haruichi, Many-pole amplitudes and elementarity. II., 20: 15490
YAGER, P. M., Study of the A and B mesons, 20: 15408
YAKHYAEV, R. Sh., Neutrino-nucleon interactions with lepton production, 20: 15387
YAKOVLEV, G. N., Preparation of ^{242}Pu and ^{242}Cm from neutron-irradiated ^{241}Am, 20: 14631
YAKOVLEVA, G. V., Radioactivity of air over Atlantic Ocean in May to July, 1964, 20: 14743
YAKUBSON, K. I., Application of similitude theory to study of radiation transfer processes, 20: 14776
YAMADA, Y., Penetration of organic compounds through isolated cuticular membranes with special reference to ^{14}C urea, 20: 16146 (COO-888-39)
YAMADA, Y., Permeability of iron and iron chelates through cuticular membranes, 20: 16147 (COO-888-45)
YAMAMOTO, Hisao, Moessbauer effect of ferromagnetic intermetallic compounds in Fe_3Ge and Fe_6Ge_5, 20: 15950
YAMAMOTO, S. S., Search for decay $\eta \rightarrow \pi^0 + e^+ + e^-$, 20: 15333
YAMAMOTO, Sadaaki, Tritium-hydrogen exchange of poly-l-glutamic acid in aqueous solutions, 20: 14628
YAMANOUCHI, T., π-meson production in p-p collisions, 20: 15336
YAMASAKI, Fumio, Vertical distributions of fallout gamma-ray sources in ground soil in eastern Japan, 20: 14751
YAMAGAWA, Sadaaki, Relativistic dynamical theory of electron diffraction containing inelastic scatterings, 20: 15959
YANG, C. N., CP violation in K decay, 20: 15434
YANG, C. N., πp Charge-exchange scattering and coherent droplet model of high-energy exchange processes, 20: 15342
YANG, L., Prog. rpt. on thermionic materials for space power applications, 10/63, 20: 14959 (N65-20797)
YANG, L., Prog. rpt. on thermionic materials for space power applications, 9/63, 20: 14960 (N65-20798)
YANG, L., Prog. rpt. on thermionic materials for space power application, 12/63, 20: 14961 (N65-20801)
YANG, L., Prog. rpt. on thermionic materials for space power applications, 1/64, 20: 14962 (N65-20803)
YANG, L., Prog. rpt. on cathodes for thermionic reactors, 4/63, 20: 15046 (N65-15820)
YAO, Chi-chuan, Neutron resonances of Yb isotopes, 20: 15839
YAO, York-Peng, Reciprocity, normality of K^0-K^0 mass matrix, and CP violation in weak interactions, 20: 15350
YAREMBASH, E. I., Roentgenographic studies of lanthanum tellurides, 20: 14530
YARMUSH, David Leon, Transfer-matrix method for γ and neutron penetration, 20: 15934
YAVORSKY, P. M., Process for producing tritiated organic compounds, 20: 14633
YAZAKI, Koichi, Energy dependence and non-locality of the optical potential, 20: 15829
YAZVITSKII, Yu. S., Neutron resonances of Yb isotopes, 20: 15839
YEARIAN, M. R., Proton form factors from elastic electron-proton scattering, 20: 15337
YEH, N., p-p Annihilations into K and π mesons at 3.7 Bev/c, 20: 15338
YIP, Sidney, Brillouin scattering by gases as test of Boltzmann equation,

20: 15580
YIP, Sidney, Time-dependent correlations in Maxwell gas, 20: 15579
YONEI, Katsumi, Energy levels in Thomas-Fermi dirac atom, 20: 15267
YOSHIZAWA, Yasuo, Skin contamination by radioactive substances, 20: 14253
YOUNG, Alexander Gillies, Pressure vessels, 20: 16009
YOUNGBLOOD, Dave Harper, Reaction $^{40}Ca(p,\gamma)^{41}Sc$, 20: 15849
YU, C. .., Convective stability in a plasma with horizontal magnetic fields, 20: 15907
YUAN, L. C. L., π-meson production in p-p collisions, 20: 15336

Z

ZABORENKO, K. B., Study of $NaBeF_3$–$NaPO_3$ system by emanation method, 20: 14557
ZABORENKO, K. B., Study of $KBeF_3$–KPO_3 system by emanation method, 20: 14558
ZACHARIASEN, F., What, if anything, is the bootstrap? 20: 15554
ZAGANESCU, M., Uniformization of the scalar self-energy diagram, 20: 15495
ZAHN, Robert E., Air intake stack and filter cartridge for fallout shelters, 20: 14722
ZAKHAROV, V. M., Flaw detection in thin-walled tubes, 20: 14713
ZAMORA, Pedro, Bibliography on conversion of salt and brackish waters into fresh water (1954–1964), 20: 14510 (NP-15834)
ZARNOWIECKI, Krzysztof, Application of motor-car engine for control of air pollution with radioactive aerosols, 20: 14672
ZARNOWIECKI, Krzysztof, Use of α-particles for measurement of mica thickness in end window counter, 20: 14826
ZATSEPINA, L. N., ^{90}Sr, stable strontium and calcium in soil and vegetable food products, 20: 14236
ZDANIS, R., Single-particle exchange in 3-particle final states of the reaction K+p at 2.26 Bev/c, 20: 15422
ZDANSKY, K., Electron spin resonance of NO_3 in irradiated $NaNO_3$, 20: 15965
ZEHNPFENNIG, T., Solar x-ray images obtained using grazing incidence optics, 20: 15203
ZELDOVICH, Ya. B., Quarks: astrophysical and physico-chemical aspects, 20: 15435
ZELLER, H., Large volume impactor collector, 20: 14815 (COO-401-139)
ZELLOS, Spyridon, Comparative studies of effect of methods of sterilization on absorption of chromic catgut, 20: 14932
ZETKIN, V. I., Structure of radiation chlorinated and sulfochlorinated polyethylene, 20: 14621
ZGANJAR, E. F., E2 conversion coefficients in ^{152}Sm, ^{154}Gd and ^{160}Dy, 20: 15705 (CONF-233(Vol.2), pp 177-90)
ZHITNIKOV, R. A., Paramagnetic resonance of free silver atoms formed in frozen solutions of silver salts irradiated at 77°K, 20: 15975
ZHUKOVSKII, N. N., Gamma radiation of ^{152}Eu in energy range 1380 to 1900 kev, 20: 15832
ZHUZE, V. P., Transport mechanism in samarium sulfide, 20: 15981
ZICHA, B., Influence of x-radiation, on urinary excretion of inorganic phosphates and ammonia, 20: 14270
ZICHA, Blahoslav, Influence of radiation on activity of some dehydrogenases in liver homogenates and in mitochondria of rats, 20: 14284
ZICHA, Blahoslav, Influence of cortisone and ACTH treatment on serum glycoprotein levels in x-irradiated rats, 20: 14378
ZICHA, Blahoslav, Oxidation products of unsaturated fatty acids in irradiated organism, 20: 14379
ZIEGLER, C. A., Low-level radiation altimeter system study, 20: 14817 (N65-20421)
ZIEGLER, Charles A., Rocket-bome air density measurement system utilizing electron-bremsstrahlung, 20: 15588 (AD-620682)
ZIETEMANN, H., Development of a laser amplifier and application in plasma diagnostics, 20: 15873 (IPP-1/42)
ZIMA, G. E., Recent zirconium fire experience at Hanford and the general zirconium fire problem, 20: 15001 (HW-66930)
ZINGERMAN, Yu. P., Characteristics of interaction of oxygen with surface of a tungsten single crystal, 20: 15986
ZINGG, E., Vesico-ureteral reflux after irradiation of urinary bladder, 20: 14411
ZINGL, H., Remarks on regularization, 20: 15320
ZIPF, K., Deoxyribonuclease II and deoxyribonucleic acid in rat thymus after action of radiomimetic drugs and x irradiation, 20: 14311
ZIPF, K., Effect of pyridoxal on strontium content of skeleton, 20: 14246
ZIPOY, David M., Light fluctuations due to an intergalactic flux of gravitational waves, 20: 15636
ZIVADINOVIC, M. S., Neutron coherent scattering amplitude of cesium, 20: 15736
ZLATIN, Norman, Machining difficult materials—molybdenum alloys, 20: 15014
ZOLOTAVIN, A. V., Decay of ^{90}Mo, 20: 15751
ZORIN, V. M., Influence of atmospheric precipitation on fallout of radioactive substances from atmosphere, 20: 14746
ZOVKO, N., Pion-nucleon scattering at high energies, 20: 15376
ZUBER, A., Influence of composition and density of soils on readings of neutron moisture meters, 20: 14771
ZUMBRUNN, Kurt, Exact and approximate solutions of many-group transport equations in even geometry, 20: 15667 (EIR-72)
ZUMINO, B., Interpretations of spin and unitary spin symmetry, 20: 15545
ZWEIFEL, P. F., Exact solution of equations of radiative transfer for local thermodynamic equilibrium in the nongray case, 20: 15572

SUBJECT INDEX

Main entries in this index are generally specific materials, things, and processes. These are followed by modifiers that describe the properties of, and processes applied to, the main entries.

The number preceding the colon is the *NSA* volume number, and the number following is the abstract number. The designation (R) following the abstract number indicates that the abstract is of a progress report; (P) indicates a patent; and (T) indicates a translation. Abstracts for reports other than progress reports carry no letter designation. References to report numbers, where appropriate, are included after the abstract number of the citation. Published literature (journal article or book) is identifiable by the absence of a report number.

The user should bear in mind that the ideas presented in the original literature, rather than key words, have been indexed. The indexers have tried to select what seemed the most probable and logical place to look for typical information. Since it is not possible to anticipate where a user would look for information, numerous cross references are included in cumulative indexes to assist him in his search.

Experience in using an index of this type will be the best guide in obtaining the desired information, and a consideration of synonymous or closely related terms will prove valuable.

Information must be so indexed as to be of the greatest use to the greatest number of users. This requires that a topic be indexed to headings that most specifically describe it and not ordinarily to the headings that describe its ultimate use, nor to the general class headings that include the specific headings. For example, information on the treatment of thyroid disease with I-131 would be indexed under Thyroid Gland and under Iodine Isotopes I-131, but not necessarily under Radiotherapy. A study of the effects of x radiation on hair would be indexed under both X Radiation and Hair. However, the information would not be indexed under the experimental animal, e.g., Rats, unless the report discusses the effects on rat hair as compared with the effect on the hair of other animals.

The broad, general class headings are used only for general information or for comprehensive reports or articles.

Subject Heading Styles

Generally, the direct form of subject entry is used rather than inverted headings, e.g., Amino Acids rather than Acids, Amino; Helium Isotopes He-4 rather than Helium—isotopes He-4 or Helium—He-4 isotopes. Note, however, that in some cases parenthetic modifying terms or inverted headings of the form Neutrons, Fast are used in preference to a direct entry that would result in the scattering of information. Organic compounds are usually entered in the index in the inverted form so that substituted compounds can be listed near the parent compound; e.g., Benzene, Bromo- rather than Bromobenzene. In general, the style of nomenclature used is that of Chemical Abstracts, except that some items listed in that publication as subheadings are elevated to form part of the main heading; e.g., Butyric Acid, Methyl Ester rather than Butyric Acid—methyl ester.

Alphabetization

Main headings are alphabetized word-by-word. A parenthetic qualifier following a main heading is disregarded in alphabetizing unless there are two or more headings identical except for the parenthetic qualifier, in which case the qualifier determines the order. Headings involving Greek letters are arranged as if the names of the letters were spelled out.

Examples:

M-Capture
  see Electron Capture
Magnesium
Magnesium Alloys
Manganese Fluorides
Manganese(II) Fluorides
Mesons
Mesons (π)
Mesons (ρ)
3-Pentanol, 2,4-Dimethyl-
2-Pentanol, 2-Methyl-
2-Pentanol, 4-Methyl-

Nomenclature of Inorganic Compounds

Inorganic compounds are indexed in the direct form, listing cations in the order of increasing valence in the case of polycationic salts of varying valence and in alphabetic order for polycationic salts in which all cations have the same valence; e.g., Sodium Aluminum Silicates and Potassium Sodium Sulfates.

Multicomponent Alloys and Other Systems

Multicomponent alloys, except well-known trade names, are indexed under a main heading in the form "element alloy" for each element in the alloy. The modifier begins with element symbols for each component arranged alphabetically as if the English name for the element were spelled out.

Example: Copper-Gold Alloy is indexed
  Copper Alloys
    Cu-Au...
  Gold Alloys
    Cu-Au...

Well-known alloys such as Zircaloy-2 are indexed directly to the trade name; cross references referring from each component of the alloy to the entry for the trade name appear in cumulative indexes.

Multicomponent systems of non-metallic elements are indexed in a manner similar to alloys except the main heading used contains the word "Systems" in place of "Alloys."

Example: Silicon–Tungsten Systems are indexed
  Silicon Systems
    Si-W...
  Tungsten Systems
    Si-W...

Multicompound systems and mixtures of compounds are indexed under the main heading for each component com-

pound; the modifiers begin with an alphabetical listing of compound formulas.

Example: Lead Titanate–Lead Zirconate is indexed
Lead Titanates
$PbTiO_3$-$PbZrO_3$...
Lead Zirconates
$PbTiO_3$-$PbZrO_3$...

A mixed system of compounds and elements is indexed using a combined form of the above conventions, e.g., a dispersion of copper and alumina would be indexed

Aluminum Oxides
Al_2O_3-Cu...
Copper Systems
Al_2O_3-Cu..

Physical States and Configurations of Materials

Specification of the physical state, if other than normal, or geometric configuration of the material is included in the modifying phrase, i.e., liquid metals would be indexed to the metal with "liquid" in the modifier, and carbon crucibles would be indexed to Carbon with "crucibles" appropriately placed in the modifier and also to Crucibles if appropriate.

Modifying Phrases

The modifiers appearing under a main heading are written specifically to describe the relation of the item being indexed to that main heading. The modifier, therefore, will generally contain more useful information about that relation than will a title or a phrase written to be used under every main heading assigned to the item. Effort is exerted to begin the modifier with the word judged to be of greatest use to the greatest number of users; this, however, does not obviate the need to consider all modifiers under the main heading(s) of interest.

Modifiers are usually intended to form a meaningful phrase when combined with the main heading. Some are intended to be read following the main heading, e.g., the entry Hydrogen—sorption by charcoal is read "hydrogen sorption by charcoal"; however, as a result of placing the important word first, many modifiers must be arranged for smooth reading, e.g., Formaldehyde—yields in radiolysis of ethyl ether, effects of deuterium on is read "effects of deuterium on formaldehyde yields in radiolysis of ethyl ether" and Uranium—crystal structure of, effect of cooling rate on allotropic transformations in is read "effect of cooling rate on allotropic transformations in crystal structure of uranium." Prepositions are sometimes omitted if no ambiguity results.

Special characters are added to modifiers in the field of physics; if the modifier does not establish the experimental or theoretical character of a reference, a symbol (E), (T), or (E/T) is placed immediately after the modifying phrase and before the journal reference number. The value of this identification has been established by the American Institute of Physics.

A

ABSTRACTS
on plutonium, 20: 16145 (BNWL-113-7)
on wave diffraction, 20: 15149(T) (JPRS-33458)
ACCELERATORS
beam deflector and rotator for, 20: 15189(P)
beam injection in cyclic, charge transfer in proton, (E), 20: 15162 (NP-15785)
beam stability in intersecting storage rings, proton, (T), 20: 15174 (SLAC-49, pp 71-3)
beam transport in electron-positron storage rings, 20: 15173 (SLAC-49, pp 61-8)
bubble and spark chambers for electron, 20: 15187
development, 20: 15156 (BNL-741(Rev.))
magnets for, short-pulse excitation of delay-type, 20: 15157 (CERN-66-1)
neutron field measurements for, threshold detector uses for, 20: 15175 (UCRL-16312)
storage rings for, instrument for measuring, 20: 15160 (LNF-65/44)
ACCIDENTS
fission products release in reactor, food contamination by, 20: 14748
nuclear, properties of wastes from, 20: 16136
radiation protection program for nuclear, USAEC, 20: 14808
ACETALDEHYDE
decomposition in ion source of mass spectrometer, mechanism of, 20: 14584(R) (TID-22444)
ACETATES
determination of carbon-14-labeled, by liquid scintillation counting on paper chromatograms, 20: 14479
ACETIC ACID, [(CARBOXYMETHYLIMINO)BIS(ETHYLENENITRILO)] TETRA-
analytical use in fission product recoveries, 20: 14436 (BNWL-SA-504)
ACETIC ACID, [1,2-DIMETHYLETHYLENE)DINITRILO]TETRA-
complexes with lanthanides, stability constants of, 20: 14521
ACETIC ACID, (ETHYLENEDIAMINE)TETRA-
analytical use in fission product recoveries, 20: 14436 (BNWL-SA-504)
chelates with iron-59 of carbon-14-labeled, penetration in cuticular membranes of tomatoes, 20: 16147 (COO-888-45)
effects on spectrophotometric determination of thorium using Chrome Azurol S, 20: 14485
spectra of, infrared, 20: 14499
use for demineralization of hard tissues by chelation with calcium, 20: 16149 (NYO-2779-10)
ACETIC ACID, (ETHYLENEDIAMINE)TETRA- COMPLEXES
with cobalt, effects of neutron reactions (n,γ) on, 20: 14584(R) (TID-22444)
with metals, infrared spectra of, 20: 14499
ACETIC ACID, (ETHYLENEDIIMINO)BIS(*o*-HYDROXYPHENYL)-
chelates with iron-59 of carbon-14-labeled, penetration in cuticular membranes of tomatoes, 20: 16147 (COO-888-45)
ACETIC ACID, (*N*-HYDROXYETHYLETHYLENEDIAMINE)TRI-
analytical use in fission product recoveries, 20: 14436 (BNWL-SA-504)
ACETIC ACID, METHYL ESTER
decomposition in ion source of mass spectrometer, mechanism of, 20: 14584(R) (TID-22444)
ACETIC ACID, TRICHLORO-
production in gamma radiolysis of aqueous carbon tetrachloride and chloroform solutions saturated with carbon dioxide, 20: 14582 (SGAE-CH-25/1965)
ACETIC ACID, VINYL ESTER
radiation effects on charcoal catalyst for preparation of, electron and gamma, 20: 14609
ACETONE
effects of impurity of, on positron annihilation spectra in argon, (E), 20: 15436
ACETONE, THENOYLTRIFLUORO-
solvent properties for curium and fermium, 20: 14654
ACOUSTIC WAVES
diffraction, (T), 20: 15149(T) (JPRS-33458)
dispersion of long-period gravity-, from nuclear explosions, (T), 20: 15611
pressure oscillation from heat generated, in closed-end pipes, (E/T), 20: 14690 (SC-DC-66-1293)
propagation in helium-3, properties of, (E), 20: 15583
ACRYLIC ACID, 2,2-DINITROPROPYL ESTERS
determination in explosives, methods for, 20: 14470 (UCRL-7873)
ACRYLIC ACID, DIPHENYL-
radioinduced isomerization of, effects of metal bromides and organic bromine compounds on, 20: 14596
ACTINIDES
atomic structure and suggested changes in positions of, in periodic table, 20: 14549
ACTINIUM ISOTOPES Ac-223
alpha decay, (E), 20: 15864
ACTIVATION ANALYSIS
method of, for determining arsenic poisoning, 20: 14478
methods and sensitivity of derivative, 20: 14502
methods and uses of, 20: 14477
of alkali metals for oxygen, 20: 14454(R) (ORNL-3889, pp 17-24)
performance of neutron, with elements yielding short-lived radionuclides, 20: 14661(R) (ORNL-3889, pp 48-70)
use in scientific crime detection, 20: 14439(R) (GA-5556)
ACTIVATION DETECTORS
development for neutron dosimetry, 20: 14862
properties of aluminum–cobalt and cobalt, 20: 14867
uses for neutron spectroscopy in reactors, 20: 14860 (RT/FI(65)-33)
ADENOSINEPHOSPHORIC ACIDS
content in rat blood and liver, effects of methioninesulfoximine on, 20: 14270
radiation effects on content of, in rat blood and liver, x, 20: 14270
ADIPIC ACID
uses in determination of ytterbium, 20: 14490
ADRENAL GLANDS
radiation effects on dog, x, 20: 14280
ADRENOCORTICOTROPIC HORMONE
effects on content of glycoprotein in blood serum of x-irradiated rats, 20: 14378
AERIAL SURVEYING
equipment for, engineering drawings for, 20: 14902
AERODYNAMICS
conference on aeronautical sciences, 20: 14729
AEROSOLS
alpha-emitter content in, spectrometer for determining, 20: 14857 (NP-15448)
deposition in respiratory tract, model for, 20: 14796
filter system for radioactive, use of automobile engine in, 20: 14672
radioactive, measurement in air, survey of methods for, 20: 14745
radioactivity of atmospheric, in Czechoslovakia, 20: 14813
AGE
effects of fetal, on strontium-85 uptake in mice, 20: 14244
effects of maternal, on leukemogenesis, 20: 14346
AGE ESTIMATION
method for glaciers, radiometric, 20: 14740
AGRICULTURE
research programs in, at Juelich Research Center, Germany, 20: 16156
AIR
analysis for tritium, Kanne ionization chamber for, 20: 14905
filter system for radioactive, use of automobile engine in, 20: 14672
gamma spectra in, from uranium-235 fission products, 20: 14733 (AD-628982)
radiosensitivity effects on DNA, x, 20: 14283
radiosensitivity effects on Salmonella infections in eggs, γ, 20: 14395
sampling using automated aperture cards, 20: 14791 (Y-1501)
AIRCRAFT
conference on aeronautical sciences, 20: 14729
materials for, evaluation of, 20: 15129
ALANINE
determination of carbon-14-labeled, by liquid scintillation counting on paper chromatograms, 20: 14479
ALANINE, 3,3'-DISELENODI-
labeling with selenium-75 by neutron activation, 20: 14630
ALARM SYSTEMS
design for radiochemical processing cells, 20: 14853 (CNEA-159)
design of gamma, for HFIR facility, 20: 16125 (ORNL-TM-1393)
ALBUMINS
amino acids in, effects of lipid peroxidation on, 20: 14587
radiosensitivity effects on DNA in deoxynucleoprotein, 20: 14277
ALCOHOLS
analysis of rice whiskey, activation, 20: 14439(R) (GA-5556)
radioinduced pyrolysis of, in water-d_2, 20: 14623
ALDOSTERONE
radioinduced decomposition of tritiated, effects of molecular structure on, 20: 14578 (EUR-2435.f)
ALGAE
productivity of, effects of accumulated radium on, 20: 14381
radiation effects on productivity of, radium, 20: 14381
ALKALI METALS
analysis and determination, 20: 14500
analysis for carbon, hydrogen, and oxygen, methods for, 20: 14454(R) (ORNL-3889, pp 17-24)
properties of, measurement of thermodynamic and transport, 20: 15028(R) (AGN-8166)
ALKALINE EARTH METALS
analysis and determination, 20: 14500
determination by spectroscopy using plasma jet, 20: 14492
determination in uranium tetrafluoride, spectrographic, 20: 14473

separation by ion exchange in mixed and non-aqueous media, review on, 20: 14469(R) (TID-22650)

ALKENES

radioinduced pyrolysis of, in water-i_2, electron, 20: 14623

ALLOYS

analysis by x-ray-fluorescence, computer code for, 20: 14457(R) (ORNL-3889, pp 36-9)
heat treatment of liquid, method for, 20: 15020
superconductivity of ferromagnetic, (T), 20: 15648
thermodynamic properties of binary, 20: 14514 (UCRL-11821)
thermodynamic properties of superconducting, approximation method for, 20: 15654
wear evaluation of soft, against SAP, 20: 15998 (EUR-2117.n)

ALPHA DECAY

energies of, calculation of, 20: 15853

ALPHA PARTICLES

angular distribution from nickel-58 (He-3,α) reactions, (E), 20: 15860
detection and measurement in radiochemical analysis, 20: 14488
detection and measurement in flowing solutions using proportional counter, 20: 14871
detection and measurement using nuclear emulsions, 20: 14877
detection in products from nuclear reactions, engineering drawings of apparatus for, 20: 14906
doses in space vehicles, computer programs for calculating, 20: 15930 (NP-15697(Vol.2))
effects on gases, luminescent, 20: 14617
effects on plant cells, diurnal variations in, 20: 14361
effects on sodium selenate crystals, ESR of paramagnetic centers from, (E), 20: 15972
emission from nuclei, fractional parentage coefficients for, (T), 20: 15741
interactions at 20 to 120 Mev, differential cross sections for, 20: 15689 (CEA-R-2786)
interactions with protons at 30 to 50 Mev, phase-shift analysis of, (T), 20: 15730(R) (RHEL/R-112, pp 67-98)
monitoring in laboratories, development of equipment for, 20: 14872
reactions (α,n) with boron-11 at 2.38 to 3.67 Mev, nitrogen-15 levels from, (E), 20: 15790
reactions (α,2α) with beryllium-9, carbon-12, and oxygen-16 at intermediate energies, final-state interaction effects on, (T), 20: 15825
reactions with anthracene and p-terphenyl monocrystals, scintillation decay time in, 20: 15989
scattering by carbon-12, polarization in inelastic, (E), 20: 15862
scattering by lithium-7 at 1.6–12 Mev, elastic and inelastic, 20: 15859
use for measuring mica thickness in end-window counters, 20: 14826

ALPHA SOURCES

content in aerosols, spectrometer for measuring, 20: 14857 (NP-15448)
preparation of plutonium-238, by deposition from solution, 20: 14444(R) (MLM-1268)
use in hygrometers, 20: 14840

ALPHA SPECTROMETERS

design and operation of ionization, 20: 14857 (NP-15448)

ALTIMETERS

use of radiometric, on moon, 20: 14817 (N65-20421)

ALTITUDE

measurement on moon using radiation sources and detectors, 20: 14817 (N65-20421)

ALUMINUM

analysis and determination, 20: 14500
cascade showers in, structure of electron-photon, (T), 20: 15938
cladding of, microradiographic method for, 20: 14704
compatibility with water in reactor environment, 20: 14996
determination in automobile lubricants, activation, 20: 14439(R) (GA-5556)
determination in automobile tire rubber, activation, 20: 14439(R) (GA-5556)
determination in automobile paint, activation, 20: 14439(R) (GA-5556)
determination in commercial plastics, activation, 20: 14439(R) (GA-5556)
determination in plutonium fluorides and peroxides, review on spectrographic, 20: 14464 (RFP-599)
determination in paper samples in criminal cases, activation, 20: 14439(R) (GA-5556)
determination in rice whiskey, activation, 20: 14439(R) (GA-5556)
determination in thumbnail clippings, activation, 20: 14439(R) (GA-5556)
determination in wood in criminal cases, activation, 20: 14439(R) (GA-5556)
determination of trace amounts of, in iron, activation, 20: 14471
effects on spectrofluorimetric determination of scandium, 20: 14476
effects on spectrophotometric determination of thorium using Chrome Azurol S, 20: 14485
effects on thermal conductivity of Springfields uranium at 160 to 620°C, 20: 15084
electron diffusion in slabs of, differential energy spectra and number transmission for, (T), 20: 15936
electron reactions at 6 to 60 kev, transient radiation from, (E), 20: 15268
electron transmission through thin foils of, plasmon excitation in, (E), 20: 15951
gamma transmission through slabs of, transfer-matrix method for, (T), 20: 15934
leaching from alumina–phosphate glass prepared from calcined alumina waste, 20: 16133 (IDO-14672)
neutron elastic scattering at 0.8 Mev, cross sections for, (T), 20: 15770
proton reactions (p,n) at 30 to 50 Mev, distributions from, 20: 15729(R) (RHEL/R-112, pp 37-66)
reactions with sodium, high-temperature, 20: 15033(R) (ANL-7152, pp 87-96)
separation from scandium by gas chromatography of trifluoroacetylacetonates, 20: 14486
superconducting energy gaps in pure and silver-doped, microwave studies of, (E), 20: 15658
testing finned cladding of, eddy-current method for, 20: 14703

ALUMINUM ALLOYS

preparation of homogeneous, by levitation melting, 20: 15013
Al–Au, preparation of stoichiometric, 20: 14511(R) (ORNL-3889, pp 71-3)
Al–Be, electron plasma oscillations in thin foil eutectoid, properties of, (E), 20: 15952
Al–Co, analysis for cobalt in wire of, comparison of activation and spectrophotometric, 20: 14433(R) (BAW-298)
Al–Co, use for neutron flux measurements, 20: 14867
Al–Fe–U, fabrication for nuclear fuel, 20: 15022(P)
Al–Fe–U, fabrication for nuclear fuel, 20: 15023(P)
Al–Fe–U, fabrication for nuclear fuel, 20: 15024(P)
Al–Ge, electron plasma oscillations in thin foil eutectoid, properties of, (E), 20: 15952
Al–Hf, solvent properties for carbon, 20: 15047(R) (N65-15919)
Al–Mg, radioinduced dislocation loops in, effects of magnesium concentration on fission-fragment, (E), 20: 15145
Al–Nb, fabrication of sintered bodies of, 20: 15026(P)
Al–Nb, superconductivity of fused, 20: 15123
Al–Ni–Nb, oxidation of, phase distributions in layers from studies of, 20: 14990
Al–Ni–Nb, phase studies at 1140°C, 20: 15121
Al–Sm, magnetic hyperfine interactions in samarium-149 in, 20: 15992
Al–Sn, electron plasma oscillations in thin foil eutectoid, properties of, (E), 20: 15952
Al–Ta, fabrication of sintered bodies of, 20: 15026(P)
Al–Ti–V, corrosion by oxygen-contaminated sodium, 20: 16060(R) (ANL-7152, pp 1-49)
Al–U, eddy-current method for testing finned aluminum cladding on, 20: 14703
Al–U, microradiographic method for testing aluminum-clad, 20: 14704
Al–U, separation of rare earth fission products from irradiated, by solvent extraction using TBP, 20: 14635 (CONF-660305-5)

ALUMINUM IONS

effects on corrosion of type 304L stainless steel by hydrofluoric acid–nitric acid solutions, 20: 14982(R) (NLCO-970, pp 6.1-4)

ALUMINUM ISOTOPES Al-26

energy levels of, unified model wave function for low-lying rotational, (T), 20: 15814

ALUMINUM ISOTOPES Al-27

energy levels from magnesium-26 (p,γ) reactions, (E), 20: 15761
neutron reactions (n,2n) at 12 to 18 Mev, cross sections for, (E), 20: 15863
proton reactions (p,n) at 30 to 50 Mev, distributions from, 20: 15792(R) (RHEL/R-112, pp 37-66)

ALUMINUM ISOTOPES Al-28

energy levels of, unified model wave function for low-lying rotational, (T), 20: 15814

ALUMINUM NITRATES

density and viscosity of aqueous solutions of, 20: 14648
$Al(NO_3)_3$–$Nd(NO_3)_3$, density and viscosity of solutions of, 20: 14648
$Al(NO_3)_3$–$La(NO_3)_3$, density and viscosity of solutions of, 20: 14648
$Al(NO_3)_3$–La_2O_3, compound formation in, at 1200°C, 20: 14539
$Al(NO_3)_3$–Nd_2O_3, compound formation in, at 1200°C, 20: 14539
$Al(NO_3)_3$–Pr_2O_3, compound formation in, at 1200°C, 20: 14539

ALUMINUM NITRIDES

reactions with basalt, copper matte, slags, and molten salts, 20: 14989

ALUMINUM OXIDES

effects on crystal growth in optical glasses, 20: 15075
effects on sorption of cesium and strontium by clay minerals and soils, 20: 14652
fixation of calcined, in phosphate glass, 20: 16133 (IDO-14672)
stability in dry hydrogen at 1100 to 2000°C, 20: 14986
Al_2O_3–$Al_2Ti_3O_9$, performance as space radiator coating on niobium–1 zirconium at 1700°F, 20: 15057(R) (PWA-2750)
Al_2O_3–La_2O_3, compound formation in, at 1600 to 1650°C, 20: 14539

Al_2O_3–Nd_2O_3, compound formation in, at 1600 to 1650°C, 20: 14539
Al_2O_3–Pr_2O_3, compound formation in, at 1600 to 1650°C, 20: 14539

ALUMINUM SILICATES
properties for sorption and storage of cesium-137 and strontium-90, 20: 14466 (RL-SA-58)

ALUMINUM SYSTEMS
Al–C–Co–Nb, phase studies, 20: 15103
Al–C–Co–Ta, phase studies, 20: 15103
Al–C–Cr–Nb, phase studies, 20: 15103
Al–C–Cr–Ta, phase studies, 20: 15103
Al–C–Cu–Nb, phase studies, 20: 15103
Al–C–Cu–Ta, phase studies, 20: 15103
Al–C–Fe–Nb, phase studies, 20: 15103
Al–C–Fe–Ta, phase studies, 20: 15103
Al–C–Fe–U, mechanical properties at intermediate strain rates and temperatures, 20: 15081
Al–C–Mn–Nb, phase studies, 20: 15103
Al–C–Mn–Ta, phase studies, 20: 15103
Al–C–Nb, phase studies, 20: 15103
Al–C–Nb–V, phase studies, 20: 15103
Al–C–Nb–Zn, phase studies, 20: 15103
Al–C–Ni–Nb, phase studies, 20: 15103
Al–C–Ni–Ta, phase studies, 20: 15103
Al–C–Ta, phase studies, 20: 15103
Al–C–Ta–V, phase studies, 20: 15103
Al–C–Ta–Zn, phase studies, 20: 15103
Al–Si, annealing and growth of films of, 20: 15030 (ANL-7102)
Al–Si, ductility of two-phase, effects of composition and particle size on, 20: 15055(R) (NYO-2394-19)
Al–Si, sample preparation for electron transmission studies, 20: 15055(R) (NYO-2394-19)

ALUMINUM TITANATES
Al_2O_3–$Al_2Ti_3O_9$, performance as space radiator coating on niobium–1 zirconium at 1700°F, 20: 15057(R) (PWA-2750)

ALUMINUM, TRIMETHYL-
decomposition in ion source of mass spectrometer, mechanism of, 20: 14584(R) (TID-22444)

ALUMS
preparation of deuterated and iron-substituted, 20: 14511(R) (ORNL-3889, pp 71-3)

AMERICIUM
separation from curium, chemical process for, 20: 14636 (CONF-660305-7)
separation from rare earth fission products, 20: 14659(P)

AMERICIUM COMPOUNDS
properties, 20: 14509 (NP-15826)

AMERICIUM ISOTOPES Am-241
content in spent power reactor fuels, evaluation of, 20: 14435 (BNWL-SA-503)
neutron reactions with, yields of americium-242, curium-242, and plutonium-242 from thermal, 20: 14631
separation from plutonium-238, methods for, 20: 14509 (NP-15826)

AMERICIUM ISOTOPES Am-242
neutron reactions with, yields of americium-243, curium-242, and plutonium-242 from thermal, 20: 14631

AMERICIUM ISOTOPES Am-243
preparation by neutron irradiation of americium-242, 20: 14631
separation from curium-244 in fission product solutions by Clanex-Tramex process, 20: 14639 (ORNL-P-1968)

AMINES
solvent properties for beryllium, 20: 14658(P)

AMINO ACIDS
effects of lipid peroxidation on, 20: 14587
radiation effects solid state polymers of, gamma, 20: 14588
radiation effects on *B. cereus* content of, x, 20: 14263
radioinduced pyrolysis of, in water-t_2, electron, 20: 14623
radiolysis of, effects of peptide bond on γ, 20: 14616
radiosensitivity effects in DNA, uv, 20: 14272

AMMONIA
content in rat urine, effects of burns, cytostatics, or methionine-sulfoximine on, 20: 14270
deuterium exchange between, and hydrogen, dual-temperature process for, 20: 14519
radiation effects on urinary excretion by rats, x, 20: 14270

AMMONIUM CARBONATES
reactions with lanthanum nitrate in aqueous solution, 20: 14535

AMMONIUM COMPOUNDS, QUATERNARY
electric conductivity in light and heavy water at 25°C, 20: 14540

AMMONIUM NITRATES
use of fertilizer-grade, as explosive, 20: 14753 (BNWL-47)

AMOEBA
radiation effects on nucleic acid synthesis in, γ and uv, 20: 14259(R) (NP-15855)
radiation effects on protein synthesis in, γ and uv, 20: 14259(R) (NP-15855)

AMPLIFIERS
analog circuit response to transistorized common-base, 20: 14822(R) (RHEL/R-112, pp 99-128)
design and performance of low-noise pre-, for boron–fluoride counters, 20: 14863
design of charge-sensitive pre-, for semiconductor detectors, 20: 14851 (BNL-9980)
design of differential, with high common-mode rejection, 20: 14822(R) (RHEL/R-112, pp 99-128)
design of pre-, for boron trifluoride detectors, 20: 14859 (ORNL-TM-1390)

ANALYSIS
book: *Analytical Chemistry of Selected Metallic Elements*, 20: 14500
electron microprobe, corrections for x-ray intensities from, 20: 14431 (ANL-7078)
electron pyrolysis methods of, 20: 14623

ANDROSTENONE, HYDROXYMETHYL-
protective effects against x ray-induced diseases in rats, 20: 14392

ANEMIA
effects of genes on, in mice, 20: 14290(R) (NYO-1800-12)
radiosensitivity effects of hereditary, in mice, 20: 14290(R) (NYO-1800-12)

ANIMAL CELLS
radiation effects on thymidine index in rat kidney, x, 20: 14258 (AD-627569)
radiation effects on fetal rat, x, 20: 14262
radiation effects on Chinese hamster cell, protective effects of serum in media against x, 20: 14400
radiation effects on cytoplasm in chick embryo muscle, effects of dose on x, 20: 14321
radiation effects on survival of 5-bromo-deoxycytidine-treated bone marrow, fast-neutron and x, 20: 14333
radiation effects on nucleic acid metabolism in cultured, uv, 20: 14355
radiation effects on, metabolic theory for, 20: 14359
radiation effects on leukemic, in culture, lethal γ, 20: 14367
radiosensitivity effects of disulfides and sulfhydryls in mammalian, 20: 14351
radiosensitivity of, in culture, 20: 14385

ANIMALS
physiology of, tracer studies, 20: 14386
radiation dosimetry in, using hematological changes, 20: 14314
radiation effects on normal and tumorous, effects of RNA on electron, 20: 14397

ANION EXCHANGE MATERIALS
efficiency of, for fission product separation, 20: 14643

ANIONS
formation in decomposition of carbonyls in ion source of mass spectrometer, 20: 14584(R) (TID-22444)

ANOXIA
effects of methandrostenolon on, in rats, 20: 14402

ANTARCTIC REGION
fallout contamination of Indo-Antarctic Ocean from 1961 thermonuclear tests, 20: 14749

ANTHRACENE
alpha reactions with, scintillation decay time from, 20: 15989
electron transitions in, oscillator strengths for probability of, (T), 20: 15275
scintillation intensity in crystals of, time dependence, (T), 20: 14615

ANTIBARYONS
interactions with baryons in S-wave state, many-pole amplitudes and elementarity in, (T), 20: 15490

ANTIBODIES
titer of mouse, effects of irradiated Schistosoma cercariae on, 20: 14304
titer of mouse, effects of purified Schistosoma eggs on, 20: 14304

ANTIGENS
effects of lymphoreticular system on, 20: 14354

ANTIMONY
analysis and determination, 20: 14500
determination in automobile tire rubber, activation, 20: 14439(R) (GA-5556)
determination in commercial plastics, activation, 20: 14439(R) (GA-5556)
determination in gunpowder residues on hands, activation, 20: 14439(R) (GA-5556)
determination in glass samples, activation, 20: 14439(R) (GA-5556)
determination in oils and silts in water, activation, 20: 14439(R) (GA-5556)
determination in paper samples in criminal cases, activation, 20: 14439(R) (GA-5556)
electron transmission through thin foils of, plasmon excitation in, (E), 20: 15951
neutron elastic scattering at 0.8 Mev, cross sections for, (T), 20: 15770
separation from fission products by solvent extraction on fine-grained carrier, 20: 14656

separation from protactinium by solvent extraction on fine-grained carrier, 20: 14656
separation from tellurium by solvent extraction on fine-grained carrier, 20: 14656
ANTIMONY ALLOYS
Sb–In, radioinduced defects in intermetallic compounds of, energy spectra of gamma, 20: 15979(T)
ANTIMONY FLUORIDES
reactions with xenon oxyfluorides, complex formation in, 20: 14523
ANTIMONY ISOTOPES Sb-119
energy levels from tellurium-119 decay, (E), 20: 15762
ANTIMONY ISOTOPES Sb-121
proton reactions (p,n) at 2.3 to 11.0 Mev, excitation of isobaric analog states in, (E), 20: 15804
ANTIMONY ISOTOPES Sb-122
decay of, beta-neutrino angular correlation and nuclear matrix elements in, (E), 20: 15857
ANTIMONY ISOTOPES Sb-123
proton reactions (p,n) at 2.3 to 11.0 Mev, excitation of isobaric analog states in, (E), 20: 15804
ANTIMONY ISOTOPES Sb-124
beta transitions in, matrix elements for first-forbidden, (E), 20: 15824
ANTIMONY OXIDES
sorptive properties for chloride and potassium ions, effects of pH on, 20: 14651
ANTIMONY SYSTEMS
Sb–B–Co, crystal structure, 20: 14532
Sb–B–Ni, crystal structure, 20: 14532
ANTINEUTRINOS
Fermi boundary of sea of, from effects on tritium beta spectra, (T), 20: 15326
interactions with protons, cross section and position spectra from, (E), 20: 15330
ANTINUCLEONS
interactions with antinucleons and nucleons, one-boson-exchange model of, 20: 15345
interactions with nucleons, one-boson-exchange model of, 20: 15345
photoproduction at high energies, review on, (T), 20: 15442
ANTIPROTONS
interactions with protons at 3.7 Bev/c, cross section for mesons (K) and (π) production in, (E), 20: 15338
interactions with protons, $\bar{U}$(12) symmetry in annihilation, 20: 15346
interactions with deuterons at 0.13 to 17.1 Bev, cross sections and amplitudes for, (T), 20: 15361
APATITES
separation of rare earths from, from Kola Peninsula, 20: 14520
ARGON
electron spectra from, j-j coupling for L Auger, (T), 20: 15237 (CONF-233(Vol.3), pp 371-97)
energy and mass transfer between gas coolant and plasma of, 20: 15584
energy level widths for, K, (T), 20: 15239 (CONF-233(Vol.3), pp 419-39)
ionization in mass spectrometer, formation of multiply charged ions in, 20: 14584(R) (TID-22444)
ionization of liquid, by x-rays, 20: 15259
ionization of, cross sections for ruby-laser-multiphonon, (T), 20: 15276
positron annihilation spectrum in, impurity effects on, (E), 20: 15436
production of cylindrically symmetric plasma of, in electric arcs, 20: 15914
reactions with cesium, excitation transfer in, (E), 20: 15253
shock propagation in, electron precursor phenomena in, (T), 20: 15577
ARGON IONS
reactions with copper and gold at 60, 80, and 90 kev, electron energy spectra from, (E), 20: 15261
ARGON ISOTOPES
content in meteorites, 20: 15193 (NP-15654)
separation by thermal diffusion, 20: 14444(R) (MLM-1268)
ARGON ISOTOPES Ar-36
proton inelastic scattering at 3 Mev, gamma polarization from, (E), 20: 15760
ARGON ISOTOPES Ar-37
decay of, K/L ratio for electron-capture, (E/T), 20: 15713 (CONF-233 (Vol.2), pp 365-8)
ARGON ISOTOPES Ar-41
determination in copra and desiccated-coconut oils, activation, 20: 14463 (PAEC(D)CH-652)
ARGON SYSTEMS
Ar–K, electron temperature in plasma of, (E/T), 20: 15874 (IPP-3/31)
ARGONNE ADVANCED RESEARCH REACTOR
component development for, 20: 16119(R) (ANL-7152, pp 73-86)
control blades for, reactivity worth of, 20: 16119(R) (ANL-7152, pp 73-86)
ARGONNE NATIONAL LAB., LEMONT, ILL.
nuclear safety program at, review of, 20: 14800
ARSENIC
analysis and determination, 20: 14500
content in Napoleon's hair, activation analysis of, 20: 14478
determination in automobile lubricants, activation, 20: 14439(R) (GA-5556)
determination in commercial plastics, activation, 20: 14439(R) (GA-5556)
determination in hair in criminal cases, activation, 20: 14439(R) (GA-5556)
determination in oil samples in water, activation, 20: 14439(R) (GA-5556)
determination of trace amounts of, in iron, activation, 20: 14471
energy level transitions in, Coster-Kronig, (T), 20: 15238 (CONF-233 (Vol.3), pp 398-418)
energy level widths for, K, (T), 20: 15239 (CONF-233(Vol.3), pp 419-39)
ARSENIC FLUORIDES
reactions with xenon oxyfluorides, complex formation in, 20: 14523
ARSENIC ISOTOPES As-75
neutron reactions (n,He-3) at 14.8 Mev, effective cross sections for, (E), 20: 15739
ARSENIC ISOTOPES As-77
half life, (E), 20: 14461(R) (ORNL-3889, pp 48-70)
ASBESTOS
use in laminated shielding panels, 20: 14680(P)
ASPHALT
radium-uranium equilibrium shifts in solid bitumen deposits, 20: 14781
ASTATINE
energy level transitions in, Coster-Kronig, (T), 20: 15238 (CONF-233 (Vol.3), pp 398-418)
ASTROPHYSICS
adiabatic invariants of stars in galactic field, (T), 20: 14950(R) (COO-614-41)
theory of cosmic radio sources, 20: 15225
ATLANTIC OCEAN
fallout monitoring over, 1964, 20: 14743
ATMOSPHERE
analysis for cosmic rays, fission products, and natural and radioinduced activity, methods for radiochemical, 20: 14430 (AD-620219)
analysis for polyphenyls, colorimetric and uv spectrophotometric methods for, 20: 14467 (RT/PROT(64)-20)
contamination of, value of threshold-limit values for, 20: 14805
density measurements at 100 to 200 km, radiometric system for, 20: 15588 (AD-620682)
fallout content in, effects of air exchange rates between stratosphere and troposphere on, 20: 14742
fallout monitoring of Canadian, October 1965, 20: 14737 (NP-15853, pp 8-20)
monitoring for radioactivity in radiochemical processing plants, 20: 14811
monitoring for radioactivity in Czechoslovakia, 20: 14813
monitoring in buildings, uses of automated aperture cards for, 20: 14791 (Y-1501)
radiation monitoring of, at McMaster University, 20: 14738 (NP-15853, pp 21-33)
radioactivity in, over Atlantic Ocean, 1964, 20: 14743
radioactivity measurements in, survey of methods for, 20: 14745
radioactivity of uranium-mine, 20: 14747
radioactivity of, over Black Sea, 1964, 20: 14741
sampling of, design of large-volume impactor collector for, 20: 14815 (COO-401-139)
ATMOSPHERES
radiosensitivity effects of gaseous, on phage inactivation and thymine dimerization, uv, 20: 14356
ATOMIC BEAMS
scattering in hard-sphere gases, effects on beam velocity distribution, (T), 20: 15247 (N65-15530)
ATOMIC ENERGY
bibliography of bibliographies on, Oct. to Nov. 1965, 20: 16152 (TID-3732)
book: *Directory of the Nuclear Industry, USA*, 20: 16144 (AED-C-32-1 (Vol.1 and Vol.2))
book: *Survey of Chemical Technology in the Nuclear Industry*, in Czech., 20: 14429
radiation hazards in peaceful uses of, evaluation of, 20: 14802
uses of, nonmilitary, 20: 14665
ATOMIC ENERGY COMMISSION
radiation protection program for nuclear accidents, 20: 14808
ATOMIC ENERGY, LEGAL ASPECTS
international cooperation in, conference on, 20: 14940
personnel radiation exposure records in, 20: 14801
radiation processing plant, gamma, 20: 14944
ATOMIC EXPLOSIONS
bibliography on underground, 20: 14661 (NP-15867)
effects of radiation from, on electronic equipment, 20: 14921
radiation effects on electronics from, instrumentation for studying, 20: 14918(R) (ECOM-01313-1)
sampling of material in vicinity of, jet system for, 20: 14662(R)

(ORNL-TM-1394)
water wave propagation from, simulation using explosives, 20: 14660 (AD-620468)
ATOMIC MODELS
energy levels in Thomas-Fermi-Dirac, (T), 20: 15267
for excited states, applications to photoionization calculations, 20: 15270
ATOMS
diffusion in monatomic gases, time-dependent moments equations for, 20: 15675
electron inner-shell vacancies in, readjustment for, 20: 15245 (CONF-233(Vol.3), pp 494-504)
electron spectra from, review of Auger, 20: 15240 (CONF-233(Vol.3), pp 440-53)
electron transitions in, many-body theory for probability of, 20: 15275
energy level transitions for $21 \leq Z \leq 90$, Coster-Kronig, (T), 20: 15238 (CONF-233(Vol.3), pp 398-418)
energy level widths for $16 \leq Z \leq 83$, K, (T), 20: 15239 (CONF-233(Vol.3), pp 419-39)
energy levels of, research, 20: 15236 (CONF-233(Vol.3))
hyperfine structure of, relativistic effects in, (T), 20: 15264
properties of, solution for Brownian motion of random-matrix eigenvalues for, (T), 20: 15785
reactions of, bibliography on, 20: 15248 (ORNL-AMPIC-3)
reactions with unlike atoms, excitation-transfer cross sections for, (T), 20: 15255
AUGER ELECTRONS
spectra for light elements, properties of, (E), 20: 15244 (CONF-233 (Vol.3), pp 487-93)
spectra of L, M, and N, review of, 20: 15240 (CONF-233(Vol.3), pp 440-53)
AURORAL STORMS
electron detection and measurement in, instrumentation for, 20: 15589(R) (ASE-1125)
AVIATION PERSONNEL
radiation hazards to supersonic-transport, 20: 14797
AVR REACTOR
development, 20: 16156
AZO DYES
analytical use for spectrophotometric determination of metals, 20: 14469(R) (TID-22650)
preparation of Calcichrome and chlorophosphazo III, 20: 14576(R) (ORNL-3889, pp 73-7)

B

BACTERIA
isolation of *Streptococcus equi* from burros, 20: 14288 (AD-627986)
mutants of *Staphylococcus aureus*, genetic studies of, 20: 14243(R) (TID-22626)
radiation control of, on frozen chickens and ducks, γ, 20: 14933
radiation effects on cell wall permeability in *Bacillus cereus*, x, 20: 14263
radiation effects on *Bacillus subtilis*, uv, 20: 14267
radiation effects on vegetative, review of, 20: 14388
radiation effects on *Micrococcus radiodurans*, mathematical models for, 20: 14388
radiation effects on spores of, review, 20: 14389
radiation effects on Pseudomonas, mechanism of protective effects of freezing against x, 20: 14394
radiation effects on morphology and physiology of *Staphylococcus aureus* effects of streptomycin on γ, 20: 14313
radiation effects on survival of staphylococcus, grown on sterilized crab meat, 20: 14936
radiation effects on, in medical supplies, electron, 20: 14941
radioinduced inactivation of, factors affecting mechanisms for, 20: 14390
BACTERIOPHAGES
effects of nitrogen mustards on, inactivating, 20: 14267
radiation effects on DNA transfer to progeny from, uv, 20: 14285
radiation effects on T4, genetic map length of reactivated uv, 20: 14328
radiation effects on, effects of gaseous environment and thymine dimerization on, 20: 14356
radiation effects on, host-cell reactivation of uv, 20: 14357
radioinduced inactivation of, x, 20: 14260 (NP-15856)
radiosensitivity of, infecting *Escherichia coli*, uv, 20: 14271
BARIUM
content in red-colored Paleozoic deposits in Northern Tien Shan, 20: 14780(T) (AEC-tr-6579)
determination by spectroscopy using plasma jet, 20: 14492
determination in automobile lubricants, activation, 20: 14439(R) (GA-5556)
determination in commercial plastics, activation, 20: 14439(R) (GA-5556)
determination in gunpowder residues on hands, activation, 20: 14439(R) (GA-5556)
determination in glass samples, activation, 20: 14439(R) (GA-5556)
determination in plutonium fluorides and peroxides, review on spectrographic, 20: 14464 (RFP-599)
mass of, spectrometric determination of, 20: 15853
neutron elastic scattering at 0.8 Mev, cross sections for, (T), 20: 15770
precipitation from tap water by magnesium carrier, 20: 14457(R) (ORNL-3889, pp 36-39)
transport across, intestinal membranes, tracer study, 20: 14243(R) (TID-22626)
BARIUM CHLORIDES
$BaCl_2$–NaCl, reactions with refractory metal borides, carbides, nitrides, and oxides, 20: 14989
BARIUM FLUORIDES
ion localized vibrations in, spectra of deuterium and hydrogen, 20: 15969
BARIUM HYDRIDES
energy levels of deuterated and ordinary, C and D, 20: 14517
BARIUM ISOTOPES
deuteron reactions at 15 Mev, isomeric states from, (E), 20: 15856
BARIUM ISOTOPES Ba-133
production in deuteron reactions with cesium-133, isomeric cross-section ratios for, (E), 20: 15778
BARIUM ISOTOPES Ba-140
determination in atmospheric and precipitation samples, methods for radiochemical, 20: 14430 (AD-620219)
exchange between barium sulfate crystals and solutions, 20: 14572
uptake by aortic wall of rats, 20: 14252
BARIUM NITRATES
determination in mock explosive, method for, 20: 14470 (UCRL-7873)
BARIUM OXIDES
$BaO–B_2O_3–SiO_2$, effects of aluminum, lanthanum, and thorium oxides on crystallization of, 20: 15075
BARIUM SULFATES
barium-140 exchange between crystals and solutions, 20: 14572
sulfur-35 exchange between crystals and solutions, 20: 14572
BARLEY
effects of radiation and diethyl sulfate on seeds of, 20: 14384
radioinduced mutations in, effects of ethylenimine on γ, 20: 14334
BARYONS
electromagnetic properties in composite model, 20: 15550
electromagnetic properties in relativistic composite models, (T), 20: 15551
form factors of octet, electromagnetic, (T), 20: 15492
interactions with mesons (π), model for isotopic symmetry for, (T), 20: 15454
interactions with antibaryons in S-wave state, many-pole amplitudes and elementarity in, (T), 20: 15490
interactions with mesons, SU(n) crossing matrices for, (T), 20: 15322
interactions with mesons, $\bar{U}(12)$ symmetry for strong, 20: 15390
magnetic moments in SU(3), (T), 20: 15492
magnetic moments in SU(3) and SU(6) symmetry, (T), 20: 15535
mass formulas in SU(3) and SU(6) symmetry, (T), 20: 15535
model for $P_{1/2}$ octet, SU(3) symmetry-breaking effects in composite, (T), 20: 15509
model for, nonrelativistic quark, 20: 15477
BARYONS, RESONANCE
classification in $S\bar{U}(12)$ representations, 20: 15496
conference, 20: 15398
form factors for $N^*_{33}N$, current algebra for, 20: 15308 (IC/66/18)
mass and widths of N^*_{33}, self-consistent determination of, (T), 20: 15353
model for $P_{3/2}$ decuplet, SU(3) symmetry-breaking effects in composite, (T), 20: 15509
models for, quasi-molecular rotator, 20: 15399
parity and spin of $Y^*_0(1815)$, (E), 20: 15414
parity and spin of, method for determining, 20: 15431
parity and spin of $Y^*_1(1660)$, determination from deuteron-meson (K^-) interaction, 20: 15397
photoproduction of N* and N**, at 4.8 to 6.0 Bev, (E), 20: 15425
production in meson (π^-)-deuteron interactions at 3.7 Bev/c, (E), 20: 15409
production in meson (K^-)-proton interactions at 2.1 to 2.7 Bev/c, (E), 20: 15412
production in meson (K^-)-proton interactions at 1.80 and 1.95 Bev/c, (E), 20: 15420
production in meson (π)-proton interactions, (T), 20: 15382
production in photoproduction of mesons (K*), (E), 20: 15424
production of (1630) and (1680), in meson (π^-)-proton interactions, (T), 20: 15392
production of N^*_{33}, in meson (π^-)-proton interactions at 600 to 900 Mev, (E/T), 20: 15411
production of N*0, in meson (K^-)-proton interactions at 3.8 Bev/c, (E),

20: 15418
production of N^*_{33} in meson (π)- nucleon interactions, position and width of, 20: 15352
production of N*, in meson (π^-)-proton interactions at 2.7 Bev/c, (E/T), 20: 15410
production of N*, in meson (K^+)-proton interactions at 2.26 Bev/c, (E/T), 20: 15422
production of N*, in meson (π^+)-proton interactions at 2.08 Bev/c, (E), 20: 15334
production of N*, in meson (π)-proton interactions, (T), 20: 15381
production of N*(1238), in meson (K^+)-proton interactions at 3.6 Bev/c, (E), 20: 15407
production of N*(1425), in meson (K^-)-proton interactions at 1.5 Bev/c, (E/T), 20: 15429
production of N*(1238), in meson (π^-)-proton interactions at 300 to 1000 Mev, (E/T), 20: 15375
production of Ξ^*(1530) in meson (K^-) interactions with protons, spin-parity analysis of, (E/T), 20: 15464
production of Y^{*-}, in meson (π^-)-proton interactions at 1.0 to 1.9 Bev, (E), 20: 15417
production of Y^{*+}(1385), in meson (K^-)-proton interactions at 5.5 Bev/c, (E), 20: 15416
production of Y*(1765), in meson (K^-)-nucleon interactions at high energies, (E), 20: 15414
properties of, review of, 20: 15371
spin of Y_0^*(1405) and Y_1^*(1358), (E), 20: 15404
theory of, using current algebra, 20: 15488
theory of, using non-compact algebras, 20: 15506

BEANS
radioinduced sterility in female *Phaseolus mungo*, 20: 14347

BEHAVIOR
radiation effects on monkey, γ, neutron, and x, 20: 14286 (AD-625837)
radiation effects on rabbit, γ, 20: 14326
radiation effects on rabbit, x, 20: 14350
radiation effects on rat spatial avoidance, x, 20: 14366

BELLOWS
design of flexible metal by, for particle beam deflector, 20: 15189(P)

BENTONITES
sorptive properties for radioactive wastes, effects of flocculants on, 20: 16138

BENZENE
effects on solvent properties for uranium in TBP system, 20: 14655
neutron diffusion in, parameters for, (T), 20: 15676
reactions with iodine, chromatographic analyses of products from, 20: 14454(R) (ORNL-3889, pp 17-24)
yields from gamma radiolysis of 1,3- and 1,4-cyclohexadienes, 20: 14610

BENZENE, HEXABROMO-
effects on radioinduced isomerization of α-phenylcinnamic acid, 20: 14596

m-BENZENEDISULFONIC ACID, 4,5-DIHYDROXY-
complexes with uranium, preparation of, 20: 14522

m-BENZENEDISULFONIC ACID, 4,5-DIHYDROXY-, SODIUM SALT
uses in determination of uranium, 20: 14482

BENZENESULFONIC ACID, 3,4-DIHYDROXY-
complexes with uranium, preparation of, 20: 14522

BENZOIC ACID, POTASSIUM SALTS
electric conductivity in light and heavy water at 25°C, 20: 14540

BENZOQUINONE
effects on radioinduced polymerization of triallyl cyanurate, 20: 14586

BERKELIUM
production in heavy-ion nuclear reactions, review of, 20: 15740

BERYLLIUM
book: *Beryllium, Its Metallurgy and Properties*, 20: 15125
deformation properties of polycrystalline, 20: 15067
diffusion of carbon-14 and radioactive iron and silver in, tracer studies on, 20: 15037 (CEA-R-2621)
effects on spectrophotometric determination of thorium using Chrome Azurol S, 20: 14485
electron diffusion in slabs of, differential energy spectra and number transmission for, (T), 20: 15936
electron transitions in, oscillator strengths for probability of, (T), 20: 15275
electron transmission through thin foils of, plasmon excitation in, (E), 20: 15951
emissivity of titanate coatings on, 20: 15057(R) (PWA-2750)
properties of arc-melted ingots of, 20: 15118
separation from aqueous solutions by solvent extraction using amines, 20: 14658(P)
separation from scandium by gas chromatography of trifluoro-acetylacetonates, 20: 14486
testing claddings of, nondestructive method for, 20: 14711

BERYLLIUM ALLOYS
Al–Be, electron plasma oscillations in thin foil eutectoid, properties of, (E), 20: 15952
Be–Pu, spectra of alpha source of, 20: 14444(R) (MLM-1268)

BERYLLIUM ALUMINUM SILICATES
radiation effects on crystalline, EPR and hfs from x, 20: 15982(T)

BERYLLIUM FLUORIDES
BeF_2–LiF–ThF_4–UF_4–ZrF_4, spectra of irradiated, absorption and reflectance, 20: 14453(R) (ORNL-3889, pp 12-14)
BeF_2–LiF–UF_4–ZrF_4, analysis for uranium, polarographic, 20: 14454(R) (ORNL-3889, pp 17-24)

BERYLLIUM ISOTOPES Be-6
energy levels, (E), 20: 15729(R) (RHEL/R-112, pp 37-66)

BERYLLIUM ISOTOPES Be-7
determination in atmospheric and precipitation samples, methods for radiochemical, 20: 14430 (AD-620219)
energy levels, (E), 20: 15729(R) (RHEL/R-112, pp 37-66)
nucleon emission from, reduced widths in shell-model intermediate coupling, (T), 20: 15830

BERYLLIUM ISOTOPES Be-8
nuclear properties in alpha-particle model, 20: 15689 (CEA-R-2786)
nucleon emission from, reduced widths in shell-model intermediate coupling, (T), 20: 15830

BERYLLIUM ISOTOPES Be-9
alpha reactions (α,2α) at intermediate energies, final-state interaction effects on, (T), 20: 15825
meson (π^+) reactions, double-charge-exchange cross sections for, (T), 20: 15813

BERYLLIUM ISOTOPES Be-10
half life, (E), 20: 14461(R) (ORNL-3889, pp 48-70)
nucleon emission from, reduced widths in shell-model intermediate coupling, (T), 20: 15830

BERYLLIUM OXIDES
radiation effects on stored energy release of, effects of dosage on neutron, 20: 15142
reactions with copper and nickel mattes, slags, molten salts, and refractory metals, 20: 14989

BETA DECAY
beta-neutrino angular correlation in first-forbidden, (E), 20: 15857
energies of, calculation of, 20: 15853
gamma spectrum in, continuous, (T), 20: 15801
lepton symmetry refraction from, 20: 15448
matrix elements for first-forbidden transitions in, measurement of, (E/T), 20: 15824
matrix elements for first-forbidden, (E), 20: 15857
properties of, effect of Coulomb field on, (T), 20: 15716 (CONF-233 (Vol.3), pp 529-37)
transition probabilities for, effects of strong interaction between nucleons in, 20: 15836

BETA PARTICLES
angular correlation with neutrinos in first-forbidden nonunique beta decay, (E), 20: 15857
detection and measurement in radiochemical analysis, 20: 14488
detection and measurement in plant effluents, methods for, 20: 14450(R) (NLCO-970, pp 8.1-4)
detection and measurement of background, scintillation counter for, 20: 14873
detection and measurement of, development of scintillation counter for, 20: 14874
detection and measurement of low-energy, performance of proportional counter for, 20: 14879
detection and measurement of low energy, engineering drawings of Kanne ionization chamber for, 20: 14905
detection and measurement of low-energy, solid-state detection for, 20: 14910(R)
detection and measurement of, instrument design combining proportional multiplier and scintillation counting for, 20: 14912(P)
detection of, multiple-junction semiconductor detector for, 20: 14909(P)
detection of, portable hand and shoe monitor for, 20: 14866
dose distributions in tissues, 20: 14403 (NP-15714)
dosimetry in animals using hematological changes, 20: 14314
dosimetry of, performance of lithium-drifted silicon p-i-n junctions for, 20: 14886
effects on auditory structures in rabbits, 20: 14316
effects on bladder tumors, vesico-ureteral reflux from, 20: 14411
effects on heart following thyrotoxicosis therapy, 20: 14424
effects on uptake of sulfate by aortic mucopolysaccharides in rabbits, tracer study, 20: 14295
monitoring in laboratories, development of equipment for, 20: 14872

BETA SOURCES
monitoring on air filters at McMaster University, 20: 14738 (NP-15853, pp 21-33)
use for exposure of nerve tissue, 20: 14332
use of monomolecular films as standard, 20: 16143 (AD-620276)

BETA SPECTRA

analysis of, using cross electric and magnetic fields, 20: 14882
BETA SPECTROMETERS
design using lithium-drifted germanium detector, engineering drawings for, 20: 14904
use of lens type, for conversion coefficient measurements, 20: 15710 (CONF-233(Vol.2), pp 252-5)
BETA SPECTROSCOPY
methods for, using crossed electric and magnetic fields, 20: 14882
BETATRONS
design and performance of 30-Mev flux-forced field-biased, 20: 15181
electron runaway in plasma, 20: 15919
BEVATRON
beam spill by amplitude modulation for, 20: 15185
neutron field measurements for, threshold detector uses for, 20: 15175 (UCRL-16312)
BEVERAGES
cesium-137 content of, in Norway, 20: 14739 (TID-22655)
BIBLIOGRAPHIES
of bibliographies on atomic energy literature, Oct. to Nov. 1965, 20: 16152 (TID-3732)
on alpha–alpha interaction cross sections, 20: 15689 (CEA-R-2786)
on analysis of accidents in boiling-water and pressurized-water power reactors, 20: 16019(R) (BMI-X-10154)
on atomic and molecular processes, 20: 15248 (ORNL-AMPIC-3)
on conversion of brackish and salt waters into fresh waters, 20: 14510 (NP-15834)
on diffusion, properties, and trapping of radioactive iodine in waste gases, 20: 14787 (CEA-Bib-64)
on effects of particle and short-wave radiation on glasses, 20: 15134 (N65-15819)
on flooding in perforated-plate pulsed extraction columns, 20: 14462 (ORNL-3890)
on materials research, 20: 14506 (CRDL-SP-5-7)
on ORNL research results, 20: 14428(R) (ORNL-3889)
on plutonium, 20: 16145 (BNWL-113-7)
on plutonium detection and metabolism in man, 20: 14239 (JUL-312-ST)
on preferred orientation in wrought and annealed metals, 20: 15099
on preparation and roentgenography of highly radioactive materials, 20: 14509 (NP-15826)
on radiation effects on solid uranium-base nuclear fuel materials, 20: 15137 (VDIT-16(5.4))
on separation of lanthanides, thorium, and other elements by ion exchange in mixed and non-aqueous media, 20: 14469(R) (TID-22650)
on strong interactions at high energies, 20: 15438
on underground nuclear explosions, 20: 14661 (NP-15867)
on welding methods, 20: 15005 (NASA-SP-5024)
one mechanisms of hot reactions, 20: 14620
BIOLOGICAL MATERIALS
radiation dosimetry in, calorimetric method for, 20: 15858
radiation dosimetry in, physical factors affecting, 20: 14814
BIOLOGICAL MODELS
for bone marrow cell maturation, 20: 14248
for iodine metabolism in man, 20: 14249
for iodine metabolism in man, 20: 14250
of deposition and retention of dusts in respiratory tract of man, 20: 14796
BIOLOGY
research programs in, at Juelich Research Center, Germany, 20: 16156
BIOMETRY
analysis of genetic map length in reactivated complexes of uv-irradiated T4 phage, 20: 14328
methods for estimation of time of acute radiation sickness as a function of dose, 20: 14287 (AD-626996)
BISMUTH
analysis and determination, 20: 14500
bremsstrahlung reactions (γ,n) at 8 to 16 Mev, spectra from, (E), 20: 15723 (MIT-2098-162)
bremsstrahlung reactions (γ,n) with, neutron emission in, (E), 20: 15724 (MIT-2098-224)
determination in airborne dusts, spectrochemical, 20: 14457(R) (ORNL-3889, pp 36-39)
determination in iron–niobium alloys, chromatographic, 20: 14455(R) (ORNL-3889, pp 25-32)
effects on spectrofluorimetric determination of scandium, 20: 14476
electron transmission through thin foils of, plasmon excitation in, (E), 20: 15951
energy level widths for, K, (T), 20: 15239 (CONF-233(Vol.3), pp 419-39)
neutron elastic scattering at 0.8 Mev, cross sections for, (T), 20: 15770
BISMUTH ISOTOPES Bi-207
detection of, response of semiconductor radiation detector response for, 20: 14444(R) (MLM-1268)
BISMUTH ISOTOPES Bi-214
beta decay of, gamma spectrum from, (E), 20: 15844
content in uranium-mine air, 20: 14747
BISMUTH OXIDES
sorptive properties for chloride and potassium ions, effects of pH on, 20: 14651
BLACK SEA
fallout monitoring on, 1964, 20: 14741
BLADDER
radiotherapy of carcinomas of, γ, 20: 14414
radiotherapy of carcinomas in, effect on ureteric valves of gamma, 20: 14298
radiotherapy of tumors of, vesico-ureteral reflux from β and γ, 20: 14411
BLOOD
adenine nucleotide content in rat, effects of methioninesulfoximine on, 20: 14270
effects of exercise and inhaled yttrium oxide on, of dogs, 20: 14257
hematocrit relation to xenon-133 solubility in, 20: 14415
radiation effects on adenine nucleotide content in rat, x, 20: 14270
radiation effects on pulmonary volume of, methods for measuring, 20: 14292(R) (TID-22563)
solvent properties for xenon-133, 20: 14415
BLOOD CELLS
volume distribution measurements using Coulter counters, computer analysis of data from, 20: 14232 (LA-3440)
BLOOD CIRCULATION
effects of x-irradiated prostheses on dog arterial, 20: 14344
measurement in carcinoma implants, tracer method for, 20: 14405 (COO-1305-2)
tracer study using xenon-133, 20: 14415
BLOOD PICTURE
radiation effects on monkey, whole-body x, 20: 14302
radiation effects on animal, use in dosimetry, 20: 14314
radiation effects on bovine, fractionated-dose whole-body x, 20: 14336
BLOOD PLASMA
effects of methyl palmitate on lipids in mouse, 20: 14241 (TID-21437)
radiation effects on proteins in rat, effects on Hamolsky's test of γ, 20: 14276
radiation effects on corticosteroid levels in dog, x, 20: 14280
technetium clearance in human, tracer study, 20: 14423
BLOOD SERUM
content in culture media of Chinese hamster cells, radiosensitivity effects of, 20: 14400
radiation effects on glycoprotein content of rat, x, 20: 14378
BLOOD VESSELS
barium-140 uptake by aortic wall of rats, 20: 14252
radiation effects on sulfate uptake by rabbit aorta, β, 20: 14295
radiation effects on prostheses for, x, 20: 14344
radiation effects on dacron prostheses for, x, 20: 14345
radiation effects on, review, 20: 14345
strontium-85 uptake by aortic wall of rats, 20: 14252
BODY FLUIDS
radiation effects on pulmonary fluid volumes in dogs, methods for measuring, 20: 14292(R) (TID-22563)
BOILERS
design and fabrication of modular, for sodium-cooled reactors, 20: 15999 (NAA-SR-11739)
tube holding device for, 20: 14698(P)
BOILING
burnout detection method for water, 20: 14694
burnout in steam-water flows with axially nonuniform heat flux, (E), 20: 14696
burnout in water in internally cooled tubes, 20: 14686(R) (EURAEC-1448)
critical heat flux in internally heated eccentric annuli, (E), 20: 16086 (TID-22651)
effects of heat transfer in transition, on fluid flow in single rod test sections, 20: 14687 (GEAP-4785)
heat fluxes during burnout of water, (E), 20: 14694
hydrodynamic oscillations in natural-circulation two-phase, 20: 14684 (ANL-7073)
BOILING REACTORS
accidents in high-power, analytic studies of, 20: 16019(R) (BMI-X-10154)
coolant decompression in, shock waves from, 20: 16023(R) (IITRI-578P21-16)
design with superheated breeding blanket, 20: 16105(P)
BONE FRACTURES
radioinduced costal, by breast cancer therapy, 20: 14369
BONE MARROW
cell development in, tracer study in rats, 20: 14248
cell maturation in, biological model of, 20: 14248
physiology of mouse, genetic control in, 20: 14290(R) (NYO-1800-12)
radiation effects on survival of 5-bromo-deoxycytidine-treated, fast-neutron and x, 20: 14333
radiation effects on content of nucleated cells in, of young mice, γ, 20: 14365
sulfhydryl content in, of radioresistant mice, 20: 14351

BONES
radiation dose rates to human, from radium D, 20: 14353
radiation dose to facial, during extraoral radiography, 20: 14412
strontium metabolism in rat, effects of pyridoxal on, 20: 14246
BORIC ACID
effects on incompatibility in *Oenothera organensis*, 20: 14382
boric acid–H_2O, neutron diffusion length at 18 to 255°C, thermal, (E), 20: 15679
BORON
determination in plutonium fluorides and peroxides, review on spectrographic, 20: 14464 (RFP-599)
determination in uranium tetrafluoride, spectrographic, 20: 14473
BORON CARBIDES
preparation of spherical particles of, procedure and apparatus for, 20: 14971(P)
B_4C–graphite, fabrication of neutron shielding of, 20: 15027(P)
BORON HYDRIDES
preparation of boron-10-labeled dibomane, 20: 14576(R) (ORNL-3889, pp 73-7)
BORON ISOTOPES
separation of boron-10 from mixtures of, by exchange distillation, 20: 14629
BORON ISOTOPES B-9
energy levels, (E), 20: 15729(R) (RHEL/R-112, pp 37-66)
BORON ISOTOPES B-10
energy levels, (E), 20: 15729(R) (RHEL/R-112, pp 37-66)
helium-3 reactions (He-3,n) with, angular distributions for, (T), 20: 15798
nucleon emission from, reduced widths in shell-model intermediate coupling, (T), 20: 15830
separation from other boron isotopes by exchange distillation, 20: 14629
triton reactions (t,p) with, angular distributions for, (T), 20: 15798
BORON ISOTOPES B-11
alpha reactions (α,n) at 2.38 to 3.67 Mev, nitrogen-15 levels from, (E), 20: 15790
deuteron reactions (d,p) at 0.7 to 1.7 Mev, angular distribution from, (E), 20: 15847
deuteron reactions (d,n) at 1 to 11 Mev, (E), 20: 15858
energy levels of, rotator model for excited, 20: 15859
BORON ISOTOPES B-12
nucleon emission from, reduced widths in shell-model intermediate coupling, (T), 20: 15830
BORON NITRIDES
spectra of translucent, absorption, 20: 14453(R) (ORNL-3889, pp 12-14)
BORON OXIDES
preparation of spherical particles of, procedure and apparatus for, 20: 14971(P)
BaO–B_2O_3–SiO_2, effects of aluminum, lanthanum, and thorium oxides on crystallization of, 20: 15075
BORON SYSTEMS
B–Cd–Co, crystal structure, 20: 14532
B–Cd–Ni, crystal structure, 20: 14532
B–Co–Ag, crystal structure, 20: 14532
B–Co–Nb, phase studies, 20: 15100
B–Co–Pb, crystal structure, 20: 14532
B–Co–U, crystal structure, 20: 14532
B–Co–Y, crystal structure, 20: 14532
B–Co–Zr, phase studies, 20: 14533
B–Cu–Mn, crystal structure, 20: 14532
B–Cu–Mo, crystal structure, 20: 14532
B–Cu–Nb, crystal structure, 20: 14532
B–Cu–Zr, crystal structure, 20: 14532
B–Fe–Mo, crystal structure, 20: 14532
B–Fe–Nb, crystal structure, 20: 14532
B–Fe–V, crystal structure, 20: 14532
B–Fe–W, crystal structure, 20: 14532
B–Fe–Zr, crystal structure, 20: 14532
B–H_2O, neutron spectra in, (E), 20: 15731(R) (RPI-328-49)
B–Ni–Ag, crystal structure, 20: 14532
B–Ni–U, crystal structure, 20: 14532
B–Ni–Y, crystal structure, 20: 14532
B–Pb–Ni, crystal structure, 20: 14532
B–stainless steel, radiation effects on poison elements of, in-pile, 20: 16089(R) (WAPD-MRP-114)
Sb–B–Co, crystal structure, 20: 14532
Sb–B–Ni, crystal structure, 20: 14532
BOSONS
decay of intermediate vector, SU(3) symmetry for nonleptonic, (T), 20: 15362
decay of vector, beta, (E), 20: 15406
exchange in mesons (K^-)-proton interactions at 1.80 and 1.95 Bev/c, (E), 20: 15420
interactions of weak intermediate, with hadrons, (T), 20: 15396
interactions with fermions in Lee model, bound states in, (T), 20: 15459
production and detection of vector, in Adone, (E), 20: 15311 (LNF-65/47)
stability of many-particle systems of, (T), 20: 15151
symmetry scheme for, A-selection rule and parity in G_2, 20: 15473
theory of intermediate, in SU(6) symmetry, 20: 15497
theory of many-body systems of, 20: 15560
BRAIN
nucleic acid metabolism in rat, tracer study, 20: 14242(R) (TID-22591)
radiation effects on electrical activity of rabbit, γ, 20: 14326
BREASTS
radiotherapy of cancer of, costal fractures from, 20: 14369
BREEDER REACTORS
design of boiling-water, with superheated breeder blanket, 20: 16105(P)
design of fast molten-salt, 20: 16037
design of fast, fused-salt-fueled, liquid-metal-cooled, 20: 16036
design parameters of large, effects on breeding in, (T), 20: 16093
BREMSSTRAHLUNG
emission from electron reactions with thin silver foils, (E), 20: 15968
interactions with protons at 550 to 1000 Mev, cross sections for meson (π) pair production in, (E), 20: 15332
interactions with protons at 225 to 350 Mev, meson (π^+) production in, (E), 20: 15340
performance for cross-section measurements in wire fabrication, (E/T), 20: 14838
production of double, cross sections for, 20: 15318
reactions (γ,n) with nuclei at 8 to 16 Mev, spectra from, (E), 20: 15723 (MIT-2098-162)
reactions (γ,n) with heavy elements, neutron emission in, (E), 20: 15724 (MIT-2098-224)
reactions with elements $14 \leq Z \leq 50$ detection efficiency for x-ray emission in, (E), 20: 15258
BREMSSTRAHLUNG SOURCES
performance of thallium-204, for wire cross-section measurements, 20: 14838
BRITTANY POWER REACTOR (EL-4)
construction of, nondestructive methods for testing materials used in, 20: 14711
BROMINATION
radioinduced, of 2,3-dimethylbutane, gamma, 20: 14591
BROMINE
determination in automobile lubricants, activation, 20: 14439(R) (GA-5556)
determination in automobile paint, activation, 20: 14439(R) (GA-5556)
determination in commercial plastics, activation, 20: 14439(R) (GA-5556)
determination in cigarette tobacco, activation, 20: 14439(R) (GA-5556)
effects on NMR spectra of bromine-79 and -81 in potassium and sodium bromides, 20: 14573
energy level transitions in, Coster-Kronig, (T), 20: 15238 (CONF-233 (Vol.3), pp 398-418)
energy level widths for, K, (T), 20: 15239 (CONF-233(Vol.3), pp 419-39)
reactions of recoil, mechanisms of, 20: 14620
BROMINE ISOTOPES Br-79
electron spectra from, Auger, (E), 20: 15244 (CONF-233(Vol.3), pp 487-93)
energy levels from gamma resonance scattering, (E), 20: 15802
nuclear magnetic resonance spectra in potassium and sodium bromides, effects of bromine on, 20: 14573
BROMINE ISOTOPES Br-81
nuclear magnetic resonance spectra in potassium and sodium bromides, effects of bromine on, 20: 14573
BROWNIAN MOVEMENT
of random-matrix eigenvalues, asymptotic solution for, (T), 20: 15785
BUBBLE CHAMBERS
particle track analysis in photographs from, using flying-spot digitizers, 20: 14850 (BNL-9763)
particle track measurements in, computer-controlled system for, 20: 14861 (UCRL-16555)
scanning and measuring projector for, engineering drawings of, 20: 14898
use at electron accelerators, 20: 15187
BUBBLES
diffusion and coalescence in solids, theory of, 20: 15132 (ANL-7079)
BURNS
effects of skin, on electrolyte and water transport, 20: 14255
effects on urinary excretion of ammonia and phosphates in rats, 20: 14270
BURROS
radiation effects on incidence of *Streptococcus equi* infections in, x, 20: 14288 (AD-627986)
BUTADIENE, CHLORO- POLYMERS
radiation effects on molecular structure of various types of, infrared spectral studies on, 20: 14585 (TID-22652)
BUTANE, 2,3-DIMETHYL-
radioinduced bromination of, gamma, 20: 14591

2-BUTENE-1,4-DIONE, 1,4-DIPHENYL-
radioinduced isomerization of, effects of potassium bromide on, 20: 14576
BUTYL PHOSPHATE COMPLEXES
with rare earth nitrates, chemical bonding in, Roman polarization measurements of, 20: 14529
with thorium nitrate, chemical bonding in, Roman polarization measurements of, 20: 14529
BUTYL PHOSPHATES
density and viscosity, 20: 14648
radiation effects in Thorex short decay runs, dose calculations, 20: 14580 (ORNL-2764)
solvent properties for uranium, 20: 14655
solvent properties for promethium-147 and other rare earth fission products, 20: 14635 (CONF-660305-5)
solvent properties for thorium, 20: 14448(R) (NLCO-970, pp 1.1-22)
$La(NO_3)_3$–tributyl phosphate, density and viscosity of, 20: 14648
$Th(NO_3)_4$–TBP, thorium distribution in, 20: 14448(R) (NLCO-970, pp 1.1-22)
tributyl phosphate–xylene, density and viscosity of, 20: 14648

C

CABLES
development for power supply and pulse transmission for radiation detectors, 20: 14876
CADMIUM
analysis and determination, 20: 14500
determination in airborne dusts, spectrochemical, 20: 14475(R) (ORNL-3889, pp 36-39)
determination in commercial plastics, activation, 20: 14439(R) (GA-5556)
energy level transitions in, Coster-Kronig, (T), 20: 15238 (CONF-233 (Vol.3), pp 398-418)
energy level widths for, K, (T), 20: 15239 (CONF-233(Vol.3), pp 419-39)
erosive effects of flowing molten, of uranium, 20: 14975 (ANL-7091)
neutron elastic scattering at 0.8 Mev, cross sections for, (T), 20: 15770
CADMIUM ISOTOPES Cd-109
determination in atmospheric and precipitation samples, methods for radiochemical, 20: 14430 (AD-620219)
CADMIUM ISOTOPES Cd-110
energy level transitions in, conversion coefficients for E2, (E), 20: 15704 (CONF-233(Vol.2), pp 164-76)
CADMIUM SULFATES
cadmium sulfate–H_2O, neutron diffusion length at 18 to 255°C, thermal, (E), 20: 15679
CADMIUM SYSTEMS
B–Cd–Co, crystal structure, 20: 14532
B–Cd–Ni, crystal structure, 20: 14532
CALCIUM
content in red-colored Paleozoic deposits in Northern Tien Shan, 20: 14780(T) (AEC-tr-6579)
determination by spectroscopy using plasma jet, 20: 14492
determination in automobile lubricants, activation, 20: 14439(R) (GA-5556)
determination in plutonium fluorides and peroxides, review on spectrographic, 20: 14464 (RFP-599)
determination in thorium compounds, spectrochemical methods for, 20: 14443(R) (MCW-1493, pp 27-30)
determination of trace amounts of, in uranium dioxide, 20: 14494
effects on incompatibility in *Oenothera organensis*, 20: 14382
energy level widths for, K, (T), 20: 15239 (CONF-233(Vol.3), pp 419-39)
meson (μ^-) capture by, neutron angular distributions from, (E), 20: 15721 (JINR-E-2517)
proton elastic scattering at 25 to 50 Mev, polarization from, (E), 20: 15728(R) (RHEL/R-112, pp 23-36)
sorption from gastrointestinal tract, calcium-47 tracer analysis of, 20: 14247
transport across, intestinal membranes, tracer study, 20: 14243(R) (TID-22626)
CALCIUM CHLORIDES
$CaCl_2$–NaCl, reactions with refractory metal borides, carbides, nitrides, and oxides, 20: 14989
CALCIUM COMPLEXES
with EDTA, demineralization of hard tissues by, 20: 16149 (NYO-2779-10)
CALCIUM FLUORIDES
ion localized vibrations in, spectra of deuterium and hydrogen, 20: 15969
CALCIUM ISOTOPES
deuteron reactions at 15 Mev, isomeric states from, (E), 20: 15856
CALCIUM ISOTOPES Ca-40
electron elastic scattering at 250 Mev, (E), 20: 15439
helium-3 reactions (He-3,α) with, measurement and distorted wave analysis of, 20: 15855
neutron compound elastic scattering at 3.15 Mev, cross sections for, (E/T), 20: 15865
neutron reactions (n,2n) at 12 to 18 Mev, cross sections for, (E), 20: 15863
nuclear properties in shell model, 20: 15730(R) (RHEL/R-112, pp 67-98)
proton elastic scattering at 30 Mev, models for, 20: 15730(R) (RHEL/R-112, pp 67-98)
proton reactions (p,γ) at 0.6 to 5.2 Mev, energy levels from, 20: 15849
CALCIUM ISOTOPES Ca-42
nuclear properties in shell model, 20: 15730(R) (RHEL/R-112, pp 67-98)
CALCIUM ISOTOPES Ca-44
electron elastic scattering at 250 Mev, (E), 20: 15439
CALCIUM ISOTOPES Ca-45
incorporation in human chromosomes, 20: 14243(R) (TID-22626)
CALCIUM ISOTOPES Ca-47
metabolism by rats, effects of dietary strontium on, 20: 14251
use for determining gastrointestinal sorption of calcium, 20: 14247
CALCIUM OXIDES
effects on in-pile properties of uranio–zirconia fuels, 20: 15138 (WAPD-292)
sorptive properties for chloride and potassium ions, effects of pH on, 20: 14651
CaO–CeO_2–ZrO_2, electric conductivity and structure of, at 500 to 1000°C, 20: 14536
CaO–Nb_2O_5, density and surface ductility of fused at 1200 to 1650°C, 20: 15076
CaO–Sm_2O_3–UO_2–ZrO_2, corrosion and surface properties of, 20: 16089(R) (WAPD-MRP-114)
CaO–UO_2–ZrO_2, corrosion and surface properties of, 20: 16089(R) (WAPD-MRP-114)
CaO–UO_2–ZrO, properties of, in-pile, 20: 15138 (WAPD-292)
CaO–V_2O_5, density and surface ductility of fused, at 1200 to 1650°C, 20: 15076
CALCIUM TITANATES
performance as space radiator coating on beryllium, niobium–1 zirconium, and type 310 stainless steel, 20: 15057(R) (PWA-2750)
CALIFORNIUM
production in heavy-ion nuclear reactions, review of, 20: 15740
separation from curium, chemical process for, 20: 14636 (CONF-660305-7)
CALIFORNIUM ISOTOPES Cf-252
fission of, neutron spectra from spontaneous, (E/T), 20: 15032(R) (ANL-7152, pp 50-72)
CALORIMETERS
current integrators for, development of, 20: 14444(R) (MLM-1268)
design and performance of total-absorption thermal x-ray, 20: 14908
design of twin isothermal, engineering drawings for, 20: 14833
CALORIMETRY
use in radiation dosimetry, 20: 15858
CAMBRIDGE SYNCHROTRON
research operations, 20: 15306(R) (CEAL-1026)
CANADA
fallout measurements in, October 1965, 20: 14737 (NP-15853, pp 8-20)
strontium-90 contamination of wheat in, 1964, 20: 14736 (NP-15853, pp 3-7)
CANDU REACTOR
environs monitoring, 20: 14738 (NP-15853, pp 21-33)
radioactive contamination of milk near, 20: 14738 (NP-15853, pp 21-33)
CAPROIC ACID
determination in commercial coconut oils, gas chromatographic, 20: 14463 (PAEC(D)CH-652)
CAPRYLIC ACID
determination in commercial coconut oils, gas chromatographic, 20: 14463 (PAEC(D)CH-652)
CARBIDES
properties of, at high temperature during fusion crystal growth, 20: 15047(R) (N65-15919)
CARBON
compatibility of coatings of pyrolytic, with plutonia at 1800°C, 20: 14957(R) (BMI-1754)
determination in alkali metals, methods for, 20: 14454(R) (ORNL-3889 (pp 17-24)
determination of simultaneously with carbon-14 in samples, 20: 14474
determination of trace amounts of, in uranium dioxide, 20: 14494
diffusion in niobium carbide at 1700°K, coefficient for, 20: 14992
diffusion in titanium and zirconium nitrates, carbide film formation in, 20: 15072
effects on microstructure of molybdenum–uranium alloy, 20: 15070
effects on thermal conductivity of Springfields uranium at 160 to 620°C, 20: 15084
meson (π^-) reactions (π^-,γ), energy spectra and yields from, (E), 20: 15794
microscopy of pyrolytic, polarized light, 20: 15089
reactions with niobium, tantalum, and vanadium diborides, 20: 14555
solubility in germanium and in hafnium alloys, 20: 15047(R) (N65-15919)
CARBON (ACTIVATED)

sorptive properties for iodine, potentiometric studies at 0 and 50°C on, 20: 15065(T) (ORNL-tr-1018)

CARBON DIOXIDES
concentration of carbon-13-enriched, methods for, 20: 14444(R) (MLM-1268)
decomposition in ion source of mass spectrometer, formation of multiply charged ions in, 20: 14584(R) (TID-22444)
formation in radioinduced oxidation of cyclohexane, 20: 14625
CO_2–glass–N_2, heat transfer in glass-bead suspensions, 20: 14671(R) (TID-22394)

CARBON IONS
electron transitions in, oscillator strengths for probability of, (T), 20: 15275

CARBON ISOTOPES C-11
energy levels, (E), 20: 15729(R) (RHEL/R-112, pp 37-66)
energy levels from carbon-12 (γ,n) reactions at 21.7 to 26.7 Mev, (E), 20: 15861
energy levels of, rotator model for excited, 20: 15859
reactions of recoil, mechanisms of, 20: 14620

CARBON ISOTOPES C-12
alpha inelastic scattering by, polarization in, (E), 20: 15862
alpha reactions (α,2α) at intermediate energies, final-state interaction effects on, (T), 20: 15825
energy levels from alpha inelastic scattering, (E), 20: 15862
energy levels in, from boron-11 (d,n) reaction, (T), 20: 15858
gamma reactions (γ,n) at 21.7 to 26.7 Mev, (E), 20: 15861
helium-3 reactions (He-3,n) at 1.97 to 4.70 Mev, angular distributions in, (E), 20: 15854
helium-3 reactions (He-3,n) with, angular distributions for, (T), 20: 15798
nuclear properties in shell model, 20: 15730(R) (RHEL/R-112, pp 67-98)
nuclear properties in alpha-particle model, 20: 15689 (CEA-R-2786)
nucleon emission from, reduced widths in shell-model intermediate coupling, (T), 20: 15830
proton elastic and inelastic scattering at 20 to 28 Mev, polarization in, (E), 20: 15805
proton elastic scattering at 30 to 50 Mev, models for, 20: 15730(R) (RHEL/R-112, pp 67-98)
proton reactions (p,d) at 155 Mev, models for, 20: 15730(R) (RHEL/R-112, pp 67-98)
proton reactions at 20 to 40 Mev, distributions from, (E), 20: 15729(R) (RHEL/P-112, pp 37-66)
proton scattering at 20 to 50 Mev, distributions from, (E), 20: 15728(R) (RHEL/R-112, pp 23-36)
scattering by lead-208, level excitation by, (E), 20: 15719 (INP-431/PL)
triton reactions (t,p) with, angular distributions for, (T), 20: 15798

CARBON ISOTOPES C-13
concentration in carbon dioxide, methods for, 20: 14444(R) (MLM-1268)
concentration in methane, methods for, 20: 14444(R) (MLM-1268)
energy levels in, from boron-11 (d,n) reaction, (T), 20: 15858
helium-3 reactions (He-3,n) with, angular distributions for, (T), 20: 15798

CARBON ISOTOPES C-14
determination in organic compounds and proteins by liquid scintillation counting on paper chromatograms, 20: 14479
determination simultaneously with total carbon in samples, 20: 14474
diffusion in beryllium, tracer studies on, 20: 15037 (CEA-R-2621)
iron-59 chelated with EDTA-incorporated, penetration in cuticular membrane of tomatoes, 20: 16147 (COO-888-45)
iron-59 chelated with EDDHA-incorporated, penetration in cuticular membranes of tomatoes, 20: 16147 (COO-888-45)
penetration of dimethylaminosuccinamide-incorporated, through cuticular membranes, 20: 16146 (COO-888-39)
penetration of maleic hydrazide-incorporated, through cuticular membranes, 20: 16146 (COO-888-39)
penetration of urea-incorporated, through cuticular membranes, 20: 16146 (COO-888-39)
production of high-purity, radiochemistry of, 20: 14461(R) (ORNL-3889, pp 48-70)
reactions of recoil, mechanisms of, 20: 14620

CARBON MONOXIDES
vapor pressure of, from chemical reactions in sol-gel fuels, 20: 14512 (ORNL-TM-1418)

CARBON STEEL
corrosion of Creusot 1.2 MD07, by water at 300°C, effects of flow rate and surface treatment on, 20: 14978 (EURAEC-1546)

CARBON SULFIDES
decomposition in ion source of mass spectrometer, formation of multiply charged ions in, 20: 14584(R) (TID-22444)

CARBON SYSTEMS
Al–C–Co–Nb, phase studies, 20: 15103
Al–C–Co–Ta, phase studies, 20: 15103
Al–C–Cr–Nb, phase studies, 20: 15103
Al–C–Cr–Ta, phase studies, 20: 15103
Al–C–Cu–Nb, phase studies, 20: 15103
Al–C–Cu–Ta, phase studies, 20: 15103
Al–C–Fe–Nb, phase studies, 20: 15103
Al–C–Fe–Ta, phase studies, 20: 15103
Al–C–Fe–U, mechanical properties at intermediate strain rates and temperatures, 20: 15081
Al–C–Mn–Nb, phase studies, 20: 15103
Al–C–Mn–Ta, phase studies, 20: 15103
Al–C–Nb, phase studies, 20: 15103
Al–C–Nb–V, phase studies, 20: 15103
Al–C–Nb–Zn, phase studies, 20: 15103
Al–C–Ni–Nb, phase studies, 20: 15103
Al–C–Ni–Ta, phase studies, 20: 15103
Al–C–Ta, phase studies, 20: 15103
Al–C–Ta–V, phase studies, 20: 15103
Al–C–Ta–Zn, phase studies, 20: 15103
C–Co–Nb, phase studies, 20: 15077
C–Cr–Mo, phase studies, 20: 15111
C–Cr–Nb, phase studies, 20: 15108
C–Cr–Ta, phase studies, 20: 15108
C–Mo–Nb–Zr, heat treatment of, 20: 14972(P)
C–Nb–Ta–Zr, heat treatment of, 20: 14972(P)
C–Nb–Ti–Zr, heat treatment of, 20: 14972(P)
C–Nb–V–Zr, heat treatment of, 20: 14972(P)
C–Nb–W–Zr, heat treatment of, 20: 14972(P)
C–Nb–W–Zr, tensile properties of D-43, 20: 15068
C-O-Th, vapor pressure of carbon monoxide in sol-gel fuels of, 20: 14512 (ORNL-TM-1418)
C–O–U, phase studies at 1700°C, 20: 14968(R) (USBM-RC-1220)
C–O–U, vapor pressure of carbon monoxide in sol-gel fuels of, 20: 14512 (ORNL-TM-1418)
C–Ta, magnetic susceptibility, 20: 15045 (N65-15624)

CARBON TETRABROMIDE
decomposition in ion source of mass spectrometer, mechanism of, 20: 14584(R) (TID-22444)

CARBON TETRACHLORIDE
decomposition in ion source of mass spectrometer, mechanism of, 20: 14584(R) (TID-22444)
effects on mice, carcinogenic, 20: 14373
effects on solvent properties for uranium in TBP system, 20: 14655
radiolysis of aqueous, carbon dioxide-saturated solutions of, formation of trichloroacetic acid in, 20: 14582 (SGAE-CH-25/1965)
reactions with gallium–plutonium alloys, critical temperature of, 20: 14513 (RFP-688)

CARBON TETRAFLUORIDE
decomposition in ion source of mass spectrometer, mechanism of, 20: 14584(R) (TID-22444)

CARBON TETRAIODIDE
decomposition in ion source of mass spectrometer, mechanism of, 20: 14584(R) (TID-22444)

CARBONATES
radioactivity of rocks of, 20: 14752

CARBONIC ACID, DIETHYL ESTER
decomposition in ion source of mass spectrometer, mechanism of, 20: 14584(R) (TID-22444)

CARBONYL SULFIDE
decomposition in ion source of mass spectrometer, formation of multiply charged ions in, 20: 14584(R) (TID-22444)

CARBONYLS
decomposition in ion source of mass spectrometer, negative ion formation in, 20: 14584(R) (TID-22444)

CARCINOGENESIS
concepts of, review on, 20: 14373
radioinduced, mechanisms for, 20: 14360

CARCINOMAS
blood circulation in implants of, tracer study, 20: 14405 (COO-1305-2)
radioactive microsphere uptake by liver, after intravascular introduction, 20: 14405 (COO-1305-2)
radioinduced in rabbits after strontium-90 injection, 20: 14316
radiotherapy of bladder, vesico-ureteral reflux from β and γ, 20: 14411
radiotherapy of bladder, γ, 20: 14414
radiotherapy of bladder, effects on ureteric valves of gamma, 20: 14298
radiotherapy of cervical, tumorigenic effects of, 20: 14300
radiotherapy of cervical, complications from surgery combined with radium and x, 20: 14377
radiotherapy of cervical, surgery combined with radium and x, 20: 14409
radiotherapy of lung, evaluation of procedures for γ and x, 20: 14420
radiotherapy of palatine arch and tonsilar, x, 20: 14416

CARNOTITES
analysis for uranium, spectrophotometric, 20: 14455(R) (ORNL-3889, pp 25-32)

CAROLINAS-VIRGINIA TUBE REACTOR

control rod performance testing, 20: 16062 (CVNA-175)
experimental facilities for, feasibility of organic-cooled loop, 20: 16063 (CVNA-241)
fuel assembly testing for, transient DNB in, 20: 16101
meteorological analyses of site of, 20: 14732 (CVNA-172)
CARTILAGE
histology of rat epiphyseal, 20: 14291(R) (TID-22494)
radiation effects on rat epiphyseal, 20: 14291(R) (TID-22494)
CASCADE SHOWERS
structure of electron-photon, Monte Carlo method for, (T), 20: 15938
CATALASES
amino acids in, effects of lipid peroxidation on, 20: 14587
CATHODES
testing of carbide, for thermionic space power systems, 20: 15046(R) (N65-15820)
CATS
radiation effects on unconditioned reflexes in lungs of, effects on cardiovascular system of x, 20: 14371
CATTLE
iodine-131 content in milk of, 20: 14243(R) (TID-22626)
radiation effects on sperm production and testicular histology in, fractionated-dose whole-body x, 20: 14336
radioinduced skeletal anomalies in, exposed *in utero*, γ, 20: 14337
radium content in teeth and thyroids of, 20: 14254
CELLULOSE
methyl ether of, effects on sintered density of plutonia–urania and urania of additions of, 20: 14965(R) (NUMEC-3524-12)
CEMENTS
properties of portland, effects of temperature on, 20: 15051 (NP-15876)
CENTRIFUGES
band withdrawal apparatus for, engineering drawings for, 20: 14673
CERAMIC MATERIALS
casting of fiber-reinforced fused silica, process development for slip-, 20: 15058(R) (SC-DC-66-1130)
conference on science of, Noordwijk aan Zee, Netherlands, May 13 to 17, 1963, 20: 14970
mechanical properties for high-temperature uses, 20: 15129
use of inorganic fibrous, with colloidal inorganic oxides as refractory composition, 20: 14974(P)
CERIUM
determination in dust samples by microchemical methods and autoradiography, 20: 14472
mass of, spectrometric determination of, 20: 15853
polarization during electrolysis in lithium chloride–potassium chloride, effects of lithium fluoride additions on, 20: 14564
polarization during electrolysis on fused salts, 20: 14561
separation from fission products, methods for, 20: 15722 (KR-76)
spectra in lanthanum chlorides, crystal-field splitting of, 20: 14553
CERIUM ALLOYS
Ce–Co, cobalt ion EPR in intermetallic compounds of, 20: 15963
Ce–Co–Pu, solvent properties for niobium at 500 to 900°C, 20: 15043 (LA-3436)
Ce–Y, electric conductivity of dilute, at low temperatures, (E), 20: 15098
CERIUM CHLORIDES
effects on molybdenum polarization during electrolysis in fused salts, 20: 14562
CERIUM ETHYL SULFATES
cerium ion interactions in, 20: 15991
CERIUM IONS
electron transfer between trivalent and tetravalent, effects of sulfate ions on, 20: 14574
magnetic interactions in cerium ethyl sulfate, 20: 15991
reactions with fluoride ions in fused salts, 20: 14563
CERIUM ISOTOPES Ce-136
atomic mass, (E), 20: 15769
CERIUM ISOTOPES Ce-137
burnup calculations for, in reactor fuels, 20: 16061(R) (BAW-296)
content in Lake Huron and Ottawa River, 20: 14738 (NP-15853, pp 21-33)
CERIUM ISOTOPES Ce-138
atomic mass, (E), 20: 15769
CERIUM ISOTOPES Ce-140
atomic mass, (E), 20: 15769
CERIUM ISOTOPES Ce-141
determination in atmospheric and precipitation samples, methods for radiochemical, 20: 14430 (AD-620219)
CERIUM ISOTOPES Ce-142
atomic mass, (E), 20: 15769
CERIUM ISOTOPES Ce-144
content in fallout over Black Sea, 1964, 20: 14741
content in Indo-Antarctic Ocean, 1962, 20: 14749
content in stratosphere and troposphere, 1962 and 1963, 20: 14742
determination in atmospheric and precipitation samples, methods for radiochemical, 20: 14430 (AD-620219)
leaching from alumina–phosphate glass prepared from calcined alumina waste, 20: 16133 (IDO-14672)
production of high-purity, radiochemistry of, 20: 14461(R) (ORNL-3889, pp 48-70)
separation from Purex waste solutions by lead carrier sulfate precipitation, 20: 14641 (RL-SA-59)
separation from rare earth fission products by isotopic exchange and reduction, 20: 14635 (CONF-660305-5)
separation from water by sorption by bentonites and diatomaceous earth, effects of flocculants on, 20: 16138
CERIUM ISOTOPES Ce-145
beta decay, (E), 20: 15722 (KR-76)
CERIUM ISOTOPES Ce-146
beta decay, (E), 20: 15722 (KR-76)
CERIUM ISOTOPES Ce-147
beta decay, (E), 20: 15722 (KR-76)
CERIUM OXIDES
sorptive properties for chloride and potassium ions, effects of pH on, 20: 14651
$CaO–CeO_2–ZrO_2$, electric conductivity and structure of, at 500 to 1000°C, 20: 14536
$Ce_2O_3–WO_3$, preparation and properties, 20: 14534
CERMETS
fabrication of tungsten–uranium dioxide–vanadium, by isostatic cold pressing, 20: 14962(R) (N65-20803)
CESIUM
atom reactions with, excitation transfer in inert-gas, (E), 20: 15253
determination in dust samples by microchemical methods and autoradiography, 20: 14472
impurities in thermionic cell, hydrogen and oxygen, 20: 15298 (FEI-22)
neutron coherent scattering amplitude of, 20: 15736
separation from fission products, review on methods for, 20: 14436 (BNWL-SA-504)
sorption by soils and clay minerals, effects of aluminum oxide and iron oxide on, 20: 14652
stability of plasma of, Kelvin-Helmholtz, (E), 20: 15906
CESIUM CARBONATES
preparation by tetraoxalate process, review on, 20: 14626 (ORNL-P-1944)
CESIUM CHLORIDES
electric conductivity in light and heavy water at 25°C, 20: 14540
CESIUM COMPOUNDS
preparation of cesium-137-labeled, review on, 20: 14626 (ORNL-P-1944)
CESIUM FLUORIDES
effects of vapor of, on performance of thermionic cells, 20: 15297 (CONF-640921, pp 101-9)
reactions with xenon oxyfluorides, complex formation in, 20: 14523
CESIUM IODIDES
radioinduced luminescence of thallium-activated, composition of, 20: 14611(T)
CESIUM ISOTOPES Cs-133
deuteron reactions (d,2n) and (d,p) with, isomeric cross-section ratios in, 20: 15778
neutron reactions (n,p) at 14.6 Mev, isomeric cross section ratio for, (E/T), 20: 15773
yields in neutron fission of plutonium-239, uranium-233, and uranium-235, 20: 15133(R) (GEAP-4893)
CESIUM ISOTOPES Cs-134
metabolism in rats, 20: 14243(R) (TID-22626)
production in deuteron reactions with cesium-133, isomeric cross-section ratios for, (E), 20: 15778
CESIUM ISOTOPES Cs-137
content in Canadian fallout, October 1965, 20: 14737 (NP-15853, pp 8-20)
content in fallout over Black Sea, 1964, 20: 14741
content in food and people in Norway, 1963 through 1965, 20: 14739 (TID-22655)
content in foods, 1963-5, 20: 14243(R) (TID-22626)
content in grass, herbage, milk, and soils in vicinity of AERE, 20: 14784(R) (AERE-R-5015)
content in Indo-Antarctic Ocean, 1962, 20: 14749
content in man, whole-body, 20: 14243(R) (TID-22626)
content in spent power reactor fuels, evaluation of, 20: 14435 (BNWL-SA-503)
content in stratosphere and troposphere, 1962 and 1963, 20: 14742
detection of, response of semiconductor radiation detector response for, 20: 14444(R) (MLM-1268)
determination in urine, 20: 14243(R) (TID-22626)
determination of, review of methods for, 20: 14483
disposal by in-pile activation to stable or shortlived isotopes, (T), 20: 16132 (BNL-8558)
energy level transitions in, internal Compton effect in M4, (E), 20: 15815
half life, (E), 20: 14461(R) (ORNL-3889, pp 48-70)
incorporation in cesium source compounds, review on, 20: 14626

(ORNL-P-1944)
leaching from alumina–phosphate glass prepared from calcined alumina waste, 20: 16133 (IDO-14672)
performance in density meters for coal and soil, measurement errors for, 20: 14837
separation from fission products by Decalso process, review on, 20: 14626 (ORNL-P-1944)
separation from Purex alkaline waste solutions by ion exchange, 20: 14641 (RL-SA-59)
separation from solutions by ion exchange, 20: 14483
separation from water by sorption by bentonites and diatomaceous earth, effects of flocculants on, 20: 16138
separation from wastes, engineering drawings of WAFRAX facilities for, 20: 16139
sorption and storage on aluminum silicate zeolites, 20: 14466 (RL-SA-58)
sorption from radioactive wastes by ion exchange, 20: 14434 (BNWL-180)
use in internal therapy, survey of techniques for, 20: 14406
yields in neutron fission of plutonium-239, uranium-233, and uranium-235, 20: 15133(R) (GEAP-4893)

CHARCOAL
radiation effects on catalytic activity of, electron and gamma, 20: 14609

CHARGED PARTICLE BEAMS
analysis of, electrostatic prism spectrometer for, (T), 20: 14868
electromagnetic fields of bunched, in straight circular pipes, (T), 20: 15167 (SLAC-49, pp 18-22)
electromagnetic fields of oscillating bunched, in straight rectangular pipes, (T), 20: 15168 (SLAC-49, pp 29-31)
electromagnetic fields of bunched, in straight circular vacuum chambers, (T), 20: 15169 (SLAC-49, pp 32-5)
electromagnetic fields of, effects of dielectric media on, (T), 20: 15172 (SLAC-49, pp 52-8)
interactions with beams and media, (T), 20: 15166 (SLAC-49)
rotation frequency in isochronous cyclotron, effect of radial betatron oscillations on, (T), 20: 15186
stability of azimuthally bunched, (T), 20: 15166 (SLAC-49)
stability of bunched circulating, in toroidal vacuum chambers, (T), 20: 15170 (SLAC-49, pp 36-48)
stability of bunched relativistic, computer analysis of, (T), 20: 15171 (SLAC-49, pp 49-51)

CHARGED PARTICLES
electromagnetic radiation from moving, at dielectric interfaces, (E), 20: 15317(T) (ORNL-tr-677)
ionization losses and invariant form factors for spin $^3/_2$, (T), 20: 15269
motion in periodic dielectric medium, radiation emitted by, 20: 15558
scattering by nuclei, analytic expressions for inelastic, (T), 20: 15743
scattering by nuclei, collective-state excitation in, (T), 20: 15763
stability of many-body systems of, (T), 20: 15151

CHELATES
effects on radioisotope excretion in man, 20: 14256
of EDTA and 8-quinolinol, infrared spectra of, 20: 14499
toxicity of, review, 20: 14256

CHEMICAL ANALYSIS
book: *Methods for Analysis of Radioactive Preparations*, in Russian, 20: 14501
summary of, for ORNL process support, 20: 14428(R) (ORNL-3889)

CHEMICAL RADIATION DETECTORS
performance of chloral hydrate solutions as, at 80 to 800 rads, 20: 14583 (TID-21634)
performance of Fricke and nitrous oxide, 20: 14870

CHEMISTRY
book: *Survey of Chemical Technology in the Nuclear Industry*, in Czech., 20: 14429
research programs in, at Juelich Research Center, Germany, 20: 16156

CHERENKOV DETECTORS
reflectors for internal-sample aqueous, optical, 20: 14893

CHERENKOV RADIATION
emission by charged particles moving in periodic dielectric medium, 20: 15558

CHICKENS
radiation effects on embryos of, effects of inoculation with smallpox virus vaccine on x, 20: 14281

CHILE
copper reconnaissance in, 20: 14779 (RME-4569(Rev.))
uranium reconnaissance in, 20: 14779 (RME-4569(Rev.))

CHINA
composition of red-colored Paleozoic deposits in Northern Tien Shan, 20: 14780(T) (AEC-tr-6579)

CHINON REACTORS
construction of, nondestructive methods for testing materials used in, 20: 14711

CHLORAL
radiation effects on, at 80 to 800 rads, 20: 14583 (TID-21634)

CHLORIDE IONS
effects on isotope exchange between iron(II) and iron(III), 20: 14571
sorption by tetra-, penta-, and hexavalent metal oxides, effects of pH on, 20: 14651

CHLORINE
determination in automobile lubricants, activation, 20: 14439(R) (GA-5556)
determination in automobile tire rubber, activation, 20: 14439(R) (GA-5556)
determination in automobile paint, activation, 20: 14439(R) (GA-5556)
determination in commercial plastics, activation, 20: 14439(R) (GA-5556)
determination in hair samples in criminal cases, activation, 20: 14439(R) (GA-5556)
determination in paper samples in criminal cases, activation, 20: 14439(R) (GA-5556)
determination in thumbnail clippings, activation, 20: 14439(R) (GA-5556)
determination in wood in criminal cases, activation, 20: 14439(R) (GA-5556)
determination of trace amounts of, in uranium dioxide, 20: 14494
effects of impurity of, on positron annihilation spectrum in argon, (E), 20: 15436
energy level widths for, K, (T), 20: 15239 (CONF-233(Vol.3), pp 419-39)
mass of, spectrometric determination of, 20: 15853
neutron capture by, gamma spectra from thermal, (E), 20: 15787
radioinduced reactions with polyethylene, 20: 14621
reactions of recoil, mechanisms of, 20: 14620

CHLORINE ISOTOPES Cl-35
neutron reactions (n,2n) at 12 to 18 Mev, cross sections for, (E), 20: 15863
spectra of yttrium monochloride containing, visible, 20: 14569

CHLORINE ISOTOPES Cl-36
decay of, K/L ratio for electron-capture, (E/T), 20: 15713 (CONF-233 (Vol.2), pp 365-8)
exchange between silver chloride crystals and solutions, 20: 14572
half life, (E), 20: 14461(R) (ORNL-3889, pp 48-70)
sorption by burned and normal skin, 20: 14255

CHLORINE ISOTOPES Cl-37
electron spectra from, Auger, (E), 20: 15244 (CONF-233(Vol.3), pp 487-93)
electron vacancies in K-shell of, multiple ionization from, 20: 15245 (CONF-233(Vol.3), pp 494-504)
spectra of yttrium monochloride containing, visible, 20: 14569

CHLORINE ISOTOPES Cl-38
determination in copra and desiccated-coconut oils, activation, 20: 14463 (PAEC(D)CH-652)

CHLOROFORM
effects on solvent properties for uranium in TBP system, 20: 14655
radiolysis of aqueous, carbon dioxide-saturated solutions of, formation of trichloroacetic acid in, 20: 14582 (SGAE-CH-25/1965)

CHROMATES
radiolysis of, yields of molecular hydrogen from gamma, 20: 14589

CHROMATOGRAPHY
analysis of irradiated hydrochloric acid–methanol mixtures by, 20: 14581(R) (ORNL-3889, pp 14-16)
use of acetylacetone and 8-quinolinol chelates in gas, 20: 14499

CHROME AZUROL S
use for spectrophotometric determination of thorium, 20: 14485

CHROMITES
radiolysis of, yields of molecular hydrogen from gamma, 20: 14589

CHROMIUM
analysis and determination, 20: 14500
content in red-colored Paleozoic deposits in Northern Tien Shan, 20: 14780(T) (AEC-tr-6579)
determination in automobile paint, activation, 20: 14439(R) (GA-5556)
determination in hair samples in criminal cases, activation, 20: 14439(R) (GA-5556)
determination in MSRE fuel, spectrographic, 20: 14457(R) (ORNL-3889, pp 36-39)
determination in plutonium fluorides and peroxides, review on spectrographic, 20: 14464 (RFP-599)
determination in soils, activation, 20: 14439(R) (GA-5556)
determination in silts in water, activation, 20: 14439(R) (GA-5556)
determination of trace amounts of, in iron, activation, 20: 14471
effects on spectrofluorimetric determination of scandium, 20: 14476
energy level fluorescence yields from, K, (E), 20: 15242 (CONF-233 (Vol.3), pp 465-79)
energy level transitions in, Coster-Kronig, (T), 20: 15238 (CONF-233 (Vol.3), pp 398-418)
energy level widths for, K, (T), 20: 15239 (CONF-233(Vol.3), pp 419-39)
neutron elastic scattering at 0.8 Mev, cross sections for, (T), 20: 15770

CHROMIUM ALLOYS
Cr–Fe–Mo, strain aging of, 20: 15063 (UCRL-16585)
Cr–Fe–Zr, corrosion by steam at 300 to 500°C, effects of nitrogen

impurity content on, 20: 14980(R) (GEAP-5065)
Cr–Fe–Zr, corrosion by steam at 500°C, effects of metallurgical processing variables on, 20: 14980(R) (GEAP-5065)
Cr–Nb–Ti, phase diagrams, 20: 15078
Cr–Re, precipitation of Cr_2N at grain boundaries in nitrogen-doped, 20: 14957(R) (BMI-1754)
CHROMIUM ARSENIDES
magnetic properties of, spin structures in, (E), 20: 15954
CHROMIUM BORIDES
abrasive properties, 20: 15109
CHROMIUM CARBIDES
abrasive properties, 20: 15109
reactions with basalt, copper matte, slags, and molten salts, 20: 14989
CHROMIUM CARBONYLS
decomposition in ion source of mass spectrometer, mechanism of, 20: 14584(R) (TID-22444)
CHROMIUM ISOTOPES Cr-50
deuteron reactions (d,n) at 2 to 12 Mev, cross sections for, (E), 20: 15808
CHROMIUM ISOTOPES Cr-51
decay of, K/L ratio for electron-capture, (E/T), 20: 15713 (CONF-233 (Vol.2), pp 365-8)
decay of, x-ray emission rates for electron-capture, (E), 20: 15242 (CONF-233(Vol.3), pp 465-79)
radioactivity of, absolute measurement of, 20: 15690 (CEA-R-2813)
CHROMIUM ISOTOPES Cr-52
deuteron reactions (d,2n) at 2 to 12 Mev, cross sections for, (E), 20: 15808
CHROMIUM OXIDES
Cr_2O_3–Nb_2O_5, density and surface ductility of fused, at 1200 to 1650°C, 20: 15076
Cr_2O_3–V_2O_5, density and surface ductility of fused, at 1200 to 1650°C, 20: 15076
CHROMIUM STEEL
Cr–Mo, corrosion by sodium at 700°F, 20: 14979 (GEAP-4835)
CHROMIUM SYSTEMS
Al–C–Cr–Nb, phase studies, 20: 15103
Al–C–Cr–Ta, phase studies, 20: 15103
C–Cr–Mo, phase studies, 20: 15111
C–Cr–Nb, phase studies, 20: 15108
C–Cr–Ta, phase studies, 20: 15108
CHROMOSOMES
aberrations induced by diethyl sulfate and radiation in barley, 20: 14384
analysis of, uses of Maniac III for Karyotyping, 20: 14950(R) (COO-614-41)
effects of trisomy in number 21, leukemogenic, 20: 14346
haploidy of coconut palm, 20: 14320
labeling with calcium-45 and tritium, 20: 14243(R) (TID-22626)
radiation effects on ploidy in coconut palm, 20: 14320
radioinduced aberrations in mouse sperm, effects of streptomycin on, 20: 14404
CIRCUITS
design of solution output processor for network analysis tapes, engineering drawings for, 20: 14834
development of integrated, for digital-computer uses, 20: 14950(R) (COO-614-41)
performance reliability of, computer program for analyzing, 20: 14824 (SC-TM-65-523)
radiation effects on, instrumentation for analyzing, 20: 14918(R) (ECOM-01313-1)
response of analog, to transistorized common-base amplifiers, 20: 14822(R) (RHEL/R-112, pp 99-128)
CITRIC ACID
acetate of tributyl ester of, method for determination of, in explosives, 20: 14470 (UCRL-7873)
CLANEX PROCESS
use with Tramex process for separation of americium and curium isotopes, 20: 14639 (ORNL-P-1968)
CLAYS
sorptive properties for cesium and strontium, effects of aluminum oxide and iron oxide on, 20: 14652
CLOUD CHAMBERS
performance for absolute activity measurements, 20: 14896
COAL
density determinations for, gamma-scattering-meter errors in, 20: 14837
performance as fuel for gas turbines, 20: 14671(R) (TID-22394)
COATINGS
fabrication of boron-free radiation-resistant vitreous, 20: 15131(P)
testing fuel element, microradiographic method for, 20: 14704
testing of fuel-element, automatic device for ultrasonic, 20: 14715
COAXIAL CABLES
pulse transmission in, 20: 14822(R) (RHEL/R-112, pp 99-128)
COBALT
analysis and determination, 20: 14500
content in red-colored Paleozoic deposits in Northern Tien Shan, 20: 14780(T) (AEC-tr-6579)
determination in aluminum–cobalt wires, comparison of activation and spectrophotometric, 20: 14433(R) (BAW-298)
determination in ferromagnetic films, activation, 20: 14489
determination in oil samples in water, activation, 20: 14439(R) (GA-5556)
determination in soils, activation, 20: 14439(R) (GA-5556)
determination in uranium tetrafluoride, spectrographic, 20: 14473
determination of trace amounts of, in iron, activation, 20: 14471
energy level transitions in, Coster-Kronig, (T), 20: 15238 (CONF-233 (Vol.3), pp 398-418)
energy level widths for, K, (T), 20: 15239 (CONF-233(Vol.3), pp 419-39)
machining of, particle size distribution from, 20: 15015
neutron capture by, gamma spectra from thermal, (E), 20: 15787
neutron resonance absorption integrals for, (E), 20: 15691 (CEA-R-2840)
spectra of, effects of magnesium on radiation emission, 20: 14444(R) (MLM-1268)
use for neutron flux measurement, 20: 14867
COBALT ALLOYS
Al–Co, analysis for cobalt in wire of, comparison of activation and spectrophotometric, 20: 14433(R) (BAW-298)
Al–Co, use for neutron flux measurements, 20: 14867
Ce–Co, cobalt ion EPR in intermetallic compounds of, 20: 15963
Ce–Co–Pu, solvent properties for niobium at 500 to 900°C, 20: 15043 (LA-3436)
Co–Er, cobalt ion EPR in intermetallic compounds of, 20: 15963
Co–Nd, cobalt ion EPR in intermetallic compounds of, 20: 15963
Co–Pr, cobalt ion EPR in intermetallic compounds of, 20: 15963
Co–rare earth, cobalt ion EPR in intermetallic compounds of, 20: 15963
Co–Sc, cobalt ion EPR in intermetallic compounds of, 20: 15963
Co–Tm, cobalt ion EPR in intermetallic compounds of, 20: 15963
Co–U, cobalt ion EPR in intermetallic compounds of, 20: 15963
Co–Y, cobalt ion EPR in intermetallic compounds of, 20: 15963
Co–Zr, cobalt ion EPR in intermetallic compounds of, 20: 15963
Co–Zr, phase studies, 20: 14533
COBALT CARBONYLS
decomposition in ion source of mass spectrometer, mechanism of, 20: 14584(R) (TID-22444)
COBALT COMPLEXES
neutron reactions (n,γ) with, cobalt-60 recoils in, 20: 14584(R) (TID-22444)
COBALT IONS
electron paramagnetic resonance in cobalt–rare earth, cobalt–scandium and cobalt–yttrium intermetallic compounds, 20: 15963
spectra in systems of molten fluorides of lithium, potassium, and sodium, absorption, 20: 14453(R) (ORNL-3889, pp 12-14)
COBALT ISOTOPES Co-57
decay of, K/L ratio for electron-capture, (E/T), 20: 15713 (CONF-233 (Vol.2), pp 365-8)
COBALT ISOTOPES Co-58
decay of, K/L ratio for electron-capture, (E/T), 20: 15713 (CONF-233 (Vol.2), pp 365-8)
uptake of, whole-body counter for measuring, 20: 14422
COBALT ISOTOPES Co-59
neutron reactions (n,γ) in cobalt complexes, effects of cobalt-60 recoil atoms in, 20: 14584(R) (TID-22444)
neutron reactions (n,He-3) at 14.8 Mev, effective cross sections for, (E), 20: 15739
proton reactions (p,n) at 30 to 50 Mev, distributions from, 20: 15729(R) (RHEL/R-112, pp 37-66)
proton total cross sections at 30 and 50 Mev, (E), 20: 15729(R) (RHEL/R-112, pp 37-66)
COBALT ISOTOPES Co-60
calibration by comparison with weak radium standard, 20: 14927
effects on bladder tumors, vesico-ureteral reflux from, 20: 14411
separation from manganese-54 by ion exchange, 20: 14433(R) (BAW-298)
use as radiographic source, advantages of, 20: 14705
use in internal therapy, survey of techniques for, 20: 14406
use in thermal radiation sources, 20: 14945 (CONF-660305-14)
COBALT NITRATES
hexammine complexes of, effects of neutron reactions (n,γ) on, 20: 14584(R) (TID-22444)
COBALT SYSTEMS
Al–C–Co–Nb, phase studies, 20: 15103
Al–C–Co–Ta, phase studies, 20: 15103
B–Cd–Co, crystal structure, 20: 14532
B–Co–Ag, crystal structure, 20: 14532
B–Co–Nb, phase studies, 20: 15100
B–Co–Pb, crystal structure, 20: 14532
B–Co–U, crystal structure, 20: 14532
B–Co–Y, crystal structure, 20: 14532
B–Co–Zr, phase studies, 20: 14533

C–Co–Nb, phase studies, 20: 15077
Co–WC, machining of, particle size distribution from, 20: 15015
Sb–B–Co, crystal structure, 20: 14532
COINCIDENCE CIRCUITS
design and performance of multiple, using avalanche transistors, 20: 14880
COINCIDENCE COUNTERS
design and performance for low-level activity, 20: 14885
design and testing of anticoincidence gamma, 20: 14865
COLLAGEN
radioinduced dissolution of, x, 20: 14593
COLLOIDS
preparation of gold-198, 20: 14627 (PAEC(D)IS-651)
radioinduced dissolution of collagen, x, 20: 14593
COMPRESSORS
testing gas-lubricated turbocompressors, 20: 14671(R) (TID-22394)
COMPTON EFFECT
measurement of internal, at small angles, 20: 15815
COMPUTER PROGRAMS
APT, subroutines for machine tool design, 20: 16154 (Y-1420(Rev.1))
ARØL, for blood cell volume distribution calculations, 20: 14232 (LA-3440)
CDC-1604-A, for analysis of alloys, 20: 14457(R) (ORNL-3889, pp 36-9)
CELVØL, for blood cell volume distribution, 20: 14232 (LA-3440)
CHRONOGRM, for analysis of chronopotentiograms, 20: 14452(R) (ORNL-3889, pp 1-12)
development for calculation of reactions of high-energy neutrons and protons in standard-man phantoms, 20: 14330
development for calculating correlation coefficients, 20: 14461(R) (ORNL-3889, pp 48-70)
development for calculating neutron flux, 20: 14661(R) (ORNL-3889 (pp 48-70)
development for gamma spectra in activation analyses, 20: 14461(R) (ORNL-3889, pp 48-70)
DYNAMIKA REAKTORU, for reactor accident dynamics, ALGOL, 20: 16026 (UJV-1459/65)
FETMOC, for shielding, FORTRAN, 20: 15937
FILTER, for flying-spot analysis of particle tracks in photographs, 20: 14849 (BNL-9720)
for calculation of gamma spectra of uranium-235 fission products, 20: 14733 (AD-628982)
for calculation of group-averaged neutron cross sections, FORTRAN for IBM 7030, 20: 15665 (AWRE-O-103/65)
for checker-playing in IPL-V for IPL-VC, 20: 14949 (ANL-7109)
for determining neutron-neutron scattering length, 20: 15511
for electric circuit reliability analysis, 20: 14824 (SC-TM-65-523)
for fuel depletion and heavy-isotope buildup, descriptions of, 20: 14438 (CEND-540)
for magnetic fields from even Ioffe bars, ALGOL, 20: 15878 (IPP-6/42)
for maintenance of nuclear data files, 20: 15995 (BNL-966)
for radiation doses in space vehicles, 20: 15930 (NP-15697(Vol.2))
for simulating Vela satellite system for nuclear-explosion detection, FORTRAN for CDC 1604, 20: 15599
for stability analysis of relativistic bunched charged-particle beams, (T), 20: 15171 (SLAC-49, pp 49-51)
for well logging borehole and formation parameters, 20: 14775
LIMIT, for activation analysis detection limits, 20: 14661(R) (ORNL-3889, pp 48-70)
NETAREA, for gamma spectra photopeaks, 20: 14661(R) (ORNL-3889 (pp 48-70)
NURLOC, for analysis of coolant-loss accidents in water-cooled high-power reactors, 20: 16019(R) (BMI-X-10154)
POLARGRM, for analysis of polarograms, 20: 14452(R) (ORNL-3889, pp 1-12)
RAD 2, for calculation of fission-product activity distributions in high-temperature gas-cooled reactors, in FORTRAN IV, 20: 16075 (GAMD-6519)
RESTORE, for re-entry trajectories, FORTRAN, 20: 16113 (SC-RR-66-22)
RHOLOG, for rock density of uranium deposits, FORTRAN, 20: 14778
SHREW, for neutron scattering by spinless targets, FORTRAN, 20: 15670 (WAPD-TM-524)
subroutines for, error-function and gamma-function library, in FORTRAN IV, 20: 14950(R) (COO-614-41)
TENSOR, for numerical simulation of seismic disturbances, 20: 14755 (UCRL-7929)
TIJ, one-group neutron collision probabilities in cylinders and slabs, 20: 15668 (EUR-2624.e)
TTA, for re-entry trajectories, for CDC 3600, 20: 16113 (SC-RR-66-22)
COMPUTERS
engineering and operations of Maniac III, 20: 14950(R) (COO-614-41)
integer programming problems in, decomposition of, 20: 14950(R) (COO-614-41)
use of PDP-4, in measurement of particle tracks in bubble chambers, 20: 14861 (UCRL-16555)
uses with flying-spot digitizers for analysis of bubble-chamber photographs, 20: 14850 (BNL-9963)
CONCRETES
gamma streaming through ducts in, analysis using Monte Carlo method, 20: 15929 (AD-627890)
properties of, effects of temperature on, 20: 15051 (NP-15876)
CONDUCTOMETRIC ANALYSIS
instrument for, design of electrodeless toroidal, 20: 14465 (RFP-657)
CONFERENCES
see also introduction to Report Number Index
Atomic Electrons in Nuclear Transformations, Role of, Vol. 3, Warsaw, Poland, Sept. 1963, 20: 15236 (CONF-233(Vol.3))
Atomic Electrons in Nuclear Transformations, Role of, Vol. 2, Warsaw, Poland, Sept. 1963, 20: 15697 (CONF-233(Vol.2))
Radiation and Terrestrial Ecosystems, Richland, Washington, May 3 to 5, 1965, summary of, 20: 14237
Radiological Monitoring of the Environment, Berkeley, Gloucestershire, Oct. 1963, 20: 14810
Resonant Particles, Proceedings of the Second Topical Conference, Athens, Ohio, June 10–12, 1965, 20: 15398
CONNECTORS (ELECTRIC)
design of contact assembly for, 20: 14842(P)
CONSTITUTION DIAGRAMS
determination of, design of automatic recording low-temperature dilatometer for, 20: 14821 (RFP-668)
CONTAMINATION
pathways of food, 20: 14748
threshold-limit values for, of atmosphere, 20: 14805
COPPER
analysis and determination, 20: 14500
content in red-colored Paleozoic deposits in Northern Tien Shan, 20: 14780(T) (AEC-tr-6579)
determination in automobile paint, activation, 20: 14439(R) (GA-5556)
determination in commercial plastics, activation, 20: 14439(R) (GA-5556)
determination in gunpowder residues on hands, activation, 20: 14439(R) (GA-5556)
determination in iron-containing ores, x-ray fluorescence, 20: 14487
determination in iron–niobium alloys, chromatographic, 20: 14455(R) (ORNL-3889, pp 25-32)
determination in oils and silts in water, activation, 20: 14439(R) (GA-5556)
determination in plutonium fluorides and peroxides, review on spectrographic, 20: 14464 (RFP-599)
determination in paper samples in criminal cases, activation, 20: 14439(R) (GA-5556)
determination in rice whiskey, activation, 20: 14439(R) (GA-5556)
determination in solutions by atomic absorption, 20: 14457(R) (ORNL-3889, pp 36-39)
determination in thumbnail clippings, activation, 20: 14439(R) (GA-5556)
determination in uranium tetrafluoride, spectrographic, 20: 14473
determination in wood in criminal cases, activation, 20: 14439(R) (GA-5556)
determination of trace amounts of, in iron, activation, 20: 14471
effects on spectrofluorimetric determination of scandium, 20: 14476
electron showers in, energy-loss distributions in, (E), 20: 15439
energy level fluorescence yields from, K, (E), 20: 15242 (CONF-233 (Vol.3), pp 465-79)
energy level transitions in, Coster-Kronig, (T), 20: 15238 (CONF-233 (Vol.3), pp 398-418)
energy level widths for, K, (T), 20: 15239 (CONF-233(Vol.3), pp 419-39)
heat transfer to liquid hydrogen, film boiling in, 20: 14697
ion reactions at 60, 80, and 90 kev, electron energy spectra from argon and neon, (E), 20: 15261
meson (π^-) reactions (π^-,γ), energy spectra and yields from, (E), 20: 15794
neutron elastic scattering at 0.8 Mev, cross sections for, (T), 20: 15770
neutron resonance absorption integrals for, (E), 20: 15691 (CEA-R-2840)
plasma production by hypervelocity jets of, 20: 15920
proton reactions (p,n) at 30 to 50 Mev, distributions from, 20: 15729(R) (RHEL/R-112, pp 37-66)
proton total cross sections at 30 and 50 Mev, (E), 20: 15729(R) (RHEL/R-112, pp 37-66)
radiation effects on wear resistance of, fast-neutron, 20: 15140
radioinduced defects in foils of, ion, 20: 15146
separation from radioactive contaminants in mining by nuclear explosives, 20: 14662(R) (ORNL-TM-1394)
use of interlayer foil of, in metal-clad reactor fuel elements, 20: 16056(P)
wetting properties for uranium monocarbide, 20: 14551
COPPER ALLOYS
Cu–Pb–Zn, radiation effects on wear resistance of lead bronze, fast-neutron, 20: 15140
COPPER BROMIDES

effects on radioinduced isomerization of α-phenylcinnamic acid, 20: 14596
COPPER ISOTOPES Cu-65
proton reactions (p,n) at 2.3 to 11.0 Mev, excitation of isobaric analog states in, (E), 20: 15804
COPPER MINERALS
mining with nuclear explosives, behavior and removal of radioactive products in, 20: 14662(R) (ORNL-TM-1394)
radioinduced isotopes in, behavior of, 20: 14662(R) (ORNL-TM-1394)
reconnaissance of, in Chile, 20: 14779 (RME-4569(Rev.))
COPPER SYSTEMS
Al–C–Cu–Nb, phase studies, 20: 15103
Al–C–Cu–Ta, phase studies, 20: 15103
B–Cu–Mn, crystal structure, 20: 14532
B–Cu–Mo, crystal structure, 20: 14532
B–Cu–Nb, crystal structure, 20: 14532
B–Cu–Zr, crystal structure, 20: 14532
CORROSION
conference on stress corrosion, delayed failures, and fatigue corrosion, 20: 14998
CORTICOSTEROIDS
effects of Decortilen on mitosis in HeLa cells in culture, 20: 14375
radiation effects on dog plasma levels of, x, 20: 14280
CORTICOSTERONES
radioinduced decomposition of tritiated, effects of molecular structure on, 20: 14578 (EUR-2435.f)
CORTISONE
effects on content of glycoprotein in blood serum of x-irradiated rats, 20: 14378
radioinduced decomposition of tritiated, effects of molecular structure on, 20: 14578 (EUR-2435.f)
COSMIC MESONS (μ)
flux intensity under sea water, energy range relation from, (E), 20: 15289
COSMIC NEUTRONS
detection of, time distributions of, (E), 20: 15233
flux intensity of, hourly counting rate from Jan.–March, 1965, 20: 15277
flux intensity of, hourly counting rate from Jan.–March, 1965, 20: 15278
flux intensity of, for April to June, 1964, 20: 15279
flux intensity of, for April to June, 1964, 20: 15280
flux intensity of, hourly counting rate from April–June, 1965, 20: 15281
flux intensity of, hourly counting rate from April–June, 1965, 20: 15282
flux intensity of, hourly counting rate from Jan.–Sept., 1964 for, 20: 15283
flux intensity of, hourly counting rate from July–Sept., 1964, 20: 15284
intensity of, hourly counting rate for, 20: 15285
intensity of, hourly counting rate for, 20: 15286
COSMIC NUCLEONS
interactions of primary, momentum spectra of long-lived heavy triplets from, (T), 20: 15287
COSMIC PHOTONS
flux of, upper limits for, (E), 20: 15291
interactions with photons at energies $\gtrsim 10^{14}$ ev, (T), 20: 15226
COSMIC RADIATION
absorption of h-f noise, effects of ionization from nuclear explosions on, (T), 20: 15607
determination in atmospheric and precipitation samples, methods for radiochemical, 20: 14430 (AD-620219)
dosimetry of, for crew and passengers during supersonic flight, 20: 14797
effects on glasses, bibliography on, 20: 15134 (N65-15819)
hydromagnetic wave propagation in interstellar, equations for, (T), 20: 15198
momentum spectra of long-lived heavy triplets from primary, (T), 20: 15287
COSMIC-RAY SPECTROMETERS
design calculations for ionization, 20: 14892
COSMIC SHOWERS
electromagnetic radiation from, (T), 20: 15288
particle angular distributions in emulsions, 20: 15290
production by cosmic photons at energies $\gtrsim 10^{14}$ ev, (T), 20: 15226
COSMOLOGY
black-body radiation in evolutionary, effects on galactic formation, (T), 20: 15204
gravitational collapse of uniform spheroid in, (T), 20: 15206
model for magnitudes of radio galaxies in, red shift for static, (T), 20: 15224
photons in, opacity of universe to high-energy, (T), 20: 15226
quark production and conservation in galactic evolution, 20: 15435
universe in, orbits in magnetic, 20: 15634
COTTON
radiosterilization of, electron, 20: 14941
COULOMETERS
circuitry for controlled-potential, differentiating, 20: 14452(R) (ORNL-3889, pp 1-12)
COULOMETRY
development of controlled-potential, for microanalysis, 20: 14452(R) (ORNL-3889, pp 1-12)
COUNTING DEVICES
use in activation analysis in scientific crime detection, 20: 14439(R) (GA-5556)
CREEP
properties of refractory metals, numerical methods for analysis of, 20: 15041 (GEMP-397)
CRITICAL ASSEMBLIES
design and operation of, review, 20: 16123 (KFK-350)
fuel element fabrication for ZPPR, 20: 16060(R) (ANL-7152, pp 1-49)
reactivity calculations for ZPR-III assembly 47, 20: 16060(R) (ANL-7152, pp 1-49)
reactivity measurements in FR0, 20: 16118 (AE-212)
reactivity worth calculations for ZPR-VI assembly 42, 20: 16060(R) (ANL-7152, pp 1-49)
reactivity worth calculations for ZPR-IX assemblies 8 and 9, 20: 16060(R) (ANL-7152, pp 1-49)
CRITICALITY STUDIES
administration of out-of-pile criticality controls at Hanford Plant, 20: 14790 (RL-SA-43A)
of interacting arrays of spheres, model for, (T), 20: 16034
CRUSTACEA
distribution in deep scattering layers of Santa Barbara Channel, Calif., 20: 14235 (SAN-584-1)
CRYOGENICS
equipment for thermal expansion measurements at 300 to 94°K, 20: 15660
CRYOSTATS
design for use with lithium-drifted germanium detectors, 20: 14845 (AD-620434)
CRYSTAL STRUCTURE
lattice parameter determination by x-ray back-reflection, method for, 20: 15660
CRYSTALLOGRAPHY
cameras for, design of precision back-reflection Laue, 20: 14820 (RFP-636)
CRYSTALS
electron diffraction in, relativistic dynamic theory with inelastic scattering for, 20: 15959
electron inelastic scattering at high energies, (T), 20: 15956
gamma scattering on single, phonon properties from Mössbauer effect in, 20: 15948
molecular oscillations in fcc, rotational tetrahedral, 20: 15940 (JUL-292-RW)
neutron scattering by single, coherent extinction and second order, 20: 15671
nuclear polarization by electron-nucleus dipolar coupling, (T), 20: 15819
scintillation intensity in organic, time dependence of, (T), 20: 14615
CULTURE MEDIA
radiosensitivity effects on bacteria, 20: 14388
serum content in Chinese hamster cell, radiosensitivity effects of, 20: 14400
CURIUM
separation from acetate and 2-hydroxyisobutyric acid solutions by solvent extraction using thenoyltrifluoroacetone, 20: 14654
separation from contaminants by solvent extraction using bis(2-ethylhexyl) phosphate, 20: 14457(R) (ORNL-3889, pp 36-39)
separation from rare earth fission products, 20: 14659(P)
separation in microquantities, method for, 20: 14509 (NP-15826)
CURIUM ISOTOPES Cm-242
content in spent power reactor fuels, evaluation of, 20: 14435 (BNWL-SA-503)
preparation by neutron irradiation of americium-241, 20: 14631
preparation neutron irradiation of americium-242, 20: 14631
separation from fission product solutions by Clanex-Tramex process, 20: 14639 (ORNL-P-1968)
CURIUM ISOTOPES Cm-244
content in spent power reactor fuels, evaluation of, 20: 14435 (BNWL-SA-503)
production in U. S. power reactors, estimates for future, 20: 14946 (DP-1015)
separation from americium-243 in fission product solutions by Clanex-Tramex process, 20: 14639 (ORNL-P-1968)
separation from irradiated fuel elements, chemical process for, 20: 14636 (CONF-660305-7)
CURIUM OXIDES
properties for use as heat sources, facility for studying, 20: 15038 (CONF-660305-12)
purification by separation and calcination, 20: 14636 (CONF-660305-7)
CURIUM PHOSPHATES
determination by x-ray diagram, 20: 14509 (NP-15826)
preparation and structure of, 20: 14509 (NP-15826)

CURRENT INTEGRATORS
development of, for use with calorimeters, 20: 14444(R) (MLM-1268)
CUTTING TOOLS
effects of thermoelectric cooling on life of carbide, during uranium machining, 20: 14689(R) (NLCO-970, pp 5.1-7)
CYANAMIDES
effects on synthesis of dipeptides, under primitive earth conditions, 20: 14233 (UCRL-16566)
CYANIDES
halide, formation of multiply charged ions in decomposition of, in ion source, 20: 14584(R) (TID-22444)
CYANOGEN IODIDES
decomposition in ion source of mass spectrometer, formation of multiply charged ions in, 20: 14584(R) (TID-22444)
CYANURIC ACID
determination in mock explosive, method for, 20: 14470 (UCRL-7873)
1,3-CYCLOHEXADIENE
radiolysis of, G-values of products from gamma, 20: 14610
1,4-CYCLOHEXADIENE
radiolysis of, G-values of products from gamma, 20: 14610
CYCLOHEXANE
radioinduced oxidation of, effects of oxygen pressure and temperature on gamma, 20: 14625
reactions with iodine, chromatographic analyses of products from, 20: 14454(R) (ORNL-3889, pp 17-24)
CYCLOHEXANOL
formation in radioinduced oxidation of cyclohexane, 20: 14625
radioinduced pyrolysis of, in water-t_2, electron, 20: 14623
CYCLOHEXANONE
formation in radioinduced oxidation of cyclohexane, 20: 14625
CYCLOHEXANONES
2,6-dioximino-, preparation, 20: 14576(R) (ORNL-3889, pp 73-7)
CYCLOHEXENE
yields from gamma radiolysis of 1,3- and 1,4-cyclohexodienes, 20: 14610
CYCLOPENTADIENYL COMPOUNDS
with nickel, decomposition in ion source of mass spectrometer, 20: 14584(R) (TID-22444)
with transition-metal carbonyls, decomposition in ion source of mass spectrometer, 20: 14584(R) (TID-22444)
CYCLOPENTANE
radiolysis of deuterated, rates of hydrogen transfer in, 20: 14599
CYCLOTRONS
design modification and performance of AVF, for negative hydrogen ion acceleration, 20: 15180
particle rotation frequency in isochronous, effect of radial betatron oscillations on, (T), 20: 15186
voltage regulator for 88-in., design of three-phase, 20: 15183
CYLINDERS
neutron transport in, one-group collision-probability code for, 20: 15668 (EUR-2624.e)
CYSTEIC ACID
neutron reactions with sulfur in, recoil atom retention in products from, 20: 14584(R) (TID-22444)
CYSTEINE
neutron reactions with sulfur in, recoil atom retention in products from, 20: 14584(R) (TID-22444)
CYSTINE
lability of, in lipid-protein reaction systems, 20: 14587
neutron reactions with sulfur in, recoil atom retention in products from, 20: 14584(R) (TID-22444)
CYTIDINE, 5-BROMO-2'-DEOXY-
radiosensitivity effects on bone marrow cells, fast-neutron and x, 20: 14333
CYTOLOGY
radiation effects on fetal rat cell, x, 20: 14262
radiation effects on animal cells in culture, 20: 14385
radiation effects on intestinal mucosa, x, 20: 14339
CYTOPLASM
radiation effects on chick muscle, effects of dose on x, 20: 14321
CZECHOSLOVAKIA
fallout monitoring in, 20: 14813

D

DATA RECORDING SYSTEMS
design for spectrophotometer, engineering drawings for, 20: 14901
design for stationary-field teletherapy, 20: 14408
design of automatic, for use with foil detectors, 20: 14846 (AECL-2517)
development for radiobiological studies, 20: 14238 (CONF-650560-13)
output processor for network analysis tapes, engineering drawings for solution, 20: 14834
DATA TABULATIONS
Auger spectra and Coster-Kronig transitions of heavy elements, 20: 15240 (CONF-233(Vol.3), pp 440-53)
binomial sampling tables, 20: 16150 (ORNL-2909)
cosmic neutron flux-intensity from April to June, 1964, 20: 15279
cosmic neutron flux-intensity from April to June, 1964, 20: 15280
cosmic neutron flux intensity hourly counting rate, April–June, 1965, 20: 15281
cosmic neutron intensity counting rate, 20: 15285
cosmic neutron intensity counting rate, 20: 15286
cosmic-neutron flux-intensity hourly counting rate, Jan.–March, 1965, 20: 15277
cosmic-neutron flux-intensity hourly counting rate, Jan.–March, 1965, 20: 15278
cosmic-neutron flux intensity hourly counting rate, April–June, 1965, 20: 15282
cosmic-neutron flux-intensity hourly counting rate, Jan.–Sept., 1964, 20: 15283
cosmic-neutron flux-intensity hourly counting rate, July–Sept., 1964, 20: 15284
criticality parameters of water-reflected fissile materials, 20: 16031
neutron flux-shape eigenfunctions for two-zone slabs, 20: 16024 (RFR-231)
neutron flux-shape eigenfunctions for two-zone cylinders, 20: 16025 (RFR-232)
reactor physics facilities, burst, critical, and subcritical, 20: 16123 (KFK-350)
thermodynamic properties of binary alloys, 20: 14514 (UCRL-11821)
DECANOIC ACID
determination in commercial coconut oils, gas chromatographic, 20: 14463 (PAEC(D)CH-652)
DEHYDROGENASES
radiation effects on activity of, in rat liver homogenates and mitochondria, γ, 20: 14284
DENSITOMETERS
design and performance of gamma-scattering, 20: 14837
development of radiometric, for atmosphere at 100 to 200 km, 20: 15588 (AD-620682)
use of radioisotope, review of industrial, 20: 14835
DETERGENTS
analysis for constituents, methods for, 20: 14455(R) (ORNL-3889, pp 25-32)
DETONATION WAVES
pressure profiles of, use of hydrodynamic machine calculations for, (T), 20: 15571 (UCRL-14531)
DEUTERIUM
abundance in stars, upper limits for, (T), 20: 15197
concentration by high-pressure exchange between hydrogen and liquid ammonia, 20: 14519
deuteron reactions (d,n) with deuterium at 57.3 to 116.8 kev, neutron polarization in, (E), 20: 15735(T) (ANL-Trans-265)
effects on ESR spectra irradiated dimethylglyoxime single crystals at 77°K, 20: 14598
effects on mechanism of electrophilic aromatic substitution, 20: 14577
effects on radioinduced ESR spectra of iodoethane, 20: 14597
electron paramagnetic resonance of atomic, in x-irradiated beryl crystals, 20: 15982(T)
exchange with hydrogen in methane, catalytic effects of palladium alloys on, 20: 14542
leak control of gaseous, development of membrane for vacuum, 20: 14730 (AWRE-O-10/66)
origin for terrestrial, noncosmic, (E), 20: 15197
polarization, (E), 20: 15262
production of, review of methods for, 20: 14948
proton reactions (p,n) at 30 to 50 Mev, distributions from, 20: 15729(R) (RHEL/R-112, pp 37-66)
reactions with hydrogen, angular distributions from atom-molecule, (T), 20: 15252
reactions with hydrogen atoms, excitation-transfer cross sections for, (T), 20: 15255
DEUTERIUM COMPOUNDS
production of, review of methods for, 20: 14948
DEUTERIUM HYDRIDES
polarization, (E), 20: 15262
DEUTERIUM IONS
vibrations in alkaline earth fluoride crystals, spectra of localized, 20: 15969
DEUTERON BEAMS
acceleration in linacs, 20: 15165(R) (RHEL/R-112, pp 12-22)
DEUTERONS
binding energy and quadrupole moment of, Eriksson theory for, 20: 15323
detection in products from nuclear reactions, engineering drawings of apparatus for, 20: 14906
form factors, (E), 20: 15306(R) (CEAL-1026)
form factors of, determination using electron scattering, 20: 15439

interactions at high energy, cross sections and amplitudes for, (T), 20: 15361
interactions with mesons (π^-) at 3.2 Bev/c, resonance production in, (E), 20: 15405
interactions with mesons (π^-) at 3.7 Bev/c, resonances in, 20: 15409
interactions with electrons, determination of nucleon form factors by, 20: 15440
interactions with mesons (π^-), neutron-neutron S-wave scattering length from, (E), 20: 15511
interactions with neutrons, Faddeev equations for, (T), 20: 15343
interactions with electrons, relativistic corrections to impulse approximation in elastic, (T), 20: 15348
interactions with antiprotons at 0.13 to 17.1 Bev, cross sections and amplitudes for, (T), 20: 15361
interactions with neutrons, Padé approximant for S-matrix for inelastic, 20: 15363
interactions with nucleons, amplitude for inelastic, (T), 20: 15386
interactions with mesons (K^-) at 670 to 770 Mev/c, Y_1^* (1660) production in, 20: 15397
interactions with gamma rays at 2.504 to 54.0 Mev, disintegration cross sections for, (T), 20: 15789
interactions with protons at 30 Mev, distributions from, (E), 20: 15728(R) (RHEL/R-112, pp 23-36)
magnetic resonance in polycrystalline glycine and glycine compounds, quadrupole coupling constants from, (E), 20: 15957
reactions (d,α) with zirconium-92 at 12.0 Mev, yttrium-90 levels from, (E), 20: 15799
reactions (d,n) with deuterium at 57.3 to 116.8 kev, neutron polarization in, (E), 20: 15735(T) (ANL-Trans-265)
reactions (d,n) with boron-11 at 1 to 11 Mev, (E), 20: 15858
reactions (d,n) with chromium-50 at 2 to 12 Mev, cross sections for, (E), 20: 15808
reactions (d,p) with boron-11 at 0.7 to 1.7 Mev, angular distribution from, (E), 20: 15847
reactions (d,p) with nuclei, models for, 20: 15730(R) (RHEL/R-112, pp 67-98)
reactions (d,p) with yttrium-89 at 11.95 Mev, yttrium-90 levels from, (E), 20: 15799
reactions (d,2n) and (d,p) with cesium-133, isomeric cross-section ratios in, (E), 20: 15778
reactions (d,2n) with chromium-52 at 2 to 12 Mev, cross sections for, (E), 20: 15808
reactions with nitrogen, electron-capture cross sections for, (E/T), 20: 15886(R) (UCRL-14285)
reactions with nuclei at 15 Mev, isomer production in, (E), 20: 15856
reactions with thorium 232, fission fragment mass and energy distributions from, (E), 20: 15840
scattering by nuclei at 15 Mev, elastic and inelastic, (E/T), 20: 15850

DIATOMACEOUS EARTH
sorptive properties for radioactive wastes, effects of flocculants on, 20: 16138

DIELECTRICS
charged particle motion in, radiation emission in, 20: 15558
dispersion forces between plates of, classical treatment for, (T), 20: 15152
electromagnetic field distributions in, near charged-particle beams, (T), 20: 15172 (SLAC-49, pp 52-8)
neutron detection and measurement by track imaging in, 20: 14854 (CONF-660304-3)

DIET
effects on content of cesium-137 and strontium-90 in urine, 20: 14243(R) (TID-22626)
strontium content in rat, effects on strontium-90 metabolism of, 20: 14251

DIETHYLAMINE, 2,2'-DICHLORO-N-METHYL-
hydrochloride, effects on urinary excretion of ammonia and phosphates in rats, 20: 14270

DIFFERENTIAL EQUATIONS
hypergeometric function of two-variables in perturbation theory, 20: 14952

DIFFUSION PUMPS
trap for, engineering drawings of cold, 20: 14674
traps for, in ALICE, engineering drawings of, 20: 15924

DILATOMETERS
design of automatic recording low-temperature, for phase diagram determinations, 20: 14821 (RFP-668)

DIPICOLINIC ACID
radiation effects on *B. cereus* content of, x, 20: 14263

DIRECT ENERGY CONVERSION DEVICES
theory of MHD squeeze film, 20: 15304

DISEASES
radiation effects on *Lupus erythematosus*, uv, 20: 14309
radioinduced atrial fibrillation, following thyrotoxicosis therapy, β, 20: 14424
radioinduced canine nephritis, effects on renal concentrating ability of x, 20: 14342

DISULFIDES
radiosensitivity effects in mammalian cells, effects of content on, 20: 14351

DODEWAARD POWER REACTOR
design, 20: 16094

DOGS
effects of exercise and inhaled yttrium oxide on blood and lungs of, 20: 14257
iodine metabolism in, tracer study, 20: 14249
radiation effects on adrenal cortex in, x, 20: 14280
radiation effects on kidney function in, x, 20: 14342
radiation effects on artificial grafts in, x, 20: 14344
radiation effects on arterial prostheses in, x, 20: 14345
radiation effects on cardiac function in, methods for measuring, 20: 14292(R) (TID-22563)
radioisotope metabolism in, automatic processing of data on, 20: 14238 (CONF-650560-13)
strontium-90 metabolism in, effects of age on, 20: 14243(R) (TID-22626)

DOLOMITES
radioactivity of, 20: 14752

DOSIMETERS
description of multiglass personnel, 20: 14907
design and performance of total-absorption thermal x-ray, 20: 14908
design of portable neutron, 20: 14915(P)
development of neutron activation, 20: 14862
performance and properties of photographic and solid-state, 20: 14907
performance of chemical, effects of temperature on, 20: 14581(R) (ORNL-3889, pp 14-16)
performance of film, for gamma exposure, 20: 14806
performance of Fricke and nitrous oxide, 20: 14870
response of lithium fluoride thermoluminescent, to electrons and gamma and x radiation, 20: 14887
response of lithium–fluoride, to electrons and gamma radiation, 20: 14888
shield design for thermoluminescent, 20: 14914(P)

DROSOPHILA
radioinduced dominant lethality in, combined with acceleration, 20: 14343
radioinduced dominant lethality in, combined with vibration, 20: 14343
radioinduced mutations in, effects of serotonin on, 20: 14398

DRUGS
analysis in criminal cases, activation, 20: 14439(R) (GA-5556)
analysis of labeled, 20: 14501
use in treating gynecologic cancer, review, 20: 14413

DUSTS
analysis for bismuth, cadmium, lead, tin, and zinc using Paschev direct reader, 20: 14457(R) (ORNL-3889, pp 36-39)
analysis for long-lived fission products, 20: 14472
analysis of cosmic, for gold, activation, 20: 14475
deposition in respiratory tract, model for, 20: 14796
effects on fallout, 20: 14746

DYSPROSIUM ALLOYS
Dy–Fe, preparation and structure, 20: 15110
Dy–Mn, preparation and structure, 20: 15110
Dy–Y, electric conductivity of dilute, at low temperatures, 20: 15098

DYSPROSIUM IONS
paramagnetic resonance of trivalent, in rare earth ethyl sulfates, 20: 15991

DYSPROSIUM ISOTOPES Dy-160
energy level transitions in, conversion coefficients for E2, (E), 20: 15705 (CONF-233(Vol.2), pp 177-90)
energy level transitions in, conversion coefficients for E2, (E), 20: 15706 (CONF-233(Vol.2), pp 191-7)
internal conversion coefficients of $2^+ \rightarrow 0^+$ transitions in, E2, (E), 20: 15745

DYSPROSIUM ISOTOPES Dy-161
energy level transition probabilities in, pairing correlations in E1, (T), 20: 15766
energy level transitions in, conversion electrons from E1, (E), 20: 15703 (CONF-233(Vol.2), pp 148-57)
energy level transitions in, delayed E-1, (T), 20: 15765

E

EARTH
biogenesis under primitive conditions on, 20: 14233 (UCRL-16566)
deuterium source for, noncosmic, (E), 20: 15197
potassium, thorium, and uranium abundance in, neutrino detection for determinating, (T), 20: 14750

ECOLOGY
radioisotope sources and paths through foodchains, 20: 14237

EGGS

radiation effects on Drosophila, combined with acceleration, 20: 14343
radiation effects on Drosophila, combined with vibration, 20: 14343

EINSTEINIUM
production in heavy-ion nuclear reactions, review of, 20: 15740

ELECTRIC ARCS
plasma production by gas-discharge, 20: 15887(T) (AD-625789)
plasma production in, cylindrically symmetric, 20: 15914
plasma transport properties in, validity conditions for, (T), 20: 15926

ELECTRIC CHARGES
oscillations of dipole, between dielectric plates, (T), 20: 15152

ELECTRIC CONDENSERS
development of capacitor banks, for research in plasma physics, 20: 15882(R) (NP-15868)
radiation effects on, nuclear-explosion, 20: 14921

ELECTRIC DISCHARGE
kinetics of high-frequency resonance, in gases, (T), 20: 15575
plasma wave excitation in r-f, (E), 20: 15912
properties of flash x-ray, electric and x-ray-emission, (E), 20: 15573

ELECTRIC FIELDS
effects on electron energy distribution in homogeneous weakly ionized plasma, (T), 20: 15889(T) (SC-T-65-776)
plasma stability in d-c, (T), 20: 15883 (SU-IPR-31)
properties of crossed magnetic and, for beta and mass spectroscopy, 20: 14882

ELECTRIC INSULATORS
fabrication of boron-free radiation-resistant vitreous, 20: 15131(P)

ELECTRIC PROBES
use in identification of low-Z elements, 20: 14457(R) (ORNL-3889, pp 36-9)
use of spherical resonance, in plasma diagnostics, (E/T), 20: 15868 (AD-628186)

ELECTRODEPOSITION
design considerations for ion, 20: 14670 (SC-R-65-997)

ELECTRODES
development of fueled emitter, for thermionic space power plants, 20: 14962(R) (N65-20803)

ELECTROMAGNETIC FIELDS
distributions in dielectric media near charged-particle beams, (T), 20: 15172 (SLAC-49, pp 52-8)
distributions in toroidal vacuum vessels containing bunched charged-particle beams, (T), 20: 15170 (SLAC-49, pp 36-48)
Einstein-Maxwell equations for dipole, exact solution of, 20: 15155
field theory exuension for null, unified, 20: 15624
interactions with electron-positron field, vacuum polarization in, (T), 20: 15639
propagation by bunched charged-particle beams in straight circular pipes, (T), 20: 15167 (SLAC-49, pp 18-22)
propagation by bunched charged-particle beams in straight circular vacuum chambers, (T), 20: 15169 (SLAC-49, pp 32-5)
propagation by oscillating bunched charged-particle beams in straight rectangular pipes, (T), 20: 15168 (SLAC-49, pp 23-31)

ELECTROMAGNETIC WAVES
diffraction, (T), 20: 15149(T) (JPRS-33458)
emission by moving charged particles at dielectric interfaces, (E), 20: 15317(T) (ORNL-tr-677)
emission from cosmic showers, (T), 20: 15288
propagation in metals, (T), 20: 15941 (NP-15698)
propagation in plasma containing heavy ions, (T), 20: 15910
propagation of h-f pulsed, from nuclear explosions, (T), 20: 15605
propagation of low-frequency ground-wave, from nuclear explosions, (T), 20: 15606

ELECTROMAGNETISM
field theory for, geometrical aspects of unified, 20: 15624
relativity theory for, metrical lattice in, 20: 15633

ELECTROMETERS
design for fallout-shelter monitor, engineering drawings for, 20: 14903

ELECTRON BEAMS
analysis of, electrostatic prism spectrometer for, (T), 20: 14868
deflection and rotation of, apparatus for, 20: 15189(P)
dose distribution from pulsed, on irradiated surfaces, (T), 20: 15178
effects of 1.5-Mev, on n-channel MOS transistors, 20: 14924
effects on bacterial populations in prepacked cotton and plastic medical supplies, 20: 14941
effects on catalytic activity of charcoal, 20: 14609
effects on germanium, apparatus for measurement of dimensional, 20: 15147
effects on normal and tumorous animals, effects of RNA on, 20: 14397
effects on thermoluminescence of lithium fluoride phosphors, 20: 14887
effects on thermoluminescence of lithium–fluoride phosphors, energy dependence of, 20: 14888
electromagnetic wave production by, use of, in determining low-Z elements, 20: 14442(R) (MCW-1493, p. 5-13)
energy measurement in low-energy linear accelerators, mean, 20: 15179
energy monitor for, 20: 15184
interactions with plasma, amplification and instabilities from, (T), 20: 15880 (ML-1292)
interactions with plasma, diagnostic uses of, (E/T), 20: 15884 (SU-IPR-33)
interactions with electron and positron beams, (T), 20: 15443
interactions with positron beams, vector boson production in, (E), 20: 15311 (LNF-65/47)
irradiation with high-energy, method for, 20: 15188(P)
production of high-current small-diameter, device for, 20: 14843(P)
reactions with compounds, x-ray corrections for, 20: 14431 (ANL-7078)
transport in electron-positron storage rings, 20: 15173 (SLAC-49, pp 61-8)

ELECTRON CAPTURE
radioactivity from, absolute measurement of, 20: 15690 (CEA-R-2813)
review, 20: 15695 (CONF-233(Vol.1), pp 30-59)

ELECTRON-DIFFRACTION ANALYSIS
theory for, with inelastic scattering, 20: 15959

ELECTRON MICROSCOPY
development of analytical, 20: 14460(R) (ORNL-3889, pp 46-8)

ELECTRON PAIRS
interactions with external electromagnetic fields, vacuum polarization in, (T), 20: 15639
photoproduction on carbon, testing of quantum electrodynamics by, (E), 20: 15306(R) (CEAL-1026)
production in electron gases, effects on degeneracy from, (T), 20: 15229
production of internal, review, (E/T), 20: 15696 (CONF-233(Vol.1), pp 60-86)

ELECTRON SHOWERS
energy-loss distributions in copper, (E), 20: 15439

ELECTRON TUBES
development of grounded-grid triode for use as valve in proton linac, 20: 15165(R) (RHEL/R-112, pp 12-22)
fabrication of discharge, in gas containing tritium, 20: 14825(T) (CEA-tr-X-356)
radiation effects on, from nuclear-explosion, 20: 14921

ELECTRONIC EQUIPMENT
development for research in plasma physics, 20: 15882(R) (NP-15868)
radiation effects on, instrumentation for analyzing, 20: 14918(R) (ECON-01313-1)
radiation effects on, from nuclear-explosion, 20: 14921

ELECTRONS
acceleration of solar, by nonlinear waves, (T), 20: 15593
capture by nuclei, processes from, 20: 15693 (CONF-233(Vol.1))
capture by nuclei, review of orbital, (E/T), 20: 15695 (CONF-233(Vol.1), pp 30-69)
degeneracy of gases of, at extremely high temperatures, (T), 20: 15229
density and temperature in nonthermal hydrogen plasma, (T), 20: 15875 (IPP-3/32)
density distribution in ionospheric F2 layer, (T), 20: 15586 (AD-620243)
density distribution in ionospheric D region, v-l-f propagation for determining, 20: 15604
density in plasma, determination by spectral line merging, 20: 15881 (MPI-PAE/PL-7/65)
density in θ-pinch plasma, measurement of, (E), 20: 15871 (IPP-1/38)
density irregularities in ionosphere, (E), 20: 15622
detection and measurement in auroral storms and radiation belts, instrumentation for, 20: 15589(R) (ASE-1125)
detection of, semiconductor radiation detector response for, 20: 14444(R) (MLM-1268)
diffraction in crystals, relativistic dynamic theory with inelastic scattering for, 20: 15959
diffusion in metallic slabs at 0.4- to 10-Mev, differential energy spectra and number transmission for, (T), 20: 15936
distributions in thermionic cells, Langmuir-Child analysis of, (T), 20: 15295 (CONF-640921, pp 47-77)
dosimetry of, for space vehicles, (T), 20: 15936
effects on alcohols, amino acids, carboxylic acids, and olefins in tritium-labeled water, 20: 14623
effects on germanium, low-temperature annealing of, 20: 15984(T)
effects on graft copolymerization of polyethylene and polyvinyl chloride films with styrene, 20: 14618
effects on molecules, distribution of ionization energy in, 20: 14595
effects on oxygenated water and aqueous solutions, 20: 14614
effects on production of Lichtenberg Figures in lucite at 6 Mev, 20: 14607
effects on silicon, energy dependence of, 20: 14925
effects on sodium selenate crystals, ESR of paramagnetic centers from, (E), 20: 15972
emission of secondary, fission fragment detection by, (E/T), 20: 14852 (CEA-R-2862)
energy distribution in homogeneous weakly ionized plasma, (T),

20: 15889(T) (SC-T-65-776)
energy spectra and fluxes in inner Van Allen belt, review of, 20: 15621
equation of state for degenerate gases of, (T), 20: 15213
escape from plasma, use of silicon solar cells for detection of, 20: 15916
interactions at high energies, lectures on, 20: 15437
interactions of free gas of, in metals, collective theory for, 20: 15987
interactions with phonons in metals in magnetic fields, effects on electron mass, (T), 20: 15939 (AD-620189)
interactions with deuterons and protons, form factors from, 20: 15439
interactions with deuterons and nucleons, determination of nucleon form factors by, 20: 15440
interactions with positrons in colliding-beam experiments, (T), 20: 15443
interactions with neutrinos (ν_e), S-operator theory for, 20: 15481
interactions with phonons, electric conductivity of polarons in, (T), 20: 15988
interactions with protons, recoil polarization measurement in elastic, (E), 20: 15313 (NP-15822)
interactions with protons, radiative corrections for, (T), 20: 15319
interactions with protons, form factors from elastic, (E), 20: 15337
interactions with deuterons, relativistic corrections to impulse approximation in elastic, (T), 20: 15348
interactions with positrons in gases of, gamma momentum distributions from, (T), 20: 15383
interactions with protons at forward angles, Rosenbluth formula for, 20: 15391
interactions with phonons in superconductors, effects on structure, 20: 15664
kinetics in collisional plasma in linear electric field, (T), 20: 15904
mass of, conformal group representations in space-time for, 20: 15470
motion in external magnetic fields, relativistic, (T), 20: 15640
oscillations and steady-state structure of sheet of relativistic, in plasma, (T), 20: 15905
polarization in magnetic field, radiative, (T), 20: 15638
reactions with aluminum, nickel, and silver at 6 to 60 kev, transient radiation from, (E), 20: 15268
reactions with gases, equipment for measuring ionization in, 20: 15235(R) (AD-620289)
reactions with lead, gold, silver, tin, and tungsten at 100 to 500 kev, cross sections for K ionization in, (E), 20: 15257
reactions with molecules in homogeneous weakly ionized plasma, elastic, (T), 20: 15888(T) (SC-T-65-775)
reactions with molecules at low energies, vibration excitation from, (T), 20: 15256
reactions with nuclei, internal pair production in, (E/T), 20: 15696 (CONF-233(Vol.1), pp 60-86)
reactions with plastic scintillators at 3 to 11 kev, light yield, 20: 14895
reactions with thin silver foils, transition radiation from, (E), 20: 15968
runaway in plasma betatrons, behavior of, 20: 15919
scattering by calcium-40 and calcium-44 at 250 Mev, (E), 20: 15439
scattering by helium-3, inelastic, 20: 15439
scattering by light nuclei, relations between E1 sum rules and form factors for inelastic, (T), 20: 15746
scattering by lithium-6, single oscillator parameter for elastic, (T), 20: 15866
scattering by thin crystals at high energies, inelastic, (T), 20: 15956
scattering in high-temperature stars, opacity from Compton, (T), 20: 15209
spin coupling in molecular system, 20: 14543
temperature in argon–potassium plasma, (E/T), 20: 15874 (IPP-3/31)
temperature in helium plasma, spectroscopic determination of, (E), 20: 15908
transmission through thin metal foils, plasmon excitation in, (E), 20: 15951
transmission through alkali halide foils, excitons and plasma oscillations in, (E), 20: 15953
transmission through sodium films, plasma oscillation from, (E), 20: 15955
uses for radiation preservation of food, 20: 14938
velocity in gas-filled thermionic diodes, drift, 20: 15303

ELECTROPHORESIS
development of high-voltage paper, 20: 14461(R) (ORNL-3889, pp 48-70)

ELECTROPLATING
design considerations for ion, 20: 14670 (SC-R-65-997)

ELEMENT ONE HUNDRED AND THREE
production in heavy-ion nuclear reactions, review of, 20: 15740

ELEMENT ONE HUNDRED AND FOUR
production in heavy-ion nuclear reactions, review of, 20: 15740

ELEMENTARY PARTICLES
bound states in axiomatic field theory, 20: 15516
classification of strongly interacting, representations in SŪ(12) for, 20: 15496
decay and production in nuclear Coulomb fields, (T), 20: 15562
detection and properties of quarks, (T), 20: 15435
Dirac equation for spin-½, in Cartan frames, (T), 20: 15457
field theory for composite, axiomatic, 20: 15516
field theory for, conformal group in space-time for, 20: 15470
field theory of, zero-mass particles in, 20: 15552
interaction amplitudes for, analyticity and unitarity of, (T), 20: 15518
interaction amplitudes at high energies, (T), 20: 15519
interaction amplitudes at high energies, analyticity in energy variables for, (T), 20: 15520
interaction amplitudes for, differential properties of Feynman, (T), 20: 15525
interaction amplitudes for, Kronecker-delta singularities in angular momentum plane, (T), 20: 15521
interactions at high energies, strong, (T), 20: 15438
interactions of hadrons, C and P invariance in, (T), 20: 15486
interactions of noncomposite, many-pole amplitudes and elementarity in two-body, (T), 20: 15490
interactions of, analytic S-matrix theory of, 20: 15512
interactions of, analytic properties of Feynman integrals in theory of, 20: 15523
interactions of, approximate symmetries of strong, (T), 20: 15548
interactions of, bootstrap mechanism and charge independence for strong, (T), 20: 15454
interactions of, CP-violating nonleptonic, (T), 20: 15433
interactions of, crossing matrices for meson-quark, (T), 20: 15322
interactions of, Faddeev-type equations for four-body, (T), 20: 15456
interactions of, G_2 symmetry scheme for weak, 20: 15474
interactions of, G_2 symmetry for electromagnetic, 20: 15475
interactions of, gauge theory and geometry of, 20: 15561
interactions of, integral representations for amplitudes of, (T), 20: 15451
interactions of, inversion expansion with non-Abelian group of parity tripod for, (T), 20: 15494
interactions of, kinematic-singularity-free helicity amplitudes for, (T), 20: 15482
interactions of, linear integral equations for relativistic multichannel, 20: 15351
interactions of, rescattering correction for three-body final-state, 20: 15476
interactions of, reciprocity principle for, 20: 15350
interactions of, S-operator theory of weak, 20: 15481
interactions of, S-matrix perturbation theory for, 20: 15526
interactions of, testing SU(3) symmetry by, (T), 20: 15532
interactions of, uniformization of scalar self-energy diagram for, (T), 20: 15495
interactions of, unitary symmetry in weak, (T), 20: 15533
interactions with photons, CP violation in, (T), 20: 15309 (JINR-E-2563)
ionization losses and invariant form factors for spin $^3/_2$, (T), 20: 15269
lectures, (T), 20: 15315 (STI/PUB/117)
magnetic moments in SU(3) and SU(6) symmetry, (T), 20: 15535
mass formulas in ISL(6) group, 20: 15499
mass formulas in SU(3) and SU(6) symmetry, (T), 20: 15535
mass relations and symmetry for strongly interacting, irreducible spin equation for, 20: 15471
model for, contraction of Lorentz-group to Euclidean-group representations for, 20: 14953
model for, vertex poles and bound states in Lee, 20: 15469
model of, VΘ-bound state in three-particle sector of Lee, 20: 15459
models for, composite, (T), 20: 15550
models for, CP nonconservation in neutral a-particle, (T), 20: 15504
models for, de Sitter-group contraction for inhomogeneous Lorentz group for, 20: 14954
models for, elastic sphere and quadri-local field, 20: 15493
models for, electromagnetic form factors in relativistic composite, (T), 20: 15551
models for, higher symmetries and composite, (T), 20: 15550
models for, Lie-group theory in, 20: 14955
models for, unitary representations of pseudo-orthogonal groups for, 20: 14951
production in proton-proton interactions, (E), 20: 15426
production of, mechanisms for, (T), 20: 15510
properties of noncomposite, bootstrap theory and Regge trajectories for, (T), 20: 15491
resonances of, conference on, 20: 15398
S-matrix in axiomatic field theory, causal, (T), 20: 15515
symmetries of, dispersion methods for, (T), 20: 15549
symmetries of, interpretation of Ū, (T), 20: 15507
symmetries of, massless particles in broken, (T), 20: 15487
symmetries of, relativistic formulations of SU(6), 20: 15546
symmetries of, self-consistent broken, (T), 20: 15557
symmetries of, spin and unitary-spin, (T), 20: 15545
symmetries of, spin and spin-orbit effects in, (T), 20: 15547
symmetries of, using Jordan algebra, (T), 20: 15543
symmetries using Poincare group with charge, space, and time reflections, 20: 15544

symmetry for, Gel'fand-Moshinsky bases for unitary, 20: 15455
symmetry for, SU(12) subgroups and W-spin in, 20: 15539
symmetry for, W-spin and rotation group in, 20: 15467
symmetry group for, R(11), (T), 20: 15508
symmetry group ISL(6) for, representations and invariants in, 20: 15498
symmetry groups for, algebra of currents for exact U(6) and W(6), (T), 20: 15444 (IC/66/14)
symmetry groups for, mass splitting among multiplets in, 20: 15461
symmetry groups for, relativistic extension of noncompact, (T), 20: 15370
symmetry groups for, unitary representations of non-compact, 20: 15540
symmetry models for, irreducible representations of SU(n), 20: 15458
symmetry of, properties of SU(3), (T), 20: 15531
symmetry of, review of U(12), (T), 20: 15537
symmetry of, SL(6,c) model as a relativistically invariant formulation of SU(6), (T), 20: 15536
symmetry of, SU(3), (T), 20: 15529
symmetry of, SU(6), (T), 20: 15534
symmetry theory for, review of, 20: 15445 (RHEL/R-102)
theory of strongly interacting, using non-compact algebras, 20: 15506
theory of strongly interacting, bootstrap, 20: 15553
theory of strongly interacting, bootstrap, 20: 15554
theory of strongly interacting, symmetries in bootstrap, 20: 15556
theory of strongly interacting, bootstrap, 20: 15555
theory of, approximate dynamical symmetries for scattering and bound-state problems in, 20: 15483
theory of, Lorentz-covariant, 20: 15538
theory of, representations of non-compact Lie algebras in, 20: 15541
theory of, representations of non-compact groups in, 20: 15542
wave equations for nonzero-mass and arbitrary-spin, relativistic Schroedinger, (T), 20: 15567

ELEMENTS
book: *Analytical Chemistry of Selected Metallic Elements*, 20: 14500
bremsstrahlung reactions (γ,n) with heavy, neutron emission in, (E), 20: 15724 (MIT-2098-224)
origin in stars, review of processes for, 20: 15231
periodic chart of, suggested changes in, 20: 14549
separation of uranium from, by combined ion exchange-solvent extraction in nitric acid–tetrahydrofuran mixture, 20: 14469(R) (TID-22650)
x-ray emission in bremsstrahlung excitation of $14 \leq Z \leq 50$, detection efficiency for, (E), 20: 15258

ELK RIVER POWER REACTOR
pressure vessel inspection and testing, 20: 16085(R) (SWRI-1228-4-15)

EMBRYOS
radiation effects on chick, effects of inoculation with smallpox virus vaccine on x, 20: 14281
radiation effects on mouse, delayed pathological x, 20: 14315

EMISSIVITY
measurement of total hemispherical, method for, 20: 15088

ENERGY
transfer between plasma jets and coolant gases, 20: 15584

ENGLAND
radiation monitoring of grass, herbage, milk, and soils in vicinity of AERE, 20: 14784(R) (AERE-R-5015)

ENZYMES
effects of lipid peroxidation on, 20: 14587
radiation effects on activity of lipolytic, x, 20: 14279
radiation effects on activity of, in mitochondria from rat liver, spleen, and thymus, x, 20: 14376
radiation effects on pyridine nucleotidase activity of rat liver and spleen, x, 20: 14362

EQUATION OF STATE
evaluation for degenerate electron gas, numerical, (T), 20: 15213
of matter at supernuclear density, 20: 15212

ERBIUM
bremsstrahlung reactions (γ,n) at 8 to 16 Mev, spectra from, (E), 20: 15723 (MIT-2098-162)
bremsstrahlung reactions (γ,n) with, neutron emission in, (E), 20: 15724 (MIT-2098-224)
electric and thermal conductivity of polycrystalline, temperature dependence of, (E), 20: 15107
thermal conductivity of polycrystalline, temperature dependence of, 20: 15117(T)

ERBIUM ALLOYS
Co–Er, cobalt in EPR in intermetallic compounds of, 20: 15963
Er–Au, electric conductivity at 4.2 to 300°K, effects of erbium content on, 20: 15083
Er–Fe, preparation and structure, 20: 15110
Er–Mn, preparation and structure, 20: 15110
Er–Y, electric conductivity of dilute, at low temperatures, 20: 15098

ERBIUM ISOTOPES
deuteron reactions at 15 Mev, isomeric states from, (E), 20: 15856

ERBIUM ISOTOPES Er-166
energy level transitions in, conversion coefficients for E2, (E), 20: 15706 (CONF-233(Vol.2), pp 191-7)
internal conversion coefficients of $2^+ \rightarrow 0^+$ transitions in, E2, (E), 20: 15745

ERBIUM ISOTOPES Er-167
neutron reactions (n,γ) with, gamma spectra from thermal, (E), 20: 15757

ERBIUM ISOTOPES Er-168
energy levels from erbium-167 (n,γ) reactions, (E), 20: 15757

ERBIUM OXIDES
crystal lattice constants at 300 and 102°K, 20: 15660
thermal expansion at 94 to 300°K, 20: 15660

ERBIUM SILICATES
structure of, polymorphic, 20: 14537

ERBIUM SULFIDES
preparation, 20: 14511(R) (ORNL-3889, pp 71-3)

ERYTHROCYTES
iron-59 content of lamb, after natural exposure, 20: 14243(R) (TID-22626)
production in mice, genetic and physiological factors affecting, 20: 14290(R) (NYO-1800-12)
radiation effects on iodine-131 incorporation in rat, γ, 20: 14276
radioinduced hemolysis of, x, 20: 14275

ERYTHROPOIETIN
effects on anemias in mice, 20: 14290(R) (NYO-1800-12)

ESCHERICHIA COLI
effects on uv-irradiated phages, 20: 14357
radiation effects on DNA in, x, 20: 14265
radiation effects on conjugation in, uv, 20: 14329
radioinduced inactivation of isolated ribosomes of, γ, 20: 14363
radiosensitivity of bacteriophages infecting, uv, 20: 14271
ribonucleic acid production in, 20: 14456(R) (ORNL-3889, pp 32-5)

ESTERS
decomposition in ion source of mass spectrometer, mechanism of, 20: 14584(R) (TID-22444)

ETHANE, DIBROMOTETRAFLUORO-
decomposition in ion source of mass spectrometer, mechanism of, 20: 14584(R) (TID-22444)

ETHANE, 1,2-DICHLORO-
effects on solvent properties for uranium in TBP system, 20: 14655

ETHANE, 1,2-DICHLORO-1,1,2,2-TETRAFLUORO-
decomposition in ion source of mass spectrometer, mechanism of, 20: 14584(R) (TID-22444)

ETHANE, HEXABROMO-
effects on radioinduced isomerization of α-phenylcinnamic acid, 20: 14596

ETHANE, HEXAFLUORO-
decomposition in ion source of mass spectrometer, mechanism of, 20: 14584(R) (TID-22444)

ETHANE, IODO-
radioinduced ESR spectra in, at 77°K, effects of deuterium and iodine-129 on, 20: 14597

ETHANE, NITRO-
photolysis of liquid and vaporous, yields from uv, 20: 14613
radiolysis of liquid and vaporous, yields from gamma, 20: 14613

ETHANE, TRICHLORO-
reactions with gallium–plutonium alloys, critical temperature of, 20: 14513 (RFP-688)

ETHANOL
ethanol–$AgNO_3$, radioinduced free silver atoms in solid solutions of, EPR of x, (E), 20: 15975(T)
ethanol–Ag_2SO_4, radioinduced free silver atoms in solid solutions of, EOR of x, (E), 20: 15975(T)
ethanol–AgF, radioinduced free silver atoms in solid solutions of, EPR of x, (E), 20: 15975(T)
ethanol–$AgClO_4$, radioinduced free silver atoms in solid solutions of, EPR of x, (E), 20: 15975(T)

ETHANOL, TRIFLUORO-
radiolysis of, gamma, 20: 14590

ETHYL ACETATE
decomposition in ion source of mass spectrometer, mechanism of, 20: 14584(R) (TID-22444)

ETHYL PHOSPHATES
chloro-, method for determination of, in mock explosive, 20: 14470 (UCRL-7873)

ETHYL SULFATES
effects of, combined with radiation on barley seeds, 20: 14384

ETHYLENE, CHLORO-
radioinduced polymerization of, at –78 and –196°C, gamma, 20: 14594

ETHYLENE, CHLORO- POLYMERS
styrene radioinduced polymerization with styrene, 20: 14618

ETHYLENE, CHLOROTRIFLUORO- POLYMERS
uses as carrier for solvents in separation processes, 20: 14656

ETHYLENE GLYCOL
dibenzoate, radiolysis of, ESR spectra of free radicals from gamma, 20: 14606

yields in gamma radiolysis of deaerated methanol, effects of sulfuric acid on, 20: 14579(R) (NYO-2303-15)
ETHYLENE OXIDE
effects of, combined with heat on sterility of catgut sutures, 20: 14932
ETHYLENE POLYMERS
radioinduced chlorination and sulfochlorination of, in solid phase, 20: 14621
radioinduced graft polymerization with styrene, radical lifetime in gamma, 20: 14624
radioinduced polymerization with styrene, 20: 14618
ETHYLENE, TETRACHLORO-
reactions with gallium–plutonium alloys, critical temperature of, 20: 14513 (RFP-688)
ETHYLENE, TETRAFLUORO-
radioinduced polymerization with isobutylene, 20: 14608
ETHYLENE, TETRAFLUORO- POLYMERS
radiation effects on prostheses of, x, 20: 14344
ETHYLENE, TRICHLORO-
reactions with gallium–plutonium alloys, critical temperature of, 20: 14513 (RFP-688)
ETHYLENIMINE
radiosensitivity effects on mutations in barley seed, γ, 20: 14334
EUROPIUM
hyperfine structure, (T), 20: 15263
hyperfine structure of, relativistic dipole and quadrupole interaction in, (E/T), 20: 15266
separation from ytterbium using organic acids, 20: 14490
spectra of, in liquid ammonia, electronic, 20: 14526
EUROPIUM ISOTOPES
deuteron reactions at 15 Mev, isomeric states from, (E), 20: 15856
EUROPIUM ISOTOPES Eu-151
nuclear magnetic dipole moment of, (E/T), 20: 15266
EUROPIUM ISOTOPES Eu-152
gamma spectra at 1380 to 1900 kev, gadolinium-152 and samarium-152 energy levels from, (E), 20: 15832
properties of short-lived gamma emitting, for use in detection of hidden materials, 20: 14451 (NYO-2586-2)
EUROPIUM ISOTOPES Eu-153
energy level transitions in, (E), 20: 15734 (ZfK-PhA-18)
energy levels from samarium-153 decay, (E), 20: 15795
nuclear magnetic dipole moment of, (E/T), 20: 15266
EUROPIUM ISOTOPES Eu-159
beta and decay of, gadolinium-159 levels from, (E), 20: 15782
half life, (E), 20: 15782
EUROPIUM TELLURIDES
crystal phase transition at high pressure, 20: 15974
EVANS BLUE
diffusion through hemato-encephalic barrier in rats, 20: 14312
EVOLUTION
mechanisms for biogenesis, 20: 14233 (UCRL-16566)
EXERCISE
effects on blood and lungs of dogs, 20: 14257
EXOSPHERE
hydromagnetic wave propagation in lower, (T), 20: 15591 (RM-4858)
EXPERIMENTAL BREEDER REACTOR-II
component development for, 20: 16060(R) (ANL-7152, pp 1-49)
fuel cladding for, irradiation testing of, 20: 16060(R) (ANL-7152, pp 1-49)
EXPERIMENTAL GAS COOLED REACTOR
coolant mixing device for, steam–water, 20: 16011(P)
power-rating distribution for, method for obtaining asymmetrical, 20: 16104(P)
EXPLOSIVES
analysis of extrusible and plastic-bonded, methods for, 20: 14470 (UCRL-7873)
analysis of gunpowder residues on hands, activation, 20: 14439(R) (GA-5556)
properties of, use of hydrodynamic machine calculations for determining, (T), 20: 15571 (UCRL-14531)
EXPONENTIAL PILES
design and operation of, review, 20: 16123 (KFK-350)
reactivity of cylindrical, spatial dependent impulse response for, (T), 20: 16020 (CEA-R-2836)
EYES
radiation effects on, following therapy of facial skin lesions, 20: 14297

F

FALLOUT
beta dose distributions in tissues from, 20: 14403 (NP-15714)
content in Indo-Antarctic Ocean, 1962, 20: 14749
content in stratosphere and troposphere, 1962 and 1963, 20: 14742
distribution vertically in Japanese soils, 20: 14751
effects of atmospheric precipitation on, 20: 14746
gamma dose rates in cylindrical and rectangular steel structures from, 20: 15931 (TO-B-65-27)
hazards from, review, 20: 14427
monitoring of, Black Sea, 1964, 20: 14741
monitoring in Czechoslovakia, 20: 14813
monitoring in New Zealand, 1965, 20: 14734(R) (NP-15844)
monitoring in Norway, 1963 through 1965, 20: 14739 (TID-22655)
monitoring of, survey of methods for, 20: 14745
monitoring over Atlantic Ocean, 1964, 20: 14743
monitoring worldwide, 1964, 20: 14243(R) (TID-22626)
protection against, shelter design for, 20: 14723(P)
uptake by Canadian wheat, 1964, 20: 14736 (NP-15853, pp 3-7)
FAST REACTORS
design and operation of, review, 20: 16123 (KFK-350)
design of fused-salt-fueled, liquid-metal-cooled, breeder, 20: 16036
design of molten-salt breeder, 20: 16037
design of power breeder, 20: 16102(P)
design parameters of large, effects on breeding in, (T), 20: 16093
economics of dual-purpose desalination–power, 20: 16108(T) (JPRS-33459)
fuel and canning materials for, characteristics of, 20: 16047
fuel cladding for, irradiation testing of, 20: 16060(R) (ANL-7152, pp 1-49)
fuel development for, 20: 16060(R) (ANL-7152, pp 1-49)
fuel economics for, 20: 16087 (TRG-Report-1115)
fuel processing development for, 20: 16060(R) (ANL-7152, pp 1-49)
FAST TEST REACTOR
fuel elements for, neutron physics of driver, 20: 16121 (BNWL-197)
FATTY ACIDS
radiation effects on metabolism in rats, x, 20: 14379
FECES
technetium-99 elimination in human, 20: 14423
FERMI FAST BREEDER REACTOR
fuel element fabrication for, 20: 16100
FERMIONS
interactions in many-body systems of, analysis by linked-cluster techniques for, 20: 15564
interactions with bosons in Lee model, bound states in, (T), 20: 15459
properties of beams of, coherence, (T), 20: 15328
stability of many-particle systems of, (T), 20: 15151
FERMIUM
production in heavy-ion nuclear reactions, review of, 20: 15740
separation from acetate and 2-hydroxyisobutyric acid solutions by solvent extraction using thenoyltrifluoroacetone, 20: 14654
FERROMAGNETIC MATERIALS
superconductivity, (T), 20: 15648
FERTILIZERS
sorption by rice seedlings, tracer study of foliar, 20: 14240 (NP-15670)
FETUSES
radiation effects on cytology in rat, x, 20: 14262
radiation effects on liver cells of rat, x, 20: 14294
radiation effects on skeletal development in cattle, sheep, and swine, γ, 20: 14337
radiation effects on human, fission product, 20: 14372
strontium-85 uptake by mouse, effects of fetal age at maternal injection on, 20: 14244
FFAG SYNCHROTRONS
development of 100-Mev electron synchrotron, electrode broad-band adaptation for, 20: 15161 (NP-15273)
FIELD THEORY
book: *Introduction to Dispersion Techniques in Field Theory*, 20: 15565
bound states in axiomatic, 20: 15516
charged fields in quantum, using local algebras, 20: 15517
elementary particles in, zero-mass, 20: 15552
elementary particle interactions in, gauge theory and geometry of, 20: 15561
formalism of axiomatic, 20: 15514
formulation of nonrenormalizable quantum, 20: 15527
lectures, 20: 15315 (STI/PUB/117)
Lie algebras in, representations of non-compact, 20: 15541
locality and paralocality in free para-, equivalence of, 20: 15468
point functions in quantum, 20: 15513
quantum, conformal group in space-time for, 20: 15470
quantum, problems in, 20: 15489
quantum, reduction formulas for S-matrix elements in axiomatic, 20: 15502
retarded functions in LSZ perturbation theory, ambiguities in, (T), 20: 15452
S-matrix in axiomatic, causal, 20: 15515
symmetries in, relativistic formulations of SU(6), 20: 15546
symmetries in, spin and unitary-spin, 20: 15545
symmetry groups in, unitary representations of non-compact, 20: 15540

testing of local, by scattering at high energies, 20: 15519
vertex function radiative corrections in nonrenormalizable, 20: 15528
wave function renormalization constants in, using partially conserved axial-vector current, 20: 15402

FILMS
evaporation of thin, device for monitoring, 20: 14819 (RFP-602)
superconducting transition temperatures of, calculation of, 20: 15655
use of monomolecular, as standard beta sources, 20: 16143 (AD-620276)

FILTERS
design for fallout shelters, 20: 14722(P)
radioactivity on air, at McMaster University, β, 20: 14738 (NP-15853, pp 21-33)
use of differential, in x-ray fluorescence analysis for copper in ores, 20: 14487
use of wedge, in gamma teletherapy, 20: 14426

FILTRATION
systems for atmospheric, use of automobile engines in, 20: 14672

FINNED TUBES
testing of, eddy-current method for nondestructive, 20: 14703
testing SAP, nondestructive methods for, 20: 14712
testing thin-walled, nondestructive methods for, 20: 14713

FIRES
protection against, design of sandwich-type structural panel for, 20: 14682(P)

FISH
radiation effects on gonad development in, effects on season and temperature on x, 20: 14307

FISSION FRAGMENTS
detection by secondary electron emission from foils, (E/T), 20: 14852 (CEA-R-2862)
effects on aluminum–magnesium alloys, dislocation loops in, 20: 15145
energy and mass distributions from deuteron reactions with thorium-232, (E), 20: 15840

FISSION PRODUCTS
activity distributions in high-temperature gas-cooled reactors, computer program for calculating, 20: 16075 (GAMD-6519)
beta dose distributions in tissues from, 20: 14403 (NP-15714)
content in food chain of man, 20: 14243(R) (TID-22626)
detection and measurement from failed fuel elements, using chemical methods, 20: 14847 (BMwF-FBK-65-01)
determination in atmospheric and precipitation samples, methods for radiochemical, 20: 14430 (AD-620219)
diffusion and coalescence in solids, theory of gaseous, 20: 15032 (ANL-7079)
diffusion from uranium dioxide, effects of radioinduced defects and temperature on, 20: 15144
diffusion in tungsten, 20: 14959(R) (N65-20797)
diffusion in tungsten, 20: 14960(R) (N65-20798)
diffusion through reactor fuel element coatings, equations for, 20: 15114
distributions from coolant-loss accidents in water-cooled power reactors, 20: 16019(R) (BMI-X-10154)
effects on human fetuses, 20: 14372
food contamination by, from reactor accidents, 20: 14748
gamma spectra of uranium-235, for calculating, 20: 14733 (AD-628982)
metabolism in animals, 20: 14243(R) (TID-22626)
radiation dose from ingested, 20: 14243(R) (TID-22626)
release from uranium carbide–zirconium carbide at high temperatures, 20: 14959(R) (N65-20797)
release from uranium carbide–zirconium carbide at high temperatures, 20: 14960(R) (N65-20798)
release from uranium carbide–zirconium carbide at 1800°C, 20: 14961(R) (N65-20801)
separation by ion exchange, kinetics of, 20: 14643
separation from waste solutions at Hanford, methods for, 20: 14641 (RL-SA-59)
separation of americium and curium from rare earth, 20: 14659(P)
separation of antimony from, by solvent extraction on fine-grained carrier, 20: 14656
separation of cerium from, method for, 20: 15722 (KR-76)
separation of promethium-147 from rare earth, ion exchange, 20: 14635 (CONF-660305-5)
separation of rare earth, from irradiated aluminum–uranium alloy by solvent extraction using TBP, 20: 14635 (CONF-660305-5)
separations of, developments in methods for, 20: 14436 (BNWL-SA-504)

FISSIUM
fissium–Pu–U, phase studies, 20: 15085

FLOCCULATION
effects on sorption of radioactive wastes by bentonites and diatomaceous earth, 20: 16138

FLOWMETERS
development for suspensions of glass beads in carbon dioxide–nitrogen mixtures, 20: 14671(R) (TID-22394)
properties for use in fused salt or molten metal systems, ultrasonic, 20: 14700(R) (NYO-3622-1)

FLUID FLOW
boundary layer in nuclear rocket motor nozzles, 20: 14727 (NASA-TM-X-1208)
dispersion in ring- and sphere-packed columns, single-phase axial, 20: 14691 (UCRL-10696(Rev.)(Pt.2))
effects of transition-boiling heat transfer on, in single rod test sections, 20: 14687 (GEAP-4785)
heat transfer by herring-bone finned surfaces to axial, (E/T), 20: 14685 (CEA-R-2471)
heat transfer in, in suspensions of glass beads in carbon dioxide–nitrogen mixtures, 20: 14671(R) (TID-22394)
magnetohydrodynamic, Rayleigh's problem in, (T), 20: 15578

FLUID FLOW (LAMINAR)
magnetohydrodynamic, boundary layer between parallel streams in, (T), 20: 15570 (N65-21084)

FLUID FLOW (TURBULENT)
critical heat flux for boiling-water, in long tubes, 20: 14695

FLUID FUEL REACTORS
design of power breeder, 20: 16102(P)

FLUID PROPELLANTS
heating of liquid hydrogen in nuclear rockets, 20: 14728 (NASA-TN-D-3328)

FLUIDS
neutron diffusion parameters in, determination of, using pulsed source, 20: 14772

FLUORIDE IONS
reactions with trivalent cerium in fused salts, 20: 14563

FLUORIDE VOLATILITY PROCESSES
efficiency of fluidized-bed separation of uranium from graphite-base fuels, 20: 14647

FLUORINE
determination in potassium dioxodifluoroiodate(V), titrimetric, 20: 14455(R) (ORNL-3889, pp 25-32)
determination of trace amounts of, in uranium dioxide, 20: 14494
photochemical reactions with krypton, 20: 14527
reactions of recoil, mechanisms of, 20: 14620

FLUORINE ISOTOPES F-18
energy levels of, unified model wave function for low-lying rotational, (T), 20: 15814

FLUORINE ISOTOPES F-19
proton inelastic scattering at 1.422 Mev, mean lifetime of first excited state from, (E), 20: 15780

FLUORINE ISOTOPES F-20
energy levels of, unified model wave function for low-lying rotational, (T), 20: 15814

FOAMS
shock wave impingement on crushable foamglass, 20: 16023(R) (IITRI-578P21-16)

FOOD
cesium-137 content of, in Norway, 20: 14739 (TID-22655)
cesium-137 content in, 1963-5, 20: 14243(R) (TID-22626)
radiation preservation of, review of methods and problems in, 20: 14938
radiation processing of chicken and duck, effects on wholesomeness of, 20: 14933
radiation processing of tropical fruits and vegetables, effects on insect infestations, 20: 14935
radioactive contamination in, methods for estimating, 20: 14243(R) (TID-22626)
radioactive contamination of, from reactor accidents, 20: 14748
radiopreservation of, status of program for, 20: 14937
strontium-90 content in, 1963-5, 20: 14243(R) (TID-22626)
tritium content in water in vegetables, 20: 14744

FORMALDEHYDE
decomposition in ion source of mass spectrometer, mechanism of, 20: 14584(R) (TID-22444)
production of, gamma radiolysis of aerated methanol, effects of sulfuric acid on, 20: 14579(R) (NYO-2383-15)
yields in gamma radiolysis of deaerated methanol, effects of sulfuric acid on, 20: 14579(R) (NYO-2383-15)
yields in uv photolysis of methanolic hydrogen peroxide, 20: 14579(R) (NYO-2383-15)

FORMIC ACID
propyl ester of, decomposition in ion source of mass spectrometer, 20: 14584(R) (TID-22444)
yields in uv photolysis of methanolic hydrogen peroxide, 20: 14579(R) (NYO-2383-15)

FORMIC ACID, METHYL ESTER
decomposition in ion source of mass spectrometer, mechanism of, 20: 14584(R) (TID-22444)

FORMIC ACID, VINYL ESTER
decomposition in ion source of mass spectrometer, mechanism of, 20: 14584(R) (TID-22444)

FOWLS
radiation processing of chickens and ducks, effects on wholesomeness of γ, 20: 14933
FREE RADICALS
lifetime in radioinduced copolymerization of polyethylene and styrene, 20: 14624
production in oxygenated water and aqueous solutions, 20: 14614
radioinduced in crystalline trypsin, γ and uv, 20: 14273
radioinduced in nucleohistone, x, 20: 14592
radioinduced in *Phleum pratense*, γ and x, 20: 14349
yields from gamma radiolysis of ethylene glycol dibenzoate and poly(ethylene terephthalate), ESR study of, 20: 14606
FREONS
reactions of Freon-TB-1 with plutonium, critical temperature of, 20: 14513 (RFP-688)
FRUITS
radiation processing of tropical, effects on insect infestations on, 20: 14935
FUMARIC ACID
effects on radioinduced isomerization of α-phenylcinnamic acid, 20: 14596
FUNGI
radiation effects on phosphate metabolism in Phycomyces, x, 20: 14264
FURAN, TETRAHYDRO-
HNO_3–tetrahydrofuran, analytical use for combined ion exchange-solvent extraction separation of uranium, 20: 14469(R) (TID-22650)
FUSED SALTS
analysis of MSRE, for chromium, 20: 14457(R) (ORNL-3889, pp 36-39)

G

GADOLINIUM
crystal structure at 120 to 370°K, 20: 15124
GADOLINIUM ALLOYS
Gd–Fe, preparation and structure, 20: 15110
Gd–Mn, preparation and structure, 20: 15110
Gd–OS–Y, thermal capacity of intermetallic compounds of, at 0.25 to 20.0°K, 20: 15061 (UCRL-11580)
Gd–Y, electric conductivity of dilute, at low temperatures, 20: 15098
GADOLINIUM IONS
paramagnetic resonance of trivalent, in rare earth ethyl sulfates, 20: 15991
GADOLINIUM ISOTOPES Gd-152
energy levels from europium-152 decay, (E), 20: 15832
GADOLINIUM ISOTOPES Gd-154
energy level transitions in, conversion coefficients for E2, (E), 20: 15705 (CONF-233(Vol.2), pp 177-90)
GADOLINIUM ISOTOPES Gd-155
energy level transitions in, delayed E1, (T), 20: 15765
energy level transition probabilities in, pairing correlations in E1, (T), 20: 15766
GADOLINIUM ISOTOPES Gd-159
energy level transitions in, conversion electrons from E1, (E), 20: 15703 (CONF-233(Vol.2), pp 148-57)
energy levels, (E), 20: 15782
GADOLINIUM SYSTEMS
Gd–H–Y, crystal structure, 20: 14546
GAGES
performance of radiometric, scale linearity in, 20: 14836
use of radioisotope, review of industrial, 20: 14835
GALAXIES
explosion in NGC 1275, optical evidence for, (E), 20: 15205
formation of, effects of black-body radiation content of universe on, (T), 20: 15204
magnitudes of radio, static cosmological model and red shift for, (T), 20: 15224
GALLIUM
determination in plutonium fluorides and peroxides, review on spectrographic, 20: 14464 (RFP-599)
effects on spectrofluorimetric determination of scandium, 20: 14476
energy level transitions in, Coster-Kronig, (T), 20: 15238 (CONF-233 (Vol.3), pp 398-418)
energy level widths for, K, (T), 20: 15239 (CONF-233(Vol.3), pp 419-39)
GALLIUM ALLOYS
Ga–Nb, superconductivity of fused, 20: 15123
Ga–Pu, critical temperature of reactions with chlorinated solvents, 20: 14513 (RFP-688)
Ga–Pu, effects of composition on corrosion of, 20: 14984 (RFP-511)
Ga–V, superconductivity of fused, 20: 15123
GALLIUM ISOTOPES Ga-69
neutron reactions (n,p) at 14.6 Mev, isomeric cross section ratio for, (E/T), 20: 15773
nitrogen-ion scattering at 16.2 and 17.7 Mev, gamma polarization from, (E), 20: 15759
GALLIUM ISOTOPES Ga-72
beta decay of, pair producing conversion transitions in, (E), 20: 15834
GAMES THEORY
computer program for playing checkers, 20: 14949 (ANL-7109)
GAMMA RADIATION
detection and measurement in radiochemical analysis, 20: 14488
detection and measurement using dual-crystal scintillation detectors, pulse-shape discrimination in, 20: 14844 (AD-620395)
detection and measurement using lithium-drifted germanium detectors, 20: 14845 (AD-620434)
detection and measurement of low-energy, performance of proportional counter for, 20: 14879
detection and measurement of absorbed dose, performance of ionization chambers for, 20: 14894
detection and measurement of low-energy, solid-state detector for, 20: 14910(P)
detection of, portable hand and shoe monitor for, 20: 14866
detection using scintillation crystals, calculation of efficiencies of, 20: 14897
distribution in complex media, similitude theory for energy and space, 20: 14776
dose buildup factors for steel, 20: 15933(T) (ORNL-tr-1060)
dose control using wedge filters, 20: 14426
dose rates in cylindrical and rectangular structures from fallout, 20: 15931 (TO-B-65-27)
dosimetry in animals using hematological changes, 20: 14314
dosimetry of, calorimetric method for, 20: 15858
dosimetry of, comparison of Fricke and nitrous oxide, 20: 14870
dosimetry using film badges, 20: 14806
effect, on cyclohexane, effects of oxygen pressure and temperature on oxidizing, 20: 14625
effects of, combined with surgery and x radiation on cervical carcinomas, complications from, 20: 14377
effects of, combined with diethyl sulfate on barley seeds, 20: 14384
effects of, combined with surgery and x radiation on cervical carcinomas, 20: 14409
effects of, combined with acceleration on Drosophila genetics, 20: 14343
effects of, combined with vibration on Drosophila genetics, 20: 14343
effects on aerated methanol, effects of sulfuric acid on formaldehyde and hydrogen peroxide yields in, 20: 14579(R) (NYO-2383-15)
effects on aliphatic peptides in aqueous solution, 20: 14616
effects on aqueous carbon tetrachloride and chloroform solutions saturated with carbon dioxide, formation of trichloroacetic acid in, 20: 14582 (SGAE-CH-25/1965)
effects on bacteria on processed frozen chickens and ducks, 20: 14933
effects on behavior in monkeys, 20: 14286 (AD-625837)
effects on behavior of rabbits, 20: 14326
effects on bladder tumors, vesico-ureteral reflux from, 20: 14411
effects on bladder carcinomas, 20: 14414
effects on bromination of 2,3-dimethylbutane, 20: 14591
effects on catalytic activity of charcoal, 20: 14609
effects on central nervous system in rabbits, 20: 14350
effects on cervical carcinomas, 20: 14409
effects on chloral hydrate at 80 to 800 rads, 20: 14583 (TID-21634)
effects on chromite and chromate solutions, 20: 14589
effects on crystalline trypsin ESR signal, 20: 14273
effects on deaerated methanol, effects of sulfuric acid on yields from, 20: 14579(R) (NYO-2383-15)
effects on decomposition of liquid and vaporous nitroethane and nitromethane, 20: 14613
effects on dehydrogenase activity in rat liver homogenates and mitochondria, 20: 14284
effects on devitrification of alumina–phosphate glass prepared from calcined waste, 20: 16133 (IDO-14672)
effects on electrical activity of brain in rabbits, 20: 14326
effects on ESR spectra of polycrystalline alkyl iodides at 77°K, 20: 14597
effects on fecundity of male and female *Platynota stultana*, 20: 14340
effects on formation of free radicals in ethylene glycol dibenzoate and poly(ethylene terephthalate), 20: 14606
effects on fruit fly populations infesting tropical fruits and vegetables, 20: 14935
effects on fuel and poison elements, in-pile measurements of, 20: 16089(R) (WAPD-MRP-114)
effects on human populations, low-dose, 20: 14331
effects on immune reactions to *Treponema pallidum*, 20: 14308
effects on indium antimonide, defect energy spectrum from, 20: 15979(T)
effects on infectivity of Schistosoma larvae in mice, 20: 14304
effects on isolated *Escherichia coli* ribosomes, inactivating, 20: 14363
effects on isomerization in solid matrices, 20: 14596
effects on leukemic mouse cells in culture, lethal, 20: 14367

effects on lung cancer, 20: 14420
effects on man, effects of polyvinylpyrrolidone on, 20: 14396
effects on meat, acceptance tests for radiopreservation, 20: 14930 (NP-15676)
effects on meat, acceptance tests for radiopreservation, 20: 14931 (NP-15677)
effects on methanol, spectral studies on, 20: 14579(R) (NYO-2383-15)
effects on molecules, distribution of ionization energy in, 20: 14595
effects on molecular structure of different types of neoprenes, infrared spectral studies on, 20: 14585 (TID-22652)
effects on morphology and physiology of *Staphylococcus aureus*, 20: 14313
effects on mouth following facial therapy, 20: 14324
effects on mutations in barley seed, effects of ethylenimine on, 20: 14334
effects on neutral and alkaline solutions of sodium acid phosphite, 20: 14600
effects on nucleated cell depletion in bone marrow, spleen, and thymus of young mice, γ, 20: 14365
effects on oak leaves, chronic low-dose, 20: 14289 (BNL-9509)
effects on oxidation of paraffin, 20: 14612(T)
effects on p-type silicon, damage effects on carrier lifetime from, (E), 20: 14922
effects on *Phleum pratense*, 20: 14349
effects on phospholipids in rabbit mitochondria, γ, 20: 14278
effects on plasma proteins in rats, 20: 14276
effects on polyethylene and styrene, radical lifetime in polymerizing, 20: 14624
effects on polymerization of triallyl cyanurate in liquid and solid states, 20: 14586
effects on polymerization of vinyl chloride at −78 and −196°C, 20: 14594
effects on polymerization of tetrafluoroethylene with isobutylene, 20: 14608
effects on potassium release through cell walls, 20: 14282
effects on productivity of algae, 20: 14381
effects on reproduction of wood-boring insects, 20: 14305
effects on reproduction of *Psila rosae* after exposure of pupae, 20: 14317
effects on Salmonella, effects of temperature and vitamin K_5 on, 20: 14395
effects on Schistosoma infectivity in mice, 20: 14304
effects on silicon detectors, noise from, (E), 20: 14923
effects on skeletal development of cattle, sheep, and swine exposed *in utero*, 20: 14337
effects on sodium acid phosphite in sodium nitrate solutions, 20: 14601
effects on sodium selenate crystals, ESR of paramagnetic centers from, (E), 20: 15972
effects on solid state polyamino acids, 20: 14588
effects on sperm production and testicular histology in bulls, fractionated-dose whole-body exposure, 20: 14336
effects on synthesis of nucleic acids and proteins in amoeba, 20: 14259(R) (NP-15855)
effects on thermoluminescence of lithium fluoride phosphors, 20: 14887
effects on thermoluminescence of lithium–fluoride phosphors, energy dependence of, 20: 14888
effects on tooth structure, 20: 14323
effects on *trans-cis* isomerization of stilbene in methanol solutions, 20: 14579(R) (NYO-2383-15)
effects on trifluoroethanol, 20: 14590
effects on ureteric valves following bladder radiotherapy, 20: 14298
effects on uterine sarcomas, therapeutic, 20: 14301
effects on 1,3- and 1,4-cyclohexadiene, 20: 14610
interactions with mesons (π), analysis of 2π production in, (T), 20: 15389
interactions with protons at 1100–1300 Mev, hyperon (Λ)-meson (K^+) production in, (E), 20: 15393
interactions with nucleons at medium energies, effects of inelastic channel on, (T), 20: 15394
interactions with deuterons at 2.504 to 50.0 Mev, disintegration cross sections for, (T), 20: 15789
monitoring in laboratories, development of equipment for, 20: 14872
monitoring of scattered, in exposure facilities, 20: 14812
production by fast neutron capture and scattering reactions, tabulations for, 20: 15725 (NP-14855)
production in meson (η) decay, (E), 20: 15395
reactions (γ,γ') with indium-113, cross section for isomer formation in, 20: 15748
reactions (γ,n) with carbon-12 at 21.7 to 26.7 Mev, (E), 20: 15861
scattering on monocrystals, phonon properties from Mössbauer effect in, 20: 15948
spectra in nuclear beta decay, continuous, (T), 20: 15801
streaming through ducts, analysis using Monte Carlo method, 20: 15929 (AD-627890)
transmission through aluminum slabs, transfer-matrix method for, (T), 20: 15934
transmission through steel pipes in nuclear powered ships, Monte Carlo calculation of, 20: 16114
use for measurement of ash content of lignite, 20: 14493
uses for radiation preservation of food, 20: 14938

GAMMA SHIELDING
thickness of steel, gamma dose buildup factors for calculating, 20: 15933(T) (ORNL-tr-1060)
use of lead plates for nuclear-powered ships, (E/T), 20: 15932(T) (ORNL-tr-843)

GAMMA SOURCES
calibration of cobalt-60, 20: 14927
content in Japanese soils, 20: 14751
distribution vertically in Japanese soils, 20: 14751
filters for cobalt-60 teletherapy, wedge, 20: 14426
performance in density meters for coal and soil, measurement errors for, 20: 14837
preparation by waste oxide fixation in glass, 20: 16141(P)
properties of short-lived, for detecting hidden materials, 20: 14451 (NYO-2586-2)
use in altitude measurements on moon, 20: 14817 (N65-20421)
use of gaseous, for surface area measurements of powders, 20: 14973(P)

GAMMA SPECTRA
analysis of, method for, 20: 14845 (AD-620434)
of uranium-235 fission products, method for calculating, 20: 14733 (AD-628982)
resolution by computer, 20: 14461(R) (ORNL-3889, pp 48-70)

GAMMA SPECTROMETERS
calibration and uses, 20: 15747
design and performance of coincident, for low-level activity, 20: 14885
design and testing of germanium (lithium) and sodium iodide anticoincidence, 20: 14865
design using lithium-drifted germanium detector, engineering drawings for, 20: 14904
performance of curved-crystal, for tungsten-187 decay spectra, 20: 15807
spectral line shape from single-crystal scintillation, reconstruction of, (T), 20: 14869
uses with activation detectors for intermediate-energy neutron spectroscopy in reactors, 20: 14860 (RT/FI(65)-33)

GAMMA SPECTROSCOPY
artifacts and errors in, 20: 14461(R) (ORNL-3889, pp 48-70)
background estimation in short-lived-source counting, 20: 14878
use in determining high-energy gamma radiation from isotopes, (E/T), 20: 14461(R) (ORNL-3889, pp 48-70)
uses for measurement of fuel burnup, 20: 14504

GARIGLIANO POWER REACTOR
control rod drive system for, design and performance of, 20: 16074 (EUR-2420.d,f,i,n,e, pp 227-48)
control rod system for, design of, 20: 16069 (EUR-2420.d,f,i,n,e, pp 147-80)
control system for, design of, 20: 16068 (EUR-2420.d,f,i,n,e, pp 133-45)
control system for regulating power output of, 20: 16073 (EUR-2420.d,f,i,n,e, pp 215-25)
development, 20: 16064 (EUR-2420.d,f,i,n,e)
instrumentation design for, in-core, 20: 16065 (EUR-2420.d,f,i,n,e, pp 17-49)
neutron flux monitoring instruments for, in-core, 20: 16068 (EUR-2420.d,f,i,n,e, pp 133-45)
turbine for, startup and operation of, 20: 16071 (EUR-2420.d,f,i,n,e, pp 191-202)

GAS COOLED REACTORS
accidents in heavy water moderated, computer program for dynamics of, 20: 16026 (UJV-1459/65)
coolant decontamination system for, 20: 16010(P)
development of graphite-moderated, review of, 20: 16035
fission-product activity distributions in high-temperature, computer program for calculating, 20: 16075 (GAMD-6519)
fuel economics for graphite-moderated, 20: 16087 (TRG-Report-1115)
loading vertical-channel, design of devices for, 20: 16003(P)
power density of high-temperature, method for obtaining uniform, 20: 16103(P)
use in thermionic space power systems, 20: 16110 (AD-620650)

GAS FLOW
magnetohydrodynamic, Hall effect in two-dimensional, along insulating plane, (T), 20: 15568 (AD-620324)

GASES
atomic beam scattering in hard-sphere, effects on beam velocity distribution, (T), 20: 15247 (N65-15530)
degeneracy of electron, with pair-creation effects at extremely high temperatures, (T), 20: 15229
density correlation functions for Maxwell, time-dependent, (T), 20: 15579
diffusion and coalescence in solids, theory of, 20: 15132 (ANL-7079)

diffusion of atoms in monatomic, time-dependent moments equations solutions for, 20: 15675
diffusion, properties, and trapping of radioactive iodine in waste, review on, 20: 14787 (CEA-Bib-64)
electric discharge system for plasma production from, 20: 15887(T) (AD-625789)
electric discharge in, kinetic theory of high-frequency resonance, (T), 20: 15575
equation of state for electron, numerical evaluation of, (T), 20: 15213
hydromagnetic wave propagation in suprathermal and thermal, equations for, (T), 20: 15198
hydrostatic equations for spheres of, in general relativity, (T), 20: 15211
ionization by electrons, equipment for measuring, 20: 15235(R) (AD-620289)
ionization by laser beams, 20: 15882(R) (NP-15868)
light scattering by, as test of Boltzmann equation, 20: 15580
magnetohydrodynamic shocks in nonaligned flow in perfect, (T), 20: 15576
neutron diffusion and distributions in heavy, thermal, (T), 20: 15677
neutron scattering in real, cluster expansion for inelastic, (T), 20: 15672
positron annihilation in electron, gamma momentum distributions from, (T), 20: 15383
radioactive, sampling and monitoring of waste, 20: 16137
radioinduced luminescence in, α, 20: 14617
stability of spherical, magnetic fields and rotation effects on thermal, (T), 20: 15876 (IPP-6/33)

GASTROINTESTINAL TRACT
calcium sorption in, calcium-47 tracer analysis of, 20: 14247
food retention time and mass of standard-man, 20: 14794
physiology of, in man, 20: 14794
radiation dose to, from ingested radioactive materials, 20: 14795

GEIGER-MUELLER TUBES
positioning ion-exchange column, engineering drawings of equipment for, 20: 14832

GENERAL ELECTRIC TEST REACTOR
design and experimental facilities of, 20: 16129

GENES
effects on anemias in mice, 20: 14290(R) (NYO-1800-12)

GENETICS
control of differentiation, theories on, 20: 14231 (BNL-931)
effects on cancer incidence in twins, 20: 14319
radiation and human, contributions of diagnostic procedures to significant dose in, 20: 14799
radiation effects on animal, review, 20: 14427
radiation effects on *E. coli* conjugation, uv, 20: 14329
radiation effects on human, review, 20: 14331
radiation effects on, in offspring of women given radiotherapy for ovarian cancer, 20: 14348
radioinduced dominant lethality in Drosophila, combined with acceleration, 20: 14343
radioinduced dominant lethality in Drosophila, combined with vibrations, 20: 14343

GEOMAGNETIC FIELDS
hydromagnetic waves in, anisotropic ionospheric effects on, (T), 20: 15619
parameters of, correlation with solar radiation time distributions, (E), 20: 15233
plasma resonances in, toroidal-mode, (T), 20: 15592
pulsation in, solar corpuscular beam and total eclipse effects on micro-, (E), 20: 15618
pulsation polarization in, mechanism for pc 5, (T), 20: 15616
pulsations in auroral zone, solar eclipse effects on micro-, (E), 20: 15617
pulsations in, classification and statistics of continuous, 20: 15613
pulsations in, polarization of long-period pc 5, (T), 20: 15615
pulsations in, transmission through lower exosphere and ionosphere, (T), 20: 15591 (RM-4858)
solar wind interactions with, particle trajectory distributions from, (T), 20: 15620

GEOPHYSICAL PROSPECTING
development, 20: 14770

GEOPHYSICS
seismic methods in, for studying liquid waste discharge to ground, 20: 14753 (BNWL-47)

GERMANIUM
determination in uranium tetrafluoride, spectrographic, 20: 14473
electron transmission through thin foils of, plasmon excitation in, (E), 20: 15951
energy level transitions in, Coster-Kronig, (T), 20: 15238 (CONF-233 (Vol.3), pp 398-418)
energy level widths for, K, (T), 20: 15239 (CONF-233(Vol.3), pp 419-39)
radiation effects on, neutron, 20: 14920 (TID-22664)
radiation effects on electric conductivity of, potassium ion, 20: 15978(T)
radiation effects on, low-temperature annealing of electron, 20: 15984(T)
radioinduced length changes in, apparatus for measurement of electron, 20: 15147
solvent properties for carbon, 20: 15047(R) (N65-15919)

GERMANIUM ALLOYS
Al–Ge, electron plasma oscillations in thin foil eutectoid, properties of, (E), 20: 15952
Ge–Fe, iron atom hyperfine fields in intermetallic compounds of, Mössbauer effect for determining, (E), 20: 15950
Ge–Hf, solvent properties for carbon, 20: 15047(R) (N65-15919)
Ge–Mg, thermodynamic properties, 20: 15056(R) (NYO-2916-10)

GERMANIUM ISOTOPES Ge-71
decay of, K/L ratio for electron-capture, (E/T), 20: 15713 (CONF-233 (Vol.2), pp 365-8)

GERMANIUM ISOTOPES Ge-72
energy level transitions from gallium-72 decay, electron pair production from, (E), 20: 15834
neutron reactions (n,α) at 14.6 Mev, isomeric cross section ratio for, (E/T), 20: 15773

GERMANIUM ISOTOPES Ge-76
proton reactions (p,n) at 2.3 to 11.0 Mev, excitation of isobaric analog states in, (E), 20: 15804

GERMANY
sea water desalination program in, 20: 16157

GLACIERS
snow layers of Alpine, radiometric dating of, 20: 14740

GLANDS
radiotherapy of epithelial tumors of lacrimal, x, 20: 14410

GLASS
analysis of, activation, 20: 14439(R) (GA-5556)
crystallization of barium oxide–borosilicate, effects of aluminum, lanthanum, and thorium oxides on, 20: 15075
effects of heat treatment and radiation on devitrification of alumina–phosphate, 20: 16133 (IDO-14672)
leachability of alumina–phosphate, prepared from radioactive calcined alumina waste, 20: 16133 (IDO-14672)
performance and properties of radiothermoluminescent, for dosimeters, 20: 14907
radiation effects on, bibliography on particle and short-wave, 20: 15134 (N65-15819)
radioinduced flow and stress relaxation in silica, proton, (T), 20: 15971
shock wave impingement on crushable foamglass, 20: 16023(R) (IITRI-578P21-16)
use in radiation source fabrication, 20: 14634(P)
waste oxide fixation in, 20: 16141(P)
CO_2–glass–N_2, heat transfer in glass-bead suspensions, 20: 14671(R) (TID-22394)

GLOBULIN
amino acids in, effects of lipid peroxidation on, 20: 14587

GLOVE BOXES
hot press design for, 20: 14666 (ORNL-P-1946)

GLUCOSE
determination of carbon-14-labeled, by liquid scintillation counting on on paper chromatograms, 20: 14479

GLUTAMIC ACID POLYMERS
tritium exchange reactions with hydrogen in, 20: 14628

GLUTATHIONE
radiosensitivity effects in Pseudomonas, 20: 14394

GLYCINE
complexes with cobalt, effects of neutron reactions (n,γ) on, 20: 14584(R) (TID-22444)
deuteron magnetic resonances in partially deuterated polycrystalline compounds of, quadrupole coupling constants from, (E), 20: 15957

GLYCOLIC ACID COMPLEXES
with neptunium, preparation and properties of, 20: 14556

GLYCOSIDES
radiation effects on content in rat blood serum, x, 20: 14378

GLYOXIME
radioinduced ESR spectra in single crystals of, at 77°K, 20: 14598

GLYOXIME, DIMETHYL-
radioinduced ESR spectra in single crystals of deuterated, at 77°K, 20: 14598

GLYOXIME, METHYL-
radioinduced ESR spectra in single crystals of, at 77°K, 20: 14598

GOATS
iodine-131 content in milk of, 20: 14243(R) (TID-22626)

GOLD
bremsstrahlung reactions (γ,n) at 8 to 16 Mev, spectra from, (E), 20: 15723 (MIT-2098-162)
bremsstrahlung reactions (γ,n) with, neutron emission in, (E), 20: 15724 (MIT-2098-224)
density of coatings on Mylar, measurement by x-ray fluorescence, 20: 14457(R) (ORNL-3889, pp 36-39)

determination in cosmic dust, activation, 20: 14475
determination in commercial plastics, activation, 20: 14439(R) (GA-5556)
determination in hair samples in criminal cases, activation, 20: 14439(R) (GA-5556)
determination in plutonium fluorides and peroxides, review on spectrographic, 20: 14464 (RFP-599)
determination in solutions by atomic absorption, 20: 14457(R) (ORNL-3889, pp 36-39)
determination in thumbnail clippings, activation, 20: 14439(R) (GA-5556)
effects of foils of, on charge states of oxygen-16 ions, 20: 15854
electron and positron reactions at 200 to 550 kev, excitation cross sections for K ionization in, 20: 15257
energy level transitions in, Coster-Kronig, (T), 20: 15238 (CONF-233 (Vol.3), pp 398-418)
energy level widths for, K, (T), 20: 15239 (CONF-233(Vol.3), pp 419-39)
gold-197 Mössbauer effect in crystals of, effects of crystal size on, (E), 20: 15962
ion reactions at 60, 80, and 90 kev, electron energy spectra from argon and neon, (E), 20: 15261
neutron resonance absorption by, method for measuring, 20: 15731(R) (RPI-328-49)
proton reactions (p,n) at 30 to 50 Mev, distributions from, 20: 15729(R) (RHEL/R-112, pp 37-66)
sputtering from neutron-irradiated foils of, 20: 14661(R) (ORNL-3889, pp 48-70)
wetting properties for uranium monocarbide, 20: 14551

GOLD ALLOYS
Al–Au, preparation of stoichiometric, 20: 14511(R) (ORNL-3889, pp 71-3)
Au–Y, crystal structure of intermetallic compound YAu_2 in, 20: 15102
Er–Au, electric conductivity at 4.2 to 300°K, effects of erbium content on, 20: 15083

GOLD COUPLES
Au–Sn, electric and thermal conductivity in superconducting, (E), 20: 15656

GOLD ISOTOPES Au-189
decay of, platinum-189 transitions from, (E), 20: 15781

GOLD ISOTOPES Au-197
energy-level parameters for, core-particle model for, 20: 15803
Mössbauer effect in gold crystals, effects of crystal size on, (E), 20: 15962
neutron reactions (n,γ) with, gamma spectra from thermal, (E), 20: 15756
proton reactions (p,n) at 2.3 to 11.0 Mev, excitation of isobaric analog states in, (E), 20: 15804

GOLD ISOTOPES Au-198
dosimetry in animals using hematological changes, 20: 14314
energy levels from gold-197 (n,γ) reactions, (E), 20: 15756
half life, (E), 20: 14461(R) (ORNL-3889, pp 48-70)
preparation of colloidal, 20: 14627 (PAEC(D)IS-651)
sorption by rat skin, 20: 14253
use in internal therapy, survey of techniques for, 20: 14406

GONADOTROPIC HORMONES
radiation effects on secretion of fish, x, 20: 14307

GONADS
radiation dose to, during extraoral radiography, 20: 14412
radiation effects on development of fish, effects of season and temperature on x, 20: 14307
radiation effects on cattle testicular, fractionated-dose whole-body x, 20: 14336
radiotherapy of cancer in ovarian, genetic damage to offspring from, 20: 14348

GRAPHITE
coating for, preparation of refractory, 20: 14974(P)
diffusion of uranium into, from uranium carbide pellets, 20: 15087
diffusion, permeability, and pore-size distribution in, model for correlating, (T), 20: 15104
electron reactions with, K electromagnetic wave spectra from, 20: 14442(R) (MCW-1493, pp 5-13)
neutron diffusion in, calculation of, 20: 15685
neutron pulse propagation in, thermalization effects in one-group analysis for thermal, (T), 20: 15678
performance of metal-impregnated, as ion source in thermionic cells, 20: 15296 (CONF-640921, pp 81-99)
radioinduced dimensional changes of, effects of specimen size on reactor, 20: 15143
reactions with hydrogen at 1550 to 2660°C, rate of, 20: 14508 (N65-20481)
reactions with refractory metal borides, carbides, nitrides, and oxides, 20: 14989

GRAPHITE (IMPREGNATED)
diffusion, permeability, and pore-size distribution in, model for correlating, (T), 20: 15104

GRAPHITE MODERATED REACTORS
design of pebble-bed, 20: 16043(P)
development of gas-cooled, review of, 20: 16035
performance of Beloyarsk type, for power–desalination uses, 20: 16107(T) (JPRS-33406)

GRAPHITE SYSTEMS
B_4C–graphite, fabrication of neutron shielding of, 20: 15027(P)

GRASS
radioactivity in vicinity of AERE, cesium-137 and strontium-90, 20: 14784(R) (AERE-R-5015)

GRAVITATION
collapse of uniform spheroid, (T), 20: 15206
dispersion of long-period acoustic-gravity waves from nuclear explosions, (T), 20: 15611
effect on convective stability of plasma in horizontal magnetic field, 20: 15907
field interactions with light beams, time-dependent intensity fluctuations from, (T), 20: 15636
field of magnetic universe, particle orbits in, 20: 15634
gravitational waves from isolated axially symmetric sources, (T), 20: 15637
theory of, quantum, 20: 15642

GREAT BRITAIN
sea water desalination program in, 20: 16157

GROUND
motion from underground explosions in salt, 20: 14663 (UCRL-14463 (Rev. 1))
waste disposal in, use of seismic methods for studying movement in, 20: 14753 (BNWL-47)

GROUND WATERS
tritium content, 20: 14744

GROWTH
effects of fetal, on strontium-85 uptake in mice, 20: 14244
radiation effects on plant-cell, indirect, 20: 14383

GUINEA PIGS
iodine-131 uptake by thyroid gland of, 20: 14245
isothiocyanate uptake by thyroid gland of, tracer study, 20: 14245

H

HAFNIUM
determination in glass samples, activation, 20: 14439(R) (GA-5556)
determination in zirconium dioxide, x-ray-fluorescence, 20: 14496
separation from zirconium by ion exchange, 20: 14657(P)

HAFNIUM ALLOYS
Al–Hf, solvent properties for carbon, 20: 15047(R) (N65-15919)
Ge–Hf, solvent properties for carbon, 20: 15047(R) (N65-15919)
Hf–Fe, solvent properties for carbon, 20: 15047(R) (N65-15919)
Hf–Nb–W–Y, properties for use in aerospace vehicles, 20: 15119
Hf–W, extrusion and swaging, 20: 15101
Hf–W, properties for high-temperature uses, 20: 15101
Hf–W, sintering, 20: 15021

HAFNIUM BORIDES
abrasive properties, 20: 15109

HAFNIUM CARBIDES
abrasive properties, 20: 15109
casting of, process development for, 20: 14968(R) (USBM-RC-1220)
hardness at 20 to 1500°C, 20: 14968(R) (USBM-RC-1220)
preparation of spherical particles of, procedure and apparatus for, 20: 14971(P)
reactions with copper and nickel mattes, slags, molten salts, and refractory metals, 20: 14989
tensile properties at 2150 and 2400°C, 20: 14968(R) (USBM-RC-1220)
thermodynamic properties of, at high temperatures, 20: 15052 (NP-15880)
HfC–ZrC, crystal structure of solid solutions in, x-ray studies of, 20: 15074

HAFNIUM ISOTOPES
deuteron reactions at 15 Mev, isomeric states from, (E), 20: 15856

HAFNIUM ISOTOPES Hf-176
energy level transitions in, conversion coefficients for E2, (E), 20: 15706 (CONF-233(Vol.2), pp 191-7)

HAFNIUM ISOTOPES Hf-177
energy level transitions in, delayed E1, (T), 20: 15765
energy level transition probabilities in, pairing correlations in E1, (T), 20: 15766
energy level transitions in, conversion electrons from E1, (E), 20: 15703 (CONF-233(Vol.2), pp 148-57)

HAFNIUM ISOTOPES Hf-178
half life of isomeric, (E), 20: 15688 (AD-620384)

HAFNIUM ISOTOPES Hf-179
energy level transitions in, delayed E1, (T), 20: 15765
energy level transition probabilities in, pairing correlations in E1, (T), 20: 15766
half life of isomeric, (E), 20: 15688 (AD-620384)

HAFNIUM OXIDES
preparation of spherical particles of, procedure and apparatus for, 20: 14971(P)
HAIR
analysis in criminal cases, activation, 20: 14439(R) (GA-5556)
analysis, forensic applications of activation, 20: 14661(R) (ORNL-3889, (pp 48-70)
arsenic content of Napoleon's, activation analysis, 20: 14478
HALOHYDROCARBONS
decomposition in ion source of mass spectrometer, mechanism of, 20: 14584(R) (TID-22444)
HANDBOOKS AND MANUALS
book: *Directory of the Nuclear Industry, USA*, 20: 16144 (AED-C-32-1 (Vol.1 and Vol.2))
for operation of JRR-4 experimental facilities, 20: 16122 (JAERI-6016)
of analytical methods used at ORNL, 20: 14428(R) (ORNL-3889)
HANDLING AND STORAGE
container design for spent fuel element, 20: 14679(P)
facility for spent reactor fuel element, 20: 16007(P)
HANDS
analysis of gunpowder residues on, activation, 20: 14439(R) (GA-5556)
analysis of nail clippings from, activation, 20: 14439(R) (GA-5556)
HANFORD WORKS, RICHLAND, WASH.
environs monitoring program at, 20: 14786 (BNWL-SA-465)
HASTELLOY X
reactions with plutonia, 20: 14965(R) (NUMEC-3524-12)
Hastelloy X–UO_2, sintering of, 20: 14965(R) (NUMEC-3524-12)
HAYNES 25 ALLOY
diffusion of hydrogen through coatings on, effects of base metal-coating reactions on, 20: 14987
HEALTH PHYSICS
safety regulations for Atomic Energy Center, Dacca, Pakistan, 20: 14783 (AECD/HP/2)
waste sampling and monitoring for studies in, instrumentation and techniques for, 20: 16137
HEART
radiation effects on function of dog, methods for measuring, 20: 14292(R) (TID-22563)
radioinduced atrial fibrillation in, following thyrotoxicosis therapy, β, 20: 14424
HEAT
effects of, combined with ethylene oxide on sterility of catgut sutures, 20: 14932
sources of, facility for studying curium oxide properties for use as, 20: 15038 (CONF-660305-12)
HEAT EXCHANGERS
tube holding device for, 20: 14698(P)
HEAT-RESISTING ALLOYS
creep and rupture of, numerical methods for analysis of, 20: 15041 (GEMP-397)
developments in research on, bibliography on, 20: 14506 (CRDL-SP-5-7)
HEAT TRANSFER
boiling burnout in water in internally cooled tubes, 20: 14686(R) (EURAEC-1448)
effects of transition-boiling, on fluid flow in single rod test sections, 20: 14687 (GEAP-4785)
film coefficients of, for suspensions of glass beads in carbon dioxide–nitrogen mixtures, 20: 14671(R) (TID-22394)
in nuclear rocket motor nozzles, effects of core position on, 20: 14727 (NASA-TM-X-1208)
in pressurized water systems, effects of vibrations on, (E), 20: 16000 (NYO-2655-1)
of finned surfaces with herring-boned patterns, (E/T), 20: 14685 (CEA-R-2471)
radiative equations for local thermodynamic equilibrium in nongray case, exact solution for, (T), 20: 15572
HEAT TRANSFER SYSTEMS
boiling in CVTR mockup, departure from nucleate, 20: 16101
design for storage facility for Hanford high-level wastes, 20: 16135 (RL-SA-62)
design of niobium-zirconium sealed tube, 20: 14699(P)
fluid flow in single rod, effect of transition boiling on, 20: 14687 (GEAP-4785)
heat transfer in pressurized water, effects of vibrations on, (E), 20: 16000 (NYO-2655-1)
pressure oscillations in pipes with closed end, (E/T), 20: 14690 (SC-DC-66-1293)
HEATERS
development of niobium carbide and zirconium carbide, 20: 15112
HEAVY WATER REACTORS
accidents in gas-cooled, computer program for dynamics of, 20: 16026 (UJV-1459/65)
development of organic-cooled power and process-heat, 20: 16109
heat transfer boiling burnout in eccentric annuli, (E), 20: 16086 (TID-22651)
HELIUM
corrosive effects on plutonium alloy and metal, effects of composition on, 20: 14984 (RFP-511)
electric discharges in, collision frequency measurements in afterglow of, (E), 20: 15867 (AD-620664)
electron temperature in plasma of, spectroscopic determination of, (E), 20: 15908
intermediate state between liquid I and liquid II, (E), 20: 15582
ionization of, cross sections for ruby-laser-multiphonon, (T), 20: 15276
meson (K^-) and (π^-) cascade and moderation times in liquid, (E), 20: 15273
microwave scattering by underdense cylindrical plasma of, phase-shift analysis for, (T), 20: 15894
reactions in O stars, burning, (T), 20: 15218
reactions with cesium, excitation transfer in, (E), 20: 15253
spectra of shock-heated plasma of, (E), 20: 15896
theory of rotating liquid II, measurement of mutual friction parameters in, 20: 15661
thermodynamic properties of Bose-Einstein assemblies of thin films of, (T), 20: 15645
vortex ring formation in superfluid, quantum theory of, 20: 15647
HELIUM FLUORIDES
wave functions of HeF, 20: 14541
HELIUM HYDRIDES
energy levels of, populations of vibrational, (T), 20: 15886(R) (UCRL-14285)
HELIUM IONS
hyperfine structure of monovalent positive helium-3, 20: 15260
HELIUM ISOTOPES
content in meteorites, 20: 15193 (NP-15654)
HELIUM ISOTOPES He-3
acoustic impedance and viscosity of, (E), 20: 15583
detection in products from nuclear reactions, engineering drawings of apparatus for, 20: 14906
electron inelastic scattering by, 20: 15439
hyperfine structure of monovalent positive ions of, (E), 20: 15260
leak control of gaseous, development of membrane for vacuum, 20: 14730 (AWRE-O-10/66)
polarization and relaxation processes in gaseous, 20: 15274
reactions (He-3,α) with nitrogen-14, association replacement amplitudes for, (T), 20: 15838
reactions (He-3,α) with nuclei, measurement and distorted wave analysis of, 20: 15855
reactions (He-3,α) with nickel-58 at 15 and 18 Mev, (E), 20: 15860
reactions (He-3,n) with carbon-12 at 1.97 to 4.70 Mev, angular distributions in, (E), 20: 15854
reactions (He-3,n) with light nuclei, angular distributions for direct, (T), 20: 15798
reactions (He,3,n) with boron-10, carbon-12, and carbon-13, angular distributions for, (T), 20: 15798
separation from tritium by sorption on carbon, 20: 14444(R) (MLM-1268)
thermal conductivity of solid, (T), 20: 15652
use in activation determination of, oxygen, 20: 14661(R) (ORNL-3889, pp 48-70)
HELIUM ISOTOPES He-4
phonon density in liquid, temperature dependence of, (E), 20: 15646
reactions in stellar cores during evolution, burning, (T), 20: 15207
thermal conductivity of solid, (T), 20: 15652
viscosity coefficients of liquid, temperature dependence of, (E), 20: 15646
HELIUM ISOTOPES He-6
beta decay of, double ionization in, (T), 20: 15715 (CONF-233(Vol.3), pp 505-9)
HELIUM OXIDES
wave functions of HeO, 20: 14541
HEMATO-ENCEPHALIC BARRIER
effects of radiomimetic compounds on permeability of, in rats, 20: 14312
radiation effects on permeability of rat, x, 20: 14312
HEMATOLOGY
computer analysis of cell volume distributions, 20: 14232 (LA-3440)
HEMOGLOBIN
amino acids in, effects of lipid peroxidation on, 20: 14587
radiation effects on bovine, fractionated-dose whole-body x, 20: 14336
HEMOLYSIS
radioinduced in erythrocytes, x, 20: 14275
HEPTADECYLAMINE
preparation, 20: 14576(R) (ORNL-3889, pp 73-7)
HETEROGENEOUS REACTORS
design of vapor-cooled, 20: 16106(P)
neutron flux measurements in, 20: 16028
HIGH-ALTITUDE EXPLOSIONS

acoustic-gravity wave production in atmosphere by, (T), 20: 15611
detection and identification in atmosphere and space, 20: 15594
detection by air fluorescence from emitted x rays, (T), 20: 15610
detection by emitted h-f electromagnetic radiation, (T), 20: 15605
detection by emitted low-frequency ground-wave electromagnetic pulses, (T), 20: 15606
detection of daytime, by prompt v-l-f phase anomalies, (T), 20: 15602
detection of deep-space, ground-based air-fluorescence system for, (T), 20: 15608
detection of, air fluorescence system for, 20: 15609
detection of, computer simulation of Vela satellite system for, 20: 15599
detection of, detector electronics of Vela satellite program for, 20: 15596
detection of, modular logic system for Vela program for, 20: 15597
detection of, redundancy design of Vela spacecraft for, 20: 15598
detection of, replenishment of spacecraft for, (T), 20: 15600
detection of, techniques for, 20: 15612
detection of, Vela satellite program for, 20: 15595
electromagnetic wave emission from, v-l-f, 20: 15601
properties of, 20: 15601
x-ray bursts from, discrimination from solar x-ray flares, 20: 15603

HIGH ENERGY INJECTION DEVICES
design of coaxial, engineering drawings for, 20: 15921
pump traps for ALICE, engineering drawings of high-conductance, 20: 15924
pumps for ALICE, engineering drawings of evaporative, 20: 15922
valves for ALICE, engineering drawings of bakeable, 20: 15923

HISTIDINE
iodine-131 exchange reactions between iodine and, chromatographic studies on, 20: 14632
lability of, in lipid-protein reaction systems, 20: 14587

HISTOLOGY
radiation effects on intestinal mucosa, x, 20: 14339

HOLMIUM
bremsstrahlung reactions (γ,n) at 8 to 16 Mev, spectra from, (E), 20: 15723 (MIT-2098-162)
bremsstrahlung reactions (γ,n) with, neutron emission in, (E), 20: 15724 (MIT-2098-224)
galvanomagnetic properties, 20: 15983(T)
thermal conductivity of polycrystalline, temperature dependence of, 20: 15117(T)

HOLMIUM ALLOYS
Ho–Fe, preparation and structure, 20: 15110
Ho–Mn, preparation and structure, 20: 15110
Ho–Y, electric conductivity of dilute, at low temperatures, 20: 15098

HOLMIUM ISOTOPES Ho-163
decay of, conversion electron spectra from, (E), 20: 15727 (PPAD-572F)

HOLMIUM ISOTOPES Ho-165
neutron capture at 0 to 55 ev with polarized, resonance spins from, (E), 20: 15681
neutron reactions (n,γ) with, gamma spectra from thermal, (E), 20: 15758

HOLMIUM ISOTOPES Ho-166
energy levels from holmium-165 (n,γ) reactions, (E), 20: 15758
energy levels from neutron capture by polarized holmium-165, spins of resonance, (E), 20: 15681

HOLMIUM NITRIDES
preparation, 20: 14511(R) (ORNL-3889, pp 71-3)

HOLMIUM OXIDES
crystal lattice constants at 296 and 94°K, 20: 15660
thermal expansion at 94 to 300°K, 20: 15660

HOLMIUM SULFIDES
preparation, 20: 14511(R) (ORNL-3889, pp 71-3)

HOMOGENEOUS REACTORS
book: *Critical Parameters of Homogeneous Multiplying Systems*, (T), 20: 16030
convection effects in, model for, (E), 20: 15996

HOSPITALS
radiosterilization in, value of, 20: 14943

HURON, LAKE
cesium-137 content in, 20: 14738 (NP-15853, pp 21-33)
radiation monitoring, α and β, 20: 14738 (NP-15853, pp 21-33)
strontium-89 content in, 20: 14738 (NP-15853, pp 21-33)
strontium-90 content in, 20: 14738 (NP-15853, pp 21-33)

HYDRAZYL, DIPHENYLPICRYL-
effects on radioinduced polymerization of triallyl cyanurate, 20: 14586

HYDROAROMATIC COMPOUNDS
reactions of, deuterium and tritium effects on electrophilic substitution, 20: 14577

HYDROCARBONS
analysis for hydrogen, activation, 20: 14480
effects on radiolysis of cyclopentane, 20: 14599

HYDROCHLORIC ACID
corrosive effects on types 416 and 430F stainless steels, effects of uranium on, 20: 14983 (NP-15875)
corrosive effects on niobium-base alloys, effects of alloy composition on, 20: 14997
effects on isotope exchange between uranium(IV) and uranium(VI), 20: 14570
HCl–methanol, effects on titanium and zirconium, corrosive, 20: 14988
HCl–methanol, radiolysis products from, analysis of, 20: 14581(R) (ORNL-3889, pp 14-16)
HCl–methanol, spectrophotometric analysis for metals, 20: 14469(R) (TID-22650)

HYDRODYNAMICS
equations for explosions, computer calculations for, (T), 20: 15571 (UCRL-14531)
equations of, in general relativity, (T), 20: 15626
stability in natural-circulation two-phase boiling loop, 20: 14684 (ANL-7073)

HYDROFLUORIC ACID
$HF–HNO_3$, corrosive effects on type-304L stainless steel, effects of aluminum, iron, and thorium ions on, 20: 14982(R) (NLCO-970, pp 6.1-4))

HYDROGEN
determination in alkali metals, methods for, 20: 14454(R) (ORNL-3889, pp 17-24)
determination in hydrocarbons, activation, 20: 14480
deuterium exchange between, and liquid ammonia, dual-temperature process for, 20: 14519
diffusion and permeation in molybdenum, coefficients for, 20: 14976 (AWRE-O-16/66)
diffusion through coatings on Haynes 25 alloy and stainless steel, effects of base metal-coating reactions on, 20: 14987
effects on alumina and zirconia at 1100 to 2000°C, 20: 14986
effects on brittleness of tantalum, 20: 15130
electron density and temperature in nonthermal plasma of, (T), 20: 15875 (IPP-3/32)
electron paramagnetic resonance of atomic, in x-irradiated beryl crystals, 20: 15982(T)
electron reactions with molecular, vibration excitation from, (T), 20: 15256
embrittlement of zirconium by, in slow-bend tests, 20: 14993
exchange of atomic and molecular, quantum mechanical model for, 20: 14518
exchange with deuterium in methane, catalytic effects of palladium alloys on, 20: 14542
exchange with tritium in poly-L-glutamic acid, 20: 14628
exchange with tritium in methane–water vapor mixtures, rate of, 20: 14662(R) (ORNL-TM-1394)
excitation in plasma, (T), 20: 15886(R) (UCRL-14285)
flow in copper test section, film boiling in, 20: 14697
heating of liquid, in nuclear rockets, 20: 14728 (NASA-TN-D-3328)
hydrogen ion reactions with molecules of, charge transfer in, (E), 20: 15250 (UCRL-6987(Rev.1))
ionization of, cross sections for ruby-laser-multiphonon, (T), 20: 15276
mass of, spectrometric determination of, 20: 15853
models for atomic, Lie-group theory in, 20: 14955
neutron diffusion in monatomic, time-dependent moments equations solutions for, 20: 15675
neutron diffusion and distribution in, thermal, (T), 20: 15677
nuclear spin relaxation in gaseous, at low densities, (E), 20: 15574
polarization of normal, ortho, and para, (E), 20: 15262
reactions in stars during evolution, burning, (T), 20: 15207
reactions with deuterium, angular distributions from atom-molecule, (T), 20: 15252
reactions with deuterium atoms, excitation-transfer cross sections for, (T), 20: 15255
reactions with graphite at 1550 to 2660°C, rate of, 20: 14508 (N65-20481)
reactions with hydrogen ions, Schroedinger equation for, 20: 14545
reactions with products from radiolysis of cyclopentane, 20: 14599
solubility in molybdenum, 20: 14976 (AWRE-O-16/66)
yields from gamma radiolysis of alkaline chromite and chromate solutions, 20: 14589
yields from gamma radiolysis of 1,3- and 1,4-cyclohexadienes, 20: 14610
yields from radiolysis of sodium acid phosphite solutions in sodium nitrate, effects of pH on, 20: 14601
yields in gamma radiolysis of deaerated methanol, effects of sulfuric acid on, 20: 14579(R) (NYO-2383-15)

HYDROGEN ION CONCENTRATION
effects on damage to barley seeds induced by diethyl sulfate and radiation, 20: 14384
radiosensitivity effects on phage inactivation and thymine dimerization, uv, 20: 14356

HYDROGEN IONS

acceleration of negative, in AVF cyclotron, 20: 15180
reactions with hydrogen molecules, charge transfer in, (E), 20: 15250 (UCRL-6987(Rev.1))
reactions with hydrogen, Schroedinger equation for, 20: 14545
reactions with nitrogen, cross sections for, (E/T), 20: 15886(R) (UCRL-14285)
vibrations in alkaline earth fluoride crystals, spectra of localized, 20: 15969

HYDROGEN PEROXIDES
formation in radioinduced oxidation of cyclohexane, 20: 14625
photolysis of methanolic, mechanism of, 20: 14579(R) (NYO-2383-15)
production of gamma radiolysis of aerated methanol, effects of sulfuric acid on, 20: 14579(R) (NYO-2383-15)

HYDROGEN SELENIDES
vibrational potential function of bent molecules of, third-order, 20: 14559
vibrational potential function of deuterium-labeled bent molecules of, third-order, 20: 14559

HYDROGEN SULFIDES
reactions with niobium and tantalum at 1000 to 1400°C, 20: 14554
vibrational potential function of bent molecules of, third-order, 20: 14559

HYDROGEN SYSTEMS
Gd–H–Y, crystal structure, 20: 14546

HYDROMAGNETIC WAVES
polarization and power spectrum in geomagnetic fields, anisotropic ionospheric effects on, (T), 20: 15619
production by dielectric sphere oscillations in mercury, 20: 15581
propagation in lower exosphere and ionosphere, (T), 20: 15591 (RM-4858)
propagation in magnetoplasma waveguides, viscous effects on, (T), 20: 15925
propagation in nonuniform plasma, (T), 20: 15890
propagation in suprathermal and thermal gases, equations for, (T), 20: 15198

HYDROXYL RADICAL
electric dipole moment, 20: 15272
hyperfine structure in oxygen-17, 20: 15272

HYGROMETERS
design and performance of radiometric, using alpha sources, 20: 14840

HYPERFRAGMENTS
decay rates of, effects of nuclear contraction on, (T), 20: 15826
wave functions for, effects of compressibility on, (T), 20: 15826

HYPERONS
decay of, nonleptonic, (T), 20: 15369
interactions with protons at low energies, (T), 20: 15413

HYPERONS (Λ)
interactions with nucleons in hypernuclei, nuclear contraction effects from, (T), 20: 15826
photoproduction on proton at 1100–1300 Mev, cross sections for, (E), 20: 15393
production in meson (π^-) reactions with xenon at 9 Bev/c, cross sections for, (E), 20: 15841
production in meson (π)-proton interactions, two-resonance model for, (T), 20: 15392

HYPERONS (Λ^0)
isospin mixing with hyperons (Σ^0), methods for determining, 20: 15401

HYPERONS (Σ^0)
isospin mixing with hyperons (Λ^0), methods for determining, 20: 15401

HYPERONS (Σ^+)
decay of, G_2 symmetry scheme for, 20: 15474
production in meson (π^+)-proton interactions, (E/T), 20: 15400

HYPERTHYROIDISM
radiotherapy of, thyrotropin treatment of hypothyroidism following iodine-131, 20: 14338

HYPOTHYROIDISM
radioinduced, thyrotropin treatment for iodine-131, 20: 14338

I

IMMUNE REACTIONS
radiation effects, combined with thymectomy on, 20: 14354

IMMUNITY
radiation effects on anti-syphilis, in man and rabbits, γ, 20: 14308

INCONEL
radiation embrittlement of types 600, 625, and X750, thermal-neutron, 20: 15141

INDIA
power reactor fuel development programs in, 20: 16099

INDIAN OCEAN
fallout contamination of southern, from 1961 thermonuclear tests, 20: 14749

INDIUM
bremsstrahlung reactions (γ,n) at 8 to 16 Mev, spectra from, (E), 20: 15723 (MIT-2098-162)
bremsstrahlung reactions (γ,n) with, neutron emission in, (E), 20: 15724 (MIT-2098-224)
conductivity in superconducting films of, electric and thermal, (E), 20: 15656
electron tunneling in thick films of superconducting, geometrical resonances in, (E/T), 20: 15650
energy level transitions in, Coster-Kronig, (T), 20: 15238 (CONF-233 (Vol.3), pp 398-418)
proton reactions (p,n) at 30 to 50 Mev, distributions from, 20: 15729(R) (RHEL/R-37-66)

INDIUM ALLOYS
In–Pb, heat absorption and emission by superconducting, Peltier effect in, (E), 20: 15649
In–Pb, superconductivity of, critical field of, 20: 15105
Sb–In, radioinduced defects in intermetallic compounds of, energy spectra of gamma, 20: 15979(T)

INDIUM ISOTOPES
beta decay of, effect of Coulomb field on, (T), 20: 15716 (CONF-233 (Vol.3), pp 529-37)

INDIUM ISOTOPES In-109
energy levels from tin-109 decay, (E), 20: 15752

INDIUM ISOTOPES In-113
gamma reactions (γ,γ'), cross section for isomer formation in, 20: 15748
half life of isomeric, 20: 15748

INDIUM ISOTOPES In-114
isomeric transitions in, multipolarity of, (E), 20: 15753

5-INDOLOL, 3-(2-AMINOETHYL)-
radiosensitivity effects on *Drosophila melanogaster*, 20: 14398

INDUCTION FURNACES
design for melting and casting uranium-233, 20: 15003 (LA-DC-7510)
equipment for levitation melting and casting of aluminum alloys, 20: 15013

INFECTIONS
radiation effects on bacteriophage, in *Escherichia coli*, uv, 20: 14271
radiation effects on incidence of *Streptococcus equi*, in burros, 20: 14288 (AD-627986)
radiation effects on immune reaction to *Treponema pallidum*, γ, 20: 14308
radioinduced by radical neck dissection, x, 20: 14303
surgically-induced by radical neck dissection, 20: 14303

INFRARED SPECTROSCOPY
use of, in examination of inorganic and organic compounds, summary on, 20: 14459(R) (ORNL-3889, pp 44-6)

INK
analysis in criminal cases, activation, 20: 14439(R) (GA-5556)

INSECTS
radiation control of populations of wood-boring, γ, 20: 14305
radiation control of populations of *Psila rosae*, γ, 20: 14317
radiation control of *Platynota stultana*, γ, 20: 14340
radiation effects on Musca emergence from pupae, x, 20: 14306
radiosensitivity of Mediterranean and oriental fruit flies and parasites, γ, 20: 14935

INSTRUMENTATION
power supplies for reactor, with positive and negative outputs, 20: 14818 (ORNL-TM-1391)

INSTRUMENTS
design for detecting high-altitude explosions, 20: 15612
design for monitoring evaporation of thin films, 20: 14819 (RFP-602)
design for studying radiation effects on electronics, 20: 14918(R) (ECOM-01313-1)
design of electrodeless toroidal, for conductometric analysis, 20: 14465 (RFP-657)
performance of radiometric, scale linearity in, 20: 14836
tariffs on nuclear, European, 20: 16155
use of radioisotope, review of industrial, 20: 14835

INTERMETALLIC COMPOUNDS
solubility of semiconducting AB, theory of retrograde, 20: 15056(R) (NYO-2916-10)

INTERNAL COMBUSTION ENGINES
use of automobile, in air filtration system, 20: 14672

INTERNAL CONVERSION
measurement by internal-external method, photoelectric angular distributions in, 20: 15709 (CONF-233(Vol.2), pp 247-51)
measurement using lens type spectrometers, properties of, 20: 15710 (CONF-233(Vol.2), pp 252-5)
research on, 20: 15697 (CONF-233(Vol.2))
transitions in, review of, 20: 15694 (CONF-233(Vol.1), pp 1-29)

INTESTINE
ion transport across membrane of rabbit, 20: 14243(R) (TID-22626)
radiation effects on phospholipids in rabbit, γ, 20: 14278
radiation effects on, after abdominal therapy, x, 20: 14339
radiation effects on mucosa of exteriorized rat, x, 20: 14364

IODIDES

determination in off-gases from uranium irradiation, chromatographic, 20: 14454(R) (ORNL-3889, pp 17-24)
IODINE
bremsstrahlung reactions (γ,n) at 8 to 16 Mev, spectra from, (E), 20: 15723 (MIT-2098-162)
bremsstrahlung reactions (γ,n) with, neutron emission in, (E), 20: 15724 (MIT-2098-224)
determination in potassium dioxodifluoroiodate(V), titrimetric, 20: 14455(R) (ORNL-3889, pp 25-32)
diffusion, properties, and trapping of radioactive, in waste gases, 20: 14787 (CEA-Bib-64)
effects on NMR spectra of iodine-127 in potassium and sodium iodides, 20: 14573
iodine-131 exchange reactions between amino acids and, chromatographic studies on, 20: 14632
metabolism in dogs, tracer study, 20: 14249
metabolism in man, mathematical model of, 20: 14249
metabolism in man, tracer study, 20: 14249
metabolism in man, mathematical model of, 20: 14250
reactions in aqueous media, chronopotentiometry and voltammetry of, 20: 14455(R) (ORNL-3889, pp 25-32)
reactions of recoil, mechanisms of, 20: 14620
sorption by activated carbon, potentiometric studies at 0 and 50°C on, 20: 15065(T) (ORNL-tr-1018)
stability in benzene and cyclohexane, determination of, 20: 14454(R) (ORNL-3889, pp 17-24)
IODINE COMPOUNDS
diffusion, properties, and trapping of radioactive, in waste gases, 20: 14787 (CEA-Bib-64)
IODINE ISOTOPES I-123
production by proton reactions with tellurium-123, (E), 20: 14461(R) (ORNL-3889, pp 48-70)
IODINE ISOTOPES I-125
energy level transitions in, conversion coefficients for, (E), 20: 15701 (CONF-233(Vol.2), pp 128-41)
use in miniature x-ray device, 20: 14677(P)
IODINE ISOTOPES I-126
decay of, beta-gamma directional correlations in, (E), 20: 15845
IODINE ISOTOPES I-127
energy level transitions in, conversion coefficients for, (E), 20: 15701 (CONF-233(Vol.2), pp 128-41)
neutron capture by, iodine-128 low-lying levels from thermal, (E), 20: 15831
nuclear magnetic resonance spectra in potassium and sodium iodides, effects of iodine on, 20: 14573
IODINE ISOTOPES I-128
energy levels of, parities and spins of low-lying, (E), 20: 15831
IODINE ISOTOPES I-129
effects on radioinduced ESR spectra of iodoethane, 20: 14597
neutron reactions with, production of iodine-130 isomer in, (E), 20: 15772
IODINE ISOTOPES I-130
production of isomeric, (E), 20: 15772
IODINE ISOTOPES I-131
beta emissions from, duplication of energy distribution of, 20: 14928
content in milk in vicinity of AERE, 20: 14784(R) (AERE-R-5015)
content in milk, assessment of, 20: 14243(R) (TID-22626)
dosimetry in animals using hematological changes, 20: 14314
effects on heart following thyrotoxicosis therapy, 20: 14424
effects on hyperthyroidism, hypothroidism induced by, 20: 14338
exchange between amino acids and iodine, chromatographic studies on, 20: 14632
ingestion in milk, 1965, 20: 14243(R) (TID-22626)
production of high-purity, radiochemistry of, 20: 14461(R) (ORNL-3889, pp 48-70)
production, release, and transport of, in reactor containment systems, 20: 14804
radiation effects on uptake by rat erythrocytes, γ, 20: 14276
uptake by thyroid gland of guinea pigs, 20: 14245
use in internal therapy, survey of techniques for, 20: 14406
IODINE ISOTOPES I-132
beta emissions from, duplication of energy distribution of, 20: 14928
IODINE ISOTOPES I-133
half life, (E), 20: 14461(R) (ORNL-3889, pp 48-70)
ION BEAMS
optical properties in double-focusing spectrometer, 20: 14822(R) (RHEL/R-112, pp 99-128)
ION EXCHANGE MATERIALS
properties of aluminum silicate zeolites for sorption and storage of cesium-137 and strontium-90, 20: 14466 (RL-SA-58)
properties of, for sorption of cesium-137 and strontium-90 from waste solutions, 20: 14434
sorptive properties of synthetic zeolite for krypton and xenon, 20: 14444(R) (MLM-1268)
ION EXCHANGE PROCESSES
methods for fission product recovery, review on developments in, 20: 14436 (BNWL-SA-504)
ION EXCHANGERS
instrumentation of, remote-control positioner for, 20: 14832
ION SOURCES
design for reactor fuel burnup analysis by mass spectrography, 20: 16046
design of crossed-beam, 20: 15235(R) (AD-620289)
IONIZATION
calculations for photo-, model for atomic excited states used in, 20: 15270
research programs on surface, 20: 14458(R) (ORNL-3889, pp 39-43)
IONIZATION CHAMBERS
calibration, 20: 14894
design for fallout-shelter monitor, engineering drawings for, 20: 14903
design of Kanne, for low-energy beta particles, engineering drawings for, 20: 14905
design with control grid, 20: 14917(P)
performance for measurement of absorbed dose, 20: 14894
performance in alpha spectrometers, 20: 14857 (NP-15448)
performance of argon liquid-filled, for x rays, 20: 15259
saturation characteristics of cylindrical and spherical, 20: 14884
IONOSPHERE
effects of anisotropic, on geomagnetic field oscillations, (T), 20: 15619
electron density distribution in F2 layer of, (T), 20: 15586 (AD-620243)
electron density distribution in D region of, v-l-f measurements for determining, 20: 15604
electron density irregularities and plasma resonances in, (E), 20: 15622
hydromagnetic wave propagation in, (T), 20: 15591 (RM-4858)
ionization in sporadic E polar region, spiral distribution of, (E), 20: 15614
plasma resonances in dipole field in, toroidal-mode, (T), 20: 15592
IONS
oscillations in bounded plasma, hydrodynamic model for, (T), 20: 15900
reactions of heavy, with heavy nuclei, production of transcurium elements by, 20: 15740
scattering by nuclei, collective-state excitation in, (T), 20: 15763
scattering by nuclei, gamma-ion angular correlations in inelastic, (T), 20: 15767
IRIDIUM
deposition on niobium and tantalum, methods for, 20: 15004(R) (N65-20790)
determination in uranium oxides, activation, 20: 14495
energy level transitions in, Coster-Kronig, (T), 20: 15238 (CONF-233 (Vol.3), pp 398-418)
neutron capture by, gamma spectra from thermal, (E), 20: 15787
properties of, for use as protective coating on niobium and tantalum, 20: 15004(R) (N65-20790)
IRIDIUM ISOTOPES Ir-192
gamma spectra, (E), 20: 14845 (AD-620434)
use as radiographic source, limitations in, 20: 14705
use in internal therapy, survey of techniques for, 20: 14406
IRON
analysis and determination, 20: 14500
analysis for trace impurities, activation, 20: 14471
determination in ferromagnetic films, activation, 20: 14489
determination in plutonium fluorides and peroxides, review on spectrographic, 20: 14464 (RFP-599)
determination in silts in water, activation, 20: 14439(R) (GA-5556)
determination in uranium tetrafluoride, spectrographic, 20: 14473
effects on spectrofluorimetric determination of scandium, 20: 14476
effects on spectrophotometric determination of thorium using Chrome Azurol S, 20: 14485
effects on thermal conductivity of Springfields uranium at 160 to 620°C, 20: 15084
electric fields in germanium–iron intermetallic compounds, Mössbauer effect for determining hyperfine, (E), 20: 15950
electron diffusion in slabs of, differential energy spectra and number transmission for, (T), 20: 15936
electron reactions with, K and L x-ray spectra from, 20: 14442(R) (MCW-1493, pp 5-13)
energy level transitions in, Coster-Kronig, (T), 20: 15238 (CONF-233 (Vol.3), pp 398-418)
energy level widths for, K, (T), 20: 15239 (CONF-233(Vol.3), pp 419-39)
gamma spectra in, from uranium-235 fission products, 20: 14733 (AD-628982)
neutron capture by, gamma spectra from resonance, (E), 20: 15731(R) (RPI-328-49)
neutron elastic scattering at 0.8 Mev, cross sections for, (T), 20: 15770
neutron resonance absorption integrals for, (E), 20: 15691 (CEA-R-2840)
radiation effects on wear-resistance of cast and wrought, fast-neutron, 20: 15140

separation of manganese-54 from irradiated, by ion exchange, 20: 14433(R) (BAW-298)
IRON ALLOYS
Al–Fe–U, fabrication for nuclear fuel, 20: 15022(P)
Al–Fe–U, fabrication for nuclear fuel, 20: 15023(P)
Al–Fe–U, fabrication for nuclear fuel, 20: 15024(P)
Cr–Fe–Mo, strain aging of, 20: 15063 (UCRL-16585)
Cr–Fe–Zr, corrosion by steam at 300 to 500°C, effects of nitrogen impurity content on, 20: 14980(R) (GEAP-5065)
Cr–Fe–Zr, corrosion by steam at 500°C, effects of metallurgical processing variables on, 20: 14980(R) (GEAP-5065)
Dy–Fe, preparation and structure, 20: 15110
Er–Fe, preparation and structure, 20: 15110
Fe–Lu, preparation and structure, 20: 15110
Fe–Mo, strain aging of, 20: 15063 (UCRL-16585)
Fe–Nb, analysis for trace metals, polarographic, 20: 14455(R) (ORNL-3889, pp 25-32)
Fe–Ni, analysis of films of, for iron and nickel, 20: 14489
Fe–rare earths, preparation and structure, 20: 15110
Fe–Th, preparation and structure, 20: 15110
Fe–Ti, thermal capacity at 0.24 to 4.20°K, 20: 15061 (UCRL-11580)
Fe–Tm, preparation and structure, 20: 15110
Fe–Y, preparation and structure, 20: 15110
Fe–Yb, preparation and structure, 20: 15110
Gd–Fe, preparation and structure, 20: 15110
Ge–Fe, iron atom hyperfine fields in intermetallic compounds of, Mössbauer effect for determining, (E), 20: 15950
Hf–Fe, solvent properties for carbon, 20: 15047(R) (N65-15919)
Ho–Fe, preparation and structure, 20: 15110
IRON, BISCYCLOPENTADIENYL-
decomposition in ion source of mass spectrometer, mechanism of, 20: 14584(R) (TID-22444)
IRON CARBIDES
Fe–Fe_3C, ductility of two-phase, effects of composition and particle size on, 20: 15055(R) (NYO-2394-19)
IRON CARBONYLS
decomposition in ion source of mass spectrometer, mechanism of, 20: 14584(R) (TID-22444)
IRON(III) CHLORIDES
corrosive effects on types 416 and 430F stainless steels, effects of uranium on, 20: 14983 (NP-15875)
IRON IONS
effects on corrosion of type 304L stainless steel by hydrofluoric acid–nitric acid solutions, 20: 14982(R) (NLCO-970, pp 6.1-4)
electron transfer between divalent and trivalent, effects of sulfate ions on, 20: 14574
isotopic exchange between divalent and trivalent, effects of chloride ions on, 20: 14571
IRON ISOTOPES
diffusion in beryllium, tracer studies on, 20: 15037 (CEA-R-2621)
exchange between iron(II) and iron(III) in dimethyl sulfoxide, effects of chloride ions on, 20: 14571
IRON ISOTOPES Fe-54
proton inelastic scattering at 7.0 to 8.5 Mev, excited state decay from, (E), 20: 15786
IRON ISOTOPES Fe-55
decay of, K/L ratio for electron-capture, (E/T), 20: 15713 (CONF-233 (Vol.2), pp 365-8)
decay of, K/L ratio for electron-capture, (E/T), 20: 15713 (CONF-233 (Vol.2),pp 365-8)
use in determining automotive engine wear rates, 20: 14661(R) (ORNL-3889, pp 48-70)
IRON ISOTOPES Fe-56
proton scattering at 150 to 180 Mev, models for, 20: 15730(R) (RHEL/R-112, pp 67-98)
proton total cross sections at 30 and 50 Mev, (E), 20: 15729(R) (RHEL/R-112, pp 37-66)
IRON ISOTOPES Fe-57
energy levels of, hyperfine structure of 14.4 kev, 20: 15775
Mössbauer effect in iron sulfates of jarosite group, 20: 15775
nitrogen-ion scattering at 16.2 and 17.7 Mev, gamma polarization from, (E), 20: 15759
IRON ISOTOPES Fe-59
chelated with carbon-14-labeled EDTA, penetration in cuticular membrane of tomatoes, 20: 16147 (COO-888-45)
chelated with carbon-14-labeled EDDHA, penetration in cuticular membranes of tomatoes, 20: 16147 (COO-888-45)
content in lambs after natural exposure, 20: 14243(R) (TID-22626)
separation from manganese-54 by ion exchange, 20: 14433(R) (BAW-298)
uptake of, whole-body counter for measuring, 20: 14422
IRON OXIDES
effects on sorption of cesium and strontium by clay minerals and soils, 20: 14652
use of paste of radioactive, in magnetic-particle inspection, 20: 14721(P)
FeO_2O_3–Nb_2O_5, density and surface ductility of fused, at 1200 to 1650°C, 20: 15076
Fe_2O_3–V_2O_5, density and surface ductility of fused, at 1200 to 1650°C, 20: 15076
IRON SULFATES
iron-57 Mössbauer effect in, of jarosite group, 20: 15775
penetration of iron-59-labeled, in cuticular membranes of tomatoes, 20: 16147 (COO-888-45)
IRON SULFIDES
iron-57 Mössbauer spectra in, performance of on-line computer for studying, 20: 15973
IRON SYSTEMS
Al–C–Fe–Nb, phase studies, 20: 15103
Al–C–Fe–Ta, phase studies, 20: 15103
Al–C–Fe–U, mechanical properties at intermediate strain rates and temperatures, 20: 15081
B–Fe–Mo, crystal structure, 20: 14532
B–Fe–Nb, crystal structure, 20: 14532
B–Fe–V, crystal structure, 20: 14532
B–Fe–W, crystal structure, 20: 14532
B–Fe–Zr, crystal structure, 20: 14532
Fe–Fe_3C, ductility of two-phase, effects of composition and particle size on, 20: 15055(R) (NYO-2394-19)
IRON TITANATES
performance as space radiator coating on beryllium, niobium–1 zirconium, and type 310 stainless steel, 20: 15057(R) (PWA-2750)
IRRADIATION FACILITIES
development and use of, for teletherapy in France, 20: 14425
for nerve ganglion using beta applicator, 20: 14332
inspection and licensing procedures for gamma, 20: 14944
radiation monitoring of, 20: 14812
IRRADIATION TECHNIQUES
development of high-energy electron, 20: 15188(P)
dose distribution from pulsed electron beams on surfaces, uniformity of, (T), 20: 15178
ISOTHIOCYANATES
uptake by thyroid gland of guinea pigs, tracer study, 20: 14245
ISOTOPE EFFECTS
of deuterium and iodine-129 on radioinduced ESR spectra of iodoethane, 20: 14597
of deuterium and tritium on mechanism of electrophilic aromatic substitutions, 20: 14577
of deuterium on electric conductivity of ions in water at 25°C, 20: 14540
on rate constants for unimolecular reactions, temperature-independent factor in, 20: 14544
separations in aqueous solutions using electrolytic countercurrent exchange processes, 20: 14947
ISOTOPE SEPARATION METHODS
efficiency of countercurrent electrolysis, 20: 14947
ISOTOPES
separation in aqueous solution using electrolytic countercurrent exchange processes, 20: 14947
ISOTOPIC EXCHANGE
between hydrogen and liquid ammonia, dual temperature process for, 20: 14519
between iron(II) and iron(III) in dimethyl sulfoxide, effects of chloride ions on, 20: 14571
kinetics of, on surface of ionic crystals, 20: 14572
of uranium-235 between uranium(IV) and uranium(VI), 20: 14570
ISRAEL
oceanography of continental shelf of Mediterranean Sea adjoining, 20: 14731(R) (NP-159861)
sea water desalination program in, 20: 16157
ITALY
sea water desalination program in, 20: 16157

J

JAPAN
fallout distribution in soils of, 20: 14751
radiation dose to population in, genetically-significant, 20: 14799
sea water desalination program in, 20: 16157
JAPANESE POWER DEMONSTRATION REACTOR (II)
core design for, hydraulic and thermal calculations for, 20: 16076 (JAERI-1088)
JAWS
radiation dose to, during extraoral radiography, 20: 14412
radiation effects on, following facial therapy, γ and x, 20: 14324
JETS
plasma production by hypervelocity copper, 20: 15920

K

KIDNEYS
function tests on, evaluation of radioisotope, 20: 14296
radiation effects on thymidine index in cells of rat, x, 20: 14258 (AD-627569)
radiation effects on function of, following radiotherapy of abdominal and pelvic tumors, 20: 14296
radiation effects on function of rabbit, combined with trauma, x, 20: 14325
radiation effects on function of canine, x, 20: 14342

KRYPTON
electron spectra from, j-j coupling for L Auger, (T), 20: 15237 (CONF-233(Vol.3), pp 371-97)
energy level transitions in, Coster-Kronig, (T), 20: 15238 (CONF-233 (Vol.3), pp 398-418)
energy level widths for, K, (T), 20: 15239 (CONF-233(Vol.3), pp 419-39)
ionization in mass spectrometer, formation of multiply charged ions in, 20: 14584(R) (TID-22444)
ionization of, cross sections for ruby-laser-multiphonon, (T), 20: 15276
oxygen ion reactions with atoms of, at 25 to 230 kev, (E), 20: 15249 (TID-22648)
photochemical reactions with fluorine or oxygen difluoride, 20: 14527
reactions with cesium, excitation transfer in, (E), 20: 15253
recovery from irradiated reactor fuels during dissolution, 20: 15133(R) (GEAP-4893)
sorption by synthetic zeolite, 20: 14444(R) (MLM-1268)

KRYPTON FLUORIDES
production from krypton and fluorine or oxygen difluoride, photochemical, 20: 14527

KRYPTON ISOTOPES Kr-79
decay of, K/L ratio for electron-capture, (E/T), 20: 15713 (CONF-233 (Vol.2), pp 365-8)
decay scheme, (E), 20: 15802

KRYPTON ISOTOPES Kr-85
disposal by in-pile activation to stable or short-lived isotopes, (T), 20: 16132 (BNL-8558)

L

LABORATORIES
operation of ORNL spectrochemical analytical, 20: 14428(R) (ORNL-3889)
radiation monitoring equipment for, 20: 14872

LACTATES
determination of carbon-14-labeled, by liquid scintillation counting on paper chromatograms, 20: 14479

LACTIC ACID
content in dog blood, effects of exercise and inhaled yttrium oxide on, 20: 14257

LACTIC ACID COMPLEXES
with neptunium, preparation and properties of, 20: 14556

LAMINATES
design of, for radiation shielding, 20: 14680(P)

LANTHANUM
bremsstrahlung reactions (γ,n) at 8 to 16 Mev, spectra from, (E), 20: 15723 (MIT-2098-162)
bremsstrahlung reactions (γ,n) with, neutron emission in, (E), 20: 15724 (MIT-2098-224)
determination by conductometric titration using selenious acid, 20: 14484
determination in paper samples in criminal cases, activation, 20: 14439(R) (GA-5556)
determination in silts in water, activation, 20: 14439(R) (GA-5556)
determination in soils, activation, 20: 14439(R) (GA-5556)

LANTHANUM ALLOYS
La–Y, electric conductivity of dilute, at low temperatures, (E), 20: 15098

LANTHANUM CHLORIDES
reactions with fused lithium chloride–potassium chloride eutectic, 20: 14565
spectra of single crystals of, crystal-field splitting of cerium-doped, 20: 14553

LANTHANUM COMPLEXES
with [(1,2-dimethylethylene)dinitrilo]tetraacetic acid, stability constants of, 20: 14521

LANTHANUM FLUORIDES
vapor pressure studies at 1325 to 1650°K, 20: 14515 (UCRL-16649)

LANTHANUM ISOTOPES
deuteron reactions at 15 Mev, isomeric states from, (E), 20: 15856

LANTHANUM ISOTOPES La-138
atomic mass, (E), 20: 15769

LANTHANUM ISOTOPES La-139
atomic mass, (E), 20: 15769

LANTHANUM ISOTOPES La-140
beta transitions in, matrix elements for first-forbidden, (E), 20: 15824

LANTHANUM NITRATES
density and viscosity of aqueous solutions of, 20: 14648
reactions with ammonium carbonate in aqueous solution, 20: 14535
$Al(NO_3)_3$–$La(NO_3)_3$, density and viscosity of solutions of, 20: 14648
$La(NO_3)_3$–tributyl phosphate, density and viscosity of, 20: 14648

LANTHANUM OXIDES
effects on crystal growth in optical glasses, 20: 15075
$Al(NO_3)_3$–La_2O_3, compound formation in, at 1200°C, 20: 14539
Al_2O_3–La_2O_3, compound formation in, at 1600 to 1650°C, 20: 14539
La_2O_3–WO_3, preparation and properties, 20: 14534

LANTHANUM TELLURIDES
crystal structure, 20: 14524
phase studies, 20: 14530

LARVAE
radiation effects on infectivity of Schistosoma, effects on mouse antibody titer of gamma, 20: 14304

LATINA POWER REACTOR
control and safety devices for, 20: 16067 (EUR-2420.d,f,i,n,e, pp 117-31)
control system for regulating power output of, 20: 16072 (EUR-2420.d,f,i,n,e, pp 203-14)
control systems for, design of, 20: 16066 (EUR-2420.d,f,i,n,e, pp 51-115)
development, 20: 16064 (EUR-2420.d,f,i,n,e)
fuel can ruptures in, detection system for, 20: 16070 (EUR-2420.d,f,i,n,e, pp 181-9)

LAURIC ACID
determination in commercial coconut oils, gas chromatographic, 20: 14463 (PAEC(D)CH-652)

LEAD
analysis and determination, 20: 14500
conductivity in superconducting films of, electric and thermal, (E), 20: 15656
content in red-colored Paleozoic deposits in Northern Tien Shan, 20: 14780(T) (AEC-tr-6579)
determination by radiometry using iodine-131, 20: 14661(R) (ORNL-3889, pp 48-70)
determination in airborne dusts, spectrochemical, 20: 14457(R) (ORNL-3889, pp 36-39)
determination in iron–niobium alloys, chromatographic, 20: 14455(R) (ORNL-3889, pp 25-32)
determination in plutonium fluorides and peroxides, review on spectrographic, 20: 14464 (RFP-599)
determination in uranium tetrafluoride, spectrographic, 20: 14473
electron and positron reactions at 200 to 550 kev, excitation cross sections for K ionization in, (E), 20: 15257
electron diffusion in slabs of, differential energy spectra and number transmission for, (T), 20: 15936
electron tunneling in junctions of superconducting, subharmonic structure in, (E/T), 20: 15651
isotopic distribution in impact crater tektites, 20: 14458(R) (ORNL-3889, pp 39-43)
leaching from alumina–phosphate glass prepared from calcined alumina waste, 20: 16133 (IDO-14672)
neutron elastic scattering at 0.8 Mev, cross sections for, (T), 20: 15770
neutron scattering by, cross sections for free and coherent, 20: 15682
stress analysis of radioisotope containers of, from internal pressures, 20: 14667 (ORNL-TM-1312(Vol.1))
ultrasonic attenuation in superconducting, amplitude dependence of, 20: 15657
use in laminated shielding panels, 20: 14680(P)
use in shield for thermoluminescent dosimeter, 20: 14914(P)
use of plates of, for gamma shielding in nuclear-powered ships, (E/T), 20: 15932(T) (ORNL-tr-843)
vapor pressure at 950 to 1105°K, 20: 15062 (UCRL-16514)

LEAD ALLOYS
Cu–Pb–Zn, radiation effects on wear resistance of lead bronze, fast-neutron, 20: 15140
In–Pb, heat absorption and emission by superconducting, Peltier effect in, (E), 20: 15649
In–Pb, superconductivity of, critical field of, 20: 15105
Pb–Sn, thermodynamic properties, 20: 15062 (UCRL-16514)
Pb–Sn, vapor pressure of lead over, effects of composition on, 20: 15062 (UCRL-16514)

LEAD ISOTOPES Pb-205
decay of, M/L ratio for electron-capture, (E), 20: 15714 (CONF-233 (Vol.2), pp 369-70)
gamma emission of 2.3-kev isomeric state in, design of low-energy proportional detector for measuring, 20: 14444(R) (MLM-1268)

LEAD ISOTOPES Pb-206
bremsstrahlung reactions (γ,n) at 8 to 16 Mev, neutron spectra from, (E),

20: 15723 (MIT-2098-162)
bremsstrahlung reactions (γ,n) with, neutron emission in, (E), 20: 15724 (MIT-2098-224)
LEAD ISOTOPES Pb-207
bremsstrahlung reactions (γ,n) at 8 to 16 Mev, neutron spectra from, (E), 20: 15723 (MIT-2098-162)
bremsstrahlung reactions (γ,n) with, neutron emission in, (E), 20: 15724 (MIT-2098-224)
LEAD ISOTOPES Pb-208
bremsstrahlung reactions (γ,n) at 8 to 16 Mev, neutron spectra from, (E), 20: 15723 (MIT-2098-162)
bremsstrahlung reactions (γ,n) with, neutron emission in, (E), 20: 15724 (MIT-2098-224)
energy level excitation by scattering of carbon-12 ions, (E), 20: 15719 (INP-431/PL)
proton elastic scattering at 25 to 50 Mev, polarization from, (E), 20: 15728(R) (RHEL/R-112, pp 23-36)
proton total cross sections at 30 and 50 Mev, (E), 20: 15729(R) (RHEL/R-112, pp 37-66)
LEAD ISOTOPES Pb-210
activity of, performance of diffusion chamber for measuring absolute, 20: 14896
content in human bone, radiation dose from, 20: 14353
determination in atmospheric and precipitation samples, methods for radiochemical, 20: 14430 (AD-620219)
distribution in auto exhaust, 20: 14461(R) (ORNL-3889, pp 48-70)
LEAD ISOTOPES Pb-214
content in uranium-mine air, 20: 14747
LEAD OXIDES
thermal decomposition of, at 400 to 500°C, DTA and radon release studies of, 20: 14548
LEAD SYSTEMS
B–Co–Pb, crystal structure, 20: 14532
B–Pb–Ni, crystal structure, 20: 14532
LEAK DETECTORS
design of variable specific gravity radioactive source holder for, for fluid-filled conduits, 20: 14683(P)
LEAKS
control by vacuum, development of membrane for, 20: 14730 (AWRE-O-10/66)
detection in shielded cells at reprocessing facility, 20: 14788 (JAERI-1089)
LEAVES
radiation effects on oak, chronic γ, 20: 14289 (BNL-9509)
sorption of fertilizers by rice, tracer study, 20: 14240 (NP-15670)
LECTURES
on electron and photon interactions at high energies, 20: 15437
on elementary particles and field theory, 20: 15315 (STI/PUB/117)
LEPTONS
interactions of, model for, 20: 15360
pair production in neutrino ($\nu\mu$) interactions with protons, effect of W meson on, (T), 20: 15347
production in neutrino interactions with nucleons, (T), 20: 15387
propagators of, structure effects on regularization of, (T), 20: 15320
symmetry for, higher, 20: 15448
LEUKEMIA
radiation effects on mouse, γ, 20: 14367
radioinduced in children, etiology of, 20: 14346
radioinduced in twins, x, 20: 14319
LEUKOCYTES
radiation effects on rat lymphatic, protective effects of methyl-androstenolone against x, 20: 14392
radiation effects on distribution of splenic and thymic, effects of cell size on x, 20: 14318
radiation effects on ultrastructure in lymphocytic, 20: 14335
LEVEL INDICATORS
use of radioisotope, review of industrial, 20: 14835
LIBRARIES
nuclear data files for reactor engineering, computer programs for maintaining, 20: 15995 (BNL-966)
LIGHT
effects on sodium chlorate crystal paramagnetic color centers, (E), 20: 15961
interactions with gravitational waves, time-dependent intensity fluctuations from, (T), 20: 15636
production by x rays from nuclear explosions in deep space, (T), 20: 15608
production by x rays from nuclear explosions, fluorescence, (T), 20: 15610
radiosensitivity effects on Neurospora, 20: 14358
reflection from strontium chloride, far-infrared vibration mode from, (E), 20: 15958
scattering by gases as test of Boltzmann equation, 20: 15580
scattering by plasma, 20: 15882(R) (NP-15868)
spectra of, from oxygen excitation by protons, (E), 20: 15271
LIGNITES
analysis for ash content by gamma irradiation techniques using thulium-170, 20: 14493
LIMESTONE
radioactivity of, 20: 14752
LINEAR ACCELERATORS
beam energy monitor for 15-Mev electron, 20: 15184
beam mean energy in electron, device for measuring, 20: 15179
design and development of proton, 20: 15165 (RHEL/R-112, pp 12-22)
design modifications and operations of proton, 20: 15164(R) (RHEL/R-112)
LINOLEIC ACID
determination in commercial coconut oils, gas chromatographic, 20: 14463 (PAEC(D)CH-652)
LIPIDS
effects of methyl palmitate on, in mouse liver, lung, plasma, and spleen, 20: 14241 (TID-21437)
effects of peroxidizing, and amino acids, enzymes, and proteins, 20: 14587
effects of tissue hydration on liver content of, in mice, 20: 14268
radiation effects on content in mouse liver, x, 20: 14268
radiation effects on metabolism in rats, 20: 14293
LIQUID METAL COOLED REACTORS
design, 20: 16040(P)
design of fused-salt-fueled, fast-breeder, 20: 16036
steam generator for sodium, design and fabrication of modular, 20: 15999 (NAA-SR-11739)
valve design for, 20: 16004(P)
LITHIUM
determination in thorium compounds, spectrochemical methods for, 20: 14443(R) (MCW-1493, pp 27-30)
determination of trace amounts of, in uranium dioxide, 20: 14494
equation of state, 20: 15096
LITHIUM BROMIDES
radiation effects on single crystals of, role of temperature in, 20: 14603
LITHIUM CHLORIDES
LiCl–KCl, lanthanum trichloride reactions with fused eutectic mix of, 20: 14565
LiCl–KCl, polarization of cerium during electrolysis in fused, 20: 14561
LiCl–KCl, polarization of molybdenum during electrolysis in fused, 20: 14562
LiCl–KCl, polarization of cerium during electrolysis in, effects of lithium fluoride additions on, 20: 14564
LiCl–KCl, reactions of trivalent cerium with fluoride ions in fused, 20: 14563
LiCl–KCl–$ZnCl_2$, reactions with uranium monocarbide–zinc at 500 to 800°C, 20: 14991
LiCl–KCl, thermodynamic properties of plutonium chloride from emf measurements in, 20: 14507 (LA-3399)
LITHIUM COMPLEXES
LiCl–KCl, analysis for uranyl chlorides at 400°C using voltammetry, 20: 14437 (CEA-R-2879)
LITHIUM FLUORIDES
effects on cerium polarization during electrolysis in lithium chloride–potassium chloride, 20: 14564
effects on magnesium oxide fabrication by hot-pressing, 20: 15010 (UCRL-16534)
electron transmission through films of, excitons and plasma oscillations in, (E), 20: 15953
performance and properties for dosimeters, 20: 14907
radiation effects on single crystals of, role of temperature in, 20: 14603
radioinduced thermoluminescence of, electron, gamma, and x, 20: 14887
radioinduced thermoluminescence in, energy dependence of gamma and electron, 20: 14888
radiolysis of, NMR studies of neutron, 20: 14602
thermal conductivity of, isotope effects on, (T), 20: 15970
BeF_2–LiF–ThF_4–UF_4–ZrF_4, spectra of irradiated, absorption and reflectance, 20: 14453(R) (ORNL-3889, pp 12-14)
BeF_2–LiF–UF_4–ZrF_4, analysis for uranium, polarographic, 20: 14454(R) (ORNL-3889, pp 17-24)
LiF–KF–NaF, spectra of cobalt ions in, absorption, 20: 14453(R) (ORNL-3889, pp 12-14)
LITHIUM HYPOBROMITES
preparation, 20: 14511(R) (ORNL-3889, pp 71-3)
LITHIUM ISOTOPES Li-6
electron elastic scattering by, single oscillator parameter for, (T), 20: 15866
meson (π^-) reactions (π^-,2n) at rest, angular distributions and energy spectra from, (E), 20: 15793

meson (π^-) reactions (π^-,γ), energy spectra and yields from, (E), 20: 15794
nuclear properties in shell model, 20: 15730(R) (RHEL/R-112, pp 67-98)
production in helium-6 decay, double ionization in, (T), 20: 15715 (CONF-233(Vol.3), pp 505-9)
proton reactions (p,n) at 30 to 50 Mev, distributions from, 20: 15729(R) (RHEL/R-112, pp 37-66)

LITHIUM ISOTOPES Li-7
alpha elastic and inelastic scattering at 1.6–12 Mev, compound-nucleus energy levels in, 20: 15859
meson (π^-) reactions (π^-,2n) at rest, angular distributions and energy spectra from, (E), 20: 15793
meson (π^-) reactions (π^-,γ), energy spectra and yields from, (E), 20: 15794
meson (π^+) reactions, double-charge-exchange cross sections for, (T), 20: 15813
nuclear properties in shell model, 20: 15730(R) (RHEL/R-112, pp 67-98)
nucleon emission from, reduced widths in shell-model intermediate coupling, (T), 20: 15830
proton reactions (p,n) at 30 to 50 Mev, distributions from, 20: 15729(R) (RHEL/R-112, pp 37-66)

LITHIUM ISOTOPES Li-8
nucleon emission from, reduced widths in shell-model intermediate coupling, (T), 20: 15830
production in meson and proton reactions with heavy emulsion nuclei at 1.5 to 25 Bev, energy spectra from, (E), 20: 15792

LITHIUM SYSTEMS
Li–Mg–Si, fabrication and properties of cast, 20: 15007 (NP-15881)

LIVER
adenine nucleotide content in rat, effects of methioninesulfoximine on, 20: 14270
effects of methyl palmitate on lipids in mouse, 20: 14241 (TID-21437)
effects of tissue hydration in mouse, on lipid content, 20: 14268
nucleic acid metabolism in rat, tracer study, 20: 14242(R) (TID-22591)
radiation effects on lipid content in mouse, x, 20: 14268
radiation effects on adenine nucleotide content in rat, x, 20: 14270
radiation effects on phospholipids in rabbit, γ, 20: 14278
radiation effects on dehydrogenase activity in homogenates and mitochondria of rat, γ, 20: 14284
radiation effects on cells of, in fetal and pregnant rats, x, 20: 14294
radiation effects on enzyme activity in mitochondria of rat, x, 20: 14376
radiation effects on pyridine nucleotidase activity of rat, x, 20: 14362
radiation exposure of mouse, effects on reticulo-endothelial function, 20: 14374
radioinduced tumors in mouse, x, 20: 14373

LOS ALAMOS TURRET REACTOR
fabrication of coated particle fuel elements for, 20: 15002 (LA-3378)

LUBRICANTS
analysis of automobile, methods for activation, 20: 14439(R) (GA-5556)

LUMINESCENCE
radioinduced in gases, α, 20: 14617

LUNGS
effects of exercise and inhaled yttrium oxide on, of dogs, 20: 14257
effects of methyl palmitate on lipids in mouse, 20: 14241 (TID-21437)
polonium-210 content and distribution in human, after cigarette smoking, 20: 14798
radiation effects on unconditioned reflexes in cat, effects on cardiovascular system of x, 20: 14371
radiation effects on blood volume and fluid spaces in dog, methods for measuring, 20: 14292(R) (TID-22563)
radiotherapy of cancer of, evaluation of procedures for γ and x, 20: 14420

LUTETIUM ALLOYS
Fe–Lu, preparation and structure, 20: 15110
Lu–Mn, preparation and structure, 20: 15110
Lu–Y, electric conductivity of dilute, at low temperatures, 20: 15098

LUTETIUM ISOTOPES Lu-175
energy level transition probabilities in, pairing correlations in E1, (T), 20: 15766
energy level transitions in, conversion electrons from E1, (E), 20: 15703 (CONF-233(Vol.2), pp 148-57)
energy level transitions in, delayed E-1, (T), 20: 15765

LUTETIUM ISOTOPES Lu-177
energy level transition probabilities in, pairing correlations in E1, (T), 20: 15766
energy level transitions in, conversion electrons from E1, (E), 20: 15703 (CONF-233(Vol.2), pp 148-57)
energy level transitions in, delayed E-1, (T), 20: 15765

LYMPH SYSTEM
radiotherapy of tonsilar carcinomas in, x, 20: 14416

LYSINE
lability of, in lipid-protein reaction systems, 20: 14587

M

MACHINE TOOLS
design of, computer programs for, 20: 16154 (Y-1420(Rev.1))

MAGNESIUM
analysis and determination, 20: 14500
determination by spectroscopy using plasma jet, 20: 14492
determination in plutonium fluorides and peroxides, review on spectrographic, 20: 14464 (RFP-599)
effects on cobalt radiation emission spectroscopy, 20: 14444(R) (MLM-1268)
electron transmission through thin foils of, plasmon excitation in, (E), 20: 15951
neutron elastic scattering at 0.8 Mev, cross sections for, (T), 20: 15770
neutron resonance absorption integrals for, (E), 20: 15691 (CEA-R-2840)
reduction of uranium tetrafluoride to metal by, comparison of electrolytic and ferrosilicon-process, 20: 15050(R) (NLCO-970, pp 3.1-4)

MAGNESIUM ALLOYS
Al–Mg, radioinduced dislocation loops in, effects of magnesium concentration on fission-fragment, (E), 20: 15145
Ge–Mg, thermodynamic properties, 20: 15056(R) (NYO-2916-10)
Mg–Sn, preparation of single-crystal, 20: 15056(R) (NYO-2916-10)
Mg–Sn, studies of equilibration in monocrystals of, 20: 15056(R) (NYO-2916-10)
Mg–Zr, development and fabrication of EdF2, for fuel cans, 20: 15018
Mg–Zr, nondestructive method for testing cladding of, 20: 14711

MAGNESIUM ISOTOPES Mg-24
neutron reactions (n,2n) at 12 to 18 Mev, cross sections for, (E), 20: 15863
proton elastic and inelastic scattering at 5.8 Mev, polarization in, (E), 20: 15806

MAGNESIUM ISOTOPES Mg-25
proton inelastic scattering at 1.96 Mev, mean lifetime of first excited state from, (E), 20: 15780

MAGNESIUM ISOTOPES Mg-26
proton reactions (p,γ) and (p,p$'\gamma$) at 2.298 Mev, gamma spectra from, (E), 20: 15761

MAGNESIUM OXIDES
fabrication by hot-pressing, effects of lithium fluoride on, 20: 15010 (UCRL-16534)
reactions with copper and nickel mattes, slags, molten salts, and refractory metals, 20: 14989

MAGNESIUM SYSTEMS
Li–Mg–Si, fabrication and properties of cast, 20: 15007 (NP-15881)

MAGNET COILS
design for high-gradient cusp geometry for plasma containment, 20: 15928(P)

MAGNETIC FIELDS
adiabatic invariants of gyrating particles in, (T), 20: 15623 (MPI-PAE/P1.15/65)
calculation of even Ioffe bar, (T), 20: 15878 (IPP-6/42)
design of plasma-containment apparatus using annular, 20: 15927(P)
effects on critical currents in superconducting tin films, 20: 15662
effects on electrostatic oscillations in collisionless electron plasma, (T), 20: 15879 (IPP-6/43)
effects on thermal instability of spherical gases, (T), 20: 15876 (IPP-6/33)
Einstein-Maxwell equations for dipole, exact solution of, 20: 15155
electron radiative polarization in, (T), 20: 15638
electron relativistic motion in external, (T), 20: 15640
evolution of solar, (T), 20: 15223
interactions with shock waves, 20: 15882(R) (NP-15868)
measurement of 0.01 to 20 G, instrument for, 20: 15160 (LNF-65/44)
measurement of, equipment for, 20: 15882(R) (NP-15868)
penetration of solar photospheric, into interplanetary space, (E), 20: 15215
plasma containment by, research progress on, 20: 15882(R) (NP-15868)
plasma resonances in dipole, toroidal-mode, (T), 20: 15592
properties of crossed electric and, for beta and mass spectroscopy, 20: 14882
properties of interplanetary, review of, 20: 15232

MAGNETIC RESONANCE
measurement in rare earth ethyl sulfates, equipment for, 20: 15991
radioinduced in crystalline trypsin, γ and uv, 20: 14273

MAGNETOHYDRODYNAMIC CELLS
development, 20: 15300
plasma conductivity measurements in, methods for, 20: 15897
research progress, 20: 15882(R) (NP-15868)

MAGNETOHYDRODYNAMICS
fluid flow boundary layer between parallel streams in magnetic fields, (T), 20: 15570 (N65-21084)
fluid flow in, compressible dissipative, (T), 20: 15585

fluid flow in, Rayleigh's problem in, (T), 20: 15578
gas flow along insulating plane in magnetic fields, Hall effect in two-dimensional, (T), 20: 15568 (AD-620324)
plasma diagnostics using noise analysis, 20: 15569 (INR-626/IX/R)
shock waves in nonaligned flow in perfect gases, (T), 20: 15576

MAGNETOMETERS
design for 0.01- to 20-G measurements, 20: 15160 (LNF-65/44)
design of high-stability Hall-effect, 20: 14822(R) (RHEL/R-112, pp 99-128)
design of, engineering drawings for, 20: 14831

MAGNETOSPHERE
interaction with solar plasma, (T), 20: 15593
model, (T), 20: 15587 (AD-620244)
properties of, review of, 20: 15232

MAGNETS
design of momentum-analyzing, for magnetic spectrometer, 20: 14822(R) (RHEL/R-112, pp 99-128)
excitation method for delay-type, short-pulse, 20: 15157 (CERN-66-1)

MALEIC ACID
effects on radioinduced isomerization of α-phenylcinnamic acid, 20: 14596

MALEIC ACID, DIHYDROXY-
uses in determination of ytterbium, 20: 14490

MALEIC ACID, DIMETHYL ESTER
radioinduced isomerization of, effects of alkali metal bromides on, 20: 14596

MALEIC ACID, HYDRAZIDES
penetration of carbon-14-labeled, through cuticular membranes, 20: 16146 (COO-588-39)

MAN
analysis for plutonium, review on, 20: 14239 (JUL-312-ST)
cesium-137 content of, in Norway, 20: 14739 (TID-22655)
iodine metabolism in, mathematical model of, 20: 14249
iodine metabolism in, tracer study, 20: 14249
iodine metabolism in, mathematical model of, 20: 14250
lead-210 content in bones of, radiation dose rates from, 20: 14353
plutonium metabolism and properties in, review on, 20: 14239 (JUL-312-ST)
radiation dose to, from ingested radioactive materials, 20: 14794
radiation dose to, from ingested radioactive materials, 20: 14795
radiation effects on immune reaction to *Treponema pallidum*, γ, 20: 14308
radiation effects on tooth structure, 20: 14323
radiation effects on, low-dose γ and x, 20: 14331
radiation effects on, at very low dose rates, 20: 14352
radioinduced erythema in, uv, 20: 14310
radiotherapy of tumors in, dosimetry in epithermal-neutron, 20: 14421

MAN (STANDARD)
gastrointestinal tract food retention time and mass of, 20: 14794

MANDELIC ACID, *p*-BROMO-
uses in determination of ytterbium, 20: 14490

MANDELIC ACID, CHLORO-
uses in determination of ytterbium, 20: 14490

MANGANESE
analysis and determination, 20: 14500
content in red-colored Paleozoic deposits in Northern Tien Shan, 20: 14780(T) (AEC-tr-6579)
determination in automobile lubricants, activation, 20: 14439(R) (GA-5556)
determination in automobile tire rubber, activation, 20: 14439(R) (GA-5556)
determination in automobile paint, activation, 20: 14439(R) (GA-5556)
determination in cigarette tobacco, activation, 20: 14439(R) (GA-5556)
determination in commercial plastics, activation, 20: 14439(R) (GA-5556)
determination in hair samples in criminal cases, activation, 20: 14439(R) (GA-5556)
determination in oils and silts in water, activation, 20: 14439(R) (GA-5556)
determination in plutonium fluorides and peroxides, review on spectrographic, 20: 14464 (RFP-599)
determination in paper samples in criminal cases, activation, 20: 14439(R) (GA-5556)
determination in soils, activation, 20: 14439(R) (GA-5556)
determination in thumbnail clippings, activation, 20: 14493(R) (GA-5556)
determination in uranium tetrafluoride, spectrographic, 20: 14473
determination in wood in criminal cases, activation, 20: 14439(R) (GA-5556)
determination of trace amounts of, in iron, activation, 20: 14471
electron spectra from, KLL-Auger, (E), 20: 15243 (CONF-233(Vol.3), pp 480-6)
energy level transitions in, Coster-Kronig, (T), 20: 15238 (CONF-233 (Vol.3), pp 398-418)
energy level widths for, K, (T), 20: 15239 (CONF-233(Vol.3), pp 419-39)
hyperfine structure of, relativistic quadrupole interaction in, (E/T), 20: 15265 (RPI-328-49)

MANGANESE ALLOYS
Dy–Mn, preparation and structure, 20: 15110
Er–Mn, preparation and structure, 20: 15110
Gd–Mn, preparation and structure, 20: 15110
Ho–Mn, preparation and structure, 20: 15110
Lu–Mn, preparation and structure, 20: 15110
Mn–Nd, preparation and structure, 20: 15110
Mn–Pr, preparation and structure, 20: 15110
Mn–rare earths, preparation and structure, 20: 15110
Mn–Sm, preparation and structure, 20: 15110
Mn–Tb, preparation and structure, 20: 15110
Mn–Tm, preparation and structure, 20: 15110
Mn–Y, preparation and structure, 20: 15110

MANGANESE CARBONYLS
decomposition in ion source of mass spectrometer, mechanism of, 20: 14584(R) (TID-22444)

MANGANESE COUPLES
Mn–Sn, electric and thermal conductivity in superconducting, (E), 20: 15656

MANGANESE ISOTOPES Mn-52
decay of, K-capture to positron ratios for, (E), 20: 15711 (CONF-233 (Vol.2), pp 345-58)

MANGANESE ISOTOPES Mn-54
content in fallout over Black Sea, 1964, 20: 14741
decay of, K/L ratio for electron-capture, (E/T), 20: 15713 (CONF-233 (Vol.2), pp 365-8)
decay of, x-ray emission rates for electron-capture, (E), 20: 15242 (CONF-233(Vol.3), pp 465-79)
determination in atmospheric and precipitation samples, methods for radiochemical, 20: 14430 (AD-620219)
radioactivity of, absolute measurement of, 20: 15690 (CEA-R-2813)
separation from cobalt-60 and iron-59 by ion exchange, 20: 14433(R) (BAW-298)

MANGANESE ISOTOPES Mn-55
neutron reactions (n,He-3) at 14.8 Mev, effective cross sections for, (E), 20: 15739

MANGANESE ISOTOPES Mn-56
determination in copra and desiccated-coconut oils, activation, 20: 14463 (PAEC(D)CH-652)

MANGANESE OXIDES
sorptive properties for chloride and potassium ions, effects of pH on, 20: 14651

MANGANESE STEEL
Mn–Mo, embrittlement by plastic fatigue of A302B, 20: 15039 (EURAEC-1475)
Mn–Mo, fatigue strength of A302B, effects of weld defects on, 20: 15059(R) (SWRI-1228-1-20)
Mn–Mo, welding thick plates of LMS2V, cracking and hardness changes from, 20: 15000 (EURAEC-1517)

MANGANESE SYSTEMS
Al–C–Mn–Nb, phase studies, 20: 15103
Al–C–Mn–Ta, phase studies, 20: 15103
B–Cu–Mn, crystal structure, 20: 14532

MASERS (OPTICAL)
beam reactions with hydrogen and rare gases, cross sections for multi-phonon ionization, (T), 20: 15276
beam scattering by plasma, cooperative effects in, (E), 20: 15911
development and use in plasma diagnostics, 20: 15873 (IPP-1/42)
use in plasma diagnostics and heating, 20: 15882(R) (NP-15868)
use in production of polarized photons, 20: 15306(R) (CEAL-1026)

MASS SPECTROGRAPHY
analytical uses at ORNL, 20: 14428(R) (ORNL-3889)
development for transplutonic elements and uranium, 20: 14458(R) (ORNL-3889, pp 39-43)
methods for, using crossed electric and magnetic fields, 20: 14882
use in reactor fuel burnup analysis, 20: 16046

MASS SPECTROMETERS
design and performance of spark-source, 20: 14458(R) (ORNL-3889, pp 39-43)
power supply for double-focusing, design of, 20: 14830
sample changer for, description of, 20: 14829
use as sampling probe for discharge plasma, 20: 15915
use in atomic mass determinations, 20: 15853

MASS TRANSFER
between confined plasma jets and gas coolants, 20: 15584
design of equipment for study of, between liquid metals and solids, 20: 14975 (ANL-7091)

MATERIALS TESTING
conference on nondestructive, 20: 14701 (STI/PUB/105(Vol.1))
eddy-current methods for, of finned fuel cladding, 20: 14703

eddy-current methods for multi-parameter, of structural components, 20: 14708
eddy-current methods for, of reactor tubes during processing and production, 20: 14720
equipment and methods for nondestructive, of finned SAP tubing, 20: 14712
equipment and method for, of Zircaloy-2 canning tubes by ultrasonics, 20: 14714
equipment and methods for, of irradiated reactor components, 20: 14719
method for magnetic-particle, using radioactive iron oxide paste, 20: 14721(P)
nondestructive methods plutonium-enriched fuel rods, 20: 14707
nondestructive methods for, of reactor pressure vessel, 20: 14709
nondestructive methods for, of pressure vessels during fabrication, 20: 14710
nondestructive methods for, 20: 14711
nondestructive methods for, of thin-walled tubes, 20: 14713
penetration tests of high-strength materials, equipment and method for, 20: 14702 (Y-1490)

MATHEMATICS
book: *Lie Groups for Physicists*, 20: 14955
groups in, unitary representations of pseudo-orthogonal, 20: 14951
integer programming problems in, decomposition of, 20: 14950(R) (COO-614-41)
Lie groups in, direct products of irreducible representations of SU(n), 20: 15458
operators in Banach spaces, uses in fixed-point theorems, 20: 14950(R) (COO-614-41)
representations of inhomogeneous Lorentz group using contraction of (1 + 4) de Sitter group, 20: 14954
representations of Lorentz group, contraction to representations of Euclidean group, 20: 14953
theorem in switching theory, 20: 14950(R) (COO-614-41)

MATTER
equation of state at supernuclear density, (T), 20: 15212

MEATS
radiopreservation of, acceptance tests for γ, 20: 14930 (NP-15676)
radiopreservation of, acceptance tests for γ, 20: 14931 (NP-15677)
radiosterilization of crab, bacterial growth after, 20: 14936

MECHANICS
particle interactions in classical relativistic, conservation laws for point-, 20: 15154

MEDICAL SUPPLIES
packaging for radiosterilization, standards for, 20: 14942
radiation effects on prosthesic, x, 20: 14345
radiosterilization of, 20: 14389
radiosterilization of catgut sutures, 20: 14932
radiosterilization of, conference on, 20: 14940
radiosterilization of, 20: 14943
radiosterilization of prepacked, electrons, 20: 14941

MEDICINE
radiation hazards in dental, control of x, 20: 14419
research programs in, at Juelich Research Center, Germany, 20: 16156
review of nuclear, 20: 14427

MEDITERRANEAN SEA
oceanography of Israel shelf of, 20: 14731(R) (NP-159861)
oceanography of, effects of Nile River floods on, 20: 14731(R) (NP-159861)

MELAMINE
determination in mock explosive, method for, 20: 14470 (UCRL-7873)

MEMBRANES
ion transport across rabbit duodenum, 20: 14243(R) (TID-22626)
permeability of cuticular, to organic compounds, 20: 16146 (COO-588-39)
permeability of tomato cuticular, to iron and iron chelates, 20: 16147 (COO-888-45)
radiation effects on polymer, used in leak control, 20: 14730 (AWRE-O-10/66)

MENDELEVIUM
production in heavy-ion nuclear reactions, review of, 20: 15740

MERCAPTO GROUP
radiosensitivity effects in mammalian cells, effects of content on, 20: 14351
radiosensitivity effects in mice, mechanism for, 20: 14351

MERCHANT VESSELS
gamma shielding for nuclear-powered, use of lead plates for secondary, (E/T), 20: 15932(T) (ORNL-tr-843)
gamma transmission through steel pipes of nuclear powered, 20: 16114

MERCURY
analysis and determination, 20: 14500
bremsstrahlung reactions (γ,n) at 8 to 16 Mev, spectra from (E), 20: 15723 (MIT-2098-162)
bremsstrahlung reactions (γ,n) with, neutron emission in, (E), 20: 15724 (MIT-2098-224)
electric conductivity of turbulent plasma of, (E), 20: 15895
energy level transitions in, Coster-Kronig, (T), 20: 15238 (CONF-233 (Vol.3), pp 398-418)
energy level widths for, K, (T), 20: 15239 (CONF-233(Vol.3), pp 419-39)
hydromagnetic wave generation by dielectric sphere in spherical shell of, 20: 15581
ionization in mass spectrometer, formation of multiply charged ions in, 20: 14584(R) (TID-22444)
neutron elastic scattering at 0.8 Mev, cross sections for, (T), 20: 15770

MERCURY ISOTOPES
internal conversion probabilities in, reduced M and N E0, (T), 20: 15771

MERCURY ISOTOPES Hg-197
half life, (E), 20: 14461(R) (ORNL-3889, pp 48-70)

MERCURY ISOTOPES Hg-198
energy level transitions in, conversion coefficients for E2, (E), 20: 15707 (CONF-233(Vol.2), pp 198-212)
energy level transitions in, conversion coefficients for E2, (E/T), 20: 15708 (CONF-233(Vol.2), pp 213-19)

MERCURY ISOTOPES Hg-199
energy level transitions in, conversion electron-gamma correlations in, (E/T), 20: 15699 (CONF-233(Vol.2), pp 117-19)

MESIC ATOMS
meson (K^-) and (π^-) moderation and cascade times in levels of helium, (E), 20: 15273
polarization in (μ), vacuum, (T), 20: 15246 (CONF-233(Vol.3), pp 520-8)

MESITYLENE
effects on solvent properties for uranium in TBP system, 20: 14655

MESON PAIRS
photoproduction of mu, on carbon, (E), 20: 15306(R) (CEAL-1026)

MESONS
decay of vector, SU(6) symmetry for radiative, 20: 15472
decays of vector, partially conserved axial-vector current in, (T), 20: 15485
electromagnetic properties in composite model, 20: 15550
electromagnetic properties in relativistic composite models, (T), 20: 15551
interactions of fields of, renormalization theory for, 20: 15453
interactions of scalar, many-pole amplitudes and elementarity in two-body, (T), 20: 15490
interactions with baryons, SU(n) crossing matrices for, (T), 20: 15322
interactions with baryons, $\bar{U}(12)$ symmetry for strong, 20: 15390
interactions with nucleons, peripheral model for, (T), 20: 15419
interactions with nucleons, renormalization theory for, 20: 15453
interactions with nucleons, N/D method for, 20: 15466
interactions with nucleons, classical limit of cross sections for, (T), 20: 15563
interactions with quarks, crossing matrices for, (T), 20: 15322
mass of 1^+, current algebra for, 20: 15308 (IC/66/18)
motion of, sub-algebras generating relations in Duffin-Kemmer algebra for, (T), 20: 15462
photoproduction on protons, (E), 20: 15306(R) (CEAL-1026)
production of antiproton-proton annihilations, $\bar{U}(12)$ symmetry breaking in two-body, 20: 15346
production of vector, Regge-pole contribution to, 20: 15354
properties in SU(3) symmetry, (T), 20: 15530
symmetry for, W-spin and rotation group in, 20: 15467
theory for scalar and vector, gauge approximation in dynamic, 20: 15460
theory of neutral vector, formalism of gauge, 20: 15561
wave equations for vector, in spherically symmetric potential, (T), 20: 15447 (UCRL-14698-T)

MESONS, RESONANCE
classification in $SU(12)$ representations, 20: 15496
classification of higher, as kinetic supermultiplets of $\bar{U}(12)$, 20: 15479
conference, 20: 15398
existence of $\eta\pi$ and $\pi\pi$, from $\eta\pi\pi$ model of meson (X^0), 20: 15355
isospin of A_1 and A_2, (E), 20: 15408
mass formulas for 189 multiplet of SU(6) for, 20: 15478
models for, quasi-molecular rotator, 20: 15399
models for, quasi-molecular rotator, 20: 15399
parity and spin of, method for determining, 20: 15431
photoproduction at 4.8 to 6.0 Bev, (E), 20: 15425
production in antiproton-proton annihilation at 3.7 Bev/c, cross section for, (E), 20: 15338
production in meson (π^-)-deuteron interactions at 3.2 Bev/c, (E), 20: 15405
production in meson (π^+) interactions with protons at 2.08 Bev/c, cross sections for, (E), 20: 15334
production of K^*0, in meson (K^-)-proton interactions at 3.8 Bev/c, (E), 20: 15418
production of K^*, in meson (K^-)-proton interactions at 1.80 and 1.95 Bev/c, (E), 20: 15420
production of K^*, in meson (K^+)-proton interactions at 2.26 Bev/c, (E/T), 20: 15422

production of K*, in meson (K+)-proton interactions at 3.6 Bev/c, (E), 20: 15407
production of K*(890), in meson (K-)-proton interactions at 2.1 to 2.7 Bev/c, (E), 20: 15412
production of K*(890), in meson (K-)-proton interactions at 5.5 Bev/c, 20: 15416
production of K*(888), in meson (K-)-proton interactions at 1.5 Bev/c, (E/T), 20: 15429
MESONS (B)
exchange in meson (π)-mesons (ω) interactions, (T), 20: 15357
MESONS (η)
decay modes of, neutral, (E), 20: 15395
decay of, C violation in, (E), 20: 15430
decay of, search ($\pi^0 e^+ e^-$), (E), 20: 15333
effects on nuclear forces, 20: 15817
production in meson (K-)-proton interactions at 3.8 Bev/c, (E), 20: 15418
production in meson (π^-)-proton charge-exchange interactions, (E), 20: 15380
MESONS (η')
decay of, $e^+e^-\pi^0$, (E), 20: 15427
decay of, $\pi^+\pi^-\gamma$, (E), 20: 15367
MESONS (K)
decay of, nonleptonic, (T), 20: 15366
decay of, 2π, (T), 20: 15369
decay rate from meson (μ) mass, maximum, 20: 15344
interactions of, inversion expansion with non-Abelian group of parity tripod for strong, (T), 20: 15494
interactions of, research on, (E/T), 20: 15307(R) (COO-1261-22)
interactions with nucleons, testing broken M(12) symmetry by vector exchange in, (T), 20: 15421
interactions with nucleons, $\bar{U}(12)$ symmetry for, 20: 15390
photoproduction at high energies, review on, (T), 20: 15442
production in antiproton-proton annihilation at 3.7 Bev/c, cross section for, (E), 20: 15338
MESONS (K^-)
cascade and moderation times in liquid helium, (E), 20: 15273
interactions with deuterons at 670 to 770 Mev/c, Y$_1^*$(1660) production in, 20: 15397
interactions with nucleons at high energies, resonances in, 20: 15414
interactions with protons at 2.1 to 2.7 Bev/c, meson (ϕ) production in, (E/T), 20: 15316 (UCRL-16526)
interactions with protons at 2.1 to 2.7 Bev/c, resonance production in, (E), 20: 15412
interactions with protons at 5.5 Bev/c, resonance production in, (E), 20: 15416
interactions with protons at 3.8 Bev/c, resonance production in, (E), 20: 15418
interactions with protons at 1.80 and 1.95 Bev/c, boson exchange in, (E), 20: 15420
interactions with protons, total cross section for, (E/T), 20: 15428
interactions with protons at 1.5 Bev/c, K*(888) and N*(1425) production in, (E/T), 20: 15429
interactions with protons, spin-parity analysis of Ξ^*(1530) from, (E/T), 20: 15464
interactions with protons, $\bar{U}(12)$ symmetry for, 20: 15390
photoproduction at high energies, (E), 20: 15306(R) (CEAL-1026)
photoproduction of, baryon resonances in, (E), 20: 15424
reactions with heavy emulsion nuclei at 1.5 to 25 Bev, lithium-8 energy spectra from, (E), 20: 15792
MESONS (K^0)
decay of K_2^0, branching ratio for neutral current, (E), 20: 15331
decay of K_2^0, CP noninvariance in 2π, (T), 20: 15446 (UCRL-12380-T)
decay of K_2^0, G_2 symmetry scheme for, 20: 15474
decay of K_2^0, neutral a-particle model for 2π, (T), 20: 15504
decay of, CP violation in, (T), 20: 15432
decay of, CP violation in, (T), 20: 15434
decay of, CP-violating nonleptonic, (T), 20: 15433
decay of, nonleptonic, (T), 20: 15307(R) (COO-1261-22)
decay of, reciprocity principle and CP violation in, 20: 15350
mass matrix for K^0-$\bar{K}^0$, reciprocity principle for, 20: 15350
production in meson (π^-) reactions with xenon at 9 Bev/c, cross sections for, (E), 20: 15841
production in meson (π)-proton interactions, two-resonance model for, (T), 20: 15392
MESONS (K^+)
decay ($\pi^+ + \pi^- + \gamma$) 20: 15396
decay ($\pi^+ + \pi^- + \gamma$), rate of, 20: 15396
decay of, G_2 symmetry scheme for weak, 20: 15474
detection of, equipment for, 20: 15393
interactions with protons at 3.6 Bev/c, resonance production in, (E), 20: 15407
interactions with protons at 3.6 Bev/c, (E), 20: 15415
interactions with protons at 2.26 Bev/c, resonance production in, (E/T), 20: 15422
interactions with protons, total cross section for, (E/T), 20: 15428
interactions with protons at 1.96 Bev/c, single-meson (π) production in, (E), 20: 15335
photoproduction at high energies, (E), 20: 15306(R) (CEAL-1026)
photoproduction of, baryon resonances in, (E), 20: 15424
photoproduction on proton at 1100–1300 Mev, cross sections for, (E), 20: 15393
MESONS (K_e^-)
decay rate and spectra of, radiative corrections to, 20: 15349
MESONS (K_{2e}^0)
decay of, G_2 symmetry scheme for, 20: 15474
MESONS (K_{e3}^+)
decay of, G_2 symmetry scheme for, 20: 15474
decay rate and spectra of, radiative corrections to, 20: 15349
MESONS ($K_{\mu 3}^-$)
decay rate and spectra of, radiative corrections to, 20: 15349
MESONS ($K_{2\mu}^0$)
decay spectra, (E), 20: 15331
MESONS ($K_{\mu 3}^+$)
decay rate and spectra of, radiative corrections to, 20: 15349
MESONS (κ)
production in meson (K+)-proton interactions at 3.6 Bev/c, (E), 20: 15415
MESONS (μ)
decay of, lepton symmetry refraction from, 20: 15448
decay of, model for leptonic, 20: 15360
mass of, charged-meson maximum decay rate from, 20: 15344
photoproduction of pairs of, on carbon, (E), 20: 15306(R) (CEAL-1026)
MESONS (μ^-)
capture by calcium, neutron angular distributions from, (E), 20: 15721 (JINR-E-2517)
capture by sulfur, neutron angular distributions from, (E), 20: 15720 (JINR-E-2516)
MESONS (ω)
decay of, SU(6) symmetry for radiative, 20: 15472
effects on nuclear forces, 20: 15817
interactions with mesons (π), meson (B) exchange in, (T), 20: 15357
production and decay in meson ($\pi^\pm$)-nucleon interactions at 1.7 Bev/c, (E), 20: 15403
production of, Regge-pole contribution to, 20: 15354
MESONS (ω')
decay of, beta, (E), 20: 15406
MESONS (ϕ)
decay modes for, (E/T), 20: 15316 (UCRL-16526)
decay of, beta, (E), 20: 15406
production of, (E/T), 20: 15316 (UCRL-16526)
MESONS (π)
decay rate from meson (μ) mass, maximum, 20: 15344
interactions of, inversion expansion with non-Abelian group of parity tripod for, (T), 20: 15494
interactions with nucleons, amplitudes for, (T), 20: 15312 (MIT-2098-86)
interactions with baryons, model for isotopic symmetry for, (T), 20: 15454
interactions with nucleons, rescattering correction for three-body final-state, 20: 15476
interactions with mesons (π), amplitudes for, (T), 20: 15518
interactions with mesons (π) and nucleons at low energies, dispersion theory of, 20: 15522
interactions with nucleons, pseudoscalar and scalar, (T), 20: 15325
interactions with mesons (π), linear integral equations for low-energy, 20: 15351
interactions with nucleons, nucleon mass and coupling constant for, 20: 15352
interactions with mesons (ω), meson (B) exchange in, (T), 20: 15357
interactions with mesons (π), strip approximation for S-wave amplitudes for, (T), 20: 15358
interactions with mesons (π), strip approximation for amplitudes for, (T), 20: 15359
interactions with nucleons, meson (ρ) exchange in, 20: 15364
interactions with mesons (π), in meson (π^-)-proton interactions at 378 Mev, (E), 20: 15368
interactions with nucleons, review of, 20: 15371
interactions with protons, phase shift analyses of, (T), 20: 15382
interactions with nucleons, dispersion relations for low-energy, (T), 20: 15385
interactions with gamma radiation, analysis of 2π production in, (T), 20: 15389
interactions with mesons (π), analysis of meson (π)-gamma production in, 20: 15389
interactions with nucleons, $\bar{U}(12)$ symmetry for, 20: 15390

interactions with nucleons at 1.68 Bev/c, $Y_0^*(1405)$ and $Y_1^*(1358)$ production in, (E), 20: 15404
photoproduction at low energies, (T), 20: 15441
photoproduction at high energies, review on, (T), 20: 15442
photoproduction on protons, E1 and M2 amplitudes in single, (T), 20: 15365
photoproduction on nucleons, dispersion sum rules for, (T), 20: 15503
production amplitudes for, isospin exchange relations for, (T), 20: 15449
production in antiproton-proton annihilation at 3.7 Bev/c, cross section for, (E), 20: 15338
production of single, in meson (K^+) interactions with protons at 1.96 Bev/c, (E), 20: 15335
scattering by nuclei, nucleon correlation effects on quasi-elastic, (T), 20: 15827
wave functions with definite symmetry for, many-body configurational, (T), 20: 15450
wave-function renormalization constant for fields of, using partially conserved axial-vector current, (T), 20: 15402

MESONS (π^-)
cascade and moderation times in liquid helium, (E), 20: 15273
interactions with deuterons at 3.2 Bev/c, resonance production in, (E), 20: 15405
interactions with protons at 3.0 and 7.0 Bev, beta decay of vector bosons from, (E), 20: 15406
interactions with deuterons at 3.7 Bev/c, resonances in, (E), 20: 15409
interactions with protons at 2.7 Bev/c, resonances in, (E/T), 20: 15410
interactions with protons at 600 to 900 Mev, single meson (π) production in, (E/T), 20: 15411
interactions with protons at 1.0 to 1.9 Bev, Y^{*-} production in, (E), 20: 15417
interactions with protons, total cross section for, (E/T), 20: 15428
interactions with deuterons, neutron-neutron S-wave scattering length from, (E), 20: 15511
interactions with protons at 9 to 18 Bev/c, meson (ρ) exchange in, (T), 20: 15364
interactions with protons at 378 Mev, π-π interaction in, (E), 20: 15368
interactions with protons at 875 to 1579 Mev/c, differential cross sections and polarization in elastic, (E), 20: 15372
interactions with protons at 500 to 1150 Mev, charge-exchange, (E), 20: 15374
interactions with protons at 300 to 1000 Mev, $N^*(1238)$ production in, (E/T), 20: 15375
interactions with protons at high energies, forward amplitude for charge-exchange, (T), 20: 15376
interactions with protons at 1.72 and 2.07 Bev/c, differential cross sections for elastic, (E), 20: 15377
interactions with protons at 2.0 Bev/c, cross sections for charge-exchange, (E), 20: 15378
interactions with protons at 2.1 to 6.9 Bev/c, resonance effects on total cross sections for, (E/T), 20: 15379
interactions with protons at 5.9 to 18.2 Mev/c, charge-exchange, (E), 20: 15380
interactions with protons at 300 to 700 Mev, isobar production in, (T), 20: 15381
interactions with protons at 9 Bev/c, meson (π^0) multiplicity and photon yields from, (E), 20: 15384
interactions with protons at 240 Mev, phase-shift analysis of elastic, (T), 20: 15388
interactions with protons, $\bar{U}(12)$ symmetry for, 20: 15390
interactions with protons, two-resonance model for hyperon (Λ)-meson (K^0) production in, (T), 20: 15392
interactions with protons, neutral decay modes of mesons (η) from, (E), 20: 15395
interactions with protons at 1.7 Bev/c, meson (ω) and (ρ^0) production and decay in, (E), 20: 15403
photoproduction at high energies, (E), 20: 15306(R) (CEAL-1026)
photoproduction on protons at high energies, (E), 20: 15306(R) (CEAL-1026)
photoproduction on protons at 550 to 1000 Mev, cross sections for, (E), 20: 15332
production in neutron-proton interactions at 585 Mev, cross sections for, 20: 15310 (JINR-P-2508)
production in proton-proton interactions at 2.0, 2.4, and 2.85 Bev, momentum spectra of, (E), 20: 15336
reactions (π^-,2n) with lithium-6 and -7 at rest, angular distributions and energy spectra from, (E), 20: 15793
reactions (π^-,γ) with complex nuclei, energy spectra and yields from, (E), 20: 15794
reactions with heavy emulsion nuclei at 1.5 to 25 Bev, lithium-8 energy spectra from, (E), 20: 15792
reactions with xenon at 9 Bev/c, hyperon (Λ) and meson (K^0) production in, (E), 20: 15841

MESONS (π^0)
production in meson (π^-)-proton charge-exchange interactions, (E), 20: 15380
production in meson (π^-)-proton interactions at 9 Bev/c, multiplicity of, (E), 20: 15384
production in meson (η) decay, (E), 20: 15395

MESONS (π^+)
interactions with protons, mesons (A) and (B) production in, 20: 15408
interactions with protons, total cross section for, (E/T), 20: 15428
interactions with protons at 4 and 8 Bev, absorption corrections to exchange term for elastic, (T), 20: 15324
interactions with protons at 208 Bev/c, cross sections for elastic scattering and meson production in, (E), 20: 15334
interactions with protons at 781 Mev, cross sections for single- and multiple-pion production in, 20: 15341
interactions with protons, model for high-energy charge-exchange, 20: 15342
interactions with protons at 875 to 1579 Mev/c, differential cross sections and polarization in elastic, (E), 20: 15372
interactions with protons at 410 and 492 Mev, recoil proton polarization in, (E), 20: 15373
interactions with protons at 2.1 to 6.0 Bev/c, resonance effects on total cross sections for, (E/T), 20: 15379
interactions with protons at 300 to 700 Mev, isobar production in, (T), 20: 15381
interactions with protons at 240 Mev, phase-shift analysis of elastic, (T), 20: 15388
interactions with protons, hyperon (Σ^+) production in, (E/T), 20: 15400
interactions with neutrons at 1.7 Bev/c, meson (ω) and (ρ^0) production and decay in, (E), 20: 15403
photoproduction at high energies, (E), 20: 15306(R) (CEAL-1026)
photoproduction on protons at high energies, (E), 20: 15306(R) (CEAL-1026)
photoproduction on protons at 550 to 1000 Mev, cross sections for, (E), 20: 15332
photoproduction on protons at 225 to 350 Mev, (E), 20: 15340
production in neutron-proton interactions at 585 Mev, cross sections for, (E), 20: 15310 (JINR-P-2508)
production in proton-proton interactions at 2.80 Bev/c, single, (T), 20: 15423
production in proton-proton interactions at 2.0, 2.4, and 2.85 Bev, momentum spectra of, (E), 20: 15336
reactions with beryllium-9 and lithium-7, double-charge-exchange cross sections for, (T), 20: 15813
reactions with nuclei, double-charge-exchange cross sections for, (T), 20: 15813

MESONS (ρ)
decay of, analysis of $\pi\gamma$, (T), 20: 15389
effects on nuclear forces, 20: 15817
exchange in meson (π)-nucleon interactions, (T), 20: 15364
production of, Regge-pole contribution to, 20: 15354

MESONS (ρ^+)
decay of, beta, (E), 20: 15406
photoproduction at 4.8 to 6.0 Bev, (E), 20: 15425
production and decay in meson ($\pi^\pm$)-nucleon interactions at 1.7 Bev/c, (E), 20: 15403

MESONS (X^0)
model of, $\eta\pi\pi$, 20: 15344

METABOLISM
radiation effects on gas, protective effects of methylandrostenolone in rats against x, 20: 14392
radiation effects on rat, neutron and x, 20: 14368

METAL COATINGS
thickness distribution of evaporated, effects of crucible shape on, 20: 16151 (RFP-647)

METAL-FOIL DETECTORS
development for fission fragments, 20: 14852 (CEA-R-2862)
sample changing systems for use with, design of automatic, 20: 14846 (AECL-2517)

METALLIC FILMS
analysis of ferromagnetic, for cobalt, iron, and nickel, activation, 20: 14489
electron tunneling excitation spectra in laminates of normal and superconducting, (T), 20: 15653

METALLIC FILTERS
cleaning of, use of ejector nozzle for, 20: 14645

METALLOGRAPHY
x-ray diffraction analysis in, conference on, 20: 15943 (RL-REA-2595)

METALLURGICAL EQUIPMENT
hot press design for glove boxes and manipulator cells, 20: 14666 (ORNL-P-1946)

METALLURGY
conference on stress corrosion, delayed failures, and fatigue corrosion, 20: 14998

measurement of depth of defects by replication techniques, 20: 14966 (RFP-673)
METALS
book: *Preferred Orientation in Wrought and Annealed Metals*, 20: 15099
coating for, fabrication of vitreous insulating, 20: 15131(P)
coating for, preparation of refractory, 20: 14974(P)
deformation of, effects of inclusions on plastic, 20: 15055(R) (NYO-2394-19)
deposition on solid electrodes by voltammetry, 20: 14453(R) (ORNL-3889, pp 12-14)
determination in methanol–mineral acid media using azo dyes, spectrophotometric, 20: 14469(R) (TID-22650)
developments in research on, bibliography on, 20: 14506 (CRDL-SP-5-7)
diffusion and coalescence of bubbles in, theory of, 20: 15132 (ANL-7079)
distribution and excretion of biologically important trace, effects of chelates on, 20: 14256
electromagnetic wave propagation in, (T), 20: 15941 (NP-15698)
electron interaction in, collective theory for free, 20: 15987
electron-phonon interactions in magnetic fields, effects on electron mass, (T), 20: 15939 (AD-620189)
evaporation of films of, device for monitoring, 20: 14819 (RFP-602)
mechanical properties for high-temperature uses, 20: 15129
penetration resistance of high-strength, equipment and methods for testing, 20: 14702 (Y-1490)
physical properties of, equipment and methods for measuring, 20: 14719
separation from solutions by solvent extraction using trialkylphosphoric triamides, 20: 14461(R) (ORNL-3889, pp 48-70)
separation of trace, from uranium by chromatography, 20: 14461(R) (ORNL-3889, pp 48-70)
technology of high-temperature liquid, review, 20: 14958 (BNL-972)
METEORITES
ages of, argon–potassium, helium-4–thorium, and uranium methods for estimating, 20: 15193 (NP-15654)
analysis for argon, helium, and neon content and isotopic composition, 20: 15193 (NP-15654)
METEOROLOGY
analysis of data from Parr, South Carolina, 20: 14732 (CVNA-172)
METERS
performance of radiometric, scale linearity in, 20: 14836
METHACRYLIC ACID, METHYL ESTER POLYMERS
radioinduced production of Lichtenberg Figures in, by 6-Mev electrons, 20: 14607
METHANE
concentration of carbon-13-enriched, methods for, 20: 14444(R) (MLM-1268)
deuterium exchange reactions with hydrogen in, catalytic effects of palladium alloys on, 20: 14542
methane–water vapor, rate of tritium-exchange reactions with hydrogen in, 20: 14662(R) (ORNL-TM-1394)
reactions with tritiated water, chromatography and scintillation spectra of products from, 20: 14455(R) (ORNL-3889, pp 25-32)
yields in gamma radiolysis of deaerated methanol, effects of sulfuric acid on, 20: 14579(R) (NYO-2383-15)
METHANE, DIIODO-
radioinduced ESR spectra in, at 77°K, 20: 14597
METHANE, NITRO-
photolysis of liquid and vaporous, yields from uv, 20: 14613
radiolysis of liquid and vaporous, yields from gamma, 20: 14613
METHANESULFONIC ACID, METHYL ESTER
preparation, 20: 14576(R) (ORNL-3889, pp 73-7)
METHANOL
effects on spectra of neodymium complexes, 20: 14560
effects on *trans-cis* isomerization of stilbene in solutions of, 20: 14579(R) (NYO-2383-15)
radiation effects on, spectral studies on gamma, 20: 14579(R) (NYO-2383-15)
radiolysis of aerated, effects of sulfuric acid on formaldehyde and hydrogen peroxide yields in, 20: 14579(R) (NYO-2383-15)
radiolysis of deaerated, effects of sulfuric acid on yields in gamma, 20: 14579(R) (NYO-2383-15)
HCl–methanol, effects on titanium and zirconium, corrosive, 20: 14988
HCl–methanol, radiolysis products from, analysis of, 20: 14581(R) (ORNL-3889, pp 14-16)
HCl–methanol, spectrophotometric analysis for metals, 20: 14469(R) (TID-22650)
methanol–$AgNO_3$, radioinduced free silver atoms in solid solutions of, EPR of x, (E), 20: 15975(T)
methanol–Ag_2SO_4, radioinduced free silver atoms in solid solutions of, EPR of x, (E), 20: 15975(T)
methanol–AgF, radioinduced free silver atoms in solid solutions of, EPR of x, (E), 20: 15975(T)
methanol–$AgClO_4$, radioinduced free silver atoms in solid solutions of, EPR of x, (E), 20: 15975(T)
methanol–HNO_3, spectrophotometric analysis for metals, 20: 14469(R) (TID-22650)
METHIONINE
lability of, in lipid-protein reaction systems, 20: 14587
METHIONINESULFOXIMINE
effects on adenine nucleotide content in rat blood and liver, 20: 14270
effects on urinary excretion of ammonia and phosphates in rats, 20: 14270
METHYL SULFOXIDE
iron isotope exchange between iron(II) and iron(III) in, 20: 14571
MICA
thickness of, in end-window counters, use of alpha particles for measuring, 20: 14826
MICE
anemias in, effects of genes on, 20: 14290(R) (NYO-1800-12)
antibody titers in, effects of egg purification on, 20: 14304
effects of carbon tetrachloride on, carcinogenic, 20: 14373
lipid content in livers of, effects of tissue hydration on, 20: 14268
metabolism of carbon-14-labeled methyl palmitate in reticulo-endothelial system in, 20: 14241 (TID-21437)
radiation effects on survival in, electrolytic balance as predictor of x, 20: 14266
radiation effects on lipid content in liver of, x, 20: 14268
radiation effects on activity of lipolytic enzymes in, x, 20: 14279
radiation effects on reticulo-endothelial function of, x, 20: 14374
radiation effects on, protective effects of sodium hyposulfite against x, 20: 14393
radiation effects on normal and tumorous tissues of, effects of RNA on x, 20: 14401
radiation effects on Schistosoma infectivity in, effects on antibody titer of, 20: 14304
radiation effects on embryos of, delayed pathological x, 20: 14315
radiation effects on survival of 5-bromo-deoxycytidine-treated bone marrow cells in, fast-neutron and x, 20: 14333
radiation effects on leukemic cells from, γ, 20: 14367
radioinduced depletion of nucleated cells in bone marrow, spleen, and thymus of young, γ, 20: 14365
radioinduced tumors in, x, 20: 14373
radiosensitivity of sperm of, effects of streptomycin on, 20: 14404
radiosensitivity of, effects of tissue sulfhydryl ratios on, 20: 14351
strontium-85 transfer through placenta in, 20: 14244
MICHIGAN RESEARCH REACTOR
reflector design modification and performance for, 20: 16128
MICROORGANISMS
radiation effects on immune reaction to *Treponema pallidum*, γ, 20: 14308
survival curves of, effects on radiation dosimetry of, 20: 14814
MICROSOMES
radioinduced inactivation of isolated *Escherichia coli*, γ, 20: 14363
MICROWAVE EQUIPMENT
hydromagnetic wave propagation in magnetoplasma waveguide, viscous effects on, (T), 20: 15925
MICROWAVE SPECTROMETERS
description of, for free-radical studies, 20: 15272
MICROWAVES
absorption in superconducting aluminum, frequency and temperature dependence of, (E), 20: 15658
emission from plasma, properties of, (T), 20: 15870 (CEA-R-2881)
emission from plasma column, structure in, (E/T), 20: 15893
scattering by underdense cylindrical helium plasma, phase-shift analysis for, (T), 20: 15894
use in plasma diagnostics, 20: 15882(R) (NP-15868)
MILITARY PERSONNEL
radiation effects on, dose and time factors after nuclear-explosion, 20: 14287 (AD-626996)
MILK
cesium-137 content of, in Norway, 20: 14739 (TID-22655)
consumption of cow's and goat's, by human populations, 20: 14243(R) (TID-22626)
fallout monitoring of Canadian, October 1965, 20: 14737 (NP-15853, pp 8-20)
iodine-131 content of, assessment of, 20: 14243(R) (TID-22626)
radioactive contamination of, near CANDU and WNRE sites, 20: 14738 (NP-15853, pp 21-33)
radioactivity of, AERE monitoring of cesium-137, iodine-131, and strontium-90, 20: 14784(R) (AERE-R-5015)
MINERALS
separation of alkaline earths, rare earths, thorium, and uranium from, by ion exchange, 20: 14469(R) (TID-22650)
MINING
atmospheric radioactivity in uranium, 20: 14747
equipment and excavations for, on Nevada Test Site, 20: 14754 (NVO-38-1)
use of nuclear explosives in, 20: 14665

MISSISSIPPI
radiation protection in, program for, 20: 14807
MITOCHONDRIA
radiation effects on phospholipids in rabbit liver, γ, 20: 14278
radiation effects on dehydrogenase activity in rat liver, γ, 20: 14284
radiation effects on enzyme activity in, from rat liver, spleen, and thymus, x, 20: 14376
radiation effects on ultrastructure of, 20: 14335
MITOSIS
effects of Decortilen on, in HeLa cells in culture, 20: 14375
radiation effects on, in HeLa cells in culture, 20: 14375
radiation effects on animal, x, 20: 14397
MIXERS
design of remote-control, for blending thorium dioxide–uranium dioxide powders, 20: 14668 (ORNL-TM-1397)
MOLECULES
electron elastic collisions with, in homogeneous weakly ionized plasma, (T), 20: 15888(T) (SC-T-65-775)
electron reactions at low energies, vibration excitation from, (T), 20: 15256
electron transitions in, many-body theory for probability of, 20: 15275
oscillations of tetragonal, in fcc crystals, 20: 15940 (JUL-292-RW)
radiation effects on, distribution of energy in, 20: 14595
reactions of, bibliography on, 20: 15248 (ORNL-AMPIC-3)
vibrational potential constants of bent xy_2, third-order, 20: 14559
MOLTEN SALT REACTOR EXPERIMENT
fuel analysis, methods for, 20: 14454(R) (ORNL-3889, pp 17-24)
MOLTEN SALT REACTORS
design of fast-breeder, 20: 16037
design of liquid-metal-cooled fast-breeder, 20: 16036
MOLYBDENUM
analysis and determination, 20: 14500
content in red-colored Paleozoic deposits in Northern Tien Shan, 20: 14780(T) (AEC-tr-6579)
creep and rupture of, numerical methods for analysis of, 20: 15041 (GEMP-397)
determination in automobile lubricants, activation, 20: 14439(R) (GA-5556)
determination in plutonium fluorides and peroxides, review on spectrographic, 20: 14464 (RFP-599)
determination in solutions, x-ray-fluorescence, 20: 14497
determination in uranium tetrafluoride, spectrographic, 20: 14473
determination of trace amounts of, in iron, activation, 20: 14471
diffusion and permeation coefficients for hydrogen in, 20: 14976 (AWRE-O-16/66)
diffusion of rhenium in, at 1700 to 2100°C, tracer studies of, 20: 15127
diffusion of tungsten in, at 1700 to 2100°C, 20: 15126
dislocation mechanisms in single-crystal, 20: 15946 (UCRL-16643)
energy level transitions in, Coster-Kronig, (T), 20: 15238 (CONF-233 (Vol.3), pp 398-418)
energy level widths for, K, (T), 20: 15239 (CONF-233(Vol.3), pp 419-39)
grain boundary structure in, internal friction studies of, 20: 15128
neutron elastic scattering at 0.8 Mev, cross sections for, (T), 20: 15770
neutron resonance absorption integrals for, (E), 20: 15691 (CEA-R-2840)
polarization during electrolysis in fused salts containing cerium trichloride, 20: 14562
radiation effects on crystal structure of, neutron, 20: 15136 (RL-REA-2595, pp 51-62)
reactions with refractory metal borides, carbides, nitrides, and oxides, 20: 14989
reactions with sodium, high-temperature, 20: 15033(R) (ANL-7152, pp 87-96)
separation from sulfate solutions by solvent extraction using tri-n-octylamine, 20: 14653
solvent properties for hydrogen, 20: 14976 (AWRE-O-16/66)
welding of, electron-beam, 20: 15012
work function of, effects of cesium-fluoride vapor on, 20: 15297 (CONF-640921, pp 101-9)
MOLYBDENUM ALLOYS
Cr–Fe–Mo, strain aging of, 20: 15063 (UCRL-16585)
Fe–Mo, strain aging of, 20: 15063 (UCRL-16585)
Mo–Nb, corrosion by hydrochloric, phosphoric, and sulfuric acids, effects of alloy composition on, 20: 14997
Mo–Nb, hardness, 20: 15073
Mo–Nb–U–Zr, mechanical properties of gamma-phase uranium-base, 20: 15060 (UCRL-7771)
Mo–Pu–U, fabrication for ZPR fuel elements, 20: 16060(R) (ANL-7152, pp 1-49)
Mo–Re, grain boundary structure in, internal friction studies of, 20: 15128
Mo–Ti, machining, 20: 15014
Mo–Ti–Zr, machining of TZM, 20: 15014
Mo–U, mechanical properties of gamma-phase uranium-base, 20: 15060 (UCRL-7771)
Mo–U, microstructure of, effects of carbon on, 20: 15070
Mo–W, electric transport in, for wide composition ratio and temperature range, 20: 15116(T)
Mo–W, mechanical properties of Oremet HPC, 20: 15069
Mo–Zr, grain boundary structure in, internal friction studies of, 20: 15128
MOLYBDENUM BORIDES
abrasive properties, 20: 15109
reactions with copper and nickel mattes, slags, molten salts, and refractory metals, 20: 14989
MOLYBDENUM CARBIDES
abrasive properties, 20: 15109
preparation of spherical particles of, procedure and apparatus for, 20: 14971(P)
reactions with copper and nickel mattes, slags, molten salts, and refractory metals, 20: 14989
MOLYBDENUM CARBONYLS
decomposition in ion source of mass spectrometer, mechanism of, 20: 14584(R) (TID-22444)
MOLYBDENUM ISOTOPES Mo-99
decay of, conversion-electron spectra from, (E), 20: 15751
MOLYBDENUM ISOTOPES Mo-93
internal conversion spectra of isomeric, (E), 20: 15751
MOLYBDENUM ISOTOPES Mo-97
burnup calculations for, in reactor fuels, 20: 16061(R) (BAW-296)
MOLYBDENUM ISOTOPES Mo-98
burnup calculations for, in reactor fuels, 20: 16061(R) (BAW-296)
MOLYBDENUM ISOTOPES Mo-100
burnup calculations for, in reactor fuels, 20: 16061(R) (BAW-296)
MOLYBDENUM OXIDES
preparation of spherical particles of, procedure and apparatus for, 20: 14971(P)
sorptive properties for chloride and potassium ions, effects of pH on, 20: 14651
MOLYBDENUM SILICIDES
reactions with copper and nickel mattes and molten salts, 20: 14989
MOLYBDENUM STEEL
Cr–Mo, corrosion by sodium at 700°F, 20: 14979 (GEAP-4835)
Mn–Mo, embrittlement by plastic fatigue of A302B, 20: 15039 (EURAEC-1475)
Mn–Mo, fatigue strength of A302B, effects of weld defects on, 20: 15059(R) (SWRI-1228-1-20)
Mn–Mo, welding thick plates of LMS2V, cracking and hardness changes from, 20: 15000 (EURAEC-1517)
MOLYBDENUM SYSTEMS
B–Cu–Mo, crystal structure, 20: 14532
B–Fe–Mo, crystal structure, 20: 14532
C–Cr–Mo, phase studies, 20: 15111
C–Mo–Nb–Zr, heat treatment of, 20: 14972(P)
Mo–Nb–N–Zr, heat treatment of, 20: 14972(P)
Mo–Nb–O–Zr, heat treatment of, 20: 14972(P)
Mo–UP, compatibility, 20: 15032(R) (ANL-7152, pp 50-72)
MONAZITES
analysis for thorium and uranium, 20: 14491
MONKEYS
radiation effects on behavior in, γ, neutron, and x, 20: 14286 (AD-625837)
radiation effects on blood picture and survival in, whole-body x, 20: 14302
MONOCHROMATORS
development of electron, 20: 15235(R) (AD-620289)
review on photon, 20: 14841
MONTE CARLO METHOD
for criticality of interacting systems of complex geometry, 20: 16034
for electron-photon cascade shower structure, (T), 20: 15938
shielding calculations using, exponential transformation for, 20: 15937
use in analysis of gamma streaming through ducts, 20: 15929 (AD-627890)
use in efficiency calculations for gamma scintillation detectors, 20: 14897
MOON
altitude measurements on, using radiation sources and detectors, 20: 14817 (N65-20421)
MÖSSBAUER EFFECT
data acquisition system for, 20: 15973
velocity drives for studying, triangle and square wave generators for, 20: 14827
MOUTH
radiation effects on, following facial therapy, γ and x, 20: 14324
radiotherapy of palatine arch carcinomas in, x, 20: 14416
MUCIC ACID
uses in determination of ytterbium, 20: 14490

MUCOSA
radiation effects on intestinal, after abdominal therapy, x, 20: 14339
radiation effects on, of exteriorized rat intestine, x, 20: 14364
MUTATIONS
induced in barley by diethyl sulfate and radiation, 20: 14384
radioinduced in barley, effects of ethylenimine on γ, 20: 14334
radioinduced in *Vigna sinensis*, neutron and x, 20: 14341
radioinduced in yeast, uv, 20: 14327
MYRISTIC ACID
determination in commercial coconut oils, gas chromatographic, 20: 14463 (PAEC(D)CH-652)

N

NAPHTHACENE
electron transitions in, oscillator strengths for probability of, (T), 20: 15275
NAPHTHALENE
electron transitions in, oscillator strengths for probability of, (T), 20: 15275
2,7-NAPHTHALENEDISULFONIC ACID, 4,5-DIHYDROXY-
uses for spectrophotometric determination of uranium, 20: 14481
NAPHTHALENE-6-SULFONIC ACID, 2,3-DIHYDROXY-
uses for spectrophotometric determination of uranium, 20: 14481
NAPHTHENIC ACIDS
solvent properties for uranium, 20: 14642
NAVAL REACTORS
book: *Naval Nuclear Power Installations*, 20: 16116
NECK
effects of surgery on wound healing in, 20: 14303
radiation effects on wound healing in, x, 20: 14303
NEODYMIUM
mass of, spectrometric determination of, 20: 15853
NEODYMIUM ALLOYS
Co–Nd, cobalt ion EPR in intermetallic compounds of, 20: 15963
Mn–Nd, preparation and structure, 20: 15110
Nd–Y, electric conductivity of dilute, at low temperatures, (E), 20: 15098
NEODYMIUM COMPLEXES
spectra of, solvent effects of methanol on light on heavy water on, 20: 14560
NEODYMIUM HYDRIDES
spectra of, effects of deuterium on infrared, 20: 14568
NEODYMIUM ISOTOPES Nd-142
atomic mass, (E), 20: 15769
NEODYMIUM ISOTOPES Nd-143
atomic mass, (E), 20: 15769
burnup calculations for, in reactor fuels, 20: 16061(R) (BAW-296)
yields in neutron fission of plutonium-239, uranium-233, and uranium-235, 20: 15133(R) (GEAP-4893)
NEODYMIUM ISOTOPES Nd-144
atomic mass, (E), 20: 15769
yields in neutron fission of plutonium-239, uranium-233, and uranium-235, 20: 15133(R) (GEAP-4893)
NEODYMIUM ISOTOPES Nd-145
atomic mass, (E), 20: 15769
yields in neutron fission of plutonium-239, uranium-233, and uranium-235, 20: 15133(R) (GEAP-4893)
NEODYMIUM ISOTOPES Nd-146
atomic mass, (E), 20: 15769
yields in neutron fission of plutonium-239, uranium-233, and uranium-235, 20: 15133(R) (GEAP-4893)
NEODYMIUM ISOTOPES Nd-147
beta decay, (E), 20: 15810
NEODYMIUM ISOTOPES Nd-148
atomic mass, (E), 20: 15769
NEODYMIUM ISOTOPES Nd-149
half life, (E), 20: 15779
NEODYMIUM ISOTOPES Nd-150
atomic mass, (E), 20: 15769
yields in neutron fission of plutonium-239, uranium-233, and uranium-235, 20: 15133(R) (GEAP-4893)
NEODYMIUM NITRATES
density and viscosity of aqueous solutions of, 20: 14648
$Al(NO_3)_3$–$La(NO_3)_3$, density and viscosity of solutions of, 20: 14648
NEODYMIUM OXIDES
reactions with water, infrared spectra of products of, 20: 14568
spectra of hydrates of, effects of deuterium on infrared, 20: 14568
$Al(NO_3)_3$–Nd_2O_3, compound formation in, at 1200°C, 20: 14539
Al_2O_3–Nd_2O_3, compound formation in, at 1600 to 1650°C, 20: 14539
Nd_2O_3–WO_3, preparation and properties, 20: 14534
NEON
ionization in mass spectrometer, formation of multiply charged ions in, 20: 14584(R) (TID-22444)
ionization of, cross sections for ruby-laser-multiphonon, (T), 20: 15276
reactions with cesium, excitation transfer in, (E), 20: 15253
NEON FLUORIDES
wave functions of NeF and NeF_2, 20: 14541
NEON IONS
reactions with copper and gold at 60, 80, and 90 kev, electron energy spectra from, (E), 20: 15261
NEON ISOTOPES
content in meteorites, 20: 15193 (NP-15654)
separation by thermal diffusion, 20: 14444(R) (MLM-1268)
NEON OXIDES
wave functions of NeO, 20: 14541
NEPTUNIUM COMPLEXES
with glycolic and lactic acids, preparation and properties of, 20: 14556
NEPTUNIUM ISOTOPES Np-237
content in spent power reactor fuels, evaluation of, 20: 14435 (BNWL-SA-503)
NERVES
radiation exposure of isolated ganglion of, β, 20: 14332
NERVOUS SYSTEM
defects in human, leukemogenic effects of, 20: 14346
radiation effects on rat, after neonatal spinal cord exposure, proton, 20: 14299
radiation effects on rabbit, x, 20: 14350
NEUROSPORA
radiosensitivity of, photoprotection against x, 20: 14358
NEUTRINOS
angular correlation with beta particles in first forbidden nonunique beta decay, (E), 20: 15857
detection of, for determination of terrestrial abundances of radioactive potassium, thorium, and uranium, (T), 20: 14750
emission from neutron stars, cooling-time effects of, (T), 20: 15201
emission processes in carbon-burning stars, effects of energy-loss, (T), 20: 15194
interactions with neutrons, charge-retention currents for elastic, (T), 20: 15327
interactions with nucleons, lepton production in, (T), 20: 15387
theory of, in geometrodynamics, 20: 15561
NEUTRINOS (ν_e)
interactions with electrons, S-operator theory for, 20: 15481
NEUTRINOS (ν_μ)
interactions with protons, effects of W meson on lepton pair production in, (T), 20: 15347
NEUTRON BEAMS
dosimetry of epithermal, for radiotherapy, 20: 14421
effects on behavior in monkeys, 20: 14286 (AD-625837)
production of regular flat-spectrum, device for, 20: 15687(P)
properties of, coherence, (T), 20: 15328
NEUTRON CROSS SECTIONS
calculation of group-averaged, computer programs for, 20: 15665 (AWRE-O-103/65)
calculation using compound nucleus model, parameters for, 20: 15863
measurement of, instrumentation development for, 20: 15731(R) (RPI-328-49)
NEUTRON SHIELDING
fabrication of high-density borated graphite, 20: 15027(P)
NEUTRON SOURCES
design of regular flat-spectrum, using heavy water diffuser, 20: 15687(P)
spectra from polonium–beryllium, in paraffin moderator, (E), 20: 15683
use in soil moisture meters, 20: 14771
use of pulsed, for determining neutron diffusion parameters in fluids and rocks, 20: 14772
uses in soil moisture determinations, 20: 14756
NEUTRON SPECTROMETERS
design and performance for polarization analysis, 20: 14856 (KFK-345)
performance of, using proton recoils, 20: 14444(R) (MLM-1268)
spectral line shape from single-crystal scintillation, reconstruction of, (T), 20: 14869
NEUTRON SPECTROSCOPY
detectors for, performance and uses of threshold, 20: 15175 (UCRL-16312)
methods for intermediate-energy, using activation detectors, 20: 14860 (RT/FI(65)-33)
NEUTRONS
absorption by gold, method for measuring resonance, 20: 15731(R) (RPI-328-49)
absorption by nuclei, resonance integrals for, (E), 20: 15691 (CEA-R-2840)
absorption of, pulsed technique for measuring resonance, 20: 15731(R) (RPI-328-49)
activation of nickel-64 by 14-Mev, 20: 14461(R) (ORNL-3889, pp 48-70)
angular distribution and energy of, from boron-11 (d,n) reaction, (E),

20: 15858
angular distributions from meson (μ^-) capture by sulfur, asymmetry in, (E), 20: 15720 (JINR-E-2516)
angular distributions from meson (μ^-) capture by calcium, (E), 20: 15721 (JINR-E-2517)
capture by holmium-165 at 0 to 55 ev, resonance spins from, (E), 20: 15681
capture by iron and manganese, gamma spectra from resonance, (E), 20: 15731(R) (RPI-328-49)
decay of, model for leptonic, 20: 15360
detection and measurement by track imaging in insulating materials, 20: 14854 (CONF-660304-3)
detection and measurement in reactors, using activation detectors, 20: 14860 (RT/FI(65)-33)
detection and measurement at low-counting rates, performance of boron–fluoride counter for, 20: 14863
detection of, stilbene scintillation detector for, 20: 14900
diffusion in benzene, parameters for, (T), 20: 15676
diffusion in monatomic hydrogen, time-dependent moments equations solutions for, 20: 15675
diffusion in water in spherical containers, parameters for, (T), 20: 15686
diffusion theory representation for control rods of thermal reactors, (T), 20: 16090 (WAPD-T-1841)
distributions in reactors, variational calculations of, 20: 15666 (CONF-660204-4)
dosimetry of, system for, 20: 14915(P)
effects on fuel and poison elements, in-pile measurements of, 20: 16089(R) (WAPD-MRP-114)
effects on lithium fluoride, NMR studies of, 20: 14602
effects on molybdenum crystal structure, 20: 15136 (RL-REA-2595, pp 51-62)
effects on semiconductors and transistors, 20: 14920 (TID-22664)
effects on sodium selenate crystals, ESR of paramagnetic centers from, (E), 20: 15972
effects on stored energy release of beryllia, effects of dosage on, 20: 15142
emission in bremsstrahlung reactions (γ,n) with heavy elements, (E), 20: 15724 (MIT-2098-224)
energy and flux measurements on, methods of, 20: 14883
flux distributions in natural uranium–water matrices, 20: 16028
flux measurements, standardization of, 20: 14461(R) (ORNL-3889, pp 48-70)
flux of, use of cobalt and aluminum–cobalt wires for measuring, 20: 14867
flux-shape eigenfunctions for two-zone slabs, tables of, 20: 16024 (RFR-231)
flux-shape eigenfunctions for two-zone cylinders, tables of, 20: 16025 (RFR-232)
interactions with neutrons in triton-triton reactions, (T), 20: 15733 (UCRL-7769)
interactions with protons at 585 Mev, mesons (π^+) and (π^-) production cross sections for, (E), 20: 15310 (JINR-P-2508)
interactions with neutrinos, charge-retention currents for elastic, (T), 20: 15327
interactions with neutrons and protons, charge independence in scattering lengths for, 20: 15356
interactions with deuterons, Padé approximant for S-matrix for inelastic, 20: 15363
interactions with gamma radiation at medium energies, effects of inelastic channel on, (T), 20: 15394
interactions with mesons (π^+) at 1.7 Bev/c, meson (ω) and (ρ^0) production and decay in, (E), 20: 15403
penetration and slowing-down in reactor shielding, method for predicting, (T), 20: 15935
photoproduction on nuclei at 8 to 16 Mev, spectra from, (E), 20: 15723 (MIT-2098-162)
polarization of, analyzer for measurement of, 20: 14856 (KFK-345)
reactions (n,α) with oxygen-16 at 14 Mev, mechanisms for, (E), 20: 15738
reactions (n,α) with germanium-72 at 14.6 Mev, isomeric cross section ratio for, (E/T), 20: 15773
reactions (n,α) with silicon-29 at 13.4 to 15.0 Mev, excitation function for, (E), 20: 15800
reactions (n,γ) with cobalt-59 in cobalt complexes, chemical effects of, 20: 14584(R) (TID-22444)
reactions (n,γ) and (n,p) with sulfur in cysteic acid, cysteine, and cystine, recoil chemistry of, 20: 14584(R) (TID-22444)
reactions (n,γ) with ytterbium isotopes, resonances in, (E), 20: 15839
reactions (n,γ) with rhodium-103, gamma spectra from, (E), 20: 15754
reactions (n,γ) with palladium-110 and tellurium-130, isomeric cross-section ratios in, (E), 20: 15777
reactions (n,He-3) with nuclei at 14.8 Mev, effective cross sections for, (E), 20: 15739
reactions (n,p) with sulfur-33, cross sections for, (E), 20: 14461(R) (ORNL-3889, pp 48-70)
reactions (n,p) with cesium-133 and gallium-69 at 14.6 Mev, isomeric cross section ratio for, (E/T), 20: 15773
reactions (n,p) with cesium-133 and gallium-69 at 14.6 Mev, isomeric cross section ratio for, (E/T), 20: 15773
reactions (n,2n) with nuclei at 12 to 18 Mev, cross sections for, (E), 20: 15863
reactions (n,2n) with rubidium-85, cross section for, (E), 20: 14461(R) (ORNL-3889, pp 48-70)
reactions (n,2n) with osmium-192 at 14.6 Mev, isomeric cross section ratio for, (E/T), 20: 15773
reactions in tissue phantom at high energies, 20: 14330
reactions with iodine-129, production of iodine-130 isomer in, (E), 20: 15772
reactions with technetium at 14 Mev, activation cross sections for, (E), 20: 14461(R) (ORNL-3889, pp 48-70)
reactions with uranium-235 at 0.1 to 2 Mev, cross sections for elastic, (E/T), 20: 15032(R) (ANL-7152, pp 50-72)
reactions with uranium-235 at 150 to 335 kev, fission cross section for, (E), 20: 15818
scattering by calcium-40 at 3.15 Mev, cross sections for compound elastic, (E/T), 20: 15865
scattering by cesium, amplitude for coherent, 20: 15736
scattering by lead and silicon, cross sections for free and coherent, 20: 15682
scattering by nuclei at 0.8 Mev, cross sections for elastic, (T), 20: 15770
scattering by silicon-28 and sulfur-32 at 2.45 to 5.80 Mev, cross sections for elastic and inelastic, (E), 20: 15811
scattering by single crystals, coherent extinction and second-order, 20: 15671
scattering by spinless targets, computer program for, 20: 15670 (WAPD-TM-524)
scattering length from deuteron-meson (π^-) interactions, (E), 20: 15511
scattering of, facility for low energy inelastic, 20: 15731(R) (RPI-328-49)
spectra in borated water, (E), 20: 15731(R) (RPI-328-49)
transmission through slabs, transfer-matrix method for, (T), 20: 15934
transport effects in neutron wave experiment, (T), 20: 15685
transport equation in plane multiregion geometries, first-order solutions of, 20: 15674
transport in cylinders and slabs, one-group collision-probability code for, 20: 15668 (EUR-2624.e)
transport in homogeneous multiplying systems, (T), 20: 16030
transport in plane geometry, orthogonality relations for, 20: 15684
transport in plane geometry, solutions of multigroup equations for, (T), 20: 15667 (EIR-72)
transport in plane parallel plate, separation of spatial and angular variables in equation for, 20: 15673
transport in spherical reactors, j_N analysis of, 20: 16022 (EUR-2627.e)
transport of, radiative transfer equation solutions for, (T), 20: 15572
transport with anisotropic scattering, geometrical effects on, (T), 20: 16021 (CEA-R-2890)

NEUTRONS, EPITHERMAL

distribution in homogeneous media, energy and space, (T), 20: 14774
dosimeter for, development of activation, 20: 14862
dosimetry of, using tissue-equivalent chamber, 20: 14421
spectra in complex media, similitude theory for, 20: 14776

NEUTRONS, FAST

capture by nuclei, gamma production data for, 20: 15725 (NP-14855)
detection and measurement of, boron trifluoride probe for, 20: 14913(P)
effects on electric conductivity of tungsten, 20: 15040(R) (GA-6721)
effects on metabolism of rats, delayed, 20: 14368
effects on survival of 5-bromo-deoxycytidine-treated bone marrow cells, 20: 14333
effects on wear resistance of copper, iron, lead bronze, and steel, 20: 15140
flux measurements using iron wires, developments in, 20: 14433(R) (BAW-298)
scattering by nuclei, gamma production data for, 20: 15725 (NP-14855)

NEUTRONS, FISSION

yields from plutonium-239, uranium-233, and uranium-235, (E), 20: 15718 (IDO-17083)

NEUTRONS, THERMAL

capture by erbium-167, gamma spectra from, (E), 20: 15757
capture by gold-197, gamma spectra from, (E), 20: 15756
capture by holmium-165, gamma spectra from, (E), 20: 15758
capture by iodine-127, iodine-128 low-lying levels from, (E), 20: 15831
capture by nuclei, gamma spectra from, (E), 20: 15787
capture by palladium, gamma spectra from, (E), 20: 15755
detection and measurement of, boron trifluoride probe for, 20: 14913(P)
diffusion and distribution in hydrogen and heavy gases, (T), 20: 15677
diffusion coefficients in petroleum and silicate, determination of, using pulsed source, 20: 14772

diffusion coefficients in fluids and rocks, determination of, using pulsed source, 20: 14772
diffusion length in water at 18 to 255°C, (E), 20: 15679
diffusion lengths in Santowax-R at 200 to 400°C, 20: 15680
distribution in homogeneous media, energy and space, (T), 20: 14774
dosimeter for, development of activation, 20: 14862
effects on lithium bromide and fluoride single crystals, 20: 14603
effects on plutonia–uranía fuels, 20: 15135(R) (NUMEC-3432-18)
effects on seeds of *Vigna sinensis*, biological, 20: 14341
embrittlement of Inconel alloys and austenitic stainless steels, 20: 15141
flux distributions in paraffin, (E), 20: 15683
flux in water and uranyl fluoride–water solutions, perturbation by aluminum–dysprosium foils, 20: 15669 (NASA-TN-D-3237)
flux measurements using aluminum–cobalt wires, developments in, 20: 14433(R) (BAW-298)
lifetime in infinite medium, determination of, using pulsed source, 20: 14772
lifetime in well-logging experiments, computer program for calculating, 20: 14775
propagation in graphite, thermalization effects in one-group analysis for pulse, (T), 20: 15678
reactions with americium-241, yields of americium-242, curium-242, and plutonium-242 from, 20: 14631
reactions with americium-242, yields of americium-243, curium-242, and plutonium-242 from, 20: 14631
reactions with plutonium-241, capture-to-fission ratio for, (E), 20: 15774
scattering in real gases, cluster expansion for inelastic, (T), 20: 15672
spectra in complex media, similitude theory for, 20: 14776

NEVADA TEST SITE
mining on, equipment and excavations for, 20: 14754 (NVO-38-1)

NEW ZEALAND
fallout monitoring, 1965, 20: 14734(R) (NP-15844)

NICKEL
analysis and determination, 20: 14500
content in red-colored Paleozoic deposits in Northern Tien Shan, 20: 14780(T) (AEC-tr-6579)
determination in ferromagnetic films, activation, 20: 14489
determination in MSRE fuel, polarographic, 20: 14454(R) (ORNL-3889, pp 17-24)
determination in plutonium fluorides and peroxides, review on spectrographic, 20: 14464 (RFP-597)
determination in uranium tetrafluoride, spectrographic, 20: 14473
determination of trace amounts of, in iron, activation, 20: 14471
effects of foils of, on charge states of oxygen-16 ions, 20: 15854
electron reactions at 6 to 60 kev, transient radiation from, (E), 20: 15268
energy level transitions in, Coster-Kronig, (T), 20: 15238 (CONF-233 (Vol.3), pp 398-418)
energy level widths for, K, (T), 20: 15239 (CONF-233(Vol.3), pp 419-39)
neutron elastic scattering at 0.8 Mev, cross sections for, (T), 20: 15770
neutron resonance absorption integrals for, (E), 20: 15691 (CEA-R-2840)
reactions with sodium, high-temperature, 20: 15033(R) (ANL-7152, pp 87-96)

NICKEL ALLOYS
Al–Ni–Nb, oxidation of, phase distributions in layers from studies of, 20: 14990
Al–Ni–Nb, phase studies at 1140°C, 20: 15121
Fe–Ni, analysis of films of, for iron and nickel, 20: 14489
Ni–Nb, phase diagrams, 20: 15115

NICKEL CARBONYLS
decomposition in ion source of mass spectrometer, mechanism of, 20: 14584(R) (TID-22444)

NICKEL COMPOUNDS
cyclopentadienyl, decomposition in ion source of mass spectrometer, 20: 14584(R) (TID-22444)

NICKEL ISOTOPES
energy levels in even, calculations of vibrational, 20: 15851

NICKEL ISOTOPES Ni-57
energy levels from nickel-58 (He-3,α) reactions, spins of, (E), 20: 15860

NICKEL ISOTOPES Ni-58
helium-3 reactions (He-3,α) at 15 and 18 Mev, (E), 20: 15860
proton elastic scattering at 25 to 50 Mev, polarization from, (E), 20: 15728(R) (RHEL/R-112, pp 23-36)
proton total cross sections at 30 and 50 Mev, (E), 20: 15729(R) (RHEL/R-112, pp 37-66)

NICKEL ISOTOPES Ni-60
parity and spin of, from deuteron scattering data, 20: 15850
proton elastic scattering at 25 to 50 Mev, polarization from, (E), 20: 15728(R) (RHEL/R-112, pp 23-36)
proton total cross sections at 30 and 50 Mev, (E), 20: 15729(R) (RHEL/R-112, pp 37-66)

NICKEL ISOTOPES Ni-64
activation using 14-Mev neutrons, 20: 14461(R) (ORNL-3889, pp 48-70)

NICKEL SYSTEMS
Al–C–Ni–Nb, phase studies, 20: 15103
Al–C–Ni–Ta, phase studies, 20: 15103
B–Cd–Ni, crystal structure, 20: 14532
B–Ni–Ag, crystal structure, 20: 14532
B–Ni–U, crystal structure, 20: 14532
B–Ni–Y, crystal structure, 20: 14532
B–Pb–Ni, crystal structure, 20: 14532
Sb–B–Ni, crystal structure, 20: 14532

NIOBIUM
coating by iridium, protective effects of, 20: 15004(R) (N65-20790)
creep and rupture of, numerical methods for analysis of, 20: 15041 (GEMP-397)
determination in the presence of fluoride, spectrophotometric, 20: 14455(R) (ORNL-3889, pp 25-32)
determination in uranium tetrafluoride, spectrographic, 20: 14473
diffusion of tantalum in liquid, coefficient for, 20: 14969
energy level transitions in, Coster-Kronig, (T), 20: 15238 (CONF-233 (Vol.3), pp 398-418)
energy level widths for, K, (T), 20: 15239 (CONF-233(Vol.3), pp 419-39)
internal friction peak in, dislocation-relaxation, 20: 15122
oxygen ion reactions with surface of, secondary oxide ion from, (E), 20: 15976(T)
production from tin slags, 20: 14956
reactions with hydrogen sulfide at 1000 to 1400°C, 20: 14554
reactions with refractory metal borides, carbides, nitrides, and oxides, 20: 14989
reactions with sodium, high-temperature, 20: 15033(R) (ANL-7152, pp 87-96)
solubility in liquid plutonium at 700 to 1000°C, 20: 15043 (LA-3436)
solubility in liquid cerium–cobalt–plutonium alloy at 500 to 900°C, 20: 15043 (LA-3436)
tensile properties of, effects of mechanical twinning on, 20: 15049(R) (N65-16256)

NIOBIUM ALLOYS
Al–Nb, fabrication of sintered bodies of, 20: 15026(P)
Al–Nb, superconductivity of fused, 20: 15123
Al–Ni–Nb, oxidation of, phase distributions in layers from studies of, 20: 14990
Al–Ni–Nb, phase studies at 1140°C, 20: 15121
Cr–Nb–Ti, phase diagrams, 20: 15078
Fe–Nb, analysis for trace metals, polarographic, 20: 14455(R) (ORNL-3889, pp 25-32)
Ga–Nb, superconductivity of fused, 20: 15123
Hf–Nb–W–Y, properties for use in aerospace vehicles, 20: 15119
Mo–Nb, corrosion by hydrochloric, phosphoric, and sulfuric acids, effects of alloy composition on, 20: 14997
Mo–Nb, hardness, 20: 15073
Mo–Nb–U–Zr, mechanical properties of gamma-phase uranium-base, 20: 15060 (UCRL-7771)
Nb–Sn, crystallization of chemical-vapor-deposited crystals of Nb_3Sn, 20: 15113
Nb–Sn, superconductivity of fused, 20: 15123
Nb–Sn–Ti, superconductivity of fused, 20: 15123
Nb–Sn–V, superconductivity of fused, 20: 15123
Nb–Sn–Zr, superconductivity of fused, 20: 15123
Nb–Ta, corrosion by hydrochloric, phosphoric, and sulfuric acids, effects of alloy composition on, 20: 14997
Nb–Ta, hardness, 20: 15073
Nb–Ta, segregation of tantalum by controlled solidification of, effects of titanium additions on, 20: 14969
Nb–Ta–Sn, superconductivity of fused, 20: 15123
Nb–Ti, corrosion by hydrochloric, phosphoric, and sulfuric acids, effects of alloy composition on, 20: 14997
Nb–Ti, hardness, 20: 15073
Nb–U, mechanical properties of gamma-phase uranium-base, 20: 15060 (UCRL-7771)
Nb–U–Zr, mechanical properties of gamma-phase uranium-base, 20: 15060 (UCRL-7771)
Nb–V, corrosion by hydrochloric, phosphoric, and sulfuric acids, effects of alloy composition on, 20: 14997
Nb–V, creep strength and ductility of, effects of mechanical twinning on, 20: 15049(R) (N65-16256)
Nb–V, hardness, 20: 15073
Nb–W, extrusion and swaging, 20: 15101
Nb–W, hardness, 20: 15073
Nb–W, properties for high-temperature uses, 20: 15101
Nb–Zr, analysis for zirconium by spectrography of solutions, 20: 14446 (N64-25607)
Nb–Zr, corrosion by hydrochloric, phosphoric, and sulfuric acids, effects of alloy composition on, 20: 14997
Nb–Zr, emissivity of titanate coatings on, 20: 15057(R) (PWA-2750)
Nb–Zr, formation of niobium carbide surface films on, activation energies

for, 20: 14992
Nb–Zr, hardness, 20: 15073
Nb–Zr, internal friction peak in, dislocation-relaxation, 20: 15122
Nb–Zr, reactions with sodium, high-temperature, 20: 15033(R) (ANL-7152, pp 87-96)
Nb–Zr, use in heat transfer tube, 20: 14699(P)
Ni–Nb, phase diagrams, 20: 15115

NIOBIUM BORIDES
reactions with carbon, 20: 14555

NIOBIUM CARBIDES
diffusion of carbon in, at 1700°K, coefficient for, 20: 14992
formation on niobium–1 zirconium alloy, activation energies for, 20: 14992
reactions with copper and nickel mattes, slags, molten salts, and refractory metals, 20: 14989
testing as high-temperature heater for electric resistance furnaces, 20: 15112
thermal capacity at 10 to 320°K, 20: 15097
NbC–UC, properties for cathodes in thermionic space power plants, 20: 15046(R) (N65-15820)

NIOBIUM ISOTOPES Nb-90
decay of, conversion electron spectra from, (E), 20: 15751
energy levels of, multipolarity of, (E), 20: 15751

NIOBIUM ISOTOPES Nb-93
proton reactions (p,n) at 2.3 to 11.0 Mev, excitation of isobaric analog states in, (E), 20: 15804

NIOBIUM OXIDES
sorptive properties for chloride and potassium ions, effects of pH on, 20: 14651
$CaO–Nb_2O_5$, density and surface ductility of fused, at 1200 to 1650°C, 20: 15076
$Cr_2O_3–Nb_2O_5$, density and surface ductility of fused, at 1200 to 1650°C, 20: 15076
$Fe_2O_3–Nb_2O_5$, density and surface ductility of fused, at 1200 to 1650°C, 20: 15076
$Nb_2O_5–K_2O$, density and surface ductility of fused, at 1200 to 1650°C, 20: 15076
$Nb_2O_5–ZrO_2$, phase studies, 20: 15079

NIOBIUM SULFIDES
preparation and properties, 20: 14554

NIOBIUM SYSTEMS
Al–C–Co–Nb, phase studies, 20: 15103
Al–C–Cr–Nb, phase studies, 20: 15103
Al–C–Cu–Nb, phase studies, 20: 15103
Al–C–Fe–Nb, phase studies, 20: 15103
Al–C–Mn–Nb, phase studies, 20: 15103
Al–C–Nb, phase studies, 20: 15103
Al–C–Nb–V, phase studies, 20: 15103
Al–C–Nb–Zn, phase studies, 20: 15103
Al–C–Ni–Nb, phase studies, 20: 15103
B–Co–Nb, phase studies, 20: 15100
B–Cu–Nb, crystal structure, 20: 14532
B–Fe–Nb, crystal structure, 20: 14532
C–Co–Nb, phase studies, 20: 15077
C–Cr–Nb, phase studies, 20: 15108
C–Mo–Nb–Zr, heat treatment of, 20: 14972(P)
C–Nb–Ta–Zr, heat treatment of, 20: 14972(P)
C–Nb–Ti–Zr, heat treatment of, 20: 14972(P)
C–Nb–V–Zr, heat treatment of, 20: 14972(P)
C–Nb–W–Zr, heat treatment of, 20: 14972(P)
C–Nb–W–Zr, tensile properties of D-43, 20: 15068
Mo–Nb–N–Zr, heat treatment of, 20: 14972(P)
Mo–Nb–O–Zr, heat treatment of, 20: 14972(P)
Nb–N–Ta–Zr, heat treatment of, 20: 14972(P)
Nb–N–Ti–Zr, heat treatment of, 20: 14972(P)
Nb–N–V–Zr, heat treatment of, 20: 14972(P)
Nb–N–W–Zr, heat treatment of, 20: 14972(P)
Nb–O–Ta–Zr, heat treatment of, 20: 14972(P)
Nb–O–Ti–Zr, heat treatment of, 20: 14972(P)
Nb–O–V–Zr, heat treatment of, 20: 14972(P)
Nb–O–W–Zr, heat treatment of, 20: 14972(P)
Nb–UP, compatibility, 20: 15032(R) (ANL-7152, pp 50-72)

NITRATE IONS
electron spin resonance in x-irradiated sodium nitrate crystals, hyperfine structure from, (E), 20: 15965

NITRATES
determination by coulometric titration, 20: 14455(R) (ORNL-3889, pp 25-32)
determination in fired thoria, infrared spectroscopic, 20: 14468 (TID-22505)
determination in 4-*sec*-butyl-2(α-methylbenzyl)phenol, spectrophotometric, 20: 14455(R) (ORNL-3889, pp 25-32)
yields from radiolysis of sodium acid phosphite solutions in sodium nitrate, effects of pH on, 20: 14601

NITRIC ACID
corrosive effects on types 416 and 430F stainless steels, effects of uranium on, 20: 14983 (NP-15875)
$HF–HNO_3$, corrosive effects on type-304L stainless steel, effects of aluminum, iron, and thorium ions on, 20: 14982(R) (NLCO-970, pp 6.1-4)
HNO_3–Pu, criticality parameters of water-reflected spheres of, (T), 20: 16031
HNO_3–tetrahydrofuran, analytical use for combined exchange-solvent extraction separation of uranium, 20: 14469(R) (TID-22650)
HNO_3–U, criticality parameters of water-reflected spheres of, (T), 20: 16031
methanol–HNO_3, spectrophotometric analysis for metals, 20: 14469(R) (TID-22650)

NITRITES
determination in nitrate-containing potassium iodide solutions, titrimetric, 20: 14455(R) (ORNL-3889, pp 25-32)

NITROCELLULOSE
determination in mock explosive, method for, 20: 14470 (UCRL-7873)

NITROGEN
determination in plasmas, time-resolved profile measurements of, (E), 20: 15872 (IPP-1/41)
determination in plutonium metal, alloys, and compounds, 20: 14440 (LA-3452)
deuteron reactions with, electron-capture cross sections for, (E/T), 20: 15886(R) (UCRL-14285)
diagnostics of discharge plasma of, mass spectrometric sampling probe for, 20: 15915
effects on brittleness of tantalum, 20: 15130
effects on corrosion of zirconium-base alloys by steam, 20: 14980(R) (GEAP-5065)
energy and mass transfer between argon plasma jet and, 20: 15584
hydrogen ion reactions with, cross sections for, (E/T), 20: 15886(R) (UCRL-14285)
proton reactions with, electron-capture cross sections for, (E/T), 20: 15886(R) (UCRL-14285)
reactions with uranium carbide at 550 to 1050°C, 20: 14994
vapor pressure of, from chemical reactions in sol-gel fuels, 20: 14512 (ORNL-TM-1418)

NITROGEN IONS
electron transitions in, oscillator strengths for probability of, (T), 20: 15275
radioinduced N_2^- as defect in sodium azide, ESR spectral studies on, 20: 15942 (NYO-2150-11)
scattering by odd-A nuclei at 16.2 and 17.7 Mev, Coulomb excitation in, (E), 20: 15759

NITROGEN ISOTOPES N-13
decay of, K-capture to positron ratios for, (E), 20: 15712 (CONF-233 (Vol.2), pp 359-64)
nucleon emission from, reduced widths in shell-model intermediate coupling, (T), 20: 15830

NITROGEN ISOTOPES N-14
helium-3 reactions (He-3, α) with, association replacement amplitudes for, (T), 20: 15838
proton elastic scattering at 4.9 Mev to 10.1 Mev, polarization from elastic, (E), 20: 15783
scattering by samarium-152 and selenium-78, 2^+ level excitation in, (T), 20: 15768

NITROGEN ISOTOPES N-15
energy levels from boron-11 (α,n) reactions, parity and spin of, (E), 20: 15790

NITROGEN MUSTARDS
effects on bacteriophages, inactivating, 20: 14267

NITROGEN OXIDES
effects on radiolysis of cyclopentane, 20: 14599
properties as gamma dosimeter, 20: 14870

NITROGEN SYSTEMS
CO_2–glass–N_2, heat transfer in glass-bead suspensions, 20: 14671(R) (TID-22394)
Mo–Nb–N–Zr, heat treatment of, 20: 14972(P)
Nb–N–Ta–Zr, heat treatment of, 20: 14972(P)
Nb–N–Ti–Zr, heat treatment of, 20: 14972(P)
Nb–N–V–Zr, heat treatment of, 20: 14972(P)
Nb–N–W–Zr, heat treatment of, 20: 14972(P)
N–Pu–U, properties of hot-pressed powders of, 20: 14957(R) (BMI-1754)

NOBELIUM
production in heavy-ion nuclear reactions, review of, 20: 15740

NORWAY
fallout monitoring, 1963 through 1965, 20: 14739 (TID-22655)

NOZZLES
uses of ejector, for cleaning metallic filters, 20: 14645

NPD REACTOR

environs monitoring, 20: 14738 (NP-15853, pp 21-33)
operation of, review of experience in, 20: 16097
NUCLEAR BATTERIES
development of isotope-heated thermionic cells, 20: 15294 (CONF-640921, pp 9-45)
NUCLEAR EMULSIONS
mesons (K^-) and (π^-) and proton reactions at 1.5 to 25 Bev, lithium-8 energy spectra from, (E), 20: 15792
preparation of thorium- and uranium-containing, 20: 14877
proton scattering in, small-angle elastic, (E/T), 20: 15314 (RT/FI(65)35)
NUCLEAR ISOMERS
gamma energies and half lives of 5- to 1000-μsec, (E), 20: 15856
half lives of hafnium-178, hafnium-179, tungsten-183, and ytterbium-177, (E), 20: 15688 (AD-620384)
NUCLEAR MAGNETIC RESONANCE
spectra of organic compounds, data recordings of, 20: 14459(R) (ORNL-3889, pp 44-6)
NUCLEAR MATERIALS MANAGEMENT
burnup calculations for reactor fuels, 20: 16061(R) (BAW-296)
determination of plutonium and uranium in nuclear fuel cycles, evaluation of methods for, 20: 14447 (NBL-231)
sampling program for, in uranium refining and machining, 20: 16140
NUCLEAR MODELS
book: *Coulomb Excitation*, 20: 15848
compound nucleus, parameters for calculation of neutron cross sections using, 20: 15863
for vibrational states, microscopic, 20: 15851
perturbation theory for deformation in light nuclei in Nilsson, 20: 15809
rotation in cranking, unified derivation for, 20: 15828
NUCLEAR MODELS (COLLECTIVE)
use for level parity and spin assignments, 20: 15726 (ORNL-P-1957)
NUCLEAR MODELS (OPTICAL)
potentials in, energy dependence and nonlocality of, (T), 20: 15829
relativistic characteristics of, 20: 15730(R) (RHEL/R-112, pp 67-98)
use for level parity and spin assignments, 20: 15726 (ORNL-P-1957)
uses for nuclear analyses, 20: 15730(R) (RHEL/R-112, pp 67-98)
NUCLEAR MODELS (SHELL)
potential for one-nucleon definite j-value state in, (T), 20: 15791
use in study of core polarization in transfer reactions, 20: 15852
uses for nuclear analyses, 20: 15730(R) (RHEL/R-112, pp 67-98)
NUCLEAR PHYSICS
research at Seibersdorf, 20: 16127
NUCLEAR POWER PLANTS
design using vapor-cooled heterogeneous reactor, 20: 16106(P)
development of nuclear-thermionic, 20: 15294 (CONF-640921, pp 9-45)
radiation monitoring in, instrumentation for, 20: 14864
NUCLEAR REACTIONS
analysis of (d,p) and (p,d), effects of D-wave deuteron states on, 20: 15730(R) (RHEL/R-112, pp 67-98)
core polarization in, shell-model and sum-rule calculations of, 20: 15852
cross sections for helium-3, table on, (E), 20: 14661(R) (ORNL-3889, pp 48-70)
energies of, calculation of, 20: 15853
nucleon potentials in photo-dipole approximation in nonlocal, (T), 20: 15842
rates of nonresonant, at stellar temperatures, (T), 20: 15221
theory for, channels projection operator and Pauli principle in, 20: 15744
NUCLEAR SPIN
coupling constant for, alternant molecular orbital expressions for, 20: 14543
NUCLEAR STRUCTURE
book: *Coulomb Excitation*, 20: 15848
conference, 20: 15749
deformations in rare earth and light nuclei, self consistent calculation for, 20: 15843
systematics of, calculation of, 20: 15853
NUCLEAR THEORY
decay theory of closely coupled unstable states, 20: 15816
forces in, meson resonance effects on, 20: 15817
nucleon pairing in finite nuclei, variational derivation of equation for, 20: 15742
NUCLEI
alpha emission from 1p shell of fractional parentage, coefficients for, (T), 20: 15741
beta decay of, effects of strong interactions between nucleons on forbidden, 20: 15836
beta decay of, effect of Coulomb field on, (T), 20: 15716 (CONF-233 (Vol.3), pp 529-37)
beta decay of, effect of Coulomb field on, (T), 20: 15716 (CONF-233 (Vol.3), pp 529-37)
charged-particle inelastic scattering by, analytic expressions for, (T), 20: 15743
charged-particle scattering by, collective-state excitation in, (T), 20: 15763
conference on spectroscopy and structure of, 20: 15749
decay by electron capture, use of calibrated gamma spectrometer for measuring, 20: 15747
decay theory of closely coupled unstable states in, 20: 15816
deformation in light, perturbation theory for, 20: 15809
deformation shapes of rare earth and light, self-consistent calculation for, 20: 15843
deuteron elastic and inelastic scattering at 15 Mev, (E/T), 20: 15850
deuteron reactions at 15-Mev, isomer production in, (E), 20: 15856
deuteron reactions (d,p) with, effects of D-wave deuteron states on, (T), 20: 15730(R) (RHEL/R-112, pp 67-98)
electron capture by, processes from, 20: 15693 (CONF-233(Vol.1))
electron capture by, review of orbital, (E/T), 20: 15695 (CONF-233 (Vol.1), pp 30-56)
electron inelastic scattering by light, relations between E1 sum rules and form factors for, (T), 20: 15746
electron reactions with, internal pair production in, (E/T), 20: 15696 (CONF-233(Vol.1), pp 60-86)
elementary particle reactions in nuclear Coulomb fields of, (T), 20: 15562
energy level in odd-A deformed, in rare earth region, collective, 20: 15833
energy level transitions in deformed, effect of pairing correlations on E-1, (T), 20: 15764
energy level transitions in deformed odd, delayed E1, (T), 20: 15765
energy level transition probabilities in deformed odd, pairing correlations in E1, (T), 20: 15766
energy levels in, microscopic models for vibrational, (T), 20: 15851
energy levels of neutron deficient, for $39 \leq Z \leq 49$, 20: 15727 (PPAD-572F)
energy levels of odd-odd light deformed, unified model wave functions for low-lying rotational, (T), 20: 15814
energy levels of, parity and spin assignment by DWBA method, 20: 15726 (ORNL-P-1957)
energy levels of, unified derivation of cranking model and Peierls-Yoccoz method for rotational, (T), 20: 15828
energy levels of, statistics of random-matrix eigenvalues for, (T), 20: 15784
excitation of 2^+ levels in even-even, interference effects in Coulomb, (T), 20: 15768
forces in, effect of meson resonances on, 20: 15817
heavy-ion reactions with heavy, production of transcurium elements by, 20: 15740
helium-3 reactions (He-3,n) with light, angular distributions for direct, (T), 20: 15798
internal conversion coefficients for $2^+ \rightarrow 0^+$ transitions in deformed, E2, (E), 20: 15745
ion inelastic scattering by, gamma-ion angular correlations in, (T), 20: 15767
magnetic moments of light, 20: 15439
meson (π^+) reactions, double-charge-exchange cross sections for, (T), 20: 15813
meson (π) quasi-elastic scattering by, nucleon correlation effects on, (T), 20: 15827
moment of inertia of, Fermi theory for, 20: 15835
neutron capture by, gamma production data for, 20: 15725 (NP-14855)
neutron definite j-value state for, shell model for single, (T), 20: 15791
neutron elastic scattering at 0.8 Mev, cross sections for, (T), 20: 15770
nucleon pairing in finite, variational derivation of equation for, (T), 20: 15742
parities of, use of deuteron scattering data in calculating, 20: 15850
photon absorption by, giant quadrupole resonance in, (T), 20: 15823
photon reactions with, dipole approximation in nonlocal potential for, (T), 20: 15842
photon splitting in electric field of, cross section for, (T), 20: 15339
polarization by electron-nucleus dipolar coupling, (T), 20: 15819
properties of, solution for Brownian motion of random-matrix eigenvalues 20: 15785
proton inelastic scattering at 155 Mev by light even, cross sections for, (T), 20: 15897
proton reactions (p,d) with, effects of D-wave deuteron states on, (T), 20: 15730(R) (RHEL/R-112, pp 67-98)
proton reactions (p,2p) with, diprotons model for, 20: 15730(R) (RHEL/R-112, pp 67-98)
radioactivity of electron-capturing, absolute measurement of, 20: 15690 (CEA-R-2813)
triton reactions (t,p) with light, angular distributions for direct, (T), 20: 15798
NUCLEI (CELLS)
radiation effects on ultrastructure of, 20: 14335
radioinduced depletion of, in bone marrow, spleen, and thymus of young mice, γ, 20: 14365
NUCLEIC ACIDS

content in viruses, effects on radioinduced inactivation, 20: 14387
radiation effects on phosphate levels in Phycomyces, x, 20: 14264
radiation effects on, in growing plant cells, 20: 14383

NUCLEONS
emission from nuclei, reduced widths in shell model intermediate coupling, (T), 20: 15830
form factors for, current algebra for coupling constants for, 20: 15308 (IC/66/18)
form factors of, determination using electron scattering, 20: 15439
form factors of, determination using electron scattering, 20: 15440
form factors of, electromagnetic, (E), 20: 15306(R) (CEAL-1026)
form factors of, isospin exchange relations for, (T), 20: 15449
form factors of, relations for, (T), 20: 15492
interactions in nuclei, effects on meson (π)-induced nuclear reactions, (T), 20: 15827
interactions in nuclei, effects on forbidden beta transitions of strong, 20: 15836
interactions in nuclei, statistics of random-matrix eigenvalues for, (T), 20: 15784
interactions of, Faddeev equations for three-body, (T), 20: 15343
interactions with mesons, (π), amplitudes for, (T), 20: 15312 (MIT-2096-86)
interactions with nucleons, effect of meson-resonance exchange on, 20: 15817
interactions with hyperons (Λ) in hypernuclei, nuclear contractions effects from, (T), 20: 15826
interactions with mesons (K^-) at high energies, resonances in, (E), 20: 15414
interactions with mesons, peripheral model for, (T), 20: 15419
interactions with mesons (K), testing broken M(12) symmetry by vector exchange in, (T), 20: 15421
interactions with photons at low energies, meson (π) production in, (T), 20: 15441
interactions with mesons, renormalization theory for, 20: 15453
interactions with mesons, N/D method for, 20: 15466
interactions with mesons (π), rescattering correction for three-body final-state, (T), 20: 15476
interactions with photons, dispersion sum rules for meson (π) production in, (T), 20: 15503
interactions with mesons (π) at low energies, dispersion theory of, 20: 15522
interactions with mesons, classical limit of cross sections for, (T), 20: 15563
interactions with mesons (π), pseudoscalar and scalar, (T), 20: 15325
interactions with mesons (π), mass and coupling constant for, 20: 15352
interactions with mesons (π), meson (ρ) exchange in, (T), 20: 15364
interactions with mesons (π), review of, 20: 15371
interactions with mesons (π), dispersion relations for low-energy, (T), 20: 15385
interactions with deuteron, amplitude for inelastic, (T), 20: 15386
interactions with neutrinos, lepton production in, (T), 20: 15387
interactions with mesons (π) and (K) $\bar{U}(12)$ symmetry for, 20: 15390
interactions with weak intermediate bosons, (T), 20: 15396
interactions with mesons ($\pi^\pm$) at 1.7 Bev/c, meson (ω) and (ρ^0) production and decay in, (E), 20: 15403
interactions with mesons (π) at 1.68 Bev/c, $Y_0^*(1405)$ and $Y_1^*(1358)$ production in, (E), 20: 15404
pairing in finite nuclei, variational derivation of equation for, (T), 20: 15742
reactions with nuclei, core polarization effects in, (T), 20: 15852

NUCLEOPROTEINS
radiation effects on DNA in deoxy-, protective effects of albumin against, 20: 14277
radioinduced free radicals in nucleohistone, x, 20: 14592

NUCLEOTIDES, PYRIDINE DIPHOSPHATE
radiation effects on content in sarcoma cells, x, 20: 14370

O

OCEANOGRAPHY
of Mediterranean Sea along the Israel shelf, 20: 14731(R) (NP-159861)

ODOR
radiation effects on meat, γ, 20: 14930 (NP-15676)
radiation effects on meat, γ, 20: 14931 (NP-15677)

OILS
analysis for radioisotopes in copra and desiccated-coconut oils, activation, 20: 14463 (PAEC(D)CH-652)
analysis of commercial coconut, gas chromatographic, 20: 14463 (PAEC(D)CH-652)

OLEIC ACID
determination in commercial coconut oils, gas chromatographic, 20: 14463 (PAEC(D)CH-652)

ONIONS
cuticular membranes in, permeability to organic compounds, 20: 16146 (COO-588-39)

OPTICAL SYSTEMS
description of flying-spot digitizer for analysis of bubble-chamber photographs, 20: 14850 (BNL-9763)
uses of flying-spot digitizers with FILTER code for particle-track analysis, 20: 14849 (BNL-9720)

ORGANIC ACIDS
radioinduced pyrolysis of, in water-t_2, electron, 20: 14623
yields from radioinduced oxidation of paraffin, 20: 14612(T)

ORGANIC COMPOUNDS
analysis of labeled, 20: 14501
determination of, by electron-induced pyrolysis, 20: 14623
labeling with tritium by recoil reactions, 20: 14620
labeling with tritium, method for, 20: 14633(P)

ORGANIC COOLED REACTORS
development of heavy water-moderated power and process-heat, 20: 16109

ORGANIC MODERATED REACTORS
control of polyphenyls in working environments of, methods for, 20: 14467 (RT/PROT(64)-20)

ORGANISMS
distribution of migrating mesopelagic, in deep scattering layers of ocean waters, 20: 14235 (SAN-584-1)

ORNL HIGH FLUX ISOTOPE REACTOR
fuel cladding failure detector for, design of, 20: 16124 (ORNL-TM-1388)
radiation alarm and monitoring systems for, design of, 20: 16125 (ORNL-TM-1393)

OSMIUM
energy level transitions in, Coster-Kronig, (T), 20: 15238 (CONF-233 (Vol.3), pp 398-418)

OSMIUM ALLOYS
Gd–Os–Y, thermal capacity of intermetallic compounds of, at 0.25 to 20.0°K, 20: 15061 (UCRL-11580)

OSMIUM ISOTOPES Os-186
energy level transitions in, conversion coefficients for E2, (E), 20: 15706 (CONF-233(Vol.2), pp191-7)

OSMIUM ISOTOPES Os-188
energy level transitions in, conversion coefficients for E2, (E), 20: 15706 (CONF-233(Vol.2), pp 191-7)

OSMIUM ISOTOPES Os-192
neutron reactions (n,2n) at 14.6 Mev, isomeric cross section ratio for, (E/T), 20: 15773

OTTAWA RIVER
cesium-137 content in, 20: 14738 (NP-15853, pp 21-33)
radiation monitoring, α and β, 20: 14738 (NP-15853, pp 21-33)
strontium-89 content in, 20: 14738 (NP-15853, pp 21-33)
strontium-90 content in, 20: 14738 (NP-15853, pp 21-33)

OXAMIDE
determination in explosives, method for, 20: 14470 (UCRL-7873)

OXIDES
diffusion and particle size of, from ignited plutonium, 20: 15036 (BNWL-205)

OXYGEN
determination in alkali metals, activation, 20: 14454(R) (ORNL-3889 pp 17-24)
determination in other elements by helium-3 activation, 20: 14661(R) (ORNL-3889, pp 48-70)
determination in plasmas, time-resolved profile measurements of, (E), 20: 15872 (IPP-1/41)
determination in potassium by surface tension method, 20: 14445(R) (MSAR-66-10)
determination in potassium and sodium, amalgamation method for, 20: 14432 (ANL-7123)
determination in uranium dioxide using electron microprobe, 20: 14442(R) (MCW-1493, pp 5-13)
effects of impurity of, on positron annihilation spectrum in argon, (E), 20: 15436
effects on brittleness of tantalum, 20: 15130
effects on oxidation of cyclohexane by gamma radiation, 20: 14625
effects on radiolysis of cyclopentane, 20: 14599
electric discharges in, collision frequency measurements in afterglow of, (E), 20: 15867 (AD-620664)
production in helium star cores, (T), 20: 15195
proton excitation at 18 to 102 kev, (E), 20: 15271
radiosensitivity effects on DNA, x, 20: 14283
radiosensitivity effects on yeasts, 20: 14399
reaction with tungsten single crystals, penetration and sorption in, (E), 20: 15986(T)
reactions with uranium monocarbide *in vacuo* at 900 to 1000°C and at 1800°C, 20: 14985

OXYGEN FLUORIDES
photochemical reactions with krypton, 20: 14527

vibrational potential function of bent molecules of, third-order, 20: 14559
OXYGEN IONS
charge states of oxygen-16, after passage through gold and nickel foils, 20: 15854
electron transitions in, oscillator strengths for probability of, (T), 20: 15275
reactions with krypton atoms at 25 to 230 kev, (E), 20: 15249 (TID-22648)
reactions with niobium surface, secondary oxide ion emission from, (E), 20: 15976(T)
OXYGEN ISOTOPES O-15
energy levels, (E), 20: 15729(R) (RHEL/R-112, pp 37-66)
OXYGEN ISOTOPES O-16
alpha reactions (α,2α) at intermediate energies, final-state interaction effects on, (T), 20: 15825
charge states of ions of, after passage through gold and nickel foils, 20: 15854
helium-3 reactions (He-3,α) with, measurement and distorted wave analysis of, 20: 15855
neutron reactions (n,α) at 14 Mev, mechanisms for, (E), 20: 15738
nuclear properties in shell model, 20: 15730 (RHEL/R-112, pp 67-98)
proton reactions (p,d) at 30 Mev, distributions from, (E), 20: 15729(R) (RHEL/R-112, pp 37-66)
proton scattering at 50 Mev, differential cross sections for, (E), 20: 15728(R) (RHEL/R-112, pp 23-36)
triton reactions (t,p) with, angular distributions for, (T), 20: 15798
OXYGEN ISOTOPES O-17
hyperfine structure in hydroxyl radicals, 20: 15272
OXYGEN ISOTOPES O-18
exchange between orthotungstate or 12-tungstocobaltate(III) and water at 25°C, 20: 14525
OXYGEN SYSTEMS
C–O–Th, vapor pressure of carbon monoxide in sol-gel fuels of, 20: 14512 (ORNL-TM-1418)
C–O–U, phase studies at 1700°C, 20: 14968(R) (USBM-RC-1220)
C–O–U, vapor pressure of carbon monoxide in sol-gel fuels of, 20: 14512 (ORNL-TM-1418)
Mo–Nb–O–Zr, heat treatment of, 20: 14972(P)
Nb–O–Ta–Zr, heat treatment of, 20: 14972(P)
Nb–O–Ti–Zr, heat treatment of, 20: 14972(P)
Nb–O–V–Zr, heat treatment of, 20: 14972(P)
Nb–O–W–Zr, heat treatment of, 20: 14972(P)

P

PACIFIC OCEAN
mesopelagic organisms in deep scattering layers of Santa Barbara Channel of, distribution of migrating, 20: 14235 (SAN-584-1)
PACKAGING
standards of, for radiosterilized items, 20: 14942
PACKED COLUMNS
fluid flow through ring- and sphere-, dispersion in single-phase, 20: 14691 (UCRL-10696(Rev.)(Pt.2))
PAINTS
analysis of automobile, activation, 20: 14439(R) (GA-5556)
diffusion of tritium from tritiated, 20: 14461(R) (ORNL-3889, pp 48-70)
PALLADIUM
content in spent power reactor fuels, evaluation of, 20: 14435 (BNWL-SA-503)
energy level transitions in, Coster-Kronig, (T), 20: 15238 (CONF-233 (Vol.3), pp 398-418)
energy level widths for, K, (T), 20: 15239 (CONF-233(Vol.3), pp 419-39)
radiochemistry of, 20: 15727 (PPAD-572F)
PALLADIUM ALLOYS
Pd–Pt, catalytic effects on deuterium-methane exchange and propane cracking reactions, 20: 14542
Pd–Rh, catalytic effects on deuterium-methane exchange and propane cracking reactions, 20: 14542
PALLADIUM ISOTOPES
neutron reactions (n,γ) with, gamma spectra from thermal, (E), 20: 15755
PALLADIUM ISOTOPES Pd-105
energy levels, (E), 20: 15755
PALLADIUM ISOTOPES Pd-106
energy levels, (E), 20: 15755
PALLADIUM ISOTOPES Pd-110
neutron reactions (n,γ) with, isomeric cross-section ratios in, (E), 20: 15777
PALLADIUM ISOTOPES Pd-111
production of isomeric, cross sections for neutron-capture, (E), 20: 15777
PALMITIC ACID
determination in commercial coconut oils, gas chromatographic, 20: 14463 (PAEC(D)CH-652)
PALMITIC ACID, METHYL ESTER
effects on lipid levels in mouse liver, lung, plasma, and spleen, 20: 14241 (TID-21437)
metabolism of carbon-14-labeled, in mouse reticulo-endothelial system, 20: 14241 (TID-21437)
PAPER
analysis in criminal cases, activation, 20: 14439(R) (GA-5556)
PARABIOSIS
effects on anemias in mice, 20: 14290(R) (NYO-1800-12)
PARAFFIN
composition and quality of mixtures of commercial, evaluation of, 20: 14637 (DP-1034)
neutron flux distributions in, (E), 20: 15683
radioinduced oxidation of, effects of dose rate on, 20: 14612(T)
PARASITES
radiosensitivity of fruit fly, γ, 20: 14935
PARTICLE COLLECTORS
design of large-volume impactor, for atmospheric sampling, 20: 14815 (COO-401-139)
development for monitoring in radiochemical processing plants, 20: 14811
PARTICLE STATISTICS
many-body problem in, Liouville's equation for, (T), 20: 15148 (N65-20165)
PARTICLE TRACKS
analysis in bubble-chamber photographs, flying-spot digitizers for, 20: 14850 (BNL-9763)
analysis in photographs using flying-spot digitizers and FILTER program, 20: 14849 (BNL-9720)
measurement in bubble chambers, computer-controlled system for, 20: 14861 (UCRL-16555)
PARTICLE TRAJECTORIES
analysis of, from beam–beam collisions, 20: 15166 (SLAC-49)
distribution functions of, in plain magnetic fields, (T), 20: 15620
PARTICLES
adiabatic invariants of gyrating, in magnetic fields, (T), 20: 15623 (MPI-PAE/P1.15/65)
distributions of injested or inhaled radioactive, 20: 14785 (BNWL-182)
interactions of point, conservation laws for classical relativistic mechanics of, 20: 15154
kinetics of classical hamiltonian, invariance transformations for, (T), 20: 15150
motion equations for pole-dipole test, in general relativity, 20: 15641
motion of classical, Poincare-invariant equations for, 20: 15153
motion of many-body systems of, (T), 20: 15148 (N65-20165)
orbits in gravitational field of magnetic universe, 20: 15634
PEAS
radioinduced mutations in *Vigna sinensis*, neutron and x, 20: 14341
PEAT
moisture content of, neutron method for measuring, 20: 14756
PEBBLE BED REACTORS
design of graphite-moderated, 20: 16043(P)
PENTACENE
electron transitions in, oscillator strengths for probability of, (T), 20: 15275
PENTAERYTHRITOL
determination in mock explosive, method for, 20: 14470 (UCRL-7873)
PENTAERYTHRITOL TETRANITRATE
determination in explosives, methods for, 20: 14470 (UCRL-7873)
2,4-PENTANEDIONE
uses in gas chromatographic separation of aluminum, beryllium, and scandium, 20: 14486
2,4-PENTANEDIONE COMPLEXES
properties and use in gas chromatography, 20: 14499
with cobalt, effects of neutron reactions (n,γ) on, 20: 14584(R) (TID-22444)
with uranium, controlled-potential coulometric analysis for uranium in, 20: 14444(R) (MLM-1268)
2,4-PENTANEDIONE, TRIFLUORO-
uses in gas chromatographic separation of aluminum, beryllium, and scandium, 20: 14486
PEPTIDES
radiation chemistry of aqueous solutions of aliphatic, γ, 20: 14616
synthesis under primitive earth conditions, role of cyanamides in, 20: 14233 (UCRL-16566)
PERISCOPES
design of tele-, for photographing and viewing irradiated fuel elements, engineering drawings for, 20: 14675
PERMEABILITY
radiation effects on cell-wall, in *B. cereus*, x, 20: 14263
PEROXIDES
photolysis of diacyl, redistribution of energy in, 20: 14619
radiation effects on formation of, in rat tissue homogenates, 20: 14261
radiolysis of diacyl, redistribution of energy in, 20: 14619

PERSONNEL
radiation exposure of, legal aspects of records of, 20: 14801
radiation monitoring of, engineering drawings of alpha hand and foot counter for, 20: 14809
PERTECHNETATES
use of technetium-99-labeled, in plasma clearance tests, 20: 14423
PERTURBATION THEORY
hypergeometric function of two variables in, 20: 14952
quantum field theory formulation in LSZ, ambiguities in, 20: 15452
S-matrix formalism in, 20: 15526
PERU
radiation protection in, program for, 20: 14793
PETROLEUM
determination in rock strata using well logging, 20: 14777
neutron diffusion parameters in, determination of, using pulsed source, 20: 14772
PHANTOMS
neutron dosimetry in whole-body, epithermal, 20: 14421
neutron reactions in standard-man, high-energy, 20: 14330
proton reactions in standard-man, high-energy, 20: 14330
use of water, for ionization chamber testing, 20: 14894
PHENOL, 4-*sec*-BUTYL-2-α-METHYLBENZYL-
analysis for nitrates, spectrophotometric, 20: 14455(R) (ORNL-3889, pp 25-32)
PHENOTHIAZINE, 3-CHLORO-10-(3'-DIMETHYLAMINOPROPYL)-
radiosensitivity effects in rats, 20: 14293
radiosensitivity effects in rats, 20: 14391
PHONONS
interactions with electrons in metals in magnetic fields, effects on electron mass, (T), 20: 15939 (AD-620189)
interactions with electrons in metals, collective theory for, 20: 15987
interactions with electrons, electric conductivity of polarons in, (T), 20: 15988
interactions with electrons in superconductors, effects on structure, 20: 15664
properties from gamma resonant scattering in monocrystals, 20: 15948
PHOSPHATE GLASS
leachability of alumina-containing, prepared from radioactive calcined alumina waste, 20: 16133 (IDO-14672)
PHOSPHATES
content in rat urine, effects of burns, cytostatics, or methionine-sulfoximine on, 20: 14270
effects on spectrophotometric determination of thorium using Chrome Azurol S, 20: 14485
radiation effects on Phycomyces metabolism of, x, 20: 14264
radiation effects on urinary excretion by rats, x, 20: 14270
yields from radiolysis of sodium acid phosphite solutions in sodium nitrate, effects of pH on, 20: 14601
PHOSPHATIDES
radiation effects on rabbit mitochondrial, γ, 20: 14278
PHOSPHINE OXIDE, TRIOCTYL-
analysis for uranium, polarographic, 20: 14452(R) (ORNL-3889, pp 1-12)
PHOSPHONIC ACID, PENTYL-, DIPENTYL ESTER
solvent properties for thorium, 20: 14448(R) (NLCO-970, pp 1.1-22)
dipentyl pentylphosphonate–$Th(NO_3)_4$, thorium distribution in, 20: 14448(R) (NLCO-970, pp 1.1-22)
PHOSPHONIC ACID, PHENYL-, DI-*sec*-BUTYL ESTER
solvent properties for thorium, 20: 14448(R) (NLCO-970, pp 1.1-22)
PHOSPHONIUM BROMIDES
benzyltributyl-, preparation, 20: 14576(R) (ORNL-3889, pp 73-7)
PHOSPHONIUM CHLORIDES
benzyltributyl-, preparation, 20: 14576(R) (ORNL-3889, pp 73-7)
PHOSPHORIC ACID
corrosive effects on niobium-base alloys, effects of alloy composition on, 20: 14997
PHOSPHORIC ACID, BIS(2-ETHYLHEXYL) ESTER
solvent properties for strontium-90, 20: 14641 (RL-SA-59)
solvent properties for curium, 20: 14457(R) (ORNL-3889, pp 36-39)
PHOSPHORS
scintillation intensity in organic, time dependence of, (T), 20: 14615
scintillation response of plastic, for 3 to 11-kev electrons, 20: 14895
PHOSPHORUS
determination in plutonium fluorides and peroxides, review on spectrographic, 20: 14464 (RFP-599)
determination of trace amounts of, in iron, activation, 20: 14471
determination of trace amounts of, in uranium dioxide, 20: 14494
PHOSPHORUS IONS
reactions with p-type silicon, for production of solar batteries, 20: 15302(T)
PHOSPHORUS ISOTOPES P-30
energy levels of, unified model wave function for low-lying rotational, (T), 20: 15814
PHOSPHORUS ISOTOPES P-31
nuclear properties in shell model, 20: 15730 (RHEL/R-112, pp 67-98)
PHOSPHORUS ISOTOPES P-32
determination in atmospheric and precipitation samples, methods for radiochemical, 20: 14430 (AD-620219)
dosimetry in animals using hematological changes, 20: 14314
recoil chemistry in neutron reactions (n,p) in cysteic acid, cysteine, and cystine, 20: 14584(R) (TID-22444)
sorption by rat skin, 20: 14253
uptake by bone marrow cells in rats, 20: 14248
use in internal therapy, survey of techniques for, 20: 14406
PHOSPHORUS ISOTOPES P-33
determination in atmospheric and precipitation samples, methods for radiochemical, 20: 14430 (AD-620219)
half life, (E), 20: 14461(R) (ORNL-3889, pp 48-70)
PHOTOCHEMISTRY
photoinactivation of trypsin, dye-sensitized, 20: 14274
reaction mechanisms for dehydration condensation in aqueous solutions under primitive earth conditions, 20: 14233 (UCRL-16566)
PHOTOELECTRIC CELLS
development of photovoltaic cells, 20: 15305
PHOTOELECTRIC EFFECT
use for internal conversion measurements, 20: 15709 (CONF-233(Vol.2), pp 247-51)
PHOTOGRAPHIC FILM
analysis for particle tracks using flying-spot digitizers, 20: 14850 (BNL-9763)
particle track analysis in, using flying-spot digitizers and FILTER program, 20: 14849 (BNL-9720)
PHOTOGRAPHIC FILM DETECTORS
performance and properties, 20: 14907
performance as personnel dosimeters for gamma radiation, 20: 14806
PHOTOGRAPHY
equipment for bubble-chamber, engineering drawings of, 20: 14898
PHOTOMULTIPLIER TUBES
design for detection of air fluorescence from nuclear explosions, 20: 15609
enclosures for, design of temperature-sensitive, 20: 14822(R) (RHEL/R-112, pp 99-128)
performance for detection of air fluorescence from nuclear explosions, (T), 20: 15608
PHOTONS
absorption by nuclei, giant quadrupole resonance in, (T), 20: 15823
interactions at high energies, lectures on, 20: 15437
interactions in nuclear electric field, cross section for splitting, (T), 20: 15339
interactions with protons, meson production in, (E), 20: 15306(R) (CEAL-1026)
interactions with protons at high energies, meson ($K^{\pm}$) and meson ($\pi^{\pm}$) production in, (E), 20: 15306(R) (CEAL-1026)
interactions with protons at high energies, meson ($\pi^{\pm}$) production in, (E), 20: 15306(R) (CEAL-1026)
interactions with nucleons at low energies, meson (π) production in, (T), 20: 15441
interactions with nucleons, dispersion sum rules for meson (π) production in, (T), 20: 15503
interactions with elementary particles, CP violation in, (T), 20: 15309 (JINR-E-2563)
interactions with protons, E1 and M2 amplitudes in single-pion-production, (T), 20: 15365
production of monochromatic beams of, review on, 20: 14841
production of polarized, using laser beams, 20: 15306(R) (CEAL-1026)
properties of beams of, coherence, (T), 20: 15328
reactions with nuclei, dipole approximation in nonlocal potential for, (T), 20: 15842
scattering by protons, Compton, (E), 20: 15306(R) (CEAL-1026)
yields from meson (π^-)-proton interactions at 9 Bev/c, (E), 20: 15384
PHYSIOLOGY
tracer studies of animal, 20: 14386
PINCH EFFECT
research progress, 20: 15882(R) (NP-15868)
PIPES
gamma transmission through steel, Monte Carlo calculation of, 20: 16114
hydrogen flow in copper, film boiling in cooldown, 20: 14697
PIQUA POWER REACTOR
auxiliaries and components operations in, 20: 16080(R) (NAA-SR-11628, pp 51-78)
coolant chemistry parameters of, through May 1965, 20: 16081(R) (NAA-SR-11628, pp 79-104)
coolant filters for, examination of used, 20: 16084(R) (NAA-SR-11628, pp 124-34)
coolant oxidation in, effects of irradiation on, 20: 16082(R) (NAA-SR-11628, pp 105-7)
development and operations of, 20: 16077(R) (NAA-SR-11628)

fuel elements of, post-irradiation inspection of malfunctioning, 20: 16083(R) (NAA-SR-11628, pp 108-23)
kinetics analysis and evaluation for, 20: 16079(R) (NAA-SR-11628, pp 17-50)
operations of, 20: 16078(R) (NAA-SR-11628, pp 9-16)

PITUITARY HORMONES
radiation effects on secretion of fish, x, 20: 14307

PLACENTA
radioisotope diffusion through human, 20: 14372
strontium-85 transfer through mouse, factors affecting, 20: 14244

PLANKTON
distribution in deep scattering layers of Santa Barbara Channel, Calif., 20: 14235 (SAN-584-1)

PLANT CELLS
radiation effects on potassium diffusion through walls of, γ, 20: 14282
radiation effects on growth in, 20: 14383
radiosensitivity of, diurnal variations in α, 20: 14361

PLANT METABOLISM
effects of radium on, in algae, 20: 14381

PLANTS
radiation effects on incompatibility in *Oenothera organensis*, uv and x, 20: 14382
radiation effects on *Phleum pratense*, factors affecting γ and x, 20: 14349
radioactivity in vicinity of AERE, cesium-137 and strontium-90, 20: 14784(R) (AERE-R-5015)
strontium-90 uptake by, from soils, 20: 14236
tritium content in water in, 20: 14744

PLASMA
acceleration and heating of, multistage, (E), 20: 15892
collision frequency measurements in helium and oxygen after, (E), 20: 15867 (AD-620664)
containment and production of thermonuclear, summary, 20: 15886(R) (UCRL-14285)
containment of, apparatus for magnetic, 20: 15927(P)
containment of, magnetic coils with high-gradient cusp for, 20: 15928(P)
containment of, research progress on, (E/T), 20: 15882(R) (NP-15868)
containment using Ioffe bars, magnetic field calculations for, (T), 20: 15878 (IPP-6/42)
current density in, generation of third-harmonic, 20: 15909
diagnostics in MHD flow, using noise analysis, 20: 15569 (INR-626/IX/R)
diagnostics of nitrogen discharge, mass spectrometric sampling probe for, 20: 15915
diagnostics of θ-pinch, laser amplifier for, 20: 15873 (IPP-1/42)
diagnostics of, electron beam probing for, (E/T), 20: 15884 (SU-IPR-33)
diagnostics of, methods development for, 20: 15882(R) (NP-15868)
diagnostics using spherical resonance probe, (E/T), 20: 15868 (AD-628186)
electric conductivity of turbulent, (E), 20: 15895
electric conductivity of, in MGD generators, 20: 15897
electromagnetic wave propagation in, containing heavy ions, (T), 20: 15910
electromagnetic wave propagation in quantized, (T), 20: 15941 (NP-15698)
electromagnetic-wave diffraction and propagation in, (T), 20: 15149(T) (JPRS-33458)
electron beam interaction with, amplification and instabilities from, (T), 20: 15880 (ML-1292)
electron bursts from, use of silicon solar cells for detection of, 20: 15916
electron density and temperature in nonthermal hydrogen, (T), 20: 15875 (IPP-3/32)
electron density determination by spectral line merging in, 20: 15881 (MPI-PAE/PL-7/65)
electron density in θ-pinch, measurement of, (E), 20: 15871 (IPP-1/38)
electron energy distribution in homogeneous weakly ionized, (T), 20: 15889(T) (SC-T-65-776)
electron kinetics in collisional, in linear electric field, (T), 20: 15904
electron runaway in betatron, 20: 15919
electron sheets in, steady-state structure and low-frequency oscillations of, (T), 20: 15905
electron temperature in argon–potassium, (E/T), 20: 15874 (IPP-3/31)
electron temperature in helium, spectroscopic determination of, (E), 20: 15908
electron-molecule collisions in homogeneous weakly ionized, elastic, (T), 20: 15888(T) (SC-T-65-775)
equations for collisionless, relation between kinetic and moment, 20: 15917
hydromagnetic oscillations of nonuniform, (T), 20: 15890
hydromagnetic wave propagation in waveguides of magneto-, viscous effects on, (T), 20: 15925
ion acoustic waves in bounded cylindrical, (T), 20: 15901
ion waves in bounded, hydrodynamic model for, (T), 20: 15900
kinetic equation for warm fully ionized, 20: 15918
kinetic theory of, (T), 20: 15899
laser beam scattering by, cooperative effects in, (E), 20: 15911
light scattering by, 20: 15882(R) (NP-15868)
magnetohydrostatic equilibria in toroidal systems, (T), 20: 15877 (IPP-6/41)
microwave emission from, properties of, (T), 20: 15870 (CEA-R-2881)
microwave emission from column of, structure in, (E/T), 20: 15893
microwave scattering by underdense cylindrical helium, phase-shift analysis for, (T), 20: 15894
oscillations in collisionless electron, magnetic field effects on electrostatic, (T), 20: 15879 (IPP-6/43)
oscillations of finite, dispersion relation for longitudinal, (T), 20: 15885 (UCRL-12207(Rev.1))
pinch effect in, stability of sheet, (T), 20: 15903
pinch effect in, time-resolved profile impurity line measurements in, (E), 20: 15872 (IPP-1/41)
production by kinetic impact of copper jets, 20: 15920
production of accelerated, engineering drawings of gun for, 20: 15921
production of cylindrically symmetric, by electric arcs, 20: 15914
production of, design of gas-discharge source for, 20: 15887(T) (AD-625789)
radiation from current strip in uniaxially anisotropic, (T), 20: 15891
research programs on, at Juelich Research Center, Germany, 20: 16156
resonances in static dipole field, toroidal mode, (T), 20: 15592
sheath properties of cathode, electron beam probing of, (E/T), 20: 15884 (SU-IPR-33)
spectra line merging in, electron density determination by, 20: 15881 (MPI-PAE/PL-7/65)
spectra of shock-heated helium, (E), 20: 15896
stability in d-c electric field, (T), 20: 15883 (SU-IPR-31)
stability in horizontal magnetic field, convective, 20: 15907
stability of cesium, Kelvin-Helmholtz, (E), 20: 15906
stability of guiding-center, variational principle for, (T), 20: 15898
stability of spherical, magnetic fields and rotation effects on thermal, (T), 20: 15876 (IPP-6/33)
stability of, research progress on, (E/T), 20: 15882(R) (NP-15868)
thermodynamic properties of electron, (T), 20: 15869 (AD-628317)
transport properties of arc, validity conditions for, (T), 20: 15926
wave equation for compressible anisotropic, (T), 20: 15913
wave excitation in r-f discharge, standing, (E), 20: 15912
wave propagation in low-frequency limit, longitudinal, (T), 20: 15902

PLASMA JETS
energy and mass transfer between gas coolant and, 20: 15584
tests on, for sampling in vicinity of nuclear detonation, 20: 14662(R) (ORNL-TM-1394)
use in space propulsion, 20: 14726 (NASA-CR-54746)
uses in spectroscopic determination of alkaline earth metals, 20: 14492

PLASTICS
analysis of commercial, identification by activation, 20: 14439(R) (GA-5556)
determination of Viton content in PBX mock explosives, methods for, 20: 14470 (UCRL-7873)
developments in research on, bibliography on, 20: 14506 (CRDL-SP-5-7)
radiosterilization of, electron, 20: 14941

PLATES
dispersion forces between dielectric, classical treatment for, (T), 20: 15152
neutron transport in, one-group collision-probability code for, 20: 15668 (EUR-2624.e)

PLATINUM
energy level transitions in, Coster-Kronig, (T), 20: 15238 (CONF-233 (Vol.3), pp 398-418)
proton reactions (p,n) at 30 to 50 Mev, distributions from, 20: 15729(R) (RHEL/R-112, pp 37-66)

PLATINUM ALLOYS
Pd–Pt, catalytic effects on deuterium-methane exchange and propane cracking reactions, 20: 14542

PLATINUM ISOTOPES Pt-189
energy level transitions in, (E), 20: 15781

PLOWSHARE PROJECT
mining copper ores using nuclear explosives, developments in, 20: 14662(R) (ORNL-TM-1394)

PLUTONIUM
analysis for nitride nitrogen, 20: 14440 (LA-3452)
bibliography on, 20: 16145 (BNWL-113-7)
compressibility of alpha-, effects of crystallographic orientation on, 20: 15095
content in operating power reactor fuel elements, methods for determining, 20: 14438 (CEND-540)
content in spent reactor fuels, evaluation of, 20: 14435 (BNWL-SA-503)
corrosion of, effects of composition on, 20: 14984 (RFP-511)
creep properties of six allotropes of, 20: 15034 (BNWL-49)

crystallographic textures of monoclinic, 20: 15944 (RL-REA-2595, pp 12-14)
determination in man, review on, 20: 14239 (JUL-312-ST)
determination in nuclear fuel cycles, evaluation of methods for, 20: 14447 (NBL-231)
emissivity at 89°C, total hemispherical, 20: 15088
grain size, effects of pressure and temperature on, 20: 15053(R) (NUMEC-3428-17)
metabolism and properties in man, review on, 20: 14239 (JUL-312-ST)
oxidation by ignition in dry air, oxide fractional release and particle size in, 20: 15036 (BNWL-205)
phase transformations in, kinetics of low-temperature, 20: 15034 (BNWL-49)
refining of, equipment and procedure for batch electro-, 20: 14967(R) (RL-SEP-503-1)
solvent properties for niobium at 700 to 1000°C, 20: 15043 (LA-3436)
testing enriched fuel rods of, nondestructive methods for, 20: 14707

PLUTONIUM ALLOYS
analysis for nitride nitrogen, 20: 14440 (LA-3452)
Be–Pu, spectra of alpha source of, 20: 14444(R) (MLM-1268)
Ce–Co–Pu, solvent properties for niobium at 500 to 900°C, 20: 15043 (LA-3436)
fissium–Pu–U, phase studies, 20: 15085
Ga–Pu, critical temperature of reactions with chlorinated solvents, 20: 14513 (RFP-688)
Ga–Pu, effects of composition on corrosion of, 20: 14984 (RFP-511)
Mo–Pu–U, fabrication for ZPR fuel elements, 20: 16060(R) (ANL-7152, pp 1-49)
Pu–Ti–U, density and structure of, 20: 16060(R) (ANL-7152, pp 1-49)
Pu–U–Zr, density and structure of, 20: 16060(R) (ANL-7152, pp 1-49)

PLUTONIUM CARBIDES
PuC–UC, burnup, 20: 15032(R) (ANL-7152, pp 50-72)

PLUTONIUM CHLORIDES
thermodynamic properties of, from emf measurements in lithium chloride–potassium chloride eutectic, 20: 14507 (LA-3399)

PLUTONIUM(III) CHLORIDES
preparation from oxide, stirred-bed gas-solids reactor for, 20: 14669 (RL-SEP-414)

PLUTONIUM COMPOUNDS
analysis for nitride nitrogen, 20: 14440 (LA-3452)

PLUTONIUM FLUORIDES
analysis for impurities, review on spectrographic, 20: 14464 (RFP-599)

PLUTONIUM ISOTOPES Pu-236
content in irradiated uranium dioxide, 20: 15133(R) (GEAP-4893)
content in spent reactor fuels, evaluation of, 20: 14435 (BNWL-SA-503)

PLUTONIUM ISOTOPES Pu-238
content in spent reactor fuels, evaluation of, 20: 14435 (BNWL-SA-503)
effects of ingested particles containing, biological, 20: 14785 (BNWL-182)
preparation of alpha source of, by deposition from solution, 20: 14444(R) (MLM-1268)
production in U. S. power reactors, estimates for future, 20: 14946 (DP-1015)
separation from americium-241, methods for, 20: 14509 (NP-15826)
separation of uranium-234 from solutions of, ion exchange and solvent extraction method for, 20: 14444(R) (MLM-1268)

PLUTONIUM ISOTOPES Pu-239
content in spent power reactor fuels, evaluation of, 20: 14435 (BNWL-SA-503)
neutron capture-to-fission ratio for, 20: 15717(R) (GEAP-4950)
neutron fission of, yields of cesium isotopes and neodymium isotopes in, 20: 15133(R) (GEAP-4893)
neutron fission of, neutron yields in, (E), 20: 15718 (IDO-17083)

PLUTONIUM ISOTOPES Pu-240
content in spent power reactor fuels, evaluation of, 20: 14435 (BNWL-SA-503)

PLUTONIUM ISOTOPES Pu-241
content in spent power reactor fuels, evaluation of, 20: 14435 (BNWL-SA-503)
neutron capture-to-fission ratio for, thermal, (E), 20: 15774

PLUTONIUM ISOTOPES Pu-242
content in spent power reactor fuels, evaluation of, 20: 14435 (BNWL-SA-503)
preparation by neutron irradiation of americium-241, 20: 14631
preparation by neutron irradiation of americium-242, 20: 14631

PLUTONIUM NITRATES
criticality parameters of water-reflected solutions of, (T), 20: 16031

PLUTONIUM NITRIDES
thermal decomposition of microspheres of, nitrogen vapor pressure in, 20: 14512 (ORNL-TM-1418)

PLUTONIUM OXALATES
criticality parameters of water-reflected solutions of, (T), 20: 16031

PLUTONIUM OXIDES
chlorination of, stirred-bed gas-solids reactor for, 20: 14669 (RL-SEP-414)
diffusion and particle size of, from ignited plutonium, 20: 15036 (BNWL-205)
PuO_2–H_2O, criticality parameters for plutonium-240 enriched, (T), 20: 16031

PLUTONIUM(IV) OXIDES
performance of stainless-steel-clad fuel elements of, for FTR, 20: 16121 (BNWL-197)
reactions with Hastelloy X and type 316L stainless steel, 20: 14965(R) (NUMEC-3524-12)
PuO_2–ThO_2, preparation of compacts of, 20: 15025(P)
PuO_2–UO_2, density of, effects of methyl cellulose additions on sintered, 20: 14965(R) (NUMEC-3524-12)
PuO_2–UO_2, development and testing as fast reactor fuel, 20: 14965(R) (NUMEC-3524-12)
PuO_2–UO_2, oxidation and fluorination of, two-zone, 20: 15032(R) (ANL-7152, pp 50-72)
PuO_2–UO_2, performance as FTR fuel elements, 20: 16121 (BNWL-197)
PuO_2–UO_2, radiation effects on fuels of, thermal-neutron, 20: 15135(R) (NUMEC-3432-18)
PuO_2–UO_2, sintering of coprecipitated powders of, process development for, 20: 14965(R) (NUMEC-3524-12)
PuO_2–UO_2–H_2O, criticality parameters for, containing enriched and natural uranium, (T), 20: 16032
PuO_2–UO_2–ZrO_2, preparation and thermophysical properties, 20: 15054(R) (NUMEC-3505-11)

PLUTONIUM PEROXIDES
analysis for impurities, review on spectrographic, 20: 14464 (RFP-599)

PLUTONIUM RECYCLE TEST REACTOR
pressure tube power for, determination of maximum, (T), 20: 16120 (BNWL-176)

PLUTONIUM SULFIDES
PuS–US, preparation and properties, 20: 15032(R) (ANL-7152, pp 50-72)

PLUTONIUM SYSTEMS
HNO_3–Pu, criticality parameters of water-reflected spheres of, (T), 20: 16031
N–Pu–U, properties of hot-pressed powders of, 20: 14957(R) (BMI-1754)

PLUTONYL IONS
hydrolysis of, in aqueous solutions, 20: 14444(R) (MLM-1268)

POLAROGRAPHS
design and performance of ORNL model Q-2792, 20: 14452(R) (ORNL-3839, pp 1-12)
design of controlled-potential differential d-c, 20: 14452(R) (ORNL-3889, pp 1-12)
design of square-wave, 20: 14452(R) (ORNL-3889, pp 1-12)
performance of comparative-amperometric d-c, 20: 14452(R) (ORNL-3839, pp 1-12)

POLAROGRAPHY
development of controlled-potential, for microanalysis, 20: 14452(R) (ORNL-3889, pp 1-12)
electrode for, development of Teflon dropping-mercury, 20: 14455(R) (ORNL-3889, pp 25-32)

POLARONS
electric conductivity and quasi-particle spectrum of, (T), 20: 15988

POLLEN
radiation effects on haploidy-induction in coconut palm, 20: 14320

POLONIUM ISOTOPES Po-210
content and distribution in human lungs after cigarette smoking, 20: 14798
production in U. S. power reactors, estimates for future, 20: 14946 (DP-1015)

POLONIUM ISOTOPES Po-214
energy levels from bismuth-214 beta decay, (E), 20: 15844

POLONIUM ISOTOPES Po-218
content in uranium-mine air, 20: 14747

POLYMERS
developments in research on, bibliography on, 20: 14506 (CRDL-SP-5-7)
yields from gamma radiolysis of 1,3- and 1,4-cyclohexadienes, 20: 14610

POLYPHENYL SYSTEMS
neutron diffusion lengths in Santowax-R, at 200 to 400°C, thermal, 20: 15680

POLYPHENYLS
determination in working environments, colorimetric and uv spectrophotometric methods for, 20: 14467 (RT/PROT(64)-20)

POLYSACCHARIDES
radiation effects on sulfate uptake by, in rabbit aorta, β, 20: 14295

POPULATIONS
iodine-131 consumption in milk by, prediction of, 20: 14243(R) (TID-22626)
radiation control of wood-boring insect, γ, 20: 14305
radiation control of *Psila rosae*, by exposure of pupae, γ, 20: 14317
radiation control of *Platynota stultana*, 20: 14340

radiation effects on human, low-dose γ and x, 20: 14331
POSITRON BEAMS
interactions with electron beams, vector boson production in, (E), 20: 15311 (LNF-65/47)
production of high-current, design of source for, (T), 20: 15176
transport in electron-positron storage rings, 20: 15173 (SLAC-49, pp 61-8)
POSITRONS
annihilation spectrum in argon, impurity effects on, (E), 20: 15436
energy spectra from fission-antineutrino interactions with protons, (E), 20: 15330
interactions in electron gases, gamma distributions from annihilation, (T), 20: 15383
interactions with protons, elastic, (E), 20: 15306(R) (CEAL-1026)
interactions with electrons in colliding-beam experiments, 20: 15443
reactions with lead, gold, silver, tin, and tungsten at 100 to 500 kev, cross sections for K ionization in, (E), 20: 15257
POTASSIUM
analysis for oxygen by surface tension method, 20: 14445(R) (MSAR-66-10)
analysis for oxygen, amalgamation method for, 20: 14432 (ANL-7123)
content in man, whole-body, 20: 14243(R) (TID-22626)
determination in cigarette tobacco, activation, 20: 14439(R) (GA-5556)
determination in plutonium fluorides and peroxides, review on spectrographic, 20: 14464 (RFP-599)
determination in thorium compounds, spectrochemical methods for, 20: 14443(R) (MCW-1493, pp 27-30)
determination in wood in criminal cases, activation, 20: 14439(R) (GA-5556)
determination of terrestrial abundance of, neutrino detection for, (T), 20: 14750
energy level widths for, K, (T), 20: 15239 (CONF-233(Vol.3), pp 419-39)
ratio to sodium in mouse urine, prediction of x-radiation response by, 20: 14266
POTASSIUM ALLOYS
K–Na, atomic structure of, x-ray- and neutron-diffraction studies of, 20: 15080
POTASSIUM BROMIDES
bromine-79 and -81 NMR spectra in, effects of bromine on, 20: 14573
effects on radioinduced isomerization of dimethyl maleate, 20: 14596
electric conductivity in light and heavy water at 25°C, 20: 14540
electron transmission through films of, excitons and plasma oscillations in, (E), 20: 15953
radioinduced V center formation in, at 200°K, x, 20: 14604
radioinduced vacancies in, strontium impurity effects on F-centers from proton, (E), 20: 15977(T)
POTASSIUM CHLORIDES
effects on radioinduced isomerization of α-phenylcinnamic acid, 20: 14596
effects on radioinduced isomerization of dimethyl maleate, 20: 14596
electric conductivity in light and heavy water at 25°C, 20: 14540
electron transmission through films of, excitons and plasma oscillations in, (E), 20: 15953
preparation of high-purity, 20: 14511(R) (ORNL-3889, pp 71-3)
radioinduced F centers in pure and strontium-doped, kinetics of accumulation of, (E), 20: 15980(T)
radioinduced V center formation in, at 200°K, x, 20: 14604
KCl–NaCl, polarization of molybdenum during electrolysis in fused, 20: 14562
LiCl–KCl, lanthanum trichloride reactions with fused eutectic mix of, 20: 14565
LiCl–KCl, polarization of cerium during electrolysis in fused, 20: 14561
LiCl–KCl, polarization of molybdenum during electrolysis in fused, 20: 14562
LiCl–KCl, polarization of cerium during electrolysis in, effects of lithium fluoride additions on, 20: 14564
LiCl–KCl, reactions of trivalent cerium with fluoride ions in fused, 20: 14563
LiCl–KCl–$ZnCl_2$, reactions with uranium monocarbide–zinc at 500 to 800°C, 20: 14991
LiCl–KCl, thermodynamic properties of plutonium chloride from emf measurements in, 20: 14507 (LA-3399)
POTASSIUM COMPLEXES
LiCl–KCl, analysis for uranyl chlorides at 400°C using voltammetry, 20: 14437 (CEA-R-2879)
POTASSIUM DIOXODIFLUOROIODATE(V)
analysis for fluorine and iodine, titrimetric, 20: 14455(R) (ORNL-3889, pp 25-32)
POTASSIUM FLUOBERYLLATES
$KBeF_3$–KPO_3, phase studies of, by radiation emission method, 20: 14558
POTASSIUM FLUORIDES
electric conductivity in light and heavy water at 25°C, 20: 14540
reactions with xenon oxyfluorides, complex formation in, 20: 14523
LiF–KF–NaF, spectra of cobalt ions in, absorption, 20: 14453(R) (ORNL-3889, pp 12-14)
POTASSIUM HYDROXIDES
KOH–H_2O, radiolysis of oxygenated solutions of, 20: 14614
POTASSIUM IODIDES
effects on radioinduced isomerization of α-phenylcinnamic acid, 20: 14596
electric conductivity in light and heavy water at 25°C, 20: 14540
iodine-127 NMR spectra in, effects of iodine on, 20: 14573
POTASSIUM IONS
effects on electric conductivity of germanium, 20: 15978(T)
radiation effects on diffusion through cell walls, γ, 20: 14282
sorption by tetra-, penta-, and hexavalent metal oxides, effects of pH on, 20: 14651
POTASSIUM ISOTOPES K-39
helium-3 reactions with, distorted wave analysis of, 20: 15855
neutron reactions (n,2n) at 12 to 18 Mev, cross sections for, (E), 20: 15863
POTASSIUM ISOTOPES K-40
content in carbonate rocks, 20: 14752
content in man, whole-body, 20: 14243(R) (TID-22626)
POTASSIUM NIOBATES
preparation, 20: 14511(R) (ORNL-3889, pp 71-3)
POTASSIUM OXALATES
complexes with cobalt, effects of neutron reactions (n,γ) on, 20: 14584(R) (TID-22444)
POTASSIUM OXIDES
preparation, 20: 14511(R) (ORNL-3889, pp 71-3)
Nb_2O_5–K_2O, density and surface ductility of fused, at 1200 to 1650°C, 20: 15076
POTASSIUM PHOSPHATES
$KBeF_3$–KPO_3, phase studies of, by radiation emission method, 20: 14558
POTASSIUM RHENIUM CHLORIDES
preparation, 20: 14511(R) (ORNL-3889, pp 71-3)
POTASSIUM SYSTEMS
Ar–K, electron temperature in plasma of, (E/T), 20: 15874 (IPP-3/31)
POTENTIOMETERS
design and operation of current-compensated chrono-, 20: 14452(R) (ORNL-3839, pp 1-12)
POTENTIOMETRIC ANALYSIS
development of derivative chrono-, 20: 14452(R) (ORNL-3889, pp 1-12)
POWDER METALLURGY
equipment for blending and transferring thorium dioxide–uranium dioxide fuels, 20: 14668 (ORNL-TM-1397)
POWDERS
surface area measurements of, radiometric method for, 20: 14973(P)
POWER BREEDER REACTORS
design, 20: 16102(P)
POWER CYCLES
use of Rankine, in space power systems, 20: 16111 (N65-16315)
POWER PLANTS
radiator weight for space, using steam cycles, 20: 14688 (N65-20692)
POWER REACTORS
accidents in boiling-water and pressurized-water, analytic studies of, 20: 16019(R) (BMI-X-10154)
control-rod drive testing for, 20: 16096
design of boiling-water, with superheated breeder blanket, 20: 16105(P)
development of heavy water-moderated, organic-cooled, 20: 16109
economics of dual-purpose desalination–power, 20: 16108(T) (JPRS-33459)
fuel element development for, in India, 20: 16099
heat transfer in heavy water moderated, burnout in eccentric annuli, (E), 20: 16086 (TID-22651)
isotopic content in operating fuel elements in, methods for determining heavy-, 20: 14438 (CEND-540)
performance of Beloyarsk type, for power–desalination uses, 20: 16107(T) (JPRS-33406)
pressure tube mounting device for, design of, 20: 16017(P)
radioisotope production in, estimates for future, 20: 14946 (DP-1015)
shutdown of, secondary system for, 20: 16095
spent fuel analysis for fission products and heavy element isotopes, evaluation of chemical, 20: 14435 (BNWL-SA-503)
POWER SUPPLIES
design for double-focusing mass spectrometers, 20: 14830
design with positive and negative outputs, 20: 14818 (ORNL-TM-1391)
PRASEODYMIUM
bremsstrahlung reactions (γ,n) at 8 to 16 Mev, spectra from, (E), 20: 15723 (MIT-2098-162)
bremsstrahlung reactions (γ,n) with, neutron emission in, (E), 20: 15724 (MIT-2098-224)
PRASEODYMIUM ALLOYS

Co–Pr, cobalt ion EPR in intermetallic compounds of, 20: 15963
Mn–Pr, preparation and structure, 20: 15110
Pr–Y, electric conductivity of dilute, at low temperatures, (E), 20: 15098
PRASEODYMIUM ISOTOPES
deuteron reactions at 15 Mev, isomeric states from, (E), 20: 15856
PRASEODYMIUM ISOTOPES Pr-141
atomic mass, (E), 20: 15769
PRASEODYMIUM ISOTOPES Pr-145
energy levels, (E), 20: 15722 (KR-76)
PRASEODYMIUM ISOTOPES Pr-146
energy levels, (E), 20: 15722 (KR-76)
PRASEODYMIUM OXIDES
$Al(NO_3)_3$–Pr_2O_3, compound formation in, at 1200°C, 20: 14539
Al_2O_3–Pr_2O_3, compound formation in, at 1600 to 1650°C, 20: 14539
Pr_2O_3–WO_3, preparation and properties, 20: 14534
PRECIPITATION, ATMOSPHERIC
effects on fallout, 20: 14746
fallout monitoring of Canadian, October 1965, 20: 14737 (NP-15853, pp 8-20)
PREDNISOLONE
radioinduced decomposition of tritiated, effects of molecular structure on, 20: 14578 (EUR-2435.f)
PREGNANCY
radiation hazards during, x, 20: 14380
radioinduced cancer in twins from exposure during, x, 20: 14319
PRESSURE GAGES
calibration for helium vapor pressure thermometry, 20: 14444(R) (MLM-1268)
PRESSURE VESSELS
design of concrete, with grid-type framework for fluid-tight liner, 20: 16009(P)
design of prestressed-concrete, 20: 16013(P)
feasibility of cable-wrapped, (T), 20: 16002
inspection of ERR, methods development for, 20: 16085(R) (SWRI-1228-4-15)
radiography of, properties of cobalt-60 and iridium-192 sources for, 20: 14705
testing during fabrication of, program outline for nondestructive, 20: 14710
testing of, nondestructive methods for, 20: 14709
PRESSURIZED WATER REACTORS
accidents in high-power, analytic studies of, 20: 16019(R) (BMI-X-10154)
coolant decompression in, shock waves from, 20: 16023(R) (IITRI-578P21-16)
PRINCETON SYNCHROTRON
design and operational parameters, 20: 15163 (PPAD-279D(Rev.))
PROCESS HEAT REACTORS
development of heavy water-moderated, organic-cooled, 20: 16109
economics of dual-purpose desalination–power, 20: 16108(T) (JPRS-33459)
performance of Beloyarsk type, for power–desalination uses, 20: 16107(T) (JPRS-33406)
PROGESTERONE
radioinduced decomposition of tritiated, effects of molecular structure on, 20: 14578 (EUR-2435.f)
PROMETHIUM
production and purification of, methods for, 20: 14509 (NP-15826)
separation from fission products, review on method for, 20: 14436 (BNWL-SA-504)
separation in microquantities, method for, 20: 14509 (NP-15826)
PROMETHIUM CHLORIDES
preparation and structure of, 20: 14509 (NP-15826)
PROMETHIUM COMPOUNDS
preparation and structure of arsenate, carbonate, hydroxide, iodate, oxalate, oxyfluoride, and phosphate, 20: 14509 (NP-15826)
PROMETHIUM FLUORIDES
preparation and structure of, 20: 14509 (NP-15826)
PROMETHIUM ISOTOPES
composition in spent power reactor fuels, evaluation of, 20: 14435 (BNWL-SA-503)
PROMETHIUM ISOTOPES Pm-146
content in spent power reactor fuels, evaluation of, 20: 14435 (BNWL-SA-503)
PROMETHIUM ISOTOPES Pm-147
content in spent power reactor fuels, evaluation of, 20: 14435 (BNWL-SA-503)
production in U. S. power reactors, estimates for future, 20: 14946 (DP-1015)
separation from Purex waste solutions by lead carrier sulfate precipitation, 20: 14641 (RL-SA-59)
separation from rare earth fission products by storage and ion exchange, 20: 14635 (CONF-660305-5)
PROMETHIUM NITRATES
preparation and structure of, 20: 14509 (NP-15826)
PROMETHIUM OXIDES
preparation and structure of, 20: 14509 (NP-15826)
PROPANE
decomposition by cracking, catalytic effects of palladium alloys on, 20: 14542
PROPANE, 2-IODO-
radioinduced ESR spectra in, at 77°K, 20: 14597
2-PROPANONE, HEXAFLUORO-
decomposition in ion source of mass spectrometer, mechanism of, 20: 14584(R) (TID-22444)
2-PROPANONE, 1,1,1-TRIFLUORO-
decomposition in ion source of mass spectrometer, 20: 14584(R) (TID-22444)
PROPENE, 2-METHYL-
radioinduced polymerization with isobutylene, 20: 14608
PROPIONALDEHYDE
decomposition in ion source of mass spectrometer, mechanism of, 20: 14584(R) (TID-22444)
PROPORTIONAL DETECTORS
amplifier for boron trifluoride, design of pre-, 20: 14859 (ORNL-TM-1390)
cable system for power supply and pulse transmission, 20: 14876
construction and performance for low-energy beta and gamma spectroscopy, 20: 14879
description of low-energy, for measuring gamma emission of 2.3-kev isomeric state in lead-205, 20: 14444(R) (MLM-1268)
design for continuous measurement of alpha activity of flowing solutions, 20: 14871
design of portable boron trifluoride, for fast and slow neutrons, 20: 14913(P)
operation of boron trifluoride, for HFIR fuel cladding failure detection, 20: 16124 (ORNL-TM-1388)
performance for absolute radioactivity measurements, 20: 15690 (CEA-R-2813)
PROPULSION
electric systems for space, mission performance of nuclear, 20: 14724 (65SD5322-A)
electric, charged colloid sources for, 20: 14725 (N65-15876)
plasma-jet systems for space, testing of, 20: 14726 (NASA-CR-54746)
PROTACTINIUM
separation from uranium by solvent extraction on fine-grained carrier, 20: 14656
PROTACTINIUM ISOTOPES Pa-227
alpha decay, (E), 20: 15864
PROTACTINIUM ISOTOPES Pa-229
alpha decay, (E), 20: 15864
PROTACTINIUM ISOTOPES Pa-231
alpha decay, (E), 20: 15864
PROTACTINIUM ISOTOPES Pa-233
effects on TBP during short decay runs, dose calculations in, 20: 14580 (ORNL-2764)
PROTEINS
determination of carbon-14-labeled, by liquid scintillation counting on paper chromatograms, 20: 14479
effects of lipid peroxidation on, 20: 14587
radiation effects on synthesis in amoeba, tracer study, 20: 14259(R) (NP-15855)
radiation effects on rat plasma, effects on Hamolsky's test of γ, 20: 14276
synthesis of, relation to cell growth, 20: 14383
PROTON BEAMS
effects on rat nervous system after neonatal spinal cord exposure, 20: 14299
energy measurement of, from linacs, 20: 15165(R) (RHEL/R-112, pp 12-22)
injection into storage rings, charge-exchange, (E), 20: 15177
optical properties in double-focusing spectrometer, 20: 14822(R) (RHEL/R-112, pp 99-128)
stability in intersecting storage rings, (T), 20: 15174 (SLAC-49, pp 71-3)
PROTON SOURCES
ionizer development for polarized-proton, 20: 15165(R) (RHEL/R-112, pp 12-22)
PROTONS
density in inner Van Allen belt, effects of solar cycle variations on, (T), 20: 15590 (NASA-TN-D-3086)
detection in products from nuclear reactions, engineering drawings of apparatus for, 20: 14906
detection of, equipment for, 20: 15393
distributions of solar, in space, 20: 15191 (N65-20996)
doses in space vehicles, computer programs for calculating, 20: 15930 (NP-15697(Vol.2))

dosimetry in biological solutions, calorimetric method for, 20: 15858
effects on n-p and p-n solar cells, annealing of, 20: 14919(R) (N65-20653)
effects on potassium bromide crystals, vacancies from, (E), 20: 15977(T)
effects on vitreous silica flow and stress relaxation, (T), 20: 15971
electric dipole and magnetic quadrupole moments for, sum rules for, (T), 20: 15365
energy loss in sodium iodide scintillators, ionization curves from, 20: 14891
energy spectra and fluxes in inner Van Allen belt, review of, 20: 15621
form factors from elastic proton-electron interactions, (E), 20: 15337
injection into cyclic accelerators and storage rings, charge-exchange, (E), 20: 15162 (NP-15785)
interactions with photons, meson production in, (E), 20: 15306(R) (CEAL-1026)
interactions with photons at high energies, meson ($K^{\pm}$) and meson ($\pi^{\pm}$) production in, (E), 20: 15306(R) (CEAL-1026)
interactions with photons at high energies, meson ($\pi^{\pm}$) production in, (E), 20: 15306(R) (CEAL-1026)
interactions with positrons, elastic, (E), 20: 15306(R) (CEAL-1026)
interactions with mesons (K^-) at 2.1 to 2.7 Bev/c, meson (ϕ) production in, (E/T), 20: 15316 (UCRL-16526)
interactions with mesons (π^-) at 3.0 and 7.0 Bev, beta decay of vector bosons from, (E), 20: 15406
interactions with mesons (K^+) at 3.6 Bev/c, resonance production in, (E), 20: 15407
interactions with mesons (π^+), mesons (A) and (B) production in, (E), 20: 15408
interactions with mesons (π^-) at 2.7 Bev/c, resonances in, (E/T), 20: 15410
interactions with mesons (K^-) at 2.1 to 2.7 Bev/c, resonance production in, (E), 20: 15412
interactions with hyperons at low energies, (T), 20: 15413
interactions with mesons (K^+) at 3.6 Bev/c, (E), 20: 15415
interactions with mesons (K^-) at 5.5 Bev/c, resonance production in, (E), 20: 15416
interactions with mesons (π^-) at 1.0 to 1.9 Bev, Y^*- production in, (E), 20: 15417
interactions with mesons (K^-) at 1.80 and 1.95 Bev/c, boson exchange in, (E), 20: 15420
interactions with mesons (K^+) at 2.26 Bev/c, resonance production in, (E/T), 20: 15422
interactions with protons at 2.8 Bev/c, single meson (π^+) production in, (T), 20: 15423
interactions with protons, particle production in, 20: 15426
interactions with mesons ($K^{\pm}$) and mesons ($\pi^{\pm}$), total cross sections for, (E/T), 20: 15428
interactions with mesons (K^-) at 1.5 Bev/c, $K^*(888)$ and $N^*(1425)$ production in, (E/T), 20: 15429
interactions with mesons (K^-), spin-parity analysis of $\Xi^*(1530)$ from, (E/T), 20: 15464
interactions with neutrons at 585 Mev, mesons (π^+) and (π^-) production cross sections for, (E), 20: 15310 (JINR-P-2508)
interactions with electrons, recoil polarization measurement in elastic, (E), 20: 15313 (NP-15822)
interactions with electrons, radiative corrections for, (T), 20: 15319
interactions with protons, integral representations for amplitudes of elastic, (T), 20: 15321
interactions with mesons (π^+) at 4 and 8 Bev, absorption corrections to exchange term for elastic, (T), 20: 15324
interactions with antineutrinos, cross section and positron spectra from, (E), 20: 15330
interactions with protons at 550 to 1000 Mev, cross sections for meson (π) pair production in, (E), 20: 15332
interactions with mesons (K^+) at 1.96 Bev/c, single-meson (π) production in, (E), 20: 15335
interactions with protons at 2.0, 2.4, and 2.85 Bev, meson (π) production in, (E), 20: 15336
interactions with electrons, form factors from elastic, (E), 20: 15337
interactions with antiprotons at 3.7 Bev/c, cross section for mesons (K) and (π) production in, (E), 20: 15338
interactions with mesons (π^+) at 781 Mev, cross sections for single- and multiple-pion production in, 20: 15341
interactions with mesons (π), model for high-energy charge-exchange, 20: 15342
interactions with antiprotons, $\bar{U}(12)$ symmetry breaking in annihilation, 20: 15346
interactions with neutrons, charge independence in scattering lengths for, 20: 15356
interactions with mesons (π^-) at 9 to 18 Bev/c, meson (ρ) exchange in, (T), 20: 15364
interactions with photons, E1 and M2 amplitudes in single-pion-production, (T), 20: 15365
interactions with mesons (π^-) at 378 Mev, π-π interaction, (E), 20: 15368
interactions with mesons (π^-) and (π^+) at 875 to 1579 Mev/c, differential cross sections and polarization in elastic, (E), 20: 15372
interactions with mesons (π^+) at 410 and 492 Mev, recoil proton polarization in, (E), 20: 15373
interactions with mesons (π^-) at 500 to 1150 Mev, charge-exchange, (E), 20: 15374
interactions with mesons (π^-) at 300 to 1000 Mev, $N^*(1238)$ production in, (E/T), 20: 15375
interactions with mesons (π^-) at high energies, forward amplitude for charge-exchange, (T), 20: 15376
interactions with mesons (π^-) at 1.72 and 2.07 Bev/c, differential cross sections for elastic, (E), 20: 15377
interactions with mesons (π^-) at 2.0 Bev/c, cross sections for charge-exchange, (E), 20: 15378
interactions with mesons (π^-) and (π^+) at 2.1 to 6.9 Bev/c, resonance effects on total cross sections for, (E/T), 20: 15379
interactions with mesons (π^-) at 5.9 to 18.2 Mev/c, charge-exchange, (E), 20: 15380
interactions with mesons (π^-) and (π^+) at 300 to 700 Mev, isobar production in, (T), 20: 15381
interactions with mesons (π), phase shift analyses of, (T), 20: 15382
interactions with mesons (π^-) at 9 Bev/c, meson (π^0) multiplicity and photon yields from, (E), 20: 15384
interactions with mesons (π^+) at 240 Mev, phase-shift analysis of elastic, (T), 20: 15388
interactions with mesons (π^-), $\bar{U}(12)$ symmetry for, 20: 15390
interactions with mesons (K^-), $\bar{U}(12)$ symmetry for, 20: 15390
interactions with electrons at forward angles, Rosenbluth formula for, 20: 15391
interactions with mesons (π^-), two-resonance model for hyperon (Λ)-meson (K^0) production in, (T), 20: 15392
interactions with gamma radiation at 1100–1300 Mev, hyperon (Λ)-meson (K^+) production in, (E), 20: 15393
interactions with gamma radiation at medium energies, effects of inelastic channel on, (T), 20: 15394
interactions with mesons (π^-), neutral decay modes of mesons (η) from, (E), 20: 15395
interactions with mesons (π^+), hyperon (Σ^+) production in, (E/T), 20: 15400
interactions with mesons (π^-) at 1.7 Bev/c, meson (ω) and (ρ^0) production and decay in, (E), 20: 15403
interactions with mesons (π^-) at 600 to 900 Mev, single meson (π) production in, (E/T), 20: 15411
interactions with mesons (K^-) at 3.8 Bev/c, resonance production in, (E), 20: 15418
interactions with alpha particles at 30 to 50 Mev, phase-shift analysis of, (T), 20: 15730(R) (RHEL/R-112, pp 67-98)
interactions with neutrinos ($\nu\mu$), effect of W meson on lepton pair production in, (T), 20: 15347
interactions with deuterons at 30 Mev, distributions from, (E), 20: 15728(R) (RHEL/R-112, pp 23-36)
interactions with mesons (π^+) at 2.08 Bev/c, cross sections for elastic scattering and meson production in, (E), 20: 15334
interactions with photons at 225 to 350 Mev, meson (π^+) production in, 20: 15340
photon scattering by, Compton, (E), 20: 15306(R) (CEAL-1026)
polarization in ytterbium-doped crystals of yttrium ethyl sulfate, (E), 20: 15964
production of polarized targets of, (E), 20: 15692 (CERN-66-3)
reactions (p,d) and (p,2p) with nuclei, models for, 20: 15730(R) (RHEL/R-112, pp 67-98)
reactions (p,d) with nuclei at 30 Mev, distributions from, (E), 20: 15729(R) (RHEL/R-112, pp 37-66)
reactions (p,γ) with calcium-40 at 0.6 to 5.2 Mev, energy levels from, 20: 15849
reactions (p,γ) and (p,p'γ) with magnesium-26 at 2.298 Mev, gamma spectra from, (E), 20: 15761
reactions (p,n) with nuclei at 30 to 50 Mev, distributions from, (E), 20: 15729(R) (RHEL/R-112, pp 37-66)
reactions (p,n) with nuclei at 2.3 to 11.0 Mev, excitation of isobaric analog states in, (E), 20: 15804
reactions (p,p'γ) with sodium-23 at 1281 and 1456 kev, gamma angular distribution from, 20: 15846
reactions and scattering on nuclei, models for, 20: 15730(R) (RHEL/R-112, pp 67-98)
reactions in tissue phantom at high energies, 20: 14330
reactions with carbon-12 at 20 to 40 Mev, distributions from, (E), 20: 15729(R) (RHEL/R-112, pp 37-66)
reactions with heavy emulsion nuclei at 1.5 to 25 Bev, lithium-8 energy spectra from, (E), 20: 15792
reactions with nitrogen, electron-capture cross sections for, (E/T), 20: 15886(R) (UCRL-14285)

reactions with nuclei at 30 and 50 Mev, total cross sections for, (E), 20: 15729(R) (RHEL/R-112, pp 37-66)
reactions with oxygen at 18 to 102 kev, excitation and light spectra produced by, (E), 20: 15271
reactions with tellurium-123, production of iodine-123 in, (E), 20: 14461(R) (ORNL-3889, pp 48-70)
scattering by argon-36 at 3 Mev, gamma polarization from inelastic, (E), 20: 15760
scattering by carbon-12 at 20 to 28 Mev, polarization in elastic and inelastic, (E), 20: 15805
scattering by fluorine-19 at 1.422 Mev, mean lifetime of first excited state from, (E), 20: 15780
scattering by iron-54 at 7.0 to 8.5 Mev, excited state decay from, (E), 20: 15786
scattering by light even nuclei at 155 Mev, cross sections for inelastic, (T), 20: 15797
scattering by magnesium-25 at 1.96 Mev, mean lifetime of first excited state from, (E), 20: 15780
scattering by magnesium-24 at 5.8 Mev, polarization in elastic and inelastic, (E), 20: 15806
scattering by nitrogen-14 at 4.9 to 10.1 Mev, polarization from elastic, (E), 20: 15783
scattering by nuclei at 20 to 50 Mev, distributions from, (E), 20: 15728(R) (RHEL/R-112, pp 23-36)
scattering in emulsions, small-angle elastic, (E/T), 20: 15314 (RT/FI(65)35)

PSEUDOUREA, 2-(2-AMINOETHYL)-2-THIO-
radiosensitivity effects on potassium diffusion through cell walls, γ, 20: 14282
radiosensitivity effects in rats, 20: 14391
radiosensitivity effects in mice, mechanism for, 20: 14351

PUERTO RICO POWER REACTOR
reactivity transient in, superheater assembly failure in, 20: 16098

PULMONARY ABSORPTION
model for dust, 20: 14796

PULMONARY EXCRETION
model for dust, 20: 14796

PULSE ANALYZERS
adapter design for selective storage units of, 20: 14822(R) (RHEL/R-112, pp 99-128)
design of analog pulse-ratio measurement systems, 20: 14822(R) (RHEL/R-112, pp 99-128)
design of fast discriminators, 20: 14822(R) (RHEL/R-112, pp 99-128)
design of synchronizing discriminators, 20: 14822(R) (RHEL/R-112, pp 99-128)
performance of multichannel, statistics of scaled pulsed for, (T), 20: 14890
pulse overlap-to-pulse height converter for, detection of pulse pile-up using, 20: 14828

PULSE COLUMNS
flooding in perforated-plate extraction, geometry, operating variables, and physical properties of, 20: 14462 (ORNL-3890)

PULSE GENERATORS (ELECTRONICS)
description of triangle and square wave, for Mössbauer velocity drives, 20: 14827
design of pedestal, 20: 14822(R) (RHEL/R-112, pp 99-128)

PULSES
scaling of, statistics of, (T), 20: 14890

PUPAE
radiation effects on emergence of adult flies from, x, 20: 14306
radiosensitivity of *Psila rosae*, γ, 20: 14317

PUREX PROCESS
diluent for, composition and quality of commercial *n*-paraffin mixtures for use as, 20: 14637 (DP-1034)
separation of fission products from, methods for, 20: 14641 (RL-SA-59)

PURINES
pyrolysis products of, chromatographic analysis of, 20: 14456(R) (ORNL-3889, pp 32-5)

PYRIDOXAL
hydrochloride, effects on strontium metabolism in rat bones, 20: 14246

PYRIMIDINES
pyrolysis products of, chromatographic analysis of, 20: 14456(R) (ORNL-3889, pp 32-5)

PYROCATECHOL
uses in determination of uranium, 20: 14482

PYROMETERS
use of infrared, for furnace melting cycle control in casting large uranium ingots, 20: 15006(R) (NLCO-970, pp 4.1-5)

PYRROLIDONE, VINYL-
radiosensitivity effects on potassium diffusion through cell walls, γ, 20: 14282

PYRROLIDONE, VINYL- POLYMERS
effects on radiation sickness in man, 20: 14396

Q

QUALITY CONTROL
of chemical analyses at ORNL, 20: 14428(R) (ORNL-3889)

QUANTUM ELECTRODYNAMICS
S-operator theory for, 20: 15635
test for, electron-pair photoproduction on carbon as, (E), 20: 15306(R) (CEAL-1026)

QUANTUM MECHANICS
barrier transmission in, JWKB approximation for, 20: 15625
decay functions for relativistic scalar particles in, 20: 15630
Dirac delta function in, 20: 15628
oscillators in, adiabatic invariants of harmonic, (T), 20: 15623 (MPI-PAE/P1.15/65)
scattering of relativistic scalar particles in Galois field, 20: 15629
theory of fields in, problems in, 20: 15489
theory of, axiomatic foundations of, 20: 15631
wave equations in, quasiclassical solution to Dirac, 20: 15559
wave functions in, space-time behavior of Schroedinger, 20: 15632

8-QUINOLINOL
spectra of, infrared, 20: 14499

8-QUINOLINOL COMPLEXES
properties and use in gas chromatography, 20: 14499
with metals, infrared spectra of, 20: 14499

R

RABBITS
blood supply to hepatic carcinoma implants in, tracer study, 20: 14405 (COO-1305-2)
effects in animals, mechanisms for carcinogenic, 20: 14360
radiation effects on mitochondrial phospholipids in liver of, γ, 20: 14278
radiation effects on activity of lipolytic enzymes in, x, 20: 14279
radiation effects on uptake of sulfate by aortic mucopolysaccharides in, β, 20: 14295
radiation effects on immune reaction to *Treponema pallidum*, γ, 20: 14308
radiation effects on kidney function in, combined with trauma, 20: 14325
radiation effects on electrical activity of brain of, γ, 20: 14326
radiation effects on behavior of, γ, 20: 14326
radiation effects on central nervous system in, γ, 20: 14350
radioinduced carcinogenesis in, effects of dose and time on, 20: 14316

RADIATION
attenuation coefficient for, definition of, 20: 15329
detection of high-energy, multiple-junction semiconductor detector for, 20: 14909(P)
dose rates to human bones from radium D, 20: 14353
dosimetry in animals using hematological changes, 20: 14314
dosimetry of, from ingested radioactive materials, 20: 14794
dosimetry of, in complex samples, 20: 14814
effects of whole-body, combined with thymectomy on immune competence, 20: 14354
effects on amino acids, enzymes, and proteins, 20: 14587
effects on animal cells, pathological, 20: 14385
effects on animal cells, metabolic theory for, 20: 14359
effects on bacterial spores, review, 20: 14389
effects on bacteria, factors affecting mechanisms of inactivation, 20: 14390
effects on bones after breast cancer therapy, 20: 14369
effects on cardiac function in dogs, methods for measuring, 20: 14292(R) (TID-22563)
effects on catgut sutures, 20: 14932
effects on children, leukemogenic, 20: 14346
effects on chlorination and sulfochlorination of polyethylene, 20: 14621
effects on crystal structure and properties of solids, review of, 20: 15139
effects on deuterated cyclopentane, 20: 14599
effects on DNA in deoxynucleoprotein, protective effects of albumin against, 20: 14277
effects on electronics, instrumentation for measuring, 20: 14918(R) (ECOM-01313-1)
effects on eyes following therapy of facial skin lesions, 20: 14297
effects on growing plant cells, indirect, 20: 14383
effects on human genetics in offspring of women given ovarian cancer therapy, 20: 14348
effects on lipid metabolism in rats, 20: 14293
effects on man at very low dose rates, 20: 14352
effects on man, dose–effect relations at various post-exposure times, 20: 14287 (AD-626996)
effects on *Micrococcus radiodurans*, mathematical models for, 20: 14388
effects on mixed mesodermal tumors, 20: 14300
effects on ploidy in coconut palms, 20: 14320
effects on rats, effects of AET and largactil on, 20: 14391

effects on reactor components, equipment and methods for measuring, 20: 14719
effects on *S. aureus* growth on cmb meat, 20: 14936
effects on solid uranium-base nuclear fuel materials, bibliography on, 20: 15137 (VDIT-16(5.4))
effects on sterility of medical supplies, 20: 14389
effects on tissue homogenates, metabolic, 20: 14261
effects on ultrastructure in lymphocytes, 20: 14335
effects on vegetative bacteria, review of, 20: 14388
effects on viruses, inactivation, 20: 14387
effects on yeasts, effects of oxygen on recovery from, 20: 14399
emission from current strip in uniaxially anisotropic plasma, (T), 20: 15891
emission in electron reactions with aluminum, nickel, and silver at 6 to 60 kev, (E), 20: 15268

RADIATION CHEMISTRY
reactor fuel design for, 20: 16053(P)
reactor fuel design for, 20: 16054(P)
reactor fuel design for, 20: 16055(P)

RADIATION DETECTION INSTRUMENTS
design for alpha counting of hands and feet, engineering drawings for, 20: 14809
design for identification of particles from nuclear reactions, engineering drawings for, 20: 14906
design for remote monitoring of high-level radiation, 20: 14911(P)
design of beta-gamma portable hand and shoe monitor, 20: 14866
design using multiple detectors and single amplifier and analyzer, 20: 14916(P)
development for monitoring, 20: 14864

RADIATION DETECTION INSTRUMENTS (ION CURRENT TYPE)
design for aerial surveying, engineering drawings for, 20: 14902

RADIATION DETECTION INSTRUMENTS (PULSE TYPE)
coincidence circuits for, design and performance of multiple-transistorized, 20: 14880
design and operation of G-M, for processing cell monitoring, 20: 14853 (CNEA-159)
design and performance of whole-body, for cobalt-58 and iron-59 uptake measurements, 20: 14422
design for low-energy beta particles, 20: 14912(P)
design of solid-state, for low-energy radiations, 20: 14910(P)
performance of boron–fluoride, for neutrons at low-counting rate, 20: 14863
uses in radiochemical analysis, 20: 14488

RADIATION DETECTORS
design and performance of portable, for use with low-radioactivity tracer system, 20: 14451 (NYO-2586-2)
design of Vela satellite program, 20: 15596
performance for neutron flux and energy measurement in radiology, 20: 14883
performance of, statistical confidence test for, 20: 14889
pulse transmission from, by cable supplying voltage, 20: 14876

RADIATION EXPOSURE CHAMBERS
design for cobalt-60 sources, 20: 14581(R) (ORNL-3889, pp 14-16)
design for cobalt-60 sources, 20: 14452(R) (ORNL-3889, pp 1-12)

RADIATION INJURIES
pathology of, in exteriorized rat intestine, x, 20: 14364

RADIATION MONITORING
air sampling for, automated aperture cards for, 20: 14791 (Y-1501)
conference on, 20: 14810
equipment design for, 20: 14872
equipment for HFIR facility, 20: 16125 (ORNL-TM-1393)
equipment for remote high-level, 20: 14911(P)
equipment for, in chemical processing cells, 20: 14853 (CNEA-159)
instrumentation development for, 20: 14864
methods of, in radiochemical processing plants and reactor areas, 20: 14811
program at Hanford Works, Richland, Wash., 20: 14786 (BNWL-SA-465)
system design for fallout-shelter, engineering drawings for, 20: 14903
system for nuclear installations, centralized field, 20: 14855 (JAERI-1090)

RADIATION PROTECTION
measures for, following reactor accidents, 20: 14748
methods for, during facial therapy, 20: 14324
methods for, in hemangioma therapy, 20: 14418
methods for, in irradiation facilities, 20: 14812
panels for, design of barrier-type, 20: 14682(P)
program at AB Atomenergi, 1964, 20: 14782(R) (AE-211)
program for nuclear-accident, USAEC, 20: 14808
program in Mississippi, 20: 14807
program in Peru, 20: 14793
safety regulations for Atomic Energy Center, Dacca, Pakistan, 20: 14783 (AECD/HP/2)

RADIATION SICKNESS
etiology of, time and dose factors for acute, 20: 14287 (AD-626996)
pathogenesis of, 20: 14396
therapy of, using polyvinylpyrrolidone, 20: 14396

RADIATION SOURCES
calibration of, calorimetric method for, 20: 15858
container for, design of variable specific gravity, 20: 14683(P)
design for radiometric gages, 20: 14835
fabrication of, method for, 20: 14634(P)
sample holder for cobalt-60, 20: 14452(R) (ORNL-3889, pp 1-12)

RADIATION TARGETS
production of polarized-proton, (E), 20: 15692 (CERN-66-3)

RADIATORS
weight for space power plants using steam cycles, 20: 14688 (N65-20692)

RADIO WAVES
absorption of h-f cosmic, effects of ionization from nuclear explosions on, (T), 20: 15607
emission from cosmic sources, (T), 20: 15225
phase anomalies of, nuclear-explosion detection by prompt v-l-f, (T), 20: 15602
phase anomalies of v-l-f, nuclear-detonation and solar x-ray detection by sudden, 20: 15603
propagation of low-frequency ground-wave, from nuclear explosions, (T), 20: 15606
propagation of v-l-f, in lower ionosphere, 20: 15604

RADIOACTIVE MATERIALS
dosimetry of deposited, in respiratory tract, 20: 14796
hazards from, in consumer products, 20: 14792
microscopy of, equipment and methods for electron, 20: 14460(R) (ORNL-3889, pp 46-8)
radiation dose from ingested, 20: 14794
radiation dose from ingested, 20: 14795
safety regulations for handling, in Atomic Energy Center, Dacca, Pakistan, 20: 14783 (AECD/HP/2)
sample preparation for 4π counting, 20: 14461(R) (ORNL-3889, pp 48-70)
shipping containers for, classification system for, 20: 14789 (ORNL-P-1910)
uptake of intravascularly introduced microspheres of, by tumors, 20: 14405 (COO-1305-2)

RADIOACTIVITY
background estimation for short-lived-source counting, 20: 14878
decay coefficient for, definition of, 20: 15329
determination in atmospheric and precipitation samples, methods for radiochemical, 20: 14430 (AD-620219)
measurement in snow layers of Alpine glaciers, dating by, 20: 14740
measurement of, from electron-capture-decaying nuclei, 20: 15690 (CEA-R-2813)
monitoring at AERE, 1963–4, 20: 14784(R) (AERE-R-5015)
monitoring atmospheric, in Czechoslovakia, 20: 14813

RADIOBIOLOGY
data on, computer analysis of, 20: 14238 (CONF-650560-13)
research in, effects of cryobiological research on, 20: 14394

RADIOCHEMICAL PROCESSING PLANTS
criticality control at Hanford, administrative setup for, 20: 14790 (RL-SA-43A)
development in Europe, review of, 20: 14646
radiation monitoring in, 20: 14811

RADIOCHEMISTRY
book: *Methods for Analysis of Radioactive Preparations*, in Russian, 20: 14501

RADIODIAGNOSIS
contribution to genetically significant doses in Japan, 20: 14799
methods in, equipment for shadow-shield, 20: 14422
radioisotopes for, review, 20: 14427

RADIOGRAPHY
dosimetry during extraoral, 20: 14412
effects of prenatal diagnostic, on cancer incidence in twins, 20: 14319
equipment and methods for testing of finned SAP tubing, 20: 14712
equipment for, design of miniature iodine-125 x-ray, 20: 14677(P)
hazards from dental, control of, 20: 14419
method for reactor pressure vessels, 20: 14709
method for thin layers, 20: 14704
methods for testing reactor building materials and fuel elements, 20: 14711
methods for thin-walled SAP tubes, low-voltage, 20: 14706
sources for, properties of cobalt-60 and iridium-192, 20: 14705

RADIOISOTOPES
activity of gamma-emitting, use of calibrated spectrometer for measuring, 20: 15747
analysis and characterization of, methods for, 20: 14461(R) (ORNL-3889, pp 48-70)
beta emissions from long-lived, energy distribution of, 20: 14928
containers for, stress analysis from internal pressures in, 20: 14667

(ORNL-TM-1312(Vol.1))
counting short-lived, method for estimating background in, 20: 14878
decay coefficient for, definition of, 20: 15329
detection of natural, by well-type scintillation counters, 20: 14461(R) (ORNL-3889, pp 48-70)
determination of beta-emitting, in air, Kanne ionization chamber for, 20: 14905
development and uses of, 20: 14929 (CONF-651132-1)
development of, medical aspects of, 20: 14427
dose distributions in tissues from beta-emitting, 20: 14403 (NP-15714)
metabolism in dogs, automatic processing of data on, 20: 14238 (CONF-650560-13)
passage through foodchain, 20: 14237
production and uses in Spain, 1964, 20: 14926
production of, properties of wastes from, 20: 16136
properties of short-lived gamma emitting, for use in detection of hidden materials, 20: 14451 (NYO-2586-2)
radiation dosimetry for diagnostic, in Japan, 20: 14799
shipping containers for, classification system for, 20: 14789 (ORNL-P-1910)
toxicity in dogs, computer analysis of data on, 20: 14238 (CONF-650560-13)
use in cancer therapy, 20: 14406
use in industrial instruments, design review for, 20: 14835
use in treating gynecologic cancer, review, 20: 14413
uses in radiochemical analysis, 20: 14488
uses in study of open-hearth steel production process, 20: 14939

RADIOLOGY
neutron energy and flux measurements for, methods for, 20: 14883

RADIOMIMETIC SUBSTANCES
effects on desoxyribonucleic acid content in rat thymus, 20: 14311
effects on DNAse activity in rat thymus, 20: 14311
effects on hemato-encephalic barrier permeability in rats, 20: 14312

RADIOSENSITIVITY
effects of hereditary anemia on, in mice, 20: 14290(R) (NYO-1800-12)
effects of light on Neurospora x, 20: 14358
effects of ploidy on animal-cell, in culture, 20: 14385
variations in plant, diurnal, 20: 14361

RADIOSTERILIZATION
acceptance tests for meat, 20: 14930 (NP-15676)
acceptance tests for meat, 20: 14931 (NP-15677)
conference on, of medical products, 20: 14940
dosimetry in, criteria for, 20: 14814
factors affecting, 20: 14390
packaging materials for, standards for, 20: 14942
program for food, status of, 20: 14937
use in hospitals, 20: 14943

RADIOTHERAPY
control of telecobalt, television equipment for, 20: 14407
data recording in stationary-field, 20: 14408
dosimetry in neutron, 20: 14421
effects on chemodectomas, 20: 14417
effects on pseudouridine excretion, 20: 14269
equipment and facilities for, in France, 20: 14425
filters for cobalt-60 teletherapy, wedge, 20: 14426
methods for hemangioma, evaluation of, 20: 14418
methods for internal, using isotopes, 20: 14406
procedures for γ and x, evaluation of, 20: 14420
radioisotopes for, review, 20: 14427

RADIUM
abundance ratio to uranium in bitumen deposits, 20: 14781
content in carbonate rocks, 20: 14752
effects of accumulated, on productivity of algae, 20: 14381
effects of, combined with surgery and x radiation on cervical carcinomas, complications from, 20: 14377
effects of, combined with surgery and x radiation on cervical carcinomas, 20: 14409

RADIUM ISOTOPES Ra-226
use in internal therapy, survey of techniques for, 20: 14406

RADON
diffusion from lead dioxide at 400 to 500°C, 20: 14548
dosimetry of deposited, in respiratory tract, 20: 14796
separation from water supplies in England by aeration, design of pilot plant for, 20: 14649

RADON ISOTOPES Rn-222
determination of, preparation of scintillation cells for, 20: 14881

RAIN WATER
analysis for cosmic rays, fission products, and natural and radioinduced activity, methods for radiochemical, 20: 14430 (AD-620219)
effects on fallout, 20: 14746
tritium content, 20: 14744

RAMJET ENGINES
conference on aeronautical sciences, 20: 14729

RARE EARTH ALLOYS
Co–rare earth, cobalt ion EPR in intermetallic compounds of, 20: 15963
Fe–rare earths, preparation and structure, 20: 15110
Mn–rare earths, preparation and structure, 20: 15110

RARE EARTH COMPLEXES
nitrate, chemical bonding in, Roman polarization measurements of, 20: 14529
with [(1,2-dimethylethylene)dinitrilo]tetraacetic acid, stability constants of, 20: 14521

RARE EARTH ETHYL SULFATES
rare earth ion magnetic interactions in, 20: 15991

RARE EARTH ISOTOPES
energy level transitions in deformed, effect of pairing correlations on E-1, (T), 20: 15764
energy levels of neutron-deficient radioactive, (E), 20: 14461(R) (ORNL-3889, pp 48-70)
energy levels of odd-A deformed, collective, 20: 15833
energy levels of, equilibrium deformation and E2 moments of, (T), 20: 15788
nuclear deformations of, self-consistent calculation for, 20: 15843
spectra of alpha-emitting, (E), 20: 14461(R) (ORNL-3889, pp 48-70)

RARE EARTH SILICATES
structure of, polymorphic, 20: 14537

RARE EARTH TELLURIDES
phase studies, 20: 14530

RARE EARTHS
atomic structure and suggested changes in positions of, in periodic table, 20: 14549
determination in methanol–mineral acid media using azo dyes, spectrophotometric, 20: 14469(R) (TID-22650)
electron density of states near Fermi level of, (E), 20: 15106
electron exchange interactions in, calculation of nonisotropic contribution to, (T), 20: 15990
excretion of, effects of radiostrontium chelates on, 20: 14256
production of, from apatites from Kola Peninsula, 20: 14520
separation by ion exchange in mixed and non-aqueous media, review on, 20: 14469(R) (TID-22650)
separation from fission products, review on methods for, 20: 14436 (BNWL-SA-504)
separation from thorium by solvent extraction using alkyl phosphonates, 20: 14448(R) (NLCO-970, pp 1.1-22)
separation from waste solutions by solvent extraction using TBP, 20: 14635 (CONF-550305-5)
separation of americium and curium from, 20: 14659(P)

RATS
adenine nucleotide content in blood and liver of, effects of methionine-sulfoximine on, 20: 14270
anoxia in, effects of methandrostenolon on, 20: 14402
barium-140 uptake by aortic wall of, 20: 14252
bone marrow cells development in, tracer study, 20: 14248
cesium-134 metabolism in, 20: 14243(R) (TID-22626)
effects of radiomimetic drugs on, physiological, 20: 14311
effects of radiomimetic drugs on hemato-encephalic barrier permeability in, 20: 14312
nucleic acid metabolism in brain and liver of, tracer study, 20: 14242(R) (TID-22591)
radiation effects on thymidine index in nephrectomized, x, 20: 14258 (AD-627569)
radiation effects on fetal cells from, x, 20: 14262
radiation effects on urinary excretion of ammonia and phosphates in, x, 20: 14270
radiation effects on adenine nucleotide content in blood and liver of, x, 20: 14270
radiation effects on plasma proteins in, Hamolsky's test for γ, 20: 14276
radiation effects on activity of lipolytic enzymes in, x, 20: 14279
radiation effects on lipid metabolism in, 20: 14293
radiation effects on liver cells of fetal and pregnant, x, 20: 14294
radiation effects on nervous system in, after neonatal spinal cord exposure, proton, 20: 14299
radiation effects on enzyme activity in mitochondria of liver, spleen, and thymus of, x, 20: 14376
radiation effects on content of glycoprotein in blood serum of, x, 20: 14378
radiation effects on fatty acid metabolism in, x, 20: 14379
radiation effects on, protective effects of methylandrostenolone against x, 20: 14392
radiation effects on, physiological x, 20: 14311
radiation effects on hemato-encephalic barrier permeability in, x, 20: 14312
radiation effects on lymphocyte distribution in spleen and thymus of, effects of cell size on x, 20: 14318
radiation effects on teeth in, head and whole-body exposure x,

20: 14322
radiation effects on enzyme activity of liver and spleen of, x, 20: 14362
radiation effects on mucosa of exteriorized intestine of, pathological x, 20: 14364
radiation effects on spatial avoidance behavior of, x, 20: 14366
radiation effects on, metabolic neutron and x, 20: 14368
radiation effects on peroxide formation in tissue homogenates of, 20: 14261
radiation effects on epiphyseal cartilage of, 20: 14291(R) (TID-22494)
radioisotope sorption by skin of, 20: 14253
radiosensitivity of, effects of largactil on, 20: 14391
radiosensitivity of, effects of methandrostenolon on, 20: 14402
skeletal growth in, effects of vitamins A and D on, 20: 16148 (NYO-2779-9)
strontium metabolism in bones of, effects of pyridoxal on, 20: 14246
strontium-85 uptake by aortic wall of, 20: 14252
strontium-90 metabolism in, effects on stable strontium feeding on, 20: 14251
urinary excretion of ammonia and phosphates, effects of burns, cytostatics, or methioninesulfoximine on, 20: 14270

REACTION MECHANISMS
isotope effects on, temperature-independent factor in, 20: 14544

REACTOR BREEDING BLANKETS
design parameters of, effects on breeding in, (T), 20: 16093

REACTOR BREEDING ELEMENTS
efficiency of carbide and oxide, comparison of, (T), 20: 16093

REACTOR COMPONENTS
physical properties of, equipment and methods for measuring, 20: 14719
research programs on, at Juelich Research Center, Germany, 20: 16156
wear evaluation of SAP, 20: 15998 (EUR-2117.n)

REACTOR CONTROL ELEMENTS
design, 20: 16012(P)
design, 20: 16016(P)
design using flowing particles, 20: 16014(P)

REACTOR CONTROL RODS
drive mechanisms for, testing of, 20: 16096
performance testing of CVTR, 20: 16062 (CVNA-175)
reactivity worth of, variation approach to boundary perturbation effects for, (T), 20: 16033

REACTOR CONTROL SYSTEMS
design of, using poison rods controlled by velocity of fluid in closed circuits, 20: 16018(P)
electric circuit design for, shut-down, 20: 16006(P)
testing rod drive mechanisms for, 20: 16096

REACTOR COOLANTS
flow in internal- and external-cooled fuel elements, aerodynamics of, (T), 20: 15997 (CEA-R-2856)

REACTOR COOLING SYSTEMS
vibrations in pressurized water, effects on heat transfer in, (T), 20: 16000 (NYO-2655-1)

REACTOR ENGINEERING
containment studies, summary, 20: 16023(R) (IITRI-578P21-16)
nuclear data files for, computer program for maintaining, 20: 15995 (BNL-966)

REACTOR FUEL ALLOYS
fabrication of β-quenched and α-annealed aluminum–iron–uranium, 20: 15022(P)
fabrication of β-quenched and α-annealed aluminum–iron–uranium, 20: 15023(P)
fabrication of β-quenched and α-annealed aluminum–iron–uranium, 20: 15024(P)

REACTOR FUEL ELEMENTS
analysis of spent, activation, 20: 14461(R) (ORNL-3889, pp 48-70)
assembly of strings of, for charging vertical-channel gas-cooled reactors, 20: 16003(P)
burnup of, mass spectrometric determination of, 20: 16046
burnup of, use of gamma spectroscopy for nondestructive measurements of, 20: 14504
coolant flow in, aerodynamics of, (T), 20: 15997 (CEA-R-2856)
design, 20: 16038(P)
design for neutron flux flattening, 20: 16052(P)
design of assemblies of, 20: 16050(P)
design of assembly of, 20: 16051(P)
design of metal-clad, with copper foil interlayer, 20: 16056(P)
development for Indian power reactors, 20: 16099
diffusion of fission products through coatings of, equations for, 20: 15114
failure detection systems for, feasibility of chemical, 20: 14847 (BMwF-FBK-65-01)
failure of, tracer methods for detecting, 20: 14848 (BMwF-FBK-65-02)
instrumentation of, design of electrical contact assembly for, 20: 14842(P)
isotopic content in operating power, methods for determining heavy-, 20: 14438 (CEND-540)
photographing and viewing irradiated, engineering drawing of teleperiscope for, 20: 14675
positioning device for, for stacked arrangement, 20: 16005(P)
processing of irradiated, equipment for, 20: 14644
processing of irradiated, research and development on, in Europe, 20: 14646
processing of irradiated, efficiency of fluidized-bed fluoride volatility method for, 20: 14647
processing of irradiated, properties of wastes from, 20: 16136
properties and performance for fast reactors, 20: 16047
radiation effects on solid uranium-base, bibliography on, 20: 15137 (VDIT-16(5.4))
separation of curium-244 from irradiated, chemical process for, 20: 14636 (CONF-660305-7)
shipping container for spent, design of air- or water-cooled, 20: 14678(P)
shipping of irradiated, economics of, in Europe, 20: 14646
shipping spent, container for, 20: 14679(P)
storage facility for spent, design of, 20: 16007(P)
storage of irradiated, survey of methods for, 20: 14803
testing clad, microradiographic method for, 20: 14704
testing clad, nondestructive methods for, 20: 14711
testing cladding on, eddy-current method for, 20: 14703
testing claddings on, automatic device for ultrasonic, 20: 14715

REACTOR FUEL ELEMENTS (CERAMIC)
burnup of plutonium and uranium carbide and uranium sulfide, 20: 15032(R) (ANL-7152, pp 50-72)
criticality parameters for water-reflected plutonium dioxide–uranium dioxide, (T), 20: 16032
design with metallic-fuel-wire insert, 20: 16057(P)
fabrication of thorium dioxide–uranium dioxide, machine for use in, 20: 14668 (ORNL-TM-1397)
processing carbide–graphite, methods for aqueous, 20: 14638 (NP-15753)
production of Zircaloy-2-clad vibratory-compacted uranie powder, process development for, 20: 14999(R) (EURAEC-1466)
radiation effects on urania and urania–zirconia, in-pile, 20: 16089(R) (WAPD-MRP-114)

REACTOR FUEL ELEMENTS (DISPERSION)
fabrication of graphite matrix containing pyrolytic-carbon-coated uranium dicarbide particles, 20: 15002 (LA-3378)

REACTOR FUEL PLATES
boiling phenomena near, simulation of, 20: 16029
radiation effects on, in-pile, 20: 16089(R) (WAPD-MRP-114)
testing of, nondestructive method for, 20: 14711

REACTOR FUEL RODS
criticality parameters for water-reflected plutonium dioxide–uranium dioxide, (T), 20: 16032
design of compartmented, 20: 16058(P)
design of grooved and canned, 20: 16048(P)
design of sheathed, with radial appendages for improved heat transfer, 20: 16049(P)
testing of thin-walled cladding tubes for, ultrasonic equipment and methods for, 20: 14716
testing plutonium-enriched, nondestructive methods for, 20: 14707
testing SAP cladding on, nondestructive methods for, 20: 14712
testing Zircaloy-2 cladding for, ultrasonic equipment and method for, 20: 14714

REACTOR FUEL TUBES
testing of, nondestructive method for, 20: 14711

REACTOR FUELS
analysis for fission products and heavy element isotopes in spent, evaluation of chemical, 20: 14435 (BNWL-SA-503)
analysis for plutonium and uranium, evaluation of methods for, 20: 14447 (NBL-231)
burnup determination for, methods for, 20: 15717(R) (GEAP-4950)
burnup of, calculations and monitors for, (E/T), 20: 16061(R) (BAW-296)
burnup of, methods development for determining, 20: 15133(R) (GEAP-4893)
criticality parameters for, (T), 20: 16031
design of porous particulate, for chemo-nuclear reactors, 20: 16053(P)
design of porous particulate, for use in chemo-nuclear reactors, 20: 16054(P)
design of porous particulate, for use in chemo-nuclear reactors, 20: 16055(P)
development for fast reactors, 20: 16060(R) (ANL-7152, pp 1-49)
economics for fast and gas-cooled graphite moderated reactors, 20: 16087 (TRG-Report-1115)
effects of ingested or inhaled SNAP, biological, 20: 14785 (BNWL-182)
homogeneity of, determination by track imaging, 20: 14854 (CONF-660304-3)
preparation of spherical granules for, 20: 14575(P)
processing for fast reactors, development of, 20: 16060(R) (ANL-7152,

pp 1-49)
processing graphite-base, for thorium and uranium recovery, 20: 14640 (ORNL-TM-1411)
properties and performance for fast reactors, 20: 16047
research on coated-particle, at Seibersdorf, 20: 16127
REACTOR MATERIALS
research programs on, at Juelich Research Center, Germany, 20: 16156
tariffs on, European, 20: 16155
testing of, nondestructive methods for, 20: 14711
REACTOR MATRICES
design with variable-pitch lattices, 20: 16015(P)
neutron flux distributions in natural uranium–water, 20: 16028
REACTOR REFLECTORS
design modification and performance for Michigan Research Reactor, 20: 16128
REACTOR SAFETY
accident analysis in boiling-water and pressurized-water high-power reactors, 20: 16019(R) (BMI-X-10154)
containment studies, summary, 20: 16023(R) (IITRI-578P21-16)
control of polyphenyls in working environments, methods for, 20: 14467 (RT/PROT(64)-20)
electric circuit design for, shut-down, 20: 16006(P)
evaluation, 20: 16001
REACTOR SAFETY EXPERIMENTS
accident analyses in LOFT, 20: 16019(R) (BMI-X-10154)
operation of TREAT, 20: 15033(R) (ANL-7152, pp 87-96)
REACTOR SHIELDING
neutron penetration and slowing-down in, method for predicting, (T), 20: 15935
REACTOR TUBES
mounting device for pressurized, 20: 16017(P)
power determination of, maximum, (T), 20: 16120 (BNWL-176)
testing during processing and production, use of eddy-current methods for, 20: 14720
testing Zircaloy-2, nondestructive method for, 20: 14711
REACTORS
accidents in, hazards of food contamination in, 20: 14748
containment and safety of, review of design practice and philosophy for, 20: 16001
containment studies for, summary, 20: 16023(R) (IITRI-578P21-16)
coolant flow in, aerodynamics of, (T), 20: 15997 (CEA-R-2856)
core design with variable-pitch lattices, 20: 16015(P)
design, 20: 16042(P)
design, 20: 16045(P)
design of liquid moderated, 20: 16044(P)
design of thin-walled, 20: 16013(P)
design with variable moderator, 20: 16041(P)
design, using plutonium-240-fuel moderation, 20: 16039(P)
design, with control by fuel element rotation, 20: 16038(P)
development, 20: 15994(R) (ANL-7152)
fuel element design for neutron flux flattening, 20: 16052(P)
fuel element failure detection systems for, feasibility of chemical, 20: 14847 (BMwF-FBK-65-01)
fuel element failure detection systems for, using tracer methods, 20: 14848 (BMwF-FBK-65-02)
iodine-131 production, transport, and deposition in containment systems of, 20: 14804
loading device for, design of, 20: 16008(P)
neutron distributions in, variational calculations of, 20: 15666 (CONF-660204-4)
neutron flux measurements in, use of cobalt and aluminum–cobalt wires for, 20: 14867
neutron flux-shape eigenfunctions for two-zone slab, 20: 16024 (RFR-231)
neutron flux-shape eigenfunctions for two-zone cylindrical, 20: 16025 (RFR-232)
neutron spectra in, activation analysis of intermediate, 20: 14860 (RT/FI(65)-33)
neutron transport in, geometrical effects on anisotropic scattering of, (T), 20: 16021 (CEA-R-2890)
neutron transport in spherical, j_N analysis of, 20: 16022 (EUR-2627.e)
neutron transport in, one-group collision-probability code for, 20: 15668 (EUR-2624.e)
pressure vessels for, feasibility of cable-wrapped, (T), 20: 16002
radiation monitoring, 20: 14811
reactivity measurements on subcritical, by noise analysis, 20: 16027
waste disposal from, by in-pile activation of long-lived radioisotopes to stable or short-lived isotopes, (T), 20: 16132 (BNL-8558)
wastes from, properties of, 20: 16136
xenon stability calculations for, tables for, 20: 16024 (RFR-231)
REFRACTORY COATINGS
development for metals and graphite, 20: 14974(P)
REFRACTORY MATERIALS
preparation from mixtures of ground inorganic fibers and colloidal inorganic oxides, 20: 14974(P)
preparation of spherical particles of, procedure and apparatus for, 20: 14971(P)
RELATIVITY THEORY
equations of motion for pole-dipole test particles in, 20: 15641
field theory in, geometrical aspects of unified, 20: 15624
gravitation theory in general, quantum, 20: 15642
gravitational waves from isolated axially symmetric sources, (T), 20: 15637
hydrodynamic equations in general, (T), 20: 15626
invariance transformations in, for classical hamiltonian particle dynamics, 20: 15150
metrical lattice in, for electromagnetism, 20: 15633
spheroid equilibrium in general, uniformly rotating, (T), 20: 15627
REMOTE-CONTROL EQUIPMENT
design for pipetting corrosive solutions, 20: 14454(R) (ORNL-3889, pp 17-24)
design for receiving, blending, and transferring thorium–uranium oxide powders, 20: 14668 (ORNL-TM-1397)
design of G-M tube positioner for ion exchange columns, engineering drawings for, 20: 14832
design of manipulator, 20: 14681(P)
RESEARCH REACTORS
control system of ISPRA-2, design of, 20: 16126
design using heavy and light water moderator, 20: 16131(P)
development and operation of FRJ-1 and FRJ-2, at Juelich Research Center, Germany, 20: 16156
experimental facilities of JRR-4, manual for operation of, 20: 16122 (JAERI-6016)
experimental facilities for IRL, thermal column pneumatic rabbit, 20: 16130
reactivity measurements in FR0 assemblies, 20: 16118 (AE-212)
use of TRIGA Mark I, for activation analysis in scientific crime detection, 20: 14439(R) (GA-5556)
RESINS
use in laminated shielding panels, 20: 14680(P)
RESISTANCE FURNACES
effects of heating element arrangement in, on uranium metal quality, 20: 14964(R) (NLCO-970, pp 2.1-7)
use of infrared pyrometers for melting cycle control in, during uranium ingot casting, 20: 15006(R) (NLCO-970, pp 4.1-5)
RESISTORS
efficiency of, for measuring enthalpies of reactions on solid surfaces, 20: 16153 (UCRL-16472)
radiation effects on, nuclear-explosion, 20: 14921
RESPIRATORY TRACTS
deposition of dusts in, 20: 14796
RETICULO-ENDOTHELIAL SYSTEM
effects of antigen stimulus on, 20: 14354
metabolism of carbon-14-labeled methyl palmitate in mouse, 20: 14241 (TID-21437)
radiation effects on function of, x, 20: 14374
RHENIUM
coatings of, uses of electrodeposited, 20: 15016
deposition of, electrolytic, 20: 15016
diffusion in molybdenum at 1700 to 2100°C, tracer studies of, 20: 15127
work function of, effects of cesium-fluoride vapor on, 20: 15297 (CONF-640921, pp 101-9)
RHENIUM ALLOYS
Cr–Re, precipitation of Cr_2N at grain boundaries in nitrogen-doped, 20: 14957(R) (BMI-1754)
Mo–Re, grain boundary structure in, internal friction studies of, 20: 15128
Re–W, fabrication of sheets from extruded bars of, 20: 14968(R) (USBM-RC-1220)
RHENIUM ISOTOPES
deuteron reactions at 15 Mev, isomeric states from, (E), 20: 15856
RHENIUM ISOTOPES Re-184
decay of isomeric, conversion electron spectra of, (E), 20: 15750
RHENIUM ISOTOPES Re-187
energy levels, 20: 15807
RHODIUM
energy level transitions in, Coster-Kronig, (T), 20: 15238 (CONF-233 (Vol.3), pp 398-418)
energy level widths for, K, (T), 20: 15239 (CONF-233(Vol.3), pp 419-39)
radiochemistry of, 20: 15727 (PPAD-572F)
separation from fission products, review on method for, 20: 14436 (BNWL-SA-504)
RHODIUM ALLOYS
Pd–Rh, catalytic effects on deuterium-methane exchange and propane cracking reactions, 20: 14542
RHODIUM ISOTOPES Rh-100

energy levels of, g-factor and lifetime of 75-kev, 20: 15727 (PPAD-572F)
RHODIUM ISOTOPES Rh-102
determination in atmospheric and precipitation samples, methods for radiochemical, 20: 14430 (AD-620219)
RHODIUM ISOTOPES Rh-103
neutron reactions (n,He-3) at 14.8 Mev, effective cross sections for, (E), 20: 15739
neutron reactions (n,γ) with, gamma spectra from, (E), 20: 15754
RHODIUM ISOTOPES Rh-104
energy levels, (E), 20: 15754
RHODIUM ISOTOPES Rh-105
yields from uranium-238 spontaneous fission, 20: 15776
RHODIUM ISOTOPES Rh-106
content in fallout over Black Sea, 1964, 20: 14741
RIBONUCLEASE, DEOXY-
effects of radiomimetic drugs on activity of, in rat thymus, 20: 14311
radiation effects on activity of, in rat thymus, x, 20: 14311
RIBONUCLEIC ACID
charging reactions of phenylalanyl-, factors affecting, 20: 14456(R) (ORNL-3889, pp 32-5)
determination in *E. coli*, methods for, 20: 14456(R) (ORNL-3889, pp 32-5)
metabolism in rat brain and liver, tracer study, 20: 14242(R) (TID-22591)
radiation effects on synthesis in amoeba, tracer study, 20: 14259(R) (NP-15855)
radiosensitivity effects in animals, electron, 20: 14397
radiosensitivity effects of injected, in mice, 20: 14401
RIBONUCLEIC ACID, DESOXY-
effects of radiomimetic drugs on content in rat thymus, 20: 14311
metabolism in rat liver, tracer study, 20: 14242(R) (TID-22591)
radiation effects on synthesis in amoeba, tracer study, 20: 14259(R) (NP-15855)
radiation effects on phosphate levels in Phycomyces, x, 20: 14264
radiation effects on, effects of amino acids on uv, 20: 14272
radiation effects on, in deoxynucleoprotein, 20: 14277
radiation effects on, direct x, 20: 14283
radiation effects on content in rat thymus, 20: 14311
radiation effects on metabolism in animal cells in culture, uv, 20: 14355
radioinduced breakdown, x, 20: 14265
radiosensitivity of, in bacteria, 20: 14267
transfer from uv-irradiated T4 bacteriophages to progeny, 20: 14285
RICE
nutrient absorption by seedlings of, tracer study of foliar, 20: 14240 (NP-15670)
ROCKET MOTOR NOZZLES
boundary layer in nuclear, effects of core position on, 20: 14727 (NASA-TM-X-1208)
heat transfer in nuclear, effects of core position on, 20: 14727 (NASA-TM-X-1208)
ROCKET MOTORS
spray systems for liquid fueled, droplet properties in, (T), 20: 14692 (UCRL-16656)
ROCKET REACTORS
core position effects on heat transfer and boundary layer in nozzles for, 20: 14727 (NASA-TM-X-1208)
ROCKET REACTORS (KIWI)
destruct systems for ROVER/NERVA, development testing of, 20: 16112 (SC-RR-65-551)
ROCKETS
development of nuclear-powered, 20: 16115
heating of liquid hydrogen in nuclear, 20: 14728 (NASA-TN-D-3328)
ROCKS
gamma and neutron distributions in, similitude theory for, 20: 14776
separation of alkaline earths, rare earths, thorium, and uranium from, by ion exchange, 20: 14469(R) (TID-22650)
RODS
anchor for rows of, 20: 14698(P)
RUBBER
analysis of automobile tire, activation, 20: 14439(R) (GA-5556)
RUBIDIUM
coupling with helium-3, atomic, 20: 15274
energy level transitions in, Coster-Kronig, (T), 20: 15238 (CONF-233 (Vol.3), pp 398-418)
energy level widths for, K, (T), 20: 15239 (CONF-233(Vol.3), pp 419-39)
RUBIDIUM FLUORIDES
reactions with xenon oxyfluorides, complex formation in, 20: 14523
RUBIDIUM ISOTOPES Rb-85
neutron reactions (n,2n), cross sections for, (E), 20: 14461(R) (ORNL-3889, pp 48-70)
RUBIDIUM OXIDES
preparation, 20: 14511(R) (ORNL-3899, pp 71-3)
RUPTURE
properties of refractory metals, numerical methods for analysis of, 20: 15041 (GEMP-397)
RUTHENIUM
determination in dust samples by microchemical methods and autoradiography, 20: 14472
energy level transitions in, Coster-Kronig, (T), 20: 15238 (CONF-233 (Vol.3), pp 398-418)
energy level widths for, K, (T), 20: 15239 (CONF-233(Vol.3), pp 419-39)
separation from hydrochloric acid solutions by solvent extraction using trioctylamine–xylene, 20: 14650
thermal capacity at 0.27 to 1.20°K, 20: 15061 (UCRL-11580)
RUTHENIUM ISOTOPES Ru-105
yields from uranium-238 spontaneous fission, 20: 15776
RUTHENIUM ISOTOPES Ru-106
content in fallout over Black Sea, 1964, 20: 14741
content in stratosphere and troposphere, 1962 and 1963, 20: 14742
separation from copper ores mined by nuclear explosives, 20: 14662(R) (ORNL-TM-1394)

S

SACCHARIC ACID
uses in determination of ytterbium, 20: 14490
SAFETY
administration of, at Argonne National Lab., 20: 14800
radiation exposure records in program for, legal aspects of, 20: 14801
SAFETY HAZARDS
determination of, from radioactive consumer products, 20: 14792
evaluation of, in peaceful uses of atomic energy, 20: 14802
SALMONELLA
radiation effects on, effects of temperature and vitamin K_5 on γ, 20: 14395
SALT DEPOSITS
nuclear explosion in, decoupling in Salmon, 20: 14664 (UCRL-14487 (Rev.1))
SAMARIUM
bremsstrahlung reactions (γ,n) at 8 to 16 Mev, spectra from, (E), 20: 15723 (MIT-2098-162)
bremsstrahlung reactions (γ,n) with, neutron emission in, (E), 20: 15724 (MIT-2098-224)
separation from ytterbium using organic acids, 20: 14490
SAMARIUM ALLOYS
Al–Sm, magnetic hyperfine interactions in samarium-149 in, 20: 15992
Mn–Sm, preparation and structure, 20: 15110
SAMARIUM ISOTOPES Sm-149
magnetic hyperfine interactions in $SmAl_2$, 20: 15992
SAMARIUM ISOTOPES Sm-151
electron energy level widths for, M, (E/T), 20: 15241 (CONF-233(Vol.3), pp 454-64)
energy level transitions in, multipolarity of 4.821-kev, (E/T), 20: 15241 (CONF-233(Vol.3), pp 454-64)
SAMARIUM ISOTOPES Sm-152
energy level transitions in, conversion coefficients for E2, (E), 20: 15698 (CONF-233(Vol.2), pp 109-16)
energy level transitions in, conversion coefficients for E2, (E), 20: 15705 (CONF-233(Vol.2), pp 177-90)
energy levels from europium-152 decay, (E), 20: 15832
nitrogen-14 scattering at 52 Mev, interference effects in 2+ level excitation in, (T), 20: 15768
SAMARIUM ISOTOPES Sm-153
decay of, gamma transitions in, (E), 20: 15795
gamma spectra, (E), 20: 15734 (ZfK-PhA-18)
half life, (E), 20: 14461(R) (ORNL-3889, pp 48-70)
SAMARIUM OXIDES
$CaO–Sm_2O_3–UO_2–ZrO_2$, corrosion and surface properties of, 20: 16089(R) (WAPD-MRP-114)
SAMARIUM SULFIDES
electric properties and transport mechanism, (E), 20: 15981(T)
SAMPLING
collector design for atmospheric, 20: 14815 (COO-401-139)
system for jet, of material in vicinity of nuclear detonation, 20: 14662(R) (ORNL-TM-1394)
SANDS
use in laminated shielding panels, 20: 14680(P)
SAP (SINTERED ALUMINUM PRODUCTS)
testing cladding of, nondestructive methods for, 20: 14712
testing finned cladding of, eddy-current method for, 20: 14703
testing tubes of, low-voltage radiographic methods for, 20: 14706
wear against SAP and steels, 20: 15998 (EUR-2117.n)
SARCOMAS
radiation effects on DPN content in, x, 20: 14370
radioinduced uterine, 20: 14300
radioinduced uterine, following pelvic irradiation, 20: 14301

radiotherapy of uterine, efficiency of, 20: 14301
SATELLITES
use for nuclear-explosion detection, replenishment statistics for, (T), 20: 15600
SCALERS
design with readout system, engineering drawings for, 20: 14899
SCANDIUM
determination in cigarette tobacco, activation, 20: 14439(R) (GA-5556)
determination in glass samples, activation, 20: 14439(R) (GA-5556)
determination in presence of aluminum and beryllium by gas chromatography of trifluoroacetylacetonates, 20: 14486
determination in paper samples in criminal cases, activation, 20: 14439(R) (GA-5556)
determination in soils, activation, 20: 14439(R) (GA-5556)
determination in silts in water, activation, 20: 14439(R) (GA-5556)
determination of trace amounts of, in iron, activation, 20: 14471
determination using salicylaldehyde semicarbazone, spectrofluorimetric, 20: 14476
energy level transitions in, Coster-Kronig, (T), 20: 15238 (CONF-233 (Vol.3), pp 398-418)
energy level widths for, K, (T), 20: 15239 (CONF-233(Vol.3), pp 419-39)
neutron capture by, gamma spectra from thermal, (E), 20: 15787
precipitation from hydrochloric acid solutions by sodium silicofluoride, 20: 14566
SCANDIUM ALLOYS
Co–Sc, cobalt ion EPR in intermetallic compounds of, 20: 15963
SCANDIUM BORIDES
stability of, chemical and thermal, 20: 14531
SCANDIUM CARBIDES
ScC–TiC–WC, preparation and hardness, 20: 15017
SCANDIUM ISOTOPES
deuteron reactions at 15 Mev, isomeric states from, (E), 20: 15856
energy levels of, weak-coupling model for $d_{3/2}$-hole states in, 20: 15852
SCANDIUM ISOTOPES Sc-41
energy levels from calcium-40 (p,γ) reactions at 0.6 to 5.2 Mev, 20: 15849
SCANDIUM SILICATES
structure of, polymorphic, 20: 14537
SCATTERING
amplitudes at high energy, ladder approximation for asymptotic behavior of, 20: 15501
amplitudes at high energies, (T), 20: 15519
amplitudes for high-energy, analyticity in energy variables for, (T), 20: 15520
amplitudes for inelastic, threshold behavior of partial, 20: 15500
amplitudes for, analyticity and unitarity of, (T), 20: 15518
amplitudes for, differential properties for Feynman, (T), 20: 15525
amplitudes for, Kronecker-delta singularities in angular momentum plane, (T), 20: 15521
amplitudes in, integral representations for, (T), 20: 15451
amplitudes in, Kronecker-delta-type singularities and Regge poles in, (T), 20: 15465
amplitudes in, removal of kinematic singularities from helicity, (T), 20: 15482
book: *Potential Scattering*, 20: 15566
Dirac equation for high-energy attractive Coulomb, quasiclassical solution to, 20: 15559
dispersion theory of low-energy, 20: 15522
Feynman integrals in, analytic properties of, 20: 15523
Feynman diagrams in, uniformization of Riemann surface for, (T), 20: 15495
potential, perturbed bound-state poles in, 20: 15480
potentials in elastic, phase-shift analysis of, (T), 20: 15463
quantum theory for elastic, space structure and relativistic, 20: 15629
S-matrices in, Padé approximant for unitary, 20: 15363
S-matrix elements for, cluster decomposition of, 20: 15484
S-matrix elements in, reduction formulas in axiomatic quantum field theory for, 20: 15502
S-matrix formalism in perturbation theory, 20: 15526
S-matrix in axiomatic field theory, causal, (T), 20: 15515
S-matrix in many-channel, analytic properties of, 20: 15505
S-matrix singularities in, 20: 15524
S-matrix theory for, N/D method for mass shifts in, 20: 15466
symmetries in, spin and spin-orbit effects in, (T), 20: 15547
testing of SU(3) symmetry by, (T), 20: 15532
theory of high-energy, 20: 15438
theory of, analytic S-matrix, 20: 15512
theory of, approximate dynamical symmetries for, 20: 15483
SCHISTOSOMA
effects of egg purification in, on cercariae infectivity, 20: 14304
radiation effects on infectivity of cercariae of, effects on mouse antibody titer of gamma, 20: 14304
SCINTILLATION DETECTORS
cable system for power supply and pulse transmission, 20: 14876
design for low-background beta counting without lead shielding, 20: 14873
design of stilbene, for neutrons, 20: 14900
design of wedge-shaped, for magnetic spectrometer, 20: 14822(R) (RHEL/R-112, pp 99-128)
development of plastic–phosphor, for beta detection, 20: 14874
efficiency for gamma radiation, calculation of, 20: 14897
performance for absolute radioactivity measurements, 20: 15690 (CEA-R-2813)
performance for detection of air fluorescence from nuclear explosions, (T), 20: 15608
performance in anticoincidence gamma spectrometers, 20: 14865
preparation for radon-222 determination, 20: 14881
pulse-shape discrimination in dual-crystal, for gamma radiation, 20: 14844 (AD-620395)
response to 150-Mev protons, measurement of ionization curves from, 20: 14891
SEA WATER
analysis for titanium, polarographic, 20: 14455(R) (ORNL-3889, pp 25-32)
desalination of, bibliography on, 20: 14510 (NP-15834)
desalination of, conference on, 20: 16157
desalination using dual-purpose reactors of Beloyarsk type, 20: 16107(T) (JPRS-33406)
desalination using dual-purpose fast reactors, 20: 16108(T) (JPRS-33459)
mesopelagic organisms in deep scattering layers of, distribution of migrating, 20: 14235 (SAN-584-1)
SEALS AND GLANDS
performance of boron-free, radiation-resistant, insulating vitreous, 20: 15131(P)
SEED
effects of radiation and diethyl sulfate on barley, 20: 14384
radiation effects on *Vigna sinensis*, neutron and x, 20: 14341
radiation effects on germination of *Phleum pratense*, γ and x, 20: 14349
SEEDLINGS
fertilizer absorption by rice, tracer study of foliar, 20: 14240 (NP-15670)
radiation effects on development of *Vigna sinensis*, neutron and x, 20: 14341
SEISMIC WAVES
detection and discrimination of underground explosion, 20: 14768
propagation from nuclear explosions in salt formations, 20: 14663 (UCRL-14463(Rev.1))
SEISMOLOGY
data processing in, noise correlations for multichannel, 20: 14763
data processing methods for detection and interpretation of teleseismic signals, (E/T), 20: 14762
decoupling in Salmon nuclear detonation, 20: 14664 (UCRL-14487 (Rev.1))
development for underground explosion discrimination, 20: 14768
simulation of seismic disturbances, computer program for, 20: 14755 (UCRL-7929)
use in geophysical studies on liquid waste discharge to ground, 20: 14753 (BNWL-47)
SEISMOMETERS
coherence measurements with time-sampling ocean-bottom, 20: 14766
data processing and recording for large-aperture arrays, 20: 14761
design and signal handling system of large-aperture arrays, 20: 14760
design for detection and discrimination of underground explosions, 20: 14769
design, installation, and operation of large-aperture arrays, 20: 14759
development and performance of ocean-bottom, 20: 14765
development and testing of unattended, 20: 14764
development of arrays of, review of, 20: 14757
operation and performance of large-aperture arrays, 20: 14758
operation and performance of ocean-bottom, (E/T), 20: 14767
SELENIOUS ACID
uses in conductometric titration lanthanum, 20: 14484
SELENIUM
energy level transitions in, Coster-Kronig, (T), 20: 15238 (CONF-233 (Vol.3), pp 398-418)
energy level widths for, K, (T), 20: 15239 (CONF-233(Vol.3), pp 419-39)
neutron elastic scattering at 0.8 Mev, cross sections for, (T), 20: 15770
SELENIUM ISOTOPES Se-75
incorporation in selenocystine by neutron activation, 20: 14630
SELENIUM ISOTOPES Se-77
nitrogen-ion scattering at 16.2 and 17.7 Mev, gamma polarization from, (E), 20: 15759
SELENIUM ISOTOPES Se-78
nitrogen-14 scattering at 36 Mev, interference effects in 2^+ level excitation in, (T), 20: 15768
SEMICONDUCTOR DETECTORS
amplifiers for, design of charge-sensitive pre-, 20: 14851 (BNL-9980)
design of lithium-drifted germanium, engineering drawings for, 20: 14904

design of multiple-junction, for high energy radiations, 20: 14909(P)
performance and properties, 20: 14907
performance in anticoincidence gamma spectrometers, 20: 14865
performance of, equations for, 20: 14875
radioinduced noise in silicon, electromagnetic, (E), 20: 14923
response of lithium-drifted silicon, to conversion electrons in bismuth-207 and cesium-137, 20: 14444(R) (MLM-1268)
response of lithium-drifted silicon p-i-n, to beta particles, 20: 14886
surface contours of p-n junctions in, properties of, 20: 14858(R) (NYO-3246-5)
use in hygrometers, 20: 14840
use of lithium-drifted germanium, in gamma detection and measurement, 20: 14845 (AD-620434)

SEMICONDUCTORS
effects on life of cutting tools during uranium machining by cooling, 20: 14689(R) (NLCO-970, pp 5.1-7)
radiation effects on, instrumentation for analyzing, 20: 14918(R) (ECOM-01313-1)
radiation effects on, nuclear-explosion, 20: 14921

SEPARATION PROCESSES
equipment for Eurex, testing of, 20: 14644
flooding in perforated-plate extraction columns, geometry, operating variables, and physical properties of, 20: 14462 (ORNL-3890)
methods for fission product recovery, review on developments in, 20: 14436 (BNWL-SA-504)
radiation monitoring equipment for, 20: 14853 (CNEA-159)
shielded cells for radioactive, leak detection in, 20: 14788 (JAERI-1089)

SHEEP
iron-59 content in young, after natural exposure, 20: 14243(R) (TID-22626)
radioinduced skeletal anomalies in, exposed *in utero*, γ, 20: 14337

SHELTERS
air intake stack and filter cartridge for fallout, 20: 14722(P)
design of prefabricated fallout, 20: 14723(P)
monitor system for fallout, engineering drawings for, 20: 14903

SHIELDED CONTAINERS
design for shipping spent fuel elements, 20: 14678(P)
design for shipping and storage of spent fuel elements, 20: 14679(P)
design for studying properties of actinides, 20: 15038 (CONF-660305-12)
leak detection in, at reprocessing facility, 20: 14788 (JAERI-1089)
stress analysis of radioisotope, from internal pressures, 20: 14667 (ORNL-TM-1312(Vol.1))

SHIELDING
calculations for, exponential transformation in Monte Carlo, 20: 15937
gamma dose rates in cylindrical and rectangular steel structures from fallout, 20: 15931 (TO-B-65-27)
radiation doses in space vehicle, computer programs for calculating, 20: 15930 (NP-15697(Vol.2))

SHIELDING MATERIALS
design of laminated, 20: 14680(P)

SHIPPING
container for spent fuel-element, 20: 14678(P)
containers for radioisotopes, stress analysis from internal pressures in, 20: 14667 (ORNL-TM-1312(Vol.1))
containers for radioactive materials, classification system for, 20: 14789 (ORNL-P-1910)

SHIPPINGPORT PRESSURIZED WATER REACTOR
decontamination of, 20: 16088 (WAPD-299)
development and operations of Core 1 and 2, 20: 16089(R) (WAPD-MRP-114)
fuel element failure detection systems for, feasibility of chemical, 20: 14847 (BMwF-FBK-65-01)
neutron diffusion theory for, control rod representation of, (T), 20: 16090 (WAPD-T-1841)

SHOCK WAVES
interactions with magnetic fields, 20: 15882(R) (NP-15868)
kinetics of interactions with crushable foamglass, 20: 16023(R) (IITRI-578P21-16)
magnetohydrodynamic, in nonaligned flow in perfect gases, (T), 20: 15576
production by water decompression in air, one-dimensional analysis of, 20: 16023(R) (IITRI-578P21-16)
propagation from nuclear explosions in salt formations, 20: 14663 (UCRL-14463(Rev.1))
propagation in argon, electron precursor phenomena in, (T), 20: 15577
propagation in exponentially decreasing atmospheres, (T), 20: 15217
propagation in helium plasma, heating from, (E), 20: 15896

SILICATE ROCKS
neutron diffusion parameters in, determination of, using pulsed source, 20: 14772

SILICON
determination in plutonium fluorides and peroxides, review on spectrographic, 20: 14464 (RFP-599)
determination in uranium tetrafluoride, spectrographic, 20: 14473
determination in uranium silicides using electron microprobe, 20: 14442(R) (MCW-1493, pp 5-13)
determination of trace amounts of, in uranium dioxide, 20: 14494
electron transmission through thin foils of, plasmon excitation in, (E), 20: 15951
neutron elastic scattering at 0.8 Mev, cross sections for, (T), 20: 15770
neutron scattering by, cross sections for free and coherent, 20: 15682
performance of lithium-drifted p-i-n junction of, in beta dosimetry, 20: 14886
performance of solar cells of, for detection of electron bursts from plasma, 20: 15916
phosphorus ion reactions with p-type, for production of solar cells, 20: 15302(T)
proton elastic scattering at 30 to 50 Mev, models for, 20: 15730(R) (RHEL/R-112, pp 67-98)
radiation effects on, neutron, 20: 14920 (TID-22664)
radioinduced damage effects on carrier lifetime in p-type, gamma, (E), 20: 14922
radioinduced defects in, energy dependence of electron, 20: 14925
radioinduced noise in detectors of, electromagnetic, (E), 20: 14923
use in photovoltaic cells, 20: 15305

SILICON CARBIDES
radioinduced conductivity and n-p effect in, x, (E), 20: 15967

SILICON ISOTOPES Si-28
neutron elastic and inelastic scattering at 2.45 to 5.80 Mev, cross sections for, (E), 20: 15811
neutron reactions (n,2n) at 12 to 18 Mev, cross sections for, (E), 20: 15863
nuclear properties in shell model, 20: 15730 (RHEL/R-112, pp 67-98)

SILICON ISOTOPES Si-29
neutron reactions (n,α) at 13.4 to 15.0 Mev, excitation function for, (E), 20: 15800

SILICON NITRIDES
reactions with basalt, copper matte, slags, and molten salts, 20: 14989

SILICON OXIDES
casting of fiber-reinforced fused, process development for slip-, 20: 15058(R) (SC-DC-66-1130)
determination in explosives, methods for, 20: 14470 (UCRL-7873)
mechanical properties of fiber-reinforced slip-cast fused, 20: 15058(R) (SC-DC-66-1130)
radioinduced flow and stress relaxation in vitreous, proton, (T), 20: 15971
sorptive properties for chloride and potassium ions, effects of pH on, 20: 14651
$BaO-B_2O_3-SiO_2$, effects of aluminum, lanthanum, and thorium oxides on crystallization of, 20: 15075

SILICON SYSTEMS
Al–Si, annealing and growth of films of, 20: 15030 (ANL-7102)
Al–Si, ductility of two-phase, effects of composition and particle size on, 20: 15055(R) (NYO-2394-19)
Al–Si, sample preparation for electron transmission studies, 20: 15055(R) (NYO-2394-19)
Li–Mg–Si, fabrication and properties of cast, 20: 15007 (NP-15881)
Si–V, superconductivity of fused, 20: 15123

SILTS
analysis of river, activation, 20: 14439(R) (GA-5556)
separation of alkaline earths, rare earths, thorium, and uranium from, by ion exchange, 20: 14469(R) (TID-22650)

SILVER
analysis and determination, 20: 14500
determination by x-ray absorption analysis, evaluation of gamma-emitter activity in, 20: 14498
determination in solutions by atomic absorption, 20: 14457(R) (ORNL-3889, pp 36-39)
determination in thumbnail clippings, activation, 20: 14439(R) (GA-5556)
determination in uranium tetrafluoride, spectrographic, 20: 14473
effects on superconducting energy gap in aluminum, (E), 20: 15658
electron and positron reactions at 100 to 400 kev, excitation cross sections for K ionization in, 20: 15257
electron diffusion in slabs of, differential energy spectra and number transmission for, (T), 20: 15936
electron paramagnetic resonance of free atoms of, in solid solutions of silver salts, (E), 20: 15975(T)
electron reactions with thin foils of, transition radiation from, (E), 20: 15968
electron reactions at 6 to 60 kev, transient radiation from, (E), 20: 15268
electron spectra from, j-j coupling for L Auger, 20: 15237 (CONF-233(Vol.3), pp 371-97)
energy level transitions in, Coster-Kronig, (T), 20: 15238 (CONF-233 (Vol.3), pp 398-418)
energy level widths for, K, (T), 20: 15239 (CONF-233(Vol.3), pp 419-39)
energy levels of, from Thomas-Fermi-Dirac potential, (T), 20: 15267
proton reactions (p,n) at 30 to 50 Mev, distributions from, 20: 15729(R) (RHEL/R-112, pp 37-66)

reactions with sodium, high-temperature, 20: 15033(R) (ANL-7152, pp 87-96)
SILVER ALLOYS
Ag–Y, crystal structure of intermetallic compound YAg_2 in, 20: 15102
SILVER CHLORIDES
chlorine-36 exchange between crystals and solutions, 20: 14572
diffusion of sodium ions in crystals of, mechanism for, (E), 20: 15966
silver-110$_m$ exchange between crystals and solutions, 20: 14572
SILVER FLUORIDES
AgF–D_2O, radioinduced free silver atoms in solid solutions of, EPR of x, (E), 20: 15975(T)
AgF–H_2O, radioinduced free silver atoms in solid solutions of, EPR of x, (E), 20: 15975(T)
ethanol–AgF, radioinduced free silver atoms in solid solutions of, EPR of x, (E), 20: 15975(T)
methanol–AgF, radioinduced free silver atoms in solid solutions of, EPR of x, (E), 20: 15975(T)
SILVER ISOTOPES
deuteron reactions at 15 Mev, isomeric states from, (E), 20: 15856
diffusion in beryllium, tracer studies on, 20: 15037 (CEA-R-2621)
SILVER ISOTOPES Ag-105
gamma spectra, (E), 20: 14845 (AD-620434)
SILVER ISOTOPES Ag-110
determination in atmospheric and precipitation samples, methods for radiochemical, 20: 14430 (AD-620219)
exchange between silver chloride crystals and solutions, 20: 14572
SILVER NITRATES
$AgNO_3$–D_2O, radioinduced free silver atoms in solid solutions of, EPR of x, (E), 20: 15975(T)
$AgNO_3$–H_2O, radioinduced free silver atoms in solid solutions of, EPR of x, (E), 20: 15975(T)
ethanol–$AgNO_3$, radioinduced free silver atoms in solid solutions of, EPR of x, (E), 20: 15975(T)
methanol–$AgNO_3$, radioinduced free silver atoms in solid solutions of, EPR of x, (E), 20: 15975(T)
SILVER PERCHLORATES
$AgClO_4$–D_2O, radioinduced free silver atoms in solid solutions of, EPR of x, (E), 20: 15975(T)
$AgClO_4$–H_2O, radioinduced free silver atoms in solid solutions of, EPR of x, (E), 20: 15975(T)
ethanol–$AgClO_4$, radioinduced free silver atoms in solid solutions of, EPR of x, (E), 20: 15975(T)
methanol–$AgClO_4$, radioinduced free silver atoms in solid solutions of, EPR of x, (E), 20: 15975(T)
SILVER SULFATES
Ag_2SO_4–D_2O, radioinduced free silver atoms in solid solutions of, EPR of x, (E), 20: 15975(T)
Ag_2SO_4–H_2O, radioinduced free silver atoms in solid solutions of, EPR of x, (E), 20: 15975(T)
ethanol–Ag_2SO_4, radioinduced free silver atoms in solid solutions of, EPR of x, (E), 20: 15975(T)
methanol–Ag_2SO_4, radioinduced free silver atoms in solid solutions of, EPR of x, (E), 20: 15975(T)
SILVER SYSTEMS
B–Co–Ag, crystal structure, 20: 14532
B–Ni–Ag, crystal structure, 20: 14532
SINTERING
equation for one-mechanism diffusion, 20: 15009 (TID-22491)
SIOUX FALLS POWER REACTOR
core flooding, pressurization, and temperature coefficients, 20: 16059 (ACNP-65600)
SKELETON
effects of vitamins A and D deficiency on growth and maturation of rat, 20: 16148 (NYO-2779-9)
radioinduced anomalies of, in cattle, sheep, and swine exposed *in utero*, 20: 14337
SKIN
chlorine-36 sorption by burned and normal, 20: 14255
radiation dose to, during extraoral radiography, 20: 14412
radioinduced *Lupus erythematosus* in human, uv, 20: 14309
radioisotope sorption by rat, 20: 14253
sodium-22 sorption by burned and normal, 20: 14255
tritiated water sorption by burned and normal, 20: 14255
SKIN LESIONS
radioinduced erythemic, uv, 20: 14310
radiotherapy of facial, choroido-retinal damage following, 20: 14297
radiotherapy of hemangioma, safety measures for, 20: 14418
SLUGS
testing of, nondestructive method for, 20: 14711
SMOKES
polonium-210 content in cigarette, uptake and distribution in lung tissues of, 20: 14798
SNOW
effects on fallout, 20: 14746
radioactivity of Alpine glacier, dating from, 20: 14740
SODIUM
analysis for impurities using mass spectrometry, solvent extraction, and surface tension, 20: 14445(R) (MSAR-66-10)
analysis for oxygen, amalgamation method for, 20: 14432 (ANL-7123)
boiling on heating surface at free convection, (E/T), 20: 14693(T) (AD-625791)
corrosive effects on aluminum–titanium–vanadium alloys, 20: 16060(R) (ANL-7152, pp 1-49)
corrosive effects on mechanical properties of type 304 stainless steel at 1200°F, 20: 14981(R) (MSAR-66-09)
corrosive effects on chromium–molybdenum steel and type 316 stainless steel, 20: 14979 (GEAP-4835)
determination in automobile lubricants, activation, 20: 14439(R) (GA-5556)
determination in automobile tire rubber, activation, 20: 14439(R) (GA-5556)
determination in automobile paint, activation, 20: 14439(R) (GA-5556)
determination in commercial plastics, activation, 20: 14439(R) (GA-5556)
determination in cigarette tobacco, activation, 20: 14439(R) (GA-5556)
determination in glass samples, activation, 20: 14439(R) (GA-5556)
determination in hair samples in criminal cases, activation, 20: 14439(R) (GA-5556)
determination in oils and silts in water, activation, 20: 14439(R) (GA-5556)
determination in plutonium fluorides and peroxides, review on spectrographic, 20: 14464 (RFP-599)
determination in paper samples in criminal cases, activation, 20: 14439(R) (GA-5556)
determination in rice whiskey, activation, 20: 14439(R) (GA-5556)
determination in soils, activation, 20: 14439(R) (GA-5556)
determination in thumbnail clippings, activation, 20: 14439(R) (GA-5556)
determination in wood in criminal cases, activation, 20: 14439(R) (GA-5556)
determination of trace amounts of, in uranium dioxide, 20: 14494
electron transmission through foils of, plasma oscillations from, (E), 20: 15955
hyperfine spectra in x-irradiated beryl crystals, 20: 15982(T)
neutron elastic scattering at 0.8 Mev, cross sections for, (T), 20: 15770
ratio to potassium in mouse urine, prediction of x-radiation response by, 20: 14266
reactions with metals at high temperatures, 20: 15033(R) (ANL-7152, pp 87-96)
SODIUM ACID PHOSPHITES
radiolysis of, effects of pH on gamma, 20: 14600
radiolysis of, in sodium nitrate solutions, effects of pH on yields from, 20: 14601
SODIUM ALLOYS
K–Na, atomic structure of, x-ray- and neutron-diffraction studies of, 20: 15080
SODIUM AZIDES
radioinduced defects in, ESR spectral studies on, 20: 15942 (NYO-2150-11)
SODIUM BROMIDES
bromine-79 and -81 NMR spectra in, effects of bromine on, 20: 14573
NaBr–NaCl, radioinduced F-bands in, effects of Schottky defects on, 20: 14605
SODIUM CARBONATES
Na_2CO_3–H_2O, radiolysis of oxygenated solutions of, 20: 14614
SODIUM CHLORATES
radioinduced color centers in, paramagnetism of x, (E), 20: 15961
SODIUM CHLORIDES
electric conductivity in light and heavy water at 25°C, 20: 14540
electron transmission through films of, excitons and plasma oscillations in, (E), 20: 15953
$BaCl_2$–NaCl, reactions with refractory metal borides, carbides, nitrides, and oxides, 20: 14989
$CaCl_2$–NaCl, reactions with refractory metal borides, carbides, nitrides, and oxides, 20: 14989
KCl–NaCl, polarization of molybdenum during electrolysis in fused, 20: 14562
NaBr–NaCl, radioinduced F-bands in, effects of Schottky defects on, 20: 14605
SODIUM FLUOBERYLLATES
$NaBeF_3$–$NaPO_3$, phase diagrams of, 20: 14557
SODIUM FLUORIDES
reactions with xenon oxyfluorides, 20: 14523
LiF–KF–NaF, spectra of cobalt ions in, absorption, 20: 14453(R) (ORNL-3889, pp 12-14)
SODIUM FLUOSILICATES
reactions with scandium in hydrochloric acid solutions, 20: 14566
SODIUM HYDROXIDES

NaOH–H_2O, radiolysis of oxygenated systems of, 20: 14614
SODIUM IODIDES
iodine-127 NMR spectra in, effects of iodine on, 20: 14573
radioinduced luminescence of thallium-activated, spectral composition of, 20: 14611(T)
response to 150-Mev protons, ionization curves from, 20: 14891
SODIUM IONS
diffusion in silver chloride crystals, mechanism for, (E), 20: 15966
SODIUM ISOTOPES Na-22
decay of, K-capture to positron ratios for, (E), 20: 15711 (CONF-233 (Vol. 2), pp 345-58)
determination in atmospheric and precipitation samples, methods for radiochemical, 20: 14430 (AD-620219)
effects on sodium ion diffusion in silver chloride, (E), 20: 15966
energy levels of, unified model wave function for low-lying rotational, (T), 20: 15814
sorption by burned and normal skin, 20: 14255
SODIUM ISOTOPES Na-23
nitrogen-ion scattering at 16.2 and 17.7 Mev, gamma polarization from, (E), 20: 15759
proton reactions (p,p′γ) at 1281 and 1456 kev, gamma angular distribution from, 20: 15846
SODIUM ISOTOPES Na-24
determination in copra and desiccated-coconut oils, activation, 20: 14463 (PAEC(D)CH-652)
dosimetry in animals using hematological changes, 20: 14314
effects on sodium ion diffusion in silver chloride, (E), 20: 15966
energy levels of, unified model wave function for low-lying rotational, (T), 20: 15814
SODIUM NITRATES
radioinduced nitrate ions in, ESR and hfs of x, (E), 20: 15965
SODIUM OXIDES
preparation, 20: 14511(R) (ORNL-3889, pp 71-3)
SODIUM PHOSPHATES
$NaBeF_3$–$NaPO_3$, phase diagrams of, 20: 14557
SODIUM SELENITES
radioinduced paramagnetic centers in, ESR spectra from alpha, beta, gamma, and neutron, (E), 20: 15972
SODIUM SULFITES
radiosensitivity effects in mice, x, 20: 14393
SOILS
analysis in criminal cases, activation, 20: 14439(R) (GA-5556)
density determinations for, gamma-scattering-meter errors in, 20: 14837
fallout distribution in Japanese, 20: 14751
moisture content in organic, neutron method for measuring, 20: 14756
moisture meters for, composition and density effects on neutron, 20: 14771
physical properties of, radiometric probe for determining, 20: 14773
radioactive contamination of, effects on foods, 20: 14243(R) (TID-22626)
radioactivity in vicinity of AERE, cesium-137 and strontium-90, 20: 14784(R) (AERE-R-5015)
sorptive properties for cesium and strontium, effects of aluminum oxide and iron oxide on, 20: 14652
strontium-90 content in, effects on plant content of, 20: 14236
SOLAR BATTERIES
development, 20: 15305
development of solar-thermionic, 20: 15294 (CONF-640921, pp 9-45)
performance of silicon, for detection of electron bursts from plasma, 20: 15916
production of silicon, by phosphorus-ion bombardment, 20: 15302(T)
radiation effects on n-p and p-n, annealing of proton, 20: 14919(R) (N65-20653)
SOLAR FLARES
effects on ionospheric D region, v-l-f propagation for determining, 20: 15604
model, (T), 20: 15214
proton distributions from, in space, 20: 15191 (N65-20996)
radiation dose to crew and passengers during supersonic flight from, 20: 14797
radiation hazards for space flight, protection against, (T), 20: 15192 (N65-21000)
SOLAR RADIATION
conference on, 20: 15234
detection of proton, time distributions of terrestrial, (E), 20: 15233
effects of corpuscular-beam eclipse on geomagnetic micropulsations, (E), 20: 15618
effects of protons on n-p and p-n solar cells, annealing of, 20: 14919(R) (N65-20653)
effects of solar wind, on long-period geomagnetic pulsation polarization, (T), 20: 15615
effects on element abundances in solar corona and photosphere, (T), 20: 15222
effects on *Lupus erythematosus*, 20: 14309
emission of x-ray, discrimination from nuclear-detonation x rays, 20: 15603
interaction of solar plasma with magnetosphere, (T), 20: 15593
interactions of solar wind with magnetopause, (T), 20: 15620
magnetic fields in wind, (E), 20: 15215
properties of solar wind, review of, 20: 15232
properties of solar wind, models for, (T), 20: 15190 (AD-620407)
wave propagation in solar wind, (T), 20: 15216
SOLIDS
centroids and inertias for solids of revolution, computer program for, 20: 16154 (Y-1420(Rev.1))
conference on mechanical properties of, for high-temperature uses, 20: 15129
diffusion and coalescence of bubbles in, theory of, 20: 15132 (ANL-7079)
enthalpies of surface reactions on, instrumentation for, 20: 16153 (UCRL-16472)
radiation effects on crystal structure and properties of, review of, 20: 15139
SOLVENT EXTRACTION PROCESSES
use in analysis of explosives and explosive simulants, 20: 14470 (UCRL-7873)
SOLVENTS
review on, for ion exchange separation of alkaline earths, lanthanides, thorium, and uranium, 20: 14469(R) (TID-22650)
SONIC INSPECTION
equipment and methods for testing thin-walled tubes, 20: 14713
SOUND
absorption in type II superconductors, theory of, 20: 15663
SOUTH CAROLINA
meteorological analyses in Parr, Fairfield County, 20: 14732 (CVNA-172)
SOUTHWEST EXPERIMENTAL FAST OXIDE REACTOR
reactivity of, 20: 16060(R) (ANL-7152, pp 1-49)
SOVIET UNION
fallout in Vitebsk, 1962–3, 20: 14746
SPACE
radiation environment in, review of, 20: 15232
SPACE FLIGHT
conference on aeronautical sciences, 20: 14729
radiation hazards from solar proton events, 20: 15191 (N65-20996)
radiation hazards from solar flares, protection against, (T), 20: 15192 (N65-21000)
SPACE VEHICLES
conference on aeronautical sciences, 20: 14729
electric power for, development of isotopic generators for, 20: 16115
electron dosimetry for, (T), 20: 15936
materials for, evaluation of, 20: 15129
power plants for, weight of radiators for steam-cycle, 20: 14688 (N65-20692)
power plants for, development of uranium carbide–zirconium carbide fuels for thermionic, 20: 14959(R) (N65-20797)
power plants for, development of uranium carbide–zirconium carbide fuel for thermionic, 20: 14960(R) (N65-20798)
power plants for, development of uranium carbide–zirconium carbide fuel for, 20: 14961(R) (N65-20801)
power plants for, development of thermionic, 20: 14962(R) (N65-20803)
power systems for, use of gas-cooled reactors in thermionic, 20: 16110 (AD-620650)
power systems for, using Rankine cycle, 20: 16111 (N65-16315)
power systems for, performance of thermionic, (T), 20: 15292 (AD-620511)
power systems for, testing of carbide cathodes for thermionic, 20: 15046(R) (N65-15820)
propulsion systems for, mission performance of nuclear-electric, 20: 14724(65SD5322-A)
propulsion systems for, charged colloid sources for electrostatic, 20: 14725 (N65-15876)
propulsion systems for, testing of plasma-jet, 20: 14726 (NASA-CR-54746)
radiation doses in, computer programs for calculating, 20: 15930 (NP-15697(Vol.2))
re-entry trajectories for, computer programs for calculating, 20: 16113 (SC-RR-66-22)
SPAIN
radioisotope production and uses in, 1964, 20: 14926
SPARK CHAMBERS
use at electron accelerators, 20: 15187
SPECTROMETERS
beam analysis and optics in double-focusing "n½", 20: 14822(R) (RHEL/R-112, pp 99-128)
components design for double-focusing magnetic "n½", 20: 14822(R) (RHEL/R-112, pp 99-128)
deflecting and dispersion properties of electrostatic prism, for charged-particle beam analysis, (T), 20: 14868
design and use of magnetic, review on, 20: 14841

design calculations for ionization, 20: 14892
SPECTROPHOTOMETERS
data readout system for, engineering drawings for, 20: 14901
SPECTROSCOPY
development of semiquantitative visual, 20: 14457(R) (ORNL-3889, pp 36-39)
SPERM
radiation effects on bull production of, fractionated-dose whole-body x, 20: 14336
radiation effects on Drosophila, combined with acceleration, 20: 14343
radiation effects on Drosophila, combined with vibration, 20: 14343
radiosensitivity of mouse, effects of streptomycin on, 20: 14404
SPHERES
criticality of interacting arrays of, model for, (T), 20: 16034
hydrostatic equations for gaseous, in general relativity, (T), 20: 15211
neutron transport in, j_N analysis of, 20: 16022 (EUR-2627.e)
SPHEROIDS
equilibrium of uniformly rotating, general relativity effects on, (T), 20: 15627
SPINAL CORD
neonatal proton irradiation of, effects on nervous system of rats, 20: 14299
SPLEEN
effects of methyl palmitate on lipids in mouse, 20: 14241 (TID-21437)
radiation effects on enzyme activity in mitochondria of rat, x, 20: 14376
radiation effects on distribution of lymphocytes by cell size in rat, x, 20: 14318
radiation effects on pyridine nucleotidase activity of rat, x, 20: 14362
radiation effects on content of nucleated cells in, of young mice, y, 20: 14365
sulfhydryl content in, of radioresistant mice, 20: 14351
surgical removal of mouse, effects on reticulo-endothelial function, 20: 14374
SPORES
radiation effects on bacterial, review, 20: 14389
radiosensitivity of *B. cereus*, mechanism for, 20: 14263
SPRAYS
droplet evaporation in high temperature convective environments, properties of, (T), 20: 14692 (UCRL-16656)
SPUTTERING
use in surface preparation for plating, 20: 14670 (SC-R-65-997)
STACK DISPOSAL
monitoring for radioactivity in, 20: 14811
STAINLESS STEEL
compatibility with water in reactor environment, 20: 14996
corrosion by hydrofluoric acid–nitric acid solutions, effects of aluminum, iron, and thorium ions on, 20: 14982(R) (NLCO-970, pp 6.1-4)
corrosion of type 304, by water at 300°C, effects of flow rate and surface treatment on, 20: 14978 (EURAEC-1546)
corrosion of type 316, by sodium at 1200°F, 20: 14979 (GEAP-4835)
corrosion of types 416 and 430F, by aqueous mineral acid solutions, effects of uranium on, 20: 14983 (NP-15875)
diffusion of hydrogen through coatings on, effects of base metal-coating reactions on, 20: 14987
emissivity of titanate coatings on type 310, 20: 15057(R) (PWA-2750)
mechanical properties of type 304, effects of high-carbon sodium at 1200°F on, 20: 14981(R) (MSAR-66-09)
mechanical properties of type 304, effects of high-oxygen sodium at 1200°F on, 20: 14981(R) (MSAR-66-09)
oxidation of types 304, 321, and 410 by steam at 400 to 600°C, effects of surface work-hardening on, 20: 14977(R) (EURAEC-1500)
physical properties of, equipment and methods for measuring, 20: 14719
radiation embrittlement of austenitic, thermal-neutron, 20: 15141
reaction of 304, with sodium, high-temperature, 20: 15033(R) (ANL-7152, pp 87-96)
reactions of type 316L, with plutonia, 20: 14965(R) (NUMEC-3524-12)
reactions with water during reactor accidents, 20: 16019(R) (BMI-X-10154)
testing cladding of, nondestructive methods for, 20: 14711
testing of cladding tubes of, automatic device for ultrasonic, 20: 14717
welding of tube sheets of, to Zircaloy-2 tubes, 20: 15019
B–stainless steel, radiation effects on poison elements of, in-pile, 20: 16089(R) (WAPD-MRP-114)
stainless steel–UO_2, sintering of, 20: 14965(R) (NUMEC-3524-12)
STANDARDS
use of monomolecular films as beta sources, 20: 16143 (AD-620276)
STARS
adiabatic invariants of, in galactic field, (T), 20: 14950(R) (COO-614-41)
collapse of, exterior metric for, (T), 20: 15228
cooling of neutron, effects of neutrino emission on, (T), 20: 15201
core motion in, overshooting in convective, (T), 20: 15208
deuterium abundance in, upper limits for, (E), 20: 15197
electron Compton scattering in semidegenerate region of, opacity from, (T), 20: 15209
electron degeneracy in, pair production effects on, (T), 20: 15229
element production in, review of processes for, 20: 15231
equation of state for interior of, numerical evaluation of, (T), 20: 15213
evolution and structure of helium, (T), 20: 15195
evolution from main sequence through core-helium burning, (T), 20: 15207
evolution of extended radio sources, (T), 20: 15200
evolution of helium, internal, (T), 20: 15202
evolution of hydrogen ion region in, (T), 20: 15199
evolution of O, during helium burning, (T), 20: 15218
evolution of population II, carbon core growth and shell helium flashes in, (T), 20: 15227
evolution of rotating nonmagnetic, pre-main-sequence, (T), 20: 15219
evolution of, model envelopes for superadiabatic layers in, (T), 20: 15196
gravitational collapse of, (T), 20: 15230
hydromagnetic wave propagation in supernova, equations for, (T), 20: 15198
hydrostatic equations for degenerate and neutron, in general relativity, (T), 20: 15211
models for carbon-burning, neutrino energy-loss effects on, (T), 20: 15194
nuclear reactions in, rates of nonresonant, (T), 20: 15221
origin of binary, fission theory for, 20: 15219
shock propagation in exponentially decreasing atmospheres of, (T), 20: 15217
spectra and location of x-ray sources, (E), 20: 15220
stability and wave propagation in corona and wind of, (T), 20: 15216
stability of, general relativity for nonradial and radial, (T), 20: 15210
STATISTICS
binomial sampling in, tables for, 20: 16150 (ORNL-2909)
formalism for scaled pulses, (T), 20: 14890
STEAM
corrosive effects on zirconium-base alloys, effects of nitrogen impurity content on, 20: 14980(R) (GEAP-5065)
corrosive effects on zirconium-base alloys, effects of metallurgical processing variables on, 20: 14980(R) (GEAP-5065)
reactions with stainless steels at 400 to 600°C, effects of surface work-hardening on, 20: 14977(R) (EURAEC-1500)
steam-water, burnout in flows with axially nonuniform heat flux, (E), 20: 14696
STEARIC ACID
determination in commercial coconut oils, gas chromatographic, 20: 14463 (PAEC(D)CH-652)
STEEL
embrittlement by plastic fatigue of Ducol W30 and Soudotenax 56, 20: 15039 (EURAEC-1475)
gamma dose buildup factors for, 20: 15933(T) (ORNL-tr-1060)
gamma transmission through pipes of, Monte Carlo calculation of, 20: 16114
production by open-hearth process, use of radioisotopes for studying, 20: 14939
radiation effects on wear resistance of, fast-neutron, 20: 15140
separation of alkaline earths, rare earths, thorium, and uranium from, by ion exchange, 20: 14469(R) (TID-22650)
testing pressure-vessel, nondestructive methods for, 20: 14709
wear against SAP and steels, 20: 15998 (EUR-2117.n)
STERILIZATION
goals and standards for, 20: 14234
STEROIDS
radioinduced decomposition of tritiated cortexolone, effects of molecular structure on, 20: 14578 (EUR-2435.f)
radiosensitivity effects of methandrostenolon on rats, 20: 14402
STIBINE, TRIMETHYL-
decomposition in ion source of mass spectrometer, mechanism of, 20: 14584(R) (TID-22444)
STILBENE
radiation effects on *trans-cis* isomerization of, in methanol solutions, 20: 14579(R) (NYO-2383-15)
scintillation intensity in crystals of, time dependence of, (T), 20: 14615
STRATOSPHERE
fallout transport from northern to southern hemisphere in 1961 and 62, 20: 14749
STREPTOMYCIN
radiosensitivity effects on mouse sperm, 20: 14404
radiosensitivity effects in *Staphylococcus aureus*, y, 20: 14313
STRESS ANALYSIS
of radioisotope transport containers, from internal pressures, 20: 14667 (ORNL-TM-1312(Vol.1))
STRONTIUM
content in rat diet, effects on calcium-47 and strontium-85 metabolism, 20: 14251
content in red-colored Paleozoic deposits in Northern Tien Shan,

20: 14780(T) (AEC-tr-6579)
determination by spectroscopy using plasma jet, 20: 14492
determination in dust samples by microchemical methods and autoradiography, 20: 14472
determination in plutonium fluorides and peroxides, review on spectrographic, 20: 14464 (RFP-597)
effects of impurity of, on radioinduced F centers in potassium chloride crystals, (E), 20: 15980(T)
effects on proton-induced vacancies in potassium bromide doped with, (E), 20: 15977(T)
energy level transitions in, Coster-Kronig, (T), 20: 15238 (CONF-233 (Vol.3), pp 398-418)
energy level widths for, K, (T), 20: 15239 (CONF-233(Vol.3), pp 419-39)
metabolism in bone of rats, effects of pyridoxal on, 20: 14246
separation from fission products, review on method for, 20: 14436 (BNWL-SA-504)
sorption by soils and clay minerals, effects of aluminum oxide and iron oxide on, 20: 14652
transport across, intestinal membranes, tracer study, 20: 14243(R) (TID-22626)
STRONTIUM CHLORIDES
light reflection from, far-infrared vibration mode from, (E), 20: 15958
STRONTIUM FLUORIDES
ion localized vibrations in, spectra of deuterium and hydrogen, 20: 15969
STRONTIUM ISOTOPES Sr-85
chelates of, effects on rare earth excretion, 20: 14256
exchange between strontium sulfate crystals and solutions, 20: 14572
metabolism by rats, effects of dietary strontium on, 20: 14251
placental transfer in mice, 20: 14244
uptake by aortic wall of rats, 20: 14252
STRONTIUM ISOTOPES Sr-89
content in Lake Huron and Ottawa River, 20: 14738 (NP-15853, pp 21-33)
determination in atmospheric and precipitation samples, methods for radiochemical, 20: 14430 (AD-620219)
STRONTIUM ISOTOPES Sr-90
beta emission by, scintillation counter for measuring, 20: 14874
chelates of, effects on rare earth excretion, 20: 14256
content in Canadian wheat, 1964, 20: 14736 (NP-15853, pp 3-7)
content in Canadian fallout, October 1965, 20: 14737 (NP-15853, pp 8-20)
content in foods, 1963-5, 20: 14243(R) (TID-22626)
content in grass, herbage, milk, and soils in vicinity of AERE, 20: 14784(R) (AERE-R-5015)
content in Indo-Antarctic Ocean, 1962, 20: 14749
content in Lake Huron and Ottawa River, 20: 14738 (NP-15853, pp 21-33)
content in soils, 20: 14236
content in spent power reactor fuels, evaluation of, 20: 14435 (BNWL-SA-503)
determination in atmospheric and precipitation samples, methods for radiochemical, 20: 14430 (AD-620219)
determination in urine, 20: 14243(R) (TID-22626)
disposal by in-pile activation to stable or short-lived isotopes, (T), 20: 16132 (BNL-8558)
effects on auditory structures in rabbits, 20: 14316
leaching from alumina–phosphate glass prepared from calcined alumina waste, 20: 16133 (IDO-14672)
metabolism in dogs, effects of age on, 20: 14243(R) (TID-22626)
purification by solvent extraction using bis(2-ethylhexyl) phosphate, 20: 14641 (RL-SA-59)
separation from Purex waste solutions by lead carrier sulfate precipitation, 20: 14641 (RL-SA-59)
separation from wastes, engineering drawings of WAFRAX facilities for, 20: 16139
sorption and storage on aluminum silicate zeolites, 20: 14466 (RL-SA-58)
sorption from radioactive wastes by ion exchange, 20: 14434 (BNWL-180)
uptake from soils by plants, 20: 14236
STRONTIUM SULFATES
strontium-85 exchange between crystals and solutions, 20: 14572
sulfur-35 exchange between crystals and solutions, 20: 14572
STRUCTURAL PANELS
design of laminated, for radiation shielding, 20: 14680(P)
design of sandwich-type, for radiation and fire protection, 20: 14682(P)
STRUCTURES
conference on high-temperature, 20: 15129
gamma dose rates in cylindrical and rectangular steel, from fallout, 20: 15931 (TO-B-65-27)
STYRENE
radioinduced graft polymerization with polyethylene, radical lifetime in gamma, 20: 14624
radioinduced polymerization with polyethylene and polyvinylchloride, 20: 14618
STYRENE POLYMERS
pyrolysis products from, chromatographic determination of, 20: 14455(R) (ORNL-3889, pp 25-32)
SUBMARINE REACTORS
design, 20: 16117(P)
SUCCINAMIC ACID, *N,N*-DIMETHYL-
penetration of carbon-14-labeled, through cuticular membranes, 20: 16146 (COO-888-39)
SUCCINATES
determination of carbon-14-labeled, by liquid scintillation counting on paper chromatograms, 20: 14479
SUCROSE
determination of carbon-14-labeled, by liquid scintillation counting on paper chromatograms, 20: 14479
SULFATE IONS
effects on valence states of cerium, iron, and uranium ions, 20: 14574
SULFATES
radiation effects on uptake by aortic mucopolysaccharides in rabbits, tracer study, 20: 14295
SULFUR
determination in automobile tire rubber, activation, 20: 14439(R) (GA-5556)
determination of trace amounts of, in iron, activation, 20: 14471
effects on stainless steel corrosion with and without uranium additions by aqueous mineral acid solutions, 20: 14983 (NP-15875)
energy level widths for, K, (T), 20: 15239 (CONF-233(Vol.3), pp 419-39)
meson (μ^-) capture by, angular distributions from, (E), 20: 15720 (JINR-E-2516)
meson (π^-) reactions (π^-,γ), energy spectra and yields from, (E), 20: 15794
radioinduced reactions with polyethylene and chlorine, 20: 14621
SULFUR DIOXIDES
vibrational potential function of bent molecules of, third-order, 20: 14559
SULFUR ISOTOPES S-32
neutron elastic and inelastic scattering at 2.45 to 5.80 Mev, cross sections for, (E), 20: 15811
neutron reactions (n,p) with, in cysteic acid, cysteine, and cystine, recoil atom retention in products from, 20: 14584(R) (TID-22444)
neutron reactions (n,2n) at 12 to 18 Mev, cross sections for, (E), 20: 15863
nuclear properties in shell model, 20: 15730(R) (RHEL/R-112, pp 67-98)
SULFUR ISOTOPES S-33
neutron reactions (n,p), cross sections for, (E), 20: 14461(R) (ORNL-3889, (pp 48-70)
SULFUR ISOTOPES S-34
neutron reactions (n,γ) with, in cysteic acid, cysteine, and cystine, sulfur-35 recoil atom retention in products in, 20: 14584(R) (TID-22444)
SULFUR ISOTOPES S-35
decay of, continuous spectrum from internal bremsstrahlung in, (T), 20: 15801
determination in atmospheric and precipitation samples, methods for radiochemical, 20: 14430 (AD-620219)
exchange between barium sulfate crystals and solutions, 20: 14572
exchange between strontium sulfate crystals and solutions, 20: 14572
recoil chemistry in neutron reactions (n,γ) in cysteic acid, cysteine, and cystine, 20: 14584(R) (TID-22444)
SULFURIC ACID
corrosive effects on types 416 and 430F stainless steels, effects of uranium on, 20: 14983 (NP-15875)
corrosive effects on niobium-base alloys, effects of alloy composition on, 20: 14997
effects on formaldehyde and hydrogen peroxide yields in gamma radiolysis of serated methanol, 20: 14579(R) (NYO-2383-15)
effects on radiolysis yields in deaerated methanol, 20: 14579(R) (NYO-2383-15)
leaching nuclear test debris in copper ores, 20: 14662(R) (ORNL-TM-1394)
H_2SO_4–H_2O, radiolysis of oxygenated solutions of, 20: 14614
SUN
core motion in, overshooting in convective, (T), 20: 15208
eclipse effects on geomagnetic micropulsations, (E), 20: 15617
eclipse effects on geomagnetic micropulsations, (E), 20: 15618
element abundances in corona and photosphere, solar wind effects on, (T), 20: 15222
magnetic field of, evolution of, (T), 20: 15223
magnetic fields of, interplanetary space extension of photospheric, (E), 20: 15215
shock propagation in exponentially decreasing atmospheres of, (T), 20: 15217
spectra of, conference on, 20: 15234
stability and wave propagation in corona and wind of, (T), 20: 15216
x-ray images of, using grazing incidence optics, 20: 15203
SUPERCONDUCTIVITY

properties of ferromagnetic alloy, (T), 20: 15648
theory of, with pairs in triplet of spins, 20: 15644
SUPERCONDUCTORS
conductivity in, electric and thermal, (E), 20: 15656
critical currents in tin, effects of magnetic field and temperature on, 20: 15662
current distribution in thin film arrays of, (T), 20: 15643 (NASA-TN-D-3293)
electron tunneling in thick films of indium, geometrical resonances in, (E/T), 20: 15650
electron tunneling in junctions of lead, subharmonic structure in, (E/T), 20: 15651
electron tunneling excitation spectra in laminates of normal metals with, (T), 20: 15653
energy gap in aluminum, microwave studies of, (E), 20: 15658
heat absorption and emission by type II, Peltier effect in, (E), 20: 15649
phonon effects in, 20: 15664
preparation by rapid quenching of molten alloys, 20: 15020
sound attenuation in type II, formula for, 20: 15663
structure of type II, suggested experiments on, 20: 15663
theory of nonhomogeneous, 20: 15655
thermodynamic properties of alloy, approximation method for, 20: 15654
ultrasonic attenuation in lead, amplitude dependence of, 20: 15657
ultrasonic wave attenuation in tin, frequency and temperature dependence of, (E/T), 20: 15659
SUPERHEATERS (NUCLEAR)
design, 20: 16106(P)
design of breeding, for boiling reactors, 20: 16105(P)
SURFACE WATERS
tritium content, 20: 14744
SURFACES
centroids and inertias for surfaces of revolution, computer program for, 20: 16154 (Y-1420(Rev.1))
enthalpies of reactions on solid, instrumentation for, 20: 16153 (UCRL-16472)
SURGERY
effects of, combined with radium and x radiation on cervical carcinomas, complications from, 20: 14377
effects of, combined with radium and x radiation on cervical carcinomas, 20: 14409
effects on cervical carcinomas, 20: 14409
effects on wound healing after radical neck dissection, 20: 14303
SWEDEN
personnel monitoring at AB Atomenergi, 1964, 20: 14782(R) (AE-211)
SWIMMING POOL REACTORS
description of ASTRA, 20: 16127
SWINE
radioinduced skeletal anomalies in, exposed *in utero*, γ, 20: 14337
SYNCHROCYCLOTRONS
beam currents and space charge limit in, improvements for, 20: 15182
SYNCHROTRONS
beam extraction from Frascati electron, (E/T), 20: 15159 (LNF-65/36)
magnets for CERN, excitation by short pulses, 20: 15157 (CERN-66-1)
storage ring for CERN, design of intersecting, 20: 15158 (CERN-542)
SYSTEMS FOR NUCLEAR AUXILIARY POWER
development of, review, 20: 16115
fuel particles from, biological effects of ingestion or inhalation of, 20: 14785 (BNWL-182)
re-entry trajectories for, computer programs for calculating, 20: 16113 (SC-RR-66-22)

T

TANTALUM
bremsstrahlung reactions (γ,n) at 8 to 16 Mev, spectra from, (E), 20: 15723 (MIT-2098-162)
bremsstrahlung reactions (γ,n) with, neutron emission in, (E), 20: 15724 (MIT-2098-224)
coating by iridium, protective effects of, 20: 15004(R) (N65-20790)
creep and rupture of, numerical methods for analysis of, 20: 15041 (GEMP-397)
diffusion in liquid niobium at melting point, coefficient for, 20: 14969
dislocation motion in, impurity and intrinsic barriers to, 20: 15040(R) (GA-6721)
embrittlement by hydrogen, effects of nitrogen and oxygen on, 20: 15130
magnetic susceptibility, 20: 15045 (N65-15634)
production from tin slags, 20: 14956
proton reactions (p,n) at 30 to 50 Mev, distributions from, 20: 15729(R) (RHEL/R-112, pp 37-66)
reactions with hydrogen sulfide at 1000 to 1400°C, 20: 14554
reactions with refractory metal borides, carbides, nitrides, and oxides, 20: 14989
reactions with sodium, high-temperature, 20: 15033(R) (ANL-7152, pp 87-96)
slip in single-crystal, rate controlling mechanism for, 20: 15947 (UCRL-16645)
work function of, effects of cesium-fluoride vapor on, 20: 15297 (CONF-640921, pp 101-9)
TANTALUM ALLOYS
Al–Ta, fabrication of sintered bodies of, 20: 15026(P)
Nb–Ta, corrosion by hydrochloric, phosphoric, and sulfuric acids, effects of alloy composition on, 20: 14997
Nb–Ta, hardness, 20: 15073
Nb–Ta, segregation of tantalum by controlled solidification of, effects of titanium additions on, 20: 14969
Nb–Ta–Sn, superconductivity of fused, 20: 15123
TANTALUM BORIDES
abrasive properties, 20: 15109
reactions with carbon, 20: 14555
reactions with copper and nickel mattes, slags, molten salts, and refractory metals, 20: 14989
TANTALUM CARBIDES
abrasive properties, 20: 15109
magnetic susceptibility, 20: 15045 (N65-15624)
preparation of spherical particles of, procedure and apparatus for, 20: 14971(P)
reactions with copper and nickel mattes, slags, molten salts, and refractory metals, 20: 14989
thermodynamic properties of, at high temperatures, 20: 15052 (NP-15880)
TaC–UC, properties for cathodes in thermionic space power plants, 20: 15046(R) (N65-15820)
TANTALUM ISOTOPES Ta-179
energy level transitions in, delayed E1, (T), 20: 15765
energy level transition probabilities in, pairing correlations in E1, (T), 20: 15766
energy level transitions in, anomalous E1, (E), 20: 15702 (CONF-233 (Vol.2), pp 142-7)
TANTALUM ISOTOPES Ta-181
energy level transitions in, delayed E1, (T), 20: 15765
energy level transition probabilities in, pairing correlations in E1, (T), 20: 15766
TANTALUM OXIDES
preparation of spherical particles of, procedure and apparatus for, 20: 14971(P)
sorptive properties for chloride and potassium ions, effects of pH on, 20: 14651
TANTALUM SULFIDES
preparation and properties, 20: 14554
TANTALUM SYSTEMS
Al–C–Co–Ta, phase studies, 20: 15103
Al–C–Cr–Ta, phase studies, 20: 15103
Al–C–Cu–Ta, phase studies, 20: 15103
Al–C–Fe–Ta, phase studies, 20: 15103
Al–C–Mn–Ta, phase studies, 20: 15103
Al–C–Ni–Ta, phase studies, 20: 15103
Al–C–Ta, phase studies, 20: 15103
Al–C–Ta–V, phase studies, 20: 15103
Al–C–Ta–Zn, phase studies, 20: 15103
C–Cr–Ta, phase studies, 20: 15108
C–Nb–Ta–Zr, heat treatment of, 20: 14972(P)
C–Ta, magnetic susceptibility, 20: 15045 (N65-15624)
Nb–N–Ta–Zr, heat treatment of, 20: 14972(P)
Nb–O–Ta–Zr, heat treatment of, 20: 14972(P)
Ta–UP, compatibility, 20: 15032(R) (ANL-7152, pp 50-72)
TASTE
radiation effects on meat, γ, 20: 14930 (NP-15676)
radiation effects on meat, γ, 20: 14931 (NP-15677)
TECHNETIUM
determination in solutions, x-ray-fluorescence, 20: 14497
energy level transitions in, Coster-Kronig, (T), 20: 15238 (CONF-233 (Vol.3), pp 398-418)
energy level widths for, K, (T), 20: 15239 (CONF-233(Vol.3), pp 419-39)
rolling of, hot, 20: 15035(R) (BNWL-196)
separation from fission products, review on method for, 20: 14436 (BNWL-SA-504)
TECHNETIUM ALLOYS
Tc–W, density, effects of composition on, 20: 15035(R) (BNWL-196)
Tc–W, microstructure, effects of composition on, 20: 15035(R) (BNWL-196)
TECHNETIUM ISOTOPES Tc-99
burnup calculations for, in reactor fuels, 20: 16061(R) (BAW-296)
content in spent power reactor fuels, evaluation of, 20: 14435 (BNWL-SA-503)
determination, activation, 20: 14661(R) (ORNL-3889, pp 48-70)
neutron reactions at 14 Mev, activation cross sections for, (E), 20: 14461(R) (ORNL-3889, pp 48-70)

separation from Purex alkaline waste solutions by ion exchange, 20: 14641 (RL-SA-59)
use as clinical tracer, 20: 14423

TEETH
radiation effects on rat, head and whole-body exposure x, 20: 14322
radiation effects on structure of, y, 20: 14323
radiography of human, hazards from x, 20: 14419
radium content in animal, 20: 14254

TEKTITES
lead isotope distribution in impact crater, 20: 14458(R) (ORNL-3889, pp 39-43)

TELEVISION EQUIPMENT
design and performance for monitoring cobalt-60 therapy, 20: 14407

TELLURIUM
effects on spectrofluorimetric determination of scandium, 20: 14476
neutron elastic scattering at 0.8 Mev, cross sections for, (T), 20: 15770
separation from antimony by solvent extraction on fine-grained carrier, 20: 14656

TELLURIUM ISOTOPES Te-115
beta spectra, (E), 20: 15753
energy levels of, parity and spin of, (E), 20: 15753
isomeric transitions in, multipolarity of, (E), 20: 15753

TELLURIUM ISOTOPES Te-119
decay of ground-state and isomeric, beta and gamma spectra from, (E), 20: 15762

TELLURIUM ISOTOPES Te-122
energy levels of, mean life of 564-kev, (E), 20: 15857

TELLURIUM ISOTOPES Te-123
proton reactions, production of iodine-132 in, (E), 20: 14461(R) (ORNL-3889, pp 48-70)

TELLURIUM ISOTOPES Te-125
proton reactions (p,n) at 2.3 to 11.0 Mev, excitation of isobaric analog states in, (E), 20: 15704

TELLURIUM ISOTOPES Te-126
proton reactions (p,n) at 2.3 to 11.0 Mev, excitation of isobaric analog states in, (E), 20: 15804

TELLURIUM ISOTOPES Te-130
neutron reactions (n,γ) with, isomeric cross-section ratios in, (E), 20: 15777
proton reactions (p,n) at 2.3 to 11.0 Mev, excitation of isobaric analog states in, (E), 20: 15804

TELLURIUM ISOTOPES Te-131
production of isomeric, cross sections for neutron-capture, (E), 20: 15777

TEMPERATURE
control and measurement at 300 to 94°K, equipment for, 20: 15660
effects on critical currents in superconducting tin films, 20: 15662
effects on incompatibility in *Oenothera organensis*, 20: 14382
effects on oxidation of cyclohexane by gamma radiation, 20: 14625
effects on radiosensitizing effects of vitamin K_5, 20: 14395
Pseudomonas sensitivity to freezing, effects of oxygen on, 20: 14394
radiosensitivity effects in Pseudomonas, 20: 14394
radiosensitivity effects of K_5 on Salmonellae infections in eggs, 20: 14395
radiosensitivity effects of storage, on growth of *S. aureus* in crab meat, 20: 14936

TERBIUM
electron band structure, (E), 20: 15106
Hall effect in, effects of temperature on, 20: 15071
hyperfine structure of low-lying levels of $4f^85d6s^2$ configuration of, (E), 20: 15254

TERBIUM ALLOYS
Fe–Tb, preparation and structure, 20: 15110
Mn–Tb, preparation and structure, 20: 15110
Tb–Y, electric conductivity of dilute, at low temperatures, 20: 15098

TERBIUM ISOTOPES
deuteron reactions at 15 Mev, isomeric states from, (E), 20: 15856
internal conversion probabilities in, reduced M and N E0, (T), 20: 15771

TERBIUM ISOTOPES Tb-159
energy level transition probabilities in, pairing correlations in E1, (T), 20: 15766
energy level transitions in, delayed E-1, (T), 20: 15765
nuclear moment of, M2, (E), 20: 15254

TEREPHTHALIC ACID, ETHYLENE POLYMER ESTERS
radiation effects on prostheses of, x, 20: 14344
radiation effects on prostheses of, x, 20: 14345
radiolysis of, ESR spectra of free radicals from gamma, 20: 14606

TERPENES
alpha reactions with p-, scintillation decay time from, 20: 15989

TERPHENYL
determination in working environments, colorimetric and uv spectrophotometric methods for, 20: 14467 (RT/PROT(64)-20)

TESTOSTERONE
radioinduced decomposition of tritiated, effects of molecular structure on, 20: 14578 (EUR-2435.f)

1,3,5,7-TETRAZOCINE, OCTAHYDRO-1,3,5,7-TETRANITRO-
determination in explosives, methods for, 20: 14470 (UCRL-7873)

THALLIUM
bremsstrahlung reactions (γ,n) at 8 to 16 Mev, spectra from, (E), 20: 15723 (MIT-2098-162)
bremsstrahlung reactions (γ,n) with, neutron emission in, (E), 20: 15724 (MIT-2098-224)

THALLIUM BROMIDES
effects on radioinduced isomerization of α-phenylcinnamic acid, 20: 14596
effects on radioinduced isomerization of dimethyl maleate, 20: 14596

THALLIUM ISOTOPES
internal conversion probabilities in, reduced M and N E0, (T), 20: 15771

THALLIUM ISOTOPES Tl-204
decay of, electron capture ratios in, (E), 20: 15796
performance of bremsstrahlung sources of, for wire cross-section measurements, 20: 14838

THERMAL CAPACITY
measurement at 0.24 to 20°K, equipment for, 20: 15061 (UCRL-11580)

THERMAL DIFFUSION
column transport coefficient calculations, design of apparatus of, 20: 14444(R) (MLM-1268)

THERMAL PROPERTIES
measurement at low temperatures, equipment for, 20: 15660

THERMAL RADIATION
effects on galactic formation, 20: 15204

THERMAL RADIATION SOURCES
development using cobalt-60, 20: 14945 (CONF-660305-14)

THERMAL REACTORS
design of boiling-water, with superheated breeder blanket, 20: 16105(P)
neutron diffusion theory for, control rod representation of, (T), 20: 16090 (WAPD-T-1841)

THERMIONIC CELLS
current-voltage characteristics of cesium, at 860 to 1320°K, 20: 15301
development, 20: 15294 (CONF-640921, pp 9-45)
development for space power plants, 20: 14962(R) (N65-20803)
development of, conference on, 20: 15293 (CONF-640921)
efficiency of, effects of cesium-fluoride vapor on, (E), 20: 15297 (CONF-640921, pp 101-9)
electrodes for, performance of metal-impregnated graphite as, 20: 15296 (CONF-640921, pp 81-99)
electron distributions in, Langmuir-Child analysis of, (T), 20: 15295 (CONF-640921, pp 47-77)
electron drift velocity measurement in gas-filled, 20: 15303
performance, (T), 20: 15299 (NASA-TN-D-3324)
performance of power systems of, (T), 20: 15292 (AD-620511)
properties of cesium, impurity effects on, 20: 15298 (FEI-22)
testing of carbide cathodes for space power systems, 20: 15046(R) (N65-15820)
testing of cesium, 20: 14960(R) (N65-20798)
testing of cesium, for space power plants, 20: 14959(R) (N65-20797)

THERMOCOUPLES
electric contact design for, 20: 14842(P)

THERMODYNAMIC PROPERTIES
equilibrium in nongray case, radiative transfer equation solutions for, (T), 20: 15572

THERMODYNAMICS
calculations for reactions on solid surfaces, instrumentation for, 20: 16153 (UCRL-16472)

THERMOELECTRIC CELLS
development of, conference on, 20: 15293 (CONF-640921)
electron distributions in, Langmuir-Child analysis of, (T), 20: 15292 (CONF-640921, pp 47-77)

THERMOELECTRIC PROPERTIES
calculation of miscibility of vanadium with other elements, 20: 14538

THERMOLUMINESCENT DETECTORS
performance and properties, 20: 14907
response of lithium–fluoride, to electrons and gamma and x radiation, 20: 14887
response of lithium–fluoride, to electrons and gamma and x radiation, 20: 14888
shield design for, 20: 14914(P)

THERMOMETERS
efficiency of thin film resistance, for measuring reactions on solid surfaces, 20: 16153 (UCRL-16472)

THERMOMETRY
gage calibration system for helium vapor pressure, 20: 14444(R) (MLM-1268)

THERMONUCLEAR EXPLOSIONS
effects on military personnel, time factors in, 20: 14287 (AD-626996)
fallout in Indo-Antarctic Ocean from 1961 Soviet, 20: 14749

THERMONUCLEAR REACTIONS

neutron-neutron interactions in triton-triton, (T), 20: 15733 (UCRL-7769)
THERMONUCLEAR REACTORS
development of, summary, 20: 15886(R) (UCRL-14285)
THERMOPILES
efficiency of, for measuring enthalpies of reactions on solid surfaces, 20: 16153 (UCRL-16472)
THICKNESS GAGES
automation of ultrasonic, for measurements on tubes, 20: 14718
design for thin films, 20: 14819 (RFP-602)
design of beta, for measurements on multi-finned SAP tubing, 20: 14712
design of semi-automatic radiometric, for measurements on long straight tubes, 20: 14816 (EUR-2512.n)
development of radiometric, for cross-section measurements on wires, 20: 14838
performance of beta-backscattering, zinc coating measurement, 20: 14839
use of radioisotope, review of industrial, 20: 14835
THIOCYANATES
methyl-, formation of multiply charged ions in decomposition of, in ion source, 20: 14584(R) (TID-22444)
THIOCYANIC ACID
reactions with zirconium at 25°C, 20: 14995
THOREX PROCESS
radiation effects on TBP during short decay runs in, dose calculations in, 20: 14580 (ORNL-2764)
THORIUM
content in animal teeth and thyroids, 20: 14254
content in carbonate rocks, 20: 14752
determination in monazites, 20: 14491
determination in methanol–mineral acid media using azo dyes, spectrophotometric, 20: 14469(R) (TID-22650)
determination of terrestrial abundance of, neutrino detection for, (T), 20: 14750
determination using Chrome Azurol S, spectrophotometric, 20: 14485
electric charge of sorbed, in tungsten, (E), 20: 15985(T)
energy level transitions in, Coster-Kronig, (T), 20: 15238 (CONF-233 (Vol.3), pp 398-418)
enthalpy of alpha- and beta-phase and molten, 20: 14550
incorporation in nuclear emulsions, estimation of maximum, 20: 14877
purification by solvent extraction using alkyl phosphoorganic compounds, 20: 14448(R) (NLCO-970, pp 1.1-22)
separation by ion exchange in mixed and non-aqueous media, review on, 20: 14469(R) (TID-22650)
separation from graphite-base reactor fuels, 20: 14640 (ORNL-TM-1411)
separation from rare earths and uranium by solvent extraction using alkyl phosphonates, 20: 14448(R) (NLCO-970, pp 1.1-22)
solvent distribution between dipentyl pentylphosphonate or TBP and thorium nitrate, 20: 14448(R) (NLCO-970, pp 1.1-22)
THORIUM CARBIDES
preparation of spherical particles of, procedure and apparatus for, 20: 14971(P)
ThC_2–UC_2, aqueous processing of graphite- and silicon dicarbide-coated fuel elements of, 20: 14638 (NP-15753)
THORIUM CHLORIDES
use of radioactive, in determination of phase diagrams in sodium beryllium fluoride–sodium phosphate system, 20: 14557
THORIUM COMPOUNDS
analysis for calcium, lithium, and potassium, spectrochemical methods for, 20: 14443(R) (MCW-1493, pp 27-30)
THORIUM(IV) FLUORIDES
BeF_2–LiF–ThF_4–UF_4–ZrF_4, spectra of irradiated, absorption and reflectance, 20: 14453(R) (ORNL-3889, pp 12-14)
THORIUM IONS
effects on corrosion of type 304L stainless steel by hydrofluoric acid–nitric acid solutions, 20: 14982(R) (NLCO-970, pp 6.1-4)
THORIUM ISOTOPES Th-226
alpha decay of, charge and energy distributions of recoils from, (E), 20: 15822
THORIUM ISOTOPES Th-232
deuteron fission of, fragment mass and energy distributions from, (E), 20: 15840
THORIUM NITRATE COMPLEXES
with TBP, chemical bonding in, Roman polarization measurements of, 20: 14529
THORIUM NITRATES
dipentyl pentylphosphonate–$Th(NO_3)_4$, thorium distribution in, 20: 14448(R) (NLCO-970, pp 1.1-22)
$Th(NO_3)_4$–TBP, thorium distribution in, 20: 14448(R) (NLCO-970, pp 1.1-22)
THORIUM OXIDES
effects on crystal growth in optical glasses, 20: 15075
preparation of spherical particles of, procedure and apparatus for, 20: 14971(P)
sorptive properties for chloride and potassium ions, effects of pH on, 20: 14651
THORIUM(IV) OXIDES
analysis for nitrates, infrared spectroscopic, 20: 14468 (TID-22505)
grain size of crystalline, determination of, by x-ray diffraction, 20: 15044(R) (MCW-1493, pp 15-25)
neutron Doppler coefficient for, (E), 20: 15732 (TID-21654)
reactions with copper and nickel mattes, slags, molten salts, and refractory metals, 20: 14989
sintering of sol-gel, mechanisms of, 20: 15009 (TID-22491)
PuO_2–ThO_2, preparation of compacts of, 20: 15025(P)
ThO_2–UO_2, analysis for uranium, polarographic, 20: 14455(R) (ORNL-3889, pp 25-32)
ThO_2–UO_2, machine design for receiving, blending, and transferring powdered, 20: 14668 (ORNL-TM-1397)
Th–ThO_2, development of cermets of, 20: 14968(R) (USBM-RC-1220)
THORIUM SYSTEMS
C–O–Th, vapor pressure of carbon monoxide in sol-gel fuels of, 20: 14512 (ORNL-TM-1418)
Th–ThO_2, development of cermets of, 20: 14968(R) (USBM-RC-1220)
THRESHOLD DETECTORS
performance for neutron spectroscopy at accelerators, 20: 15175 (UCRL-16312)
THULIUM
Hall effect in, effects of temperature on, 20: 15071
THULIUM ALLOYS
Co–Tm, cobalt ion EPR in intermetallic compounds of, 20: 15963
Fe–Tm, preparation and structure, 20: 15110
Mn–Tm, preparation and structure, 20: 15110
THULIUM ETHYL SULFATES
crystal structure of, EPR study of defects in, 20: 14547
THULIUM ISOTOPES
deuteron reactions at 15 Mev, isomeric states from, (E), 20: 15856
THULIUM ISOTOPES Tm-170
beta transitions in, matrix elements for first-forbidden, (E), 20: 15824
THULIUM ISOTOPES Tm-171
energy level transitions in, conversion electrons from E1, (E), 20: 15703 (CONF-233(Vol.2), pp 148-57)
THULIUM NITRIDES
preparation, 20: 14511(R) (ORNL-3889, pp 71-3)
THULIUM PHOSPHIDES
preparation, 20: 14511(R) (ORNL-3889, pp 71-3)
THYMIDINE
radiation effects on uptake of tritium-labeled-, by rat kidney cells, x, 20: 14258 (AD-627569)
THYMINE
radioinduction in DNA, effects of amino acids on uv, 20: 14272
THYMUS GLAND
effects of radiomimetic drugs on DNAse activity in rat, 20: 14311
effects of radiomimetic drugs on DNA content in rat, 20: 14311
radiation effects on enzyme activity in mitochondria of rat, x, 20: 14376
radiation effects on DNAse activity in rat, x, 20: 14311
radiation effects on content of DNA in rat, x, 20: 14311
radiation effects on distribution of lymphocytes by cell size in rat, x, 20: 14318
radiation effects on content of nucleated cells in, of young mice, y, 20: 14365
THYROID GLAND
iodine-131 uptake by guinea pig, 20: 14245
isothiocyanate uptake by guinea pig, tracer study, 20: 14245
pathology and physiology in rat, Hamolsky's test for, 20: 14276
radiotherapy of thyrotoxicosis of, effects on heart of, 20: 14424
radium content in animal, 20: 14254
THYROID HORMONES
effects of thyrotropin, on radioinduced hypothyroidism, 20: 14338
THYROXINE
metabolism in man, mathematical model of, 20: 14249
metabolism in man, mathematical model for, 20: 14250
TIMING CIRCUITS
design for digital-voltmeter readout, 20: 14822(R) (RHEL/R-112, pp 99-128)
TIN
analysis and determination, 20: 14500
bremsstrahlung reactions (γ,n) at 8 to 16 Mev, spectra from, (E), 20: 15723 (MIT-2098-162)
bremsstrahlung reactions (γ,n) with, neutron emission in, (E), 20: 15724 (MIT-2098-224)
conductivity in superconducting films of, electric and thermal, (E), 20: 15656
content in red-colored Paleozoic deposits in Northern Tien Shan, 20: 14780(T) (AEC-tr-6579)
critical currents in superconducting films of, effects of magnetic field and temperature on, 20: 15662
determination in airborne dusts, spectrochemical, 20: 14475(R) (ORNL-

3889, pp 36-39)
determination in plutonium fluorides and peroxides, review on spectrographic, 20: 14464 (RFP-599)
effects on spectrofluorimetric determination of scandium, 20: 14476
electron and positron reactions at 100 to 400 kev, excitation cross sections for K ionization in, 20: 15257
electron transmission through thin foils of, plasmon excitation in, (E), 20: 15951
energy level transitions in, Coster-Kronig, (T), 20: 15238 (CONF-233 (Vol.3), pp 398-418)
ultrasonic wave attenuation in superconducting, frequency and temperature dependence of, (E/T), 20: 15659
use in shield for thermoluminescent dosimeter, 20: 14914(P)
TIN ALLOYS
Al–Be, electron plasma oscillations in thin foil eutectoid, properties of, (E), 20: 15952
Mg–Sn, preparation of single-crystal, 20: 15056(R) (NYO-2916-10)
Mg–Sn, studies of equilibration in monocrystals of, 20: 15056(R) (NYO-2916-10)
Nb–Sn, crystallization of chemical-vapor-deposited crystals of Nb_3Sn, 20: 15113
Nb–Sn, superconductivity of fused, 20: 15123
Nb–Sn–Ti, superconductivity of fused, 20: 15123
Nb–Sn–V, superconductivity of fused, 20: 15123
Nb–Sn–Zr, superconductivity of fused, 20: 15123
Nb–Ta–Sn, superconductivity of fused, 20: 15123
Pb–Sn, thermodynamic properties, 20: 15062 (UCRL-16514)
Pb–Sn, vapor pressure of lead over, effects of composition on, 20: 15062 (UCRL-16514)
TIN COUPLES
Au–Sn, electric and thermal conductivity in superconducting, (E), 20: 15656
Mn–Sn, electric and thermal conductivity in superconducting, (E), 20: 15656
TIN HYDRIDES
Mössbauer effect in, 20: 14567
spectra of deuterated and normal, absorption, (E/T), 20: 15251
TIN ISOTOPES
deuteron reactions at 15 Mev, isomeric states from, (E), 20: 15856
TIN ISOTOPES Sn-109
beta decay of, branching ratios and conversion electron and gamma spectra from, (E), 20: 15752
TIN ISOTOPES Sn-112
proton reactions (p,d) at 30 Mev, distributions from, (E), 20: 15729(R) (RHEL/R-112, pp 37-66)
TIN ISOTOPES Sn-114
proton reactions (p,d) at 30 Mev, distributions from, (E), 20: 15729(R) (RHEL/R-112, pp 37-66)
TIN ISOTOPES Sn-116
proton reactions (p,d) at 30 Mev, distributions from, (E), 20: 15729(R) (RHEL/R-112, pp 37-66)
proton reactions (p,n) at 2.3 to 11.0 Mev, excitation of isobaric analog states in, (E), 20: 15804
TIN ISOTOPES Sn-118
proton reactions (p,d) at 30 Mev, distributions from, (E), 20: 15729(R) (RHEL/R-112, pp 37-66)
proton reactions (p,n) at 2.3 to 11.0 Mev, excitation of isobaric analog states in, (E), 20: 15804
TIN ISOTOPES Sn-119
proton reactions (p,n) at 2.3 to 11.0 Mev, excitation of isobaric analog states in, (E), 20: 15804
TIN ISOTOPES Sn-120
parity and spin of, from deuteron scattering data, 20: 15850
proton reactions (p,d) at 30 Mev, distributions from, (E), 20: 15729(R) (RHEL/R-112, pp 37-66)
proton total cross sections at 30 and 50 Mev, (E), 20: 15729(R) (RHEL/R-112, pp 37-66)
TIN ISOTOPES Sn-122
proton reactions (p,d) at 30 Mev, distributions from, (E), 20: 15729(R) (RHEL/R-112, pp 37-66)
proton reactions (p,n) at 2.3 to 11.0 Mev, excitation of isobaric analog states in, (E), 20: 15804
TIN ISOTOPES Sn-124
proton reactions (p,d) at 30 Mev, distributions from, (E), 20: 15729(R) (RHEL/R-112, pp 37-66)
proton reactions (p,n) at 2.3 to 11.0 Mev, excitation of isobaric analog states in, (E), 20: 15804
TIN OXIDES
sorptive properties for chloride and potassium ions, effects of pH on, 20: 14651
TIN, TRIETHYLIODO-
radioinduced ESR spectra in, at 77°K, 20: 14597
TISSUE CULTURES
effects of Decortilen on mitosis of HeLa cells in, 20: 14375
radiation effects on mitosis of HeLa cells in, x, 20: 14375
radiation effects on Chinese hamster cell, protective effects of serum in media against x, 20: 14400
radiation effects on cytoplasm in chick embryo muscle, effects of dose on x, 20: 14321
radiation effects on nucleic acid metabolism in, uv, 20: 14355
radiation effects on mouse leukemic cells in, lethal y, 20: 14367
radiosensitivity of animal cells in, 20: 14385
TISSUE HOMOGENATES
radiation effects on peroxide formation in rat, 20: 14261
radiation effects on dehydrogenase activity in rat liver, y, 20: 14284
TISSUE TRANSPLANTS
effects of hematopoietic, on anemic mice, 20: 14290(R) (NYO-1800-12)
TISSUES
analysis for elemental composition, spectrographic, 20: 14457(R) (ORNL-3889, pp 36-39)
demineralization of hard, using EDTA for calcium chelation, 20: 16149 (NYO-2779-10)
dose distributions in, from beta-emitting isotopes, 20: 14403 (NP-15714)
hydration in mouse liver, effects on lipid content of, 20: 14268
neutron reactions at high energies, 20: 14330
proton reactions at high energies, 20: 14330
radiation effects on lipolytic enzyme activities in fatty, x, 20: 14279
radiation effects on normal and tumorous mouse, effects of injected RNA on x, 20: 14401
TITANIUM
analysis and determination, 20: 14500
content in red-colored Paleozoic deposits in Northern Tien Shan, 20: 14780(T) (AEC-tr-6579)
corrosion cracking in alcohol–acid solution, effects of water on stress, 20: 14988
creep and rupture of, numerical methods for analysis of, 20: 15041 (GEMP-397)
determination in automobile tire rubber, activation, 20: 14439(R) (GA-5556)
determination in automobile paint, activation, 20: 14439(R) (GA-5556)
determination in commercial plastics, activation, 20: 14439(R) (GA-5556)
determination in sea water, polarographic, 20: 14455(R) (ORNL-3889, pp 25-32)
determination in uranium tetrafluoride, spectrographic, 20: 14473
determination of trace amounts of, in iron, activation, 20: 14471
effects on spectrofluorimetric determination of scandium, 20: 14476
effects on tantalum segregation in niobium by controlled solidification of additions of, 20: 14969
energy level transitions in, Coster-Kronig, (T), 20: 15238 (CONF-233 (Vol.3), pp 398-418)
energy level widths for, K, (T), 20: 15239 (CONF-233(Vol.3), pp 419-39)
reactions with sodium, high-temperature, 20: 15033(R) (ANL-7152, pp 87-96)
thermal capacity at 0.24 to 4.20°K, 20: 15061 (UCRL-11580)
TITANIUM ALLOYS
Al–Ti–V, corrosion by oxygen-contaminated sodium, 20: 16060(R) (ANL-7152, pp 1-49)
Cr–Nb–Ti, phase diagrams, 20: 15078
Fe–Ti, thermal capacity at 0.24 to 4.20°K, 20: 15061 (UCRL-11580)
Mo–Ti, machining, 20: 15014
Mo–Ti–Zr, machining of TZM, 20: 15014
Nb–Sn–Ti, superconductivity of fused, 20: 15123
Nb–Ti, corrosion by hydrochloric, phosphoric, and sulfuric acids, effects of alloy composition on, 20: 14997
Nb–Ti, hardness, 20: 15073
Pu–Ti–U, density and structure of, 20: 16060(R) (ANL-7152, pp 1-49)
Ti–Va, reactions with sodium, high-temperature, 20: 15033(R) (ANL-7152, pp 87-96)
TITANIUM BORIDES
abrasive properties, 20: 15109
reactions with copper and nickel mattes, slags, molten salts, and refractory metals, 20: 14989
TITANIUM CARBIDES
abrasive properties, 20: 15109
preparation of spherical particles of, procedure and apparatus for, 20: 14971(P)
reactions with copper and nickel mattes, slags, molten salts, and refractory metals, 20: 14989
ScC–TiC–WC, preparation and hardness, 20: 15017
TITANIUM ISOTOPES
deuteron reactions at 15 Mev, isomeric states from, (E), 20: 15856
energy levels of, weak-coupling model for $d_{3/2}$-hole states in, 20: 15852
TITANIUM NITRIDES
reactions with copper and nickel mattes, slags, molten salts, and refractory metals, 20: 14989

TITANIUM NITRATES
diffusion of carbon in, carbide film formation in, 20: 15072
TITANIUM OXIDES
preparation of spherical particles of, procedure and apparatus for, 20: 14971(P)
TITANIUM(IV) OXIDES
sorptive properties for chloride and potassium ions, effects of pH on, 20: 14651
TITANIUM SYSTEMS
C–Nb–Ti–Zr, heat treatment of, 20: 14972(P)
Nb–N–Ti–Zr, heat treatment of, 20: 14972(P)
Nb–O–Ti–Zr, heat treatment of, 20: 14972(P)
Ti–UP, compatibility, 20: 15032(R) (ANL-7152, pp 50-72)
TITRATION EQUIPMENT
development of ORNL model Q-2564 coulometric, 20: 14452(R) (ORNL-3889(p.1-12)
TOBACCO
analysis of cigarette, activation, 20: 14439(R) (GA-5556)
polonium-210 uptake by lungs from smoke of, 20: 14798
TOLUENESULFONIC ACID, POTASSIUM SALTS
electric conductivity in light and heavy water at 25°C, 20: 14540
TOMATOES
cuticular membranes in, permeability to organic compounds, 20: 16146 (COO-888-39)
cuticular membranes in, permeability to iron and iron chelates of, 20: 16147 (COO-888-45)
TRACER TECHNIQUES
feasibility for detecting failed reactor fuel elements, 20: 14848 (BMwF-FBK-65-02)
for permeability of cuticular membranes to organic compounds, carbon-14, 20: 16146 (COO-888-39)
TRACER TECHNIQUES (AGRICULTURE)
foliar absorption of fertilizers by plants, 20: 14240 (NP-15670)
TRACER TECHNIQUES (BIOLOGY)
development for physiological studies, 20: 14386
TRACER TECHNIQUES (BOTANY)
for permeability of cuticular membranes, 20: 16147 (COO-888-45)
TRACER TECHNIQUES (CHEMISTRY)
evaluation of short-lived radioisotopes for detection of hidden materials, 20: 14451 (NYO-2586-2)
for determination of lead, 20: 14661(R) (ORNL-3889, pp 48-70)
TRACER TECHNIQUES (ENGINEERING)
for wear rates in automotive engines, 20: 14661(R) (ORNL-3889, pp 48-70)
methods and uses, 20: 14934
TRACER TECHNIQUES (MEDICINE)
blood circulation studies, xenon-131, 20: 14415
for determining kidney function after radiotherapy of abdominal and pelvic tumors, 20: 14296
for gastrointestinal sorption of calcium, calcium-47, 20: 14247
TRAMEX PROCESS
use with Clanex process for separation of americium and curium isotopes, 20: 14639 (ORNL-P-1968)
TRANSCURIUM ELEMENTS
production in heavy-ion nuclear reactions, review of, 20: 15740
TRANSISTORS
electric and radiation storage time in junction, (E/T), 20: 15993
radiation effects on performance of, 20: 14920 (TID-22664)
radiation effects on n-channel MOS, electron, 20: 14924
TRANSITION METALS
dislocation motion in bcc, model for, 20: 15040(R) (GA-6721)
TRANSPLUTONIC ELEMENTS
determination, mass spectrometric, 20: 14458(R) (ORNL-3889, pp 39-43)
TRANSURANIC ELEMENTS
processing of, analytical equipment and methods for, 20: 14454(R) (ORNL-3889, pp 17-24)
TRAPS
design of bakeable cold, engineering drawings for, 20: 14674
design of high-conductance, for pumps in ALICE, engineering drawings for, 20: 15924
use of, for radioactive iodine in waste gases, 20: 14787 (CEA-Bib-64)
TRAUMA
effects of, combined with x-irradiation on kidney function in rabbits, 20: 14325
effects on sorptive properties of rat skin, 20: 14253
TREES
haploid embryos in coconut palm, 20: 14320
radiation effects on ploidy in coconut palm, 20: 14320
s-TRIAZINE, HEXAHYDROTRINITRO-
determination in explosives, methods for, 20: 14470 (UCRL-7873)
s-TRIAZINE, 2,4,6-TRIS-(ALLYLOXY)-
radioinduced polymerization of, in liquid and solid states, gamma, 20: 14586
TRIMETHYLAMINE
effects on radiolysis of cyclopentane, 20: 14599
TRIOCTYLAMINE
solvent properties for molybdenum and uranium in sulfate solutions, 20: 14653
trioctylamine–xylene, solvent properties for ruthenium, 20: 14650
TRITIUM
beta spectra of, effects of antineutrino sea on, (T), 20: 15326
content in lakes, rain water, vegetable water, and underground water, 20: 14744
determination by beta counting using proportional or scintillation detectors, 20: 14503
determination in air, Kanne ionization chamber for, 20: 14905
diffusion from tritiated paints, 20: 14461(R) (ORNL-3889, pp 48-70)
effects on mechanism of electrophilic aromatic substitution, 20: 14577
exchange with hydrogen in poly-L-glutamic acid, 20: 14628
exchange with hydrogen in methane–water vapor mixtures, rate of, 20: 14662(R) (ORNL-TM-1394)
incorporation in human chromosomes, 20: 14243(R) (TID-22626)
incorporation in organic compounds by recoil reactions, 20: 14620
incorporation in organic compounds, method for, 20: 14633(P)
leak control of gaseous, development of membrane for vacuum, 20: 14730 (AWRE-O-10/66)
production of, review of methods for, 20: 14948
properties of, induced in copper ore by nuclear explosives, 20: 14662(R) (ORNL-TM-1394)
proton reactions (p,n) at 30 to 50 Mev, distributions from, 20: 15729(R) (RHEL/R-112, pp 37-66)
radiation effects on uptake of thymidine-incorporated, by rat kidney cells, x, 20: 14258 (AD-627569)
reactions of recoil, mechanisms of, 20: 14620
separation from helium-3 by sorption on carbon, 20: 14444(R) (MLM-1268)
TRITIUM COMPOUNDS
production of, review of methods for, 20: 14948
TRITONS
binding energy of, Faddeev equations for, (T), 20: 15343
detection in products from nuclear reactions, engineering drawings of apparatus for, 20: 14906
reactions (t,p) with light nuclei, angular distributions for direct, (T), 20: 15798
reactions (t,p) with boron-10, carbon-12, and oxygen-16, angular distributions for, (T), 20: 15798
reactions with tritons, neutron-neutron interactions in, (T), 20: 15733 (UCRL-7769)
TRYPSIN
photoinactivation of dye-sensitized, 20: 14274
radioinduced free radicals in crystalline, γ and uv, 20: 14273
TUBES
anchor for rows of, 20: 14698(P)
burnout heat flux in circular, axial distribution and inlet enthalpy effects on, (E), 20: 14696
charged-particle beam reactions with, electromagnetic fields from, (T), 20: 15168 (SLAC-49, pp 23-31)
critical heat flux in long, with boiling water flow, 20: 14695
interactions with charged-particle beams, electromagnetic fields from, (T), 20: 15167 (SLAC-49, pp 18-22)
pressure oscillations from closed end, heat-generated, (E/T), 20: 14690 (SC-DC-66-1293)
testing of stainless steel cladding, automatic device for ultrasonic, 20: 14717
testing of, eddy-current methods for multiparameter, 20: 14708
testing SAP, low-voltage radiographic methods for, 20: 14706
testing thin-walled, nondestructive methods for, 20: 14713
testing thin-walled, ultrasonic equipment and methods for, 20: 14716
testing vapor-deposited tungsten, 20: 15048 (N65-16231)
testing Zircaloy-2, ultrasonic equipment and method for, 20: 14714
thickness measurements on, automatic equipment and methods for ultrasonic, 20: 14718
thickness measurements on long straight, design of semi-automatic device for, 20: 14816 (EUR-2512.n)
TUMORS
chemotherapy of gynecologic, 20: 14413
induced by carbon tetrachloride, in mice, 20: 14373
radiation effects on animals bearing, effects of RNA on electron, 20: 14397
radiation effects on mouse, effects of injected RNA on x, 20: 14401
radioinduced in mice, x, 20: 14373
radioinduced in twins, x, 20: 14319
radioinduced, mechanisms for, 20: 14360
radiotherapy of abdominal and pelvic, isotope test for kidney function following, 20: 14296
radiotherapy of bladder, vesico-ureteral reflux from β and γ, 20: 14411
radiotherapy of breast, costal fractures from, 20: 14369
radiotherapy of chemodectomas, 20: 14417

radiotherapy of gynecologic, review of hyperbaric and radioisotope, 20: 14413
radiotherapy of hemangioma, safety measures for, 20: 14418
radiotherapy of lacrimal gland, x, 20: 14410
radiotherapy of ovarian, genetic damage to offspring from, 20: 14348
radiotherapy of, dosimetry in neutron, 20: 14421
radiotherapy of, using isotopes, 20: 14406
radiotherapy using cobalt-60 and wedge filters, 20: 14426
TUNGSTATES
oxygen-18 exchange between water and, 20: 14525
TUNGSTEN
analysis and determination, 20: 14500
bremsstrahlung reactions (y,n) at 8 to 16 Mev, spectra from, (E), 20: 15723 (MIT-2098-162)
bremsstrahlung reactions (y,n) with, neutron emission in, (E), 20: 15724 (MIT-2098-224)
creep and rupture of, numerical methods for analysis of, 20: 15041 (GEMP-397)
deformation mechanisms in, 20: 15040(R) (GA-6721)
determination in explosives, method for, 20: 14470 (UCRL-7873)
determination in uranium tetrafluoride, spectrographic, 20: 14473
determination of trace amounts of, in iron, activation, 20: 14471
diffusion in molybdenum at 1700 to 2100°C, 20: 15126
diffusion of fission products in, 20: 14959(R) (N65-20797)
diffusion of fission products in, 20: 14960(R) (N65-20798)
dislocation motion in, impurity and intrinsic barriers to, 20: 15040(R) (GA-6721)
electric charge of sorbed thorium in, (E), 20: 15985(T)
electric conductivity of cold-worked, effects of annealing temperature on, 20: 15040(R) (GA-6721)
electron and positron reactions at 200 to 550 kev, excitation cross sections for K ionization in, 20: 15257
energy level widths for, K, (T), 20: 15239 (CONF-233(Vol.3), pp 419-39)
fabrication and high-temperature properties, 20: 15101
neutron elastic scattering at 0.8 Mev, cross sections for, (T), 20: 15770
oxygen molecule reactions with single crystals of, penetration and sorption in, (E), 20: 15986(T)
radiation effects on electric conductivity of, fast-neutron, 20: 15040(R) (GA-6721)
reactions with refractory metal borides, carbides, nitrides, and oxides, 20: 14989
tensile properties of, effects of mechanical twinning on, 20: 15049(R) (N65-16256)
testing vapor-deposited tubing of, 20: 15048 (N65-16231)
work function of, effects of cesium-fluoride vapor on, 20: 15297 (CONF-640921, pp 101-9)
TUNGSTEN ALLOYS
Hf–Nb–W–Y, properties for use in aerospace vehicles, 20: 15119
Hf–W, extrusion and swaging, 20: 15101
Hf–W, properties for high-temperature uses, 20: 15101
Hf–W, sintering, 20: 15021
Mo–W, electric transport in, for wide composition ratio and temperature range, 20: 15116(T)
Mo–W, mechanical properties of Oremet HPC, 20: 15069
Nb–W, extrusion and swaging, 20: 15101
Nb–W, hardness, 20: 15073
Nb–W, properties for high-temperature uses, 20: 15101
Re–W, fabrication of sheets from extruded bars of, 20: 14968(R) (USBM-RC-1220)
Tc–W, density, effects of composition on, 20: 15035(R) (BNWL-196)
Tc–W, microstructure, effects of composition on, 20: 15035(R) (BNWL-196)
W–Zr, extrusion and swaging, 20: 15101
W–Zr, properties for high-temperature uses, 20: 15101
TUNGSTEN BORIDES
abrasive properties, 20: 15109
reactions with copper and nickel mattes, slags, molten salts, and refractory metals, 20: 14989
TUNGSTEN CARBIDES
abrasive properties, 20: 15109
machining of, particle size distribution from, 20: 15015
preparation of spherical particles of, procedure and apparatus for, 20: 14971(P)
reactions with copper and nickel mattes, slags, molten salts, and refractory metals, 20: 14989
Co–WC, machining of, particle size distribution from, 20: 15015
ScC–TiC–WC, preparation and hardness, 20: 15017
TUNGSTEN CARBONYLS
decomposition in ion source of mass spectrometer, mechanism of, 20: 14584(R) (TID-22444)
TUNGSTEN ISOTOPES W-176
decay of, gamma spectra from electron-capture, (E), 20: 1502 (CONF-233 (Vol.2), pp 142-7)
TUNGSTEN ISOTOPES W-179
decay of, anomalous E1 transition in electron-capture, (E), 20: 15702 (CONF-233(Vol.2), pp 142-7)
TUNGSTEN ISOTOPES W-181
determination in atmospheric and precipitation samples, methods for radiochemical, 20: 14430 (AD-620219)
TUNGSTEN ISOTOPES W-182
energy level structure of, centrifugal-stretching and Coriolis-force antipairing effects in, (T), 20: 15821
energy levels transition in, isomeric shift of, (E), 20: 15820
internal conversion coefficients of $2^+ \rightarrow 0^+$ transitions in, E2, (E), 20: 15745
TUNGSTEN ISOTOPES W-183
half life of isomeric, (E), 20: 15688 (AD-620384)
Mössbauer effect of 46.5 kev line of, 20: 15737
TUNGSTEN ISOTOPES W-184
energy levels from rhenium-184 decay, (E), 20: 15750
energy levels transition in, isomeric shift of, (E), 20: 15820
TUNGSTEN ISOTOPES W-185
determination in atmospheric and precipitation samples, methods for radiochemical, 20: 14430 (AD-620219)
TUNGSTEN ISOTOPES W-186
energy level transitions in, conversion coefficients for E2, (E), 20: 15706 (CONF-233(Vol.2), pp 191-7)
energy levels transition in, isomeric shift of, (E), 20: 15820
TUNGSTEN ISOTOPES W-187
gamma spectra of, performance of curved-crystal spectrometer for, 20: 15807
TUNGSTEN OXIDES
preparation of spherical particles of, procedure and apparatus for, 20: 14971(P)
sorptive properties for chloride and potassium ions, effects of pH on, 20: 14651
Ce_2O_3–WO_3, preparation and properties, 20: 14534
La_2O_3–WO_3, preparation and properties, 20: 14534
Nd_2O_3–WO_3, preparation and properties, 20: 14534
Pr_2O_3–WO_3, preparation and properties, 20: 14534
TUNGSTEN SELENIDES
reactions with copper and nickel mattes and molten salts, 20: 14989
TUNGSTEN SYSTEMS
B–Fe–W, crystal structure, 20: 14532
C–Nb–W–Zr, heat treatment of, 20: 14972(P)
C–Nb–W–Zr, tensile properties of D-43, 20: 15068
Nb–N–W–Zr, heat treatment of, 20: 14972(P)
Nb–O–W–Zr, heat treatment of, 20: 14972(P)
W–UO_2–V, fabrication of cermets of, by isostatic cold pressing, 20: 14962(R) (N65-20803)
W–UP, compatibility, 20: 15032(R) (ANL-7152, pp 50-72)
TUNGSTOCOBALTATES
oxygen-18 exchange between water and, 20: 14525
TURBINES
development of coal-fired, 20: 14671(R) (TID-22394)
testing gas-lubricated turbocompressors, 20: 14671(R) (TID-22394)
TYROSINE
iodine-131 exchange reactions between iodine and, chromatographic studies on, 20: 14632
TYROSINE, 3,5-DIIODO-
iodine-131 exchange reactions between iodine and, chromatographic studies on, 20: 14632
TYROSINE, TRIIODO-
iodine-131 exchange reactions between iodine and, chromatographic studies on, 20: 14632

U

ULTRASONICS
attenuation in superconducting lead, amplitude dependence of, 20: 15657
attenuation in superconducting tin, frequency and temperature dependence of, (E/T), 20: 15659
attenuation in type II superconductors, formula for, 20: 15663
equipment and method for tests on Zircaloy-2 canning tubes, 20: 14714
equipment and method for tests on fuel claddings, 20: 14715
equipment and methods for testing of thin-walled cladding tubes, 20: 14716
equipment and methods for tube-thickness measurements by, 20: 14718
equipment for testing stainless steel cladding tubes by, design of automatic, 20: 14717
instruments for nuclear uses, development of, 20: 14700(R) (NYO-3622-1)
method for testing reactor pressure vessels, 20: 14709
methods for testing reactor building materials and fuel elements, 20: 14711
methods for testing of finned SAP tubing, 20: 14712
use for detection of incipient boiling in molten metals, 20: 14700(R)

(NYO-3622-1)
ULTRAVIOLET RADIATION
effects in *Bacillus subtilis*, 20: 14267
effects on bacteriophages, host-cell reactivation of, 20: 14357
effects on conjugation in *E. coli*, 20: 14329
effects on crystalline trypsin ESR signal, 20: 14273
effects on decomposition of liquid and vaporous nitroethane and nitromethane, 20: 14613
effects on DNA transfer from T4 bacteriophages to progeny, 20: 14285
effects on DNA, effects of amino acids on, 20: 14272
effects on glasses, bibliography on, 20: 15134 (N65-15819)
effects on human skin, 20: 14310
effects on incompatibility in *Oenothera organensis*, 20: 14382
effects on *Lupus erythematosus*, 20: 14309
effects on methanolic hydrogen peroxide, mechanism of, 20: 14579(R) (NYO-2383-15)
effects on nucleic acid metabolism in cultured animal cells, 20: 14355
effects on phage inactivation and thymine dimerization, effects of pH and gases against, 20: 14356
effects on reproduction of bacteriophages infecting *Escherichia coli*, 20: 14271
effects on *Schizosaccharomyces pombe*, genetic, 20: 14327
effects on silicon detectors, noise from, (E), 20: 14923
effects on synthesis of nucleic acids and proteins in amoeba, 20: 14259(R) (NP-15855)
effects on T4 phage, genetic map length of reactivated, 20: 14328
UNDERGROUND EXPLOSIONS
bibliography on nuclear, 20: 14661 (NP-15867)
decoupling in Salmon event, 20: 14664 (UCRL-14487(Rev.1))
detection and discrimination of, research on, 20: 14768
detection and discrimination of, seismometers for, 20: 14769
ground motion from atomic, in salt, 20: 14663 (UCRL-14463(Rev.1))
seismic disturbances from, computer program for simulating, 20: 14755 (UCRL-7929)
use in mining copper ores, behavior and removal of radioactive products in, 20: 14662(R) (ORNL-TM-1394)
uses for excavation and mining, 20: 14665
UNDERWATER EXPLOSIONS
water wave propagation from atomic simulation using explosives, 20: 14660 (AD-620468)
UNITED STATES
sea water desalination program in, 20: 16157
URANIUM
abundance ratio to radium in bitumen deposits, 20: 14781
analysis and determination, 20: 14500
analysis for uranium-235 in solutions of, gamma spectrometric, 20: 14449(R) (NLCO-970, pp 7.1-5)
casting large ingots of, use of infrared pyrometers for furnace melting cycle control in, 20: 15006(R) (NLCO-970, pp 4.1-5)
compatibility with water in reactor environment, 20: 14996
content in animal teeth and thyroids, 20: 14254
content in waste precipitate cakes and machining scraps, 20: 16140
crystallization and deformation, 20: 15099
crystallographic analysis using double-diffracting and standard x-ray diffractometers, 20: 14823 (RL-REA-2595, pp 73-9)
determination in carnotite, spectrophotometric, 20: 14455(R) (ORNL-3889, pp 25-32)
determination in methanol–mineral acid media using azo dyes, spectrophotometric, 20: 14469(R) (TID-22650)
determination in monazites, 20: 14491
determination in nuclear fuel cycles, evaluation of methods for, 20: 14447 (NBL-231)
determination in red-colored Paleozoic deposits in Northern Tien Shan by fluorescent method, 20: 14780(T) (AEC-tr-6579)
determination in synthetic MSRE fuel, coulometric, 20: 14454(R) (ORNL-3889, pp 17-24)
determination in thoria–urania fuels, polarographic, 20: 14455(R) (ORNL-3889, pp 25-32)
determination in tri-*n*-octylphosphine oxide, polarographic, 20: 14452(R) (ORNL-3889, pp 1-12)
determination in uranyl complex with 2,4-pentanedione, controlled-potential coulometric, 20: 14444(R) (MLM-1268)
determination in water, activation, 20: 14461(R) (ORNL-3889, pp 48-70)
determination of terrestrial abundance of, neutrino detection for, (T), 20: 14750
determination of trace amounts of, by naphthenic acid extraction, 20: 14642
determination of, evaluation of pyrocatechol and tiron for spectrophotometric, 20: 14482
determination using chromotropic acid and 2,3-dihydroxynaphthalene-6-sulfonic acid, spectrophotometric, 20: 14481
determination, mass spectrometric, 20: 14458(R) (ORNL-3889, pp 39-43)
diffusion from uranium carbide pellets into graphite, 20: 15087
diffusion in urania, model for, 20: 15091
diffusion of xenon in, at 950 and 1000°C, coefficient for, 20: 15090
effects on corrosion behavior of types 416 and 430F stainless steels in aqueous mineral acid solutions, 20: 14983 (NP-15875)
effects on spectrofluorimetric determination of scandium, 20: 14476
electric conductivity of quenched, effects of low-temperature annealing on, 20: 15066
erosion by flowing molten cadmium, 20: 14975 (ANL-7091)
incorporation in nuclear emulsions, estimation of maximum, 20: 14877
machining of, effects of thermoelectric cooling on life of carbide cutting tools during, 20: 14689(R) (NLCO-970, pp 5.1-7)
machining of, nuclear materials management in, 20: 16140
neutron elastic scattering at 0.8 Mev, cross sections for, (T), 20: 15770
phase transformation in, beta-to-alpha, 20: 15092
production by uranium tetrafluoride reduction, comparison of electrolytic and ferrosilicon-process magnesium for, 20: 15050(R) (NLCO-970, pp 3.1-4)
production by uranium tetrafluoride reduction, effects of furnace heating element arrangement on, 20: 14964(R) (NLCO-970, pp 2.1-7)
proton reactions (p,n) at 30 to 50 Mev, distributions from, 20: 15729(R) (RHEL/R-112, pp 37-66)
radiation effects on nuclear fuel elements of, bibliography on, 20: 15137 (VDIT-16(5.4))
reactions with sodium, high-temperature, 20: 15033(R) (ANL-7152, pp 87-96)
separation by ion exchange in mixed and non-aqueous media, review on, 20: 14469(R) (TID-22650)
separation from aqueous solutions by solvent extraction using naphthenic acid, 20: 14642
separation from elements by combined ion exchange-solvent extraction in nitric acid–tetrahydrofuran mixture, 20: 14469(R) (TID-22650)
separation from fission products by ion exchange, kinetics of, 20: 14643
separation from graphite-base reactor fuels, 20: 14640 (ORNL-TM-1411)
separation from irradiated graphite-base fuels by fluidized-bed fluoride volatility process, 20: 14647
separation from protactinium by solvent extraction on fine-grained carrier, 20: 14656
separation from sulfate solutions by solvent extraction using tri-*n*-octylamine, 20: 14653
separation from thorium by solvent extraction using alkyl phosphonates, 20: 14448(R) (NLCO-970, pp 1.1-22)
separation from trace metals by chromatography, 20: 14461(R) (ORNL-3889, pp 48-70)
separation from tributyl phosphate solutions by solvent extraction, kinetics of, 20: 14655
stress analysis in, performance of x-ray diffractometry for residual, 20: 15945 (RL-REA-2595, pp 43-50)
testing finned aluminum cladding on, eddy-current method for, 20: 14703
testing reactor tubes of, nondestructive method for, 20: 14711
thermal conductivity of Springfields, at 160 to 620°C, effects of aluminum, carbon, or iron content on, 20: 15084
URANIUM ALLOYS
radiation effects on solid fuel elements of, bibliography on, 20: 15137 (VDIT-16(5.4))
testing reactor tubes of, nondestructive method for, 20: 14711
Al–Fe–U, fabrication for nuclear fuel, 20: 15022(P)
Al–Fe–U, fabrication for nuclear fuel, 20: 15023(P)
Al–Fe–U, fabrication for nuclear fuel, 20: 15024(P)
Al–U, eddy-current method for testing finned aluminum cladding on, 20: 14703
Al–U, microradiographic method for testing aluminum-clad, 20: 14704
Al–U, separation of rare earth fission products from irradiated, by solvent extraction using TBP, 20: 14635 (CONF-660305-5)
Co–U, cobalt ion EPR in intermetallic compounds of, 20: 15963
fissium–Pu–U, phase studies, 20: 15085
Mo–Nb–U–Zr, mechanical properties of gamma-phase uranium-base, 20: 15060 (UCRL-7771)
Mo–Pu–U, fabrication for ZPR fuel elements, 20: 16060(R) (ANL-7152, pp 1-49)
Mo–U, mechanical properties of gamma-phase uranium-base, 20: 15060 (UCRL-7771)
Mo–U, microstructure of, effects of carbon on, 20: 15070
Nb–U, mechanical properties of gamma-phase uranium-base, 20: 15060 (UCRL-7771)
Nb–U–Zr, mechanical properties of gamma-phase uranium-base, 20: 15060 (UCRL-7771)
Pu–Ti–U, density and structure of, 20: 16060(R) (ANL-7152, pp 1-49)
Pu–U–Zr, density and structure of, 20: 16060(R) (ANL-7152, pp 1-49)
U–Zr, mechanical properties of gamma-phase uranium-base, 20: 15060 (UCRL-7771)
URANIUM ARSENIDES
crystal and magnetic structure below Néel point, (E), 20: 15949
URANIUM CARBIDES

diffusion of uranium from pellets of, into graphite, 20: 15087
electron emission by rhenium-clad and tungsten-clad, thermionic, 20: 14961(R) (N65-20801)
oxidation by oxygen *in vacuo* at 900 to 1000°C and at 1800°C, 20: 14985
preparation and properties of, 20: 15011
preparation of spherical particles of, procedure and apparatus for, 20: 14971(P)
reactions with nitrogen at 550 to 1050°C, 20: 14994
reactions with zinc at 500 to 800°C, 20: 14991
thermal expansion of dicarbide and sesquicarbide, 20: 15093
wetting by copper and gold, 20: 14551
NbC–UC, properties for cathodes in thermionic space power plants, 20: 15046(R) (N65-15820)
PuC–UC, burnup, 20: 15032(R) (ANL-7152, pp 50-72)
TaC–UC, properties for cathodes in thermionic space power plants, 20: 15046(R) (N65-15820)
ThC_2–UC_2, aqueous processing of graphite- and silicon dicarbide-coated fuel elements of, 20: 14638 (NP-15753)
UC–Zn, reactions with potassium chloride–lithium chloride–zinc chloride at 500 to 800°C, 20: 14991
UC–ZrC, aqueous processing of graphite- and silicon dicarbide-coated fuel elements of, 20: 14638 (NP-15753)
UC–ZrC, development as fuel for thermionic space power plants, 20: 14959(R) (N65-20797)
UC–ZrC, development as fuel for thermionic space power plants, 20: 14960(R) (N65-20798)
UC–ZrC, development as fuel for thermionic space power plants, 20: 14961(R) (N65-20801)
UC–ZrC, fabrication into fuel for thermionic space power plants, 20: 14962(R) (N65-20803)
UC–ZrC, fission product release at high temperatures, 20: 14959(R) (N65-20797)
UC–ZrC, fission product release at 1800°C, 20: 14961(R) (N65-20801)
UC–ZrC, fission product release at high temperatures, 20: 14960(R) (N65-20798)
UC–ZrC, properties for cathodes in thermionic space power plants, 20: 15046(R) (N65-15820)

URANIUM CHLORIDES
preparation, 20: 14511(R) (ORNL-3889, pp 71-3)

URANIUM COMPLEXES
with dihydroxybenzenedisulfonic acid and dihydroxybenzenesulfonic acid, preparation of, 20: 14522
with phenolic ligands, preparation of, 20: 14481
with tiron and pyrocatechol, preparation of, 20: 14482
with 2,4-pentanedione, controlled-potential coulometric analysis for uranium in, 20: 14444(R) (MLM-1268)

URANIUM COMPOUNDS
preparation of spherical granules of, 20: 14575(P)

URANIUM DEPOSITS
rock density in, computer program and logging system for determining, 20: 14778

URANIUM DEPOSITS (CHILE)
reconnaissance, 20: 14779 (RME-4569(Rev.))

URANIUM FLUORIDES
spectra of solid, reflectance, 20: 14453(R) (ORNL-3889, pp 12-14)

URANIUM(IV) FLUORIDES
analysis for impurities by direct spectrography, 20: 14473
reduction to metal, comparison of electrolytic and ferrosilicon-process magnesium for, 20: 15050(R) (NLCO-970, pp 3.1-4)
spectra of crystalline, transmission, 20: 14453(R) (ORNL-3889, pp 12-14)
BeF_2–LiF–ThF_4–UF_4–ZrF_4, spectra of irradiated, absorption and reflectance, 20: 14453(R) (ORNL-3889, pp 12-14)
BeF_2–LiF–UF_4–ZrF_4, analysis for uranium, polarographic, 20: 14454(R) (ORNL-3889, pp 17-24)

URANIUM(VI) FLUORIDES
crystal structure of, electron diffraction studies of, 20: 14516

URANIUM IODIDES
preparation, 20: 14511(R) (ORNL-3889, pp 71-3)

URANIUM IONS
electron transfer between tetravalent and hexavalent, effects of sulfate ions on, 20: 14574
uranium-235 exchange between tetravalent and hexavalent, effect of hydrochloric acid on, 20: 14570

URANIUM ISOTOPES
content in operating power reactor fuel elements, methods for determining, 20: 14438 (CEND-540)
internal conversion probabilities in, reduced M and N E0, (T), 20: 15771

URANIUM ISOTOPES U-233
casting of, equipment and procedures for, 20: 15003 (LA-DC-7510)
determination of trace amounts in flowing solutions using proportional counter, 20: 14871
neutron fission of, yields of cesium isotopes and neodymium isotopes in, 20: 15133(R) (GEAP-4893)
neutron fission of, neutron yields in, (E), 20: 15718 (IDO-17083)

URANIUM ISOTOPES U-234
content in spent reactor fuels, evaluation of, 20: 14435 (BNWL-SA-503)
internal conversion probabilities in, reduced M and N E0, (T), 20: 15771
separation from plutonium-238 solutions, ion exchange and solvent extraction method for, 20: 14444(R) (MLM-1268)

URANIUM ISOTOPES U-235
content in spent reactor fuels, evaluation of, 20: 14435 (BNWL-SA-503)
determination in uranium solutions, gamma spectrometric, 20: 14449(R) (NLCO-970, pp 7.1-5)
exchange between uranium(IV) and uranium(VI), effects of hydrochloric acid on, 20: 14570
fission products of, method for calculating gamma spectra of, 20: 14733 (AD-628982)
neutron capture-to-fission ratio for, 20: 15717(R) (GEAP-4950)
neutron fission at 150 to 335 kev, cross section for, (E), 20: 15818
neutron fission of, yields of cesium isotopes and neodymium isotopes in, 20: 15133(R) (GEAP-4893)
neutron fission of, neutron yields in, (E), 20: 15718 (IDO-17083)
neutron reactions at 0.1 to 2 Mev, cross sections for elastic, (E/T), 20: 15032(R) (ANL-7152, pp 50-72)

URANIUM ISOTOPES U-236
content in spent reactor fuels, evaluation of, 20: 14435 (BNWL-SA-503)

URANIUM ISOTOPES U-237
decay of, gamma branchings in, (E), 20: 14461(R) (ORNL-3889, pp 48-70)

URANIUM ISOTOPES U-238
content in irradiated uranium dioxide, 20: 15133(R) (GEAP-4893)
fission of, rhodium-105 and ruthenium-105 from spontaneous, 20: 15776

URANIUM MINERALS
composition of red-colored Paleozoic, in Northern Tien Shan, 20: 14780(T) (AEC-tr-6579)
processing of, nuclear materials management in wastes from, 20: 16140

URANIUM NITRIDES
thermal decomposition of microspheres of, nitrogen vapor pressure in, 20: 14512 (ORNL-TM-1418)

URANIUM ORES
processing of, properties of wastes from, 20: 16136

URANIUM OXIDES
analysis for iridium, activation, 20: 14495
preparation of spherical particles of, procedure and apparatus for, 20: 14971(P)

URANIUM(IV) OXIDES
analysis for oxygen using electron microprobe, 20: 14442(R) (MCW-1493, pp 5-13)
analysis for trace impurities, 20: 14494
creep of single-crystal, at 1340 to 1685°C, 20: 15086
density of extruded, effects of wetting agents on, 20: 14965(R) (NUMEC-3524-12)
density of vibratory-compacted powders of, effects of fuel can dimensions on, 20: 14999(R) (EURAEC-1466)
density of, effects of additions of dead-burned uranias or methyl cellulose on sintered, 20: 14965(R) (NUMEC-3524-12)
diffusion of fission products from, effects of radioinduced defects and temperature on, 20: 15144
diffusion of pores in, 20: 15094
diffusion of uranium in, model for self-, 20: 15091
grain size of crystalline, determination of, by x-ray diffraction, 20: 15044(R) (MCW-1493, pp 15-25)
mechanical properties, 20: 15029 (ANL-7070)
melting in crucibles, 20: 14999(R) (EURAEC-14666)
performance of stainless-steel-clad fuel elements of, for FTR, 20: 16121 (BNWL-197)
plutonium-236 and plutonium-238 content in irradiated, 20: 15133(R) (GEAP-4893)
preparation of microspheres of, by sol-gel technique, 20: 15008 (ORNL-8874)
pressing of tungsten-clad, hot-, 20: 14962(R) (N65-20803)
production by electrochemical reduction of uranium(VI) solutions, 20: 14552
radiation effects on plates of, in-pile, 20: 16089(R) (WAPD-MRP-114)
reactions with sodium, high-temperature, 20: 15033(R) (ANL-7152, pp 87-96)
sintering at 950 to 1500°C in hydrogen, kinetics of, 20: 15082
thermal conductivity of, under transient conditions, method for measuring, 20: 15031 (ANL-7116)
CaO–Sm_2O_3–UO_2–ZrO_2, corrosion and surface properties of, 20: 16089(R) (WAPD-MRP-114)
CaO–UO_2–ZrO_2, corrosion and surface properties of, 20: 16089(R) (WAPD-MRP-114)
CaO–UO_2–ZrO_2, properties of, in-pile, 20: 15138 (WAPD-292)
Hastelloy X–UO_2, sintering of, 20: 14965(R) (NUMEC-3524-12)
PuO_2–UO_2, density of, effects of methyl cellulose additions on sintered, 20: 14965(R) (NUMEC-3524-12)

PuO_2–UO_2, development and testing as fast reactor fuel, 20: 14965(R) (NUMEC-3524-12)
PuO_2–UO_2, oxidation and fluorination of, two-zone, 20: 15032(R) (ANL-7152, pp 50-72)
PuO_2–UO_2, performance as FTR fuel elements, 20: 16121 (BNWL-197)
PuO_2–UO_2, radiation effects on fuels of, thermal-neutron, 20: 15135(R) (NUMEC-3432-18)
PuO_2–UO_2, sintering of coprecipitated powders of, process development for, 20: 14965(R) (NUMEC-3524-12)
PuO_2–UO_2–H_2O, criticality parameters for, containing enriched and natural uranium, (T), 20: 16032
PuO_2–UO_2–ZrO_2, preparation and thermophysical properties, 20: 15054(R) (NUMEC-3505-11)
stainless steel–UO_2, sintering of, 20: 14965(R) (NUMEC-3524-12)
ThO_2–UO_2, analysis for uranium, polarographic, 20: 14455(R) (ORNL-3889, pp 25-32)
ThO_2–UO_2, machine design for receiving, blending, and transferring powdered, 20: 14668 (ORNL-TM-1397)
UO_2–H_2O, criticality parameters for, (T), 20: 16031
UO_2–ZrO_2, properties of, effects of calcia additions on in-pile, 20: 15138 (WAPD-292)
UO_2–ZrO_2, radiation effects on plates of, in-pile, 20: 16089(R) (WAPD-MRP-114)
W–UO_2–V, fabrication of cermets of, by isostatic cold pressing, 20: 14962(R) (N65-20803)

URANIUM PHOSPHIDES
mechanical properties of, effects of impurities on, 20: 15029 (ANL-7070)
Mo–UP, compatibility, 20: 15032(R) (ANL-7152, pp 50-72)
Nb–UP, compatibility, 20: 15032(R) (ANL-7152, pp 50-72)
Ta–UP, compatibility, 20: 15032(R) (ANL-7152, pp 50-72)
Ti–UP, compatibility, 20: 15032(R) (ANL-7152, pp 50-72)
UP–Zr, compatibility, 20: 15032(R) (ANL-7152, pp 50-72)
W–UP, compatibility, 20: 15032(R) (ANL-7152, pp 50-72)

URANIUM SILICIDES
analysis for silicon using electron microprobe, 20: 14442(R) (MCW-1493, pp 5-13)

URANIUM SULFIDES
burnup of fuel elements of, 20: 15032(R) (ANL-7152, pp 50-72)
mechanical properties of, effects of impurities on, 20: 15029 (ANL-7070)
PuS–US, preparation and properties, 20: 15032(R) (ANL-7152, pp 50-72)

URANIUM SYSTEMS
radiation effects on solid fuel elements of, bibliography on, 20: 15137 (VDIT-16(5.4))
Al–C–Fe–U, mechanical properties at intermediate strain rates and temperatures, 20: 15081
B–Co–U, crystal structure, 20: 14532
B–Ni–U, crystal structure, 20: 14532
C–O–U, phase studies at 1700°C, 20: 14968(R) (USBM-RC-1220)
C–O–U, vapor pressure of carbon monoxide in sol-gel fuels of, 20: 14512 (ORNL-TM-1418)
HNO_3–U, criticality parameters of water-reflected spheres of, (T), 20: 16031
N–Pu–U, properties of hot-pressed powders of, 20: 14957(R) (BMI-1754)
U–H_2O, criticality parameters for, (T), 20: 16031

URANYL CHLORIDES
determination in lithium chloride–potassium chloride eutectic at 400°C using voltammetry, 20: 14437 (CEA-R-2879)

URANYL FLUORIDES
UO_2F_2–H_2O, neutron flux perturbation by aluminum–dysprosium foils in, thermal, 20: 15669 (NASA-TN-D-3237)

URANYL IONS
hydrolysis of, in aqueous solutions, 20: 14444(R) (MLM-1268)

UREA
penetration of carbon-14-labeled, through cuticular membranes, 20: 16146 (COO-888-39)

UREA, THIO-
radiosensitivity effects in Pseudomonas, 20: 14394

URIDINE
radiation effects on excretion of pseudo-, after cancer therapy, x, 20: 14269

URINARY TRACT
radiation effects on ureteric valves in, after bladder carcinoma therapy, gamma, 20: 14298
radiation effects on, surgery combined with radium and x, 20: 14377

URINE
ammonia and phosphate excretion in rat, effects of burns, cytostatics, or methionine sulfoximine on, 20: 14270
analysis for cesium-137, 20: 14243(R) (TID-22626)
analysis for strontium-90, 20: 14243(R) (TID-22626)
potassium/sodium ratio in mouse, prediction of x-radiation response by, 20: 14266
radiation effects on pseudouridine content in, after radiotherapy, 20: 14269
radiation effects on ammonia and phosphate excretion in rat, x, 20: 14270
radioisotope excretion in human, effects of chelates on, 20: 14256
technetium-99 elimination in human, 20: 14423

UTERUS
radioinduced mesenchymal sarcomas in, following pelvic irradiation, 20: 14301
radioinduced sarcomas in human, 20: 14300
radiotherapy of carcinomas, tumorigenic effects of, 20: 14300
radiotherapy of carcinomas of, complications from surgery combined with radium and x, 20: 14377

V

V PARTICLES
production in meson (K⁻)-proton interactions at 5.5 Bev/c, (E), 20: 15416

VACCINES
radiosensitivity effects of smallpox virus, on chick embryos, x, 20: 14281

VACUUM PUMPS
design of evaporative, for ALICE, engineering drawings for, 20: 15922

VACUUM SYSTEMS
development, 20: 15882(R) (NP-15868)

VACUUM VESSELS
beam reactions with circular, electromagnetic fields from, (T), 20: 15169 (SLAC-49, pp 32-5)
charged-particle beam stability in toroidal, (T), 20: 15170 (SLAC-49, pp 36-48)

VALERIC ACID, 4,4-DINITRO-, ETHYL ESTER
determination in explosives, method for, 20: 14470 (UCRL-7873)

VALERIC ACID, 4,4-DINITRO-, METHYL ESTER
determination in explosives, method for, 20: 14470 (UCRL-7873)

VALLECITOS BOILING WATER REACTOR
spent fuel analysis for fission products and heavy element isotopes, evaluation of chemical, 20: 14435 (BNWL-SA-503)

VALVES
design of bakeable, for ALICE, 20: 15923
design of flow-regulator, for sodium cooled fast reactors, 20: 16004(P)
design of lift and non-rotatable spindle-type flow-control, 20: 14676(P)

VAN ALLEN RADIATION BELTS
charged-particle energy spectra and flux in, 20: 15232
electron and proton energy spectra and fluxes in inner, review of, 20: 15621
electron detection and measurement in, instrumentation for, 20: 15589(R) (ASE-1125)
origin, (T), 20: 15593
proton density in inner, effects of solar cycle variations on, (T), 20: 15590 (NASA-TN-D-3086)

VANADATES
alkyl ortho-, decomposition in ion source of mass spectrometer, 20: 14584(R) (TID-22444)

VANADIUM
analysis and determination, 20: 14500
content in red-colored Paleozoic deposits in Northern Tien Shan, 20: 14780(T) (AEC-tr-6579)
creep and rupture of, numerical methods for analysis of, 20: 15041 (GEMP-397)
determination in automobile lubricants, activation, 20: 14439(R) (GA-5556)
determination in oil samples in water, activation, 20: 14439(R) (GA-5556)
determination in uranium tetrafluoride, spectrographic, 20: 14473
determination of trace amounts of, in iron, activation, 20: 14471
effects on spectrofluorimetric determination of scandium, 20: 14476
energy level fluorescence yields from, K, (E), 20: 15242 (CONF-233 (Vol.3), pp 465-79)
energy level transitions in, Coster-Kronig, (T), 20: 15238 (CONF-233 (Vol.3), pp 398-418)
energy level widths for, K, (T), 20: 15239 (CONF-233(Vol.3), pp 419-39)
miscibility with other elements, calculation of, 20: 14538
neutron capture by, gamma spectra from thermal, (E), 20: 15787
proton reactions (p,n) at 30 to 50 Mev, distributions from, 20: 15729(R) (RHEL/R-112, pp 37-66)
reactions with sodium, high-temperature, 20: 15033(R) (ANL-7152, pp 87-96)

VANADIUM ALLOYS
miscibility with other elements, calculation of, 20: 14538
Al–Ti–V, corrosion by oxygen-contaminated sodium, 20: 16060(R) (ANL-7152, pp 1-49)
Ga–V, superconductivity of fused, 20: 15123
Nb–Sn–V, superconductivity of fused, 20: 15123
Nb–V, corrosion by hydrochloric, phosphoric, and sulfuric acids, effects of alloy composition on, 20: 14997

Nb–V, creep strength and ductility of, effects of mechanical twinning on, 20: 15049(R) (N65-16256)
Nb–V, hardness, 20: 15073
Ti–Va, reactions with sodium, high-temperature, 20: 15033(R) (ANL-7152, pp 87-96)

VANADIUM BORIDES
abrasive properties, 20: 15109
reactions with carbon, 20: 14555

VANADIUM CARBIDES
abrasive properties, 20: 15109

VANADIUM COMPOUNDS
decomposition of tetraalkoxides in ion source of mass spectrometer, mechanism of, 20: 14584(R) (TID-22444)

VANADIUM ISOTOPES V-48
decay of, K-capture to positron ratios for, (E), 20: 15711 (CONF-233 (Vol.2), pp 345-58)

VANADIUM ISOTOPES V-51
proton scattering at 50 Mev, differential cross sections for, (E), 20: 15728(R) (RHEL/R-112, pp 23-36)

VANADIUM OXIDES
$CaO–V_2O_5$, density and surface ductility of fused, at 1200 to 1650°C, 20: 15076
$Cr_2O_3–V_2O_5$, density and surface ductility of fused, at 1200 to 1650°C, 20: 15076
$Fe_2O_3–V_2O_5$, density and surface ductility of fused, at 1200 to 1650°C, 20: 15076

VANADIUM SYSTEMS
miscibility with other elements, calculation of, 20: 14538
Al–C–Nb–V, phase studies, 20: 15103
Al–C–Ta–V, phase studies, 20: 15103
B–Fe–V, crystal structure, 20: 14532
C–Nb–V–Zr, heat treatment of, 20: 14972(P)
Nb–N–V–Zr, heat treatment of, 20: 14972(P)
Nb–O–V–Zr, heat treatment of, 20: 14972(P)
Si–V, superconductivity of fused, 20: 15123
W–UO_2–V, fabrication of cermets of, by isostatic cold pressing, 20: 14962(R) (N65-20803)

VELA PROJECT
data processing for satellite program, modular logic system for, 20: 15597
decoupling in Salmon detonation, seismology of, 20: 14664 (UCRL-14487(Rev.1))
design of satellite and systems for, redundancy, 20: 15598
development of satellite program, 20: 15595
performance of satellite system, computer simulation for, 20: 15599
radiation detector electronics for satellite program, 20: 15596

VELOCITY
effects of, combined with γ radiation on Drosophila genetics, 20: 14343

VESSELS
design for storage and shipping of spent fuel elements, 20: 14679(P)

VIBRATIONS
effects of, combined with γ radiation on Drosophila genetics, 20: 14343

VIRUSES
radioinduced inactivation of, mechanisms for, 20: 14387

VISCOSITY
radiation effects on, in solid state polyamino acids, 20: 14588

VITAMIN A
effects on skeletal growth in rats, 20: 16148 (NYO-2779-9)

VITAMIN D
effects on calcium transport across intestinal membrane, tracer study, 20: 14243(R) (TID-22626)
effects on skeletal growth in rats, 20: 16148 (NYO-2779-9)

VITAMIN K
radiosensitivity effects of K_5 on Salmonellae infections in eggs, 20: 14395

VITREOUS MATERIALS
fabrication of boron-free, for radiation-resistant insulation, 20: 15131(P)

VOLTAGE REGULATORS
design and construction of three-phase, for 88-in. cyclotron, 20: 15183

VOLTMETERS
design of, engineering drawings for, 20: 14831
timing systems for readout of digital, 20: 14822(R) (RHEL/R-112, pp 99-128)

W

WASTE DISPOSAL
activation, for in-pile conversion of long-lived isotopes to stable or short-lived isotopes, (T), 20: 16132 (BNL-8558)
fixation in glass, 20: 16141(P)
ground, use of seismic methods for studying, 20: 14753 (BNWL-47)
problems in liquid, at Institute of Atomic Energy, Brazil, 20: 16134 (IEA-102)
storage, design of facility for Hanford, 20: 16135 (RL-SA-62)

WASTE PROCESSING
facilities for, engineering drawings of WAFRAX, 20: 16139
ion exchange methods of, 20: 14643
methods for, at Institute of Atomic Energy, Brazil, 20: 16134 (IEA-102)
solidification methods for, 20: 16142(P)
sorption methods for, use of flocculants in, 20: 16138

WASTE SOLUTIONS
analysis for beta activity, methods for, 20: 14450(R) (NLCO-970, pp 8.1-4)
sampling and monitoring of, instrumentation and techniques for, 20: 16137
separation of cesium-137 and strontium-90 from, by sorption on ion exchange materials, 20: 14434 (BNWL-180)
separation of rare earth fission products from, by solvent extraction using TBP, 20: 14635 (CONF-660305-5)

WATER
analysis for uranium, activation, 20: 14461(R) (ORNL-3889, pp 48-70)
boiling burnout detection method for, 20: 14694
boiling burnout in water in internally cooled tubes, 20: 14686(R) (EURAEC-1448)
boiling in natural circulation loop, oscillations in, 20: 14684 (ANL-7073)
content in organic soils, measurement of, using neutron method, 20: 14756
corrosive effects on carbon and stainless steels, effects of flow rate and surface treatments on, 20: 14978 (EURAEC-1546)
decompression into air, one-dimensional analysis of shock waves from, 20: 16023(R) (IITRI-578P21-16)
determination in rock strata using well logging, 20: 14777
determination in soils, neutron meter for, 20: 14771
effects on aluminum, stainless steel, uranium, and zirconium in reactor environment, 20: 14996
effects on radioinduced paramagnetic centers in sodium selenite, (E), 20: 15972
effects on spectra of neodymium complexes, 20: 14560
effects on stress corrosion cracking of titanium and zirconium in alcohol–acid solutions, 20: 14988
electric conductivity of ions in, at 25°C, 20: 14540
flow of boiling, critical heat flux in long tubes for, 20: 14695
heat fluxes during burnout, (E), 20: 14694
neutron diffusion in spherical containers of, parameters for, (E), 20: 15686
neutron diffusion length at 18 to 255°C, thermal, (E), 20: 15679
neutron flux perturbation by alumiaum–dysprosium foils in, thermal, 20: 15669 (NASA-TN-D-3237)
oxygen-18 exchange with orthotungstate or 12-tungstocobaltate at 25°C, 20: 14525
radiolysis of oxygenated, transient species in, 20: 14614
radiolysis of, in sodium acid phosphite–sodium nitrate solutions, effects of pH on, 20: 14601
radiosensitivity effects on germination in *Phleum pratense*, γ and x, 20: 14349
reactions with neodymium oxide, infrared spectra of products of, 20: 14568
reactions with stainless steel and zirconium during reactor accidents, 20: 16019(R) (BMI-X-10154)
separation of radioisotopes from, by sorption by bentonites and diatomaceous earth, 20: 16138
vibrational potential function of bent molecules of, third-order, 20: 14559
$AgClO_4–H_2O$, radioinduced free silver atoms in solid solutions of, EPR of x, (E), 20: 15975(T)
$AgF–H_2O$, radioinduced free silver atoms in solid solutions of, EPR of x, (E), 20: 15975(T)
$AgNO_3–H_2O$, radioinduced free silver atoms in solid solution of, EPR of x, (E), 20: 15975(T)
$Ag_2SO_4–H_2O$, radioinduced free silver atoms in solid solutions of, EPR of x, (E), 20: 15975(T)
$B–H_2O$, neutron spectra in, (E), 20: 15731(R) (RPI-328-49)
boric acid–H_2O, neutron diffusion length at 18 to 255°C, thermal, (E), 20: 15679
cadmium sulfate–H_2O, neutron diffusion length at 18 to 255°C, thermal, (E), 20: 15679
$H_2SO_4–H_2O$, radiolysis of oxygenated solutions of, 20: 14614
$KOH–H_2O$, radiolysis of oxygenated solutions of, 20: 14614
$Na_2CO_3–H_2O$, radiolysis of oxygenated solutions of, 20: 14614
$NaOH–H_2O$, radiolysis of oxygenated systems of, 20: 14614
$PuO_2–H_2O$, criticality parameters for plutonium-240 enriched, (T), 20: 16031
$PuO_2–UO_2–H_2O$, criticality parameters for, containing enriched and natural uranium, (T), 20: 16032
steam-water, burnout in flows with axially nonuniform heat flux, (E), 20: 14696
$U–H_2O$, criticality parameters for, (T), 20: 16031

UO_2F_2–H_2O, neutron flux perturbation by aluminum–dysprosium foils in, thermal, 20: 15669 (NASA-TN-D-3237)
UO_2–H_2O, criticality parameters for, (T), 20: 16031
WATER-d_2
effects on spectra of neodymium complexes, 20: 14560
electric conductivity of ions in, at 25°C, 20: 14540
vibrational potential function of bent molecules of, third-order, 20: 14559
$AgClO_4$–D_2O, radioinduced free silver atoms in solid solutions of, EPR of x, (E), 20: 15975(T)
AgF–D_2O, radioinduced free silver atoms in solid solutions of, EPR of x, (E), 20: 15975(T)
$AgNO_3$–D_2O, radioinduced free silver atoms in solid solutions of, EPR of x, (E), 20: 15975(T)
Ag_2SO_4–D_2O, radioinduced free silver atoms in solid solutions of, EPR of x, (E), 20: 15975(T)
WATER-t
sorption by burned and normal skin, 20: 14255
WATER-t_2
reactions with methane, effects of tritium on products from, 20: 14455(R) (ORNL-3889, pp 25-32)
WATER COOLED REACTORS
accidents in, metal-water reaction data for predicting, 20: 14996
coolant mixing device for, steam–water, 20: 16011(P)
reactivity excursion simulation in, 20: 16029
WATER MODERATED REACTORS
reactivity excursion simulation in, 20: 16029
WATER SUPPLIES
separation of radon from, by aeration, design of pilot plant for, 20: 14649
WATER VAPOR
water vapor, rate of tritium exchange reactions with hydrogen in, 20: 14662(R) (ORNL-TM-1394)
WATER WAVES
propagation from atomic explosions, simulation using explosions, 20: 14660 (AD-620468)
WELDED JOINTS
testing pressure-vessel, nondestructive methods for, 20: 14709
WELDING
bibliography on methods of, 20: 15005 (NASA-SP-5024)
dissimilar metals, process development for explosive, 20: 14957(R) (BMI-1754)
equipment for TIG-MIG, with visual inspection device, 20: 15019
thick steel plates, cracking and hardness changes from, 20: 15000 (EURAEC-1517)
WELL LOGGING
borehole and formation parameters in, computer code for, 20: 14775
development, 20: 14770
method for determining uranium-deposit rock density using computer program and system, 20: 14778
method using computer learning program, 20: 14777
neutron diffusion theory for, 20: 14774
probe design for, 20: 14773
WHEAT
strontium-90 content in Canadian, 1964, 20: 14736 (NP-15853, pp 3-7)
WHITESHELL REACTOR NO. 1
environs monitoring, 20: 14738 (NP-15853, pp 21-33)
radioactive contamination of milk near, 20: 14738 (NP-15853, pp 21-33)
WINDOWS
thickness of mica, in end-window counters, use of alpha particles for measuring, 20: 14826
WINDSCALE ADVANCED GAS COOLED REACTOR
design and operation, 20: 16092
fuel economics for, 20: 16087 (TRG-Report-1115)
WINNIPEG RIVER
radiation monitoring, 20: 14738 (NP-15853, pp 21-33)
WIRES
fabrication of, bremsstrahlung measurement of cross-section variations for, (E/T), 20: 14838
WOOD
analysis in criminal cases, activation, 20: 14439(R) (GA-5556)
WOUNDS
radiation effects on healing of, after radical neck dissection, x, 20: 14303
radioisotope sorption in rat, 20: 14253

X

X AGENT
directional properties, 20: 14622
X RADIATION
detection and measurement of low-energy, performance of proportional counter for, 20: 14879
detection and measurement of absorbed dose, performance of ionization chambers for, 20: 14894
detection and measurement of low-energy, solid-state detection for, 20: 14910(P)
detection of, calorimeter design and performance for, 20: 14908
detection of, performance of liquid argon-filled chambers for, 20: 15259
diffraction by molybdenum, radioinduced line-width changes in, 20: 15136 (RL-REA-2595, pp 51-62)
dosimetry for dental procedures, 20: 14419
dosimetry of diagnostic, in Japan, 20: 14799
dosimetry of, calorimetric method for, 20: 15858
effects during pregnancy, 20: 14380
effects of, combined with radium therapy and surgery on cervical carcinomas, complications from, 20: 14377
effects of, combined with diethyl sulfate on barley seeds, 20: 14384
effects of, combined with radium therapy and surgery on cervical carcinomas, 20: 14409
effects of, combined with trauma on function of rabbit kidney, 20: 14325
effects on activity of lipolytic enzymes, 20: 14279
effects on adenine nucleotide content in rat blood and liver, 20: 14270
effects on adrenal cortex in dogs, 20: 14280
effects on arterial prostheses in dogs, 20: 14344
effects on arterial prostheses in dogs, 20: 14345
effects on *Bacillus cereus*, biochemical, 20: 14263
effects on bacteriophage, inactivating, 20: 14260 (NP-15856)
effects on behavior in monkeys, 20: 14286 (AD-625837)
effects on beryl crystals, EPR and hfs from, 20: 15982(T)
effects on blood picture and survival in monkeys, 20: 14302
effects on cartilage of rats, biological, 20: 14291(R) (TID-22494)
effects on cervical carcinomas, 20: 14409
effects on chick embryos, effects of inoculation with smallpox virus vaccine on, 20: 14281
effects on Chinese hamster cells, protective effects of serum in media against, 20: 14400
effects on collagen gel, 20: 14593
effects on content of glycoprotein in blood serum of rats, 20: 14378
effects on cytoplasm in chick embryo muscle, effects of dose on, 20: 14321
effects on dacron prostheses, 20: 14345
effects on defect induction in sodium azide, ESR spectral studies on, 20: 15942 (NYO-2150-11)
effects on desoxyribonucleic acid content in rat thymus, 20: 14311
effects on DNA, 20: 14283
effects on DNA in *E. coli*, 20: 14265
effects on DNAse activity in rat thymus, 20: 14311
effects on DPN content in sarcoma cells, 20: 14370
effects on embryos of mice, delayed pathological, 20: 14315
effects on emergence of house flies from pupae, 20: 14306
effects on enzyme activity of mitochondria from rat liver, spleen, and thymus, 20: 14376
effects on epithelial tumors of lacrimal glands, 20: 14410
effects on erythrocytes, hemolytic, 20: 14275
effects on ESR spectra in single crystals of dimethylglyoxime-d_2, glyoxime, and methylglyoxime at 77°K, 20: 14598
effects on F-bands in sodium bromide–sodium chloride mixed crystals, 20: 14605
effects on fatty acid metabolism in rats, 20: 14379
effects on fine structure in fetal rat cells, 20: 14262
effects on glasses, bibliography on, 20: 15134 (N65-15819)
effects on gonad development in fish, effects of season and temperature on, 20: 14307
effects on hemato-encephalic barrier permeability in rats, 20: 14312
effects on human populations, low-dose, 20: 14331
effects on incidence of *Streptococcus equi* infections in burros, 20: 14288 (AD-627986)
effects on incompatibility in *Oenothera organensis*, 20: 14382
effects on intestinal mucosa after abdominal therapy, 20: 14339
effects on kidney function in dogs, 20: 14342
effects on lipid content in fetal rat cells, 20: 14262
effects on lipid content in mouse liver, 20: 14268
effects on liver cells of pregnant rats, pathological, 20: 14294
effects on liver cells of fetal rats, pathological, 20: 14294
effects on luminescence of thallium-activated cesium iodide and sodium iodide crystals, 20: 14611(T)
effects on lung cancer, 20: 14420
effects on lung reflexes in cats, effects on cardiovascular system of, 20: 14371
effects on lymphocyte distribution in rat spleen and thymus, effects of cell size on, 20: 14318
effects on man, effects of polyvinylpyrrolidone on, 20: 14396
effects on metabolism of rats, delayed, 20: 14368
effects on mice, carcinogenic, 20: 14373
effects on mice, effects of hereditary anemia on, 20: 14290(R) (NYO-

1800-12)
effects on mice, protective effects of sodium hyposulfite against, 20: 14393
effects on mitosis in HeLa cells in culture, 20: 14375
effects on mouse gonads, pathological, 20: 14404
effects on mouse survival, electrolytic balance as predictor of, 20: 14266
effects on mouth following facial therapy, 20: 14324
effects on mucosa of exteriorized rat intestine, pathological, 20: 14364
effects on mutation rate in *Drosophila melanogaster* in presence of serotonin, 20: 14398
effects on Neurospora, photoprotection against, 20: 14358
effects on nucleohistone, 20: 14592
effects on palatine arch and tonsilar carcinomas, 20: 14416
effects on *Phleum pratense*, 20: 14349
effects on phosphate metabolism in Phycomyces, 20: 14264
effects on potassium chloride crystals, F center accumulation kinetics in, (E), 20: 15980(T)
effects on Pseudomonas, mechanism of protective effects of freezing against, 20: 14394
effects on pseudouridine excretion, 20: 14269
effects on pyridine nucleotidase activity of rat liver and spleen, 20: 14362
effects on rats, protective effects of methylandrostenolone against, 20: 14392
effects on reticulo-endothelial function in mice, 20: 14374
effects on seeds of *Vigna sinensis*, biological, 20: 14341
effects on silicon carbide conductivity and n-p effect, (E), 20: 15967
effects on silicon detectors, noise from, (E), 20: 14923
effects on sodium chlorate crystals, color center paramagnetism from, (E), 20: 15961
effects on sodium nitrate crystals, nitrate ion ESR and hfs from, (E), 20: 15965
effects on solid solutions of silver salts, EPR of free atoms in, (E), 20: 15975(T)
effects on spatial avoidance behavior of rats, 20: 14366
effects on sterility in female *Phaseolus mungo*, 20: 14347
effects on survival of 5-bromo-deoxycytidine-treated bone marrow cells, 20: 14333
effects on teeth in newborn rats, head and whole-body exposure, 20: 14322
effects on thermoluminescence of lithium fluoride phosphors, 20: 14887
effects on thymidine index in nephrectomized rats, tracer study, 20: 14258 (AD-627569)
effects on urinary excretion of ammonia and phosphates in rats, 20: 14270
effects on uterine sarcomas, therapeutic, 20: 14301
effects on V center formation in alkali halides at 200°K, 20: 14604
effects on wound healing after radical neck dissection, 20: 14303
emission from electron reactions with compounds, intensity corrections for, 20: 14431 (ANL-7078)
emission in bremsstrahlung excitation of $14 \leq Z \leq 50$ elements, detection efficiency for, (E), 20: 15258
emission in flash x-ray discharges, (E), 20: 15573
monitoring of scattered, in exposure facilities, 20: 14812
reactions with atoms, model for ionization, 20: 15270
reactions with liquid argon, measurement of ionization in, 20: 15259
spectra and location of stellar sources of, (E), 20: 15220
uses for radiation preservation of food, 20: 14938

X-RAY-ABSORPTION ANALYSIS
equipment for monochromatic, of mixed samples, 20: 14505(P)
gamma-emitter activity in, method for calculating, 20: 14498

X-RAY CAMERAS
design of precision back-reflection Laue, 20: 14820 (RFP-636)

X-RAY-DIFFRACTION ANALYSIS
development for thoria and urania crystallite size determination, 20: 15044(R) (MCW-1493, pp 15-25)
uses in metallography, conference on, 20: 15943 (RL-REA-2595)

X-RAY DIFFRACTOMETERS
design, 20: 15064(T) (AD-625748)
performance for residual-stress analysis in uranium, 20: 15945 (RL-REA-2595, pp 43-50)
performance of double-diffracting and standard, comparison, 20: 14823 (RL-SA-2595, pp 73-9)

X-RAY EQUIPMENT
design of miniature, using iodine-125, 20: 14677(P)

X-RAY FLUORESCENCE ANALYSIS
filter systems for, differential, 20: 14487

XENON
diffusion in uranium at 950 and 1000°C, coefficient for, 20: 15090
energy level widths for, K, (T), 20: 15239 (CONF-233(Vol.3), pp 419-39)
ionization in mass spectrometer, formation of multiply charged ions in, 20: 14584(R) (TID-22444)
ionization of, cross sections for ruby-laser-multiphonon, (T), 20: 15276
meson (π^-) interactions at 9 Bev/c, hyperon (Λ) and meson (K^0) production in, (E), 20: 15841
photoabsorption calculations for, using model for atomic excited states, 20: 15270
reactions with cesium, excitation transfer in, (E), 20: 15253
recovery from irradiated reactor fuels during dissolution, 20: 15133(R) (GEAP-4893)
sorption by synthetic zeolite, 20: 14444(R) (MLM-1268)

XENON ISOTOPES
separation by thermal diffusion, 20: 14444(R) (MLM-1268)

XENON ISOTOPES Xe-125
decay of, conversion electron spectra from K-capture, (E), 20: 15701 (CONF-233(Vol.2), pp 128-41)
energy levels in, five-particle isomeric, (T), 20: 15837

XENON ISOTOPES Xe-126
energy levels, (E), 20: 15845

XENON ISOTOPES Xe-127
decay of, conversion electron spectra from K-capture, (E), 20: 15701 (CONF-233(Vol.2), pp 128-41)

XENON ISOTOPES Xe-132
energy level transitions in, conversion coefficients for E2, (E), 20: 15704 (CONF-233(Vol.2), pp 164-76)

XENON ISOTOPES Xe-133
solubility in blood, 20: 14415

XENON OXYFLUORIDES
density and refractive index, 20: 14528
properties of, chemical and physical, 20: 14523
reactions with alkali metal, antimony, and arsenic fluorides, 20: 14523

XYLENE
density and viscosity, 20: 14648
tributyl phosphate–xylene, density and viscosity of, 20: 14648
trioctylamine–xylene, solvent properties for ruthenium, 20: 14650

Y

YANKEE POWER REACTOR
core performance analysis for, (E), 20: 16091(R) (WCAP-6078)
spent fuel analysis for fission products and heavy element isotopes, evaluation of chemical, 20: 14435 (BNWL-SA-503)

YEASTS
radiation effects on, effects of oxygen on recovery from, 20: 14399
radioinduced mutations of *Schizosaccharomyces pombe*, recombination among uv, 20: 14327

YTTERBIUM
determination of, use of organic acids for, 20: 14490
energy level widths for, K, (T), 20: 15239 (CONF-233(Vol.3), pp 419-39)
separation from europium and samarium using organic acids, 20: 14490
spectra of, in liquid ammonia, electronic, 20: 14526

YTTERBIUM ALLOYS
Fe–Yb, preparation and structure, 20: 15110

YTTERBIUM ISOTOPES
deuteron reactions at 15 Mev, isomeric states from, (E), 20: 15856

YTTERBIUM ISOTOPES Yb-170
energy level transitions in, conversion coefficients for E2, (E), 20: 15700 (CONF-233(Vol.2), pp 120-7)
energy level transitions in, conversion coefficients for E2, (E), 20: 15706 (CONF-233(Vol.2), pp 191-7)
internal conversion coefficients of $2^+ \rightarrow 0^+$ transitions in, E2, (E), 20: 15745

YTTERBIUM ISOTOPES Yb-171
neutron resonances at 0 to 150 ev, (E), 20: 15839

YTTERBIUM ISOTOPES Yb-172
neutron resonances at 0 to 150 ev, (E), 20: 15839

YTTERBIUM ISOTOPES Yb-173
energy level transition probabilities in, pairing correlations in E1, (T), 20: 15766
energy level transitions in, delayed E-1, (T), 20: 15765
neutron resonances at 0 to 150 ev, (E), 20: 15839

YTTERBIUM ISOTOPES Yb-174
neutron resonances at 0 to 150 ev, (E), 20: 15839

YTTERBIUM ISOTOPES Yb-176
neutron resonances at 0 to 150 ev, (E), 20: 15839

YTTERBIUM ISOTOPES Yb-177
energy level transitions in, delayed E-1, (T), 20: 15765
half life of isomeric, (E), 20: 15688 (AD-620384)

YTTRIUM
chelates of, urinary excretion of, 20: 14256
content in red-colored Paleozoic deposits in Northern Tien Shan, 20: 14780(T) (AEC-tr-6579)
effects on spectrofluorimetric determination of scandium, 20: 14476
energy level transitions in, Coster-Kronig, (T), 20: 15238 (CONF-233 (Vol.3), pp 398-418)

YTTRIUM ALLOYS
Ag–Y, crystal structure of intermetallic compound YAg_2 in, 20: 15102
Au–Y, crystal structure of intermetallic compound YAu_2 in, 20: 15102
Ce–Y, electric conductivity of dilute, at low temperatures, (E), 20: 15098
Co–Y, cobalt ion EPR in intermetallic compounds of, 20: 15963
Dy–Y, electric conductivity of dilute, at low temperatures, 20: 15098
Er–Y, electric conductivity of dilute, at low temperatures, 20: 15098
Fe–Y, preparation and structure, 20: 15110
Gd–Os–Y, thermal capacity of intermetallic compounds of, at 0.25 to 20.0°K, 20: 15061 (UCRL-11580)
Gd–Y, electric conductivity of dilute, at low temperatures, 20: 15098
Hf–Nb–W–Y, properties for use in aerospace vehicles, 20: 15119
Ho–Y, electric conductivity of dilute, at low temperatures, 20: 15098
La–Y, electric conductivity of dilute, at low temperatures, (E), 20: 15098
Lu–Y, electric conductivity of dilute, at low temperatures, 20: 15098
Mn–Y, preparation and structure, 20: 15110
Nd–Y, electric conductivity of dilute, at low temperatures, (E), 20: 15098
Pr–Y, electric conductivity of dilute, at low temperatures, (E), 20: 15098
Tb–Y, electric conductivity of dilute, at low temperatures, 20: 15098
Y–Zn, crystal structure of intermetallic compound YZn_{12} in, 20: 15102
YTTRIUM CHLORIDES
spectra of chlorine-35- and -37 containing, visible, 20: 14569
YTTRIUM ETHYL SULFATES
proton polarization in ytterbium-doped crystals of, (E), 20: 15964
YTTRIUM ISOTOPES Y-89
deuteron reactions (d,p) at 11.95 Mev, yttrium-90 levels from, (E), 20: 15799
YTTRIUM ISOTOPES Y-90
beta emission by, scintillation counter for measuring, 20: 14874
energy levels from deuteron reactions (d,p) with yttrium-89 at 11.95 Mev, (E), 20: 15799
energy levels from deuteron reactions (d,α) with zirconium-92 at 12.0 Mev, (E), 20: 15799
sorption by rat skin, 20: 14253
use in internal therapy, survey of techniques for, 20: 14406
YTTRIUM OXIDES
effects of inhaled, on blood and lungs of dogs, 20: 14257
YTTRIUM SILICATES
structure of, polymorphic, 20: 14537
YTTRIUM SYSTEMS
B–Co–Y, crystal structure, 20: 14532
B–Ni–Y, crystal structure, 20: 14532
Gd–H–Y, crystal structure, 20: 14546

Z

ZINC
analysis and determination, 20: 14500
coatings of, beta-backscattering gage for measuring thickness of, 20: 14839
content in red-colored Paleozoic deposits in Northern Tien Shan, 20: 14780(T) (AEC-tr-6579)
determination in airborne dusts, spectrochemical, 20: 14475(R) (ORNL-3889, pp 36-39)
determination in automobile lubricants, activation, 20: 14439(R) (GA-5556)
determination in automobile tire rubber, activation, 20: 14439(R) (GA-5556)
determination in automobile paint, activation, 20: 14439(R) (GA-5556)
determination in commercial plastics, activation, 20: 14439(R) (GA-5556)
determination in iron–niobium alloys, chromatographic, 20: 14455(R) (ORNL-3889, pp 25-32)
determination of trace amounts of, in iron, activation, 20: 14471
energy level transitions in, Coster-Kronig, (T), 20: 15238 (CONF-233 (Vol.3), pp 398-418)
energy level widths for, K, (T), 20: 15239 (CONF-233(Vol.3), pp 419-39)
neutron elastic scattering at 0.8 Mev, cross sections for, (T), 20: 15770
neutron elastic scattering at 0.8 Mev, cross sections for, (T), 20: 15770
reactions with uranium monocarbide at 500 to 800°C, 20: 14991
ZINC ALLOYS
Cu–Pb–Zn, radiation effects on wear resistance of lead bronze, fast-neutron, 20: 15140
Y–Zn, crystal structure of intermetallic compound YZn_{12} in, 20: 15102
Zn–Zr, ferromagnetic resonance in intermetallic compounds of, (E), 20: 15960
ZINC CHLORIDES
LiCl–KCl–$ZnCl_2$, reactions with uranium monocarbide–zinc at 500 to 800°C, 20: 14991
ZINC, DIMETHYL-
decomposition in ion source of mass spectrometer, mechanism of, 20: 14584(R) (TID-22444)
ZINC IONS
effects on foils of copper, 20: 15146
ZINC ISOTOPES Zn-65
decay of, K/L ratio for electron-capture, (E/T), 20: 15713 (CONF-233 (Vol.2), pp 365-8)
decay of, x-ray emission rates for electron-capture, (E), 20: 15242 (CONF-233(Vol.3), pp 465-79)
radioactivity of, absolute measurement of, 20: 15690 (CEA-R-2813)
ZINC SYSTEMS
Al–C–Nb–Zn, phase studies, 20: 15103
Al–C–Ta–Zn, phase studies, 20: 15103
UC–Zn, reactions with potassium chloride–lithium chloride–zinc chloride at 500 to 800°C, 20: 14991
ZIRCALOY-2
hydride precipitate orientation in, effects of stress on, 20: 15120
ignition properties of wastes from machining operations on, 20: 15001 (HW-66930)
testing of tubes of, ultrasonic equipment and method for nondestructive, 20: 14714
testing reactor tubes of, nondestructive method for, 20: 14711
welding of tubes of, to stainless steel tube sheets, 20: 15019
ZIRCALOY-4
ignition properties of wastes from machining operations on, 20: 15001 (HW-66930)
ZIRCONIUM
compatibility with water in reactor environment, 20: 14996
corrosion cracking in alcohol–acid solution, effects of water on stress, 20: 14988
determination in dust samples by microchemical methods and autoradiography, 20: 14472
determination in glass samples, activation, 20: 14439(R) (GA-5556)
determination in niobium–zirconium alloys by spectrography of solutions on cored graphite, 20: 14446 (N64-25607)
determination in uranium tetrafluoride, spectrographic, 20: 14473
ductility of, combined grain size and temperature effects on, 20: 15042(R) (IITRI-578-P27-14)
effects on spectrofluorimetric determination of scandium, 20: 14476
embrittlement by hydrogen during slow-bend tests, 20: 14993
energy level transitions in, Coster-Kronig, (T), 20: 15238 (CONF-233 (Vol.3), pp 398-418)
energy level widths for, K, (T), 20: 15239 (CONF-233(Vol.3), pp 419-39)
neutron elastic scattering at 0.8 Mev, cross sections for, (T), 20: 15770
neutron resonance absorption integrals for, (E), 20: 15691 (CEA-R-2840)
oxidation in thiocyanic acid at 25°C, 20: 14995
proton reactions (p,n) at 30 to 50 Mev, distributions from, 20: 15729(R) (RHEL/R-112, pp 37-66)
reactions with sodium, high-temperature, 20: 15033(R) (ANL-7152, pp 87-96)
reactions with water during reactor accidents, 20: 16019(T) (BMI-X-10154)
separation from hafnium by ion exchange, 20: 14657(P)
UC–ZrC, fission product release at high temperatures, 20: 14959(R) (N65-20797)
ZIRCONIUM ALLOYS
ignition properties of wastes from machining operations on, 20: 15001 (HW-66930)
Co–Zr, cobalt ion EPR in intermetallic compounds of, 20: 15963
Co–Zr, phase studies, 20: 14533
Cr–Fe–Zr, corrosion by steam at 300 to 500°C, effects of nitrogen impurity content on, 20: 14980(R) (GEAP-5065)
Cr–Fe–Zr, corrosion by steam at 500°C, effects of metallurgical processing variables on, 20: 14980(R) (GEAP-5065)
Mg–Zr, development and fabrication of EdF2, for fuel cans, 20: 15018
Mg–Zr, nondestructive method for testing cladding of, 20: 14711
Mo–Nb–U–Zr, mechanical properties of gamma-phase uranium-base, 20: 15060 (UCRL-7771)
Mo–Ti–Zr, machining of TZM, 20: 15014
Mo–Zr, grain boundary structure in, internal friction studies of, 20: 15128
Nb–Sn–Zr, superconductivity of fused, 20: 15123
Nb–U–Zr, mechanical properties of gamma-phase uranium-base, 20: 15060 (UCRL-7771)
Nb–Zr, analysis for zirconium by spectrography of solutions, 20: 14446 (N64-25607)
Nb–Zr, corrosion by hydrochloric, phosphoric, and sulfuric acids, effects of alloy composition on, 20: 14997
Nb–Zr, emissivity of titanate coatings on, 20: 15057(R) (PWA-2750)
Nb–Zr, formation of niobium carbide surface films on, activation energies for, 20: 14992
Nb–Zr, hardness, 20: 15073
Nb–Zr, internal friction peak in, dislocation-relaxation, 20: 15122
Nb–Zr, reactions with sodium, high-temperature, 20: 15033(R) (ANL-

7152, pp 87-96)
Nb–Zr, use in heat transfer tube, 20: 14699(P)
Pu–U–Zr, density and structure of, 20: 16060(R) (ANL-7152, pp 1-49)
U–Zr, mechanical properties of gamma-phase uranium-base, 20: 15060 (UCRL-7771)
W–Zr, extrusion and swaging, 20: 15101
W–Zr, properties for high-temperature uses, 20: 15101
Zn–Zr, ferromagnetic resonance in intermetallic compounds of, (E), 20: 15960

ZIRCONIUM BORIDES
abrasive properties, 20: 15109
reactions with copper and nickel mattes, slags, molten salts, and refractory metals, 20: 14989

ZIRCONIUM CARBIDES
abrasive properties, 20: 15109
preparation of spherical particles of, procedure and apparatus for, 20: 14971(P)
reactions with copper and nickel mattes, slags, molten salts, and refractory metals, 20: 14989
testing as high-temperature heater for electric resistance furnaces, 20: 15112
thermodynamic properties of, at high temperatures, 20: 15052 (NP-15880)
HfC–ZrC, crystal structure of solid solutions in, x-ray studies of, 20: 15074
UC–ZrC, aqueous processing of graphite- and silicon dicarbide-coated fuel elements of, 20: 14638 (NP-15753)
UC–ZrC, development as fuel for thermionic space power plants, 20: 14959(R) (N65-20797)
UC–ZrC, development as fuel for thermionic space power plants, 20: 14960(R) (N65-20798)
UC–ZrC, development as fuel for thermionic space power plants, 20: 14961(R) (N65-20801)
UC–ZrC, fabrication into fuel for thermionic space power plants, 20: 14962(R) (N65-20803)
UC–ZrC, fission product release at high temperatures, 20: 14960(R) (N65-20798)
UC–ZrC, fission product release at 1800°C, 20: 14961(R) (N65-20801)
UC–ZrC, properties for cathodes in thermionic space power plants, 20: 15046(R) (N65-15820)

ZIRCONIUM FLUORIDES
BeF_2–LiF–ThF_4–UF_4–ZrF_4, spectra of irradiated, absorption and reflectance, 20: 14453(R) (ORNL-3889, pp 12-14)
BeF_2–LiF–UF_4–ZrF_4, analysis for uranium, polarographic, 20: 14454(R) (ORNL-3889, pp 17-24)

ZIRCONIUM HYDRIDES
precipitation in Zircaloy-2 crystals, effects of stress on, 20: 15120

ZIRCONIUM ISOTOPES
deuteron reactions at 15 Mev, isomeric states from, (E), 20: 15856

ZIRCONIUM ISOTOPES Zr-90
internal conversion probabilities in, reduced M and N E0, (T), 20: 15771
proton reactions (p,n) at 30 to 50 Mev, distributions from, 20: 15729(R) (RHEL/R-112, pp 37-66)

ZIRCONIUM ISOTOPES Zr-92
deuteron reactions (d,α) at 120 Mev, yttrium-90 levels from, (E), 20: 15799
parity and spin of, from deuteron scattering data, 20: 15850

ZIRCONIUM ISOTOPES Zr-95
determination in atmospheric and precipitation samples, methods for radiochemical, 20: 14430 (AD-620219)

ZIRCONIUM NITRATES
diffusion of carbon in, carbide film formation in, 20: 15072

ZIRCONIUM NITRIDES
reactions with copper and nickel mattes, slags, molten salts, and refractory metals, 20: 14989

ZIRCONIUM OXIDES
analysis for hafnium, x-ray-fluorescence, 20: 14496
preparation of spherical particles of, procedure and apparatus for, 20: 14971(P)
reactions with copper and nickel mattes, slags, molten salts, and refractory metals, 20: 14989
sorptive properties for chloride and potassium ions, effects of pH on, 20: 14651
stability in dry hydrogen at 1100 to 2000°C, 20: 14986
CaO–CeO_2–ZrO_2, electric conductivity and structure of, at 500 to 1000°C, 20: 14536
CaO–Sm_2O_3–UO_2–ZrO_2, corrosion and surface properties of, 20: 16089(R) (WAPD-MRP-114)
CaO–UO_2–ZrO_2, corrosion and surface properties of, 20: 16089(R) (WAPD-MRP-114)
CaO–UO_2–ZrO_2, properties of, in-pile, 20: 15138 (WAPD-392)
Nb_2O_5–ZrO_2, phase studies, 20: 15079
PuO_2–UO_2–ZrO_2, preparation and thermophysical properties, 20: 15054(R) (NUMEC-3505-11)
UO_2–ZrO_2, properties of, effects of calcia additions on in-pile, 20: 15138 (WAPD-292)
UO_2–ZrO_2, radiation effects on plates of, in-pile, 20: 16089(R) (WAPD-MRP-114)

ZIRCONIUM SYSTEMS
B–Co–Zr, phase studies, 20: 14533
B–Cu–Zr, crystal structure, 20: 14532
B–Fe–Zr, crystal structure, 20: 14532
C–Mo–Nb–Zr, heat treatment of, 20: 14972(P)
C–Nb–Ta–Zr, heat treatment of, 20: 14972(P)
C–Nb–Ti–Zr, heat treatment of, 20: 14972(P)
C–Nb–V–Zr, heat treatment of, 20: 14972(P)
C–Nb–W–Zr, heat treatment of, 20: 14972(P)
C–Nb–W–Zr, tensile properties of D-43, 20: 15068
Mo–Nb–N–Zr, heat treatment of, 20: 14972(P)
Mo–Nb–O–Zr, heat treatment of, 20: 14972(P)
Nb–N–Ta–Zr, heat treatment of, 20: 14972(P)
Nb–N–Ti–Zr, heat treatment of, 20: 14972(P)
Nb–N–V–Zr, heat treatment of, 20: 14972(P)
Nb–N–W–Zr, heat treatment of, 20: 14972(P)
Nb–O–Ta–Zr, heat treatment of, 20: 14972(P)
Nb–O–Ti–Zr, heat treatment of, 20: 14972(P)
Nb–O–V–Zr, heat treatment of, 20: 14972(P)
Nb–O–W–Zr, heat treatment of, 20: 14972(P)
UP–Zr, compatibility, 20: 15032(R) (ANL-7152, pp 50-72)

REPORT NUMBER INDEX

Reports, conference papers and proceedings, numbered translations, and patents abstracted during the period are included in this index. Each item is listed by report number; this is followed by the abstract number and a brief notation regarding public availability. The index entries show which reports are on file in the depository libraries, which reports have been published in open-literature journals (journal citation given), and which reports can be purchased (source and price). Whenever a report is identified by more than one number, cross references from secondary to primary report numbers are cited.

The report number codes apply to AEC reports unless designated otherwise. Non-AEC reports are identified by parenthetical notes after the report codes; e.g., (non-AEC), (British), (Canadian), (French). The note (Misc.) identifies those codes used for both USAEC and non-AEC reports. Patents are listed under the heading "PATENTS"; the country of origin is included in parentheses.

A comprehensive listing of both AEC and non-AEC report codes is contained in TID-8505(5th Rev.), *Report Number Series Used by the Division of Technical Information in Cataloging Reports*. This information is also included in the Cumulative Report Number Index (issued annually).

Public Availability of USAEC Reports

All USAEC reports abstracted in *NSA* are available to the public through one or more of the following sources:

(1) Depository libraries in the United States, in other countries, and in international agencies. A list of these depositories appears on the inside covers of each issue of *NSA*.

(2) Scientific and technical journals or other publications.

(3) Microcard Editions, Inc., in Microcard and micronegative form. Orders and inquiries should be sent to: Accounting and Shipping Department, West Salem, Wisconsin 54669.

(4) Clearinghouse for Federal Scientific and Technical Information, U. S. Department of Commerce, Springfield, Virginia 22151.

(5) Superintendent of Documents, U.S. Government Printing Office, Washington, D. C. 20402.

Public Availability of Non-AEC Reports

U. S. Reports. Many reports of U. S. Government agencies are available to the public from the Clearinghouse for Federal Scientific and Technical Information (CFSTI). This availability is given when known. Such reports should be ordered by AD number or NASA-N number. If availability is not shown, inquiries may be directed to CFSTI. In the case of NP numbers, inquiries should be by title and author.

Non-U. S. Reports. Many reports of atomic energy establishments of other countries are deposited in the libraries listed on the inside covers of each issue of *NSA*.

Additionally, the following have made their reports available as indicated.

AUSTRALIA

Australian Atomic Energy Commission Research Establishment. Available upon request from the Library, Australian Atomic Research Establishment, Private Mail Bag, Sutherland, New South Wales, Australia.

BELGIUM

Centre d'Étude de l'Énergie Nucléaire. Available upon request to individuals and organizations, from the Centre d'Étude de l'Énergie Nucléaire (CEN), 31, Rue Belliard, Bruxelles, Belgium.

CANADA

Atomic Energy of Canada Limited. For sale by the Technical Information Officer, Atomic Energy of Canada Limited, Chalk River, Ontario, Canada. Copies are also deposited in libraries in the United Kingdom.

National Research Council of Canada. Available from the National Research Council of Canada, Ottawa 2, Ontario, Canada.

DENMARK

Atomic Energy Commission Research Establishment, Risø. Available on exchange from the Library, Danish Atomic Energy Commission, Risø, Roskilde, Denmark. Also for sale by Jul. Gjellerup, Booksellers, 87 Sölvgade, København K., Denmark.

Danatom. Available on loan from Research Establishment, Risø, Roskilde, Denmark. Copies are available from Danatom, Aurehøjvej 2, Hellerup, Denmark.

EURATOM

Reports from the Commission of the European Atomic Energy Community are available from: Presses academiques europeennes, 98, chaussee de Charleroi, Brussels 6, Belgium; and Office central de vente des publications des Communautes eurodeennes 2, place de Metz, Luxemburg.

FRANCE

Commissariat à l'Énergie Atomique. Inquiries for reports numbered 1-2199 should be addressed to Commissariat à l'Énergie Atomique, Service Central de Documentation, Centre d'Études Nucléaires de Saclay, Boite Postale No. 2, Gif-sur-Yvette (S. et O.), France. Reports numbered 2200 and above are available from La Documentation Francaise, 16 Rue Lord-Byron, Paris VIII, France.

Service Central de Protection contre les Rayonnements Ionisants. Copies are available from Ministère de la Santé Publique, Service Central de Protection contre les Rayonnements Ionisants, B. P. n° 35—LE VESINET (S. et O.), France.

GERMANY

Deutsches Elektronen-Synchrotron DESY. Copies are available from Deutsches Elektronen-Synchrotron Desy, Dokumentation, 2000 Hamburg-Gr. Flottbek 1, Notkestieg 1, Germany.

Gesellschaft für Kernforschung mbH (KFK). Copies are available from Gesellschaft für Kernforschung mbH, 75 Karlsruhe, Postfach 947, Germany. Copies are also deposited in many national nuclear centers in the world.

Kernforschungsanlage. Copies may be ordered from Zentralbibliothek der Kernforschungsanlage Jülich, Jülich, Bundesrepublik Deutschland.

Hahn-Meitner-Institute für Kernforschung. Available without charge from Hahn-Meitner-Institute für Kernforschung Berlin, Bibliothek, Glienicker Strasse 100, 1 Berlin

39, Germany. Copies are deposited in many national nuclear centers in the world.

Johann-Wolfgang-Goethe Universität, Frankfurt Am Main, Institut für Kernphysik, (IKF). Copies are available from Gmelin Institut, 40-42 Varrentrappstrasse, Frankfurt (Main), West Germany.

ISRAEL

Israel Atomic Energy Commission. Available without charge from Ministry of Defence/Atomic Energy Commission, Soreq Research Establishment, Yavne, Israel. Copies are deposited in libraries in Israel and in other countries.

ITALY

Centro Informazioni Studi Esperienze (CISE). For sale at CISE Press Office, Casella Postale 3986, Milano, Italy. Copies are deposited in libraries in Italy.

Comitato Nazionale per l'Energia Nucleare. Copies are available from Comitato Nazionale per l'Energia Nucleare, Divisione Affari Internazionali e Studi Economici, Ufficio Pubblicazioni, Via Belisario, 15, Roma, Italy.

JAPAN

Japan Atomic Energy Research Institute (JAERI). Available from the Staff Supply Cooperative of Japan Atomic Energy Research Institute (JAERI), 1-1 Tamura-Cho, Shiba, Minato-Ku, Tokyo, Japan. Copies are deposited in depositories in Tokyo, Nagoya, and Osaka.

Nagoya University. Copies are available from Research Information Center, Institute of Plasma Physics, Nagoya University, Nagoya, Japan.

University of Tokyo. Available free of charge from Institute for Nuclear Study, University of Tokyo, Tanashi-Machi, Kitatama-gun, Tokyo, Japan.

NETHERLANDS

Reactor Centrum Nederland. For sale by Reactor Centrum Nederland, 112 Scheveningseweg, 's-Gravenhage, The Netherlands. Copies are deposited in university libraries in Holland and in many national nuclear centers in the world.

NEW ZEALAND

Institute of Nuclear Sciences. Copies are available from Librarian, Institute of Nuclear Sciences, D.S.I.R., Private Bag, Lower Hutt, New Zealand. Copies are deposited in other countries.

NORWAY

Forsvarets Forskningsinstitutt. Copies available from Norwegian Defence Research Establishment, Library, P. O. Box 25, Kjeller, Norway.

Institutt for Atomenergi. "KR" reports are available on an exchange basis from the Library, Institutt for Atomenergi, Box 40, Kjeller, Norway. Other series are not generally available to the public.

Norwegian Reactor School. Copies are available from The Library, Institutt for Atomenergi, P. O. Box 40, Kjeller, Norway.

PAKISTAN

Atomic Energy Center. Copies are available from Atomic Energy Center, P. O. Box 658, Lahore, (West Pakistan).

POLAND

Reports of the Polish nuclear institutes are published by the Nuclear Energy Information Center of the Government Commissioner for Use of Nuclear Energy. Copies are available from Ośrodek Informacji o Energii Jądrowej, Warszawa, PKiN, Poland.

SPAIN

Junta de Energia Nuclear. "JEN" reports are available without charge from Servicio de Documentation, Junta de Energia Nuclear, Ciudad Universitaria, Madrid (3), Spain.

SWEDEN

Aktiebolaget Atomenergi. "AE" reports are for sale from Aktiebolaget Atomenergi, Library Section, Box 43041, Stockholm 43, Sweden. Bibliographies and literature surveys of the VDDIT- series may be obtained from Aktiebolaget Atomenergi, Information Office, Scientific and Technical Information, Box 43041, Stockholm 43, Sweden. Other series are not generally available to the public. Organizations in the atomic energy field may obtain copies from Aktiebolaget Atomenergi. Microcopy of AE reports is available from the International Documentation Centre, Tumba, Sweden.

SWITZERLAND

CERN European Organization for Nuclear Research. Available without charge from CERN European Organization for Nuclear Research, Geneva 23, Switzerland. Copies are deposited in libraries in 13 countries.

Eidgenössisches Institut für Reaktorforschung. "EIR" reports are available from Eidgenössiches Institut für Reaktorforschung, c/o Bibliothek, Würenlingen/Ag, Switzerland.

TURKEY

Turkish Atomic Energy Commission. Copies are available free of charge from T.A.E.C., Çekmece Nuclear Research Center, P. O. Box 1, Airport, Istanbul, Turkey.

UNITED KINGDOM

United Kingdom Atomic Energy Authority. Some reports are for sale in the United States by the British Information Service (BIS), 845 Third Avenue, New York, N. Y. 10022. United Kingdom reports generally may be purchased from Her Majesty's Stationery Office, London. Copies not for sale by Her Majesty's Stationery Office may be purchased in microcopy form from Micro Methods Limited, East Ardsley, Wakefield, Yorks, England. Report copies are deposited in a large number of libraries in England.

Conferences

Published conference proceedings as well as individual unpublished papers from conferences are included in this index. A CONF number is assigned to the conference if published proceedings are received and also if only a single paper is received. The base number used is year-month-sequence. Thus, the number CONF-650101 would indicate that the conference was held in 1965, in January, and that this was the first January 1965 conference so received. This number would be assigned to complete published proceedings, or if individual papers are received, the base number would be extended to include a paper number, i.e., CONF-650101-1. As additional papers are received, they will be assigned consecutive numbers in the series, CONF-650101-1, 2, 3, 4, etc. This numbering system ensures that all papers received from a conference will be associated with that conference in this index.

If published proceedings are received after the receipt of individual papers, the complete proceedings will be abstracted and the abstract number will appear in this index with the base CONF number.

Abbreviations Used in Availability Column

AECL	For sale by Atomic Energy of Canada Ltd., Chalk River, Ontario, Canada.
BIS	For sale by British Information Service, 845 Third Avenue, New York, N. Y. 10022
CFSTI	For sale by the Clearinghouse for Federal Scientific and Technical Information, U. S. Department of Commerce, Spring-

field, Virginia 22151. The symbol "cy" indicates that the format of the item sold may be either a printed document or a photographic reproduction (two-thirds of original size) depending upon the availability of printed stock. The indicated price is for either format. The symbol "mn" is used to indicate that copy is also available in the form of micronegatives (microfiche).

Dep. — AEC reports: Full-size copy is on deposit in the depository libraries both inside and outside the United States. These reports are also for sale by Microcard Editions, Inc., Accounting and Shipping Department, West Salem, Wisconsin 54669.

Non-AEC reports: Full-size copy on deposit in the depository libraries in the United States only.

Dep.(mc) — Same as for Dep., except copy is in Microcard form.

Dep.(mn) — Same as for Dep., except copy is in micronegative (microfiche) form.

DSIR — For sale by the National Lending Library for Science and Technology (D.S.I.R.), Boston Spa, Yorkshire, England.

DTI Extension — Available from the U. S. Atomic Energy Commission, Division of Technical Information Extension, P. O. Box 62, Oak Ridge, Tennessee 37830.

EM — Blueprints and microcopy of AEC engineering drawings are available from Clearinghouse for Federal Scientific and Technical Information, U. S. Department of Commerce, Springfield, Virginia 22151. Current prices of the CAPE- packages may be obtained from this address. TID-4100, available from the Division of Technical Information Extension, P. O. Box 62, Oak Ridge, Tennessee 37831, contains information on all the CAPE- packages for sale.

Gmelin — Available at a nominal charge and under the AED- number shown from Atomic Energy Documentation Center, Gmelin Institute, 40-42 Varrentrappstrasse Frankfurt (Main), West Germany.

GPO — For sale by the Superintendent of Documents, Government Printing Office, Washington, D. C. 20402.

HMSO — Her Majesty's Stationery Office, London.

IAEA — Available from the International Atomic Energy Agency, Vienna, Austria, and from its sales agencies in various countries throughout the world. A list of these agencies is found in each STI/DOC and STI/PUB publication.

JCL — For sale by the Special Libraries Association Translation Center, John Crerar Library, 35 West 33rd Street, Chicago, Illinois 60616.

LC — For sale by the Library of Congress, Photoduplication Service, Washington, D. C. 20540.

NAS — National Academy of Sciences, National Research Council, Washington, D. C. 20418.

NRC — For sale by the National Research Council of Canada, Ottawa, Ontario, Canada.

ORINS — Available on interlibrary loan from the Library, Oak Ridge Associated Universities, Post Office Box 117, Oak Ridge, Tennessee 37830.

OTS — See CFSTI.

UKAEA, London — Available from United Kingdom Atomic Energy Authority, 11 Charles II Street, London, S. W. 1.

UN — United Nations Bookshop, United Nations Headquarters, New York, New York.

USGS — Available free of charge from the U. S. Geological Survey, Washington, D. C. 20242.

[The symbols "ph," "mf," and "fs" are used to designate that copy is available only in photostat, microfilm, or facsimile form. The symbol "mn" is used to designate that copy is available in micronegative (microfiche) form. The symbol "cy" is used to designate full size or photographically enlarged copy (two-thirds of original size).]

Report No.	Abstract No.	Availability
NUMERICAL	**(Misc.)**	
65SD5322-A	20-14724	
ACNP–	**(Misc.)**	
65600	20-16059	Dep. mn. CFSTI $2.00 cy, $0.50 mn
AD–	**(Misc.)**	
620189	20-15939	CFSTI $2.00 cy, $0.50 mn
620219	20-14430	CFSTI $3.00 cy, $0.75 mn
620243	20-15586	CFSTI $1.00 cy, $0.50 mn
620244	20-15587	CFSTI $2.00 cy, $0.50 mn
620276	20-16143	CFSTI $1.00 cy, $0.50 mn
620289	20-15235	CFSTI $2.00 cy, $0.50 mn
620324	20-15568	CFSTI $2.00 cy, $0.50 mn
620384	20-15688	CFSTI $3.00 cy, $0.50 mn
620395	20-14844	CFSTI $3.00 cy, $0.75 mn
620407	20-15190	CFSTI $6.00 cy, $1.25 mn
620434	20-14845	CFSTI $3.00 cy, $0.75 mn
620468	20-14660	CFSTI $3.00 cy, $0.75 mn
620511	20-15292	CFSTI $1.00 cy, $0.50 mn
620650	20-16110	CFSTI $2.00 cy, $0.50 mn
620664	20-15867	CFSTI $2.00 cy, $0.50 mn
620682	20-15588	CFSTI $3.00 cy, $0.75 mn
625748	20-15064	CFSTI $1.00 cy, $0.50 mn
625789	20-15887	CFSTI $1.00 cy, $0.50 mn
625791	20-14693	CFSTI $1.00 cy, $0.50 mn
625837	20-14286	CFSTI $1.00 cy, $0.30 mn
626996	20-14287	CFSTI $2.00 cy, $0.50 mn
627569	20-14258	CFSTI $1.00 cy, $0.50 mn
627890	20-15929	CFSTI $2.00 cy, $0.50 mn
627986	20-14288	CFSTI $1.00 cy, $0.50 mn
628186	20-15868	CFSTI $3.00 cy, $0.75 mn
628317	20-15869	CFSTI $2.00 cy, $0.50 mn
628982	20-14733	CFSTI $3.00 cy, $0.75 mn
AE–	**(Non-AEC)**	
211	20-14782	Dep. mn
212	20-16118	Dep. mn
AEC-tr–	**(For complete listing see TID-4025)**	
6579	20-14780	CFSTI $1.00 cy, $0.50 mn. JCL $1.60 fs, $0.80 mf
AECD-HP–	**(Pakistani)**	
2	20-14783	Dep. mn
AECL–	**(Canadian)**	
2517	20-14846	Dep. AECL $1.00
AED-C–	**(Non-AEC)**	
32-1(Vol.1 and Vol.2)	20-16144	Gmelin, Frankfurt, W. Ger. or Larchmont, N. Y. $5.00
AERE-R–	**(British)**	
4831	20-14883	Phys. Med. Biol., 11: 1-14(1966)
4843	20-14551	J. Nucl. Mater., 19: 117-19(1966)
4865	20-15774	J. Inorg. Nucl. Chem., 27: 2481-91(1965)
5015	20-14784	Dep. BIS $0.60. HMSO 3s.
5035	20-15145	Phys. Status Solidi, 12: 877-90(1965)
AFCRL–	**(Non-AEC)**	
65-410	20-14430	See AD-620219
65-453	20-15867	See AD-620664
65-507	20-15588	See AD-620682
65-621	20-15586	See AD-620243
65-622	20-15587	See AD-620244
65-856	20-15589	See ASE-1125
65-858	20-15868	See AD-628186
AFOSR–	**(Misc.)**	
65-1192	20-15939	See AD-620189
65-1201	20-15568	See AD-620324
AGN–	**(Misc.)**	
8166	20-15028	Dep. mn. CFSTI $1.00 cy, $0.50 mn
ANL–		
7070	20-15029	Dep. mn. CFSTI $2.00 cy, $0.50 mn
7073	20-14684	CFSTI $4.00 cy, $0.75 mn
7078	20-14431	Dep. mn. CFSTI $1.00 cy, $0.50 mn
7079	20-15132	Dep. mn. CFSTI $1.00 cy, $0.50 mn
7091	20-14975	Dep. mn. CFSTI $5.00 cy, $1.00 mn
7102	20-15030	Dep. mn. CFSTI $1.00 cy, $0.50 mn
7109	20-14949	Dep. mn. CFSTI $1.00 cy, $0.50 mn
7116	20-15031	Dep. mn. CFSTI $2.00 cy, $0.50 mn
7123	20-14432	Dep. mn. CFSTI $1.00 cy, $0.50 mn
7152	20-15994	Dep. mn. CFSTI $4.00 cy, $0.75 mn
ANL-Trans–		
265	20-15735	Dep. mn. JCL $1.10 fs, $0.80 mf
ASE–	**(Non-AEC)**	
1125	20-15589	CFSTI
ASTRA-G–	**(Non-AEC)**	
71	20-14688	See N65-20692
AWRE-O–	**(British)**	
10/66	20-14730	Dep. BIS $0.60. HMSO 3s. 0d.
16/66	20-14976	Dep. BIS $0.50. HMSO 2s. 6d.
103/65	20-15665	Dep. BIS $1.20. HMSO 6s.
BAW–	**(Misc.)**	
296	20-16061	Dep. mn. CFSTI $2.00 cy, $0.50 mn
298	20-14433	Dep. mn. CFSTI $1.00 cy, $0.50 mn
BM-RI–	**(Misc.)**	
6734	20-14956	Bureau of Mines Free
BMI–	**(Misc.)**	
1754	20-14957	Dep. mn. CFSTI $2.00 cy, $0.50 mn
BMI-X–		
10154	20-16019	Dep. mn. CFSTI $3.00 cy, $0.50 mn
BMwF-FBK–	**(German)**	
65-01	20-14847	Dep. mn. Gmelin
65-02	20-14848	Dep. mn. Gmelin
BNL–		
741(Rev.)	20-15156	Dep. mn. CFSTI $1.00 cy, $0.50 mn
931	20-14231	Dep. mn. CFSTI $3.00 cy, $1.50 mn
966	20-15995	Dep. mn. CFSTI $4.00 cy, $0.75 mn
972	20-14958	Dep. mn. CFSTI $2.00 cy, $0.50 mn
8558	20-16132	Dep. mn; CFSTI $2.00 cy, $0.50 mn
9292	20-15677	Nucl. Sci. Eng., 24: 212-16(1966)
9410	20-15428	pp. 524-6 of Resonant Particles. Athens, Ohio, Fazl-i-Umar Research Inst., 1965
9415	20-14647	Ind. Eng. Chem., Process Design Develop., 5: 51-9(1966)
9467	20-15287	Phys. Rev., 142: 844-51(1966)
9509	20-14289	ORAU
9571	20-15333	Phys. Rev., 142: 893-5(1966)
9582	20-14891	Rev. Sci. Instrum., 37: 291-3(1966)
9596	20-15677	See BNL-9292
9720	20-14849	Dep. mn. CFSTI $1.00 cy, $0.50 mn
9763	20-14850	Dep. mn. CFSTI $1.00 cy, $0.50 mn
9980	20-14851	Dep. mn. CFSTI $1.00 cy, $0.50 mn
BNWL–		
47	20-14753	Dep. mn. CFSTI $3.00 cy, $0.50 mn
49	20-15034	Dep. mn. CFSTI $6.00 cy, $1.25 mn
113-7	20-16145	Dep. mn. CFSTI $1.00 cy, $0.50 mn
176	20-16120	Dep. mn. CFSTI $1.00 cy, $0.50 mn
180	20-14434	Dep. mn. CFSTI $2.00 cy, $0.50 mn
182	20-14785	Dep. mn. CFSTI $1.00 cy, $0.50 mn
196	20-15035	Dep. mn. CFSTI $1.00 cy, $0.50 mn
197	20-16121	Dep. mn. CFSTI $3.00 cy, $0.50 mn
205	20-15036	Dep. mn. CFSTI $2.00 cy, $0.50 mn
BNWL-SA–		
219	20-14237	Nucl. Safety, 7: 92-9;102(1965)
465	20-14786	Dep. mn. CFSTI $3.00 cy, $0.75 mn
503	20-14435	Dep. mn. CFSTI $1.00 cy, $0.50 mn
504	20-14436	Dep. mn. CFSTI $1.00 cy, $0.50 mn
CALT–		
68-41	20-15506	pp 17-32 of Resonant Particles. Athens, Ohio, Fazl-i-Umar Research Inst., 1965
68-55	20-15365	Phys. Rev., 142: 1258-62(1966)
CAPE–		
1060	20-14898	
1263	20-14899	

Report No.	Abstract No.	Availability
1269	20-16139	
1282	20-14900	
1283	20-14901	
1287	20-14831	
1288	20-14902	
1293	20-14903	
1300	20-14832	
1308	20-14833	
1311	20-14906	
1312	20-14673	
1316	20-14834	
1317	20-14904	
1319	20-15922	
1320	20-15924	
1321	20-14675	
1324	20-15923	
1326	20-14809	
1328	20-15921	
1329	20-14674	
1330	20-14905	
CEA-Bib–	**(French)**	
64	20-14787	Dep. mn
CEA-R–	**(French)**	
2471	20-14685	Dep. mn
2621	20-15037	Dep. mn
2786	20-15689	Dep. mn
2813	20-15690	Dep. mn
2836	20-16020	Dep. mn
2840	20-15691	Dep. mn
2856	20-15997	Dep. mn
2862	20-14852	Dep. mn
2879	20-14437	Dep. mn
2881	20-15870	Dep. mn
2890	20-16021	Dep. mn
CEA-tr–	**(French)**	
X-356	20-14825	Dep. mn. JCL $1.60 fs, $0.80 mn
CEAL–		
1026	20-15306	Dep. mn. CFSTI $1.00 cy, $0.50 mn
CEND–	**(Misc.)**	
540	20-14438	Dep. mn. CFSTI $5.00 cy, $1.00 mn
CERN–	**(European Organization for Nuclear Research)**	
66-1	20-15157	Dep. mn
66-3	20-15692	Dep. mn
542	20-15158	Dep. mn
CNEA–	**(Argentinian)**	
159	20-14853	Dep. mn
CONF-233–	**(Conference on the Role of Atomic Electrons in Nuclear Transformations, Warsaw, Sept. 1963)**	
Vol.1	20-15693	Dep. ORAU
Vol.2	20-15697	Dep. URAU
Vol.3	20-15236	Dep. ORAU
CONF-365–	**20-14810**	**(Symposium on Environmental Monitoring, Berkeley, Gloucestershire, England, Oct. 1963) $17.50**
CONF-620804–	**20-14729**	**(Conference on Aeronautical Sciences, Stockholm, Aug. 27–31, 1962)**
CONF-630101–	**20-15129**	**(3rd Symposium on Naval Structural Mechanics, New York, Jan. 23–25, 1963) 5£; $15.00**
CONF-630506–	**(Conference on Science of Ceramics, Noordwijk ann Zee, Netherlands, May 13–17, 1963)**	
Vol.2	20-14970	London, Academic Press Inc., 1965. 434p. $13.50.
CONF-630806–	**20-15234**	**(Symposium on the Solar Spectrum, Utrecht, Aug. 26–31, 1963)**
CONF-631104–	**(Meeting on the Utilization of Research Reactors, Sao Paulo, Brazil, Nov. 4–8, 1963)**	
9	20-16134	See IEA-102
CONF-640408–	**(Wear Congress "Assocn. for Knowledge of Materials," Utrecht, Apr. 22, 1964)**	
1	20-15998	See EUR-2117.n
CONF-640415–	**20-16157**	**(Symposium on Fresh Water from the Sea, Milan, Apr. 20–21, 1964) $9.00**
CONF-640416–	**(Joint Working Group Meeting, Aldermaston, Berks., England, Apr. 27–29, 1964)**	
1	20-15060	See UCRL-7771
CONF-640626–	**20-14998**	**(8th Symposium on Metallurgy, Cadarache, France, June 25–26, 1964)**
CONF-640921–	**20-15293**	**(Symposium on Thermionic Conversion, Saclay, France, Sept. 10–11, 1964) Dep. mn**
CONF-640926–	**(3rd All-Union Symposium on Wave Diffraction, Tbilisi, U.S.S.R., Sept. 24–30, 1964)**	
Absts.	20-15149	See JPRS-33458
CONF-641222–	**20-14940**	**(1st International Symposium on the Use of Ionizing Radiation for the Sterilization of Medical Products, Roskilde, Denmark, Dec. 6–9, 1964)**
CONF-650119–	**20-15749**	**(15th Annual Conference on Nuclear Spectroscopy and the Structure of the Atomic Nucleus, Minsk, U.S.S.R., Jan. 25–Feb. 2, 1965)**
CONF-650210–	**20-15943**	**(Application of X-Ray Diffraction in the Atomic Energy Field Meeting, Richland, Wash., Feb. 23–24, 1965) See RL-REA-2595**
CONF-650221–	**(Biophysical Society, 9th Annual Meeting, San Francisco, Feb. 24–26, 1965)**	
4	20-14265	Biophys. J., 6: 113-22(1966)
CONF-650422–	**(American Geophysical Union, Program for Section of Seismology Annual Meeting, Washington, D. C., Apr. 19–22, 1965)**	
17	20-15622	ORINS. Gmelin, AED-CONF-65-118-56
18	20-15291	ORINS. Gmelin, AED-CONF-65-118-53
CONF-650509–	**(IAEA Symposium on Nondestructive Testing in Nuclear Technology, Bucharest, May 17–21, 1965)**	
Vol.1	20-14701	See STI/PUB/105(Vol.1)
CONF-650534–	**(6th International Space Science Symposium, Buenos Aires, May 17, 1965)**	
2	20-15291	See CONF-650422-18
CONF-650549–	**(International Atomic Energy Agency, Symposium on Exchange Reactions, Upton, N. Y., May 31–June 4, 1965)**	
4	20-14570	ORINS
6	20-14574	ORINS
7	20-14572	ORINS
10	20-14571	ORINS
18	20-14573	ORINS
CONF-650553–	**20-15315**	**(Seminar on High Energy Physics and Elementary Particles, Trieste, Italy, May 3–June 30, 1965) See STI/PUB/117**
CONF-650560–	**(13th Annual Meeting of the Radiation Research Society, Philadelphia, May 23–26, 1965)**	
13	20-14238	Dep. mn. CFSTI $1.00 cy, $0.50 mn
CONF-650602–	**(American Nuclear Society 11th Annual Meeting, Gatlinburg, Tenn., June 20–24, 1965)**	
62	20-14502	Gmelin, AED-CONF-65-125-44
70	20-15686	ORINS. Gmelin, AED-CONF-65-125-109
71	20-16033	ORINS. Gmelin, AED-CONF-65-125-107
CONF-650606–	**(EURATOM Symposium on Fuel Cycles of High-Temperature Gas-Cooled Reactors, Brussels,**	

Report No.	Abstract No.	Availability
	June 10–11, 1965)	
10	20-14638	See NP-15753
CONF-650616–	(Health Physics Society, Annual Meeting, Los Angeles, June 14–17, 1965)	
15	20-14907	ORINS
CONF-650636–	20-15437	(International Symposium on Electron and Photon Interactions at High Energies, Hamburg, June 8–12, 1965)
CONF-650638–	(Physics of Quantum Electronics Conference, San Juan, Puerto Rico, June 28–30, 1965)	
3	20-15276	ORINS. Gmelin, AED-CONF-65-156-6
CONF-650652–	(6th International Conference on Radiocarbon and Tritium Dating, Pullman, Wash., June 7–11, 1965)	
1	20-14503	Gmelin, AED-CONF-65-158-6
CONF-650653–	(American Physical Society, Summer Meeting, New York, June 23–25, 1965)	
9	20-15866	ORINS. Gmelin, AED-CONF-65-170-25
11	20-15925	ORINS. Gmelin, AED-CONF-65-170-23
12	20-15567	ORINS. Gmelin, AED-CONF-65-170-18
CONF-650661–	(Symposium on Molecular Structure and Spectroscopy, Columbus, Ohio, June 14–18, 1965)	
1	20-15275	ORINS. Gmelin, AED-CONF-65-150-9
CONF-650665–	20-14231	(Brookhaven Symposia in Biology, Upton, N. Y., June 4–10, 1965) See BNL-931
CONF-650707–	(IEEE Annual Conference on Nuclear and Space Radiation Effects, Ann Arbor, Mich., July 12–15, 1965)	
8	20-14925	ORINS. Gmelin, AED-CONF-65-152-16
10	20-15993	ORINS. Gmelin, AED-CONF-65-152-17
15	20-15232	ORINS. Gmelin, AED-CONF-65-96-83
CONF-650710–	19-43507	(American Nuclear Society, Meeting on Reactor Operating Experience, Jackson Lake Lodge, Wyo., July 28–30, 1965)
14	20-16128	ORINS. Gmelin, AED-CONF-65-192-11
15	20-16130	ORINS. Gmelin, AED-CONF-65-192-12
CONF-650711–	(AIAA 2nd Annual Meeting and Technical Demonstration, San Francisco, July 26–29, 1965)	
52	20-15926	ORINS
54	20-15621	ORINS. Gmelin, AED-CONF-65-200-1
CONF-650720–	(Symposium on Extra-terrestrial Influences on Atmospheric Circulation, Boulder, Colo., July 29–30, 1965)	
1	20-15233	ORINS. Gmelin, AED-CONF-65-198-1
CONF-650721–	(Positron Annihilation Conference, Detroit, July 27–29, 1965)	
1	20-15436	ORINS. Gmelin, AED-CONF-65-211-1
CONF-650803–	(IAEA Symposium on Nuclear Materials Management, Vienna, Aug. 30–Sept. 3, 1965)	
36	20-16140	ORINS
40	20-14504	ORINS
CONF-650817–	(Gordon Research Conference on Ion Exchange, New London, N. H., Aug. 2–6, 1965)	
2	20-15723	See MIT-2098-162
CONF-650825–	(20th Annual Calorimetry Conference, Ames, Iowa, Aug. 11–13, 1965)	
1	20-14908	ORINS. Gmelin, AED-CONF-65-196-2
CONF-650826–	(International Conference on Energetics, Rochester, N. Y., Aug. 18–20, 1965)	
1	20-15304	ORINS. Gmelin, AED-CONF-65-210-3
26	20-15305	ORINS. Gmelin, AED-CONF-65-210-1
CONF-650827–	(Western Electronics Show and Conference, San Francisco, Aug. 24–27, 1965)	
1	20-14665	ORINS. Gmelin, AED-CONF-65-213-1
CONF-650923–	(5th International Conference on High Energy Accelerators, Frascati, Italy, Sept. 9–16, 1965)	
26	20-15159	See LNF-65/36
CONF-651023–	(Symposium on Radioisotope Instruments in Industry and Geophysics, Warsaw, Oct. 18–22, 1965)	
1	20-14770	ORINS
4	20-14775	ORINS
5	20-14835	ORINS
8	20-14840	ORINS
9	20-14839	ORINS
21	20-14772	ORINS
24	20-14773	ORINS
25	20-14836	ORINS
28	20-14778	ORINS
30	20-14776	ORINS
31	20-14777	ORINS
34	20-14774	ORINS
35	20-14838	ORINS
36	20-14752	ORINS
37	20-14771	ORINS
38	20-14837	ORINS
CONF-651044–	(Conference on Programming for Flying Spot Devices, New York, Oct. 24–26, 1965)	
4	20-14850	See BNL-9763
5	20-14849	See BNL-9720
CONF-651101–	20-3647 20-9102	(American Nuclear Society, Winter Meeting, Washington, D. C., Nov. 15–18, 1965) (Revised 11-8-65)
69	20-16090	See WAPD-T-1841
CONF-651103–	(IAEA Symposium on Criticality Control of Fissile Materials, Stockholm, Nov. 1–5, 1965)	
1	20-14790	See RL-SA-43A
16	20-16034	ORINS
18	20-16031	ORINS
19	20-16032	ORINS
CONF-651109–	(1st Symposium on Accelerator Radiation Dosimetry and Experience, Upton, N. Y., Nov. 3–5, 1965)	
19	20-15175	See UCRL-16312
CONF-651110–	(American Society of Mechanical Engineers, Annual Winter Meeting, Chicago, Nov. 7–11, 1965)	
13	20-14695	ORINS
14	20-14697	ORINS
15	20-14696	ORINS
16	20-14694	ORINS
17	20-16129	ORINS
18	20-16101	ORINS
19	20-16002	ORINS
CONF-651118–	(American Physical Society, Gatlinburg, Tenn., Nov. 11–13, 1965)	
9	20-15726	See ORNL-P-1957
CONF-651130–	(DECUS Symposium, Stanford, Calif., Nov. 29–30, 1965)	
2	20-14861	See UCRL-16555
CONF-651132–	(Atomic Industrial Forum, 12th Annual Conference, Washington, D. C., Nov. 17, 1965)	
1	20-14929	Dep. mn. CFSTI $2.00 cy, $0.50 mn
CONF-660204–	(American Nuclear Society Meeting, San Diego, Calif., Feb. 7–9, 1966)	
4	20-15666	Dep. mn. CFSTI $2.00 cy, $0.50 mn
CONF-660205–	(Metallurgical Society of the American Institute of Mining, Metallurgical, and Petroleum Engineers, New York, Feb. 1966)	
3	20-14754	See NVO-38-1
CONF-660207–	(Radioisotope Applications in Aerospace Symposium, Dayton, Ohio, Feb. 15–17, 1966)	
1	20-14789	See ORNL-P-1910
CONF-660208–	(Symposium on Solidification and Long-Term Storage of Highly Radioactive Wastes, Richland, Wash., Feb. 14–18, 1966)	
2	20-16135	See RL-SA-62
3	20-14466	See RL-SA-58

Report No.	Abstract No.	Availability
CONF-660304–	**(Institute of Electrical and Electronics Engineers, Scintillation and Semiconductor Counter Symposium, Washington, D. C., Mar. 2–4, 1966)**	
2	20-14851	See BNL-9980
3	20-14854	Dep. mn. CFSTI $2.00 cy, $0.50 mn
CONF-660305–	**(American Nuclear Society, Topical Meeting, Augusta, Ga., Mar. 21–23, 1966)**	
3	20-14641	See RL-SA-59
4	20-14626	See ORNL-P-1944
5	20-14635	Dep. mn. CFSTI $1.00 cy, $0.50 mn
6	20-14436	See BNWL-SA-504
7	20-14636	Dep. mn. CFSTI $1.00 cy, $0.50 mn
10	20-14666	See ORNL-P-1946
11	20-14435	See BNWL-SA-503
12	20-15038	Dep. mn. CFSTI $1.00 cy, $0.50 mn
13	20-14639	See ORNL-P-1968
14	20-14945	Dep. mn. CFSTI $1.00 cy, $0.50 mn
CONF-660501–	**(American Foundrymen's Society Convention, Cleveland, May 9–13, 1966)**	
1	20-15003	See LA-DC-7510
COO–		
32-114	20-14597	J. Amer. Chem. Soc., 88: 412-16(1966)
264-273	20-15354	Phys. Rev., 142: 1088-91(1966)
264-282	20-15451	Ann. Phys. (N. Y.), 36: 228-49(1966)
264-284	20-15321	Ann. Phys. (N. Y.), 36: 250-66(1966)
401-139	20-14815	Dep. mn. CFSTI $3.00 cy, $0.75 mn
614-41	20-14950	Dep. mn; CFSTI $5.00 cy, $1.00 mn
875-43	20-14274	Radiat. Res., 27: 237-49(1966)
888-39	20-16146	Dep. mn. CFSTI $1.00 cy, $0.50 mn
888-45	20-16147	Dep. mn. CFSTI $1.00 cy, $0.50 mn
1001-6	20-14525	Inorg. Chem., 5: 321-2(1966)
1195-43	20-15331	Phys. Rev., 142: 871-82(1966)
1261-16	20-15472	Phys. Rev., 142: 1087-8(1966)
1261-22	20-15307	Dep. mn. CFSTI $1.00 cy, $0.50 mn
1305-2	20-14405	Dep. mn. CFSTI $1.00 cy, $0.50 mn
CRDL-SP–	**(Non-AEC)**	
5-7	20-14506	
CVNA–	**(Misc.)**	
172	20-14732	
175	20-16062	
241	20-16063	Dep. mn. CFSTI $1.00 cy, $0.50 mn
DP–		
1015	20-14946	Dep. mn. CFSTI $2.00 cy, $0.50 mn
1034	20-14637	Dep. mn. CFSTI $1.00 cy, $0.50 mn
DUBNA REPORTS	**(Russian)**	
See JINR (Russian)		
ECOM–	**(Non-AEC)**	
01313-1	20-14918	CFSTI $3.00 cy, $0.50 mn
EIR–	**(Swiss)**	
72	20-15667	Dep. mn
ER–	**(Misc.)**	
65-10-182	20-14918	See ECOM-01313-1
7777(Vol.2)	20-15930	See NP-15697(Vol.2)
ETR–	**(Belgian)**	
172	20-14638	See NP-15753
EUR–	**(European Atomic Energy Community)**	
2117.n	20-15998	Dep. mn
2382	20-14686	See EURAEC-1448
2390	20-14999	See EURAEC-1466
2396	20-15039	See EURAEC-1475
2420.d,f,i,n,e	20-16064	Dep. mn
2435.f	20-14578	Dep. mn
2512.n	20-14816	Dep. mn
2624.e	20-15668	Dep. mn
2627.e	20-16022	Dep. mn
2658	20-14977	See EURAEC-1500
2669	20-15000	See EURAEC-1517
2688	20-14978	See EURAEC-1546

Report No.	Abstract No.	Availability
EURAEC–		
1448	20-14686	ORAU
1466	20-14999	Dep. mn. CFSTI $1.00 cy, $0.50 mn
1475	20-15039	Dep. mn. CFSTI $2.00 cy, $0.50 mn
1500	20-14977	Dep. mn. CFSTI $3.00 cy, $0.75 mn
1517	20-15000	Dep. mn. CFSTI $3.00 cy, $0.75 mn
1540	20-14687	See GEAP-4785
1546	20-14978	Dep. mn. CFSTI $2.00 cy, $0.50 mn
1563	20-15054	See NUMEC-3505-11
1571	20-16019	See BMI-X-10154
1574	20-14980	See GEAP-5065
1576	20-15042	See IITRI-578-P27-14
FEI–	**(Russian)**	
22	20-15298	Dep. mn
FTD-TT–	**(Non-AEC)**	
65-806	20-15887	For translation see AD-625789
65-907	20-14693	For translation see AD-625791
65-977	20-15064	For translation see AD-625748
GA–	**(Misc.)**	
5556	20-14439	Dep. mn. CFSTI $3.00 cy, $0.75 mn
5721	20-15048	See N65-16231
6373	20-15292	See AD-620511
6721	20-15040	Dep. mn. CFSTI $3.00 cy, $0.75 mn
GACD–	**(Non-AEC)**	
43-12	20-15046	See N65-15820
4730	20-14960	See N65-20798
4768	20-14959	See N65-20797
4923	20-14961	See N65-20801
4990	20-14962	See N65-20803
GAMD–	**(Misc.)**	
6519	20-16075	Dep. mn. CFSTI $2.00 cy, $0.50 mn
GE–	**(Non-AEC)**	
214-252	20-14726	See NASA-CR-54746
GEAP–	**(Misc.)**	
4785	20-14687	Dep. mn. CFSTI $3.00 cy, $0.75 mn
4835	20-14979	Dep. mn. CFSTI $4.00 cy, $0.75 mn
4893	20-15133	Dep. mn. CFSTI $2.00 cy, $0.50 mn
4950	20-15717	Dep. mn. CFSTI $2.00 cy, $0.50 mn
5065	20-14980	Dep. mn. CFSTI $1.00 cy, $0.50 mn
GEMP–	**(Misc.)**	
397	20-15041	Dep. mn. CFSTI $6.00 cy, $1.50 mn
HW–		
66930	20-15001	ORAU
IBJ–	**(Polish)**	
See INR		
IC–	**(Misc.)**	
65/72	20-15370	Proc. Roy. Soc. (London), Ser. A, 289: 177-91(1966)
66/13	20-15308	Dep. mn
66/14	20-15444	Dep. mn
IDO–		
14672	20-16133	Dep. mn. CFSTI $2.00 cy, $0.50 mn
17083	20-15718	Dep. mn. CFSTI $3.00 cy, $0.50 mn
IEA–	**(Brazilian)**	
102	20-16134	Dep. mn
IFJ–	**(Polish)**	
See INP		
IITRI–	**(Misc.)**	
578P21-16	20-16023	Dep. mn. CFSTI $3.00 cy, $0.50 mn
578P27-14	20-15042	Dep. mn. CFSTI $1.00 cy, $0.50 mn
T6042-16	20-16023	See IITRI-578P21-16
INP–	**(Polish)**	
431/PL	20-15719	Dep.
INR–	**(Non-AEC)**	
626/IX/R	20-15569	Dep.

Report No.	Abstract No.	Availability
IP–	**(Non-AEC)**	
68	20-14430	See AD-620219
IPP–	**(Non-AEC)**	
1/38	20-15871	Dep. mn
1/41	20-15872	Dep. mn
1/42	20-15873	Dep. mn
3/31	20-15874	Dep. mn
3/32	20-15875	Dep. mn
6/33	20-15876	Dep. mn
6/41	20-15877	Dep. mn
6/42	20-15878	Dep. mn
6/43	20-15879	Dep. mn
IS–		
1250	20-14991	J. Less-Common Metals, 10: 190-9(1966)
1302	20-15963	Phys. Rev. Lett., 16: 233-4(1966)
JAERI–	**(Japanese)**	
1088	20-16076	Dep. mn
1089	20-14788	Dep. mn
1090	20-14855	Dep. mn
6016	20-16122	Dep. mn
JINR–	**(Russian)**	
E-2516	20-15720	Dep. mn
E-2517	20-15721	Dep. mn
E-2563	20-15309	Dep. mn
P-2508	20-15310	Dep. mn
JPRS–	**(Non-AEC)**	
33406	20-16107	CFSTI $1.00 cy, $0.50 mn
33458	20-15149	CFSTI $7.00 cy, $1.75 mn
33459	20-16108	CFSTI $1.00 cy, $0.50 mn
JUL–	**(German)**	
292-RW	20-15940	Dep. mn
312-ST	20-14239	Dep. mn
KAPL-P–		
3129	20-14830	Rev. Sci. Instrum., 37: 369-70(1966)
KFK–	**(German)**	
345	20-14856	Dep. mn
350	20-16123	Dep. mn
KR–	**(Norwegian)**	
76	20-15722	Dep. mn
LA–		
3378	20-15002	Dep. mn. CFSTI $2.00 cy, $0.50 mn
3399	20-14507	Dep. mn. CFSTI $1.00 cy, $0.50 mn
3436	20-15043	Dep. mn. CFSTI $1.00 cy, $0.50 mn
3440	20-14232	Dep. mn. CFSTI $3.00 cy, $0.50 mn
3452	20-14440	Dep. mn. CFSTI $1.00 cy, $0.50 mn
LA-DC–		
7136	20-14550	J. Nucl. Mater., 19: 50-2(1966)
7447	20-15095	J. Nucl. Mater., 19: 115-16(1966)
7508	20-15595	Proc. IEEE (Inst. Elec. Electron. Eng.), 53: 1935-48(1965)
7510	20-15003	Dep. mn. CFSTI $1.00 cy, $0.50 mn
7512	20-15596	Proc. IEEE (Inst. Elec. Electron. Eng.), 53: 1949-58(1965)
7543	20-15093	J. Nucl. Mater., 19: 111-12(1966)
LNF–	**(Italian)**	
65/36	20-15159	Dep. mn
65/44	20-15160	Dep. mn
65/47	20-15311	Dep. mn
MATT–		
352	20-15906	Phys. Fluids, 9: 309-13(1966)
395	20-15899	Phys. Fluids, 9: 252-64(1966)
MCW–		
1493	20-14441	Dep. mn. CFSTI $2.00 cy, $0.50 mn
MIT–	**(Misc.)**	
2098-86	20-15312	Dep. mn. CFSTI $1.00 cy, $0.50 mn
2098-161	20-15744	Ann. Phys. (N. Y.), 36: 217-27(1966)
2098-162	20-15723	Dep. mn. CFSTI $1.00 cy, $0.50 mn
2098-165	20-15361	Phys. Rev., 142: 1195-1214(1966)
2098-207	20-15820	Phys. Rev. Lett., 16: 322-5(1966)
2098-224	20-15724	Dep. mn. CFSTI $7.00 cy, $1.50 mn
ML–	**(Misc.)**	
1292	20-15880	Dep. mn. CFSTI $2.00 cy, $0.50 mn
MLM–		
1268	20-14444	Dep. mn. CFSTI $2.00 cy, $0.50 mn
MPI-PAE–	**(German)**	
P1.15/65	20-15623	Dep. mn
PL-7/65	20-15881	Dep. mn
MSAR–	**(Misc.)**	
66-09	20-14981	Dep. mn. CFSTI $2.00 cy, $0.50 mn
66-10	20-14445	Dep. mn. CFSTI $1.00 cy, $0.50 mn
N–	**(Misc.)**	
64-25607	20-14446	Dep. mn
65-15530	20-15247	CFSTI $1.00 cy, $0.50 mn
65-15534	20-15045	CFSTI $1.00 cy, $0.50 mn
65-15819	20-15134	CFSTI $1.00 cy, $0.50 mn
65-15820	20-15046	CFSTI $2.00 cy, $0.50 mn
65-15876	20-14725	CFSTI $3.00 cy, $0.75 mn
65-15919	20-15047	CFSTI $2.00 cy, $0.50 mn
65-16231	20-15048	CFSTI $2.00 cy, $0.50 mn
65-16256	20-15049	CFSTI $1.00 cy, $0.50 mn
65-16315	20-16111	CFSTI $6.00 cy, $1.25 mn
65-20165	20-15148	CFSTI $3.00 cy, $0.50 mn
65-20421	20-14817	CFSTI $3.00 cy, $0.75 mn
65-20481	20-14508	CFSTI $1.00 cy, $0.50 mn
65-20653	20-14919	CFSTI $1.00 cy, $0.50 mn
65-20692	20-14688	
65-20790	20-15004	CFSTI $2.00 cy, $0.50 mn
65-20797	20-14959	CFSTI $2.00 cy, $0.50 mn
65-20798	20-14960	CFSTI $1.00 cy, $0.50 mn
65-20801	20-14961	CFSTI $2.00 cy, $0.50 mn
65-20803	20-14962	CFSTI $2.00 cy, $0.50 mn
65-20996	20-15191	CFSTI $1.00 cy, $0.50 mn
65-21000	20-15192	CFSTI $2.00 cy, $0.50 mn
65-21084	20-15570	CFSTI $2.00 cy, $0.50 mn
NAA-SR–		
11628	20-16077	Dep. mn. CFSTI $4.00 cy, $1.00 mn
11739	20-15999	Dep. mn. CFSTI $3.00 cy, $0.50 mn
NASA-CR–	**(Misc.)**	
54176	20-14725	See N65-15876
54277	20-15048	See N65-16231
54746	20-14726	
54891	20-15057	See PWA-2750
57558	20-14919	See N65-20653
57637	20-14817	See N65-20421
57653	20-14961	See N65-20801
57654	20-14962	See N65-20803
57655	20-14959	See N65-20797
57657	20-14960	See N65-20798
57768	20-15004	See N65-20790
57845	20-15570	See N65-21084
60404	20-15046	See N65-15820
60407	20-15134	See N65-15819
60437	20-15047	See N65-15919
60540	20-15049	See N65-16256
60553	20-16111	See N65-16315
NASA-SP–	**(Misc.)**	
5024	20-15005	CFSTI $1.00 cy, $0.50 mn
NASA-TM–	**(Misc.)**	
X-1208	20-14727	CFSTI $1.00 cy, $0.50 mn
X-53216	20-15192	See N65-21000
NASA-TN–	**(Misc.)**	
D-2617	20-15247	See N65-15530
D-2638	20-15045	See N65-15534
D-2738	20-14508	See N65-20481
D-2746	20-15191	See N65-20996
D-3086	20-15590	CFSTI $2.00 cy, $0.50 mn
D-3237	20-15669	CFSTI $1.00 cy, $0.50 mn
D-3293	20-15643	CFSTI $1.00 cy, $0.50 mn
D-3324	20-15299	CFSTI $0.70 cy, $0.50 mn

Report No.	Abstract No.	Availability
D-3328	20-14728	CFSTI $2.00 cy, $0.50 mn
NASA-TR–	**(Non-AEC)**	
R-217	20-15148	See N65-20165
NBL–		
231	20-14447	Dep. mn. CFSTI $4.00 cy, $1.00 mn
NLCO–		
970	20-14963	Dep. mn. CFSTI $3.00 cy, $0.75 mn
NM–	**(Misc.)**	
001-059.16-03	20-16143	See AD-620276
NMC-ONR–	**(Non-AEC)**	
65	20-14660	See AD-620468
NP–	**(AEC File No. for Non-AEC Reports)**	
14855	20-15725	Dep. mn
15273	20-15161	Dep. mn
15448	20-14857	Dep. mn
15654	20-15193	Dep. mn
15670	20-14240	Dep. mn
15676	20-14930	
15677	20-14931	
15697(Vol.2)	20-15930	
15698	20-15941	
15714	20-14403	
15753	20-14638	Dep. mn. CFSTI $3.00 cy, $0.75 mn
15785	20-15162	Dep. mn
15822	20-15313	Dep. mn
15826	20-14509	Dep. mn
15834	20-14510	Dep. mn
15844	20-14734	Dep. mn
15853	20-14735	Dep. mn
15855	20-14259	Dep. mn
15856	20-14260	Dep. mn
15861	20-14731	Dep. mn
15867	20-14661	Dep. mn
15868	20-15882	Dep. mn
15875	20-14983	Dept. of Mines and Technical Surveys, Ottawa $0.75
15876	20-15051	Dep. mn
15880	20-15052	
15881	20-15007	CFSTI $1.00 cy, $0.50 mn
NRL–	**(Misc.)**	
F18	20-14734	See NP-15844
NUMEC–		
3428-17	20-15053	Dep. mn. CFSTI $1.00 cy, $0.50 mn
3432-18	20-15135	Dep. mn. CFSTI $1.00 cy, $0.50 mn
3505-11	20-15054	Dep. mn. CFSTI $2.00 cy, $0.50 mn
3524-12	20-14965	Dep. mn. CFSTI $2.00 cy, $0.50 mn
NYO–		
38-1	20-14754	Dep. mn. CFSTI $1.00 cy, $0.50 mn
NYO–		
1800-12	20-14290	Dep. mn. CFSTI $1.00 cy, $0.50 mn
2150-11	20-15942	Dep. mn. CFSTI $3.00 cy, $0.75 mn
2383-15	20-14579	Dep. mn. CFSTI $1.00 cy, $0.50 mn
2394-19	20-15055	Dep. mn. CFSTI $1.00 cy, $0.50 mn
2586-2	20-14451	Dep. mn. CFSTI $3.00 cy, $0.50 mn
2655-1	20-16000	Dep. mn. CFSTI $4.00 cy, $0.75 mn
2779-9	20-16148	Dep. mn. CFSTI $1.00 cy, $0.50 mn
2779-10	20-16149	Dep. mn. CFSTI $1.00 cy, $0.50 mn
2916-10	20-15056	Dep. mn. CFSTI $1.00 cy, $0.50 mn
3246-5	20-14858	Dep. mn. CFSTI $3.00 cy, $0.50 mn
3622-1	20-14700	Dep. mn. CFSTI $1.00 cy, $0.50 mn
ORNL–		
2764	20-14580	Dep. mn. CFSTI $1.00 cy, $0.50 mn
3874	20-15008	Dep. mn. CFSTI $3.00 cy, $0.75 mn
3889	20-14428	Dep. mn. CFSTI $5.00 cy, $1.00 mn
3890	20-14462	Dep. mn. CFSTI $7.00 cy, $1.50 mn
3909	20-16150	Dep. mn. CFSTI $3.00 cy, $0.75 mn
ORNL-AMPIC–		
3	20-15248	Dep. ORNL Free

Report No.	Abstract No.	Availability
ORNL-P–	**(Misc.)**	
931	20-16100	Weld. J. (N. Y.), 44: 1027-34(1965)
1101	20-15139	Amer. Ceram. Soc. Bull., 44: 963-70(1965)
1328	20-15461	J. Math. Phys. (N. Y.), 7: 395-8(1966)
1403	20-15089	J. Nucl. Mater., 19: 81-9(1966)
1491	20-15797	Nucl. Phys., 79: 33-45(1966)
1537	20-15339	Phys. Rev., 142: 944-56(1966)
1584	20-14330	Health Phys., 12: 227-37(1966)
1726	20-14829	Rev. Sci. Instrum., 37: 336-7(1966)
1865	20-15818	Phys. Rev. Lett., 16: 248-9(1966)
1910	20-14789	Dep. mn. CFSTI $1.00 cy, $0.50 mn
1944	20-14626	Dep. mn. CFSTI $1.00 cy, $0.50 mn
1946	20-14666	Dep. mn. CFSTI $1.00 cy, $0.50 mn
1957	20-15726	Dep. mn. CFSTI $2.00 cy, $0.50 mn
1968	20-14639	Dep. mn. CFSTI $1.00 cy, $0.50 mn
ORNL-TM–		
1312(Vol.1)	20-14667	Dep. mn. CFSTI $3.00 cy, $0.75 mn
1388	20-16124	Dep. mn. CFSTI $1.00 cy, $0.50 mn
1390	20-14859	Dep. mn. CFSTI $1.00 cy, $0.50 mn
1391	20-14818	Dep. mn. CFSTI $1.00 cy, $0.50 mn
1393	20-16125	Dep. mn. CFSTI $1.00 cy, $0.50 mn
1394	20-14662	Dep. mn. CFSTI $1.00 cy, $0.50 mn
1397	20-14668	Dep. mn. CFSTI $1.00 cy, $0.50 mn
1411	20-14640	Dep. mn. CFSTI $1.00 cy, $0.50 mn
1418	20-14512	Dep. mn. CFSTI $1.00 cy, $0.50 mn
ORNL-tr–		
677	20-15317	Dep. mn. CFSTI $4.00 cy, $0.75 mn. JCL $10.10 fs, $3.86 mf
843	20-15932	Dep. mn. JCL $3.60 fs, $1.10 mf
1018	20-15065	Dep. mn. JCL $1.60 fs, $0.80 mf
1060	20-15933	Dep. mn. JCL $1.60 fs, $0.80 mf
PAEC(D)CH–	**(Philippines)**	
652	20-14463	Dep. mn
PAEC(D)IS–	**(Phillipines)**	
651	20-14627	Dep. mn
PAN–	**(Polish)**	**(This series of reports was terminated in 1965. Subsequent reports are identified by the code INR.)**
PATENTS	**(British)**	**(4s. 6d. each, U. K. Patent Office)**
1,017,201	20-16048	
1,017,237	20-16003	
1,017,350	20-16004	
1,017,401	20-16005	
1,017,455	20-14698	
1,017,539	20-15022	
1,017,540	20-15023	
1,017,595	20-14505	
1,017,713	20-15188	
1,017,789	20-15687	
1,017,981	20-15024	
1,017,992	20-16006	
1,018,021	20-15131	
1,018,402	20-14909	
1,018,432	20-16049	
1,018,471	20-14676	
1,018,493	20-14910	
1,018,618	20-16007	
1,018,662	20-16008	
1,018,723	20-14677	
1,018,783	20-14842	
1,018,874	20-14971	
1,019,282	20-16009	
1,019,373	20-16141	
PATENTS	**(Canadian)**	
724,080	20-14657	
PATENTS	**(French)**	
1,190,253	20-16102	
1,304,929	20-16038	
1,305,299	20-16103	
1,314,117	20-16117	
1,327,306	20-16039	
1,329,610	20-16050	
1,329,611	20-16051	
1,345,862	20-16010	
1,351,029	20-16104	

Report No.	Abstract No.	Availability
1,353,703	20-16040	
1,355,945	20-16041	
1,359,123	20-16011	
1,360,063	20-16042	
1,361,744	20-16052	
1,365,532	20-16043	
1,367,389	20-16012	
1,367,390	20-16044	
1,368,813	20-16013	
1,369,644	20-16131	
1,370,966	20-16045	
PATENTS	**(German)**	
1,199,414	20-16142	
1,203,745	20-14658	
PATENTS	**(U. S.)**	**($0.25 each, U. S. Patent Office)**
3,228,175	20-14722	
3,228,749	20-14575	
3,228,846	20-16105	
3,228,847	20-16014	
3,228,848	20-16053	
3,228,849	20-16054	
3,228,850	20-16055	
3,228,886	20-15025	
3,229,090	20-14911	
3,229,091	20-14912	
3,229,092	20-14913	
3,229,096	20-14678	
3,229,097	20-14914	
3,229,759	20-14699	
3,230,036	20-14659	
3,230,119	20-14972	
3,230,145	20-15927	
3,230,146	20-16015	
3,230,147	20-16016	
3,230,149	20-16017	
3,230,150	20-16056	
3,230,151	20-16057	
3,230,152	20-16058	
3,230,176	20-14721	
3,230,261	20-14633	
3,230,364	20-14973	
3,230,369	20-14915	
3,230,371	20-14916	
3,230,372	20-14917	
3,230,373	20-14679	
3,230,374	20-14634	
3,230,375	20-14680	
3,230,409	20-15189	
3,230,418	20-15928	
3,230,419	20-14843	
3,230,911	20-14723	
3,231,098	20-14681	
3,231,344	20-15026	
3,231,401	20-14974	
3,231,451	20-14682	
3,231,473	20-16018	
3,231,475	20-16106	
3,231,521	20-15027	
3,231,739	20-14683	
PPAD–		
279D(Rev.)	20-15163	Dep. mn. CFSTI $1.00 cy, $0.50 mn
572F	20-15727	Dep. mn. CFSTI $6.00 cy, $1.25 mn
PUC–		
937-170	20-15809	Nucl. Phys., 79: 209-19(1966)
PWA–	**(Non-AEC)**	
2750	20-15057	
R–	**(Misc.)**	
113	20-16111	See N65-16315
166	20-14983	See NP-15875
276	20-15869	See AD-628317
412	20-15929	See AD-627890
1785	20-15007	See NP-15881
RFP–		
511	20-14984	Dep. mn. CFSTI $1.00 cy, $0.50 mn
599	20-14464	Dep. mn. CFSTI $1.00 cy, $0.50 mn
602	20-14819	Dep. mn. CFSTI $2.00 cy, $0.50 mn
636	20-14820	Dep. mn. CFSTI $1.00 cy, $0.50 mn
647	20-16151	Dep. mn. CFSTI $1.00 cy, $0.50 mn
657	20-14465	Dep. mn. CFSTI $1.00 cy, $0.50 mn
668	20-14821	Dep. mn. CFSTI $1.00 cy, $0.50 mn
673	20-14966	Dep. mn. CFSTI $1.00 cy, $0.50 mn
688	20-14513	Dep. mn. CFSTI $1.00 cy, $0.50 mn
RFR–	**(Swedish)**	
231	20-16024	Dep. mn
232	20-16025	Dep. mn
RHEL-R–	**(British)**	
102	20-15445	Dep. mn
112	20-15164	Dep. mn
RL-REA–		
2595	20-15943	Dep. mn. CFSTI $3.00 cy, $0.75 mn
RL-SA–		
43A	20-14790	Dep. mn. CFSTI $1.00 cy, $0.50 mn
58	20-14466	Dep. mn. CFSTI $1.00 cy, $0.50 mn
59	20-14641	Dep. mn. CFSTI $1.00 cy, $0.50 mn
62	20-16135	Dep. mn. CFSTI $1.00 cy, $0.50 mn
RL-SEP–		
414	20-14669	Dep. mn. CFSTI $1.00 cy, $0.50 mn
503-1	20-14967	Dep. mn. CFSTI $2.00 cy, $0.50 mn
RM–	**(Misc.)**	
4469-PR	20-16110	See AD-620650
4858	20-15591	
RME–		
4569(Rev.)	20-14779	Dep. mn. CFSTI $2.00 cy, $0.50 mn
RPI–	**(Misc.)**	
328-49	20-15731	Dep. mn. CFSTI $3.00 cy, $0.75 mn
RT-FI–	**(Italian)**	
(65)33	20-14860	Dep. mn
(65)35	20-15314	Dep. mn
RT-PROT–	**(Italian)**	
(64)-20	20-14467	Dep. mn
SAN–		
584-1	20-14235	Dep. mn. CFSTI $2.00 cy, $0.50 mn
SC-DC–		
66-1130	20-15058	Dep. mn. CFSTI $2.00 cy, $0.50 mn
66-1293	20-14690	Dep. mn. CFSTI $6.00 cy, $1.25 mn
SC-R–		
65-997	20-14670	Dep. mn. CFSTI $3.00 cy, $0.50 mn
SC-RR–		
65-551	20-16112	Dep. mn. CFSTI $4.00 cy, $1.00 mn
66-22	20-16113	Dep. mn. CFSTI $3.00 cy, $0.75 mn
SC-T–		
65-775	20-15888	Dep. mn. JCL $2.60 fs, $0.86 mf
65-776	20-15889	Dep. mn. JCL $1.60 fs, $0.80 mf
SC-TM–		
65-523	20-14824	Dep. mn. CFSTI $2.00 cy, $0.50 mn
SGAE-CH–	**(Austrian)**	
25/1965	20-14582	Dep. mn
SLAC–		
49	20-15166	Dep. mn. CFSTI $3.00 cy, $0.75 mn
STI-PUB–	**(International Atomic Energy Agency)**	
105(Vol.1)	20-14701	IAEA: $8.00; S 168,-; £2.8.0; F Fr 32,-; DM 28,-.
117	20-15315	IAEA: $15.00; S 315,-; £4.10.0; F Fr 60,-; DM 52,50.
SU-IPR–		
31	20-15883	Dep. mn. CFSTI $2.00 cy, $0.50 mn
33	20-15884	Dep. mn. CFSTI $3.00 cy, $0.75 mn

Report No.	Abstract No.	Availability
SWRI–		
1228-1-20	20-15059	Dep. mn. CFSTI $2.00 cy, $0.50 mn
1228-2-20	20-15059	See SWRI-1228-1-20
1228-4-15	20-16085	Dep. mn. CFSTI $1.00 cy, $0.50 mn
1228-5-20	20-15059	See SWRI-1228-1-20
TID–		
3732	20-16152	DTI Extension Free
20987	20-14866	Health Phys., 11: 314-16(1965)
21437	20-14241	Dep. mn. CFSTI $2.00 cy, $0.50 mn
21634	20-14583	Dep. mn. CFSTI $1.00 cy, $0.50 mn
21654	20-15732	Dep. mn. CFSTI $1.00 cy, $0.50 mn
21655	20-15674	J. Math. Phys. (N. Y.), 7: 345-55(1966)
21956	20-15463	Nucl. Phys., 79: 77-107(1966)
22182	20-15338	Phys. Rev., 142: 932-43(1966)
22237	20-15120	Trans. Met. Soc. AIME, 236: 221-2(1966)
22297	20-15783	Nucl. Phys., 78: 492-6(1966)
22394	20-14671	Dep. mn. CFSTI $1.00 cy, $0.50 mn
22444	20-14584	Dep. mn. CFSTI $1.00 cy, $0.50 mn
22491	20-15009	Dep. mn. CFSTI $5.00 cy, $1.00 mn
22494	20-14291	Dep. mn. CFSTI $1.00 cy, $0.50 mn
22505	20-14468	Dep. mn. CFSTI $1.00 cy, $0.50 mn
22563	20-14292	Dep. mn. CFSTI $1.00 cy, $0.50 mn
22591	20-14242	Dep. mn. CFSTI $1.00 cy, $0.50 mn
22626	20-14243	Dep. mn. CFSTI $5.00 cy, $1.00 mn
22648	20-15249	Dep. mn. CFSTI $1.00 cy, $0.50 mn
22650	20-14469	Dep. mn. CFSTI $5.00 cy, $1.00 mn
22651	20-16086	Dep. mn. CFSTI $1.00 cy, $0.50 mn
22652	20-14585	Dep. mn. CFSTI $2.00 cy, $0.50 mn
22655	20-14739	Dep. mn. CFSTI $3.00 cy, $0.75 mn
22664	20-14920	Dep. mn. CFSTI $5.00 cy, $1.00 mn
TO-B–	**(Non-AEC)**	
65-27	20-15931	
TR–	**(Misc.)**	
66-02	20-14235	See SAN-584-1
TRG-Report–	**(British)**	
1115	20-16087	Dep. BIS $1.60. HMSO 8s.
TT–	**(Canadian)**	
65-33980	20-16107	See JPRS-33406
65-34032	20-15149	See JPRS-33458
65-34033	20-16108	See JPRS-33459
UCRL–		
6987(Rev.1)	20-15250	Dep. mn. CFSTI $1.00 cy, $0.50 mn
7769	20-15733	Dep. mn. CFSTI $2.00 cy, $0.50 mn
7771	20-15060	Dep. mn. CFSTI $1.00 cy, $0.50 mn
7873	20-14470	Dep. mn. CFSTI $3.00 cy, $0.75 mn
7929	20-14755	Dep. mn. CFSTI $2.00 cy, $0.50 mn
10696(Rev.)(Pt.2)	20-14691	Dep. mn. CFSTI $1.00 cy, $0.50 mn
11436(Rev.)	20-15464	Phys. Rev., 142: 883-7(1966)
11580	20-15061	Dep. mn. CFSTI $3.00 cy, $0.75 mn
11745	20-15263	Proc. Roy. Soc. (London), Ser. A, 289: 81-96(1965)
11821	20-14514	Dep. mn. CFSTI $4.00 cy, $1.00 mn
12207(Rev.1)	20-15885	Dep. mn. CFSTI $1.00 cy, $0.50 mn
12380-T	20-15446	Dep. mn. CFSTI $1.00 cy, $0.50 mn
14260-T	20-15363	Phys. Rev., 142: 1245-54(1966)
14285	20-15886	Dep. mn; CFSTI $4.00 cy, $1.00 mn
14392	20-15905	Phys. Fluids, 9: 299-308(1966)
14463(Rev.1)	20-14663	Dep. mn. CFSTI $2.00 cy, $0.50 mn
14487(Rev.1)	20-14664	Dep. mn. CFSTI $1.00 cy, $0.50 mn
14531	20-15571	Dep. mn. CFSTI $1.00 cy, $0.50 mn
14698-T	20-15447	Dep. mn. CFSTI $1.00 cy, $0.50 mn
16062	20-15183	Rev. Sci. Instrum., 37: 279-83(1966)
16158	20-15456	J. Math. Phys. (N. Y.), 7: 215-20(1966)
16219	20-15185	Rev. Sci. Instrum., 37: 358-61(1966)
16240	20-15482	Phys. Rev., 142: 1187-94(1966)
16276	20-15335	Phys. Rev., 142: 913-17(1966)
16312	20-15175	Dep. mn. CFSTI $3.00 cy, $0.75 mn
16339	20-15358	Phys. Rev., 142: 1156-63(1966)
16347	20-15359	Phys. Rev., 142: 1163-72(1966)
16374	20-15904	Phys. Fluids, 9: 292-8(1966)
16444	20-15368	Phys. Rev. Lett., 16: 374-7(1966)
16472	20-16153	Dep. mn. CFSTI $2.00 cy, $0.50 mn
16514	20-15062	Dep. mn. CFSTI $2.00 cy, $0.50 mn
16526	20-15316	Dep. mn. CFSTI $3.00 cy, $0.75 mn
16534	20-15010	Dep. mn. CFSTI $2.00 cy, $0.50 mn
16555	20-14861	Dep. mn. CFSTI $2.00 cy, $0.50 mn
16566	20-14233	Dep. mn. CFSTI $6.00 cy, $1.25 mn
16585	20-15063	Dep. mn. CFSTI $3.00 cy, $0.50 mn
16643	20-15946	Dep. mn. CFSTI $2.00 cy, $0.50 mn
16645	20-15947	Dep. mn. CFSTI $2.00 cy, $0.50 mn
16649	20-14515	Dep. mn. CFSTI $1.00 cy, $0.50 mn
16656	20-14692	Dep. mn. CFSTI $3.00 cy, $0.75 mn
UJV–	**(Czechoslovakian)**	
1459/65	20-16026	Dep. mn
UR–		
875-92	20-15336	Phys. Rev., 142: 918-22(1966)
USBM-RC–		
1220	20-14968	Dep. mn. CFSTI $2.00 cy, $0.50 mn
USNRDL-TR–	**(Misc.)**	
905	20-14287	See AD-626996
942	20-14733	See AD-628982
945	20-14258	See AD-627569
960	20-14288	See AD-627986
VDIT–	**(Swedish)**	
16(5.4)	20-15137	Dep. mn
WAPD–	**(Misc.)**	
292	20-15138	Dep. mn. CFSTI $3.00 cy, $0.50 mn
299	20-16088	Dep. mn. CFSTI $3.00 cy, $0.75 mn
WAPD-MRP–		
114	20-16089	Dep. mn; CFSTI $2.50 cy, $0.75 mn
WAPD-T–		
1841	20-16090	Dep. mn. CFSTI $1.00 cy, $0.50 mn
WAPD-TM–	**(Misc.)**	
524	20-15670	Dep. mn. CFSTI $1.00 cy, $0.50 mn
WCAP–	**(Misc.)**	
6078	20-16091	Dep. mn; CFSTI $3.00 cy, $0.75 mn
Y–		
1420(Rev.1)	20-16154	Dep. mn. CFSTI $2.00 cy, $0.50 mn
1490	20-14702	Dep. mn. CFSTI $1.00 cy, $0.50 mn
1501	20-14791	Dep. mn. CFSTI $1.00 cy, $0.50 mn
ZFK-PHA–	**(German)**	
18	20-15734	Dep. mn

DEPOSITORIES OF USAEC REPORTS

In Countries Other than the U.S.

ARGENTINA
Buenos Aires, Comisión Nacional de Energía Atómica
AUSTRALIA
Canberra, Australian National Library
Sutherland, New South Wales, Australian Atomic Energy Commission
AUSTRIA
Vienna, Zentral Bibliothek der Physikalischen Institute der Universität
BELGIUM
Mol-Donk, Centre d'Etude de l'Energie Nucleaire
BOLIVIA
La Paz, Comisión Nacional de Energiá Nuclear
BRAZIL
Rio de Janeiro, Instituto Brasileiro de Bibliografia e Documentacao
São Paulo, Instituto de Energia Atomica, Cidade Universitaria São Paulo
BURMA
Rangoon, Union of Burma Applied Research Institute, Atomic Energy Center Library
CANADA
Hamilton, McMaster University
Ottawa, National Research Council Library
Vancouver, University of British Columbia
CHILE
Santiago, Instituto de Fisica y Matematicas, Universidad de Chile
CHINA
Hsinchu, Taiwan, Free China, National Tsing Hua University
COLOMBIA
Bogota, Instituto De Asuntos Nucleares
COSTA RICA
San Pedro, University of Costa Rica Library
DENMARK
Risö, Danish Atomic Energy Commission
ECUADOR
Quito, Escuela Politécnica Nacional
EL SALVADOR
San Salvador, Universidad de El Salvador, Biblioteca de Energia Nuclear
FINLAND
Helsinki, Teknillisen Korkeakoulun Kirjasto
FRANCE
Gif-sur-Yvette, Centre d'Etudes Nucléaires de Saclay
Paris, Académie des Sciences
GERMANY
Berlin, Hahn-Meitner-Institut für Kernforschung Berlin
Frankfurt/Main, Gmelin-Institut
Munich, Technische Hochschule, Bibliothek
GHANA
Accra, University College of Ghana
GREECE
Athens, Nuclear Research Center "Democritus"
GUATEMALA
Guatemala, Comisión Nacional de Energía Nuclear
INDIA
Bombay, Department of Atomic Energy
IRAN
Tehran, Tehran University Nuclear Centre
IRAQ
Baghdad, Iraqi Atomic Energy Commission
IRELAND
Dublin, University College
ISRAEL
Rehovoth, Israel Atomic Energy Commission
ITALY
Rome, Centro di Studi Nucleari della Casaccia
Rome, Comitato Nazionale per l'Energia Nucleare
JAPAN
Tokyo, National Diet Library
KOREA
Seoul, Office of Atomic Energy
LEBANON
Beirut, Lebanese National Council for Scientific Research
LUXEMBOURG
Luxembourg, Ministry of Transport and Electricity
MALAYSIA
Kuala Lumpur, University of Malaysia
MEXICO
Mexico, D.F., Comisión Nacional de Energía Nuclear
NETHERLANDS
The Hague, Reactor Centrum Nederland
NEW ZEALAND
Lower Hutt, Institute of Nuclear Sciences
NIGERIA
Ibadan, University of Ibadan
NORWAY
Lillestrom, Institutt för Atomenergi
PAKISTAN
Lahore, West Pakistan, Atomic Energy Centre
PERU
Lima, Junta de Control de Energia Atomica
PHILIPPINE REPUBLIC
Manila, Philippine Atomic Energy Commission
POLAND
Warsaw, Biura Pelnomocnika Rzadu do Spraw Wykorzystania Energii Jadrowej
PORTUGAL
Sacavem, Junta de Energía Nuclear
REPUBLIC OF SOUTH AFRICA
Pretoria, Atomic Energy Board Library
REPUBLIC OF THE CONGO
Leopoldville, Université Lovanium
SPAIN
Madrid, Junta de Energía Nuclear, Biblioteca Documentación y Publicaciones, Ciudad Universitaria
SWEDEN
Nyköping, Aktiebolaget Atomenergi
SWITZERLAND
Zürich, Eidgenössische Technische Hochschule, Bibliothek
THAILAND
Bangkok, Office of the Thai Atomic Energy Commission, Department of Science
TURKEY
Ankara, Turkish Atomic Energy Commission, Atomic Energy Library
UNITED ARAB REPUBLIC
Cairo, Atomic Energy Commission
UNITED KINGDOM
Birmingham, Central Library
Boston Spa, National Lending Library for Science and Technology
Kingston upon Hull, Central Library
Liverpool, Central Library
London, Central Library, Acton
London, National Reference Library
London, Science Museum Library, South Kensington
Manchester, Central Library
Newcastle upon Tyne, Central Library
Nottingham, Central Library
Sheffield, Central Library
URUGUAY
Montevideo, Comision Nacional de Energia Atomica
VENEZUELA
Caracas, Instituto Venezolano de Investigaciones Científicas
VIET-NAM
Saigon, Atomic Energy Office
YUGOSLAVIA
Belgrade, Federal Commission for Nuclear Energy

In International Agencies

AUSTRIA
Vienna, International Atomic Energy Agency
BELGIUM
Brussels, La Bibliotheque EURATOM
FRANCE
Paris, European Nuclear Energy Agency, O.E.C.D.
ITALY
Ispra, EURATOM Research Center
SWITZERLAND
Geneva, United Nations Library

UNITED STATES
GOVERNMENT PRINTING OFFICE
DIVISION OF PUBLIC DOCUMENTS
WASHINGTON, D.C. 20402

OFFICIAL BUSINESS

POSTAGE AND FEES PAID
U.S. GOVERNMENT PRINTING OFFICE

TECHNICAL PROGRESS REVIEWS

The Division of Technical Information, U. S. Atomic Energy Commission, also publishes the Technical Progress Reviews, a series of five quarterly journals on nuclear technology. These journals, compiled by specialists and recognized authorities, summarize, evaluate, and reference the progress of development in five important fields.

Isotopes and Radiation Technology P. S. Baker, A. F. Rupp, and associates, Oak Ridge National Laboratory. Reviews AEC-sponsored projects and related significant worldwide developments in radioisotopes and radiation technology.

Nuclear Safety Wm. B. Cottrell, W. H. Jordan, and associates, Oak Ridge National Laboratory. Covers topics relevant to the analysis and control of hazards associated with nuclear reactors and with operations involving fissionable materials and the products of nuclear fission.

Power Reactor Technology Argonne National Laboratory. Reviews research, development, design practices, and operating experiences associated with power reactors, including aerospace applications.

Reactor Fuel Processing Stephen Lawroski and associates, Argonne National Laboratory. Reviews all aspects of the fuel-processing field, including aqueous and nonaqueous processing and waste disposal.

Reactor Materials R. W. Dayton, E. M. Simons, and associates, Battelle Memorial Institute. Covers the properties, behavior, and fabrication processes of materials used in nuclear reactors and associated equipment.

Availability

SUBSCRIPTION RATE: The Technical Progress Reviews may be purchased from the Superintendent of Documents, U. S. Government Printing Office, Washington, D. C. 20402, at $2.50 per year for each subscription or $0.70 per issue.

POSTAGE: Postpaid within the United States, Canada, Mexico, and all Central and South American countries except Argentina, Brazil, British and French Guiana, Surinam, and British Honduras. For these Central and South American countries and all other countries, add $0.75 per year or $0.20 per single issue.

REMITTANCE: Payment should be by check, money order, or document coupons and MUST accompany order. Remittances from foreign countries should be made by international money order or draft on an American bank payable to the Superintendent of Documents or by UNESCO book coupons.